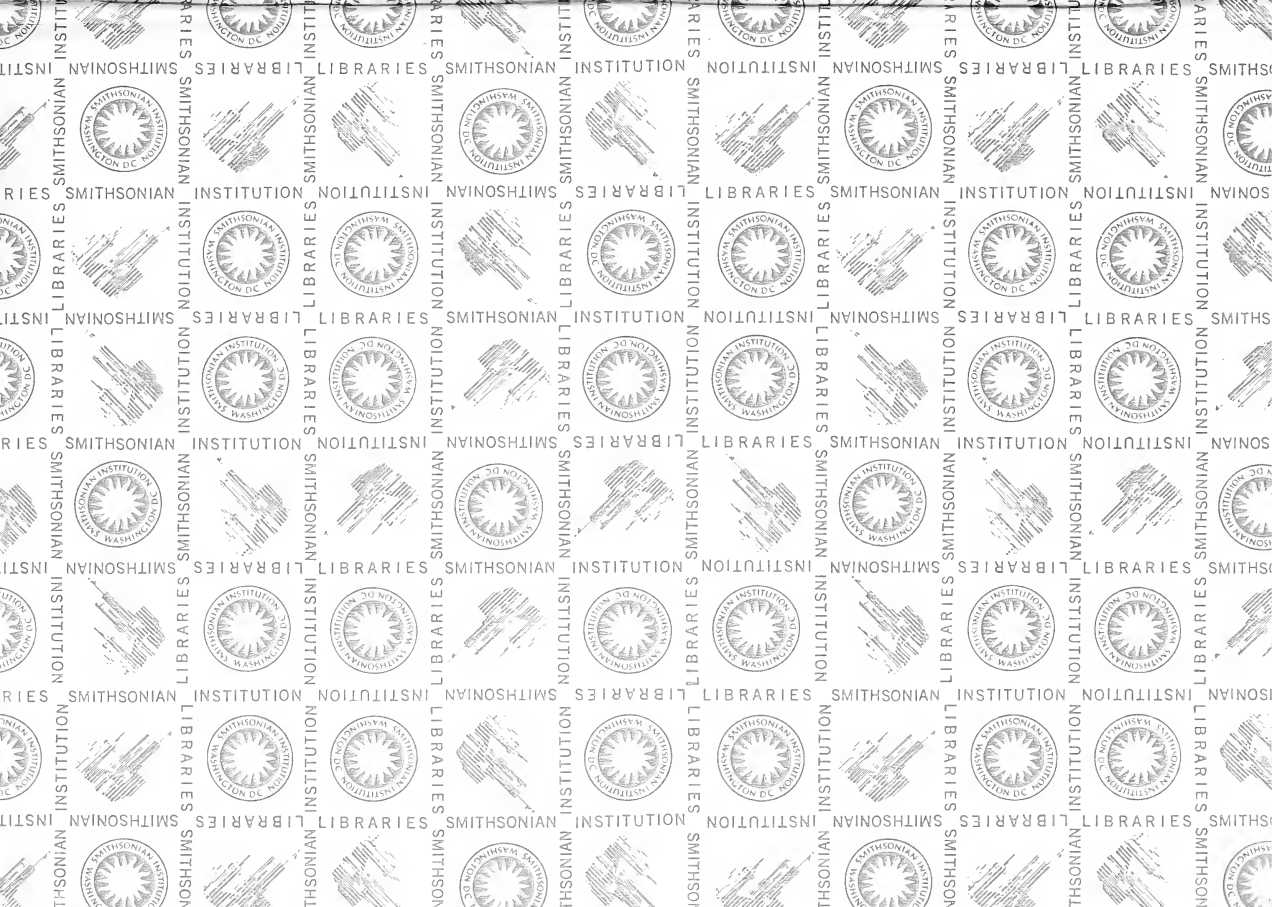
SMITHSONIAN INSTITUTION LIBRARIES

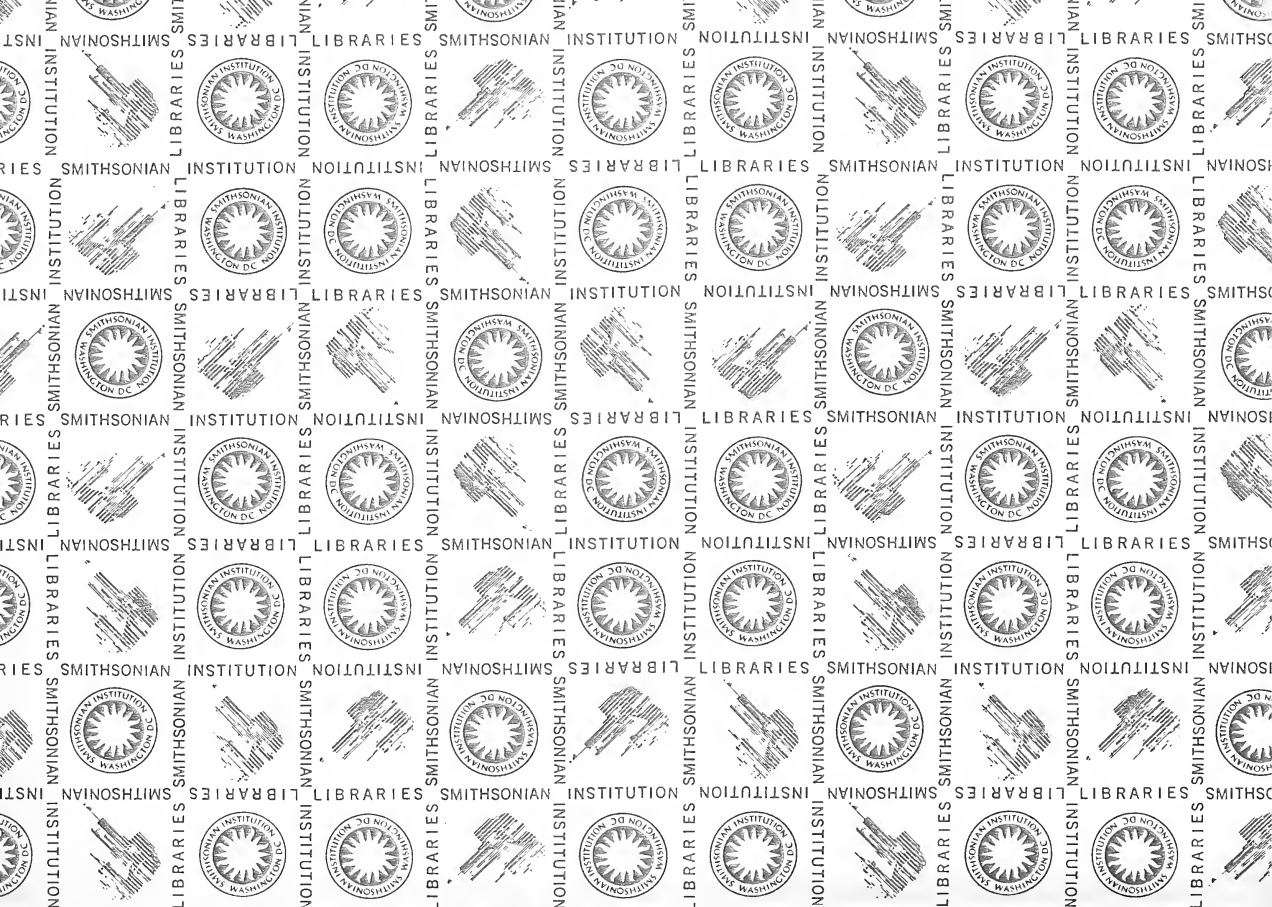
SMITHSONIAN INSTITUTION LIBRARIES

VOLUME 13

Palaeontology

1970

PUBLISHED BY THE
PALAEONTOLOGICAL ASSOCIATION
LONDON

Dates of publication of parts of Volume 13

Part 1, pp. 1–173, pls. 1–34	22 March 1970
Part 2, pp. 175–333, pls. 35–62	26 August 1970
Part 3, pp. 335–510, pls. 63–102	30 October 1970
Part 4, pp. 511–700, pls. 103–128	22 December 1970

THIS VOLUME EDITED BY N. F. HUGHES, GWYN THOMAS, ISLES STRACHAN, ROLAND GOLDRING, M. R. HOUSE AND J. D. HUDSON

Dates of publication of Special Papers in Palaeontology

Special Paper No. 1	21 June 1967
Special Paper No. 2	31 January 1968
Special Paper No. 3	7 October 1968
Special Paper No. 4	1 May 1969
Special Paper No. 5	17 October 1969
Special Paper No. 6	26 April 1970
Special Paper No. 7	6 August 1970

PRINTED IN GREAT BRITAIN

CONTENTS

VOLUME 13 · PART 1

Palaeontology

MARCH 1970

PUBLISHED BY THE
PALAEONTOLOGICAL ASSOCIATION
LONDON

Price £3

THE PALAEONTOLOGICAL ASSOCIATION

The Association was founded in 1957 to further the study of palaeontology. It holds meetings and demonstrations, and publishes the quarterly journal *Palaeontology* and *Special Papers in Palaeontology*. Membership is open to individuals, institutions, libraries, etc., on payment of the appropriate annual subscription:

Institute membership	£7. 0*s*. (U.S. $20.00)
Ordinary membership	£5. 0*s*. (U.S. $13.00)
Student membership	£3. 0*s*. (U.S. $8.00)

There is no admission fee. Institute membership is only available by direct application, not through agents. Student members are persons receiving full-time instruction at educational institutions recognized by the Council; on first applying for membership, they should obtain an application form from the Membership Treasurer. All subscriptions are due each January, and should be sent to the Membership Treasurer, Dr. A. J. Lloyd, Department of Geology, University College, Gower Street, London, W.C. 1, England.

STATISTICAL ANALYSIS AND PRESENTATION OF TRINUCLEID (TRILOBITA) FRINGE DATA

by C. P. HUGHES

ABSTRACT. The current notation and methods of data presentation for the pits of the trinucleid fringe are reviewed and some shortcomings noted. Using a sample of *Trinucleus fimbriatus* Murchison investigations show that (i) operator errors in selecting half-fringes were negligible, (ii) major features of the pit distribution are not dependent on the size of specimen, (iii) statistically there are no significant differences between the left and right half-fringes, although particular individuals commonly exhibit some asymmetry. It is considered most probable that these conditions hold true in all trinucleids and that numerical studies should be applied throughout taxonomic studies of the group.

SINCE Bancroft (1929) introduced a notation for describing the trinucleid fringe and the use of the fringe characteristics in systematic studies, the taxonomic importance of the pit distribution on the fringe of trinucleids has increased enormously. However, the most favoured system of pit enumeration at the present day is still that proposed by Bancroft (1929, pp. 69–72) and subsequently emended by Whittard (1955, pp. 27–8). That this system has remained unchanged in its essentials since its inception is surprising, as several authors have experienced some difficulties in using it. Williams (1948), in studying the marrolithids of South Wales, found it difficult to apply Bancroft's scheme to the variable numbers of swollen pits typical of these trinucleids. Cave (1957) in a population study of *Salterolithus caractaci* found even Whittard's emended form of notation unsatisfactory to deal adequately with the variation he found within the population. More recently Whittington (1966, pp. 86–90) found a similar degree of variation in *Broeggerolithus nicholsoni* and recognized the need for some new means of documenting the variation present and, while working within the general framework of the traditional notation, presented data on the variation by means of simple histograms rather than attempting to use the standard half-fringe formula. Whittington (1968) again raised the problem of documenting the characteristics of the pit distribution when describing some North American species of *Cryptolithus* where the preservation is such that data are available for complete fringes. In that study he concluded that the full use of Whittard's notation was unnecessary and he concentrated on the number of pits in the complete E_1 arc and the appearance of the inner I arcs, I_3 and I_4, since these three aspects of the fringe pit distribution were the most important for distinguishing the species under consideration. He also (p. 703) raised the problem, often apparently ignored when half-fringe data have been given in the past, that even in such well preserved material the selection of the midline of the fringe is often difficult.

The main aim of the present paper is to record the methods and results of an analysis of the distribution of pits on a trinucleid fringe made as a preliminary to the application of statistical techniques in taxonomic studies of the trinucleids. This analysis showed that the half-fringe may in fact be used satisfactorily to represent the characteristics of the whole fringe and that it does not show any dependence on the size of the individual. Although the details of the methods used here were closely linked to one particular

[Palaeontology, Vol. 13, Part 1, 1970, pp. 1–9.]

trinucleid, namely *Trinucleus fimbriatus*, this type of approach is, it is believed, applicable to all trinucleid fringes as well as to many problems concerning numerical symmetry and size dependence of morphological features in palaeontological studies. The main purpose of presenting these results here as a separate entity divorced from any accompanying systematic studies is that by so doing it is hoped to be more readily accessible to workers in other fields, for although such techniques as employed here have on occasion been used over the last 30 or 40 years, there is still a need for their much wider application.

The present study was made as a preliminary to the redescription of the trinucleids of the Builth region (Hughes in press) and was carried out entirely independently of Whittington and prior to the appearance of his 1968 paper. It is of interest therefore to note that although the types of material and approaches used were different, the conclusions are basically very similar. The approach adopted here has tended to be more numerical than graphical, for although graphs and histograms of the type used by Whittington are a very useful means of illustration, the purely statistical presentation enables direct objective comparisons to be made between various sets of data; such comparisons are not possible directly from histograms. On the other hand the statistical presentation adopted here could be attacked as being too abstract, and it is believed that in systematic studies the most satisfactory method may well be a conjunct use of both methods, using the graphical aids to illustrate appropriate features. Finally, in this paper the possibilities of extending the results of this study towards a more mathematical approach to the description of the pit distribution of trinucleid fringes are assessed.

As mentioned by Whittington (1968, p. 704) it is chiefly because of the incomplete preservation of the fringe in the bulk of trinucleid material that the vast majority of trinucleid species have been based on half-fringe descriptions, even in species where some complete fringes were known. This reliance on the half-fringe has assumed a symmetrical distribution of the pits of the fringe about the sagittal line—an assumption that has never been put to any real test. Another possible weakness of the traditional 'half-fringe formula' for describing trinucleid fringes is that it has never made any allowance for the possibility that the pit distribution may be dependent on the size of the individual. Although ontogenetic studies (Whittington 1941, pp. 510–11; 1959, pp. 443 ff.) show that the fringe apparently assumes the essential adult characteristics early in the meraspid stage of development, this does not preclude the possibility that there may be some change in the pit distribution with increasing size.

A sample of some three hundred and fifty internal moulds of cephala of *Trinucleus fimbriatus* Murchison 1839 from the black shales of basal Caradoc (*N. gracilis*) age exposed in the middle quarry, Llanfawr, Llandrindod Wells, Radnorshire was collected for this study. This sample consisted of slightly flattened, generally well-preserved, though incomplete remains. Despite the fragmentary nature of many specimens, samples of about 30 were generally obtainable for any particular aspect of the pit distribution. Although these samples were not as large as one could have hoped for, they were, it is believed, sufficient to give adequate data of the fringe characteristics. Apart from the obvious criterion of availability, *Trinucleus fimbriatus* was selected on account of its pit distribution being relatively simple with well-developed radial and concentric elements (see text-fig. 1).

Terminology. The terminology used throughout this study is that in standard use for trinucleids with the exception that Bancroft's term 'concentric row' is replaced by the term 'arc'. This avoids the possibility of confusion which has in the past occurred through some authors abbreviating one or both Bancroft's terms 'concentric row' and 'radial row' to 'row'. It has been found that the standard convention of numbering radial rows and arcs is both useful and generally satisfactory (except where there is a complete lack of radial and concentric arrangement) in defining the various elements of the pit distribution, although as is shown below the continued use of the 'half-fringe formula' should not be encouraged. Throughout this study, symmetry is only considered with respect to the number of pits, not their size or exact relative positioning.

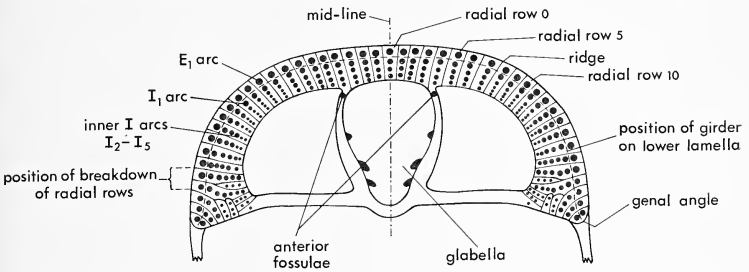

TEXT-FIG. 1. Diagram of *Trinucleus fimbriatus* Murchison showing the distribution of pits on the fringe and the terminology used. The diagram shows radial row 0 and slight asymmetry developed.

STATISTICAL INVESTIGATION

Because of the nature of much trinucleid material it is highly desirable that species should be definable without the necessity of recourse to details of the pit distribution of the full fringe. However, this may only be done if the fringe is symmetrical, or if it is not, any asymmetries must be small enough so as to have no significance. Further, any errors in selecting the mid-line of the fringe must not be significant either. Preliminary observations showed that slight asymmetry of the fringe was common and data were collected to assess the magnitude and characteristics of the asymmetries. In the collection of half-fringe data from material in which the complete fringe is preserved some care must be taken to avoid biasing the data. Such bias may be caused by the systematic misidentification of the mid-line or a personal tendency to select half-fringes showing some atypical feature. In the collection of data therefore one half-fringe only must be included from any one individual and some system should be used for selecting the half-fringe to be considered; in this study left and right half-fringes were selected alternately.

It is seen from Table 1 that of any of the three elements considered, i.e. the E_1, I_1 arcs and the number of radial rows developed, only about one-third of the specimens show symmetrical fringes. If however all three elements are considered simultaneously, then the percentage of bilaterally symmetrical specimens falls to 10%. Thus, although due to the non-perfect preservation it is difficult to consider all elements of the fringe at once, it is clear that perfectly symmetrical fringes rarely, if ever, occur.

As mentioned above it is important to remember that some specimens may show apparent symmetry, or asymmetry, due to the misidentification of the mid-line of the fringe. Thus a specimen having $2n+1$ pits (full-fringe) in a particular arc would appear symmetrical (with regard to that particular arc) if the mid-line were taken along the central radial row, but asymmetrical if taken along either of the adjacent ridges or rows.

TABLE 1. Data giving the number of complete specimens of *Trinucleus fimbriatus* Murchison symmetrical and asymmetrical about the sagittal line with respect to the number of pits in the E_1 and I_1 arcs and the number of radial rows developed.

	E_1	I_1	*Radial rows*
No. of symmetrical specimens	10	9	6
No. of asymmetrical specimens	21	22	16
% of symmetrical specimens	32	29	37

In order to reduce such misidentifications to a minimum the mid-line was taken as passing through the mid-point between the anterior fossulae. Specimens in which this differed markedly from the mid-line as estimated by eye on the glabella, were rejected as being too deformed for symmetry studies, and also for the collection of any precise half-fringe data. Even if small errors due to mid-line misidentification are occasionally included they will, in most cases, be sufficiently rare so as not to have any significant effect on the final outcome, as the two half-fringe pit counts commonly differed by more than one.

In practice the only common case that had to be decided concerning the placing of the mid-line was whether it lay along a radial row of pits (row 0) or along the ridge to one side of that row (which would then be row 1). If there was any systematic error being made in the positioning of the mid-line it could cause a correlation, either positive or negative, between symmetry and the positioning of the mid-line along the row of pits, row 0 or along the ridge on one side. The 2×2 contingency tables given in Table 2 show that no such correlation exists for the E_1 and I_1 arcs considered separately or combined together. Insufficient data are available on the inner I arcs, but the same result is anticipated if such data were available.

Thus it is established that some asymmetry (in the actual numbers and not exact positioning or size of pits) is present in the vast majority of specimens and that this asymmetry is not to be explained by the misidentification of the mid-line of the fringe.

Before considering how much effect these asymmetries may or may not have on the use of half-fringe data it is convenient to investigate on full-fringe data whether there is any correlation between the pit distribution and size of the individual. Since relatively few data were available for arcs internal to I_1, the E_1 and I_1, arcs were again taken as representative of the arc elements of the fringe. Data showing that no correlation with size is present are given in Table 3.

Although relatively few data are available, observations indicate that the major factor that varies in the inner arcs is the row in which the particular arc commences (that is also true in *Cryptolithus tessellatus* (Whittington 1968, pp. 709–10) and in *Bettonia chamberlaini* (Hughes in press). Observations on *Trinucleus fimbriatus* show that this variation only affects the pit counts in the five antero-median rows, data for each half-fringe being given in Table 4, which indicates that this variation is not correlated with the

size of specimen. Again in the case of these data small errors may occur due to the misidentification of the mid-line, but since the variation between the rows is small, the effect of any such errors will be insignificant. Any attempt to number the rows from the position of radial breakdown near the genal angles would introduce far greater uncertainties owing to the imprecise way the radial nature of the pits is lost.

TABLE 2. 2×2 tables illustrating the lack of correlation in *Trinucleus fimbriatus* Murchison between the symmetry of the fringe for the E_1, I_1 and E_1+I_1 arcs and the development of radial row 0. The value of P gives the probability that inhomogeneities as great or greater than those observed would occur by chance in a random sample drawn from a homogeneous population. Conventionally a value of $P < 0{\cdot}05$ is considered as 'significant', that is, there is a better than 19 in 20 chance that the inhomogeneities observed are truly present in the source population. In this and all other 2×2 tables χ^2 has been calculated by the unadjusted method (see Simpson, Roe, and Lewontin 1960, pp. 189, 322–3). The values of P obtained here by this method never indicate a significant correlation. The adjusted method always errs on the 'safe side' and would never give a significant value for P when the unadjusted method did not. Thus although the samples are small it is considered unnecessary to calculate the more refined adjusted values (in Table 7 cell values of zero are present and so exact probability tests were applied).

	E_1		I_1		E_1+I_1	
Radial row 0	*present*	*absent*	*present*	*absent*	*present*	*absent*
Symmetrical	4	6	4	5	3	5
Asymmetrical	11	10	10	12	11	12*
	$P = 0{\cdot}50$		$P \simeq 1{\cdot}00$		$P = 0{\cdot}70$	

* This figure includes one specimen with a pit of radial row 0 present in the E_1 arc but absent in the I_1 arc.

TABLE 3. 2×2 tables showing the lack of correlation in *Trinucleus fimbriatus* Murchison between the number of pits developed in the E_1 and I_1 arcs and size as measured by the maximum cephalic width (*tr.*), excluding the fringe. For explanation of P see Table 2.

size in mm.	*9–13*	*14–19*	*size in mm.*	*9–13*	*14–19*
38–42 E_1 pits	13	10	*38–42 I_1 pits*	9	14
43–47 E_1 pits	5	2	*43–47 I_1 pits*	3	3
	$P = 0{\cdot}67$			$P = 0{\cdot}68$	

Thus it is seen from Tables 3 and 4 that for the E_1 and I_1 arcs and for rows 1–5 of each half-fringe there is no correlation between the number of pits developed and the size of the individual. Although the sample considered only includes a few, probably fairly advanced meraspides, this finding is in general agreement with what has been inferred in the past from ontogenetic studies.

Now that the lack of size correlation has been demonstrated, the problem as to whether the asymmetries in the pit distribution have any significant effect on the use of half-fringe data may be examined. If, as might be expected, the irregularities causing the asymmetries occur randomly on left and right halves of the fringe and are also generally small compared to any inherent variability of the species, then, provided that the data are taken from a random sample of half-fringes, the asymmetry should not affect the final outcome. In order to check this, left and right half-fringe counts were made for the E_1 and I_1 arcs and the data summarized in Table 5.

TABLE 4. 2 × 2 tables showing the lack of correlation between the number of pits occurring in the radial rows 1–5 of each half-fringe and size in *Trinucleus fimbriatus* Murchison. Size in this table is taken as the maximum width (*tr.*) of the left or right gena. For explanation of *P* see Table 2.

Row 1

Left half-fringe			*Right half-fringe*		
Size in mm.	*6–7*	*8–10*	*Size in mm.*	*6–7*	*8–10*
5 pits	4	9	*4–5 pits*	4	14
6 pits	0	2	*6 pits*	0	4
	$P \simeq 1{\cdot}00$			$P \simeq 0{\cdot}56$	

Row 2

Left half-fringe			*Right half-fringe*		
Size in mm.	*6–7*	*8–10*	*Size in mm.*	*6–7*	*8–10*
5 pits	5	8	*2–5 pits*	5	15
6 pits	1	5	*6 pits*	1	5
	$P \simeq 0{\cdot}60$			$P \simeq 1{\cdot}00$	

Row 3

Left half-fringe			*Right half-fringe*		
Size in mm.	*6–7*	*8–10*	*Size in mm.*	*5–7*	*8–11*
4–5 pits	5	9	*4–5 pits*	3	13
6 pits	2	9	*6 pits*	4	12
	$P \simeq 0{\cdot}40$			$P \simeq 1{\cdot}00$	

Row 4

Left half-fringe			*Right half-fringe*		
Size in mm.	*6–7*	*8–11*	*Size in mm.*	*5–7*	*8–11*
3–5 pits	1	7	*3–5 pits*	3	10
6 pits	6	11	*6 pits*	6	16
	$P \simeq 0{\cdot}46$			$P \simeq 1{\cdot}00$	

Row 5

Left half-fringe			*Right half-fringe*		
Size in mm.	*5–7*	*8–11*	*Size in mm.*	*5–7*	*8–11*
3–5 pits	0	1	*5 pits*	1	2
6–7 pits	6	15	*6–7 pits*	6	20
	$P = 0{\cdot}70$			$P = 1{\cdot}00$	

TABLE 5. Data showing the lack of significant difference between the left and right half-fringe pit counts for the E_1 and I_1 arcs of *Trinucleus fimbriatus* Murchison. For explanation of *P* see Table 2.

	E_1			I_1		
	mean	*var.*	*n*	*mean*	*var.*	*n*
Left half-fringe	20·70	1·89	55	20·62	1·64	54
Right half-fringe	20·81	1·23	62	20·74	1·35	62
	$P > 0{\cdot}9$			$P > 0{\cdot}9$		

In this and subsequent half-fringe counts, row 0 when present, was taken as having half a pit in each half-fringe. From the data of this table it is seen that for these two arcs there are no significant differences between the two half-fringes. Table 6 gives data

comparing the number of pits in the radial rows 1–5, for both half-fringes and again it is seen that there are no significant differences between the two.

TABLE 6. Modes and ranges for the number of pits developed in radial rows 1–5 of both half-fringes of *Trinucleus fimbriatus* Murchison.

	Row 1					
	mode	*range*	*n*			
Left half-fringe	5	5–6	15			
Right half-fringe	5	4–6	22			
	Row 2			Row 3		
	mode	*range*	*n*	*mode*	*range*	*n*
Left half-fringe	5	5–6	18	5	4–6	25
Right half-fringe	5	2–6	26	6	4–6	32
	Row 4			Row 5		
	mode	*range*	*n*	*mode*	*range*	*n*
Left half-fringe	6	3–6	25	6	3–7	22
Right half-fringe	6	3–6	35	6	5–7	29

Table 7, however, shows that the number of radial rows developed is significantly correlated to the number of pits present in the E_1 arc. That is, a specimen having a high E_1 pit count does not have all the extra pits accommodated posterolaterally to enlarge the genal flange where the pit distribution does not show radial arrangement. This correlation indicates that since the E_1 pit counts are not dependent on size, nor do the counts for the two half-fringes show any significant differences, then the same will hold true for the number of radial rows developed and formal tests need not be made.

Thus it has been shown in *Trinucleus fimbriatus* that for the E_1 and I_1 arcs, the numbers of pits in rows 1–5 and the total number of radial rows developed, the half-fringe may be taken as representative of the entire fringe, and it seems reasonable to assume that this

TABLE 7. 2×2 tables showing the significant correlation between the number of pits developed in the E_1 arc in each half-fringe and the number of radial rows present. Since cell values of zero are present exact probability tests were used in place of χ^2 tests.

Left half-fringe

Number of E_1 pits	*18–20*	*21–24*
12–17 rows	19	0
18–20 rows	0	12

$P \simeq 0$

Right half-fringe

Number of E_1 pits	*18–20*	*21–23*
15–17 rows	17	12
18–20 rows	0	11

$P \simeq 0$

should also be true for the other inner arcs and the more laterally placed radial rows (the few data that are available do in fact support this). This is supported by other studies on trinucleids, including *Bettonia* and *Cryptolithus* (Hughes in press), and it seems likely that these general results hold true throughout the Trinucleidae. Although much of this other work on trinucleid fringes has suffered from a similar paucity of data for the inner regions of the fringe, some data on the appearance of the inner arcs (I_3 and I_4) in *Cryptolithus tessellatus* and *Cryptolithus lorettensis* have been presented by Whittington (1968, text-figs. 3–5). Formal tests on his data show that there are no significant differences between the two half-fringes.

Thus the continued use of the half-fringe in trinucleid studies appears to be justified, provided the variation within a population and the asymmetry exhibited by some individuals are borne in mind. Particular caution should be exercised in assessing the significance of the pit distribution when only a few specimens are available, and no new taxa should be erected on slight differences in the distribution of the pits in single specimens or small groups of individuals as has on occasion been done in the past.

In order to facilitate comparisons, it is desirable to have some convention both as to the fringe data selected and as to the manner of their presentation. For the identification of individual pits it is proposed to retain Whittard's notation, but the continued use of the half-fringe formula in specific descriptions cannot be justified, since it cannot express the variation encountered within a species in a manner which enables direct objective comparisons with other samples or species. The data cited will vary in detail from one species to another but they should always be as comprehensive as possible. It is suggested that data for the various arcs and for those radial rows in which variation occurs should always be given. Data for other elements such as the number of radial rows present, distribution of adventitious pits, numbers of pits along the posterior border of the fringe, etc., should be given where appropriate, together with suitable summarizing statistics (see below) and, where useful, illustrated by means of graphical aids such as simple graphs and histograms. In view of the fact that most samples are such that the bulk of the data available are for half-fringes, it is proposed that in order to facilitate comparisons, half-fringe data are given even in cases where the full-fringe data are also available. This ensures that in all data the error sources are, as far as is possible, the same and differing samples are comparable. Although in this study it has been shown that the 'operator variation' due to the misidentification of the mid-line of the fringe has no significant effect, this might not always be the case for all trinucleids, since its magnitude depends on the state of preservation and form of the pit distribution medially as well as the skill of the operator.

The type of summarizing statistics cited will vary depending on the element of the fringe being considered. For elements such as the various arcs where the range in the possible number of pits present is relatively large, continuous variable statistics may be applied, and the mean and variance given. Comparisons between samples may then be made by the use of the 't' test. This test assumes that the distribution does not depart significantly from normality; inspection of distributions obtained shows this condition is satisfied. In elements such as the number of pits in a radial row, where the total number and range is small, continuous variable statistics are not applicable and the mode and range should be quoted. Comparisons between data may then be made with non-parametric tests (see Siegel 1956). In some cases where relatively few data are available

summary statistics may be misleading and it would be more satisfactory to present the raw data.

While the above proposals for the description and documentation of the trinucleid fringe are more complex than the half-fringe formulae of Whittard, it is believed that they give a sound basis for the description of any trinucleid fringe, for they are easily adaptable to special features that may be present (e.g. the frontal adventitious pits of *Bettonia*, the data for which may be given or suitable summarizing statistics presented) and to the type and amount of material available. Furthermore it is thought that coupled with some qualitative description and appropriate use of graphical aids a much more comprehensive picture of the distribution and variation of the fringe pits in a population is obtained than could be from the traditional half-fringe formulae.

Acknowledgements. The bulk of this work was undertaken at the Queen's University of Belfast during the tenure of a N.E.R.C. Research Studentship, to whom thanks are given for financial support. I am most grateful to Professor A. Williams and Dr. A. D. Wright for their encouragement and help during my studentship. I am also indebted to Professor H. B. Whittington for allowing me access to his raw data on *Cryptolithus* and for much helpful discussion. Useful discussion on the statistical techniques has been provided by Drs. D. B. Williams and J. L. Cutbill, to whom I render my thanks.

REFERENCES

BANCROFT, B. B. 1929. Some new species of *Cryptolithus* (s.l.), from the Upper Ordovician. *Mem. Proc. Manchr. lit. phil. Soc.* **73**, 67–98, pl. 1, 2.

CAVE, R. 1957. *Salterolithus caractaci* (Murchison) from Caradoc Strata near Welshpool, Montgomeryshire. *Geol. Mag.* **94**, 281–90, pl. 10.

HUGHES, C. P. (in press). The Ordovician Trilobite Faunas of the Builth-Llandrindod Inlier, Central Wales, Part II. *Bull. Br. Mus. nat. Hist. (Geol.)*.

MURCHISON, R. I. 1839. *The Silurian System founded on geological researches in the counties of Salop, Hereford, Radnor, Montgomery, Caermarthen, Brecon, Pembroke, Monmouth, Gloucester, Worcester and Stafford; with descriptions of the coal-fields and overlying formations.* xxxii+768 pp., 40 pls. London.

SIEGEL, S. 1956. *Nonparametric statistics for the behavioral sciences.* xvii+312 pp. McGraw-Hill, New York.

SIMPSON, G. G., ROF, A. and LEWONTIN, R. C. 1960. *Quantitative zoology.* 440 pp. New York.

WHITTARD, W. F. 1955. The Ordovician Trilobites of the Shelve Inlier, West Shropshire. Part 1. *Palaeontogr. Soc. (Monogr.)*, 1–40, pl. 1–4.

WHITTINGTON, H. B. 1941. Silicified Trenton Trilobites. *J. Paleont.* **15**, 492–522, pl. 72–5.

—— 1959. Silicified Middle Ordovician Trilobites: Remopleuridae, Trinucleidae, Raphiophoridae, Endymionidae. *Bull. Mus. comp. Zool.* **121**, 371–496, pl. 1–36.

—— 1966. The Ordovician Trilobites of the Bala area, Merioneth. Part III. *Palaeontogr. Soc. (Monogr.)*, 63–92, pl. 19–28.

—— 1968. *Cryptolithus* (Trilobita): specific characters and occurrence in the Ordovician of eastern North America. *J. Paleont.* **42**, 702–14, pl. 87–9.

WILLIAMS, A. 1948. The Lower Ordovician Cryptolithids of the Llandeilo District. *Geol. Mag.* **85**, 65–88, pl. 6.

C. P. HUGHES
Department of Geology
Sedgwick Museum
Cambridge

Final typescript received 9 June 1969

PALAEOSMUNDA, A NEW GENUS OF SIPHONOSTELIC OSMUNDACEOUS TRUNKS FROM THE UPPER PERMIAN OF QUEENSLAND

by R. E. GOULD

ABSTRACT. Petrified osmundaceous trunks from the Upper Permian coal measures of the Bowen Basin, Queensland, are assigned to a new genus, *Palaeosmunda*, which possesses an ectophloic, sometimes almost simple but usually dictyoxylic, siphonostele with parenchymatous pith; the stems bear stipulate petiole bases which contain sclerotic rings that are rhomboidal in transverse section, upwards becoming laterally extended into flanges. These are the first Permian Osmundaceae definitely known to exhibit a distinct pith and leaf gaps. A table of morphological comparisons of all known Permian osmundaceous axes is presented. Discovery of *Palaeosmunda* indicates that the family had a greater structural diversity and a wider geographic distribution in the Upper Permian than was previously realized; and hence the Osmundaceae probably developed before the Permian. Two species, *P. williamsii* (type species) and *P. playfordii*, are described in detail; the inner cortex, and sometimes the stipules of the petiole bases of *P. williamsii* contain strands of sclerenchyma, while stipules and inner cortex of the petiole bases of *P. playfordii* consist only of parenchyma. Evidence from association indicates that the trunks probably bore fronds of the types referred to *Sphenopteris lobifolia* Morris 1845, *S. polymorpha* Feistmantel 1876, and *Cladophlebis roylei* Arber 1901.

TRUNKS and rhizomes characteristic of the Osmundaceae are apparently well suited to preservation as fossils and the geological history of the family, based on petrified stems, extends from Upper Permian to Recent (Andrews 1961, Miller 1967). Prior to the present work, all known specimens of Permian osmundaceous stems came from the Soviet Union; where the stele is preserved, these contain a protostele or at least an ectophloic siphonostele without well-developed leaf gaps.

Osmundaceous trunks, petrified with silica, calcite, and ferruginous material, occur at many localities in the Upper Permian coal measures of the Bowen Basin, Queensland (text-fig. 1). These are described as two species of a new genus, *Palaeosmunda* gen. nov., in which the stele is usually an ectophloic dictyoxylic siphonostele, but can appear almost simply siphonostelic; the petiole bases are very similar to those of other stipulate Permian osmundaceous stem genera. The new genus is unusual in that it is the first Permian member of the family definitely known to exhibit a distinct pith and leaf gaps.

The specimens on which the study is based were collected by Dr. J. Armstrong, Mr. R. Lees, Dr. B. Runnegar, Dr. F. W. Whitehouse, Mr. J. H. Williams, and the author. Mr. W. A. Hansen and the management and staff of Utah Development Company provided considerable assistance in the location and collection of specimens from Utah's Blackwater coal-mining lease. One specimen, collected in June 1956, was already held in the collections of the Department of Geology and Mineralogy, University of Queensland. All specimens are housed in the Department and catalogue numbers are prefixed UQ.

In his study of the morphology of the living Osmundaceae, Hewitson (1962, p. 80) used the term 'bundle' when describing the stem xylem in transverse section; he considered two (or more) xylem strands connected by even one tracheid as a single bundle. This terminology avoids any confusion when counting the xylem strands, and is very

[Palaeontology, Vol. 13, Part 1, 1970, pp. 10–28, pls. 1–8.]

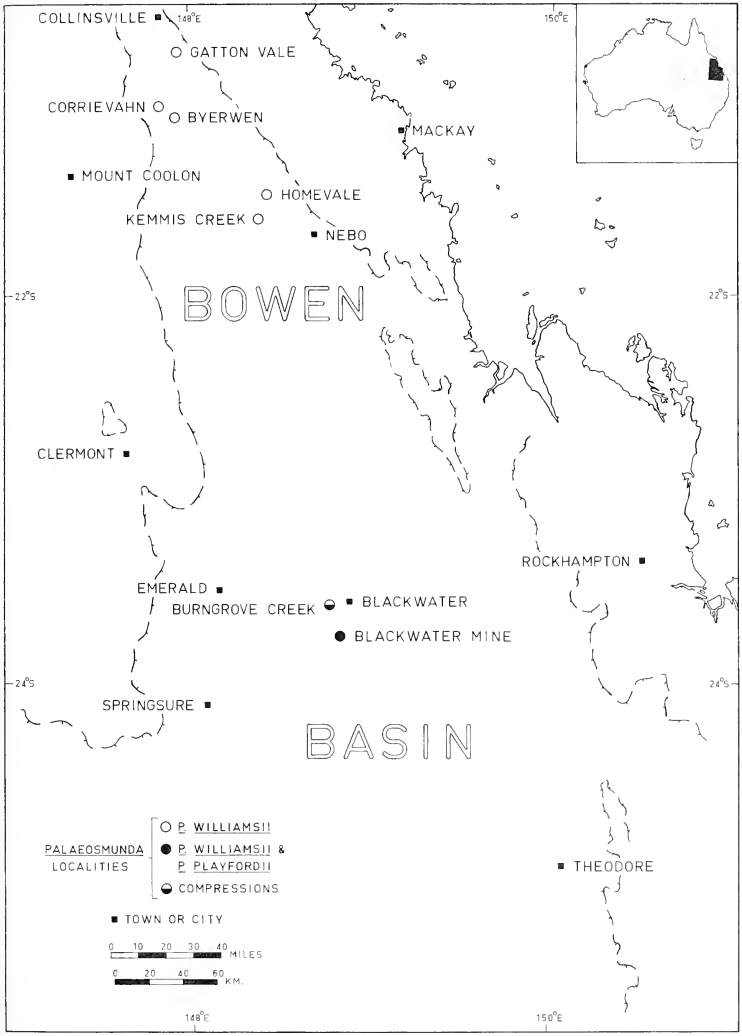

TEXT-FIG. 1. Locality map.

useful in describing the stems of the family where the dictyoxylic stele is well developed. However, where the number of gaps in the xylem ring is small, the number of 'bundles' does not give a complete indication of the structure of the ring. Instead, in the following descriptions, the number of gaps appearing in a transverse section of the xylem cylinder is given. This is equal to the number of bundles in the sense of Hewitson, provided that there are two or more gaps; no gap, or one, results in one 'bundle'. The term 'radial strand' is used in this paper to designate any group of stelar xylem tracheids with a prominent radial dimension when seen in transverse section, regardless of whether the group is connected to adjacent strands or not.

Previous literature. In the second and third parts of their classic memoir on the fossil Osmundaceae, Kidston and Gwynne-Vaughan (1908, 1909) published the first detailed anatomical accounts of Upper Permian osmundaceous stems. They described five species from the Upper Permian of the U.S.S.R., *Zalesskya gracilis* (Eichwald) Kidston and Gwynne-Vaughan 1908, *Z. diploxylon* Kidston and Gwynne-Vaughan 1908, *Thamnopteris schlechtendalii* (Eichwald) Brongniart 1849, *Bathypteris rhomboidea* (Kutorga) Eichwald 1860, and *Anomorrhoea fischeri* Eichwald 1860. The steles of *B. rhomboidea* and *A. fischeri* were not present in their specimens and that of *B. rhomboidea* was described later by Zalessky (1924). Seward (1910) figured some of Kidston and Gwynne-Vaughan's slides and one of these, his frontispiece of *T. schlechtendalii*, had not been figured previously.

In a series of papers, Zalessky (1924, 1927, 1931*a*, *b*, 1935) described and figured further examples from the Upper Permian of the U.S.S.R.; these comprise *B. rhomboidea*, *T. kidstoni* Zalessky 1924, *T. gwynne-vaughani* Zalessky 1924, *Z. uralica* Zalessky 1924, *A. fischeri*, *T. schlechtendalii*, *Z. gracilis*, *Z. diploxylon*, *T. kazanensis* Zalessky 1927, *Z. fistulosa* (Eichwald) Zalessky 1927, *Petcheropteris splendida* Zalessky 1931*a*, *Chasmatopteris principalis* Zalessky 1931*b*, and *Iegosigopteris javorskii* Zalessky 1935. *Thamnopteris kazanensis* was not formally described but a transverse section and some details were figured with explanation (Zalessky 1927, pp. 26, 44, pl. 24, figs. 1–4); the specimen is poorly preserved. Knowledge of *Z. fistulosa* is limited to a photograph of its external surface (Zalessky 1927, pp. 31, 48, pl. 32, fig. 3).

Posthumus (1931) compiled synonymy lists for the genera and species of Permian and other osmundaceous stems that had been described prior to 1928.

STRATIGRAPHY

All specimens of *Palaeosmunda* were collected from the Bowen Basin in freshwater sediments which have been referred to as the Upper Bowen Coal Measures (Smith 1958, Hill and Denmead 1960). Devine and Power (1967) have assigned these sediments in the central western Bowen Basin, including the Blackwater district, to the Bandanna Formation (Power 1967 usage, formerly Upper Bandanna Formation of Patterson *in* Webb 1956, p. 2330). The localities for the osmundaceous fossils (text-fig. 1) are all within the Blackwater Group (Malone 1966) as shown on the geological map of the basin compiled by Malone, Olgers, Mollan, and Jensen (1967); in the Blackwater district the fossil trunks occur in the upper two units of the group, the Burngrove Formation and the Rangal Coal Measures. The Blackwater Group and Bandanna Formation are the same lithological unit in the Blackwater–Springsure area (Power 1967,

Devine and Power 1967). The age of the Upper Bowen Coal Measures, Bandanna Formation, and Blackwater Group is generally considered to be Upper Permian (e.g. Runnegar 1968). Webb and McDougall (1967, pp. 483–4) reported an isotopic age of 240 m.y. for a basal part of the Blackwater Group. Ammonoids from horizons below the coal measures in the northern part of the basin are considered to be of Artinskian (Aktastinian–Baigendzhinian) age (Armstrong, Dear, and Runnegar 1967), while microfloras from the Rewan Formation, which overlies the coal measures, are probably in part of Scythian (Otoceratan) age (Evans 1966, p. 59).

SYSTEMATIC PALAEOBOTANY

Division PTEROPHYTA
Order FILICALES
Family OSMUNDACEAE
Genus PALAEOSMUNDA gen. nov.

Type species. Palaeosmunda williamsii sp. nov.

Diagnosis. Arborescent osmundaceous trunks, each with a stem surrounded by a mantle of leaf bases and adventitious roots; branching of stem dichotomous. Stele an ectophloic, generally dictyoxylic, siphonostele, sometimes almost simply siphonostelic; pith parenchymatous; xylem ring with 0–13 gaps, consisting of 14–28 more or less contiguous radial strands, 9–19 tracheids thick; development of leaf gaps immediate, delayed, or incomplete; gaps very short to long; phloem, pericycle, and endodermis external only. Cortex differentiated into inner parenchymatous zone and outer sclerotic fibrous layer, the latter with short, wide, sclerenchyma cells lining leaf traces and inner cortex; inner cortex about as wide as outer cortex; leaf traces arise at 10–35° to stele, initially with 1 or 2 endarch protoxylem groups; 12–43 traces in a transverse section of cortex. Petiole bases stipulate, containing an adaxially curved, C-shaped vascular strand, inner cortex, and sclerotic ring; sclerotic rings somewhat rhomboidal in cross-section, upwards becoming laterally extended into flanges which partially or completely replace the stipules; rings with gradual increase of fibre diameter towards inner cortex of petiole base, otherwise homogeneous; lateral extremities of ring usually thinner than abaxial and adaxial portions. Roots with diarch xylem strand, arising in pairs from each departing leaf trace usually before it enters inner cortex, or rarely singly, directly from stele; roots often branched and forming dense mat outside mantle.

Discussion. Palaeosmunda differs from the Permian osmundaceous stem genera *Bathypteris* Eichwald 1860, *Chasmatopteris* Zalessky 1931*b*, *Iegosigopteris* Zalessky 1935, *Petcheropteris* Zalessky 1931*a*, *Thamnopteris* Brongniart 1849, and *Zalesskya* Kidston and Gwynne-Vaughan 1908, in that the stele is an ectophloic, usually dictyoxylic, siphonostele with homogeneous metaxylem and a parenchymatous pith; the leaf traces in *Palaeosmunda* initially have one or two endarch protoxylem groups whereas the leaf traces of these other genera are initially mesarch. *Palaeosmunda* lacks both the wide cortex of *Zalesskya* and the spinose petiole bases of *Bathypteris*. There is insufficient information available on *Anomorrhoea* Eichwald 1860, for any useful generic distinction

to be made. A table of comparisons of the species of Upper Permian osmundaceous stems is given in folder.

Osmundacaulis Miller 1967 (an organ genus based on '*Osmundites*' *skidegatensis* Penhallow 1902), which occurs in Mesozoic and Tertiary strata, would include stems similar to those of the new genus, but the petiole bases of *Palaeosmunda* are quite different. Besides being of specific importance, the arrangement of sclerenchyma within the petiole base in the Osmundaceae, as well as the anatomy of the stele, is of generic and subgeneric significance (Kidston and Gwynne-Vaughan 1907, Hewitson 1962, Miller 1967). The leaf bases of *Palaeosmunda* can be more closely compared with those of *Anomorrhoea*, *Chasmatopteris*, *Iegosigopteris*, *Petcheropteris*, and *Thamnopteris* than with those of *Osmundacaulis*. The generally rhomboidal to laterally extended shape of the sclerotic ring in transverse section is exhibited by all the Permian genera except *Zalesskya*, in which the leaf bases are unknown. In contrast, the sclerotic rings of *Osmundacaulis* are generally rounded; the leaf traces in the outer cortex of the Jurassic *O. gibbiana* (Kidston and Gwynne-Vaughan) Miller 1967, are, however, rhomboidal in transverse section (Kidston and Gwynne-Vaughan 1907). The initial rhomboidal shape, small stipules, and upward lateral extension of the sclerotic ring into flanges which replace the stipules are well developed in *Palaeosmunda*; the shape is not solely due to the close arrangement of the bases around the stem, as they retain and even increase the laterally flanged shape in the outer part of the mantle where they are free of any restriction. The gradual increase in diameter of the fibres of the sclerotic ring towards the inner cortex of the petiole base is also exhibited by *T. schlechtendalii*, *B. rhomboidea*, and possibly by *A. fischeri* and *I. javorskii* (see Kidston and Gwynne-Vaughan 1909, pl. 5, fig. 36; pl. 7, fig. 48; pl. 8, fig. 63; Zalessky 1935, pl. 2, fig. 7), as well as some post-Palaeozoic species of Osmundaceae. At least *I. javorskii* and *P. splendida*, and possibly also *A. fischeri*, *C. principalis*, and *T. schlechtendalii* (see Zalessky 1927, pl. 23, fig. 1), show relatively thin lateral extremities of the sclerotic ring as in *Palaeosmunda*.

The development of the ectophloic dictyoxylic siphonostele in Osmundaceae by Upper Permian is somewhat earlier than had been previously thought (e.g. Hewitson 1962, p. 84), but is not altogether surprising. Leaf gaps are partially formed in the Upper Permian *C. principalis*, and *T. kidstoni*, also of Upper Permian age, contains some parenchyma cells in the inner xylem. Triassic representatives of osmundaceous stems include *Osmundacaulis herbstii* (Archangelsky and de la Sota) Miller 1967, '*Osmundites*' *tuhajkuensis* Prynada (Orlov 1963, pl. 29, fig. 10), and probably '*Osmundites*' *winterpockensis* Bock 1960; all of these are of Upper Triassic age and *O. herbstii*, and probably '*O.*' *tuhajkuensis*, exhibit dictyoxylic siphonosteles. The shape of the transverse section of the sclerotic ring in the leaf bases of '*O.*' *tuhajkuensis* is somewhat intermediate between those of the Permian examples and *Osmundacaulis*; the two masses of sclerenchyma in each arm of the C-shaped petiolar strand of '*O.*' *tuhajkuensis* has, however, only been found in *Osmundacaulis* and *Osmunda*. '*Osmundites*' *winterpockensis* is based on a sandstone cast with no internal structure preserved (C. N. Miller, pers. comm. 1969). Other Triassic fossil stems referred to the Osmundaceae, and used as examples to explain the evolution of the dictyoxylic siphonostele from the protostele (e.g. Daugherty 1960, Emberger 1962, Arnold 1964, Surange 1966), actually belong to other groups. These include *Chinlea campii* Daugherty 1941, and *Osmundites walkeri* Daugherty 1941, which are synonymous and belong to the Lepidophyta (Miller 1968), and the ectophloic

	ANOMORRHOEA FISCHERI	BATHYPTERIS RHOMBOIDEA	CHASMATOPTERIS PRINCIPALIS	IEGOSIGOPTERIS JAVORSKII	PALAEOSMUNDA WILLIAMSII	PALAEOSMUNDA PLAYFORDII	PETCHEROPTERIS SPLENDIDA	THAMNOPTERIS SCHLECHTENDALII	THAMNOPTERIS GWYNNE-VAUGHANI	THAMNOPTERIS KAZANENSIS	THAMNOPTERIS KIDSTONI	ZALESSKYA GRACILIS	ZALESSKYA DIPLOXYLON	ZALESSKYA URALICA
TRANSVERSE SECTION OF STELE	?	 RECONSTRUCTION				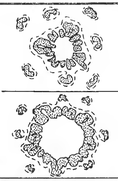				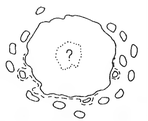	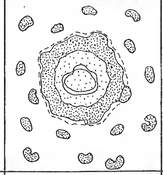		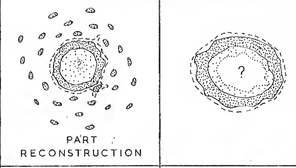 PART RECONSTRUCTION	
NUMBER & POSITION OF PROTOXYLEM GROUPS IN LEAF TRACE AS IT LEAVES STELE	?	1 ENDARCH IN INNER CORTEX	1 ADAXIALLY MESARCH	1 MESARCH	1-2 ENDARCH	1 ENDARCH	1 MESARCH	1(2) MESARCH	1 MESARCH	?1 MESARCH	1 MESARCH	1 MESARCH	PROBABLY 1 MESARCH	1 MESARCH
NUMBER & POSITION OF PROTOXYLEM GROUPS IN LEAF TRACE AS IT ENTERS OUTER CORTEX OF STEM	1 ENDARCH	?	4 ENDARCH	2 ENDARCH	(1)2-4 ENDARCH	(1)2 ENDARCH	SEVERAL (>1-2) ENDARCH	4-5 ENDARCH	2-3 ENDARCH	AT LEAST 2 ENDARCH	4-5 ENDARCH	2-3 ENDARCH	SEVERAL ENDARCH	2-3 ENDARCH
NUMBER OF PROTOXYLEM GROUPS IN LEAF TRACE AS IT ENTERS BASE OF PETICLE	?(>2)	?	10-12+	6-10+	4-12	4-10	?MANY	10-12+	?5-9	?	?	?	?	?(>4)
ROOTS:— XYLEM TRACE: ORIGIN:	DIARCH ?	DIARCH & TRIARCH PROBABLY FROM STELE	DIARCH FROM STELE	DIARCH RARELY TRIARCH FROM STELE OR DEPARTING LEAF TRACES	DIARCH MAINLY FROM DEPARTING LEAF TRACES ALSO FROM STELE	DIARCH RARELY TRIARCH MAINLY FROM DEPARTING LEAF TRACES ALSO FROM STELE	DIARCH FROM STELE	DIARCH FROM STELE OR LEAF TRACES	DIARCH FROM LEAF TRACES	DIARCH ?	DIARCH FROM LEAF TRACES	DIARCH FROM STELE BELOW DEPARTING LEAF TRACES	DIARCH FROM STELE BELOW DEPARTING LEAF TRACES	DIARCH FROM STELE
NUMBER OF LEAF TRACES IN A TRANSVERSE SECTION OF INNER CORTEX OF STEM	?	?	?14-16	20-26	5-25	6-21	?	20-24	40-44	MANY	23-25	140-160	60-65+	100+
NUMBER OF LEAF TRACES IN A TRANSVERSE SECTION OF OUTER CORTEX OF STEM	?20-24	?	?10-12	29-34	7-26	9-19	?	16-20	?20-30	?	?5-6	?(7-8+)	?	?(12-16+)
TRANSVERSE SECTION OF PETIOLE BASE									? NO SCLERENCHYMA IN STIPULES			?	?	?
PETIOLE BASES IN MANTLE:	CLOSELY ADPRESSED	LOOSELY ADPRESSED, BUT NOT OPEN	CLOSELY ADPRESSED	CLOSELY ADPRESSED	CLOSELY ADPRESSED NEAR STEM; CAN BE OPEN FURTHER OUT	CLOSELY ADPRESSED NEAR STEM, USUALLY OPEN FURTHER OUT	CLOSELY ADPRESSED NEAR STEM, OPEN FURTHER OUT	CLOSELY ADPRESSED	CLOSELY ADPRESSED NEAR STEM, OPEN FURTHER OUT	CLOSELY ADPRESSED	?CLOSELY ADPRESSED NEAR STEM	?	?	?
REMARKS	POSSIBLY REFERABLE TO THAMNOPTERIS		PROBABLY REFERABLE TO THAMNOPTERIS	PROBABLY REFERABLE TO THAMNOPTERIS			PROBABLY REFERABLE TO THAMNOPTERIS					CORTEX	COMPARATIVELY	CLOSELY COMPARABLE TO Z. GRACILIS WIDE
SOURCES OF DATA	KIDSTON & GWYNNE-VAUGHAN 1909 ZALESSKY 1927	KIDSTON & GWYNNE-VAUGHAN 1909 ZALESSKY 1924, 1927	ZALESSKY 1931b	ZALESSKY 1935	THIS PAPER	THIS PAPER	ZALESSKY 1931a	KIDSTON & GWYNNE-VAUGHAN 1909 SEWARD 1910 ZALESSKY 1927	ZALESSKY 1924, 1927	ZALESSKY 1927	ZALESSKY 1924, 1927	KIDSTON & GWYNNE-VAUGHAN 1908 ZALESSKY 1924, 1927	KIDSTON & GWYNNE-VAUGHAN 1908 ZALESSKY 1927	ZALESSKY 1924, 1927

TEXT-FIG. 2. Morphological comparisons of Upper Permian osmundaceous stems; *Zalesskya fistulosa* (Eichwald) Zalessky, 1927, is omitted as no details are known. Transverse sections of stele *c.* ×2; inner xylem open stipple, cells not preserved in central portions containing question marks; outer xylem close stipple; details of *Thamnopteris kazanensis* Zalessky, 1927, unknown. Transverse sections of leaf bases *ca.* × 1·55; sclerenchyma black; stippled area in inner cortex of *Anomorrhoea fischeri* Eichwald, 1860, may be sclerenchymatous; outlines show alternate shapes of sclerotic rings.

siphonostelic *Itopsidema vancleavii* Daugherty 1960, which is also probably not a member of the Osmundaceae (Miller 1969). On the other hand, the plants with protosteles and those with ectophloic dictyoxylic siphonosteles may have already been separate groups by the Upper Permian.

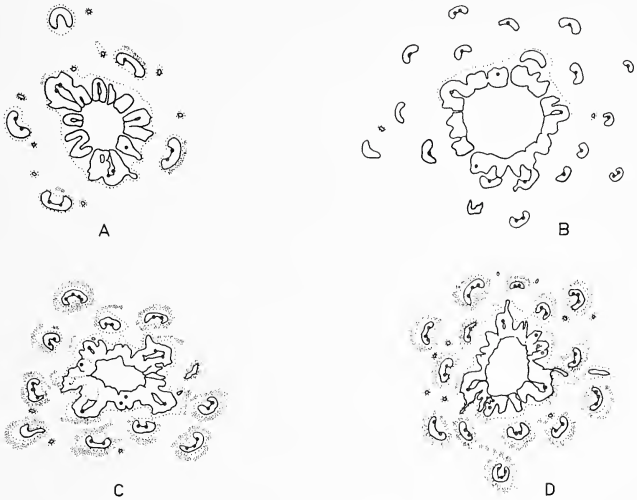

TEXT-FIG. 3. *Palaeosmunda williamsii* gen. et sp. nov. Transverse sections of stele and inner cortex, *c.* ×3·5; where discernible, protoxylem groups of xylem ring and leaf traces represented as black dots; endodermis by a dotted line; and generalized position of sclerenchyma strands in inner cortex by close stipple. A, UQF53542; B, UQF50620; C, D, UQF21571 (holotype).

The oldest known petrified axes referable to the Osmundaceae all occur in Upper Permian strata and these are compared in text-fig. 2. In view of the structural diversity and wide geographic distribution exhibited by these axes, and the relatively stable development of the family from Mesozoic to Recent, it is reasonable to assume that the Osmundaceae originated well before the Upper Permian, probably even before the Permian.

Absence of cataphylls in all specimens of *Palaeosmunda* from the Bowen Basin probably indicates that the climate in which the plant grew lacked severe winters (Steeves and Wetmore 1953; Miller 1967, p. 144). It is interesting to note that cataphylls have not been found in any of the Permian osmundaceous axes.

Palaeosmunda williamsii sp. nov.

Plate 1, figs. 1, 2; Plate 2, figs. 1–7; Plate 3, figs. 1–8; Plate 4, figs. 1–10; text-figs. 2, 3

Holotype. UQF21571; figured in Plate 1, figs. 1, 2; Plate 2, figs. 1, 2, 6, 7.

Type locality. Beside the Collinsville–Mt. Coolon Road in Portion 4, Parish of Corrievahn, central Queensland (shown on text-fig. 1 as Corrievahn); Blackwater Group (formerly Upper Bowen Coal Measures).

Derivation of name. The species is named in honour of Mr. J. H. Williams (Mackay) who kindly assisted in the collection of specimens from the northern part of the Bowen Basin.

Diagnosis. *Palaeosmunda* trunks up to 22 cm. in diameter; stems 1–3·6 cm. wide. Stele an ectophloic dictyoxylic siphonostele, sometimes appearing simply siphonostelic, 3·5–8 mm. in diameter; pith diameter 1–4 mm.; xylem ring 0·7–2·2 mm. wide, with 0–9 gaps, composed of 15–28 radial strands, 9–17 tracheids thick; metaxylem tracheids 35–260 μ (usually 50–150 μ) in diameter, with regular scalariform pitting in 1–5 vertical series on each wall. Inner cortex parenchymatous, sometimes with fibrous sclerenchyma strands surrounding leaf traces; inner cortex 0·8–5·5 mm. wide, including 5–25 leaf traces in a given transverse section; fibrous outer cortex 2·5–9 mm. wide, with 7–26 leaf traces in a transverse section. Leaf traces arise with 1 or 2 endarch protoxylem groups which usually bifurcate before they enter outer cortex; strands of sclerenchyma surround leaf trace in outer cortex of stem, and vascular trace in inner cortex of petiole base. Stipules parenchymatous, or with up to 30, generally small, scattered strands of sclerenchyma fibres.

Description

General. There are 16 specimens, each consisting of a stem surrounded by a mantle of adhering leaf bases and adventitious roots (e.g. Pl. 1, fig. 1; Pl. 3, figs. 1, 7). The specimens are up to 21 cm. long and 22 cm. in diameter, and both ends are broken across. Some trunks are circular in cross-section, but others are oval, presumably due to compression. Three specimens show dichotomy of the stem, but only one contains the actual branching region. The stems, bounded by the sclerotic outer cortex, are 1–3·6 cm. in diameter; the outline in transverse section is undulose due to the emerging petioles.

Stele. The pith is 1–4 mm. in diameter (Pl. 2, figs. 4–7; Pl. 3, figs. 4–6), and consists of vertically elongated, rounded to polygonal, parenchyma cells, measuring 20–110 μ in diameter and 40–300 μ in length; the wall between two adjacent cells is 1–6 μ thick. The parenchyma cells have sometimes partially decayed and separated before preservation.

EXPLANATION OF PLATE 1

Figs. 1, 2. *Palaeosmunda williamsii* gen. et. sp. nov. 1, Transverse section of holotype, UQF21571, from Corrievahn, ×2; section from midway along specimen (top of Plate 2, fig. 1); transmitted and reflected light. 2, Details of stele, inner cortex, and part of outer cortex of fig. 1, ×8; most of pith and inner cortex not preserved; leaf traces depart from stele with 2 protoxylem groups; transmitted light.

EXPLANATION OF PLATE 2

Figs. 1–7. *Palaeosmunda williamsii* gen. et. sp. nov. 1, 2, 6, 7, Holotype, UQF21571. 1, Longitudinal section, ×1; lower half of specimen, details of pith not preserved. 2, Transverse section of petioles showing stipules, ×5. 6, Transverse section from upper part of specimen, ×2. 7, Central portion of fig. 6, ×6; pith partly displaced; note endodermis of stem continuous with sclerotic cortex of root trace at right centre. 3–5, UQF53542, from Homevale. 3, Transverse section, ×2. 4, Detail of stele, ×8; leaf traces leave stele with 2 protoxylem groups. 5, Longitudinal section of pith and xylem of stem, ×16. (1, 3, 6, 7, transmitted and reflected light; 2, 4, 5, transmitted light.)

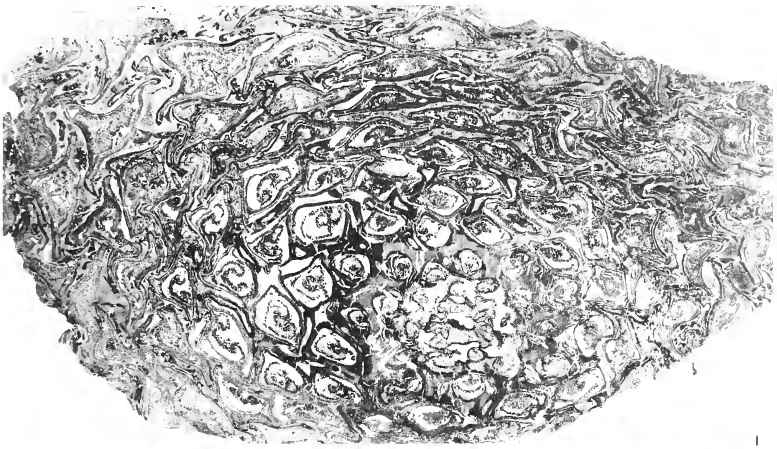

1

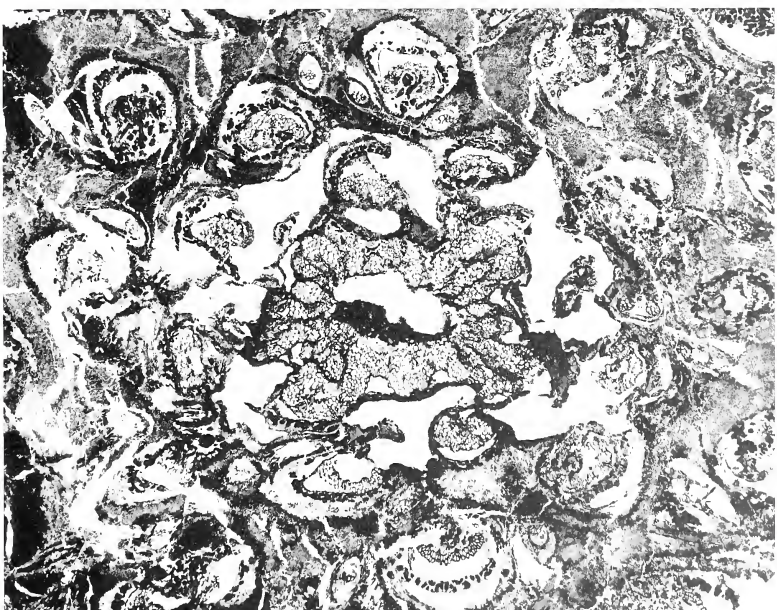

2

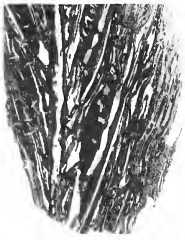
1

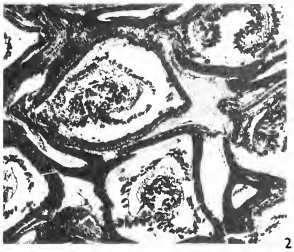
2


3

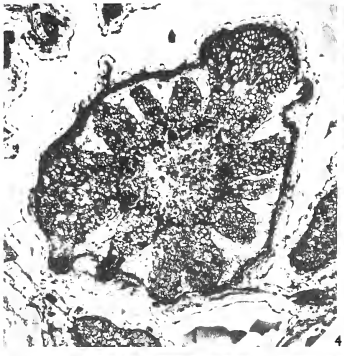
4


5


7

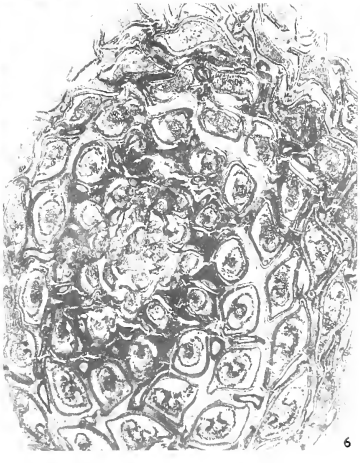
6

GOULD, Late Permian osmundaceous trunks

In one specimen, a few short tracheids are present in the pith (Pl. 4, figs. 1, 2), but these occur where the stem is twisted and are associated with nearby metaxylem strands (cf. Hewitson 1962, p. 81). No internal endodermis is present.

The xylem cylinder is generally similar to that in *Osmunda* and *Osmundacaulis*. It is 0·7–2·2 mm. wide and in transverse section exhibits 0–9 gaps; i.e. in some specimens the xylem is a continuous, but indented ring (Pl. 1, fig. 2; text-fig. 3C, D), while in others it is dissected (Pl. 2, fig. 4; text-fig. 3A, B) and similar to those in most post-Palaeozoic forms of the Osmundaceae. In transverse section the xylem cylinder has 9–24 external lobes, while the cylinder itself consists of 15–28 radial strands, each 9–17 tracheids thick. The protoxylem tracheids, initially mesarch in metaxylem strands below departing leaf traces, are 6–40 μ in diameter, with a wall thickness of 3–14 μ between adjacent cells, and exhibit one series of scalariform pits on each longitudinal wall. Metaxylem tracheids are 35–260 μ in diameter (commonly 50–150 μ), with a wall thickness of 6–23 μ between two adjacent cells. The metaxylem tracheids show regular scalariform pitting in 1–5 vertical series on each wall (Pl. 3, fig. 8); the transverse bars of thickening are 1·1–4 μ thick and 1·5–7 μ apart.

In most of the specimens, except for a dark line marking the position of the endodermis, and strands of sclerenchyma, little cellular detail is preserved between the xylem cylinder and the outer cortex of the stem (Pl. 1, fig. 2; Pl. 2, figs. 3, 4; Pl. 3, fig. 2). A parenchyma xylem sheath, 1–3 cells thick, may be present. Phloem is only preserved in one specimen; it probably formed a continuous layer around the xylem. Metaphloem cells in the wedges between the xylem lobes have a diameter of 27–100 μ with a wall thickness of 3–6 μ. Outside the phloem is a layer of flattened cells up to 7 cells thick, which probably represents the protophloem and pericycle. The endodermis is marked by a dark line or a stained zone, and an abrupt change from pericycle tissue to inner cortex, but cellular detail is lacking. The endodermal diameter is 3·5–8 mm.

Cortex. The inner cortex is 0·8–5·5 mm. wide and consists of parenchyma with, in some specimens, bundles of sclerenchyma fibres. The parenchyma is polygonal to rounded in transverse section, and may be tangentially elongated, measuring 25–70 μ $\times$ 10–60 μ; thickness of the wall between two adjacent cells is 0·7–4 μ, but may appear up to 14 μ thick with deposits of organic and mineral matter. Where present, the bundles of sclerenchyma fibres occur in an intermittent peripheral zone around the endodermis below and adjacent to abaxial surfaces of the departing leaf traces (Pl. 1, fig. 2; Pl. 2, fig. 7); the bundles usually surround the endodermis of the leaf trace as it leaves the stele and they accompany it through the inner and outer cortex of the stem and into the petiole bases. In other cases however, the sclerenchyma does not appear until further out in the inner or outer cortex. In transverse section the bundles measure up to 540 μ tangentially, and up to 210 μ radially. They are composed of sclerenchyma fibres which have a diameter of 13–38 μ, a length of at least 850 μ, and a wall thickness between adjacent cells of 6–18 μ. The primary and secondary walls are clearly shown and the secondary wall may almost completely fill the cell. The inner cortex contains 5–24 leaf traces in a given transverse section.

The dense outer cortex is 2·5–9 mm. wide and consists of sclerenchyma fibres which are polygonal in cross section (Pl. 4, figs. 6, 7). The majority of these fibres have a diameter of 12–45 μ, sometimes up to 70 μ, and length of 270 μ to at least 1100 μ; the end walls are transverse, oblique, or tapering. The primary and secondary

walls are clearly preserved and the secondary wall may consist of several layers. Total thickness of wall between two adjacent fibres is 6–30 μ; intercellular spaces of up to 4 μ are sometimes present at the angles. The longitudinal walls may be smooth or exhibit simple, small (3–7 μ), round to oval, irregularly scattered pits. Large, irregularly defined rectangular (3×7 μ–7×23 μ, 1·5–8 μ apart) or annular pits may also be present, but these appear to be formed by shrinkage of the original cell wall. Rare transverse septations may occur. Sometimes the lumen of a fibre is almost filled with secondary wall. A few layers of relatively larger and shorter, although otherwise similar, fibres occur adjacent to the inner cortex of the stem and leaf traces (Pl. 1, fig. 2), and also on the outside of the stem in the depressions behind the departing petioles (Pl. 4, fig. 8); these cells usually have a diameter of 40–85 μ, and a length of 70–300 μ. Part of the outer cortex of one specimen appears inhomogeneous with rings of light-coloured (in thin section) fibres surrounding the leaf traces, and darker, somewhat larger fibres in the areas between the rings (Pl. 3, fig. 1). The outer cortex contains 7–26 leaf traces in a given transverse section. Total number of leaf traces in any one transverse section of the whole cortex is 12–43.

Leaf traces. Traces are formed from the metaxylem strands of the stem in a manner generally similar to that in the subgenera *Osmunda* and *Osmundastrum* of the genus *Osmunda* (Hewitson 1962, Miller 1967). A protoxylem group develops approximately in the centre of the metaxylem strand which gives rise to the leaf trace. Above this point an island of parenchyma develops adaxially to the protoxylem group. This island enlarges upwards and usually becomes connected by a narrow gap with the pith. Thus the xylem strand assumes a U-shape with the narrow open end of the 'U' directed

EXPLANATION OF PLATE 3

Figs. 1–8. *Palaeosmunda williamsii* gen. et sp. nov. 1–3, UQF57604, from Byerwen. 1, Transverse section, ×1. 2, Transverse section of stele; most of pith and inner cortex filled with silica; leaf traces arise with 1 protoxylem group, ×6. 3, Transverse section of parts of petiole bases showing irregular mass of sclerenchyma in sclerotic ring, and sclerenchyma strands in stipules, ×10·6. 4–6, UQF50624, from Blackwater district. 4, 5, Transverse sections of pith. 4, ×42; 5, ×67·5. 6, Longitudinal section of pith, ×67·5. 7, 8, UQF50620, from Blackwater district. 7, Transverse section, ×1·5; numerous roots and petioles loosely adpressed in outer part of mantle. 8, Longitudinal view of xylem tracheids of stem, ×42. (1, transmitted and reflected light; 2–8, transmitted light).

EXPLANATION OF PLATE 4

Figs. 1–10. *Palaeosmunda williamsii* gen. et. sp. nov. 1, 2, Longitudinal sections showing tracheids in pith, UQF50620. 1, ×42; 2, ×66. 3, Transverse section of roots, UQF53549, from Blackwater Mine, ×10·6. 4, 5, Longitudinal sections of xylem of root. 4, UQF50624, ×99; 5, UQF57604, ×63. 6, 7, Transverse sections of sclerenchyma fibres of outer cortex. 6, UQF53552, from Blackwater Mine, ×60, showing intercellular spaces; 7, UQF53549, ×60. 8, Longitudinal section of outer cortex and part of sclerotic ring of departing petiole, showing shorter fibres at outside of stem; longitudinal axis of section tilted to left; UQF53552, ×40. 9, Longitudinal section of sclerenchyma strand in inner cortex of petiole, showing pitting, UQF50624, ×99. 10, Transverse section of part of petiole base, UQF53541, from Homevale, ×42; note increase in diameter of fibres of sclerotic ring towards inner cortext of petiole.

Fig. 11. *Palaeosmunda playfordii* gen. et. sp. nov. Transverse surface of holotype, UQF53544, from Blackwater Mine, ×0·75; loosely adpressed petioles and numerous roots in outer part of mantle. (1–10, transmitted light; 11, reflected light.)

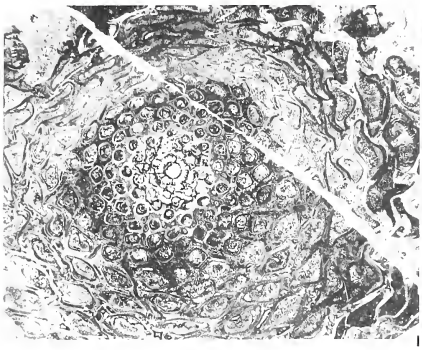
1

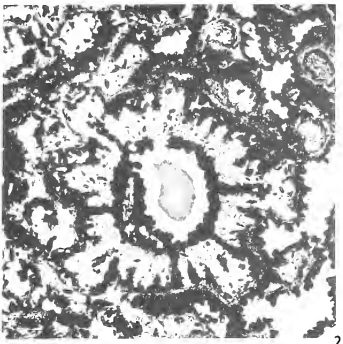
2

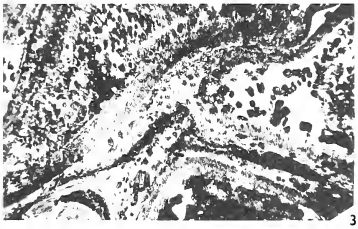
3

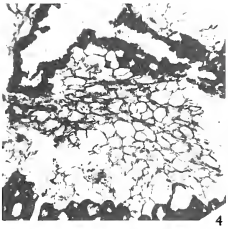
4

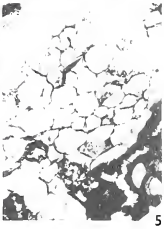
5

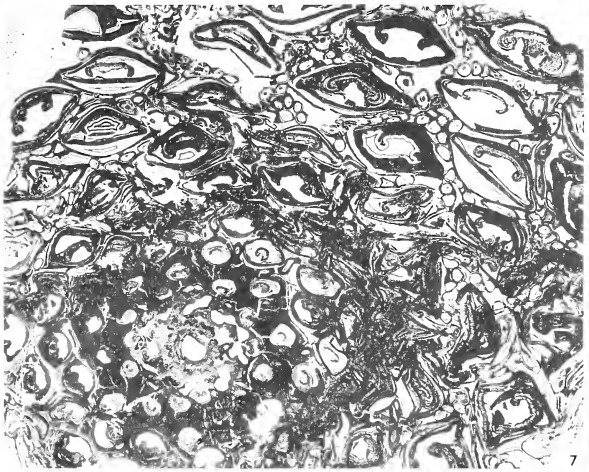
7

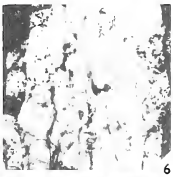
6


8

GOULD, Late Permian osmundaceous trunks

1

2

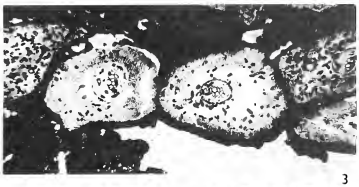

3

4

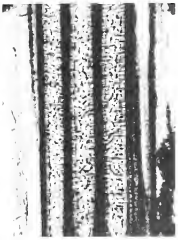

5

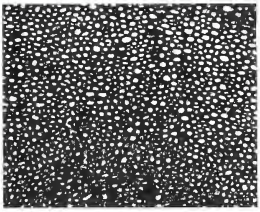

6

9

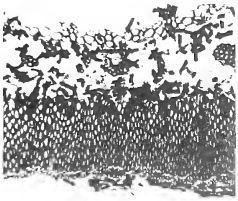

10

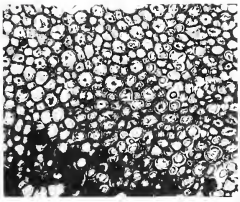

7

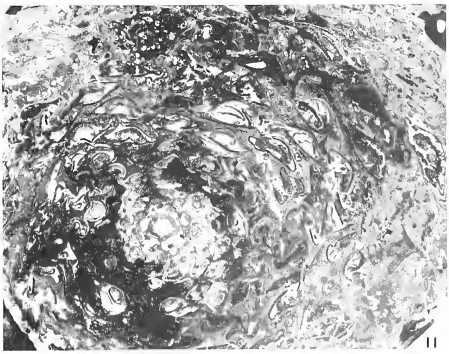

11

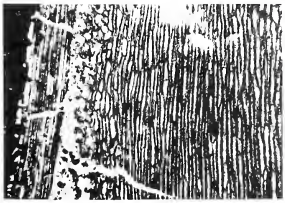

8

GOULD, Late Permian osmundaceous trunks

toward the pith, and the protoxylem group in the centre of the concave surface; the protoxylem group may bifurcate at this stage. The curved part of the 'U' with the adaxial protoxylem group (or groups) then breaks away to form the leaf trace. The leaf gap in the stem xylem may be closed before the leaf trace breaks away, and hence the gap is not evident in any one transverse section, the stem xylem being continuous within the strand or through the departing leaf trace. In other cases the formation of the gap may be delayed until after the leaf trace has entered the inner cortex; sometimes it appears that no complete gap forms although the island of parenchyma is still well developed. A pair of root traces usually arise with the departing leaf trace, one root trace arising from each abaxial lateral angle of the 'U'. However root traces may also be derived from 1 or 2 adjacent strands which partly coalesce with the original radial metaxylem strand.

The leaf traces become progressively larger and more C-shaped as they move out. There are 1–2 adaxial protoxylem groups in the trace when it enters the inner cortex, (1) 2–4 groups as it passes from the inner to the outer cortex, and 4–12 groups when it enters the petiole base. The trace gains encircling layers of phloem, pericycle, endodermis, inner cortex (sometimes including sclerenchyma strands), and outer cortex as it passes through these zones of the stem; except for the sclerenchyma strands around the endodermis, no gaps are left in the tissues concerned. Where sclerenchyma strands are present in the stem, they surround the endodermis of the leaf trace as soon as it enters the inner cortex (Pl. 1, fig. 2); in other cases the sclerenchyma appears further out in the inner or outer cortex, either initially located within the arms of the 'C' or surrounding the leaf trace. The strands of sclerenchyma fibres are always present around the endodermis of the leaf traces within the outer cortex of the stem.

Petioles. The petiole bases arise from the stem at angles of 10–35°; they are usually tightly packed near to the stem, but may be closely or loosely adpressed further out in the mantle (Pl. 2, fig. 6; Pl. 3, fig. 7). The bases consist of a C-shaped vascular strand surrounded by the endodermis, the inner cortex including bundles of sclerenchyma fibres just outside the endodermis, the sclerotic ring, and the stipules (Pl. 2, fig. 2); apart from the stipules, which arise with the petiole, these tissues are continuous with the corresponding zones of the stem. The petiole bases enlarge upwards, ranging from a minimum of 2·5 mm. in radial thickness by 4 mm. wide near the stem, up to 14 mm. thick by 32 mm. wide at the periphery of the mantle of leaf bases, and the ends of the vascular strand become more incurved.

Towards the periphery of the mantle the xylem of the petiolar strand becomes narrower, being 3–4 tracheids thick radially near the stem and only 1–3 tracheids thick further out; the metaxylem tracheids generally decrease in diameter from up to 100–140 μ to 25–70 μ. In one specimen, secondary thickening similar to that of the sclerenchyma fibres occurs in a few tracheids; these have a wall thickness of 13–28 μ. Up to 44 protoxylem groups project on the adaxial sides of the xylem traces in the outermost petioles. In two specimens it appears that there is an intermittent parenchyma sheath around the xylem, consisting of polygonal cells 12–20 μ in diameter. The xylem trace is then completely surrounded by phloem, containing cells which are polygonal in transverse section and 14–40 μ in diameter. The pericycle consists of 2 to 5 layers of polygonal cells 17–30 μ in diameter. Large, apparently schizogenous, mucilage cavities with a diameter of 95–140 μ sometimes occur in the adaxial pericycle region.

The endodermis is often well marked by a dark line or a colour change, but is rarely

preserved in detail; it is 1 or 2 cells thick, the cells measuring 14–45 $\mu \times 12$–30 μ in transverse section, and showing distinct Casparian strips.

The parenchyma cells of the inner cortex of the petiole are polygonal in transverse section with a diameter of 27–95 μ and a wall thickness of 0·8–5 μ. The strands of sclerenchyma that surround the endodermis consist of fibres with a diameter of 13–55 μ, a length of 130 μ to at least 1300 μ, and a wall thickness of 10–34 μ; in some fibres, the secondary wall completely fills the lumen. The end walls may be transverse, oblique, or tapering. The longitudinal walls are usually pitted (pits 2·5–4 μ; Pl. 4, fig. 9) similarly to those of the outer cortex of the stem. Extending up the petiole, the groups at first increase and irregularly coalesce, and then diminish in numbers and size. The concentration of strands varies from a complete spread almost filling the inner cortex, to a single row just surrounding the endodermis. Sometimes 1–4 strands of fibres occur discrete from the others in the lateral extremities of the inner cortex.

The sclerotic ring is usually rhomboidal in cross-section, upwards becoming tangentially elongated; the lateral extremities extend well into the stipules and eventually replace them (Pl. 1, fig. 1; Pl. 3, figs. 1, 7). Adjacent to the stem the size of the ring varies from $3 \times 2{\cdot}5$ mm. to 9×6 mm. with an average thickness of 0·3–0·6 mm.; toward the periphery of the mantle the rings are up to $31{\cdot}5 \times 14$ mm. with a thickness of up to 0·9 mm. The lateral extremities of the rings are usually markedly thinner than the abaxial and adaxial portions. The constituent fibres are similar to those forming the outer cortex of the stem. The fibre diameter increases gradually toward the inner cortex of the petiole base (Pl. 4, fig. 10), although occasionally only a few layers lining the inside of the ring are distinctly larger; the wall thickness (6–24 μ) of all the cells is approximately the same in any one ring. In one specimen, some sclerotic rings contain 1 or 2 masses of large, but short, irregularly arranged, sclerenchyma cells; these are usually in the thin lateral extremities of the ring and appear to have developed where the ring has been broken (Pl. 3, fig. 3).

The stipules consist of polygonal parenchyma cells 14–80 μ in transverse diameter with walls 0·8–3 μ thick, although in many specimens little cellular detail is preserved (Pl. 2, fig. 2). Up to 30, generally small, strands of sclerenchyma develop in the stipular wings of two specimens (Pl. 3, fig. 3). These strands contain fibres with a diameter of 12–55 μ, and a wall thickness between two adjacent cells of 6–28 μ. The secondary wall may completely fill the lumen. The stipular tissue extends well up the petiole base and at least to the periphery of the closely packed mantle of leaf bases. However, the lateral extension of the sclerotic ring replaces more of the stipules further up the petiole base, although in some cases the stipules also increase in length; poor preservation and penetration by adventitious roots prevents definite identification of the parenchymatous stipules at this level.

Roots. The roots usually arise in pairs from the leaf trace before, as, or just after it leaves the stem xylem but before it enters the inner cortex; in one specimen, however, some root traces originate from leaf traces in the inner cortex. Roots occasionally arise from stem xylem strands immediately above, below, or adjacent to departing leaf traces. The xylem trace is diarch (Pl. 1, fig. 2; Pl. 4, fig. 3) and it gains the tissues of the phloem, pericycle, and endodermis as it passes through these zones of the stem. The xylem tracheids are similar to those in the stem (Pl. 4, figs. 4, 5). In the inner cortex the root trace may have a narrow sclerenchyma sheath continuous with the endodermis of the stem,

but this is replaced by a sclerotic cortex as the trace enters the outer cortex of the stem (Pl. 2, fig. 7). A few layers of the cells of the inner cortex may accompany the root trace into the outer cortex as there is a gap between the endodermis and the sclerenchyma, but in several cases no inner cortical cells are present. Towards the outside of the mantle, the walls of the cortical fibres nearest to the endodermis usually become progressively thinner, thus giving the appearance of a parenchymatous inner cortex. The endodermis often shows well-defined Casparian strips. The roots vary from less than 1 mm. to 2·5 mm. in diameter and in the majority of specimens, except for the region near the stem, most are cut transversely by a transverse section of the trunk (Pl. 3, fig. 7); this is probably indicative of an arborescent habit (Miller, pers. comm. 1969). They are often branched within the mantle and outside it, sometimes forming an external mat up to 3 cm. wide. The roots freely penetrate the cortex of the stem and the stipules, but not the sclerotic rings or inner cortex of the petiole bases.

Branching. The branching of the stem does not show any abnormal characteristics. However the single specimen containing the branching region is not well preserved.

Discussion. The species is characterized by the sclerotic strands surrounding the leaf traces in the inner cortex of the petiole base. The stele (e.g. Pl. 3, fig. 2; text-fig. 3) is somewhat similar to that in the Jurassic *Osmundacaulis dunlopi* (Kidston and Gwynne-Vaughan) Miller 1967 (see Kidston and Gwynne-Vaughan 1907; Marshall 1926; Edwards 1933, 1934) in that leaf gaps may or may not be completely developed in the xylem ring. Unlike some members of the Osmundaceae, the steles of *P. williamsii* which show the continuous xylem ring are not just associated with branching of the stem (cf. Hewitson 1962). Further variability of the stele is exhibited by the number of protoxylem groups in the developing leaf traces; those which arise from the stele with 2 protoxylems are, like those containing only 1 protoxylem, derived from a single original metaxylem strand of the stele and not from 2 adjacent crozier-shaped strands as is the case in the subgenus *Plenasium* of the genus *Osmunda* (Hewitson 1962, Miller 1967).

Other occurrences. Bowen River crossing, near Gatton Vale Homestead (Blackwater Group); Byerwen Station (Blackwater Group); south-western boundary of Homevale Station (Blackwater Group); Kemmis Creek (Blackwater Group); and south of Utah Development Company's Blackwater Mine, Blackwater district (Rangal Coal Measures of Blackwater Group; or Bandanna Formation). The localities are shown on text-fig. 1.

Palaeosmunda playfordii sp. nov.

Plate 4, fig. 11; Plate 5, figs. 1–5; Plate 6, figs. 1–10; Plate 7, figs. 1–9; Plate 8, figs. 1–7; text-figs. 2, 4

Holotype. UQF53544; figured in Plate 4, fig. 11; Plate 5, fig. 1; Plate 6, figs. 2–4, 9, 10; Plate 8, figs. 6, 7.

Type locality. South of Utah Development Company's Blackwater Mine, Portion 3, Parish of Stewarton, near Blackwater, central Queensland; Bandanna Formation, or Rangal Coal Measures of Blackwater Group (formerly Upper Bowen Coal Measures). Locality shown as Blackwater Mine in text-fig. 1.

Diagnosis. Palaeosmunda trunks up to 18 cm. in diameter; stems 18–37 mm. wide. Stele an ectophloic dictyoxylic siphonostele, 3·5–11 mm. in diameter; pith diameter 2–6 mm.; xylem ring 1–2 mm. wide, with (?0)3–13 gaps, consisting of 14–20, 27 radial strands,

9–19 tracheids thick; metaxylem tracheids 30–160 μ in diameter, with regular scalariform pitting in 1–7 vertical series on each wall. Inner cortex parenchymatous, 1–6 mm. wide, including 6–21 leaf traces in a given transverse section; fibrous outer cortex 1–10 mm. wide, containing 9–19 leaf traces in a transverse section. Leaf traces arise with one adaxial protoxylem group which usually bifurcates in inner cortex of stem. Stipules and inner cortex of petiole bases parenchymatous.

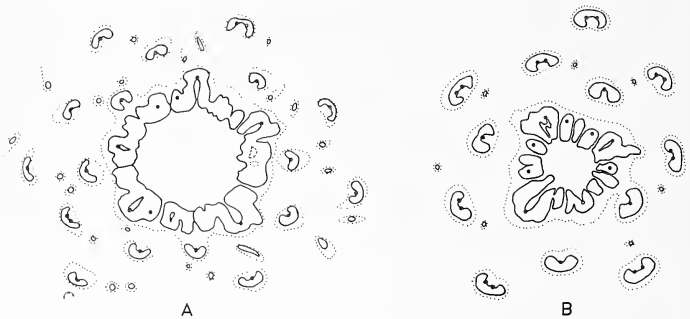

TEXT-FIG. 4. *Palaeosmunda playfordii* gen. et sp. nov. Transverse sections of stele and inner cortex, *c.* ×3·5; protoxylem groups, where discernible, represented as black dots; endodermis by a dotted line. A, UQF50622; B, UQF53566.

Description

General. This species is the most common in the material collected from the Blackwater district; more than 30 trunks, consisting of a central stem with a mantle of petiole bases and adventitious roots (e.g. Pl. 4, fig. 11; Pl. 5, figs. 1, 3), were used for the description. The specimens are up to 28 cm. long and 18 cm. in diameter with one or both ends broken across. The stems may be dichotomously branched but, although

EXPLANATION OF PLATE 5

Figs. 1–5. *Palaeosmunda playfordii* gen. et sp. nov. 1, Transverse section of holotype, UQF53544, ×1·5; pith and some of inner cortex not preserved. 2, Transverse section of UQF53553, from Blackwater Mine, ×2. 3–5, UQF53566, from Blackwater Mine. 3, Transverse section ×1. 4, Detail of stele and inner cortex, ×5. 5, Longitudinal section of pith and xylem of stem, ×24. (1, transmitted and reflected light; 2–5, transmitted light.)

EXPLANATION OF PLATE 6

Figs. 1–10. *Palaeosmunda playfordii* gen. et sp. nov. 1, Transverse surface of axis above dichotomy (actual branching region not present in specimen), UQF53560, from Blackwater Mine, ×1. 2–4, 9, 10, Holotype, UQF53544. 2, Transverse section of inner cortex, ×66. 3, Longitudinal section of inner cortex, ×66. 4, Longitudinal section of outer cortex showing pitting. ×99. 9, Transverse section of petiole base at point of departure from stem, ×16. 10, Detail of vascular trace in fig. 9, ×66. 5, 6, Longitudinal sections of outer cortex. 5, UQF53566, ×44; 6, UQF53567, from Blackwater Mine, ×63. 7, 8, UQF50622, from Blackwater district. 7, Transverse section of leaf trace at outside of inner cortex, ×16. 8, Transverse section of leaf trace in inner cortex, ×10·6. (1, reflected light; 2–10, transmitted light.)

1

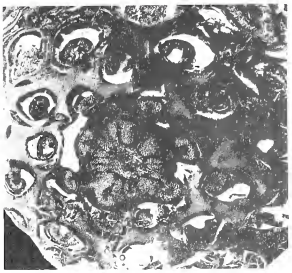

2

5

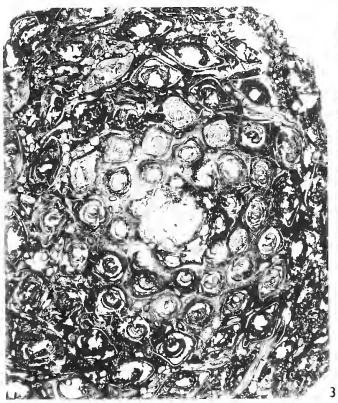

3

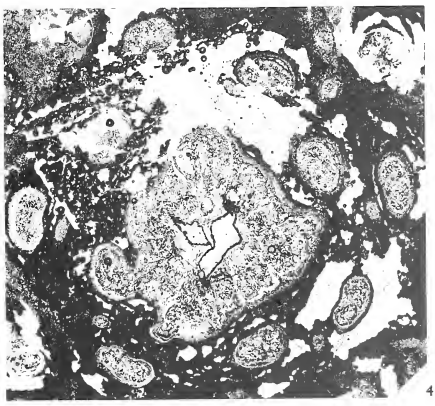

4

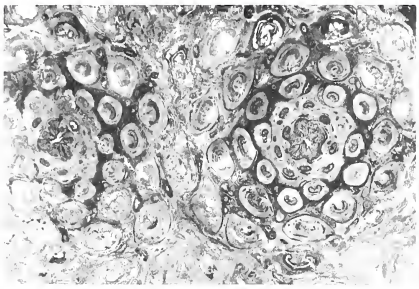

1

4

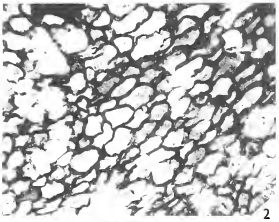

2

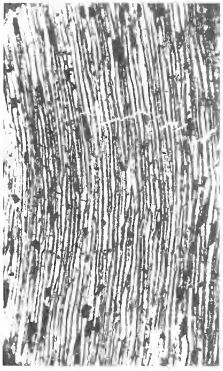

5

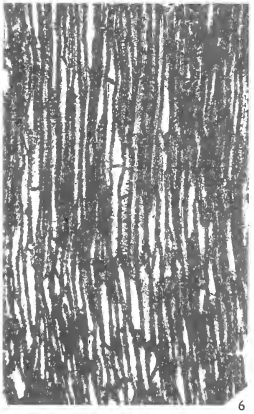

6

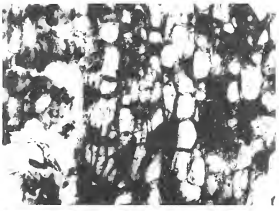

3

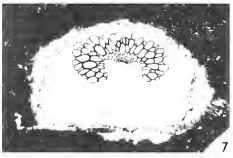

7

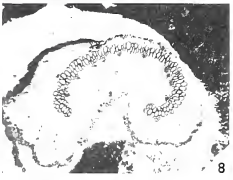

8

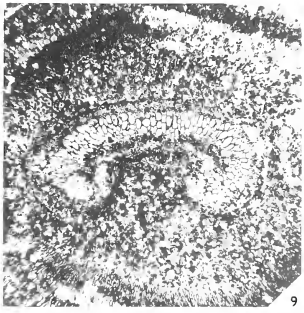

9

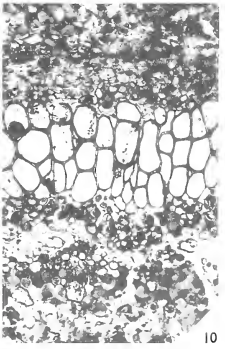

10

GOULD, Late Permian osmundaceous trunks

some specimens contain 2–4 axes in close proximity, the actual branching region is not present (Pl. 6, fig. 1).

Stele. The pith is 2–6 mm. wide and consists of longitudinally elongated, polygonal parenchyma cells with a diameter of 20–83 μ, and a length of 68–300 μ (Pl. 5, fig. 5); wall thickness between two adjacent cells is 1·5–3·5 μ, but may appear up to 10 μ due to organic and mineral matter. There is a slight decrease in the transverse diameter of the pith cells toward the xylem ring.

The xylem cylinder is 1–2 mm. wide and in transverse section exhibits 3–13 gaps (text-fig. 4). It consists of 14–20 (one with 27) radial metaxylem strands, 9–19 tracheids thick, and shows 10–16 external lobes. The protoxylem groups, which appear subcentrally in the metaxylem strands below the departure of leaf traces, consist of tracheids with a diameter of 7–27 μ and a wall thickness of 4–13 μ. Metaxylem tracheids have a diameter of 30–160 μ and a total wall thickness between two adjacent cells of 6–27 μ. These tracheids have 1–7 vertical series of regular scalariform pits on each wall; the bars of thickening are 1–3 μ thick and 2·5–8 μ apart. As in *P. williamsii*, the xylem is dissected by gaps in some specimens (Pl. 5, figs. 2, 4), while in others it is an almost continuous but externally indented ring (Pl. 7, fig. 9). A parenchyma sheath 2–8 cells thick is present in two specimens which both have fully dissected xylem rings. The sheath is prominently developed on the outside of, and in the gaps between, the xylem strands; it does not appear to be present between pith and xylem. The sheath consists of elongated polygonal cells which have a diameter of 13–40 μ, a length of 40–120 μ, and a wall thickness of 1·6–5 μ.

The phloem forms a continuous layer around the xylem and xylem sheath. The metaphloem, which has its greatest development in the indentations between the metaxylem strands, contain cells which are polygonal in transverse section, and presumed to be sieve cells with a diameter of 35–96 μ, a length of at least 550 μ, and a wall thickness between adjacent strands of 1·6–6·8 μ; no sieve areas, however, could definitely be distinguished. Associated with these are some smaller cells, which are rectangular to polygonal in transverse view; these measure from 14–27 μ in diameter to 40 $\mu \times 14$ μ. The metaphloem is surrounded by a continuous zone, 68–130 μ wide, of crushed cells, which probably represents the protophloem and pericycle. Some polygonal and tangentially elongated cells, 13–70 μ in diameter with a wall thickness of 3–13 μ, can be distinguished; these have a length of 54–270 μ.

The endodermis is marked by a different colouration and a change from the pericycle to the larger cells of the inner cortex. It consists of slighly darker coloured, more resistant cells which are rounded-polygonal to tangentially elongated in cross-section with a diameter of 12–55 μ; they are rectangular in longitudinal view and up to 200 μ long. No definite Casparian strips are visible. The total diameter of the stele to the endodermis is 3·5–11 mm.

Cortex. The inner cortex consists of slightly tangentially and longitudinally elongated rounded to polygonal parenchyma cells with a transverse diameter of 25–110 μ and a length of 40–170 μ (Pl. 6, figs. 2, 3). The walls may be straight or sinuous, with a thickness between two adjacent cells of 1·5–4 μ. The inner cortex is 1–6 mm. wide; in most specimens this zone contains 6–13 leaf traces in a given transverse section, but one shows 20–1 traces.

The dense sclerotic outer cortical region is 1–10 mm. wide, and consists of fibres

which are polygonal in cross-section. The walls between two adjacent cells are 10–30 μ thick and clearly show the primary and secondary walls; intercellular spaces of up to 6 μ commonly occur at the angles. The majority of cells are 13–55 μ in diameter with a length of at least 1300–1800 μ (Pl. 6, figs. 5, 6); the end walls may be transverse, oblique, or tapering. Some relatively wider (28–85 μ, but up to 160 μ) and shorter (200 μ) cells occur on the boundary with the inner cortex of the stem and the leaf traces, and in the depressions beneath the departing petiole bases on the outside of the stem. The longitudinal walls of the fibres may be smooth or with round to oval pits (2·5–8 μ; Pl. 6, fig. 4) as in *P. williamsii*. Larger, more or less rectangular or annular pits appear to be caused by shrinkage of the original wall material. The outer cortex contains 9–19 leaf traces in a given transverse section; total number of traces in the whole cortex in any one section is 18–38.

Leaf traces. These arise from the stem xylem similarly to the traces in the Tertiary–Recent subgenera *Osmunda* and *Osmundastrum*; leaf gaps are usually developed. A mesarch protoxylem group appears in the metaxylem strand of the stem and then an island of parenchyma develops adaxially to the protoxylem. The island of parenchyma enlarges upwards and connects with the pith to form the leaf gap while the outer endarch arch of the xylem breaks away to form the leaf trace. The trace gains the encircling tissues of the xylem sheath, phloem, pericycle, endodermis, inner cortex, and outer cortex as it passes through these respective zones of the stem; each zone of the stem fills in behind the trace and no gaps are formed.

The leaf trace arises with one endarch protoxylem group which usually bifurcates in the inner cortex of the stem (Pl. 6, figs. 7, 8); 4–10 adaxial protoxylem groups are present

EXPLANATION OF PLATE 7

Figs. 1–9. *Palaeosmunda playfordii* gen. et sp. nov. 1–8, UQF53547, from Blackwater Mine. 1, Transverse section of petioles in outer part of mantle, ×1·5. 2, Part of vascular trace and inner cortex of petiole at left centre of fig. 1, ×10·6. 3, Transverse section of part of vascular trace and inner cortex of petiole (not shown in fig. 1), ×16. 4, Detail of vascular trace from fig. 3, ×42. 5, Further enlargement of part of vascular trace with the adaxial schizogenous mucilage cavities, ×66. 6, Longitudinal section of part of vascular trace of petiole, showing zone of crushed parenchyma cells, ×99. 7, Detail of endodermis of petiolar trace, showing Casparian strips on the radial walls, ×270. 8, Transverse section of sclerotic ring of petiole base; note increase in fibre diameter toward the inner cortex, ×42. 9, Transverse section of stele, UQF50622, ×6; pith and inner cortex not preserved. (1, transmitted and reflected light; 2–9, transmitted light.)

EXPLANATION OF PLATE 8

Figs. 1–7. *Palaeosmunda playfordii* gen. et sp. nov. 1–5, Transverse sections of roots. 1, UQF53564, from Blackwater Mine, ×26·5; 2, Shows triarch xylem trace, UQF59129, from Blackwater Mine, ×10·6. 3–5, Show 2 diarch xylem strands in section, UQF53547. 3, ×16; 4, ×31·5; 5, ×26·5. 6, 7, Xylem tracheids of petiole containing Basidiomycete hyphae with clamp connections, holotype, UQF53544, ×480.

Figs. 8, 9. Dissociated, flanged petioles, with fronds of *Sphenopteris lobifolia–Cladophlebis roylei–S. polymorpha*, and *Glossopteris* sp., from the Burngrove Formation at Burngrove Creek. 8, UQF53582, ×0·66 (the line is a saw cut—see figs. 10, 11); 9, UQF53575, ×0·44.

Figs. 10, 11. Sections of dissociated petioles in specimen shown in fig. 8, ×2.

Figs. 12, 13. Compressions of osmundaceous trunks (probably *Palaeosmunda*) from the Burngrove Formation at Burngrove Creek. 12, UQF53581, ×0·66; 13, UQF53577, ×0·55. (1–7, transmitted light; 8–13, reflected light.)


1

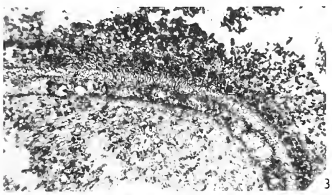
3

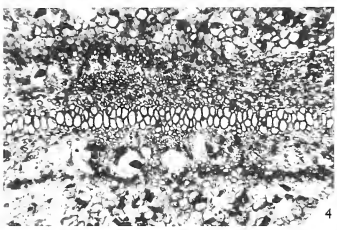
4

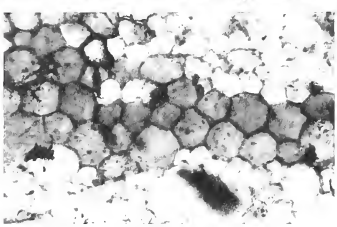
7

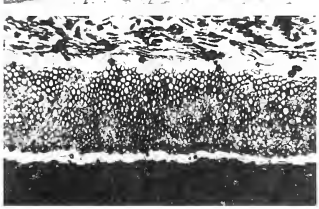
8

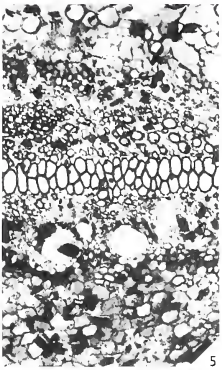
5


6

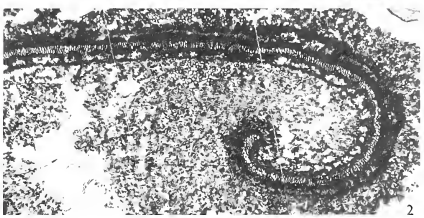
2

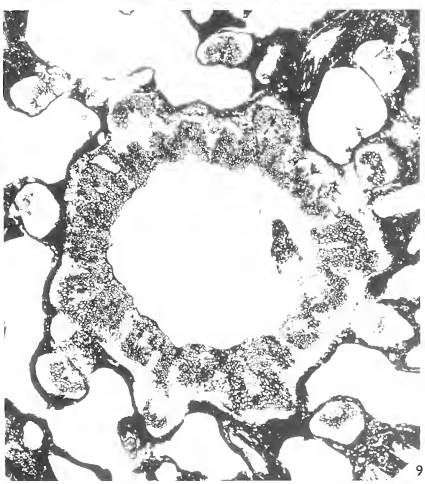
9

GOULD, Late Permian osmundaceous trunks


1

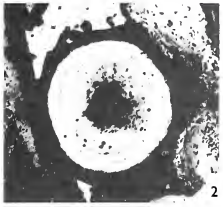
2

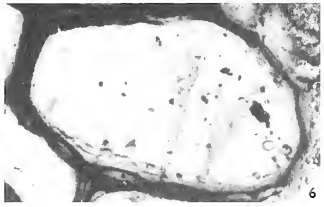
6


3

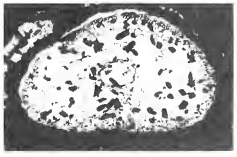
4

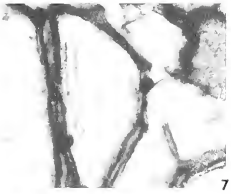
7

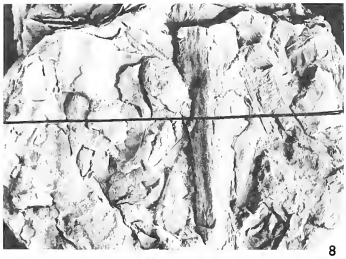
8


5

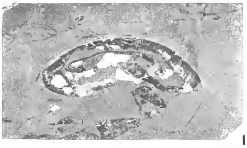
10


11


9


12


13

GOULD, Late Permian Osmundaceae

when the trace enters the base of the petiole. There are up to 44 groups in the trace in the outer zones of the mantle.

Petioles. The petioles arise from the stem at angles of 15–30° and are usually closely adpressed near the stem but loosely arranged in the outer part of the mantle (Pl. 4, fig. 11). The petiole bases consist of a C-shaped vascular trace surrounded by a parenchymatous inner cortex, a sclerotic ring, and lateral stipules; except for the stipules which arise as the petiole emerges from the stem, these tissues are derived from, and continuous with, the corresponding zones of the stem. The bases enlarge upwards, ranging in transverse section from 3·5 mm. thick by 7 mm. wide near the stem, up to 12·5 mm. thick and 35 mm. wide near the periphery of the mantle.

Upwards the C-shaped xylem strands become larger, but thinner, the constituent tracheids narrower, and the ends become more incurved (cf. Pl. 6, figs. 9, 10 and Pl. 7, figs. 1–5). The strands are 1–4 tracheids thick, and the metaxylem tracheids are 30–110 μ in diameter, rarely up to 160 μ. Basidiomycete hyphae showing clamp connections occur within some tracheids in the holotype (Pl. 8, figs. 6, 7). The xylem is surrrounded by a xylem sheath up to 6 cells thick, the phloem, the pericycle, and the endodermis. The pericycle is 2–6 cells thick, and usually contains numerous, apparently schizogenous, mucilage cavities with a diameter of 68–164 μ (Pl. 7, fig. 5; cf. Seward and Ford 1903, p. 247, pl. 30, fig. 45); these cavities are most common on the adaxial side of the trace, but are occasionally present on the abaxial side. Groups of compressed, irregularly arranged parenchyma cells occur in the adaxial xylem sheath, phloem, and pericycle. The groups are quite distinctive in longitudinal section (Pl. 7, fig. 6) and compression probably resulted from the formation of the schizogenous cavities.

The endodermis is 1–2 cells thick (Pl. 7, fig. 7). The cells are polygonal in transverse section (diameter 14–35 μ) and elongated to rectangular in longitudinal view (length 80–330 μ). Casparian strips 6–17 μ wide are present.

The inner cortex of the petiole base consists of parenchyma cells (Pl. 6, fig. 9; Pl. 7, figs. 2, 3) which are polygonal in transverse section with a diameter of 25–100 μ, and rectangular in longitudinal section with a length of 40–280 μ; wall thickness between two adjacent cells is 1–3·5 μ. Sometimes the cells have been partially macerated and separated before preservation.

The sclerotic ring contains sclerenchyma fibres similar to those in the outer cortex of the stem. The fibres are polygonal in transverse section and generally range from 13 to 40 μ in diameter; in any one ring there is usually a gradual increase in diameter towards the inner cortex (Pl. 7, fig. 8). The walls between adjacent fibres are 6–17 μ thick. The sclerotic rings are circular to rhomboidal in shape when they arise and they broaden upwards, contributing greatly to the stipules, eventually replacing them. They range in size from 3–7 mm. in diameter near the stem to 34·5 × 12 mm. in the periphery of the mantle; the thickness of the ring varies from 0·2 mm. to 1 mm. and the lateral extremities are usually thinner than the adaxial and abaxial portions.

The sclerotic ring is surrounded by a sheath of parenchymatous tissue which is extended laterally to form the stipules; the cells have diameters of 25–60 μ.

Roots. The adventitious roots have a diameter of 0·7–2·5 mm. and usually arise in pairs from the leaf traces before their departure from the stele. Roots may also arise irregularly from the metaxylem strands of the stem, especially those immediately below a departing leaf trace. The xylem trace gains the surrounding tissues of phloem,

pericycle, endodermis, and sclerotic outer cortex as it passes through these zones of the stem. In most cases no cells of the inner cortex accompany the trace into the outer cortex of the stem, the sclerenchyma being contiguous with the endodermis. In a few examples, however, there is a narrow gap between the endodermis of the root trace and the sclerotic outer cortex as if a layer of inner cortex was present, but no cells are preserved. In a cross-section of the trunk, most roots, except those in the region near the stem, are seen in transverse section (Pl. 4, fig. 11) and this is probably indicative of an arborescent habit (Miller pers. comm. 1969). The root usually has a diarch xylem trace (Pl. 8, fig. 1), but in one case it is triarch (Pl. 8, fig. 2); some show two diarch xylem strands in a section (Pl. 8, figs. 3–5), possibly prior to branching. Sections of roots from the inside to the outside of the mantle show the inner layers of cortical fibres progressively becoming thin-walled, thus appearing as a parenchymatous inner cortex. The roots, which are often branched, penetrate freely throughout the mantle of leaf bases between the sclerotic rings; in one specimen they penetrate through the sclerotic rings into the inner cortex of some of the outer leaf bases, possibly because these were injured while the plant was still living. In several specimens the trunk is surrounded by a mat of roots up to 6 cm. wide; the silt- to very fine sand-sized sediment enclosed within this zone is in contrast to the medium to very coarse sandstone in which the specimens occur.

Discussion. *Palaeosmunda playfordii* differs from *P. williamsii* in lacking sclerenchyma strands in the stipules and inner cortex of the petiole bases. Speciation on the distribution of sclerenchyma in the leaf bases in Osmundaceae is a well-established principle (e.g. Miller 1967) and the distinction by presence or absence of sclerenchyma is a useful one. The xylem ring in the specimens of *P. playfordii* studied, unlike that in *P. williamsii*, always exhibits some leaf gaps (text-fig. 4); however, the variation shown is of a magnitude that suggests it would be possible for a xylem ring with no gaps to occur. The leaf traces have only been found to arise with 1 protoxylem group.

ASSOCIATED FOLIAGE

The fossil flora of the Upper Bowen Coal Measures has been described and figured by Walkom (1922), Rigby (1962, 1963), Hill and Woods (1964), and White (1964; *in* Malone, Corbett, and Jensen 1964, pp. 70–7, pl. 3–13; *in* Olgers, Webb, Smit, and Coxhead 1966, pp. 49–52, pl. A–D).

Many compressions of osmundaceous trunks, probably referable to *Palaeosmunda*, occur in the silicified, abundantly fossiliferous siltstones of the Burngrove Formation (Blackwater Group) outcropping in a small tributary of Burngrove Creek on 'Tolmies Creek' Station, near Blackwater (Portion 10, Parish of Blackwater; locality shown as Burngrove Creek on text-fig. 1). These specimens show the typical mantle of flanged petiole bases, although other anatomical details are not preserved (Pl. 8, figs. 12, 13). The strata also contain impressions of plants of the types which Walkom (1922) described as *Phyllotheca* sp., *Cladophlebis roylei* Arber 1901, *Sphenopteris polymorpha* Feistmantel 1876, *S. lobifolia* Morris 1845, and *Glossopteris* spp. The portions of fronds referred to *S. lobifolia*, *C. roylei*, and *S. polymorpha* vary from bipinnate to tripinnate and appear to intergrade. Unfortunately, no fertile examples of these fronds have been reported. Some layers of the Burngrove Formation contain masses of the *S. lobifolia–C. roylei–S. polymorpha* fronds, flattened osmundaceous trunks, and dissociated, flanged petioles

(Pl. 8, figs. 8, 9). Transverse sections of some of these dissociated petioles show the sclerotic ring and characteristic C-shaped vascular trace which have been replaced by calcite (Pl. 8, figs. 10, 11). It is thus probable that *Palaeosmunda* trunks bore foliage of this type, but this can only be inferred by association.

Acknowledgements. The author thanks Dr. G. Playford (Department of Geology and Mineralogy, University of Queensland) for his guidance and helpful criticism of the manuscript. Dr. C. N. Miller, Jr. (Department of Botany, University of Montana, Missoula) kindly allowed the author to examine slides of *Itopsidema vancleavii*, and also read the typescript. The investigation was carried out at the Department of Geology and Mineralogy, University of Queensland, while the author was in receipt of a Commonwealth Post-graduate Award.

REFERENCES

ANDREWS, H. N. 1961. *Studies in Paleobotany*. New York.

ARBER, E. A. N. 1901. Notes on Royle's types of fossil plants from India. *Geol. Mag.* **8**, 546–9.

ARMSTRONG, J. D., DEAR, J. F., and RUNNEGAR, B. 1967. Permian ammonoids from eastern Australia. *J. geol. Soc. Aust.* **14**, 87–97, 2 pls.

ARNOLD, C. A. 1964. Mesozoic and Tertiary fern evolution and distribution. *Mem. Torrey bot. Club* **21** (5), 58–66.

BOCK, W. 1960. New American Triassic tree ferns. *Proc. Pa Acad. Sci.* **34**, 92–5.

BRONGNIART, A. 1849. *Tableau des genres de végétaux fossiles considérés sous le point de vue de leur classification botanique et de leur distribution géologique: dictionnaire univ. histoire nat.* **13**, 1–127. Paris.

DAUGHERTY, L. H. 1941. The Upper Triassic flora of Arizona. *Publs. Carneg. Instn* **526**, 108 pp., 34 pls.

—— 1960. *Itopsidema*, a new genus of the Osmundaceae from the Triassic of Arizona. *Am. J. Bot.* **47**, 771–7.

DEVINE, S. B. and POWER, P. E. 1967. Permian stratigraphic revisions and rock-unit correlations, central western Bowen Basin, Queensland. *Qd. Govt. Min. J.* **68**, 511–20.

EDWARDS, W. N. 1933. *Osmundites* from central Australia. *Ann. Mag. nat. Hist.*, ser. 10, **11**, 661–3.

—— 1934. Jurassic plants from New Zealand. Ibid., ser. 10, **13**, 81–109, pl. 4, 5.

EICHWALD, E. 1860. *Lethaea Rossica ou paleontologie de la Russie*. **1**. Stuttgart.

EMBERGER, L. 1962. L'intérêt des Osmundacées Triassiques récemment découvertes. *Naturalia monspel.* ser. Bot. **14**, 41–5.

EVANS, P. R. 1966. Mesozoic stratigraphic palynology in Australia. *Australas. Oil Gas J.* **12** (6), 58–63

FEISTMANTEL, O. 1876. On some fossil plants from the Damuda Series in the Raniganj coalfield, collected by Mr. J. Wood-Mason. *J. Asiat. Soc. Beng.* **45** (2), 329–82.

HEWITSON, W. 1962. Comparative morphology of the Osmundaceae. *Ann. Mo. bot. Gdn.* **49**, 57–93.

HILL, D. and DENMEAD, A. K. (eds.). 1960. The geology of Queensland. *J. geol. Soc. Aust.* **7**, 474 pp., 8 pls., 2 maps.

—— and WOODS, J. T. (eds.). 1964. *Permian index fossils of Queensland*. Brisbane.

KIDSTON, R. and GWYNNE-VAUGHAN, D. T. 1907–9. On the fossil Osmundaceae. Part I. *Trans. R. Soc. Edinb.* **45**, 759–80, pl. 1–6. Part II. Ibid. **46**, 213–32, pl. 1–4. Part III. Ibid. **46**, 651–67, pl. 1–8.

MALONE, E. J. 1966. *Geology. Fitzroy region, Queensland. Resources series*. Canberra.

—— CORBETT, D. W. P., and JENSEN, A. R. 1964. Geology of the Mount Coolon 1:250,000 sheet area. *Rep. Bur. Miner. Resour. Geol. Geophys. Aust.* **64**, 78 pp., 15+4 pls.

—— OLGERS, F., MOLLAN, R. G., and JENSEN, A. R. 1967. *Geological map, Bowen Basin, Queensland*. Scale 1:500,000. Canberra.

MARSHALL, P. 1926. A new species of *Osmundites* from Kawhia, New Zealand. *Trans. N.Z. Inst.* **56**, 210–13, pl. 48–54.

MILLER, C. N., JR. 1967. Evolution of the fern genus *Osmunda*. *Contr. Mus. Paleont. Univ. Mich.* **21**, 139–203, pl. 1–4.

—— 1968. The lepidophytic affinities of the genus *Chinlea* and *Osmundites walkeri*. *Am. J. Bot.* **55**, 109–15.

MILLER, C. N., JR. 1969. (In press.) The evolution of the fern family Osmundaceae. *Contr. Mus. Paleont. Univ. Mich.*

MORRIS, J. 1845. *Fossil Flora.* Pp. 245–4, pl. 6, 7, in STRZELECKI, P. E. de. *Physical descriptions of New South Wales and Van Diemen's Land.* London.

OLGERS, F., WEBB, A. W., SMIT, J. A. J., and COXHEAD, B. A., 1966. Geology of the Baralaba 1:250,000 sheet area, Queensland. *Rep. Bur. Miner. Resour. Geol. Geophys. Aust.* **102,** 58 pp., D+3 pls.

ORLOV, YU. A. 1963. *Osnovy paleontologii.* (**14**) *Vodorosli, Mokhoobraznye, Psilofitovye, Plaunovidnye, Chlenistostebel'nye, Paporotniki.* Moscow (in Russian).

PENHALLOW, D. P. 1902. *Osmundites skidegatensis* n.sp. *Trans. R. Soc. Can.* Sect. 4, 2nd ser., **8,** 3–18, pl. 1–6.

POSTHUMUS, O. 1931. *Catalogue of the fossil remains, described as fern stems and petioles.* Malang.

POWER, P. E. 1967. Geology and hydrocarbons, Denison Trough, Australia. *Bull. Am. Ass. Petrol. Geol.* **51,** 1320–45.

RIGBY, J. F. 1962. The taxonomic position of *Actinopteris indica* Srivastava. *Proc. Linn. Soc. N.S.W.* **86,** 299–304, pl. 10A.

—— 1963. On a collection of plants of Permian age from Baralaba, Queensland. Ibid. **87,** 341–51, pl. 11, 12.

RUNNEGAR, B. 1968. (In press.) The Permian faunal succession in eastern Australia. *Proc. Specialist Symposium, Geol. Soc. Aust., Canberra, 1968.*

SEWARD, A. C. 1910. *Fossil Plants. A Text-book for Students of Botany and Geology. II.* Cambridge.

—— and FORD, S. O. 1903. The anatomy of *Todea*, with notes on the geological history and affinities of the Osmundaceae. *Trans. Linn. Soc. Lond.* 2nd ser. Bot. **6,** 237–60, pl. 27–30.

SMITH, E. M. 1958. *Queensland. Lexique stratigraphique international* **6** (5a). Paris.

STEEVES, T. A., and WETMORE, R. H. 1953. Morphogenetic studies on *Osmunda cinnamomea* L.: some aspects of the general morphology. *Phytomorphology* **3,** 339–54.

SURANGE, K. R. 1966. *Indian fossil Pteridophytes.* New Delhi.

WALKOM, A. B. 1922. Palaeozoic floras of Queensland. Part I. The flora of the Lower and Upper Bowen Series. *Publs. geol. Surv. Qd.* **270,** 65 pp.

WEBB, A. W., and MCDOUGALL, I. 1967. Isotopic dating evidence on the age of the Upper Permian and Middle Triassic. *Earth Planet. Sci. Letters* **2,** 483–8.

WEBB, E. A. 1956. Review of exploratory oil wells penetrating Permian section in central Queensland, Australia. *Bull. Am. Ass. Petrol. Geol.* **40,** 2329–53.

WHITE, M. E. 1964. Reproductive structures in Australian Upper Permian Glossopteridae. *Proc. Linn. Soc. N.S.W.* **88,** 392–6, pl. 22–4.

ZALESSKY, M. D. 1924. On new species of Permian Osmundaceae. *J. Linn. Soc.*, Bot. **46,** 347–58, pl. 32–4.

—— 1927. Permskaya flora ural'skikh predelov Angaridy. Atlas. Flore Permienne des limites ouraliennes de l'Angaride. Atlas. *Trudy geol. Kom.* **176,** 152 pp., 46 pls. (in Russian and French.)

—— 1931*a*. Structure anatomique du stipe du *Petcheropteris splendida* n. g. et sp., un nouveau représentant des Osmundacées Permiennes. *Izv. Akad. Nauk. SSSR* 7th ser. (1931), 705–10, pl. 1, 2.

—— 1931*b*. Structure anatomique du stipe du *Chasmatopteris principalis* n. g. et sp., un nouveau représentant des Osmundacées Permiennes. Ibid. 715–20, pls. 1, 2.

—— 1935. Structure anatomique du stipe d'une nouvelle Osmondée du terrain Permian du Basin de Kousnetzk. Ibid. (1935) 747–52, pls. 1–3.

R. E. GOULD
Department of Geology and Mineralogy
University of Queensland
St. Lucia, Queensland
Australia 4067

Typescript received 6 February 1969

ON THE STRUCTURE OF *CORDAITES FELICIS* BENSON FROM THE LOWER PENNSYLVANIAN OF NORTH AMERICA

by CHARLES W. GOOD *and* THOMAS N. TAYLOR

ABSTRACT. New material of *Cordaites felicis* Benson is described from lower Pennsylvanian petrifactions collected in eastern Kentucky. Additional information about the anatomy and epidermal pattern is provided and an emended diagnosis is presented together with a discussion of other structurally preserved cordaitean leaves.

IN 1912 Margaret Benson described a new anatomical species of cordaite leaf, *Cordaites felicis*, from British petrifaction material equivalent to lower Pennsylvanian in age. Of petrified cordaitean leaf forms, *C. felicis* is similar to three species which had been distinguished as *C. loculosus* Felix (1886), *C. robustus* Felix (1886), and *C. wedekindi* Felix (1886). Subsequent to Benson's work, Koopmans (1928) made a comparative study of Felix's species from material collected from the Netherlands and regards them as synonyms of *C. felicis*. Seward (1917) considered *C. felicis* as probably being equivalent to petrified specimens of *C. principalis* (Germar) Geinitz (Germar 1848, Geinitz 1855, Renault 1879, Stopes 1903, Harms and Leisman 1961). Harms and Leisman (1961) have suggested that another cordaite leaf which they studied, *C. crassus* Renault (Renault 1879, Seward and Sahni 1920, Darrah 1940), might also be equivalent to *C. felicis* because the vascular bundles are sometimes completely separated by fibrous tissue, a characteristic that has been generally used to delimit *C. felicis*. Darrah (1940) has also mentioned a similarity between *C. crassus* and *C. felicis*, and has reported the presence of *C. felicis* in a check list of an Iowa coal ball flora (Darrah 1941).

SYSTEMATIC DESCRIPTION

Order CORDAITALES

Genus CORDAITES Unger 1850

Cordaites felicis Benson 1912

Emended diagnosis. Leaves 0·1–1·0 mm. thick with irregular surfaces and rounded margins. Vein frequency of 10–25 per cm. determined by distance from point of attachment; veins separated by longitudinally directed fibrous partitions (primary ribs) that are continuous from abaxial to adaxial surfaces. Identical thick-walled fibres in longitudinal bands above and below veins (primary ribs) and similar hypodermal fibrous masses occasionally between vein and intervein partitions (secondary ribs), dichotomizing veins in basal sections, decreasing in frequency toward tip. Mesophyll constructed of parenchyma plates of laterally elongate cells, vertically attached to lower and upper epidermis, laterally to vein and intervein partitions; vein surrounded by outer sheath 2–7 cells thick and continuous with mesophyll plates. Mesarch xylem of 1–10 larger centripetal metaxylem tracheids (20–57 μ diam.) with secondary wall thickenings of closely spaced

[Palaeontology, Vol. 13, Part 1, 1970, pp. 29–39, pls. 9–11.]

scalariform bars and multiseriate circular bordered pits, and smaller (7–12 μ diam.) less well-developed centrifugal metaxylem tracheids that partially surround centripetal elements, protoxylem tracheids 3–6 μ in diam. and difficult to delimit in all veins, presumed phloem elements typically crushed; inner sheath tracheids present on flanks and abaxial side of bundle. Stomata sunken and longitudinally oriented in rows, 1–2 rows between vein and intervein partition on the adaxial epidermis and up to 8 rows on the abaxial epidermis.

Type locality. The Colliery at Shore-Littleborough, Lancashire.

Stratigraphic position and age. Westphalian A.

Type material. (Lectotype) Specimen designated 365.2 (fig. 2 of Benson 1912), Palaeontological Collection, British Museum (Natural History).

MATERIALS AND METHODS

New material of *C. felicis*, which forms the basis of this study, provides additional information about the structure and phylogenetic relationships of this species. The specimens were collected from the Lewis Creek and Shack Branch localities in eastern Kentucky (Schopf 1961).

Anatomical features of the leaves were determined by the use of cellulose acetate peels. Additional foliage fragments were macerated from coal balls with dilute HCl and provided information on the three-dimensional structure and the surface ribbing patterns of the individual leaves. Surface configurations of the leaves were also observed by chipping coal away from leaves near the surface of the coal balls. Following the technique of Florin (1931), Ledran (1960), and Harms and Leisman (1961), small pieces of coal ball containing only cordaite leaves were completely macerated in Schulze's solution. Cuticles obtained by this process were examined to determine epidermal features. Because of the nature of the material no additional clearing or staining was necessary.

Material used in this study includes slides 3460–3745, cellulose acetate peels, and macerated cuticles from Coal Balls 121, 144, 145, 493, 1460, and 1744, all of which are included in the Paleobotanical Collection, Department of Biological Sciences, University of Illinois at Chicago Circle. Specific designations of figured specimens in this paper are included with plate explanations.

STRATIGRAPHY

Benson's specimens of *C. felicis* were obtained from the mine at Shore Littleborough, Lancashire. The stratigraphic position of this coal, according to Hoskins and Cross (1943) is in the Gannister beds, and is equivalent to deposits of lower Westphalian A, while the material of *C. felicis* described by Koopmans (1928) is from the Finefrau and Katharina horizons which are regarded as being equivalent to lower and upper Westphalian A respectively. Darrah (1941) has recorded *C. felicis* in a check-list of species of coal ball plants from Iowa which he indicates are equivalent to deposits of Westphalian C. An examination of the correlation chart prepared by Moore *et al.* (1940), however, shows these deposits equivalent to Westphalian D. The specimens of *C. felicis* used as the basis of this paper were collected at the Lewis Creek and Shack Branch localities in

Leslie County, Kentucky (Schopf 1961). According to Schopf, the coal balls occupy the position of the Copland Coal, immediately below the Magoffin marine zone, and are considered the oldest coal balls known in North America, intermediate in age between petrifactions recovered from the Lower Coal Measures of Britain and the Eastern Interior Basin deposits of North America. Moore *et al.* (1940) include the Copland Coa as equivalent to upper Westphalian B deposits. Huddle, Lyons, Smith, and Ferm (1963) regard the stratigraphic position of the Copland Coal as equivalent to rocks of middle Pennsylvanian age, while Prostka (1965) indicates that the Copland Coal is in strata of either lower or middle Pennsylvanian age, but makes no precise distinction.

One approach to determining the exact stratigraphic position of the Kentucky coal balls is to examine the floral components contained in these petrifactions. To date the described members of the flora from the Lewis Creek and Shack Branch localities include *Mitrospermum compressum* (Taylor and Stewart 1964), *Calamostachys binneyana* (Taylor 1967), *Bowmanites dawsoni* (Taylor 1969), and *Cordaites felicis*. All of these taxa, in addition to several studies currently in progress (e.g. *Conostoma anglo-germanicum*, *Medullosa* cf. *anglica*, *Pachytesta* cf. *olivaeformis*), are known from the Lower Coal Measures or equivalent strata. *Mitrospermum compressum* and *Cordaites felicis* have been reported but not described from Iowa coal balls of middle Pennsylvanian age (Darrah 1941). While the precise stratigraphic position of the beds containing the eastern Kentucky petrifactions is known, the application of the time stratigraphic terms lower and middle Pennsylvanian to these deposits is in dispute. On the basis of the floristics, however, it is our opinion that the floral components which are so unlike the well-known middle and upper Pennsylvanian age coal ball floras of North America, and so similar to the floras of Westphalian A in Europe, should be regarded as representing time equivalent strata of Westphalian A (= lower Pennsylvanian) in eastern Kentucky.

DESCRIPTION

External morphology. All of the specimens examined were leaf fragments; therefore no complete transverse sections of entire leaves were available. Leaf length, width, and shape are still incompletely known. In transverse section, the most complete leaf measures 32·0 mm. wide and is twice the maximum width reported by Benson in her description of *C. felicis*. According to the magnifications accompanying Benson's photographs of *C. felicis* (1912), the leaves illustrated agree in size with the specimens reported here. The data in the text portion of Benson's paper, however, appear to be $\frac{1}{10}$ of the size indicated by the photographs. It is therefore assumed that Benson's data must be multiplied by a factor of ten in order to correlate with the photographs. Leaf thickness in the Kentucky specimens ranges from 0·1 to 1·0 mm. Toward the margins the leaves gradually become thinner, but are not as thin as Benson's reported margin thickness of 19 microns (taken now as 190 μ).

Leaf margins are bluntly rounded (Pl. 10, fig. 2) and do not agree with the drawing of a supposedly young leaf similar to *C. felicis* which shows pointed margins (Scott 1924). The leaf epidermis, as exposed on the coal ball surfaces and by maceration with HCl, typically exhibits straight, axially oriented rows of ribs of uniform breadth (Pl. 10, fig. 1). According to the terminology of earlier workers, these structures are referred to as primary ribs, because they are the most prominent surface feature, and account for

raised areas on the left surface (Pl. 9, fig. 2). Macerated leaves indicate that the primary ribs are the result of longitudinally disposed fibrous hypodermal tissue associated with the veins and partitions between veins. From the surface it is impossible to tell whether a primary rib is associated with a vein or an intervein partition. Thinner secondary ribs are occasionally seen between these primary ribs (Pl. 10, fig. 1) and consist of smaller masses of fibrous hypodermal tissue often situated between the veins and intervein partitions (Pl. 9, fig. 2).

The leaves show a considerable variation in degree of surface relief in transverse section. Some have almost smooth external surfaces (Pl. 10, fig. 3), while others show an undulating surface, apparently due to crushing thinner walled cells except where the veins and intervein partitions give additional support (Pl. 9, fig. 1). Since many of the leaves have a smooth external surface in transverse section, it seems probable that originally there was little or no surface relief.

Internal anatomy. The most conspicuous characteristic of the internal anatomy of *Cordaites felicis* is the presence of complete epidermis-to-epidermis partitions between most of the veins (Pl. 9, figs. 1, 2). In transverse section these partitions resemble 'I' beams (Pl. 9, fig. 1); the top and bottom consisting of hypodermal masses of fibres which are 5–15 cell layers deep and 3–10 cells wide. Individual fibres are axially elongate (Pl. 9, fig. 5) and have small lumens. Fibre diameters range from 35 to 124 μ. In thicker fragments the partition consists entirely of these fibre-like cells, although the lumina of those cells in the centre of the partition are broader than the lumina of cells near an epidermis (Pl. 9, figs. 1, 2). In transverse sections that measure no more than about 0·75 mm. thick the fibres only extend about $\frac{1}{4}$ of the distance across the leaf from both the upper and lower epidermis (Pl. 10, fig. 3). The remaining central portion of the partition is made up of thin-walled rectangular cells with somewhat thickened corners and diameters that range between 23 and 46 μ. In paradermal section these cells measure 105–240 μ in length and 20–35 μ in width. Individual partitions extend uninterrupted throughout the length of the leaf fragments studied.

Approximately 10 % of the veins have neither hypodermal fibrous tissue nor thin-walled cells between them, although they are surrounded by a common sheath. This absence of partitions varies considerably with leaf thickness; leaf fragments thicker than 0·6 mm. have approximately 17 % of their veins unpartitioned. Leaves between 0·3 and 0·6 mm. thick have approximately 7 % unpartitioned veins. Specimens less than 0·3 mm. thick have about 4 % unpartitioned veins. It is assumed that the thicker leaf fragments represent the basal portion of the leaf, as has been suggested by Benson

EXPLANATION OF PLATE 9

Figs. 1–5. *Cordaites felicis*. 1, Transverse section of portion of leaf showing fibrous ribs, disposition of veins, and intervein partitions (IP); arrow indicates position of inner sheath; C.B. 145A bot, # 39, ×60. 2, Transverse section of portion of leaf showing hypodermal fibrous masses responsible for primary (PR) and secondary (SR) surface ribs; C.B. 145A bot, # 31, ×115. 3, Oblique section of leaf showing mesophyll plates (MP); C.B. 145A bot, # 31, ×120. 4, Transverse section of vein and position of outer sheath (OS); C.B. 145F (2) top, # 67, ×130. 5, Longitudinal section of leaf showing thick-walled fibres of hypodermal masses and secondary wall thickenings of centripetal xylem elements; C.B. 145F (1) bot, # 9, ×155.

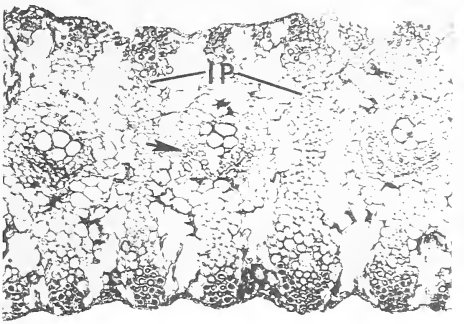

1

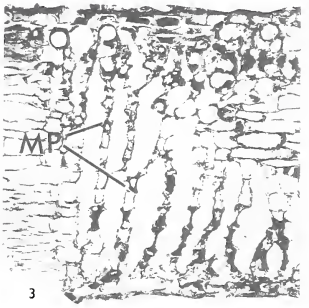

3

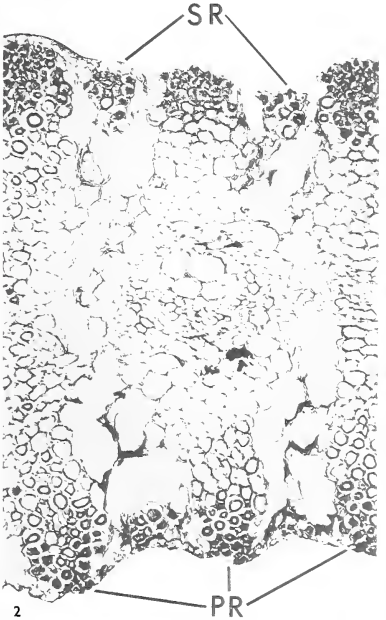

2

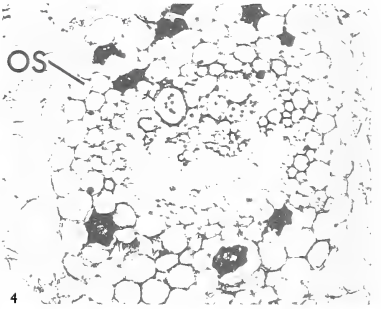

4

5

GOOD and TAYLOR, Pennsylvanian *Cordaites* leaves

(1912), Harms and Leisman (1961), and other authors who have described various structurally preserved cordaite leaf species. The frequency of unpartitioned veins further supports the conclusion that divisions occur most frequently at the basal region of the leaf (Pl. 10, fig. 3). This feature of vein frequency is consistent with Benson's description of *Cordaites felicis*, and agrees with the presumed pattern of vein dichotomy in other structurally preserved cordaite leaf species (Harms and Leisman 1961) as well as those known only from compression specimens. Successive transverse sections indicate that when vein dichotomy occurs it is at a very acute angle.

Incomplete partitions that do not extend from epidermis to epidermis occur between less than 0·1 % of the veins. This frequency of incomplete partitions is not the case with *C. crassus* and *C. principalis* (Harms and Leisman 1961) which are otherwise described as being very similar to *C. felicis* in their internal organization.

The distribution of the veins of *C. felicis* is typical of most cordaite leaf species. The number of veins and associated tissues (vascular bundle sheath) ranges from 10 to 25 per cm. and in transverse section occupies 50–75 % of the leaf thickness. Masses of fibrous hypodermal tissue are located above and below the veins (Pl. 9, figs. 1, 2) and have the same general dimensions as those which form part of the intervein partitions (Pl. 9, figs. 1, 2). Vascular elements are surrounded by a sheath of thin-walled cells 4–7 cell layers thick that thins laterally to 2–3 cells in thickness (Pl. 9, fig. 4). In transverse section sheath cells are approximately circular in outline and have diameters that range from 20 to 40 μ while in paradermal section they are rectangular and measure 115–305 μ long and appear identical to those cells found in the centre of the intervein partitions.

The xylem in *C. felicis* is mesarch. One to ten broad (20–57 μ) thick-walled metaxylem elements are situated on the adaxial side of the bundle (Pl. 10, fig. 5). Protoxylem elements (3–6 μ diam.) occur as a small strand immediately below these cells (Pl. 10, fig. 5) but are not identifiable in all of the bundles. Centrifugal metaxylem elements, of smaller diameters than the centripetal metaxylem cells and larger diameters than the protoxylem tracheids, radiate out to the side of the centripetal cells from below the protoxylem (Pl. 10, fig. 5). Radial sections of veins show the centripetal elements to be very long and characterized by secondary wall thickenings that range from closely spaced scalariform bars to multiseriate circular bordered pits (Pl. 11, fig. 3). Centrifugal elements are smaller and more circular in outline than the centripetal elements and have diameters that range from 7 to 12 μ. These cells occasionally form an arc that laterally encloses the centripetal xylem. Often, small areas of centrifugal xylem are present only on the lateral sides of the centripetal elements (Pl. 10, fig. 5).

Additional xylem elements often occur just inside the thin-walled vein sheath (Pl. 9, fig. 1; Pl. 10, fig. 5). These cells, that range in diameter between 9 and 23 μ, have been referred to as the 'inner sheath' by early workers (Renault 1879, Stopes 1903). They intermittently occur below and to the side of the centripetal and centrifugal metaxylem elements (Pl. 10, fig. 5) and often merge with the centrifugal xylem present laterally and adjacent to the centripetal tracheids (Pl. 10, fig. 5). Cells presumed to be phloem can occasionally be distinguished between the inner sheath and the central portion of the centrifugal xylem (Pl. 10, fig. 5), but their general poor preservation precludes a detailed description.

Hypodermal masses of fibrous tissue sometimes occur between the veins and intervein partitions associated with both surfaces of the leaf (Pl. 10, fig. 1). These masses are usually

smaller groups of fibres than those associated with the veins or partitions. They are sometimes attached to the outer sheath of veins and may be associated with a new intervein partition that has arisen just distal to the point of a vein dichotomy. No constant relationship exists between vein division and these masses of fibres. These small fibrous masses usually occur in the thicker leaf fragments, and are responsible for the so-called secondary ribs sometimes seen in surface and sectional views (Pl. 9, fig. 2).

Palisade parenchyma is absent in *Cordaites felicis*, as has been reported in *C. principalis* and *C. crassus*; however, it is present in other petrified forms. The entire internal tissue between the veins and intervein partitions of *C. felicis* consists of spongy mesophyll making up parenchyma plates that are perpendicular to the leaf surfaces, and to the axially oriented veins and intervein partitions (Pl. 9, fig. 3; Pl. 10, fig. 1). Each plate is a single cell layer in thickness and is attached to both the upper and lower epidermis (Pl. 10, fig. 1). The plates extend laterally between a vein and adjacent intervein partition and in this direction can be seen to have 5 to 9 cells (Pl. 10, fig. 1). In some specimens these plates consist of flattened, laterally elongate cells suggestive of a flaccid condition of the mesophyll tissue (Pl. 10, fig. 1). Other plates, however, consist of apparently turgid cells that are isodiametric and measure 20–30 μ in diameter (Pl. 10, fig. 4). Between plates are conspicuous lacunar areas that approximate the width of the turgid mesophyll parenchyma cells. Toward the veins and intervein partitions these spaces become smaller, with the plates of parenchyma cells adjoining the intervein partition or outer sheath of a vein (Pl. 10, fig. 3). Similar appearing mesophyll cells that make up plates of photosynthetic tissue have been described by Cross (1940) in *Taxodium distichum* and Esau (1965) in *Pinus*. Studies of *T. distichum* indicate that the lacunar spaces are the result of cell separation brought about by a slower rate of cell enlargement in the mesophyll as compared with that of the surrounding tissues. The absence of extensive foliar specimens at this time precludes a developmental interpretation of this kind for *C. felicis*.

In transverse section, cells of the mesophyll parenchyma appear similar to the cells of the outer sheath, and in some instances the two cannot be distinguished (Pl. 10, fig. 3). The difference is only seen in paradermal view, where the sheath cells appear more axially elongated than the cells of the parenchyma plates.

Epidermal structure. The epidermis consists of longitudinal rows of stomata located above the regions where there is no hypodermal fibrous tissue, and intervening rows of rectangular accessory cells above the fibrous tissue (Pl. 11, figs. 1, 4). Accessory epidermal cells are oriented parallel to the long axis of the leaf, measure 60–150 μ long and

EXPLANATION OF PLATE 10

Figs. 1–6. *Cordaites felicis*. 1, Slightly oblique paradermal section of leaf showing position of primary ribs (PR) and mesophyll plates; arrow indicates secondary rib; C.B. 1460 bot, # 37, × 100. 2, Transverse section of leaf at margin; C.B. 145D (1) top, # 30, × 150. 3, Transverse section of leaf showing smooth adaxial surface and vein at level of dichotomy (arrows); note continuity of cells of outer sheath (OS) and those of mesophyll plates; C.B. 145F (2) top, # 67, × 120. 4, Paradermal section of leaf showing turgid nature of mesophyll plate cells; C.B. 121J top, # 20, × 200. 5, Transverse section of vascular bundle indicating position of centripetal (X) and centrifugal metaxylem (X′), protoxylem elements (PX), phloem (P), and inner sheath (IS); C.B. 145A bot, # 39, × 250. 6, Transverse section through two guard cells (G) and lateral subsidiary cells; arrow indicates cuticular extension over stoma; C.B. 145D (1), # 31, × 1000.

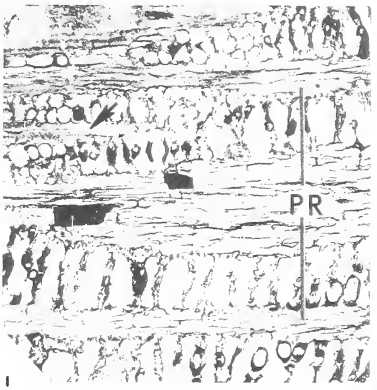

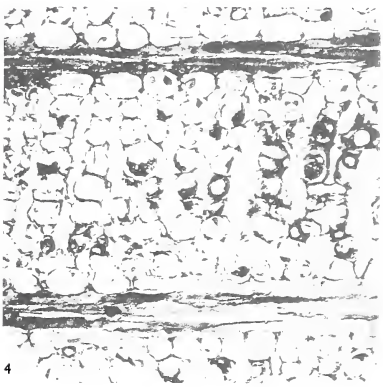

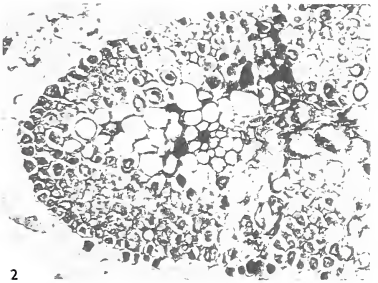

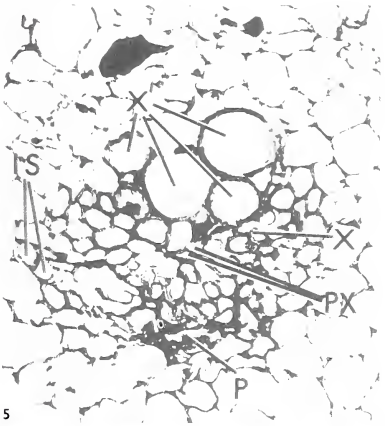

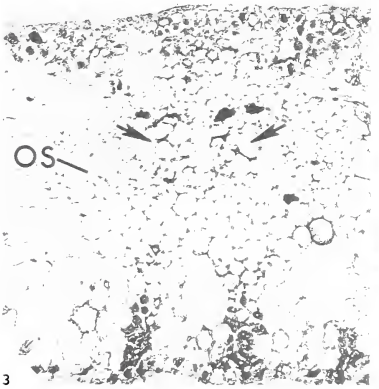

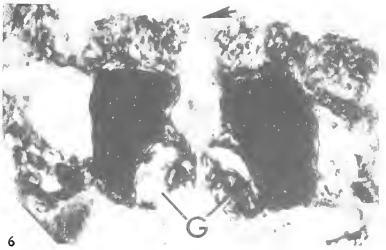

GOOD and TAYLOR, Pennsylvanian *Cordaites* leaves

12–28 μ wide, and occur in easily identifiable bands across the epidermis (Pl. 11, fig. 1). Cuticles show a faint longitudinal median line associated with some of the accessory cells (Pl. 11, fig. 2). This feature occurs only on isolated cuticles and appears to be a property of the cuticle since no evidence of such a thickening can be seen in the same position on sections of the epidermis. The accessory cells have end walls that are straight, while the radial walls are irregularly thickened and exhibit primary pits (Pl. 11, fig. 2).

The epidermal cells which occur over the regions between the fibrous tissue are variable in shape (Pl. 11, fig. 5). They are usually shorter than the accessory cells over fibrous areas and tend to be more isodiametric, often having bluntly rounded end walls. These cells are associated with the stomatal apparatus.

Regions at the presumed basal (thick) part of the leaf which have narrow areas between the relatively massive zones of fibrous tissue have few stomata. At all other regions both the upper and lower epidermis contain stomata. This is not consistent with Benson's (1912) description of *C. felicis* in which stomata are reported as occurring only on the lower epidermis.

The upper epidermis has bands that contain one or two rows of stomata (Pl. 11, fig. 1). Slightly narrower bands containing only accessory cells alternate with stomatiferous bands (Pl. 11, fig. 1). Superficially, the stomata appear scattered, but upon close examination are seen to arise from the same row or rows of cells showing no sharing of terminal subsidiary cells.

The lower epidermis contains one or two rows of stomata positioned between the hypodermal fibrous masses in basal areas of the leaf. The stomata are more closely spaced than are those of the upper epidermis, often having adjacent terminal subsidiary cells. On the thinner, presumably more distal parts of the leaf, where there are few fibrous masses between the veins and intervein partitions, more rows of stomata appear (Pl. 11, fig. 4). Often 5–7, and occasionally 8 rows of stomata occur between a vein and an adjacent intervein partition (Pl. 11, fig. 4). The rows are usually staggered, all the stomata of adjacent rows are not lined up in transverse bands as in *Cordaites principalis* (Harms and Leisman 1961) and *C. affinis* (Reed and Sandoe 1951). Under these crowded conditions terminal subsidiary cells are often shared with adjacent stomata in the same cell row for several consecutive stomata. When there are fewer than 5 rows of stomata on the lower epidermis subsidiary cell sharing is not common.

The stomatal apparatus consists of two bean-shaped guard cells (Pl. 11, fig. 7), two bean-shaped lateral subsidiary cells (Pl. 11, fig. 6), and two terminal subsidiary cells (Pl. 11, fig. 7). The lateral subsidiary cells of both the upper and lower epidermis range between 39–69 μ long and 11–23 μ wide. The terminal subsidiary cells of the upper epidermis measure 14–70 μ long and 11–21 μ wide; those of the lower epidermis measure 20–40 μ long and 11–18 μ wide. The terminal subsidiary cells of both the upper and lower epidermis measure approximately 20 μ in depth. In general, the terminal subsidiary cells are small when there is another stoma nearby in the same row, as is typical of the lower epidermis where the density of stomata is considerably greater. In cases where the same terminal subsidiary cell is shared by two stomata, the cell is almost circular in outline.

Guard cells measure 35–46 μ long and approximately 10–12 μ wide. In transverse section these cells appear noticeably depressed below the surrounding subsidiary cells (Pl. 10, fig. 6). The thick cuticle does not extend downward into the epistomal chamber

(Pl. 10, fig. 6). No hairs or other cuticular appendages are present on the epidermis of *C. felicis*.

DISCUSSION

Several anatomical species of cordaite leaves are similar to *C. felicis*. Of these taxa, anatomical specimens of *C. principalis* from the Carboniferous and Permian of Europe, and *C. crassus*, known from the Carboniferous of France and North America (Pennsylvanian of Iowa), have been suggested as being closely related if not equivalent to *C. felicis*. The present study indicates, however, that although these 3 species are similar in several important features including leaf thickness, vein frequency, and stomatal apparatus, *C. felicis* differs from *C. principalis* and *C. crassus* in the following important features. The maturation pattern of the primary xylem in *C. felicis* and *C. crassus* is mesarch, whereas in *C. principalis* it is exarch. Complete intervein partitions apparently run the length of the *C. felicis* leaf whereas these are infrequent and generally of limited extent in *C. crassus*, and are completely absent in *C. principalis*. In *C. felicis* a maximum of 8 rows of stomata are present between the vein and intervein partition, while in *C. crassus* only 8 rows are present between 2 veins. A maximum of 5 rows of stomata occur between hypodermal fibrous masses in *C. principalis*, with stomata aligned between adjacent rows; in *C. felicis* adjacent rows of stomata are staggered. Hypodermal fibrous masses project far into the mesophyll between the veins only in the thicker areas of the leaf in *C. felicis*, but extend from the abaxial surface through one-half of the leaf regardless of the total thickness in *C. crassus*. The outer bundle sheath in *C. crassus* is 6–7 cells wide on its adaxial or upper surface, narrowing on the sides and abaxial portion. In *C. felicis* the sheath is 4–7 cells thick; in *C. principalis* it consists of 1–3 cell layers.

The petrified foliage forms *C. rotundinervis* Grand'Eury (1877), *C. rhombinervis* Grand'Eury (1877) from the Carboniferous of France are immediately distinguished from *C. felicis* by the exarch nature of the primary xylem. In addition, *C. rhombinervis* and *C. tenuistriatus* are characterized by a mesophyll that is differentiated into a distinct palisade and spongy region, as is *C. lingulatus* Grand'Eury (1877) from the Carboniferous and Permian of Europe. The occurrence of forms designated as *C. loculosus*, *C. robustus*, and *C. wedekindi* by Felix (1886), and *C. weristeri* Leclercq (1927) from petrifaction material collected from the same stratigraphic level and in some instances occurring in the same coal ball, as well as a tendency for one species to grade into another, caused Koopmans (1928) to regard all as synonyms of *C. felicis*. Benson (1912)

EXPLANATION OF PLATE 11

Figs. 1–7. *Cordaites felicis*. 1, Cuticle of upper epidermis showing bands of rectangular cells above fibrous masses with bands of stomata between; C.B. 145F (1) Maceration slide # 18, ×130. 2, Enlargement of epidermal cells from fig. 1 showing irregular radial wall thickenings; C.B. 145F (1) Maceration slide # 18, ×400. 3, Multiseriate circular bordered pits and scalariform bars of centripetal xylem elements; C.B. 145F (1) bot, # 2, ×600. 4, Paradermal section just beneath cuticle of lower epidermis showing primary ribs (arrows) and stomatal rows between; C.B. 145F (1) side # 17, ×130. 5, Epidermal cells associated with stomatal bands from upper epidermis; C.B. 145F (1) Maceration slide # 18, ×400. 6, Stoma and subsidiary cells of upper epidermis; C.B. 145F (1) Maceration slide # 18, ×500. 7, Two stomata and shared terminal subsidiary cells from lower epidermis; C.B. 145F (1) side, # 17, ×625.

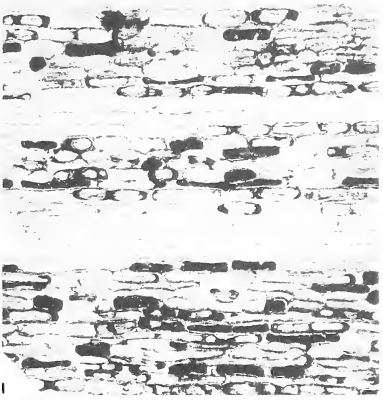

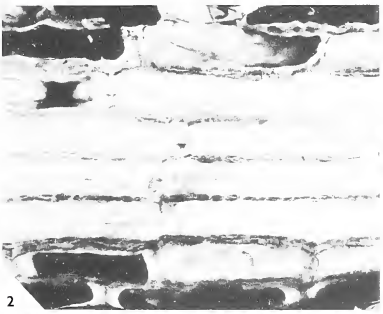

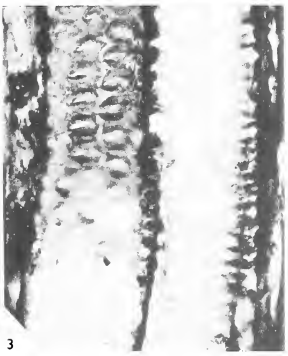

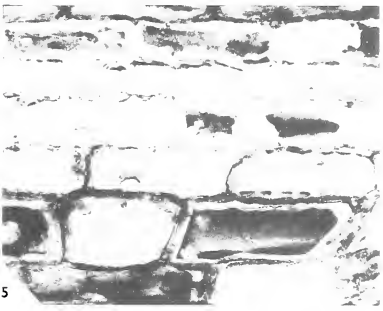

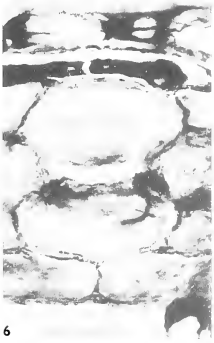

GOOD and TAYLOR, Pennsylvanian *Cordaites* leaves

notes the general similarity of the presumed upper or distal part of *C. felicis* to *C. wedekindi*, while sections closer to the base more closely resemble material of the *C. loculosus* and *C. robustus* types.

Although the probability exists that several recognized cordaite foliage species represent different parts of the same leaf our studies with the Kentucky specimens of *C. felicis* do not show either a gradual or marked anatomical change taking place through many centimetres of lamina presumably representing all parts of the leaf. For example, intervein partitions, a feature used to delimit numerous anatomical species, were incomplete in only 0·1 % of all of the sections of leaves examined. The consistent absence of complete partitions in *C. weristeri* and *C. robustus* still provides a means of distinguishing them from *C. felicis*. Specimens of *C. loculosus* are described with complete intervein partitions, however, material of this type is readily recognized by the absence of a bundle sheath. General leaf thickness, extent of bundle sheath, and slender intervein partitions are features that Benson (1912) used to delimit *C. wedekindi* from *C. felicis*.

In alluding to the ultimate solution of delimiting cordaite foliage through the organic attachment of leaves to stems, Benson (1912) notes the consistent mutual occurrence of the cordaitalean seed *Mitrospermum compressum* and *C. felicis* foliage. Whereas such an association can have limited value in studies involving petrifaction material, such a correlation becomes more meaningful as identical species associations are discovered and recorded. It is, therefore, of interest that *Mitrospermum compressum* was reported and described for the first time in North America (Taylor and Stewart 1964) from the same petrifaction material that has provided the specimens of *C. felicis* used in this study.

Cuticular studies of cordaite foliage by Renault (1879), Wills (1914), Florin (1931), Reed and Sandoe (1951), and Harms and Leisman (1961) have demonstrated epidermal patterns similar to the *C. felicis* type. Patterns that are unlike this type have recently been reported in cordaitean leaves by Ledran (1958, 1960) for petrified specimens of *C. angulostriatus* Grand'Eury (1877) and *C. lingulatus*. In *C. angulostriatus* the shape and orientation of the stomata is not as consistent as it is in species such as *C. felicis*. Moreover, in *C. angulostriatus* each pair of guard cells has 4–5 subsidiary cells and the stomata are aligned in single rows. In *C. lingulatus* the stomata are randomly arranged, each with 3–8 subsidiary cells. Florin (1931) has shown prominent cuticular papillae associated with the subsidiary cells of *C. lingulatus*.

There appear to be at least two general types of cuticular patterns known for cordaitean leaves. The pattern demonstrated by *C. felicis*, *C. principalis*, *C. crassus*, *C. affinis*, and a number of described but unnamed forms by Renault (1879), Wills (1914), and Florin (1931), have guard cells and subsidiary cells oriented parallel to the long axis of the leaf. Cuticular papillae are absent and the stomatal apparatus of all of these forms are almost indistinguishable from one another.

The epidermal cell pattern characterized by *C. angulostriatus* and *C. lingulatus* shows a consistent irregular orientation of the stomata and a wide range in the number of subsidiary cells. Cuticular papillae are associated with subsidiary cells of this type.

When these two types of epidermis are considered along with internal structural features and the stratigraphic position of the leaves, a potential basis for interpreting the phylogeny of cordaitean foliage emerges. Taxa with the more regular epidermal cell

patterns tend to be characterized by prominent hypodermal fibrous masses separating veins, and are generally found in lower and middle Pennsylvanian age sediments. Cordaite leaves with less well-developed hypodermal bands between the veins and more irregular cuticular patterns extend on into Permian age rocks. It is clear that epidermal features of cordaitean leaves may not only be useful taxonomically, but may provide a means of comparison between structurally preserved leaves and the large number of presently meaningless compression species.

It is worth while here to mention the similarity between the irregular pattern of stomata disposition in some cordaite foliage species and the epidermal cell arrangements of some of the earliest coniferophyte leaves discussed by Florin (1944, 1951). In general, *Lebachia* has stomata with 4–10 subsidiary cells, each typically associated with a cuticular papilla. The orientation of the individual stoma is random within two band-like regions on each surface of the leaf. Foliage of *Ernestiodendron* has stomata in single rows. Each stoma is randomly oriented within the row and has 4–8 subsidiary cells with papillae. The epidermal cell patterns of *Lebachia* and *Ernestiodendron* more closely resemble the type of cordaite cuticles described by Ledran (1958, 1960) than the type characterized by *Cordaites felicis*. In particular the cell patterns of *C. angulostriatus* and those of *Ernestiodendron* foliage are almost identical. It is also interesting to note the similarity between the arrangement and structure of stomata on the seed scales of *Araucaria cutchensis* (Pant and Srivastava 1968), an Upper Jurassic compression from India, and the arrangement and structure of stomata in *C. angulostriatus*. A comparison of epidermal patterns may ultimately provide a clue to the group of Carboniferous cordaites from which some Permian conifers have evolved.

Acknowledgements. This study was supported by National Science Foundation Grants GB–6834 and GY–4525. We are grateful to Dr. John M. Pettitt, British Museum (Natural History), for making Benson's material of *Cordaites felicis* available for investigation.

REFERENCES

BENSON, M. 1912. *Cordaites felicis*, sp. nov., a cordaitean leaf from the lower coal measures of England. *Ann. Bot.* **26,** 201–7.

CROSS, G. L. 1940. Development of the foliage leaves of *Taxodium distichum*. *Am. J. Bot.* **27,** 471–82.

DARRAH, W. C. 1940. The fossil flora of Iowa coal balls III: *Cordaianthus*. *Harvard Univ. Bot. Mus. Leaflets*, **8,** 1–20.

—— 1941. Studies of American coal balls. *Am. J. Sci.* **239,** 33–53.

ESAU, K. 1965. *Plant anatomy*, second edition. John Wiley & Sons, New York. 767 pp.

FELIX, J. 1886. Untersuchungen über den inneren Bau Westfalisher Carbonpflanzen. *Abhandl. zur Geol. Spezialkarte von Preussen*, **7,** 1–73.

FLORIN, R. 1931. Untersuchungen zur Stammesgeschichte der Coniferales und Cordaitales. *Kungl. Svenska Vetenskapsakad. Handl.* **III,** 10.

—— 1944. Die Koniferen des Oberkarbons und des Unteren Perms. *Palaeontographica*, **85,** 366–456.

—— 1951. Evolution in Cordaites and Conifers. *Acta Horti Bergiani*. **15,** 285–388.

GEINITZ, H. B. 1855. *Die Versteinerungen der Steinkohlenformation in Sachsen, II*. Leipzig.

GERMER, E. F. 1848. *Die Versteinerungen der Steinkohlenformation in Wettin und Loebejun in Saalkreis, IV*. Loebejun, Halle.

GRAND'EURY, C. 1877. La flore carbonifère du Département de la Loire et du centre de la France. *Mem. Acad. Sci. Inst. Fr.* **24.**

HARMS, V. L. and LEISMAN, G. A. 1961. The anatomy and morphology of certain *Cordaites* leaves. *J. Paleont.* **35,** 1041–64.

HOSKINS, J. H. and CROSS, A. T. 1943. Monograph of the Paleozoic cone genus *Bowmanites* (Sphenophyllales). *Am. Midl. Nat.* **30,** 113–63.

HUDDLE, J. W., LYONS, E. J., SMITH, H. L., and FERN, J. C. 1963. Coal reserves of eastern Kentucky. *U.S. Geol. Survey Bull.* **1120,** 247 pp.

KOOPMANS, R. G. 1928. Researches on the floras of the coal balls from the 'Finefrau-Nebenband' horizon in the province of Limburg (The Netherlands). *Geol. Bur. Nederland,* **1,** 1–54.

LECLERCQ, S. 1927. Les végétaux à structure conservée du houiller Belge. Note I. Feuilles et racines de cordaitales des coalballs de la couche Bouxharmont. *Ann. Soc. Géol. Belgique,* **51,** 53–66.

LEDRAN, C. 1958. Sur la nervation de quelque feuilles de *Cordaites. Bull. Soc. Géol. Fr.* 6 série, **8,** 39–43.

—— 1960. Sur les cuticules de Cordaitales. Ibid. 7 série, **2,** 653–6.

MOORE, R., *et al.* 1944. Correlation of Pennsylvanian formations of North America. *Bull. Geol. Soc. Am.* **55,** 657–706.

PANT, D. D. and SRIVASTAVA, G. K. 1968. On the cuticular structure of *Araucaria* (*Araucarites*) *cutchensis* (Feistmantel) comb. nov. from the Jabalpur series, India. *J. Linn. Soc.* (Bot.) **61,** 201–6.

PROSTKA, H. 1965. Geology of the Hyden East Quadrangle, Kentucky. *U.S. Geol. Survey* map GQ–423.

REED, F. D. and SANDOE, M. T. 1951. *Cordaites affinis*: a new species of cordaitean leaf from American coal fields. *Bull. Torrey Bot. Club,* **78,** 449–57.

RENAULT, B. 1879. Structure comparée de quelques tiges de la flore carbonifère. *Nouv. Archives Mus. Hist. Nat. Paris,* **2,** 213–326.

SCHOPF, J. M. 1961. Coal-ball occurrences in eastern Kentucky. *Geol. Survey Research* (Short papers in the geologic and hydrologic sciences, 1–146) **95,** B228–B230.

SCOTT, D. H. 1924. *Extinct Plants and Problems of Evolution.* Macmillan & Co., London. 240 pp.

SEWARD, A. C. 1917. *Fossil Plants,* III. Cambridge University Press, London. 656 pp.

—— and SAHNI, B. 1920. Indian Gondwana plants. *Mem. Geol. Survey India,* **7,** 1–41.

STOPES, M. C. 1903. On the leaf-structure of *Cordaites. New Phytol.* **2,** 91–8.

TAYLOR, T. N. 1967. On the structure of *Calamostachys binneyana* from the lower Pennsylvanian of North America. *Am. J. Bot.* **54,** 298–305.

—— 1969. On the structure of *Bowmanites dawsoni* from the lower Pennsylvanian of North America. *Palaeontographica,* **125 B,** 65–72.

—— and STEWART, W. N. 1964. The Paleozoic seed *Mitrospermum* in American coal balls. Ibid. **115 B,** 51–8.

UNGER, F. 1850. *Genera et species plantarum fossilium.* Vienna. 627 pp.

WILLS, L. J. 1914. Plant cuticles from the coal measures of Britain. *Geol. Mag.* N.S. **1,** 385–90.

CHARLES W. GOOD
THOMAS N. TAYLOR
Department of Biological Sciences
University of Illinois at Chicago Circle
Chicago, Illinois 60680
U.S.A.

Typescript received 18 January 1969

A DIMORPHIC GONIATITE FROM THE NAMURIAN OF CHESHIRE

by N. H. TREWIN

ABSTRACT. *Eumorphoceras yatesae* sp. nov. is described from a high E2a Carboniferous horizon at Croker Hill, Cheshire. Dimorphs A and B are described under the same specific name since the initial stages of each are identical and they are both confined to the same horizon. Possible dimorphism in the goniatite genus *Eumorphoceras* is considered.

MANY authors have described dimorphism in ammonite genera, for example, Callomon (1963), Makowski (1962), and Palframan (1966, 1967). In general the dimorphs differ in size at maturity and the smaller form is usually taken as the male. The development of special modifications of aperture takes place at maturity—lappets, rostra, and apertral constrictions being frequently described. The general ornament of the shell is often different in the two dimorphs, usually after an initial period of development where the ornament of the two dimorphs is similar.

Dimorphism has been described in the Devonian goniatite genera *Manticoceras*, *Tornoceras*, and *Cheiloceras* (Makowski 1962) involving differences in size at maturity. Demanet (1943) described dimorphism in *Gastrioceras* species found in association where one form is characterized by a wide umbilicus and ventrally flattened whorl section and the other by a narrower umbilicus and higher whorl section. The form with the wide umbilicus is interpreted by him as the female, but he gives no indication of the relative sizes of the forms at maturity. Ramsbottom and Calver (1962) also consider it possible that dimorphism is shown by species of *Gastrioceras* from the *G. subcrenatum* and *G. listeri* horizons.

Absolute differences in size at maturity cannot be demonstrated for the dimorphs of *Eumorphoceras yatesae* as the specimens are always crushed. It can be demonstrated that in each of three marine bands two forms of *Eumorphoceras* are present with similar differences in ornamentation and that in the case of the *erinense–ferrimontanum* pair, and the *yatesae* A and B pair, the initial stages of development appear to be identical.

SYSTEMATIC DESCRIPTION

Order AMMONOIDEA Zittel 1825
Suborder GONIATITINA Hyatt 1884
Superfamily GONIATITACEA de Haan 1825
Family GONIATITIDAE de Haan 1825
Subfamily GIRTYOCERATINAE Wedekind 1918
Genus EUMORPHOCERAS Girty 1909

Eumorphoceras yatesae sp. nov.

Plate 12, figs. 1–5

[Palaeontology, Vol. 13, Part 1, 1970, pp. 40–6, pl. 12]

Material. All specimens are crushed in shale and preserved mainly as external moulds. Holotype: *E. yatesae* dimorph A. LZ 5779. Paratypes dimorph A: LZ 5782; LZ 5783. Paratypes dimorph B: *E. yatesae* dimorph B. LZ 5780; LZ 5784. Paratypes dimorph indeterminate *E. yatesae* LZ 5781; LZ 5785–90.

The specimen numbers quoted throughout the text refer to specimens deposited with the Institute of Geological Sciences, Leeds.

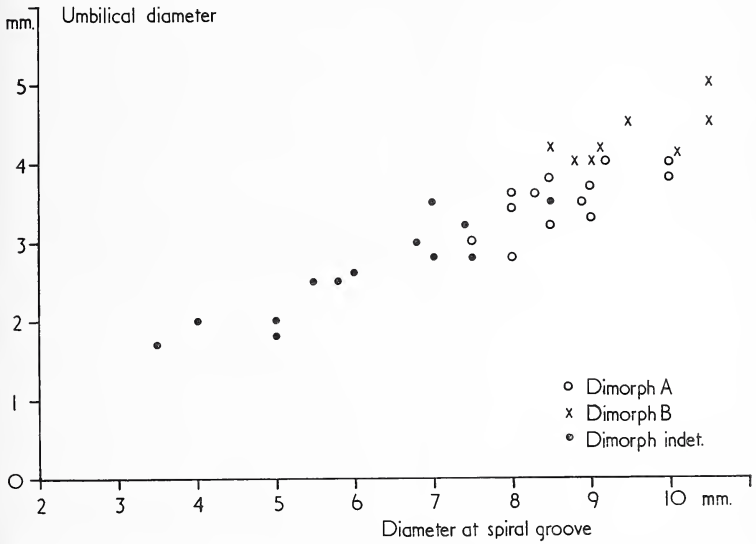

TEXT-FIG. 1. The relation between umbilical diameter and spiral groove diameter for *Eumorphoceras yatesae* sp. nov.

Description. The crushed nature of the material does not allow an accurate measurement of the over-all diameter to be made and so diameter measurements have been made at the spiral groove.

Up to 8 mm. spiral groove diameter, all specimens have similar features (LZ 5781; Pl. 12, fig. 4). Ribs are present on the second whorl where there are about 12 per half whorl. With increase in diameter ribs become more numerous until there are 17–20 per half whorl at 7–8 mm. spiral groove diameter. The ribs arise within the umbilicus and are radial or slightly forwardly directed for the first part of their course over the flanks. At a point about halfway from the umbilicus to the spiral groove the ribs bend evenly forward to meet the spiral groove.

At 8 mm. spiral groove diameter the umbilicus is 3 mm. wide and at 4 mm. diameter it measures 2 mm. The umbilical diameter is difficult to measure in this crushed material,

but text-fig. 1 illustrates the general relation between umbilical and spiral groove diameter for the species.

The spiral groove is present at 5 mm. diameter and persists to the largest diameters seen on all specimens. Constrictions are present on some specimens which appear as deep grooves between two sharp ribs, they are best seen at the umbilical margin or at the spiral groove. Constrictions are not invariably present and do not appear to be regularly spaced. On specimens larger than 8 mm. diameter dimorphs A and B can be distinguished.

Dimorph A. In this form the ribs begin to die out at 8 mm. diameter and are represented by umbilical nodes. These are clearly seen on the holotype LZ 5779 (Pl. 12, fig. 1) and paratype LZ 5783 (Pl. 12, fig. 2), where nodes are well developed and only growth-lines are present on the flanks. The spiral groove is still strong and has a subsidiary groove ventral to it. In the last part of the shell there are 13–14 nodes per half whorl before the flanks become smooth at about 11 mm. diameter.

Dimorph B. Dimorph B is characterized by ribs which persist to at least 11 mm. diameter but which are weak in comparison with those on the early part of the shell. The ribs are strongest near the umbilicus (Paratype LZ 5784; Pl. 12, fig. 5) but nodes are not developed. The ribs number about 17 per half whorl in the latter part of the shell. The spiral groove is still strong at 11 mm. diameter. These features are all seen on paratype LZ 5780 (Pl. 12, fig. 3).

The measurements of umbilical diameter made on the specimens of Dimorphs A and B vary considerably and it appears that Dimorph A has the smaller umbilicus, but the data are insufficient for this to be proved with certainty.

Discussion. This species falls within the original range of *Eumorphoceras bisulcatum* Girty (1909), but the redescription of part of Girty's original *E. bisulcatum* material by Elias (1956) as *Eumorphoceras girtyi* restricts the definition of *E. bisulcatum* to a *Eumorphoceras* with strong ribs present at 11 mm. diameter (9 mm. spiral groove diameter). The ribs in Girty's material are clearly sickle-shaped. According to McCaleb *et al.* (1964) the ribs on *E. bisulcatum* die out at an early intermediate stage of 25–30 mm. diameter. Thus *E. yatesae* is considered distinct from *E. bisulcatum* in its rib shape and in the diameter at which the ribs begin to die out. *E. yatesae* can be clearly distinguished from the described 'subspecies', 'mutation', and 'varieties' of *E. bisulcatum.*

EXPLANATION OF PLATE 12

Fig. 1. *Eumorphoceras yatesae* sp. nov. Dimorph A. Holotype LZ 5779, ×5: ribs reduce to nodes on umbilical margin at 8 mm. spiral groove diameter. Locality 354, Croker Hill, Cheshire.

Fig. 2. *Eumorphoceras yatesae* sp. nov. Dimorph A. Paratype LZ 5783, ×5: ribs reduce to nodes on umbilical margin at 8 mm. spiral groove diameter. Locality 354, Croker Hill, Cheshire.

Fig. 3. *Eumorphoceras yatesae* sp. nov. Dimorph B. Paratype LZ 5780, ×5: ribs persist weakly beyond 8 mm. spiral groove diameter. Locality 354, Croker Hill, Cheshire.

Fig. 4. *Eumorphoceras yatesae* sp. nov. Dimorph indeterminate. Paratype LZ 5781, ×5: small specimen showing numerous ribs. Locality 354, Croker Hill, Cheshire.

Fig. 5. *Eumorphoceras yatesae* sp. nov. Dimorph B. Paratype LZ 5784, ×5: ribs persist to about 11 mm. spiral groove diameter. Locality 354, Croker Hill, Cheshire.

Fig. 6. *Eumorphoceras* sp. LZ 5778, ×5: small undescribed form from *E. bisulcatum grassingtonense* horizon at Croker Hill, Cheshire. (Grid Ref. 93336675, north-west side of gully 630 yd. W. 7° S. from Dawsons.) This is possibly the 'A' dimorph of *E. bisulcatum grassingtonense*: note reduction of ribs to nodes on the umbilical margin at an early stage.

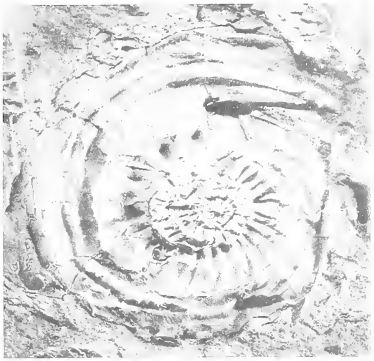

1

2

3

4

5

6

TREWIN, *Eumorphoceras yatesae*

Yates (1962) subspecies *E. bisulcatum erinense* and *E. bisulcatum ferrimontanum* differ from *E. yatesae* in having ribs that persist to larger diameters, and which are nearer to the sickle-shaped ribs of *E. bisulcatum* Girty.

E. bisulcatum grassingtonense Dunham and Stubblefield (1944) differs in having markedly fewer ribs, a tendency for rib bifurcation and for thickening of ribs in the mid-flank region.

E. bisulcatum leitrimense Yates (1962) is similar in being of small size, having ribs that die out early, and possessing constrictions. However it appears from Yates's figures to have only 12–13 ribs per half whorl.

The forms described by Schmidt (1934) as *E. bisulcatum* var. *varicata* and *E. bisulcatum mut.* β differ markedly from *E. yatesae* in having fewer ribs. Moreover *varicata* is described as having short ribs which do not reach the spiral groove and *mut.* β is characterized by pairing of the ribs.

E. stubblefieldi Moore (1946) has ribbing that dies at 8 mm. diameter, and also constrictions, but the spiral groove does not appear until 8 mm. diameter and the ribs are not so numerous or as strong as in *E. yatesae*.

The combination of small size, up to 20 strong ribs per half whorl at 7–8 mm. diameter and the presence of constrictions immediately distinguishes both these dimorphs from any described *Eumorphoceras*. It is considered best to regard these specimens as being dimorphs of the same species as they are both found in the same horizon, appear to be confined to that horizon, and have identical initial stages.

Fauna associated with E. yatesae. The only other goniatite specimens present with *E. yatesae* include rare fragments of an unidentifiable *Cravenoceras* and specimens of *Anthracoceras* or *Dimorphoceras* which cannot be distinguished without sutural evidence. *P. corrugata* (Etheridge jun.) is abundant and *Posidoniella variabilis* Hind appears in the north Staffordshire basin succession for the first time at this level.

Stratigraphic position of the E. yatesae *band.* The horizon containing *E. yatesae* occurs between the main E2a marine band which contains *E. bisulcatum ferrimontanum* Yates and *E. bisulcatum erinense* Yates and E2b1 marine band with *Cravenoceratoides edalensis* (Bisat) and *Cravenoceratoides bisati* Hudson. The *E. yatesae* band is separated from the main E2a band by a unit of protoquartzitic sandstones and shale-mudstones which is about 40 m. thick and from the E2b1 band by shales and shale-mudstones 7 m. thick. The marker horizon with *Leiopteria longirostris* Hind lies about 0·5 m. below *E. yatesae* and K-bentonite B4 (Trewin 1968, fig. 2) lies 3·5 m. above *E. yatesae* in the Pyecliough section (Loc. 101). At Loc. 355 *E. yatesae* occurs from 1–1·5 m. above *L. longirostris*. The *E. yatesi* horizon is of limited stratigraphic value as it appears to be discontinuous within the north Staffordshire basin area.

Zonal position of E. yatesae. The horizon with *E. yatesae* is considered to be highest E2a faunal band present in the north Staffordshire basin area since its goniatite fauna is dominated by *Eumorphoceras*, and *Cravenoceratoides* is absent. Thus there are three *Eumorphoceras*-bearing horizons in the E2a succession of the north Staffordshire basin area. The lowest contains *E. bisulcatum grassingtonense* Dunham and Stubblefield, the middle band contains *E. bisulcatum ferrimontanum* Yates and *E. bisulcatum erinense* Yates, and the highest band *E. yatesae* sp. nov.

CORRELATION WITH OTHER AREAS

No other described faunas can be correlated with certainty with the *E. yatesae* band, but several records of '*E. bisulcatum*' close below *Ct. edalensis* may represent this horizon. The *Eumorphoceras* specimen (Zh 1023) from 368 to 369 ft. in the Alport Derbyshire borehole (Hudson and Cotton 1943) is too poorly preserved to permit useful comparison with *E. yatesae*, but the occurrence of a *Cravenoceratoides* fragment (Zh 1022) only a foot above may indicate that this horizon is slightly younger than the *E. yatesae* band.

The author has examined the exposures in Edale, Derbyshire, but has not found any *Eumorphoceras* at this level although a faunal band with *Anthracoceras* sp. or *Dimorphoceras* sp., *Posidoniella variabilis*, and *Posidonia corrugata* is present which probably correlates with this horizon. The fauna is found in a bank of a small tributary stream about 12 yards from the junction with the main stream near Loc 112 of Hudson and Cotton (1945).

Hudson (1944) records *E. bisulcatum*, *Posidonia* and *Anthracoceras* 25 ft. below a band with *Ct. edalensis* and *C. subplicatum* in Coppice Beck, Harrogate, Yorkshire. A *Eumorphoceras* fragment (RM 412) from this locality shows only the spiral groove and comparison with *E. yatesae* is not possible, but this fauna must lie very close to the position of the *E. yatesae* band.

A *Eumorphoceras* specimen (RS 1543) described by Evans *et al.* (1968, p. 80) from the stream section in which the *E. yatesae* specimens described here were found appears to have been obtained from higher in the succession, above the *Ct. edalensis* band. The specimen is small and has 30–40 ribs per whorl, and the ribs die out at 7–8 mm. spiral groove diameter. (The figure of 30 ribs per whorl mentioned on p. 80 of Evans *et al.* (1968) is a misprint (W. H. C. Ramsbottom pers. comm.).)

Yates (1962) does not record a *Eumorphoceras*-bearing band equivalent to this band, thus it is probably absent on Slieve Anierin, Eire.

Localities. Specimens have been obtained from the following localities, all the type material is from Loc. 354.

Locality no.	Notes
101 Pyeclough Brook	250 yd. south of Bradshaw, Staffordshire. (Grid. Ref. 04656488) Stream bank exposure upstream of bridge.
201 Blake Brook	450 yd. north of Upper-Hay Corner, Staffordshire. (Grid. Ref. 05726088) Near base of section exposed at upstream end.
354 Croker Hill	450 yd. north of Dawsons, Cheshire. (Grid. Ref. 92806723) Shale scar under tree upstream of tributary ditch.

NOTE ON APPARENT DIMORPHISM IN ARNSBERGIAN GONIATITES

The described differences between the dimorphs A and B of *E. yatesae* are of exactly the same type as the differences between the subspecies *E. bisulcatum erinense* Yates and *E. bisulcatum ferrimontanum* Yates. Both *erinense* and *ferrimontanum* appear to have identical initial stages of development, but in *ferrimontanum* the ribs die out at *c.* 10 mm. spiral groove diameter to leave umbilical nodes, and in *erinense* the ribs persist to 15 mm. spiral groove diameter. These features are seen on Yates's (1962) illustrations of these subspecies. Comparing with *E. yatesae*, *ferrimontanum* is the 'A' dimorph and *erinense*

the 'B' dimorph. Both *erinense* and *ferrimontanum* occur in the same marine band and are confined to the base of the band in north Staffordshire. Yates (1962) states that *erinense* occurs slightly above *ferrimontanum* on Slieve Anierin within the same marine band, but this is not the case in north Staffordshire.

The lowest Arnsbergian marine band in the north Staffordshire basin area is the *Eumorphoceras bisulcatum grassingtonense* band. Well-preserved *Eumorphoceras* specimens are scarce in this band, but apart from individuals which are identical with the specimen figured by Yates (1962, pl. 52, fig. 3) in which the ribs die out at about 12 mm. spiral groove diameter, there are also some small undescribed forms in which the ribs reduce to small plications on the umbilical margin at 6 mm. spiral groove diameter, and by 9 mm. spiral groove diameter only small nodes are present on the umbilical margin (see Pl. 12, fig. 6). Of these two forms *grassingtonense* is the 'B' dimorph and the small undescribed form is the 'A' dimorph.

Thus in each of the three *Eumorphoceras*-bearing horizons of E2a in the north Staffordshire basin area there exists two forms of *Eumorphoceras*, and in all three horizons the differences between the two forms are of a very similar kind. While the present evidence is somewhat inconclusive there appear to be increasing grounds for believing that in the Carboniferous goniatite genera *Eumorphoceras* and *Gastrioceras* dimorphic species existed.

Acknowledgements. The author wishes to thank Dr. W. H. C. Ramsbottom for critically reading the manuscript and offering many useful suggestions, and also for the loan of specimens from the Institute of Geological Sciences collection.

REFERENCES

CALLOMON, J. H. 1963. Sexual dimorphism in Jurassic ammonites. *Trans. Leicester lit. phil. Soc.* **57**, 21–56.

DEMANET, F. 1943. Les horizons Marins du Westphalien de la Belgique et leurs Faunes. *Mem. Mus. Hist. nat. Belg.* **101**, 1–166, pl. 1–9.

DUNHAM, K. C. and STUBBLEFIELD, C. J. 1944. The stratigraphy, structure and mineralization of the Greenhow mining area, Yorkshire. *Quart. Jl geol. Soc. Lond.* **100**, 209–68, pl. 21, 22.

ELIAS, M. K. 1956. Upper Mississippian and Lower Pennsylvanian formations of south-central Oklahoma. *In* Petroleum Geology of Southern Oklahoma. Symposium: *Amer. Ass. Petrol. Geol.* 56–134, pl. 1–6.

EVANS, W. B., WILSON, A. A., TAYLOR, B. J., and PRICE, D. 1968. Geology of the Country around Macclesfield, Congleton, Crewe and Middlewich. 2nd ed. *Mem. Geol. Surv. Great Britain*, **110**, x+328 pp. pl. 1–8.

GIRTY, G. H. 1909. The fauna of the Caney Shale of Oklahoma. *Bull. U.S. geol. Surv.* **377**, 5–106, pl. 1–13.

HUDSON, R. G. S. 1944. The faunal succession in the *Ct. nitidus* zone in the mid-Pennines. *Proc. Leeds phil. lit. Soc.* **4**, 233–42.

—— and COTTON, G. 1943. The Namurian of Alport Dale, Derbyshire. *Proc. Yorks. Geol. Soc.* **25**, 142–73.

—— —— 1945. The Carboniferous rocks of the Edale anticline, Derbyshire. *Quart. Jl geol. Soc. Lond.* **101**, 1–36, pl. 1.

MAKOWSKI, H. 1962. Problem of sexual dimorphism in ammonites. *Palaeont. pol.* **12**, 1–92.

MCCALEB, J. A., QUINN, J. H., and FURNISH, W. M. 1964. Girtyoceratidae in the Southern Midcontinent. *Oklahoma Geol. Surv., Circ.* **67**, 1–41.

MOORE, E. W. J. 1946. The Carboniferous goniatite genera *Girtyoceras* and *Eumorphoceras*. *Proc. Yorks. geol. Soc.* **25**, 387–445, pl. 22–7.

PALFRAMAN, D. F. B. 1966. Variation and ontogeny of some Oxford Clay ammonites: *Taramelliceras richei* (de Loriol) and *Creniceras renggeri* (Oppel), from Woodham, Buckinghamshire. *Palaeontology*, **9**, 290–311, pl. 48–52.

—— 1967. Variation and ontogeny of some Oxford Clay ammonites: *Distichoceras bicostatum* (Stahl) and *Horioceras baugieri* (D'Orbigny), from England. Ibid. **10**, 60–94, pl. 9–13.

RAMSBOTTOM, W. H. C. and CALVER, M. A. 1962. Some marine horizons containing *Gastrioceras* in North West Europe. *Compte Rendu 4^e Congrès Strat. et Geol. Carbon. Heerlen 1958*. **3**, 571–6, pl. 14–15.

SCHMIDT, H. 1934. Cephalopodenfaunen des alteren Namur aus der Umgegend von Arnsberg in Westfalen. *Jb. preuss. geol. Landesanst*. **54**, 440–61.

TREWIN, N. H. 1968. Potassium bentonites in the Namurian of Staffordshire and Derbyshire. *Proc. Yorks. geol. Soc*. **37**, 73–91.

YATES, P. J. 1962. The palaeontology of the Namurian rocks of Slieve Anierin, Co. Leitrim, Eire. *Palaeontology*, **5**, 355–443, pl. 51–62.

N. H. TREWIN
Department of Geology and Mineralogy
Marischal College
Aberdeen, AB9 1AS

Final typescript received 13 June 1969

A NEW *ORIONASTRAEA* (RUGOSA) FROM THE LOWER CARBONIFEROUS OF NORTHERN ENGLAND

by M. KATO *and* M. MITCHELL

ABSTRACT. *Orionastraea magna* sp. nov. is described from the *Orionastraea* Band, Upper *Dibunophyllum* (D_2) Zone, near Settle, Yorkshire, and the genus is briefly discussed.

Orionastraea was erected by Smith (1916, p. 3) for Carboniferous corals previously assigned to the Devonian genus *Phillipsastraea* d'Orbigny. The genus has since been broadly interpreted to include many divergent stocks. Some of the Upper Carboniferous and Lower Permian forms are closely related to the *Protowentzelella* Porfiriev–*Stylastraea* Lonsdale group, whereas the true *Orionastraea* is believed to be phylogenetically connected with the massive forms of *Lithostrotion* Fleming.

SYSTEMATIC DESCRIPTION

Class ANTHOZOA Ehrenberg 1834
Order RUGOSA Milne Edwards and Haime 1850
Family LITHOSTROTIONIDAE d'Orbigny 1851
Genus ORIONASTRAEA Smith 1916

1916 *Orionastraea* Smith, p. 3.
1917 *Orionastraea*; Smith, p. 294.
1926 *Orionastraea*; Hudson, p. 145.
1929 *Orionastraea*; Hudson, p. 441.
1934 *Orionastraea*; Hill, p. 90.
non 1936 *Orionastraea*; Dobrolyubova, p. 17.
1940 *Orionastraea*; Hill, p. 187.
non 1941 *Orionastraea*; Soshkina, Dobrolyubova and Porfiriev, p. 151.
1950 *Orionastraea*; Wang, p. 222 (pars).
1952 *Orionastraea*; Lecompte, p. 473.
1956 *Orionastraea*; Hill, p. F283.
1958 *Orionastraea*; Dobrolyubova, p. 199.
1964 *Orionastraea*; Yoh and Wu, p. 102.
1967 *Orionastraea*; Ivanovsky, p. 33.

Type species (selected by Smith 1917, p. 295). *Sarciuula phillipsii* McCoy 1849, p. 125, from the Carboniferous Limestone (D_2), of Corwen, Merionethshire, Wales.

Diagnosis. Astreoid, thamnasterioid or aphroid Lithostrotionidae; columella weakly developed or absent; septa withdrawn from axis and in some from periphery also, when dissepiments become lonsdaleoid.

Distribution. The genus is known from the upper part of the Viséan of Australia, China, Russian Platform, and Britain. Some of the Asiatic and Australian forms may be slightly

[Palaeontology, Vol. 13, Part 1, 1970, pp. 47–51, pl. 13.]

older than those from Europe, possibly due to difference of origin of species within the genus. Bassler (1950, p. 247) lists '*Orionastraea phillipsi?*' from the Permian of Chitral region, W. Pakistan, and Dobrolyubova (1958, p. 201) also gives the genus as ranging into the Permian. These Permian records are considered to be erroneous and should be referred either to *Lonsdaleiastraea* Gerth or *Wentzelellites* Wu of the Waagenophyllidae (Minato and Kato 1965). The record of the genus in Japan (Hayasaka 1932, p. 273) is doubtful and the form may belong to *Pseudopavona* Yabe, Sugiyama, and Eguchi 1943.

Remarks. The following nominal species are referable to *Orionastraea*, although not all are regarded as valid: *Erismolithus tubiporites? (radiatus)* Martin 1809; *Sarcinula tuberosa, placenta* and *phillipsii* McCoy 1849; *Lithostrotion ensifer* Milne Edwards and Haime 1851; *Phillipsastraea clissiophylloides* [*sic*], *clissiophylloides stellata* and *fasciculata* Thomson 1898; *Lithostrotion? columnare* R. Etheridge jun. 1900; *Orionastraea indivisa* Hudson 1926; *O. ensifer matura, edmondsi, edmondsi laciniosa, prerete, rete, garwoodi, garwoodi sera* and *garwoodi pristina* Hudson 1929; *O. lonsdaleoides* Hill 1934; *O. kurakovensis, rareseptata* and *heteroseptata* Dobrolyubova 1958; *O. huaitoutalaensis, minor* and *gigantea* Lo 1962; *Arachnastraea minor* Wu 1964; and *Lithostrotion parvicolumnare* and *O. columellaris* Pickett 1966.

Orionastraea is considered to be restricted to the Lower Carboniferous and to be phylogenetically connected with the massive forms of *Lithostrotion*. The Upper Carboniferous and Permian species from the boreal province which have been referred to *Orionastraea* have rudimentary walls, ill-defined minor septa, lack columella and have thin skeletal elements, and are related to the *Protowentzelella–Stylastraea* lineage. The suggested genera for the following species are given in brackets:

Columnaria solida Stuckenberg 1895, *non* Ludwig 1862 ('*Uralastraea*' Fomitchev); *C. zitteli* Stuckenberg 1895 ('*Uralastraea*'); *C. toulai* Stuckenberg 1895 (*Stylastraea*); *Protolonsdaleiastraea atbassarica* Gorsky 1832 (*Protolonsdaleiastraea* Gorsky); *Orionastraea asiatica* Lee and Yu 1934 (*Arachnastraea* Yabe and Hayasaka); *O. campophylloides, Columnaria stuckenbergi* Gerasimov (MS), *O. breviseptata, O. breviseptata major* Dobrolyubova 1936; and *O. hudsoni* Wilson and Langenheim 1962 (all '*Uralastraea*').

'*Uralastraea*' was proposed by Fomitchev (1953) for *Orionastraea* of Upper Carboniferous and Lower Permian age but no type species was designated and the genus is a *nomen nudum* (Hill 1957, p. 51).

EXPLANATION OF PLATE 13

Figs. 1–5. *Orionastraea magna* sp. nov. ×1·5. *Orionastraea* Band, Upper *Dibunophyllum* (D_2) Zone, low escarpment, $\frac{1}{3}$ mile NE. of Brunton House, $\frac{1}{2}$ mile S. of Feizor, which is 3 miles NW. of Settle, Yorkshire. 1, L.S. slide PF 3387 of paratype GSM 65803. 2–5, Sections of holotype, GSM 65802; 2, L.S. slide PL 309; 3–5, T.S. slides PL 310, 312–13.

Figs. 6, 7. *Orionastraea ensifer* (Milne Edwards and Haime). 6, ×3; 7, ×2. Limestone band of Round Point, Upper Cromhall Sandstone, Upper *Dibunophyllum* (D_2) Zone, Clifton side of Avon Gorge, Bristol, Gloucestershire. Sections of topotype; 6, T.S. UHR 18931*a*; 7, L.S. UHR 18931*b*.

Figs. 8, 9. *Orionastraea phillipsii* (McCoy). ×2. Upper *Dibunophyllum* (D_2) Zone, Hafod-y-Calch, Corwen, Merionethshire. Sections of topotype; 8, T.S. UHR 18932; 9, L.S. UHR 18934.

Figs. 6–9 are for comparison. Note the presence of 'annular growth' in figs. 1, 2, 7, and 9.

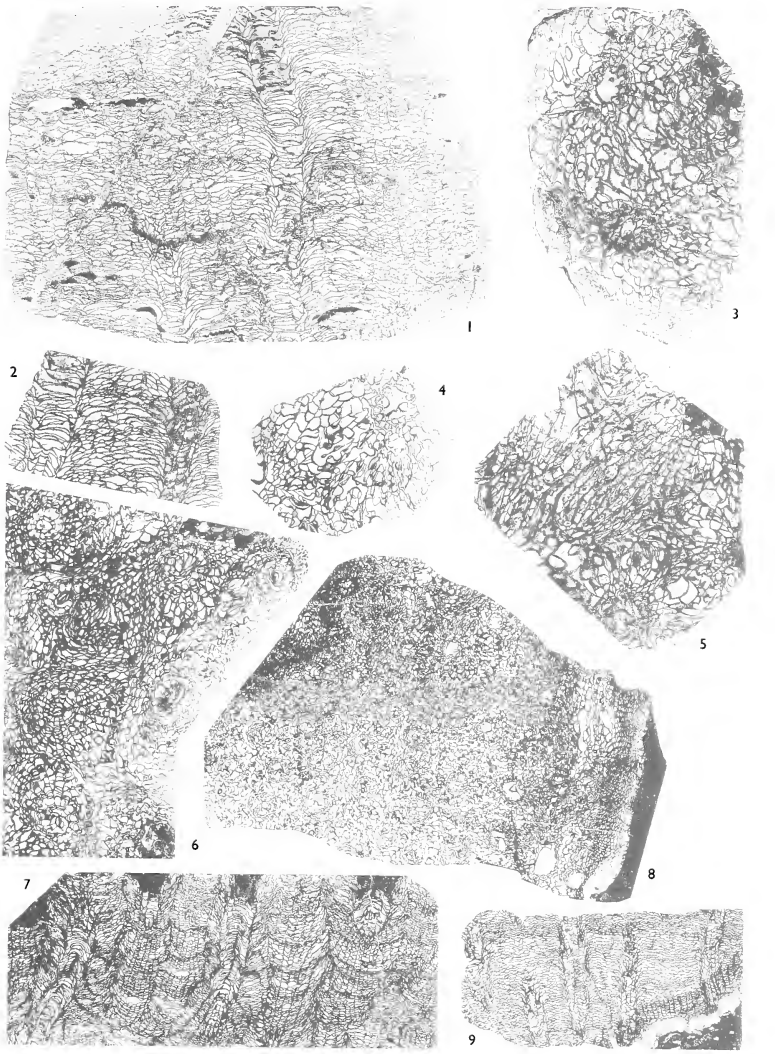

KATO and MITCHELL, *Orionastraea*

Orionastraea magna sp. nov.

Plate 13, figs. 1–5

1924 *Orionastraea phillipsi*, exceptionally large variety; Garwood and Goodyear, pp. 219, 227, 232 (in text only).

cf. 1958 *Orionastraea phillipsi* (McCoy); Dobrolyubova, p. 201, pl. 34, fig. 2; pl. 35.

Name. Refers to large size of tabularia.

Holotype. GSM 65802, from the *Orionastraea* Band, Upper *Dibunophyllum* (D_2) Zone, low escarpment, $\frac{1}{4}$ mile NE. of Brunton House, $\frac{1}{8}$ mile S. of Feizor, which is 3 miles NW. of Settle, Yorkshire.

Paratypes. GSM 65800–1, 65803, horizon and locality as for holotype; GSM 66699, 66700, 66703–6, from *Orionastraea* Band, Low South Bank, south side of Stockdale Beck, opposite Stockdale Farm, 2 miles E. of Settle; SME 13857, from *Orionastraea* Band, right bank of Cow Gill, $\frac{1}{4}$ mile N. of New Houses, $\frac{2}{3}$ mile SW. of Bordley, which is $7\frac{1}{2}$ miles E. of Settle. All the GSM material is in the Garwood Collection.

Diagnosis. Corallum platy, mainly thamnasterioid, with tabularia exceptionally large, 4–5 mm. in diameter. Skeletal elements notably thin. Major septa 15. Columella absent.

Description. External characters. Corallum is compound, large, flat, expanded and platy. The size of the corallum is not known, only broken specimens being preserved. The largest fragments have an area of 129×91 mm. (GSM 66699) and a thickness of at least 44 mm. (GSM 65800–1).

Numerous fine concentric striations or wrinkles are present on the epitheca of the corallum's lower surface. These wrinkles indicate rapid lateral expansion of the coral. The upper surface is comparatively smooth.

Internal characters. (*a*) In transverse section. The corallum is mainly thamnasterioid, and sometimes aphroid. All internal skeletal elements are very thin.

The tabularia are round or oval and weakly differentiated from the dissepimentaria by somewhat crowded concentric vertically inclined inner margins of dissepiments. The diameter of tabularia is 4–5 mm., a little less in SME 13857, and their centres are 15–20 mm. apart.

Septa are very thin, but may be finely trabecular. There are 14 or 15, rarely 17, slightly flexuous major septa. They fall short of the centre of the tabularia which are open due to the lack of axial structure. Septa are confluent with corresponding ones of neighbouring corallites. The columella is absent in specimens from Feizor. A few major septa extend to the centre of tabularia in SME 13857 and also in specimens from Low South Bank but without thickening into a columella. Minor septa are of variable length, rarely extending to the tabularia and may sometimes not be developed.

The dissepimentaria which form the greater part of the corallum consist of confluent septa and some large irregular dissepiments that prevent the thamnasterioid elongation of septa. The aphroid tendency is marked in SME 13857.

(*b*) In longitudinal section. The tabularia are clearly differentiated from the dissepimentaria. The tabulae, 25 in 10 mm., are flat or slightly dome shaped and are incomplete. No columella is present. The dissepimentaria are composed of numerous fine, horizontally elongate dissepiments and are often penetrated by the cut ends of the septa. Weak 'periodicity' may be discernible with slight crowding of dissepiments occurring three times in 10 mm. (Pl. 13, fig. 2).

Remarks. The present form was listed by Garwood and Goodyear (1924, pp. 219, 227, 232) as *O. phillipsi*, exceptionally large variety, and the label on GSM 65801 reads '*Orionastraea phillipsi* (McCoy), this specimen has been identified by Mr. S. Smith'. However, McCoy's species has a tabularium diameter of about 2·5 mm. and the large size of the tabularia of *O. magna* makes it easily recognizable. It is probable that *O. phillipsii* is not present at Settle (Hudson 1929, p. 452).

Hudson (1929, pp. 451–2) lists *O. indivisa*, *prerete* and *rete* from the *Orionastraea* Band of the Settle district but the large size and thamnasterioid corallites distinguish *O. magna* from these species.

In general appearance, the form resembles *Orionastraea phillipsi* of late D_2 age described and figured by Dobrolyubova (1958, p. 201; pl. 34, fig. 2; pl. 35) from the Russian Platform. The Russian form, however, has slightly smaller tabularia in comparison with *O. magna*, a less pronounced aphroid tendency, and also a weakly developed columella. Dobrolyubova's *phillipsi* may stand between *phillipsii* McCoy and *garwoodi* Hudson, although it has much larger tabularia.

Distribution. *O. magna* is known only from the *Orionastraea* Band (D_2 Zone) of the Settle district. The conflicting views on the correlation of the *Orionastraea* Band with the Hardraw or Simonstone Limestones of Wensleydale are discussed by Garwood and Goodyear (1924, pp. 205–6). Hicks (1959, pp. 33–7) re-examined the evidence in the Ingleborough area and confirmed the view of the Geological Survey (Dakyns and others 1890, pp. 25–8) that this horizon at Settle is the equivalent of the Hardraw Limestone.

Acknowledgements. The authors acknowledge the assistance of the following: the late Dr. H. Dighton Thomas, British Museum (Natural History), Dr. F. W. Anderson, Institute of Geological Sciences (GSM), Professor M. Minato, Hokkaido University (UHR), and Dr. C. L. Forbes, Sedgwick Museum, Cambridge (SME). Initials in brackets are prefixes of specimens in the respective museums. Mr. Mitchell publishes with the permission of the Director of the Institute of Geological Sciences.

REFERENCES

BASSLER, R. S. 1950. Faunal lists and description of Palaeozoic corals. *Mem. geol. Soc. Am.* **44,** 1–315, pl. 1–20.

DAKYNS, J. K., TIDDEMAN, R. H., GUNN, W., and STRAHAN, A. 1890. The geology of the country around Ingleborough, with parts of Wensleydale and Wharfedale. *Mem. geol. Surv. U.K.*

DOBROLYUBOVA, T. A. 1936. The corals of the Upper Carboniferous of the western slope of the Middle Urals and their stratigraphic importance. *Trudȳ vses. nauchno-issled. Inst. miner. Sȳr'ya.* **103,** 1–68, pl. 1–37 (in Russian).

—— 1958. Lower Carboniferous colonial tetracorals of the Russian Platform. *Trudȳ paleont. Inst.* **70,** 1–224, pl. 1–38 (in Russian).

FOMITCHEV, V. D. 1953. Rugose corals and stratigraphy of Middle–Upper Carboniferous and Permian deposits of the Donetz Basin. *Trudȳ vses. nauchno-issled. geol. Inst.* (VSEGEI), 1–622, pl. 1–44 (in Russian).

GARWOOD, E. J. and GOODYEAR, E. 1924. The Lower Carboniferous succession in the Settle district. *Q. Jl geol. Soc. Lond.* **80,** 184–273, pl. 10–21.

HAYASAKA, I. 1932. An astraeiform coral from Central Japan. *Geol. Mag.* **69,** 273–5.

HICKS, P. F. 1959. The Yoredale rocks of Ingleborough, Yorkshire. *Proc. Yorks. geol. Soc.* **32,** 31–43.

HILL, D. 1934. The Lower Carboniferous corals of Australia. *Proc. R. Soc. Qd.* **45** (12), 63–115, pl. 7–11.

—— 1940. A monograph on the Carboniferous Rugose Corals of Scotland. *Palaeontogr. Soc.* [*Monogr.*] (3), 115–204, pl. 6–11.

HILL, D. 1956. Rugosa: In *Treatise on invertebrate paleontology* (ed. R. C. MOORE). Part F, *Coelenterata*, 233–324, Univ. Kansas Press and Geol. Soc. Am.

—— 1957. The sequence and distribution of Upper Palaeozoic coral faunas. *Aust. J. Sci.* **19** (3*a*), 42–60.

HUDSON, R. G. S. 1926. On the Lower Carboniferous corals; *Orionastraea indivisa*, sp. n., and *Thysanophyllum praedictum*, sp. n. *Ann. Mag. nat. Hist.* (Ser. 9), **18**, 144–51, pl. 8.

—— 1929. On the Lower Carboniferous corals—*Orionastraea* and its distribution in the north of England. *Proc. Leeds phil. Lit. Soc.* (Sci. Sect.), **1** (9), 440–57, pl. 1–4.

IVANOVSKY, A. B. 1967. *Étude de Lower Carboniferous Rugosa*. 92 pp., 22 pl. Moscow. Nauka (Akad. Nauk SSSR, Sib. Otd. Inst. Geol. Geofiz.) (in Russian).

LECOMPTE, M. 1952. I. Madréporaires Palézoiques: In *Traité de Paléontologie* (ed. J. Piveteau), Part 1, 419–538. Paris.

MCCOY, F. 1849. On some new genera and species of Palaeozoic corals and foraminifera. *Ann. Mag. nat. Hist.* (Ser. 2), **3**, 1–20, 119–36.

MINATO, M. and KATO, M. 1965. Waagenophyllidae. *J. Fac. Sci. Hokkaido Univ.* (Ser. 4), **12** (3–4), i–xiii, 1–241, pl. 1–20.

SMITH, S. 1916. *Aulina rotiformis*, gen. et sp. nov., *Phillipsastraea hennahi* (Lonsdale), and the genus *Orionastraea*. *Abstr. Proc. geol. Soc. Lond.* No. 995, 2–5.

—— 1917. *Aulina rotiformis*, gen. et sp. nov., *Phillipsastraea hennahi* (Lonsdale), and *Orionastraea*, gen. nov. *Q. Jl geol. Soc. Lond.* **72**, 280–307, pl. 12–14.

SOSHKINA, E. D., DOBROLYUBOVA, T. A., and PORFIRIEV, G. 1941. The Permian rugose corals of the European part of the USSR. *Paleontologiya SSSR*. **5** (3) (1), 1–304, pl. 1–63.

WANG, H. C. 1950. A revision of the zoantharia rugosa in the light of their minute skeletal structures. *Phil. Trans. R. Soc.* (Ser. B), (611) **234**, 175–246, pl. 4–9.

YABE, H., SUGIYAMA, T., and EGUCHI, M. 1943. A new hexacoral-like Carboniferous coral (preliminary note). *J. geol. Soc. Japan*, **50** (600), 242–5.

YOH, S. S. and WU, W. S. 1964. *Fossil corals* (*Tetracorals*). Science Press, Peking, 234 pp., 5 pl. (in Chinese).

M. KATO
Department of Geology and Mineralogy
Hokkaido University
Japan

M. MITCHELL
Institute of Geological Sciences
Ring Road Halton
Leeds, LS15 8TQ

Typescript received 17 March 1969

VARIATION IN THE VISÉAN CORAL *CANINIA BENBURBENSIS* FROM NORTH-WEST IRELAND

by O. A. DIXON

ABSTRACT. *Caninia benburbensis* Lewis occurs in abundance in upper Viséan marine limestones and shales in north-western Ireland. Study of a single assemblage reveals a range of variation which expands Lewis's concept of the species. The morphological affinity of certain variants to *C. cylindrica* (Scouler) strongly suggests that this Tournaisian or lower Viséan species is ancestral to *C. benburbensis*. The morphological mode clearly distinguishes this species from all earlier caniniid populations.

CERTAIN Lower Carboniferous formations in north-western Ireland contain large, caniniid corals in a profusion that has inspired repeated comment by geologists for more than a century. The coral-rich strata are magnificently exposed at several localities along the coast of County Sligo and have been recognized at inland exposures in several areas of Counties Sligo, Leitrim, and Roscommon. Hubbard (1966, p. 253) summarized the important coastal exposures and, supported by Hubbard and Sheridan (1965, pp. 193–4), strongly substantiated the idea that many of the important caniniid-rich beds in the region are synchronous and of late Viséan age.

However, large caniniid corals occur throughout the Lower Carboniferous in north-western Ireland (generally more than 1150 m. thick) and elsewhere in the British Isles. Attempts in the past to utilize the caniniids for stratigraphical purposes have been inconclusive, probably due in part to misinterpretations of local stratigraphy and in part to intraspecific variation, which impedes the precise identification of isolated specimens. In an attempt to define the limits of variation within a single assemblage, a collection from one of the best-known localities, Streedagh Point in Co. Sligo, was studied.

A narrow strip of gently dipping limestones and shales is exposed along the sea coast at Streedagh Point (text-fig. 1). The strata are cut by several, small, vertical faults with displacements up to 6·5 m. The faults are made obvious by offset of beds containing rich accumulations of species of the compound coral *Lithostrotion*—useful marker beds for stratigraphical control within the area. The caniniid assemblage was collected systematically through the sequence represented by the generalized stratigraphical column in text-fig. 2. All but six specimens came from richly fossiliferous beds between 18 and 22·6 m. More extensive collecting was limited, as many of the corals are intractably set in thick and resistant limestone beds.

The fossils generally are well preserved, although it is common to find the epitheca and a thin layer of the adjacent rock silicified, while the remainder of the fossil is calcitic. In addition, some specimens in outcrop are missing parts of the epitheca and dissepimentarium. Where some of the matrix still adheres to the fossil, it is possible to demonstrate in many instances that these parts of the skeleton were removed by abrasion before final burial in the sediment.

The collected specimens clearly are not contemporaneous but represent several successive palaeobiological populations. Initial attempts to attribute observed morpho-

[Palaeontology, Vol. 13, Part 1, 1970, pp. 52–63.]

logical variations to changes of facies or to phylogenetic change were unsuccessful, and consequently the specimens were grouped and studied as a single population. The areal distribution of the assemblage is sufficiently limited that each included population may

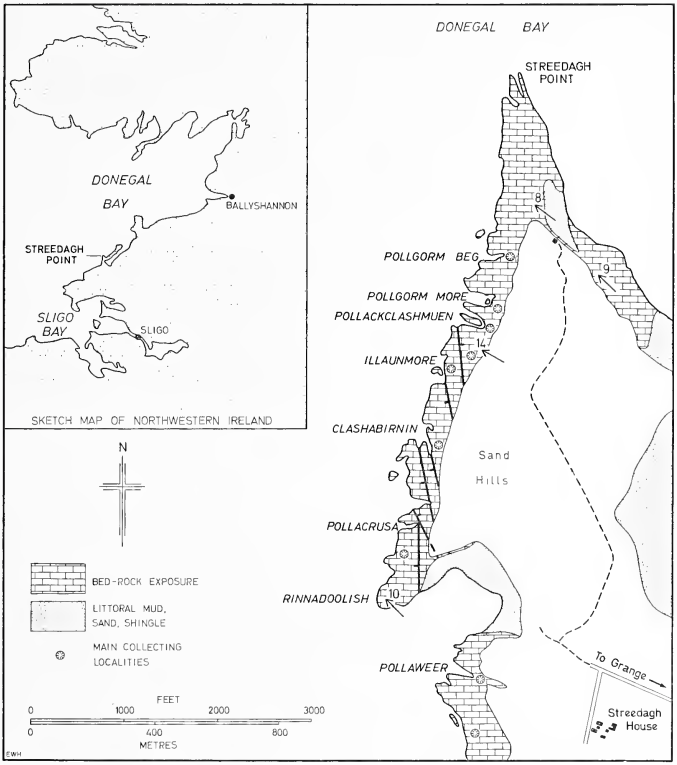

TEXT-FIG. 1. Streedagh Point, north-western Ireland. Hachured open circles mark the principal collecting localities. Base map courtesy of the Ordnance Survey, Phoenix Park, Dublin.

be assumed to have experienced free panmixis. The profusion of caniniids in limestones and shales throughout this limited succession suggests, too, that the area was continually populated, and favours the treatment of the assemblage as a unit having a very restricted time range within the entire caniniid lineage.

Foraminiferan evidence places the rocks at Streedagh Point in the lower D_1 subzone

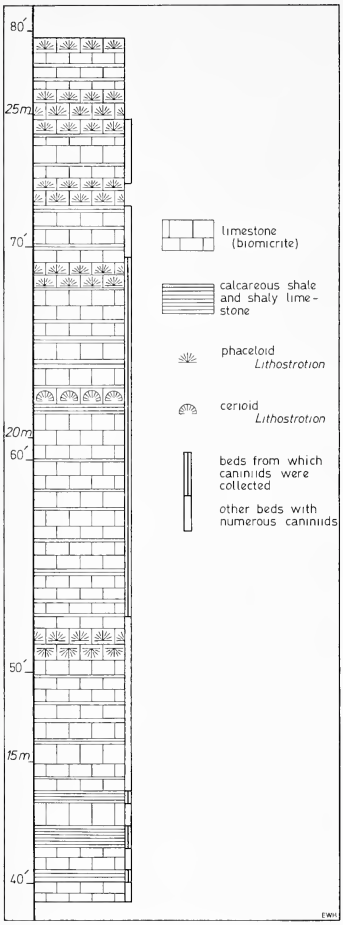

TEXT-FIG. 2. Diagrammatic section representing the top 13 m. of strata exposed on Streedagh Point. The column incorporates (and extends about 3 m. below) the 'coral limestone horizon' of Hubbard (1966, fig. 11).

of late Viséan age (Oldroyd 1965, p. 195), and specimens of *Dibunophyllum* found with the caniniids support this. The suggested correlation is with the Benbulben Shale–Glencar Limestone transition (Hubbard 1966, pp. 267–8; Oswald 1955, pp. 175–6).

SYSTEMATIC DESCRIPTION

Superfamily ZAPHRENTICAE Milne-Edwards and Haime 1850
Family CYATHOPSIDAE Dybowski 1873
Genus CANINIA Michelin 1840

Caninia benburbensis Lewis

Text-figs. 3–11

1925 *Caninia* cf. *samsonensis* Salée; Lewis, in L. B. Smyth, pp. 145–6.

1927 *Caninia benburbensis* Lewis, pp. 378–80, pl. 16, figs. 5–6; pl. 17, figs. 1–4.

1930 *Caninia benburbensis* Lewis; Lewis, p. 267, pl. 20, figs. 2*a–c*.

1939 *Caninia benburbensis* Lewis; Hill, p. 112.

Material. Adult portions of 149 coralla, the majority lacking juvenile apical portions.

Diagnosis. Large solitary rugosans. Diameter of tabularium 28–46 mm. Major septa commonly number 56–78, extend well into tabularium, mostly continuous extrathecally, may be sinuous and split along axial planes to various extents; transition to a few forms with septal crests on dissepiments. Minor septa commonly semi-continuous extrathecally (continuous near theca), few project intrathecally; transition to a few forms lacking minor septa and a few with many minor septa projecting intrathecally. Dissepiments mainly concentric or herringboned; transition to a few forms with predominantly lonsdaleoid dissepiments. Large, well-defined cardinal fossula.

Description. The specimens are large, solitary rugosans, mainly 50–70 mm. in diameter (maximum more than 80 mm.), and as much as 0·9 m. long. The corallum may be straight,

uniformly curved, sharply geniculated (one or more times), or developed in a loose spiral. In the initial conical stage, the corallum expands at angles between 13 and 25°. The adult corallum may continue to increase in diameter very gradually, may maintain a fairly uniform diameter (except for rugae), or may be marked by constrictions of varying magnitude.

The coral polyps rested in a deep, beaker-shaped calice, the vertical inner wall of which is formed by the theca, or boundary between the dissepimentarium and tabularium (cf. text-fig. 3*b*). The diameter of the fully developed tabularium may range from 28 to 46 mm. However, in an adult corallum, this diameter remains fairly constant (variations of 1 or 2 mm.) despite marked constrictions of the dissepimentarium. The constrictions were produced when the polyp contracted inward from the inclined lip of the calice, interrupting the formation of dissepimental tissue, but not of intrathecal skeletal elements.

The number of major septa is commonly 56 to 78, but up to 82 may be present. The number of septa remains nearly constant in the adult stage of a corallum. The septa form continuous, blade-like, vertical partitions intrathecally, but vary in their continuity extrathecally. Where the septa are continuous extrathecally, the dissepiments are of simple or herringbone type; where the septa are discontinuous, the dissepiments are larger and lonsdaleoid. Minor septa may be semi-continuous extrathecally, or poorly developed (represented only by isolated septal crests on the dissepiments), or absent. Only in a few individuals do the minor septa project intrathecally.

During ontogeny, the polyp secreted and rested on a succession of medially flattened (or very slightly depressed) tabulae, which are sharply curved down at the margins. A rhythmic arrangement of closely spaced incomplete tabulae and more widely spaced complete tabulae is discernible in many specimens. The tabulae are deeply depressed in the cardinal fossula, into which projects a short cardinal septum.

The skeletal elements within the tabularium (most commonly the septa in the cardinal quadrants) show varied stereoplasmic thickening. In some individuals, this affects the septa and tabulae in all quadrants, but the development is not consistent during ontogeny. Juvenile portions tend to show more thickening than adults (compare Salée 1910, pl. 3, fig. 1*b–f*), and in adults, the skeletal structures are usually thinner in areas of constrictions and geniculations.

Variation. It becomes evident from detailed examination of the coral morphology that certain biocharacters were markedly affected by environmental conditions. The curves and geniculations which the coralla show have been attributed to instability of the bottom sediments in which the corals rested (Hubbard, *in litt.*). Periodic constrictions of the epitheca in some instances are associated with geniculations and may have a related cause. The groups of widely spaced tabulae correspond in age to constrictions of the dissepimental zone, and Ma (1937, p. 9) related such changes in growth form to seasonal temperature variations. Clearly, the dependence on environment of features such as total diameter, geniculations, spacing of tabulae, and intrathecal stereoplasmic thickening, renders them of little use in classification. Other biocharacters apparently remained unchanged during what evidently were crises in the ontogeny of individuals. The most significant of these are the intrathecal diameter, the number of septa, and certain septal characteristics, such as extrathecal continuity. Closely related to continuity of the septa

was the nature of the dissepiments, and these apparently were fairly consistent in form throughout ontogeny.

The Streedagh assemblage comprises a wide group of variants, some recognized before (Lewis 1927, p. 380) and others (not distinguished by Lewis) which significantly expand his concept of the species. The main variations are summarized below. About 10 % of the studied assemblage were not classified because of poor or incomplete preservation. All figured specimens bear catalogue numbers of the Hunterian Museum, University of Glasgow.

Form A (Specimen C. 7471a–e). Individuals included in this group are few in number (less than 5% of the Streedagh assemblage). They characteristically possess a predominantly lonsdaleoid dissepimentarium and consequently markedly discontinuous septa extrathecally (text-fig. 3*a* and *b*). However, the minor septa are commonly as poorly developed as in more typical examples of *C. benburbensis*. The average intrathecal diameter and number of septa are both less than for the remainder of the assemblage (text-figs. 12 and 13) but the number of specimens measured may not be representative.

Form B (Specimens C. 7474a–f and C. 7475a–c). About 10 % of the assemblage are closely similar to the holotype of *C. benburbensis* (Lewis 1927, p. 380, pl. 17, figs. 1*a–b*) and show clearly all the diagnostic features (text-fig. 7). The major septa are mostly continuous extrathecally. Minor septa are well developed near the theca but are reduced to septal crests on the outer dissepiments, and usually few of these septa project intrathecally. The dissepiments are of concentric or herringbone type, and show an irregular spacing, generally quite closely crowded near the theca.

In a few individuals otherwise identical, many of the minor septa project 1–2 mm. into the tabularium. Another morphological variation is shown by several consistently smaller individuals (text-fig. 6*a* and *b*) with finer skeletal elements (although they have the same range in numbers of septa as larger forms).

Form C (Specimen C. 7477a–e). About 10 % of the assemblage lack minor septa, but are otherwise similar to Form B in having more or less continuous major septa and concentric or herringboned dissepiments (text-fig. 9*a* and *b*).

Form D (Specimens C. 7478a–l and C. 7479a–e). About 10 % of the assemblage can be referred to this distinctive form. Specimens are generally of large size, and usually the major septa are split along their axial planes and contorted in the dissepimentarium (text-fig. 10). The dissepiments commonly have lost their concentric or herringbone aspect and appear as sinuous or angulated plates between the septa. In a few otherwise similar forms (text-fig. 11*a* and *b*), the major septa are split less commonly. The skeletal distortions are not a result of geronticism as they are evident in more juvenile stages of the few complete coralla studied.

Measurements of number of septa and adult intrathecal diameter fall within the range of variation of the assemblage, but both measurements average consistently greater than the assemblage average (text-figs. 12 and 13).

Transitional forms (Specimens C. 7472a–c, C. 7473 and C. 7476a–e). The complete artificiality of separating the assemblage into distinct morphological types is obvious from examination of the remaining specimens. Approximately 25 % of the total may be described as morphologically transitional between Forms A and B, i.e. showing a skeletal development intermediate between those with lonsdaleoid dissepiments and

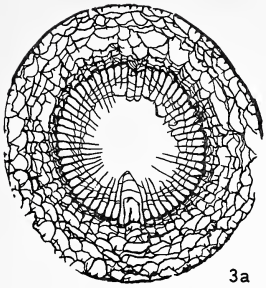

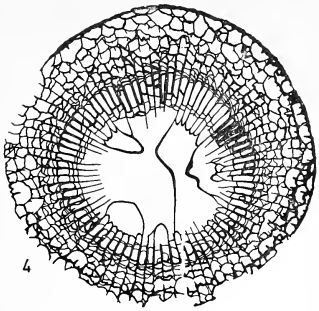

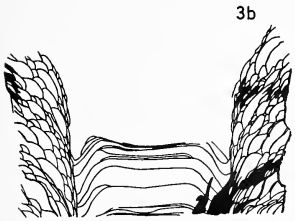

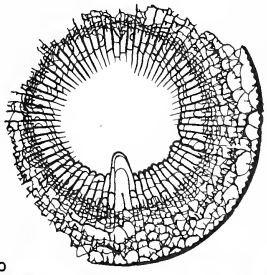

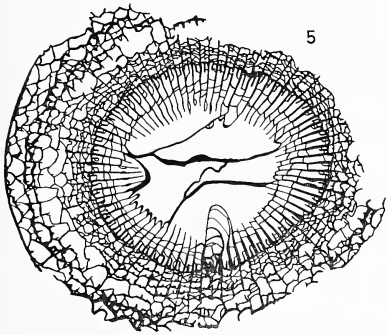

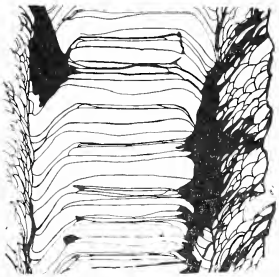

TEXT-FIGS. 3–6. *Caninia benburbensis*. Figured specimens bear catalogue numbers of the Hunterian Museum, University of Glasgow. All are at natural size. *3a, b*. Form A. C. 7471b, C. 7471d. Transverse and longitudinal sections. Epitheca complete but partly obscured by silicification. 4, 5. Intermediate forms A–B. C. 7472b, C. 7473. Transverse sections. *6a, b*. Form B. C. 7474b, C. 7474d. Transverse and longitudinal sections. Specimens represented by text-figs. 4–6 all show the effects of penecontemporaneous abrasion.

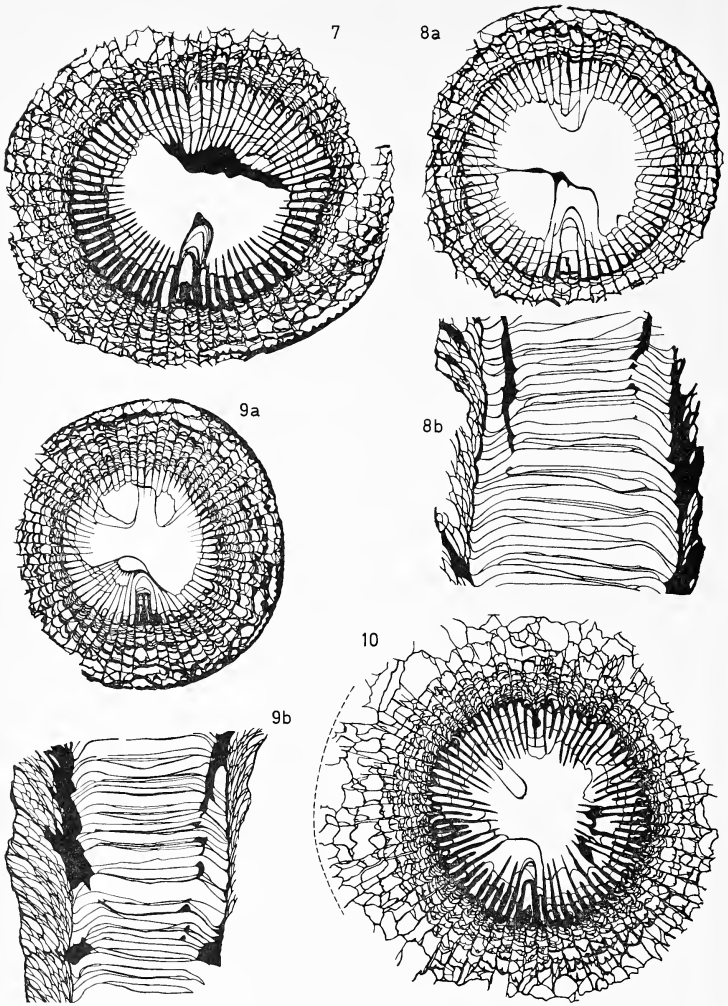

TEXT-FIGS. 7–10. *Caninia benburbensis*. 7. Form B. C. 7475b. Transverse section. Epitheca mostly obscured by silicification. 8*a*, *b*. Intermediate form B–C. C. 7476b, C. 7476d. Transverse and longitudinal sections. 9*a*, *b*. Form C. C. 7477d, C. 7477b. Transverse and longitudinal sections. Specimens represented by text-figs. 8 and 9 both show the effects of penecontemporaneous abrasion. 10. Form D. C. 7478i. Transverse section. Dissepimentarium partly abraded. Silicified epitheca approximately at dashed line.

septal crests, and those with concentric dissepiments and fairly continuous major septa. In this group, the minor septa show varied development—virtually absent in some (text-fig. 4) and well developed in others (text-fig. 5).

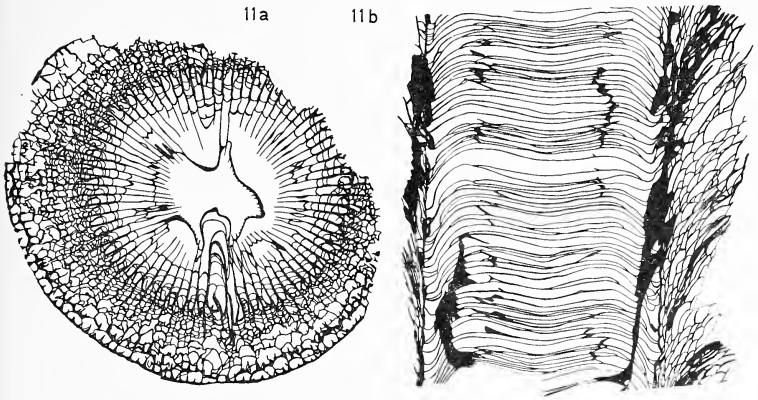

TEXT-FIG. 11*a*, *b*. *Caninia benburbensis*. Form D. C. 7479d. C. 7479b. Transverse and longitudinal sections. Deep penecontemporaneous abrasion on counter-cardinal surface.

Approximately 30% of the assemblage are individuals morphologically intermediate between Forms B and C (text-fig. 8*a* and *b*). A series of individuals may be recognized in which the minor septa gradually diminish and ultimately disappear (as in Form C). Among these are specimens showing progressively finer skeletal elements, and generally smaller size (as some of Form B).

Similarly, Form D cannot be separated distinctly from the remainder of the assemblage. Characters such as bifurcating major septa and irregular dissepiments can be seen (although much less prominently) in various specimens which have been included in the preceding Forms (e.g. text-fig. 7).

Remarks. The variations evident in the assemblage are most reasonably regarded as variations within a single species. Any or all of the variants may be found on a single bedding plane within the section, and there are no significant differences in the vertical distribution of the various forms. The identification of complete intermediate series among the recognized forms makes any systematic division of little practical value.

Lewis (1927, p. 380) concluded that the ancestry of *C. benburbensis* may be found among earlier forms of *C. cylindrica* (Scouler). The latter has been reported in several nearby areas in rocks of early Viséan age (Caldwell 1959, p. 174; George and Oswald 1957, p. 173; Simpson 1955, p. 399), and this has been confirmed by personal examination of a complete Viséan sequence in the Ballymote syncline south of Sligo. In this sequence, *C. cylindrica* is quite common in rocks of Seminulan and pre-Seminulan age,

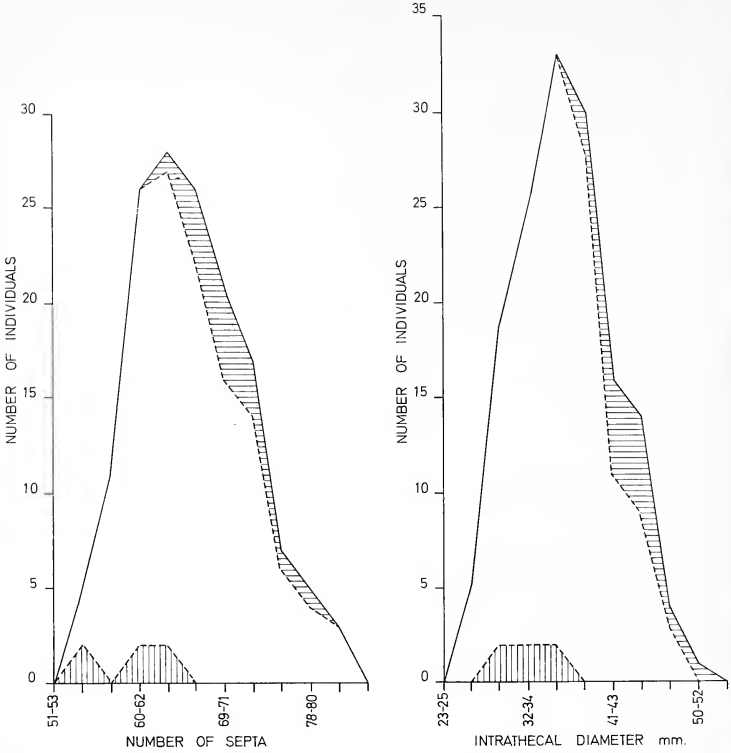

TEXT-FIGS. 12–13. Frequency curves of *Caninia benburbensis*. Vertical and horizontal ruling represents the frequency of Form A and Form D, respectively.

and *C. benburbensis* is found in rocks of late Seminulan age but most commonly in those of the *Dibunophyllum* Zone. The essential characters which have been used to distinguish the two species are as follows:

Caninia cylindrica

1. Tooth-like septal crests on the dissepiments (no continuous septa outside the theca).
2. Minor septa projecting about 2 mm. intrathecally.
3. Large and irregular interdissepimental spaces becoming smaller inwards and formed by lonsdaleoid dissepiments.

Caninia benburbensis

1. Major septa predominantly continuous extrathecally and sinuous.
2. Minor septa discontinuous for one-half to two-thirds of the extrathecal distance (do not typically project intrathecally).
3. Interseptal spaces with concentric or herringbone dissepiments.

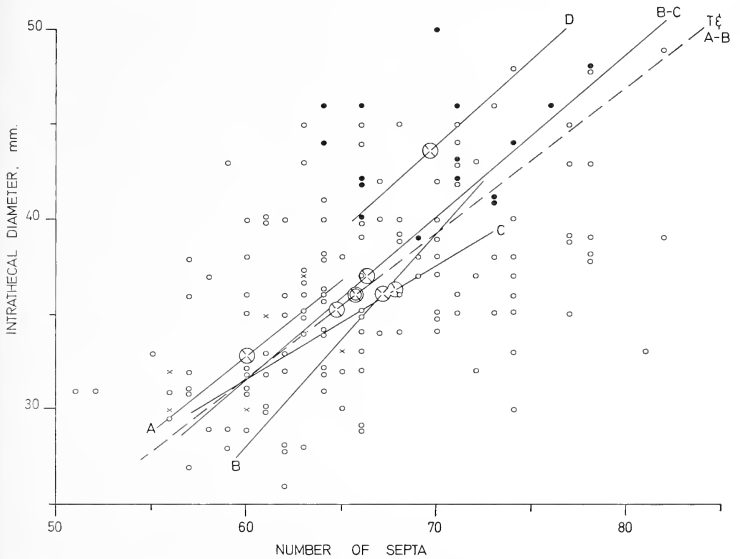

TEXT-FIG. 14. Scatter diagram of number of septa–intrathecal diameter of *Caninia benburbensis*. Crosses represent individuals of Form A; closed circles, Form D; small open circles, the remainder of the population. The reduced major axis for the transitional group A–B coincides with that for the total population (T). The total population mean is marked by the large double circle; others by large single circles.

Of significance is the presence within the Streedagh assemblage of a few specimens (Form A) with certain morphological features in common with *C. cylindrica* (compare the 'transitional forms' of Lewis 1927, p. 380, pl. 16, fig. 6; pl. 17, fig. 4). Statistical analysis of two readily measured parameters, number of septa and intrathecal diameter, indicate that these forms are slightly smaller and have fewer septa than the bulk of the assemblage (text-figs. 12, 13, and 14). Although the specimens may be too few to be representative, they are similar in dimensions to *C. cylindrica* from Tournai (Salée 1910, p. 31, pl. 2–5).

Perhaps also significant are the specimens which Salée (1910, pp. 37–9) described as

Caninia cylindrica var. *Herculina* (De Koninck). In a collection otherwise typical of the species *cylindrica*, the two specimens referred to this subspecies show an extrathecal development strikingly similar to that in typical forms of *C. benburbensis*, namely, greater continuity of the major septa, and considerable reduction of the zone of large lonsdaleoid dissepiments in favour of smaller concentric or herringbone dissepiments.

The specimens ascribed to Form A appear to possess certain distinctive morphological characters which were retained as the caniniid lineage evolved. These characters persisted through Viséan time as the population mode gradually changed toward larger adult individuals with more major septa, with concentric rather than lonsdaleoid dissepiments, and with diminished minor septa.

Text-figs. 12, 13, and 14 show the distinct and perhaps significant departure of Form D from the assemblage average. This may represent a new variation which became established as the lineage evolved. Further study of caniniid populations higher in the *Dibunophyllum* Zone may reveal whether or not this type was successful and increased in proportion with time. As it forms an integral part of the *C. benburbensis* assemblage in the lower D_1 subzone, there is no justification yet for its establishment as a new species. Lewis (1927, p. 380, pl. 17, figs. 2*a–b*, 3*a–c*) described such forms as 'senescent', or a final senile evolutionary stage of the species before it became extinct. This is questionable, as the supposedly senescent forms appeared early in Dibunophyllidan time in extremely successful populations, such as the ones at Streedagh Point, and the caniniid line continued to flourish well into D_2 time.

There is no general agreement on the relationship between *Caninia* Michelin 1840 (type species: *C. cornucopiae*) and *Siphonophyllia* Scouler *in* McCoy 1844 (type species: *S. cylindrica*). Both Salée (1910, p. 27) and Lewis (1927, p. 374) regarded *Siphonophyllia* as a synonym of *Caninia*. Both genera are recognized by Hill (1956, p. F292), in which *Siphonophyllia* is distinguished only on the basis of a wide lonsdaleoid dissepimentarium. In view of the wide range of septal and dissepimental development in *C. benburbensis*, and the as yet incomplete understanding of caniniid phylogeny, both *benburbensis* and *cylindrica* have been referred herein to the genus *Caninia* (*sensu lato*).

CONCLUSIONS

1. A wide range of morphological variation occurs in the Streedagh Point assemblage of *Caninia benburbensis*, and clearly distinguishes it from all earlier assemblages.

2. Certain characters, such as total diameter, geniculations, spacing of tabulae, and stereoplasmic thickening were distinctly dependent on ecological conditions, and varied during ontogeny.

3. Biocharacters such as intrathecal diameter, number of septa, extrathecal continuity of septa, and nature of the dissepiments show a regularity or constancy throughout ontogeny which favours their use in classification.

4. Certain members of the population possess morphological features which strongly affirm an earlier idea that *C. benburbensis* evolved from *C. cylindrica* (Lewis 1927, p. 380). In agreement with this are their respective stratigraphical ranges in Ireland.

5. Certain members of the population show features which may presage the divergence of a new species from the evolving caniniid lineage.

Acknowledgements. The author is indebted to Dr. W. G. E. Caldwell of the University of Saskatchewan for critically reading the manuscript and to Dr. J. Hubbard of King's College, London, for helpful discussions and comments on the manuscript. Technical assistance provided by the University of Glasgow in the initial specimen preparation, and the assistance of E. W. Hearn (Ottawa) in the preparation of text-figures, are both gratefully acknowledged.

REFERENCES

CALDWELL, W. G. E. 1959. The Lower Carboniferous rocks of the Carrick-on-Shannon syncline. *Q. Jl geol. Soc. Lond.* **115,** 163–88, pl. 6.

GEORGE, T. N. and OSWALD, D. H. 1957. The Carboniferous rocks of the Donegal syncline. Ibid. **113,** 137–79, pl. 14–16.

HILL, D. 1938–41. The Carboniferous rugose corals of Scotland. *Palaeontographical Soc. Mon.* (London), 213 pp., 11 pls.

—— 1956. Systematic descriptions. In MOORE, R. C. (ed.), *Treatise on invertebrate paleontology*, Part F, *Coelenterata*, F256–F321. Univ. Kansas Press and Geol. Soc. Am.

HUBBARD, J. A. E. B. 1966. Population studies in the Ballyshannon Limestone, Ballina Limestone, and Rinn Point Beds (Viséan) of NW. Ireland. *Palaeontology,* **9,** 252–69, pl. 40–1.

HUBBARD, W. F. and SHERIDAN, D. J. R. 1965. The Lower Carboniferous stratigraphy of some coastal exposures in Co. Sligo, Ireland. *Sci. Proc. R. Dublin Soc.* ser. A, **2,** 189–95, pl. 16–17.

LEWIS, H. P. 1927. *Caninia cylindrica* Scouler and other large *Caninias* from the Carboniferous Limestone of Ireland. Ibid. **18**, 373–82, pl. 16–17.

—— 1930. The Avonian succession in the south of the Isle of Man. *Q. Jl geol. Soc. Lond.* **86,** 234–90, pl. 20–5.

MA, T. Y. H. 1937. On the seasonal growth in Paleozoic tetracorals and the climate during the Devonian Period. *Paleontologia Sinica*, ser. B. **2,** fasc. 3, 1–106, 22 pl.

OLDROYD, R. W. L. 1965. A summary of the micropalaeontology of the Lower Carboniferous of Co. Sligo, Ireland. In HUBBARD, W. F. and SHERIDAN, D. J. R. The Lower Carboniferous stratigraphy of some coastal exposures in Co. Sligo, Ireland. *Sci. Proc. R. Dublin Soc.* ser. A, **2,** 189–95, pl. 16, 17.

OSWALD, D. H. 1955. The Carboniferous rocks between the Ox Mountains and Donegal Bay. *Q. Jl geol. Soc. Lond.* **111,** 167–86, pl. 11.

SALÉE, A. 1910. Contribution à l'étude des polypiers du Calcaire Carbonifère de la Belgique. Le genre *Caninia. Soc. Belge Géol.*, Nouv. Mém. Sér. 4, Mém. **3,** 62 pp., 9 pls.

SIMPSON, I. M. 1955. The Lower Carboniferous stratigraphy of the Omagh syncline, Northern Ireland. *Q. Jl geol. Soc. Lond.* **110,** 391–408, pl. 18.

SMYTH, L. B. 1925. A contribution to the geology of Great Orme's Head. *Sci. Proc. R. Dublin Soc.* **18,** 141–64, pl. 3–7.

O. A. DIXON
Department of Geology
University of Ottawa
Ottawa, 2
Canada

Final typescript received 15 July 1969

AMPHIPORA AND *EURYAMPHIPORA* (STROMATOPOROIDEA) FROM THE DEVONIAN OF WESTERN CANADA

by N. R. FISCHBUCH

ABSTRACT. Subsurface diamond cores of the Devonian Swan Hills Formation of central Alberta contain well-preserved specimens of *Amphipora* Schulz and *Euryamphipora* Klovan. Three varieties of *Amphipora* are recognized in the Swan Hills material, and are referred to the species *A. angusta*, *A. pervesiculata*, and *A. ramosa*; a new species of *Euryamphipora* (*E. mollis*) and the type species *E. platyformis* also are present. *Amphipora* is placed in the Clathrodictyidae with *Euryamphipora* since they have identical tissue. 'Juvenile' forms, which may represent an early astogenetic stage, are found associated with mature *Amphipora* coenostea. The concept that some forms of *Amphipora* grew without producing a peripheral rim is rejected and the absence of this feature s considered the result of abrasion.

THE stromatoporoid genus *Amphipora*, so common in the Devonian carbonate rocks of western Canada, has aroused only passing interest among Canadian palaeontologists. Those specimens described have been referred mainly to *Amphipora ramosa* (Phillips), and have been commonly considered in conjunction with other stromatoporoids as aberrant forms. The presence and abundance of *Amphipora*, however, has been noted in several recent sedimentological studies (Edie 1961; Fischbuch 1960, 1962, 1968; Thomas and Rhodes 1961; Murray 1966; Jenik and Lerbekmo 1968; Leavitt 1968).

The Swan Hills reef complexes, which are found deep in the subsurface of the central plains of Alberta, contain exceptionally well-preserved specimens of *Amphipora* which abound in the lagoon and platform carbonates. *Amphipora* coenostea constitute up to 70 % of these rocks, are commonly oriented horizontally, and appear to have been transported over longer or shorter distances after death. The specimens used in this study were taken from diamond cores of the Devonian Swan Hills Formation which straddles the Givetian–Frasnian boundary (Fischbuch 1968, p. 523) and contains nine stages of reef growth; these have been informally designated from bottom to top as Divisions I–IX (Fischbuch 1968, p. 452). *Amphipora* and *Euryamphipora* are present in all but Division I. Three species of *Amphipora* and two species of *Euryamphipora* are recognized in the Swan Hills material; both genera are placed in the family Clathrodictyidae.

TAXONOMIC CONSIDERATIONS

The classification of *Amphipora* as a stromatoporoid has been rejected by some palaeontologists: for example, Öpik (1935, p. 3) regarded *Amphipora* as a calcareous sponge. Nicholson (1886, p. 99) also believed that it should be regarded in a separate category. Lecompte (1952) classified *Amphipora* with the dendroid stromatoporoids but cautioned that 'Dans l'état présent des observations, le genre *Amphipora* apparaît entièrement aberrant dans le groupe des Stromatoporoïdes' (1952, p. 324). Later (1956, p. F142), he removed *Amphipora* and classified it as Incertae sedis. Its relatively slender, cylindrical, growth form and consistently fibrous tissue is somewhat anomalous amidst

[Palaeontology, Vol. 13, Part 1, 1970, pp. 64–75, pls. 14–17.]

other genera of the Idiostromatidae and certainly anomalous compared to the families that exhibit melanospheric, cellular, compact, and flocculent tissue. Unfortunately it was not assigned originally to the Clathrodictyidae, which are typified by fibrous tissue, but rather, due to its uniformly cylindrical growth form, was conveniently placed in the

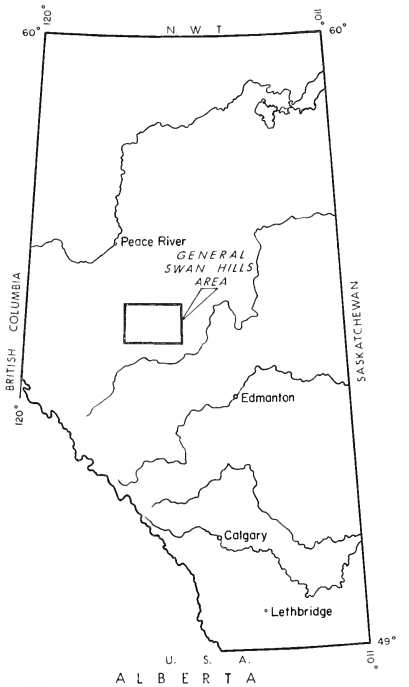

TEXT-FIG. 1. Location of Swan Hills area.

Idiostromatidae. The discovery of a tabular counterpart, *Euryamphipora*, by Klovan (1966, p. 14) sheds new light on this problem. In his description, he left little doubt that the fibrous tissue allies his genus to the family Clathrodictyidae. This, consequently, paves the way for the entry of *Amphipora* into that same family, since both genera have indistinguishable tissue. Furthermore, Birkhead (1967, pp. 31, 32), in reviewing stromatoporoid phylogeny, suggested a relationship between *Amphipora* and *Anostylostroma*. This evidence supports the inclusion of the genus *Amphipora* in the Stromatoporoidea.

Leavitt (1968, p. 325) discussed some aspects of reproduction in *Amphipora* and illustrated marginal cysts or buds and 'juvenile' coenostea (Leavitt 1968, pl. 8). Other Swan Hills limestones contain similar forms, which grade from small spherical bodies, 0·15–0·6 mm. in diameter, through incipient *Amphipora*-like stems, containing a simple

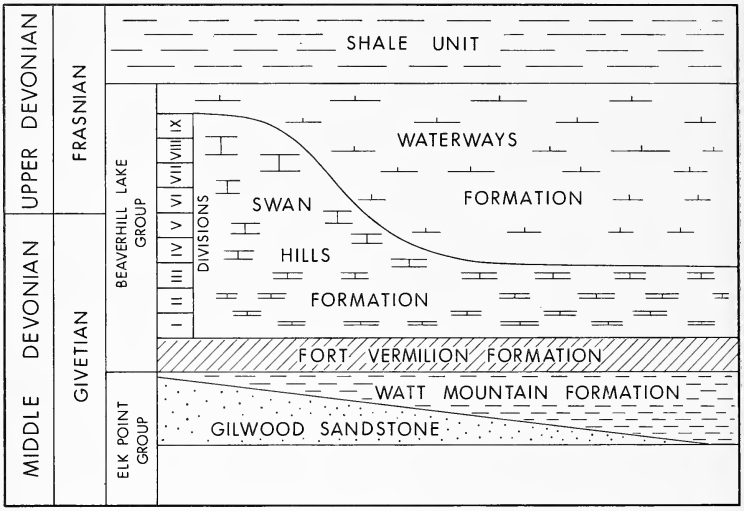

TEXT-FIG. 2. Stratigraphic position of the Swan Hills Formation.

arrangement of one or two structural elements, to mature *Amphipora* stems (Pl. 14, figs. 1–8). The outer rim in all specimens is formed by a single layer of transversely fibrous tissue. The small spheres may have been formed on the outer margins of the coenostea (Leavitt 1968, pl. 8, fig. 5). If this were so, subsequently they may have become detached, floated freely in the water, and then attached themselves to the substrate to develop into adult forms. This hypothesis, however, is conjectural, since nothing is known of the reproductive habits of stromatoporoids.

The function of the axial canal remains problematic. Lecompte (1952, p. 323) rejected the contention that it is an astrorhizal tube on the basis that there is no ramification from it throughout the tissue. Several workers, however, have reported openings connecting it to the galleries. The function of the marginal vesicles is also open to question. Nicholson (1886, p. 110) suggested that they may have been used in reproduction. Some workers (Nicholson 1886, p. 110; Lecompte 1952, p. 323) also maintain that marginal vesicles are not present in all forms. Convinced that some forms grew without producing a peripheral rim, based on his observations of the Ardennes material, Lecompte (1952, pp. 329, 330) erected two species (*A. rudis*, *A. laxeperforata*) to include such coenostea.

In the many specimens from the Swan Hills Formation, however, there seems to be little doubt that absence of the outer rim is the result of abrasion. This outer envelope of tissue is relatively thin and the slightest erosion would disrupt it or remove it completely. Most coenostea have been transported some distance and a complete sequence of forms, ranging from those with the outer rim intact, to slightly broken, and finally completely removed, can be observed in the Swan Hills material (Pl. 14, figs. 9–13).

Specimens of *Amphipora* described from Canada have been referred mainly to the type species *Amphipora ramosa* (Phillips). There are, however, several distinct varieties which can be grouped as follows:

1. Those with a narrow zone of marginal vesicles, stout pillar-laminar architecture, and relatively small axial canal.
2. Those with a narrow zone of marginal vesicles, stout pillar-laminar architecture, and no axial canal.
3. Those with a wide zone of marginal vesicles, delicate pillar-laminar architecture, and relatively large axial canal.

To represent the above three types, the species *Amphipora ramosa* (Phillips), *Amphipora angusta* Lecompte, and *Amphipora pervesiculata* Lecompte respectively, were selected from over thirty described species. They usually occur closely associated with each other in the Swan Hills Formation, but generally one species is dominant in any *Amphipora*-rich bed.

Some poorly-preserved Swan Hills specimens do not portray the dark-coloured median line in the structural elements. These were not referred to the genus *Paramphipora*, proposed by Yavorsky (1955) for specimens with tissue lacking a dark-coloured median line, since the absence of this feature is probably a function of preservation. The validity of Yavorsky's genus has also been questioned by other workers (Klovan 1966, p. 14; Stearn 1966*a*, p. 109).

KEY TO LOCATION OF SPECIMENS

The locations of wells are given in an abbreviated form, e.g. the Atlantic Kaybob 4–14 well, is 4–14–64–19 W5, which should be read as Legal Subdivision 4, Section 14, Township 64, Range 19, West of the fifth Meridian. Depths are measured from the Kelly Bushing (K.B.).

The type and other specimens described in this paper have been deposited at the Geological Museum of the University of Saskatchewan under Coelenterata, Stromatoporoidea, and are numbered with the prefix GMUS Cs. Under occurrences only well numbers are given, followed by depths in feet and GMUS Cs numbers in parentheses.

Well number	*Well name and location*
1	Phillips *et al.*, Kaybob 2–5–64–19 W5
2	Atlantic Kaybob 4–14–64–19 W5
3	S.O.B.C. Snipe Lake 10–21–70–18 W5
4	Phillips *et al.*, Kaybob 10–4–64–19 W5
5	Home Regent 'A' Swan Hills 10–4–67–10 W5
6	Phillips *et al.*, Kaybob 2–9–64–19 W5
7	Pan American B.A. Swan Hills 10–32–66–10 W5
8	Pan American B.A. Swan Hills 12–19–66–10 W5
9	Imperial Goose River 4–15–67–18 W5
10	Imperial Goose River 10–15–67–18 W5

11 Canadian Superior Sakwatamau 10–4–63–15 W5
12 Canadian Kewanee Swan Hills 4–16–68–10 W5
13 California Standard S.O.B.C. Snipe Lake 10–35–70–18 W5
14 Pan American 'A–1' Sunset House 4–16–70–19 W5
15 Pan American B.A. Swan Hills 12–29–66–10 W5
16 B.A. Goose River 10–5–67–18 W5
17 Shell Virginia Hills 12–35–64–13 W5
18 Canadian Kewanee Swan Hills 4–7–69–10 W5
19 California Standard S.O.B.C. House Mountain 4–6–70–10 W5
20 Shell Swan Hills 6–34–64–13 W5
21 Pure Sakwatamau 7–7–63–14 W5
22 Pan American B.A. 'U–12' Swan Hills 4–8–66–10 W5
23 Canadian Kewanee Swan Hills 10–32–68–10 W5

SYSTEMATIC DESCRIPTIONS

Family CLATHRODICTYIDAE Kühn 1939
Genus AMPHIPORA Schulz 1883

Type species. Caunopora ramosa Phillips 1841.

Diagnosis. Coenosteum cylindrical, rod-shaped, and very rarely branching. It may or may not have an axial canal with or without irregular tabulae. Pillars and laminae cannot be distinguished but rather are commonly amalgamated to form a coarse network, which is separated from a thin outer rim by a zone of marginal vesicles. Tissue is transversely fibrous and the structural elements (amalgamated pillars and laminae) contain a dark-coloured median line. The outer rim does not have a median line and is only about half as thick as the pillar-laminar elements.

EXPLANATION OF PLATE 14

All figures × 10.

Figs. 1–8. Progressive development from possible immature to mature *Amphipora* coenostea.

Fig. 1. Concentration of small and irregular immature *Amphipora* forms composed mainly of an outer rim with little or no internal development of structural elements; well no. 10, 9335.

Figs. 2–4. Initial stage with vague internal tissue apparent in figs. 3 and 4; well no. 10, 9335.

Fig. 5. Irregular intermediate form with definite, but separate, internal skeletal elements; well no. 10, 9335.

Figs. 6–7. Development of axial canal surrounded by an intermittent network of structural elements; well no. 10, 9335.

Fig. 8. Mature, completely developed *Amphipora* coenostea; well no. 10, 9284.

Figs. 9–13. Progressive erosion of *Amphipora* coenostea.

Fig. 9. Cross-section of *Amphipora* coenosteum with outer rim broken in two places; well no. 4, 9801.

Fig. 10. Cross-section of *Amphipora* coenosteum with right side of peripheral rim removed by erosion; well no. 4, 9801.

Fig. 11. Cross-section of *Amphipora* coenosteum with only a remnant of outer rim preserved (right side of photo). Sediment has penetrated into the galleries and axial canal; well no. 4, 9801.

Fig. 12. Cross-section of *Amphipora* coenosteum with outer rim partly collapsed; well no. 6, 9884.

Fig. 13. Cross-section of *Amphipora* coenosteum with outer rim completely removed by erosion; well no. 6, 9884.

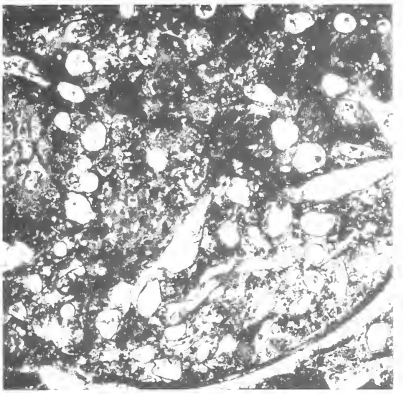

1

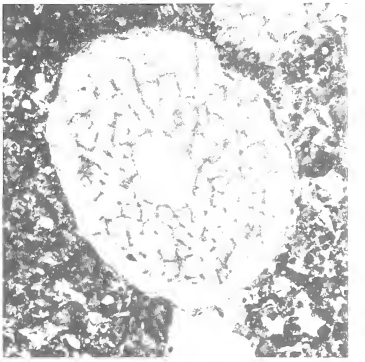

8

2

3

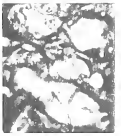

4

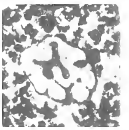

5

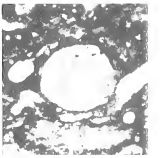

6

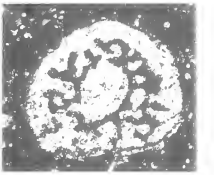

7

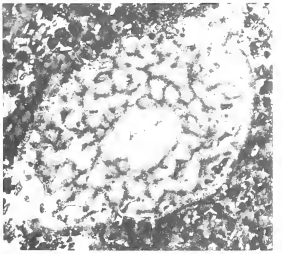

9

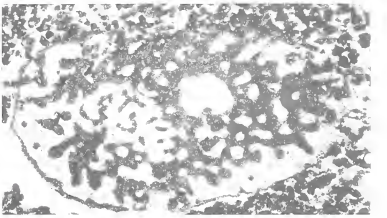

10

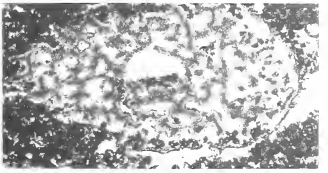

11

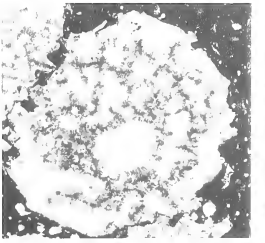

12

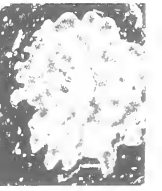

13

FISCHBUCH, *Amphipora*

Amphipora ramosa (Phillips 1841)

Plate 15, figs. 1–5

For synonymy to 1957 see Galloway (1957, p. 442).

1957 *Amphipora ramosa* (Phillips), Yavorsky, p. 63, pl. xli, figs. 1–9 (Lower Devonian, Kuznetsk Basin, Russia).
1957 *Amphipora intexta* Yavorsky, p. 62, pl. xxxiv, figs. 5–9 (Middle Devonian, Kuznetsk Basin, Russia).
?1960 *Amphipora ramosa* (Phillips), Galloway and Ehlers, p. 98, pl. xi, figs. 1*a*, 1*b* (Middle Devonian, Michigan, U.S.A.).
1961 *Amphipora ramosa* (Phillips), Yavorsky, p. 58, pl. xxxvi, fig. 15; pl. xxxvii, figs. 1–10 (Middle Devonian, Kuznetsk Basin, Russia).
?1961 *Amphipora ramosa* (Phillips), Stearn, p. 946, pl. 107, figs. 9, 10 (Upper Devonian, Alberta, Canada).
?1963 *Amphipora ramosa* (Phillips), Stearn, p. 663, pl. 87, fig. 2 (Swan Hills Formation, Alberta, Canada).
1963 *Amphipora intexta* (Yavorsky), Stearn, p. 663, pl. 87, figs. 3, 4, 5 (Swan Hills Formation, Alberta, Canada).
1966*a* *Amphipora ramosa* (Phillips), Stearn, p. 109.
?1966 *Amphipora* sp. Klovan, p. 30, pl. x, figs. 1–6 (Cooking Lake and Leduc Formations, Alberta, Canada).
?1966*b* *Amphipora ramosa* (Phillips), Stearn, p. 63, pl. xxiv, fig. 2 (Hay River Formation, Northwest Territories, Canada).
1967 *Amphipora ramosa* (Phillips), Birkhead, p. 84, pl. 16, figs. 2*a*, 2*b* (Callaway Formation, Missouri, U.S.A.).

Diagnosis. The coenostea are cylindrical, rarely branching, and contain an axial canal. Coenosteal diameter ranges from 2·5 to 4·6 mm. (averaging 3·47 mm.). Structural elements consist of fibrous tissue.

Description. This species is represented in the Swan Hills collection by 65 rock specimens, each of which contains many coenostea. Sixteen of these specimens were used in this description.

Cross-section. An axial canal always is present, but is not as prominent as in some other species. It ranges in diameter from 0·4 to 1·1 mm., with an average of 0·66 mm. Pillars and laminae are amalgamated to form an irregular network surrounding the axial canal. The structural elements forming this network are stout, measuring 0·1–0·25 mm. (averaging 0·2 mm.) in diameter. They are composed of light-brown tissue and contain a dark-coloured, median line with fibres extending from the line toward the perimeter of the skeletal elements. Between the pillar-laminar entanglement and the outer rim is a zone of round or oval marginal vesicles, 0·1–0·3 mm. thick. The vesicles are formed by structural elements extending, at regular intervals, across the relatively open space immediately within the outer rim. The outer rim is composed of a single layer of radially fibrous tissue that does not have a dark-coloured median line and is about half as thick as the structural elements. Dissepiments, in the marginal vesicles, galleries, and axial tube, are rare.

Axial section. The structural elements of the pillar-laminar network are commonly unoriented, but rarely appear to splay upward and outward from the axial canal and toward the periphery. The elements that pass through the zone of marginal vesicles meet the outer rim at oblique angles.

Discussion. *Amphipora ramosa*, as here defined, always possesses an axial canal, and thus differs from *A. angusta* Lecompte, which does not have this feature. It has thicker structural elements, a narrower zone of marginal vesicles, and fewer dissepiments than *A. pervesiculata* Lecompte. Coenostea exhibiting a splay pattern of the structural elements in some axial sections, such as those referred to *A. intexta* Yavorsky, are interpreted as variants of *A. ramosa*.

Occurrence. This species is found in Divisions II–VI of the Swan Hills Formation. In Divisions II–III it is associated with *A. pervesiculata*, and *A. angusta*, and fragmented subspherical stromatoporoids, but is one of the dominant fossils in the lagoonal facies of Divisions IV–VII. *A. ramosa* occurs in the calcirudites, calcarenites, and calcilutites in the following wells: 1, 9725 (267), 9762 (268); 2, 9759·5 (269), 9749 (270); 3, 8798 (271); 4, 9778 (272), 9801 (273); 5, 8591 (274); 6, 9884 (275), 9854 (276); 7, 9071 (277), 8977 (278); 8, 8618 (279); 9, 9192 (280); 10, 9284 (281); 11, 9735 (282).

Amphipora angusta Lecompte 1952

Plate 15, figs. 6–9

1952 *Amphipora angusta* Lecompte, p. 324, pl. lxvii, fig. 2 (Middle Devonian, Dinant Basin, Belgium).

Diagnosis. The coenosteum is cylindrical and does not contain an axial canal. Coenosteal thickness ranges from 2·2 to 4·7 mm. (averaging 3·19 mm.). Structural elements consist of fibrous tissue.

Description. Description of this species is based on fourteen rock specimens, all of which contain many coenostea.

Cross-section. An axial canal is lacking in all specimens, and the central portion of the coenosteum is composed of an amalgamated pillar-laminar system. Galleries are irregular in outline but continuous open areas can be traced completely through the skeletal system. The structural elements range from 0·1 to 0·3 mm. (averaging 0·16 mm.) in diameter, and form a continuous network. This network is surrounded by a zone of marginal vesicles, 0·1–0·4 mm. (averaging 0·3 mm.) in depth. It is crossed at regular intervals by structural elements that are commonly of equal diameter to those of the interior network but rarely thin to the point of disappearance as they cross the vesicular zone. In the rare instances in which the median part of these elements has disappeared, the elements are reduced to two 'barbs', which project into the vesicular zone from opposite sides. Skeletal tissue is light brown, transversely fibrous, and contains a dark-coloured median line. The outer rim, which is about half as thick as the structural elements, is composed of one layer of radially fibrous tissue. Dissepiments are rare.

Axial section. The interior network of intertwined structural elements is generally completely amalgamated but rarely displays a vague upward splay pattern. The elements pass through the zone of marginal vesicles and join the outer rim at an oblique angle.

EXPLANATION OF PLATE 15

Figs. 1–5. *Amphipora ramosa* (Phillips). 1, Hand specimen containing numerous coenostea, ×1; well no. 11, 9735 (282). 2, Cross-section, ×50; well no. 11, 9735 (282). 3, Cross-section, ×20; well no. 11, 9735 (282). 4, Cross-section, ×10; well no. 11, 9735 (282). 5, Cross and axial section, ×10; well no. 11, 9735 (282).

Figs. 6–9. *Amphipora angusta* Lecompte. 6, Hand specimen containing numerous coenostea, ×1; well no. 6, 9915 (285). 7, Cross-section, ×10; well no. 6, 9915 (285). 8, Fibrous microstructure, ×50; well no. 6, 9915 (285). 9, Cross and axial sections, ×10; well no. 6, 9915 (285).

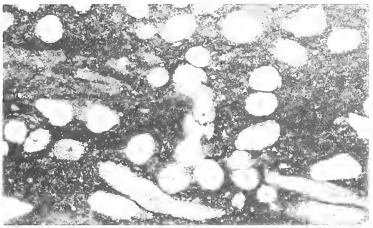

1

2

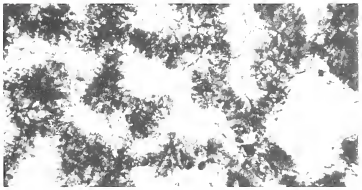

3

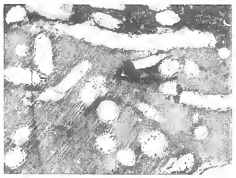

6

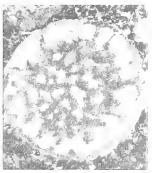

7

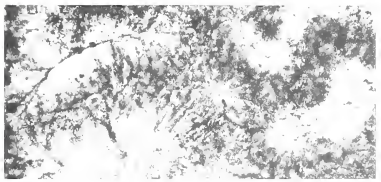

8

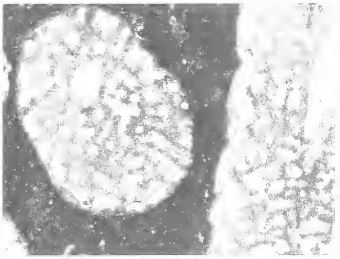

4

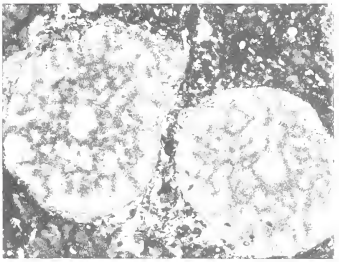

5

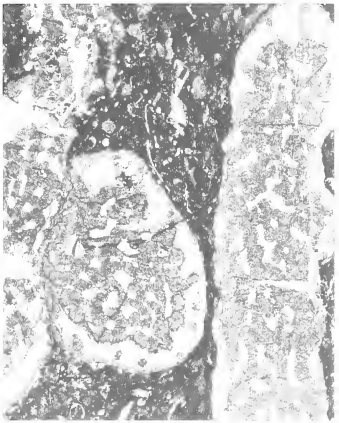

9

FISCHBUCH, *Amphipora*

Discussion. The Swan Hills specimens are similar to the Belgian holotype described by Lecompte in that they lack an axial canal, but the average diameter of the Swan Hills specimens is considerably greater (3·19 mm.) compared to a diameter range of 0·5–2·0 mm. given by Lecompte. The conspicuous absence of an axial canal, however, appears sufficient to ally the Swan Hills specimens to this species. *A. angusta* has slightly thinner structural elements than, and lacks the axial canal of, *A. ramosa.* It is easily distinguished from *A. pervesiculata*, which has thinner structural elements and a relatively large axial canal and marginal vesicles.

Occurrence. This species is found in Divisions II–VII of the Swan Hills Formation. In Divisions II and III it is associated with *A. pervesiculata*, *A. ramosa*, and other stromatoporoids, but in the lagoonal facies of Divisions IV–VII the above three species of *Amphipora* occur in great abundance to the complete exclusion of other stromatoporoids. *A. angusta* occurs in the calcirudites, calcarenites, and calcilutites in the following wells: 6, 9912 (283), 9913 (284), 9915 (285); 2, 9752 (286), 9762 (287); 12, 7957 (288); 13, 8651 (289); 14, 9093 (290); 15, 8811 (291); 7, 9099 (292); 16, 9189 (293); 17, 9341 (294); 10, 9333 (295); 18, 7842 (296).

Amphipora pervesiculata Lecompte 1952

Plate 16, figs. 1–5

1952 *Amphipora pervesiculata* Lecompte, p. 331, pl. lxx, figs. 3, 4, 5 (Upper Devonian, Dinant Basin, Belgium).

?1952 *Amphipora laxeperforata* Lecompte, p. 330, pl. lxx, figs. 1, 2 (Upper Devonian, Dinant Basin, Belgium).

1957 *Amphipora pinguis* Yavorsky, p. 63, pl. xxxv, figs. 1–5 (Middle Devonian, Kuznetsk Basin, Russia).

Description. This species is represented in the Swan Hills collection by 43 rock specimens, 19 of which are used in this description, and all contain many coenostea. The cylindrical skeleton ranges from 2·0 to 4·9 mm. (averaging 3·3 mm.) in diameter.

Cross-section. A relatively large axial canal, 0·5–1·5 mm. (averaging 0·82 mm.) in diameter, is a dominant feature of all coenostea. Undifferentiated structural elements form a continuous but relatively narrow network around the axial canal. The diameter of these structural elements ranges from 0·1 to 0·24 mm. (averaging 0·13 mm.). They are slightly thinner than those of other species but appear even more so due to their reduced numbers. The conspicuous zone of marginal vesicles, 0·2–0·6 mm. wide, is crossed by structural elements which thin perceptibly, and commonly do not extend completely across the zone, but are broken to form opposing 'barbs'. In some cross-sections, most, or even all, of the marginal vesicles are joined to form a continuous open area between the outer rim and the interior skeletal system. The outer rim, 0·03–0·06 mm. in thickness, is composed of a single layer of transversely fibrous tissue, differing from the other elements which are also transversely fibrous but are thicker and contain a dark-coloured median line. Dissepiments are common in most coenostea but are especially noticeable in the large axial canal and zone of marginal vesicles.

Axial section. Structural elements are uncommon in the zone of marginal vesicles, giving the impression of an annulus between the outer rim and the pillar-laminar network.

Discussion. The Swan Hills specimens structurally are indistinguishable from the Belgian holotype described by Lecompte but have a greater over-all diameter. Considerable variation in size, however, seems to be characteristic of mature specimens of amphiporoid species. *A. pervesiculata* differs from *A. ramosa* in having a larger axial canal and a much wider zone of marginal vesicles. It is easily distinguished from *A. angusta*, which has no axial canal. *A. pinguis* Yavorsky is indistinguishable from the Swan Hills specimens in size of the coenosteum and axial canal. Width of the marginal vesicular zone was not given by Yavorsky but measures about 0·25 mm. on the illustrations, and this compares favourably with the Swan Hills specimens. *A. pinguis* is, therefore, a junior subjective synonym of *A. pervesiculata*. *A. laxeperforata* Lecompte appears to be an *A. pervesiculata* or *A. ramosa* in which the outer rim has been destroyed by abrasion.

Occurrence. This species is found in Divisions II–IX of the Swan Hills Formation. *A. pervesiculata* is associated with *A. ramosa*, *A. angusta*, fragmented subspherical, and dendroid stromatoporoids in Divisions II and III. In Divisions IV–IX it is found associated only with *A. ramosa* and *A. angusta*. It occurs in the calcirudites, calcarenites, and calcilutites in the following wells: 5, 8472·5 (297), 8409 (298); 17, 9495 (299), 9372 (300); 15, 8931 (301), 9001 (302), 8739 (303), 8813 (304); 10, 9317 (305); 4, 9737 (306), 9729 (307); 2, 9756 (308), 9764 (309); 1, 9751 (310); 14, 9104 (311); 6, 9727·5 (312); 12, 7927 (313); 3, 8716 (314); 19, 7516 (315).

Genus EURYAMPHIPORA Klovan 1966

Type species. *Euryamphipora platyformis* Klovan 1966.

Diagnosis. Coenosteum thin, tabular, undulating, and composed of a median zone of undifferentiated structural elements representing amalgamated pillars and laminae, which is flanked above and below by marginal vesicles. Tissue of the structural elements is transversely fibrous and contains a dark-coloured median line.

Euryamphipora platyformis Klovan 1966

Plate 17, figs. 1–5

1966 *Euryamphipora platyformis* Klovan, p. 15, pl. iii, figs. 4*a*, 4*b*; pl. iv, figs. 1–7 (Cooking Lake and Leduc Formations, Alberta, Canada).

Diagnosis. Coenostea are flat, tabular forms, ranging from 1 to 3 mm. in thickness. Astrorhizal canals, mamelons, and latilaminae are not present.

Description. This species is represented in the Swan Hills collection by nine specimens.

EXPLANATION OF PLATE 16

Figs. 1–5. *Amphipora pervesiculata* Lecompte. 1, Hand specimen containing numerous coenostea, ×1; well no. 5, 8472·5 (297). 2, Cross-section, ×10; well no. 10, 9317 (305). 3, Cross-section showing fibrous microstructure, ×50; well no. 5, 8472·5 (297). 4, Cross-section, ×20; well no. 5, 8472·5 (297). 5, Axial section showing a vague upward splay pattern of the structural elements, ×10; well no. 5, 8472·5 (297).

Figs. 6–10. *Euryamphipora mollis* sp. nov. 6, Hand specimen containing tabular coenostea of *Euryamphipora mollis* sp. nov. associated with *Amphipora* and dendroid stromatoporoids, ×1; well no. 6, 9924 (325). 7, Vertical section of *E. mollis* showing fibrous microstructure and zone of marginal vesicles crossed by dissepiments, ×50; well no. 6, 9924·5 (325). 8, Tangential section showing cross-sections of structural elements, ×50; well no. 6, 9924·5 (325). 9, Vertical section, ×10; well no. 6, 9924·5 (325). 10, Tangential section, ×10; well no. 6, 9924·5 (325).

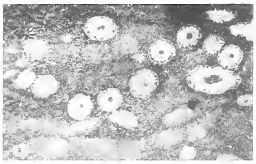

1

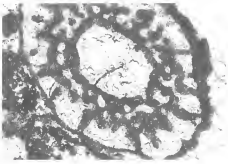

2

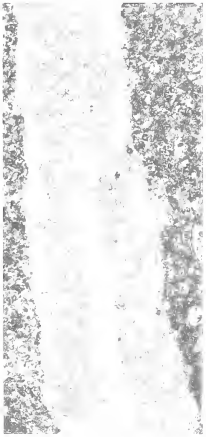

5

3

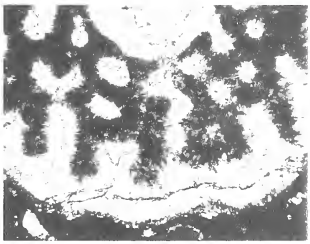

4

6

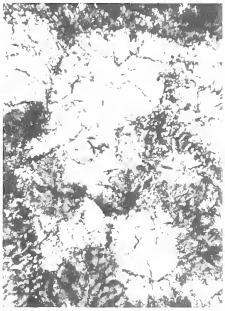

7

8

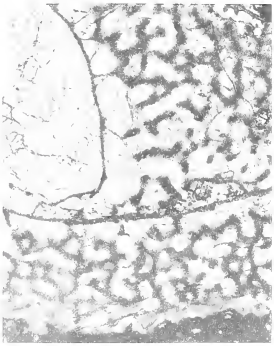

9

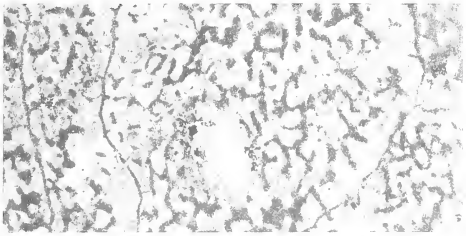

10

Vertical section. The upper and lower surfaces of the coenosteum are bordered by a thin (0·05 mm.) layer of transversely fibrous tissue, which does not contain a dark-coloured median line. In some coenostea, the upper layer has been disrupted or removed by erosion allowing sediment or algal (?) material to accumulate directly on the pillar-laminar network (Pl. 17, fig. 1). The pillar-laminar entanglement occupies the median portion of the skeleton, and its elements range from 0·1 to 0·2 mm. in diameter. They are composed of light-brown, transversely fibrous tissue and contain a dark-coloured median line. The interior network is joined, at regular intervals, to the outer layer of tissue by vertical elements (pillars?), forming a continuous row of marginal vesicles 0·25–0·35 mm. in thickness. Dissepiments are rare.

Tangential section. Where sections cut the median zone, the skeletal elements not uncommonly are crudely oriented in subparallel rows at right angles to each other, forming a coarse, screen-like pattern. This differs from the sheet-like laminae of other stromatoporoids, which are pierced only by foramina and vacuoles. Tangential sections through the relatively open marginal vesicle zone reveal the structural elements as discrete dots, 0·1–0·15 mm. in diameter, which are joined by dissepiments.

Discussion. The Swan Hills specimens are closely similar to the holotype described by Klovan from the Upper Devonian Redwater reef complex, although they have a slightly thinner outer layer of tissue. This difference, however, is negligible and not of specific significance. *E. platyformis* differs from *E. mollis*, which has more dissepiments, thinner structural elements, and larger marginal vesicles.

Occurrence. E. platyformis is found in Divisions II–VII of the Swan Hills Formation, where it is associated with *Amphipora*, fragmented brachiopods, and disarticulated ostracode carapaces. It occurs in growth position and in the calcarenites and calcirudites in the following wells: 20, 9447 (316), 9644 (317); 21, 9408 (318); 22, 8613 (319), 8616 (320); 23, 8247 (321), 8249 (322); 8, 8777 (323); 12, 7910 (324).

Euryamphipora mollis sp. nov.

Plate 16, figs. 6–10

Holotype. 6, 9924·5 (325).

Diagnosis. Coenostea have a tabular growth habit and occur singly or in superposed layers of several coenostea, which encrust and over-ride each other giving the whole mass a latilaminar aspect. Some coenostea persist laterally for only short distances and have the appearance of large 'cysts' formed on the underlying coenosteum. These, in turn, are engulfed by the coenosteum above, which may have similar 'cysts' on its upper surface.

Description. Euryamphipora mollis is represented in the Swan Hills collection by six specimens.

Vertical section. Coenosteum consists of a median pillar-laminar system, 1–1·5 mm. thick, in which pillars cannot be distinguished from laminae. These structural elements range from 0·1 to 0·15 mm. in diameter, are transversely fibrous, and contain a dark-coloured median line. The median zone of undifferentiated structural elements is flanked above and below by a zone of marginal vesicles, 0·4–0·8 mm. in thickness, which is crossed at regular intervals by vertical or oblique structural elements. These elements

thin perceptibly and commonly do not extend across the zone, but are broken completely to form opposing 'barbs'. The coenosteum is covered by a thin layer of transversely fibrous tissue, 0·04–0·08 mm. in thickness. Where coenostea are superposed, the line of contact can be traced by a dark-coloured median line, identical to that in the interior elements. Dissepiments are common, especially in the marginal vesicles, where they curve and branch outward, linking the median skeletal system to the outer, covering layer.

Tangential section. Structural elements in the median zone are represented by discrete, irregular masses of fibrous tissue surrounded by continuous gallery space, which is interrupted only by dissepiments. Where sections cut the zone of marginal vesicles, widely spaced skeletal elements are represented by dots, 0·1 mm. or less in diameter, not uncommonly joined by dissepiments.

Discussion. E. mollis differs from the only other species of *Euryamphipora*, *E. platyformis*, in having more dissepiments, a more delicate pillar-laminar system, and a larger zone of marginal vesicles. It has a slightly 'knotted' structure reminiscent of *Hammatostroma nodosum*, described by Klovan from the Redwater reef complex, but the laminae in the latter species are much more closely spaced than the units described here as individual coenostea. The genera *Euryamphipora* and *Hammatostroma* have similar fibrous microstructure but differ markedly in laminar spacing (or coenosteal thickness). They eventually may be found to be related to a common ancestor.

Occurrence. This species is found in Divisions II and III of the Swan Hills Formation, where it is associated with *Amphipora*, *Euryamphipora platyformis*, subspherical stromatoporoids, and ostracode carapaces. It occurs in growth position and in the calcarenites and calcirudites in the following wells: 6, 9924·5 (325), 9902·5 (326), 9926 (327); 5, 8640 (328); 22, 8614 (329); 2, 9770 (330).

Acknowledgements. This paper is a portion of a doctoral dissertation written at the University of Saskatchewan under the direction of Drs. W. G. E. Caldwell and W. K. Braun. The writer gratefully acknowledges their guidance and criticism.

REFERENCES

BIRKHEAD, P. K. 1967. Stromatoporoidea of Missouri. *Bull. Am. Paleont.* **52,** no. 234, 23–110.

EDIE, R. W. 1961. Devonian reef reservoir, Swan Hills oilfield, Alberta. *Can. Mining and Met. Bull.* **54,** no. 590, 447–54.

FISCHBUCH, N. R. 1960. Stromatoporoids of the Kaybob reef, Alberta. *Jour. Alta. Soc. Petrol. Geol.* **8,** 113–31.

—— 1962. Stromatoporoid zones of the Kaybob reef, Alberta. Ibid. **10,** 62–72.

—— 1968. Stratigraphy, Devonian Swan Hills reef complexes of central Alberta. *Bull. Can. Petrol. Geol.* **16**, 446–587.

GALLOWAY, J. J. 1957. Structure and classification of the Stromatoporoidea. *Bull. Am. Paleont.* **37,** no. 164, 345–480.

EXPLANATION OF PLATE 17

Figs. 1–5. *Euryamphipora platyformis* Klovan. 1, Vertical section showing tabular growth habit, ×10; well no. 20, 9644 (317). 2, Tangential section showing orientation of skeletal elements in subparallel rows, ×10; well no. 22, 8616 (320). 3, Tangential section cutting median pillar-laminar entanglement and zone of marginal vesicles, ×10; well no. 22, 8616 (320). 4, Vertical section showing marginal vesicle, ×50; well no. 22, 8613 (319). 5, Tangential section showing fibrous microstructure, ×50; well no. 22, 8613 (319).

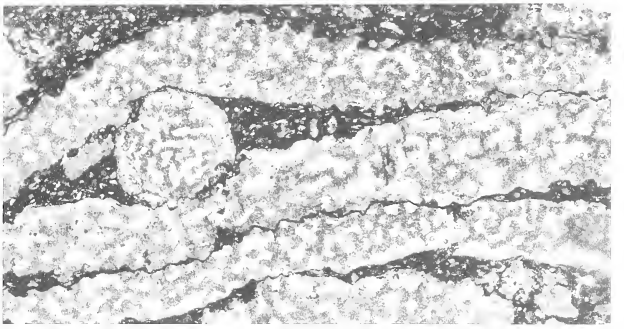

1

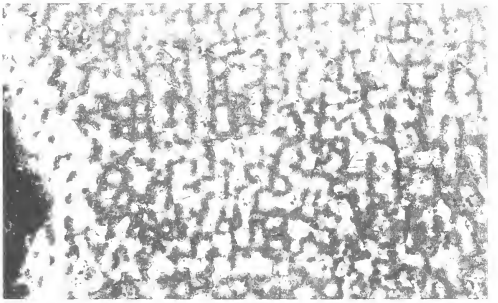

2

4

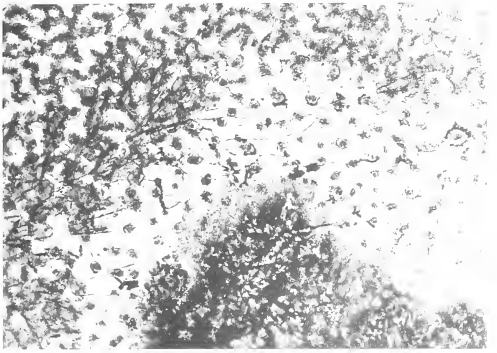

3

5

FISCHBUCH, *Euryamphipora*

GALLOWAY, J. J. and EHLERS, G. M. 1960. Some Middle Devonian stromatoporoids from Michigan and south-western Ontario, including the types described by Alexander Winchell and A. W. Grabau. *Contr. Mus. Paleont. Univ. Mich.* **15,** no. 4, 39–120.

—— and ST. JEAN, J. JR. 1957. Middle Devonian Stromatoporoidea of Indiana, Kentucky, and Ohio. *Bull. Am. Paleont.* **37,** no. 162, 29–308.

JENIK, A. J. and LERBEKMO, J. F. 1968. Facies and geometry of Swan Hills reef Member of Beaverhill Lake Formation (Upper Devonian), Goose River field, Alberta, Canada. *Bull. Am. Assoc. Petrol. Geol.* **52,** 21–56.

KLOVAN, J. E. 1966. Upper Devonian stromatoporoids from the Redwater reef complex, Alberta, Canda. *Bull. geol. Surv. Can.* **133,** 1–33.

LEAVITT, E. M. 1968. Petrology, palaeontology, Carson Creek North reef complex, Alberta. *Bull. Can. Petroleum Geol.* **16,** 298–413.

LECOMPTE, M. 1952. Les stromatoporoïdes du Dévonien moyen et supérieur du Bassin de Dinant. *Mém. Inst. r. Sci. Nat. Belg.* **117,** 216–369.

—— 1956. Stromatoporoidea. In MOORE, R. C. (ed.), *Treatise on invertebrate paleontology.* Part F, F107–44, Univ. Kansas Press and Geol. Soc. Amer.

MCCOY, F. 1884. *A synopsis of the characters of the Carboniferous limestone of Ireland.* Univ. Press, Dublin.

MURRAY, J. W. 1966. An oil-producing reef-fringed carbonate bank in the Upper Devonian Swan Hills Member, Judy Creek, Alberta. *Bull. Can. Petroleum Geol.* **14,** 1–103.

NICHOLSON, H. A. 1886, 1892. A monograph of the British stromatoporoids. *Palaeontographical Soc. London.* Pts. 1, 4, 39, 46, 1–234.

ÖPIK, A. 1935. *Amphipora ramosa* (Phillips) in the marine Devonian of Estonia. *Ann. Nat. Soc. Tartu Univ.* **41,** 1–8.

PHILLIPS, J. 1841. *Figures and descriptions of the Palaeozoic fossils of Cornwall, Devon, and West-Somerset.* Longman, Brown, Green, and Longmans, London.

RIPPER, E. A. 1937. A note on the occurrence of *Amphipora ramosa* (Phillips) in western Australia. *R. Soc. West. Aust. Jour.* **23,** 37–41.

SCHULZ, E. 1883. Die Eifelkalkemunde von Hillesheim. Nebst einem palaeontolog Anhang. *Jb. preuss. geol. Landesanst. Berg Akad. für 1882,* 160–247.

STEARN, C. W. 1961. Devonian stromatoporoids from the Canadian Rocky Mountains. *J. Paleont.* **35,** 923–48.

—— 1963. Some stromatoporoids from the Beaverhill Lake Formation (Devonian) of the Swan Hills area, Alberta. Ibid. **37,** 651–68.

—— 1966*a*. The microstructure of stromatoporoids. *Palaeontology,* **9,** 74–124.

—— 1966*b*. Upper Devonian stromatoporoids from southern Northwest Territories and northern Alberta. *Bull. geol. Surv. Can.* **133,** 35–68.

THOMAS, G. E. and RHODES, H. S. 1961. Devonian limestone bank-atoll reservoirs of the Swan Hills area, Alberta. *Jour. Alta. Soc. Petrol. Geol.* **9,** 29–38.

YAVORSKY, V. I. 1955. Stromatoporoidea Sovetskogo Soyuza, pt. 1. *Trudy Vses. Naucluo-issled. geol. Inst.*, Minist. geol. Okhr. Nedr., n. ser. **8,** 173 pp.

—— 1957. Stromatoporoidea Sovetskogo Soyuza, pt. 2. Ibid. **18,** 78 pp.

—— 1961. Stromatoporoidea Sovetskogo Soyuza, pt. 3. Ibid. **44,** 64 pp.

N. R. FISCHBUCH
33 Fernie Place S.E.
Calgary 27
Alberta, Canada

Final typescript received 15 July 1969

THE GROWTH AND SHELL MICROSTRUCTURE OF THE THECIDEACEAN BRACHIOPOD *MOORELLINA GRANULOSA* (MOORE) FROM THE MIDDLE JURASSIC OF ENGLAND

by P. G. BAKER

ABSTRACT. Analysis of the growth habit of *M. granulosa* from a functional point of view has proved to be of value in the interpretation of shell microstructure. Serial sectioning of shells at 20 μ intervals has revealed that fibre orientation may change suddenly at various levels within a shell. The paper notes the need for detailed information regarding the orientation and location of sections through shells, as study of *M. granulosa* indicates this may be of critical importance. The shell-structure differs markedly from that of *Lacazella mediterranea* (Risso), as the shells of some, if not all Inferior Oolite thecidellinids were differentiated into primary and secondary layers. Interpretation of the microstructure has taken into account the effects of shell resorption in the brachial valve and the development of crescentic tubercles in the pedicle valve. Some evidence has been obtained which indicates that the pedicle opening of *M. granulosa* occupied a supra-apical position. Despite the general spiriferoid appearance of the shell-structure, the detailed microstructure of various morphological features of the two valves, together with bulk morphological similarities, are thought to suggest strophomenoid affinity.

THE microstructure outlined in this paper is based on combined evidence from serial sections and polished blocks prepared from fifty-three specimens, comprised of brachial valves, pedicle valves, and complete shells of *Moorellina granulosa* (Moore), from the Oolite Marl of Westington Hill Quarry in the Cotswolds. The stratigraphy and location of the quarry and the exact horizon from which the material was obtained have been described in a previous paper (Baker 1969). A further horizon has been located in a yellow-orange clay at the base of the Oolite Marl on the west face of the quarry but the material recovered was not sufficiently well-preserved for the study of shell microstructure.

In the material studied, many of the shells are recrystallized but some are well preserved. Partially recrystallized material is useful for comparing and contrasting the unaltered shell with diagenetic effects.

A discussion of the thecideacean environment and a detailed account of the morphology of the brachial valve (Pl. 18, fig. 1) is given in an earlier paper (Baker 1969).

The most prominent feature of thecideidines is the elaboration of the brachial apparatus. The inevitable result of interest in this structure is that in much of the published work the pedicle valve is neglected.

The pedicle valve of thecideaceans is subject to much less variation than the brachial valve and the pedicle valve of *M. granulosa* (Pl. 18, fig. 2) is morphologically very similar to that of *Bifolium faringdonense* (Dav.), described by Elliott (1948). Attachment to the substratum is by cementation and the shape of the pedicle valve is greatly influenced by the size of the scar of the area of attachment. Ontogenetic development of the valve concerns the appearance and development of crescentic tubercles, the change in position of the hinge teeth and the change in the relative proportion of the hemispondylium.

[Palaeontology, Vol. 13, Part 1, 1970, pp. 76–99, pls. 18–21.]

The shell of *M. granulosa* is endopunctate and shows the apparently random distribution noted by Elliott (1955). However, neither the models proposed by Kemežys (1965) nor Cowen (1966), satisfactorily explain the punctation mosaic observed in thecidellinids. An account of the punctation mosaic and the proposal of a new model is to be published separately.

During analysis of the microstructure, particular care has been taken to attach significance only to structures seen in at least six different specimens. Occasional peculiar features are noted which may be important but occur so infrequently in the material studied that firm conclusions must not be drawn from them.

Acknowledgements. The author is indebted to Dr. J. D. Hudson, Geology Department, University of Leicester, for supervision of the preparation of this paper. Thanks are due to Dr. M. Talbot, Geology Department, University of Dundee, for the loan of Upper Oxfordian material for comparison purposes and to Mr. G. McTurk for preparing the stereoscan negatives. Finally I wish to thank Professor P. C. Sylvester-Bradley for use of the research facilities of the University of Leicester.

Registration of material. The material figured in this paper, in the form of etched blocks and complete specimens, together with original peels and, where available, duplicates, is to be housed in the museum collection of the Department of Geology, University of Leicester, under the catalogue numbers quoted.

PREPARATION OF MATERIAL

A comprehensive account of the preparation of Oolite Marl material is given in Baker (1969) and the material studied in the present paper was obtained by the same method. For microstructure investigation however, it has been discovered that reduction of the etching time from ten seconds in 5 % HCl, to eight seconds in 3 % HCl yields better results. In addition it was found that fresh resin does not make a good bond with plain glass slides and blocks may become detached during sectioning. A more effective bond is obtained by the use of ground glass slides.

GROWTH AND DEVELOPMENT OF THE SHELL

General. The nature of shell growth is mixoperipheral, leading to a strophic condition (Rudwick 1959, p. 18), as, contrary to the belief of Elliott (1965), a small hypercline dorsal interarea (by definition, Williams 1965, H59) is present (Pl. 18, fig. 5). The lateral profile is obscured by the area of attachment but in forms with a small area of attachment, may be described as modified plano- to concavo-convex with a rectimarginate commisure. Certain differences in the development of structures in the brachial and pedicle valves have taxonomic significance and they will be discussed separately, following an account of the general shell growth.

A comprehensive account of shell deposition in living brachiopods is given by Williams (1956, 1966, 1968*a*, *b*), Williams *et al.* (1965) and it is reasonable to suppose the shell of *Moorellina granulosa* (Moore) was deposited in the same manner. Evidence presented in this paper shows that Williams (1968*a*) is in error in regarding the single layered shell of *Lacazella mediterranea* (Risso) as typical of the thecideidine shell structure. *M. granulosa* clearly shows the development of primary and secondary shell layers.

As described in an earlier paper (Baker 1969) the brachial valve of *M. granulosa* is initially almost circular, later becoming broader than long. However, study of a number

of specimens shows that the shape of the brachial valve is really controlled by the shape of the pedicle valve, which is itself strongly influenced by the size of the scar of the area of attachment. Williams (1956) has shown that although cell division occurs throughout the epithelium the enlargement of the brachiopod shell is controlled mainly by peripheral zones of growth.

Various aspects of the mode of shell growth have been defined by Rudwick (1959, p. 2). It is convenient for the purpose of demonstrating the mode of growth in *M. granulosa* to use his second interpretation, i.e. that the shell surface represents a series of sectors which were formed continuously by different arcs of the valve edge.

At a magnification of 250× linear, the external surface of the shell of well-preserved specimens of *M. granulosa* is seen to be covered with small fibres. These fibres are inclined radially outwards from the umbo at a low angle from the shell surface and show an orientation normal to the growth-lines and commissure (Pl. 18, fig. 3). If one assumes that the fibres are associated with the deposition of primary shell, either mechanically or crystallographically, their orientation directions may be used as growth vectors for the determination of points of relatively rapid increase in various arcs of the commissure.

Rudwick has shown how growth at any point on the valve edge may be resolved into component growth rates. By assigning a value of one growth unit to an arbitrary surface area corresponding to Rudwick's growth points (1959, text-fig. 1*a*), provided that the growth vectors are known, different rates of growth in different sectors of a shell can be fairly accurately determined. To demonstrate this adequately in *M. granulosa* necessitates the introduction of additional 'momentary' and 'cumulative' terms. The growth vector may be regarded as the cumulative product of the arrangement of growth units normal to the mantle edge. The total number of growth units per growth vector may be represented as $d/\sqrt{x}$, where d represents the length of the vector and x represents the surface area of the growth unit. *Proliferation points* occur where the distance between two growth vectors has doubled and *proliferation arcs* are represented by lines joining series of new proliferation points. The growth rate in any sectors may be determined by the *growth acceleration*, v, which is represented by the number of proliferation arcs in any sector. The *relative growth index* may therefore be expressed as $v(d/\sqrt{x})$ for any sector

EXPLANATION OF PLATE 18

Stereoscan photomicrographs of specimens of *Moorellina granulosa* (Moore) from the Oolite Marl, Westington Hill Quarry near Chipping Camden. All figures are of specimens coated with evaporated aluminium before photography.

Fig. 1. Interior view of a brachial valve (37512) showing the median septum and tuberculate sub-peripheral rim. Bridge and brachial apparatus broken. ×40.

Fig. 2. Interior view of a pedicle valve (37513) showing the teeth, supported hemispondylium and the sub-peripheral crescentic tubercles. Umbonal cavity filled by the broken cardinal process. ×40.

Fig. 3. External surface of a portion of the left postero-lateral region of a brachial valve (37512) showing the oriented fibres on the surface of the primary layer. Scale represents 30 μ.

Fig. 4. Lateral view of a complete specimen (37511) showing the growth habit and large free ventral anterior surface. ×50.

Fig. 5. Posterior view of specimen (37511) showing the large, ventral and small, dorsal interareas. Angle of incidence 40°. ×40.

Fig. 6. Profile view of an enlarged portion of specimen (37513) showing the supporting septum of the hemispondylium, with the dental ridges continuous with the outer edges of the hemispondylial plates. Angle of incidence 60°. ×65.

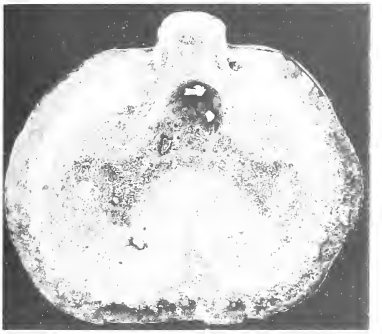

1

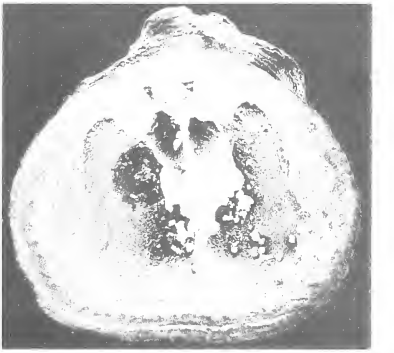

2

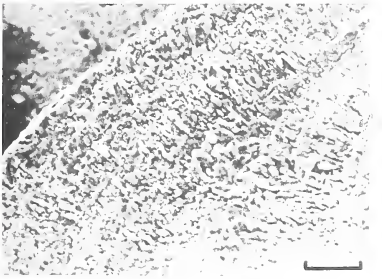

3

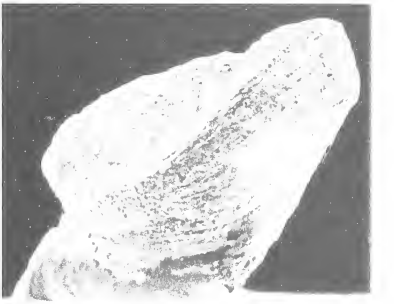

4

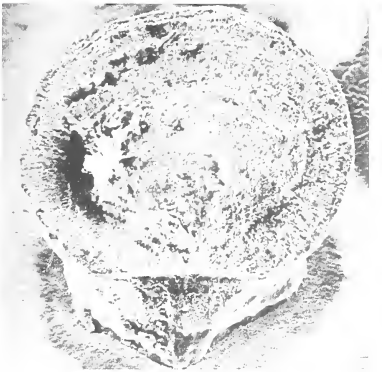

5

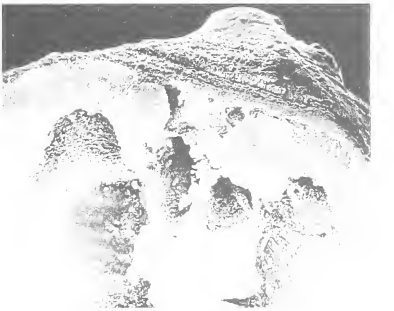

6

BAKER, *Moorellina granulosa*

of the valve. In Rudwick's terms, proliferation points and proliferation arcs are momentary and growth acceleration and relative growth index are cumulative.

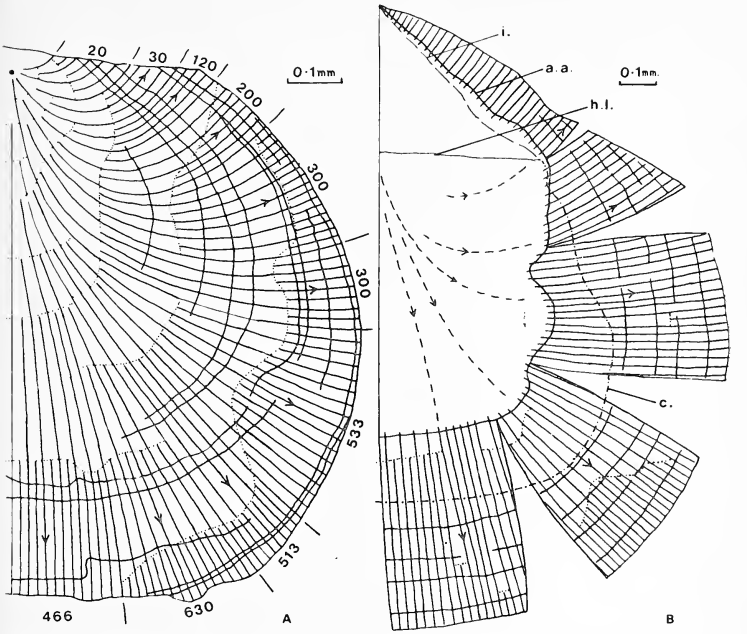

TEXT-FIG. 1. Reconstruction of the primary growth vectors of *M. granulosa*, plotted from oriented fibres. Proliferation arcs dotted. Concentric lines represent visible growth-lines. A. Right half of a brachial valve. Numbers indicate relative growth indices in different sectors. B. Right half of a pedicle valve. Broken lines within the area of attachment represent the vector mosaic inferred by the brachial valve. Commissure projected stereographically to allow plotting of the primary growth vectors. The relative position of a.a. edge of the area of attachment, c. commissure and i. edge of interarea, plotted from cellulose acetate peels. h.l. hinge-line.

Brachial valve. The growth of the brachial valve of *M. granulosa*, when expressed in the manner outlined, shows a marked radial pattern with a high relative growth-rate anterolaterally (text-fig. 1A). For the reasons outlined in Williams and Wright (1963) it is considered that it is only necessary to plot the data for one-half of the valve.

The validity of the above interpretation obviously rests on the assumption that the proposed association of fibre orientation with deposition of the primary layer is correct. The author is alive to the possibility that in the material investigated, the growth vectors

are not recorded from the exposed ends of primary fibres but from crystallites growing on their outer ends. However, the fibre orientation pattern shows a remarkable constancy in the thirty external brachial surfaces examined. Even if the development of the fibres is diagenetic, the constancy of their orientation pattern must be in some way connected with the microstructure of the primary layer, most probably the crystallographic orientation of the primary fibres themselves (Cloud 1942, p. 24).

Pedicle valve. Analysis of the growth-lines of the pedicle valve of *Thecidiopsis* (Nekvasilová 1967) has enabled determination of the mode of development. Study of *M. granulosa* shows that the pedicle valve exhibits the same development régime, which, when advanced, produces an almost linear pattern masking the radial growth typical of brachial valves. After the development of the area of attachment and presumably in response to environmental influence, material is added to the anterior and antero-lateral regions of the pedicle valve much more rapidly than in the other regions so that the angle between the plane of the commissure and the plane of the area of attachment changes rapidly and the anterior and antero-lateral regions of the shell develop rapidly without appreciably increasing the length of the commissure. This means that the deposition of the primary layer of the pedicle valve although remaining normal to the valve margin shows a distinctly linear growth orientation anteriorly (text-fig. 1B). In Rudwick's terms therefore, the growth of the shell of *M. granulosa* is characterized by a declining vertical component in the brachial valve and an increasing vertical component in the pedicle valve, a cumulative growth pattern which obviously serves to lift the anterior gape away from the substratum (Pl. 18, fig. 4).

Secondary layer. As shown by Williams the secondary shell consists essentially of fibres arranged with their long axes at a low inclination to the internal surface of the primary layer and overlapping to a greater or lesser extent according to the angle of inclination, usually about 10°. By plotting the orientation of the long axes of exposed parts of secondary fibres, Williams (1968*a*, pp. 10–15) has demonstrated a discernible lineation in several genera. Construction of a secondary growth mosaic for *M. granulosa* shows the existence of the same spiral arc arrangement in which there is a relatively constant deflexion of the secondary fibres (text-fig. 2). The pattern is modified anteriorly in the brachial valve by the development of the relatively very thickened anterior of the median septum. There is no sign of peripheral reorientation normal to the shell edge but this may simply be the result of the disruptive influence of the tubercle cores. Williams (1966, p. 1148) notes the blurring of the pattern in areas of excessive calcite deposition in terebratuloids. In the pedicle valve also, the spiral arc pattern is modified anteriorly by the development of the crescentic tubercles. However, although Williams is able to demonstrate the bulk migration of the mantle in the direction of growth (1968*a*, p. 8) in order to account for the inclination of secondary fibres, the reason for the migration has not been explained. Study of his text-figure makes it apparent that it is impossible to extend the fibre series anteriorly or posteriorly without changing their inclination. The situation is further complicated by trying to impose the model on a convex shell. There is ample figured evidence, however, to show that his account of fibre shape must be correct. The solution to the problem must, therefore, lie in the orientation of the fibres themselves. The length of the fibres in any zone of the shell seems to remain fairly constant, suggesting that the cells of the epithelium secreting them have a standard life and

secretory activity. Obviously the rate of cell division in the mantle groove must vary to account for the growth characteristics of the shell. If the organization of the cells is such that the calcite of the secondary fibres is secreted at a fairly constant rate, areas showing

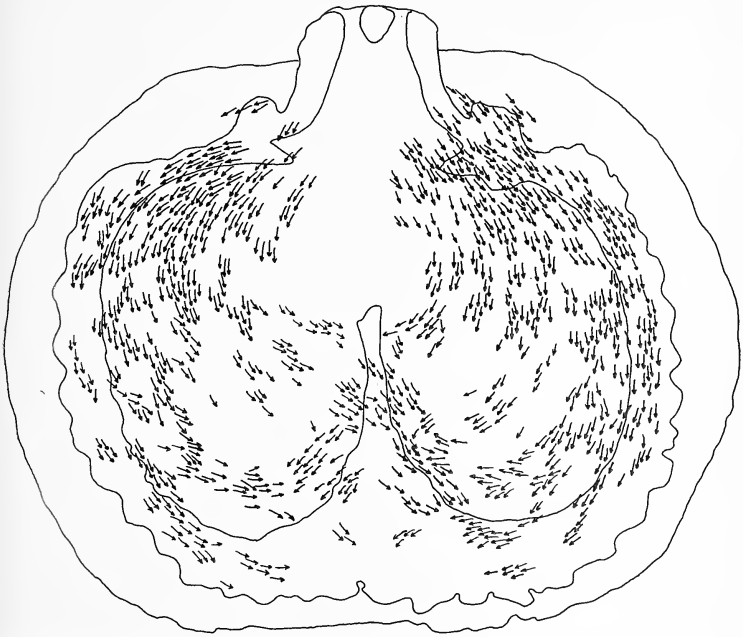

TEXT-FIG. 2. Reconstruction of the secondary growth mosaic of *M. granulosa*, plotted from twenty-five superimposed peels. Solid outline represents the position of the sub-peripheral rim, median septum, and cardinal process.

a relatively slow vectoral primary growth rate, i.e. postero-lateral sectors, must suffer from a build-up of secondary shell, unless the fibres are deflected away from the primary growth vectors in order to prevent the shell from becoming excessively thickened. Conversely the fibres may be deflected towards areas where thickening of the shell is taking place, such as the development of the median septum (text-fig. 2). This orientation deflexion of the secondary fibres away from sectors of relatively decelerated deposition of primary shell material would readily explain the forward migration of the secreting cells and the difference in orientation between the vectors of the primary and secondary layers (text-figs. 1A, 2).

DEVELOPMENT OF SPECIFIC STRUCTURES

Development of the sub-peripheral rim. Very little progress regarding the determination of the microstructure of the brachial valve was made until the mode of development of the sub-peripheral rim was appreciated. Williams (1968*a*, p. 50) described local resorption in *Lacazella* and resorption is found to play an important role in *M. granulosa*. Ontogenetic studies (Baker 1969) show that the sub-peripheral rim appears at the preforbesiform stage of development and subsequently occupies the same position relative to the valve margin, irrespective of the size of the valve. As the sub-peripheral rim is too prominent to be submerged by subsequent secondary shell deposition, it must migrate outwards. Evidence that the migration is accomplished by development at the external margin of the rim and resorption along its inner margin will be presented later. The sub-peripheral rim is tuberculate and the generative zone of the tubercles appears to be where the secretory activity of the outer epithelial cells changes from the deposition of primary to the deposition of secondary fibres.

Development of the hemispondylium. Elliott (1948) noted the presence of a structure in the floor of the pedicle valve of *Bifolium faringdonense* (Davidson) to which he gave the name hemispondylium. In his opinion, the structure was not formed by the fusion of dental plates. Elliott also noticed the presence of what might almost be called dental ridges, buttressing the hinge teeth internally but adopted the view that they played no part in the formation of the muscle supports (spondylium) as in other brachiopods, a view confirmed by the present work. Some specimens of *M. granulosa* however, show that the buttressing ridges which may represent rudimentary dental plates, are continuous with the upturned outer edges of the hemispondylial plates (Pl. 18, fig. 6). This arrangement is an interesting feature and may be homologous with the ankylosed median septum–dental ridge structure of the davidsoniacean *Orthotetes*.

Sectioned material enables resolution of the problem. Forms with a supporting septum have the appearance of possessing a spondylium simplex (text-fig. 3A–C, G). However, forms with a sessile hemispondylium show quite clearly that the dental ridges simply merge with the floor of the valve (text-fig. 3D–F, H). There can be no doubt therefore, that Elliott's interpretation is correct and that the hemispondylial plates are not formed by the fusion of dental plates but from secretion of secondary shell by the outer epithelium adjacent to the supporting septum. The dental ridges may or may not unite with them depending on the growth habit of the valve. In forms with well-developed dental ridges it is possible to obtain sections which are strikingly similar to sections through the umbonal region of pedicle valves of *Derbyia* (Williams *et al.* 1965, H404, fig. 261 D). As Nekvasilová (1964) has recorded in *Lacazella* (*B*) *lacazelliformis* (Elliott) and as Elliott has recorded in *B. faringdonense*, the hemispondylium is present in the smallest valves studied and may be sessile or supported by a median septum. Rare specimens may show the hemispondylial plates supported by a double septum anteriorly. A single specimen of *M. granulosa* shows the hemispondylial plates supported by three septa whilst another (Pl. 19, fig. 1) shows a reticulate support. The form of the hemispondylium may be correlated with the form of the area of attachment and is apparently related to muscle efficiency (Elliott 1948, p. 20).

Development of the crescentic tubercles. Post-forbesiform and adult pedicle valves are characterized by the development of structures along the internal edge of the valve

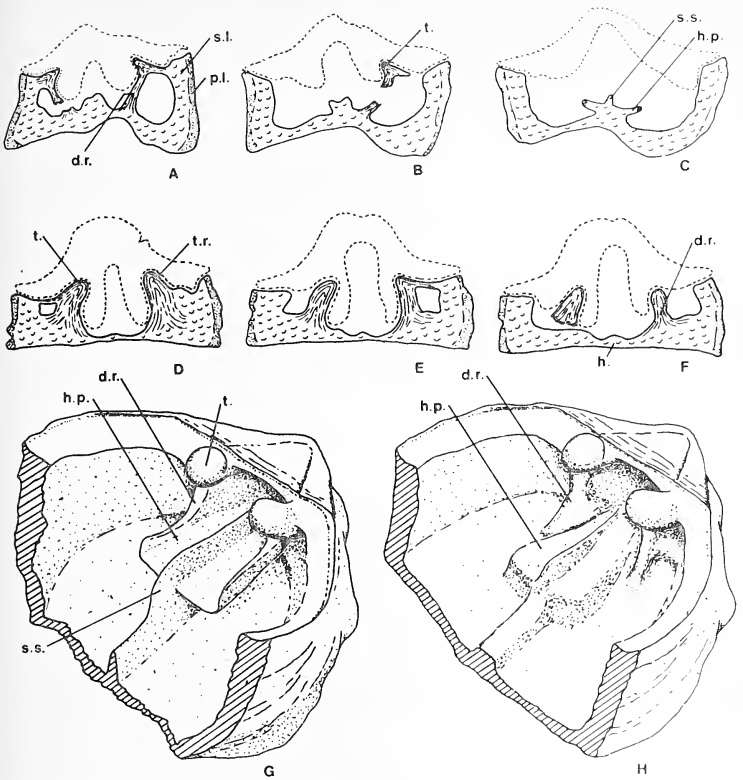

TEXT-FIG. 3. A–C. Three serial sections through *M. granulosa* to show the form of the supported hemispondylium. D–F. Three serial sections, showing the form of the sessile hemispondylium. G. Three-quarters profile reconstruction of a supported hemispondylium, showing the dental ridges continuous with the hemispondylial plates. H. Three-quarters profile reconstruction of a sessile hemispondylium, showing the dental ridges merging with the floor of the valve. Outline of brachial valve dotted. d.r. dental ridge, h. root of sessile hemispondylium, h.p. hemispondylial plate, p.l. primary layer, s.l. secondary layer, s.s. supporting septum, t. tooth, t.r. tooth ridge.

margin (Pl. 18, fig. 2; Pl. 19, fig 2). which Elliott in *B. faringdonense* has called sub-pustulose marginal ornament. In *M. granulosa* these structures can be shown to be modified tubercles and are thought to be of considerable importance. As their shape is quite characteristic it is proposed to designate them crescentic tubercles. They appear

to be most strongly developed in the anterior and antero-lateral sectors of the valve and show a development pattern entirely different from that of the tubercles of the sub-peripheral rim. Crescentic tubercles do not appear until the anterior of the pedicle valve begins to grow away from the attachment surface. They apparently grow simply by the incremental addition of material at their distal ends and the secreting cells must occupy an invagination of the outer epithelium so that the tubercle cores stay slightly in advance of adjacent outer epithelial secretory cells. Their relationship with adjacent secondary fibres would indicate that their long axes are not quite parallel with the internal shell surface but inclined dorsally inwards at an angle of about 2°. This development pattern of the crescentic tubercles is obviously related to the maintenance of a constant orientation relative to the tubercles of the sub-peripheral rim (text-fig. 6A, C).

DETAILED MICROSTRUCTURE

As already noted, *Moorellina granulosa* (Moore) offers conclusive proof that in some Jurassic thecidellinids at least, the shell was differentiated into primary and secondary layers. The primary layer is best seen in the pedicle valve where it is relatively much thicker than in the brachial valve. It is possible that in some specimens the thin primary layer may occur only sporadically as in orthoids and strophomenoids where its absence is attributable to wear of a very thin layer. The possibility of the removal of the primary layer is important in the interpretation of occasional pitted structures, described later, occurring in the outer surface of some brachial valves.

The primary crystallite mat gives the typical fibrous, transverse (Pl. 19, fig. 3) and pitted, horizontal (Pl. 19, fig. 4) sections described by Williams. Transverse sections through secondary fibres show typical cross-sections (Williams 1968*a*, p. 9) with the exception that the lateral areas are much reduced so that a sub-hexagonal pattern is produced (Pl. 19, fig. 5). This standard shape appears to persist throughout the secondary layer of the pedicle valve but shows some modification in the brachial valve. Patches of fibres in the brachial valve show dorso-ventral flattening distally so that they develop

---

EXPLANATION OF PLATE 19

Stereoscan photomicrographs of specimens of *Moorellina granulosa* (Moore). Material of all figures coated with evaporated aluminium before photography.

Fig. 1. Interior view of a broken pedicle valve (37514) showing the hemispondylial plates supported by a reticulate structure. Umbonal region missing. ×40.

Fig. 2. Enlarged portion of the margin of pedicle valve (37515), showing the position and characteristic shape of the crescentic tubercles. ×170.

Fig. 3. Etched surface prepared from polished block (37516) showing the primary layer in transverse section, lower right, and detail of the junction with the secondary layer. Section orientation: vertical, longitudinal. Section location: pedicle valve, free anterior surface, close to the area of attachment. Scale represents 4 μ.

Fig. 4. Stereoscanned cellulose acetate peel (37518), showing the primary layer in horizontal section, lower right. Section orientation: perpendicular to the plane of the commissure at 75° to the long axis. Section location: pedicle valve, left postero-lateral sector. Scale represents 8 μ.

Fig. 5. Stereoscanned cellulose acetate peel (37518) showing transverse section through secondary fibres. Section orientation and location as fig. 4. Scale represents 5 μ.

Fig. 6. Interior of the brachial valve of a pre-forbesiform individual (37503) showing endopuncta and the exposed inner ends of secondary fibres on the floor of the left brachial cavity. Scale represents 5 μ.

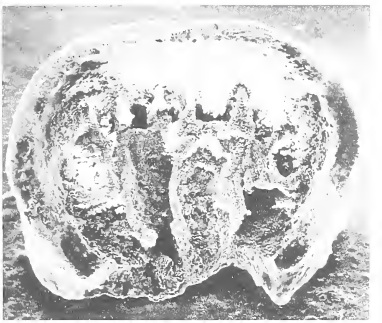

1

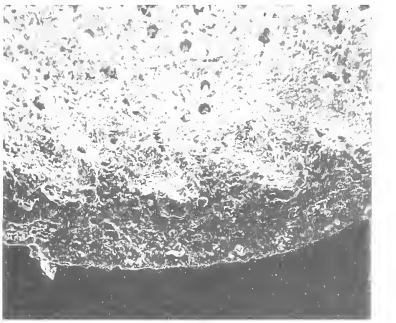

2

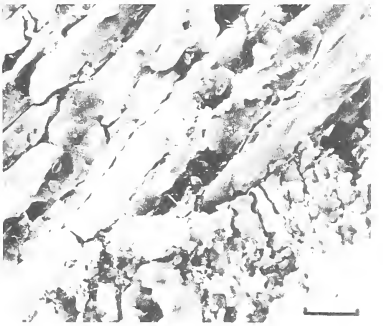

3

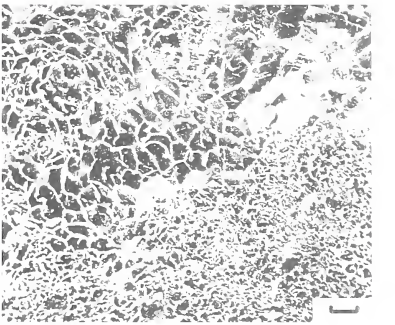

4

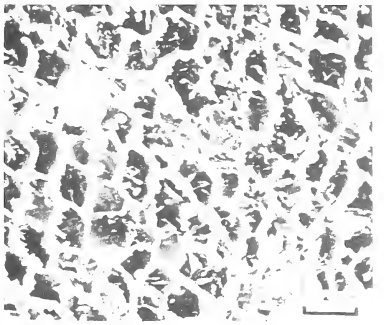

5

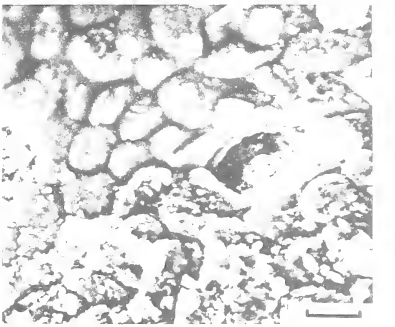

6

BAKER, *Moorellina granulosa*

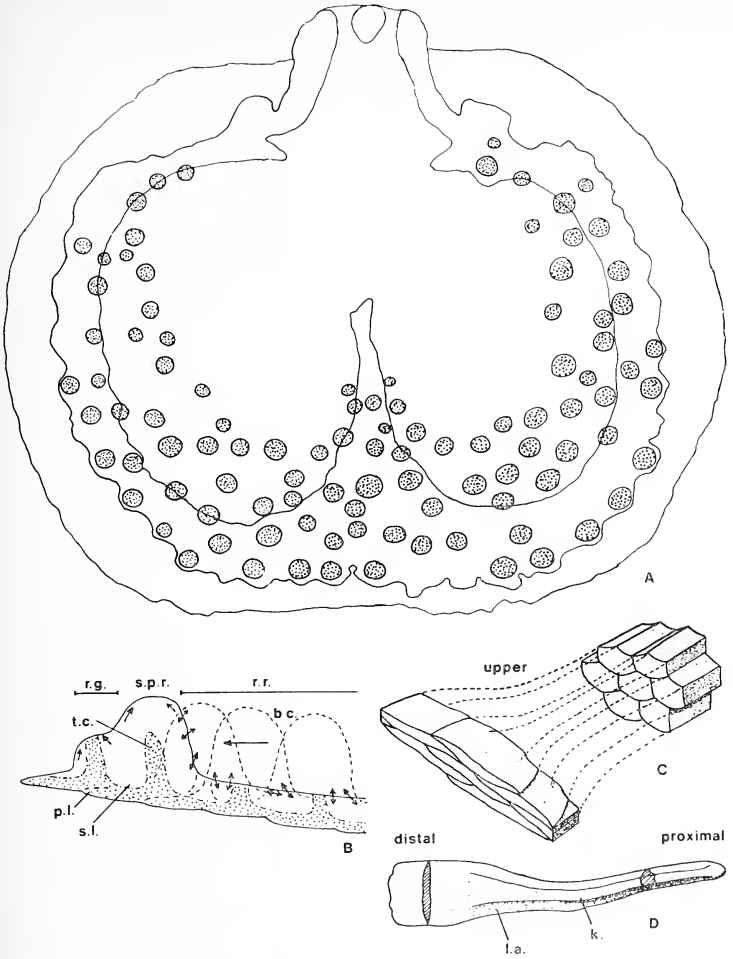

TEXT-FIG. 4. A. The distribution of the tubercle cores (dotted) in the brachial valve of *M. granulosa*, plotted from twenty-five superimposed peels. The core distribution inside the sub-peripheral rim, outlined, indicates the areas of the brachial cavities where resorption has occurred. B. Diagrammatic representation of the probable mode of migration of the sub-peripheral rim during growth. C. Normal and flared transverse mosaics. D. Diagram to show the shape of an individual fibre. b.c. brachial cavity, k. keel, l.a. lateral area, p.l. primary layer, r.g. rim generation zone, r.r. rim resorption zone, s.l. secondary layer, s.p.r. sub-peripheral rim, t.c. tubercle core.

flared ends (text-fig. 4C, D). The possibility that these were merely apparent transverse sections, produced by fibre reorientation was checked against horizontal longitudinal sections through fibres. The flared secondary fibres have a characteristic strap-like appearance and are up to three times (10–12 μ) the width of normal fibres. It is possible that the modified fibres are associated with muscle scars but this could not be confirmed in the material studied. The location of the sections however, would suggest that the fibres occur in zones of the valve which were not areas likely to be associated with muscle attachment.

The variability of the fibres in section and the consequent possibility of misinterpretation of sections has been noted by Williams (1966, p. 1148). The present work has been hindered by the same rapid changes of fibre orientation. Studies indicate that orientation variation in the secondary layer may occur at different depths, in different sectors of a valve, and that the microstructure of the brachial and pedicle valves of the same animal may show significant differences. For this reason it is felt that all future plate figures must be accompanied by accurate data concerning the orientation of sections through the specimen and the exact location of the section on the shell. The author has attempted to present such data in a concise form in the plate explanations, to enable other workers to avoid or duplicate these sections in subsequent investigations.

Relatively large areas of the brachial cavities of *M. granulosa* are formed by the progressive resorption of the sub-peripheral rim (text-fig. 4A, B). As a result of resorption in these areas, the fibre orientation persisting at the bases of former sub-peripheral rim tubercles is exposed on the internal surface of the valve, producing a very disturbed pattern (Pl. 20, figs. 1, 2). Once the significance of rim resorption had been appreciated, it was realized that undisturbed secondary mosaic would only be seen in areas which were not affected by shell resorption. This suggested three possible sites, (*a*) the border

EXPLANATION OF PLATE 20

Stereoscan photomicrographs of *Moorellina granulosa* (Moore) except figs. 7 and 8. Material of all figures coated with evaporated aluminium before photography.

Fig. 1. Interior view of a brachial valve (37519), showing an endopuncta and disturbed secondary mosaic, right, in the area affected by resorption of the sub-peripheral rim. Scale represents 5 μ.

Fig. 2. Stereoscanned cellulose acetate peel (37520), showing the disturbed secondary layer of the brachial valve and the development of flared fibres, lower centre. Section orientation: parallel with the plane of the antero-lateral surface. Section location: right antero-lateral sector 0·12 mm. from the external surface of the valve. Scale represents 25 μ.

Figs. 3–5. Stereoscanned cellulose acetate peel (37522).

Fig. 3. Section through the sub-peripheral rim showing the tubercle cores in cross section, offset by one half-phase. Two partially resorbed cores are visible along the inner margin of the rim, top left. Section orientation: parallel with the plane of the commissure. Section location: brachial valve, left antero-lateral sector 0·048 mm. from the distal ends of tubercles. Scale represents 20 μ.

Figs. 4, 5. Isolated tubercle cores in areas of the brachial cavity affected by resorption of the sub-peripheral rim (fig. 4) and tubercle cores continuous with the primary layer (fig. 5, centre and lower right). Section orientation and location as in fig. 3, but 0·144 mm. from the distal ends of tubercles. Scale represents 20 μ.

Fig. 6. Stereoscanned cellulose acetate peel (37523). Vertical section through the sub-peripheral rim showing tubercle cores in oblique section. Section orientation: perpendicular to the external shell surface at 85° from the long axis. Section location: brachial valve, right antero-lateral sector. Scale represents 30 μ.

Figs. 7, 8. Stereoscan photomicrograph of the external surface of a brachial valve of *Moorellina ornata* (Davidson) (37524), showing detail of the structures interpreted as weathered tubercle cores. × 1000.

1

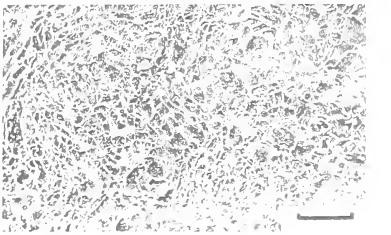

2

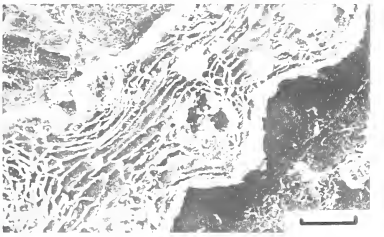

3

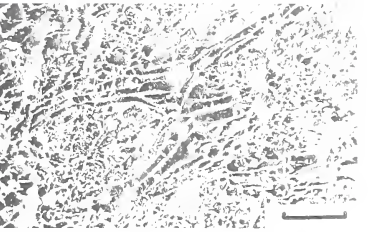

4

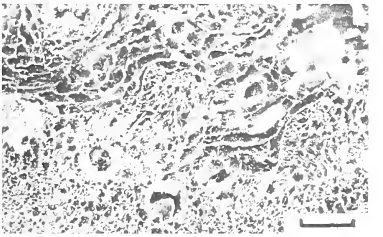

5

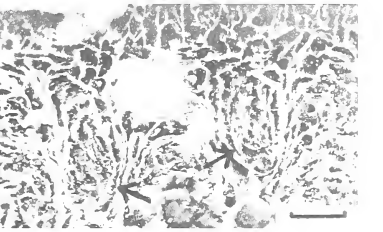

6

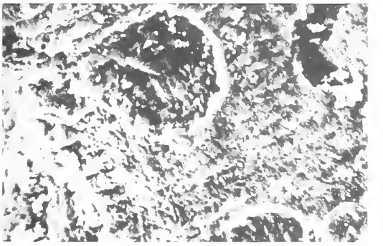

7

8

BAKER, *Moorellina granulosa*

region outside the sub-peripheral rim, (*b*) the pedicle valve, and (*c*) the brachial cavities of pre-forbesiform (Baker 1969) individuals, where rim resorption had not yet begun. A detailed examination of brachial and pedicle valves was then undertaken with these considerations in mind. The border region has proved to consist entirely of primary shell and the mosaic on the inner surface of the pedicle valve is obscured by the development of crescentic tubercles. A pre-forbesiform brachial valve (37503) however, clearly shows traces of the internal mosaic of the secondary layer (Pl. 19, fig. 6).

The observed differences in the brachial and pedicle valves of *M. granulosa* have produced significant differences in microstructure and render it necessary that the microstructure of the two valves be described separately.

Brachial valve. A thin primary and a disturbed secondary layer associated with the development and migration of the sub-peripheral rim are present.

A detailed investigation of the tubercles of the sub-peripheral rim was undertaken. If the concept of resorption is correct, it should be possible to distinguish the remains of tubercle cores in areas of the brachial cavity formerly occupied by the sub-peripheral rim. Horizontal, transverse, oblique, and longitudinal sections were prepared in order to establish their presence. Horizontal serial sections (Pl. 20, figs. 3–5) show that the tubercles are cored structures and that the tubercle cores are, in fact, continuous with the material of the primary layer (Pl. 20, fig. 5). The tubercle cores may be regarded therefore, as being composed of primary shell type material. The question of whether the primary layer has suffered diagenesis has little significance as the material of this layer and of the tubercle cores has the same characteristics and may logically be considered to have the same origin. The author envisages localized patches of outer epithelium continuing to secrete primary shell. It seems probable that the mechanism of development is similar to that which controls the initiation of punctae, as tubercles also are normally, but not universally, offset by one half-phase (Pl. 20, figs. 3, 5). A plot of the tubercle cores in superimposed serial sections through a brachial valve of *M. granulosa* shows that they persist through several sections and are intimately connected with the development of the sub-peripheral rim. They do not appear in zones of the shell which may be logically considered to have been deposited prior to the appearance of that structure (text-fig. 4A). Horizontal sections through the sub-peripheral rim (Pl. 20, fig. 3) confirm that the tubercle cores originate near the mantle edge, in fact at the outer boundary of the sub-peripheral rim itself, and close to the point where the secretion of secondary shell begins. Subsequent isolation of eroded tubercle cores in the brachial cavities is brought about by the mode of development of the sub-peripheral rim during ontogeny (Pl. 20, fig. 4). Vertical sections (Pl. 20, fig. 6) show that the tubercle cores are inclined at a high angle, almost normal to the external shell surface, with a slight outward deflection.

That the tubercle cores of the brachial valve are composed of primary shell material would appear to be confirmed by occasional curious pitted structures occurring on the external surface of valves. Although these occur in *M. granulosa* they are better preserved in the Upper Oxfordian, *Moorellina ornata* (Moore) (Pl. 20, figs. 7, 8). Each pit has a central granular mound and may possibly be interpreted as some form of exopuncta. However, in the light of observations regarding the thickness of the primary layer and the fact that the tubercle cores are shown to be continuous with it, it would appear that what is actually seen is the outer boundary of the secondary layer, exposed by the

removal of primary shell. In which case, the apparent bands are the long axes of fibres and the central mounds of the pits are really weathered tubercle cores. This is supported by: (*a*) the orientation of the fibres is correct if they constitute part of a normal spiral arc, (*b*) they are the right thickness, about 4 μ, (*c*) the granular nature of the central mound is the same as that of sectioned tubercle cores, (*d*) the diameter of the pits is the same as the diameter of tubercle cores in section, i.e. 25–30 μ, and (*e*) they are too large to be normal punctae which have a diameter of only 8–10 μ.

Pedicle valve. A well-developed primary and secondary layer are present. The primary layer thins posteriorly and the secondary layer shows modification anteriorly as a result of the growth habit of the valve.

Attempts to reconstruct a secondary mosaic in the manner described above, failed to produce a decipherable pattern because the secondary layer of the pedicle valve of *M. granulosa* is itself composed of two regions with regard to fibre orientation. There is an outer, essentially normal, spiral arc orientation and an inner layer in which the fibre orientation is intimately bound up with the development of the crescentic tubercles (Pl. 21, figs. 1, 2). In the lateral and postero-lateral sectors of the valve, the secondary fibres show a normal spiral arc arrangement. In the zones of the anterior surface adjacent to the area of attachment, the orientation of the fibres of both regions of the secondary layer appear to follow the primary growth vectors and longitudinal sections produce typical longitudinal sections through fibres (Pl. 21, fig. 3). However, as growth of the pedicle valve proceeds away from the substratum, the secondary layer is differentiated into outer and inner regions. The orientation of the fibres in the outer region changes in such a way that they come to lie almost parallel with the commissure. Longitudinal

EXPLANATION OF PLATE 21

Stereoscan photomicrographs of specimens of *Moorellina granulosa* (Moore). Material of all figures coated with evaporated aluminium before photography.

Fig. 1. Stereoscanned cellulose acetate peel (37520). Transverse section through a pedicle valve showing the orientation of the outer fibres of the secondary layer and the reniform tubercle cores. Section orientation: parallel with the plane of the commissure. Section location: left antero-lateral sector, 0·4 mm. from the distal ends of the tubercles. Scale represents 50 μ.

Fig. 2. Stereoscanned cellulose acetate peel (37521). Section through the secondary layer showing fibres deflected by the crescentic tubercles. Section orientation: parallel with the anterior surface. Section location: pedicle valve, anterior surface, 0·168 mm. from the external surface. Scale represents 20 μ.

Figs. 3, 4. Etched surface prepared from polished block (37516). Section orientation and location as in fig. 3 (Pl. 19). Fig. 3 shows the primary layer, bottom and detail of the secondary fibres in longitudinal section. Fig. 4 shows reorientation of the fibres of the outer region of the secondary layer to give almost transverse section. The elongate fibres (oblique section), upper left, represent a tubercle core sectioned near the axis. Scale represents 10 μ.

Fig. 5. Stereoscanned cellulose acetate peel (37521). Section through the secondary layer showing the fibrous cores of the crescentic tubercles. Section orientation and location as in fig. 2, but 0·096 mm. from the external surface. Scale represents 50 μ.

Fig. 6. Interior view of the anterior surface of a pedicle valve (37515) showing the arrangement of the punctae in rows relative to the crescentic tubercles. $\times$ 50.

Fig. 7. Stereoscanned cellulose acetate peel (37523). Transverse section through the ventral umbonal region showing the plugged pedicle opening and dorsally exposed pedicle sheath. Section location: 0·08 mm. from the umbo. Scale represents 50 μ.

Fig. 8. Retouched photomicrograph of fig. 7.

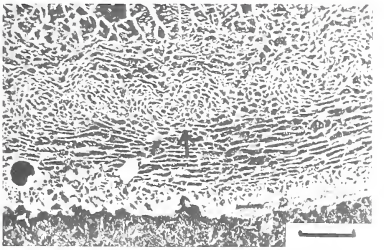

1

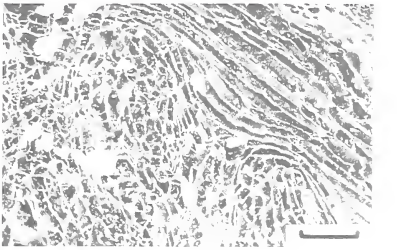

2

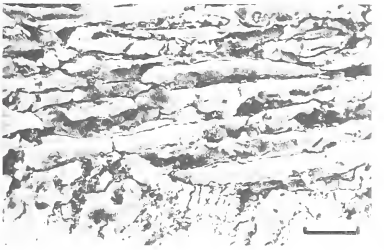

3

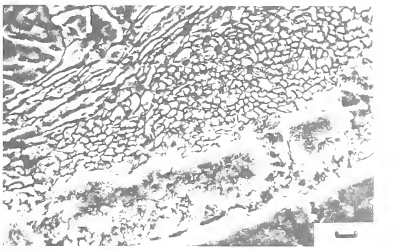

4

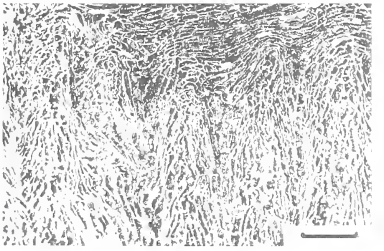

5

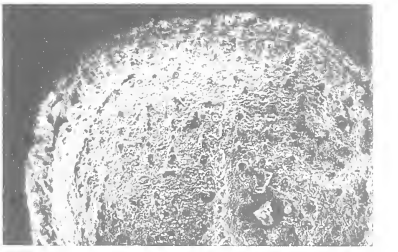

6

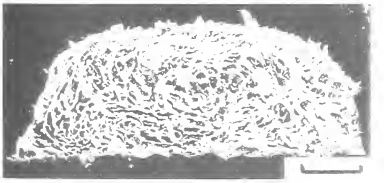

7

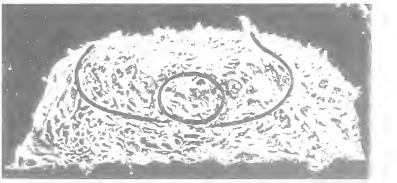

8

BAKER, *Moorellina granulosa*

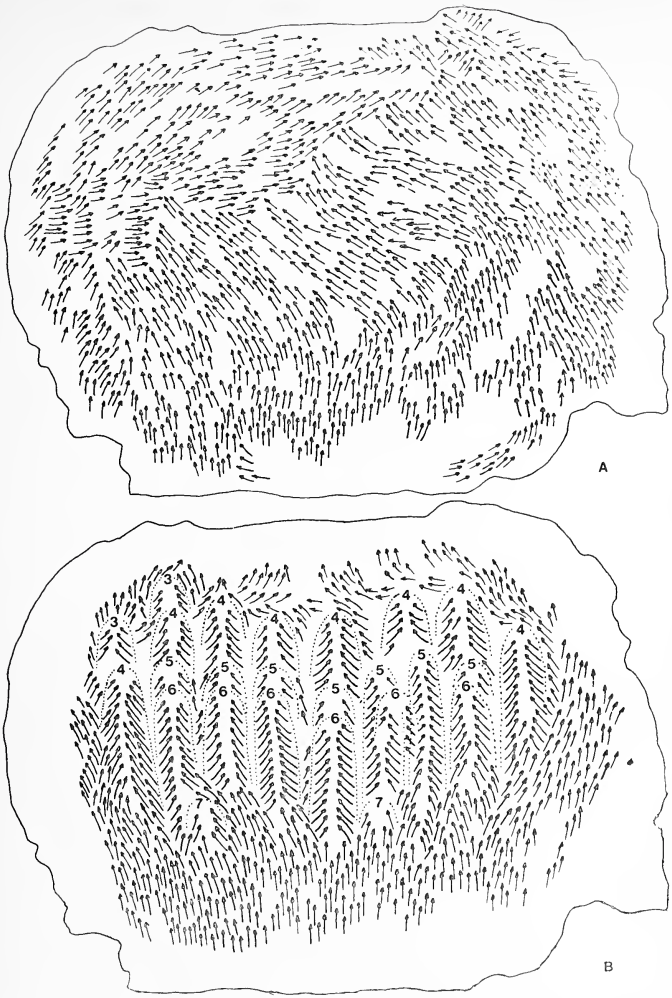

TEXT-FIG. 5. Reconstruction of the fibre orientation of the outer and inner regions of the secondary layer of the free anterior of the pedicle valve of *M. granulosa*, from eight superimposed peels. A. Fibre orientation of the outer region. B. Fibre orientation and tubercle cores of the inner region. Numbers indicate the position of the tubercles in successive peels, from the internal surface of the valve.

sections through these zones produce almost transverse sections through the fibres of this outer layer (Pl. 21, fig. 4).

With this information available the growth mosaics of the two regions were fairly easily reconstructed by plotting the fibres of the outer and inner regions separately. This was achieved by plotting the primary/secondary layer junctions of serial sections, together with the orientation direction of the fibres adjacent to the junctions. The mosaic produced (text-fig. 5A) was interpreted as representing the growth mosaic of the outer region of the secondary layer of the anterior surface of the pedicle valve. Similarly, a re-plot of the remaining fibre orientation on each serial section, i.e. omitting those plotted in text-fig. 5A, was interpreted as representing the growth mosaic of the inner region of the secondary layer (text-fig. 5B). A suggested explanation for this anterior differentiation is offered later, as it can be shown not to be present throughout the whole of the secondary layer.

As in the brachial valve, the structure of the crescentic tubercles was investigated with the aid of transverse, horizontal, oblique, and longitudinal serial sections. In longitudinal sections the tubercles are seen to be composed entirely of fibrous cones (Pl. 21, figs. 2, 5) deflecting the other fibres adjacent to them. In transverse section (Pl. 21, fig. 1) the tubercles exhibit a characteristic reniform shape. The presence of these structures may be of profound significance and their implication is discussed later.

Compilation of the features exhibited by serial sections at various orientations allows reconstruction of the microstructure of the shell of *M. granulosa* (text-fig. 6A–C).

The pseudodeltidium and pedicle sheath. Study of *Lacazella* (Williams *et al.* 1965) indicates that neither the pedicle nor its muscle system is developed. The structure of the strophomenoid pseudodeltidium is still imperfectly known but it is now generally agreed that it consists of primary and secondary material and was secreted between the teeth ridges by the outer epithelium. Ventral umbonal regions of well-preserved specimens of *M. granulosa* were carefully sectioned in an attempt to resolve the problem of the fate of the pedicle opening in Jurassic thecidellinids. Owing to the mode of growth of the area and the minute proportions of the structures involved, it was difficult to distinguish the pseudodeltidium at all. Of the limited number of specimens in which it could be recognized, only three showed any discernible microstructure. In these specimens, transverse sections close to the ventral umbo show the presence of a minute pore 50 μ in diameter and apparently plugged by calcite having a different orientation from that of the pseudodeltidium (Pl. 21, figs. 7, 8). The pore appears at about 0·06 mm. from the posterior of the pedicle valve and close to the area of attachment (text-fig. 7C) in what must be regarded as a supra-apical position (text-fig. 7H). It appears to be surrounded laterally and dorsally by a collar or ring of material in which the fibres show a concentric orientation in the plane of section. The dorsal surface of the ring is exposed externally and is obviously the structure interpreted as a pseudodeltidium. In subsequent sections the pore migrates dorsally away from the area of attachment and the ring increases in size, still maintaining its dorsally exposed surface (text-fig. 7C–F). Continuity of the structure through several sections reveals that it is really a calcareous tube, which, if the plugged pore represents the site of the atrophied pedicle opening, may be regarded as a form of pedicle sheath which initially closed the delthyrium. At about 0·14 mm. from the umbo the structure terminates (text-fig. 7G) and is replaced by the ventral umbonal cavity, housing the posterior tip of the cardinal process. The space between the tooth

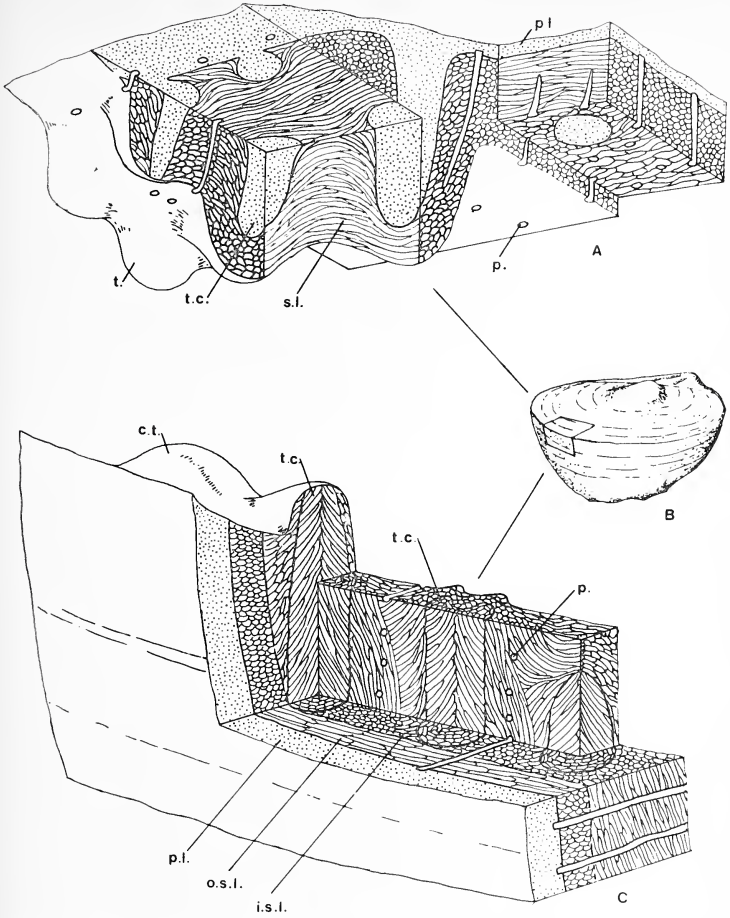

TEXT-FIG. 6. Diagrammatic reconstruction of the shell microstructure of *Moorellina granulosa* (Moore). A. Block diagram showing the microstructure of the brachial valve. B. Complete specimen showing relative position of the reconstructed segments. C. Block diagram showing the microstructure of the pedicle valve. c.t. crescentic tubercle, i.s.l. inner secondary layer, o.s.l. outer secondary layer, p. puncta, p.l. primary layer, s.l. secondary layer, t. tubercle, t.c. tubercle core.

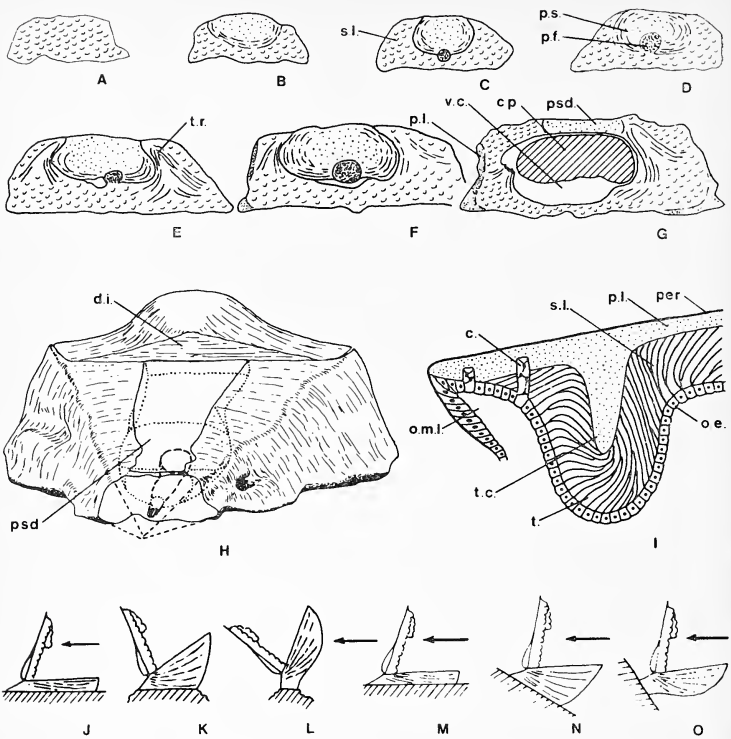

TEXT-FIG. 7. A–G. Drawings prepared from cellulose acetate peels of serial transverse sections through the ventral umbonal region of *M. granulosa* showing the continuity and anterior termination of the pedicle sheath and the plugged pedicle foramen. H. Reconstruction of the ventral umbonal region from thirteen superimposed peels. Outline of the pedicle sheath dotted and the pedicle opening, broken line. Position of umbo projected by dotted lines. I. Diagrammatic section through the sub-peripheral rim to show the difference in the development of endopunctae and tubercle cores. J–O. Series of six diagrams to show the orientation of the brachial apparatus relative to a prevailing current, arrowed. J–L, constant growth position with variable size of the attachment surface. M–O, constant orientation at various growth positions. c. caecum, c.p. cardinal process, d.i. dorsal interarea, o.e. outer epithelium, o.m.l. outer mantle lobe, per. periostracum, psd. pseudodeltidium, p.f. pedicle foramen, p.l. primary layer, p.s. pedicle sheath, s.l. secondary layer, t. tooth, t.c. tubercle core, t.r. tooth ridge, v.c. ventral umbonal cavity.

ridges is now occupied by a plate of more normal pseudodeltidial appearance. Unfortunately, at the moment there is no evidence to show whether this is a discrete plate or whether it is the product of overgrowth by the outer epithelium at the anterior termination of the calcareous tube. Atrophy of the pedicle would explain why the tube ceased to develop and only closes the posterior part of the delthyrium, an operation subsequently taken over by the outer epithelium.

SIGNIFICANCE OF THE OBSERVED GROWTH AND MICROSTRUCTURE

Growth orientation. Obviously there must be some genetic control of the proliferation of epithelial cells in the mantle fold and it is not possible to show absolute growth in *M. granulosa.* However, the use of a system of growth units makes it possible, providing one knows the primary growth orientation, to determine areas of rapid proliferation of cells and, therefore, relatively rapid increase in size. The observed external fibre orientation is clearly a topological expression of shell growth. There is a very close resemblance between the distribution of primary costae in *Rhipidomella oblata* (Hall) and the external fibre orientation of *M. granulosa* but this is to be expected if addition of material is normal to the commissure with mixoperipheral growth. This would clearly suggest that the radial ornament of the dalmanellaceids (Williams and Wright 1963, p. 22) is topological also. Work on the orientation pattern of *M. granulosa* would therefore appear to confirm their view that dalmanellaceid ornamentation patterns of 'progressive' species of *Watsella* (Bancroft 1945, p. 190) have no supra-specific taxonomic status.

The anteriorly modified spiral arc of the pedicle valve of *M. granulosa,* producing a secondary layer differentiated into two regions can only be clearly demonstrated in valves having a large free anterior surface. If one considers the thecideacean environment (Ager 1965, 1967; Nekvasilová 1967; Baker 1969) this anterior differentiation of the secondary layer is readily explained. Forms with a large free anterior surface (small area of attachment) would have relatively more of the pedicle valve exposed to the rigours of the environment. Development of crescentic tubercles would produce a structure which would secure the commissure (interlocking effect) but at the same time produce an exposed anterior surface which could be more easily breached at the relatively weak juctions between adjacent tubercles (Pl. 21, fig. 5). Differentiation of the secondary layer anteriorly into what might be described as a cross-laminate structure would greatly increase its strength. The above seems a logical explanation for the observed microstructure of the pedicle valve of *M. granulosa* and the relationship between fibre orientation and microstructure of other attached brachiopods is well worth investigating. Strophomenides, for example, may have solved the problem by the modification of fibres to produce laminae (Williams 1968*a*, p. 37). The fibres with flared ends noted in the brachial valve of *M. granulosa* may represent an attempt in this direction.

Ecology and functional morphology. Consideration of the growth habit of the pedicle valve in ecological terms is interesting. If the cumulative growth pattern is designed to lift the anterior gape away from the substratum, it is difficult to see why the characteristic is suppressed in forms with a large area of attachment. It seems probable that it is the degree of inclination, rather than the size of the surface to which the animal attaches itself, which is the major control. Elliott's (1948) paper would suggest that the relatively enormous gape (Rudwick 1968) of the thecideidines is associated with orientation of the

brachial apparatus relative to the 'prevailing' environment, probably represented by a persistent current direction.

The above relationship seems entirely probable and supports the author's argument. Individuals attaching themselves to surfaces of suitable inclination already have their commissures in the 'ideal' orientation position from an ecological standpoint. Such individuals would have no need to develop elaborate anterior surfaces, although development of even the relatively small anterior surface encountered in these specimens must inevitably require the cumulative growth pattern postulated.

There seems to be a correlation between size of animal and degree of elaboration of the brachial apparatus (Elliott 1948), interpreted as being related to the animal's food-gathering ability in a competitive sense. This may partially explain the onset of the development changes which lead to the freeing of the anterior of the pedicle valve from attachment to the substratum. Size of the animal is obviously critical where small size of the attachment surface is concerned but observations indicate that size may be critical independently. Attainment of a certain size might render necessary a change in organization, to effectively meet the increasing nutritional demands.

There are obviously other factors to be considered such as accommodation of the brachial apparatus and the developing sub-peripheral rim, the relative efficiency of the lophophore and the ecological niche (Rudwick 1962) occupied by any particular individual. However, if, as there would appear to be, there is any order associated with the growth habit of thecideidines, it is easier to reconcile this, in ecological terms, with the attainment of a certain orientation position of the gape (text-fig. 7J–O) rather than the size of the surface to which the animal was attached. One feels that the orientation of the gape, in terms of functional efficiency of the brachial apparatus, is the more satisfactory explanation for the variable growth habit observed in the pedicle valves of thecidellinids.

As *M. granulosa* is a member of the surf-zone fauna, the interlocking tubercles of the two valves on such cemented forms may have acted as accessory teeth and sockets to help secure the brachial valve in position during adverse conditions. The preponderance of brachial valves in any collection may be a measure of the relative vulnerability that the abnormally wide gape exposed in the existing hinge.

Microstructure. Williams, in his work on *Lacazella* (1968*a*, *b*) apparently abandons his earlier interpretation (1955, 1956, 1965) that a secondary layer is present, in favour of a shell composed only of primary material. The three earlier accounts are essentially similar. The 1955 paper records the presence of fibre bundles almost perpendicular to the 'lamellar' layer, producing the appearance of pseudopunctae but, in the absence of a non-fibrous core, unrelated to the strophomenid spicules. These core bundles are figured in the rather vague reconstruction of the shell of *Lacazella mediterranea* (Risso) in (1965, H67), but their orientation is apparently in the wrong direction. Attention is, however, drawn to the similarity of this type of shell structure and that of the terebratellaceid *Megerlina lamarkiana* (Dav.). The 1956 paper records the same fibrous cores in thecidaceids but offers no information as to which were studied. It is felt that the structures described must be referred to the microstructure of the crescentic tubercles of *M. granulosa* (Pl. 21, figs. 2, 5, text-fig. 6C).

The absence of a secondary layer in *Lacazella* is interpreted as being the result of

neotenous suppression (Williams 1968*a*). Although changes in the secretory habit of the epithelial cells in *M. granulosa* appear to follow a normal pattern, the stability of the thickness of the primary layer does not appear to be quite as constant as Williams has suggested and it is possible to see groups of secondary fibres apparently embedded in primary shell. This irregularity of deposition of the secondary layer in *M. granulosa* may be the first expression of its ultimate suppression.

Although *M. granulosa* is not costellate, it is worth noting that the external expression of the crescentic tubercles on the inner edge of the margin of the pedicle valve, bears a strong resemblance to the follicular eminences and embayments of the Recent *Terebratulina* and also fossil enteletacean (Williams and Wright 1963, p. 19; Williams and Rowell 1965, H81) brachiopods and may have served a similar purpose. Similar structures are seen in the cemented inarticulate *Crania anomala* (Müller) where they are not associated with setae but control the distribution of punctae. In *M. granulosa*, the crescentic tubercles appear to exercise a similar control over the distribution of punctate (Pl. 21, fig. 6).

Elliott (1953, 1955) has arrived at the conclusion that all thecideidines are enodpunctate with the possible exception of *Davidsonella*. Study of *M. granulosa* and *M. ornata* shows that although the endopunctae are formed in a terebratuloid manner, the cup-shaped distal enlargements and the deflexion of secondary fibres have not been seen.

Deeper issues are at stake with regard to the implication of the described tubercle structure. They occur together with endopunctae and the initiation of punctae and tubercle cores seems to follow the same pattern. Upon consideration of their structure, the question arises whether the tubercles are homologous with pseudopunctae. Tubercle cores must arise in a very different manner from endopunctae (text-fig. 7I), and therefore if homologous with pseudopunctae, pseudopunctae and endopunctae must be totally unrelated.

Williams (1965, H72) has stated that taleolae are comparable in texture with the terebratuloid primary layer. Sections parallel with the plane of the commissure through *M. granulosa* have shown that the tubercle cores of the brachial valve are in fact continuous with the primary layer and as far as can be ascertained, represent imperfectly developed primary shell, secreted by persistent patches of columnar epithelium, surviving from the tip of the outer mantle lobe.

Williams (1965) has shown that pseudopunctae are markedly asymmetrical in longitudinal section, with their apices directed inwardly and anteriorly to protrude from the internal surfaces of both valves as tubercles. The orientation of the tubercles in the brachial valve of *M. granulosa* shows this approximate pattern. In the pedicle valve, it only requires a slight exaggeration of this trend to produce, in *M. granulosa*, tubercle cores running almost parallel with the plane of the valve in such a way that they emerge as tubercles along the inner edge of the anterior margin. In which case, they may be regarded as homologous with the pseudopunctae of davidsoniaceans such as *Derbyia*, which consist of fibrous cones of the type shown to exist in the pedicle valve of *M. granulosa* (text-figs. 5B, 6C, Pl. 21, fig. 5).

The suspected close relationship between pseudopunctae with and without taleolae is confirmed by the presence of both types in a single animal. A careful sectioning technique, supported by the fact that the structures are located in different valves, enables one to show that the tubercles of the brachial valve have cores, whilst those of the pedicle

valve are without cores. If one considers the pure mechanics of this arrangement it would appear to be quite logical. In the brachial valve where orientation of the tubercle axis is near perpendicular to the surface of the valve, the development of the primary core in the manner suggested is the simplest way of bringing about an invagination of the outer epithelium. On the other hand, in the pedicle valve, where by virtue of the growth habit, the orientation of the tubercles must necessarily be nearly parallel with the valve inner surface, a primary core would become very attenuated. In this situation it would be far easier to produce a tubercle core by a slight change in the orientation of secondary fibres.

If one considers the tubercles in terms of this functional requirement, they may be regarded as the modified counterpart of strophomenoid pseudopunctae. They deflect secondary fibres in the same way and the similarity of the disposition of the fibres presumably indicates a similar pattern of development.

AFFINITIES

The affinities of the Thecideidina have been a subject of interest and speculation for a number of years, Elliott (1948, 1953, 1958), Rudwick (1968), and Williams (1965, 1968*a*, *b*) being notable among the later works. Demonstration of a primary and secondary shell layer in *M. granulosa* invalidates only Williams's (1968*a*, *b*) conclusion that *Lacazella* is a typical model of the thecideidine shell and in no way impairs his line of descent. If, as Williams's work suggests, the secondary layer of *Lacazella* has been neotenously suppressed to the point of exclusion, *M. granulosa* occupies an attractive position, as Jurassic forms in which this process might just be beginning, represent an important contribution to our knowledge. One feels that the diversity of shell microstructure encountered in a single specimen of *M. granulosa*, must represent a genetic disturbance which could quite easily result in the ultimate suppression of the secondary layer. The banded shell of *Lacazella* might in environmental terms, more easily satisfy the requirements for a reinforced shell and render the structurally reinforced secondary layer of *M. granulosa* obsolete, thus accounting for its disappearance. The secondary shell mosaic seems closer to terebratulide or spiriferide than any other. However, the shape of the fibres is different and also variable within an individual, so that one may see fibres with flared outer ends reminiscent of the laminae of plectambonitaceans. Still other features of the microstructure may be reconciled with davidsoniaceans.

The value of functional analysis of morphology, demonstrated by Rudwick (1968) and the significant correlation between the modification of the microstructure of *M. granulosa* and environmental influence, underlines an advance in our knowledge of taxonomic technique. Obviously, not only structures but also their significance in environmental terms must be critically examined before assigning a species to a particular systematic position, as convergence may be encountered at the microstructure level. It is felt therefore, that the taxonomic importance of some aspects of shell microstructure should not, as has happened frequently in the past on discovery of a character, be overestimated.

The value of shell microstructure from a taxonomic point of view has been discussed by Williams (1956, 1968*a*, *b*), Rudwick (1968), and Gauri and Boucot (1968). As the present investigations have shown, there are important differences between the microstructure of the brachial and pedicle valves of *M. granulosa*. That this is not a feature

peculiar to thecidellinids has been demonstrated by Gauri and Boucot (1968) who record that in the pentamerids *Antirhynchonella*, *Clorinda*, and *Zdimir*, the prismatic layer is absent from the brachial valve. Their study of pentameraceans and the gulf which exists between Williams's (1968*a*) thecideidine model and the observed microstructure of *M. granulosa* indicates that the state of our knowledge of shell microstructure in brachiopods is not yet sufficiently advanced to allow anything other than a tentative taxonomic significance to be ascribed to it.

With regard to the fate of the pedicle, it appears unlikely that *M. granulosa* will yield the quality of evidence to enable one to make categoric statements concerning the microstructure of the pedicle opening. Evidence yielded by *Lacazella mediterranea* (Risso) must remain suspect in view of the neotenous modification of this species. The main hope seems to lie in the discovery of well-preserved, larger thecideidines from other horizons. Only limited significance should therefore be attached to the pseudodeltidium of *M. granulosa* until the evidence has been strengthened. If a pedicle sheath does arise supra-apically, then it is possible to equate this with the strophomenoid pseudodeltidium. Arber (1942) has recorded a very similar solid pseudodeltidium, fused with the floor of the pedicle valve in the Orthotetinae and Rafinesquinae. However, Williams (1956) has noted an imperforate delthyrial cover in *Eospirifer*. The indication that the pseudodeltidium of *M. granulosa* was deposited by the ventral edge of the capsule of a pedicle undergoing atrophy, appears to confirm the views of Arber (1942) and Williams (1956) regarding the form of the pseudodeltidium of *Lacazella*.

Although it appears that the thecideacean pseudodeltidium is homologous with the pseudodeltidium of strophomenoids, Williams and Rowell (1965, H188) regard the similarity between strophomenoids and thecideaceans as an expression of convergence and derive the thecideidines from possible suessiacean ancestors. One must agree that the secondary mosaic is very similar to *Cyrtina* but encounters the same time-gap objection raised by Williams (1956) to the affinity proposed by Kozlowski (1929) for the lophophore platforms of some plectambonitaceids and thecidaceids.

Structurally there appears to be no significant difference between strophomenoid pseudopunctae and the tubercles of *M. granulosa*. The similarity between them and pseudopunctae of the davidsoniacean *Derbyia* is even closer. On this basis, it would not be unreasonable to conclude that the tubercles of thecidellinids are homologous with strophomenoid pseudopunctae, functionally modified.

Elimination of obscure similarities, plectambonitaceid, enteletacean, terebratellacean, etc., leaves one with the basic problem of whether the thecideidines show strophomenide or spiriferide affinity. An analysis of the literature shows that the systematic position of *Thecospira* is of critical importance as far as the thecideidines are concerned. It seems strange that Williams (1968*a*), after lengthy discussion of the low taxonomic value of a limited number of characters, should re-assign the genus to the Spiriferida solely on the basis of its shell structure and admitted non-spiriferoid calcareous spires. If one considers the points of similarity between *M. granulosa* and *Thecospira* they are most striking. Both are strophic and show the same lateral profile. *Thecospira* shows punctate and obscurely pseudopunctate representatives. *M. granulosa* is endopunctate but probably independently from terebratuloid endopunctation (Williams 1968*c*, p. 489). The similarity in *Thecospira* and *M. granulosa*, of the cardinal process, the hinge articulation, the sub-marginal structures, the coalesced punctae and lateral shift of the main adductor

muscles is thought to be more than coincidental. Differences such as the lack of costellate ornament may not be profound, as radially arranged fibres have been recognized in *M. granulosa*. As spiral brachidia apparently evolved twice among the Spiriferida, there is no reason why similar brachidia should not evolve in non-spiriferide forms, e.g. *Thecospira* and *Cadomella* (Cowen and Rudwick 1966) whose epithelia had the ability to resorb material. If one bears in mind the neotenous origin of the thecideidines and extends the posterior horns of the brachial lobes of *M. granulosa* (Baker 1969, text-fig. 3F) back to unite with the bridge extensions, one may derive or 'lose' a simple spiral brachidium as a result of the demonstrated resorptive activity taking place in the brachial cavities.

Rudwick (1968) has put forward a reasoned argument for the assignment of the Thecideacea to the Strophomenida, close to, but distinct from the Davidsoniacea. As outlined in the discussion of possible environmental influence, the possibility of a convergent origin of the davidsoniacean characters of *M. granulosa* must not be overlooked but the similarity between *Moorellina granulosa* (Moore), the spire-bearing *Thecospira*, and known davidsoniaceans such as *Derbyia* and *Orthotetes* is thought to be much too close to be merely convergent. The weight of evidence now accumulated would suggest that the thecideidines show affinity closer to the davidsoniaceans than any other group. The author must agree with Rudwick, that on the basis of our present knowledge the Thecideacea should be assigned to the Strophomenida.

REFERENCES

AGER, D. V. 1965. The adaptation of Mesozoic brachiopods to different environments. *Palaeogeography, Palaeoclimatol., Palaeoecol.* **1**, 143–72.

—— 1967. Brachiopod palaeoecology. *Earth-Sci Rev.* **3**, 157–79.

ARBER, M. A. 1942. The pseudodeltidium of the strophomenoid brachiopods. *Geol. Mag.* **79**, 179–87.

BAKER, P. G. 1969. The ontogeny of the thecideacean brachiopod *Moorellina granulosa* (Moore) from the Middle Jurassic of England. *Palaeontology*, **12**, 388–99.

BANCROFT, B. B. 1945. The brachiopod zonal indices of the stages Costonian to Onnian in Britain. *J. Paleont.* **19**, 181–252.

CLOUD, P. E. 1942. The terebratuloid Brachiopoda of the Silurian and Devonian. *Spec. Pap. geol. Soc. Amer.* **38.**

COWEN, R. 1966. The distribution of punctae on the brachiopod shell. *Geol. Mag.* **103**, 269–75.

—— and RUDWICK, M. J. S. 1966. A spiral brachidium in the Jurassic chonetoid brachiopod *Cadomella*. Ibid. **103**, 403–6.

ELLIOTT, G. F. 1948. Palingenesis in Thecidea (Brachiopoda). *Ann. Mag. nat. Hist.* **(12) 1**, 1–30.

—— 1953. The classification of the thecidean brachiopods. Ibid. **(12) 6**, 693–701.

—— 1955. Shell-structure of thecidean brachiopods. *Nature, Lond.* **175**, 1124.

—— 1965. Suborder Thecideidina. In MOORE, R. C. (ed.), *Treatise on invertebrate paleontology*, part (H) *Brachiopoda*, H857–62. Univ. Kansas and Geol. Soc. Amer.

GAURI, K. L. and BOUCOT, A. J. 1968. Shell structure and classification of the Pentameracea M'Coy, 1844. *Palaeontographica Abt. A.* **131**, 79–135.

KEMEŽYS, K. J. 1965. Significance of punctae and pustules in brachiopods. *Geol. Mag.* **102**, 315–24.

KOZLOWSKI, R. 1929. Les brachiopodes gothlandiens de la Podolie polonaise. *Palaeont. polon.* **1**, 1–254.

NEKVASILOVÁ, O. 1964. Thecideidae (Brachiopoda) der bohmischen Kreide. *Sbor. geol. ved, Praha*, **P3**, 119–62.

—— 1967. *Thecidiopsis* (*Thecidiopsis*) *bohemica imperfecta* n. subsp. (Brachiopoda) from the Upper Cretaceous of Bohemia. Ibid. **P9**, 115–36.

RUDWICK, M. J. S. 1959. The growth and form of brachiopod shells. *Geol. Mag.* **96**, 1–24.
—— 1962. Notes on the ecology of brachiopods in New Zealand. *Trans. Roy. Soc. N.Z.* **1**, 25:327–35.
—— 1968. The feeding mechanisms and affinities of the Triassic brachiopods *Thecospira* Zugmayer and *Bactrynium* Emmrich. *Palaeontology*, **11**, 329–60.
WILLIAMS, A. 1955. Shell-structure of the brachiopod *Lacazella mediterranea* (Risso). *Nature, Lond.* **175**, 1123.
—— 1956. The calcareous shell of the Brachiopoda and its importance to their classification. *Biol. Rev.* **31**, 243–87.
—— 1965. In MOORE, R. C. (ed.), *Treatise on invertebrate paleontology*, part H, *Brachiopoda*. 927 pp. Univ. Kansas and Geol. Soc. Amer.
—— 1966. Growth and structure of the shell of living articulate brachiopods. *Nature, Lond.* **211**, 1146–8.
—— 1968*a*. Evolution of the shell structure of articulate brachiopods. *Spec. Pap. Palaeont.* **2**, 55 pp.
—— 1968*b*. A history of skeletal secretion among articulate brachiopods. *Lethaia, Universitetsforlaget, Oslo* **1**, 268–87.
—— 1968*c*. Shell-structure of the billingsellacean brachiopods. *Palaeontology*, **11**, 486–90.
—— and ROWELL, A. J. 1965. Morphology. In MOORE, R. C. (ed.) *Treatise on invertebrate paleontology*, part H, *Brachiopoda*. H57–155. Univ. Kansas and Geol. Soc. Amer.
—— and WRIGHT, A. D. 1963. The classification of the '*Orthis testudinaria* Dalman' group of brachiopods. *J. Paleont.* **37**, 1–32.

P. G. BAKER
Department of Biological Sciences
Derby and District College of Technology
Kedleston Road
Derby, DE3 1GB

Typescript received 6 June 1969

ONTOGENY OF THE UPPER CAMBRIAN TRILOBITE *LEPTOPLASTUS CRASSICORNIS* (WESTERGAARD) FROM SWEDEN

by P. H. WHITWORTH

ABSTRACT. The development of the dorsal exoskeleton of the trilobite *Leptoplastus crassicornis* (Westergaard) is described from the Upper Cambrian of Andrarum, Scania, Sweden. The cranidium is represented by all stages from protaspis to holaspis, although specimens other than protaspids are disarticulated and precise degrees are unknown; they have therefore been allocated to seven morphological groups. The development of the meraspid librigena, hypostome, and pygidium is also briefly described. The growth of the cranidium is closest to *Peltura scarabeoides* but also shows similarities with *Olenus gibbosus* and *Leptoplastides salteri*. The nature and course of early facial sutures is discussed. Scatter diagrams show growth to be linear and allometric.

AMONGST the reference collections in the Birmingham University Geology Museum are several slabs of black alum-shale material from the 'Olenus Stage' (as labelled) of Andrarum, Scania, Sweden. These are crowded with specimens of the trilobite *Leptoplastus crassicornis* (Westergaard) in all stages of growth, with occasional individuals of *L. norvegicus* (Holtedahl), preserved as internal and external moulds. The specimens are labelled as *Eurycare angustatum* (transferred to *Leptoplastus* by Henningsmoen 1957) but they are considered to belong to *L. crassicornis*, and the association with *L. norvegicus* supports this. Such an assemblage suggests that the material comes from the Subzones *crassicornis* or *ovatus* of the Leptoplastus (2c) Zone (Henningsmoen 1957, chart 2). A continuous series is represented but due to fragmentation of the exoskeleton only the protaspis stages are complete, and consequently the size groups cannot be related to successive degrees.

The numerous specimens were measured using a micrometer eye-piece, but it must be remembered that the measurement of protaspid length in particular (taken when the anterior and posterior margins lie on an approximately horizontal plane) are reduced by the strong curvature of the specimens. The ratios of length and width measurements of cranidium and glabella, when plotted graphically (text-fig. 2), provide a remarkably linear scatter and also demonstrate the allometric growth of these parts. Breaks in the scatters may indicate separation of size groups by instars, but the number of these is small when compared with the number of thoracic segments in the adult and this may be due to the release of two or more segments into the thorax at some instars. It is appreciated that a certain number of young stages of *L. norvegicus* may have been included in the measurements, but such early stages of two closely related species are unlikely to show any significant differences and their possible inclusion is disregarded.

Any size limits imposed to separate the protaspis, meraspis, and holaspis stages would be entirely arbitrary and subjective, but for convenience such limits are employed. The meraspis stage is considered to commence when the posterior transverse ridge of the protaspis is fully developed and a distinct separation of the cranidium and pygidium by a transverse suture is attained. The holaspid condition is based on the evidence of

[Palaeontology, Vol. 13, Part 1, 1970, pp. 100–11, pls. 22–24.]

a specimen bearing 10 thoracic segments (Pl. 23, fig. 5). As the nature of the suture and free cheeks is not known in detail for early stages the head shield is termed a cephalon up to, and a cranidium after, the meraspid condition is reached. The axis then becomes the glabella, the axial rings and ring furrows become the glabellar lobes and furrows. The descriptions are based mainly in internal moulds, but the external moulds differ insignificantly from them in all important characters.

TABLE 1. Detailed measurements of figured cranidia. Measurements of length of cranidium and glabella include the occipital ring, of width where this is greatest. Eye-lobe measurement is of length.

	Plate	*Fig.*	*No.*	*Length shield*	*Width shield*	*Length axis*	*Width axis*	*No. of segments*
Protaspis	22	1	O6	0·20	0·20	0·19	0·06	5
		2, 3	W10	0·22	0·22	0·20	0·08	5
		4	W77	0·26	0·26	0·21	0·08	6
		5	W80	0·28	0·30	0·26	0·10	6
		6	W77	0·28	0·28	0·22	0·09	6
		7, 8	W61	0·30	0·33	0·26	0·11	7
				Length cranid.	*Width cranid.*	*Length glab.*	*Width glab.*	*Eye-lobe*
Meraspis		9	W62	0·26	0·29	0·22	0·09	(—)
		10	O14	0·27	0·36	0·26	0·11	0·20
		11	W81	0·30	0·41	0·30	0·14	0·20
		12	W47	0·30	0·42	0·30	0·12	0·20
		13	W50	0·32	0·46	0·33	0·13	0·21
		14	W32	0·34	0·48	0·30	0·14	0·22
		15	W2	0·40	0·58	0·36	0·17	0·24
		16	W9	0·42	0·60	0·40	0·19	0·26
		17	W70	0·48	0·74	0·46	0·20	0·28
		18	W40	0·48	0·70	0·46	0·22	0·26
		19	W52	0·58	0·88	0·56	0·24	0·32
		20	W53	0·68	1·20	0·63	0·32	0·40
		21	W44	0·80	1·40	0·74	0·36	0·40
	23	1	O7	0·97	1·80	0·90	0·50	0·46
		2	W55	1·28	2·60	1·16	0·68	0·68?
		3	O8	1·40	2·80	1·28	0·72	0·76
		4	O9	1·60	3·20	1·50	0·92	0·88
		5	O2	1·64	(—)	1·46	0·96	0·90
		6	O10	1·76	3·63	1·60	1·16	1·06
Holaspis		7	O3	2·14	(—)	1·84	1·26	1·10
		8	W56	2·48	5·28	2·12	1·40	1·24
		9	W17	2·60	5·92	2·36	1·72	1·40
		10	W21	2·80	6·0	2·56	1·76	1·40
		11	O11	3·20	(—)	2·80	2·0	1·60
		12	W26	5·0	9·0	4·50	3·0	1·40

Terminology. The terminology employed in this paper is a combination of that of Whittington 1957 and 1958 and that of the *Treatise* (Moore, 1959) with the additional use of the term *ring furrow* to denote the transverse furrows of the protaspid cephalic axis. As the nature of the early cephalic segmentation is not yet clear in the olenids,

Størmer's (1942) terminology referring to the segmental nature of certain characters (e.g. pre-antennal segment) is not used. Measurements of length are sagittal unless otherwise stated and of width (tr.) where this is greatest, the latter not necessarily comparable. The length of the cranidium includes the occipital ring and length of the pygidium excludes the articulating half-ring. The axial rings and furrows (excluding the occipital furrow) of the protaspis stages are numbered from back to front in accordance with the usual notation for adult trilobites by inference from the development of the respective rings in the meraspid/holaspid periods.

Technique. Photography of specimens of the order of 0·25 mm. across has often proved extremely difficult but some measure of success has been obtained here by the use of a Leitz Wetzlar biological microscope, and the depth of field problem with highly convex specimens has been overcome by using a 35 mm. Leitz objective incorporating an iris diaphragm. All specimens were whitened with ammonium chloride sublimate before photographing but the coarseness of even the finest application obscures some of the very fine ornament and structure of the protaspids.

SYSTEMATIC DESCRIPTION

Family OLENIDAE Burmeister 1843
Subfamily LEPTOPLASTINAE Angelin 1854

Leptoplastus crassicornis (Westergaard 1944)

Plate 22, figs. 1–21; Plate 23, figs. 1–12; Plate 24, figs. 1–20; text-fig. 1.

Material. The specimens are individually numbered on three slabs of rock with white (W) and orange (O) labels and are deposited in the Birmingham University Geology Museum numbered BU 395–7.

Because of the fragmentary nature of the material the descriptions have been included under five separate headings: (*a*) protaspis, (*b*) meraspis/holaspis cranidium, (*c*) librigena, (*d*) hypostome, and (*e*) pygidium. It was found most convenient to divide the series into seven morphological groups, for each of which the size-range, number of specimens measured, and the plate and figure references precede each description. A fuller list of measurements of figured cranidia is given in Table 1.

PROTASPIS

Group 1. Length (entire shield)—0·20–0·25 mm., 6 specimens (Pl. 22, figs. 1–3; text-fig. 1*a*).

The shield is circular in outline, up to 0·26 mm. wide, moderately convex becoming more strongly bent down behind. Axis essentially of 5 rings separated by straight ring furrows with the suggestion of an incipient 6th segment in later stages (Pl. 22, fig. 3).

EXPLANATION OF PLATE 22

Leptoplastus crassicornis (Westergaard). Developmental series of protaspis and early meraspis to show changes in relative dimensions (BU 395, 396). Individual specimen numbers as in Table 1. Fig. 1, ×80; figs. 2, 3, ×70; figs. 4–9, ×65; figs. 10–14, ×50; figs. 15, 16, ×40; figs. 17–19, ×30; figs. 20, 21, ×25.

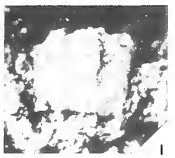
1

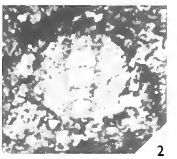
2

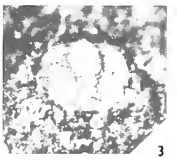
3

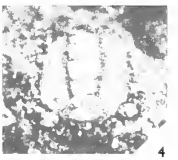
4

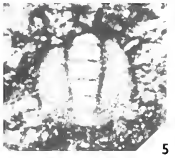
5

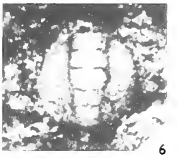
6

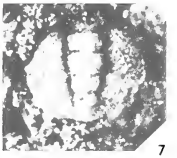
7

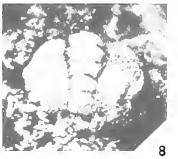
8

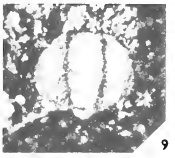
9

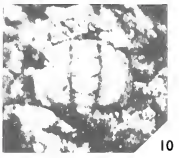
10

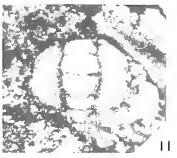
11

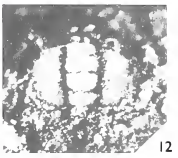
12

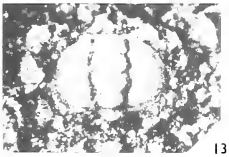
13

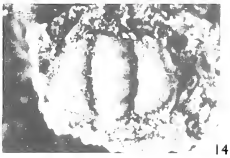
14


15


16

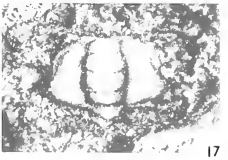
17

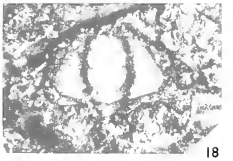
18

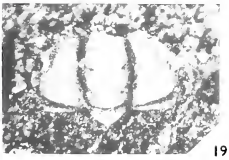
19

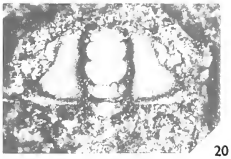
20

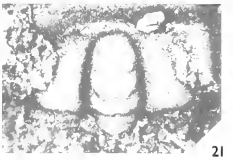
21

WHITWORTH, *Leptoplastus crassicorne* (Westergaard)

The axis is slightly constricted behind the 3p ring which is the widest. The frontal lobe is longer than the others and at its antero-lateral corners are a pair of anterior pits which continue laterally into faint furrows, bounded in front by the narrow anterior border. A lateral border extends forwards from a small fine spine (Pl. 22, figs. 2, 3) to the level

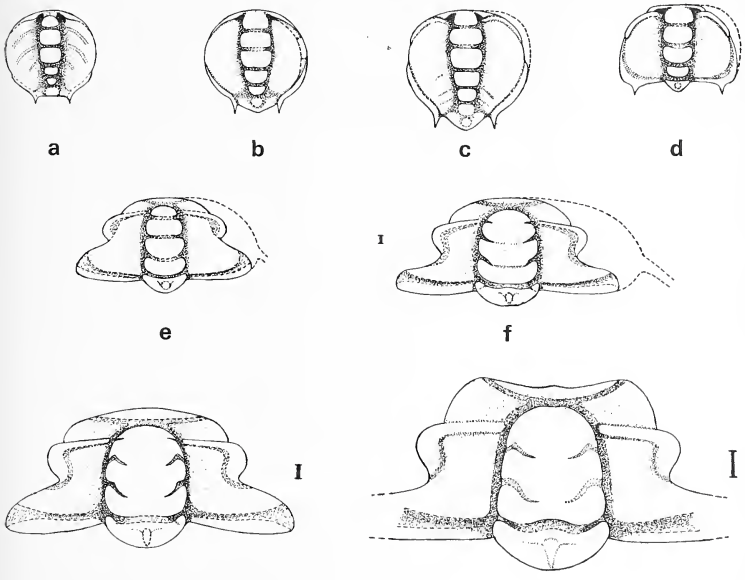

TEXT-FIG. 1. Reconstructions of some stages in the development of *Leptoplastus crassicornis* (Westergaard). *a*. W10, ×70; *b*. W80, ×65; *c*. W61, ×65; *d*. W50, ×50; *e*. W53, ×25; *f*. O9, ×12; *g*. W21, ×9; *h*. W26, ×7. Approximate natural sizes are given alongside some figures to show the over-all increase from smallest protaspis to largest holaspis. Suggested positions and shapes of librigenae are given in figs. *b–f*; those in fig. *b* occupy a ventral position, the suture being marginal.

of the 1p axial ring. There are indications on some specimens of several obliquely backwards directed and forwards convex furrows on the pleural regions, but they are very faint.

Group 2. Length (entire shield)—0·26–0·29 mm., 19 specimens (Pl. 22, figs. 4–6; text-fig. 1*b*).

Here the shield, which may be up to 0·32 mm. wide, shows a 6th axial segment behind the occipital ring representing the single segment of the protopygidium, which is developed as a flat triangular plate of minute size (Pl. 22, fig. 5; text-fig. 1*b*). The axis

is still widest, but less constricted, at the 2p ring and is more strongly convex. The anterior lobe reaches almost to the anterior margin and on either side of it the anterior pits and border continue to increase in prominence (Pl. 22, fig. 6). The lateral border is a little wider than before and reaches forwards to opposite the 1p ring furrow. The fixigenal spines are somewhat larger and directed backwards and downwards. From opposite the middle of the occipital ring a change in height of the pleural regions suggests the appearance of an oblique ridge crossing their posterior part, a feature seen better in Group 3 (Pl. 22, fig. 4). The pleural regions are often seen to have a relatively coarse reticulate ornament.

Group 3. Length (entire shield)—0·30–0·32 mm., 5 specimens (Pl. 22, figs. 7, 8; text-fig. 1*c*).

The shield, ranging in width from 0·30 to 0·34 mm., may be thus slightly wider than long and is strongly convex (tr.), being better defined by deep axial furrows than before. The frontal lobe appears to have diminished slightly in relative length and width, while the 2p and 3p rings are of about equal width and 1p and the occipital ring progressively smaller, the abrupt narrowing behind the 3p ring being less marked (Pl. 22, fig. 7). The occipital ring is raised high above the level of the descending protopygidium. Anteriorly a distinct eye-ridge is now seen to trend forwards and outwards from the axial furrow near the 3p ring furrow to the antero-lateral margin where, defined from the anterior border by a shallow furrow, it turns backwards, reaching almost to the level of the 2p ring furrow (text-fig. 1*c*). The anterior pits are very well defined and quite deep. The inflated reticulate pleural regions, still bearing traces of oblique grooves posteriorly, descend evenly outwards all round but are abruptly less convex behind the 1p ring furrow where a shallow oblique groove and faint ridge is developed (Pl. 22, fig. 7). This represents the incipient posterior border and margin of the meraspid cranidium. The lateral border is flange-like, reaches forwards to the level of the 2p axial ring and extends posteriorly into now quite strong spines. The small triangular protopygidium has 2 poorly defined circular segments (Pl. 22, fig. 8). The length of the primary axis (5 segments) is here 0·23 mm. and the cranidial width 0·34 mm. (compare values below for Group 4).

MERASPIS/HOLASPIS CRANIDIUM

Group 4. Length (cranidium)—0·26–0·39 mm., 20 specimens (Pl. 22, figs. 9–14; text-fig. 1*d*).

The width of the cranidium varies in this group from 0·35–0·60 mm., showing quite a considerable individual variation during early growth. The cranidium shows an overall shortening and widening due to the lateral growth of the posterior areas of the fixigenae. The glabella becomes distinctly barrel-shaped by the relative increase in width of the 2p and 3p glabellar lobes, the occipital ring remaining small and becoming triangular in shape with the development in later stages of a small median tubercle or node (Pl. 22,

EXPLANATION OF PLATE 23

L. crassicornis (Westergaard). Developmental series of late meraspids and of holaspids to show changes in relative dimensions (BU 395, 397). Individual specimen numbers as in Table 1. Fig. 1, ×20; fig. 2, ×16; fig. 3, ×14; figs. 4, 5, ×12; fig. 6, ×11; fig. 7, ×10; figs. 8–11, ×9; fig. 12, ×7.

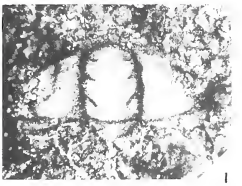
1

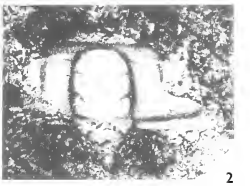
2


3

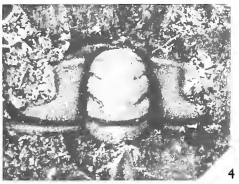
4

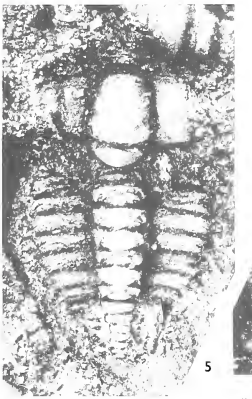
5


6

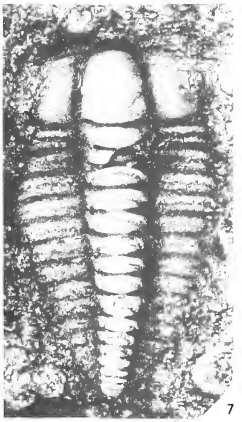
7

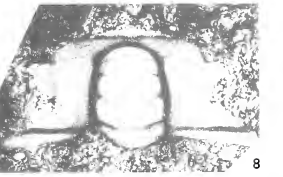
8

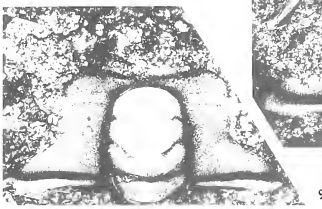
9

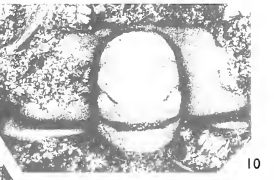
10

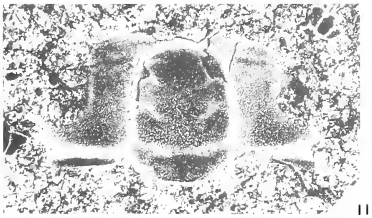
11

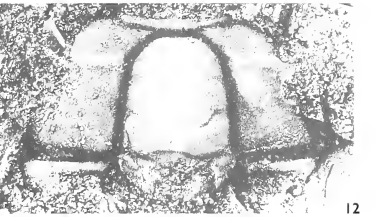
12

WHITWORTH, *Leptoplastus crassicorne* (Westergaard)

fig. 11). The 1p to 3p glabellar furrows become gradually shallower, especially medially, while the occipital furrow deepens. The initially curved anterior border becomes distinctly transverse but is still continuous axially with the frontal glabellar lobe. The anterior pits and border furrow combine to form rather large triangular depressions, and the convex anterior border extends laterally beyond the axial furrow to a distance about equal to half the width of the glabella, turning abruptly back so that the eye-ridges become marginal (Pl. 22, fig. 13). The more clearly defined and gently curved eye-ridges extend back to level with the posterior half of the 3p glabellar lobe and show a slight swelling at their posterior (abaxial) end (Pl. 22, figs. 10, 14). The oblique transverse ridge and depression on the pleural regions continue to develop from the protaspis and eventually unite with the lateral border, forming a transverse posterior margin to the cranidium (Pl. 22, fig. 14). The lateral border extends gradually further forwards from the rounded postero-lateral corners of the cranidium, becoming narrower as it does so, to meet but remain distinct from the eye-ridge, and is accompanied by a border furrow continuous with that of the posterior border (Pl. 22, fig. 13). It is clear that a facial suture and free cheek is developed at early stages in this group (see discussion at end), and indeed probably also in Group 3, but no librigenae of such dimensions have been found. As a consequence, the lateral border may now be termed the sutural ridge and the border spines are seen to be of fixigenal origin (i.e. metafixigenal). These latter move relatively outwards to, at most, four-fifths of the distance out from the axial furrow (Pl. 22, fig. 14). The fixigenal areas retain their reticulate pattern to the end of this group, but it is usually lost early in Group 5. These areas commence to inflate individually and the posterior areas to increase gradually in width, the latter also descending rather steeply behind into the posterior border furrow (Pl. 22, fig. 10).

Group 5. Length (cranidium)—0·41–1·00 mm., 53 specimens (Pl. 22, figs. 15–21; Pl. 23, fig. 1; text-fig. 1*e*).

Cranidial width ranges from 0·53 to 1·80 mm. The most important changes in this group affect the glabellar shape and segmentation and the expansion of the posterior fixigenal areas. The glabella continues to expand at the 2p and 3p lobes at first (Pl. 22, figs. 15, 18) but in later stages the 1p lobe and occipital ring take up this change and begin to widen (tr.) so that the sides of the glabella tend to become parallel (Pl. 22, fig. 21). The 2p lobe becomes the longest (sag.) with the 1p and occipital lobes remaining short; the frontal lobe is also reduced. In this group one also sees the first break in continuity of the glabellar furrows, 3p and 2p becoming very indistinct or even disappearing medially (Pl. 23, fig. 1). This is accompanied by an increase in depth of the abaxial parts of the glabellar furrows, 1p and 2p becoming almost notch-like, and by the change in direction of these parts from transverse to inwards and backwards directed. 1p is directed more sharply backwards than 2p (Pl. 22, fig. 20; Pl. 23, fig. 1). The occipital furrow remains continuous and increases in depth, turning forwards abaxially; the median occipital node is very prominent (Pl. 22, figs. 17, 19, 21).

Due to the width increase of the glabella the palpebral areas of the fixigenae become relatively narrower in relation to it than before and become less inflated. The posterior fixigenal areas grow rapidly abaxially and the ratios of cranidial to glabellar width increase, indicating that the growth of these parts does not keep pace. As the fixigenae grow so the sutural ridge is lost, the postero-lateral corners of the cranidium become

less well rounded, the posterior margin becomes straighter, and the fixigenal spines are aborted (compare Pl. 22, figs. 15 and 19). The eye-ridges increase in prominence and become more transverse, and the palpebral furrow deepens. The posterior end of the palpebral lobe is at first situated opposite the outer ends of the 2p glabellar furrows but

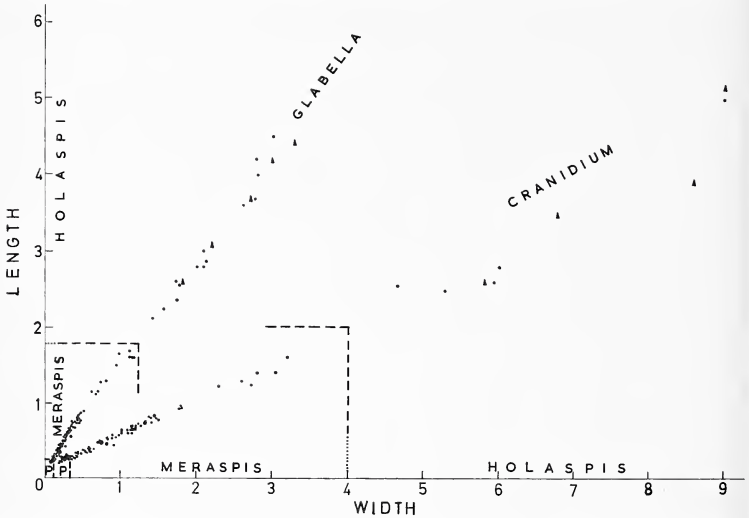

TEXT-FIG. 2. Scatter diagram showing nature of growth of cranidium and glabella of *Leptoplastus crassicornis* from 116 specimens. Those marked with a triangle are of Norwegian material, measurements being taken directly from the plates of Henningsmoen 1957. Breaks in the scatters might be interpreted as instars, but there is no conclusive evidence which can be used in support of this; no abrupt changes in the morphological development of the cranidium alone are evident. Note relative rates of growth in length and width (allometric) of cranidium and glabella. Measurements in millimetres.

in later stages it extends back to opposite the middle of the 2p glabellar lobe (Pl. 23, fig. 1). The frontal lobe becomes separated from the anterior border of earlier groups by a distinct preglabellar furrow which abaxially defines a true narrow, convex border from a narrow (exsag.) anterior fixigenal area (Pl. 22, fig. 21). The course of the posterior section of the facial suture turns at first slightly outwards behind the palpebral lobe, but in later stages more strongly so, bending back to cut the posterior margin at a distance from the axial furrow of slightly less than the length of the glabella (exc. occipital ring).

Group 6. Length (cranidium)—1·1–1·9 mm., 8 specimens (Pl. 23, figs. 2–5; text-fig. 1*f*).

In this group the cranidium attains, and further develops, the typical adult form and the changes observed are mainly due to size increase. The maximum width of the cranidium in this group is about 3·5 mm. By continued increase in width of the occipital

ring and 1p glabellar lobe the glabella soon becomes parallel sided and broadly rounded in front (Pl. 23, fig. 2). The occipital ring may even become slightly wider than the rest of the glabella and has a straighter posterior margin than previously, its abaxial margins turning strongly forwards; the median node becomes somewhat elongate and reduced in prominence. The median parts of 1p and 2p glabellar furrows are gradually lost while the lateral parts become deeper and develop a slight forwards convex curve (Pl. 23, fig. 4). The 3p furrows also continue to get fainter. The eye-ridges are no longer curved but are still directed outwards and slightly backwards. The anterior fixigenal areas and the anterior border increase slowly in length (exsag. and sag. respectively) but a preglabellar area is not yet developed. The posterior margin has become nearly straight, and the convex border widens abaxially along with the border furrow which is now very deep (Pl. 23, figs. 3, 4). The strongly inflated rear parts of the posterior fixigenal areas descend steeply into this border furrow and also into the axial furrow, but the anterior and palpebral areas are much less convex. The by now well-developed palpebral lobes extend back almost to the level of the outer ends of the 1p glabellar furrows (Pl. 23, figs. 2, 4). The course of the facial suture describes a gentle curve from a median marginal position out and back to the front end of the palpebral lobe. Thence, from the back of the palpebral lobe, it turns immediately outwards and runs back in a gentle forwards convex curve (text-fig. 1*f*), bending quite sharply back again to cut the posterior margin at a distance from the axial furrow of a little more than the length of the glabella (excluding occipital ring).

Judging by the size of the cranidium of a specimen which seems to have about 10 thoracic segments (Pl. 23, fig. 5), and that of the smallest available specimen with the full complement of 12 segments (Pl. 23, fig. 7), the holaspid condition is attained when the cranidial length reaches *c.* 2·0 mm. Group 7 is therefore considered to represent the development of the holaspis (adult) stage.

Group 7. Length (cranidium)—2·0 (approx.)–5·0 mm., 14 specimens (Pl. 23, figs. 6–12; text-figs. 1*g*, *h*).

Apart from an over-all size increase of about $2\frac{1}{2}$ times the principal changes concern the glabella. This becomes extremely convex (tr. and sag.), almost semicircular in cross-section, and is raised high above the level of the fixigenae which have been correspondingly reduced in convexity and height. The reduction in over-all convexity of the cranidium continues, and in contrast to the gently arched anterior regions the posterior fixigenae are strongly inflated behind and descend abruptly into the deep and wide posterior border furrow. The glabella continues to widen at the occipital ring and 1p lobes so that the axial furrows become forward convergent. The preglabellar furrow may or may not be confluent with the border furrow, so that a very narrow (sag.) preglabellar area may be present (cf. Pl. 23, figs. 8, 10, and fig. 12). As the glabella widens the glabellar furrows lengthen so that, from occupying only the outer one-fifth of the glabellar width in earlier Groups, they now occupy one-third of the same. 1p and 2p furrows also exhibit a marked sinuosity (Pl. 23, fig. 9) and eventually become quite strongly sigmoidal (Pl. 23, fig. 12), but the 3p furrows remain slightly curved and eventually disappear. As with the glabellar furrows in earlier groups the median part of the occipital furrow tends to weaken (Pl. 23, fig. 8); the median occipital node is more elongate and indistinct. In fig. 12 the glabellar furrows as a whole become much fainter,

especially abaxially, and are hardly continuous with the axial furrows. The eye-ridges terminate adaxially opposite the 3p glabellar furrows and are finally almost transverse.

The anterolateral parts of the anterior fixigenal areas tend to grow rather rapidly forwards and downwards, resulting in the anterior border developing a forward concave curve with a slight median expansion. The outer ends of the posterior fixigenae are also strongly bent downwards and invariably hidden, but the posterior sections of the facial suture seem to approach the posterior border at a more acute angle than before.

SUMMARY OF CRANIDIAL DEVELOPMENT

The following summary also acts as a diagnosis for each of the groups described above.

Group 1. Protaspids characterized by 5 axial segments, the absence of palpebral lobes and eye-ridges, and by a lateral border reaching forwards to opposite the occipital furrow.

Group 2. Protaspids with a definite protopygidium of 1 segment, defined by a groove and incipient ridge crossing the posterior part of the pleural regions from the axis to the fixigenal spines. Lateral border reaches forwards to opposite the 1p ring furrow.

Group 3. Late protaspids with a protopygidium of 2 segments, suggestions of eye-ridges extending back to level of 3p axial ring, and a lateral border reaching forwards to level of 2p axial ring.

Group 4. Early meraspids in which the palpebral lobes are defined and the lateral border becomes to sutural ridge by the migration of the suture to the dorsal surface; the ridge reaches forwards the meet the palpebral lobes opposite 2p glabellar furrow. Posterior cephalic border is accentuated and fixigenal spines move out relatively towards the postero-lateral angles of the cranidium. A median occipital tubercle develops.

Group 5. Meraspids showing marked lateral growth of the posterior fixigenal areas and corresponding outwards curve of the suture. Eye-ridges become less curved and less oblique. Glabella widens rapidly at 3p and 2p lobes in early stages and at 1p lobe and occipital ring in later stages, becoming almost parallel sided. Glabellar furrow gradually reduced, the median part of 3p and 2p becoming faint and disappearing. Preglabellar furrow disappears and anterior fixigenal areas develop. Fixigenal spines aborted.

Group 6. Late meraspids in which the glabella becomes parallel-sided and glabellar furrows entirely lateral. Occipital ring slightly wider than glabella, occipital furrow remains deep and continuous. Convexity (tr.) of cranidium as a whole, and of the fixigenae, is reduced except for abaxial regions of posterior areas and their posterior limits. Median part of 1p glabellar furrow obliterated, outer parts of 1p and 2p furrows

EXPLANATION OF PLATE 24

L. crassicornis (Westergaard). Developmental series of pygidium (figs. 1–7), hypostome (figs. 8–12) and librigena (figs. 13–20). Figs. 1–6, ×25; fig. 7, ×15; figs. 8–12, ×25; figs. 13–16, 18, 19, ×45; figs. 17, 20, ×8. Fig. 1, W64; fig. 2, W42; fig. 3, W30; fig. 4, W65; fig. 5, W22; fig. 6, W46; fig. 7, W36; fig. 8, O18; fig. 9, W1; fig. 10, W67; fig. 11, W13; fig. 12, W29; fig. 13, W59; fig. 14, O19; fig. 15, O22; fig. 16, O17; fig. 17, W42; fig. 18, O16; fig. 19, O27; fig. 20, O28.

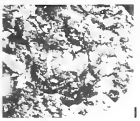
1

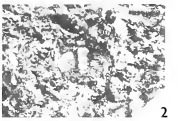
2


3


4

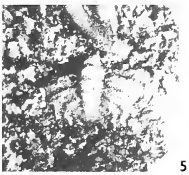
5

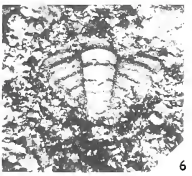
6

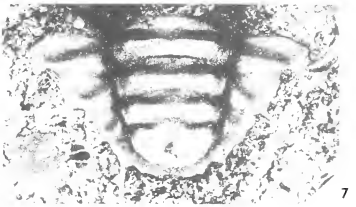
7

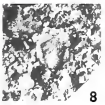
8

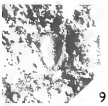
9

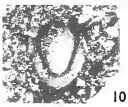
10

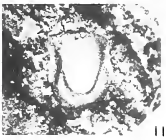
11

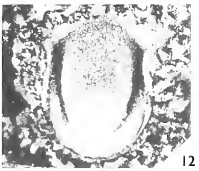
12

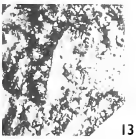
13


14

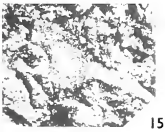
15

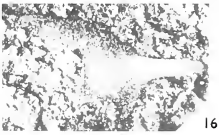
16


18

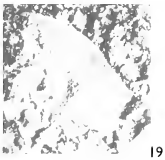
19

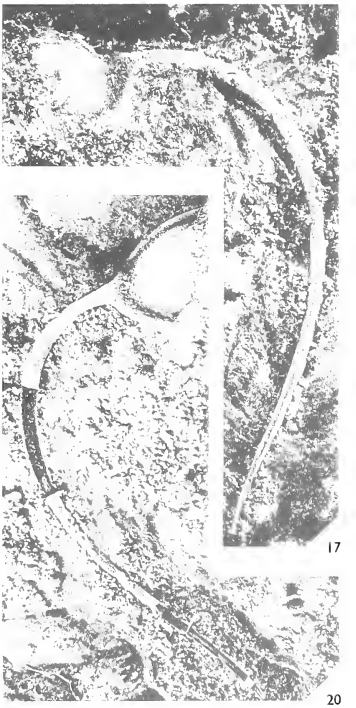
17 20

WHITWORTH, *Leptoplastus crassicorne* (Westergaard)

become curved and oblique, 3p remaining faint and transverse. Up to 11 thoracic segments present.

Group 7. Holaspids, with very strongly convex and parallel sided to forward narrowing glabella and fainter, strongly sigmoidal 1p and 2p glabellar furrows; 3p furrows may disappear. Preglabellar area may be present. Fixigenae not very convex except abaxial parts of anterior and posterior areas. Eye-ridges almost transverse, palpebral lobes reach back to level with outer ends of 1p glabellar furrows. Anterior border becomes forwards concave. Posterior sections of facial sutures cut posterior border at a more acute angle and more abruptly than before.

LIBRIGENA

There are few complete librigenae preserved but those illustrated show some of the changes which occur (Pl. 24, figs. 13–20).

The smallest fragment (Pl. 24, fig. 13), very doubtfully a free cheek, measures 0·36 mm. long and 0·10 mm. wide. The outer margin is entire but the ?sutural margin is probably not preserved in its original form. It may belong to an early meraspid stage as Plate 1, fig. 10. The ?genal spine is short and postero-lateral. During subsequent development (Pl. 24, figs. 14–18) the librigena becomes wider than long and increases strongly in convexity in the ocular region as the librigenal spine migrates forwards from a postero-lateral (Pl. 24, fig. 14) to lateral (Pl. 24, fig. 17) position. The adult genal spine is very long and robust, developing a strong outwards convex curve with a slightly reflexed tip. The lateral border and furrow do not appear until quite a late stage.

Due to imperfect preservation of the sutural margin in most cases it is almost impossible to assign the illustrated librigenae to respective cranidia, but from comparison of relative sizes it appears that Plate 24, fig. 14 might belong to a late Group 4 meraspid, Plate 24, figs. 15–18 to stages in Group 5, and Plate 24, figs. 19–20 to a late holaspid (e.g. Pl. 23, fig. 11).

HYPOSTOME

A few stages in the development of the hypostome are shown on Plate 24, figs. 8–12, taken from quite a large number of specimens. Few changes in relative dimensions occur, changes being mainly due to accentuation of the features present in the early forms. The smallest hypostome (Pl. 24, fig. 8) is about 1·28 mm. long and wide with a weakly convex middle body (strongest posteriorly) and narrow, convex borders. At a length of 0·33 mm. (Pl. 24, fig. 9) the middle body has increased in posterior convexity and is well raised above the now wider posterior border. The lateral border furrows are pit-like anteriorly and the anterior wings very small. By the time a length of 0·60 mm. is reached (Pl. 24, figs. 10, 11) its maximum width (ant.) is 0·56 mm. and the lateral borders are strongly constricted and ridge-like at one-third of their length from the front. The middle body has its highest point posteriorly at a single median apex. The posterior border is more broadly curved behind and descends almost immediately from the border furrow. The largest hypostome (Pl. 24, fig. 12) is 1·12 mm. long and wide (ant.). It differs from the earlier stages in having a very shallow anterior border furrow, deep and pit-like lateral border furrows at the constriction, and in the shape of the middle body. This latter rises very high above the posterior border, is somewhat truncated

behind, and has a double apex at its postero-lateral corners. A narrow convex rim runs around the margin of both lateral and posterior borders.

PYGIDIUM

The pygidia (Pl. 24, figs. 1–7) are considerably less common than cranidia and no advanced meraspid pygidia have been seen. The figures show most of the changes which occur during growth. It is impossible to accurately assign any but the smallest pygidia to respective cranidial sizes.

The smallest meraspid pygidium (Pl. 24, fig. 1) is 0·32 mm. wide and 0·16 mm. long with semicircular outline. The narrow axis has 2 distinct rings and an indication of a third, the pleural regions have 2 pairs of straight, oblique pleural furrows. At the lateral margin is a narrow convex rim leading into the first of 3 pairs of fine marginal spines which increase in length adaxially. The pygidium is moderately convex sagittally.

During subsequent development (Pl. 24, figs. 2–7) the pygidium is seen to develop 4 axial rings and a rounded terminal piece ((Pl. 24, figs. 4 and 7), 4 pairs of oblique pleural furrows, and 4 pairs of marginal spines. The axis increases in width at the expense of the pleurae from a quarter to a half or more (Pl. 24, figs. 2 and 7) of the total width and the median axial tubercles of the transitory pygidium are lost on the adult; the early segments are tuberculate and pass forward into the thorax, but the later true pygidial segments are smooth. The adult pygidial pleurae are relatively both shorter (exsag.) and narrower (tr.) than the early segments and the marginal spines smaller. Of the latter, all but the 4th pair, which remain long and fine, are short and triangular in the adult. An over-all change in shape from semicircular to triangular is seen and the sagittal convexity of early stages is completely lost, the adult pygidial pleural lobes being flat (in contrast to the strongly convex axis).

DISCUSSION

The development of *L. crassicornis* is similar in some respects to that of *Olenus gibbosus* (Strand 1927). The protaspid axis differs principally in the shape, size, and late-stage segmentation of the frontal lobe and in that it is widest anteriorly. The transverse suture and ridge between the cephalon and protopygidium/transitory pygidium is developed at an earlier stage and the fixigenal spines are longer. The protaspis is also somewhat larger throughout development in *O. gibbosus*. In meraspid stages the sutural ridge and fixigenal spine are retained longer, but the two species agree in the possession of a straight anterior cranidial border.

Early protaspid development of *L. crassicornis* is most like that of *Peltura scarabeoides* (Whittington 1958), especially in intermediate stages (Group 2 here), but the meraspid axial development is closer perhaps to that of *Leptoplastides salteri* (Raw 1925).

Regarding the nature and course of the facial sutures, the interpretation of Whittington (1958, pp. 203–4) for *P. scarabeoides* may be equally applied in this case. The facial suture is not clearly developed on the present material of *L. crassicornis* until early meraspid stages, but the presence and nature of the sutural ridge is identical in both species. The abrupt anterior termination of the lateral border (= sutural ridge of larger specimens) seen in Plate 22, figs. 7, 8 and in its interpretation, text-fig. 1*c*, suggests that

the facial suture, after running alongside the eye-ridge, crosses the border on to the ventral surface (?doublure). As growth proceeds its course is extended backwards to cut the border postero-laterally, and is accompanied by the loss of the metafixigenal spine. It is clear that the metafixigenal spine, which may be (as here) essentially transient, has previously been too freely equated with the fixigenal spines of adult olenids such as *Saltaspis* and *Nericiaspis*. From such an assumption *L. crassicorne* could easily be referred to the proparian condition during early meraspid development, but subsequent development shows that the final condition is opisthoparian. It is unfortunate that there are no well-preserved early meraspid librigenae (excluding the doubtful specimen in Pl. 24, fig. 13) from which one might determine the origin of the librigenal spine. It is possible, as suggested by Palmer (1958) for *Crassifimbra walcotti*, that the librigenae of protaspids may be represented at first by an entirely ventral plate, the suture thus being marginal (see text-fig. 1*b*). In later protaspids and early meraspids (text-fig. 1*c–e*) the librigena and facial suture become dorsal and the point where the posterior section cuts the border migrates slowly backwards outside the sutural ridge, which thus becomes a structure separate from the true marginal border.

Acknowledgements. Thanks go to Dr. I. Strachan for his continued assistance during the preparation of the manuscript. The work was undertaken during the tenure of a N.E.R.C. research grant which is gratefully received.

REFERENCES

HENNINGSMOEN, G. 1957. The trilobite family Olenidae. *Skr. norske Vidensk.-Akad. Mat.-naturv. Kl.* **1**, 1–303, pl. 1–31.

HOLTEDAHL, O. 1910. Über einige norwegischen Oleniden. *Norsk. geol. Tidsskr.* **2**, 1–24, pl. 1–3.

MOORE, R. C. (ed.) 1959. *Treatise on invertebrate paleontology*, Part O, *Arthropoda 1*. Geol. Soc. Am. and Univ. Kansas Press.

PALMER, A. R. 1958. Morphology and ontogeny of a Lower Cambrian Ptychoparioid trilobite from Nevada. *J. Paleont.* **32**, 154–70, pl. 25, 26.

RAW, F. 1925. The development of *Leptoplastus salteri* and other trilobites. *Q. Jl geol. Soc. Lond.* **81**, 223–324, pl. 15–18.

STØRMER, L. 1942. Studies on trilobite morphology. II. The larval development, the segmentation and the sutures, and their bearing on trilobite classification. *Norsk. geol. Tidsskr.* **21**, 49–164, pl. 1, 2.

STRAND, T. 1927. The ontogeny of *Olenus gibbosus*. *Norsk. geol. Tidsskr.* **9**, 320–9.

WHITTINGTON, H. B. 1957. The ontogeny of trilobites. *Biol. Revs.* **32**, 421–69.

—— 1958. Ontogeny of the trilobite *Peltura scarabeoides* from the Upper Cambrian, Denmark. *Palaeontology*, **1**, 200–5, pl. 38.

PETER H. WHITWORTH
Department of Geology
The University
Birmingham 15

Final typescript received 16 July 1969

A NEW CEPHALOPOD FAUNA FROM THE LOWER CARBONIFEROUS OF EAST CORNWALL

by S. C. MATTHEWS

ABSTRACT. A collection of approximately three hundred small cephalopods from a site in the Lower Carboniferous of east Cornwall includes representatives of *Gattendorfia* sp., Gen. et sp. nov. A, *Muensteroceras complanatum*, *M.* cf. *rotella*, *Ammonellipsites princeps*, *A.* sp. aff. *asiaticus*, *A.* sp. indet. and Gen. et sp. nov. B. It is argued that the fauna is of an age later than those of the Hangenbergkalk ('cuI') of Germany and possibly earlier than the late Tournaisian cephalopods of Belgium ('cuIIα'). German conodont evidence, taken together with some from Belgium, demonstrates that there is a range of Tournaisian age (Tn 2a–Tn 3b? in terms of the Belgian stratigraphy, or approximately the *Siphonodella crenulata* Zone in terms of conodonts) of which the cephalopod-based zonal standard makes no account. Certain North American (Mississippian) cephalopod faunas which show coincidences of cheiloceratacean (including gattendorfiid) and goniatitacean (including muensteroceratid and ammonellipsitid) forms have not found accommodation in the European zonal scheme. In the cases of the Chouteau limestone, Rockford limestone, and Walls Ferry limestone the evidence of conodonts suggests reference to that range of the Tournaisian where the European cephalopod standard fails.

CEPHALOPODS occur only rarely in successions of early Carboniferous age. The zonal scheme based on these fossils can be no better than the patchy record allows. So, too, with matters of phylogeny: any discussion of the emergence of the goniatitaceans (eventually the dominant group of Carboniferous goniatites) is hindered by the poverty of the evidence at present available. In these circumstances a certain degree of interest attaches to a new fauna which appears to be of Tournaisian age and which has, as contemporaries, cheiloceratacean and goniatitacean forms.

This paper is concerned mainly with the question of the age of the fauna as indicated by the most nearly mature goniatites present. A later communication will refer to the detail of immature forms and to ontogenies, and will review the current state of information on Tournaisian goniatites.

THE NEW FAUNA FROM EAST CORNWALL

A detached sheet of Lower Carboniferous rocks forms the mass of Viverdon Down south and east of Callington in east Cornwall. It emerged during mapping that the sheet includes a lower succession in which shales are predominant and an upper which has the tougher, siliceous rocks that define the topographic high. The lower succession is exposed at SX 398665 in a cutting on the narrow road which leads south-eastward down to the Tamar at Haltonquay. On the south-western side of the road thin cross-stratified siltstones occur among the dark shales, and at the north-western end of the exposure, near to the entrance to Heathfield Farm, coarse sandstones are exposed. These are taken to be associated with the finer-grained rocks in the stratigraphy of the lower part of the detached sheet. At a point approximately 30 metres south-east of the entrance to Heathfield Farm, and $2\frac{1}{2}$ m. above the present road level in the cutting, there is a lens of iron-shot, relatively coarse material disposed parallel to bedding within the shale and siltstone succession. When first discovered the remnant of the lens measured approximately

[Palaeontology, Vol. 13, Part 1, 1970, pp. 112–31, pls. 25–28.]

60 cm. by 4 cm. as exposed on the weathered face, and it proved to continue for 10 cm. maximum in the third dimension. Only the last 'tail' of the lens now remains in the exposure. Small cephalopods were visible on the site, and later preparation (under the microscope, with needle and brush) finally freed over three hundred individual fossils. Only molluscs are recognizable, and the minority of these are minute. There are no conodonts.

COMMENTS ON SIZE, AND ON BURIAL AND PRESERVATION

The range of size of the goniatites is shown in text-fig. 1. The smaller forms can be allotted to genera by continuous association of details of form down through the size-range. The graph of sizes of the generically indeterminable goniatites illustrates the obvious fact that the smallest individuals present the greatest difficulties of identification. Representatives of the ribbed ammonellipsitids and of Gen. et sp. nov. B, which is keeled at all growth stages, can nevertheless be confidently identified down to values of diameter in the neighbourhood of 1 mm. The size-frequency of all goniatites collected peaks at the 1–2 mm. grade.

There are many specimens in which living chamber and gas chambers can be distinguished. They indicate that the smallness of the fossils cannot be due to breakage during a transport–burial sequence of events or during preparation. Nor is this the kind of preservation in which only nuclei survive diagenesis in a robust state. In a majority of cases the fossils represent the stage of growth achieved at the time of death. The range of size and the range of form (evolute near-serpenticones to tightly involute near-cadicones, and orthocones and small, low-turreted gastropods are also present, if rare) suggest that this close concentration of such diverse individuals cannot have experienced any lengthy exposure to a sorting process.

The fossils are found silicified in a lens which is cut by many small siliceous veins. The more general silicification which affects the immediately higher part of the stratigraphy is, however, not developed here.

THE FAUNA AND ITS AGE

The following are identified:

Gattendorfia sp.
Gen. et sp. nov. A
Muensteroceras complanatum (de Koninck)
Muensteroceras cf. *rotella* (de Koninck)
Muensteroceras spp.
Ammonellipsites princeps (de Koninck)
Ammonellipsites sp. aff. *asiaticus* (Librovitch)
Ammonellipsites sp. indet.
Ammonellipsites spp.
Gen. et sp. nov. B

Indeterminable low-spired gastropods and small orthocones are also present.

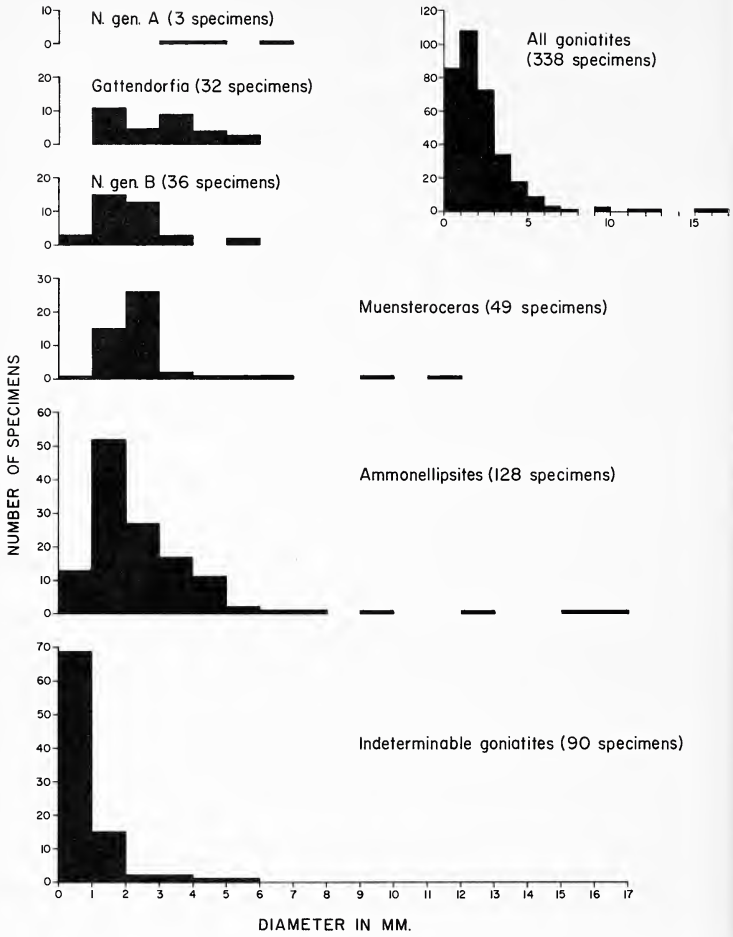

TEXT-FIG. 1. Size distribution of goniatites in the new fauna from Cornwall, by genera and (top right) for all goniatites collected.

The occurrence is stratigraphically in isolation. The nearest occurrence of any other fossils is at a point 800 m. to the west and some 100 m. higher in the succession (as judged from a map) where conodonts of the *anchoralis*-Zone are found (Matthews 1969*a*).

The cephalopods include *Ammonellipsites princeps* and *Muensteroceras complanatum*, and these are the indices to the first of the units (cuIIα) distinguished by Schmidt (1925) in the *Pericyclus*-Stufe (cuII, now the *Ammonellipsites*-Stufe—see Paproth, Teichmüller, and Remy 1960). But the Belgian original has been, until now, the sole western European occurrence of these forms, and it is therefore difficult to arrive at any understanding of stratigraphic limits for cuIIα. Also, the new fauna from Cornwall shows these two forms in an association altogether different from that found in Belgium (Delépine 1940*a*). For these reasons it becomes necessary to examine the composition of the currently accepted zonal scheme (which is in most essentials that advanced by Schmidt in 1925) in order to discover the constraints that exist in the matter of judging the age of the new fauna.

The cephalopod-based standard includes, in the Lower Carboniferous, three stages, successively the *Gattendorfia*-Stufe (cuI), *Ammonellipsites*-Stufe (cuII), and *Goniatites*-Stufe (cuIII). Schmidt's contribution of 1925 offered more detailed proposals than had been available before on the succession of faunas in cuI and cuIII and (this as a complete novelty) cuI subjoined to the two Lower Carboniferous stages previously recognized. Schindewolf (1927) would have preferred to define the beginning of the Carboniferous by reference to the entry of the distinctively Carboniferous goniatitaceans, with a median saddle as their characteristic. Schmidt was guided by altogether a different consideration. He brought forward the *Gattendorfia*-Stufe (then known as the *Protocanites*-Stufe) as the earliest Carboniferous unit because field mapping, particularly the work of Paeckelmann (1922), had indicated that the *Protocanites*-Stufe stratigraphy might be regarded as an equivalent of the Étroeungt. More recently, Vöhringer (1960) has presented a detailed analysis of the stratigraphic distribution, form and phylogenetic relationships of the cephalopods that occur in the 2 m. thick Hangenbergkalk, the type example of cuI. Vöhringer retained the definition of the lower limit of the Carboniferous as the point of entry of *Gattendorfia subinvoluta*, and added clarification by showing that *Balvia* is an imitoceratid. However, for want of any information from the stratigraphy above the Hangenbergkalk (the Liegende Alaunschiefer) he was unable to propose any upper limit to cuI. Among his cephalopods there was an example of *Karagandoceras*, a genus which possesses a median saddle, but which according to Vöhringer should be regarded as precocious in this respect, and should not be identified as the first of the major suite of goniatitaceans. Weyer (1965) has restudied the collections of *Gattendorfia*-Stufe material from Dzikowiec (Ebersdorf) in Lower Silesia, and has been able to suggest that *Paralytoceras*, too, anticipates later forms in its possession of a median saddle.

Schmidt's *Ammonellipsites*-Stufe units, cuIIα, β, γ, δ, were founded on occurrences of cephalopods in respectively Belgium, Ireland, Germany (Dillmulde), and Germany (Harz). In the case of cuIIα, the material comes from the Calcaire de Vaux–Calcaire de Calonne range of the stratigraphy according to Delépine (1940*a*). In Legrand, Mamet, and Mortelmans (1966) the site is referred to Tn 3c. The Irish cuIIβ forms (Foord 1903) cannot be given any exact stratigraphic attribution. The Erdbacherkalk, the IIγ type (Holzapfel 1889, Schmidt 1925) rests on pillow lavas. Its local stratigraphical relationships

and its content of reworked Upper Devonian conodonts have been described by Walliser and others (1958) and by Krebs (1963). The original occurrence of the cuIIδ fauna (Schmidt 1941) was in a bed of red shale, a few centimetres thick, which outcrops near Riefensbeek in the Harz Mountains. Plainly, there is no possibility of guaranteeing the cuI–cuII relationship nor the interrelationships of the cuII units by direct observation of stratigraphic superpositions. Only in the case of the cuII–cuIII transition can this be done, for the cuIIδ horizon, with *Entogonites nasutus*, has now been identified in the Rheinisches Schiefergebirge and its stratigraphic relationship to the cuIIIα marker horizons demonstrated (Nicolaus 1963). Schmidt's scheme of zones of 1925 had to depend on a presumed course of phylogenesis (based mainly on the sequence of prolecanitids) supported at one point by Belgian evidence taken to confirm the relative age of cuIIα and cuIIγ. The scheme has been available for over forty years. It can be seen to be weak in that it was based on evidence from a relatively small number of scattered localities. It has survived, free from any serious challenge, because of the continuing poverty of the evidence. But there have been occasional finds of cephalopod faunas which could not satisfactorily be dated by reference to this standard. Notable European examples are those from Zadelsdorf (Schindewolf 1922, 1926, 1939) and Iberg–Winterberg (Schindewolf 1951*a*). The early Mississippian goniatite faunas of the U.S.A. likewise have never found accommodation in Schmidt's scheme.

An alternative means of dating rock-successions of this range of age has appeared by the development in recent years of a zonal scheme based on conodonts. Voges's (1959, 1960) proposals, now confirmed and further elaborated by Meischner (in press), are based on detailed collecting from continuous sections. That information includes some obtained from sites where cephalopods occur, such as the Hangenbergkalk and the Erdbacherkalk. In 1960, Voges attempted a reconciliation of the two schemes. He claimed that cuIIα and cuIIβ were distinguishable from one another (and referred especially to Delépine's (1940*b*) treatment of Irish faunas) but that cuIIβ and cuIIγ were not. His tentative proposal was that the *Siphonodella crenulata* Zone should be equated with cuIIα, and the *anchoralis* Zone with cuIIβ/γ. It should be understood that neither cuIIα nor cuIIβ were identifiable in the sections from which his conodonts came, and also that the *anchoralis* Zone (as Voges himself showed) does not extend to the top of the Erdbacherkalk, the cuIIγ type. On the other hand, his proposals for cuI units, based on the evidence of the Hangenbergkalk, are irreproachable.

It is now possible to use conodonts as a means of distinguishing Belgian equivalents of the German stratigraphic units, and the results are immediately of relevance here. Conil, Lys, and Mauvier (1964) produced a preliminary account of the conodonts they had discovered in the Franco-Belgian Lower Carboniferous. As Paproth (1964) has pointed out, this made it possible to recognize Tn 1b as the Hangenbergkalk correlative. It follows that some hundreds of metres of the Belgian succession (Legrand, Mamet, and Mortelmans 1966) intervene between the cuI horizon and the cuIIα source. This range is unrecognized in the statement of cephalopod zones. In terms of conodonts it is approximately the *Siphonodella crenulata* Zone of Voges. Further, Conil, Lys, and Mauvier's discovery of *Scaliognathus anchoralis* in Tn 3c indicates that the cuIIα source lies within Voges's *anchoralis* Zone, and consequently that Voges was mistaken in his tentative equation of the *anchoralis* Zone with cuIIβ/γ. A new rendering of relationships linking cephalopod occurrences and conodont zones is offered in text-fig. 2.

The Hangenbergkalk record of cephalopods fails to close with that from the late Tournaisian of Belgium and the cephalopod zonal scheme is seen to be discontinuous. In the past it has been suggested that the sufficiency of the scheme was confirmed by the work of Librovitch (1940), who dealt with an unusually rich body of material from

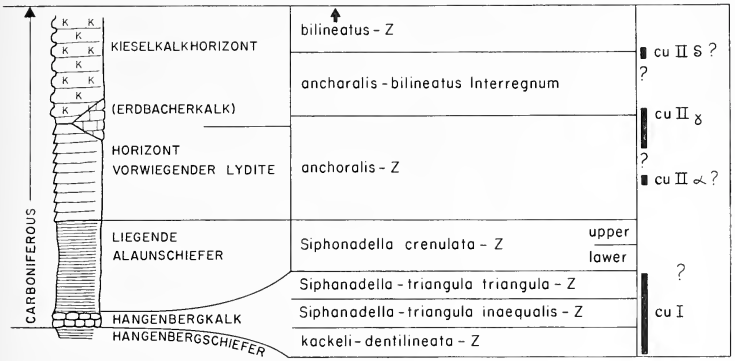

TEXT-FIG. 2. Rock-units in the Lower Carboniferous stratigraphy of Germany, and the conodont-zones established there (after Voges). Standard cephalopod occurrences may be referred to the conodont scheme as suggested on the right of the diagram.

Kazakhstan. Librovitch proposed a succession of 'faunal complexes' which appeared to repeat the sequence of stages proposed by Schmidt in 1925. The complexes do not, however, stand as independent confirmation of the standard scheme. They were modelled on the existing western European proposals, as Librovitch himself plainly admitted.

The new fauna from Cornwall may be of *Siphonodella crenulata*-Zone age, certainly later than the Hangenbergkalk faunas, possibly earlier than those of the late Tournaisian of Belgium in that there is coincidence of *Gattendorfia* and *Ammonellipsites*. This estimate of the age relative to Tn 3c is not easily made. *Ammonellipsites princeps* and *Muensteroceras complanatum* are common to the two. The new elements in the Cornish fauna, since they are unique to this case, have no part in a question of relative age. The mere presence of gattendorfiids has no immediate significance, for an argument of age based on late survival is never entirely satisfactory. But the gattendorfiids seen here resemble the small, slightly more evolute, constricted '*Kazakhstania?*' of the Walls Ferry limestone of Arkansas (see below) and in this there is an indirect suggestion that the Cornish fauna might predate Tn 3c. The fauna adds to the record of Tournaisian goniatites, and it may have its place within the gap now seen to interrupt the standard sequence of zones; but it does not by any means close that gap nor provide any justification for proposing a new zone.

The view that a coincidence of gattendorfiid and goniatitacean cephalopods exists in a post-Hangenbergkalk, pre-Calcaire de Calonne range of age is strongly encouraged

by the American evidence. It is necessary to refer here to the conodonts of the *Siphonodella quadruplicata–S. crenulata* Zone and of the *Siphonodella isosticha–S. cooperi* Zone. These may be equated with European proposals as is done in Canis (1968, table 2), but neither should be regarded as identifying cuIIα. Also, it should be noted that the *Siphonodella isosticha–S. cooperi* Zone can be found to precede the *anchoralis* Zone in Europe (Matthews 1969*b*). The Chouteau limestone, according to Miller and Collinson (1951), produces representatives of the following cephalopod genera: *Gattendorfia*, *Muensteroceras*, *Ammonellipsites*, *Imitoceras*, *Protocanites*, and *Prodromites*. Canis (1968) refers the Chouteau limestone to the *S. quadruplicata–S. crenulata* and *S. isosticha–S. cooperi* Zones. The Rockford limestone of Indiana has, at the type locality, *Imitoceras*, *Muensteroceras*, *Protocanites*, and *Prodromites* (Miller and Collinson 1951) and has produced a *Gattendorfia* species in north-western Indiana (Gutschick and Treckmann 1957). Rexroad and Scott (1964) report that the Rockford limestone has the conodonts of the *S. isosticha–S. cooperi* and *Gnathodus semiglaber–Pseudopolygnathus multistriata* Zones. Gordon (1964) lists *Gattendorfia*, '*Kazakhstania*?', *Ammonellipsites*, and *Muensteroceras* from the Walls Ferry limestone of Arkansas and observes that conodonts, dominated by siphonodellids (according to W. H. Hass), are found in a bed which lies 1 ft. below the cephalopod occurrence. Gordon (1964) reports too the existence of a *Gattendorfia* specimen from the lower part of the Lodgepole limestone of Montana and an ammonellipsitid, as yet undescribed, again from the Lodgepole. Klapper (1966) has described conodonts of the 'lower *Siphonodella crenulata* Zone' (which, misled by German practice, he equates with cuIIα) from the basal part of the Lodgepole.

The record of American information is not as full as might be desired. For example, it would be preferable to identify the exact stratigraphic provenance of cephalopod material and to refer in every case to conodont material taken from the same horizon. Again, greater fullness is desirable in that the outstanding 'misfit' (as seen from Europe), the Marshall sandstone fauna of Michigan, cannot yet be referred to a conodont-based age-standard. But the evidence so far available may be sufficient to show that there is little purpose in attempting to judge the age of these early Mississippian faunas by reference to the European scheme of cephalopod zones. They appear to belong to a range of age which goes unregarded in the cephalopod scheme and which can be distinguished only by the evidence of conodonts.

SYSTEMATIC DESCRIPTIONS

Numbers with prefix BU refer to the Geology Museum, University of Bristol.

Measurements. The dimensions given apply in every case to the stated diameter. Abbreviations are: D = diameter, U = umbilical segment of the diameter, WH = whorl height, Wh = distance from the ventral crest of the whorl to the ventral crest of the preceding whorl, WW = whorl width.

Order AMMONOIDEA Zittel 1884
Suborder GONIATITINA Hyatt 1884
Superfamily CHEILOCERATACEAE Frech 1897
Family CHEILOCERATIDAE Frech 1897
Subfamily IMITOCERATINAE Ruzhencev 1950
Genus GATTENDORFIA Schindewolf 1920

Type-species by original designation: *Gattendorfia subinvoluta* Schindewolf 1920.

1960 *Gattendorfia* Schindewolf; Vöhringer, pp. 149–50 (see also for earlier references).
1964 *Gattendorfia* Schindewolf; Gordon, pp. 168–70 (see also for earlier references).
1964 *Kazakhstania* Librovitch; Gordon, p. 171.
1965 *Gattendorfia* Schindewolf; Weyer, p. 447.

Gattendorfia sp.

Plate 25, figs. 6–18; text-fig. 3*a-e*

Material. BU 19635–BU 19666.
Dimensions (mm.)

	Plate reference	*D*	*U*	*WH*	*Wh*	*WW*	*Volutions*
BU 19635	Plate 25, figs. 17, 18	*c.* 6·5	*c.* 2·5	*c.* 2·5	*c.* 2	*c.* 2	4·5?
BU 19640	Plate 25, fig. 12	5	3	1·3	—	1·5	4·75
BU 19642	Plate 25, fig. 16	4·2	1·8	1·2	—	1·5	4·5
BU 19666	Plate 25, figs. 13, 14	4·2	2	1·2	*c.* 1·0	*c.* 1·5	4·5
BU 19637	Plate 25, figs. 7, 8	3·4	1·6	1	0·9	*c.* 0·9	3·75
BU 19645	Plate 25, figs. 9, 10	2·7	1·05	0·8	*c.* 0·7	0·7	3
	Gordon (1964, p. 172):	8·5	5·2	2·0	—	2·6	
		9·0	6·4	2·0	—	2·5	
		10·2	7·3	2·2	—	*c.* 3·0	

Description. Small evolute shells with rounded whorls which are relatively high at early stages of growth. No evidence of external ornament. Whorls each bear two conspicuous constrictions, one succeeded by another at slightly less than half-circumference. Constrictions follow a shallowly sinuous course across the flanks, are so disposed to the axis of growth that their nearest approach to the aperture is on the venter. Suture as in text-fig. 3*d*, *e*. External lobe relatively deep.

Remarks. The sutures of these evolute forms have no match among known gattendorfiids. Their character excludes a prolecanitid affinity, and so too does the presence of constrictions. The evolute shell-form and the presence of constrictions are reminiscent of what is seen in the persistently evolute gattendorfiid to which some refer as '*Kazakhstania*'. Librovitch, in 1940, proposed the subgenus *Gattendorfia* (*Kazakhstania*) on the basis of material from central Asia, and suggested it to be distinct from *Gattendorfia* by its evolute form maintained throughout growth. Further, he suggested that *Gattendorfia* (*Kazakhstania*), with its relatively deep, lanceolate external lobe, and with constrictions, need not be confused with the protocanitids, which are also evolute. Miller and Collinson (1951), without discussing the matter, referred to '*Kazakhstania*' as a genus. It was not until 1955 that Miller and Garner proposed that the form be raised to generic rank. They then added an American species to the two described by Librovitch. In 1960 Vöhringer returned these evolutes to synonymy with *Gattendorfia*, and there is much to commend his view. Vöhringer's full analysis of the Hangenbergkalk gattendorfiids has shown how variable are these involution–evolution characteristics of shell form, and it seems good to accept that the continuously evolute shell, which Librovitch saw as the definitive characteristic of his subgenus, is not sufficiently distinctive to justify a relatively elevated systematic position for '*Kazakhstania*'. Certainly, full generic status does not seem justifiable.

Gordon (1964), apparently unaware of Vöhringer's opinion, identified a small, evolute ammonoid from the Mississippian of Arkansas as '*Kazakhstania?* sp.' He suggested that '*Kazakhstania*' might receive also certain small, evolute, constricted ammonoids reported from the Mississippian of Ohio by Hyde (1953). These latter strongly resemble the

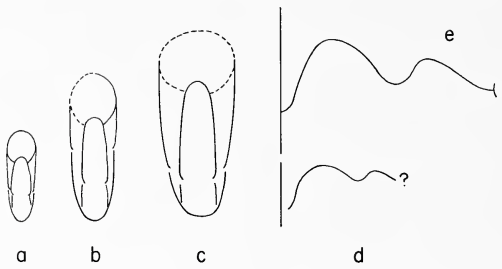

TEXT-FIG. 3. *Gattendorfia* sp. *a*, *b*, *c*. Apertural aspect of BU 19645 (terminal diameter 2·7 mm.), BU 19637 (3·4 mm.), BU 19644 (4·3 mm.) respectively. *d*. Suture of BU 19645 at diameter 1·7 mm. *e*. Suture (reversed) of BU 19643 at diameter approximately 3·7 mm. (specimen deformed).

individuals encountered in the Cornish fauna (an observation first put to the author by Professor M. R. House).

Weyer (1965), like Vöhringer, regarded '*Kazakhstania*' as synonymous with *Gattendorfia*. Vöhringer, indeed, had gone so far as to suggest that Librovitch's two species were perhaps to be identified with *Gattendorfia tenuis* (a form which ranges through most of the Hangenbergkalk and is still available in the topmost bed, as Vöhringer's table 1 shows). *G. tenuis* is, however, more involute at late stages of growth and must therefore differ from the two forms described by Librovitch. Since Vöhringer found nothing entirely comparable with '*Kazakhstania*' in the Hangenbergkalk there remains a possibility that fully evolute species may be of an age somewhat later than is represented in that sequence. The evidence from the Hangenbergkalk (which has three gattendorfiid species still extant in its uppermost part) need not be taken to account completely for the vertical range of *Gattendorfia*. Thus, although these evolute forms lose their generic rank, they may be thought to retain a special stratigraphic interest.

EXPLANATION OF PLATE 25

Figs. 1, 2. Gen. et sp. nov. A. Right (to display ornament) and left (to display early whorls) views of BU 19668. ×8.

Figs. 3, 4, 5. Gen. et sp. nov. A. Apertural, lateral and oblique ventral (to display sutures) views of BU 19667. ×8.

Figs. 6–18. *Gattendorfia* sp. 6, BU 19641. 7, 8, BU 19637. 9, 10, BU 19646. 11, BU 19643 (deformed). 12, BU 19640 (deformed). 13, 14, BU 19666. 15, BU 19638. 16, BU 19642. 17, 18, BU 19635 (deformed). All ×8.


1

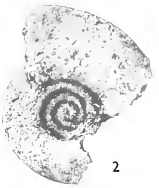
2


3


4


5


6


7

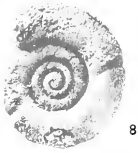
8


9


10


11

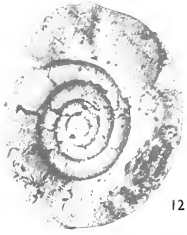
12


13


14


15


16


17

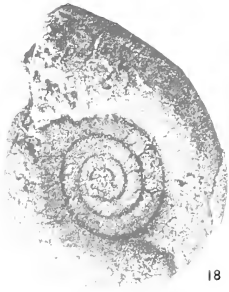
18

MATTHEWS, Carboniferous cephalopods from Cornwall

Superfamily GONIATITACEAE de Haan 1825
Family GONIATITIDAE de Haan 1825
Subfamily KARAGANDOCERATINAE Librovitch 1957
Gen. et sp. nov. A

Plate 25, figs. 1–5; text-fig. 4*a*, *b*

Material. BU 19667–BU 19669.
Dimensions (mm.)

	Plate reference	*D*	*U*	*WH*	*Wh*	*WW*	*Volutions*
BU 19667	Plate 25, figs. 3–5	5	1·6	1·8	1·3	2·6	?
BU 19668	Plate 25, figs. 1, 2	4	1·4	1·6	1·1	2·4	3·8

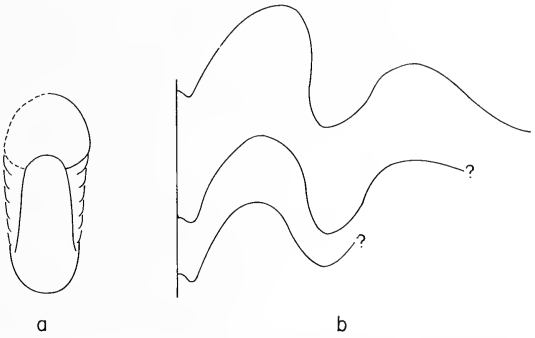

TEXT-FIG. 4. Gen. et sp. nov. A. *a.* Apertural aspect of BU 19667 (terminal diameter 5 mm.). *b.* Three successive sutures of BU 19667 at diameters 3·9–4·7 mm.

Description. Narrow, open umbilicus exposes all previous whorls. Whorls depressed, wider than high, maximum width (also overlap) at approximately one-third whorl-height. Ornament of approximately twenty robust umbilical ribs which fade as they curve concave adaperturally beyond the locus of maximum whorl-width and finally approach parallelism with the growth axis. Venter broad, rounded, unornamented. Suture (text-fig. 4*b*) has broadly splayed external lobe with median saddle.

Remarks. The form reveals its most interesting characteristic in the broad external lobe, with its median saddle. It is therefore a goniatitacean. But like *Karagandoceras* and *Paralytoceras* it has little else in common with the goniatitinids.

Weyer (1965), who re-examined *Paralytoceras* and first demonstrated its possession of goniatitacean sutural character, decided to refer both *Karagandoceras* and *Paralytoceras* provisionally to the Karagandoceratinae—this in full awareness of the possibility that the two genera might have arisen along quite independent courses. Weyer preferred to attach the subfamily Karagandoceratinae to the family Goniatitidae, rather than follow Ruzhencev (1962) in identifying a family Karagandoceratidae attached to the Praeglyphioceratacеae. The systematic affiliation of the new genus as given here is

entirely in accordance with Weyer's proceeding: a third genus is added to Karagandoceratinae, and this is done recognizing the possible artificiality of a Gen. et sp. nov. A—*Karagandoceras–Paralytoceras* combination.

The new form has a sutural character sufficient to separate it from any goniatitinid of conceivably comparable age, although in its relative robust ornament and in shell-form it appears to be closer to the goniatitinids than is *Karagandoceras* or *Paralytoceras*. The resemblance, within the Karagandoceratinae, is more with *Paralytoceras*, especially in the form of the external lobe. The lateral lobes of the two sutures differ slightly, however, and the fimbriate ornament of the more evolute, carinate *Paralytoceras* is altogether different from what is seen in Gen. et sp. nov. A. Certain umbilical ornament is seen among the ammonellipsitids, especially in the young stages of *A. rotuliformis* (Crick) and in *A. homoceratoides* (Schindewolf). In neither case is the exact form of the ornament comparable with what is seen here. The sutures (at much larger diameter) of these two are also different.

Formal proposal and precise diagnosis of the new genus and species is reserved until further, possibly relevant material has been examined. BU 19667 (which was capable of being prepared in order to expose the median saddle) and BU 19668 probably belong to one and the same species. BU 19668 offers no sutural information, but is consistent with BU 19667 in shell-form and ornament. A badly preserved, relatively large third form (BU 19669) has more sharply sculpted ribs than the other two (Pl. 27, fig. 8) and is tentatively referred to the new genus.

Subfamily MUENSTEROCERATINAE Gordon 1964

Genus MUENSTEROCERAS Hyatt 1884

Type species by original designation: *Goniatites oweni* var. *parallela* Hall 1860.

1961 *Muensteroceras* Hyatt; Kullmann, pp. 256–8 (see also for earlier references).
1961 *Munsteroceras* Hyatt; Pareyn, p. 96.
1963 *Muensteroceras* Hyatt; Campbell and Engel, p. 87.
1964 *Munsteroceras* Hyatt; Wagner-Gentis, p. 232.
1964 *Muensteroceras* Hyatt; Gordon, p. 175 (see also for earlier references).
1965 *Dzhaprakoceras* Popov, p. 36.
1965 *Muensteroceratoides* Popov, p. 36.

Muensteroceras complanatum (de Koninck 1880)

Plate 26, figs. 10, 11; text-fig. 5*c*

1884 *Goniatites complanatus* de Koninck, p. 106, pl. 46, fig. 4.
1940*a* *Muensteroceras complanatum* (de Koninck); Delépine, pp. 47–52; pl. 3, figs. 3, 4; text-fig. 8.

EXPLANATION OF PLATE 26

Figs. 1, 2. *Ammonellipsites* sp. indet. Lateral and ventral views of BU 19772. ×5.
Figs. 3–6, 9. *Muensteroceras* spp. 3, BU 19675. 4, BU 19674. 5, BU 19676. 6, BU 19672. 9, BU 19673. 6×5, others ×8.
Fig. 7. *Muensteroceras* cf. *rotella* (de Koninck). Oblique ventral (to display sutures) view of BU 19671. ×8.
Fig. 8. *Ammonellipsites princeps* (de Koninck). BU 19721. ×8.
Figs. 10, 11. *Muensteroceras complanatum* (de Koninck). Apertural and lateral views of BU 19670. ×5.

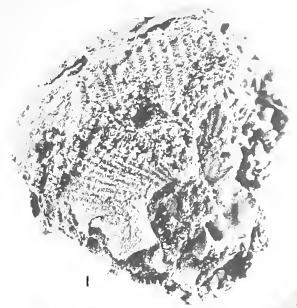

1

2

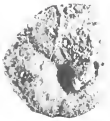

3

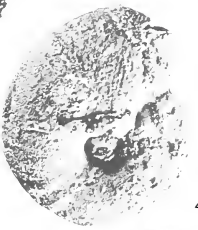

4

5

6

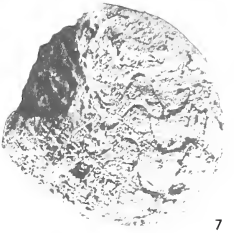

7

8

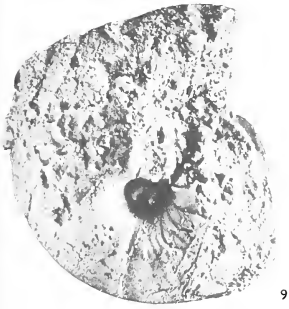

9

10

11

MATTHEWS, Carboniferous cephalopods from Cornwall

Material. BU 19670.
Dimensions (mm.)

	Plate reference	*D*	*U*	*WH*	*WW*
BU 19670	Plate 26, figs. 10, 11	*c.* 12	*c.* 1·0	*c.* 6·3	*c.* 4·5
	Delépine (1940*a*, 47):	65	6–7	33	18

Note. Delépine (1940*a*, 47) referred in his table to Plate 28, figs. 3 and 4. Obviously, a reference to Plate 27, figs. 3 and 4 was intended.

Remarks. The specimen figured shows well the involution, small umbilicus, high flanks and sutural character (text-fig. 5*c*) appropriate to this species.

Muensteroceras cf. *rotella* (de Koninck 1880)

Plate 26, fig. 7; text-fig. 5*b*

Material. BU 19671.

Remarks. One fragment provides evidence sufficient to justify comparison with *Muensteroceras rotella*. The umbilicus appears to be more open than that of *M. complanatum*; the suture line (text-fig. 5*b*), with a straight-sided external lobe stacked close to the same element of the previous suture line, as is found in *M. rotella*. In this, *Muensteroceras rotella* is close to the American *M. oweni* and *M. parallelum*.

It is worthwhile to note that Delépine (1940*a*) referred one example of *M. rotella* to a relatively early position in the Tournaisian stratigraphy, and also that an ammonoid collected from the Liegende Alaunschiefer in Germany has been suggested to be identifiable as *M. rotella* (H. Schmidt's opinion, reported in Paproth, Teichmüller and Remy 1960, p. 8).

Muensteroceras spp.

Plate 26, figs. 3–6, 9

Material. BU 19672–BU 19718.

Remarks. Several specimens are referred to the genus *Muensteroceras* on the evidence of their form. Occasionally, sutural evidence is also available. Certain small specimens may carry a hint of faint ribbing (Pl. 26, figs. 4, 9), and some constrictions (Pl. 26, figs. 3, 5).

Subfamily PERICYCLINAE Hyatt 1900
Genus AMMONELLIPSITES Parkinson 1822

Type-species by subsequent designation of Schindewolf 1951*b*: *Ellipsolithes funatus* Sowerby 1814.

1911 *Pericyclus*; Hind, pp. 107–8; pl. 4, figs. 3, 4, 5, 5*a*.
1957 *Ammonellipsites* Parkinson; Gordon, pp. 29–33.
1961 *Pericyclus* Mojsisovics 1882 emend. Hyatt 1883; Pareyn, p. 135.
1963 *Pericyclus* Mojsisovics; Campbell and Engel, p. 114.
1964 *Ammonellipsites* Parkinson; Gordon, pp. 172–3 (see also for earlier references).
1964 *Pericyclus* Mojsisovics; Wagner-Gentis, p. 229.
?1965 *Neopericyclus* Popov, pp. 45–6.

Remarks. Gordon (1957) has produced a thorough review of the history of attempts to subdivide this genus. He supplied also a key to recognition of the extant subgenera. Since

present information on the relative ages of the various occurrences of ammonellipsitids is so poor, and since sutural evidence is not available in every case, there is a danger that these subgeneric associations of ammonellipsitid species may be artificial and phylogenetically uninstructive. No subgeneric assignments are made here.

Ammonellipsites princeps (de Koninck 1844)

Plate 26, fig. 8; Plate 28, figs. 1–7; text-fig. 5*a*

1844 *Ammonites princeps* de Koninck, pp. 579–80; pl. 51, figs. 2*a*, *b*, *c*, 3*a*, *b*, *c* (de Koninck's publication is given the dates 1842–4. Delépine (1940*a*) refers de Koninck's proposal of *Ammonites princeps* to the year 1842).

1940*a* *Pericyclus princeps* (de Koninck); Delépine, pp. 38–40; pl. 1, figs. 12–15; text-fig. 7 (see also for earlier references).

Material. BU 19719–BU 19761.

Dimensions (mm.)

	Plate reference	*D*	*U*	*WH*	*Wh*	*WW*	*No. of ribs*
BU 19719	Plate 28, figs. 1, 2	*c.* 6·8	1·3	*c.* 3·4	*c.* 2·6	4·8	*c.* 60
BU 19720	Plate 28, fig. 7	*c.* 10·0	*c.* 2·0	*c.* 4·0	?	6·8	
BU 19721	Plate 28, fig. 6	*c.* 5	1·2	1·8	*c.* 2·0	3·2	*c.* 50
BU 19723	Plate 28, fig. 5	3·3	1·0	1·4	?	2·8	*c.* 40
BU 19726	Plate 28, fig. 3	2·2	0·7	0·8	?	1·4	—
	Delépine (1940*a*, 39):	35	10	—	—	—	42
	„	34	11	—	—	—	> 50

Remarks. BU 19719 shows well the sutural (text-fig. 5*a*) and sculptural characteristics of the species, although ribs may be more numerous than in the larger Belgian specimens. Other specimens (BU 19720–BU 19761), if their ornament is well preserved, may also be referred to this species. Some further small individuals possibly fit to be compared with *A. princeps* are included in *Ammonellipsites* spp. (below).

The relatively robust ribs curve convex-adapically across the venter, but their curvature is always more slight than in the American form *A. blairi*. Occasional instances of bifurcation are seen. The constrictions, up to four in number per whorl, are relatively broadly developed, and their course parallels that of the ribs.

Ammonellipsites sp. aff. *asiaticus* (Librovitch 1940)

Plate 27, figs. 5, 9, 10

1940 *Pericyclus asiaticus* Librovitch, pp. 122–30, 268–72; pl. 16, figs. 1–6; pl. 17, figs. 1–4; text-figs. 43–51.

1940 *Pericyclus asiaticus* var. *simplex* Librovitch, pp. 130–1, 272; pl. 17, figs. 5, 6; text-figs. 52, 53.

EXPLANATION OF PLATE 27

Figs. 1–4, 6, 7. *Ammonellipsites* spp. 1, 2, BU 19730 (cf. *A. princeps*). 3, BU 19724 (cf. *A. princeps*). 4, BU 19766 (cf. *A.* sp. aff. *asiaticus*). 6, BU 19729 (cf. *A. princeps*). 7, BU 19765 (cf. *A.* sp. aff. *asiaticus*). All ×8.

Fig. 8. Gen. et sp. nov. A? BU 19669. ×5.

Figs. 5, 9, 10. *Ammonellipsites* sp. aff. *asiaticus* (Librovitch). 5, BU 19764. 9, 10. Lateral and ventral (to display spiral ribbing) views of BU 19762. 5, ×8, others ×5.

1

2

3

4

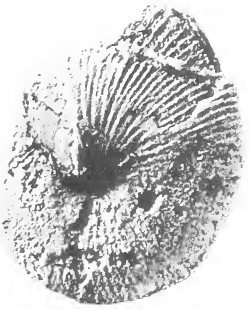

5

10

6

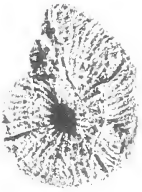

7

8

9

MATTHEWS, Carboniferous cephalopods from Cornwall

Material. BU 19762–BU 19771.
Dimensions (mm.)

	Plate reference	*D*	*U*	*WH*	*Wh*	*WW*
BU 19762	Plate 27, figs. 9, 10	17	2·4	8	5·3	9
BU 19763		*c.* 16	*c.* 1·2	*c.* 10·5	6	*c.* 7·5
BU 19764	Plate 27, fig. 5	7·7	0·6	4	2·6	*c.* 5·8
?BU 19766	Plate 27, fig. 4	4·7	0·6	2·0	?	*c.* 3·6
?BU 19765	Plate 27, fig. 7	3·8	0·5	1·8	*c.* 1·4	*c.* 2·4

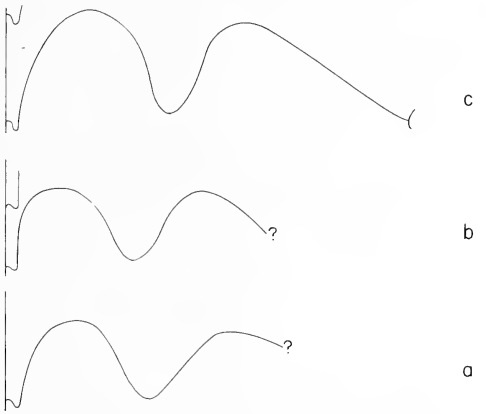

TEXT-FIG. 5. *a. Ammonellipsites princeps.* Suture of BU 19719 at diameter 4·5 mm. *b. Muensteroceras* cf. *rotella.* Suture of the incomplete specimen BU 19671, with ventral element of the succeeding suture shown. *c. Muensteroceras complanatum.* Suture of BU 19670 at diameter 10 mm., with ventral element of the succeeding suture shown.

Description. The shell is tightly involute and the narrow umbilicus has a rounded margin. The last whorl is relatively high, with extensive flanks and a rounded venter. On the largest specimen (terminal diameter 17 mm.) approximately eighty ribs can be counted on the venter. The fine ribs increase by bifurcation, and rarer intercalation, achieved near the locus of maximum whorl-width. Of the two secondary ribs produced by bifurcation one is immediately collinear with the primary rib and the other diverges adapically. The ribs follow a sinuous course across the flanks with a weak, broad, adaperturally concave curve whose turning-point is situated near half whorl-height. There is a clear ventral sinus. In addition to these transverse sculptural elements a minor spiral set is present, best seen in troughs between major ribs. The spiral elements are collinear in adjacent troughs. Interference of transverse with spiral sculptural elements results in a serrate condition seen in the better-developed transverse ribs. There are no constrictions. The suture is unknown.

Remarks. The general form resembles that seen in some of the tightly umbilicate, multicostate species described by Delépine (1940*a*). None of these is exactly similar. Gordon (1957) suggested that certain involute species described by Librovitch, *A. asiaticus*, *A. dichotonus*, *A. sokurensis*, should perhaps be united in a subgenus which, if sutural information were available, might be found fit to receive also the Belgian forms *A. divisus* and *A. ryckholti*. The Cornish species is of this character, if not strictly identical with any of the species mentioned. In the continuing absence of sutural information, Gordon's suggestion cannot be acted upon; and the view expressed above is that there may be little profit from such proposals of subgenera. It is perhaps worth while to note that *A. divisus* and *A. ryckholti* come, according to Delépine (1940*a*), from a relatively low part of the Belgian succession.

The closest similarity is to Librovitch's species *A. asiaticus*, especially to that variety which he distinguished by its lack of constrictions. There is a resemblance in general form, and some similarity in the course of the ribbing, but the umbilical margin appears to be more sharply defined in the Kazakhstan individuals. Also, they have, apparently, coarser and less numerous ribs (17–18 per cm. here at diameter 17 mm. as against 6–10 at 30–5 mm.—unfortunately, none of the Cornish forms are large enough to permit comparison at a common diameter).

Librovitch mentioned that *A. asiaticus* shows a fine spiral striation in extremely rare cases, sufficient to give a faintly reticulate character to the ornament, and spiral striae are seen in the present case. A spiral element occurs fairly commonly in the ornament of early Carboniferous cephalopods. Examples in *Gattendorfia* were mentioned by Librovitch (1940, p. 241) and Vöhringer (1960, p. 156). Vöhringer (1960, p. 148) found sculpture of this kind in *Costimitoceras*, too. Schindewolf (1951*b*, p. 306) has listed *A. trapezoidalis*, *A. hauchcornei*, *A. kochi*, *A. homoceratoides* and (possibly) *A. plicatilis* among ammonellipsitids so ornamented (he did not mention *A. asiaticus*, and in *A. homoceratoides* he included a case where the 'spiral' element is not conspicuously well organized). The spiral sculpture-element is, then, a feature of the present individuals that they share with *A. asiaticus*, but since it is one so commonly developed among early Carboniferous cephalopods it need not be taken as compelling the conclusion that the Cornish specimens and *A. asiaticus* are conspecific. In later Carboniferous ammonoids there are, of course, numerous examples of forms which display such sculpture.

It is necessary to note here Budinger and Kullmann's (1964) brief mention of what is perhaps the earliest Carboniferous goniatite fauna so far recovered in the Cantabrian Mountains. It includes '*Ammonellipsites* (*Pericyclus*) aff. *asiaticus* (sp. iuv.)' and imitoceratids. The suggestions of affinity with *A. asiaticus* advanced by these authors and again here involve some measure of coincidence. The writer is not acquainted with Budinger and Kullmann's specimen.

The small specimens BU 19765–BU 19771 are only tentatively included. The material

EXPLANATION OF PLATE 28

Figs. 1–7. *Ammonellipsites princeps* (de Koninck). 1, 2, Lateral and oblique apertural (note plug of silica filling the umbilicus) views of BU 19719. 3, BU 19726. 4, BU 19725. 5, BU 19723. 6, BU 19721. 7, BU 19722. 7, ×5, all others ×8.

Figs. 8–20. Gen. et sp. nov. B. 8, 9, BU 19854. 10, 11, BU 19853. 12, BU 19849 (deformed). 13, BU 19851. 14, BU 19852. 15, 16, BU 19850. 17, 18, BU 19847. 19, 20, BU 19848. All ×8.

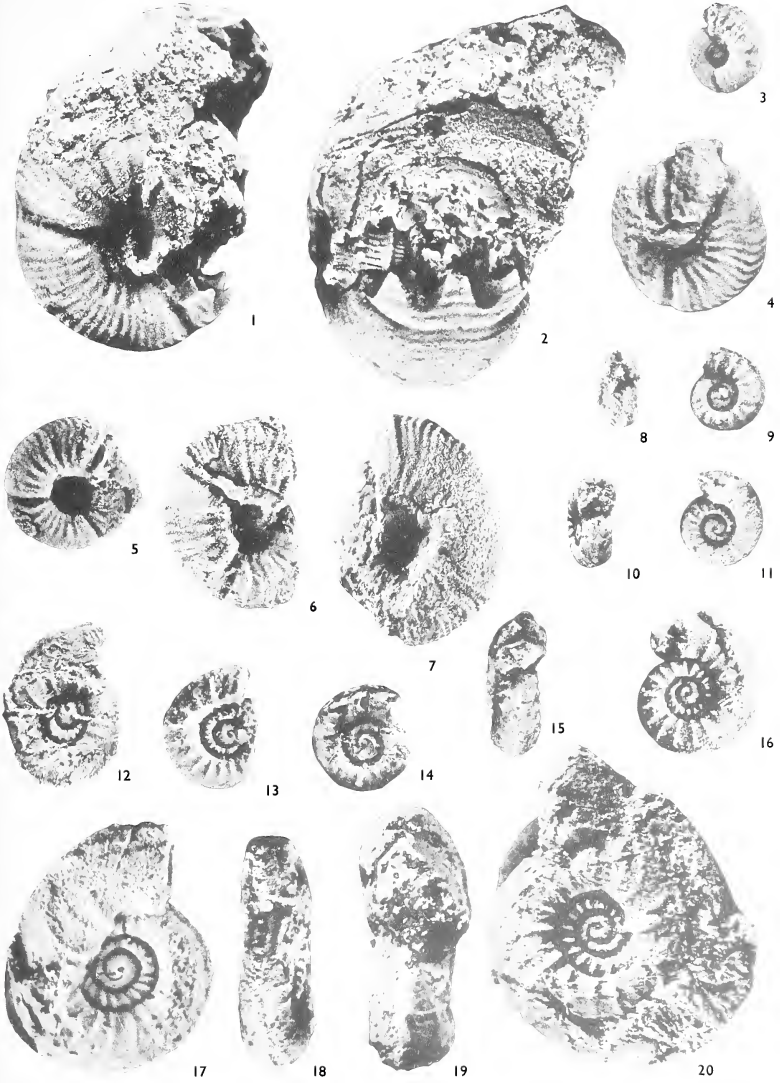

MATTHEWS, Carboniferous cephalopods from Cornwall

available is too limited to allow the form to be traced down confidently to the smaller ranges of size. Certain specimens listed under *Ammonellipsites* spp. may deserve to be compared with the form treated here.

Ammonellipsites sp. indet.

Plate 26, figs. 1, 2

Material. BU 19772.
Dimensions (mm.)

	Plate reference	*D*	*U*	*WH*	*WW*
C 75076	Plate 26, figs. 1, 2	?	*c.* 3·5	6·5	12·5

Description. A globose, multicostate, tightly umbilicate form. The flanks are restricted and the venter broadly rounded. The fine ribs bifurcate, to give equal secondaries, near the umbilical margin. Intercalation is also seen, but is less common. The course of the ribs is almost straight until the broad ventral sinus is reached. A hint of minor, spiral ribbing can be seen. No constrictions are found. The suture is unknown.

Remarks. The tight umbilicus and abundant fine ribs suggest comparison with the forms mentioned for these features above, and the presence of spiral striations suggests a comparison with *A.* sp. aff. *asiaticus.* In this present case, however, the shell is distinctively globose; but the single specimen is poorly preserved, the suture not revealed, and any justification for proposing a new specific category is lacking.

Ammonellipsites spp.

Plate 27, figs. 1–4, 6, 7

Material. BU 19773–BU 19846.

Remarks. Certain of the specimens included here may tentatively be associated with *A. princeps* or *A.* sp. aff. *asiaticus* by the character (relative robustness, curvature) of their ribbing (see remarks attached to the explanation of Pl. 27).

Subfamily PERICYCLINAE Hyatt 1900?
Gen. et sp. nov. B

Plate 28, figs. 8–20; text-figs. 6*a–d*

?1880 *Goniatites* de Koninck (partim), pp. 112–13; pl. 44, fig. 9*a, b.*
?1940*a* '*Goniatites*' (*Pericyclus?*) Delépine, pp. 42–3; pl. 3, fig. 7.

Material. BU 19847–BU 19882.
Dimensions (mm.)

	Plate reference	*D*	*U*	*WH*	*Wh*	*WW*	*Volutions*
BU 19848	Plate 28, figs. 19, 20	5	1·7	2·3	*c.* 1·8	2	4·2
BU 19847	Plate 28, figs. 17, 18	*c.* 3·8	1·4	1·3	?	*c.* 1·2	3·75
BU 19850	Plate 28, figs. 15, 16	3·5	1·4	1·3	*c.* 1·1	1·2	3·5
BU 19853	Plate 28, figs. 10, 11	2·2	0·9	0·7	*c.* 0·6	1·1	2·75
BU 19852	Plate 28, fig. 14	2·1	0·8	0·7	0·5	0·9	2·3
BU 19854	Plate 28, figs. 8, 9	2·0	0·8	0·7	0·5	0·9	2·3

Description. Relatively evolute shell with all earlier whorls displayed. Umbilical margin rounded. Early whorls depressed, wider than high, carry an umbilical ornament of elongate, edged nodes and have a ventral carina which may be noded. At later stages the umbilical ornament is weaker, the ribs gradually fade as they approach the venter (which they do not reach) and show an adaperturally concave curvature. The later whorls are higher than wide, with maximum width at approximately one-third whorl-height. The venter here is sharp rather than distinctly carinate. Suture, as in text-fig. 6, has a shallow, straight-sided, external lobe with median saddle.

Remarks. This form differs from any Lower Carboniferous cheiloceratacean genus having a keel and any umbilical or flank ornament (*Protocanites*, *Pseudarietites*) by reason of its sutural character. One pseudarietidan whose suture is unknown, *P. serratus*, is distinctly the latest of the Hangenbergkalk forms referred to *Pseudarietites* by Vöhringer (1960). Its ornament is vaguely reminiscent of what is seen at early stages of growth here.

Several goniatitids may resemble the present form in particular characteristics of form, but there is in no case complete correspondence. *Muensteroceras acutum* Librovitch and '*Brancoceras*' *enniskillense* Foord both have acute, near-carinate venters, but show no other point of resemblance. There is no agreement of sutural evidence. *Ammonellipsites? carinatus* (Schindewolf) differs in its ribbing and in the degree of its involution. Its suture is unknown. *Anmonellipsites homoceratoides* (Schindewolf) has umbilical ornament at early stages. But it is at no stage carinate, and its form is more inflated than is the case here. The *A. homoceratoides* suture is of another character and is in fact such as to have led Pareyn (1961) to suggest *A. homoceratoides* as the source from which *Beyrichoceras* sprang. It is conceivable that the *A. homoceratoides* example of umbilical ornamentation arose independently of the one under discussion here.

Two Belgian forms deserve closer attention. They are *Goniatites crenulatus* de Koninck and *Goniatites* (*Pericyclus?*) *tuberculatus* Delépine. In neither of these is the suture known, but they bear close resemblance to the new genus in shell-form. *G.* (*P.?*) *tuberculatus* appears to be at all stages more involute and more depressed, and its umbilical ornament is nodose rather than costate. The last whorl bears four clear constrictions. None of these objections apply to the more evolute *G. crenulatus*, whose umbilical tubercules show a tendency toward elongation at right angles to the umbilical border. However the venter in the case of *G. crenulatus* is rounded (de Koninck 1880, pl. 49, fig. 9*b*). Given information on the suture line and on the ventral form of juvenile stages, *G. crenulatus* and *G.* (*P.?*) *tuberculatus* might be seen to belong in this new genus.

Delépine (1940*a*, p. 43) wrote of *G. crenulatus* thus: 'Peut-être, quand la suture sera connue, pourrait-on réunir ces deux espèces dans un genre nouveau, intermédiaire entre *Pericyclus* et *Munsteroceras*, voisin de *Pericyclus* au stade jeune, mais distinct de celui-ci parce que les côtes, saillantes surtout au bord de l'ombilic, où elles sont noduleuses, s'atténuent très tôt, puis passent à des côtes fines, plûtot des stries, comme chez *Munsteroceras*'. The possibility of proposing a new genus arises now, and it may prove to include these two small problematical Belgian forms in specific categories distinct from one constructed to contain the Cornish specimens. One would acknowledge Delépine's prescience, but should forbear at this time from speculating on any phylogenetic linkage of the two Belgian forms with the one described here.

The occurrence of a median saddle in this relatively evolute goniatite is especially interesting. The near-parallel margins of the external lobe and the rounded character of the adjacent saddles are taken as possible justifications for an assignment to the subfamily Pericyclinae—this even though ventral ornament, the carina apart, fails.

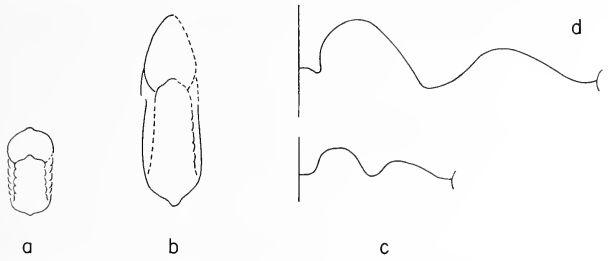

TEXT-FIG. 6. Gen. et sp. nov. B. *a*, *b*. Apertural aspect of BU 19854 (terminal diameter 2 mm.) and BU 19847 (*c*. 3·8 mm.) respectively. *c*. Suture of BU 19854 at diameter 1·7 mm. *d*. Suture of BU 19847 at diameter 3·2 mm.

The American faunas which (it is argued above) intervene between those of the Hangenbergkalk and of the late Tournaisian have as yet produced no representation of goniatites with predominantly umbilical ornament.

Acknowledgements. The cephalopod fauna described here was discovered during the author's tenure of a Shell International Petroleum Company Research Studentship. On many occasions, Professor Scott Simpson and Professor D. L. Dineley have freely offered their advice and encouragement. Professor M. R. House, Dr. R. Goldring and Dr. M. K. Howarth have kindly criticized a draft of the paper. The photographic illustrations are the work of Mr. R. Godwin of the Geology Department, University of Bristol, which is here gratefully acknowledged.

REFERENCES

BUDINGER, P., and KULLMANN, J. 1964. Zur Frage von Sedimentationsunterbrechungen im Goniatiten- und Conodonten-führenden Oberdevon und Unterkarbon des Kantabrischen Gebirges (Nordspanien). *N. Jb. Geol. Paläont., Mh.* 1964, 414–29, 2 figs.

CAMPBELL, K. S. W. and ENGEL, B. A. 1963. The faunas of the Tournaisian Tulcumba Sandstone and its members in the Werrie and Belvue synclines, New South Wales. *J. geol. Soc. Aust.* **10**, 55–122, 11 figs., pl. 1–9.

CANIS, W. F. 1968. Conodonts and biostratigraphy of the Lower Mississippian of Missouri. *J. Paleont.* **42**, 525–55, 2 figs., pl. 72–4.

CONIL, R., LYS, M., and MAUVIER, A. 1964. Critères micropaléontologiques essentiels des formations-types du Carbonifère (Dinantien) du bassin Franco-Belge. *Congrès Avanc. Étud. Stratigr. carb.* Paris, 1963, 325–32, pl. 1, 2.

DELÉPINE, G. 1940*a*. Les goniatites du Dinantien de la Belgique. *Mém. Mus. r. Hist. nat. Belg.* **91**, 1–91, 19 figs., pl. 1–10.

—— 1940*b*. Contribution à l'étude des goniatites du Waulsortien d'Irlande et de Belgique. *Annls. Soc. géol. N.* **64**, 134–49, pl. 4.

FOORD, A. H. 1897–1903. Carboniferous cephalopoda of Ireland. *Palaeontogr. Soc.* [*Monogr.*] 1–234, pl. 1–49.

GORDON, M. 1957. Mississippian cephalopods of northern and eastern Alaska. *Prof. Pap. U.S. geol. Surv.* **283**, 1–61, 26 figs., pl. 1–6.

—— 1964. Carboniferous cephalopods of Arkansas. *Prof. Pap. U.S. geol. Surv.* **460**, 1–322, 96 figs., pl. 1–30.

GUTSCHICK, R. C. and TRECKMAN, J. F. 1957. Lower Mississippian cephalopods from the Rockford limestone of northern Indiana. *J. Paleont.* **31**, 1148–53, 3 figs., pl. 143, 144.

HIND, W. 1910. On four new Carboniferous nautiloids and a goniatite new to Great Britain. *Proc. Yorks. geol. Soc.* **17**, 97–109, pl. 3–7.

HOLZAPFEL, E. 1889. Die Cephalopoden-führenden Kalke des unteren Carbon von Erdbach-Breitscheid bei Herborn. *Paläont. Abh.* (N.F. 1), **1**, 1–74, pl. 1–8.

HYDE, J. E. 1953. Mississippian formations of central and southern Ohio. *Bull. Geol. Surv. Ohio*, **51**, 1–355, pl. 1–54.

KLAPPER, G. 1966. Upper Devonian and Lower Mississippian conodont zones in Montana, Wyoming, and South Dakota. *Paleont. Contr. Univ. Kans.* **3**, 1–43, 2 figs., pl. 1–6.

KONINCK, L. G. DE, 1842–4. *Description des animaux fossiles qui se trouvent dans le terrain carbonifère de Belgique.* iv+650 pp., atlas, 55 pl. Liège.

—— 1880. Faune du calcaire carbonifère de la Belgique. II. Genres *Gyroceras*, *Gomphoceras*, *Orthoceras*, *Subclymenia* et *Goniatites*. *Annls. Mus. r. Hist. nat. Belg.* (Sér. Pal.) **5**, 2, 1–125, 28 figs., pl. 32–50.

KREBS, W. 1963. Oberdevonische Conodonten im Unterkarbon des rheinischen Schiefergebirges und des Harzes. *Z. dt. geol. Ges.* **114**, 57–84, 4 figs. pl. 9, 10.

KULLMANN, J. 1961. Die Goniatiten des Unterkarbons im Kantabrischen Gebirge (Nordspanien). I. Stratigraphie. Paläontologie der U.O. Goniatitina Hyatt. *N. Jb. Geol. Paläont. Abh.* **113**, 219–326, 12 figs., pl. 19–23.

LEGRAND, R., MAMET, B., and MORTELMANS, G. 1966. Sur la stratigraphie du Tournaisien de Tournai et de Leuze. Problèmes de l'étage Tournaisien dans sa localité-type. *Bull. Soc. belge Géol. Paléont. Hydrol.* **74**, 140–88, pl. 1.

LIBROVITCH, L. S. 1940. Carboniferous ammonoids of north Kazakhstan. *Paleontologiya SSSR*, Moscow, **4** (9), 1–394, 78 figs., pl. 1–25 [in Russian, English summary].

MATTHEWS, S. C. 1969*a*. A Lower Carboniferous conodont fauna from east Cornwall. *Palaeontology*, **12**, 262–75, 1 fig., pl. 46–50.

—— 1969*b*. Two conodont faunas from the Lower Carboniferous of Chudleigh, south Devon. Ibid. **12**, 276–80, pl. 51.

MEISCHNER, D. (in press). Conodont zonation of the German Carboniferous. *Congrès. Avanc. Étud. Stratigr. carb.* Sheffield 1967.

MILLER, A. K. and COLLINSON, C. 1951. Lower Mississippian ammonoids of Missouri. *J. Paleont.* **25**, 454–87, 14 figs., pl. 68–71.

—— and GARNER, H. F. 1955. Lower Mississippian cephalopods of Michigan. Part 3, Ammonoids and Summary. *Contr. Mus. Paleont. Univ. Mich.* **12**, 113–73, 16 figs., pl. 1–7.

NICOLAUS, H.-J. 1963. Zur Stratigraphie und Fauna der *crenistria*-Zone im Kulm des Rheinischen Schiefergebirges. *Beih. Geol. Jb.* **53**, 1–246, 32 figs., pl. 1–18.

PAECKELMANN, W. 1922. Über das Oberdevon und Unterkarbon des Südflügels der Herzkamper Mulde auf Blatt Elberfeld. *Jb. preuss. Landesanst. BergAkad.* **42**, 257–306, 2 figs., pl. 2.

PAPROTH, E. 1964. Die Untergrenze des Karbons. *Congrès Avanc. Étud. Stratigr. carb.*, Paris, 1963, **2**, 611–17, 3 figs.

—— TEICHMÜLLER, R., and REMY, W. 1960. Allemagne, Carbonifère. In PRUVOST, P. (ed.), *Lexique Stratigraphique International*, **5c** (1), 3–307, Paris.

PAREYN, C. 1961. Les massifs carbonifères du Sahara sud-Oranais, II. Paléontologie stratigraphique. *Publs. Cent. Rech. Sahar.* (sér. Géol.) **1**, 15–244, 27 figs., pl. 1–28.

POPOV, A. V. 1965. New Viséan ammonoids of the Tien-Shan. *Paleont. Zh.* Moscow 1965, **2**, 35–49, figs. 1–8, pl. 3, 4 [in Russian].

REXROAD, C. B., and SCOTT, A. J. 1964. Conodont zones in the Rockford Limestone and New Providence Shale (Mississippian) in Indiana. *Bull. Indiana Dep. Conserv. Geol. Surv.* **30**, 1–54, 6 figs.

RUZHENCEV, V. E. 1962. Mollusca-Cephalopoda 1. In ORLOV, Y. A. (ed.), *Osnovy Palaeontologii* **5**, 437 pp., 187 figs., pl. 1–32. Moscow [in Russian].

SCHINDEWOLF, O. H. 1922. Über eine Unterkarbonfauna aus Ostthüringen. *Senckenbergiana*, **4**, 8–20.
—— 1926. Beiträge zur Kenntnis der Cephalopodenfauna des oberfränkisch-ostthüringischen Unterkarbons. Ibid. **8**, 63–96, 11 figs.
—— 1927. Zur Kenntnis der Devon-Karbon-Grenze in Deutschland. *Z. dt. geol. Ges.* **78**, 88–132, 5 figs.
—— 1939. Bemerkungen zur Stratigraphie des oberfränkisch-ostthüringischen Unterkarbons. *Jb. preuss. geol. Landesanst. BergAkad.* **59**, 456–75, 8 figs., pl. 16, 17.
—— 1951*a*. Über ein neues Vorkommen unterkarbonischer *Pericyclus*-Schichten im Oberharz. *N. Jb. Geol. Paläont. Abh.* **93,** 23–116, 36 figs., pl. 3–7.
—— 1951*b*. Zur Gliederung der *Pericyclus*-Gruppe (Cephal., Goniatit.). *N. Jb. Geol. Paläont. Mh.* 1951, **10**, 305–10.
SCHMIDT, H. 1925. Die carbonischen Goniatiten Deutschlands. *Jb. preuss. Geol. Landesanst. BergAkad.* **45**, 489–609, pl. 19–26.
—— 1941. Eine neue Fauna mit *Pericyclus* von Riefensbeek im Harz. *Jb. Reichstelle Bodenforsch.* **60,** 148–56, pl. 19–20.
VOGES, A. 1959. Conodonten aus dem Untercarbon I und II (Gattendorfia- und Pericyclus-Stufe) des Sauerlandes. *Paläont. Z.* **33**, 266–314, 5 figs., pl. 33–5.
—— 1960. Die Bedeutung der Conodonten für die Stratigraphie des Unterkarbons I und II (Gattendorfia- und Pericyclus-Stufe) im Sauerland. *Fortschr. Geol. Rheinl. Westf.* **3** (1), 197–228, 5 figs.
VÖHRINGER, E. 1960. Die Goniatiten der unterkarbonischen Gattendorfia-Stufe im Hönnetal (Sauerland). Ibid. **3** (1), 107–96, 53 figs., pl. 1–7.
WAGNER-GENTIS, C. H. T. 1964. VI. Description of Goniatites. In HIGGINS, A. C., WAGNER-GENTIS, C. H. T., and WAGNER, R. H. 1964. Basal Carboniferous strata in part of northern Léon, N.W. Spain: stratigraphy, conodont and goniatite faunas. *Bull. Soc. belge Géol. Paléont. Hydrol.* **72**, 228–48, pl. 1–4.
WALLISER, O. H. *et al.* 1958. Zum Oberdevon und Unterkarbon von Erdbach-Langenaubach (SW-Dillmulde, Rheinisches Schiefergebirge). *Notizbl. hess. Landesamt. Bodenforsch. Wiesbaden*, **87**, 120–32.
WEYER, D. 1965. Zur Ammonoiden-Fauna der *Gattendorfia*-Stufe von Dzikowiec (Ebersdorf) in Dolny Śląsk (Niederschlesien), Polen. *Ber. geol. Ges. D.D.R.* **10**, 443–64, 3 figs., pl. 6–8.

S. C. MATTHEWS
Geology Department
Queen's Building
University Walk
Bristol 8

Typescript received 2 June 1969

NOTE ADDED IN PROOF

After this paper had gone to press the author became aware of Krebs's (1968) valuable restudy of the Erdbacherkalk. Krebs has been able to show that the Lower Carboniferous in the Langenaubach–Breitscheid reef complex includes Erdbach limestone facies developments at three different levels in the stratigraphy. His paper includes new identifications of the goniatites by Kullman and of the trilobites by Hahn. Krebs's information on the local stratigraphy of this important palaeontological source is entirely welcome. It will be seen that the remarks made here on the Erdbacherkalk (pp. 115–17) were written in ignorance of these most recent findings. It should be clear, however, that the author's comments on the scattered nature (geographic and stratigraphic) of the standard goniatite occurrences remain valid.

REFERENCE

KREBS, W. 1968. Die Lagerungsverhältnisse des Erdbacher Kalkes (Unterkarbon II) bei Langenaubach–Breitscheid (Rheinisches Schiefergebirge). *Geotekt. Forsch.* **28**, 72–103, 4 text-figs.

TWO NEW DICYNODONTS FROM THE TRIASSIC YERRAPALLI FORMATION OF CENTRAL INDIA

by TAPAN ROY CHOWDHURY

ABSTRACT. Two new dicynodonts recently collected from the Triassic Yerrapalli formation of India are described. The first, *Rechnisaurus cristarhynchus*, is a stahleckeriid and the first of its kind to be reported from Asia. *Rechnisaurus* shows considerable similarities to *Dinodontosaurus* of the Middle Triassic of Brazil and Argentina. The second dicynodont, *Wadiasaurus indicus* is the first kannemeyeriid to be described from India and its nearest relative is thought to be *Sangusaurus* of the Middle Triassic of Zambia.

UNTIL recently the only dicynodont reptile known from India was *Lystrosaurus*, reported from the Panchet formation of the Damodar valley Gondwanas (Robinson 1958). This dicynodont is now known from a large number of skulls and associated postcranial material and shows a close resemblance to the South African *Lystrosaurus* (Tripathi and Satsangi 1963). The occurrence of a second dicynodont reptile from India was noticed recently by Jain, Robinson, and Roy Chowdhury (1964) from the Gondwanas of the Parnhita-Godavari valley. This relatively large dicynodont was represented by the anterior ends of the lower jaws, fragments of maxillae and of basicrania, and several postcranial bones. Somewhat resembling *Kannemeyeria*, it was found in a red clay horizon overlying the Permo-Triassic Kamthi formation and which was separated from the overlying fossiliferous Upper Triassic Maleri formation by a sandstone horizon devoid of any fossil remains. This large dicynodont was found associated with a large thecodont reptile (a possible erythrosuchid), a moderately large theriodont reptile and two labyrinthodont amphibians (one was possibly a capitosaur, the other perhaps a brachyopid), thus revealing an altogether new fauna for this sub-continent. Prompted by this discovery, Jain *et al.* (1964) suggested a new formation name, the Yerrapalli formation, for the clay belt from which this new fauna was found, and tentatively suggested that this is comparable in age to the *Cynognathus* zone of the South African Karroo or possibly a little later. The barren sandstone belt immediately above the Yerrapalli formation was named the Bhimaram (sometimes spelt Bheemaram) sandstone.

The Yerrapalli fauna was first noted from an isolated outcrop of Gondwana rocks near Chinur, lying south of the main outcrop belt of Upper Gondwana formations around Maleri and Achlapur and separated from the main outcrop by an oblique fault. In 1964 when Dr. P. L. Robinson visited the main outcrop belt with Dr. E. H. Colbert and the author, she picked up some dicynodont tusks and skull bones from a red clay horizon lying south of Achlapur. Since dicynodonts are unknown in the overlying Upper Triassic fauna of the Maleri formation, these fragments indicated the presence of a distinct fauna. Chatterjee (1967) subsequently mapped the area around Achlapur and proved beyond doubt that the same geological sequence occurs in the main outcrop area as in the more southerly Chinur area. 'Immediately above the Kamthi rocks a red clay belt, with sandstones, contains representatives of the Yerrapalli fauna. Above this clay belt lies a continuous band of sandstone equivalent to Bhimaram sandstone of the

[Palaeontology, Vol. 13, Part 1, 1970, pp. 132–44.]

Chinur area. This sandstone band is succeeded by the true Maleri formation in which excellent specimens of the Upper Triassic vertebrate fauna have been found' (Chatterjee 1967, p. 40).

The dicynodonts described in this paper were collected from red clays of the Yerrapalli formation by the field party of the Geological Studies Unit, Indian Statistical Institute, during field trips of 1964 and 1965. The material consists of two skulls and many postcranial bones, but no skeleton, complete or partial, could be obtained. One skull described here as a new genus and species, *Rechnisaurus cristarhynchus*, was found in the northern area near Rechni village. The second skull, also belonging to a new genus and species described here as *Wadiasaurus indicus*, was excavated from the red clays of the southern area near Yerrapalli village. A large number of postcranial bones were also found in the latter locality but not in actual association with the skull. As it appears that two distinct genera of dicynodonts are present in the Yerrapalli formation, no attempt has been made to relate the postcranial bones to either of these two genera at present, and their description has been deferred until associated material is discovered.

SYSTEMATIC DESCRIPTIONS

Genus RECHNISAURUS gen. nov.

Derivation of name. The genus has been named after the village near which it was discovered.

Type species. *Rechnisaurus cristarhynchus* sp. nov.

Diagnosis. As for sole species at present.

Rechnisaurus cristarhynchus sp. nov.

Text-figs. 1–3

Derivation of name. This refers to the presence of a strong median ridge in the nasal region of the skull.

Material. The holotype skull only; specimen I.S.I.R.37 in the collection of the Geological Museum, Indian Statistical Institute, Calcutta.

Type locality. One kilometre south of Rechni, Pranhita Godavari valley, Andhra Pradesh, India.

Horizon. Yerrapalli formation of the Gondwana Group, Triassic.

Diagnosis. Dicynodont of moderately large size. Skull about 38 cm. long. Large canine teeth. Wide interorbital region. Blunt snout. Strong median ridge on anterior and dorsal surfaces of premaxilla which continues on dorsal surface of nasal; on either side of the ridge lies a pair of deep depressions. Powerful antero-ventrally directed caniniform process bearing rugose rounded flange on its postero-ventral edge. Short postorbital region. Short and wide temporal opening. Fairly narrow intertemporal bar, dorsally concave in cross section. No high parietal crest. Low boss immediately behind pineal foramen. Parietal forms most of the intertemporal bar. Sharp transition between dorsal and occipital surface.

The material and its preservation: The skull was found partly exposed in the red clays and was just beginning to disintegrate on a 'nala' (gully) slope. Parts of the skull were actually found on the 'nala' bed, a little removed from their original place, but could be fitted on to the skull. Most of the occiput and the zygomatic arches were probably washed away and could not be found. The preorbital half of

the skull is almost complete and only very slightly distorted. There is a break, however, along the suture between the premaxilla and the nasal, and the antero-lateral part of the nasal, where it forms the dorsal border of the nostril, is missing; the rest of the narial border is well preserved and the missing part could be restored quite easily. Similarly the anterior border of both the orbits is also broken and parts of the prefrontals, lacrymals, jugals, and squamosals, forming these borders, are missing and have been restored in dotted outline in the illustrations. Behind the orbits, there is a transverse break in front of the pineal foramen with some fitting surfaces to help restoration. Most of the superficial part of the interparietal bone is missing but the rest of the intertemporal bar is well preserved. The zygomatic arches are broken a little behind the maxillae, but the well-preserved post-orbital bar helps in restoring the continuation of the suborbital bar up to the orbit and also indicates the position of the more posterior extension of the zygomatic bar. The braincase and the central part of the palate are more or less well-preserved. In the occiput, only the condyle, the foramen magnum and the median part of the supra-occipital are preserved, with a minor break above the condyle. The squamosals are missing save for an isolated piece near the dorsal part of the lateral wing of the right squamosal. The quadrates and quadratojugals are not present. Only the symphysial part of the lower jaw was found.

Description of the skull

Dorsal view (text-fig. 1). The skull is massive and appears to have been quite broad and triangular in outline. The top of the snout is wide and there is a strong median ridge running from the tip of the snout, gradually widening and dying out behind the nasal-frontal suture. On either side of the ridge lies a pair of deep depressions which become wider posteriorly as the snout broadens; these depressions terminate where the nasals meet the frontals and prefrontals. The front of the snout is wide and blunt. The sides of the snout fall sharply vertically, and thus the external nostrils do not appear in the dorsal view of the skull. The nasals are fairly large bones with a long midline suture. The premaxilla is rather short and wide with a strongly rugose surface. The orbits are separated by the large frontals and are bordered dorsally by prefrontals, frontals, and post-orbitals. The post-orbital bar has rather delicate proportions for such a massive skull, and the post-orbital bone overlaps the parietal strongly by a process directed posteriorly along the lateral edge of the intertemporal bar.

The preparietal bone is small, and only its anterior and posterior parts are preserved, for in this region the specimen has a break in the skull roof which obscures the contact between the frontal and the parietal, lateral to the preparietal. The pineal foramen is rather small, 12 mm. long and 8 mm. wide and is quite deep. There is certainly an abrupt elevation of the level of the skull roof just behind the pineal foramen. The pineal foramen is bordered anteriorly by the preparietal and otherwise by the parietals.

The temporal opening must have been quite short as is evident by the short intertemporal bar, almost exclusively formed by the parietals. The intertemporal bar is narrow; the paired parietals meet at a long midline suture behind the pineal foramen and each has a raised lateral edge, thus making the dorsal face of the bar concave in section. There is a low but prominent median boss immediately behind the pineal foramen. At the posterior end of the parietal, on its lateral surface, the squamosal is preserved only as a broken patch of bone forming a sutural contact. Another dissociated fragment of the lateral wing of the squamosal is also present, but does not give any useful information except to locate the postero-lateral border of the temporal opening.

Ventral view (text-fig. 2). The secondary palate, formed almost entirely by the premaxilla, is rather short and its plane is set at an angle to rest of the palate, giving an arched shape for the ventral surface of the skull.

A pair of palatal ridges runs back from the tip of the premaxilla to converge into a median ridge about halfway along the secondary palate. The vomer is not preserved, but presumably continued the median ridge posteriorly on to the palate. Laterally the premaxilla is strongly overlapped by the maxilla; the latter bone is drawn out laterally into

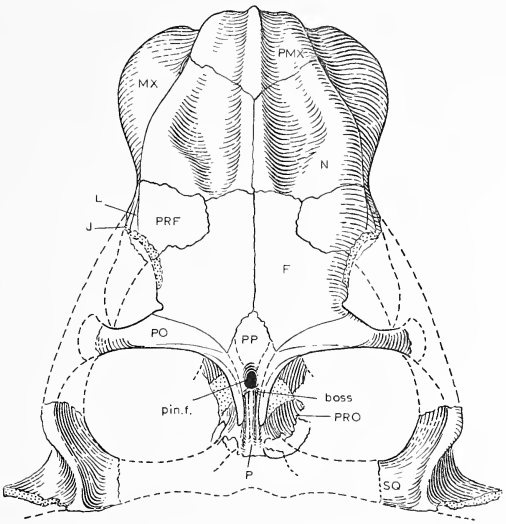

TEXT-FIG. 1. *Rechnisaurus cristarhynchus*, holotype. Dorsal view of skull, $\times\frac{1}{4}$ (for abbreviations, see pp. 143–4).

a very strong caniniform process, as already mentioned. The powerful tusks have their roots quite posteriorly placed in the maxillae, and are curved slightly inwards. Posteriorly the maxilla is bounded laterally by the jugal and medially by the pterygoid; there is a large lateral fenestra in between these three bones. On the left side of the specimen, at the root of the caniniform process, the maxilla shows on its lateral wall a sutural facet which continues on to the lateral surface of the jugal. This facet must have received the anterior extension of the squamosal overlapping the former two bones laterally. The posterior part of the sub-orbital bar is missing.

The anterior rami of the pterygoids leave the maxillae, run posteriorly and meet along a midline suture behind a short interpterygoid vacuity. The vomers are not preserved but the palatines lie on the inner sides of the anterior rami of the pterygoids and terminate anteriorly against the maxillae. The ectopterygoid is missing, but there is a distinct depressed sutural facet on the lateral side of the pterygoid which is probably for the ectopterygoid. If the above observation is correct, the ectopterygoid must have been a thin sheet of bone as observed in *Dinodontosaurus* (Cox, 1968). Behind the palate, the

parasphenoid and the basisphenoid-basioccipital complex show the normal dicynodont condition. The quadrate ramus of the pterygoid, the epipterygoid and the stapes are, however, missing.

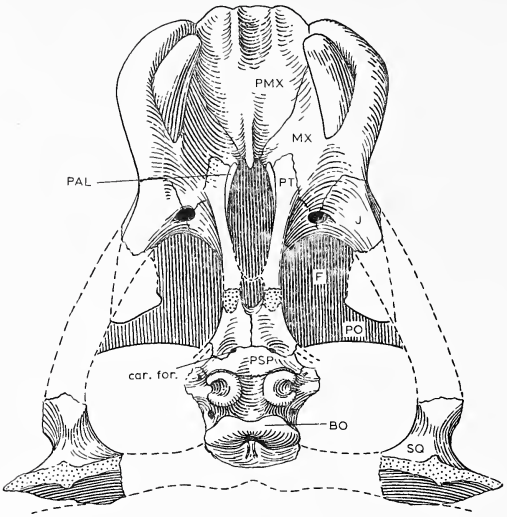

TEXT-FIG. 2. *Rechnisaurus cristarhynchus*, holotype. Ventral view of skull, $\times\frac{1}{4}$ (for abbreviations, see pp. 143–4).

Side view (text-fig. 3). The massive caniniform process of the maxilla covers most of the large tusk and only the anterior part of the tusk is visible in side view. The face is steep and high; its appearance is further accentuated by the presence of a high median dorsal ridge. The external nostrils are quite large and there is no trace of any septo-maxilla on the narial floor, the latter being formed by the maxilla. The pre-orbital region is quite long compared to the post-orbital region. Although only the postero-dorsal quarter of the orbital margin is preserved, it seems likely that the orbit was subcircular in outline. In front of the post-orbital bar, at the postero-dorsal corner of the orbit, there is a distinct bay present, formed by a notch in the frontal bone bordering the orbit.

Discussion. Cox (1965) has divided most of the Triassic dicynodonts into two families, the Kannemeyeriidae and the Stahleckeriidae. This classification is based on shape of the snout, presence or absence of a parietal crest, nature of the temporal openings, and proportion of the occiput. In *Rechnisaurus*, though the occiput is not known completely, the snout is wide and blunt, a parietal crest is absent from the short inter-temporal bar

and the temporal openings appear to be short and broad. All these features clearly indicate that this new form belongs to the Family Stahleckeriidae. On the other hand the presence of a high median ridge in the nasal region, and a prominent boss on the intertemporal bar immediately behind the pineal foramen, makes *Rechnisaurus* quite distinct from the four other Stahleckeriid genera known. Three of these genera are known from

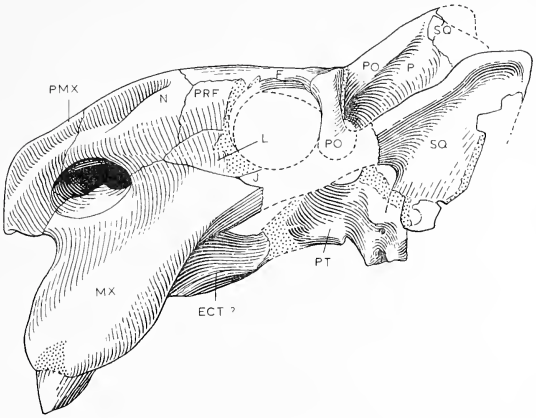

TEXT-FIG. 3. *Rechnisaurus cristarhynchus*, holotype. Lateral view of skull, $\times \frac{1}{4}$ (for abbreviations, see pp. 143–4).

the Middle Triassic of South America: *Stahleckeria* from the Santa Maria formation of Brazil (von Huene 1935–42); *Chanaria* from the Chañares formation of Argentina (Cox 1968); and *Dinodontosaurus* common to both these formations (Cox 1965, 1968). The only African genus, *Zambiasaurus*, is known from the Middle Triassic Ntawere formation of Zambia (Cox 1969). *Rechnisaurus* is the first Stahleckeriid to be reported from Asia.

In *Stahleckeria* the snout is extremely blunt, consequently the nasals are very wide bones with a very short midline suture, the preparietal bone is absent and there is no tusk. In all these respects *Zambiasaurus*, according to Cox (1969) is quite closely related to *Stahleckeria* and may actually be ancestral to the latter. On the other hand *Dinodontosaurus* and *Chanaria* are quite distinct from the above two genera. Prominent tusks are present in the maxillae, the preparietal bone has been retained and the nasals meet along a long suture. *Rechnisaurus* appears to be closer to *Dinodontosaurus* in all those respects but differs in having a high median nasal ridge and a boss behind the pineal foramen. *Chanaria*, though showing some similarity to these two genera, has certain peculiarities such as a very smooth skull without any boss or regosities and a frontal bone with a rectangular projection into the nasal.

Genus WADIASAURUS gen. nov.

Derivation of name. In recognition of the encouragement given for the past decade by Professor D. N. Wadia, F.R.S., F.N.I., National Professor, to the Research programme of the Geological Studies Unit, Indian Statistical Institute.

Type species. Wadiasaurus indicus sp. nov.

Diagnosis. As for sole species at present.

Wadiasaurus indicus sp. nov.

Text-figs. 4–7

Material. Holotype skull; specimen I.S.I.R.38 in the collection at the Geological Museum, Indian Statistical Institute, Calcutta.

Referred specimens. One isolated maxilla, I.S.I.R.39, in the same collection and two isolated quadrate bones, I.S.I.R.40 and I.S.I.R.41.

Type locality. About 2 km. east-south-east of Yerrapalli, Pranhita-Godavari valley, Andhra Pradesh, India.

Horizon. Yerrapalli formation of the Gondwana Group, Triassic.

Diagnosis. Skull of moderately large size. Upper tusks weakly developed or absent. Skull triangular in outline, widest across occiput; gradually tapers anteriorly into a blunt snout. Maxillary flange weak, laterally compressed and projecting ventrally. Nasal ridge short, low and narrow. Inter-orbital region moderately wide. Inter-temporal bar narrow anteriorly but widens posteriorly up to the occipital margin. Parietal crest high. Temporal opening long and narrow. Zygomatic arches thin and almost parallel. Occiput faces sharply downward and backward. Lateral margins of occiput rise sharply and are subparallel. Palatal surface of premaxilla bears pair of anterior ridges. Interpterygoid vacuity wide.

The material and its preservation. The skull described here comes from the same stretch of red clays which yielded the dicynodont bones mentioned by Jain *et al.* (1964). It is of a moderately large size, 40 cm. long and 32 cm. wide across the squamosals. Although nearly complete, the skull has suffered some amount of distortion after burial and has been damaged by exposure prior to its discovery. The maxillary flanges are compressed inward, the right flange is more compressed than the left. The snout is bent slightly downward causing some displacement of the premaxilla and thus obscuring the exact suture between the premaxilla and the nasals. The central part of the skull roof has been squashed, damaging the frontals and other circumorbital bones. The pineal foramen is damaged and it is not possible to be sure whether the preparietal is present or not. The posterior half of the right side of the parietal crest has been displaced ventro-laterally causing some displacement of the bones bordering the temporal opening. The post-orbital bar is fortunately very little distorted, but the posterior extension of the post-orbital bones behind the orbits has had to be restored. The palate is the least distorted part and the displacement of the right sub-orbital bar can be corrected to give the lateral border of the skull. The left side of the palate, however, is damaged. The right side of the occipital plate is very little distorted though the left side is pushed inward and somewhat damaged. The quadrates and part of the quadrato jugals have been restored from an isolated segment found near the skull which has also been given the same specimen number in the field.

Description of the skull.

Dorsal view (text-fig. 4). The skull is triangular in outline with a somewhat narrow snout ending rather bluntly. The maxillary flanges project sharply downward and are

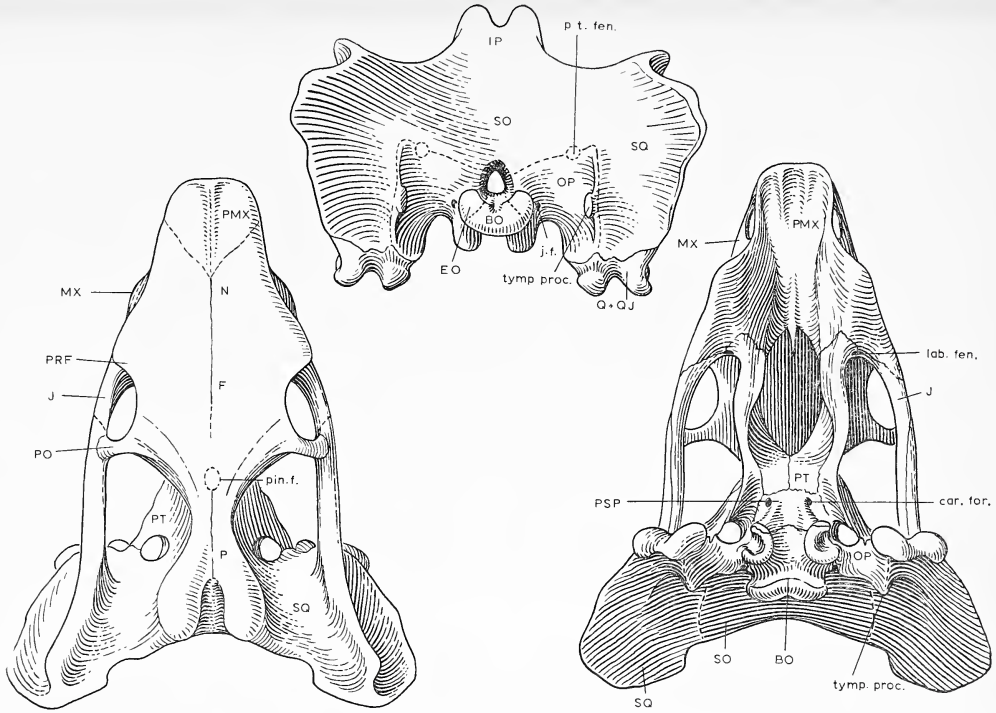

TEXT-FIGS. 4–6. *Wadiasaurus indicus*, holotype. 4. Dorsal view of skull, $\times\frac{1}{4}$. 5. Occipital view of skull, $\times\frac{1}{4}$. 6. Ventral view of skull, $\times\frac{1}{4}$ (for abbreviations, see pp. 143–4).

hardly visible in dorsal view. Behind the premaxilla, the skull broadens slowly up to the orbits, then the zygomatic arches run almost parallel, to be terminated at the level of the occiput by the laterally expanded squamosals which form the lateral margins of the rear of the skull.

There is a low but distinct median ridge on the premaxilla. The ridge has a groove in the middle which widens posteriorly. The inter-orbital region is not very broad, about 28% of the skull length. The orbits look mainly outward and slightly forward. The post-orbital bar lies halfway along the skull. The temporal openings are rather long, widest in the middle behind the pineal region, where the parietal crest is low and probably narrow, but the openings become slightly narrower posteriorly as the parietal crest widens progressively.

It is very difficult to distinguish sutures on the skull roof due to the extremely damaged nature of the bones and due to the presence of many erratic cracks. Many of these cracks seem to follow sutures but it is almost impossible to be sure. However, the suture between the post-orbital and the sub-orbital bar and zygomatic arch is clear.

Occipital view (text-fig. 5). The occiput is quite deep. Its dorsal half is inclined to the skull roof at an acute angle, while its ventral half becomes almost vertical; there is a transitional zone in between. This shape seems to be natural though it is possibly a little exaggerated by distortion. The posterior ends of the lateral wings of the squamosals bend inward in the dorsal half of the occiput so that the occiput as a whole has the form of a concave plate which faces postero-ventrally. The lateral margins of the occiput rise quite steeply and are sub-parallel, slightly diverging dorsally. As a result the occiput is wider dorsally than it is across the quadrates.

The occipital condyle is semicircular in outline and is weakly tripartite with an excavation on the upper surface and a clear notochordal pit. The foramen magnum is triangular in outline.

It is not possible to follow the sutures, hence the extent of the individual bones is difficult to delimit. However, the paroccipital process of the opisthotic projects laterally downwards below the level of the basiphenoid tubera. In the dorsal part of its distal end it is drawn into a posteriorly directed tympanic process.

Ventral view (text-fig. 6). The palatal face of the maxilla is marked by three anterior palatal grooves separated by two ridges. The groove in the middle is deeper but posteriorly is cut short by the convergence of the pair of ridges which meet to form a single ridge separating the continuation of the lateral grooves. The caniniform processes of the maxillae rise from the floor of the secondary palate and appear to be directed slightly outward.

There is no sign of the presence of a tusk in the maxilla in the holotype skull. However, an isolated maxilla, identical with the maxilla of the type skull except that it is somewhat smaller, has a tusk which is quite slender and rather weakly developed. Returning to the type skull, the inner margin of the caniniform process has two distinct faces: the anterior face looks medially whereas the posterior face is directed postero-medially. The former meets the premaxilla on the secondary palate and the latter meets the pterygoid-palatine process medially and the jugal process laterally.

Behind the premaxilla, the vomer and much of the palatine are highly crushed and the passage for the internal nostrils is completely obliterated beyond any possibility of restoration or description. The right anterior ramus of the pterygoid is much less

distorted and the suture between the pterygoid and the maxilla is quite clear. The labial fenestra is present in its usual position. Behind their contact with the maxillae, the pterygoids arch outward and finally make a long midline sutural contact. There is a raised prominence here, perhaps indicating the presence of a boss, as found in *Ischigualastia* (Cox 1965). Postero-laterally, the pterygoid extends behind the midline suture as

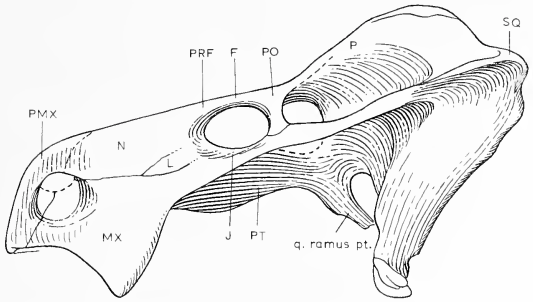

TEXT-FIG. 7. *Wadiasaurus indicus*, holotype. Lateral view of skull, $\times \frac{1}{4}$ (for abbreviations, see pp. 143–4).

the slender quadrate ramus terminating in front of the paroccipital process near the quadrate recess. Behind the pterygoids along the midline, there is a pair of carotid foramina posterior to the transverse parasphenoid-pterygoid suture. The tubera are set a little apart and their anterior faces are formed by the parasphenoid. The occiput is broadly exposed in the ventral view of the skull.

Side view (text-fig. 7). The anterior part of the parietal crest and the area around the pineal foramen have been restored, and the tilt of the parietal crest due to crushing has been corrected. The facial part of the skull is moderately long and rather low in contrast to the relatively high posterior half of the skull.

The orbits must have been oval, about 7 cm. along the antero-posterior axis, and look outward but slightly forward. The nostrils are large, rounded, and placed anteriorly just behind the tip of the snout. The premaxilla is beak-like and its anterior end rises sharply on the skull roof. Posteriorly it forms the front margin of the nostril, and meets the maxilla ventrally and the nasal postero-dorsally near the middle of the nostril. The posterior margin of the nostril is bordered by maxilla below and by nasal above and the suture between these two bones runs horizontally. When followed posteriorly this suture meets the anterior tip of the lachrymal half way between the nostril and the orbit.

On the narial floor, there is a patch of broken bits of bone resting on maxilla. These bits may be the remains of the septomaxilla but it is impossible to be sure of this. Therefore, these fragments have not been included in the figure. The lachrymal is a narrow triangular bone lying in front of the orbit. It separates the nasal and the prefrontal from the maxilla and extends to form the antero-ventral border of the orbit.

The jugal forms most of the ventral border of the orbit. Its limits at both ends are far from clear. An extensive overlap of the jugal by a thin anterior extension of the

squamosal is strongly suggested. The squamosal jugal bar is thin, compressed dorso-ventrally, and runs straight behind the orbit at a low angle, slightly rising upwards to the posterior end of the skull.

Discussion. There can be no doubt that in *Wadiasaurus*, the skull has a high parietal crest, the occiput is deep and wide, the snout is narrow with a blunt end and the temporal opening is long and narrow. These characters clearly indicate that this new form belongs to the family Kannemeyeriidae as defined by Cox (1965). *Wadiasaurus* is still very incompletely known, hence any comparison with other kannemeyeriid genera can only be very general and largely tentative.

Among the genera belonging to the family Kannemeyeriidae, *Sinokannemeyeria* and *Parakannemeyeria*, both known from the Lower Triassic Er-ma-ying formation of Shansi, China (Sun 1963), have extremely long pre-orbital regions, 46–50% of the total skull length, which makes them very distinct. The pre-orbital length of *Wadiasaurus* is more normal for the family—about 35% of the total skull length. The most widely distributed genus is *Kannemeyeria*. It is known from the lower Triassic *Cynognathus* zone of South Africa (Pearson 1924, Broom 1937), the Middle Triassic Manda beds of East Africa (Cruickshank 1965), and also from the lower Middle Triassic Puesto Viejo formation of Mendoza, Argentina (Bonaparte 1966). *Kannemeyeria* is characterized by a very narrow intertemporal bar drawn into a sharp steeply rising median crest, a situation not found in any other kannemeyeriid genera including *Wadiasaurus*. The Upper Triassic form *Placerias*, known from the Chinle formation of North America, is rather a specialized end-form with the outwardly projected caniniform processes of the maxilla drawn into a facial horn (Camp and Welles 1957, Cox 1965). A tusk is either weakly developed or absent in *Placerias* but the intertemporal bar is wide and devoid of a crest. Due to these specializations, *Placerias* also is quite distinct from *Wadiasaurus*.

The two remaining kannemeyeriid genera, *Ischigualastia*, from the Middle or Upper Triassic Ischigualasto formation of Argentina (Cox, 1965), and *Sangusaurus*, from the Middle Triassic Ntawere formation of Zambia (Cox, 1969) are however, tuskless. *Ischigualastia* differs from *Wadiasaurus* in having a pointed snout, a more anteriorly directed caniniform process and zygomatic arches which are markedly bowed outward. *Sangusaurus*, known only from its premaxilla, maxilla, and the intertemporal bar, shows some similarity with those parts of *Wadiasaurus*. The premaxilla, though generally similar in the two genera, has a pointed anterior end in the former but ends bluntly in the latter. The caniniform process of the maxilla is quite similar in the two forms but its orientation in *Sangusaurus* is not exactly known. Although the relationship between the interparietal and parietal and the exact position of the pineal foramen is not known in *Wadiasaurus*, there is some resemblance between the intertemporal bars in those two genera. In both, the inter-temporal bar widens posteriorly and their dorsal borders are concave in section. There is an abrupt change between the dorsal and occipital faces of the intertemporal bar in *Sangusaurus*, which is also, most probably, true for this region of *Wadiasaurus*.

Another kannemeyeriid genus, *Barysoma*, from the Middle Triassic Santa Maria formation of Brazil, is known very incompletely from a partial occiput and some post-cranial remains. According to Cox (1969, p. 296), *Barysoma* 'appears to be closely related to *Ischigualastia*', but any comparison of *Barysoma* with *Wadiasaurus* is not possible at this stage.

Acknowledgements. Dr. P. L. Robinson, University College, London, took a keen interest throughout the work and the paper was completed during my stay in London on an N.E.R.C. grant, given for the project 'Mesozoic vertebrates and continental sediments in Britain and India', of which the paper forms a part. I wish to thank sincerely Dr. C. B. Cox, King's College, London, for much help and useful criticism. I am also thankful to all my colleagues in the Geological Studies Unit for much help at various stages. Mr. D. Roy and Mr. A. Lee helped in completing the illustrations. Finally my thanks are due to Mr. and Mrs. N. V. Raja Reddy for hospitality in the field.

REFERENCES

BONAPARTE, J. F. 1966. Una nueva 'fauna' Triásica de Argentina (Therapsida: Cynodontia Dicynodontia); consideraciones filogenéticas y paleobiogeográficas. *Ameghiniana*, Buenos Aires, **4**, 243–96, figs. 1–29, pl. 1–2.

BROOM, R. 1937. A further contribution to our knowledge of the fossil reptiles of the Karroo. *Proc. zool. Soc. Lond.* (B) **1937,** 299–318, figs. 1–16.

CAMP, C. L. and WELLES, S. P. 1956. Triassic dicynodont reptiles. Part I. The North American genus *Placerias*. *Mem. Univ. Calif.* **13,** 255–304, figs. 1–41, pl. 30–3.

CHATTERJEE, S. 1967. New discoveries contributing to the stratigraphy of the continental Triassic sediments of the Pranhita-Godavari Valley. *Bull. geol. Soc. India*, **4** (2), 37–41, fig. 1.

COX, C.B. 1965. New Triassic dicynodonts from South America, their origins and relationships. *Phil. Trans. R. Soc.* London, **248** (B), 457–516, figs. 1–30.

—— 1968. The Chañares (Argentina) Triassic reptile fauna. IV. The dicynodont fauna. *Breviora*, Cambridge, Mass., **205,** 1–27, figs. 1–12.

—— 1969. Two new dicynodonts from the Triassic Ntawere formation, Zambia. *Bull. Br. Mus. nat. Hist.* (Geol.). **17** (6), 255–94, figs. 1–23.

CRUICKSHANK, A. R. I. 1965. On a specimen of the anomodont reptile *Kannemeyeria latifrons* (Broom) from the Manda Formation of Tanganyika, Tanzania. *Proc. Linn. Soc. Lond.* **176,** 149–57, figs. 1–5.

HUENE, F. VON. 1935–42. *Die fossilen Reptilien des Südamerikanischen Gondwanalandes an der Zeitenwende*. 332 pp., figs. 1–66, pl. 1–38, Tübingen.

JAIN, S. L., ROBINSON, P. L., and ROY CHOWDHURY, T. 1964. A new vertebrate fauna from the Triassic of Deccan-India. *Q. Jl geol. Soc. Lond.* **120,** 115–24, figs. 1–3.

PEARSON, H. S. 1924. The skull of the dicynodont reptile *Kannemeyeria*. *Proc. zool. Soc. Lond.* **1924,** 793–826, figs. 1–18.

ROBINSON, P. L. 1958. Some new vertebrate fossils from the Panchet series of West Bengal. *Nature, Lond.* **182,** 1722–3.

SUN, A. L. 1963. The Chinese kannemeyerids. *Palaeont. sinica* (N.S.) (C), **17,** 73–109, figs. 1–51.

TRIPATHI, C. and SATSANGI, P. P. 1963. *Lystrosaurus* fauna from the Panchet Series of the Ranigang Coalfields. *Palaeont. indica* (N.S.) **37,** 1–53, pl. 1–13.

List of abbreviations used in the figures

BO	basi-occipital	p.t. fen.	post-temporal fenestra
car. for.	carotid foramen	PAL	palatine
ECT?	ectopterygoid?	pin. f.	pineal foramen
EO	exoccipital	PMX	premaxilla
F	frontal	PO	post-orbital
IP	interparietal	PP	preparietal
J	jugal	PRF	prefrontal
L	lachrymal	PRO	prootic
lab. fen.	labial fenestra	PSP	parasphenoid-basisphenoid complex
MX	maxilla	PT	pterygoid
N	nasal	Q	quadrate
P	parietal	q.r. pt.	quadrate ramus of the pterygoid

QJ	quadratojugal	tymp. proc.	tympanic	process.
SO	supra-occipital			
SQ	squamosal			

TAPAN ROY CHOWDHURY
Geological Studies Unit
Indian Statistical Institute
Calcutta

Typescript received 10 May 1969

EPIDERMAL STUDIES IN THE INTERPRETATION OF *LEPIDODENDRON* SPECIES

by B. A. THOMAS

ABSTRACT. Thirteen species of *Lepidodendron* are described including two new species *L. arberi* and *L. barnsleyense*. Details of the epidermis are given and its use in species distinction and classification is considered. Cuticle information about secondary growth is also discussed.

LEPIDODENDRON is an arborescent lycopod stem genus characterized by the persistent basal parts of leaves (leaf cushions) from which the apical parts have often been shed. The compression species, like those of most other fossil lycopod genera, have been described and classified on external gross morphology. Text-fig. 1 illustrates the cushion features most useful in classification. However, the actual naming of a specimen, especially a badly preserved one, is still sometimes difficult because many species appear similar in one or more details. The lycopod cuticle has been largely ignored as a possible descriptive character even though epidermal characters have been shown to be of great importance in other plant groups. The value of the lycopod cuticle has already been discussed (Thomas 1966) but detailed descriptions of *Lepidodendron* cuticles are given here showing how a study of them can assist in the definition and distinction of species.

Whenever possible the type specimen was examined together with several other specimens to detect any variation within the species. However, specimens from which cuticle could be prepared were often difficult to find. Some type specimens and many others are preserved as impressions and some of those which are compressions have finely cracked carbon which does not yield cuticle. Examination of the cushion surface is sometimes useful when the cuticle cannot be prepared as the epidermal cells and stomata are often visible.

Cuticle was prepared by macerating portions of the carbonized compression in Schulze solution followed by clearing in dilute ammonia solution. The cuticles were mounted unstained in glycerine jelly and examined by normal transmitted light supplemented in a few instances by phase contrast illumination. The cuticle preparations have been deposited with their respective specimens.

The specimens were borrowed from or deposited in: the British Museum of Natural History, London (BMNH); the Kidston collection of the Geological Survey and Museum, London (K); the general collection of the Geological Survey and Museum, London (GSM); the Geological Survey, Leeds (GSL); the Geological Survey, Edinburgh (GSE); the Sedgwick Museum, Cambridge (SM); the Warwickshire County Museum, Warwick (WM); the Leicester City Museum (LM); the Royal Scottish Museum, Edinburgh (RSM), and the Czechoslovakian National Museum, Prague (CNM).

Acknowledgements. I would like to thank Professor T. M. Harris, F.R.S. for his help and guidance throughout much of this study; the directors and staff of the museums for allowing me to borrow and

[Palaeontology, Vol. 13, Part 1, 1970, pp. 145–73, pls. 29–34.]

make preparations from specimens in their collections; the National Coal Board and Open Cast Executive for permitting my access to their workings; the site officials who helped me to collect specimens; the Coal Board Scientific Staff for help in certain correlation problems; the University of Reading Research Board from whom I was in receipt of a research studentship, and the University of Newcastle upon Tyne and the Royal Society of London for travel grants. The work was completed during the tenure of the Lord Adams Research Fellowship at the University of Newcastle upon Tyne.

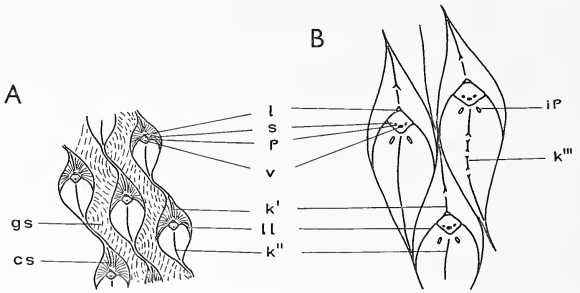

TEXT-FIG. 1. Drawings of diagrammatic leaf cushions to illustrate their main features. A, Leaf cushions continuous with other cushions above and below but separated from those on either side by wrinkled areas of bark. B, Closely packed leaf cushions not continuous with other cushions above and below. cs—cushion striations; gs—inter cushion striations; ip—infrafoliar parichnos; k′—cushion keel above the leaf scar; k″—cushion keel below the leaf scar; k‴—cushion keel broken by transverse notches; l—ligule pit aperture; ll—lateral line running from leaf scar to cushion edge; p—foliar parichnos; s—leaf scar; v—vascular print.

SYSTEMATIC DESCRIPTIONS

Lepidodendron aculeatum Sternberg

Plate 29; Plate 30, figs. 1, 5; Plate 31, figs. 1–3; text-figs. 2, 3

1820 *Lepidodendron obovatum* Sternberg, pp. 20, 23, pl. 6, fig. 1; pl. 8, figs. 1A, *a*, *b*.
1820 *Lepidodendron aculeatum* Sternberg, pp. 20, 23, pl. 6, fig. 2; pl. 8, figs. 1B, *a*, *b*.
1820 *Lepidodendron crenatum* Sternberg, pp. 20, 23, pl. 8, fig. 2B.
1821 *Lepidodendron aculeatum* Sternberg, pl. 14, figs. 1–4.
1838 *Sagenaria aculeata* Presl in Sternberg, p. 177, pl. 68, fig. 3.
1838 *Sagenaria rugosa* Presl in Sternberg, p. 177, pl. 68, fig. 4.
1838 *Sagenaria caudata* Presl in Sternberg, p. 178, pl. 68, fig. 7.
1877 *Lepidodendron aculeatum* Sternberg; Fairchild pars, p. 77, pl. 5, figs. 1–4; pl. 6, figs. 1–5; pl. 7, figs. 1–4; pl. 8, figs. 1, 2.
1886 *Lepidodendron aculeatum* Sternberg; Zeiller, p. 435, pl. 65, figs. 1–7.

EXPLANATION OF PLATE 29

Lepidodendron aculeatum Sternberg. Fig. 1, CNM ČGH 365; Type specimen of Sternberg 1820, pl. 6, fig. 2. Fig. 2, CNM ČGH 658 (= *Lepidodendron obovatum* Sternberg 1820, pl. 6, fig. 1). Fig. 3, CNM ČGH 805 (= *Sagenaria rugosum* Presl *in* Sternberg 1838, pl. 68, fig. 4). Fig. 4, CNM ČGH 792 (= *Sagenaria caudata* Presl *in* Sternberg 1838, pl. 68, fig. 7).
All at × 1.

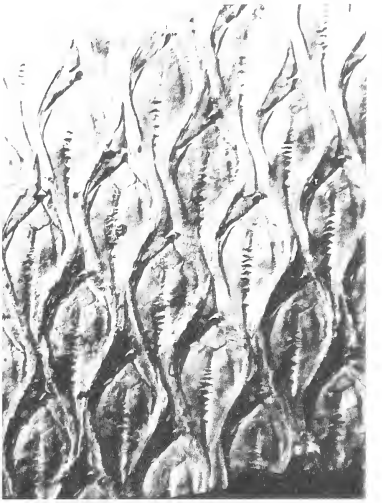

1

2

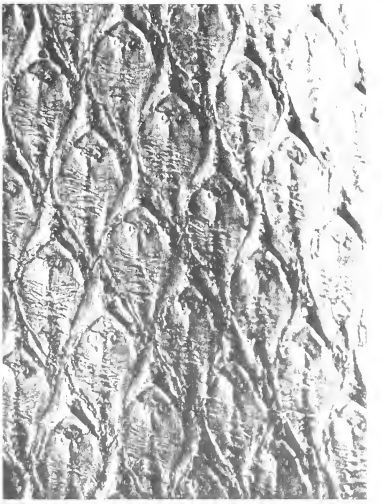

3

4

THOMAS, *Lepidodendron*

1899 *Lepidodendron aculeatum* Sternberg; Potonié, p. 220, text-fig. 211.
1904 *Lepidodendron aculeatum* Sternberg; Zalessky, p. 81, pl. 1, figs. 1–6; pl. 2, fig. 2.
1947 *Lepidodendron aculeatum* Sternberg; Němejc pars, p. 49.
1959 *Lepidodendron aculeatum* Sternberg; Remy, p. 98, text-figs. 76, *a*, *b*.
1964 *Lepidodendron aculeatum* Sternberg; Crookall, p. 233, pl. 60, fig. 6; text-fig. 77*a*.

Material. Type specimen CNM ČGH 365 from the Upper Carboniferous of Radnice, Bohemia; CNM ČGH 658 (*L. obovatum* Sternberg 1820, pl. 6, fig. 2.) from Radnice; CNM ČGH 660 (*L. crenatum* Sternberg 1820, pl. 8, fig. 2в) from Radnice; CNM ČGH 792 (*Sagenaria caudata* Presl in Sternberg 1838, pl. 68, fig. 4) from the Upper Carboniferous, Waldenburg, Silesia; CNM 23072 from the Mydlak horizon of Kladno; WM G. 541, from the Westphalian coal measures of Tamworth, Staffordshire; BMNH 1049, from the coal measures of Waldenburg, Silesia; BMNH 46685, from the Westphalian coal measures of Ebbw Vale, Monmouthshire; BMNH 41308, from the Mushett Blackband Ironstone, No. 6 pit, Monkland, near Airdrie, Scotland; Westphalian B.

All the specimens possess the same general cushion characters. The cushions have inflexed, pointed upper and lower angles and rounded lateral angles. The leaf scars are diamond-shaped, about as long as broad, and are situated about one-third the distance down the leaf cushions. There are three foliar prints, though sometimes only one can be seen, and two infrafoliar parichnos. The ligule pit aperture is adjacent to the upper angle of the leaf scar and not a short distance above as it is often figured. There are prominent keels above and below the scar and lateral lines curve from the lateral angles of the leaf scars to the edges of the leaf cushion. The keels are normally smooth and continuous above the leaf scar but are divided by notches below the scar. The leaf cushion surface is smooth. BMNH 1049 and BMNH 41308 have very plain infrafoliar parichnos but although repeated attempts have been made to prepare cuticle from them none was obtained and I am convinced there never was any. Most specimens of this species show the leaf cushions close together but some, e.g. BMNH 1049, have them separated by wrinkled areas of bark. These wrinkled areas have been thought to be of diagnostic value, for example Lesquereux (1879/80) used their presence as the main character for his *Lepidodendron modulatum*. It is now commonly accepted that they are the result of lateral expansion of the bark produced during the secondary growth of the stem (for further discussion see Eggert 1961 and Chaloner 1967). The wrinkles have been described as fissures or cracks in the bark by Fairchild (1877). However as cuticle was prepared from the whole area in BMNH 1049 it is more likely that they were formed by a secondary production of epidermis interspersed between the original epidermis of the furrow. This formation of extra epidermis seems to have been accompanied by a stretching out and shallowing of the intercushion groove. Preparation of cuticle from the intercushion areas of BMNH 1049 shows that the furrows possess roughly isodiametric epidermal cells and stomata while the interconnected ridges have epidermal cells elongate across the ridges and no stomata. The cuticle without stomata probably represents the secondary produced epidermal areas especially as those specimens with close cushions have stomata within their intercushion grooves.

CNM 23072 has many isolated leaf cushions with leaves still attached. The leaves are at least 11 cm. long but all are incomplete and only the slightest narrowing can be seen. Even though the leaves are attached three foliar prints are visible showing that their presence is not necessarily indicative of prior leaf fall. A central median vein can be clearly seen on all leaves and on a few an additional line is present on either side of the median, which probably represents a stomatal groove. Not all the leaves show stomatal

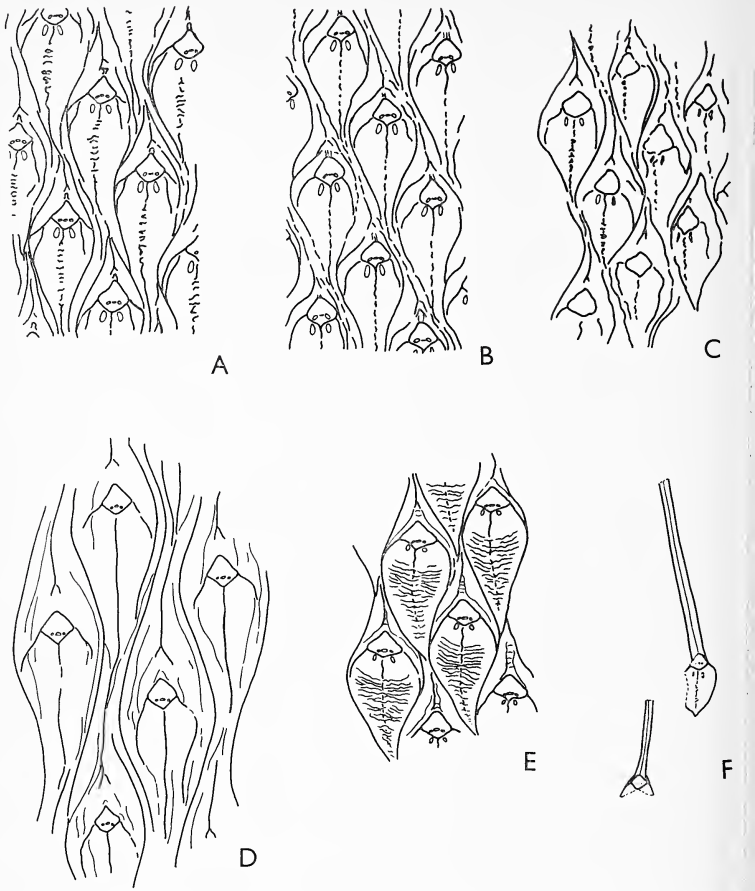

TEXT-FIG. 2. *Lepidodendron aculeatum* Sternberg. A, CNM ČGH 365; Type specimen of Sternberg 1820, pl. 6, fig. 2. B, CNM ČGH 658 (= *L. obovatum* Sternberg 1820, pl. 6, fig. 1). C, CNM ČGH 660) (= *Lepidodendron crenatum* Sternberg 1820, pl. 8, fig. 2B). D, CNM ČGH 792 (= *Sagenaria caudata* Presl *in* Sternberg 1838, pl. 68, fig. 7). E, CNM ČGH 805 (= *Sagenaria rugosa* Presl *in* Sternberg 1838, pl. 68, fig. 4). F, CNM 23072; showing leaves still attached to the leaf cushions. All illustrations at ×2.

grooves as their visibility is of course dependent on the orientation of the leaves. Such long leaves with stomatal grooves, if found detached, would undoubtedly be determined as *Cyperites bicarinatus* Lindley and Hutton, confirming the reports of the possession of such leaves by *Lepidodendron aculeatum* given by Crookall (1966, p. 535) and Chaloner (1967, p. 673). Unfortunately no cuticle could be prepared from these attached leaves and no epidermal detail could be discerned by direct observation.

Cuticle description. The epidermal cells from all over the cushion surface are roughly isodiametric and 15–20 μ across, except near the cushion edges where they are mostly 30 $\mu \times 15$ μ and elongated towards the cushion centre. However, in BMNH 46685, where the keel is more prominent and divided by many transverse notches, the epidermal cells near the keel are elongated towards the keel and are typically 30 $\mu \times 18$ μ in size. The anticlinal walls are straight, smooth and about 2 μ thick. The perclinal walls are flat and smooth. The stomata are about 200–250 per mm.^{2}, randomly distributed and orientated, but in BMNH 46685 they are absent on the keel lumps and very sparse in the keel notches. Stomatal average size is about 40 $\mu \times 18$ μ and the guard cells are sunken in pits 12–15 μ deep. There are about nine subsidiary cells to each stoma, unmodified except for sometimes being slightly elongated away from the stomata. In the wrinkled intercushion areas there are interconnecting strands of dark cuticle separating patches of lighter brown cuticle. The dark cuticle has epidermal cells 30 $\mu \times 15$ μ elongated at right angles to the strands, but the lighter cuticle has isodiametric cells about 20–30 μ broad. Stomata are about 340 per mm.^{2} in the lighter cuticle but are very few and restricted to the edges of the dark cuticle. The stomata are 25–30 $\mu \times 10$ μ in size and the guard cells are sunken in pits 10–15 μ deep. The ligule pit cuticle is about 0·45 mm. broad and at least 2 mm. long. The lining cells are rectangular, 45 $\mu \times 15$ μ, and elongated along the pit.

Comparison. Specimens similar to Sternberg's figures of *L. obovatum* and *L. aculeatum* have been commonly found and described. However, the two species have not always been interpreted in the same way and indeed many authors have changed their views from one paper to another. Some authors have accepted only part of Sternberg's descriptions and figures, others have placed some of his other species in synonymy with these two species, while a few have united the two. These varying opinions seem to have arisen as a result of differing ideas about the value of Sternberg's figures and the emphasis put on different cushion characters.

A study of Sternberg's specimens has shown that his interpretation needs to be modified. I agree basically with Němejc (1947) in his reinterpretation but differ slightly in the synonymy lists quoted. The illustration of the type specimen of *L. obovatum* (Sternberg 1820, pl. 6, fig. 1) fails to show accurately the upper angle of the cushions and the keel ornamentations. The upper angle is pointed as is the lower angle and not rounded as the illustration suggests and the keel below the leaf scar is divided by transverse notches. When *L. obovatum* is interpreted in this manner, there is no difference between it and the subsequently described *L. aculeatum*. Specimens of this form have been, and indeed still are, commonly named *L. aculeatum*. Fischer (1904) united the two species under *L. obovatum* but included in his synonymy other forms which are quite different, e.g. the *L. obovatum* of Presl. This broad interpretation of *L. obovatum* is quite unacceptable and I believe the best solution is to regard *L. obovatum* as a confused name

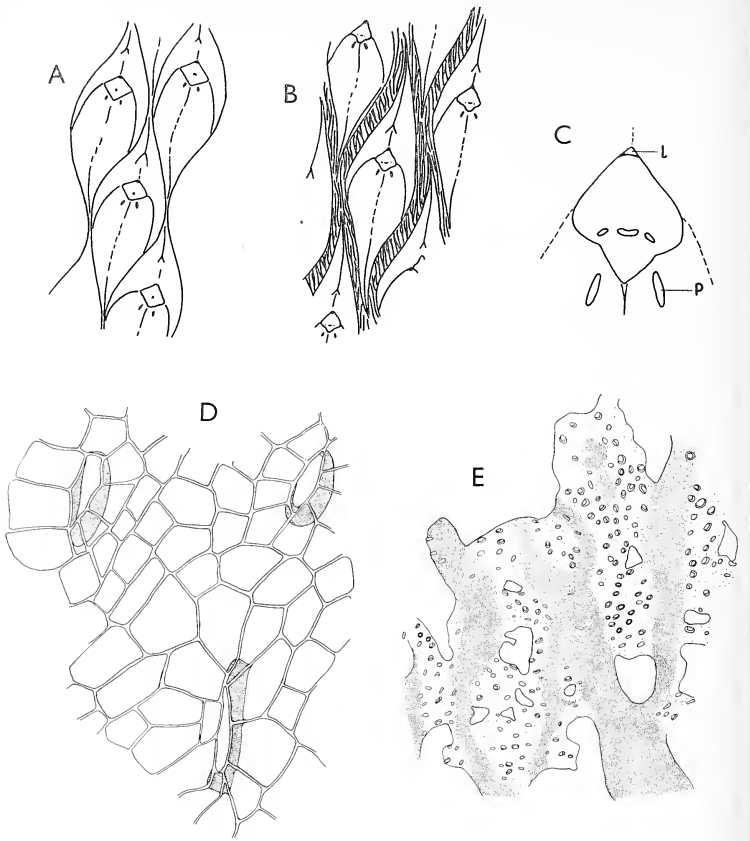

TEXT-FIG. 3. *Lepidodendron aculeatum* Sternberg. A, B, Leaf cushions before and after secondary expansion of the stem, ×1. C, Leaf scar with ligule pit (l) and infrafoliar parichnos (p). D, Leaf cushion cuticle, ×400. E, Cuticle from expanded bark between the leaf cushions showing dark cuticle with none or very few stomata and light-coloured cuticle with many stomata, ×20. A, C, E, from WM G541; B, D, from BMNH 1049.

reduced to a synonym of the more commonly used *L. aculeatum*. Presl, in Sternberg (1838), described a specimen (pl. 68, fig. 6) as *L. obovatum*. However this is not *L. obovatum* Sternberg, i.e. *L. aculeatum* Sternberg. The cushions are broader and have no drawn out inflexed upper and lower angles. The leaf scars are broader than long while in *L. aculeatum* they are about as long as broad. The cushion surface above the leaf scar is finely striated while in *L. aculeatum* it is smooth. Finally the infrafoliar parichnos are not so well defined as in *L. aculeatum*. Nevertheless, many workers have described specimens as *L. obovatum* because they resembled Presl's specimen named as *L. obovatum*. Now in an attempt to discover the name that should be applied to Presl's specimen, I found that *L. mannabachense* Presl in Sternberg (1838, pl. 68, fig. 2) is identical to the now commonly accepted form of *L. obovatum*. A description of this species is given later.

Sagenaria caudata Presl, *S. rugosa* Presl, and *Lepidodendron crenatum* Sternberg should all be referred to *L. aculeatum* Sternberg. The type specimen of *S. caudata* is an almost flat compression and, although the original illustration is not very informative, clearly shows the typical features of *L. aculeatum*. *S. rugosa* is best regarded as *L. aculeatum* although several authors have included it in *L. obovatum* sensu Presl. The type specimen differs from *L. aculeatum* only in having leaf scars which are slightly broader than long; this alone seems insufficient for species distinction. In contrast, Presl's (1838, pl. 68, fig. 5) specimen of *S. crenatum*, CNM ČGH 322, has leaf scars quite unlike those of *L. aculeatum* and is not this species. The leaf scars are as broad as the cushions and are situated just above their centres.

Lepidodendron serpentigerum Koenig

Plate 31, fig. 4; Plate 34, fig. 6; text-fig. 4

1825 *Lepidodendron serpentigerum* Koenig, pl. 16, fig. 195.
1902 *Lepidodendron serpentigerum* Koenig; Kidston, pp. 345, 371, pl. 51, fig. 2.
1906 *Lepidodendron serpentigerum* Koenig; Fischer pars, No. 75, figs. 1, 2.
1927 *Lepidodendron serpentigerum* Koenig; Hirmer, pp. 200, 204, text-fig. 237.
1964 *Lepidodendron serpentigerum* Koenig; Crookall, p. 260, pl. 61, fig. 5, text-fig. 83.

Material. Neotype, BMNH 39020 from the Westphalian Coal Measures, Newcastle upon Tyne (Crookall 1964, text-fig. 83); K 2498 from above the Stranger Coal, Granger Colliery, Kilmarnock, Ayrshire (Kidston 1902, pl. 51, fig. 2; Crookall 1964, pl. 61, fig. 5), Westphalian B; SM 3148 from the Transition Coal Measures of the Bishopsbourne Boring, Barham Down, 4 miles south-east of Canterbury, Kent.

The three specimens are very similar in having their leaf cushions connected above and below by inflexed cushion extensions and separated on either side by wrinkled areas of bark. The leaf scars are two-thirds the distance up the cushions and possess three conspicuous foliar prints. The ligule pit aperture is adjacent to the upper angle of the leaf scar and there are two plainly visible infra-foliar parichnos. The keels are more prominent below the leaf scars and are divided by many transverse grooves. No cuticle could be prepared from the neotype and only small fragments from the other two. K 2498 gave good cuticle from the wrinkled intercushion areas but poor cuticle from the leaf cushions and SM 3148 gave reasonable cuticle from the leaf cushions but none from the wrinkled areas.

Cuticle description. The cuticle is similar over the whole leaf cushion surface. The epidermal cells are about 35 μ across, roughly isodiametric or slightly elongated. The anticlinal walls are straight, smooth and about 2 μ thick. The periclinal walls are flat and granular. The stomata are about 50 $\mu \times 30$ μ in size and the guard cells are sunken

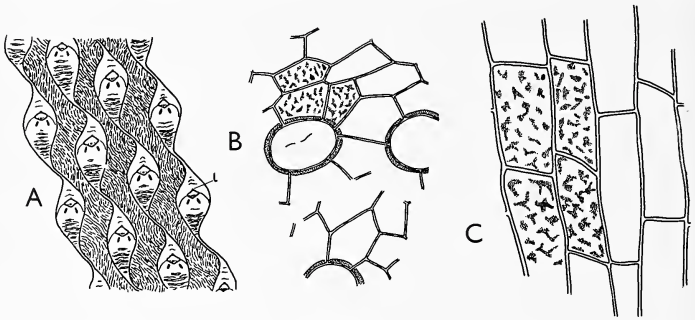

TEXT-FIG. 4. *Lepidodendron serpentigerum* Koenig. A, Leaf cushions from K2498, $\times 1$; Ligule pit (1). B, Cushion cuticle from SM 3148, $\times 400$. C, Cuticle from intercushion areas of K2498, slide PF 3144. The granular surface of the cuticle seen under phase contrast is represented in only a few cells of B and C.

in pits 4 μ deep. The cuticle from the inter-cushion areas is thicker than that from the cushion surface and has roughly rectangular cells, 60 $\mu \times 20$ μ, elongated parallel to the intercushion striations. The anticlinal walls are straight, smooth, and 3 μ thick and the periclinal walls are flat and granular. There are no stomata in the intercushion areas.

Comparison. Lepidodendron zeilleri Zalessky (1904, p. 91, pl. 4; fig. 1, 1*a*) is almost certainly a synonym of *L. serpentigerum.* The only difference between the two type specimen figures is that *L. zeilleri* has more rounded upper angles to the leaf scars which is not a distinctive enough character for species separation.

Němejc (1947, p. 62) believed that *L. serpentigerum* was similar to *L. obovatum* Presl, non Sternberg (= *L. mannabachense* Presl) and *L. aculeatum* Sternberg and that it was probably only a growth form of the latter. However the cushions of *L. serpentigerum* are more S-shaped than both these species and possess different cushion and epidermal

EXPLANATION OF PLATE 30

Fig. 1, *Lepidodendron aculeatum* Sternberg, CNM ČGH 660 (= *Lepidodendron crenatum* Sternberg 1820, pl. 8, fig. 2B).

Fig. 2, *Lepidodendron veltheimii* Sternberg, CNM ČGH 330; figured by Presl *in* Sternberg 1838, pl. 68, fig. 14.

Fig. 3, *Lepidodendron mannabachense* Presl, CNM ČGH 355 (= *Sagenaria obovatum* Presl *in* Sternberg 1838, pl. 68, fig. 2).

Fig. 4, *Lepidodendron mannabachense* Presl (type specimen), CNM ČGH 329; figured by Presl *in* Sternberg 1838, pl. 68, fig. 2.

Fig. 5, *Lepidodendron aculeatum* Sternberg, with leaves attached to leaf cushions, CNM 23072.

All at $\times 1$.

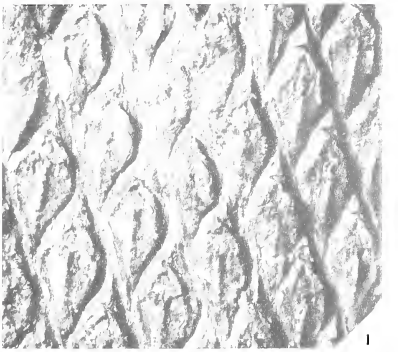

1

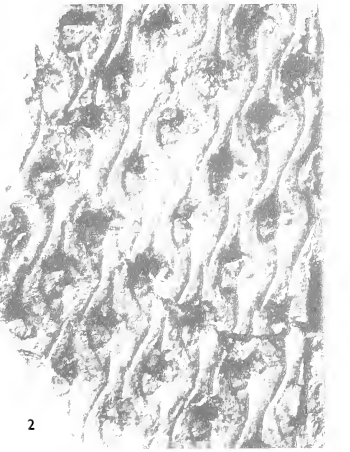

2

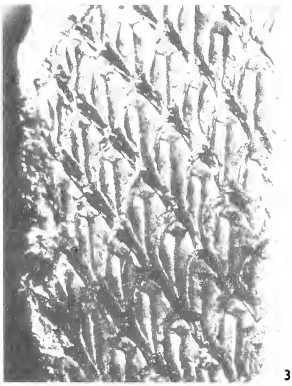

3

5

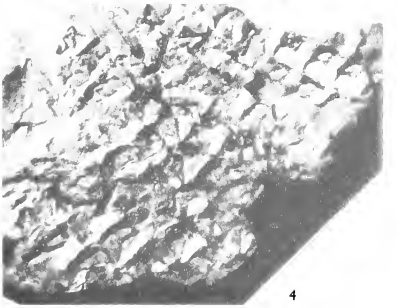

4

details. *L. mannabachense*, unlike *L. serpentigerum*, has striations on its leaf cushions and has dissimilar epidermal arrangements above and below the leaf scars. *L. aculeatum* Sternberg has broader leaf scars, more prominent keels, smaller epidermal cells, and deeper stomatal pits than *L. serpentigerum*. The form of *L. aculeatum* with separated leaf cushions also differs in the cuticle details obtained from the intercushion areas. In *L. aculeatum* there are strips of epidermis with stomata alternating with strips with no stomata whereas in *L. serpentigerum* the epidermis is all similar and possesses no stomata.

Lepidodendron veltheimii Sternberg

Plate 30, fig. 2; Plate 33, figs. 4–6; text-fig. 5

1825 *Lepidodendron Veltheimii* Sternberg, p. 43, pl. 52, fig. 3.
1838 *Lepidodendron Veltheimianum* Presl in Sternberg, p. 180, pl. 68, fig. 14.
1899 *Lepidodendron Veltheimianum* Sternberg; Hoffman and Ryba, p. 78, pl. 15, figs. 7, 8.
1926 *Lepidodendron Veltheimianum* Sternberg; Kidston, p. 147, pl. 13, fig. 2.
1964 *Lepidodendron veltheimi* Sternberg; Crookall, p. 298, pl. 64, figs. 3–5; pl. 70, fig. 8; pl. 71, figs. 1, 2; text-figs. 77*c*, 96.

Material. CNM ČGH 330 from the Lower Carboniferous of Magdeburg (probably the specimen figured by Presl 1838, although it also bears a label referring it to Sternberg 1825); K 2411 from immediately beneath the Orchard Limestone, New Brawden Quarry, Giffnock, Renfrewshire, Upper Limestone Group of the Carboniferous Limestone Series, Lower Namurian.

CNM ČGH 330 is an impression with no carbon remaining and no visible epidermal details, so all the information about the epidermis was obtained from K 2411. This is a fairly thick compression on a slab of black shale. The leaf cushions are in low-angle spirals of about 25° to the horizontal and are continuous with the cushions above and below by inflexed apical and basal angles. The leaf scar is prominent but only one foliar print can be seen and no infrafoliar parichnos are visible. The ligule pit aperture is adjacent to the upper angle of the leaf scar. The keel is prominent, but interrupted in the upper part below the leaf scar. The carbon of the compression is not cracked as in most specimens and large pieces of well-preserved cuticle could be prepared from it.

Cuticle description. The cuticle from the grooves between the cushions is about 3–4 μ thick. The epidermal cells are isodiametric, 20 μ across, or elongated up to 40 μ. The anticlinal walls are straight, smooth, and 2–3 μ thick. The periclinal walls are flat and smooth. No stomata were visible in the grooves but some are present near the edges of the cushion. The leaf cushion cuticle is 2 μ thick. The epidermal cells are isodiametric, 15–20 μ, or elongated up to 40 μ. The long axes of the cells tend to form curves running from the cushion edge towards the keel and then parallel to it. The cells do not form well-developed rows, but sometimes are in small groups appearing to have been formed by the transverse division of one cell. The anticlinal walls are straight, smooth, and 2–4 μ thick. The periclinal walls are flat and smooth. Stomata are about 60 per mm^2. on the cushion below the leaf scar but slightly less above it. They are randomly distributed over most of the cushion, but are arranged concentrically around the lumps which make up the keel just below the leaf scar. The guard cells are sunken in overhanging, thick-walled stomatal pits, 15 μ deep. The stomatal apertures are usually oval, but occasionally rounded, and of average size 60 $\mu \times 40$ μ. The subsidiary cells are usually 8–12 in number

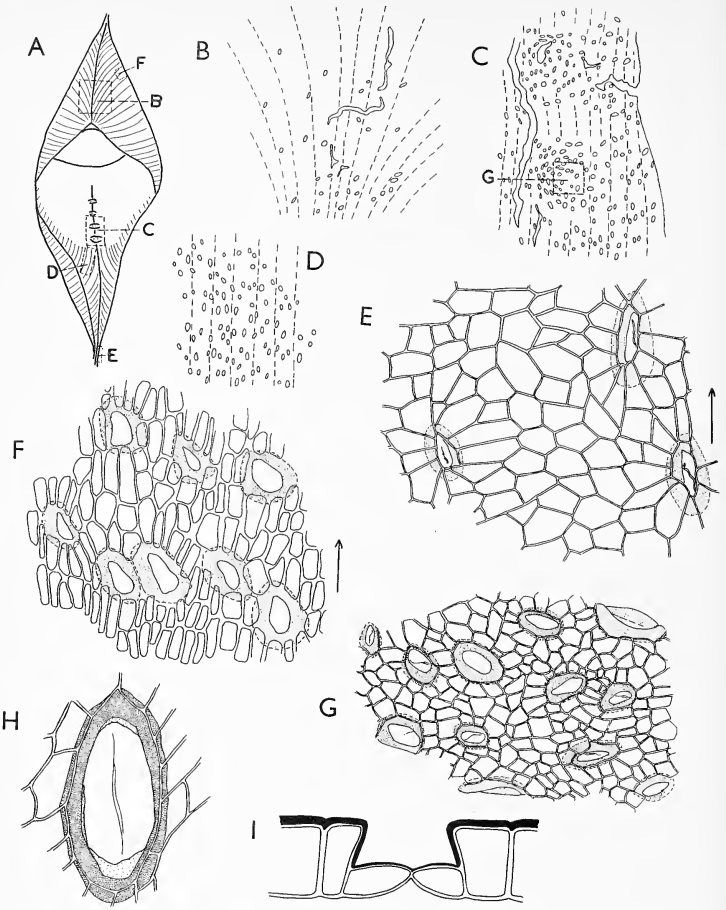

TEXT-FIG. 5. *Lepidodendron veltheimii* Sternberg. K2411. A, Leaf cushions, ×3. The lines on the cushion indicate the direction and area covered by surface striations, but they do not represent individual striations. B, C, D, Areas of cushion surface showing direction of striations and distribution of stomata, ×20. Slide nos.: B—PF 2699; C. D—PF 2700. E, Cuticle from groove between cushions, arrows directed parallel to the groove, slide PF 2701, ×200. F, Cuticle from edge of cushion, arrow directed away from groove, slide PF 2698, ×200. G, Cuticle from cushion surface, slide PF 2700, ×200. H, Stoma ×500. I, Reconstructed median transverse section of a stoma, ×500. All lettering gives the location of other figures.

and unmodified in size and orientation but sometimes are radially elongated from the stomatal aperture.

Comparison. Lacey (1962) has described a species of *Lepidodendron* from the Lower Carboniferous of North Wales as being nearest to *L. veltheimii*. His plate 16, fig. 16 shows the leaf cushions to be roughly 20×7 mm. with very little detail except a slight inflection of the upper and lower angles. The cuticle from the groove between the cushions has epidermal cells 100 μ×30 μ possessing thick (5–6 μ) anticlinal walls. These cells are larger and have thicker walls than those from the larger cushions of K 2411 so it is doubtful that the two specimens belong to the same species.

Lepidodendron feistmanteli Zalessky

Plate 33, fig. 3; Plate 34, fig. 5; text-fig. 6

1875 *Lepidodendron dichotomum* Sternberg; Feistmantel, p. 188, pl. 32, figs. 2, 4.
1904 *Lepidodendron Feistmanteli* Zalessky, p. 93, pl. 4, figs. 6, 10.
1913 *Lepidodendron Jaraczewski* Zeiller; Bureau, p. 113, pl. 40, figs. 1, 1*a*.
1944 *Lepidodendron Jaraczewski* Zeiller; Bell, p. 89, pl. 51, figs. 1, 2.

Material. GSM 77179, 77180 (part and counterpart); K 3255, 4874–6, 4946, 4993 from above the Fenton coal, Wooley and Dodworth collieries, near Barnsley, Yorkshire—communis zone, Westphalian A; K 3605 from the Bradford coal group, Bradford colliery, Lancashire—phillipsii zone, Westphalian C.

The largest piece of bark (GSM 77179) is 11 cm. broad and 33 cm. long and like all the other specimens shows no variation in cushion size or details. The leaf cushions are rhomboidal, strongly raised, and not continuous with the cushions above and below. The leaf scars are in the centre of the leaf cushions and raised above the general cushion area. The leaf scars have edges which slightly overlap the cushion and produce unequal partition of the compression when the rock is split. The carbonized compression of the scar is usually left in the counterpart producing what looks like a small unmarked scar on the elevated cushions of the other part of the specimen (text-fig. 6A). No vascular prints nor ligule pit apertures are visible on such specimens but they can be clearly seen if the compression is removed from the sunken impressions of the counterpart. The cushion surfaces are smooth but have very prominent keels above and below the leaf scars and also possess strong keel-like ridges running from the edges of the leaf scars to the edges of the cushions. No external parichnos are present.

Cuticle description. The epidermal cells on the leaf cushion surfaces are isodiametric and 15–20 μ across, but the cells on the cushion edges are slightly elongated towards the cushion centre. The anticlinal walls are straight, smooth, and 1–2 μ thick. The periclinal walls are flat and smooth. The stomata are 300–350 per mm.^{2} and are about 45–50 μ long and 15–20 μ broad. The guard cells are sunken in pits, 3–6 μ deep with very little or no overhang of the pit aperture. The ligule pit cuticles are about 0·8 mm. long with rectangular cells, 15–20 μ long and 15 μ broad, in longitudinal files.

Comparison. Fischer (1904) included *L. feistmanteli* in *L. dichotomum* Sternberg and Hirmer (1927) believed them to be related. They are, however, clearly distinct in both cushion and cuticle details. The leaf scars of *L. dichotomum* are not elevated and are relatively further up the leaf cushion. The epidermis of *L. feistmanteli* is roughly the

same over the whole cushion but in *L. dichotomum* it is different above and below the leaf scar. The epidermal cells and stomata are also larger in *L. feistmanteli*.

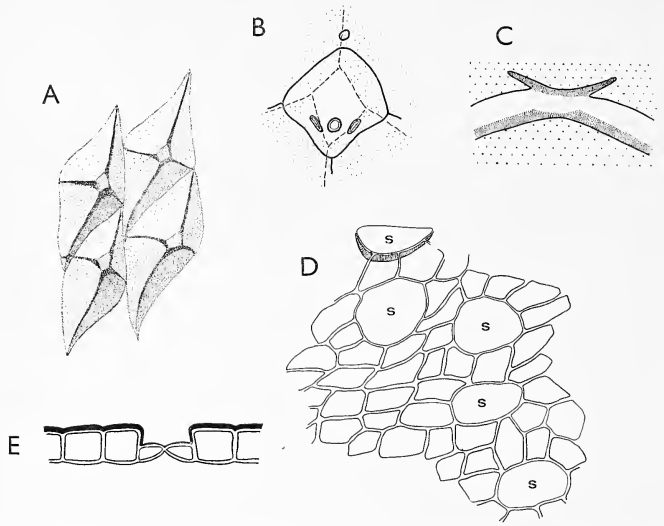

TEXT-FIG. 6. *Lepidodendron feistmanteli* Zalessky. GSM 77179. A, Leaf cushions, ×2. B, Reconstruction showing elevated leaf scar overlapping part of the leaf cushion, ×10. C, Reconstructed section through part and counterpart of a leaf cushion compression to show the raised leaf scar and the unequal splitting of the carbon. Coarse shading represents the rock matrix and the fine shading the carbonized compression. D, Leaf cushion cuticle, ×400; stomata—s; slide PF 2870. E, Reconstructed median transverse section through a stoma, ×400.

Bureau (1913) and Bell (1944) described what appear to be specimens of *L. feistmanteli* as *L. jaraczewski* Zeiller, However *L. jaraczewski* has relatively longer cushions and the leaf scars are not so raised, have no overlap over the cushion surface, and are

EXPLANATION OF PLATE 31

Figs. 1–3. *Lepidodendron aculeatum* Sternberg; illustrating variation in cushion ornamentation and the separation of cushions by lateral stem expansion; ×1. 1, WM, G 541 from Tamworth, Staffordshire. 2, BMNH 46685, from Ebbw Vale, Monmouthshire. 3, BMNH 1049, from Waldenburg, Silesia.

Fig. 4. *Lepidodendron serpentigerum* Koenig. GSM 2498 from above the Stranger Coal, Grange Colliery, Kilmarnock, Ayrshire; ×2.

Fig. 5. *Lepidodendron barnsleyense* sp. nov. Holotype, K 4131, from above the Barnsley Bed, Monkton Main Colliery, Yorkshire; ×2.

Figs. 6, 7. *Lepidodendron dichotomum* Sternberg. Unlocalized specimen in the Huddersfield Museum; ×2. 6, Portion of compressed bark. 7, Impressions of cushions in the shale.

1

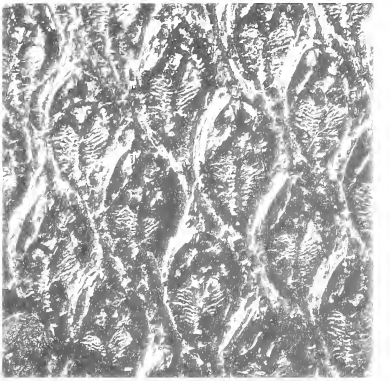

2

3

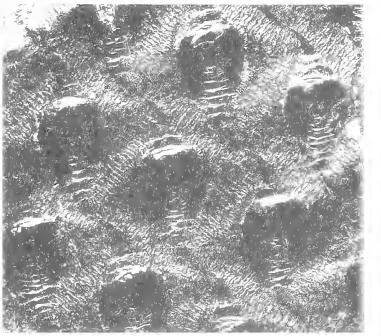

4

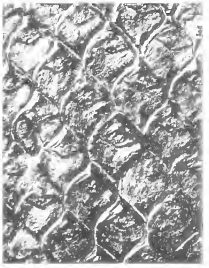

5

6

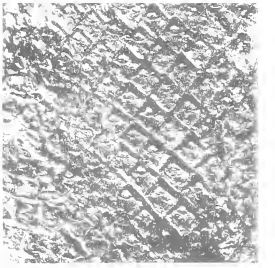

7

THOMAS, *Lepidodendron*

situated further up the leaf cushions. *L. jaraczewski* also has less prominent keels and lateral lines running from leaf scar to cushion edge. These lateral lines are also not as straight as in *L. feistmanteli* but curve downwards to meet the cushion edge below the central broadest part of the leaf cushion.

Lepidodendron mannabachense Presl

Plate 30, figs. 3, 4; Plate 32; Plate 34, figs. 1, 2, 7, 8; text-figs. 7, 8

1838 *Lepidodendron mannabachense* Presl in Sternberg, p. 177, pl. 68, fig. 2.
1838 *Sagenaria obovatum* Presl in Sternberg, p. 178, pl. 68, fig. 6.
1886 *Lepidodendron obovatum* Sternberg; Zeiller, p. 442, pl. 66, figs. 1–8.
1904 *Lepidodendron obovatum* Sternberg; Renier, pl. 1, figs. *a*, *b*.
1947 *Lepidodendron obovatum* Sternberg; Němejc (in part), p. 51.
1959 *Lepidodendron obovatum* Sternberg; Remy, p. 100, fig. 77.
1964 *Lepidodendron obovatum* Sternberg; Crookall, p. 239, pl. 60, figs. 3, 4; text-fig. 776.
1966 *Lepidodendron obovatum* Sternberg; Thomas, fig. 3.

Material. Type specimen, CNM ČGH 329, from the Upper Carboniferous of Mannabach, Thüringen; CNM ČGH 335 (*S. obovatum* Presl in Sternberg 1838, pl. 68, fig. 6) from the Upper Carboniferous of Chomle; K 3365, from the Westphalian of Trawden Forest, near Colne, Lancashire; K 2469, Low main coal, Cramlington, Northumberland—Westphalian B; K 2473, Stanley Main coal, Thome's colliery, Wakefield, Yorkshire—Westphalian B; K 2474, Low Moor, near Bradford, Yorkshire—Westphalian A; SM M378, from the coal measures of Wakefield, Yorkshire; SM M1476, Queen's seam, Broomhill colliery, near Amble, Northumberland—Westphalian B; LM 265, 1958/1, Adam Head No. 1 pit, Desford colliery, Leicestershire, probably Westphalian A.

Both the specimens described by Presl are preserved as impressions with no compression remaining. Similar cuticles were, however, prepared from the other seven specimens. The cushion outlines are distinct but in some specimens their upper angles overlap the lower parts of the cushions above which is probably a compression feature produced during fossilization. The leaf scars are within the upper halves of the leaf cushion and have three foliar prints in their lower halves. The ligule pit apertures are adjacent to the upper angles of the leaf scars where they can be easily overlooked if cuticle preparations are not made. Traces of infrafoliar parichnos can be seen on some cushions of every specimen. The keels, which are always present, are smooth above the leaf scar but sometimes notched below it. The cushion surface below the leaf scar is smooth but above it there are many fine striations running from the scar to the cushion edge.

The range of leaf cushion size is a result of the different positions of the cushions on the parent plant, as the larger shoots always bore the larger cushions. The differences in cushion shape are small and can be regarded as variation within the species.

Cuticle description. The epidermal cells above and below the leaf scars are different. The cells above the scars are about 20–40 μ long and 10–15 μ broad and elongated from the scar to the cushion edge, while the cells from below the scars are isodiametric and 15–20 μ broad or sometimes elongated towards the scar and about 30–35 $\mu \times 15$ μ in size. Cells from the intercushion grooves are isodiametric and 15 μ broad, or elongated across the groove and about 15 $\mu \times 10$ μ. The anticlinal walls are straight, smooth and 1–2 μ thick. The periclinal walls are flat and faintly granular and occasionally have striations, less than 1 μ thick, across the cells. The stomata are about 200 per mm.^{2} and randomly

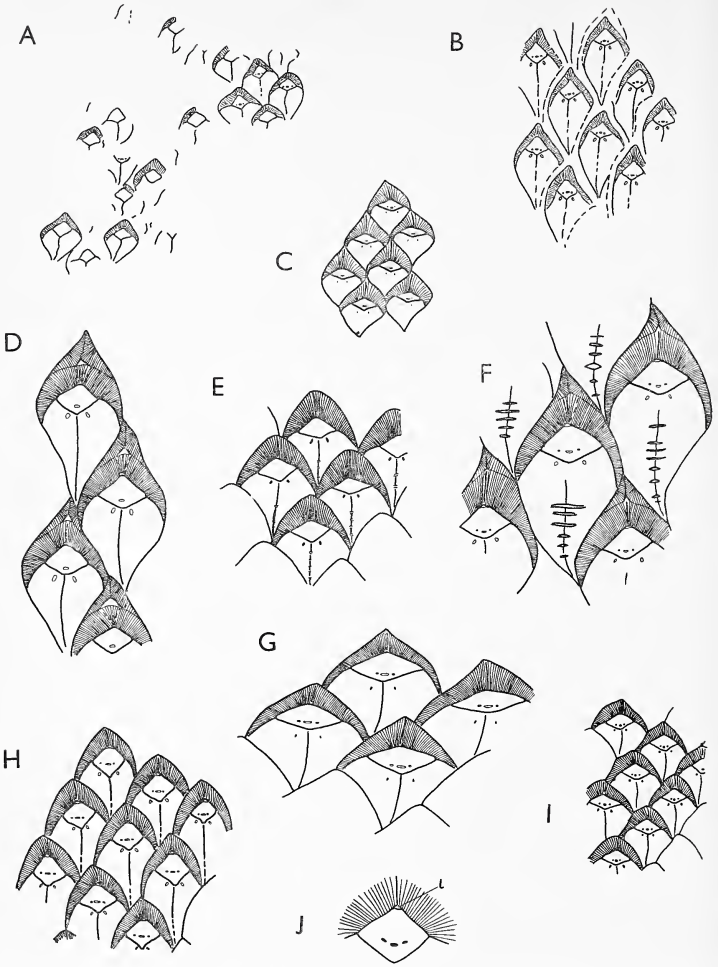

TEXT-FIG. 7. *Lepidodendron mannabachense* Presl. A, Type specimen, CNM ČGH 329. B, CNM ČGH 335. C, K 2469. D, SM M1476. E, K 2473. F, LM 256, 1958/1. G, SM, M378. H, K 3365. I, K 2474. All at ×2. J, Leaf scar with ligule pit (l), ×4. The shading lines indicate the areas covered by surface striations and their direction. They do not represent individual striations.

distributed on the cushion surface, but are absent in the intercushion grooves. Stomatal average size is about 25–30 $\mu \times 12\ \mu$ and the guard cells are sunken in pits about 6 μ deep. The subsidiary cells are unmodified and about eight per stoma. The ligule pit has rectangular cells 30 $\mu \times 10\ \mu$ along most of its length, but roughly square cells, 10 μ across, near its base.

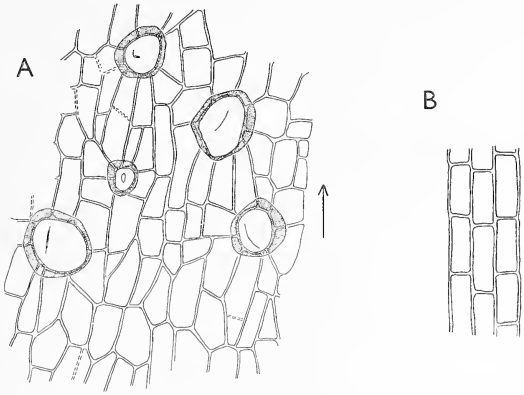

TEXT-FIG. 8. Cushion cuticle of *Lepidodendron mannabachense* Presl. A, Leaf cushion cuticle from above the leaf scar, from K 3365, slide PF 2815. B, ligule pit cuticle, from K 2469, slide PF 2810. Both at $\times 400$.

Comparison. The distinction of *L. mannabachense* has already been dealt with above in the discussion of *L. aculeatum*. Cuticle study also supports the distinction of the two species as *L. mannabachense*, unlike *L. aculeatum*, has striations on the leaf cushions above the scars and a corresponding difference in epidermal structure above and below the scars.

Lepidodendron dichotomum Sternberg

Plate 31, figs. 6, 7; text-fig. 9

1820 *Lepidodendron dichotomum* Sternberg, pars, pl. 1, 2.
1838 *Lepidodendron dichotomum* Presl in Sternberg, p. 214, pl. 68, fig. 2; pl. A, fig. 16.
1838 *Lepidodendron Sternbergii* Brongniart, p. xiv, pl. 16, figs. 2, 3.
1875 *Lepidodendron dichotomum* Sternberg; Feistmantel, p. 188, pl. 32, figs. 1,3.
1934 *Lepidodendron dichotomum* Sternberg; Němejc, p. 1, pl. 1, figs. 2, 3; pl. 2, fig. 1.
1959 *Lepidodendron dichotomum* Sternberg; Remy, p. 100, text-fig. 78, *a*, *b*.
1964 *Lepidodendron dichotomum* Sternberg; Crookall, pars, p. 236.

Material. Type specimen, CMH ČGH 315, from the Upper Carboniferous of Svinná; K. 4876, from above the Parkgate coal, Dodworth, near Barnsley—Westphalian A; an unlocalized specimen in the Huddersfield Museum.

The specimens show shoots covered with diamond-shaped leaf cushions 2–5 mm. high and broad with angled corners. Some variation is shown in K 4876, where some cushions are slightly different being 2 mm. long and broad but with rounded lateral angles. Also certain shoots show different-shaped cushions in different parts; for example one has cushions 4 mm. long and 2 mm. broad in one part while elsewhere they are 2 mm. long and broad. The leaf scars are situated near the apices of the cushions and are roughly diamond-shaped and one and a half times as broad as high. Three foliar prints and two infrafoliar parichnos are present, though they are often indistinct. The ligule pit aperture is adjacent to the upper angle of the leaf scar. A very slightly raised keel can be seen, though it is usually more definite above than below the leaf scar. The cushion surface above the leaf scar shows many fine striations running from the leaf scar to the cushion edge, but the surface below the scar is smooth.

Cuticle description. The epidermal arrangement is different above and below the leaf scars. The cells above the scars are normally about 20–30 μ long and 15 μ broad and elongated from the scar to the cushion edge, although occasionally they are roughly isodiametric. These cells are often in short longitudinal rows running from the scar to the cushion edge. The cells below the leaf scars are normally roughly isodiametric and 10–15 μ broad but are sometimes slightly elongated towards the leaf scars. The intercushion grooves have isodiametric cells 15 μ across and cells 15 $\mu \times 10$ μ elongated across the groove. Anticlinal walls are straight, smooth, and 2 μ thick except above the leaf scar where they are often 4 μ thick. The periclinal walls are flat and faintly granular. Stomata are very frequent below the leaf scar, 450 per mm.^{2}, where they are randomly distributed and orientated. However, they are normally absent above the leaf scar except occasionally in the lower angles at the sides of the scar. Very few stomata are present in the intercushion grooves. Stomatal average size is about 40 $\mu \times 20$ μ and the guard cells are sunken in pits about 6 μ deep. The subsidiary cells are unmodified and are about ten per stoma. The ligule pit is about 0·6 mm. long and 0·13 mm. broad. The cells are mostly rectangular, 30 $\mu \times 10$ μ, and elongated along the pit, but are roughly square near its base.

Comparison. Much has been written about this species. Brongniart (1828*a*) followed by Presl in Sternberg (1838) restricted *L. dichotomum* to plates 1 and 2 of Sternberg's (1820) original description, excluding his plate 3. The species in this restricted sense has been widely recorded, although Jongmans (1929) and Crookall (1964) believed many of the specimens to be misinterpreted. Other authors have interpreted *L. dichotomum* in different ways including other combinations of specimens as synonyms, but as Němejc (1947) has given a useful summary no further review will be included here. However, some authors, including Němejc (1946 and 1947) and Chaloner (1967), have included *L. dichotomum* as a synonym of *L. obovatum* (= *L. mannabachense*) believing them to be the small and large shoots of one species. Although the smallest cushions included here as

EXPLANATION OF PLATE 32

Figs. 1–7. *Lepidodendron mannabachense* Presl, illustrating variation in cushion shape and size. All at ×2. 1, SM M1476. 2, LM 256, 1958/1. 3, K 3365. 4, K 2473. 5, K 2469. 6, K 2474. 7, K 378.

The localities are given on p. 157.

1

2

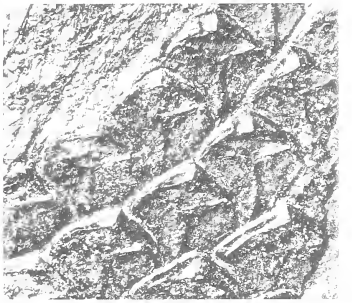

3

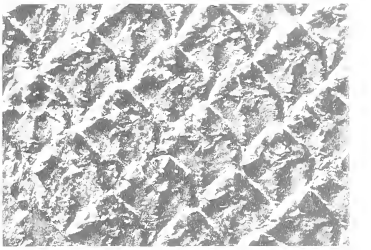

4

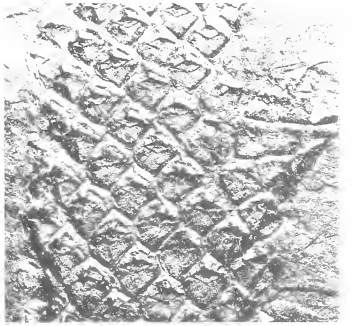

5

6

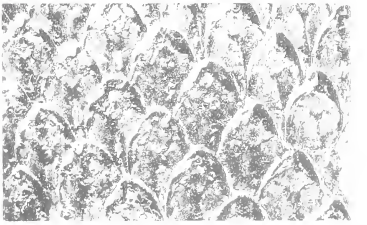

7

THOMAS, *Lepidodendron*

L. mannabachense are very similar to those of *L. dichotonum*, I favour, at least for the present, their continued separation. The leaf cushions of *L. dichotomum*, as interpreted here, are more diamond-shaped than those of *L. mannabachense* and the leaf scars are

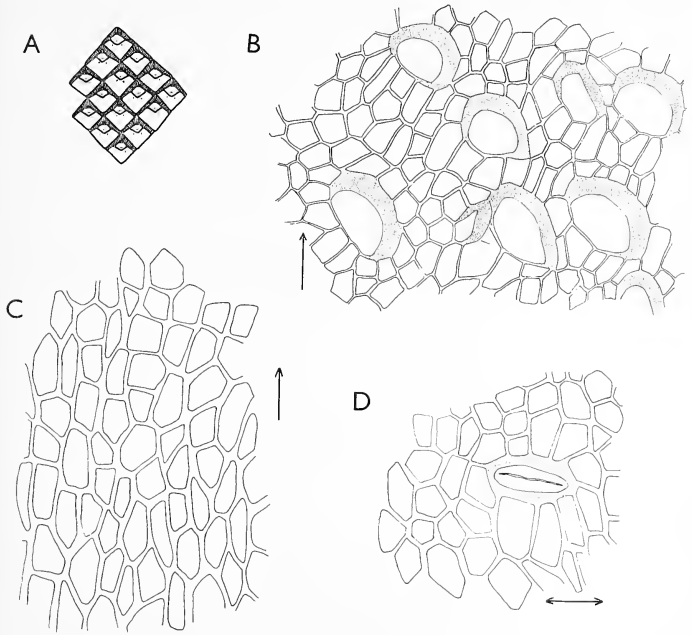

TEXT-FIG. 9. *Lepidodendron dichotomum* Sternberg. A, Unnumbered specimen in the Huddersfield Museum. B, Leaf cushion cuticle from below leaf scar. C, Leaf cushion cuticle from above leaf scar. D, Cuticle from intercushion groove; arrows are parallel to groove. Magnifications: leaf cushions $\times 2$; cuticles $\times 400$

situated relatively higher on the cushions. The epidermal cells are larger in *L. mannabachense*, but more important is the difference in stomatal frequency between the two. In *L. dichotomum* stomata are almost completely absent above the leaf scar but are 450 per mm.^{2} below the scar, in contrast to *L. mannabachense* where they are roughly 200 per mm.^{2} over the whole cushion surface.

All the typical shoots of *L. dichotomum*, as described here, are narrow. However, it is reasonable to assume that the larger shoots of the species bore larger leaf cushions since leaf cushion and shoot sizes are generally supposed to be interrelated (Eggert 1961). Therefore, if *L. mannabachense* is not the larger form of *L. dichotomum* we should look

elsewhere for such shoots. Němejc (1934) described some specimens as *L. dichotomum* which have both larger leaf cushions and broader shoots than those described here. The leaf scars are diamond-shaped and are situated centrally on the cushions and not near their apices as in the more typical specimens described above. No cuticles could be prepared from Němejc's specimens and the rough surface of the compression prevented direct observation of individual epidermal cells. Striations were, however, visible above the leaf scar suggesting that the cells in this area were elongated while those below the scar were isodiametric, but this alone is not sufficiently characteristic for species distinction as several species are known to have such epidermal arrangements. These specimens cannot therefore be regarded as being definitely conspecific with *L. dichotomum*, although such a relationship is not impossible on the available epidermal evidence. Further work is clearly needed before the larger shoots of *L. dichotomum* are known with certainty.

Lepidodendron subdichotomum Sterzel pars

Text-fig. 10, E–H

1855 *Sagenaria dichotoma* Sternberg; Geinitz pars, p. 34, pl. 3, figs. 2–5, 9.
1901 *Lepidodendron subdichotomum* Sterzel pars, p. 106.
1903 *Lepidodendron dichotomum* Zeiller (?Sternberg); Arber, pp. 20, 32, pl. 1, figs. 1, 2.
1904 *Lepidodendron dichotomum* Sternberg; Zalessky pars, pp. 9, 83, pl. 3, figs. 5, 10, 10*a*, 11.
1914 *Lepidodendron dichotomum* Sternberg; Arber, pp. 402, 445, pl. 29, fig. 36.
1922 *Lepidodendron loricatum* Arber pars, p. 201, pl. 13, figs. 27–32.
1925 *Lepidodendron loricatum* Arber; Crookall, p. 170.
1929 *Lepidodendron loricatum* Arber; Crookall, p. 25, pl. 3, fig. *h*; pl. 20, fig. *h*.
1929 *Lepidodendron loricatum* Arber; Jongmans, p. 208.
1929 *Lepidodendron subdichotomum* Sterzel; Jongmans, p. 313.
1947 *Lepidodendron subdichotomum* Sterzel; Němejc pars, p. 57, pl. 1, fig. 7.
1964 *Lepidodendron loricatum* Arber pars; Crookall pars, p. 243, pl. 64, fig. 9; text-fig. 79.

Material. Syntype of *L. loricatum*, SM 2506, from the Sulphur Coals, Transition Coal Measures, Bayton Colliery, Wyre Forest, Worcestershire, Westphalian C; K. 6340, No. 3 Llantwit Seam, Cross Inn, Llantrisant, Glamorgan, Westphalian C.

The leaf cushions are close together but not continuous with those above and below. The leaf scars are about two-thirds the distance up the leaf cushions and are often arranged obliquely on the cushions. There is no keel above the leaf scar, only a faint keel below the scar and no lateral lines running from the scars to the cushion edges. Three foliar prints can be indistinctly seen about one-third the distance up the scars but there are now visible infrafoliar parichnos. The ligule pit apertures are adjacent to the upper

EXPLANATION OF PLATE 33

Fig. 1. *Lepidodendron peachii* Kidston. K 2466, from the Lower Main Seam, Newsham, Newcastle upon Tyne, ×2.

Fig. 2. *Lepidodendron arberi* sp. nov. Holotype, K 2488, from the Lower Main Coal, Cramlington, Northumberland, ×2.

Fig. 3. *Lepidodendron feistmanteli* Zalessky. GSM 77179, from the Fenton Coal, Wooley, Yorkshire, ×2.

Figs. 4–6. *Lepidodendron veltheimii* Sternberg. K 2411, from immediately beneath the Orchard Limestone, New Brawden Quarry, Giffnock, Renfrewshire. 4, Leaf cushions, ×2. 5 and 6, Leaf cushion cuticle, slide PF 2700; 5, Epidermal cells and stomata on and near the keel below the leaf scar, ×25; 6, Obliquely compressed stomata showing pit cuticles but no guard cells, ×400.

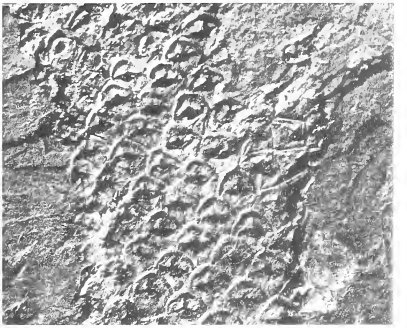

1

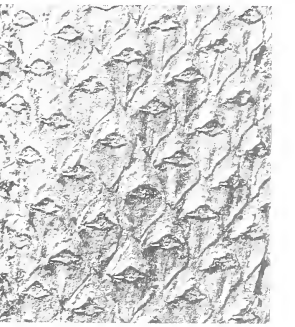

2

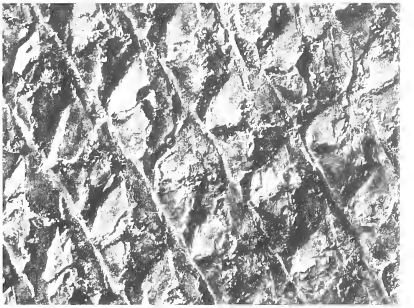

3

4

5

6

THOMAS, *Lepidodendron*

angles of the leaf scars. The leaf cushion surfaces are smooth above and below the leaf scars.

Cuticle description. The epidermal arrangements are roughly the same above and below the leaf scars. The epidermal cells from the central area of the cushions are isodiametric and about 15–20 μ across. The cells from the edges of the cushions are elongated towards the leaf scars and are about 30 μ long and 10 μ broad. The anticlinal walls are straight, smooth and about 1 μ thick. The periclinal walls are flat and smooth. The stomata are about 200 per mm.^{2} and of average size 38 $\mu \times 26$ μ, with superficial guard cells. The ligule pits have rectangular cells, in longitudinal rows, which are 40 $\mu \times 10$ μ in size along most of the pit except near the base where they are roughly 10 μ square.

Comparison. Sterzel instituted *L. subdichotomum* for some specimens from Sachsen which had been previously identified by Geinitz (1855) as *Sagenaria dichotoma* Sternberg (pl. 3, figs. 1–12) and *Sagenaria rimosa* Sternberg (pl. 3, figs. 13–15). Arber (1922) also included the *S. dichotoma* of Geinitz as a synonym of his *Lepidodendron loricatum* making no reference to Sterzel, although if both authors were correct in their determinations, his species was merely a later synonym for *L. subdichotomum*. The major problem, as usual, is deciding how much variation occurs within the species and what specimens are conspecific. Sterzel had not included in synonymy all the figures of *S. dichotoma* and *S. rimosa* given by Geinitz, while Arber suggested that possibly only two figures of *S. dichotoma* of Geinitz were the same species as his *L. loricatum*. Crookall included only a part of the *S. dichotoma* of Geinitz (pl. 3, figs. 2–5, 9) and only the plate 13, figs. 27–32 of Arber in his synonymy for *L. loricatum*, but like Arber made no reference to Sterzel. Such an acceptance of partial conspecificity of Geinitz's and Arber's specimens seems the best solution, but Sterzel's work should not be excluded as it has priority even though it is accepted in a reduced form. *L. subdichotomum* is therefore the correct name for specimens of this form.

Those figures quoted for *L. loricatum* by Crookall are given in synonymy here but three of his additional specimens are excluded. His plate 61, fig. 1 is probably *L. mannabachense* as the specimen has faint striations on the cushion surfaces above the leaf scars; plate 64, fig. 6 is described here as *Lepidodendron barnsleyense* sp. nov.; and plate 64, figs. 7, 8 has relatively highly placed leaf scars and infrafoliar parichnos making it unacceptable as *L. loricatum*, though I do not suggest another name. Three of Arber's specimens are also excluded from the present synonymy. Two (pl. 13, figs. 33–5) are described here as *L. arberi* sp. nov. and one (pl. 13, figs. 36, 37) looks more like *L. fusiformis* Corda.

Crookall (1964, p. 242) believed that most of the specimens identified by Kidston as *L. obovatum* (= *L. mannabachense*) were really *L. loricatum* (= *L. subdichotomum*) and that the latter species was the more common in Great Britain. The confusion of these two species by Crookall, as illustrated above by his plate 61, fig. 1, probably accounts for this view which appears incorrect when they are interpreted with the extra evidence afforded by epidermal studies.

Lepidodendron arberi sp. nov.

Plate 33, fig. 2; text-fig. 10, A–D

1922 *Lepidodendron loricatum* Arber pars, p. 201, pl. 13, figs. 33–5.
1964 *Lepidodendron* sp. Crookall, p. 303, pl. 72, fig. 5.

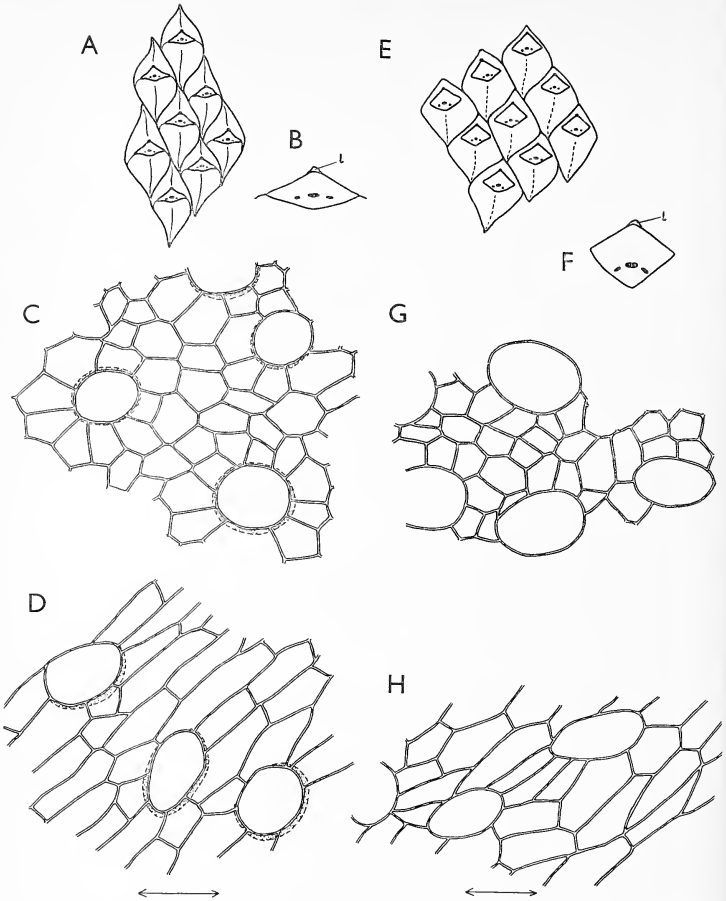

TEXT-FIG. 10. *Lepidodendron arberi* sp. nov. (A–D). and *Lepidodendron subdichotomum* Sterzel pars, (E–H). A, *L. arberi* K 2488, leaf cushions. B, Leaf scar with ligule pit aperture (l), ×6. C, Cuticle from median area of cushion, slide PF 3085. D, Cuticle from edge of cushion, arrows parallel to groove between cushions, slide PF 3086. E, *L. subdichotomum* SM 2056, leaf cushions. F, Leaf scar with ligule pit aperture (l), ×6. G. Cuticle from median area of cushion. H, Cuticle from edge of cushion, arrows parallel to groove between cushions. Magnifications: Leaf cushions ×2, Cuticles ×400.

Material. Holotype, K. 2488 from the Low Main coal, Cramlington, Northumberland, *similis-pulchra* Zone, Westphalian B. Paratypes, RSM, Dunlop collection, 1957.1.7428 from above the Kiltongue Coal, Ellismuir, Bailliestown, Lanarkshire—Westphalian A; SM. 1953, 1645, from the Upper Coal Measures of the Forest of Dean—Westphalian C.

The holotype is a small shoot preserved as a compression on dark grey shale. The shoot possesses one dichotomy of about 40°. Individual leaf cushions are about 10 mm. long and 5 mm. broad below the dichotomy and about 8 mm. long and 5 mm. broad above it. The leaf scars are all about 1 mm. long and 3 mm. broad. Reasonable cuticle was obtained from the type specimen but only fragments could be obtained from SM 1953 and RSM 1957.1.7428 and none from SM 1645.

Diagnosis. Leaf cushions close together and not continuous with those above and below. Leaf scar broader than long and just above the cushion centre. Three foliar prints slightly below the middle of the leaf scar. Ligule pit aperture adjacent to upper angle of leaf scar. No visible infrafoliar parichnos. Faint keels above and below leaf scars. Lateral lines running from leaf scars to cushion edges. Leaf cushion surface smooth above and below leaf scar.

Epidermis similar above and below the leaf scars. Cells from centre of cushions roughly isodiametric and 20 μ broad or elongated parallel to cushion length and 35 μ long. Cells from cushion edges elongated toward leaf scars and about 35 $\mu \times 15$ μ across. Anticlinal walls straight, smooth and 2 μ thick. Periclinal walls flat, smooth. Stomata about 200 per mm.^{2}, randomly orientated and distributed. Average size 35 $\mu \times 28$ μ. Guard cells sunken in pits about 5 μ deep. Ligule pit about 800 μ long and 200 μ across, with rectangular cells in longitudinal files, 30 μ long and 10 μ broad except at the base where they are 10 μ square.

Derivation of name. For the late E. A. N. Arber.

Comparison. L. arberi can be distinguished from *L. subdichotomum* by the lower position of its leaf scars and its possession of lateral lines and distinct keels. The cuticles of the two are rather similar but *L. subdichotomum* has smaller epidermal cells in the central areas of the cushion and has superficial, not sunken, guard cells.

Lepidodendron peachii Kidston

Plate 33, fig. 1; Plate 34, fig. 4; text-fig. 11, A, C, D

1885*a* *Lepidodendron Peachii* Kidston, p. 363, pl. 11, fig. 6.
1885*b* *Lepidodendron Peachii* Kidston, p. 421, pl. 21, fig. 6.
1929 *Lepidodendron Peachii* Kidston; Jongmans, p. 258.
1929 *Lepidodendron peachi* Kidston; Crookall, p. 25, pl. 6, fig. *e*.
1964 *Lepidodendron peachi* Kidston; Crookall, p. 245, pl. 60, fig. 1.

Material. K. 668 (type specimen), below the Armadale main, Glenfain or Guttenhole coal, Brickworks, Falkirk, Stirlingshire—Westphalian A; K. 2466, Lower Main Coal, Newsham, Newcastle upon Tyne—Westphalian B.

The leaf cushions are raised into hood-like structures and have rounded upper angles. The ligule pit apertures are adjacent to the upper angles of the leaf scars and three foliar prints are visible one-third the distance up the scars. No infrafoliar parichnos are visible. A keel can be seen above the leaf scars but only traces can be seen below them.

The cushion surface is finely striated above the scars, with the striations running from the scars to the cushion edges, but below the scars the surface is smooth. Cuticle could only be prepared from K 2466 as the type specimen is preserved solely as an impression.

Cuticle description. The epidermal cells are different above and below the leaf scars. The cells above the scars are about 40–60 $\mu \times 10$ μ and elongated from the scar to the cushion edge while the cells below the scars are roughly isodiametric and 10–15 μ across. The anticlinal walls are straight, smooth and about 1 μ thick. The periclinal walls are flat and smooth. Stomata are about 150 per mm.^{2} below the scar but are absent above. Individual stomata are about 40–50 $\mu \times 35$–40 μ in size and have guard cells sunken in pits 8–10 μ deep. The ligule pits are about 200 μ across with rectangular cells in longitudinal files 60 μ long and 10 μ broad except near the base where they are 20 μ long.

Comparison. Arber (1903, p. 20) suggested that *L. peachii* might be identical to the specimen that he was figuring as *L. dichotomum* Zeiller (?Sternberg) and later (1922) included both in his synonymy for *L. loricatum* (= *L. subdichotomum* Sterzel). However, *L. peachii* can be clearly separated from this other species on both cushion and epidermal characters. The cushions of *L. peachii* are strongly raised and striated above the leaf scar but those of *L. subdichotomum* are flat and smooth. The upper cushion angles are rounded in *L. peachii* but are pointed in *L. subdichotomum* and lateral lines running from cushion scar to cushion edge are only present in *L. peachii*. The epidermal arrangement is roughly the same over the whole leaf cushion in *L. subdichotomum* but in *L. peachii* it is different above and below the leaf scar and in *L. subdichotomum* the guard cells are superficial whereas in *L. peachii* they are sunken.

Lepidodendron barnsleyense sp. nov.

Plate 31, fig. 5; Plate 34, fig. 3; text-fig. 11 B, E–G

1964 *Lepidodendron loricatum* Arber; Crookall pars, p. 243, pl. 64, fig. 6.

Material. Holotype, K. 4131 from above the Barnsley Bed, Monkton Main Colliery, Yorkshire—Base of the *similis-pulchra* Zone, Westphalian B.

EXPLANATION OF PLATE 34

Figs. 1, 2. Leaf cushion cuticle of *Lepidodendron mannabachense* Presl from below the leaf scar, showing stomata and roughly isodiametric cells. Slide PF 2809 from K 2469. 1, ×200; 2, ×400.

Figs. 3, 4. Leaf cushion cuticle from above the leaf scars showing epidermal cells elongated towards the scars, ×200; 3, Slide PF 3090 from *Lepidodendron barnsleyense* sp. nov., K 4131; 4, Slide PF 2877 from *Lepidodendron peachii* Kidston, K 2466.

Fig. 5. Leaf cushion cuticle from *Lepidodendron feistmanteli* Zalessky, ×200; Slide PF 2875 from GSM 72779.

Fig. 6. Cuticle from intercushion area of *Lepidodendron serpentigerum* Koenig, showing rectangular epidermal cells and no stomata; Slide PF 3144 from K 2498.

Figs. 7–8. Ligule pit cuticle from *Lepidodendron mannabachense* Presl; Slide PF 2810 from K 2469; 7, Complete ligule pit showing the opening on to the cushion surface on the right and the opening marking the attachment position of the ligule on the left, ×100; 8, Portion of ligule pit cuticle showing the anticlinal walls standing outwards as ridges, ×600.

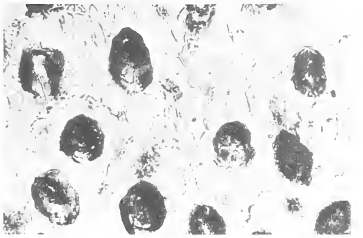

1

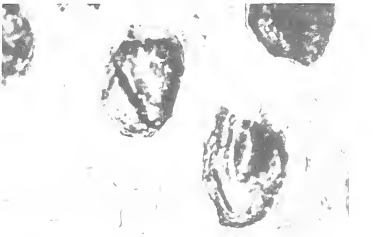

2

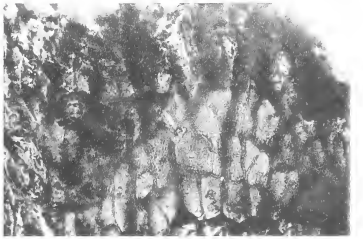

3

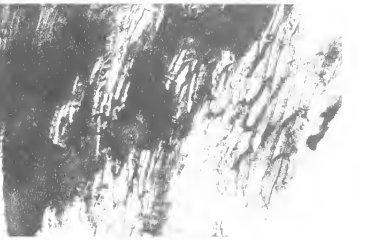

4

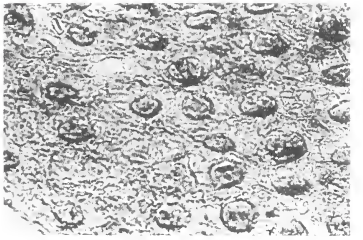

5

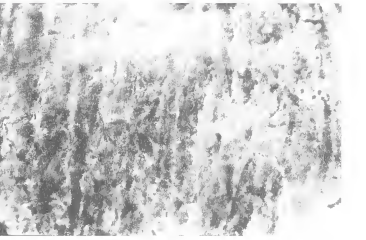

6

7

8

THOMAS, *Lepidodendron*

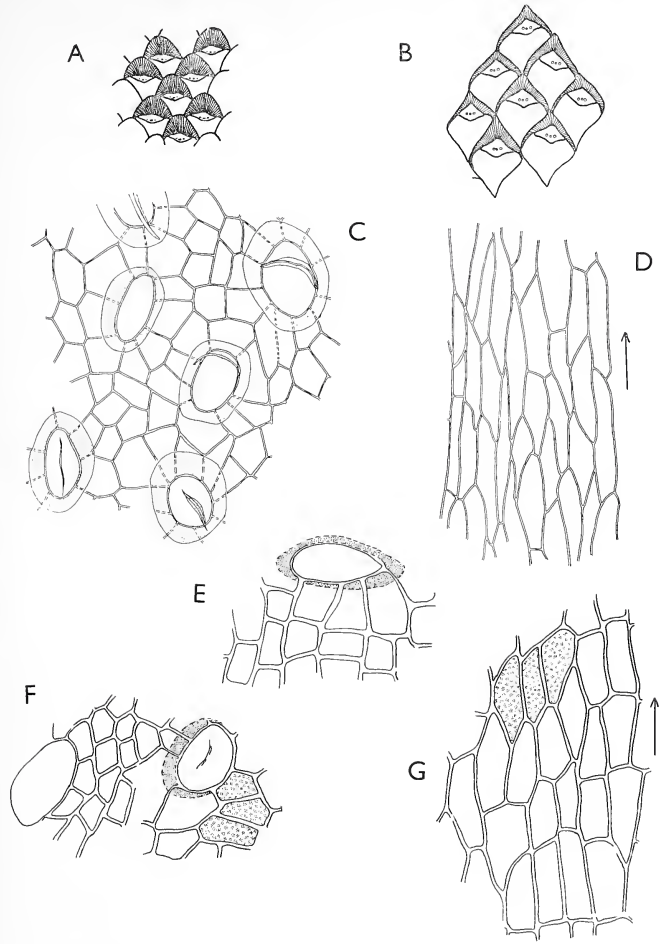

TEXT-FIG. 11. *Lepidodendron peachii* Kidston (A, C, D) and *Lepidodendron barnsleyense* sp. nov. (B, E-G). A, *L. peachii*—K 2466. C, Cuticle from below the leaf scar, figured from the underside, slide PF 2879. D, Cuticle from above the leaf scar (arrows are parallel to cushion striations), slide PF 2877. B, *L. barnsleyense*—K 4131. E, F, Cuticle from below the leaf scar, figured from above, slide PF 3089. G. Cuticle from above the leaf scar (arrows are parallel to cushion striations), slide PF 3090. Magnifications: leaf cushions ×2; cuticles ×400.

The type specimen, which is the only known one referable to this species, is a 3-cm. broad slab of compressed bark on dark grey shale. Cuticle could be easily prepared from the leaf cushions but was only obtained in very small fragments from below the leaf scars. These fragments showed epidermal cells and stomata but were too small to permit an accurate estimation of stomatal frequency. The ligule pit cuticles also broke up during maceration preventing measurement of their over-all sizes.

Diagnosis. Leaf cushions rhomboidal, not continuous with other cushions above and below with leaf scars two-thirds the distance up them. Three foliar prints one-third the distance up the leaf scars but no visible infrafoliar parichnos. Ligule pit aperture adjacent to upper angle of leaf scar. Indistinct kells above and below leaf scars. Lateral lines running from leaf scars to cushion edges. Cushion surface striated above leaf scar with striations running from scar to cushion edge; surface below leaf scar smooth. Epidermal cells above leaf scar 30–45 $\mu \times 10$–20 μ elongated from scar to cushion edge. Cells below leaf scar roughly isodiametric and 15 μ across. Cells from groove cuticle, between cushions, rectangular, about 35 $\mu \times 30$ μ in size, elongated across the groove. Anticlinal walls straight, smooth, about 1 μ thick. Periclinal walls faintly granular. Stomata present below leaf scar but absent above scar and in intercushion grooves. Stomatal average size 48 $\mu \times 30$ μ. Guard cells sunken in pits, 6 μ deep. Ligule pits about 230 μ broad with cells 30–40 μ long, 15 μ broad.

Derivation of name. From the type locality.

Comparison. L. barnsleyense can be distinguished from *L. subdichotomum* in having lateral lines running from the leaf scars to the cushion edges and surface striations above the leaf scars. Cuticle examination supports the distinction of these two species. The epidermal arrangement is different above and below the leaf scars in *L. barnsleyense* but in *L. subdichotomum* it is roughly the same over the whole cushion. Also the guard cells are sunken in pits only in *L. barnsleyense*, those in *L. subdichotomum* being superficial.

The species most similar to *L. barnsleyense* are *L. mannabachense*, *L. dichotomum*, and *L. peachii*. *L. barnsleyense* differs from *L. mannabachense* and *L. dichotomum* in having neither infrafoliar parichnos nor stomata in the cushion epidermis above the leaf scars. *L. dichotomum* also has its leaf scars placed higher on relatively broader leaf cushions. *L. peachii* can be distinguished by its strongly raised upper cushion surface which also possesses longer and narrower cells than the corresponding cushion surface in *L. barnsleyense*. The guard cells of *L. peachii* are also in deeper pits than those of *L. barnsleyense*. *L. barnsleyense* is also distinguished by having granular periclinal walls to its epidermal cells in contrast to the other three species which have smooth walls.

Lepidodendron rhodianum Sternberg

Text-fig. 12

1820 'Schuppenpflanze' Rhode, pp. 7, 8, pl. 1, figs. 1, 3.
1825 *Lepidodendron rhodianum* Sternberg, p. xi.
1877 *Lepidodendron Rhodeanum* Sternberg; Stur, p. 283, pl. 23 (40), fig. 1; pl. 24 (41), figs. 1–3.
1926 *Lepidodendron Rhodeanum* Sternberg; Kidston, p. 125, pl. 13, fig. 3.
1939 *Lepidophloios laricinus* Sternberg; Crookall pars, pp. 14, 18, pl. 2, fig. 2.
1964 *Lepidodendron rhodeanum* Sternberg; Crookall, p. 245, pl. 61, fig. 8; text-fig. 80.

Material. GSE. 1296, from a borehole at Cambus, 2 miles west of Alloa, Clackmannanshire, Scotland; 5 ft. above the Castlecary Limestone, in the lower part of the Millstone Grit, Lower Namurian.

This specimen is a small piece of dark shale with three fragments of shoot referable to *L. rhodianum*. The leaf cushions are close and slightly overlap the cushions above producing an apparent pointing of their lower angles. The original figures given by

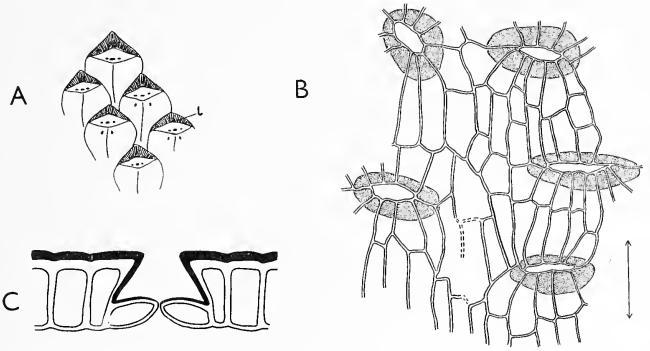

TEXT-FIG. 12. *Lepidodendron rhodianum* Sternberg. GSE, No. 1296. A, Leaf cushions ×3; Ligule pit (l). B, Cuticle from above leaf scar, ×200; arrows directed parallel to cushion striations. C, Reconstructed median transverse section through a stoma, ×400.

Rhode suggest a similar feature in his specimen. The leaf scars are three-quarters the way up the cushions and extend completely or nearly completely across their widths. The leaf cushion surface is striated above the leaf scar but is smooth below. There are three foliar prints, one-third the distance up the scars, two infrafoliar parichnos and a ligule pit aperture, adjacent to the upper angle of the leaf scar.

Cuticle description. The cushion epidermal arrangement is different above and below the leaf scars. The cells above the scars are of average size 50 $\mu \times 20\ \mu$ and elongated from the scar to the cushion edge but the cells below the scar are isodiametric and about 40 μ across. The anticlinal walls are straight, smooth, and about 2 μ thick. The periclinal walls are flat and smooth. The stomata are about 40 per mm.^{2} and randomly distributed over the whole cushion surface. They are randomly orientated below the leaf scar but above the scar the guard cell apertures are orientated at right angles to the direction of epidermal cell elongation. The guard cells are in pits about 20 μ deep and are greatly overhung by the subsidiary cells. The average size of the stomatal aperture is 43 $\mu \times 16\ \mu$ and of the guard cell pair is 77 $\mu \times 54\ \mu$. The ligule pits are at least 1·2 mm. long and 0·35 mm. broad. The pit cells are rectangular, elongated along the pit, and in vertical rows. They are about 50 $\mu \times 20\ \mu$ along most of its length but about 20 μ square near the base.

Comparison. Crookall (1939) described this specimen as *Lepidophloios laricinus* Sternberg and used it as an example of a species occurring in both the Upper and the Lower

Carboniferous. However, *L. laricinus* differs in having leaf scars at the bottom of downward-bulging leaf cushions, non-striated leaf cushions, and ligule pit apertures separated from the leaf scars. A similar confusion occurred when Kidston (1886, p. 160) recorded *L. rhodeanum* (BMNH V284) from the Upper Carboniferous although he later (1894, p. 251) confined this species to the Lower Carboniferous. Crookall (1939, p. 18; 1964, p. 247) described this specimen of Kidston as *Lepidophloios laricinus* Sternberg but it has similar leaf cushions to K3365 which is illustrated here as *Lepidodendron mannabachense* Sternberg (pl. 4, fig. 3; text-fig. 7, H) and is best considered to be this species.

L. rhodianum is similar to *L. mannabachense*, *L. dichotomum*, *L. peachii*, and *L. barnsleyense* in having leaf cushions which are striated above the scars and smooth below them. *L. rhodianum* can, however, be distinguished from these other species by its much broader leaf scars and its epidermal characters. *L. peachii* and *L. barnsleyense* have no stomata above the leaf scars; *L. dichotomum* has very few above the scars but very many more than *L. rhodianum* below the scars; *L. mannabachense* has more stomata than *L. rhodianum* and they are smaller and in shallower pits.

DISCUSSION

The main details of the lepidodendroid cuticle have been previously given (Thomas 1966); but as specific cuticle descriptions are now available for comparison certain features of the *Lepidodendron* cuticle should be discussed in greater detail.

Although the *Lepidodendron* cuticle is like that of some related lepidodendroid genera, it can still sometimes be useful in generic determinations. Lacey (1962) described the cuticle from his new species *Lepidodendron perforatum* but suggested that it may be better included in *Prelepidodendron* Danzé. Lacey's specimens have recognizable leaf cushions but the leaf scars are relatively larger than those of *Lepidodendron* and there are no stomata on the cushion cuticles. Both scar size and cuticle detail therefore support the exclusion of this species from *Lepidodendron*; unfortunately no cuticle has been described from a definite species of *Prelepidodendron* making a cuticle comparison impossible. Cuticle study also supports the removal of the southern hemisphere lycopod, *Lycopodiopsis pedroanum* (Carruthers) Edwards (1952), from *Lepidodendron* where it was originally included. The cuticle prepared from one of the paratypes, BMNH V230g, showed much larger epidermal cells ($60\,\mu \times 45\,\mu$) and much thicker anticlinal walls ($4–7\,\mu$) than any described here. The stomata also differ in distribution, being only present on the very edges of the cushions and there only rarely.

Lepidodendron compression species are normally classified on external cushion morphology and this is often satisfactory. Sometimes however, specimens may be incomplete or imperfectly preserved, making identification difficult, and knowledge of the cuticle from these specimens can be often invaluable. Epidermal cell characters can be very useful in distinguishing species: for example in *L. peachii* the cells above the leaf scar are longer and slightly narrower ($40–60\,\mu \times 10–15\,\mu$) than in the similar species *L. barnsleyense* ($30–35\,\mu \times 15\,\mu$). However, care must be taken to examine the cuticle from over the whole cushion surface as the shape and orientation of epidermal cells may vary from area to area. The arrangement of epidermal cells divides *Lepidodendron* species into two broad groups. One group has mainly isodiametric cells over the whole cushion,

e.g. *L. aculeatum*, *L. serpentigerum*, and *L. subdichotomum*, while the other group has the cells above the leaf scar elongated towards the scars, e.g. *L. mannabachense*, *L. dichotomum*, and *L. rhodianum*. Some species, e.g. *L. veltheimii*, do have areas of elongated cells below the leaf scars, but no species is known which has only isodiametric cells above and elongated cells below the scars. This cellular arrangement on the cushions probably reflects the arrangement on the abscissed distal portions of the leaves. Those cushions with dissimilar epidermal arrangements above and below the leaf scars probably bore leaves with dissimilar upper and lower epidermises, while those cushions with only one epidermal arrangement probably bore leaves with similar upper and lower epidermises. Graham (1935) described the epidermises of petrified lycopod leaves but described no specimens with distinctly different upper and lower epidermises. He did, however, show that some leaves possessed their stomata in two furrows on the lower surface, while other leaves possessed no such furrows. Perhaps some association of stomatal furrows with cushion epidermal arrangement may be proved with future work, but as yet no definite conclusions can be drawn.

The periclinal walls of the epidermal cells should also be closely examined, preferably with phase contrast illumination, as they are granular in some species. This granulation seems to be uncommon as only two of the eleven species described here, *L. serpentigerum* and *L. barnsleyense*, have such ornamentation.

Stomata vary from species to species in distribution, size, and depth of stomatal pit, for example the more frequent but smaller stomata (200 per mm.^{2} and 30 $\mu \times 18$ μ) of *L. mannabachense* distinguish it from *L. rhodianum* (48 per mm.^{2} and 77 $\mu \times 45$ μ). Here, as with epidermal cells, the whole cushion should be examined to detect any variation, as *L. peachii* and *L. barnsleyense* only have stomata on the cushion surface below the leaf scars and *L. dichotomum*, which has many stomata (450 per mm.^{2}) below the scars, has almost none above them.

Stomatal distribution is of further interest when comparing species with separated leaf cushions. The areas between such cushions in *L. aculeatum* have regions possessing stomata interspersed among the epidermis with no stomata, while in *L. serpentigerum* the whole area between the cushions is devoid of stomata. This suggests that only part of the intercushion area in *L. aculeatum* may be of secondary origin, but that all of it in *L. serpentigerum* is the result of secondary lateral growth.

Stomatal pit depth is sometimes of use in species distinction. Within the species described here is a range between the superficial guard cells in *L. subdichotomum* and the 23 μ deep stomatal pits in *L. rhodianum*. Thus *L. subdichotomum* can be further distinguished from *L. mannabachense* and *L. dichotomum*, which both have 6 μ deep pits, and *L. mannabachense* from *L. rhodianum* and *L. aculeatum*, which respectively have pits 23 μ and 15 μ deep.

Specimens are often found which have no preserved cuticle, but the possibility of obtaining details of the epidermis need not be disregarded as direct observation often reveals information. The cushion areas which possessed elongated cells often appear striated while the areas which possessed isodiametric cells conversely are not striated. Thus it can be inferred that fine striations on a cushion surface indicate the presence or former presence of elongated cells even though epidermal details may be unobtainable.

The cuticle is clearly an aid to the understanding and the classification of *Lepidodendron*, but epidermal studies should be used, as in other plant groups, in conjunction with

gross morphological characters. An attempt has been made to detect variation within the species but this is difficult and sometimes impossible due to a lack of suitable specimens. What is needed is an examination of as many specimens as possible of individual species with the ultimate aim of finding any epidermal variations possibly correlated with relative positioning on the plant as a whole. The epidermis may therefore provide a means of identifying the smallest shoots with the largest branches, a task which is otherwise usually impossible. Similarly, work on suitable specimens might enable a comparison of leaves to be made, although large cushions possessing attached leaves are very scarce. The present work therefore illustrates the value of such epidermal studies but it does not answer all the questions. It shows what can be done with cuticles and the sort of studies which should be made.

REFERENCES

ARBER, E. A. N. 1903. Notes on fossil plants from the Ardwick Series of Manchester. *Mem. Proc. Manchr lit. phil. Soc.* **48**, 1–32.

—— 1914. On the fossil floras of the Wyre Forest, with special reference to the geology of the coalfield and its relationships to the neighbouring Coal Measure areas. *Phil. Trans. R. Soc. Ser. B*, **204**, 365–445.

—— 1922. Critical studies of Coal-Measure plant impressions. *J. Linn. Soc.* **46**, 171–217.

BELL, W. A. 1944. Carboniferous rocks and fossil floras of Northern Nova Scotia. *Mem. geol. Surv. Can.* **238**, 276 pp.

BRONGNIART, A. 1828*a*. *Prodrome d'une histoire des végétaux fossiles*. Paris. 233 pp.

—— 1828–38. *Histoire des végétaux fossiles, ou recherches botaniques et géologiques sur les végétaux fossiles renfermés dans les diverses couches du globe*, pt. I, 488 pp., 166 pls.; pt. II, 72 pp., 30 pl.

BUREAU, E. M. 1913–14. *Bassin de la Basse Loire. II Description des flores fossiles*. Paris. Text 1914; Atlas 1913.

CHALONER, W. G. 1967. In BOUREAU, E. *Traité de Paléobotanique*. II. Paris. 845 pp.

CROOKALL, R. 1925. On the fossil flora of the Bristol and Somerset Coalfield. *Geol. Mag.* **62**, 145–80.

—— 1929. *Coal Measure plants*. London. 77 pp.

—— 1939. The plant 'break' in the Carboniferous rocks of Great Britain. *Bull. geol. Surv. G.B.* **1**, 13–24.

—— 1964. Fossil plants of the Carboniferous rocks of Great Britain. *Mem. Geol. Surv. G.B. Palaeontology*, IV, pt. 3, 217–354.

—— 1966. Ibid. pt. 4, 355–571.

EDWARDS, W. N. 1952. *Lycopodiopsis*, a southern hemisphere Lepidophyte. *The Palaeobotanist*, **1**, 159–64.

EGGERT, D. A. 1961. Ontogeny of Carboniferous Arborescent Lycopsida. *Palaeontographica*, **B108** 43–92.

FAIRCHILD, H. L. 1877. On the structure of *Lepidodendron* and *Sigillaria*. 2. The variation of the leaf scars of *Lepidodendron aculeatum* Sternberg. *Ann. N.Y. Acad. Sci.* **1**, 77–91.

FEISTMANTEL, O. 1875. Die Versteinerungen der Böhmischen Kohlenablagerungen. *Palaeontographica*, **23**, 175–236.

FISCHER, F. 1904. Zur Nomenclatur von *Lepidodendron* und zur Artkritik dieser Gattung. *Abh. k. preuß. geol. Landesanst.* **39**, 80 pp.

—— 1906. *In* POTONIÉ, H. Abbildungen und Beschreibungen fossiler Pflanzenreste der Paläozoischen und Mesozoischen Formationen. Lief. IV. *Abh. k. preuß. geol. Landesanst.*

GEINITZ, H. B. 1855. *Die Versteinerungen der Steinkohlenformation in Sachsen*. Leipzig. 61 pp.

GRAHAM, R. 1935. An anatomical study of the leaves of the Carboniferous Arborescent Lycopods. *Ann. Bot.* **49**, 587–608.

HIRMER, M. 1927. *Handbuch der Paläobotanik*. Munich and Berlin. 708 pp.

HOFMANN, A. and RYBA, F. 1899. *Leitpflanzen der palăozoischen Steinkohlenablagerungen in Mittel-Europa*. Prague. 104 pp.

JONGMANS, W. J. 1929. *Fossilium Catalogus* II, Plantae. Pars 15, Lycopodiales II, 53–525. Berlin.

KIDSTON, R. 1885*a*. On some new or little known Fossil Lycopods from the Carboniferous Formation. *Ann. Mag. Nat. Hist.* (5), **15,** 357–65.

—— 1885*b*. Ibid. *Proc. Roy. Phys. Soc. Edin.* **8,** 415–24.

—— 1886. *Catalogue of the Palaeozoic Plants in the Department of Geology and Palaeontology, British Museum (Natural History)*. London. 288 pp.

—— 1894. On the various Divisions of the Carboniferous Rocks as determined by their Fossil Flora. *Proc. Roy. Phys. Soc. Edin.* **12,** 183–257.

—— 1902. Flora of the Carboniferous Period. *Proc. Yorks. Geol. & Polytech. Soc.* **14,** 334–70.

—— 1926. *In* Central Coalfield of Scotland (Area V). *Mem. Geol. Surv. Scot.* 145–7.

KOENIG, C. 1825. *Icones fossilium sectiles*. London. 1 (1825), 4 pp., pl. 1–4; 2 (undated), pl. 9–19.

LACEY, W. S. 1962. Welsh Lower Carboniferous plants. I, The flora of the Lower Brown Limestone in the Vale of Clwyd, North Wales. *Palaeontographica*, **B111,** 126–60.

LESQUEREUX, L. 1879–80. Description of the coal flora of the carboniferous formation in Pennsylvania and throughout the United States. *Geol. Surv. Penn. Rept. Progress, P.* Text (1879), 1, 1–354; 2, 355–694. Atlas (1880), 85 pl.

NĚMEJC, F. 1934. Critical remarks on Sternberg's *Lepidodeudron dichotomum. Bull. int. Acad. tchéque Sci.* 35 ann., 75–79.

—— 1947. The Lepidodendraceae of the coal districts of central Bohemia (a preliminary study). *Acta Musei Nationalis Prague*, **3B,** 2, 45–87.

—— 1946. Further critical remarks on Sternberg's *Lepidodeudron dichotomum* and its relations to the cones of *Sporangiostrobus* Bode. *Bull. int. Acad. tchéque Sci.* 47 ann. (1946), 35–43.

POTONIÉ, H. 1899. *Lehrbuch der Pflanzenpalaeontologie*. Berlin. 402 pp.

REMY, W. and REMY, R. 1959. *Pflanzenfossilien*. Berlin. 285 pp.

RENIER, A. 1904. *Documents pour l'étude de Paléontologie du terrain houiller*. Liège. 26 pp.

RHODE, J. G. 1820. *Beiträge zur Pflanzenkunde der Vorwelt*. Breslau. 40 pp.

STERNBERG, C. VON. 1820–38. *Versuch einer geognotisch-botanischen Darstellung der Flora der Vorwelt*. Leipzig and Prague. pt. 1 (1820) 24 pp.; pt. 2 (1821) 33 pp.; pt. 3 (1823) 39 pp.; pt. 4 (1825) 42 pp.; pt. 5 and 6 (1833) 80 pp.; pt. 7 and 8 (1838) 291 pp.

STERZEL, J. T. 1901. *Erlauterungen zur geologischen Spezialkarte des Königreichs Sachsen*. Section Zwickau Werdau Blatt III.

STUR, D. R. J. 1877. Beiträge zur Kenntiss der Flora der Vorwelt. I, Culm-Flora. Heft 2, Die Culm-Flora der Ostrauer und Waldenburger Schichten. *Abhandl. k. k. geol. Reichanst.* Vienna, **8,** 1–366.

THOMAS, B. A. 1966. The cuticle of the Lepidodendroid stem. *New Phytol.* **65,** 296–303.

ZALESSKY, M. D. 1904. Végétaux fossiles du terrain carbonifère du Bassin du Donetz. I, Lycopodiales. *Trudy geol. Kom.* N.S. **13,** 126 pp.

ZEILLER, R. 1886–8. Bassin houiller de Valenciennes. Description de la flore fossile. Text 1888, Atlas 1886. *Étude des gîtes minéraux de France*. Paris. 731 pp.

B. A. THOMAS
Biology Department
University of London Goldsmiths' College
London, S.E. 4

Revised typescript received 3 June 1969

THE PALAEONTOLOGICAL ASSOCIATION

PALAEONTOLOGY

The journal *Palaeontology* is devoted to the publication of papers (preferably illustrated) on all aspects of palaeontology and stratigraphical palaeontology. Four parts at least are published each year and are sent free to all members of the Association. Members who join for 1970 will receive Volume 13, Parts 1 to 4.

All back numbers are still in print and may be ordered from B. H. Blackwell, Broad Street, Oxford, England, at £3 per part (post free). A complete set, Volumes 1–12, consists of 47 parts and costs £141.

SPECIAL PAPERS IN PALAEONTOLOGY

This is a series of substantial separate works published by the Association. The subscription rate is £6 (U.S. $16.00) for Institute Members and £3 (U.S. $8.00) for Ordinary and Student Members. Subscriptions and orders by members of the Association should be placed through the Membership Treasurer, Dr. A. J. Lloyd, Department of Geology, University College, Gower Street, London, W.C.1, England.

The following *Special Papers* are available. Members may obtain them at reduced rates through the Membership Treasurer. Non-members may obtain them from B. H. Blackwell, Broad Street, Oxford, England, at the prices indicated.

Special Paper No. 1 (for 1967): MIOSPORES IN THE COAL SEAMS OF THE CARBONIFEROUS OF GREAT BRITAIN, by A. H. V. Smith and M. A. Butterworth. 324 pp., 72 text-figs., 27 plates. Price £8 (U.S. $22.00), post free.

Special Paper No. 2 (for 1968): EVOLUTION OF THE SHELL STRUCTURE OF ARTICULATE BRACHIOPODS, by Alwyn Williams. 55 pp., 27 text-figs., 24 plates Price £5 (U.S. $13.00).

Special Paper No. 3 (for 1968): UPPER MAESTRICHTIAN RADIOLARIA OF CALIFORNIA, by Helen P. Foreman. 82 pp., 8 plates. Price £3 (U.S. $8.00).

Special Paper No. 4 (for 1969): LOWER TURONIAN AMMONITES FROM ISRAEL, by R. Freund and M. Raab. 83 pp., 15 text-figs., 10 plates. Price £3 (U.S. $8.00).

Special Paper No. 5 (for 1969): CHITINOZOA FROM THE ORDOVICIAN VIOLA AND FERNVALE LIMESTONES OF THE ARBUCKLE MOUNTAINS, OKLAHOMA, by W. A. M. Jenkins. 44 pp., 10 text-figs., 9 plates. Price £2 (U.S. $5.00).

Special Paper No. 6 (for 1969): AMMONOIDEA FROM THE MATA SERIES (SANTONIAN–MAASTRICHTIAN) OF NEW ZEALAND, by R. A. Henderson. 82 pp., 13 text-figs., 15 plates. Price £3 (U.S. $8.00).

SUBMISSION OF PAPERS

Typescripts on all aspects of palaeontology and stratigraphical palaeontology are invited. They should conform in style to those already published in this journal, and should be sent to Mr. N. F. Hughes, Department of Geology, Sedgwick Museum, Downing Street, Cambridge, England, who will supply detailed instructions for authors on request (these are published in *Palaeontology*, **10**, pp. 707–12). Fifty free offprints are provided to authors.

PALAEONTOLOGY

VOLUME 13 · PART 1

CONTENTS

PRINTED IN GREAT BRITAIN AT THE UNIVERSITY PRESS, OXFORD
BY VIVIAN RIDLER, PRINTER TO THE UNIVERSITY

VOLUME 13 · PART 2

Palaeontology

AUGUST 1970

PUBLISHED BY THE
PALAEONTOLOGICAL ASSOCIATION
LONDON

Price £3

THE PALAEONTOLOGICAL ASSOCIATION

The Association was founded in 1957 to further the study of palaeontology. It holds meetings and demonstrations, and publishes the quarterly journal *Palaeontology*. Membership is open to individuals, institutions, libraries, etc., on payment of the appropriate annual subscription:

Institute membership	£7. 0*s*. (U.S. $20.00)
Ordinary membership	£5. 0*s*. (U.S. $13.00)
Student membership	£3. 0*s*. (U.S. $8.00)

There is no admission fee. Institute membership is only available by direct application, not through agents. Student members are persons receiving full-time instruction at educational institutions recognized by the Council; on first applying for membership, they should obtain an application form from the Membership Treasurer. All subscriptions are due each January, and should be sent to the Membership Treasurer, Dr. A. J. Lloyd, Department of Geology, University College, Gower Street, London, W.C. 1, England.

MORPHOLOGIC VARIABILITY OF THE GENUS *SCHWAGERINA* IN THE LOWER PERMIAN WREFORD LIMESTONE OF KANSAS

by G. A. SANDERSON *and* G. J. VERVILLE

ABSTRACT. Fusulinids referable to the genus *Schwagerina* occur in the basal part of the Threemile Limestone Member of the Permian Wreford Formation in Chase County, Kansas. Three hundred specimens from six collecting localities in four townships in Chase County were used in this study. The restricted stratigraphic range and limited geographic distribution of the fusulinid fauna within the intracratonic, cyclical succession tend to minimize the effects of diachronism, and it is presumed that the collections are approximately contemporaneous.

Considerable morphologic variability is evident within the Threemile fusulinid fauna, and affinities with several previously described species of *Schwagerina* can be demonstrated. Studies of measurable morphologic parameters suggest that all the Wreford schwagerinids sampled are referable to a single population, and thus the validity of several established taxa is open to challenge.

THE Permian Wreford Limestone Formation is a cyclical, intracratonic marine unit which is exposed in Kansas along a generally north–south trending outcrop belt (text-fig. 1). Fusulinids referable to the genus *Schwagerina* have been found in the Wreford only in Chase County. The specimens used in this study are from six outcrop localities in four townships within Chase County (text-fig. 1).

Stratigraphically, the Wreford defines the base of the Wolfcampian Chase Group. It is overlain by the Matfield Shale and underlain by the Speiser Shale. The Wreford has three members, which are, in ascending order, the Threemile Limestone, the Havensville Shale, and the Schroyer Limestone (text-fig. 2). In Chase County, the thickness of the Wreford averages approximately 12 m. (Moore *et al.* 1951).

Fusulinids occur abundantly in the Wreford in central Chase County but only in the Threemile Member and only in the lowermost 3–5 cm. of that unit (Hattin 1957). The lower Threemile Member is persistently a grey, porous, cherty limestone in the area of our collections. There are no obvious indications of lithofacies differences among the collections, and we are assuming that a generally similar environment is represented throughout our samples. The geological setting suggests also that the effects of diachronism are minimal. These close stratigraphic, geographic, ecologic and temporal limits which we are able to place upon the Wreford fauna make it particularly well suited to a study of morphologic variability and population distribution.

MORPHOLOGY

The Wreford fusulinids exhibit considerable morphologic diversity. Among the specimens illustrated on Plate 35, shape is the most apparent variable (figs. 1, 3, 8, and 11), but closer examination of the fauna shows differences also in other morphologic characters, such as prolocular diameter, wall thickness, tunnel width, and nature of

[Palaeontology, Vol. 13, Part 2, 1970, pp. 175–83, pl. 35, 36.]

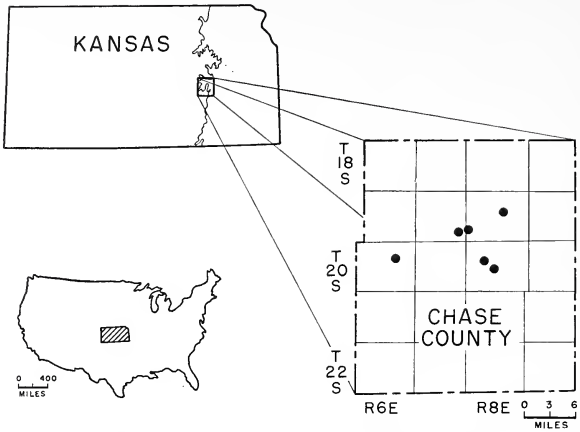

TEXT-FIG. 1. Index map of Wreford collecting localities.

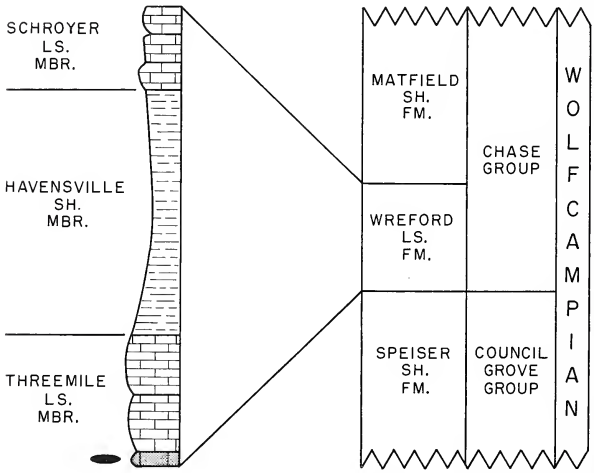

TEXT-FIG. 2. Stratigraphic chart showing position of fusulinids.

septal folding. Any attempt to evaluate the significance of these differences leads inevitably to consideration of some rather basic questions, such as:

1. How many taxa (populations) are present?
2. How may they be distinguished?
3. What is their geographic distribution?

In an effort to find answers to these questions, a representative sampling was made consisting of 50 randomly selected specimens from each of the 6 collections. Equal numbers of oriented axial and sagittal thin sections were prepared, giving a total of 300 individuals used in this study. This extensive sampling, while statistically adequate and systematically desirable, proved to be disturbing to the traditional method of taxonomic differentiation by visual examination. As might be expected, the morphologic complexity produced by the interaction of multiple variables tends to inhibit consistent differentiation by visual inspection alone.

Only a few specimens of the total Wreford fauna are illustrated on Plate 35, but even here the gradational nature of the morphologic parameters, such as form ratio, for example, is quite evident, and the distinctive individuals labelled as figs. 1, 3, 8, and 11 begin to blend into a morphologic spectrum. The difficulty of separating these forms consistently by visual means is increased progressively as the sample size is increased. Obviously, supplemental quantitative data are required to establish definable limits to the population or populations.

To this end, the following parameters were measured on the appropriate orientations of the 300 sampled specimens: prolocular diameter, length, diameter, radius vector, septal count, volution height, prothecal thickness, half length, and tunnel width. Although they do not quantify every morphologic dimension, these parameters represent the bulk of those commonly employed by fusulinid workers. In all, nearly 24 000 bits of raw quantitative data were accumulated, which subsequently have been manipulated and subjected to statistical treatment.

QUANTITATIVE ASPECTS

The quantitative aspects of the Wreford fusulinid fauna were investigated in a threefold manner: first, by considering the variability of specific parameters within the sampled specimens; second, by examining ontogenetic changes within the population or populations; and, third, by comparing all the individual specimens in the samples with one another statistically. We considered that one or more of these approaches should reveal the existence of a quantitative basis for taxonomic subdivision of the fusulinid fauna.

Parameter variability

Results of the first approach are illustrated in the frequency distribution histograms of several parameters (text-figs. 3–6). Text-fig. 3 shows the number of individuals in each size class of prolocular diameter; on the left are plots for each of the 6 collecting localities, using a common scale on the X-axis and stacked for purposes of comparison. All the histograms suggest a gradation of dimension through a fairly narrow range with a strong clustering tendency about the means, which are virtually identical in all samples. The data in each sample have a high degree of statistical correlation. On the right side

of the same figure is a composite plot of all the data on the left; measurements from all 300 fusulinid specimens are included. In this larger sampling, the distribution is naturally smoother with accentuation of the clustering tendency, but the essential characteristics are similar to those of the separate localities. It closely approaches a continuous, symmetrical distribution about a mean with no indication of bimodality. There would appear to be no reason for any taxonomic separation on the basis of this parameter.

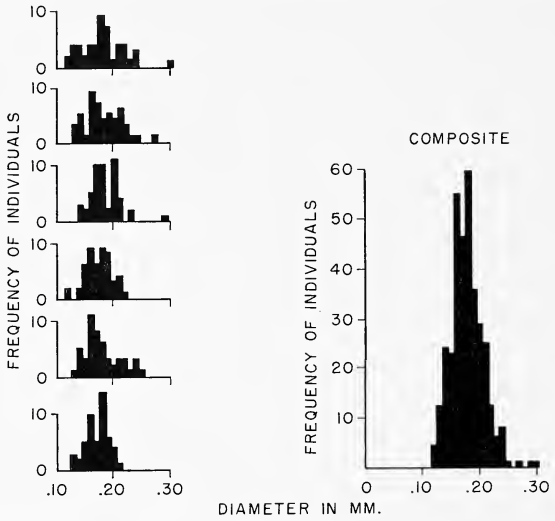

TEXT-FIG. 3. Frequency distribution histograms of prolocular diameter, composite and for individual localities.

A frequency distribution plot of septal count by volution produces similar histograms (text-fig. 4). The same bell-shaped distribution may be observed in all volutions, although the shape changes ontogenetically from more leptokurtic to more platykurtic. Representative distributions are shown for septal counts of all specimens in the second and sixth volutions. These counts are made from sagittal sections only, and the total specimen count is 150. The flattening of the distribution is progressive with growth and suggests a greater range of dimensional variability in the adult test than in the juvenile. None the less the variation seems to be essentially continuous among all the measurements for any given volution.

EXPLANATION OF PLATE 35

Morphologic gradation of Wreford schwagerinid fauna, ×8. Figs. 1–11 are specimens 226, 31, 328, 57, 209, 306, 144, 37, 43, 153, and 287, respectively.

1

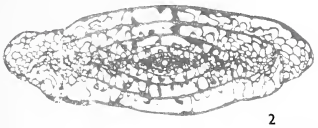

2

3

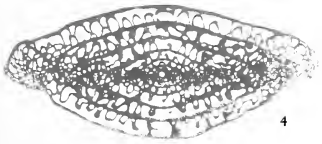

4

5

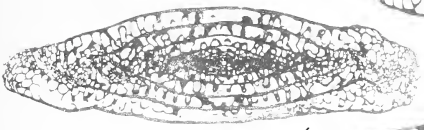

6

7

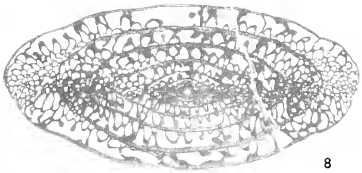

8

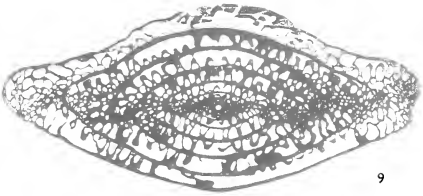

9

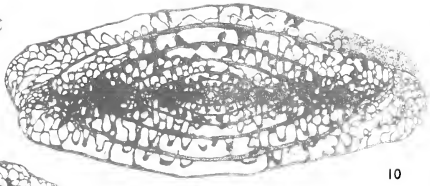

10

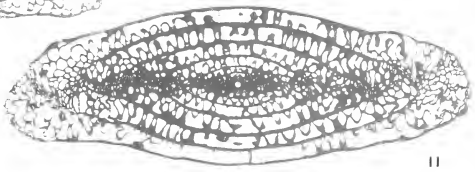

11

SANDERSON and VERVILLE, Morphologic variability of *Schwagerina*

It should be noted that these graphic illustrations were plotted from raw measurements made on a volution-by-volution basis before adjustment for position on the growth spiral. The adjusted data have an even smoother frequency distribution. A

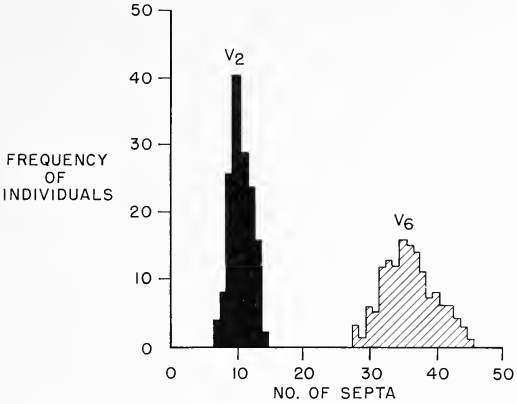

TEXT-FIG. 4. Frequency distribution histograms of septal count for volutions 2 and 6.

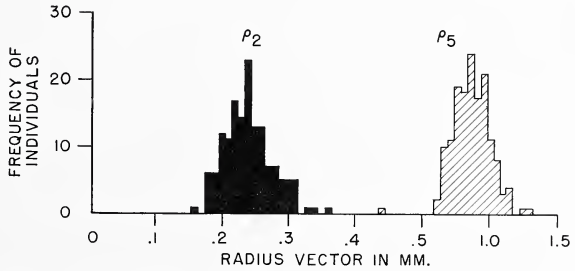

TEXT-FIG. 5. Frequency distribution histograms of radius vector (ρ) for volutions 2 and 5.

statistical evaluation of interpolated values at equal diameters made by Dr. J. L. Cutbill (personal communication) of Cambridge University showed virtually all the distributions to be statistically normal.

An analogous situation may be seen in the radius vector (ρ) distribution. Text-fig. 5 illustrates the values for volutions 2 and 5. Again the frequency histograms are essentially symmetrical and closely clustered about the mean with a tendency toward progressive flattening in outer volutions. In the case illustrated, the flattening is somewhat masked

by the scale change necessitated by size limitations of the graph. The dimensional variability is essentially continuous, and normality of distribution can be demonstrated. Similar plots of other parameters (e.g. text-fig. 6) give the same results; none has yet produced any clear indication of a quantitative basis for taxonomic separation.

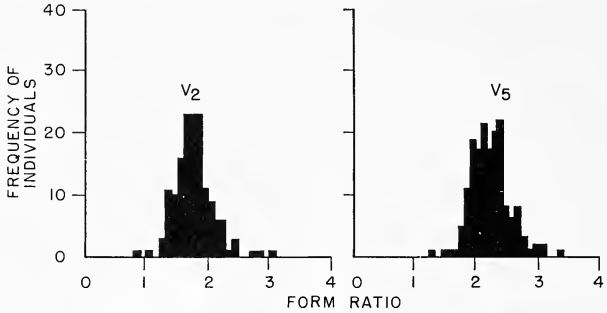

TEXT-FIG. 6. Frequency distribution histograms of form ratio for volutions 2 and 5.

Ontogenetic changes

Text-fig. 7 is a plot of increase in septal count with growth. Maximum, minimum, and mean values per volution are given for the entire sampling. With the exception of volution 1, which contains the prolocular aperture and is unique, the septal count in all other volutions increases arithmetically, resulting in the linear relationship shown. Again, there seems to be no compelling reason to attempt taxonomic subdivision of the Wreford fusulinid fauna on the basis of this parameter.

The ontogenetic increase in radius vector is illustrated in text-fig. 8 with the maximum, minimum, and mean values per volution given for all the Wreford specimens. In contrast to the septal count, the growth curve is exponential, but there is still no suggestion that more than one population is present in our samples.

Comparable results appear in other data plots, and the point need not be laboured. All other measured parameters which have not been illustrated correlate closely with those shown or exhibit similar relationships.

Statistical analyses

Various types of multivariate analysis have been used since the study of the Wreford fauna began, and, in fact, the statistical study is continuing as more sophisticated computer hardware and software become available. Our initial studies utilized raw data consisting of measurements made at single volution (e.g. 360°) increments. The volution approach does not, of course, take into account the variability in diameter of the initial chamber and, therefore, comparisons of growth characteristics are only approximate. Although other methods of adjustment have been investigated, the Cutbill data standardization method (unpublished manuscript) of relating measurements to standard reference diameters has been used in most subsequent computer applications.

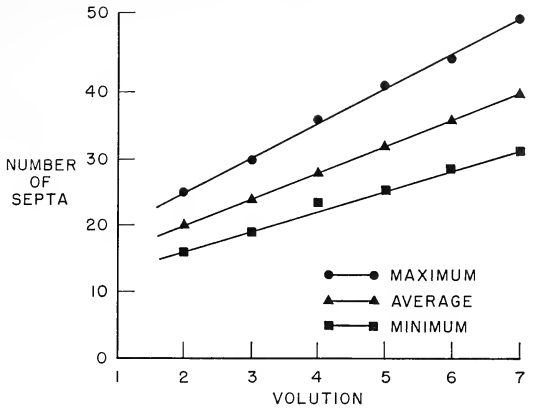

TEXT-FIG. 7. Plot of maximum, minimum, and mean septal counts per volution for the total Wreford population.

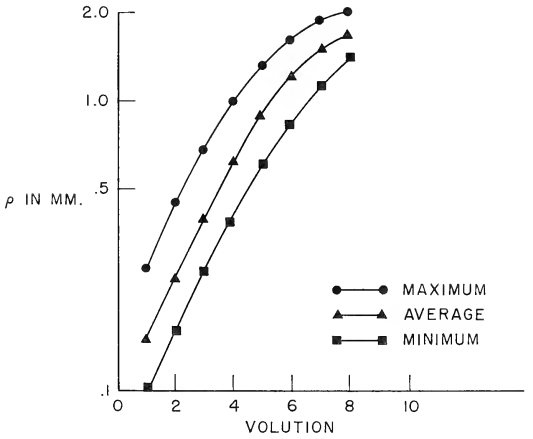

TEXT-FIG. 8. Plot of maximum, minimum, and mean radius vectors per volution for the total Wreford population.

Multivariate analyses run on both the raw data and the adjusted data include R-mode factor analysis, Q-mode factor analysis, and discriminant function analysis. Results of the tests run to date support the premise that the Wreford fusulinids probably belong to a single continuously variable population.

FAUNAL COMPARISONS

Since we have been unable to make taxonomic subdivision of the Wreford fusulinid fauna on the basis of either qualitative or quantitative criteria, our original questions seem to be answered adequately by the simple recognition of a single fusulinid population distributed essentially uniformly throughout our collections. This certainly is not a startling conclusion in view of the geologic evidence, but a disturbing ramification presents itself in the comparisons made on Plate 36, using 6 fusulinid pairs. One member of each pair is a published species, in some cases the holotype, of an age roughly comparable to that of the Wreford; the other is a selected member of the Wreford population from somewhere within the morphologic spectrum. A close degree of similarity is obvious. Perhaps these specimens are not all conspecific, but differentiation certainly would involve extremely subtle differences—of an order well within the range of variability of a single population such as that of the Wreford. Whether or not these particular specimens are conspecific is rather beside the point. What is important is that they are extremely difficult, if not impossible, to differentiate by conventional means—that is, visually or on the basis of limited measurements. In short, there is a reasonable doubt as to their validity, which in turn suggests the need for a reappraisal of commonly accepted taxonomic practices, for there is abundant evidence to indicate that similar studies could be conducted on the majority of published fusulinid faunas with comparable results. Needless to say, our criticism is directed at the present 'state of the art' and not personally at its practitioners among whom we include ourselves.

Unfortunately, there is no easy solution to the problem. Speciation among fusulinid workers is a highly subjective process unfettered by procedural standards or guidelines. Such standards are urgently needed, but it would be naïve, indeed, to assume that they will be forthcoming soon. Nevertheless it should be encumbent upon authors of new taxa to define them in such a manner that they are unequivocally distinguishable. In our view this includes extensive sampling, adequate illustration, and detailed quantitative treatment of the morphologic variability spectrum of the taxon. Cutbill and Forbes (1967) suggest possible procedures for routine taxonomic work which can be used to advantage. Whether graphic representations are used or not, the minimum sampling of twenty specimens suggested by Cutbill and Forbes should be practised whenever possible. A larger sampling would be even better.

Multivariate analysis will undoubtedly play a significant role in population studies in the future, particularly in view of increasing computer availability. Discriminant function analysis can aid in the recognition of morphologic groupings (Harbaugh and

EXPLANATION OF PLATE 36

Faunal comparison, ×8. Figs. 1*a*–6*a* are specimens 309, 49, 226, 55, 54, and 43, respectively, of the Wreford schwagerinid population. Figs. 1*b*–6*b* are *Schwagerina vervillei* Thompson 1954, *S. colemani* Thompson 1954, *S. emaciata* (Beede) 1916, *S. campensis* Thompson 1954, *S. andresensis* Thompson 1954, and *S. complexa* Thompson 1954, respectively.

1a

1b

2a

2b

3a

3b

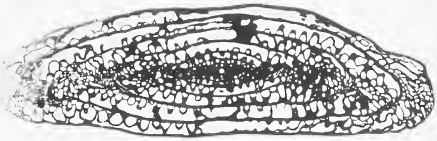

4a

4b

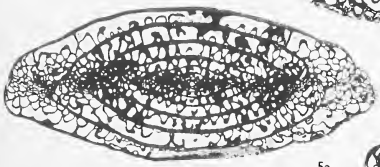

5a

5b

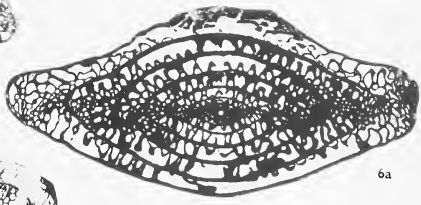

6a

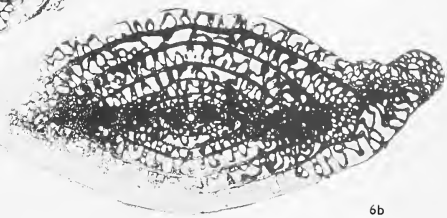

6b

SANDERSON and VERVILLE, Morphologic variability of *Schwagerina*

Merriam 1968). Factor analysis in the Q-mode and R-mode is applicable to fusulinid studies involving populations of individuals or variable morphologic parameters (Harbaugh and Merriam 1968, Merriam 1966). In fact, study of the spatial and temporal variability of particular morphologic parameters may well turn out to be of greater significance geologically than the characterization of the individual as an aggregate of many variables. In any case, the delimiting of morphologic variability is inherent in realistic taxonomy.

CONCLUSIONS

All available evidence indicates that the Wreford fusulinids studied apparently belong to a single morphologic population distributed more or less uniformly through all six collecting localities. Close similarity is demonstrable between several existing species of *Schwagerina* and specimens within the Wreford population, and it is doubtful whether all of the former represent valid species. Current taxonomic practices are in need of review, and a shift of emphasis from the typological concept to a population-oriented approach seems to be in order. Realistic and objective delineation of species requires consideration of the whole spectrum of morphologic variability, and the erection of any new taxon should entail sufficient quantitative data for adequate characterization.

Acknowledgements. We are particularly grateful to Dr. J. L. Cutbill who made the first statistical test of our data with his data standardization routine and who has also permitted us access to unpublished manuscript material. His counsel and encouragement are appreciated. Pan American Petroleum Corporation provided computer and other facilities utilized in this study and granted permission for publication. Among the Pan American colleagues who have aided materially this study, we wish to acknowledge the efforts of Messrs. L. V. Brown, N. Di Vittorio, and K. Wignall in statistical aspects of the project. We also wish to thank Dr. Alan B. Shaw with whom several fruitful discussions were held.

Repository. All specimens are filed by specimen number under Localities 2795–2800 inclusive at the Research Center of the Pan American Petroleum Corporation (address below).

REFERENCES

CUTBILL, J. L., and FORBES, C. L. 1967. Graphical aids for the description and analysis of variation in fusuline foraminifera. *Palaeontology*, **10**, 322–37.

HARBAUGH, J. W., and MERRIAM, D. F. 1968. *Computer applications in stratigraphic analysis*. 282 pp. John Wiley & Sons, Inc., New York, London, Sidney.

HATTIN, D. E. 1957. Depositional environment of the Wreford megacyclothem (Lower Permian) of Kansas. *Bull. Kans. geol. Surv.* **124**, 150 pp., 22 pl.

IMBRIE, J. 1956. Biometrical methods in the study of invertebrate fossils. *Bull. Am. Mus. Nat. Hist.* **108**, 215–52.

MERRIAM, D. F. (Ed.). 1966. Computer applications in the earth sciences: Colloquium on classification procedures. *Kans. geol. Surv. Computer Contrib.* **7**, 79 pp.

MOORE, R. C., JEWETT, J. M., and O'CONNOR, H. G. 1951. Geology, mineral resources, and ground-water resources of Chase County, Kansas; Pt. 1, Rock formations of Chase County. *Kans. geol. Surv.* **11**, 5–16, pl. 1.

THOMPSON, M. L. 1954. American Wolfcampian Fusulinids. *Paleont. Contr. Univ. Kans.* **5**, 226 pp., 52 pls.

G. A. SANDERSON
G. J. VERVILLE
Pan American Petroleum Corporation
Research Center
4502 East 41st Street
P.O. Box 591
Tulsa, Oklahoma–74102, U.S.A.

Typescript received 11 April 1969

SURFACE TEXTURES OF CALCAREOUS FORAMINIFERIDS

by J. W. MURRAY *and* C. A. WRIGHT

ABSTRACT. A comparison is made between the surface appearance of fresh calcareous foraminiferid tests, those etched artificially, and those found in fossil representatives from the Hampshire Basin. It is concluded that most fossil foraminiferids show some post-mortem etching of the test surface.

THE texture of the wall surface and the relative size of the pores have been used as specific characters in taxonomic studies of foraminiferids based on examination under the light microscope. Recent descriptions of the ultrastructure of the calcareous foraminiferid wall (Hay, Towe, and Wright 1963, Lynts and Pfister 1967, Towe and Cifelli 1967) have been illustrated by excellent electron photomicrographs of surface and internal features. With the introduction of the scanning electron microscope to the study of foraminiferids much more information on textures and structures will become available.

The preparation of material for examination in the two types of electron microscope is quite different. For the transmission electron microscope the material is replicated, usually with carbon, and it is the replica which is examined. The scanning electron microscope can be used to examine specimens directly, providing they have a conducting layer on the surface. Foraminiferids are usually coated with a gold–palladium mixture but other metals such as gold or aluminium have also been used with success. The disadvantage of the metallic coating is that it obscures detail finer than its own thickness. Hay and Sandberg (1967) state the resolution of the transmission microscope to be 5 Å and that of the scanning microscope to be 200 Å. However, this disadvantage is offset by the great depth of field of the scanning microscope.

Routine examination of Tertiary and Recent foraminiferids from the Hampshire Basin and Western Approaches at magnifications of $\times 20$ to $\times 6000$ has provided a large amount of information on the texture of foraminiferid walls. Magnifications of up to $\times 20\,000$ have been used where necessary. Altogether some 1200 photomicrographs have been taken to date.

When viewing a wall texture in detail it is important to establish whether the structures observed are primary or secondary. Two processes can lead to post-mortem changes in the surface texture: physical abrasion with sedimentary particles, and chemical etching of those walls which are calcareous. These processes may operate singly or together. The present discussion is concerned only with textures resulting from chemical etching.

A short note by Murray (1967) described how hyaline calcareous foraminiferids which appeared transparent when fresh could be made opaque by etching. In the examples described below, species of Recent foraminiferids have been studied in a fresh unetched condition and compared with forms which have been artificially etched in EDTA and with fossil forms which show comparable textures.

[Palaeontology, Vol. 13, Part 2, 1970, pp. 184–7, pl. 37–39.]

Examples

Protelphidium anglicum Murray (1965) has a radiate, perforate, calcite test wall. In living individuals the outer test surface is smooth and shows irregularly distributed circular pores about 1–1·5μ in diameter (Pl. 37, fig. 2). When such a specimen is etched for 2–3 minutes in 5% EDTA, the wall becomes white and opaque (Murray 1967). Under high magnification the pores are seen to have become polygonal and often they are located near the centre of a polygonal 'crystal' (Pl. 37, figs. 3–5). Occasionally the pore is eccentric or even peripheral to the 'crystal'. The 'crystals' have sutured contacts with one another and have an uneven etched surface. This may indicate that they are composed of bundles of fibres (R. Bradshaw, University of Bristol, pers. comm.). These may be analogous to the plate-like units observed in the radial wall of *Ammonia beccarii* (Linné) by Towe and Cifelli (1967).

The same type of etched surface has been seen in *Protelphidium* sp. from Oligocene rocks (Middle Headon Beds) of the Isle of Wight, England (Pl. 37, fig. 5).

Nummulites rectus Curry from the Lower Barton shows the same type of etched surface. Plate 38, figs. 1, 2 show these textures on the inside of the chamber wall in a broken form. The same polygonal 'crystals' can be seen with sutured contacts and a central pore. In the fossil forms, however, the 'crystal' is composed of radiating 'blocks', the number present depending on the stage to which the etching has exposed the divisions between them. Eight to ten 'blocks' are present surrounding the pore and each of these has a rough texture exhibiting the same bundle-of-fibre structure. Between the pores, 'bundles' of 'crystals' fill in the spaces, groups of 'bundles' being separated by sutured contacts.

In the umbilical region of modern examples of *Protelphidium anglicum* there are no pores in the wall. Etching does not reveal crystal boundaries although the previously smooth shell becomes pitted (Pl. 37, fig. 3).

Cibicides lobatulus (Walker and Jacob) also has a radiate calcite test wall. In fresh specimens the wall is smooth (Pl. 38, figs. 3, 4) but in specimens etched in 5% EDTA the wall becomes irregularly pitted. In this species the pores are relatively large (6–7μ in diameter) and it seems probable that the component calcite crystals of the wall surround each pore. Etching leads to pore enlargement.

The same etched surface texture has been seen in fossil forms of this species from the Upper Barton Beds of Hampshire. These forms also display large pores with complex layered internal structures separated by etched wall with irregular pitted texture best displayed in the apertural region where the pores are less abundant (Pl. 38, fig. 6).

The wall structure of *Ammonia beccarii* (Linné) was described in detail by Towe and Cifelli (1967). The greater part of the wall is made up of plate-like calcite units which are very much smaller than the wall pores. When the surface is etched, the pores are enlarged and the surface becomes uneven (Pl. 39, figs. 1, 2). Etching preferentially attacks the pores because of the large surface area of their walls.

In fossil forms of *Nonion laeve* (d'Orbigny), the effects of abrasion on the high points of the chambers can be seen. This abrasion aids the chemical etching of the test by destroying the original smooth surface. In this form (Pl. 38, fig. 7) the chamber is very severely etched to produce a rough and pitted texture compared with the smooth wall visible along the suture and on the sutural processes. The chamber wall immediately

adjacent to the suture is also smooth but the wall becomes pitted on the elevated part of the chamber.

Early stages in the etching process have been studied in fossil forms of *Melonis affine* (Reuss) which has a granular perforate calcite test wall and an open umbilicus. The wall is normally smooth and finely perforate but in some fossil forms this smooth wall is broken up by a series of interlocking cracks with a pore at the centre of each system. These cracks appear to be the first stages in the production of the sutured contacts between the 'crystals' (Pl. 39, figs. 3–5).

The common Recent miliolid *Quinqueloculina seminulum* (Linné) normally has an opaque white, imperforate test in which the surface has a porcelain-like glaze. The wall structure in general is described as 'porcellaneous'. Under a magnification of $\times 20\,000$, the 'tile-roof' pattern of calcite crystals forming the surface glaze may just be made out (see Hay, Towe, and Wright 1963 and Towe and Cifelli 1967; also the 'pavement-like pattern' of Lynts and Pfister 1967). When the wall is etched in 5% EDTA, the 'tile-roof' glaze can be readily seen and beneath it the very disorganized layers of calcite rods are revealed (Pl. 39, figs. 6, 7). The 'roof-tile' crystals average 2μ in length

---

EXPLANATION OF PLATE 37

Figs. 1–5. *Protelphidium anglicum* Murray; Recent, Christchurch Harbour, England. 1, Lateral view of specimen with attached turbellarian egg case; maximum diameter of specimen 533μ; $\times 105$. 2, Details of smooth wall with pores averaging $1–1{\cdot}5\mu$ in diameter; $\times 5600$. 3, Chamber wall etched in 5% EDTA showing 'crystals' with pores and an underlying layer; the umbilical region in the upper part of the photograph is only slightly pitted; $\times 2100$. 4, Strongly etched chamber wall (using 5% EDTA) showing layered structure, 'crystals' and pores; $\times 1950$. 5, Enlargement of fig. 4. Note sutured boundaries between 'crystals' and the polygonal pores; $\times 5900$.

Fig. 6. *Protelphidium* sp.; Middle Headon Beds (Oligocene), Headon Hill, Isle of Wight. Naturally etched wall showing many similarities with figs. 3, 4 and 5; $\times 1500$.

EXPLANATION OF PLATE 38

Figs. 1, 2. *Nummulites rectus* Curry; Lower Barton Beds, Becton Bunny, Hampshire. 1, View of inside of chamber wall to show etched 'crystals' composed of 'blocks', each 'crystal' being pierced by a pore (diameter $0{\cdot}5–1\mu$); $\times 2250$. 2, Enlargement of part of fig. 1; $\times 5550$.

Figs. 3–5. *Cibicides lobatulus* (Walker and Jacob); Recent, Western Approaches. 3, View of spiral side to show the coarsely perforate test; $\times 126$. 4, Smooth, unetched wall with pores (diameter $6–7\mu$); $\times 1050$. 5, Wall etched with 5% EDTA; $\times 2170$.

Fig. 6. *Cibicides lobatulus* (Walker and Jacob); Upper Barton Beds (Zone H), Barton Cliff, Hampshire. Natural etched wall; $\times 1650$.

Fig. 7. *Nonion laeve* (d'Orbigny); Lower Barton Beds, Becton Bunny, Hampshire. View of smooth unetched suture with adjacent chamber walls etched; $\times 2000$.

EXPLANATION OF PLATE 39

Figs. 1, 2. *Ammonia beccarii* (Linné), Recent, Western Approaches. 1, Dorsal view of complete test etched in 5% EDTA; note the pore enlargement; $\times 154$. 2, Details of pores enlarged by etching; $\times 1536$.

Figs. 3–5. *Melonis affine* (Reuss); Middle Barton Beds (Zone F), Barton Cliff, Hampshire. 3, General view; $\times 210$. 4, Incipient etching of the granular wall surface; $\times 1130$. 5, Enlargement of fig. 4; $\times 2325$.

Figs. 6, 7. *Quinqueloculina seminulum* (Linné); Recent, Western Approaches. 6, Wall etched in 5% EDTA to reveal the surface 'roof-tile' layer of rectangular crystals and the underlying layer of randomly oriented rods; $\times 4800$. 7, Details of the randomly oriented rods; $\times 9350$.

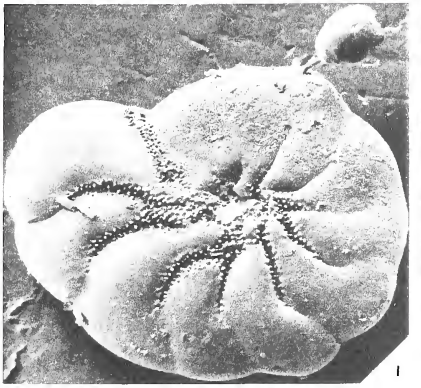

1

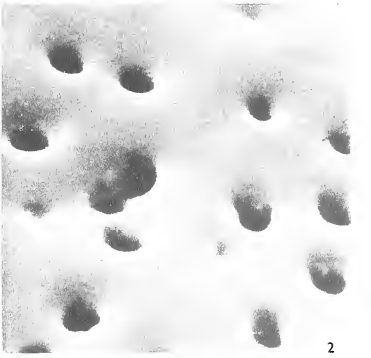

2

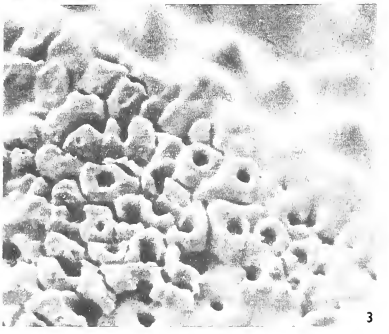

3

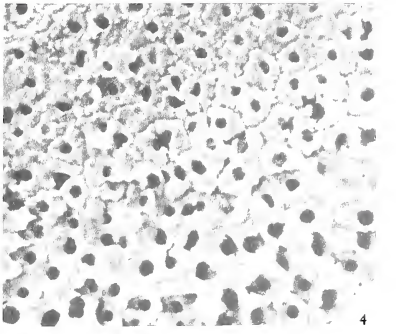

4

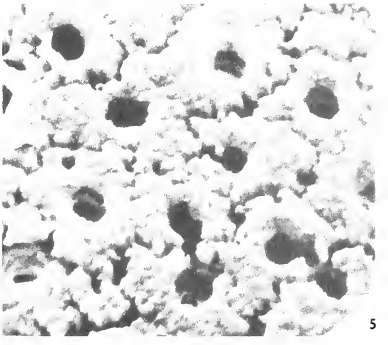

5

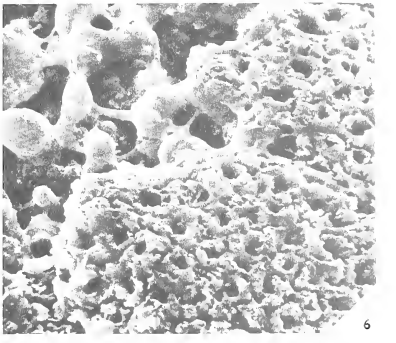

6

MURRAY and WRIGHT, Surface textures of calcareous foraminiferids

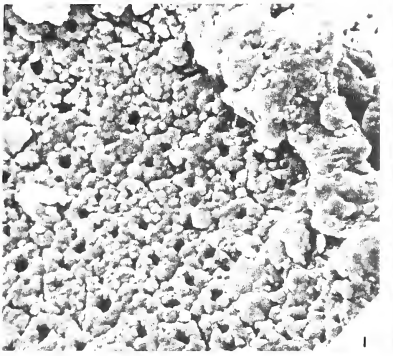
1

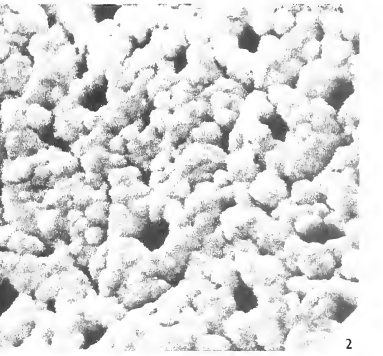
2

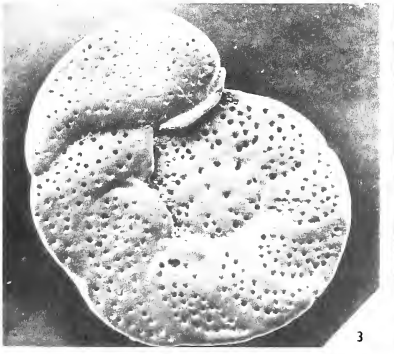
3

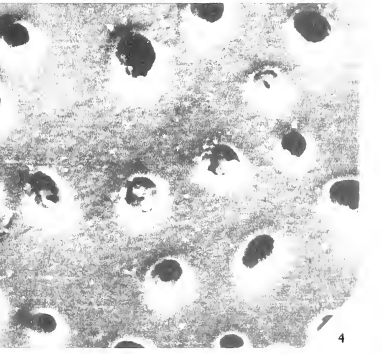
4

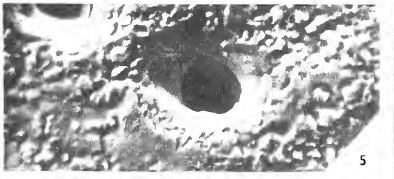
5

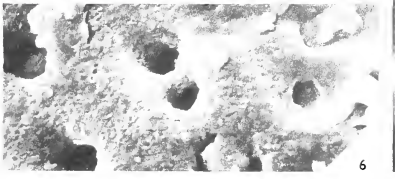
6

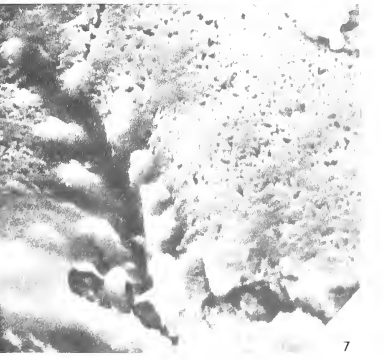
7

MURRAY and WRIGHT, Surface textures of calcareous foraminiferids

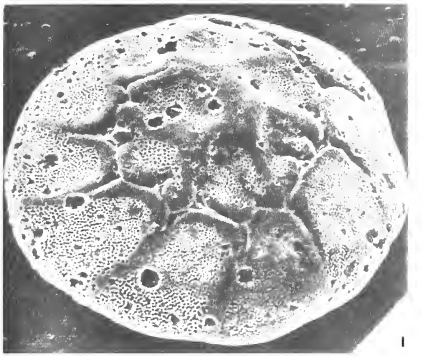

1

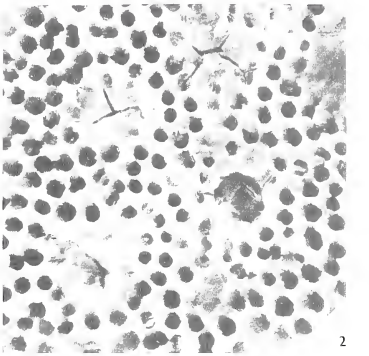

2

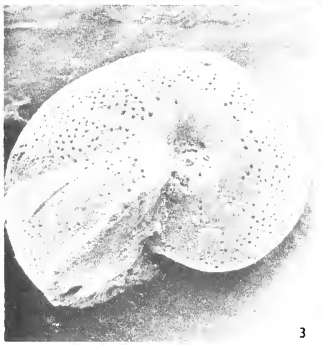

3

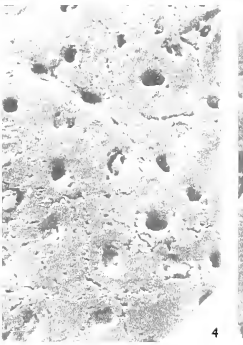

4

5

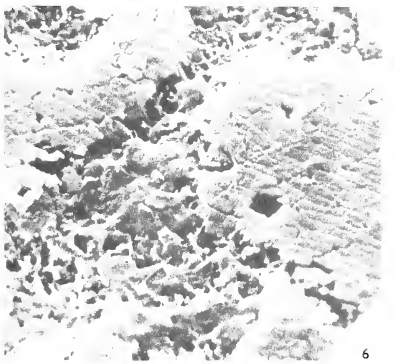

6

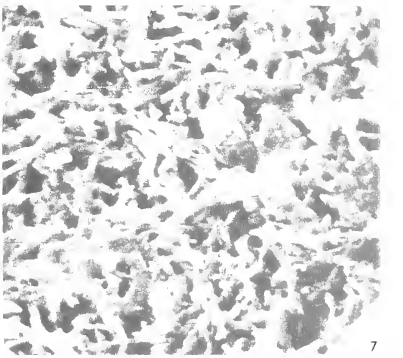

7

MURRAY and WRIGHT, Surface textures of calcareous foraminiferids

and 0·3μ in width, while the dimensions of the inner rods are 1·0 and 0·2μ respectively. Most fossil miliolids have lost their 'roof-tile' veneer.

It is probable that the specimens examined by Hay, Towe, and Wright (1963) had already been etched since they described them as 'dull and chalky' in appearance in comparison with the smooth tests of *Peneroplis planatus*. In our experience fresh miliolids have a glaze comparable with that of the peneroplids.

Conclusions

Calcareous tests are extensively altered even by short periods of etching. In hyaline types originally smooth perforate walls become rough; the platelets, or fibres within the 'crystals' become apparent, the 'crystal' boundaries are hollowed out and the pores become enlarged. When the pores have a diameter greater than that of the component 'crystals' of the wall, etching produces more pronounced pore enlargement than surface textural effects. In miliolids, the porcellaneous wall be may stripped of its veneer of 'roof-tile' crystals leaving the underlying layer of randomly oriented calcite rods exposed.

As etching is most pronounced on the topographically high parts of tests and individual chambers, and less marked along the sutural regions, there is reason to believe that slight abrasion of these highs may promote subsequent etching effects.

The majority of fossil examples examined by us show etching effects to a greater or lesser extent. The recognition of such post-mortem etching is important for the proper understanding of foraminiferid structures and for the proper interpretation of species differences.

Acknowledgements. We would like to thank R. Bradshaw for critical comments on the manuscript. The research was sponsored by the Natural Environmental Research Council.

REFERENCES

HAY, W. H., and SANDBERG, P. A. 1967. The scanning electron microscope, a major break-through for micropaleontology. *Micropaleontology*, **13**, 407–18, pl. 1, 2.

—— TOWE, K. M., and WRIGHT, R. C. 1963. Ultramicrostructure of some selected foraminiferal tests. Ibid. **9**, 171–95, pl. 1–16.

LYNTS, G. W., and PFISTER, R. M. 1967. Surface ultrastructure of some tests of recent Foraminiferida from the Dry Tortugas, Florida. *J. Protozool.* **14**, 387–99.

MURRAY, J. W. 1967. Transparent and opaque foraminiferid tests. *J. Paleont.* **41**, 791.

TOWE, K. M., and CIFELLI, R. 1967. Wall ultrastructure in the calcareous foraminifera: crystallographic aspects and a model for calcification. Ibid. **41**, 742–62, pl. 87–99.

J. W. MURRAY
C. A. WRIGHT
Department of Geology
Queen's Building
University Walk
Bristol BS8 1TR

Revised typescript received 23 October 1969

NEW XIPHOSURID TRAILS FROM THE UPPER CARBONIFEROUS OF NORTHERN ENGLAND

by P. G. HARDY

ABSTRACT. Trails from the lower surfaces of sandstone bands in the Upper Haslingden Flags (G Stage, Namurian) of the Rossendale area of Lancashire are attributed to arthropod (xiphosurid) activity. The trails are associated with *Pelecypodichnus* Seilacher which here result from the activity of non-marine bivalves. The xiphosurid trails are therefore considered of non-marine origin. The trails differ from those previously described in that in addition to walking activity, burrowing by the xiphosurid is recorded. For convenience these new trails are referred to *Kouphichnium rossendalensis* sp. nov.

TRAILS of xiphosurid origin have been found in loose blocks from the upper part of the Upper Haslingden Flags (G Stage Namurian) in Rossendale, Lancashire (for details of the stratigraphy see Wright *et al.* 1927). The trails occur on the sharply defined under surfaces of flaggy sandstone bands which generally are interbedded with siltstones. The sandstones associated with the trails exhibit a number of sedimentological structures including large-scale planar cross-bedding, small-scale asymmetrical ripples, interference ripples, micro-cross lamination, and ball and pillow structure. The Upper Haslingden Flags are essentially lens shaped, thinning in all directions from their strongest development in the Whitworth area of Rossendale where they exceed 100 ft. (30 m.) in thickness. The thickness is now known to exceed the figure quoted by Wright (in Wright *et al.* 1927). Together with the sedimentological evidence of clean, well-sorted, ripple-marked sands there seems to be evidence to suggest a sandbank type of environment during deposition of the Flags. Trails of xiphosurid origin are well known from various horizons including the Upper Carboniferous and have been described by many authors. A bibliography up to 1938 is given by Caster (1938). Subsequent papers include those of Caster (1940, 1941, 1944), Linck (1943), Brady (1947), Glaessner (1957), Häntzschel (1962), Malz (1964), King (1965), and Bandel (1967). Limulid trails previously supposed to have been of vertebrate origin have been given various names. Many earlier names are inappropriate and *Kouphichnium* (Nopcsa 1923) is now generally used for these trails (see Häntzschel 1965). Previously described trails have featured mainly evidence of walking activity e.g. appendage marks, genal spine drag marks, and telson marks. In this instance a new species of the genus *Kouphichnium* seems justified as there is clear evidence of burrowing activity which has only been described previously from modern *Limulus* trails (see Caster 1938, pl. 12, fig. 2).

DESCRIPTION

Genus KOUPHICHNIUM Nopcsa 1923

Kouphichnium rossendalensis sp. nov.

Plate 40

[Palaeontology, Vol. 13, Part 2, 1970, pp. 188–90, pl. 40.]

Holotype. Geology Department, Manchester University, SF3.

Diagnosis. Trails comprise lunate casts corresponding in outline to the shape of the xiphosuran prosoma, often in a series, and associated with appendage and telson marks.

Description. The trails are preserved as an irregularly meandering series of lunate casts the width of which is in general 16–17 mm. although some are smaller, 9–11 mm. The casts are deepest at the anterior convex end, where they project 2·5–3·5 mm. below the surface. Posteriorly each cast shallows, and most pass directly into the preceding cast at a distance of between 0·5–2·0 cm. Where the casts are less closely spaced, and in a few more or less isolated casts, they often resolve (see Pl. 40, inset) into 2 rows of appendage marks of circular plan which appear to be in a series *en echelon*. Behind many of the lunate casts there is median telson cast which is strongest 2–3 cm. behind the shallow end of the lunate casts. Groups of *en echelon* marks, each elongated in plan, occur behind some telson casts in Plate 40. Up to 6 clear elongate casts can be seen in one set. In no instance has the pusher impression of the maxillipeds been observed. Very fine wrinkle-like marks occur around the convex end of some of the lunate casts. In a few examples the convex end of the lunate cast is represented by a cloven-hoof-like mark. Similar marks have been produced by modern *Limulus* (Caster 1938; pl. 12, fig. 2) when sinking vertically into the sediment.

Interpretation. The faintness of the trails at the beginning of each series of *Kouphichnium rossendalensis* sp. nov. is interpreted as due to a xiphosurid about to touch down on the sediment surface dragging telson and appendages through the sediment for a brief interval and retracting them again before finally landing to implant the first lunate mark in the sediment. It is conceivable that telson and appendages were used as a brake prior to touch down; further the use of the telson in this way would serve to depress the prosoma towards the sediment surface. It appears that the xiphosurid having landed on the sediment surface burrowed, then moved forward some few millimetres, burrowed again and so on before finally taking off into the overlying water. Although the temporal sequence of burrowing–walking–burrowing is clear the actual time involved is unknown. Associated with *Kouphichnium rossendalensis* sp. nov. is *Pelecypodichnus* Seilacher formed, apparently, by non-marine bivalves. The evidence for this statement is, (1) *Pelecypodichnus* of the Haslingden Flags is identical in form and lithological association with *Pelecypodichnus* in the sandstones above the Lower Mountain Mine at Upholland (Lancashire). Non-marine bivalves occur within the burrows of *Pelecypodichnus* in the sandstones at Upholland, (2) *Pelecypodichnus* of the Haslingden Flags is identical to *Pelecypodichnus* at the base of the Rough Rock at Billinge Hill near Bollington, Cheshire. The base of the Rough Rock at Bollington contains non-marine bivalves, (3) the Upper Haslingden Flags are followed in upward sequence by shales known to contain a non-marine fauna (body fossils) at various localities. The conclusion is reached that *Kouphichnium rossendalensis* sp. nov. is non-marine. Two genera of xiphosurid, *Belinurus* and *Euproops*, are known from the Upper Carboniferous. *Belinurus* is often found in association with non-marine bivalves (Calver 1968) and is thought to have been responsible for the trails. Specimens of *Belinurus* from the Manchester Museum were measured across the prosoma, the width of which was found to correspond closely to the total width of the trails.

Acknowledgements. The author wishes to thank Dr. F. M. Broadhurst for allowing him to use the specimens and for advice. He is also grateful to Miss Susan Maher for the photographs.

REFERENCES

BANDEL, K. 1967. Isopod and Limulid marks and trails in Tonganoxie Sandstone (Upper Pennsylvanian) of Kansas. *Palaeont. Contr. Univ. Kans.* Paper **19,** 1–10, 4 pl.

BRADY, L. F. 1947. Invertebrate tracks from the Coconino Sandstone of Northern Arizona. *J. Paleont.* **21,** 466–72, pl. 66–8.

CALVER, M. A. 1968. In MURCHISON, D. G., and WESTOLL, T. S. *Coal and coal-bearing strata*. Oliver and Boyd, London, 147–77.

CASTER, K. E. 1938. A restudy of the tracks of *Paramphibius*. *J. Paleont.* **12,** 3–60, pl. 1–13.

—— 1940. Die sogenannten 'Wirbeltierspuren' und die Limulus-Fährten der Solnhofener Plattenkalke. *Paläont. Z.* **22,** 12–29.

—— 1941. Trails of *Limulus* and supposed vertebrates from Solnhofen Lithographic Limestone. *Pan. Am. Geol.* **76,** 241–58.

—— 1944. Limuloid trails from the Upper Triassic (Chinle) of the Petrified Forest National Monument, Arizona. *Am. J. Sci.* **242,** 74–84. 1 pl.

GLAESSNER, M. F. 1957. Paleozoic arthropod trails from Australia. *Pälaont. Z.* **31,** 103–9, pl 10–11.

HÄNTZSCHEL, W. 1962. In MOORE, R. C. (ed.) *Treatise on invertebrate Paleontology*. Pt. W: *Miscellanea*. Geol. Soc. Amer. and Univ. Kansas Press, W177–W245.

—— 1965. Vestigia Invertebratorum et Problematica. *Fossilium Catalogus*, I. Animalia, **108,** Gravenhage.

KING, A. F. 1965. Xiphosurid trails from the Upper Carboniferous of Bude, North Cornwall. *Proc. geol. Soc.* **1626,** 162–5.

LINCK, O. 1943. Die Buntsandstein Kleinfährten von Nagold. *Neues Jb. Miner. Geol. Paläont. Mh.* B, 9–27.

MALZ, H. 1964. *Kouphichnium walchi* die Geschichte einer Fährte und ihres Tieres. *Natur Mus. Frankf.* **94,** 81–97.

NOPCSA, F. 1923. Die Familien der Reptilien. *Fortschr. Geol. Palaeont.* **2,** 1–210.

WRIGHT, W. B, SHERLOCK, R. L. WRAY, D. A, LLOYD, W., and TONKS, L. H. 1927. The geology of the Rossendale Anticline. *Mem. Geol. Surv. U. K.*

P. G. HARDY
Department of Geology
The University
Manchester 13

Final typescript received 9 August 1969

EXPLANATION OF PLATE 40

Kouphichnium rossendalensis sp. nov. holotype (coll. Geology Dept., Manchester University SF3) showing appendage marks, telson marks, and lunate casts, ×2/3. Inset, paratype showing appendage marks arranged *en echelon*, ×2, specimen SF4.

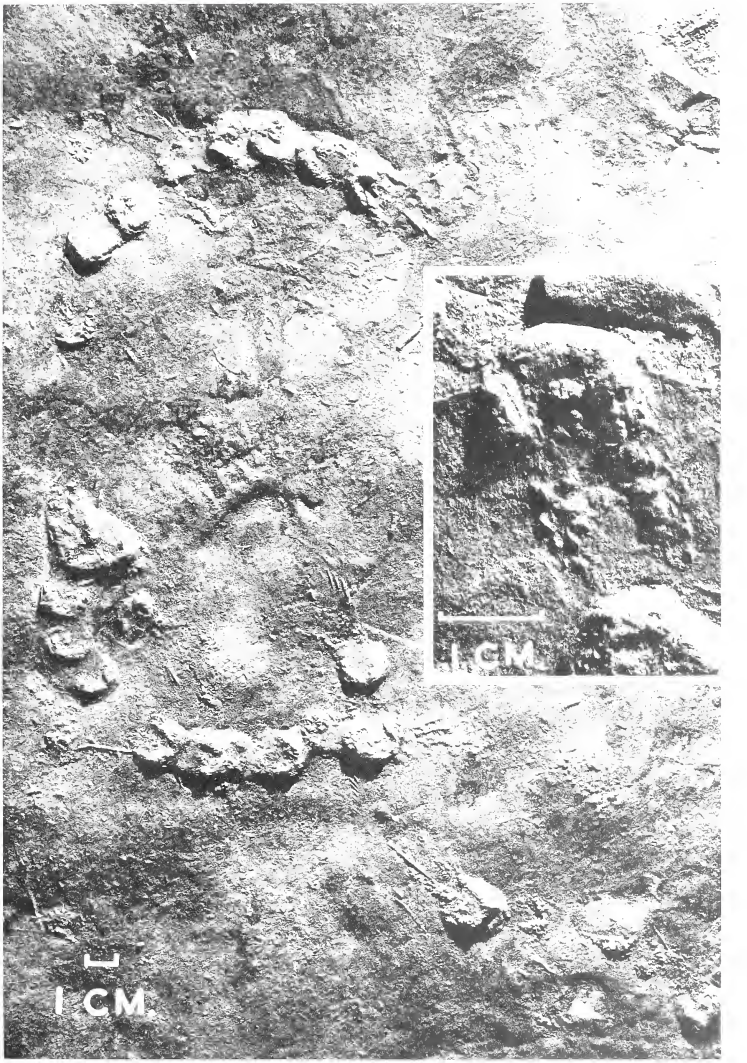

HARDY, *Kouphichnium rossendalensis*

SEDIMENTOLOGICAL FACTORS AFFECTING THE DISTRIBUTION AND GROWTH OF VISÉAN CANINIOID CORALS IN NORTH-WEST IRELAND

by J. A. E. B. HUBBARD

ABSTRACT. The Viséan limestone-shale sequences of north-west Ireland contain a characteristic distribution pattern of alternating coraliferous and 'barren strata' (called 'inter-beds'). The varied geniculation in the assemblages of prone solitary caninioids in both types of strata are interpreted from comparison with observations and experiments on modern corals, as showing a close relationship of coral growth to stability, sedimentation, and penecontemporaneous erosion of the soft lime-mud substrate. Two types of lime-mud are found in the axial region of the corals: fine homogeneous micrite flooring the tabulae is regarded as original infill, while extraneous biomicrite, introduced through openings caused by penecontemporaneous erosion and boring sponges and bryozoa is evidently of subsequent origin. Adverse environmental conditions during skeletogenesis are believed to be responsible for the widely spaced tabulae, conspicuously thin skeleton, and suppression of the dissepimentarium, which are irregularly developed and often associated. The effects of compactional loading and diagenesis are outlined. Each bedding-plane strewn with adult caninioids is regarded as a winnowed death assemblage involving many different generations and accumulating during periods of slow deposition. The difficulties for corals living on an unlithified sea bed are discussed and some wider regional implications considered.

BEDDING-PLANES strewn with large solitary cylindrical Rugose corals (Pl. 41, fig. 1) alternating with comparatively barren strata are common in the Viséan limestone–shale sequences of north-west Ireland. The coralliferous partings are particularly well known from around the shores of Donegal Bay from whence they have been described since the mid nineteenth century (see Wynne 1864, p. 38; Wynne 1885). Until now no ecological interpretation has been attempted, but this would now seem opportune in the light of recent work on ancient and modern carbonate sedimentology and on modern coral habits.

METHOD

Detailed field observations form the bulk of this work because little of the material is suitable for laboratory study. The Viséan around Donegal Bay from Easky (Irish National Grid Reference G380 385) to Muckros Head (I.N.G.R. G620 375) (see text-fig. 1) is ideally exposed in sections showing deeply weathered, almost horizontal strata. But crucial information has been derived from the comparatively poorly weathered inland escarpments of Benbulben (I.N.G.R. G684 462) and Knocknarea (I.N.G.R. G622 350). Quantitative field analyses which involved more than 3000 caninioids include data incorporated in the 100 one-metre quadrat analysis (see Hubbard 1966, p. 254) of the following localities: Easky (I.N.G.R. G380 385), Aughris (I.N.G.R. G485 350), Serpent Rock (I.N.G.R. G558 460), and Streedagh Point (I.N.G.R. G627 510). Selective laboratory studies which exposed the three-dimensional relationship of the coralla to their matrices and infilling material were implemented by means of polished and etched specimens, thin sections, and acetate peels. In addition 160 thin

[Palaeontology, Vol. 13, Part 2, 1970, pp. 191–209, pl. 41–44.]

sections and 320 acetate peels of the associated sediments at Streedagh Point and Easky were studied petrographically.

Terminologically the caninioids mentioned include the solitary specimens of *Caninia* spp. and *Siphonophyllia* spp. listed in stratigraphical accounts of the area (see Table 1). Systematic studies show that there is much intraspecific variation at Streedagh Point (Dixon 1970) but all those corals quoted are siphonophyllids, whereas outside this locality occasional caniniids are known notably in Co. Donegal.

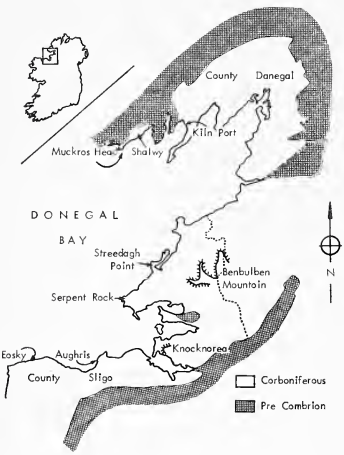

TEXT-FIG. 1. Outline map of the Sligo–Donegal coast to show the location of the most informative sections in the Viséan limestone–shale sequences in relation to their regional setting.

EVIDENCE

1. *General distribution.*

Corals occur throughout the limestone–shale sequences of north-west Ireland but are remarkably rich on certain bedding-planes. There is a tendency for one member of the fauna to predominate in each stratum, e.g. caninioid, zaphrentoid, fasciculate, or cerioid lithostrotionoid corals. But of these the caninioids are not only the most spectacular in the variability of their growth forms and distribution patterns, but are also the most ubiquitous in their sedimentary associations. They are found in biosparites and shales as well as all intermediate sediment types. Their distribution, which may be compared with other faunal elements, mirrors subtle lithological variations. Essentially their occurrence can be divided into two categories which have distinct sedimentological associations, (*a*) caninioid-dominated bedding-planes and (*b*) interbeds with sparse caninioids (see Table 2); the main difference being that whereas the former accumulates almost invariably represent condensed composite death assemblages

EXPLANATION OF PLATE 41

Fig. 1. An adult caninioid-dominated bedding-plane at Serpent Rock showing the comparatively uniform size and variability in growth forms of the partially silicified, randomly oriented, prone coralla of a composite winnowed death assemblage. The deep weathering of the present day intertidal zone has eroded the majority of the epithecae thus exposing many internal structures in longitudinal section. The corals rest on a crinoidal biomicrite, which probably equates with a high energy organic sand substrate, but are overlain by an impure dark trace fossil-riddled micrite matrix, which represents a lower energy rapidly deposited lime-mud. Scale of 1000 mm.

Fig. 2. A vertical polished section of a prone adult caninioid from a block of graded biomicrite at Streedagh Point showing extensive penecontemporaneous erosion of the upward facing surface of the coral. The caninioid's lower surface rests on a more richly organodetrital biomicrite of coral–echinoderm–brozoan debris than the overlying material which has a somewhat higher mud content. Scale of 50 mm.

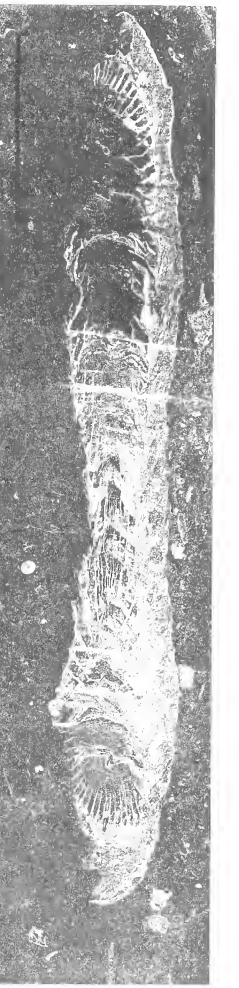

HUBBARD, Caninioid corals

the latter occasionally incorporate individuals which are thought to be preserved in positions of growth.

(*a*) *Caninioid-dominated bedding-planes.* The bedding-planes strewn with large adult prone caninioids (Pl. 41, fig. 1) are particularly conspicuous in the shore sections of Streedagh Point, Serpent Rock, Aughris, and Easky. This style of exposure usually results from differential weathering of weak partings at limestone–shale interfaces. Thus, where thin shale partings overly the corals the overlying limestone is readily

TABLE 1. The regional distribution and systematic status of the caninioids discussed according to the stratigraphical lists in 1, Oswald (1955), 2, Bowes (1957, unpublished Ph.D. thesis University of Glasgow), and 3, George and Oswald (1957).

	Co. Sligo			*Co. Donegal*	
Systematic status	*Benbulben*	*Aughris*	*Easky*	*West*	*South-east*
Caninia cornucopiae Michelin	1				3
C. benburbensis Lewis		2	2		
C. cf. *benburbensis* Lewis		2	2		
C. cf. *cylindrica* (Scouler)	1	2	2		
Caninia sp.		2	2		
amplexoii caniniids				3	
Siphonophillia cylindrica (Scouler)				3	
S. cf. *cylindrica* (Scouler)				3	
S. cf. *britoliensis* (Vaughan)				3	
S. cf. *benburbensis* (Lewis)				3	
Siphonophyllia sp. (see Lewis 1927, p. 37)					3

undermined and stripped off. The partially silicified coralla resting in or on the underlying silty biomicrites are thus left as upstanding features in the contemporary foreshore. Where the overlying shale parting is absent or limited to an unusually thin veneer the corals do not weather out so readily on the surface of bedding-planes, but are traceable in bands along the cliff. The true lateral extent of these caninioid-dominated planes is difficult to determine. Inland they give the impression of continuity over a matter of kilometres, but coast sections expose much small-scale faulting which complicates correlation. Certainly the evidence available suggests that the minimum continuity is in excess of 30 m. The distribution of caninioids within these planes is more variable and their orientation is apparently random (compare text-figs. 2 and 3). Caninioid population densities vary from four to eleven adults per square metre. Occasionally such concentrated accumulates pass abruptly into 'barren' areas within a metre, and in these cases there is usually evidence of shoaling organic debris on the lee sides of the caninioids.

There is a marked tendency for a uniformity of late neanic growth stages to predominate. These range up to 1064 mm. in length and 82 mm. in diameter, but average 505 mm. in length and 76 mm. in diameter. Juveniles are rare or absent. Growth forms, however, are highly variable and random in their associations. Thus straight, gently arcuate, and complexly geniculate forms often occur together. Though the proportion of straight to geniculate caninioids is not constant, the latter tend to be more numerous (text-fig. 4*a*). There is no correlation between the size of the corallum, the number, type, or distribution of geniculations. Thus geniculate caninioids range from simply curved

TABLE 2. A synoptic comparison of the caninioid-dominated strata and 'inter-beds' to show their contrasts in population structure, population density, epifauna, thickness, and lithological associations.

	Caninioid-dominated bedding-planes	'*Inter-beds*'
1. *Approximate frequency of 'inter-beds' to caninioid-dominated units*	1 in 16.	16 to 1.
2. *Average thickness of unit*	Variable—less than 50 mm.	100–9015 mm.
3. *Population structure*		
(*a*) *Density*	High (up to 11 adults per sq. m.).	Low.
(*b*) *Frequency*	Constant.	Sporadic.
4. *Growth stages present*	Mainly adults (*c.* > 90%).	Juveniles dominant, most growth-stages known.
5. *Growth forms recorded*	All styles from complexly geniculate in several planes to simple straight forms.	Straight or simple forms with only small simple geniculations at the apical end.
6. *Orientation*	90% prone (i.e. long axis of the corallum parallel to bedding). 10% low angle oblique to bedding.	80% prone (mainly adults). 10% inverted (mainly ephebic and young neanic). 7% in position of growth associated with fasciculate lithostrotionids (all growth stages except gerontic). 3% independently in position of growth (usually young neanic).
7. *Evidence of attachment*		
(*a*) *Scars*	None.	None.
(*b*) *Holdfasts*	Three neanic individuals attached to one adult specimen at Serpent Rock (text-fig. 5 3).	Rare: (*a*) young neanic individual attached to a spiriferid fragment by rootlets at Serpent Rock (*b*) one adult attached to linoproductid fragment in the Streedagh Shales at Streedagh Point.
8. *Epifauna*	Rare: a local feature at Easky and Pound Point (St. John's Point).	Rare.
(*a*) *Aulopora*	Encrusting upward facing surfaces of prone caninioids, linoproductoids, and davisiellоids.	Encircling the median region of one upstanding juvenile caninioid in position of growth at Largymore.
(*b*) *Boring by sponges and bryozoa*	Both types known. Penetration restricted to theca. Locally common, e.g. Streedagh Point, Easky.	Not recorded.

9. *Damage*	Sporadic epithecal erosion in some adults.	Limited to prone adults.
10. *Associated fauna*	Variable in numbers and kinds: generally not forming a significant proportion of the population. Chiefly corals, long hinged brachiopods and bryozoa, with crinoid and trilobite debris.	Variable in numbers and kinds: often forming a significant proportion of the population: generally mixed with dominance of corals and brachiopods (including short hinged forms).
(*a*) *Nos. of families and genera*	Restricted.	Diverse.
(*b*) *Nos. of individuals*	Comparatively 'high'.	Sparse.
(*c*) *Sizes and growth stages*	Uniform.	Not conspicuously uniform.
(*d*) *Preservation*	Generally transported and commonly disarticulated.	Mixed autochthonous and indigenous.
(*e*) *Commensal*	None.	Fasciculate lithostrotionids.
11. *Associated sediment*	Variable often with impurities.	Generally uniform.
(*a*) *Overlying the corals*	(*a*) Commonly dark shales and shaly biomicrites passing up into biomicrites.	
(*b*) *Underlying the corals*	(*b*) Occasionally uniform biomicrites.	Uniform, either (*a*) light-coloured barren micrite, (*b*) light-coloured crinoidal biomicrite, or (*c*) shales.
	Commonly biomicrite: composition variable, usually light-coloured biomicrite, occasionally darker and gradational towards shelly micrite.	
12. *Interpretation*	Almost invariably composite death assemblages.	(*a*) *Mainly transported death assemblages.* (*b*) Occasional individuals in position of growth, e.g. Serpent Rock, Streedagh Point, Knocknarea, and Largymore.

TABLE 2. A synoptic comparison of the caninioid-dominated strata and 'inter-beds' to show their contrasts in population structure, population density, epifauna, thickness, and lithological associations.

	Caninioid-dominated bedding-planes	*'Inter-beds'*
1. *Approximate frequency of 'inter-beds' to caninioid-dominated units*	1 in 16.	16 to 1.
2. *Average thickness of unit*	Variable—less than 50 mm.	100–9015 mm.
3. *Population structure*		
(*a*) *Density*	High (up to 11 adults per sq. m.),	Low,
(*b*) *Frequency*	Constant.	Sporadic,
4. *Growth stages present*	Mainly adults (*c.* > 90%).	Juveniles dominant, most growth-stages known.
5. *Growth forms recorded*	All styles from complexly geniculate in several planes to simple straight forms,	Straight or simple forms with only small simple geniculations at the apical end.
6. *Orientation*	90% prone (i.e. long axis of the corallum parallel to bedding). 10% low angle oblique to bedding.	80% prone (mainly adults). 10% inverted (mainly ephebic and young neanic). 7% in position of growth associated with fasciculate lithostrotionids (all growth stages except gerontic). 3% independently in position of growth (usually young neanic).
7. *Evidence of attachment*		
(*a*) *Scars*	None.	None.
(*b*) *Holdfasts*	Three neanic individuals attached to one adult specimen at Serpent Rock (text-fig. 53).	Rare: (*a*) young neanic individual attached to a spiriferid fragment by rootlets at Serpent Rock (*b*) one adult attached to linoproductid fragment in the Streedagh Shales at Streedagh Point.
8. *Epifauna*	Rare: a local feature at Easky and Pound Point (St. John's Point).	Rare.
(*a*) *Aulopora*	Encrusting upward facing surfaces of prone caninioids, linoproductoids, and davisiellоids.	Encircling the median region of one upstanding juvenile caninioid in position of growth at Largymore.
(*b*) *Boring by sponges and bryozoa*	Both types known. Penetration restricted to theca. Locally common, e.g. Streedagh Point, Easky.	Not recorded.
9. *Damage*	Sporadic epithecal erosion in some adults.	Limited to prone adults.
10. *Associated fauna*	Variable in numbers and kinds: generally not forming a significant proportion of the population. Chiefly corals, long hinged brachiopods and bryozoa, with crinoid and trilobite debris.	Variable in numbers and kinds: often forming a significant proportion of the population: generally mixed with dominance of corals and brachiopods (including short hinged forms).
(*a*) *Nos. of families and genera*	Restricted.	Diverse.
(*b*) *Nos. of individuals*	Comparatively 'high'.	Sparse.
(*c*) *Sizes and growth stages*	Uniform.	Not conspicuously uniform.
(*d*) *Preservation*	Generally transported and commonly disarticulated.	Mixed autochthonous and indigenous.
(*e*) *Commensal*	None.	Fasciculate lithostrotionids.
11. *Associated sediment*	Variable often with impurities.	Generally uniform.
(*a*) *Overlying the corals*	(*a*) Commonly dark shales and shaly biomicrites passing up into biomicrites. (*b*) Occasionally uniform biomicrites.	Uniform, either (*a*) light-coloured barren micrite, (*b*) light-coloured crinoidal biomicrite, or (*c*) shales.
(*b*) *Underlying the corals*	Commonly biomicrite: composition variable, usually light-coloured biomicrite, occasionally darker and gradational towards shelly micrite.	
12. *Interpretation*	Almost invariably composite death assemblages.	(*a*) *Mainly transported death assemblages.* (*b*) Occasional individuals in position of growth, e.g. Serpent Rock, Streedagh Point, Knocknarea, and Largymore.

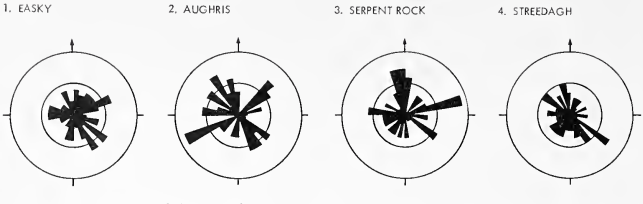

TEXT-FIG. 2. Rose diagrams to illustrate the random orientation of the geniculate caninioids in the caninioid-dominated bedding-planes. Each diagram represents 100 readings in which the angle of interception of the coral is plotted.

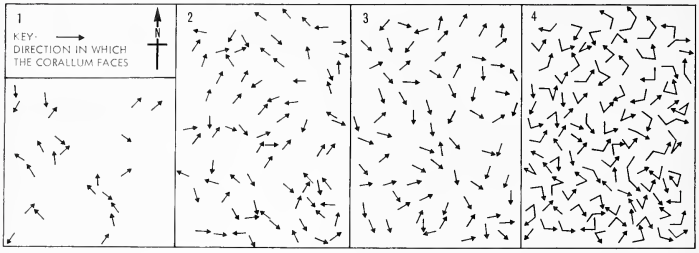

TEXT-FIG. 3. Diagrammatic illustration of an analysis of the orientation of 100 prone, adult caninioids on a single bedding-plane at the top of the Streedagh Point succession. Inset 4 represents the field evidence, in which all stages of the coral growth visible are plotted. The directions in which arrows point indicate the orientation of the calices and their geniculations are plotted to the nearest degree. The diameters of the coralla are constant but unrepresented. The relative lengths of the intergenicular regions are approximately in proportion. Inset 3 represents the final stage of growth only. Inset 2 shows the orientation of the coralla before the last geniculation, while inset 1 records only the first stage of growth visible. Thus there seems to be no apparent preferred orientation either at a particular growth stage or *in toto*.

cylindrical specimens to more complex S– and Z–shapes in which the geniculation(s) occur in one plane or at random. Similarly the genicular angle may be wide and gently arcuate or narrow and sharply V-shaped. Geniculations show no constant relation to the situation of the cardinal quadrant, apex, or calice. The epitheca is often partially removed from the upper surface of the corals as a result of penecontemporaneous

EXPLANATION OF PLATE 42

Close-up of a prone caninioid in a naturally eroded, longitudinal section resting in a bioturbated coralliferous biomicrite at Serpent Rock. This illustrates the fine detail often visible in the field as compared with laboratory preparations (Pl. 44). The corallum shows repetitive suppressions of the dissepimentarium, local asymmetrical development of the dissepimentarium, local thinning of the septa (halfway up the coral), and a gently arcuate geniculation suggesting that this coral's life was periodically fraught with the dangers of silting up during adverse conditions. Scale of 100 mm.

HUBBARD, Caninioid corals

erosion (Pl. 41, fig. 2), but this damage is seldom extensive and breakages are few numbering less than 10% of any population studied (Text-fig. 4*b*).

(*b*) '*Inter-beds*'. In contrast to the caninioid-dominated strata these are varied in thickness, lithology, and faunal content (Table 2). They contain few whole fossils but are composed of a high organo-detrital content. The population is low in numbers but more varied, containing representatives of various growth stages of a fauna which appears to be

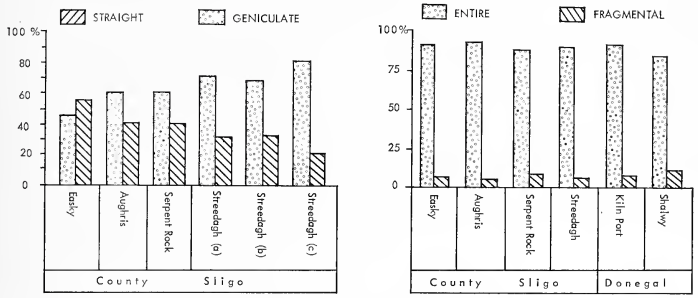

TEXT-FIG. 4. Caninioid statistics: Left, histogram to show the ratio of geniculate to straight caninioids within a single bedding-plane. Three horizons are cited at Streedagh Point. A dominance of geniculate forms is generally discernible. Right, percentage histogram of entire and fragmental caninioids calculated from 100 one-metre quadrats at each locality.

locally indigenous and occasionally in position of growth (Text-fig. 5). Whereas the caninioid-dominated bedding-planes are generally marked by an abrupt change in sedimentary style, e.g. silty biomicrite to bioturbated shale, the 'inter-beds' are conspicuous for their uniformity. At most they are graded within the individual stratum. But there is a tendency for these 'inter-beds' to be terminated abruptly at their upper surface by a caninioid-dominated bedding-plane.

2. *Caninioid growth*

Longitudinal axial sections exposing the tabularium, many of which are as well etched in the field (Pl. 43) as can be achieved in the laboratory (Pl. 44), are plentiful in the foreshores and yield important information on the growth of the corallum. The arrangement of the tabulae, though variable in detail, is generally parallel to the orientation of the external growth rings. This constancy may be used indirectly as evidence of the probable direction of growth of the live coral.

(*a*) *Geniculation*. A gradual compensational swing of both tabulae and growth rings is usual (Text-figs. 5 1, 2; Pl. 43). Abrupt changes are rare.

(*b*) *Attachment*. Evidence is seldom found as the apical region is either buried or rarely seen preserved. Three juveniles are known on the epitheca of one adult caninioid

(Text-fig. 5 3), while another juvenile attached itself to a spiriferid fragment by supporting 'rootlets'. Only one attached adult is known from Co. Sligo; it is cemented apically to a linoproductid fragment in the basal shales of Streedagh Point. In all four cases the scar is evident, but small. No evidence of attachment scars is found outside the apical region.

(*c*) *Attitude of growth.* Several young caninioids are known in upright positions which would seem to be functionally viable (Text-figs. 5 1, 2, 3; Pl. 44, fig. 1). These are recorded from 'inter-beds' and are known from similar sediments in the escarpments of Knocknarea and Benbulben as well as the shores of Easky, Aughris, Serpent Rock, Streedagh Point, and Shalwy. But they are rare occurrences limited to homogeneous biomicrite and silty biomicrite facies. Several neanic and ephebic caninioids are found in this position where they are intergrown with fasciculate lithostrotionoids as though deriving benefit from their shelter (Pl. 44, fig. 1).

3. *Preservation.*

(*a*) *Axial infill.* The advanced state of diagenesis of both corallum and matrix often obscures the original nature of the axial infill. The coralla are preserved in finely crystalline silica and carbonate, from which, by granular cementation of the carbonate crystals, the intraskeletal voids are filled. Locally coarse drusy carbonate is developed, often at the expense of the skeletal structure. Thus tabulae, septa, and dissepiments terminate abruptly against the mosaic (Pl. 43). The coarse mosaic is commonly developed in bands of less than 50 mm. deep within the tabularium. Occasionally this extends laterally into the dissepimentarium.

In addition to the crystalline infill, lime-mud is found locally in the axial region. This consists of two types, (*a*) very fine homogeneous micrite flooring the tabulae, and (*b*) extraneous silty biomicrite which frequently completely fills the intertabular space but shows no geopetal features. This latter infill often occurs in the genicular region of the corallum, where the skeleton is conspicuously thin, and/or in areas where the tabulae are disorganized.

(*b*) *Penecontemporaneous erosion.* Caninioids are seldom as extensively eroded as the one illustrated in Plate 42, but localized erosion of parts of the corals' outer surface is not uncommon. Damage is usually restricted to the upward facing sector of the corallum. Often the epitheca is breached, but penetration is known to extend as far as the tabularium thus allowing the introduction of extraneous lime-mud into the axial region. This type of damage is readily distinguished from the products of differential loading and diagenesis (compare Tables 3 and 4).

EXPLANATION OF PLATE 43

A longitudinal section of a deeply etched, prone, geniculate caninioid. The dissepimentarium shows pronounced constrictions on the convex side and a certain degree of asymmetry. The tabular region is locally confused by diagenetic rupture, while the intertabular interval is somewhat masked by the uneven distribution of carbonate mosaic and silica. Scale of 10 mm.

HUBBARD, Caninioid corals

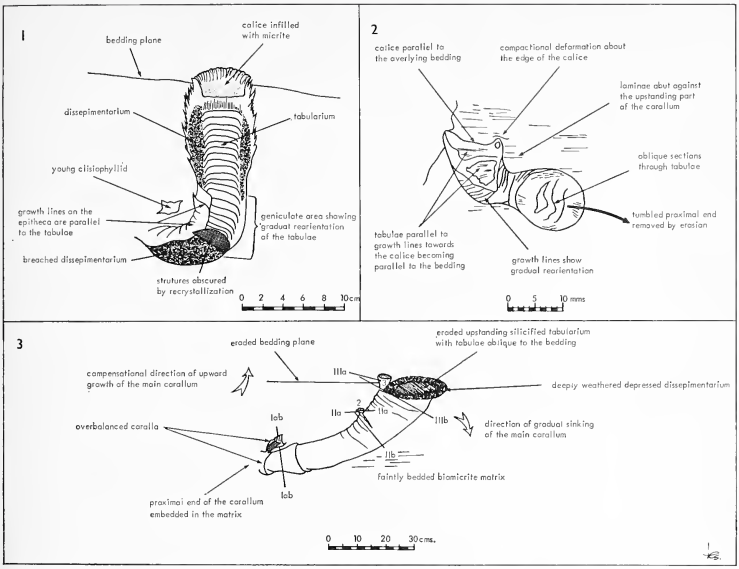

TEXT-FIG. 5. Caninioid corals preserved in their probable positions of growth.

(1) Field sketch of an adult geniculate caninioid at Serpent Rock illustrating the relationship of the calice to the axial structures and bedding. There is a conspicuous parallelism of growth-lines, tabulae, and calice, which distally are almost parallel to the bedding. The apical region is inaccessibly buried in the matrix. The geniculate development of the corallum suggests that the young coral became unbalanced and managed to reorient itself successfully with respect to its substrate by gradual upright growth, which is reflected in both growth rings and tabulae.

(2) Sketch from a peel of a young geniculate caninioid from Knocknarea illustrating the relationship between the corallum and matrix. In the upstanding portion of the corallum the bedding terminates abruptly against the epitheca indicating that deposition and coral growth were contemporaneous. The calice is at a low angle, in this case almost parallel to the succeeding sedimentary laminae. The growth history of the coral may be traced from the orientations of the tabulae and growth-lines with respect to the bedding. During its early life the coral overbalanced and came to rest obliquely on the sea bed, but compensation reorientation enabled the polyp to resume its upright position and continue growing until its premature death. This probably resulted from 'suffocation' as there seems to be little evidence of a break in sedimentation between the coral's successful readjustment and its final burial. At the calical margin the overlying bedding, which is affected by compactional deformation, and is of post-mortem origin completely transgresses the corallum.

(3) Field sketch of a caninioid life assemblage comprising an adult supporting three juveniles at Serpent Rock. The inferred directions of settling of the main corallum are indicated by the angular discordance between its growth rings (Ib, IIb, IIIc) and those of the small coralla (Ia, IIa, IIIa) which probably initially attached themselves in an erect position.

TABLE 3. A synopsis of caninioid features which result from post-mortem causes.

Feature	*Area affected*	*Frequency*	*Cause*
SKELETAL DAMAGE			
1. Thecal breaching; occasionally superficial sometimes associated with damage of contiguous internal structures, e.g. abruptly truncated tabulae (see Pl. 41, fig. 2).	Commonly confined to upper surfaces of prone adults. Locally coincident with geniculations.	Irregular.	Contemporaneous erosion while strewn over the sea bed.
2. Tabular slivers arranged *en échelon* between complete tabulae.	Random.	Irregular.	Expansional rupture during diagenesis.
3. Tabulae missing and/or represented by slivers with random orientation in biomicrite filled intertabular area.	Random. Sometimes associated with particularly thin skeletal areas.	Irregular.	Introduction of extraneous material resulting from local breaching by contemporaneous erosion.
4. Planar orientation of skeletal fragments parallel to the bedding.	Variable, often extensive or developed throughout the length of the corallum.	Common.	Crushing during compactional loading.
INFILLING MEDIUM			
1. Homogeneous micrite A.	Locally developed flooring intertabular areas.	Rare.	Original.
2. Homogeneous micrite B.	Local, usually associated with the external margin of the dissepimentarium.	Sporadic.	Diagenesis.
3. Drusy carbonate.	Local, commonly restricted to 50 mm. thick bands in the tabularium, but is also found affecting adjacent areas of the tabularium.	Sporadic (total loss of internal structures).	Diagenesis.
4. Cryptocrystalline silica.	Locally present in intertabular area.	Sporadic.	Diagenesis.
PRESERVATION OF CORALLUM			
1. Microcrystalline carbonate.	Throughout.	Usual.	Replacement.
2. Cryptocrystalline silica.	Irregular, usually best developed at the theca, from which it selectively penetrates the septa.	Variable.	Permineralization.

TABLE 4. A synopsis of caninioid features which result from the contemporaneous effects of mobile sediment on the growing corallum.

Feature	*Effects or areas affected*	*Location*	*Frequency*	*Likely cause*
GENICULATION	(*a*) External form (*b*) Tabularium (*c*) Dissepimentarium.	Random.	Irregular but common.	Negative geotropic readjustment resulting from (*a*) Instability on substrate, (*b*) Unfavourable original attachment, (*c*) Directional growth away from sediment.
TABULARIUM				
1. Intertabular distance.	(*a*) Tabulae locally crowded.	Random.	Irregular, usually limited.	Favourable conditions, with sufficient carbonate for additional growth.
	(*b*) Tabulae locally widely separated, often coincident with particularly thin tabulae and restricted dissepimentarium.	Random.	Irregular.	Adverse conditions: (*a*) Lack of carbonate for skeletal growth, (*b*) Need of rapid upward extension of the skeleton to avoid choking by mobile sediment.
2. Orientation of tabulae.	(*a*) Oblique to previous tabulae. (*b*) Off-lapping. (*c*) Overlapping. Often associated with parallel directional change in external growth rings.	Variable, most common in genicular areas.	Common.	Compensational growth resulting from readjustment of growth direction.
3. Broken tabulae.	Concentric arrangement of tabulae occupying one intertabular space. Usually associated with thin tabulae.	Irregular.	Rare.	? contemporaneous collapse of calice during adverse conditions.
DISSEPIMENTARIUM				
1. Crowding of dissepiments on concave side of geniculation.	Local, coincident with geniculations.	Variable.	Irregular.	Response to concentric growth about a curve.
2. Locally suppressed: (*a*) symmetrically, (*b*) asymmetrically.	Associated with thin distantly spaced tabulae.	Variable.	Irregular.	Adverse conditions: (*a*) Lack of carbonate for skeletal growth, (*b*) Need added height rather than sturdiness.

4. *Original skeletal peculiarities.*

Intertabular distance, suppression of the dissepimentarium and skeletal thinning (see Table 4) show random development within the coralla. They are commonly associated with one another and therefore more probably reflect the influence of environment rather then genetic factors.

(*a*) *Tabular distance.* The intertabular distance is variable. Frequently tabulae are grouped into more and less dense areas; these are not quantifiable, and thus are not explicable in terms of Ma's (1937, p. 9) seasonal growth hypothesis. In certain coralla the tabulae are locally widely spaced and unusually thin. This type of development is sometimes coincident with local suppression of the dissepimentarium.

(*b*) *Suppression of the dissepimentarium.* Whereas the tabularium retains a constant diameter, the dissepimentarium frequently shows a marked reduction. In some individuals the suppression may be sufficiently intensive that the dissepimentarium is difficult to recognize. This usually occurs in regions where the tabulae are thin and widely spaced. Often this coincides with the sharper geniculations, but it is also found at random along the length of straight caninioids.

(*c*) *Skeletal thinning.* This is highly variable in its occurrence and is most conspicuous in the tabularium, where it generally coincides with the widely spaced tabulae and restricted dissepimentarium.

These features are thus highly suggestive of temporary adverse conditions in which the coral was unable to sustain its usual rate of skeletal secretion. Hence for survival the coral would be forced to effect a restricted building programme in which it would naturally concentrate on growing upwards and away from the offending sediment, by developing widely spaced tabulae, rather than consolidating its scaffolding by dissepimentarial growth.

5. *Recent analogies.*

Deductions based on analogies between the extinct Rugosa and modern Scleractinia have obvious limitations because of fundamental differences in thecal formation and the development of tabulae. Nevertheless it is still worthwhile reviewing some of the

EXPLANATION OF PLATE 44

Fig. 1. A block of biomicrite at Serpent Rock containing a life assemblage of a slightly geniculate caninioid growing in close proximity to a fasciculate lithostrotionoid corallum suggests that the former derived shelter from the latter. The effect of uneven compactional loading causing 'pinch and flow' structures is seen in the deformed *Chrondrites* rich sedimentary laminae which can be traced from the base of the caninioid obliquely towards the right hand base of the compound coral. Scale of 100 mm.

Fig. 2. A deeply eroded marine platform reveals several different sedimentary environments within a distance of less than 15 cm. in what must have been a soft lime-mud substrate during Viséan times. The section is floored by a linoproductid-coral micrite, which passes up into a dark, bioturbated, biomicrite horizon. The latter is sharply and unevenly overlain by an impersistent uniform impure organodetrital shale, which in turn gives way to another caninioid–lithostrotionoid–linoproductoid micrite which can be traced discontinuously from the top left to the right of centre. Scale of 100 mm.

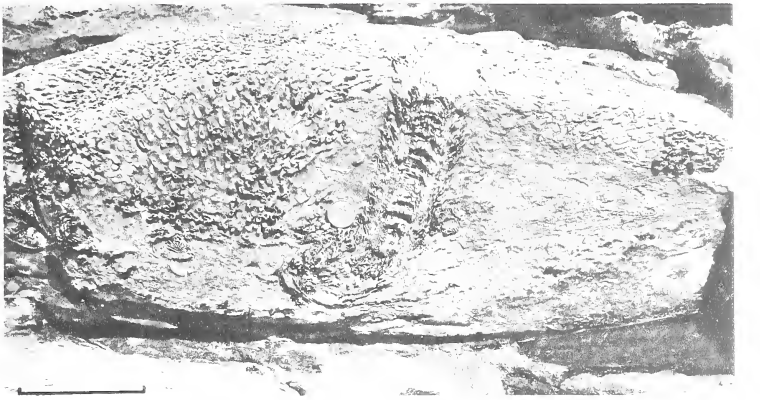

1

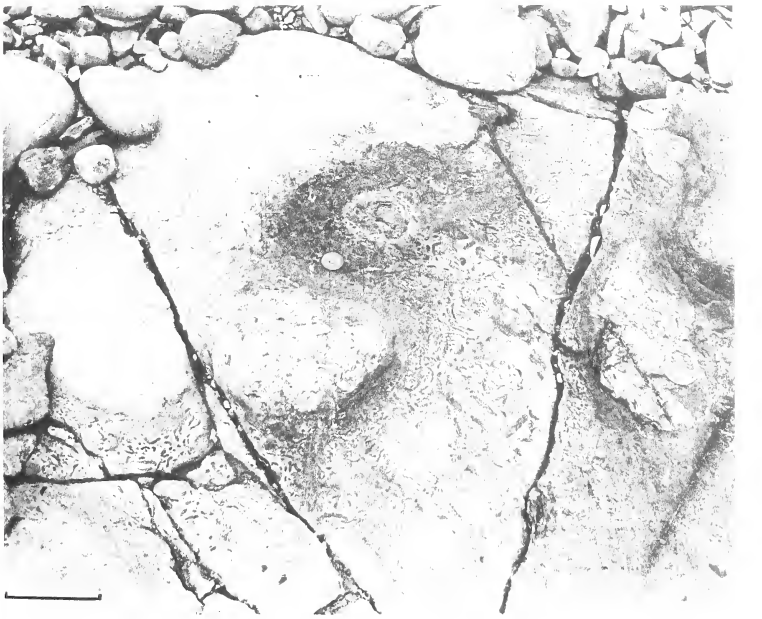

2

HUBBARD, Caninioid corals

experimental and observational findings on the habits of modern corals and considering the extent to which these may have controlled growth in caninioids.

(*a*) *Initial attachment*. Experiments with *Pocillopora* larvae indicate that attachment is readily achieved irrespective of the nature of the substrate (Edmondson 1929, p. 8). Algae, broken glass, and the smooth sides of a glass beaker were sufficient for this modern coral; thus the organo-detrital content of the Viséan biomicrites, e.g. comminuted shell, crinoid ossicles, and bryozoan debris, should have been adequate for the caninioids.

(*b*) *Later growth habits*. (i) Upward growth is a direct response of the polyps' need to be above the level where it would be 'suffocated' by moving sediment (Manton and Stephenson 1935, p. 308; Marshall and Orr 1931, pp. 130–1). Phototropism is a subsidiary factor, being an indirect response to the polyps' dependence on light (see Edmondson 1929, Roøs 1967). Thus in life the calice of the caninioid probably faced upwards, and was normally parallel to, or sometimes at a low angle to the sea floor (see text-figs. 5 1, 2, 3; Pl. 44, fig. 1).

(ii) Permanent attachment throughout the coral's life is not necessary. The modern Bahaman solitary coral *Manicena aureolata* Linnaeus (Yonge 1935, p. 187; Squires 1958, p. 258) frequently frees itself and loses all trace of its former attachment on unlithified sediments. Similarly the caninioids appear to have required anchorage only in extreme youth.

(iii) Stability is a common problem in modern unlithified lime-muds. Present-day coral populations in the West Indies tend to have slightly lower specific densities than the surrounding sediments, and it is suggested that this adaptation allows *Manicena areolata* Linnaeus in Bimini Lagoon (Squires 1958, Yonge 1935) to keep a constant proportion of the corallum above the sea water–sediment interface irrespective of the rate of sedimentation. Experimental calculations on the relative densities of caninioids and their associated sediments suggest that this was operative in the Viséan. In the Bahamas as much as 9144 mm. of unconsolidated lime-mud is recorded (Squires 1958, p. 236), a thickness which is more than adequate for the support of any known caninioid. But what proportion of the caninioid remained buried during life is speculative. It could not have survived the effects of mobile sediment in the prone condition. The stability of the coral would have been dependent on the length of the buried portion, the fluidity of the matrix, and current velocities in the surrounding sea water. Even in the ideal situation, perpendicular to the sea bed, it seems unlikely that the caninioid would be stable were more than a third of the corallum exposed above the sediment–sea water interface, and this upstanding part might be considerably smaller.

Subsidiary factors affecting the stability of the corallum include minute textural differences in the matrix and these together with the effects of penecontemporaneous crystallization and early diagenesis could have had a profound effect on the permeability, porosity and compaction of the surrounding sediment (Trask 1931, p. 275).

(iv) The effect of mobile sediment on Recent corals is crucial. In modern seas the effects of rate, type, and direction of mobile sediment is of considerable importance in coral growth and survival. Marshall and Orr (1931, pp. 130–1) show that the larger the calice, the greater is the polyps' ability to withstand temporary muddy influxes. This is paralleled by the ubiquitous caninioids in contrast to the more selective distribution of

lithostrotionoid corals in the Irish Viséan. Marshall and Orr also note a close correlation between particle size and 'suffocation' i.e. the finer the particle size the more rapid the 'suffocation'. Similarly they note that the direction of sedimentation can be crucial in *Pocillopora*, *Gallaxea*, *Symphyllia*, *Fungia*, and *Acropora*. These corals can withstand almost unlimited amounts of sediment from above, but where sediment built up around the lower reaches of the calice death followed within forty-eight hours. This apparently results from the polyps' inability to move its tentacles laterally in such circumstances. Thus during windy weather the polyps' chances of survival are somewhat hazardous as the level of the sea bed keeps changing in relation to the polyp. Hence by comparison the movement of only a small amount of Viséan lime-mud could have effectively 'suffocated' a large number of caninioids on what is now represented by a single bedding-plane. But more recently Goreau and Goreau (1959, p. 247) note that the polyps of *Porites* and *Millepora* can withstand starvation during conditions of extreme muddiness. In these conditions the polyps free themselves from the coralla and live for several weeks without a sign of skeletal building. By analogy the thin skeletal structures in some caninioids are attributed to similar, though slightly better conditions than those to which Goreau and Goreau refer.

(v) Sedimentary rates. Even in modern sediments where exact records may be taken it is difficult to distinguish sedimentary rates of consequence. Thus, where two days yield an average of 1 mm. per day, the same locality can also record an average of only 3 mm. in 15–35 days (see Bakus 1967, p. 45). Viséan sedimentary rates are thus speculative, but in comparative terms their variations are significant. Thus argillaceous bands rich in trace fossils represent periods of rapid accumulation, while well-winnowed, organo-detrital calcarenites probably represent slower accumulation, and graded silty biomocrites probably represent an intermediate and gradational rate of accumulation. Variations in the vertical combinations of these lithologies (see Pl. 44, fig. 2) leave little doubt that there were variations in depositional rate during the Viséan. The caninioid-dominated bedding-planes commonly rest on well-winnowed calcarenites and are overlain by bioturbated shales which are in turn overlain by further limestones. Some of these caninioids contain relics of extraneous biomicrite within the intertabular areas which can be matched with the overlying sediments. This suggests penecontemporaneous erosion of the sea bed between the deposition of the underlying and overlying sediments. But there is no evidence of channelling, probably because the sediments were still unlithified and highly mobile. Further indications of breaks in the sedimentary record are provided by truncated trace fossils (see Goldring 1962) and localized epifaunal developments.

The absolute rate of sedimentation during Viséan times is unknown, but indirect estimates may be hazarded using Wells's (1963) geochronometrical analysis of fine growth rings, which in modern corals are added diurnally. According to Wells there were 393 days in the Mississippian year. If this figure is accepted several counts of caninioid diurnal growth increments would suggest that their average growth rate was 65 mm. per annum which is identical to the Devonian *Cystiphyllum americanum* (Wells 1937, p. 17). Thus an age of thirteen years can be ascribed to the longest straight caninioid at Serpent Rock. Hence it is assumed that if vertical growth kept pace with sedimentation a rate of accumulation of less than 65 mm. per annum is indicated. During the life of this caninioid sediment accumulation was uninterrupted, but ultimately the supporting

sediment was winnowed away and the corallum left in a prone resting position. But though shoaling of organic debris is not uncommon few coral case histories are as simple as this.

A rate of accumulation of 65 mm. per annum is regarded as high by modern lime-mud standards and compares with lagoonal environments. But in that this rate is shown to be a temporary feature in the Viséan the comparison is plausible.

(vi) Epifauna. The distribution is characteristically local. One bedding-plane may be more affected than another at the same locality. But Easky, Serpent Rock, and Pound Point (St. John's Peninsula) sustain the highest caninioid-based epifauna. *Aupolora* is the most common encrusting creature. It generally attaches itself to the upper surface of prone caninioids on caninioid-dominated bedding-planes and inverted linoproductids and davisiellids on brachiopod-dominated bedding-planes. It is also found attached to one caninioid calice which would suggest that it is usually a post-mortem colonization to combat the adverse effects of life on the lime-mud sea bed. One upstanding caninioid, believed to be in position of growth, at Shalwy is encircled by an auloporid, in this case suggesting a commensal relationship.

Penetration by boring sponges and bryozoa (see Brunton 1966) is locally common, affecting the upper surfaces of prone caninioid thecae at Easky and Streedagh Point. But there is no evidence of contemporaneous infestation. In section the effective depth of penetration by boring creatures is obscured by diagenesis, but it is possible that these passages provided another route for the introduction of extraneous micrite into the axial region.

CONCLUSIONS

A crude, somewhat oversimplified flow diagram of the caninioids' probable life histories indicates the main factors affecting caninioid growth and distribution (Text-fig. 6) and ultimate accumulation as composite death assemblages in caninioid-dominated bedding-planes alternating with 'inter-beds'. Mobile sediment is the key inorganic factor.

1. Caninioids grew upright for preference (Text-fig. 6, 3ia–3ic; text-fig. 5; Pl. 44, fig. 1).

2. Caninioids could not live long in the prone condition as even small amounts of mobile sediment would have soon 'suffocated' them (Text-fig. 6, 3iiig–3iiih).

3. Geniculation developed wherever a righting reaction was necessary as for instance:

(*a*) Resulting from instability induced by contemporaneous winnowing of the soft lime-mud sea bed (Text-fig. 6, 3iiib–3iiic–3iiid–3iiie).

(*b*) Resulting from instability induced by oblique attachment (Text-fig. 6, 3iia–3iib–3iic).

(*c*) Resulting from instability induced by other causes not witnessed in the fossil record, e.g. behaviour of the substrate during early diagenesis, variations in current strengths due to salinity changes.

4. The wide caninioid calice renders them more tolerant of mobile sediment than the associated, mainly lithostrotionoid, corals and thus accounts for the ubiquity of the caninioids in contrast to the more environmentally restricted lithostrotionoids.

5. The corals' susceptibility to mobile sediment renders the caninioids more complex than other groups which reflect similar variations in Viséan sedimentological conditions. They indicate both the individual's responses throughout life and the effects on the mass

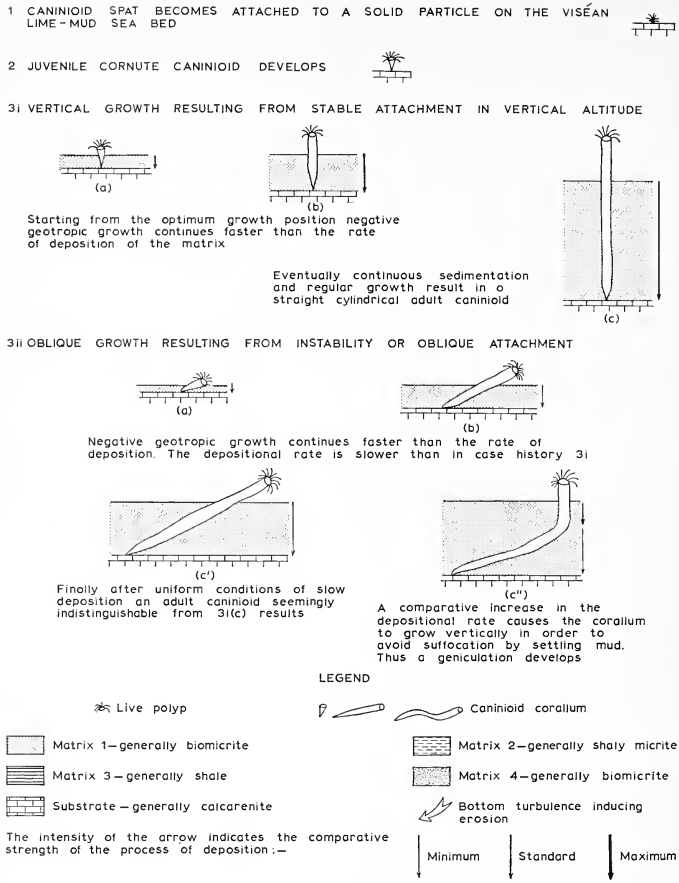

TEXT-FIG. 6. A simplified highly idealized flow diagram which accounts for some of the possible origins of the relationship of the various caninioid growth forms, their orientations, and their matrices. The relative rates of coral growth, stability, sedimentation, and penecontemporaneous erosion as reflected in individual coralla and cannot be represented accurately. A general minimal sedimentary rate is inferred and variations in sedimentary rate are thought to be variable but not in excess of 65 mm. per annum. Periodically, after the repetition of several of these phases, the winnowed accumulates of diverse growth forms of adult caninioids, now preserved in caninioid dominated bedding-planes, were buried by a renewed increase in sedimentation.

3iii VARIATION IN GENICULAR STYLE RESULTING FROM MOBILITY OF THE SUBSTRATE COMBINED WITH THE ALTERNATION OF DEPOSITION AND PENECONTEMPORANEOUS EROSION

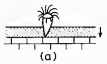

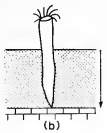

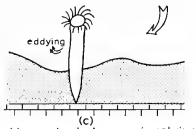

Bottom turbulence involving penecontemporaneous erosion of the matrix

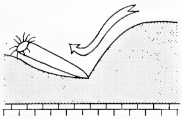

Penecontemporaneous erosion and current activity over-balance the corallum

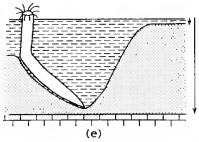

Renewed influx of sedimentation with the caninioid resuming its negative geotropic tendencies

(f) The processes involving 3iii (c)-(e) may be repeated innumerable times thus accounting for an indefinite number of geniculations and variations in curvature

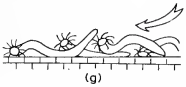

Renewed winnowing. Bottom turbulence removes all the original matrix tumbling and rolling the coralla

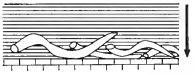

Influx of extraneous mud with rapid deposition causes final suffocation of any but the most recalcitrant caninioid

THECAL BREACHING

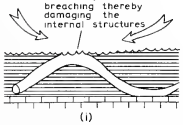

Partial burial and/or subsequent erosion may cause the upstanding geniculate area to be breached

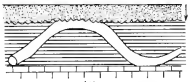

Subsequent deposition infills the buried topography of the eroded caninioid

4 RESULT

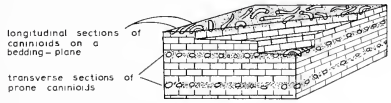

Segregations of "prone" adult caninioid-dominated bedding-planes alternate with almost "barren" units

of the population at the time of burial. These patterns of organic and sedimentological variation are mirrored in the distribution of brachiopods which occur interbedded in these sequences, of which linoproductids, pustulids, and davisellids are the most common. They are seldom seen in position of growth but often occur as dense masses of adults strewn inverted over shaly bedding-planes.

GENERAL DISCUSSION

Having reviewed the local factors, i.e. those pertaining to each caninioid assemblage now found on single bedding-planes, other major or regional factors influencing survival and distribution of all recurrent assemblages may be considered briefly. First, there are the palaeogeographical factors which control such peculiarities as the recurrent changes in sedimentary regime which are of a crude rhythmic nature. However, the absence of positive evidence of an inshore facies and adjacent shoreline precludes any definite statement as to this as a control. Further, with the exception of some limited evidence of boring algae, no algal mats, dessication cracks, or carbonate pseudomorphs after anhydrite, which would indicate extreme shallow water conditions are known. This negative evidence together with the study of the caninioids previously presented, indicates conclusively that the caninioid populations were not marginal to any shoreline but may have occupied the dysphotic zones. Other factors which have ultimately to be taken into account are those of a climatic nature whose effects can only be indirectly inferred. It is probable that the Viséan carbonate sediments of north-west Ireland accumulated under climatic conditions similar to those found in the tropical climatic belts of the present time and to be observed in such classic carbonate areas as the Bahamas. In this area seasonal effects occur when an increase in rainfall causes a sedimentary influx coupled with a decrease in salinity (cf. Squires 1958, pp. 234–5) and it is conceivable that similar effects occurred in Viséan times. However, absence of marked concentrations of growth-rings in the north-west Irish Viséan caninioids seems to indicate no seasonal control of growth although the effects of exceptionally severe tropical storms cannot be eliminated entirely.

There are wider implications to be drawn from the abundant development of Viséan caninioid assemblages in north-west Ireland. Thus favourable conditions in Ireland seem to reflect favourable conditions globally in tropical climatic belts as comparable caninioid developments occur in similar horizons not only in north-west Europe but also in the U.S.S.R. and North America. So apart from the local factors which influenced initial colonization and survival there were wider controls whose nature can only be very indirectly inferred at the present time. It is evident that caninioid growth in one and in all the recurrent assemblages was an extremely complex process which is not unique to Viséan times. In other systems, e.g. Middle Devonian of New York (Oliver 1951) and the Eifel (Birenheide 1962*a*, *b*, *c*, 1963) and the Silurian of Norway (Kiaer 1906) earlier but similar complexities governing the distribution of solitary corals seem to have been present.

Acknowledgements. The author is indebted to Dr. F. M. Broadhurst whose comments provoked this study and to Dr. J. M. Hancock and Professor G. Y. Craig whose stimulating comments offered further encouragement. Too many palaeontologists and geologists to list have afforded helpful criticisms of the manuscript but their aid is gratefully acknowledged. Specialist information on hydraulics, caninioid systematics, and the behaviour of modern corals was kindly supplied by Mr. M. J. Kenn, Drs. O. A.

Dixon, D. R. Squires, and Professor T. F. Goreau. The departmental secretarial and technical services are gratefully acknowledged. The research was facilitated by a grant from the University of London Central Research Fund, and the Geological Society of London's Daniel Pidgeon Fund.

REFERENCES

BAKUS, G. J. 1968. Sedimentation and benthonic invertebrates of Fanning Island, Central Pacific. *Mar. Geol.* **6**, 45–51.

BIRENHEIDE, R. 1962*a*. Siedlungs- und Wuchsformen mitteldevonischer Korallen aus der Eifel. *Natur Mus. Frankf.* **92** (1), 21–8, 9 figs.

—— 1962*b*. Entwicklungs-und umweltbedigte Veränderungen bei den Korallen aus dem Eifeler Devon. Teil I. Ibid. **92** (3), 87–94, 7 figs.

—— 1962*c*. Entwicklungs- und unweltbedingte Veränderungen bei den Korallen aus dem Eifeler Devon. Teil II. Ibid. **92** (4), 134–8, figs. 8–12.

—— 1963. Standortwechsel von Korallen aus dem Eifelmeer. Ibid. **93** (10), 405–9, 3 figs.

BRUNTON, H. 1966. Predation and shell damage in Viséan brachiopod fauna. *Palaeontology*, **9**, 355–9, pl. 60.

DIXON, O. A. 1970. Variation in the Viséan coral *Caninia benburbensis* from Northwest Ireland. Ibid. **13**.

EDMONDSON, C. H. 1929. Growth of Hawaiian Corals. *Bull. Bishop Mus. Honolulu*, **53**, 1–38, 5 pls.

GEORGE, T. N., and OSWALD, D. H. 1957. The Carboniferous rocks of the Donegal syncline. *Quart. J. geol. Soc. London*, **113**, 137–79, pl. 14–16.

GOLDRING, R. 1962. The trace fossils of the Baggy Beds (Upper Devonian) of North Devon, England. *Paläont. Z.* **36**, 232–51.

GOREAU, T. F., and GOREAU, NORA I. 1959. The physiology of skeleton formation in corals: II. Calcium deposition by hermatypic corals under various conditions in the reef. *Biol. Bull.* **117**, 239–50.

HUBBARD, J. A. E. B. 1966. Population studies in the Ballyshannon Limestone, Ballina Limestone and Rinn Point Beds (Viséan) of NW. Ireland. *Palaeontology*, **9**, 252–69, pl. 40–41.

KIAER, J. 1906. Das Obersilur im Kristianagebiete. *Videnskabs-Sels-kabets Skrifter, I, Math.-Naturv. Klasse* (Oslo).

MA, T. Y. H. 1937. On the seasonal growth in Palaeozoic tetracorals and the climate during the Devonian period. *Palaeont. Sinica*, Ser. B, **2**, fasc. 3, 1–106.

MANTON, S. M. and STEPHENSON, T. A. 1935. Ecological surveys of coral reefs. Great Barrier Reef Exped. 1928–29, *Sci. Rept. Brit. Mus.* (*N.H.*), **3** (10), 274–312, 2 figs. 16 pl.

MARSHAL, S. M., and ORR, A. P. 1931. Sedimentation on Low Isles Reef and its relation to coral growth: Great Barrier Reef Exped. 1928–29. Ibid. **1** (5), 94–133, 7 figs.

OLIVER, W. A. 1951. Middle Devonian coral beds of central New York. *Amer. Jour. Sci.* **249**, 705–28, 2 pl. 6 figs.

OSWALD, D. H. 1955. The Carboniferous rocks between the Ox Mountains and Donegal Bay. *Quart. J. geol. Soc. Lond.* **111**, 167–86, pl. 11.

RØØS, P. J. R. 1967. *Growth and occurrence of the reef coral* Porites astraeoides *Lamark in relation to submarine radiance distributions*. (Academic proefschrift) Utrecht.

SQUIRES, D. F. 1958. Stony corals from the vicinity of Bimini, Bahamas. *Bull. Am. Mus. Nat. Hist.* **115**, 217–62.

TRASK, P. D. 1931. Compaction of sediments. *Bull. Am. Assoc. Pet. Geol.*, **15**, 271–6.

WELLS, J. W. 1937. Individual variation in the Rugose coral species *Heliophyllum halli* Edwards and Haime. *Palaeontogr. amer.* **2** (6) 20 pp. 1 pl.

—— 1963. Coral growth and geochronometry. *Nature, Lond.* **197**, 948–50.

WYNNE, A. B., 1864. On the geology of parts of Sligo, etc. *Journ. Geol. Soc. Dublin*, 33–41.

—— 1885. Geological Survey of Ireland. Explanatory memoir to accompany sheets nos. 42 and 43.

YOUNGE, C. M. 1935. Studies on the biology of Tortugas corals. I. Observations on *Meandra areolata* Linnaeus. *Pap. Tortugas Lab.* **29**, 185–98, pl. 1–3.

JULIA A. E. B. HUBBARD,
Department of Geology
King's College (London University)
Strand
London, W.C.2

Final typescript received 14 July 1969

A NEW CAPITOSAURID LABYRINTHODONT FROM EAST AFRICA

by A. A. HOWIE

Abstract. Cranial and post-cranial amphibian remains from two localities in the Middle Triassic Manda Formation of the Ruhuhu area of Tanzania are described. A new species of *Parotosaurus*, *P. pronus* is proposed.

In the skull, the pterygoid canal is of particular interest and may have carried the VIIth nerve. The lower jaw has a well-developed pre-articular (hamate) process with behind it a pre-articular fossa.

The neural arches, intercentra, and ribs show considerable regional variation. Ossified pleurocentra are described for the first time in a capitosaur.

The dermal pectoral girdle is massive. Large trabeculae on the interclavicle and clavicles have been interpreted as a ridge system to resist a forward pull on the dorsal process of the clavicle by a cleidomastoideus muscle. Both fore and hind limbs are poorly ossified.

The problem of jaw opening is discussed in capitosaurs and brachyopids. It is thought that in capitosaurs a cleidomastoideus muscle, attached to the tabular horn and to the clavicle, was used to raise the skull, while the depressor mandibulae muscle was used to lower the mandible. In brachyopids the first part of this system was probably an occipito-vertebral muscle.

The retro-articular process and the stereospondylous vertebral column are considered.

Labyrinthodonts have been known since Jaeger in 1824 figured remains of a skull and vertebral column which were later recognized as belonging to the same animal, *Mastodonsaurus giganteus*. Subsequently, labyrinthodonts from Carboniferous, Permian, or Triassic rocks have been recovered from most parts of the world.

Since Jaeger's account of *Mastodonsaurus*, capitosaurs, in the broad sense, have been described by many authors. Contributions other than taxonomic descriptions of new species have been made especially by Watson (1919, 1951, 1958, 1962), Huene (1922), Nilsson (1937, 1943 *a*, *b*, 1944), and Romer (1947). Welles and Cosgriff (1965) revised the group and placed all members of the Family Capitosauridae in three genera, *Parotosaurus*, *Paracyclotosaurus*, and *Cyclotosaurus*, thus following Romer (1947) in excluding *Mastodonsaurus* from the family.

Capitosaurs arose in the Lower Triassic and became extinct before the Jurassic. Adults range in size from a skull length of 7 cm. in a specimen from Australia being described by Cosgriff, to approximately 70 cm. in the Upper Triassic *Cyclotosaurus hemprichi*, the latter indicating a total length of at least 280 cm.

Watson emphasized various trends associated with the evolution of the capitosaurs from Lower, through Middle to Upper Triassic times. The more obvious are: an increase in size; a decrease in ossification, especially of the brain-case and limbs; an increase in dorso-ventral flattening of the skull; and a tendency to close the otic notch. This last character, especially, divides the family, so that the Lower Triassic forms are parotosaurs with open otic notches, while the Upper Triassic types are cyclotosaurs with closed otic notches. The third capitosaur genus, *Paracyclotosaurus*, is Upper Triassic, and was considered by Watson (1958) to have a closed otic notch. Although post-cranial skeletons have rarely been described in capitosaurs, one noticeable trend throughout the group is a gradual change from a rhachitomous vertebral column to

[Palaeontology, Vol. 13, Part 2, 1970, pp. 210–53, pl. 45.]

a neorhachitomous, and finally to a stereospondylous one at least in the anterior part of the column.

The parotosaurs described here were collected by Dr. F. R. Parrington in the Manda Formation of the Ruhuhu Coalfields in Tanzania. They were mentioned in 1958 and 1962 by Watson who thought they could be ancestral to a line of deep-skulled parotosaurs, and by Welles and Cosgriff in 1965, and are especially noteworthy for the large amount of post-cranial material associated with two of the skulls.

Capitosaurs are thought to have been slow-moving animals, living on the bottom of swamps or shallow streams. The huge size of the later forms, accompanied by a decrease in ossification has led to speculation about the function of various parts of their anatomy. Watson has discussed problems concerning the opening of their jaws, and has emphasized the general flattening, together with the enormous development of dermal pectoral girdle, and several authors have commented on the strange mixture of rhachitomy and stereospondyly in the vertebral column.

The Manda beds are regarded by Watson (1958, 1962), Parrington (1946), and Crompton (1955) as being of Middle Triassic age and a detailed summary of the stratigraphy of the area is given by Charig (1963).

Material. The capitosaur material described was collected from two of Stockley's localities in the Manda Formation. Stockley's B 9, Mkongoleko, produced Dr. Parrington's field no. 48 which consists of two labyrinthodont skulls with mandibles, a labyrinthodont pterygoid, and a large amount of labyrinthodont post-cranial material, the holotype of a new pseudosuchian (this specimen is being described by Dr. A. J. Charig), and some problematical bones which are here taken to be two ischia and six sacral ribs of an early Triassic reptile. An additional labyrinthodont skull (field no. 135) of the same species as the above was recovered from Stockley's B 26, Gingama.

The labyrinthodont material will be referred to below by Parrington's field numbers. Thus the two skulls from Mkongoleko become F.R.P. 48 I (the larger) and F.R.P. 48 II (the smaller).

The material from Mkongoleko was preserved in a sandstone, undoubtedly the 'pink and purple felspathic sandstone' noted by Stockley (1932) as characteristic of the Manda Beds. The Gingama specimen is grey in colour and its matrix is a 'consolidated marl'.

Although much of the skull material is fragmented, the pieces are generally well preserved. Skull F.R.P. 48 I has almost perfectly preserved ornament but the individual bones have broken apart at their sutures, so their exact interdigitations are not always clear.

Skull F.R.P. 135 has weathered dorsally. In this specimen it was impossible to follow most suture lines because the bone and matrix were identical in colour, and because the bone is covered with a reticulum of suture-like cracks. However, the skull is particularly well preserved in the brain-case area.

All three skulls are a little dorso-ventrally distorted.

The post-cranial material is equally well preserved although pre-sacral neural arches tend to have their spines separated, while several post-sacral neural arches are split in half longitudinally. Only one intercentrum is longitudinally split.

While the skulls, lower jaws, and post-cranial material from F.R.P. 48 were not found in actual association, they were the only labyrinthodont remains recovered from the particular site, and as they all appear to belong to parotosaur-like labyrinthodonts of a comparable size, the post-cranial material is taken to belong to the two skulls.

Preparation of the specimens was carried out with a dental mallet, and an airbrasive unit, and they were reinforced with glyptal.

Parotosaurus pronus sp. nov.

The labyrinthodont material contained in F.R.P. field locality 48 is considered to belong to a new species of parotosaur which is named *P. pronus*, the specific name referring to the fact that the animal is dorso-ventrally flattened.

Holotype. A skull, no. 48 I: F. R. Parrington collection, University Museum of Zoology, Cambridge.

Paratypes. A second skull, 48 II. Four half mandibles. Labyrinthodont post cranial material designated by letters. All F. R. Parrington collection, University Museum of Zoology, Cambridge.

Referred specimen. A skull, no. 135: F. R. Parrington collection, University Museum of Zoology, Cambridge.

Type locality. F. R. Parrington field locality B 91, at Stockley's B 9, Mkongoleko, Ruhuhu Valley, Tanzania.

Horizon. Manda Formation (K8), *Teleocrater* Zone (as proposed by Charig, 1963), Middle Trias.

Diagnosis. A parotosaurus with a skull broad posteriorly (B:L approximately 75) (indices as used by Welles and Cosgriff (1965)—B = breadth of skull across quadratojugals, L = skull length, S = breadth of snout one-fifth of the skull length from the tip, H = height of the postparietals above the parasphenoid), but tapering anteriorly (S:L approximately 32); skull deep posteriorly (H:B approximately 23); nares elongate, lateral, long axes parallel to skull border; septomaxilla present; orbits close together and separated by a shallow depression, well posterior, oval, long axes parallel to midline; frontal and jugal enter orbital margin; pineal foramen rectangular, just posterior to hind border of orbits; otic notches semiclosed with tabular horns distinctive, expanded distally towards squamosal; supratemporal excluded from otic notch; posterior skull border concave.

Anterior palatal vacuity reniform; exoccipitals barely exposed on palate; pterygoids meeting palatines; pterygoid with facet for jaw articulation.

Processus lamellosus of exoccipital present.

Lower jaw with large pre-articular process and pre-articular fossa.

Vertebrae not longitudinally compressed; pre-sacral neural arches with antero-ventral nodules developed; intercentra crescentic; some pleurocentra ossified.

Ribs all with uncinate processes; most with distal expansion; all with 'knee' bend.

Dermal pectoral girdle massive, flattened; dorsal process of clavicle well developed and inclined inwards anterodorsally, scapulocoracoid poorly ossified.

Humerus tetrahedral, poorly ossified.

Pelvic elements separate; pubis apparently unossified.

Hind limb poorly ossified; femur with well-developed adductor ridge.

Skull

The skull of *Parotosaurus pronus* has the bone complement and shape characteristic of the genus as described for *P. peabodyi* by Welles and Cosgriff (1965).

One character distinguishing *P. pronus* from other parotosaur species is the shape of the tabular horn (text-fig. 1): it is expanded anteriorly as well as laterally towards the squamosal so that distally the horn is nearly one-third wider than the neck which separates it from the body of the tabular.

EXPLANATION OF PLATE 45

Parotosaurus pronus sp. nov. Type skull F.R.P. 48 I. Dorsal view. The exoccipital bones have been displaced posteriorly.

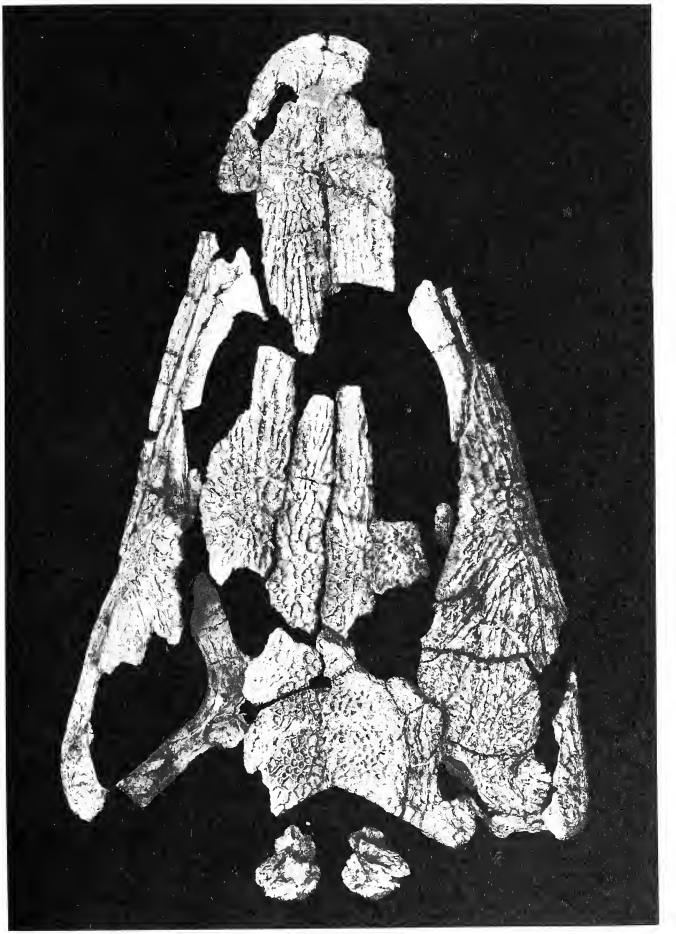

HOWIE, *Parotosaurus*

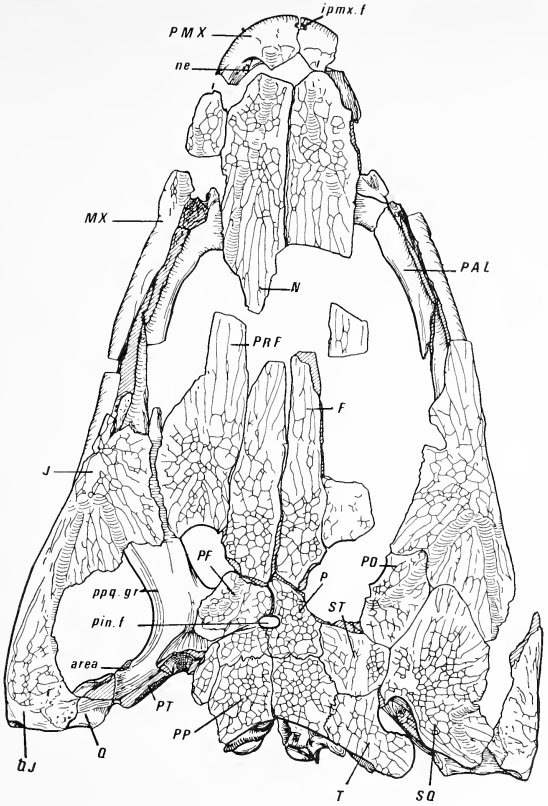

TEXT-FIG. 1. *Parotosaurus pronus* sp. nov. Skull 48 I. dorsal view (×¼).

A second distinction is a roughened area of bone on the quadrate ramus of the pterygoid in an internal position adjacent to the quadrate (text-figs. 1, 9). This appears to have been a continuation on to the pterygoid of the articular surface of the screw-shaped quadrate condyle.

Excellent preservation in some parts of the occiput and the area around the brain-case reveal several new features of capitosaur anatomy. Particularly prominent on the occiput are a pair of tabular ridges. Below the postero-medial edge of each tabular is a

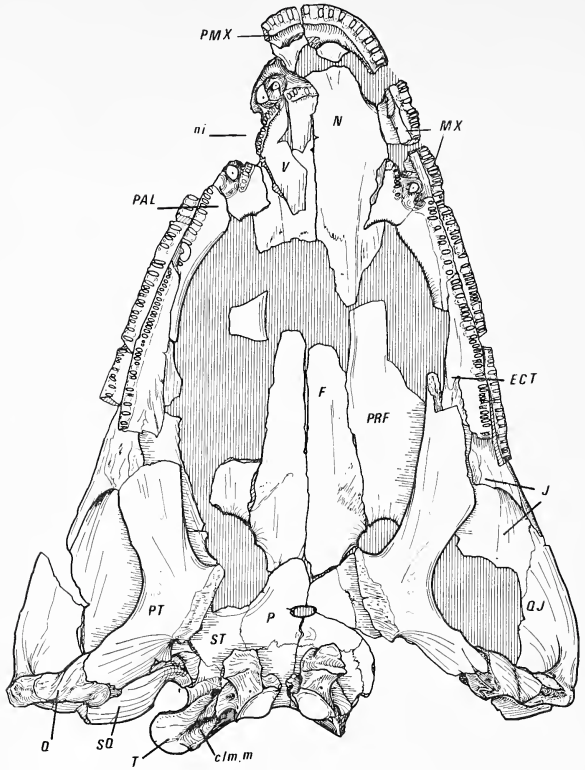

TEXT-FIG. 2. Skull 48 I. palatal view ($\times \frac{1}{2}$).

rugose ridge which runs across the occiput, narrows, and is continued on to the post-parietals. This would have served, together with a small rugosity immediately below the distal end of the tabular, as an insertion point for some of the occipito-vertebral muscles. However, the most conspicuous ridge on the tabular runs along the paroccipital process (text-figs. 3, 5) and was the insertion for the cleidomastoideus muscle (see below). In anterior view (that is, from inside the otic notch) it can be seen that this ridge is confluent with the anterior wall of the paroccipital process. Also in this view, a further ridge can be seen running down the paroccipital process along what appears to be the posterior border of the subtympanic area.

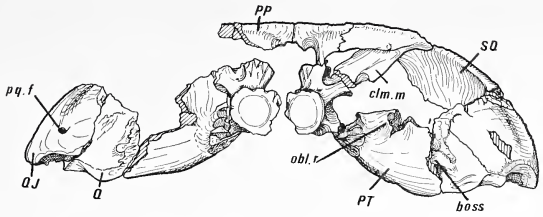

TEXT-FIG. 3. Skull 48 I. occipital view ($\times \frac{1}{4}$).

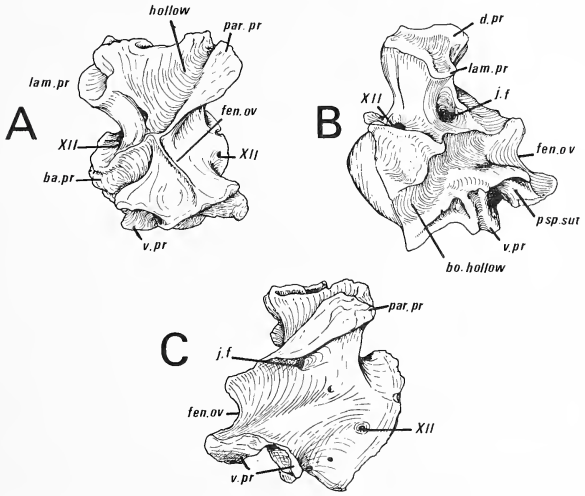

TEXT-FIG. 4. Skull 48 I. Left exoccipital ($\times \frac{2}{3}$). A, anterior view; B, medial view; C, lateral view.

At their suture on the paroccipital process both the tabular and exoccipital are hollowed: this space was filled in life by the cartilaginous opisthotic which was not exposed on the occiput. An antero-ventral expansion of the tabular has an unfinished surface and a space between it and the paroccipital process is hollowed and presumably also contained opisthotic.

The exoccipitals of the type skull are shown in three views in text-fig. 4. Text-fig. 4A shows the jugular foramen and the foramen for nerve XII entering the exoccipital from the cavity occupied by the medulla oblongata while text-fig. 4C shows their exits. Also in text-fig. 4A can be seen a longitudinal hollow for the lateral edge of the basioccipital

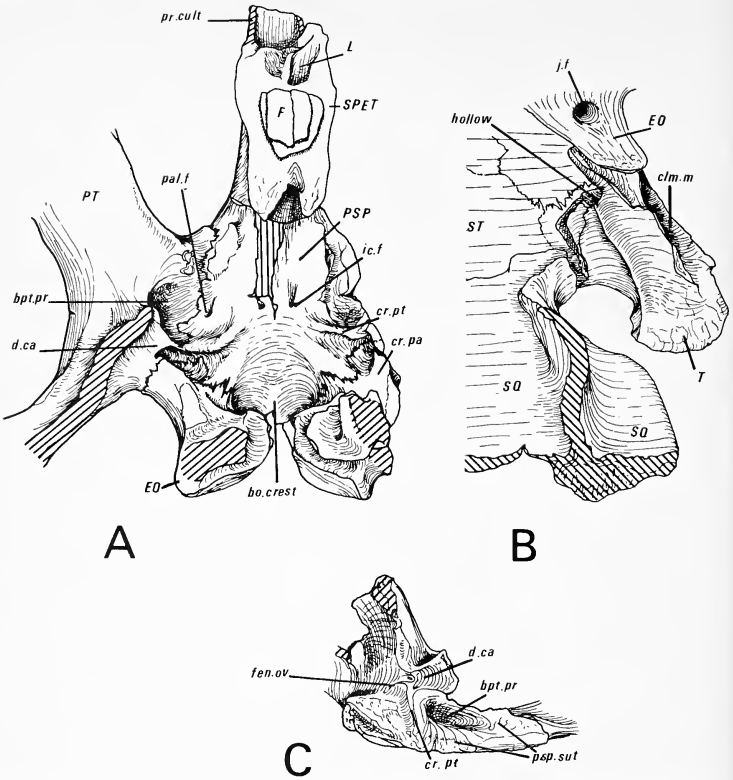

TEXT-FIG. 5. Skull ($\times \frac{1}{2}$). A, Skull 48 II, dorsal view of parasphenoid area; B, Skull 48 I, ventral view of otic notch; C, Skull 48 I, medial view of pterygoid body.

cartilage, and below this an area of suture with the parasphenoid. Anteriorly, beneath the base of the paroccipital process, an oblique ridge which connects the lateral external part of the exoccipital with the inner brain-case area is the median edge of the fenestra ovalis.

Beside the exoccipital, the pterygoid curves anteriorly to form a cupped region beneath the otic notch—the subtympanic cavity—whose postero-lateral edge is the beginning of an oblique ridge. This ridge projects less than the 'otic flange' described by Watson (1962) and in specimen 135 is recurved so that it just fails to meet the ptery-

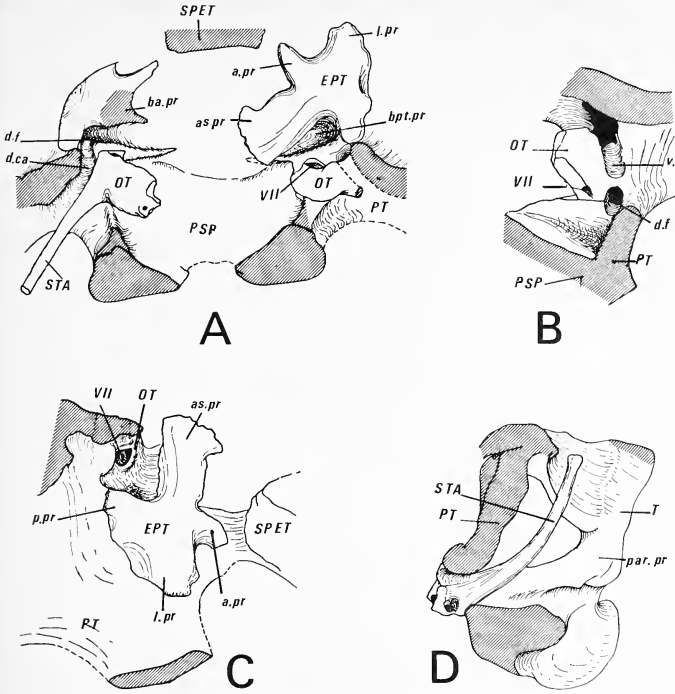

TEXT-FIG. 6. Skull 135 ($\times \frac{1}{2}$). A, dorsal view of parasphenoid area; B, anterior view of left otic area; C, antero-latero-dorsal view of right epipterygoid; D, antero-latero-ventral view of left stapes and surrounding area.

goid dorsally to form a canal. From the front of the subtympanic cavity a semicircular groove leads inwards above the exoccipital suture and ends dorsal to the conical recess in the pterygoid for the basipterygoid process of the basisphenoid. This groove is referred to as the dorsal canal of the pterygoid and its opening above the conical recess is the dorsal foramen (text-figs. 5, 6). Watson (1919, fig. 16) shows a similar groove but does not describe it.

A foramen for the vena capitis dorsalis enters skull 135 just above the dorsal canal, while in the type skull immediately below the canal and behind the parapterygoid crista, is a sharp lip of bone which marks the lateral edge of the fenestra ovalis.

In addition to the sphenethmoid complex, specimen 135 has part of the stapes, otic regions, and epipterygoids preserved on both sides (text-fig. 6). The right epipterygoid

is almost complete and differs from that of *P. peabodyi*, rather resembling the ones described by Wilson (1941) in *Buettneria*. A medial basal process of the epipterygoid (text-fig. 6A) is pierced by a foramen which probably carried the profundus nerve (V_1) and also the palatine branch of nerve VII. Just posterior to this basal process nerve V must have divided so that V_1 passed in front of the ascending process of the epipterygoid, and V_2 behind it, but there is no trace of a groove for the gasserian ganglion found in this area by Watson (1958).

Little interpretable structure can be seen in the stapes (text-fig. 6D) as its proximal end cannot be separated from the otic ossification. The head of the stapes is thus fused into the fenestra ovalis which is formed by the otic bones dorsally, the pterygoid laterally, and the exoccipital medially.

The otic ossification attached to the stapes is probably the pro-otic but it has a less well-defined shape than the pro-otic described by Welles and Cosgriff in *P. peabodyi*. It lies medially to the quadrate ramus of the pterygoid and postero-dorsally to the parapterygoid crista (which forms the rear wall of the conical recess for the basipterygoid process of the basisphenoid). On the left, laterally, the dorsal canal between the pro-otic and the underlying pterygoid marks the lateral limit to the otic area. The more antero-medial section of the pro-otic, above the parapterygoid crista is thin antero-posteriorly, and is perforated by a foramen which probably carried part of the VIIth nerve before it curved posteriorly to exit from the skull. Bystrow and Efremov (1940) in their restoration of the brain and cranial nerves in *Benthosuchus* show nerve VII passing into the pro-otic in a similar position as does Francis (1934, plate X) in the salamander.

Separate from and posterior to the otic region joined to the stapes is an opisthotic ossification which still forms a core to the paroccipital process.

Lower jaws (text-fig. 7)

The bones of the lower jaw largely follow the typical parotosauran pattern as shown by Welles and Cosgriff. One difference is that in lateral view in *P. pronus* the most posterior part of the postsplenial lies ventral to the anterior wedge of the angular, the reverse of the condition in *P. peabodyi*.

The pre-articular in *P. pronus* occupies all the median edge of the adductor fossa, and here its hinder end is drawn dorsally into an extensive pre-articular (hamate) process which rises 3·5 cm. above the fossa. The process is transversely thickened and is excavated medially by the leading edge of a pre-articular fossa. A flange of the hamate process forming the dorso-medial wall of the pre-articular fossa is continued forward inside the jaw parallel to, but a centimetre below, the margin of the adductor fossa. The pre-articular fossa has not been described in other labyrinthodonts although it was present in an unidentified mandible cf. *Parotosaurus* in Cambridge (F.R.P. 116). In other better-ossified labyrinthodonts which have a hamate process (e.g. *Paracyclotosaurus*, *Rhineceps*, *Mastodonsaurus* (Wepfer 1923)) the fossa has been filled by a more anterior ossification of Meckel's cartilage than is seen in *P. pronus*. It seems likely, as suggested by Nilsson (1943*b*) that there was also a posterior extension of Meckel's cartilage running beneath the angular and ending just medial to the most posterior point of the retro-articular process. An interior flange of the angular noted by Nilsson in *Aphaneramma* is present in *P. pronus* as a nodule of bone on the floor of the Meckelian space at the centre of ossification of the angular.

The articular forms a screw-shaped glenoid fossa for articulation with the double quadrate condyle of the skull, the articular area being increased by the hamate process which articulates with the roughened patch on the pterygoid adjacent to the quadrate.

Teeth on the skull and mandible have the typical capitosaur shape and arrangement. Alternation of teeth with replacement pits is regular on the premaxillae of all three specimens, but becomes less regular in more posterior areas. Here there seems little obvious order of teeth and pits, sometimes as many as twenty-three teeth appearing without a gap. In skull F.R.P. 48 II and in one of the mandibles work with an airbrasive

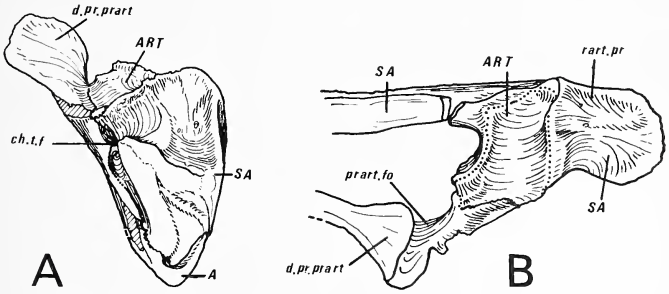

TEXT-FIG. 7. Lower jaw ($\times \frac{1}{2}$). A, posterior view; B, dorsal view of posterior end.

unit revealed tiny replacing teeth in some of the pits. These occurred in areas where pits regularly alternate with fully formed teeth and usually several replacing teeth are found in a series. Often the mature teeth between pits containing replacement teeth are old and appear to be being resorbed, showing the characteristic pattern described by Bystrow (1938) for aged teeth. The enamel in the small replacing teeth is unconvoluted.

Preparation of a section of left mandible for *Lydekkerina* sp. (specimen F.R.P. 1964/34) revealed replacement teeth in almost every pit. These were found in all stages of development from minute to mature teeth. One tooth was emerging from a partly resorbed mature tooth, while in at least five instances, two teeth were found in a single pit. One replacement tooth was found on a coronoid bone.

Reconstruction of the skull and mandible (text-figs. 8, 9)

In the skull reconstruction the parasphenoid and septomaxilla, missing in the type skull, were restored from skull 48 II.

With the articular in place against the quadrate it can be seen that the teeth of the lower jaw must fit in between the two upper tooth rows. It is evident that in this position the upper and lower jaw margins will be separated by at least the depth of the lower teeth, so that in the jaw closed position the three rows are aligned. It can be seen in the present reconstruction that the dentary tusks clear the palate without needing the extra depth afforded by the anterior palatal vacuity. Text-fig. 9 shows that the tooth rows do not meet posteriorly: this region was probably enclosed laterally by a flap of

skin which would prevent food escaping from the mouth. A similar situation can be seen in Watson's reconstruction of *Paracyclotosaurus*.

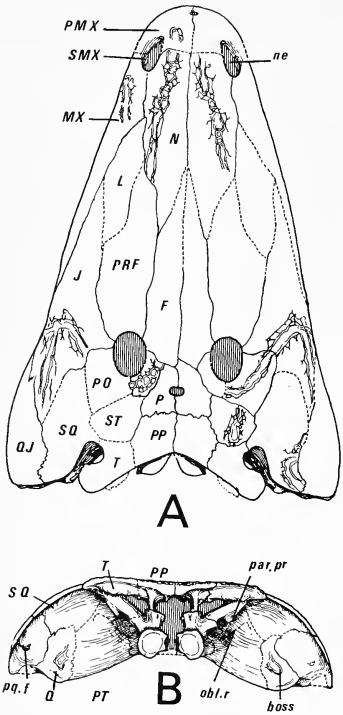

TEXT-FIG. 8. *Parotosaurus pronus* sp. nov. Restoration of skull 48 I (×⅓). A, dorsal view; B, occipital view.

Post-cranial skeleton

Vertebral column. Among the capitosaurs, *Paracyclotosaurus* and *Mastodonsaurus* (Huene 1922) have been preserved with their vertebral columns almost intact, but in other forms only scattered, dissociated elements remain.

The vertebrae in specimen F.R.P. 48 probably belonged to two animals but for descriptive purposes they are treated as a single, incomplete vertebral column. Neural arches, intercentra, and pleurocentra are present, and some regional differentiation can be seen in them, especially in the neural arches. The latter have been lettered and the intercentra and pleurocentra numbered to prevent them being inadvertently linked.

Atlas and axis are not represented in the collection.

Neural arches. One of the more anterior presacral neural arches, arch C (text-fig. 10), probably supported a massive rib above the pectoral girdle. Its spine is split longitudinally and laterally bears a vertical roughened area which marks the position of the segmental boundary (Olsen 1936, Panchen 1967). Beneath the neural spine the limits of the neural canal are clearly defined by dorsal and ventro-lateral ridges: midway along the canal on each side is a small foramen.

On the underside of the body of the neural arch on either side of the neural canal, and extending laterally as far as the transverse processes, is an almost rectangular facet (which Watson (1958) notes is for articulation with the pleurocentrum), while, almost continuous with this but on the anterior surface of the arch, is a further facet. This is deep medially beside the neural canal, but tapers laterally, and is separated from the prezygapophysis by a marked recess. This anterior facet is apparently absent in *Paracyclotosaurus* but is present in other rhachitomes and neorhachitomes and some stereospondyls. It is said (Nilsson 1943*a*) to be an articular facet for the pleurocentrum belonging to the vertebra in front. A pronounced ridge bounds both ventral and anterior

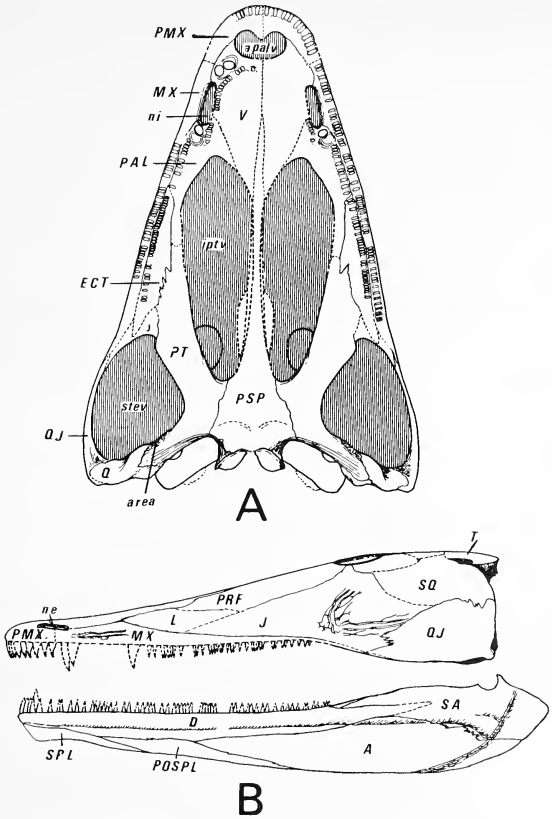

TEXT-FIG. 9. *Parotosaurus pronus* sp. nov. Restoration of skull 48 I ($\times \frac{1}{6}$). A, palatal view; B, lateral view of skull and lower jaw.

facets and separates them from the neural canal medially, from the dorsal parts of the arch body anteriorly and posteriorly, and from the transverse process laterally. Both facets are cartilage finished, but in a slight depression between them, towards the midline on each side, is a projecting nubbin which has a surface of finished bone. The bone lamellae of this knob lie in the same plane as the body of the arch, almost at right angles to the longitudinal axis of the vertebra. These antero-ventral nubbins are developed to

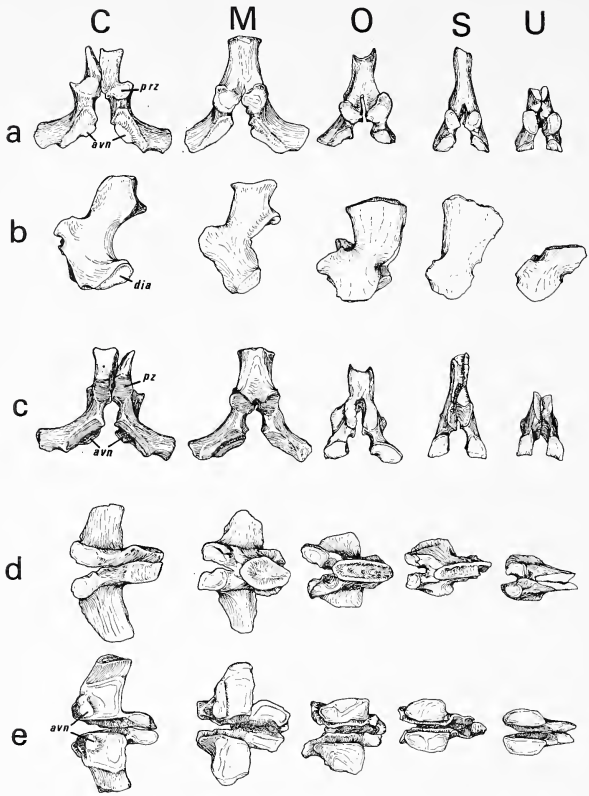

TEXT-FIG. 10. Neural arches. C, M, O, S, U. ($\times \frac{3}{4}$). *a*, anterior views; *b*, left lateral views; *c*, posterior views; *d*, dorsal views; *e*, ventral views. Where necessary in this and the following figures bones have been reversed so that all views are of the left side.

some extent in most presacral vertebrae. They vary in size and shape from a small (4 mm.) rounded nubbin, to a raised strip of bone tapering from the midline and completely separating the ventral and anterior neural arch facets. No reference can be found to them in other labyrinthodonts and they were not found in specimens of *Eryops* and *Lydekkerina* examined, or in *Paracyclotosaurus*.

The sacral neural arch, K (text-fig. 11B) has a low spine with poorly ossified zygapophyses, strongly developed body arches, and small antero-ventral bone nubbins. There is a precocious development of the diapophyses so that they are almost circular in lateral view and the transverse processes are correspondingly thickened.

Neural arch O (text-fig. 10), from the anterior caudal area, is remarkable for the altered shape of its neural spine. This is taller, longer, and better ossified than in the more anterior arches, and is narrower at the base than it is dorsally. Its post-zygapophyses are poorly developed and appear merely as swellings of the posterior wall of the neural spine immediately above the neural canal. Laterally the arch body is reduced so that it hardly exceeds the neural canal in width. On the left, the ventral and anterior facets have almost merged, with only a low swelling between. There is no transverse process, but a raised, down-facing, triangular facet lateral to the ventral articular area probably represents the diapophysis.

In the more posterior caudal arches like arch S (text-fig. 10), the post-zygapophyses have disappeared, but in the appropriate place the lower edges of the neural spine bend outwards as if to form a lateral boundary to a pair of wholly cartilaginous facets.

The more helpful criteria used in arranging the presacral neural arches are as follows: from anterior to posterior there can be seen

1. An increase in the angle between the neural spine and the body of the vertebra carrying the transverse process,
2. A decrease in length of the transverse process,
3. 1 and 2 together produce a narrowing of the total width of the neural arch,
4. A decrease in length and width of the diapophyses: this follows from a decrease in size of the ribs,
5. A slight over-all decrease in size,
6. On these criteria, presacral vertebrae with split arches fall anteriorly. This position is supported by observation of the arrangement of *Paracyclotosaurus* in which arches 1–12 are wholly or partially split.

Characters used in ordering the caudal neural arches are as follows:

1. A decrease in over-all size accompanied by a decrease in ossification, especially of the post-zygapophyses,
2. A decrease in the size of the body of the arch and transverse processes, until the latter disappear,
3. An increase in length of the spine in those arches with transverse processes, and, thereafter, its gradual decrease.

The most posterior caudals are graded purely on size.

Intercentra. It was found that *P. pronus*'s intercentra could be divided into two categories, the first containing the more anterior intercentra, and the second, the more posterior ones.

An example of the first category is intercentrum no. 7 (text-fig. 11A). This is characteristically wedge shaped in lateral view and crescentic in anterior and posterior views. Seen from in front, the intercentrum is much less massive than anterior intercentra of *Paracyclotosaurus*, its dorsal-most parts being pointed, not dorsally flattened. There

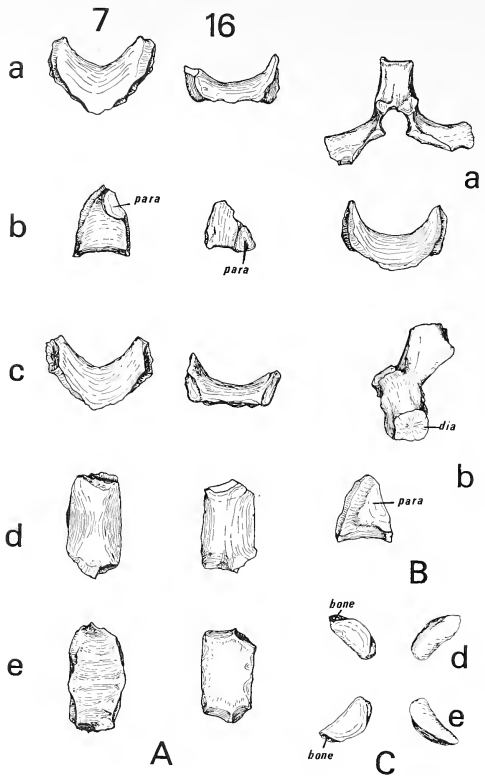

TEXT-FIG. 11. A, Intercentra 7, 16. *a*, anterior view; *b*, lateral view; *c*, posterior view; *d*, dorsal view; *e*, ventral view. B, Sacral arch K and intercentrum. *a*, anterior view; *b*, lateral view. C, Pleurocentra 1 and 2. *d*, dorsal view; *e*, ventral view. ($\times\frac{3}{8}$).

are no indications that the element is beginning to ossify around a notochord as it was in the anterior vertebrae of some Upper Triassic capitosaurs.

The ventro-lateral surface of the intercentrum is of finished bone and is concave antero-posteriorly. It is traversed by three longitudinal ridges which are similar to, though much smaller than, ridges seen beneath *Eryops* intercentra.

Between this ventral surface and the dorsal convex one there is often a groove which

runs on the anterior margin of the intercentrum. Posteriorly, a similar groove borders the intercentrum below the level of the parapophyses.

The parapophysis, the oval facet for articulation with the capitulum of the rib, is much better developed than its equivalent in *Eryops*, but less well developed than anterior *Mastodonsaurus* parapophyses. The facet in *P. pronus* lies at the back of the intercentrum in a dorso-lateral position. It is surrounded by a ridge which is especially well developed anteriorly, so that there is often a distinct groove between the parapophysis and the anterior edge of the bone. All surfaces of the intercentrum except the concave ventral and lateral ones were finished in cartilage.

An example of the second category of intercentrum is seen in no. 16 (text-fig. 11A). It differs markedly from no. 7 in being flattened ventrally so that its lateral faces have become distinct from the ventral face. It is shallower, and less well ossified than the more anterior intercentra, and only a small area on its ventral surface appears to be of finished bone. The parapophyses have moved ventrally so that their lower edges project below the ventral line of the bone and have become triangular, with the base of the triangle lying ventrally and the hypotenuse lying posteriorly. In this position the parapophysis is lying in a wider part of the intercentrum, and so the groove between it and the anterior border of the bone has become correspondingly wider.

No. 14 may belong to the sacral vertebra (text-fig. 11B). It is flattened, but not to such an extent as the apparently more posterior caudals, and its parapophyses, which are already triangular, are larger than any others in the column.

Trends used to position the intercentra are as follows: from anterior to posterior

1. There is a decrease in over-all size of intercentra.
2. There is a change in shape from deeply crescentic and ventrally pointed anteriorly to ventrally flattened and shallow posteriorly.
3. The parapophysis changes in position from dorsal to ventral, in shape from oval to triangular, and its size first decreases and then increases again with the change to triangular shape.

No haemal arches are preserved.

Pleurocentra (text-fig. 11C). Although their presence has often been postulated, and the structure of the intercentra indicate that they were present, though probably cartilaginous, ossified pleurocentra have not previously been described in the Capitosauridae. Watson (1958) has dotted them in in *Paracyclotosaurus*. According to Romer (1947) they were ossified in *Benthosuchus*, but Bystrow and Efremov (1940) noted their absence in that animal. Pleurocentra are present in many of the neorhachitomous Rhinesuchoidea, especially notable examples being *Uranocentrodon* (van Hoepen 1915), *Lydekkerina*, and *Sclerothorax* (Huene 1932). However, descriptions of pleurocentra have usually been brief, and they are commonly illustrated in side view only. Nilsson (1943*a*) does illustrate pleurocentra of the trematosaur, *Lyrocephalus*, in several views, and, except that they are less elongate, their shape is similar to the pleurocentra of *P. pronus*.

Although they were probably present throughout the column, only nine pleurocentra were found. The condition of preservation and degree of ossification of these varies, but it is possible to establish a common structure. Most surfaces are of unfinished bone. The better-formed elements have the median end expanded, the lateral end bluntly

pointed, and are narrow dorso-ventrally, so that they are roughly lens-shaped. The dorsal face is flat for articulation with the postero-ventral facet on the neural arch, while the ventral face bulges a little especially towards the midline. These two faces are separated laterally by a narrow convexly curved surface, but medially they meet in a line which is a little concave, presumably to curve around the dorsal part of the notochord. On the larger pleurocentra is a small area of finished bone which faces antero-laterally: in the smaller pleurocentra this facet is often unfinished. In some cases this area is concave and in one case it seems to be double, with one area lying above and

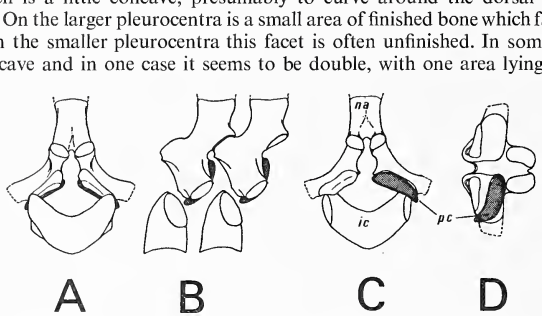

TEXT-FIG. 12. Reconstruction of presacral vertebra ($\times \frac{1}{3}$). A, anterior view; B, lateral view of two vertebrae; C, posterior view; D, ventral view. Pleurocentra are hatched.

behind the other. In one pleurocentrum the lateral strip of bone also has a partly finished surface. It seems that the pleurocentral element was probably only exposed on its lateral face, at the 'facet' and at the lateral facing strip of bone, all other surfaces being covered with cartilage.

Reconstruction of the vertebrae

Presacral region (text-fig. 12). Placing the neural arches in articulation shows that the presacral vertebrae were arranged in units which averaged 3·3 cm. in length. This leaves a gap of 0·6 cm. between successive intercentra which seems rather large in view of Watson's 1958 restoration in *Paracyclotosaurus davidi* 'with a minimum of ligament between them', but no other arrangement is possible. The intercentra are situated in front of the neural arches with their dorsal points being level, in lateral view, with the transverse processes. It can be seen from the anterior view in text-fig. 12 that the dorsal points of the intercentra are also level with the lateral edges of the anterior neural arch facets.

It follows from this loose arrangement of the neural arch and intercentrum and the small size of the pleurocentrum, that the latter could be placed in one of two ways. It could form the central core of a cartilaginous block which fills the gap between the larger elements: a rhachitomous condition; or it could adhere closely to the neural arch so that the intercentrum fills the gap: an almost stereospondylous condition. It is probable that the neorhachitomous vertebra is almost stereospondylous, the pleurocentra being placed dorsally against the ventral neural arch facet, with a minimum of cartilage between the two. In this position the rounded median end of the pleurocentrum

projected postero-medially towards the anterior neural arch facet of the vertebra behind, while its pointed lateral end extended a little below the level of the transverse process.

Caudal region (text-fig. 12). As no haemal arches are preserved there is little evidence on which to base a reconstruction of this area. However, the neural canals can be aligned, and the regions which held their cartilaginous post-zygapophyses can be placed above the prezygapophyses of the arch behind. Haemal arches probably lay between but below the neural arches, separated from them by a great deal of cartilage (as they were in *Uranocentrodon*).

Ribs (text-fig. 13)

Few rib series of the larger Triassic labyrinthodonts have been described. Among these, ribs are best known in *Paracyclotosaurus* (Watson 1958) which has an almost complete set. Huene (1922) figured a series of ribs of the large neorhachitome *Sclerothorax*. Bystrow (1944) showed a full series of ribs for the Permian seymouriamorph, *Kotlassia*, as did White (1939) for *Seymouria*. Finally, the ribs of *Eryops* are well known, and Olsen (1936) has restored their musculature.

Although there is tremendous individual variation in the ribs it is possible to establish a basic morphological plan. The ribs are single headed but the head is clearly divided into ventral capitular and dorsal tubercular areas, so that it appears slipper-shaped in proximal view. The end was cartilage capped and in life the cartilage probably divided to give a double head. One rib, probably a posterior dorsal, with two heads supports this supposition. From the tuberculum and capitulum, shafts of bone lead laterally to merge on the antero-ventral border of the rib, forming its main shaft. Just distal to this point is a 'knee' bend, so that the remainder of the bone curves postero-ventrally. The 'knee' is present in all ribs (although it is not sharp in the most posterior caudals), unlike the situation in *Paracyclotosaurus* where the posterior thoracic ribs are straight. The rib shaft terminates distally in an unfinished oval facet (the distal articulation) which would have continued as a cartilaginous connection to the sternum. Postero-dorsally, the shaft is drawn out to form a thin shelf of bone which in some cases runs the length of the rib from the tuberculum to the distal articulation, while in others it is a mere indication of a ridge. A cross-section of the rib anywhere along this shelf has a comma shape, the main shaft forming the head of the comma, and giving off the dorsal shelf as its tail. From the shelf develop the characteristic uncinate processes which are found in most larger labyrinthodonts. These processes are fairly small in F.R.P. 48*a*, but in addition to them the distal end of the shelf is expanded so that there are usually two (and in one certain case (text-fig. 13B), three) posteriorly directed processes on each rib. Thus all ribs have two heads, a shaft with a 'knee' bend, and some sort of expansion of the shaft.

Cervical ribs are apparently missing in the collection, but a cervical rib count of two seems likely.

Rib A is like rib 4 of *Paracyclotosaurus* and is the largest of all ribs preserved. Remarkable for the massiveness of its shaft and especially for the great distal expansion of the dorsal shelf, it is placed as the first thoracic rib so that it acts as a support for the shoulder girdle.

Of the ribs illustrated in text-fig. 13, rib D is fairly typical of anterior thoracic ribs,

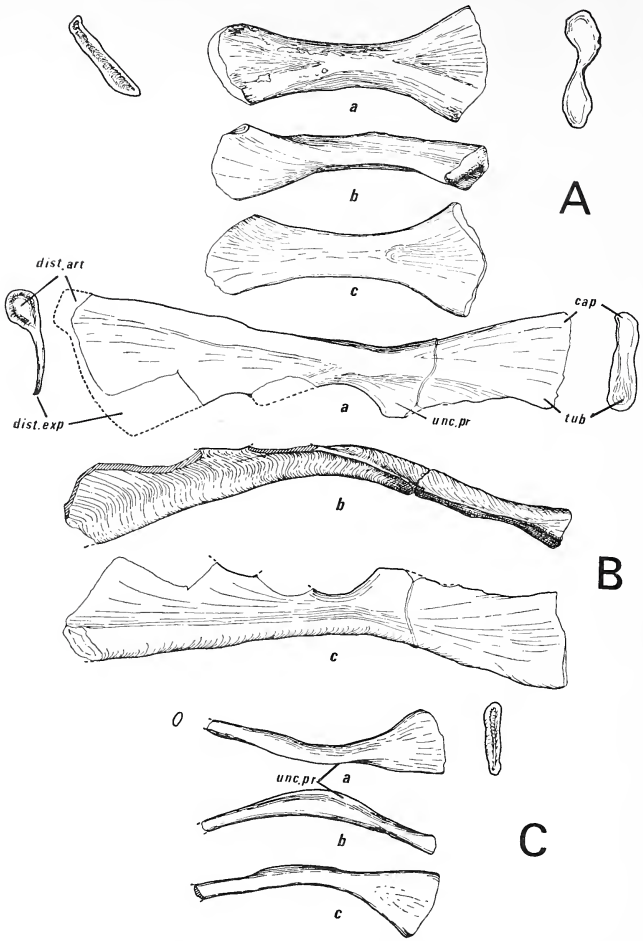

TEXT-FIG. 13. *Parotosaurus pronus* sp. nov. A, sacral rib; B, rib D; C, rib X ($\times \frac{1}{2}$). *a*, antero-dorsal views; *b*, posterior views; *c*, postero-ventral views. On the right are proximal and on the left distal outlines of the rib ends.

while rib X resembles the 32nd rib of *Paracyclotosaurus davidi* (the 4th posterior to the sacrum). Moving posteriorly along the series from rib D to rib X there is a gradual decrease in over-all size of the rib accompanied by a more distal position of the uncinate process and the reduction and eventual loss of the distal expansion.

P. pronus sacral rib (text-fig. 13) resembles both the cervical and sacral ribs of *Paracyclotosaurus davidi*. The rib has well-developed capitular and tubercular areas. Its distal end is expanded to almost the same extent as its proximal end but has twisted to face anteriorly while the proximal end faces antero-dorsally. On its anterior face, prominent ridges run from all four corners of the bone to meet near the middle of the shaft.

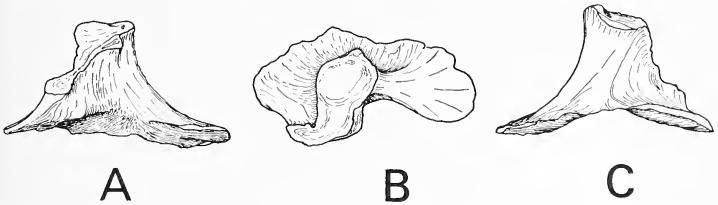

TEXT-FIG. 14. Largest sacral rib of ? reptile ($\times\frac{1}{2}$). A, ventral view; B, medial view; C, dorsal view.

This rib is remarkably like the sacral rib of *Benthosuchus sushkini* (Bystrow and Efremov 1940, fig. 41) although the extremities of the latter are less well ossified: the same muscular 'cristae' are present, and the distal ends of the two ribs are almost indistinguishable. The rib lacks the double processes for articulation with the ilium seen in *Paracyclotosaurus*, but this region was restored by Watson. A similar rib was restored in *Buettneria*'s pelvis by Sawin (1945).

In the collection from field locality F.R.P. 48 is another series of sacral ribs.

The largest of these is the best preserved (text-fig. 14). It has an extremely short, thick shaft, and the proximal and distal ends are greatly expanded at right angles to the shaft. Two proximal articular areas are apparent: a rounded capitulum, and running from this, a narrow, elongate tuberculum. Both were finished by cartilage. A strong rounded spine runs laterally from the capitulum to end medial to the anterior part of the distal expansion, while a shorter spine connects the tuberculum with the posterior part of the expansion. This distal expansion for articulation with the ilium is slipper-shaped and curves a little dorsomedially, this 'instep' leading dorsally on to the bone shaft. The proximal end of the rib is twisted roughly 50° relative to the distal end.

This second type of rib is like the one described by Romer (1947) as being typical of labyrinthodonts. Certainly, variations of this rib are seen, for example, in *Peltobatrachus* (Panchen 1959), *Parioxys* (Shawki Moustafa 1955), *Cacops* (Williston 1910), and *Kotlassia* (Bystrow 1944). However, this type of sacral rib is also seen in reptiles, especially dinosaurs and in the present case it seems more likely that the shorter type of sacral rib belonged to a reptile associated with the remains. Supporting this conclusion is the presence of two elongate bones which can only be interpreted here as ischia of a large Triassic reptile, probably an early member of the Sauropodomorpha

(Huene 1932). The sacral rib series and ischia are of a comparable size and could well have come from the same pelvic girdle.

It seems that in labyrinthodonts the sacral rib may be one of two types. The squat type described by Romer tends to be associated with mainly terrestrial labyrinthodonts with fairly well-developed locomotory powers and expanded iliac blades. In this case the animal has a deep-sided pelvis. The second, elongate type of sacral rib is found in labyrinthodonts which are larger, but flattened, and are probably totally aquatic. These have unexpanded ilia and much cartilage in the pelvis, the pubis being rarely ossified. The ischia in this case incline outwards so the pelvic girdle is dorso-ventrally flattened.

Reconstruction of the ribs

The ribs as preserved are incomplete both proximally and distally and most have some part of the dorsal shelf missing. The latter has been restored in the figures as described above. No attempt has been made to envisage the restored distal end of the ribs except to note that there was probably some cartilaginous connection to a sternum, at least in the more anterior ribs.

However, some attempt has been made to restore the proximal end of the rib, and to fit the ribs to the vertebral column. It is apparent that the rib head as preserved will not fit the arrangement of a diapophysis and parapophysis on the vertebra, and that to make this fit a greater length of cartilage will have to be added to the capitulum than to the tuberculum. The fit of the tuberculum to the diapophysis is remarkably good in *P. pronus*, and Watson has noted a similarly good fit between these facets in *Paracyclotosaurus*. Thus it seems likely that the cartilaginous caps on the tuberculum and diapophysis were thin. If it is assumed that the cartilage between the capitulum and the parapophysis belonged entirely to the capitulum then it can be seen that the capitulum of an anterior thoracic rib would need to be extended by over a centimetre of cartilage. This is approximately the situation reported by Watson in *Paracyclotosaurus*, and ribs of *Mastodonsaurus* have been preserved with an ossified capitulum which extends medially in this manner (Wepfer 1923).

Thus restored the rib head fits on to the vertebra with its dorsal shelf sloping backwards. In the anterior ribs successive uncinate processes probably overlapped, possibly so that their surfaces touched.

It was noted in reconstructing the vertebrae that while the tubercular rib head was almost the same size and shape as the diapophysis, the capitular head was much smaller than the parapophysis and seemed to lie across its long axis. Now the proximal ends of the ribs lie in an almost horizontal longitudinal plane, so that any movement made by the rib would be expected to occur in a dorso-ventral direction rather than an antero-dorsal direction. Assuming that the rib was involved in dorso-ventral movements, it becomes possible to explain the larger size of the parapophysis. As the capitulum is longer than the tuberculum it can be seen that if the rib is depressed or raised using the tuberculum–diapophysis facet as a pivot, the capitulum will move a greater distance than the tuberculum. This movement will be along an antero-dorsal to postero-ventral line, that is, in the same line as the long axis of the parapophysis. Thus, if the rib is depressed the capitulum would move dorsally on the parapophysis. Movements of ribs used, for example, in respiration are more likely to be in a downwards direction but it is probable that a little dorsal movement was also possible. The capitulum has therefore

been placed in a resting position a little above the lower limit of the diapophysis. If this interpretation is correct, and the intercentra have been arranged in their correct order, then the anterior ribs seem to have moved less than the posterior ones.

Pectoral girdle

Two interclavicles, two left and two right clavicles, one left and one right cleithrum, and one primary girdle element, a right scapulo-coracoid, were found. By inspection of their articular facets it can be shown that the interclavicles and clavicles form two complete sets, one a little larger than the other. It is less easy to fit the cleithra to their respective clavicles, but the approximate clavicle–cleithrum relationship can be deduced. The scapulocoracoid is small and badly preserved, and could belong to either of the dermal girdles. All pectoral girdle elements are reasonably well known in Triassic labyrinthodonts.

Interclavicle (text-fig. 16). The interclavicles have the typical parotosaur shape as shown by Welles and Cosgriff (1965).

The lateral interclavicular trabeculae on the ventral surface of the bones (Bystrow and Efremov 1940, Welles and Cosgriff 1965) are particularly prominent, but the sternal trabeculae are small. In the smaller specimen, an anterior trabecula arises opposite the sternal trabecula, and leads anteriorly to the base of the interclavicle's stem.

The ventral areas for articulation with the clavicles are deeply ridged especially above the lateral trabeculae. Similar ridges on the dorsal surface of the clavicles undoubtedly intermeshed with these, a system which apparently restricted movement between the elements.

Clavicle (text-fig. 15). The general shape of the clavicles is similar to that seen in *Paracyclotosaurus davidi*.

The clavicles also have well-developed trabeculae. These stretch from the median border of the clavicle, from a position below the lateral interclavicular trabeculae, to the base of the dorsal process at which point the thickened bone of the trabeculae is continued upwards and a little medially as a dorsal spine. This spine runs postero-dorsally to draw out the upper corner of the dorsal process into a backwards-facing ridged articulation for the cleithrum. On the external surface of the dorsal process an extensive antero-dorsally facing area in front of the spine is roughened according to Watson (1958) for the cleidomastoideus muscle.

Cleithrum (text-fig. 16). The cleithra show similar features to cleithra of *Benthosuchus sushkini* described by Bystrow and Efremov (1940).

In their natural orientation each cleithrum continues the postero-dorsal slope taken by the dorsal spine of the dorsal process on the clavicle. An area for attachment to the clavicle is shown by a system of coarse longitudinal ridges on the ventral half of the anterior face. Above the clavicular articulation the crista cleithralis (Bystrow and Efremov 1940) is represented by a pair of small hooked processes which expand the head of the cleithrum. Diametrically opposite this crista is a posteriorly directed flange, the lamina suprascapularis (Bystrow and Efremov 1940) which leads into a deep, vertically elongated recess in the head of the bone. The recess is continued ventrally as

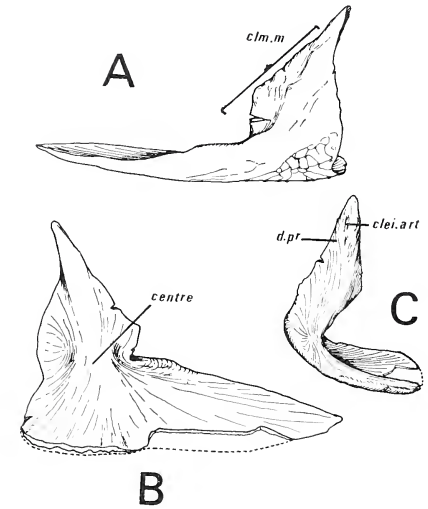

TEXT-FIG. 15. Smaller right clavicle (reversed) (×¼). A, antero-lateral view; B, postero-medial view; C, posterior view.

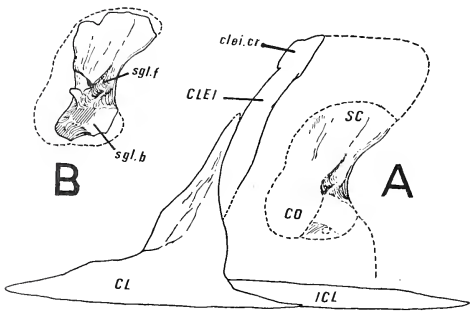

TEXT-FIG. 16. *Parotosaurus pronus* sp. nov. A, reconstruction of the smaller pectoral girdle, lateral view; B, unreconstructed scapulocoracoid, lateral view (×¼).

a groove which is at first narrow but later broadens to fill the whole width of the median surface. This area undoubtedly clasped the cartilaginous anterior border of the scapulocoracoid.

Scapulocoracoid (text-fig. 16). If, as seems likely, this bone resembled the scapulocoracoid of *Parotosaurus peabodyi* (Welles and Cosgriff 1965) or *Wetlugasaurus* sp. (Riabinin 1930) then the thinner, lateral coracoid portion of the bone is missing.

The actual glenoid region is unossified but the articular facet was undoubtedly just postero-lateral to the expanded base of the scapulocoracoid. This expanded area, the supraglenoid buttress, is more extensive than it is in *Paracyclotosaurus*, and shows an antero-ventromesial process divided from the characteristically flattened rectangular buttress by a shallow recess.

The extent of the coracoid process is variable in related types. In *Paracyclotosaurus* it is narrow. In *Parotosaurus peabodyi*, on the other hand, the process is wide ventrally, but narrow dorsally. Close examination of the area of origin of the coracoid process in the present case reveals that only a small section of bone is actually broken, the rest of the roughened surfaces being finished in cartilage. Thus, the coracoid process was probably like the smaller one in *Wetlugasaurus* sp., and even more like the immature scapulocoracoid of *Benthosuchus* (Bystrow and Efremov 1940, fig. 76, D). It is not surprising that *P. pronus* scapulocoracoid probably resembled an immature form as the whole skeleton is poorly ossified when compared with earlier or more terrestrial labyrinthodonts.

As the ventral part of the coracoid plate is missing, the lateral view of the bone is almost a longitudinal section. Thus the supracoracoid foramen is seen in section as a deep recess arising posteriorly near the middle of the bone, and extending antero-ventrally across it. The canal would probably have been closed laterally by bone (as it is in *Wetlugasaurus* sp.) and was rounded, unlike the elongate foramen closed (presumably) by cartilage in *Benthosuchus*.

The narrow dorsal and anterior edges of the scapula blade apparently supported an extensive cartilaginous cap. Dorsally this occupied the position of a suprascapula, while laterally it formed a connection with the posterior face of the cleithrum.

The posterior margin is a true edge which curves forward from just below the dorsal cartilage cap to the median edge of the supraglenoid buttress.

Medially, the existing surface is vertically flat, but falls away slightly anteriorly as the subscapular fossa (Sawin 1945). Ventro-medially, behind the supraglenoid buttress is a deep, rounded groove which was presumably finished by cartilage to form the glenoid foramen (Riabinin 1930).

Reconstruction of the pectoral girdle (text-fig. 16). In reconstructing the pectoral girdle of *P. pronus* the position of all dermal elements was easily established. It seemed best to restore the scapulocoracoid in a high position. This allows a characteristic overlap of the cleithrum dorsally, and sufficient room for the glenoid cavity to be placed so that the head of the humerus can be clear of the ground.

The girdle as a whole is extensively dorso-ventrally flattened with relatively enormous dermal elements and reduced primary girdle. The clavicles–interclavicle complex forms an immense, ventral plate beneath the pectoral region.

The poor state of ossification of the scapulocoracoid of *P. pronus* indicates a weakly

developed fore limb, a theory supported by the equally poorly ossified condition of the fore limb bones. Thus it seems that the massive dermal shoulder girdle had little to do with locomotion: consideration (below) of the thickened trabeculae on the clavicles and interclavicle indicates a function for it other than limb muscle support.

Fore limb

The fore limb bones consist of a left and a right humerus, radius, and ulna. Proximal and distal ends of all the limb bones were finished in cartilage.

Humerus (text-fig. 17). The humerus is of the reduced tetrahedral type described by Watson in *Paracyclotosaurus* (the humerus illustrated by Watson is a left one and has been incorrectly labelled right). Thus the strong muscular processes seen in *Eryops* (Miner 1925) or *Acheloma* (Romer 1922) have been reduced, and less of the distal and proximal ends of the bone are ossified. There are no ectepicondylar or entepicondylar foramina.

On the proximal-dorsal surface the deltoid crest is prominent as is the antero-distal supinator crest.

Radius (text-fig. 17). The radius has an almost straight shaft which is flattened ventrally (posteriorly) and has its ends expanded and cupped to house their terminal cartilages. The proximal end is rounded except ventrally, while the distal end is also flattened postero-dorsally so that it is almost triangular in cross-section. Low ridges lie laterally, anteriorly and medially on the shaft, and the last named forms a distal process directed towards the ulna. There are no easily identified muscle origins or insertions.

Ulna (text-fig. 17). The lateral edge of the ulna is almost vertical, but the medial border is concave, so that the proximal and distal ends of the bone are expanded towards the radius. In proximal view, the cap of the ulna is rhomboidal, and the postero-lateral corner of the rhombus is raised above the other corners as a short olecranon process. Opposite the process, on the median edge of the rhombus is a characteristic depression. The distal end is almost rectangular but narrows on the radial side and is sub-divided into median and lateral facets. The shaft of the ulna is squared proximally, becomes thin and rounded in the middle, and is expanded distally in an anterior–posterior plane. Proximally, the lateral, medial and flexor faces of the shaft are depressed and roughened for muscle attachment.

Pelvic girdle

The pelvic girdle is represented by a left and a right ilium and a left and a right ischium. As these are of comparable size it seems likely that they are from the same girdle. There is no evidence of pubes but these are rarely ossified in contemporary related forms.

Ilium (text-fig. 18). The two ilia resemble those of *Paracyclotosaurus* but the blade shows a greater posterior slope. Dorsally on the antero-medial surface of the ilium is a vertical series of ridges, presumably for ligamentous attachment.

Ischium (text-fig. 18). The ischia are unremarkable. They are almost identical, though a

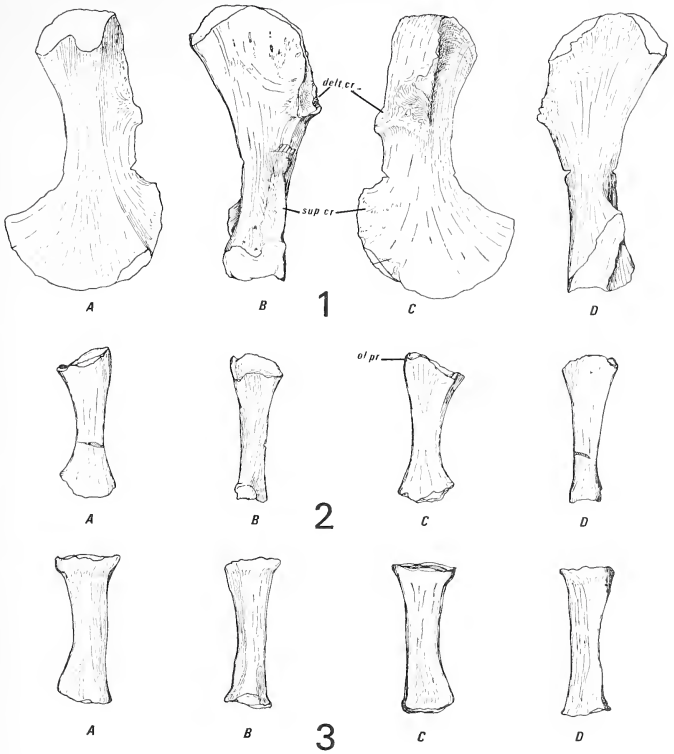

TEXT-FIG. 17. *Parotosaurus pronus* sp. nov. 1. Humerus. A, distal dorsal view; B, proximal ventral view; C, distal ventral view; D, proximal ventral view. 2, Ulna; 3, Radius. A, dorsal view; B, anterior view; C, ventral view; D, posterior view. All $\times\frac{3}{8}$ approx.

little larger, to those of *Buettneria* (Sawin 1945). *Paracyclotosaurus* has similar ischia, but they are more antero-posteriorly elongate.

The reconstructed pelvic girdle is flattened dorso-ventrally, with the iliac blades well separated dorsally. The sacral rib slopes backwards along the same lines as its neighbouring ribs: its area of contact with the ilium is vertical and narrow, but was apparently extended by cartilage in the living animal. This positioning of the sacral rib so that its iliac contact lies well behind the level of the sacral vertebra seems a weak arrangement, but other species such as the salamander *Megalobatrachus* are similarly built.

An area in front of the ischia was presumably filled by cartilaginous pubes: Watson has found impressions of flat oval elements with ossification in this region in *Paracyclotosaurus*.

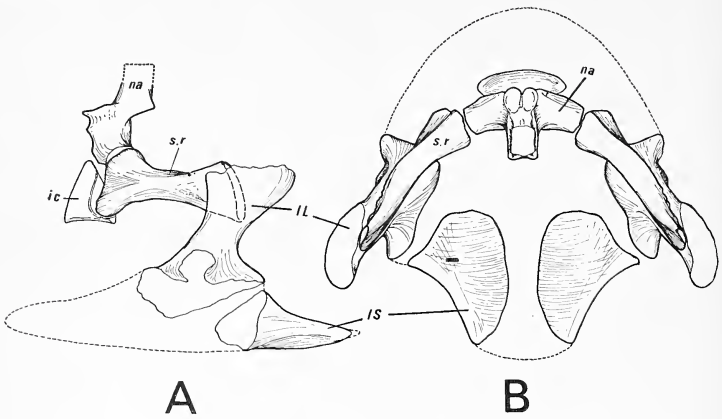

TEXT-FIG. 18. Reconstruction of the pelvic girdle (×⅓). A, lateral view; B, dorsal view.

Hind limb

The collection contains one left and two right femora, a left and a right tibia, and a right fibula.

Femur (text-fig. 19). Except for its smaller size the femur resembles the *Paracyclotosaurus* femur described by Watson.

Tibia (text-fig. 19). Proximally, the tibia is greatly expanded anteriorly (dorsally), medially and laterally but posteriorly (ventrally) the surface is concave. This massive head tapers to form a shaft which is circular but for a broad dorsal ridge leading distally from the 'knee' region to the smaller distal end. One especially prominent muscle scar covers the proximal and anterior 'knee' region and is equivalent to the tuberositas tibiae of Bystrow and Efremov (1940): their ventral crista posterior is present proximally as a sharp, low ridge anterior to the posterior concavity mentioned above, but fails to extend further along the shaft.

Fibula (text-fig. 19). The fibula is remarkably like the ones described by Bystrow and Efremov (1940) in *Benthosuchus* and Case (1932) in *Buettneria*. The most characteristic feature of this and fibulae of related types is a reflection of the distal medio-ventral corner of the bone forming a groove (the sulca fibularis of Bystrow and Efremov) between it and the shaft. Muscle scars are concentrated about the extremities of the fibula, but posteriorly there is one large scar in the middle of the shaft.

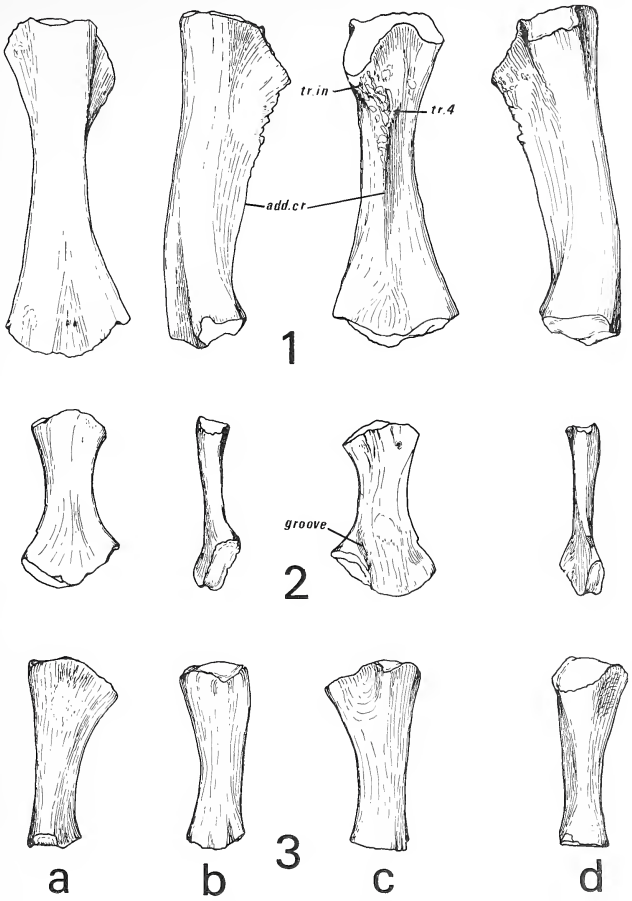

TEXT-FIG. 19. *Parotosaurus pronus* sp. nov. 1, Femur; 2, Fibula; 3, Tibia. (×$\frac{1}{2}$). *a*, dorsal view; *b*, anterior view; *c*, ventral view; *d*, posterior view.

Other limb bones

Fourteen smaller limb bones were found. Twelve of these are of roughly the same shape but of varying sizes and are probably phalangeal bones, metacarpals, and metatarsals. These are elongated, a little dorso-ventrally (antero-posteriorly) flattened, and have their ends expanded. The two remaining bones are paired and could be carpals or tarsals. They are smaller and thicker than the above and have one end compressed at right angles to the other.

DISCUSSION

Dermal pectoral girdle

Prominent on the interclavicle are the lateral trabeculae which lead from the centre of ossification of the bone to its lateral corners. It is evident that the trabeculae are thickest where they meet and underlie the postero-lateral edge of the clavicles. Here is the region of maximum contact between interclavicle and clavicles with maximum interlocking between their articular surfaces. The clavicles in their turn are thickest in this region. This is the lateral limit of the clavicular trabeculae which lead to the centre of ossification of the clavicle at the base of the dorsal process and are continued dorsally as the clavicular spine. This series of trabeculae is a system of struts well sited to counteract an upwards and forwards pull on the dorsal process of the clavicle. The cleidomastoideus muscle (if Watson's interpetation of the scar on the external antero-dorsal corner of the dorsal process of the clavicle is correct) is in a position to create just such a pull. In support of this theory is the fact that only the larger, flattened, aquatic labyrinthodonts with similar interclavicles to *P. pronus* have well-developed trabeculae, and in all these types the dorsal process of the clavicle has an enlarged cleidomastoideus muscle scar (especially *Buettneria* (Sawin 1945, fig. 9*a*), *Benthosuchus* (Bystrow and Efremov 1940, figs. 44, 45), *Paracyclotosaurus* (Watson 1958, figs. 10, 11)). A possible reason for the enlarged cleidomastoideus muscle in these flattened forms will be discussed below.

It is evident that a strong framework in this area would also be necessary because the animal is large and flat. A flattened girdle means that the legs are far apart. In this position the fore limbs, working together, could, theoretically, raise the anterior part of the body off the ground, but only if the area between them was stiff. In fact if the girdle was stiff, it would take no more effort to lift the weight above it from two points near the girdle's edges, than from two points near its centre. To prevent the animal collapsing, a system of struts would be required similar to that needed to resist the pull of a strong cleidomastoideus muscle. But in this case the pull would act on the back of the dorsal process of the clavicle, via the scapulocoracoid and cleithrum.

The girdle undoubtedly also functioned to protect thoracic organs from pressures from the ground.

The flattened dermal pectoral girdle of capitosaurs is thus of use in three ways: as a framework for a system of ridges backing up the cleidomastoideus muscle, as a strut for the pectoral region, and as a protection for the anterior viscera.

Jaw opening

When discussing the jaw musculature of *Paracyclotosaurus davidi* in 1958, Watson noted: 'The relative position of the occipital and quadrate condyles shows that if the

lower jaw rested on the ground, as must often have been the case, it would move forward as the mouth was opened by raising the skull.' In 1962 he postulates, in the same animal, a 'great muscle, the musculus depressor mandibulae', attached to the retro-articular process of the lower jaw and 'inserted onto the posterior edge of the dermal skull roof at the highest possible point, contraction of which will raise the skull *if the lower jaw rests on the ground*' (my emphasis). Panchen (1959) also uses the depressor mandibulae to raise the skull in brachyopids and plagiosaurs. But he suggests that occipital muscles combined with the depressor to lift the skull. However, there is an alternate system of muscles which could be used in jaw opening to overcome some of the difficulties inherent in the above schemes.

Watson's scheme employs both the occipital condyles and the quadrate condyles in a movement governed by a single muscle. This could function only if the two sets of condyles were in the same transverse line, otherwise, if it is assumed that the atlas does not move posteriorly when the skull is raised against the atlas using the articular as fulcrum then:

(*a*) If the occipital condyles were in the same transverse plane as, but above the quadrate condyles, the vertebral column would be depressed as the skull was raised,
(*b*) If the occipital condyles were in the same horizontal plane as, but in front of the quadrate condyles, the column would be elevated as the skull was raised, or
(*c*) If the occipital condyles were in the same horizontal plane as, but behind the quadrate condyles, the vertebral column would again be depressed as the skull was raised.

Watson realized this and employed point (*b*) when he showed that *Eryops* could not raise its skull (1951). But he disregarded it when he noted (1951) that in capitosaurs the lower jaw would move forward as the skull was raised. True, capitosaurs are approaching the ideal situation for Watson's scheme, and some of them (especially *Parotosaurus orenbergensis*, Konzhukova 1965), seem to have reached it.

Brachyopids, however, are far from it. In them, the occipital condyles are well behind and above the quadrate condyles, and it can be seen (text-fig. 20) that using the depressor mandibulae muscle to raise the skull (as shown by Panchen) must force the occipital condyle ventrally, and with it the whole vertebral column. In brachyopids this depression is considerable (more than one-quarter of the body depth) and implies that either the pectoral girdle was very loosely connected to the vertebral column, or that the pectoral area was held clear of the ground, a most unlikely position if the mandible must be grounded.

Brachyopids, having their occipital condyles behind and above the quadrate condyles, better illustrate a second difficulty: than an animal whose lower jaw shoots forward as it must in a brachyopid when it raises its skull, is unlikely to be relying on that jaw for leverage against the ground. Panchen likens the brachyopid jaw movement to that of an active, predatory fish, implying a rapid action. But for the skull to be raised by a depressor muscle, the lower jaw must be on the ground; if it was not, contraction of the depressor would lower the jaw, not raise the skull. No other system supports the lower jaw except the adductor muscles, and these are antagonistic to the depressor: if they were relaxed, and the jaw was not on the ground, again the depressor would lower the

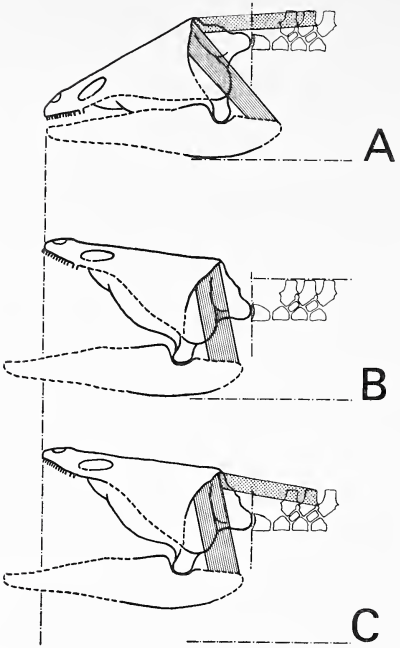

TEXT-FIG. 20. A brachyopid skull (*Batrachosuchus*) in profile. A, Skull with jaws closed. B, Skull to show the method of opening the jaws by raising the skull by contraction of the depressor mandibulae muscle as depicted by Panchen (1959). Note depression of the vertebral column. C, Skull to to show method of opening the jaws by 1, contraction of the muscles between the occiput and the vertebrae to raise the skull, and 2, contraction of the depressor mandibulae muscle to lower the lower jaw. Note that the vertebral column has not been depressed and that the lower jaw is clear of the ground. Skull outline from Watson's figure of *Batrachosuchus* (1956, text, fig. 5). Lower jaw from Panchen's (1959) reconstruction. Occipito-vertebral muscles stippled. Depressor mandibulae muscle hatched. *Batrachosuchus*'s vertebrae are restored following discussion with Dr. S. P. Welles who has a collection of intercentra which show that the brachyopids had rhachitomous vertebrae.

jaw. (Of course, when the animal was swimming it could feed by lowering the jaw, but the rapid forward movement of the jaw characteristic of predatory fish could only occur if the skull was raised.)

Finally, it is illuminating to consider the nature and attachments of the depressor mandibulae muscle itself. Watson says that the muscle should be inserted on the highest possible point of the skull roof. In capitosaurs this is the tabular. From the side, a

muscle inserted here looks feasible (Watson 1951, fig. 27). From behind, however, the angle at which the muscle would have to function is poor: the depressor would have almost as high a horizontal component as a vertical one. The situation in this case is worsened by the nature of the quadrate condyles which are slightly screw-shaped, the thread of the screw running from postero-lateral to antero-medial. A lower jaw rotating about this condyle must necessarily move laterally so that the two rami separate slightly

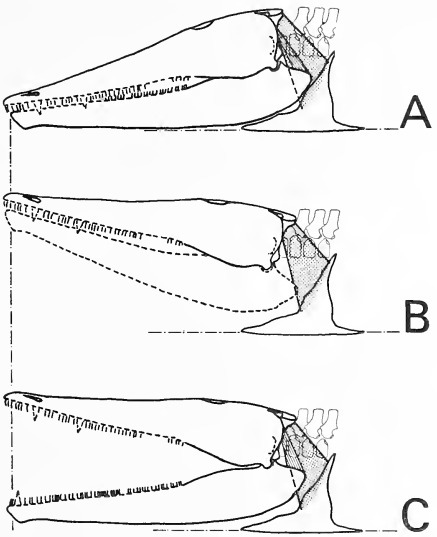

TEXT-FIG. 21. *Parotosaurus pronus* skull in profile. A, skull with jaws closed. B, C, the method of opening the jaws divided into two stages. B, contraction of the cleidomastoideus muscle to raise the skull (depressor muscles omitted); C, contraction of the depressor mandibulae muscle to lower the lower jaw. Cleidomastoideus muscle stippled. Depressor mandibulae muscle hatched.

at their median symphysis. This action would oppose the inward pull from the depressor which would then be working at a double disadvantage. (However, it should be noted that in brachyopids a depressor would have a better working angle as the cheek is deeper, and the muscle could act from directly above the lower jaw.)

The proposed solution to these problems has two aspects (text-fig. 21B, C). First, the skull is raised by specially developed occipital muscles using the occipital condyles as the fulcrum, and, second, the lower jaw is lowered by contraction of the depressor mandibulae muscle. In practice, the two muscles would work simultaneously (text-fig. 21C). The most obvious advantage of this system is that raising the skull against the occipital condyles will elevate the quadrate condyles as well (that is, the opposite effect

to the depression of the vertebral column resulting from Panchen's scheme) and so the lower jaw will be freed from the ground. Subsequent contraction of the depressor does not need ground support as it is a lowering not a raising action. Under these conditions the brachyopid jaw will shoot forward without interference from the ground.

There is evidence for a suitable occipital muscle in capitosaurs. Consideration of the dermal girdle in *Parotosaurus pronus* (above) has indicated a well-developed system of ridges which were interpreted as a support for an upwards and forwards pull by the cleidomastoideus muscle. If the girdle is placed behind the skull it can be seen that the area of attachment for the cleidomastoideus muscle on the dorsal process of the clavicle is in the same plane (but behind and below) a pronounced ventro-lateral flange of the tabular (text-figs. 3, 5). This flange runs from the tabular horn postero-ventro-medially along the paroccipital process, ending just dorsal to the suture between the tabular and the exoccipital. It is proposed that in capitosaurs this flange was the insertion of the cleidomastoideus muscle which contracted to raise the skull. In this position, the cleidomastoideus muscle would be working at an angle very similar to the depressor muscle as visualized by Watson, but the lateral component would be reduced. However, unlike the depressor, the cleidomastoideus muscle will not have to counteract the lateral movement of the lower jaw. Miner (1925) restored part of the cleidomastoideus in *Eryops*, attaching it to the squamosal and posterior part of the skull generally, with its other end on the cleithrum, clavicle, and scapula, but he did not attempt a functional explanation for it. It is interesting to note that Watson (1926) postulated, in embolomeres, a bony articulation between the tabular horn and the shoulder girdle via a post-temporal element but Romer later (1947) considered that this was more likely to be a ligamentous connection.

Use of this muscle in a skull-raising capacity may help to explain the (evolutionary) lateral movement of the tabular horns (which eventually closed the otic notch in cyclotosaurs), and the accompanying inward movement of the dorsal process of the clavicle in these flattened forms, so that the origin and insertion of the cleidomastoideus came to lie more in a longitudinal–vertical plane.

Occipito-vertebral muscles could have assisted the cleidomastoideus, but they are unlikely to have formed the main skull-raising system in a capitosaur. A capitosaur has a vertical occiput, so that the point of attachment of the occipital muscles is in the same transverse plane as the occipital condyles. Consideration of text-fig. 22 shows that a muscle attached between the occiput and the vertebral column could raise the skull a certain amount, but it would only be really effective at the very beginning of its contraction, and it is doubtful whether this would be sufficient to account for the whole range of opening. The clavicle, however, is positioned better in relation to the occiput, and, if a muscle attached to it was used to raise the skull, the muscle would be at its most effective position when the occiput had travelled backwards through approximately 25°, resulting in a narrow gape which will be shown below to be that most used by a capitosaur. It thus seems highly probable that the cleidomastoideus formed the main skull-raising muscle in a capitosaur, with the occipito-vertebral muscles perhaps assisting at the start of the movement.

The situation is different in the brachyopids. Here the occiput slopes forward (text-fig. 22) giving an occipito-vertebral muscle a greater effective range. It is probable, therefore, that the brachyopid skull was at least partly raised by occipito-vertebral

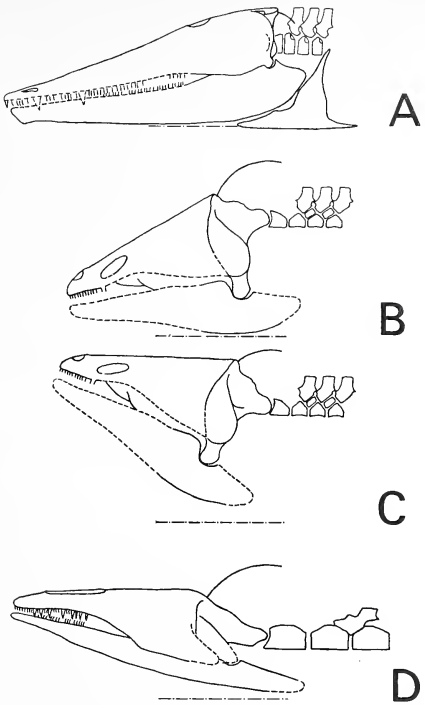

TEXT-FIG. 22. Diagrams of lateral views of the skull and anterior vertebrae of various labyrinthodonts to show the relationship of the occiput to the vertebral column and pectoral girdle. The arcs which would be described by the point of attachment of the occipital muscles on the skull when the latter is raised, are indicated. No attempt is made to indicate the extent of the gape in the brachyopid or plagiosaur but the capitosaur skull would probably not have opened further than the arc suggests. Note that in A the dorsal process of the clavicle is in a better position than the vertebrae for the attachment of a skull-raising muscle; in B the vertebral column is in a better position than a (presumably) more ventral clavicle, but that in C where the skull is held with its dorsal surface parallel to the vertebrae the position is better still; in D the plagiosaur skull is held in a similar position. A, *Parotosaurus pronus*; B, C. *Batrachosuchus* as in text-fig. 20; D, *Gerrothorax* after Panchen (1959) —vertebrae reconstructed from Nilsson's (1937) figures of *Gerrothorax rhaeticus*.

muscles (as suggested by Panchen): these would certainly have a better initial moment than a more ventral muscle from the pectoral girdle. Whether a pectoral or a vertebral muscle was used cannot be determined until the vertebrae and pectoral girdle of brachyopids are better known. It is evident that if a muscle from the clavicle was used in an animal with a forward-sloping occiput, then the dorsal process of the clavicle would have to be tall, at least as high as the vertebrae. Reconstruction of the clavicle of *Eobrachyops*, an early brachyopid, from Watson's (1956) figure and description, shows that in that animal at least, the dorsal process was too short. Watson's (1956) observation that in the brachyopid *Platyceps wilkinsoni* 'the first three vertebrae seem to be somewhat more massively ossified than those farther back, but curiously there seem to be no ossifications in the exoccipital condyles' may lend support to the case for a vertebral muscle.

The pectoral girdle is known in metoposaurs where the occiput is intermediate between capitosaurs and brachyopids, the occipital condyles projecting a little behind the quadrate condyles, but being almost on a horizontal level with them. Here the area for the cleidomastoideus muscles' attachment to the clavicle is exceptionally well developed (Sawin 1945, figs. 8*e*, 9*a*) and the muscle could apparently have been used to raise the skull.

One point which becomes obvious when studying text-fig. 22 is that in order to increase the mechanical advantage of the occipital muscles in the brachyopid and plagiosaur skulls it would be necessary to increase the height of the neural arches. But neural spines of these labyrinthodonts, where preserved, are low. However, the same result would be achieved if, instead of the dorsal surface of the skull facing anteriorly, it was horizontal, so that the vertebral column was parallel to the skull (text-fig. 22B). This position is not unknown in aquatic animals: fish such as the herring have the skull facing dorsally and the lower jaw facing antero-ventrally. This position of the skull seems a more satisfactory arrangement for labyrinthodonts such as brachyopids and plagiosaurs, with anteriorly sloping occiputs, but it would hold little advantage for a capitosaur.

Retro-articular process

It is apparent in these labyrinthodonts that, for the depressor mandibulae muscle to be effective, the greater the slope of the occiput, the longer must be the retro-articular process. A better solution would be to have a shorter process which turned upward (text-fig. 23) (as it does in capitosaurs). This would have the same effect as a long retroarticular process except that the length of the muscle would be a little less.

Text-fig. 23 illustrates the position of the mandible in capitosaurs and plagiosaurs at which the depressor mandibulae would be most effective. This indicates a narrow gape in capitosaurs and a wide one in plagiosaurs (brachyopids being intermediate). If the retro-articular process was turned dorsally (text-fig. 23C) in plagiosaurs it would be possible for the depressor muscle to reach a point of maximum efficiency, but with a straight process (text-fig. 23B) the point would not be reached. In the only brachyopid jaw preserved with the retro-articular process intact, *Bothriceps australis* (Watson 1956), the tip is turned up. In *Batrachosuchus watsoni* (Watson 1956), the retro-articular process appears to turn up, but its tip is missing. Although the retro-articular process is often said to be long in advanced Triassic labyrinthodonts no jaw has been described

where the process is complete and is longer than it is in *Bothriceps*. Panchen (1959) has reconstructed a straight retro-articular process on the lower jaw of *Gerrothorax* from Huene's (1922) figures and description of the lower jaw of *Plagiosuchus* and *Plagiosternum* but the posterior half of the process is missing in both these forms, and it is possible that they did, in fact, turn dorsally.

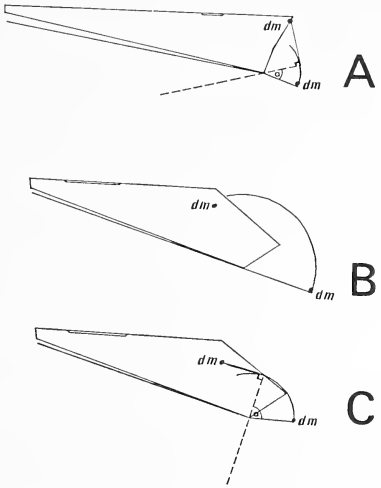

TEXT-FIG. 23. Diagrammatic representations of the skulls and lower jaws of a capitosaur and a plagiosaur to show the difference in their gapes with different retro-articular processes. *a* is the angle through which the lower jaw will move before the depressor mandibulae muscle meets the lower jaw at a right angle. According to Parrington (1955) this is the position where the depressor muscle achieves the greatest leverage on the lower jaw. dm are the points of origin and insertion of the depressor muscle. Note that in A, a capitosaur, the gape is narrow when angle a is reached. In B, a plagiosaur, the angle is never reached. In C, a plagiosaur, the retro-articular process has been turned dorsally: now the position of greatest leverage can theoretically be attained.

It was shown above that in capitosaurs the depressor mandibulae muscle would appear to be most efficient when the gape was small. Additional factors actually prevent the jaws opening far. It seems that in most capitosaurs the ventro-postero-lateral corners of the quadratojugals are not preserved, presumably because they were cartilaginous. But in one or two cases (e.g. *Cyclotosaurus posthumus*, Fraas 1913) ossification persists and it appears that the quadratojugals projected below the level of the quadrate condyle. Now, the capitosaur condylar system is screw-shaped which necessitates an outward movement of the articular along the quadrate as the jaws open. The ventro-postero-lateral projection of the quadratojugals would prevent this movement beyond

a certain point. Also limiting the gape is the post-condylar process of the surangular. There are indications that this was tall, and if so, it would have prevented too great a movement of the quadrate relative to the lower jaw.

The lateral screwing of the jaws, while not great, must increase with the gape and this movement would have been against the action of the depressor muscles which tend to pull the retro-articular process inwards as well as upwards. While the disadvantage of this action has largely been removed by using the depressor to lower the jaw rather than raise the skull, it would undoubtedly become a limiting factor were the jaws to try to open wide.

It seems, therefore, that the capitosaur cranial anatomy is adapted for keeping the gape of the jaws fairly small, rather than for allowing them to open far.

The position of the eyes may have some bearing on this question. As the eyes are placed far back and close together on the capitosaur skull, it is manifest that were the jaw to open widely (by raising the skull), the animal would be unable to see. True, the eyeball could probably be protruded as it is in modern frogs, but it is doubtful if this protrusion would be enough to enable a capitosaur to see if its skull was raised far. It seems significant that in many labyrinthodonts which are thought to have a wider gape such as brachyopids and plagiosaurs, the eyes are larger and further forward on the skull and would probably have been able to project sufficiently. Metoposaurs seem intermediate: they undoubtedly had a wider gape than capitosaurs, and their eyes were well forward.

Dorsal pterygoid canal

The floor of this canal can be seen in specimen 48 I (text-fig. 5A) and more of the canal is shown in specimen 135 (text-fig. 6A). It runs from behind to enter the skull at an abrupt face beside the stapes and above the conical recess and it is probable that the canal carried the VIIth nerve with its accompanying blood vessels. If this dorsal foramen and canal did carry nerve VII then the path of the nerve may have continued behind the ascending oblique ridge of the pterygoid which begins near the posterior section of the canal. This ridge rises obliquely and then turns laterally along the quadrate ramus of the pterygoid to end at the quadrate. On the left of specimen 135 the distal lip of the ridge almost meets the pterygoid to form a canal. On the right of the same skull, a groove above the quadrate leads down and laterally to end near the paraquadrate foramen in the quadratojugal, and this foramen has been postulated by Bystrow and Efremov (1940) as the point where the hyomandibular branch of nerve VII re-enters the skull. If this system of canals did house VII it would adequately protect that nerve from the depressor muscles. Watson (1962) describes in *Rhineceps* and *Wetlugasaurus* a stapedial groove which corresponds in position to the oblique ridge on the pterygoid and suggests that this groove housed the stapes. This may have been the case in other forms but in *P. pronus* the groove is much too small and extends too far laterally. Watson notes this lateral elongation and suggests that the outer section of the groove was to carry the ligamentous attachment of the stapes to the quadrate. But if this was its sole purpose, the groove should have run towards the quadrate 'boss', shown by Westoll (1943) to be the probable point of attachment of the quadrate ligament from the stapes. This is not the case, as study of the same specimen of *Rhineceps* shows a distinct shallow groove which originates at the lateral limit of the oblique ridge and by-passes

the quadrate boss, passing above it in just the position predicted for a nerve stretching from the end of the oblique ridge of the paraquadrate foramen. There seems no reason why in species where the oblique ridge obviously was large enough and in a position to carry the stapes it should not have also carried the VIIth nerve.

The stereospondylous vertebra

It is generally agreed that the stereospondylous centrum is an intercentrum (that is, it corresponds to the intercentrum of amniotes), and that it lies beneath, but a little in front of, the neural arch. Nilsson (1937, fig. 16) places the neural arch of *Mastodonsaurus* in this position and Watson (1958) does the same with *Paracyclotosaurus*.

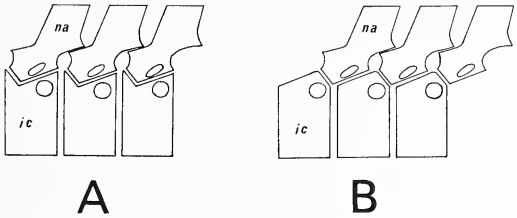

TEXT-FIG. 24. Diagrams of stereospondylous vertebrae showing the two possible arrangements of the neural arch on the intercentrum. A, conventional position, B, correct position. Note 1. The necessity to notch the intercentrum dorsally in A. 2. The relationships of the diapophysis to the parapophysis in A which would make it impossible to fit the type of rib found in stereospondylous labyrinthodonts to the vertebra.

However, Chowdhury (1965, fig. 7) notes the presence of both anterior and posterior facets in stereospondylous intercentra which he assumes belong to *Metoposaurus*, but he also suggests articulating the centrum with only the ventral (posterior) facet of the neural arch. This position agrees with conclusions reached (above) about the arrangement in *Parotosaurus pronus*. However, in this position the intercentrum is articulating with the smaller, anterior, neural arch facet, while the larger more posterior, ventral facet is not accounted for.

Watson, in 1958, notes that this ventral neural arch facet is for the pleurocentrum, a statement undoubtedly true for rhachitomes and neorhachitomes, including *P. pronus*. But in view of the fact that Chowdhury shows two articular facets on a stereospondylous intercentrum (even labelling them anterior neural arch facet and posterior neural arch facet), it seems likely that the neural arch of stereospondyls is morphologically intervertebral, so that the anterior facet of the intercentrum actually articulated with the large posterior facet of the neural arch anterior to it (text-fig. 24).

The vertebral column

Parrington (1967) has noted the disproportionate size of the head in typical labyrinthodonts and the fact that this must have resulted in a forward displacement of the centre of gravity with resulting problems when the mode of walking is considered. And

he has suggested that a rhachitomous vertebral column served the purpose of allowing considerable twist to the short presacral vertebral column enabling the animal to raise the front end of the body on the appropriate side at each step of a fore limb, and so reposition the centre of gravity of the body above the triangle of support offered by the three legs remaining on the ground. He notes, however, that the principle may not have applied to the larger Triassic forms which may have lived largely in water and never have walked with the body clear of the ground. In addition, Watson (1958) has suggested that *Paracyclotosaurus* may have been of almost neutral buoyancy and that it moved in water by touching the ground with its digits (much as does the 'walking' lungfish). It seems therefore that in capitosaurs and stereospondyls the rhachitomous type of vertebra is no longer essential for locomotion (in Parrington's sense).

It was once thought that all capitosaurs were truly stereospondylous, but work by Bystrow and Efremov and others recognized in them the neorhachitomous condition of well-developed intercentrum with reduced bony or cartilaginous pleurocentrum. Watson (1958) has dotted pleurocentra in *Paracyclotosaurus* but none have been found ossified in capitosaurs other than in *P. pronus*. These are obviously mere remnants of the true rhachitomous pleurocentra, and it seems clear that the vertebrae are becoming stereospondylous. If it is accepted that the rhachitomous condition has become unnecessary for locomotion it becomes important to try to explain the advantage of the stereospondylous condition.

Among labyrinthodonts two types of vertebrae are particularly associated with aquatic life: embolomerous and stereospondylous. Parrington (1967) has suggested that the embolomerous condition allows an eel-like form of locomotion in long-bodied types, the greater number of central units allowing a greater flexibility in a lateral plane. As far as they are known the stereospondyls were comparatively short-bodied and therefore could not have swum by lateral undulations, and so some other method must have sufficed. Probably the capitosaurs and other typical stereospondyls swam by flexion of the tail which propelled the animal forward while the body remained largely stiff, much as do tadpoles. Although Watson restored *Paracyclotosaurus* with a fairly short tail of about twenty-five vertebrae, there is evidence that some neorhachitomes at least may have had a longer tail. According to van Hoepen (1915) the neorhachitome *Uranocentrodon senekalensis* had 'at least thirty-six caudal vertebrae and may have had forty-six'. Huene (1922) figured the intercentra of *Mastodonsaurus giganteus*, only showing a representative number of caudal vertebrae but noting that in all probability the tail was very long.

Often in capitosaurs the anterior vertebrae are almost stereospondylous, but the development of the intercentra decreases towards the tail, the posterior presacral and caudal vertebrae remaining in the rhachitomous condition. This is shown in Huene's figure of *M. giganteus* (1922, fig. 2) and is also present in *Paracyclotosaurus*, and, to a much lesser extent in *Parotosaurus pronus*. In short, it seems that, during the Trias, in capitosaur-like labyrinthodonts there is a gradual tendency towards stereospondyly in the presacral vertebrae, while the tail tends to remain rhachitomous. Force produced by a tail used as a propulsive organ must be transmitted through the vertebral column, and a reasonably rigid strut will best serve to transmit this force. The tail, however, would be more flexible if it remained rhachitomous. Flexibility is no doubt increased by a large core of cartilage in the tail and Van Hoepen's photograph of *Uranocentrodon*

tail vertebrae, preserved in what appears to be their natural position, shows neural arches and haemal arches well separated, presumably by cartilage.

It seems, then, that the neorhachitomous tail could have been a flexible structure with isolated dorsal and ventral ossifications, perhaps providing a framework for the attachment of a tail fin; while the neorhachitomous presacral vertebral column was a fairly rigid strut which transmitted the propulsive force produced by the tail to the body.

Taxonomic position

As is well known, the type specimen of *Capitosaurus*, *C. arenaceus*, is indeterminate as its otic region is not preserved and, as an Upper Triassic form, it is probably a cyclotosaur. Jaekel (1922) recognized this and coined the term *Parotosaurus* to refer to capitosaurs. Romer (1947) concurs, suggesting that *Capitosaurus* be confined to the type, while *Parotosaurus* should refer to the Early Triassic '*Capitosaurus*' with open otic notch, and *Cyclotosaurus* to the Upper Triassic closed otic notch type. Welles and Cosgriff, in their much-needed (1965) revision of the family Capitosauridae, decided to follow this scheme, but dropped *Capitosaurus* altogether, the type becoming *Parotosaurus arenaceus*. Further, they lump the twenty-nine genera of Triassic 'capitosaurs' into four, of which three, *Cyclotosaurus*, *Parotosaurus*, and *Paracyclotosaurus*, are Capitosauridae.

It is manifest that the present specimens are parotosaurs, but they cannot be fitted into any of the eight parotosaur species retained by Welles and Cosgriff, nor to *P. orenbergensis* (Konzhukova 1965). They are thus deemed to belong to a new species, *Parotosaurus pronus*. The species is defined by both cranial and post-cranial material, although Welles and Crosgriff use only cranial characters (post-cranial material is not available for most parotosaur species). It is felt that the separation of a species on characters of the skull roof only, as has been done in the past, is a needless generalization when description of post-cranial bones will often clarify a species.

Parotosaurus pronus is distinguished from other parotosaurs chiefly by the shape and position of its tabular horn. In four of the ten species of *Parotosaurus* the tabulars have grown laterally towards the squamosal, like they have in *P. pronus*. Of these, *P. semiclausus* (Swinton 1927) is obviously different: the tabular is unexpanded distally, and only just fails to meet the squamosal; the choanae and orbits are more rounded, the former parallel the midline, while the latter parallel the skull margins; the pineal foramen is rounder; the jugal is excluded from the orbital margin; and the sculpture is large and coarse. Some of these characters could apply to a young individual of *P. pronus*, but in that case the otic notch could be expected to be less, not more, closed in the younger specimen.

Although the tabular horn of *P. birdi* (Brown 1933) and *P. peabodyi* have moved laterally, they still have no distal expansion. In addition, *P. peabodyi* has a much shallower occiput. Its vertebrae differ from those of *P. pronus*, both intercentrum and neural arch being extensively antero-posteriorly compressed in the former. The occiput of *P. birdi* is much nearer to *P. pronus*. However, *P. birdi* has a greater exposure of exoccipital on the palate; the orbits are far apart and slope towards the otic notch; the cultriform process is sharply keeled; and the occipital area extends farther posteriorly, behind the level of the quadrates.

The last of the four is *P. brookvalensis* (Watson 1958). This is the only other

partosaur where the tabular is expanded distally as it is in *P. pronus*, but Watson's reconstruction shows this as a bulbous swelling of the horn, increasing its surface area rather than causing it to approach the squamosal. *P. brookvalensis* could be thought a juvenile *P. pronus* but for the character of its ornament and the length of its snout, which are both adult in proportion.

In 1958, Watson divided the Capitosauridae into shallow-skulled and deep-skulled lines. The latter contained *Paracyclotosaurus davidi* and '*Paracyclotosaurus*' *hemprichi*, and he suggested that *Parotosaurus pronus* could well be their ancestor. Welles and Cosgriff dissolved this grouping, returning '*Paracyclotosaurus*' *hemprichi* to *Cyclotosaurus*. Indeed, there seems little to link the former species apart from their depth of skull, and *Parotosaurus birdi* and *P. angustifrons* seem just as deep.

It is possible that *P. pronus* is ancestral to *Paracyclotosaurus davidi*. Curiously, *Paracyclotosaurus davidi* is the only form where the otic notch is closed by unornamented bone, this area being delimited from the tabular and squamosal by well defined ridges which follow the lines of these bones. It seems possible that the notch is open, the gap being filled by matrix. Certainly, it is unlike the semiclosed *Parotosaurus semiclausus* where tabular and squamosal closely approach one another with their opposing edges parallel. No closed otic notch type has a similar concavity in the posterior skull margin behind the notch, and, if the link between tabular and squamosal be removed, *Paracyclotosaurus davidi* looks remarkably like a parotosaur. In dorsal view, its skull bone arrangement is similar to *Parotosaurus pronus*, but the tabular differs in being expanded proximally as well as distally. Such a character could, however, be advanced, and would not preclude a relationship between the two. Other advanced characters of *Paracyclotosaurus davidi* which could have come from *Parotosaurus pronus* are: a greater exposure of exoccipital on the palate, and a reduction in ossification of the brain-case region, the latter being especially noticeable in the absence of a processus lamellosus to support the supra-occipital. It is harder to envisage the evolution of the *Paracyclotosaurus davidi* rounded nostril from the oval in *Parotosaurus pronus*, or the unusually broad cultriform process from *P. pronus* narrow, almost keeled one. One curious feature of Watson's reconstruction of *Paracyclotosaurus davidi* is the absence of an anterior palatal vacuity, and a (possibly related) absence of tusks in the mandible. This would set *P. davidi* apart from all other capitosaurs, but inspection of casts of the areas shows that they were missing in the original. Unless Watson has other evidence for their absence, it seems more likely that they were present.

The post-cranial skeleton is better ossified in *P. davidi* than *Parotosaurus pronus*, and most differences in shape can be attributed to this. Intercentra have advanced towards the stereospondylous condition. Rib structure, however, distinguishes the two as *P. pronus* ribs all carry some development of uncinate process, usually accompanied by a distal expansion, while *Paracyclotosaurus davidi* ribs have no process or expansion beyond the seventh or eighth thoracic rib.

These comparisons lead to the conclusion that *Parotosaurus pronus* and *Paracyclotosaurus davidi* are remarkably similar, but, while *Parotosaurus pronus* may be more closely related to *Paracyclotosaurus davidi* than to other parotosaurs, there are some features which preclude the former being directly ancestral.

Acknowledgements. The material described in this paper is from Dr. F. R. Parrington's collection. I am deeply grateful to him for loan of the material and for his constant help and advice as supervisor

of the work which was originally submitted for the degree of Ph.D. Cambridge. Thanks are also due to Dr. A. L. Panchen, Dr. S. P. Welles, and Dr. T. S. Kemp for helpful discussions and to Mr. R. D. Norman for general assistance.

The British Museum (Natural History) kindly lent me some casts of *Paracyclotosaurus davidi*, and the Australian Museum donated a cast of *Parotosaurus brookvalensis*.

During the third year of the study the work was supported by a Commonwealth Scholarship.

REFERENCES

BRANSON, E. B., and MEHL, M. G. 1929. Triassic amphibians from the Rocky Mountain Region. *Univ. Mo. Stud.* **4**, 154–255, 15 pl.

BYSTROW, A. P. 1935. Morphologische Untersuchungen der Deckknochen des Schädels der Wirbeltiere. I. Mitteilung. Schädel der Stegocephalen. *Acta zool., Stockh.* **16**, 65–141.

—— 1938. Zahnstruktur der Labyrinthodonten. Ibid. **19**, 387–425.

—— 1944. *Kotlassia prima* Amanitsky. *Bull. geol. Soc. Am.* **55**, 379–416.

—— and EFREMOV, J. A. 1940. *Benthosuchus sushkini Efr.* A labyrinthodont from the Eotriassic of Sharjenga River. *Trudy paleozool. Inst.* **10**, 1–152 [Russian, English summary].

CASE, E. C. 1932. A collection of stegocephalians from Scurry County, Texas. *Contr. Mus. Paleont. Univ. Mich.* **4**, (1), 1–156.

CHARIG, A. J. 1963. Stratigraphical nomenclature in the Songea series of Tanganyika. *Rec. Geol. Surv. Tanganyika*, **10**, 47–53.

CHOWDHURY, T. R. 1965. A new metoposaurid amphibian from the Upper Triassic Maleri Formation of Central India. *Phil. Trans.* B, **250**, 1–52.

CROMPTON, A. W. 1955. On some Triassic cynodonts from Tanganyika. *Proc. zool. Soc. Lond.* **125**, 617–69.

FRAAS, E. 1913. Neue Labyrinthodonten aus der schwäbischen Trias. *Palaeontographica*, **60**, 275–94, 7 pl.

FRANCIS, E. T. B. 1934. *The anatomy of the salamander*. Oxford University Press.

HOEPEN, E. C. N. VAN. 1915. Stegocephalia of Senekal, O.F.S. *Ann. Transv. Mus.* **5**, 125–49, 9 pl.

HUENE, F. VON. 1922. Beiträge zur Kenntnis der Organisation einiger Stegocephalen der schwäbischen Trias. *Acta zool., Stockh.* **3**, 395–460, 2 pl.

—— 1932. Ein neuartiger Stegocephalen-Fund aus dem oberhessischen Buntsandstein. *Paläout. Z.* **14**, 200–29, 2 pl.

JAEGER, G. F. 1824. *De Ichthyosauri sive Proteosauri fossilis speciuinibus in agro Bollensi in Wurtembergia:* Stuttgart.

JAEKEL, O. 1922. Neues über Hemispondyla. *Paläont. Z.* **5**, 1–25, 1 pl.

KONZHUKOVA, E. P. 1965. New parotosaurs from the Trias of the Lower Urals. *Paleont. Zh.* 1965 (1), 97–104.

MINER, R. W. 1925. The pectoral limb of *Eryops* and other primitive tetrapods. *Bull. Am. Mus. nat. Hist.* **51**, 145–312.

NILSSON, T. 1937. Ein Plagiosauride aus dem Rhät Schonens. Beiträge zur Kenntnis der Organisation der Stegocephalengruppe Brachyopoidei. *Acta Univ. lund.* **34**, (2), 1–75, 5 pl.

—— 1943*a*. Über einige postkraniale Skelettreste der triassischen Stegocephalen Spitzbergens. *Bull. geol. Instn. Univ. Upsala*, **30**, 227–72, 4 pl.

—— 1943*b*. On the morphology of the lower jaw of Stegocephalia with special reference to Eotriassic stegocephalians from Spitzbergen. I Descriptive Part. *K. svenska Vetensk Akad. Handl.* **20** (9), 1–46, 9 pl.

—— 1944. On the morphology of the lower jaw of Stegocephalia with special reference to Eotriassic stegocephalians from Spitzbergen. II General Part. Ibid. **21**, no. 1.

OLSON, E. C. 1936. Dorsal axial musculature of certain primitive Permian Tetrapods. *J. Morph.* **59**, 265–311.

PANCHEN, A. L. 1959. A new armoured amphibian from the Upper Permian of East Africa. *Phil. Trans.* B, **242**, 207–81, pl.

—— 1966. The axial skeleton of the labyrinthodont *Eogyrinus attheyi*. *J. Zool., Lond.* **150**, 199–222.

—— 1967. The homologies of the labyrinthodont centrum. *Evolution, Lancaster, Pa.* **21**, 24–33.

PARRINGTON, F. R. 1946. On the cranial anatomy of cynodonts. *Proc. zool. Soc. Lond.* **116,** 181–97.
—— 1967. The vertebrae of early tetrapods. *Colloques Int. Cent. Natn. Rech. Scient.* **163,** 269.
RIABININ, A. N. 1930. A labyrinthodont stegocephalian *Wetlugasaurus angustifrons* nov. gen., nov. sp. from the Lower Triassic of Vetluga-Land in Northern Russia. *Ezheg. russk. paleont. Obschch.* **8,** 49–76, 5 pl.
ROMER, A. S. 1922. The locomotor apparatus of certain primitive and mammal like reptiles. *Bull. Am. Mus. nat. Hist.* **46,** 517–606, 20 pl.
—— 1947. Review of the Labyrinthodonta. *Bull. Mus. comp. zool. Harv.* **99,** 1–352.
SÄVE-SÖDERBERGH, G. 1936. On the morphology of Triassic Stegocephalians from Spitzbergen, and the interpretation of the endocranium in the Labyrinthodontia. *K. svenska Vetensk Akad. Handl.* **16,** 1–181, 22 pl.
SAWIN, H. J. 1945. Amphibians from the Dockum Triassic of Howard County, Texas. *Univ. Tex. Publs.* **4401,** 361–99.
SCHROEDER, H. 1913. Ein Stegocephalen-Schädel von Helgoland. *Jb. preuss. geol. Landesanst.* **33,** 232–64, 7 pl.
SHAWKI MOUSTAFA, Y. 1955. The skeletal structure of *Parioxys ferricolus* Cope. *Bull. Inst. Egypte*, **36,** 41–76, 9 pl.
STOCKLEY, G. M. 1932. The geology of the Ruhuhu Coalfields, Tanganyika Territory. *Q. Jl geol. Soc. Lond.* **88,** 610–22.
—— and OATES, F. 1931. The Ruhuhu Coalfields, Tanganyika Territory. *Mining. Mag.* **45,** 73–91.
WATSON, D. M. S. 1919. The structure, evolution and origin of the Amphibia.—The 'orders' Rachitomi and Stereospondyli. *Phil. Trans.* B, **209,** 1–73, 2 pl.
—— 1926. Croonian Lecture. The evolution and origin of the Amphibia. Phil. Trans. B, **214,** 189–257.
—— 1951. *Paleontology and modern biology*. New Haven: Yale University Press.
—— 1956. The brachyopid labyrinthodonts. *Bull. Br. Mus. nat. Hist.* **2,** 317–92, 1 pl.
—— 1958. A new labyrinthodont (*Paracyclotosaurus*) from the Upper Trias of New South Wales. *Bull. Br. Mus. nat. Hist.* **3,** 233–64, 5 pl.
—— 1962. The evolution of the Labyrintodontia. *Phil. Trans.* B, **245,** 219–65.
WELLES, S. P., and COSGRIFF, J. 1965. A Revision of the labyrinthodont Family Capitosauridae and a description of *Parotosaurus peabodyi* n. sp. from the Wupatki Member of the Moenkopi Formation of Northern Arizona. *Univ. Calif. Publs. geol. Sci.* **54,** 1–148, 1 pl.
WEPFER, E. 1923. *Cyclotosaurus papilio* n. sp. aus der Grenzregion Muschelkalk–Lettenkohle des nördlichen Baden, ein Beitrag zur Kenntnis des Stegocephalen–Hinterhauptes. *Mit. bad. geol. Landesanst.* **9,** 367–90, 2 pl.
WESTOLL, T. S. 1943. The hyomandibular of *Eusthenopteron* and the tetrapod middle ear. *Proc. R. Soc.* B, **131,** 393–414.
WHITE, T. E. 1939. Osteology of *Seymouria baylorensis* Broili. *Bull. Mus. comp. Zool. Harv.* **85,** 325–410, 3 pl.
WILLISTON, S. W. 1910. *Cacops*, *Desmospondylus*; new genera of Permian vertebrates. *Bull. geol. Soc. Am.* **21,** 249–84.
WILSON, J. A. 1941. An interpretation of the skull of *Buettneria*, with special reference to the cartilages and soft parts. *Contr. Mus. Palaeont. Univ. Mich.* **6,** 71–111.

LIST OF ABBREVIATIONS USED IN THE FIGURES

Nerve foramina	Roman numerals
A	angular
add. cr	adductor crest
a. pal. vac	anterior palatal vacuity
a. pr	anterior process
area	area of pterygoid which articulates with the pre-articular process
ART	articular
as. pr	ascending process
avn	antero-ventral bone nubbin
ba. pr	basal process
bo. crest	basi-occipital crest
bo. hollow	hollow in exoccipital for the basi-occipital cartilage
bone	area of finished bone on the pleurocentrum
boss	quadrate boss
pt. pr	conical recess for the basipterygoid process of the basisphenoid

C	coronoid
cap	capitulum
centre	centre of ossification
ch. t. f.	chorda tympanic foramen
CL	clavicle
CLEI	cleithrum
clei. art	area for articulation with the cleithrum
clm. m	area of attachment of the cleido-mastoideus muscle
CO	coracoid
cr. pa	paroccipital crest
cr. pt	parapterygoid crest
D	dentary
d. f	dorsal foramen
d. ca	dorsal canal
delt. cr	deltoid crest
dia	diapophysis
dist. art	distal articulation
dist. exp	distal expansion
d. pr	dorsal process
d. pr. prart	dorsal process of the pre-articular
ECT	ectopterygoid
F	frontal
fen. ov	fenestra ovalis
hollow	hollow in tabular or exoccipital for the opisthotic
ic. f	foramen for the internal carotid artery
ICL	interclavicle
IL	ilium
IS	ischium
ipmx. f	interpremaxillary foramen
ipt. v	interpterygoid vacuity
J	jugal
j. f	jugular foramen
L	lachrymal
l. pr	lateral process
lam. pr	lamellar process
MX	maxilla
N	nasal
n. a.	neural arch
ne	external nostril
ni	internal nostril
obl. r	oblique ridge
ol. pr	olecranon process
OT	pro-otic ossification
P	parietal
PAL	palatine
pal. f	foramen for the palatine branch of the internal carotid artery
para	parapophysis
par. pr	paroccipital process
pc	pleurocentrum
PF	post-frontal
pin. f	pineal foramen
PMX	premaxilla
PO	post-orbital
POSPL	post-splenial
PP	post-parietal
ppq. gr	groove on the pterygoid for the palato-pterygo-quadrate cartilage
p. pr	posterior process
pq. f	paraquadrate foramen
pr. cult	cultriform process of the parasphenoid
PRF	prefrontal
prz	prezygapophysis
PSP	parasphenoid
PT	pterygoid
psp. sut	area for suture with the parasphenoid
pz	post-zygapophysis
Q	quadrate
QJ	quadratojugal
rart. pr	retro-articular process
SA	surangular
SC	scapula
sgl. b	supraglenoid buttress
sgl. f	supraglenoid foramen
SMX	septomaxilla
SPET	sphenethmoid complex
SPL	splenial
SQ	squamosal
ST	supratemporal
STA	stapes
ste. v	subtemporal vacuity
sup. cr	supinator crest
T	tabular
tr. in	internal trochanter
tr. 4	fourth trochanter
tub	tuberculum
V	vomer
v. c. d.	groove for vena capitis dorsalis
v. pr	ventral process
unc. pr	uncinate process

Final typescript received 1 October 1969

A. A. HOWIE
School of Biological Sciences
University of Sydney
Sydney, Australia, 2006

FEEDING HABITS OF PREDATORY GASTROPODS IN A TERTIARY (EOCENE) MOLLUSCAN ASSEMBLAGE FROM THE PARIS BASIN

by JOHN D. TAYLOR

ABSTRACT. The distinctive boreholes produced by two predatory gastroped superfamilies, the Muricacea and the Naticacea, can be recognized in their molluscan prey in a fossil assemblage from the Calcaire Grossier (Eocene, Lutetian) from Dameray in the Paris Basin. Possible predators are six species of Naticacea and two of Muricacea. About 7000 mollusca representing 40 species were examined for boreholes of either type. The most common prey species of the Muricacea were the epifaunal bivalve *Ostrea plicata*, the shallow burrowing bivalve *Venericardia serrulata* and the epifaunal gastropod *Omalaxis serrata*. The Naticidae fed upon deeper burrowing bivalves as well as *Venericardia serrulata* but very rarely upon epifaunal bivalves. Their principal prey species was the burrowing gastropod *Mesalia regularis* as well as a varied selection of other burrowing gastropods with a marked tendency towards cannibalism within the superfamily. The position of the borehole upon the prey species can give information on the behaviour and mode of attack of the predator.

IT is widely known that members of several families of Recent gastropods obtain their food by boring holes through the calcareous exoskeletons of prey (Carriker and Yochelson 1968). The families with this ability are the Naticidae, Muricidae, and the Cassidae; of these, the two former feed regularly upon other molluscs and the latter usually feeds upon echinoderms. Gastropod boreholes have been recognized in molluscs and brachiopods of many ages (Fischer 1922, 1960, 1962, 1963, 1964, 1966, Bucher 1938, Hayasaka 1933, Siler 1965, Brunton 1966, Carter 1967, Carriker and Yochelson 1968). However, the holes, particularly in the Palaeozoic, need not have been produced by members of the families of Recent gastropods listed above.

To the palaeontologist the recognition of these boreholes gives one of the few pieces of positive, rather than circumstantial, evidence of feeding. Previous work on boreholes in fossils has been limited to records of their occurrence and a discussion of possible predators. The present study of predation on a molluscan assemblage, from the Calcaire Grossier (Eocene, Lutetian) of the Paris Basin shows that boreholes of the Naticacea and Muricacea can be distinguished and with certain reservations inferences about the dietary preferences and the biology of the predators can be made.

BORING IN RECENT GASTROPODS

A detailed summary of boring mechanisms and borehole morphology has recently been made by Carriker and Yochelson (1968). It appears that all Recent Naticacea bore holes, and the work of Ankel (1937), Ziegelmeier (1954, 1961), and Carriker (1961) has established that they bore by means of rotatory action of the radula assisted by a secretion from an accessory boring organ situated at the ventral tip of the proboscis. The hole produced by this process is neat and circular with a broad bevelled outside rim producing a wide conical shape (see figure in Carriker and Yochelson 1968).

[Palaeontology, Vol. 13, Part 2, 1970, pp. 254–60, pl. 46.

Incomplete borings show a characteristic central boss. Naticids are usually infaunal gastropods, highly active but usually only bore when they and the prey are buried in the sand. The foot is exceptionally broad and used as a plough when moving through the sand. The prey is grasped and virtually enveloped in the foot while being manipulated into the correct position for boring to commence. Boring takes place by alternations of rotatory rasping of the radula and the application of the accessory boring organ to the site. When the hole is complete, the proboscis is closely applied and the contents of the prey dragged out and pieces cut off by the jaws. Recent naticids usually feed upon infaunal bivalves and occasionally upon gastropods when the need and opportunity arises (Paine 1963).

Independently the Muricacea have evolved a similar method of boring using the radula with the aid of a secretion from an accessory boring organ situated in the foot. The boring process is essentially similar to that of the naticids but the resulting hole is rather different. The hole is straight-sided, or tapers slightly inwards, the outer parts may be ragged and irregular; a bevelled rim is sometimes produced but it is never as wide or neat as that of the naticids. Members of the Muricacea are almost exclusively epifaunal and movements appear rather clumsy when compared with those of the highly motile naticids. In many species the foot is poorly developed and they are unable to move rapidly in pursuit of prey and have limited, if any, powers of excavating prey from sediment (Paine 1963). However, on rocky shores muricids are very successful predators feeding upon byssate bivalves, limpets, and barnacles. Muricids such as *Urosalpinx* and *Ocenebra* are common predators of oyster beds (Carriker 1955, Hancock 1960).

The ability to drill holes enables naticids and muricids to attack and eat bivalves larger than themselves. However, when attacking gastropods the size and mobility of the prey are important limiting factors (Paine 1963). Ansell (1960) considers that naticids may not be able to hold and manipulate much larger bivalves successfully and consequently do not recognize them as suitable food.

Carter (1967) has pointed out that there have been many attempts to show a preferred boring site for naticids but that most of this has been inconclusive and conflicting. Ansell (1960) reasonably considers that the site of boring by naticids depends upon the shape of the prey and predator and in any one species of prey there would be a preferred site but that the position of the borings would be expected to differ for each prey/predator combination. Muricids generally do not show preferred sites for boring when feeding upon epifaunal prey. However, when bivalves are attached in tight byssate groups only certain portions of the prey may be available for boring.

PREDATION IN THE CALCAIRE GROSSIER ASSEMBLAGE

Part of a large block of Calcaire Grossier limestone originating from Bed iii (Abrard 1925) at Dameray, near Epernay in the Paris Basin, has been examined. It is a loosely cemented shell sand composed mainly of broken and whole mollusc shells; echinoids, *Ditrupa*, polyzoa, and foraminifera are also very common.

Preservation of the fossils is excellent; many bivalves are preserved with the valves together and all growth stages of many species are present, including even the planktonic veliger stages of the molluscs. It appears that very little post-mortem sorting has

taken place. The numbers of individuals of each species extracted from the rock gives some indication of their relative abundance in the assemblage. About 7000 molluscs were examined representing 40 species of which 29 showed evidence of predation by boring gastropods (Table 1).

Potential predators

Molluscan genera in the Calcaire Grossier assemblage are sufficiently similar to, or the same as Recent genera to assume that they probably had similar habits. Thus it is possible to pick out the potential hole-boring predators in the assemblage and make the assumption that no other gastropod genus represented in the assemblage was a borer into other molluscs. The possibility that some holes may have been drilled by octopus must not be discounted (Pilson and Taylor 1961), but these are much more irregular than those of the Muricacea.

Possible hole-borers are represented by six species of Naticacea and two Muricacea. Only two species of naticids are at all common, these being *Natica epiglottina* and *Euspira labellata*. Wrigley (1949) considers that *Lunatia*, a Recent genus, is synonymous with *Euspira*; feeding in the former has been described in detail by Zeigelmeier (1954). Three species of *Ampullina* occur, *A. patula*, *A. sigaretina*, and *A. parisiensis* but only the first occurs in any numbers. This genus became extinct during the Miocene but it is so similar in morphology to Recent naticids that it is reasonable to assume that it was a borer. The only other naticid present is *Sinum clathratum* of which only five specimens were found; feeding in a Recent species of this genus has been described by Paine (1963). Only two species of muricids were found, *Pteropurpura tricarinatus* and *Poiriera frondosus*; whilst it cannot be assumed that all muricids are borers, these two species are the only available potential borers of straight-sided holes in the assemblage. These muricids are surprisingly uncommon, only 20 specimens of *P. tricarinatus* and 16 of *P. frondosus* were found. *P. tricarinatus* shows great morphological resemblance to the Recent 'Oyster drill' *Ocenebra*.

Predation

Each mollusc was examined for presence, type (muricid or naticid), and success or failure of the boring. The results of this examination and the numbers examined are shown in Table 1. Amongst bivalves the most common and most commonly attacked species are *Venericardia serrulata* and *Ostrea plicata*. *O. plicata* is a cemented epifaunal species frequently occurring in attached groups. It is attacked exclusively by muricids; of the 103 borings seen there was a slight preference for right, upper valves (58 borings) as opposed to the lower left valve (42 borings). There is no apparent preferred site for the attacks. This behaviour is slightly puzzling, for it would be expected that attacks on the attached, more inaccessible and thicker, lower valve would be fewer than on the thin, right, upper valve, seemingly the more obvious site for attack. A similar sort of behaviour has been observed on living species by Carriker (1955) who records that in *Urosalpinx* the site of drilling is not limited to any specific region or to any position which is easier to penetrate. Another Recent muricid predator, *Nucella lapillus* (Linnaeus), will frequently attempt to bore the thick ligamental area of *Mytilus edulis* Linnaeus whilst other individuals at the same locality may be boring at the shell margins

TABLE 1

Prey species	*Number examined*	*Naticid bored*	*Muricid bored*	*Failed borings*
BIVALVES				
Nucula inixta Deshayes	19	2	5	
Nuculana galliotina Nyst.	29	0	0	
Barbatia irregularis Deshayes	45	4	0	
Glycimeris pulvinata (Lamarck)	215	9	2	
Ostrea plicata Solander	981	0	103	
Venericardia imbricata Deshayes	280	0	0	
Venericardia serrulata Deshayes	2,699	101	366	
Crassatella dilatata Deshayes	21	2	1	
Crassatella grignonensis Deshayes	51	10	0	
Crassatella trigonata (Lamarck)	177	2	2	
Crassatella tumidum (Lamarck)	20	0	3	
Loxocardium bouei (Deshayes)	200	2	6	1 muricid
Calpitaria distincta (Deshayes)	180	11	0	
Aphrodina nitidula (Lamarck)	77	13	0	2 naticid
Castacallista laevigata (Lamarck)	62	3	0	
Bicorbula gallica (Lamarck)	27	0	5	
Corbula rugosa Lamarck	179	2	22	1 muricid
GASTROPODS				
Bittium sp.				
Calyptraea aperta Solander	65	6	0	
Solarium olicatum (Lamarck)	100	0	4	
Oinalaxis serrata (Deshayes)	73	2	2	1 muricid
Mesalia regularis (Deshayes)	519	0	109	
Rimella fissurella (Linnaeus)	886	272	0	
Marginella eburnea (Lamarck)	227	12	1	
Marginella ovulata (Lamarck)	200	3	0	
Natica epiglottina (Lamarck)	31	5	0	
Euspira labellata (Lamarck)	115	9	0	10 naticid
Ampullina patula (Lamarck)	138	17	3	11 naticid
Ampullina parisiensis (d'Orbigny)	8	2	0	
Ampullina sigaretina (Deshayes)	2	0	0	
Sinum clathratus (Gmelin)	6	1	0	
Ancilla buccinoides (Lamarck)	5	0	0	
Pteropurpura tricarinatus (Lamarck)	119	9	2	
Poiriera frondosus (Lamarck)	20	0	0	
Sycostoma pirus (Solander)	16	0	0	
Clavilithes noae (Lamarck)	12	0	0	
Ficus sp.	5	0	0	
Turris sp.	145	5	0	
Athleta (*Volutospina*) *athleta* (Linn.)				
Conus parisiensis (Deshayes)	9	2	0	
Ringicula ringens (Lamarck)	66	0	0	

(personal observation). *Venericardia serrulata* is by far the most common bivalve, usually reaching a size of 15 mm. It was a shallow burrower and shows evidence of predation by both naticids and muricids; the latter making the most attacks. In attacks on this species most of the muricid bores are situated at the margin of the valves. These marginal bores at the commissure of the valves are semicircular and are frequently

situated in the interspace between the ribs. The bores are very similar to the illustrations by Carriker (1961) of boring by *Murex fulvescens* on *Mercenaria mercenaria*.

In an attempt to see if there was a preferred drilling site the shell was divided up into sectors and the frequency of attacks in each sector recorded (text-fig. 1). No preference for right or left valves was shown, but in both valves there was a very marked preference for sites in the two sectors at the ventral margin towards the midline (Pl. 46, figs. 1, 2). Naticid bores into this species are usually completely enclosed as opposed to the marginal borings of muricids and situated towards the centre of the shell. Different sizes of *Venericardia* show different predation rates, most attacks taking place in the 3–6 mm. size range and least in the 11–15 mm. range. Small *Venericardia* are drilled by small holes indicating small predators. The regular preferred position of muricid bores in this species, as opposed to the indiscriminate attacks on *O. plicata*, is probably accounted for by the fact that *Venericardia* is a burrower and always has the same orientation in the sediment so that the muricid must excavate and manipulate the prey in its foot prior to drilling. These processes probably follow fixed behaviour patterns, resulting in the apparently preferred drilling site. Epifaunal bivalves are usually byssally fixed or cemented allowing the muricids to crawl all over their prey and attack without prior manipulation with the foot.

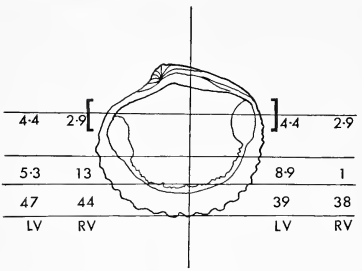

TEXT-FIG. 1. Diagram of inside of the right valve of *Venericardia serrulata* showing the percentage frequency of attacks in each sector for each valve. 215 attacked valves examined.

The larger, thicker-shelled species *Venericardia imbricata* which reaches 40 mm. in length shows no evidence of predation or even attempted borings suggesting that adults of this species are not recognized as prey. Ansell (1960) found that large, thick-shelled individuals of *Venus striatula* had neither borings nor attempted borings and suggested that *Natica alderi* may be incapable of manipulating large heavy specimens in the foot.

By comparison with Recent members of the family *Bicorbula gallica* and *Corbula rugosa* can be assumed to have been very shallow burrowers, probably with their posterior end protruding from the sediment. They are eaten almost exclusively by muricids. In *B. gallica* most of the borings took place at the protruding posterior end, but in the smaller *C. rugosa* most borings took place towards the midline of the shell.

EXPLANATION OF PLATE 46

Fig. 1. *Venericardia serrulata* Deshayes showing muricid boring, ×12.

Fig. 2. *Venericardia serrulata* Deshayes showing muricid boring at valve margin, a common occurrence in the species, ×18.

Fig. 3. Naticid boring in *Crassatella grignonensis* Deshayes, ×12.

Fig. 4. Muricid boring on flat spire of *Omalaxis serrata* Deshayes, ×20.

Fig. 5. Naticid boring in *Ampullina patula* (Lamarck) indicating cannibalism within the Naticacea, ×11.

Fig. 6. *Mesalia regularis* (Deshayes) showing a naticid boring in the mid-portion of the spire, ×14.

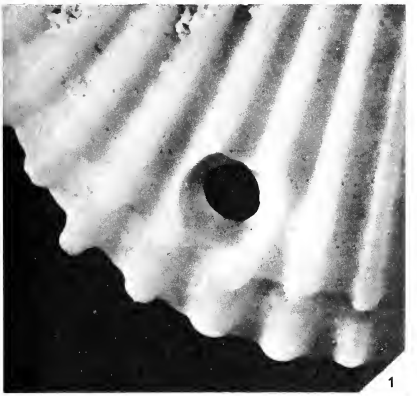
1


2


3

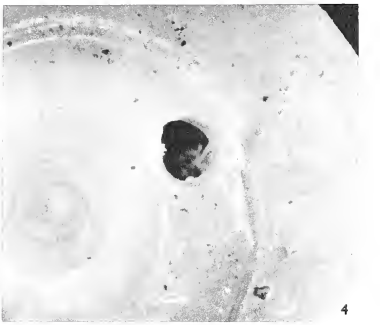
4

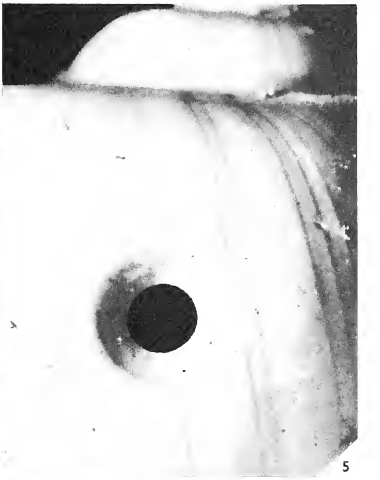
5

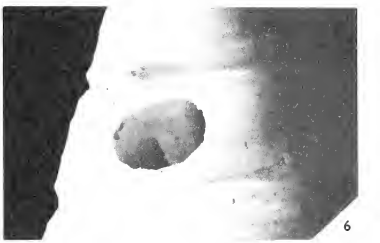
6

TAYLOR, Gastropod predation

Deeper burrowing bivalves (indicated by deep pallial sinuses), such as *Aphrodina nitidula*, *Calpitaria distincta*, are attacked by naticids alone. No particular preference for left or right valves was shown, but in *A. nitidula* all the bores fall within the area bounded by the pallial lines. All naticid attacks on the burrowing *Crassatella grignonensis* took place approximately on a line from the umbo to the midpoint of the ventral margin (Pl. 46, fig. 3). Predation on the very thin-shelled, shallow burrower *Loxocardium bouei* is less than expected. A possible reason for this is that in common with several Recent species of Cardiacea it may have had the ability to make leaping motions by rapid flexing of the foot; an effective escape mechanism. In *Nucula mixta* the muricid bores are distributed around the ventral margin, but the two naticid bores are situated at the anterior end. Four individuals of *Barbatia irregularis* were attacked by naticids. This is rather surprising as it is a byssate epifaunal bivalve and must have been attacked very close to the sediment surface.

Predation on gastropods was more exclusively by naticids, with a wide choice of prey; whereas predation by muricids is limited to a few species only. By far the most common gastropod in the fauna is a turritellid *Mesalia regularis*, a burrowing suspension feeder. This species shows a very high predation rate (Table 1) and must have been a principal item in the diet of naticids. Most of the attacks take place on individuals up to about 20 mm. in height. The hole is usually made about half-way up the spire (Pl. 46, fig. 6) with no preference for aboral or adoral sides; larger, thicker-shelled specimens of *Mesalia* show no evidence of attacks.

In all naticid attacks on gastropods there is a more definite preferred site than for attacks on bivalves. Species such as *Marginella eburnea*, *M. ovulata*, *Ancilla buccinoides*, and *Euspira labellata* show most of the attacks at the adoral surface very near to the aperture. These apparently preferred sites for boring arise possibly because gastropods are generally more active than bivalves and the ensuing struggles with predators induce stereotyped behaviour patterns on the part of both attacker and attacked. Cannibalism by naticids is common (Pl. 46, fig. 5) but it is impossible to tell if this is intra- or inter-specific, or both. An interesting feature of the cannibalism is the high incidence of failed borings, a reflection of the high mobility of this genus. Carriker (1961) records that laboratory-starved *Polynices* (naticids) exhibit a high degree of cannibalism but in the presence of bivalves will eat these first.

The only gastropod attacked by muricids to any extent is *Omalaxis serrata*. Little is known about the habits of this extinct genus, but by comparison with the related genus *Architectonica*, it is assumed to have been epifaunal. Of the muricid attacks on this species, 70 per cent took place on the flat top of the planispiral shell (Pl. 46, fig. 4), other attacks took place on the side of the whorl. The only other epifaunal gastropods, *Architectonica plicata*, *Capulus ungaricus*, and *Ringicula ringens*, show little or no predation by muricids.

It is noticeable that attacks on other gastropod predators such as *Sycum*, *Athleta*, *Clavilithes*, and *Turris* are uncommon, and where they do occur, as in *Turris*, they are confined to juveniles.

CONCLUSIONS

From an examination of the occurrence and distribution of the two different types of gastropod boreholes in the Calcaire Grossier fossil assemblage it is possible to

reconstruct, at least in part, the diets of the two gastropod superfamilies. It is possible to ascertain points of feeding overlap and possible sources of competition between the two superfamilies. Muricacea generally feed upon sedentary epifaunal prey, and Naticacea upon infaunal prey, both sedentary and motile; but shallow burrowing species are liable to be eaten by members of either superfamily. The site of the attack on the prey species can give information concerning the behaviour of the predator and prey. Study of fossil boreholes provides one of the few positive pieces of evidence in the reconstruction of food chains and trophic levels in fossil communities.

Acknowledgements. I am grateful to Dr. H. Brunton for reading the manuscript, and to Mr. P. Green of the Photographic Studio of the British Museum for the photographs.

REFERENCES

ABRARD, R. 1925. Le Lutetien du Bassin de Paris. *Essai de Monographie stratigraphique. Angers. Soc. Française d'Imp. d'Angers*, 1–388.

ANSELL, A. D. 1960. Observations on predation of *Venus striatula* (Da Costa) by *Natica alderi* (Forbes). *Proc. malac. Soc. Lond.* **34**, 157–64, 1 pl.

ANKEL, W. E. 1937. Wie böhrt *Natica*? *Biol. Zentr.* **57**, 75–82.

BRUNTON, H. 1966. Predation and shell damage in a Viséan Brachiopod Fauna. *Palaeontology*, **9**, 355–9, 1 pl.

BUCHER, W. H. 1938. A shell boring gastropod in a *Dalmanella* bed of Upper Cincinnatian age. *Am. J. Sci.* **36**, 1–7.

CARRIKER, M. R. 1955. Critical review of biology and control of oyster drills, *Urosalpinx* and *Eupleura*. *Spec. sci. Rep. U.S. Fish. Wildl. Serv.* **148**, 1–150.

—— 1961. Comparative functional morphology of boring mechanisms in gastropods. *Amer. Zool.* **1**, 263–6.

—— and YOCHELSON, E. L. 1968. Recent gastropod boreholes and Ordovician cylindrical borings. *U.S. Geol. Survey. Prof. Pap.* **593–B**, 1–23, 5 pl.

CARTER, R. M. 1967. On the biology and palaeontology of some predators of bivalved mollusca. *Palaeogeography Palaeoclimatol. Palaeoecol.* **4**, 29–65, 2 pl.

FISCHER, P.-H. 1922. Sur les gastéropodes perceurs. *J. Conchyliol.* **67**, 1–56.

—— 1960. Action des gastéropodes perceurs sur un bivalve de l'Etage Lutetien. Ibid. **100**, 129–31.

—— 1963. Corbules fossiles perforées par des gastéropodes prédateurs. Ibid. **103**, 29–31.

—— 1964. Au sujet des perforations attribuées à des gastéropodes pre-tertiares. Ibid. **104**, 45–47.

—— 1966. Perforations de fossiles tertiares par des gastéropodes prédateurs. Ibid. **605**, 66–96.

HANCOCK, D. A. 1960. The ecology of the molluscan enemies of the edible mollusc. *Proc. malac. Soc. Lond.* **34**, 123–43.

HAYASAKA, I. 1933. Fossil occurrence of pelecypod shells bored by certain gastropods. *Mem. Fac. Sci. Agric. Taihoku Imp. Univ.* **6**, 65–70.

PAINE, R. T. 1963. Trophic relationships of 8 sympatric predatory gastropods. *Ecology*, **44**, 63–73.

PILSON, M. E. Q., and TAYLOR, P. B. 1961. Hole drilling by *Octopus*. *Science*, **134**, 1366–8.

SILER, W. L. 1965. Feeding habits of some Eocene carnivorous gastropods. *Texas J. Sci.* **17**, 213–18.

WRIGLEY, A. 1949. English Eocene and Oligocene Naticidae. *Proc. malac. Soc. Lond.* **28**, 10–30.

ZIEGELMEIER, E. 1954. Beobachtungen über den Nahrungserwerb bei der Naticide *Lunatia nitida* Donovan. (Gastropoda, Prosobranchia) *Helgol. Wiss. Meeresunters.* **5**, 1–33.

—— 1961. Zur Fortpflanzungsbiologie der Naticiden (Gastropoda, Prosobranchia). Ibid. **8**, 94–188.

J. D. TAYLOR
Department of Zoology
British Museum (Natural History)
Cromwell Road
London, S.W.7

Final typescript received 15 October 1969

CHITINOZOA FROM THE ORDOVICIAN SYLVAN SHALE OF THE ARBUCKLE MOUNTAINS, OKLAHOMA

by W. A. M. JENKINS

ABSTRACT. Chitinozoa referable to nine genera and twelve species (five new) are recorded from the Sylvan Shale of the Arbuckle Mountains in southern Oklahoma. They provide for the first time a means of dating, biostratigraphically subdividing, and correlating the entire formation. Its chitinozoan fauna indicates that the Sylvan Shale is of Upper Ordovician age throughout and confirms with additional fossil evidence the age of the lower beds. No *abrupt* changes break the general continuity of the chitinozoan succession but on the basis of *gradual* changes in the composition of its chitinozoan fauna the Sylvan Shale may be divided into three biostratigraphical units. The fauna occurs throughout the Arbuckle Mountains and is recognizable in the subsurface of western Texas and in the Maquoketa Formation of eastern Iowa. It differs strikingly from the fauna in the underlying Viola and Fernvale Limestones, and from the faunas in the overlying formations of the Silurian–Devonian Hunton Group. The occurrence of reworked Sylvan chitinozoans in upper Sylvan strata indicates that during late Sylvan time uplift (hitherto unsuspected) took place, at least locally, in the southern mid-continent.

The fauna is described systematically. *Clathrochitina* Eisenack 1959 is used in its original sense; *Plectochitina* Cramer 1964 is a junior synonym. *Sagenachitina* gen. nov. is proposed for species, hitherto referred to *Clathrochitina*, whose basal margins support finely divided networks. *Acanthochitina rashidi*, *Ancyrochitina merga*, *Clathrochitina sylvanica*, *Cyathochitina agrestis*, and *Sphaerochitina lepta* are new species.

THIS account of chitinozoans from the Sylvan Shale is the second of two investigations directed primarily at establishing an Upper Ordovician chitinozoan reference section in the Arbuckle Mountains of southern Oklahoma. In a stratigraphical sense it is the continuation of an earlier study (Jenkins 1969) devoted to chitinozoans from the underlying Viola and Fernvale Limestones. An incidental objective was to provide, for the first time, a means of dating and correlating the entire formation.

The Sylvan Shale is the youngest Ordovician formation in the Arbuckle Mountains, and rests unconformably upon the slightly older Viola–Fernvale limestone succession. It was chosen for this investigation primarily because it contains large numbers of well-preserved chitinozoans at practically all stratigraphical levels, but several additional factors also favoured its selection as a standard for stratigraphical reference. In particular, it is a distinctive lithostratigraphical unit separated by regional unconformities and by its sharply contrasting lithology from thick carbonate sequences above and below. In the subsurface the Sylvan Shale extends across most of Oklahoma into north-western Texas and southern Kansas and has been widely used as a marker horizon in the subsurface mapping of an otherwise unbroken sequence of Ordovician to Devonian limestones.

The formation crops out widely within the Arbuckle Mountains, for which reason the samples were collected there. It is particularly well exposed and free from faulting in a narrow outcrop 14 miles (22 km.) long, running west-north-west from Ravia to the Washita River along the steeply dipping southern flank of the Sycamore Creek Anticline (text-fig. 1). Chitinozoans from this outcrop form the basis of the present study.

In this paper, for reasons presented elsewhere (Jenkins 1969, pp. 5, 6), the base of the *Nemagraptus gracilis* Zone (or its correlatives) is taken as the lower limit of the Upper Ordovician. Thus defined, the Upper Ordovician includes the basal beds of the North

[Palaeontology, Vol. 13, Part 2, 1970, pp. 261–288, pl. 47–51.]

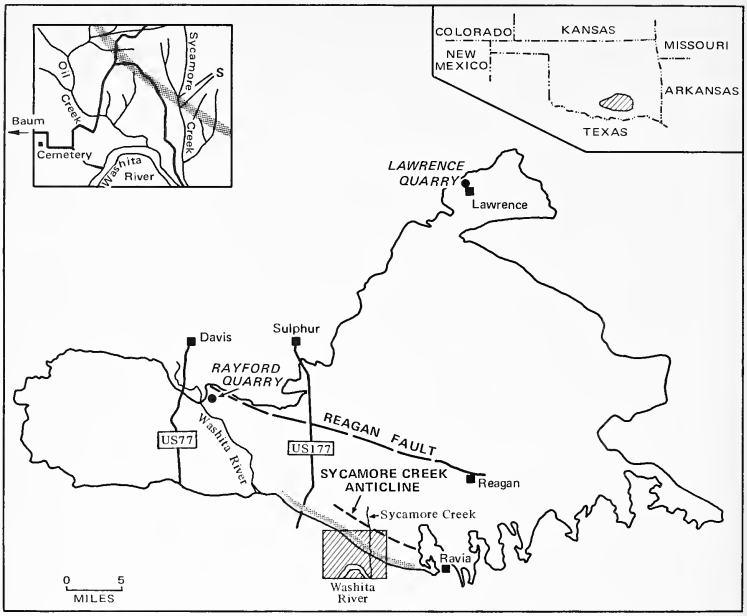

TEXT-FIG. 1. Showing the outcrop (outlined) and structural features of the pre-Pennsylvanian rocks in the Arbuckle Mountains. The shaded portion of the index map of Oklahoma delineates the area shown. The upper left inset map (represented by the shaded rectangle in the chart) shows the outcrop (stippled) of the Sylvan Shale exposed in the Sycamore Creek Anticline, and the road from Baum (on U.S. Highway 177) to the section (S) which provided the rock samples for this study. Compiled from Ham, W. E. 1955, *Geology of the Arbuckle Mountain Region*, Guide Book III; Ham, W. E. *et al.*, 1954, *Geologic Map and Sections of the Arbuckle Mountains, Oklahoma*, Guide Book III. Both published by the Oklahoma Geological Survey.

American Black River Stage and their correlatives (Twenhofel *et al.* 1954; Berry 1960*a*, *b*; Kay 1960, p. 30) at the base of the Caradoc Series in Britain.

PREVIOUS RESEARCH

Previous publications concerned with chitinozoans from the Sylvan Shale are limited to two notes (Wilson 1958, Wilson and Hedlund 1964) and an abstract (Wilson and Hedlund 1962). The latter is from Hedlund's (1960) substantial account of chitinozoans, acritarchs, and scolecodonts, which was submitted as a thesis for the Master of Science degree to the University of Oklahoma. Although unpublished, Hedlund's work has remained for a decade the chief source of information about

organic-walled microfossils in the Sylvan Shale, and the only attempt to describe them systematically.

The possibility exists, however, that chitinozoans were encountered in fossil residues of the Sylvan Shale as early as 1930. A short publication by Thomas (1930) contains (p. 87) not only a very early (perhaps the earliest) reference to organic-walled microfossils in the Lower Palaeozoic of Oklahoma, but almost certainly a passing reference to chitinozoans. I have been unable to ascertain whether or not this paper preceded Eisenack's of the same year, in which chitinozoans (though not named as such) were introduced to the scientific literature. On account of this paper's apparent obscurity outside North America the following relevant passage is reproduced.

> . . .I also have permission from Mr. S. W. Lowman, micropaleontologist for the Midcontinent Petroleum Corporation, to announce a discovery he has recently made concerning the Sylvan in Oklahoma and Kansas. He has found that after completely dissolving the shale in concentrated hydrochloric acid the residue will yield microfossils which are invisible upon ordinary microscopic examination. He discovered organisms similar to *Sporangites* found in the Woodford [Formation, which is Devonian–Mississippian]. One species is about as large as the disc-like *Sporangites huronense* and is found in the upper Sylvan from central Kansas to the Arbuckles. Another species about twice as large as the above has been found in the upper Sylvan on the outcrop and in wells near the Arbuckles. A few spindle-shaped forms have been found. There are reasons to believe that these are plant spores and there are also arguments in favor of the theory that they are graptolitic in nature (Thomas 1930, p. 87).

In all probability the 'spindle-shaped forms' are chitinozoans for, to my knowledge, no organic-walled microfossils in the Sylvan Shale other than certain chitinozoans (and possibly a few netromorph acritarchs) could be interpreted, however broadly, as spindle-shaped. It is interesting to learn from Thomas's paper that the speculation about the natural affinities of the Chitinozoa, which has continued to the present day, had already started before the group was formally established and named by Eisenack in 1931.

GENERAL STRATIGRAPHY

Lithology and fauna. Throughout the Arbuckle Mountains the lower part of the Sylvan Shale, up to *c.* 130 ft. (40 m.) thick, is a hard, splintery, very fissile, brown to dark grey shale containing graptolites which are particularly abundant near the base. By contrast, the upper part of the formation, up to 200 ft. (61 m.) thick, is mainly a soft, weakly fissile to concretionary, greenish-grey shale, and is apparently devoid of macrofossils. The topmost 30 ft. (9 m.) is a soft, massive, highly pyritic, light green claystone, which disaggregates completely in water and is, for this reason, only ever temporarily exposed. The Sylvan Shale is generally slightly calcareous, and may be highly calcareous locally, particularly in its upper 100 ft. (30 m). Dolomite beds a few inches thick occur irregularly throughout the formation, and in the lower part two beds of dense brown dolomite, each 1–3 ft. (0·30–0·91 m.) thick, extend laterally over a wide area. Outcrops of the Sylvan Shale are strikingly delineated by sharp changes in the topography, soil, and vegetation of the limestone country within which they are exposed.

The formation contains, in addition to one species of brachiopod (Cooper 1956, p. 244) and seven species of graptolites (Decker 1935, 1945; Ruedemann 1947, pp. 90–2, 100) in its lower part, a rich fauna of chitinozoans and acritarchs throughout. Generally,

however, other fossils are lacking, and the upper Sylvan in particular is seemingly devoid of macrofossils.

The lithology and fauna of the Sylvan Shale indicate that it was laid down in tranquil waters, and suggested to Ham (1969, p. 11) that it was deposited in deeper waters than all other pre-Mississippian formations in the Arbuckle Mountains. It is the only pre-Upper Devonian shale unit, moreover, to persist throughout the Arbuckle Geosyncline and to extend beyond it over much of the southern mid-continent.

Pattern of deposition. Within the Arbuckle Mountains the Sylvan Shale's broad pattern of deposition is similar to that of the Viola Limestone (Jenkins 1969, p. 3). The Sylvan sediments in the south-western Arbuckle Mountains were laid down in the rapidly subsiding basin of the Arbuckle Geosyncline, whereas those to the north and east of a line now approximately followed by the Reagan Fault (text-fig. 1) were deposited on a slowly subsiding geosynclinal shelf. This led to the accumulation of less sediment in the north-east than in the south-west and explains the general thinning of the formation north-eastward across the Arbuckle Mountains from a maximum of 325 ft. (99 m.) in the basin to 150–175 ft. (45–53 m.) on the shelf (Ham 1969, p. 10).

Stratigraphical relations. Over a large part of Oklahoma, including the Arbuckle Mountains, regional unconformities separate the Sylvan Shale from a thick sequence of older Ordovician limestones below, and a succession of Silurian and Devonian carbonate formations above. The Sylvan lies everywhere upon the Fernvale Limestone, and the sharp contact is well exposed in Sycamore Creek (text-fig. 1), map reference $SW\frac{1}{4}$ $SE\frac{1}{4}$ sec. 27, T. 3 S., R. 4 E., Johnston County, Oklahoma. The dips of the two formations appear to be the same, but close examination reveals that the top of the Fernvale Limestone is an erosion surface that had been extensively weathered before the shale was laid down. A 2–3 in. (5–8 cm.) thick band of oxidizing pyritic 'rubble', containing phosphatized pebbles, locally marks the base of the shale, as at Sycamore Creek, and (Ham, personal communication, May 1969) is particularly well developed as a pyritic phosphate conglomerate, containing dolomite pebbles, in the road-cut entrance to Rayford Quarry (text-fig. 1), map reference $NW\frac{1}{4}$ $NE\frac{1}{4}$ $NE\frac{1}{4}$ sec. 28, T. 1 S., R. 2 E., Murray County, Oklahoma. This and related late Ordovician unconformities are given some prominence, and discussed in a regional context, by Ham and Wilson (1967, pp. 350–2) in a comprehensive account of Palaeozoic tectonic disturbances in the central United States.

Almost everywhere within the Arbuckle Mountains the Sylvan Shale is unconformably overlain by Silurian or Lower Devonian limestones (Amsden 1960, panel III). These are extremely thin within the Sycamore Creek Anticline, however, and locally, as at Sycamore Creek, they have been entirely removed by mid-Devonian erosion; the black shales and bedded cherts of the Upper Devonian–Mississippian Woodford Formation lie directly upon the Sylvan Shale. The Woodford Formation, which is 350–560 ft. (107–171 m.) thick in the Arbuckle Mountains, has been dated by conodonts as ranging in age from Frasnian (Upper Devonian) to Kinderhookian (Lower Mississippian); the Mississippian part of the formation generally is less than 1 ft. (0·30 m.) thick, and exceptionally at least 10 ft. (3 m.) thick (Hass and Huddle 1965).

Age and correlation. The Sylvan Shale was dated Upper Ordovician by Decker (1935), on the basis of graptolites confined to the lower part of the formation. The greater part

of the Sylvan Shale has yielded no macrofossils, however, but was placed in the Ordovician on the basis of its association with the lower Sylvan. Although Decker's age determination for the lower graptolitic Sylvan has generally been accepted, the age of the overlying 'unfossiliferous' beds, at least 200 ft. (61 m.) thick in the south-western Arbuckle Mountains, has not hitherto been demonstrated.

Collection and preparation of material. Samples were collected at stratigraphical intervals of 20 ft. (6·10 m.) throughout the Sylvan Shale succession exposed in the bed and banks of Sycamore Creek (text-fig. 1), map reference SW¼ SE¼ sec. 27, T. 3 S., R. 4 E., Johnston County, Oklahoma, commencing 1 ft. above the Fernvale Limestone–Sylvan Shale contact. The latter serves as an easily recognizable reference datum, and samples are numbered according to their original stratigraphical positions (measured in feet) above it. For example, sample Sy280 is from a stratigraphical level 280 ft. above the contact, the prefix 'Sy' indicating that it is from Sycamore Creek. These samples are briefly described in the appendix.

The collection of regularly spaced samples was made easy at Sycamore Creek by the steep inclination of the beds and the absence of faulting. The relatively resistant shales in the lower part of the formation are well exposed in the bed and steep banks of the creek, and samples of these were collected without difficulty. To obtain samples of the softer shales and claystones near the top of the formation, however, it was necessary to dig through as much as 2 ft. (0·6 m.) of Recent alluvium. The total thickness of the Sylvan Shale at Sycamore Creek, from its sharp contact with the Fernvale limestone below, to its equally sharp contact with the Woodford Formation above, was carefully measured by Mr. J. A. Turnbull and myself, and found to be 305 ft. (93 m.), slightly less than Decker's (1935, p. 698) figure of 320 ft. (97·5 m.).

In order to determine how much the character of the Sylvan chitinozoan fauna varies regionally several samples were collected at widely scattered localities (q.v., p. 283) throughout the Arbuckle Mountains. A few figured specimens are from outcrops along U.S. Highway 77 about 4 miles (6·4 km.) south of Davis (text-fig. 1), map reference sec. 30, T. 1 S., R. 2 E., Murray County, Oklahoma. Their reference numbers are prefixed 'Da'.

The chitinozoans were prepared for microscopical examination according to the method outlined by Jenkins (1967, pp. 439–41), and furnished with reference numbers in the manner described for the Viola and Fernvale specimens of an earlier study (Jenkins 1969, p. 7). Most of the preparations, including all the type material, and portions of each rock sample, are housed in the Micropalaeontology Laboratory, Department of Geology, The University, Sheffield, England.

SYSTEMATIC PALAEONTOLOGY

Order CHITINOZOA Eisenack 1931
Genus ACANTHOCHITINA Eisenack 1931 emend. Jenkins 1967

Type species. Acanthochitina barbata Eisenack 1931 (by original designation), Ordovician, Baltic.

Acanthochitina rashidi sp. nov.

Plate 47, fig. 20; Plate 48, figs. 1, 2; text-fig. 2

Holotype. Plate 48, figs. 2*a*, *b*. Specimen Sy80/2/1/B; Sylvan Shale, 80 ft. (24·38 m.) stratigraphically above base, Sycamore Creek.

Diagnosis. Small conical to pyriform test. Maximum diameter about four-fifths total length; base convex, margin rounded. Neck weakly differentiated from chamber, short, tapering; commonly not developed. Aperture equal to, or slightly greater than, half maximum diameter. Numerous closely spaced slender processes; arms of adjacent

processes united, forming a complete reticulum that stands as high as 12 μ above surface of test wall.

Dimensions (*in microns*). 25 specimens measured.

	Total length	*Maximum diameter*	*Apertural diameter*
Holotype:	128	89	53
Range:	105–158	81–106	40–63
Mean:	123	93	51

Remarks. Acanthochitina rashidi is considered as a separate species because it falls well outside Jansonius's (1964, p. 909) definition of *Kalochitina multispinata*. Wherever it has been found, however, *A. rashidi* makes up continuously intergrading populations with *K. multispinata* and many transitional forms occur. The two species are distinguished arbitrarily and solely on the basis of their ornaments. Their close relationship is not reflected in the strictly empirical system of classification followed here, however, and they are unavoidably referred to different genera.

TEXT-FIG. 2. *Acanthochitina rashidi* sp. nov. Lateral profile, ×400. For the sake of clarity only the ornament seen in profile is shown.

Comparison. In *Hercochitina downiei* Jenkins 1967 processes stand in longitudinal rows, and most frequently are connected only to those longitudinally adjacent to them. *A. rashidi* is much smaller than the type species (total length of 25 British examples 300–485 μ, mean 408 μ), and has a much more delicate ornament; processes on the basal margin do not differ appreciably from those elsewhere and, in particular, are not connected by a membrane.

Material. Several thousand single tests, and a dozen chains of two or three tests each.

Occurrence. Sy80–Sy200. *A. rashidi* is restricted to the middle of the Sylvan Shale, although forms transitional to it, but referable to *K. multispinata*, occur at the younger horizons Sy220, Sy240, and Sy260.

EXPLANATION OF PLATE 47

Figs. 1–19. *Ancyrochitina merga* sp. nov., all but 19 ×250. 1–8, Sy80/1/1/B, Sy60/1/1/F, B, E, Sy80/1/1/A, D, C, and Sy60/1/1/H, respectively, bearing a variety of T- and Y-shaped appendices. 9–11, Sy60/1/1/D, Sy80/1/1/E and Sy60/1/1/A, respectively, with λ-shaped appendices. 12, 13, Sy80/1/1/F (holotype) and Sy60/1/1/C, respectively, each possessing T-, Y-, and λ-shaped appendices. 14–17, Sy40/1/1/A, C, B, and D, respectively, with ornaments of simple spines and λ-spines; this form represents the species near the base of the Sylvan Shale, whereas younger Sylvan strata contain only smooth-walled forms (figs. 1–13). 18, Sy60/1/1/G, cluster of three tests; two are in polar view, the upper right in lateral view. 19, Sy80/1/1/G, detail showing three simple appendices, and one with three orders of branching, in phase-contrast illumination ×400.

Fig. 20. *Acanthochitina rashidi* sp. nov., Sy100/2/1/B, in phase-contrast illumination, ×400.

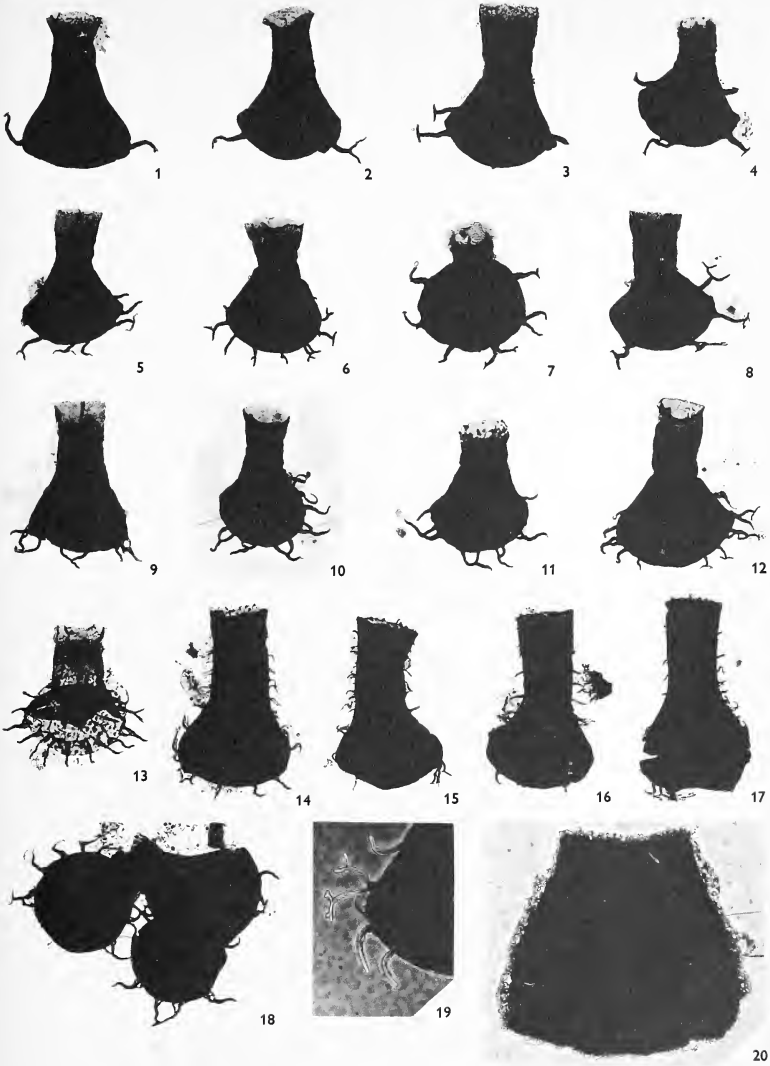

JENKINS, Ordovician chitinozoa from Oklahoma

Genus ANCYROCHITINA Eisenack 1955*a*

Type species. *Conochitina ancyrea* Eisenack 1931 (by original designation), Silurian, Baltic.

Ancyrochitina merga sp. nov.

Plate 47, figs. 1–19; text-fig. 3

Holotype. Plate 47, fig. 12. Specimen Sy80/1/1/F; Sylvan Shale, 80 ft. (24·38 m.) stratigraphically above base, Sycamore Creek.

TEXT-FIG. 3. *Ancyrochitina merga* sp. nov. Lateral view of test showing the appendices and the ornament of λ-spines and simple spines, ×400.

Diagnosis. Small fungiform test. Chamber about half total length, wider than long; base slightly convex, margin rounded. 8–24, generally fewer than 15, simple or branching appendices up to one-third of the maximum diameter in length; generally 1–3, rarely 4, orders of Y– or T–shaped branching into 2 sharply diverging, equal distal limbs. Commonly, appendices divide (λ–shaped branching) in a transverse plane to form two proximal limbs which meet the basal margin abruptly. Oral tube cylindrical or slightly flaring, one-third to half maximum diameter in width; aperture fringed with hairs up to 5μ in length. Test smooth, or bearing slender, tapering, simple or λ–spines with pointed tips, up to one-sixth maximum diameter in length; thinly distributed, absent on base and basal margin.

Dimensions (*in microns*). 25 specimens measured.

	Total length	*Chamber length*	*Maximum diameter*	*Oral tube diameter*	*Apertural diameter*	*Appendix length*
Holotype:	125	70	91	35	*c.* 35	< 30
Range:	100–155	52–71	70–98	32–46	35–55	< 35
Mean:	128	64	81	36	44	—

Description. The flanks of the short, wide chamber are almost straight and taper rapidly, but with no abrupt change of curvature, into the neck. The maximum diameter generally is 120–140% of the chamber length. Where *A. merga* first occurs (horizon Sy40) it bears slender, simple spines and λ-spines up to 12 μ in length, distributed thinly over the test (Pl. 47, figs. 14–17). Throughout the remainder of the formation, however, forms with smooth walls, or forms with very few short spines (< 2 μ in length) on the shoulder and neck, greatly predominate over the more ornate forms.

Comparison. A. merga is readily distinguished by the style and number of its appendices. *A. corniculans* Jenkins 1969 from the Viola and Fernvale Limestones is cylindro-conical rather than fungiform, and has only 4–6 appendices.

Material. Several thousand single tests.

Occurrence. Sy40–Sy305.

Genus CLATHROCHITINA Eisenack 1959

Type species. Clathrochitina clathrata Eisenack 1959 (by original designation), Wenlock, Gotland.

Diagnosis. 'Chitinozoans shaped like *Ancyrochitina ancyrea*, and furnished with appendices whose distal ends coalesce with a ring situated concentrically about the basal margin' (Eisenack 1959, p. 15).

Remarks. Clathrochitina Eisenack 1959 was conceived for cylindroconical chitinozoans possessing *distinct appendices* (generally discrete processes confined to the basal margin) that coalesce distally; *Plectochitina* Cramer 1964 is a junior synonym. Unfortunately, several species lacking distinct appendices have been referred inappropriately to *Clathrochitina* on the basis of *finely meshed networks* suspended from their basal margins, and *Plectochitina* has assumed the taxonomic role originally intended for *Clathrochitina*. Consequently, the genus *Sagenachitina* (q.v., p. 270) is here proposed for chitinozoans with *networks* suspended from their basal margins; and several species are transferred to it from *Clathrochitina*. The latter is considered to include, besides the type species, *Clathrochitina multiramosa* (Taugourdeau and Jekhowsky 1960) Taugourdeau 1967, *C. saharica* (Taugourdeau 1962) comb. nov., *C. carminae* (Cramer 1964) comb. nov., *C. rosendae* (Cramer 1964) comb. nov., and *C. combazi* (Cramer 1967*a*) comb. nov. It seems essentially a Silurian genus, being known only from the uppermost Ordovician (this paper), the Silurian (Eisenack 1959; Taugourdeau 1962, 1967; Cramer 1964, 1967*a*; Taugourdeau *et al.* 1967, p. 85, under *Plectochitina*), and, perhaps, the basal Devonian (Cramer 1964).

Cramer (1967*a*, pp. 84, 94; 1967*b*, p. 47) interpreted the structure on the basal margin of *C. clathrata* (type species of its genus) as a 'perforate cingulum' and, on the basis of this interpretation, transferred the species to *Cyathochitina* Eisenack 1955*b*. For species previously referred to *Clathrochitina*, which was abandoned through the loss of its type species, he proposed the genera *Clathrochitinella* and *Pseudoclathrochitina*. While Cramer's proposals may seem reasonable in the light of his structural interpretation, the latter is entirely inconsistent with Eisenack's (1959, p. 15, pl. 1, figs. 3, 4; text-fig. 4) clear illustrations and lucid, unambiguous description of the genus and its type species. Cramer's proposals and transfer of *C. clathrata* are, if only for this reason, unacceptable, and *Clathrochitinella* and *Pseudoclathrochitina* should be abandoned along with *Plectochitina*. Aside from the faulty interpretive basis upon which they rest, Cramer's proposals and transfer serve little more than to complicate and confuse a relatively straightforward issue, namely the generic placement of two groups of cylindroconical chitinozoans, one characterized by networks suspended from the basal margin (*Sagenachitina*), the other by appendices which coalesce distally (*Clathrochitina*). The existence of a few forms transitional between *Sagenachitina* and *Clathrochitina* is known (e.g. Taugourdeau 1967, pl. 1, fig. 9) but scarcely complicates the issue.

Clathrochitina sylvanica sp. nov.

Plate 48, figs. 3–13; text-fig. 4

Holotype. Plate 48, figs. 11*a*, *b*. Specimen Da50/12/1/A; Sylvan Shale, 50 ft. (15·24 m.) stratigraphically above base, in outcrop on west side of U.S. Highway 77, about 4 miles (6·4 km.) south of Davis, Oklahoma.

Diagnosis. Conical chamber slightly longer than oral tube, approximately as wide as long; base flat or slightly convex, margin rounded. Appendices of uniform thickness and texture, suspended at 6–15, generally 8–12, points on the basal margin; commonly anastomosing; occasionally discrete for their full lengths and connected at their tips by a continuous ring; equal to, or less than, maximum diameter in length. Oral tube cylindrical, half maximum diameter in width. Test wall smooth.

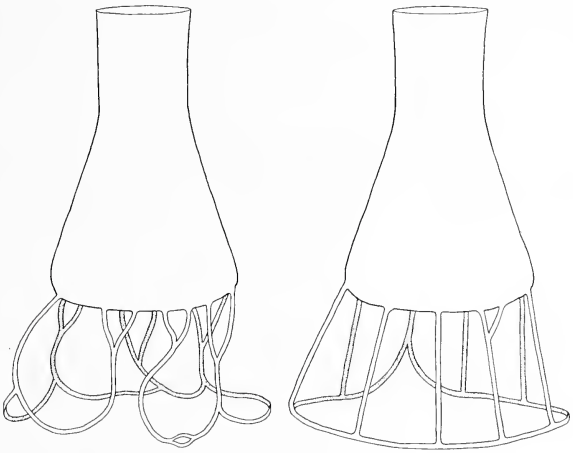

TEXT-FIG. 4. *Clathrochitina sylvanica* sp. nov. Lateral views of two variants with strongly developed appendices, ×400.

Dimensions (*in microns*). 25 specimens measured.

	Total length	*Chamber length*	*Maximum diameter*	*Oral tube diameter*	*Appendix length*
Holotype:	120	62	78	36	< 53
Range:	110–160	60–85	75–103	36–48	12–90
Mean:	131	76	84	40	—

Description. The flanks taper fairly uniformly, and the junction of the chamber and neck generally is clearly defined. The appendices are very strongly developed. Their pattern of branching and anastomosing varies considerably at each horizon, but the same, or closely similar, variants occur wherever the species has been found.

Comparison. Ancyrochitina merga is readily distinguished from *C. sylvanica* by its discrete, pitchfork-shaped appendices. Damaged specimens which have lost their appendices, however, may be exceedingly difficult to identify, but typical examples of *A. merga* are, nevertheless, fungiform rather than cylindroconical, and may bear

simple or λ-spines. Four similar species of *Clathrochitina* differ from *C. sylvanica* as follows. *C. combazi* (Cramer 1967*a*) possesses 12–24 modestly branching appendices, whereas *C. rosendae* (Cramer 1964) bears only a few. The appendices of *C. clathrata* Eisenack 1959 are very short; those of *C. carminae* (Cramer 1964) branch elaborately and may extend as far as 130 μ from the basal margin. *C. multiramosa* (Taugourdeau and Jekhowsky 1960) Taugourdeau 1967 is readily distinguished by about 12 short processes attached immediately below the aperture, and connected at their tips by a continuous ring.

Material. Approximately 400 single tests.

Occurrence. ?Syl, Sy16–Sy180. *Clathrochitina sylvanica* is a distinctive element in approximately the lower half of the Sylvan Shale.

Genus SAGENACHITINA gen. nov.

Type species. Clathrochitina oblonga Benoit and Taugourdeau 1961 (by original designation), Arenig, Algeria.

Diagnosis. Chitinozoa with cylindroconical or campanulate tests and a network suspended from the basal margin.

Remarks. Sagenachitina gen. nov. is not represented in the Sylvan Shale, but is proposed for a group of closely similar species including 5 formerly referred inappropriately to *Clathrochitina* Eisenack 1959. These are *Sagenachitina oblonga* (Benoit and Taugourdeau 1961) comb. nov., *S. aquitanica* (Taugourdeau 1961) comb. nov., *S. eisenacki* (Taugourdeau 1961) comb. nov., *S. retifera* (Taugourdeau and Jekhowsky 1960) comb. nov., and *S. striata* (Benoit and Taugourdeau 1961) comb. nov. *Sagenachitina* differs from *Clathrochitina* (q.v., p. 268) in that its basal margin supports a finely divided network, rather than a relatively small number of distinct processes which coalesce distally. Apparently it is restricted to the Ordovician (Taugourdeau *et al.* 1967, p. 78), whereas *Clathrochitina* (*sensu* Eisenack 1959) seems essentially a Silurian genus.

Acknowledgement. Sagenachitina was introduced to the literature by Jansonius (1967, p. 352) as an informal manuscript name. It is validated here, in its original sense, with the permission and approval of Dr. Jansonius.

Genus CONOCHITINA Eisenack 1931 restr. 1955*b*

Type species. Conochitina claviformis Eisenack 1931 (by original designation), Silurian, Baltic.

Conochitina elegans Eisenack 1931

Plate 49, figs. 1–17

EXPLANATION OF PLATE 48

Figs. 1, 2. *Acanthochitina rashidi* sp. nov., ×400. 1, Sy100/2/1/D, in phase-contrast illumination. 2, Sy80/2/1/B, holotype; in bright-field (2*a*) and phase-contrast (2*b*) illumination.

Figs. 3–13. *Clathrochitina sylvanica* sp. nov., illustrating variation in the size and complexity of the appendices, ×250. 3, Sy60/12/1/D. 4, Sy100/12/1/A. 5, Sy80/12/1/B. 6, Sy60/12/1/C, polar view. 7, Sy60/12/1/E. 8, Sy60/12/1/K. 9, Sy80/12/1/A. 10, Sy100/12/1/C. 11, Da50/12/1/A, holotype; in bright-field (11*a*) and phase-contrast (11*b*) illumination. 12, Sy60/12/1/H. 13, Sy60/12/1/A.

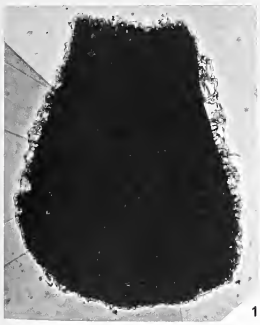
1


2a


2b


3


4


5


6


7


8


9


10


11a


11b


12


13

JENKINS, Ordovician chitinozoa from Oklahoma

1931 *Conochitina elegans* Eisenack, p. 87, pl. 2, fig. 4 (holotype).
1934 *Rhabdochitina conocephala* Eisenack, p. 61, pl. 4, figs. 10–12; text-fig. 32.
1959 *Conochitina elegans* Eisenack; Eisenack, p. 3, pl. 2, figs. 4 (neotype), 5; text-fig. 1.
1960 *Rhabdochitina conocephala* Eisenack; Taugourdeau and Jekhowsky, p. 1230, pl. 9, fig. 131.
non 1962 *Conochitina elegans* Eisenack; Beju and Dăneț, p. 531, pl. 1, figs. 31, 32.
non 1964 *Rhabdochitina conocephala* Eisenack; Cramer, p. 351, pl. 22, fig. 14; pl. 23, figs. 7, 11, 12.
1965 *Rhabdochitina hedlundi* Taugourdeau, p. 472, pl. 3, figs. 60, 66.
1965 *Conochitina elegans* Eisenack; Eisenack, p. 126, pl. 10, fig. 9.
1967 *Conochitina elegans* Eisenack; Jenkins 1967, p. 455, pl. 71, figs. 1–4.

Dimensions (*in microns*). 50 specimens measured.

		Total length	*Maximum diameter*	*Minimum diameter*	*Apertural diameter*
	Range:	204–904	62–96	50–78	61–78
	Mean:	403	78	61	69
26 specimens from Estonia (Eisenack 1959)	Range:	288–667	—	—	—
	Mean:	467	—	—	—
26 specimens from the Ostseekalk of south Finland (Eisenack 1965)	Range:	332–690	—	—	—
	Mean:	493	—	—	—
30 specimens from England (Jenkins 1967)	Range:	200–616	58–92	—	—
	Mean:	388	73	—	—

Remarks. Conochitina elegans Eisenack 1931 shows the same pattern of morphological variation in the Sylvan Shale as it does in the Caradocian Jewe and Kegel Beds, D_1–D_2, of Estonia (Eisenack 1959, p. 3, text-fig. 1), and in the Caradoc Series of England (Jenkins 1967). Throughout the Sylvan Shale, short conical or cylindroconical forms up to 400 μ in length (Pl. 49, figs. 8–15) predominate numerically over much longer cylindrical forms, up to 900 μ in length, which have pronounced aboral swellings (Pl. 49, figs. 1–7). The aperture is distinctively fringed by numerous, irregular, simple or branching processes up to 6 μ in length.

I am reasonably sure that *Conochitina elegans* and *Rhabdochitina hedlundi* Taugourdeau 1965 are conspecific. Well-preserved typical examples of *C. elegans* occur at several horizons in the Upper Ordovician Maquoketa Formation from Iowa, where Taugourdeau obtained the type material of *R. hedlundi*, but no other species comparable to *C. elegans* or *R. hedlundi* is represented.

Material. Several thousand single tests, and clusters of up to 15 tests each.

Occurrence. Syl-Sy305. The species occurs in the Caradoc Series of Estonia (Eisenack 1959, 1962*b*) and Shropshire, England (Jenkins 1967), and in the Ostseekalk of north Germany and south Finland (Eisenack 1965). Taugourdeau and Jekhowsky (1960) record it, as *Rhabdochitina conocephala*, in Algerian sediments referred with reservations (op. cit., pp. 1205, 1230) to the lower Silurian. Eisenack (1964) refers to *C.* cf. *elegans* a group of forms from the Llandovery, Wenlock, and lower Ludlow of Gotland which, while closely similar to the Ordovician type material, are not certainly conspecific with it.

Conochitina cactacea Eisenack 1937

Plate 49, figs. 18–25; text-fig. 5

1937 *Conochitina cactacea* Eisenack, p. 222, pl. 15, figs. 14, 15 (holotype).
1959 *Conochitina cactacea* Eisenack; Eisenack, p. 10, pl. 1, figs. 12 (neotype), 13; text-fig. 2*a*, *b*.
non 1965 *Conochitina* cf. *cactacea* Eisenack *typica* Taugourdeau, p. 467, pl. 1, fig. 10.
1965 *Conochitina cactacea* Eisenack; Eisenack, p. 125, pl. 9, figs. 18, 19.
1967 *Conochitina cactacea* Eisenack; Laufeld, p. 299, fig. 9.

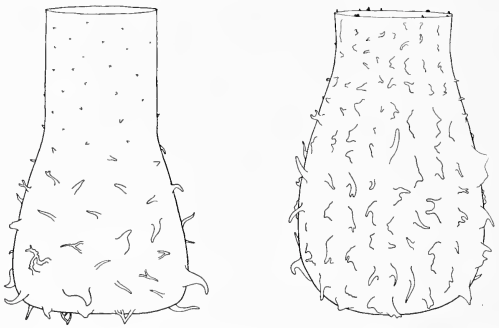

TEXT-FIG. 5. *Conochitina cactacea* Eisenack 1937. Lateral views illustrating (left) a typical cylindroconical example with randomly distributed spines, and (right) a pyriform test whose spines are expanded proximally and arranged in longitudinal rows, ×350.

Dimensions (*in microns*). 25 specimens measured.

	Total length	*Maximum diameter*	*Oral tube diameter*	*Apertural diameter*	*Spine length*
Range:	118–240	80–123	52–77	53–73	< 15
Mean:	165	97	63	62	—
Neotype (Eisenack 1959):	123	72	42	43	—

EXPLANATION OF PLATE 49

Figs. 1–17. *Conochitina elegans* Eisenack 1931, ×100. 1–7, Sy60/4/1/A, D, K, Da3/4/1/B, Sy60/4/1/R, G, and Sy100/4/1/C, respectively, long cylindrical tests with conspicuous aboral swellings. 8–10, Sy60/4/1/S, H, and J, respectively, shorter tests with neck and chamber differentiated. 11–17, Sy40/4/1/C, D, F, A, Sy60/4/1/T, Da3/4/1/D and Sy60/4/1/P, respectively, short to very short tests illustrating some of the very considerable variation that is expressed in both the large and small size-fractions of populations of *C. elegans*.

Figs. 18–25. *Conochitina cactacea* Eisenack 1937, all except 19*b* ×250. The figured specimens have been chosen to illustrate the ornament; most are distorted and none shows the typical shape of this well-known species. 18, Sy60/6/1/A. 19, Sy16/6/1/A; 19*a*, showing exceptionally well-preserved ornament in upper right quadrant of photograph; 19*b*, detail of proximally-expanded spines, in phase-contrast illumination ×1600. 20, Sy16/6/1/D. 21, Sy16/6/1/B. 22, Sy16/6/1/F. 23, Sy60/6/1/B. 24, Sy16/6/1/E. 25, Sy16/6/1/C.

JENKINS, Ordovician chitinozoa from Oklahoma

Description. The chamber is conical with straight or swollen flanks, and makes up more than half the total length. The base is flat, with a broadly rounded margin. The oral tube, which occasionally is not developed, is cylindrical and approximately two-thirds of the maximum diameter in width. The aperture is straight, or fringed with irregularly spaced processes up to 3 μ in length. Short spines, most of which are simple, cover the entire test. Branching spines with two distal limbs, and λ-spines with two or three discrete bases, however, are common. Spines may taper uniformly, or their proximal portions may be widely expanded in a plane parallel with the test's longitudinal axis. Commonly the spines show some tendency to loosely align themselves in longitudinal rows, and in some examples the expanded proximal portions of longitudinally adjacent spines occasionally coalesce, forming very short ridges up to 3 μ in height. Such ridges tend to be less strongly developed, though no less common, toward the aperture. In general, spines are largest on the basal margin and become smaller orally.

Material. Approximately 200 single tests.

Occurrence. Syl-Sy305. *C. cactacea* occurs throughout the Sylvan Shale, but nowhere is it common. The species occurs in the Ostseekalk of north Germany and Gotland (Eisenack 1965), and in the Caradocian Dalby and Slandrom Formations of central Sweden (Laufeld 1967). A few atypical examples are known from the Wesenberg Beds, E, of Estonia (Eisenack 1962*b*, 1965).

Genus CYATHOCHITINA Eisenack 1955*b*

Type species. Conochitina campanulaeformis Eisenack 1931 (by original designation), Ordovician, Baltic.

Cyathochitina agrestis sp. nov.

Plate 50, figs. 11, 18

Holotype. Plate 50, figs. 11*a*, *b*. Specimen Syl/8/1/A; Sylvan Shale, 1 ft. (0·3 m.) stratigraphically above base, Sycamore Creek.

Diagnosis. Large test. Chamber conical to swollen cylindrical, about two-thirds total length; maximum diameter in lower half or middle of chamber, about one-third chamber length; base flat, about three-quarters maximum diameter in width. Carina attached some distance aborally of maximum diameter. Oral tube cylindrical or slightly flaring, about four-fifths maximum diameter in width; aperture straight. Test wall rough.

Dimensions (*in microns*). 6 specimens measured.

	Total length	*Chamber length*	*Maximum diameter*	*Oral tube diameter*	*Apertural diameter*	*Carina width*
Holotype:	980	660	192	148	172	< 20
Range:	592–980	376–660	176–192	128–152	136–172	< 25
Mean:	784	549	184	142	153	—

Comparison. In general shape this species closely resembles *Acanthochitina barbata* Eisenack 1931 and *Cyathochitina stentor* (Eisenack 1937), but lacks the diagnostic ornament of either (Jenkins 1967, pp. 443–5; Laufeld 1967, p. 318, respectively). It is much larger than *Cyathochitina calix* (Eisenack 1931), 57 Baltic examples of which (Eisenack 1962*a*) average 299 μ in total length (min. 190 μ, max. 450 μ).

Material. 10 single tests.

Occurrence. Syl.

Cyathochitina ontariensis (Jansonius 1964) comb. nov. emend.

Plate 50, figs. 1–9

1964 *Tanuchitina ontariensis* Jansonius, p. 910, pl. 1, figs. 5, 6 (holotype).

Emended diagnosis. Elongate, cylindroconical, or campanulate test. Chamber approximately two-thirds total length; base almost flat; margin drawn out into a short sharp carina, generally directed aborally, and situated slightly below the maximum diameter. Neck cylindrical, half to two-thirds maximum diameter in width; collarette flaring; aperture serrate or fimbriate, generally 8–12 μ wider than neck. Wall smooth.

Dimensions (*in microns*). 25 specimens measured.

	Total length	*Maximum diameter*	*Neck diameter*	*Apertural diameter*	*Carina width*
Range:	268–740	102–180	56–88	64–106	< 3
Mean:	475	142	69	79	—
Holotype (Jansonius 1964):	310	—	—	—	—

Description. The flanks may taper uniformly or be slightly swollen (Pl. 50, figs. 1, 2, 4, 5), in which cases the chamber and neck are more or less clearly distinguishable. Occasionally the test is trumpet-shaped, having concave flanks which merge with the neck (Pl. 50, figs. 3, 7). Originally the base probably was flat or almost so; in most specimens, however, perhaps owing to compression, it is convex in the centre and concave toward the margin. The carina is a continuous, uniformly wide, knife-edge rim which, in lateral view, rarely protrudes more than 3 μ beyond the general silhouette of the test.

Remarks. This species was designated type species of *Tanuchitina* by Jansonius (1964), but is here considered to fall well within the scope of *Cyathochitina* Eisenack 1955*b*.

Comparison. C. agrestis sp. nov. has a much larger carina than *C. ontariensis* and the shape of its test is quite different. *C. stentor* (Eisenack 1937) is furnished with a strongly developed, skirt-like carina (up to 85 μ in width; Laufeld 1967, p. 318) and an ornament of strongly defined longitudinal ridges.

Material. Several thousand single tests.

Occurrence. Sy80-Sy305. The type material is from the subsurface Upper Ordovician of Ontario.

EXPLANATION OF PLATE 50

Figs. 1–9. *Cyathochitina ontariensis* Jansonius 1964, ×100. 1, 2, Sy100/7/1/A and B, respectively, typical examples with slender campanulate tests and weakly developed carinae. 3, Sy80/7/1/B, trumpet-shaped test. 4, 5, Sy80/7/1/A and Sy100/70/1/C, respectively, with well-developed carinae. 6–7, Sy80/7/1/C and Sy100/7/1/D, respectively, very short tests. 8, Sy80/7/1/E. 9, Sy80/7/1/D.

Figs. 10, 12–17, 19, 20. *Desmochitina minor* Eisenack 1931. 10, 14, 15, 19, 20, Sy100/9/1/A, Sy80/9/1/A, B, C, and Sy100/9/1/B, single tests each with an operculum firmly attached at the base, ×250. 12, Sy40/9/1/A, single test lacking an operculum at its base (presumably one was once present and has since been lost), but having retained the operculum sealing its own aperture (this is set squarely in the throat of the specimen), ×250. 13, 16, 17, Sy60/9/1/B, H, and Sy100/9/1/C, respectively, chains of tests connected aperture-to-base, ×100.

Figs. 11, 18. *Cyathochitina agrestis* sp. nov. 11, Syl/8/1/A, holotype; 11*a*, ×100; 11*b*, carina, ×250. 18, Syl/8/1/B, ×100.

Fig. 21. *Desmochitina scabiosa* (Wilson and Hedlund 1964), Sy60/10/1/D, cluster of four tests, ×250.

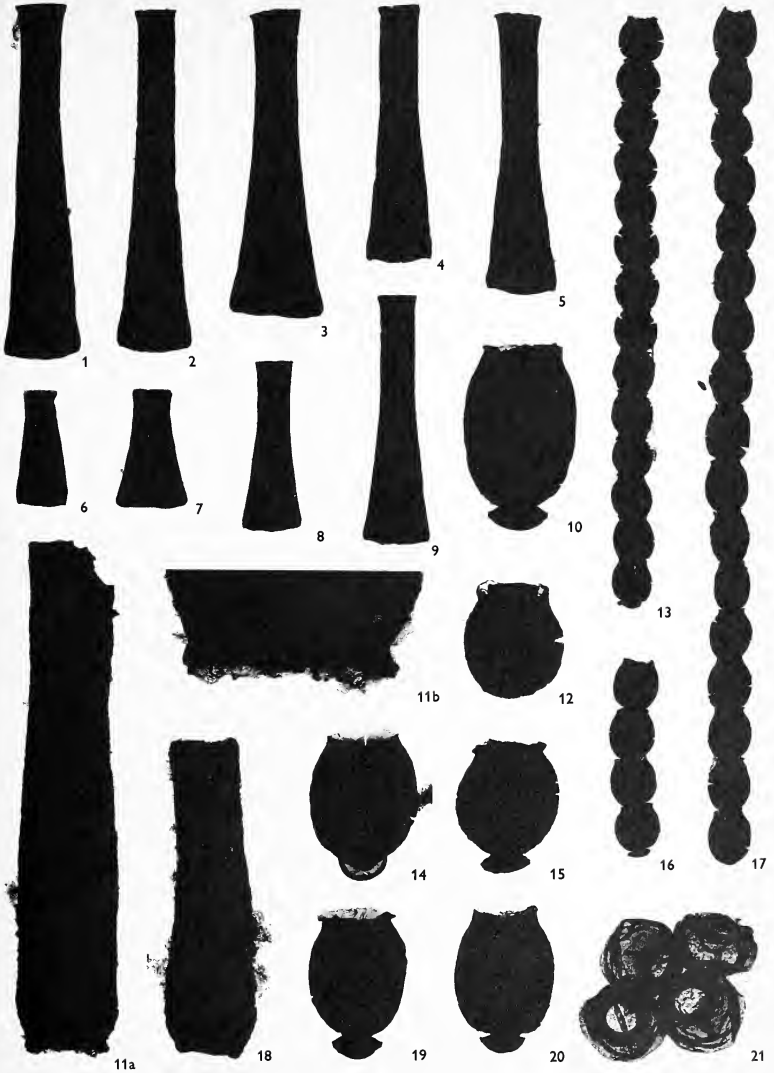

JENKINS, Ordovician chitinozoa from Oklahoma

Genus DESMOCHITINA Eisenack 1931 emend. 1962*a*

Type species. Desmochitina nodosa Eisenack 1931 (by original designation), Ordovician, Baltic.

Remarks. For the present I share Eisenack's (1968, pp. 155, 185) view that *Hoegisphaera* Staplin 1961 is superfluous, and would place it (and its junior synonym *Calpichitina* Wilson and Hedlund 1964) in synonymy with *Desmochitina* Eisenack 1931 emend. 1962*a*. *Hoegisphaera* was established by Staplin (1961) for 'a new type of Paleozoic microfossil possibly allied to the Chitinozoa' (op. cit., p. 392), in which 'The colour and texture of the wall are similar to those of Chitinozoa, but the analogy cannot be carried farther' (op. cit., p. 419). However, it is clear that the species assigned to *Hoegisphaera are* chitinozoans, and they have been widely recognized as such in the literature (Jansonius 1964, p. 913; 1967, p. 350; Taugourdeau *et al.* 1967, p. 61; Laufeld 1967, pp. 319–20, 327–8; Jenkins 1967, p. 462; Eisenack 1968, pp. 155, 185). Three years after *Hoegisphaera* had been established, Wilson and Hedlund (1964) described the genus *Calpichitina* with its type species *C. scabiosa*. This generic name, however, was proposed for a species (*C. scabiosa*) which clearly fell within Staplin's (1961) concept of *Hoegisphaera*, and was closely similar in size and shape to *Desmochitina complanata* Eisenack 1932 (for dimensions see Eisenack 1959, p. 16). Very shortly after the establishment of *Calpichitina*, Wilson and Dolly (1964), doubting its validity, abandoned it by transferring the type species (*C. scabiosa*) to *Hoegisphaera*.

Desmochitina minor Eisenack 1931

Plate 50, figs. 10, 12–17, 19, 20

1969 *Desmochitina minor* Eisenack; Jenkins, pp. 20, 21, pl. 6, figs. 1–18 (q.v. for further synonymy).

Dimensions (*in microns*). 25 specimens measured.

	Total length	*Chamber length*	*Maximum diameter*	*Minimum (neck) diameter*	*Apertural diameter*
Range:	72–120	60–108	66–86	46–60	54–64
Mean:	92	84	76	53	58

Remarks. Eight informal infraspecific taxa have been referred to *Desmochitina minor* by Eisenack (1958, 1962*a*). The form recorded here corresponds exactly to the informal taxon *D. minor* forma *typica* Eisenack 1958 but is considered to merit recognition as a separate species. It occurs widely within North America and Europe, where it is generally quite distinct. The remaining seven infraspecific taxa, and forms transitional to them, are apparently lacking in the Sylvan Shale.

Most specimens are indistinguishable from many of the examples from Bohemia (Eisenack 1948, text-figs. 14, 15), the Ordovician Rhenish Schiefergebirge (Eisenack 1939, text-figs. 1–3, 6), and the Swedish and British Caradoc (Laufeld 1967, fig. 25; Jenkins 1967, pl. 71, fig. 18). They differ appreciably, however, from Eisenack's Baltic material (1962*a*, pl. 16, figs. 1–8, 10; 1965, pl. 10, figs. 16, 17) and the Viola–Fernvale specimens recorded in an earlier study (Jenkins 1969), in that the general shape of the chamber in lateral view tends to be spherical rather than quadrangular; the oral tube is smaller and less sharply flaring; and chains of up to 20 tests are common.

In marked contrast to its broad pattern of morphological variation in the Viola and Fernvale Limestones (Jenkins 1969, p. 21, pl. 6, figs. 1–18), the species is represented

within the Sylvan Shale by a conservative form which, throughout the formation, varies little in size, shape, or surface texture.

Material. Many thousand single tests, and several hundred chains of up to 20 tests each. Clusters of up to 60 tests are common at horizon Sy60.

Occurrence. Sy16-Sy260. In the lower half of the formation (Sy16-Sy140) *D. minor* is a numerically important element in the chitinozoan fauna and occurs in long chains; thereafter its numbers are drastically reduced, and the species is missing or extremely scarce near the top of the formation (Sy280-Sy305). Its occurrence outside North America is given elsewhere (Jenkins 1969, p. 21).

Desmochitina scabiosa (Wilson and Hedlund 1964) Jenkins 1969

Plate 50, fig. 21

1958 *Desmochitina* sp. 2 Wilson, pl. 1, fig. 7.
1962*a* *Desmochitina* sp. Eisenack, p. 304, pl. 16, figs. 11, 12.
1964 *Calpichitina scabiosa* Wilson and Hedlund, p. 164, pl. 1, figs. 1 (holotype), 2–12.
1965 *Desmochitina lecaniella* Eisenack, p. 131, pl. 10, figs. 21, 22 (holotype).
1967 *Desmochitina lecaniella* Eisenack; Laufeld, p. 326, fig. 24.
1969 *Desmochitina scabiosa* (Wilson and Hedlund); Jenkins, p. 23.

Dimensions (*in microns*). 25 specimens measured.

	Total length	*Chamber length*	*Maximum diameter*	*Apertural diameter*
Range:	50–75	43–68	52–92	48–62
Mean:	61	56	73	56
Holotype (Wilson and Hedlund 1964):	60	—	79	41

Remarks. The stratigraphical ranges of *D. scabiosa* (Wilson and Hedlund 1964) and *D. lecaniella* Eisenack 1965 both lie within the Upper Ordovician, and the two species are so closely similar that it would seem impractical to continue distinguishing them. Populations from the Sylvan Shale consist largely of single tests, but clusters (*sensu* Kozlowski 1963) are common at several horizons.

Material. Several thousand single tests, and numerous clusters of up to 11 tests each.

Occurrence. Sy40-Sy305. Wilson and Hedlund (1964) illustrate several single tests particularly well, and record the species approximately 50 ft. (15·24 m.) above the base of the formation, at an outcrop on U.S. Highway 77 about 4 miles (6·4 km.) south of Davis, Oklahoma (text-fig. 1) and 20 miles (32 km.) north-west of the Sycamore Creek section. Taugourdeau records *C. scabiosa* (illustrated as *C.* cf. *scabiosa*) in the Maquoketa Formation, Richmond, of Iowa. *Desmochitina lecaniella* has been recorded in the Caradocian Kegel Beds, D_2, of Estonia (Eisenack 1962*a*, 1965); in the Ostseekalk of north Germany, Gotland, and south Finland (Eisenack 1965); and in the Dalby Formation, Caradoc, of central Sweden (Laufeld 1967).

Genus KALOCHITINA Jansonius 1964

Type species. Kalochitina multispinata Jansonius 1964 (by original designation), Upper Ordovician, Ontario.

Remarks. The chief diagnostic features of this genus are its pyriform test, reduced neck, and ornament of numerous, generally small spines which frequently are aligned in longitudinal rows.

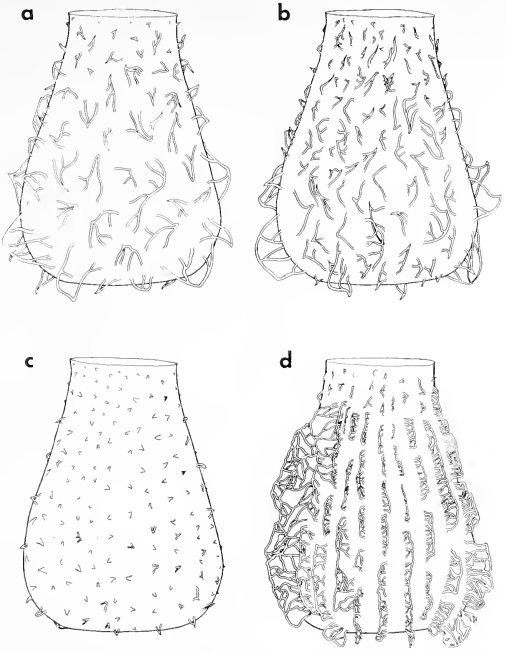

TEXT-FIG. 6. *Kalochitina multispinata* Jansonius 1964. Lateral views illustrating variation in the style of the ornament, ×400. *a*, Typical example with evenly spaced spines. *b*, Typical example with spines showing tendency to align themselves in longitudinal rows. *c*, Example with reduced ornament of short thorn-like spines. *d*, Example furnished with ridges which appear to have formed, figuratively, as if by fusion of closely spaced λ-spines.

Kalochitina multispinata Jansonius 1964

Plate 51, figs. 1–10, 15; text-fig. 6

1958 Genus B, Wilson, pl. 1, figs. 10, 11.
1964 *Kalochitina multispinata* Jansonius, p. 909, pl. 2, figs. 21 (holotype), 22.

Dimensions (*in microns*). 30 specimens measured.

	Total length	*Maximum diameter*	*Apertural diameter*	*Spine length*
Range:	102–156	82–103	42–60	< 12
Mean:	121	90	51	—
Holotype (Jansonius 1964):	140	—	—	—

Description. The test is pyriform to conical, with a maximum diameter about four-fifths of the total length. The neck is short, tapering, and rather weakly differentiated from the chamber; in most individuals it has been lost or was never developed. The apertural diameter equals or slightly exceeds half the maximum diameter.

In all populations of *K. multispinata* the ornament varies considerably, but, for the most part, its range of variation is much the same throughout the formation. The lower and upper beds (up to horizon Sy60 and above horizon Sy200) contain pure populations of *K. multispinata*, but throughout approximately the middle 140 ft. (43 m.) of the formation (horizons Sy80 to Sy200) the species makes up continuously intergrading populations with *A. rashidi*. The two species are distinguished from each other arbitrarily and solely on the basis of their ornaments (compare text-figs. 2 and 6). Typical examples of *K. multispinata* are covered with closely and evenly spaced λ-spines, up to 12 μ in length and possessing 2–6 proximal limbs (text-fig. 6*a*). In many, but by no means all, of the more typical examples, the proximal limbs of each λ-spine, and the spines as a whole, show some tendency to loosely align themselves in approximately 30 more or less clearly defined longitudinal rows (text-fig. 6*b*). In addition, each population contains individuals whose ornament is reduced to short ($< 2{\cdot}5$ μ in length) thorn-like spines (text-fig. 6*c*). A rare form, seemingly of sporadic vertical distribution, is furnished with perforate or imperforate ridges up to 8μ in height (text-fig. 6*d*), which appear to have formed, figuratively, as if by fusion of very closely spaced λ-spines. Variants transitional to *A. rashidi* (text-fig. 2) occur from horizon Sy80 to Sy260.

Material. Several thousand single tests, and 20 chains of up to 4 tests each.

Occurrence. Sy16-Sy260. The type material is from the subsurface Upper Ordovician of Ontario (Jansonius 1964).

Genus RHABDOCHITINA Eisenack 1931

Type species. *Rhabdochitina magna* Eisenack 1931 (by original designation), Ordovician, Baltic.

Rhabdochitina sp.

Plate 51, fig. 14

Remarks. A species of very large chitinozoan is present in the Sylvan Shale, but only 2 incomplete examples are recorded here, one from horizon Sy80, the other from Sy120.

EXPLANATION OF PLATE 51

Figs. 1–10, 15. *Kalochitina multispinata* Jansonius 1964, all but 10 × 250. 1–5, Sy40/3/1/C, Sy100/3/1/A, E, G and Sy60/3/1/D, respectively. 6, Sy40/3/1/A, showing ornament through translucent test. 7, 8, Sy100/3/1/B and Sy40/3/1/D, respectively. 9, Da2/3/1/D, cluster of four tests showing a roughly parallel alignment of their longitudinal axes, a particularly common phenomenon in this species. 10, Sy40/3/1/M, λ-spines, in phase-contrast illumination × 1000. 15, Sy100/3/1/D, chain of two tests.

Figs. 11–13, 16–20. *Sphaerochitina lepta* sp. nov., a series of tests illustrating *inter alia* the variable length of the neck, × 250. 11, Sy60/11/1/F, compressed so the longitudinal axis of the neck has folded into the same plane as the transverse axis of the chamber (cf. text-fig. 7*a*). 12, 13, 16–18, Sy60/11/1/K (holotype), E, M, R, and B, respectively. These specimens are not carinate, as might be erroneously assumed from the photographs. The sharp prominences on the chambers are not original features but occur in tests where accommodation during compression has involved an inward collapse of the base (cf. text-fig. 7*b*). 19, 20, Sy100/11/1/C and D, with relatively long necks.

Fig. 14. *Rhabdochitina* sp., Sy80/5/1/A, × 100.


1


2


3


4


5


6


7


8


9


10


14


15


11


12


13


16


17


18


19


20

JENKINS, Ordovician chitinozoa from Oklahoma

The tests are for the most part cylindrical, swollen at their aboral ends, and quite smooth. The larger specimen is 180 μ in width, and its original length exceeded 850 μ.

Genus SPHAEROCHITINA Eisenack 1955*a*

Type species. Lagenochitina sphaerocephala Eisenack 1932 (by original designation), Silurian, Baltic.

Sphaerochitina lepta sp. nov.

Plate 51, figs. 11–13, 16–20; text-fig. 7

Holotype. Plate 51, fig. 12. Specimen Sy60/11/1/K; Sylvan Shale, 60 ft. (18·28 m.) stratigraphically above base, Sycamore Creek.

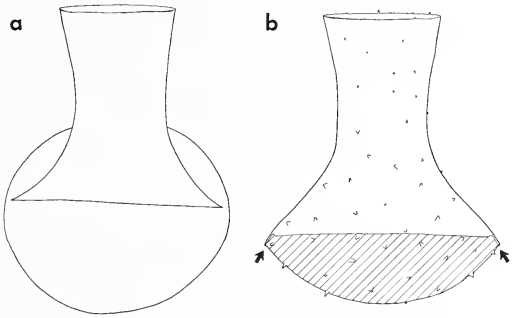

TEXT-FIG. 7. *Sphaerochitina lepta* sp. nov., × 550. *a*, Smooth form which is found in the middle and upper Sylvan Shale, compressed so the longitudinal axis of the neck has folded into the same plane as the transverse axis of the chamber. *b*, example of the ornamented form which occurs in the upper Sylvan Shale, compressed laterally. The small sharp prominences (indicated by arrows) simulate the carinae of other species. They are not original features, however, but are common in tests where accommodation during compression has involved an inward collapse of the base (shaded).

Diagnosis. Small, cylindroconical or fungiform test. Chamber and neck of approximately equal length. Maximum diameter about 150% chamber length; base flat or convex. Neck one-third to half maximum diameter in width. Aperture straight or fimbriate. Wall smooth, or bearing small, generally simple processes, thinly and uniformly distributed over entire test.

Dimensions (*in microns*). 25 specimens measured.

	Total length	*Chamber length*	*Maximum diameter*	*Neck diameter*	*Apertural diameter*	*Process length*
Holotype:	89	55	85	32	38	—
Range:	83–120	45–60	72–88	29–33	35–43	< 3·5
Mean:	97	52	79	31	39	—

Description. In size and shape, this species remains virtually the same wherever it has been found. The test wall is relatively thin and translucent, and large secondary folds

are generally present. The ornament consists of cones, simple spines, and a few λ-spines with blunt or pointed tips. The species first occurs in the middle of the formation (Sy120–Sy180) where it is represented exclusively by smooth forms. Thereafter (Sy200–Sy305) smooth and ornamented forms occur together.

Comparison. Several species are closely similar to *S. lepta*, including *S. schwalbi* Collinson and Scott 1958, *S. nodulosa* Collinson and Scott 1958, and *S. actonica* Jenkins 1967. All may be distinguished, however, by the style and distribution of their ornamental processes.

Material. Several thousand single tests, and a dozen clusters of up to 20 tests each.

Occurrence. Sy120–Sy305.

GENERAL CONCLUSIONS

The chitinozoan fauna of the Sylvan Shale has been examined at widely scattered localities throughout the Arbuckle Mountains, and at stratigraphical intervals of 20 ft. (6·10 m.) throughout the 305 ft. (93 m.) thick sequence exposed in the bed and banks of Sycamore Creek (text-fig. 1), Johnston County, Oklahoma. Preservation is generally excellent except for the reworked material in the uppermost part of the formation (p. 282), and rich assemblages occur throughout the area and at all stratigraphical levels. The fauna has been referred to the following nine genera, and twelve species of which five are new:

Acanthochitina rashidi sp. nov.
Ancyrochitina merga sp. nov.
Clathrochitina sylvanica sp. nov.
Conochitina cactacea Eisenack 1937
Conochitina elegans Eisenack 1931
Cyathochitina agrestis sp. nov.
Cyathochitina ontariensis (*Jansonius* 1964) comb. nov.
Desmochitina minor Eisenack 1931
Desmochitina scabiosa (Wilson and Hedlund 1964)
Kalochitina multispinata Jansonius 1964
Rhabdochitina sp.
Sphaerochitina lepta sp. nov.

THE FAUNAL SUCCESSION

No *abrupt* changes interrupt the general continuity of the chitinozoan succession in the Sylvan Shale sequence at Sycamore Creek, and deposition would appear to have continued without significant interruption. *Conochitina elegans* and *C. cactacea* occur throughout the formation, while several other species (*Ancyrochitina merga*, *Cyathochitina ontariensis*, *Desmochitina minor*, *D. scabiosa* and *Kalochitina multispinata*) are present at nearly all stratigraphical levels and may be considered, for most practical purposes, characteristic of the formation as a whole (Table 1).

On the basis of *gradual* changes in the composition of its chitinozoan fauna, however, the Sylvan Shale at Sycamore Creek may be divided into three biostratigraphical units. These are not formally proposed in this paper as zones but, since they can be recognized seemingly unchanged 20 miles (32 km.) north-west of the Sycamore Creek outcrop in

	HORIZON \ CHITINOZOAN	*Cyathochitina agrestis*	*Conochitina elegans*	*Conochitina cactacea*	*Clathrochitina sylvanica*	*Kalochitina multispinata*	*Desmochitina minor*	*Ancyrochitina merga*	*Desmochitina scabiosa*	*Acanthochitina rashidi*	*Cyathochitina ontariensis*	*Sphaerochitina lepta*
SYLVAN SHALE	Sy305		●	●				●	●		●	●
	Sy300		●	●				●	●		●	●
	Sy280		●	●				●	●		●	●
	Sy260		●	●		●	●	●	●		●	●
	Sy240		●	●		●	●	●	●		●	●
	Sy220		●	●		●	●	●	●		●	●
	Sy200		●	●		●	●	●	●	●	●	●
	Sy180		●	●	●	●	●	●	●	●	●	●
	Sy160		●	●	●	●	●	●	●	●	●	●
	Sy140		●	●	●	●	●	●	●	●	●	●
	Sy120		●	●	●	●	●	●	●	●	●	●
	Sy100		●	●	●	●	●	●	●	●	●	
	Sy80		●	●	●	●	●	●	●	●	●	
	Sy60		●	●	●	●	●	●	●			
	Sy40		●	●	●	●	●	●	●			
	Sy16		●	●	●	●	●					
	Sy1	●	●	●	?							

TABLE 1. Summary of the stratigraphical distribution of chitinozoan species in one section through the Sylvan Shale of Oklahoma. The two occurrences (Sy80, Sy120) of *Rhabdochitina* sp. are not shown.

exposures along U.S. Highway 77, it is not unlikely that after further study they will form the basis of a more formal, and widely applicable stratigraphical subdivision. In the lower unit, about 110 ft. (33·5 m.) thick at Sycamore Creek, the fauna diversifies steadily from 3 to 10 species, and is strikingly characterized by large numbers of *Desmochitina minor*, which are often preserved in very long chains. Only one species, *Cyathochitina agrestis*, disappears within this interval, at the top of which the fauna attains its maximum diversity.

No new forms appear above horizon Sy120, and the fauna in approximately the middle 160 ft. (48 m.) of the formation, from horizon Sy120 to Sy260, is remarkably stable. It consists initially of 10 species and changes qualitatively only in that about midway up it loses *Acanthochitina rashidi* and *Clathrochitina sylvanica*. In addition, the numbers of *Desmochitina minor* above horizon Sy160 are drastically reduced and only rarely is the species preserved in chains.

The upper biostratigraphical unit of the Sylvan Shale lies above horizon Sy260 and is between 25 and 45 ft. (7·6–13·7 m.) thick at Sycamore Creek. It contains throughout a reduced fauna of only 6 species, and its base is marked by the disappearance of *in situ* specimens of *Desmochitina minor* and *Kalochitina multispinata*. In addition, numerous chitinozoans are present which, judging from their condition and identity, are almost certainly reworked from older Sylvan sediments. Their state of preservation contrasts strikingly with that of the forms considered to be *in situ*. They are bleached, corroded, perforated by the holes of 'boring organisms', and lack all but the stumps of their ornamental processes.

The occurrence of reworked Sylvan chitinozoans in upper Sylvan strata indicates that during late Sylvan time uplift took place, at least locally, in the southern mid-continent. The area of uplifted strata is not known, however (Ham, personal communication, 1969), and will need to be determined by future work demonstrating the absence of uppermost Sylvan beds beneath the lower Llandovery Keel Formation, which is the basal unit of the Silurian–Devonian Hunton Group. Although the pre-Keel unconformity is well-known and widely distributed (though very poorly exposed) in the Arbuckle Mountains, associated uplift beginning in late Sylvan time has thus far been unsuspected.

At Sycamore Creek, the three biostratigraphical subdivisions distinguished above correspond approximately to the three units of a tripartite lithostratigraphical subdivision (q.v., p. 263) that is recognizable widely within Oklahoma and clearly apparent in the Arbuckle Mountains. These are successively, a sequence of hard, very fissile, brown to dark grey shales up to 130 ft. (40 m.) or so thick in the lower part of the formation; a succession of soft, weakly fissile, greenish-grey shales up to 200 ft. (61 m.) thick in the upper part; and a thin sequence, about 30 ft. (9 m.) thick, of soft, massive, light green claystone at the top.

LATERAL DISTRIBUTION OF THE SYLVAN CHITINOZOAN FAUNA

In order to determine how much the character of the Sylvan chitinozoan fauna varies regionally, several samples were collected at widely scattered localities throughout the Arbuckle Mountains. In addition to those from Sycamore Creek, which lies at the extreme southern end of the mountains, samples were obtained from outcrops along

U.S. Highway 77 about 4 miles (6·4 km.) south of Davis (text-fig. 1), map reference sec. 30, T. 1 S., R. 2 E., Murray County, in the western 'thumb' of the mountains; at Lawrence (Ideal Portland Cement Company) Quarry (text-fig. 1), map reference sec. 36, T. 3 N., R. 5 E., Pontotoc County, in the area's most northerly exposure of Sylvan Shale; and at several localities in between. Assemblages of chitinozoans from these samples indicate clearly that the Sylvan fauna extends throughout the Arbuckle Mountains and remains essentially unchanged 20 miles (32 km.) to the north-west, and 30 miles (48 km.) to the north, of the Sylvan outcrops on Sycamore Creek. Furthermore, the fauna is not restricted to the immediate environs of the Arbuckle Mountains. Core samples from borings in north-western Texas prove its very extensive lateral distribution, and demonstrate that its composition remains essentially unchanged up to 180 miles (288 km.) west of the Arbuckle Mountains.

Several species of Sylvan chitinozoans are present 650 miles (1050 km.) north-north-east of the Arbuckle Mountains in outcrops of the Maquoketa Formation in eastern Iowa. These include *Conochitina elegans*, *Cyathochitina ontariensis*, *Desmochitina minor*, *D. scabiosa*, and *Kalochitina multispinata*, and provide substantial fossil evidence that the Sylvan Shale of Oklahoma and the Maquoketa Formation of Iowa are, for the most part, of the same general age. In so far as they correlate the two formations, they would support Decker's (1935, p. 698) view that in the subsurface the Sylvan Shale grades north-eastward into the Maquoketa Formation. At the same time these fossils provide some palaeontological evidence to substantiate Lee's (1943, p. 40) assertion that 'The Maquoketa shale . . . in the Mississippi Valley . . . is equivalent to the Sylvan shale of Oklahoma', and (op. cit., p. 42) his view that 'The Maquoketa shale was originally deposited . . . probably across the Chautauqua arch in continuation with the Sylvan shale of Oklahoma.'

Several species not mentioned above have been identified by Taugourdeau (1965) in poorly preserved material from two samples of the Maquoketa Formation from Iowa. These are: *Ancyrochitina ancyrea* (Eisenack 1931), but Taugourdeau's doubts (op. cit., p. 465) about this identification are clearly implied, and his specimens may well be broken examples of *A. merga* sp. nov.; *Cyathochitina campanulaeformis* (Eisenack 1931); *C. kuckersiana* (Eisenack 1934); *Desmochitina minor* forma *ovulum* Eisenack 1962*a*, here considered specifically distinct from *D. minor* Eisenack 1931; and *Hoegisphaera utricula* Taugourdeau 1965. In addition, Taugourdeau (op. cit.) records *Desmochitina scabiosa* (designated *Calpichitina scabiosa* in text, but *C.* cf. *scabiosa* in plate explanations) and *Rhabdochitina hedlundi* Taugourdeau 1965 (here [p. 271] considered a junior synonym of *Conochitina elegans* Eisenack 1931).

CHITINOZOAN FAUNAS FROM ABOVE AND BELOW THE SYLVAN SHALE

The chitinozoan fauna of the Sylvan Shale differs strikingly from that which precedes it in the underlying Viola and Fernvale Limestones (Jenkins 1969), the two faunas containing only one species, *Desmochitina minor*, in common. Numerous samples of both units, collected at points throughout the Arbuckle Mountains, indicate that the differences between the two faunas persist laterally over a wide area and are everywhere essentially the same. As noted earlier (op. cit., p. 34): 'The striking difference between the Viola–Fernvale and Sylvan faunas suggests that the unconformity between the two

stratigraphical units probably represents a substantial period of time (although no reliable indication of its duration can presently be given) or that the character of chitinozoan faunas may be very much more subject to control by the environment of deposition than has hitherto been suspected.'

Chitinozoans have been cursorily examined from the several carbonate formations of the Silurian–Devonian Hunton Group, which overlie the Sylvan Shale in Kansas, Oklahoma, and Texas. It would appear from this preliminary examination that the younger faunas are entirely different from those of the Ordovician Viola, Fernvale, and Sylvan formations, and that their affinities lie with faunas which existed contemporaneously in Europe (Eisenack 1955*a*, 1955*b*, 1959, 1962*a*, 1964) and North Africa (Taugourdeau and Jekhowsky 1960, Taugourdeau 1962).

AGE AND CORRELATION OF THE SYLVAN SHALE

The Sylvan Shale has been dated uppermost Ordovician on the basis of its graptolite fauna (Decker 1935, pp. 698–700; 1936*a*, pp. 308–9; 1936*b*, pp. 1256–7; Berry 1960*a*, p. 31, table 2). Generally it has been correlated (Decker 1935, Twenhofel *et al.* 1954, Berry 1960*a*) with part of the Richmond Stage, which is typically developed in the upper valley of the Ohio River and considered approximately correlative with the Ashgill Series of Britain. It is also correlated by graptolites with the Maquoketa Formation of the upper Mississippi Valley (Decker 1935, p. 698; 1936*a*, p. 308; 1936*b*, p. 1257; Twenhofel *et al.* 1954); the upper Maravillas Chert in the Marathon Basin of western Texas (Twenhofel *et al.* 1954; Berry 1960*a*, p. 38, table 2); and the Polk Creek Shale in the Ouachita Mountains of south-eastern Oklahoma and south-western Arkansas (Decker 1936*a*, p. 308; 1936*b*, pp. 1256–7, table 1; Harlton 1953, p. 787, fig. 2; Twenhofel *et al.* 1954; Berry 1960*a*, p. 38, table 2). The fauna contains, in particular, *Dicellograptus complanatus*, which gives its name to the lower graptolite zone of the British Ashgill. Lee (1943, p. 40) asserts, but without supporting evidence, that the Maquoketa Formation and the Sylvan Shale are equivalent, and (op. cit., pp. 43, 108) uses the terms 'Maquoketa' and 'Sylvan' interchangeably.

For many years prior to the mid 1930s the age of the Sylvan Shale was in dispute, the formation being assigned alternately to the Ordovician and Silurian Systems. Although most authors expressed their opinions about the Sylvan's age cautiously, sometimes acknowledging them to be provisional, a few asserted their views with unwarranted confidence. Indeed, in 1930 (p. 306) Levorsen, making no attempt to substantiate his claim, went so far as to state categorically that 'Eventually the Sylvan shale and the underlying upper Viola limestone will undoubtedly be generally regarded as Silurian in age.' A few years later Decker (1935) recorded graptolites of unquestionable Ordovician age in the lower beds of the formation, and the debate virtually ceased.

It is important to realize, however, that Decker's discovery of graptolites did not completely solve the problem of the Sylvan Shale's age, and that for 35 years the *whole* formation has been dated and correlated on the basis of graptolites which generally are confined to the basal beds and only exceptionally extend up through the lower 100 ft. (30 m). The upper part of the Sylvan Shale, 200 ft. (60 m.) or more thick over much of southern Oklahoma, apparently lacks not only graptolites but all macrofossils, and has been placed in the Ordovician on the basis of its association with the lower Sylvan.

The present study demonstrates for the first time that the formation is Ordovician *in its entirety*, and at the same time confirms with additional fossil evidence the Upper Ordovician age of the lower beds. It is hoped, and considered likely, that when the vertical ranges of chitinozoans in the North American type sections (or other standards of stratigraphical reference) are better documented this study will provide a means of correlating and more precisely dating all parts of the formation.

TABLE 2. List of previously described species (column A) found in the Sylvan Shale and their occurrences in reliably dated sediments outside Oklahoma.

Previously described species in the Sylvan Shale \ Occurrence outside Oklahoma	Upper Ordovician			Lower Ordovician
	Northern Europe	Southern Ontario	Anticosti Island, Quebec	of Estonia and Britain
Conochitina cactacea	X			
Conochitina elegans	X			
Cyathochitina ontariensis		X		
Desmochitina minor	X		X	X
Desmochitina scabiosa	X (designated *D. lecaniella*)		X	
Kalochitina multispinata		X		
Column A	B	C	D	E

The six previously described species in the Sylvan Shale occur in Upper Ordovician sediments over a very wide area. To my knowledge only one of them, *Desmochitina minor*, has been recorded in reliably dated sediments below the Upper Ordovician (Eisenack 1958, 1962*a*, *b*; Jenkins 1967), and none is known from sediments reliably dated as Silurian. Four (Table 2, column B) are present in northern Europe (Eisenack 1962*b*, 1965; Laufeld 1967; Jenkins 1967) and two (column C) occur in the subsurface of southern Ontario (Jansonius 1964). In addition, I have encountered typical examples of *D. minor* and *D. scabiosa* in photographs of Upper Ordovician chitinozoans from the subsurface of Anticosti Island, Quebec; this record, based upon material kindly provided by Dr. Jansonius, raises to four the number of species common to the Sylvan Shale and the Upper Ordovician of eastern Canada (Table 2, columns C and D).

A new species found in the Sylvan Shale, *Acanthochitina rashidi*, is furnished with a well-developed 'raised reticulum' (q.v., text-fig. 2; and Jenkins 1967, text-fig. 3), a rare style of ornament which elsewhere, perhaps significantly, is known only from young Ordovician deposits. These are, namely, the Ostseekalk of north Germany (Eisenack 1965), the Lyckholm Beds, F_1, of Estonia (Eisenack 1962*b*), the Caradoc of Anticosti Island, Quebec (Jansonius 1967, pl. 1, fig. u), the upper Caradocian Onnia Beds in the Caradoc type section, Shropshire, England (Jenkins 1967), and the uppermost Caradoc of central Sweden (Laufeld 1967, pp. 295–6, 298).

The presence in the Sylvan Shale of cylindroconical chitinozoans with strongly developed, anastomosing appendices (*Clathrochitina sylvanica*) would appear to herald the approach of Silurian time and emphasizes the very young Ordovician age of the formation. Chitinozoans of this general type are elsewhere known only from sediments of Silurian and, perhaps, earliest Devonian age (Eisenack 1959; Taugourdeau and Jekhowsky 1960, pl. 2, fig. 32; Cramer 1964, 1967*a*; Taugourdeau 1967).

APPENDIX: DESCRIPTION OF SAMPLES

The samples used in this study are listed below in ascending stratigraphical order. They are numbered according to their original positions (measured in feet) above the Fernvale Limestone–Sylvan Shale contact. Thus sample Sy280, for example, is from a horizon 280 ft. above this datum.

The total thickness of the Sylvan Shale in Sycamore Creek was measured as 305 ft. (93 m.).

Syl	Calcareous, dark brown, hard platy shale with conchoidal fracture, containing black graptolite compressions.
Sy16	Slightly calcareous, buff- to orange-weathering brown shale.
Sy40	Slightly calcareous, dark grey shale containing abundant graptolites.
Sy60	Slightly calcareous, dark greyish-brown shale.
Sy80	Slightly calcareous, dark greenish-grey, hard splintery shale with conchoida fracture.
Sy100, Sy120	Slightly calcareous, dark brown silty shale with thin yellow and grey laminae.
Sy140	Slightly calcareous, green to greenish-brown, soft shale.
Sy160	Slightly calcareous, green, soft shale with purple-hearted concretions.
Sy180, Sy200	Slightly calcareous, dark greenish-grey, soft shale.
Sy220, Sy240, Sy260	Calcareous, greenish-grey, soft concretionary shale.
Sy280, Sy300, Sy305	Calcareous, light green, soft claystone, which disaggregates readily in water.

Acknowledgements. This work is the second part of a larger study of North American Ordovician Chitinozoa carried out at the University of Oklahoma. I am indebted to the Science Research Council of Great Britain for the award of a two-year Research Fellowship, and to Dr. L. R. Wilson for inviting me to work in his laboratory during its tenure. I wish to record my sincere gratitude to the late Dr. M. A. Rashid and Mr. J. A. Turnbull for assistance in the field, and to the latter for invaluable help in measuring the Sycamore Creek section; to Dr. J. Jansonius (Imperial Oil Ltd., Calgary) for generously permitting me to validate his manuscript genus '*Sagenachitina*'; to the American Association of Stratigraphic Palynologists for a generous donation toward the cost of publication; and to Humble Oil and Refining Company for readily agreeing to my publishing this study. I am especially grateful to Dr. R. W. Hedlund (Atlantic Richfield Company, Dallas) who, after completing a substantial study of organic-walled microfossils in the Sylvan Shale, offered me complete freedom to pursue the subject and encouraged me to publish this paper.

For their critical reading of the paper in typescript I thank Miss J. B. Stough (Esso Production Research Company, Houston), Dr. A. E. Marshall (Humble Oil and Refining Company, Houston) and Drs. T. W. Amsden and W. E. Ham (Oklahoma Geological Survey).

REFERENCES

AMSDEN, T. W. 1960. Stratigraphy and paleontology of the Hunton Group in the Arbuckle Mountain region. Pt. VI. Hunton Stratigraphy. *Bull. Okla. geol. Surv.* 311 pp., 17 pl.

BEJU, D., and DĂNEȚ, N. 1962. Chitinozoare siluriene din Platforma moldovenească și Platforma moezică. *Petrol și Gaze*, **13,** 527–36, pl. 1, 2.

BENOIT, A., and TAUGOURDEAU, P. 1961. Sur quelques chitinozoaires de l'Ordovicien du Sahara. *Revue Inst. fr. Pétrole*, **16,** 1403–21, pl. 1–5.

BERRY, W. B. N. 1960*a*. Graptolite faunas of the Marathon region, west Texas. *Univ. Tex. Publs.* **6005,** 179 pp., 20 pl.

—— 1960*b*. Correlation of Ordovician graptolite-bearing sequences. *21st Int. geol. Congr.*, pt. 7 97–108.

COOPER, G. A. 1956. Chazyan and related brachiopods. *Smithson. misc. Collns.* **127** (2 parts), 1245 pp., 269 pl.

CRAMER, F. H. 1964. Microplankton from three Palaeozoic formations in the province of León, NW–Spain. *Leid. geol. Meded.* **30,** 253–361, pl. 1–24.

—— 1967*a*. Chitinozoans of a composite section of Upper Llandoverian to basal Lower Gedinnian sediments in northern León, Spain. *Bull. Soc. belge Géol. Paléont. Hydrol.* **75** (1966), 69–129, pl. 1–5.

CRAMER, F. H. 1967*b*. An evaluation of the chitinozoan genus *Clathrochitina* Eisenack, 1959. *Notas Comun. Inst. geol. min. Esp.* **94,** 45–52.

DECKER, C. E. 1935. Graptolites of the Sylvan Shale of Oklahoma and Polk Creek Shale of Arkansas. *J. Paleont.* **9,** 697–708.

—— 1936*a*. Some tentative correlations on the basis of graptolites of Oklahoma and Arkansas. *Bull. Am. Ass. Petrol. Geol.* **20,** 301–11.

—— 1936*b*. Table of tentative Lower Paleozoic correlations on basis of graptolites. Ibid. **20,** 1252–7.

—— 1945. Graptolites on well cuttings, Carter County, Oklahoma. Ibid. **29,** 1043–5.

EISENACK, A. 1930. Neue Mikrofossilien des baltischen Silurs. (Vorläufige Mitteilung.) *Naturwissenschaften,* **18,** 880–1.

—— 1931. Neue Mikrofossilien des baltischen Silurs I. *Paläont. Z.* **13,** 74–118, pl. 1–5.

—— 1932. Neue Mikrofossilien des baltischen Silurs II. Ibid. **14,** 257–77, pl. 11, 12.

—— 1934. Neue Mikrofossilien des baltischen Silurs III und neue Mikrofossilien des böhmischen Silurs I. Ibid. **16,** 52–76, pl. 4, 5.

—— 1937. Neue Mikrofossilien des baltischen Silurs IV. Ibid. **19,** 217–43, pl. 15, 16.

—— 1939. Chitinozoen und Hystrichosphaerideen im Ordovicium des Rheinischen Schiefergebirges. *Senckenberg. leth.* **21,** 135–52, pl. A–B.

—— 1948. Mikrofossilien aus Kieselknollen des böhmischen Ordoviziums. Ibid. **28,** 105–17, pl. 1.

—— 1955*a*. Chitinozoen, Hystrichosphären und andere Mikrofossilien aus dem *Beyrichia*-Kalk. Ibid. **36,** 157–88, pl. 1–5.

—— 1955*b*. Neue Chitinozoen aus dem Silur des Baltikums und dem Devon der Eifel. Ibid. **36,** 311–19, pl. 1.

—— 1958. Mikrofossilien aus dem Ordovizium des Baltikums. 1. Markasitschicht, *Dictyonema*-Schiefer, Glaukonitsand, Glaukonitkalk. Ibid. **39,** 389–405, pl. 1, 2.

—— 1959. Neotypen baltischer Silur-Chitinozoen und neue Arten. *Neues Jb. Geol. Paläont. Abh.* **108,** 1–20, pl. 1–3.

—— 1962*a*. Neotypen baltischer Silur-Chitinozoen und neue Arten. Ibid. **114,** 291–316, pl. 14–17.

—— 1962*b*. Mikrofossilien aus dem Ordovizium des Baltikums. 2. Vaginatenkalk bis Lyckholmer Stufe. *Senckenberg. leth.* **43,** 349–66, pl. 44.

—— 1964. Mikrofossilien aus dem Silur Gotlands. Chitinozoen. *Neues Jb. Geol. Paläont. Abh.* **120,** 308–42, pl. 26–30.

—— 1965. Die Mikrofauna der Ostseekalke. 1. Chitinozoen, Hystrichosphären. Ibid. **123,** 115–48, pl. 9–13.

—— 1968. Über Chitinozoen des baltischen Gebietes. *Palaeontographica,* **131**A, 137–98, pl. 24–32.

HAM, W. E. 1969. *Regional Geology of the Arbuckle Mountains, Oklahoma.* Oklahoma Geological Survey, Guide Book 17, Univ. Oklahoma Press, Norman.

—— and WILSON, J. L. 1967. Paleozoic epeirogeny and orogeny in the central United States. *Am. J. Sci.* **265,** 332–407.

HARLTON, B. H. 1953. Ouachita chert facies, southeastern Oklahoma. *Bull. Am. Ass. Petrol. Geol.* **37,** 778–96.

HASS, W. H., and HUDDLE, J. W. 1965. Late Devonian and Early Mississippian age of the Woodford Shale in Oklahoma, as determined from conodonts. *Prof. Pap. U.S. geol. Surv.* **525–**D, D125–32.

JANSONIUS, J. 1964. Morphology and classification of some Chitinozoa. *Bull. Canad. Petrol. Geol.* **12,** 901–18, pl. 1, 2.

—— 1967. Systematics of the Chitinozoa. *Rev. Palaeobot. Palynol.* **1,** 345–60, pl. 1.

JENKINS, W. A. M. 1967. Ordovician Chitinozoa from Shropshire. *Palaeontology,* **10,** 436–88, pl. 68–75.

—— 1969. Chitinozoa from the Ordovician Viola and Fernvale Limestones of the Arbuckle Mountains, Oklahoma. *Spec. Pap. Palaeont.* no. 5, 44 pp., 9 pl.

KAY, M. 1960. Classification of the Ordovician System in North America. *21st. Int. geol. Congr.*, pt. 7, 28–33.

LAUFELD, S. 1967. Caradocian Chitinozoa from Dalarna, Sweden. *Geol. För. Stockh. Förh.* **89,** 275–349, figs. 1–34.

LEE, W. 1943. The stratigraphy and structural development of the Forest City Basin in Kansas. *Bull. Kansas Univ. geol. Surv.* **51,** 142 pp.

LEVORSEN, A. I. 1930. Geology of Seminole County. *Bull. Okla. geol. Surv.* **40** (3), 287–352.

RUEDEMANN, R. 1947. Graptolites of North America. *Mem. geol. Soc. Am.* **19,** 652 pp., 92 pl.

STAPLIN, F. L. 1961. Reef-controlled distribution of Devonian microplankton in Alberta. *Palaeontology,* **4,** 392–424, pl. 48–51.

TAUGOURDEAU, P. 1961. Chitinozoaires du Silurien d'Aquitaine. *Revue Micropaléont.* **4,** 135–54, pl. 1–6.

—— 1962. Associations de chitinozoaires dans quelques sondages de la région d'Édjelé (Sahara). Ibid. **4,** 229–36, pl. 1.

—— 1965. Chitinozoaires de l'Ordovicien des U.S.A.; comparaison avec les faunes de l'ancien monde. *Revue Inst. fr. Pétrole,* **20,** 463–85, pl. 1–3.

—— 1967. Néotypes de chitinozoaires. *Revue Micropaléont.* **9,** 258–64, pl. 1.

—— and JEKHOWSKY, B. DE. 1960. Répartition et description des chitinozoaires siluro-dévoniens de quelques sondages de la C.R.E.P.S., de la C.F.P.A. et de la S.N. REPAL au Sahara. *Revue Inst. fr. Pétrole,* **15,** 1199–1260, pl. 1–13.

—— *et al.* 1967. Microfossiles organiques du Paléozoïque. Les chitinozoaires (1). Analyse bibliographique illustrée. Published for the Commission Internationale de Microflore du Paléozoïque by the Centre National de la Recherche Scientifique, Paris.

THOMAS, H. S. 1930. Characteristics of the Sylvan Shale in widely separated areas. *Proc. Okla. Acad. Sci.* **10,** 85–87.

TWENHOFEL, W. H. *et al.* 1954. Correlation of the Ordovician formations of North America. *Bull. geol. Soc. Am.* **65,** 247–98.

WILSON, L. R. 1958. A chitinozoan faunule from the Sylvan Shale of Oklahoma. *Okla. Geol. Notes,* **18,** 67–71, pl. 1.

—— and DOLLY, E. D. 1964. Chitinozoa in the Tulip Creek Formation, Simpson Group (Ordovician), of Oklahoma. Ibid. **24,** 224–32, pl. 1.

—— and HEDLUND, R. W. 1962. Acid-resistant microfossils of the Sylvan Shale (Ordovician) of Oklahoma. *Pollen Spores,* **4,** 388.

—— —— 1964. *Calpichitina scabiosa,* a new chitinozoan from the Sylvan Shale (Ordovician) of Oklahoma. *Okla. Geol. Notes,* **24,** 161–4, pl. 1.

W. A. M. JENKINS
Humble Oil and Refining Company
P.O. Box 2189
Houston, Texas 77001, U.S.A.

Typescript received 5 July 1969

A NEW SPECIES OF *HEMICYPRIS* (OSTRACODA) FROM ANCIENT BEACH SEDIMENTS OF LAKE RUDOLF, KENYA

by R. H. BATE

ABSTRACT. A new fossil species of *Hemicypris* (*H. posterotruncata* sp. nov.) is described from ancient beach sediments of Lake Rudolf, Kenya. The presence of marginal sockets within the duplicature of the right valve, for the reception of the marginal denticles of the left valve, is recorded for the first time.

TOWARDS the end of 1968 two sieved residues of beach sand (samples M4 and M7) were received from Dr. B. Verdcourt. These samples consisted of 90% ostracod and small gastropod shells with a very subordinate amount of smooth, water worn, quartz grains. The beach sand was collected from two localities: M4 from a site 20 ft. below the beach crest (east side) and approximately 100 yards out from the ridge crest to the south of Lothagam Hill, and M7 from the west of Lothagam Hill. Both samples were collected by Dr. M. D. Gwynne during the Royal Geographical Society South Turkana Expedition. The map showing the location of the samples (text-fig. 1) is based on a sketch provided by Dr. Gwynne. This paper is no. V of the South Turkana Expedition Papers.

The ostracods, present in very large numbers, are all referable to the single new species *Hemicypris posterotruncata* sp. nov. It is difficult to give a precise age dating to the beach deposits as neither the ostracod nor the molluscs listed below are of any assistance in this matter. All that can be said is that they are sub-Recent, possibly Holocene or even Pleistocene in age. What is indicated, however, is that Lake Rudolf was very much more extensive in the past than is the case at the present time.

The following molluscs have been identified by Dr. Verdcourt from the two samples mentioned above:

Sample M3 (from which the residue M4 was obtained)

1. *Bellamya unicolor costulata* (Von Mts.)
2. *Cleopatra bulimoides pirothi* (Jiekeli)
3. *Melanoides tuberculata* (Müll)
4. *Caelatura chefneuxi* (Neuv. and Anthony)
5. *Caelatura rothschildi* (Neuv. and Anthony)
6. *Corbicula africana pusilla* (Philippi)
7. *Biomphalaria pfeifferi* (Krauss)

Sample M7. Associated molluscs were nos. 1, 2, 3 and 5 together with:

Mutella nilotica (Cailliand)
Mutella alluaudi (Germain)

All the material described in this paper is in the collections of the Department of Palaeontology, British Museum (Natural History).

The photographs were taken on the scanning electron microscope.

[Palaeontology, Vol. 13, Part 2, 1970, pp. 289 296, pl. 52.]

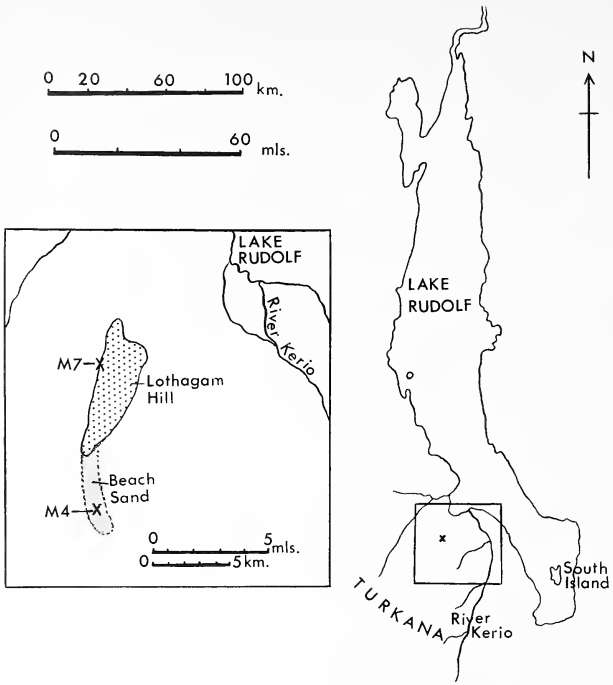

TEXT-FIG. 1. Location map of the beach sand sample, Lake Rudolf, Kenya.

SYSTEMATIC DESCRIPTION

Subclass OSTRACODA Latreille 1806
Order PODOCOPIDA Müller 1894
Suborder PODOCOPINA Sars 1866
Family CYPRIDIDAE Baird 1845
Subfamily CYPRIDINAE Baird 1845
Genus HEMICYPRIS Sars 1903

Type species. Hemicypris pyxidata (Moniez), designated Swain (1961, p. Q221).

Remarks. Sars included three species in his new genus *Hemicypris: Hemicypris pyxidata* (Moniez), *H. ovata* sp. nov., and *H. megalops* sp. nov., although he did not designate a type species (see above). His reasons for distinguishing *Hemicypris* from the closely related genus *Cyprinotus* Brady were that the right valve in each case was larger than

the left, the second pair of maxillae were devoid of a vibratory plate and that they all reproduced parthenogenetically.

The validity of *Hemicypris* was refuted by Klie (1932, p. 471) after he had examined material identified by Sars. Klie pointed out that the three species placed in *Hemicypris*

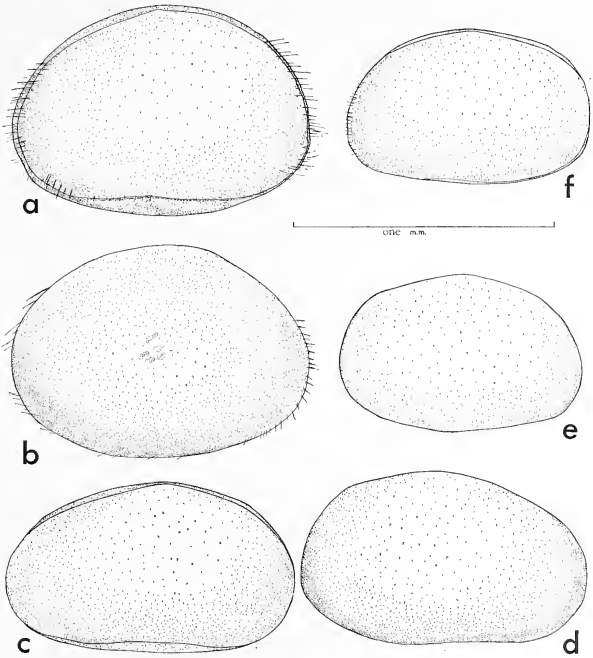

TEXT-FIG. 2. *a, b, Hemicypris pyxidata* (Moniez), F. 12294, Univ. Oslo; left and right views, complete carapace. *c, d, Hemicypris ovata* Sars, F. 12293, Univ. Oslo; left and right views, complete carapace. *e, f, Hemicypris megalops* Sars, F. 12292, Univ. Oslo; right and left views, complete carapace.

by Sars did in fact possess a vibratory plate and that this was clearly visible in both *pyxidata* and *ovata*. He further stated that, as recommended in a previous publication of his (1930), the genus *Cyprinotus* should be retained for those species in which the valves have a crenulate margin and a dorsal hump, and that *Heterocypris* should be used for those species lacking a dorsal hump whether or not the valves were crenulate at their margins. Accordingly he placed *pyxidata* and *megalops* in *Heterocypris*.

This arrangement of Klie's is not, however, satisfactory as the characters of the carapace play an important role in the grouping of ostracods into natural units, and the

possession of marginal denticles is considered here to indicate a close genetic affinity between the species. These species should not, therefore, be placed in *Heterocypris*. Coupled with a general umbonate dorsal outline the genus *Cyprinotus* may be clearly divided into those forms in which the left valve is the larger (*Cyprinotus* s.s.) and those in which the right valve is the larger (*Hemicypris* s.s.). In both groups it is the smaller valve which possesses the marginal denticles. If there was but a single species having the right valve larger than the left it would be unnecessary to retain the genus *Hemicypris*. There are, however, twelve species having a wide geographical distribution which may be assigned to the *Hemicypris* group. Should this morphological group be placed in *Cyprinotus* or separately identified? If the latter case, are the characters present sufficient for a generic or a subgeneric determination? It is considered here that the presence of at least twelve species indicates that this group has developed sufficiently for a generic determination to be made.

The following species are here placed in *Hemicypris*:

Cyprinotus pyxidatus Moniez 1892, the type species, described from a pond in Luwu in the Célèbes.
Hemicypris ovata Sars 1903, from dried mud, north-eastern Sumatra.
Hemicypris megalops Sars 1903, from dried mud, north-eastern Sumatra.
Cyprinotus (*Hemicypris*) *kaufmanni* Vávra 1906, from an ornamental fish pond, the Bronze Horse Temple, Nagasaki, Japan.
Cyprinotus fossulatus Vávra 1898, from Usaramo, Tanzania.
Cyprinotus decoratus Daday 1910, from the Zoological Gardens, Giza [Gizeh], Egypt.
Cyprinotus inversus Daday 1913, from Ku-Gudië, Kalahari, South Africa.
Cyprinotus fullerborni Daday 1910, from Lake Rukwa [Rikwa], Tanzania.
Cyprinotus humbertii Gauthier 1933, from Ambovombe, Malagassy Republic.
Heterocypris reticulatus Klie 1930, from Gran Chaco, Paraguay.
Hemicypris posterotruncata sp. nov., this paper, sub-Recent beach sediment, Lake Rudolf, Kenya.
Heterocypris dentatomarginata Kiss 1959, from Lake Tanganyika.

Hemicypris posterotruncata sp. nov.

Plate 52, figs. 1–7; text-fig. 3*d–i*, text-fig. 4*a*, *b*

Diagnosis. *Hemicypris* with strongly calcified carapace, of angular outline with truncated, broadly flattened posterior end. Dorsal margin arched, umbonate, with greatest height passing through anterior cardinal angle; greatest length passing well below mid-point.

Holotype. Io. 1410, carapace, figured Plate 52, fig. 1, text-fig. 3, figs. *d–g*. Sub-Recent beach sediment, Lake Rudolf, Kenya.

Paratypes. Io. 1411–49, carapaces and single valves from the same locality as above.

Other material. Io. 1450A, B. Topotype material contained in the original sample (M4); locality as above.

Description. Carapace strongly calcified, subrectangular in outline with broadly rounded anterior end and broad, truncated posterior end. Postero-dorsal slope long, flattened;

EXPLANATION OF PLATE 52

Hemicypris posterotruncata sp. nov. 1, left view of complete carapace, holotype, Io. 1410, ×85. 2, right valve, paratype, Io. 1419, ×85. 3, internal view of left valve showing anterior and posterior marginal denticles, paratype Io. 1415, ×85. 5, section of anterior duplicature, right valve, showing small pits (sockets) for the reception of the marginal denticles of the left valve; paratype, Io. 1416, ×500. 6, anterior duplicature, left valve, to show marginal denticles, paratype, Io. 1415, ×500. 7, central and dorsal muscle scars, internal view of right valve, paratype, Io. 1418, ×85.

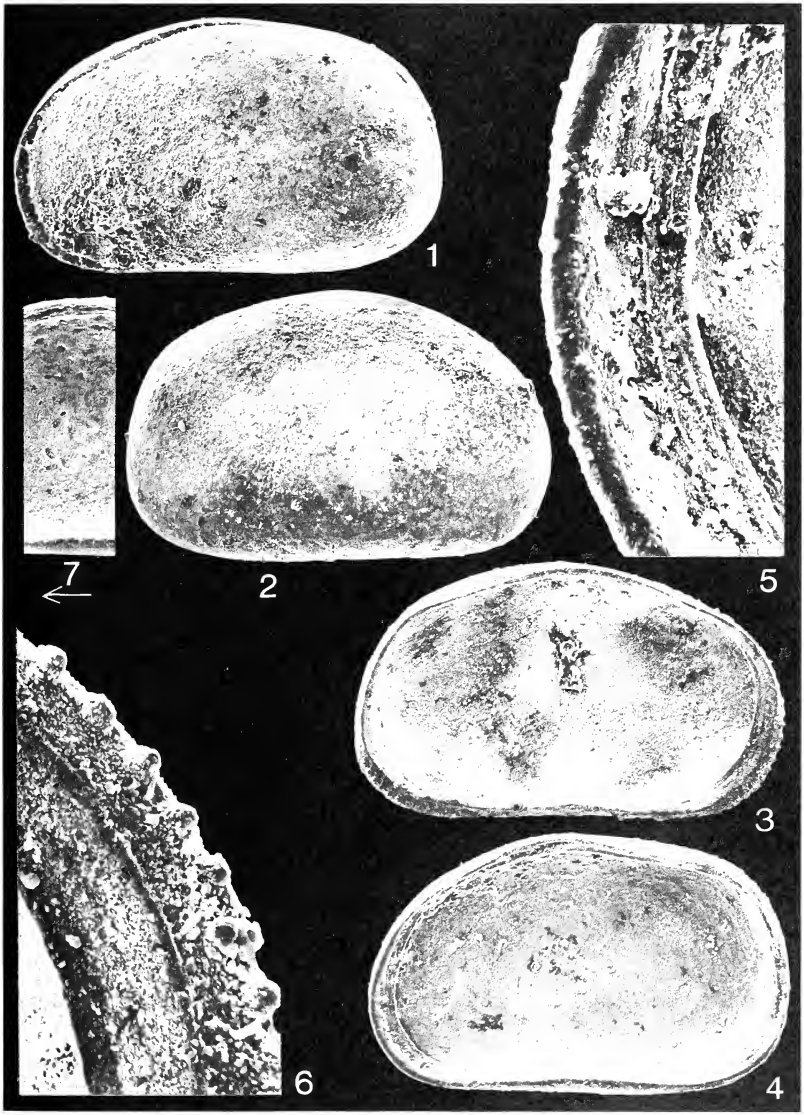

BATE, *Hemicypris posterotruncata*

postero-ventral slope convex. Posterior cardinal angle situated very close to extreme posterior end of carapace and prominently developed. Dorsal margin convex, umbonate at anterior cardinal angle which is situated above, or slightly in front of mid-point of carapace. Line of greatest height of valve passes through this cardinal angle. Extreme

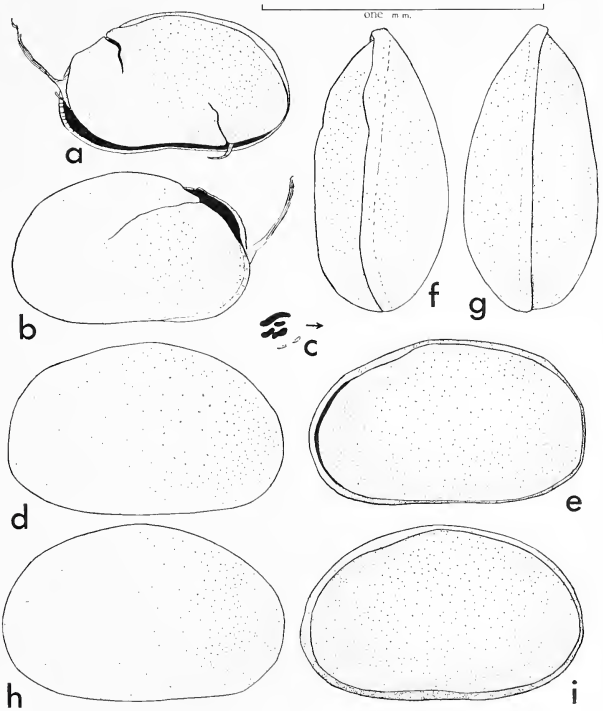

TEXT-FIG. 3. *a–c*, *Hemicypris fossulata* (Vávra), K. 19043, Zool. Staatsinstitut, Hamburg; left and right views, complete carapace and muscle scars. *d–g*, *Hemicypris posterotruncata* sp. nov. Io. 1410, holotype; right, left, dorsal and ventral views, complete carapace. *h*, *i*, *Hemicypris posterotruncata* sp. nov. Io. 1411, paratype; right and left views, complete carapace.

posterior termination of carapace is situated below mid-height and as a result line of greatest length passes well below mid-point. Line of greatest width passes through carapace slightly behind mid-point. Antero-dorsal slope long and obliquely convex. Ventral margin moderately convex with shallow median incurvature.

Right valve much larger than left, overlapping it strongly in region of antero-dorsal slope. Right valve also overlaps left along ventral margin and around posterior margin,

but anteriorly merely projects beyond the left. Mid-dorsally valves tend to diverge slightly and there is no overlap or overreach of either valve.

Shell surface granular, showing no evidence of surface pitting.

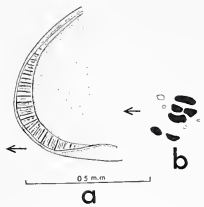

TEXT-FIG. 4. *a*, Anterior radial pore canals, paratype, Io. 1421. *b*, Muscle scars, right valve, paratype, Io. 1418, ×115.

Hinge is simple with dorsal edge of smaller left valve (terminally thickened) fitting into groove situated in dorsal margin of right valve. This dorsal groove terminally widens to produce elongate sockets which are open at their ends to interior of valve.

Duplicature is of moderate width anteriorly and slightly more narrow posteriorly; selvage is particularly well developed in left valve. Inner margin and line of concrescence do not quite coincide but a distinct vestibule is not developed. Around antero-ventral and postero-ventral parts of free margin, small marginal denticles are developed in smaller left valve (Pl. 52, figs. 3, 6). These denticles fit into small pits (sockets) situated in duplicature of right valve (Pl. 52, figs. 4, 5). Posteriorly these sockets are overhung by prominent development of selvage. Marginal denticles are a device for holding valves firmly together when closed.

Muscle scars (text-fig. 4*b*, Pl. 52, fig. 7), typical of the Cyprididae, consist of group of 4 laterally elongate adductor scars with 2 oval scars situated below. Prominent dorsal muscle scars are situated above these scars, just below hinge.

Anterior radial pore canals (text-fig. 4*a*) are straight and simple, numbering approximately 40–45.

Dimensions (in *mm*.)

	Length	*Height*	*Width*
Holotype, Io. 1410, carapace	0·95	0·59	0·48
Paratypes, Io. 1411, „	0·96	0·60	0·46
Io. 1412, „	0·98	0·60	0·45
Io. 1413, „	0·96	0·60	0·45
Io. 1415, left valve	0·95	0·55	
Io. 1416, right valve	0·93	0·59	
Io. 1418, „ „	0·88	0·54	
Io. 1419, „ „	0·93	0·59	

Remarks. Hemicypris pyxidata (Moniez) (text-fig. 2*a*, *b*) is more oval in outline and too compressed when viewed dorsally to be confused with *H. posterotruncata*. Some similarity in outline exists between the latter species and the slightly larger *H. ovata* Sars which is more oval in outline and without the truncated posterior margin. *Hemicypris megalops* Sars is close to *H. posterotruncata* in outline and size, but as is also the case for *H. ovata*, the valvular relationships when viewed from the left are completely different. This is evident in the camera lucida drawings (text-figs. 2*c*, *f*; 3*e*, *i*), in which the characteristic overlap of the left valve by the right in the antero-dorsal region of *H. posterotruncata* is clearly shown. This feature is not present in the other two species.

Hemicypris fossulata (Vávra) is distinguished from *H. posterotruncata* by the narrower, more evenly rounded anterior and posterior ends and by the less acute posterior cardinal angle. It has a punctate shell surface which is less pronounced than shown

by Vávra (1898, fig. 8), though this may be due to decalcification of the material during storage.

The specimens of *Hemicypris fossulata* (Vávra) in the collections of the Zoologisches Staatsinstitut, Hamburg, were collected from Kilimanjaro by Professor F. Fülleborn (1898–1900) and determined by Daday.

The other species placed in *Hemicypris* (*Heterocypris dentatomarginata*, *Cyprinotus fullerborni*, *C. humbertii* and *C. decoratus*) all differ from *H. posterotruncata* in carapace outline, whilst *Heterocypris reticulatus*, although of angular outline, is clearly distinguished by its surface ornamentation. *Cyprinotus inversus* Daday differs from *H. posterotruncata* not only in the possession of a more smoothly convex dorsal outline but also in the possession of straight radial pore canals in the right valve and branching canals in the left.

Conclusions. *Hemicypris* Sars is retained as a valid genus. The identification of *Hemicypris posterotruncata* sp. nov., a fossil species from ancient beach sediments of Lake Rudolf, indicates that the genus has a longer developmental history than had previously been understood. The assignment here of one fossil species and eleven living species to *Hemicypris* has extended the geographical distribution of the genus to include South America, North, South, and East Africa, Malagassy Republic, Java, Sumatra, the Célèbes and Japan. No species have yet been recorded from outside the area bounded by the latitudes 40° North and 40° South of the Equator. The genus *Cyprinotus*, on the other hand, besides being recorded from tropical climates, is also known to occur in the colder climates of the U.S.A., Canada, and Greenland.

Acknowledgements. I should like to record my thanks to Dr. B. Verdcourt, Royal Botanic Gardens, Kew and to Dr. M. D. Gwynne, Balliol College, Oxford for the opportunity to examine and describe this new ostracod species. My sincere thanks are also due to Dr. G. Hartmann, Zoologisches Staatsinstitut, Hamburg for the loan of *Hemicypris fossulata* material and to Dr. M. Christiansen, University of Oslo, for the loan of Sars's Sumatra material of *H. pyxidata*, *H. ovata*, and *H. megalops*. My colleague Dr. Ken McKenzie gave much valuable advice during the preparation of this paper.

REFERENCES

DADAY, E. 1910. Untersuchungen über die Süsswasser-Mikrofauna Deutsch-Ostafrikas. XII, Ostracoda. *Zoologica*, **59**, pp. 159–240, 15 pl. Stuttgart.

—— 1910. Ergebnisse der mit Subvention aus der Erbschaft Treitl unternommenen zoologischen Forschungsreise Dr. Franz Werner's nach dem ägyptischen Sudan und Nord Uganda. XV. Beiträge zur Kenntnis der Mikrofauna des Nils. *Akad. Wissenschft. Wien*, pp. 1–52, pl. 1, 2.

—— 1913. Cladoceren und Ostracoden aus Süd-und Südwestafrika. *Denkschr. med.-naturw. Ges. Jena*, **17**, 89–102, pl. 5, 6.

FERGUSON, E. 1966. Some freshwater ostracods from the Western United States. *Trans. Am. micros. Soc.*, Lancaster, **85**, 313–18.

GAUTHIER, H. 1933. Entomostracés de Madagascar, 2. Description d'un nouveau *Cyprinotus* (Ostracodes). *Bull. zool. Soc. France*, Paris, **58**, 305–16.

KISS, R. 1959. Quelques Ostracodes nouveaux et intéressants de la région de l'extrémité Nord du Lac Tanganika. *Rev. zool. bot. afr.*, Bruxelles, **59**, 81–105.

KLIE, W. 1930. Ostracoden aus dem paragarayischen Teile des Gran Chaco. *Arch. hydrobiol.*, Stuttgart, **22**, 221–58.

—— 1932. Die Ostracoden der deutschen limnologischen Sunda-Expedition. *Arch. hydrobiol., Suppl.*, Stuttgart, **11**, 447–502, pl. 64–69.

MONIEZ, R. 1892. Entomostracés d'eau douce de Sumatra et de Célèbes. II, Ostracodes. *Zool. Ergebnisse niederländ. Ost-Indien*. Leiden. **2,** 129–35, pl. 10.

SARS, G. O. 1903. Fresh-water Entomostraca from China and Sumatra. *Archiv for Mathematik og Naturvidenskab*, Kristiania, **25,** 3–44, pl. 1–4.

SWAIN, F. M. 1961. *In* MOORE, R. C. (ed.) *Treatise on Invertebrate Paleontology*, Pt. O, *Arthropoda*, 3, 442 pp. Univ. of Kansas and Geol. Soc. Am.

VÁVRA, V. 1898. Die Süsswasser-Ostracoden Deutsch-Ost-Afrikas. *Thierwelt Ost-Afrik. Nachbarg.*, Berlin, **4,** 1–28.

—— 1906. Ostracoden von Sumatra, Java, Siam, den Sandwich-Inseln und Japan. *Zool. Jb. system. Geogr. Biol.*, Jena, **23,** 413–38, pl. 24, 25.

R. H. BATE
Department of Palaeontology
British Museum (Natural History)
Cromwell Road
London, S.W.7

Typescript received 13 May 1969

VARIATION IN THE CARDINALIA OF THE BRACHIOPOD *PTYCHOPLEURELLA BOUCHARDI* (DAVIDSON) FROM THE WENLOCK LIMESTONE OF WENLOCK EDGE, SHROPSHIRE

by M. G. BASSETT

ABSTRACT. In specimens of the orthacean brachiopod *Ptychopleurella bouchardi* (Davidson) from the Wenlock Limestone of Wenlock Edge, Shropshire, the cardinalia display a wide range of variation, particularly in the development of the cardinal process. The variation can be explained partly by ontogeny but in some extreme cases it is suggested that it reflects environmental control due to turbulent water conditions in an area of active reef growth. These conditions led mainly to the progressive inflation of the cardinal process to produce an optimum attachment surface for the diductor muscle bases, but in two specimens no cardinal process is developed. In these the muscle bases appear to have covered the notothyrial platform from the earliest growth stage, thus preventing the secretion of a cardinal process from a central strip of epithelium. The effect of this was to employ a maximum attachment area throughout ontogeny as an alternative to the production of a bulbous cardinal process.

THE orthacean brachiopod species *Ptychopleurella bouchardi* (Davidson 1847) occurs fairly commonly throughout the Wenlock Limestone (Silurian) of the type area in the vicinity of Much Wenlock, Shropshire. Examination of the interiors of a number of brachial valves of *P. bouchardi* from this area reveals that the cardinalia display a wide range of morphological variation hitherto unrecorded in orthoid genera. This variation is seen mainly in the development of the cardinal process and to a lesser extent in the modification of the brachiophores and sockets. Since the valves studied are from collections made from single bedding planes, are associated with a single type of pedicle valve, and have a similar musculature and external morphology, the variation is regarded as being intraspecific in nature. Undoubtedly it is due partly to the ontogenetic development of the shell, but is here interpreted partially as a response to environmental control.

The observations and interpretation of the variation are based largely on a collection of 12 brachial valves from an area of about 5 sq. m. of a bedding plane in the Wenlock Limestone of Coates Quarry, Wenlock Edge, on the north side of the road approximately 1 mile south-west of Much Wenlock (Grid Ref. SO/6045.9935; text-fig. 1). Comparative evidence is provided by a collection of about 20 shells from a single bedding plane in the Wenlock Limestone of the old quarry on the west side of Lincoln Hill, Ironbridge (Grid Ref. SJ/6695.0381). Text-fig. 2 illustrates 7 representative specimens from Coates Quarry. Specimens A–E are members of a progressive growth series, indicated on the graph by a progressive increase in valve length coupled with an increase in the number of growth lamellae on the exterior of the valve. The approach to maturity of the larger specimens is further suggested by the close spacing of the growth lamellae at the anterior margin of the valve. Specimens F and G are also mature shells but the plot of the growth lamellae suggests that they are not a continuation of the growth series A–E.

[Palaeontology, Vol. 13, Part 2, 1970, pp. 297–302, pl. 53.]

The nature of the variation

1. *The cardinal process.* Figs. A–E in text-fig. 2 illustrate the progressive growth of the cardinal process in 5 of the specimens studied from Coates Quarry. At the young growth stage represented by A the floor of the notothyrial chamber is almost flat or slightly ridged and no definite cardinal process is developed. This probably indicates that at this stage the diductor muscle bases were implanted discretely on to the floor

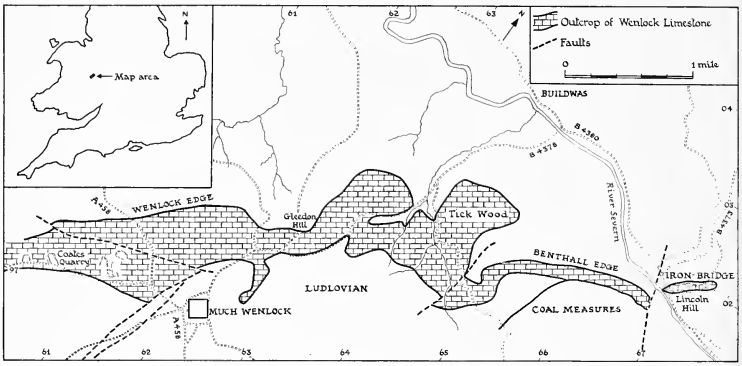

TEXT-FIG. 1. Map of the outcrop of the Wenlock Limestone along the north-east of Wenlock Edge and its continuation to Benthall Edge, showing the position of Coates Quarry and Lincoln Hill.

of the notothyrial platform. With increased shell growth, seen in B, a low, longitudinal, median ridge, representing an embryonic cardinal process is developed, presumably by the secretion of secondary calcite from the strip of outer epithelium between the muscle bases, following the pattern common to most orthoid brachiopods (Williams and Rowell, *in* Moore 1965, p. H118). In specimen C further anterior and ventral growth of the median ridge has led to the development of a clearly defined, slightly lobed cardinal process. This growth was probably accompanied by a medial migration of the diductor muscle bases from the floor of the notothyrial platform on to the lateral surfaces of the cardinal process. The further pronounced anterior and ventral inflation of the cardinal process seen in D and E must clearly reflect a response to the need for the muscle bases to be attached over a wider surface area.

In specimens collected from Lincoln Hill the stages A–C can be traced in valves at closely comparable growth stages to those described above. However, the maximum growth in the cardinal process in shells from Lincoln Hill is only slightly beyond that of stage C and even in larger specimens there is no extreme inflation comparable to that in specimens D and E from Coates Quarry. The extreme growth of the cardinal process in D and E from Coates Quarry would therefore appear to be controlled by factors other than ontogeny.

Specimens F and G in text-fig. 2 are two aberrant shells from Coates Quarry, in which

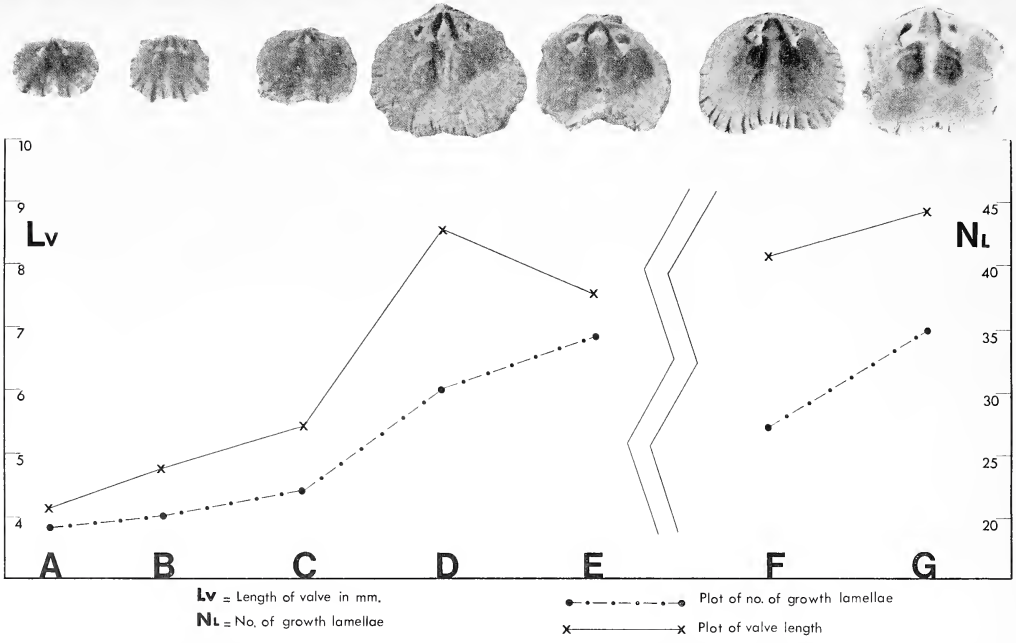

TEXT-FIG. 2. Diagram to illustrate the growth and variation of the cardinalia in 7 specimens of *P. bouchardi* from a single bedding plane in the Wenlock Limestone of Coates Quarry. Specimens A–E are part of a progressive growth series. Specimens F and G are two aberrant shells in which no cardinal process is developed.

the cardinal process is not developed. There is no evidence in these shells that the cardinal process has merely been broken off and although the two specimens are fairly large the plot of the number of growth lines does not suggest that they are gerontic members of the growth series A–E in which a condition has been reached where resorption has led to the disappearance of the cardinal process. Further evidence against this latter suggestion is presented by a study of the pattern of growth lines within the cardinalia. In the young shells A and B, for example, the fine growth lines on the floor of the notothyrial chamber are straight or very gently curved and are sub-parallel to the hinge line (see Pl. 53, fig. 9). After this stage the further pronounced ventral and anterior growth of the cardinal process is reflected in the development of a distinctive chevron-shaped pattern of growth lines across the notothyrial area, especially well seen in specimen D (see Pl. 53, fig. 10). In contrast, the growth lines seen in F and G (see Pl. 53, fig. 11) are again sub-parallel to the hinge line, similar to the pattern seen in young shells. This suggests that in these two aberrant specimens the cardinal process was never developed and implies that in their early growth stages the diductor muscle bases were attached over the whole of the central area of the notothyrial chamber so that no medial strip of epithelium was exposed to secrete secondary calcite in the form of a cardinal process. No shells from Lincoln Hill have been found in this aberrant condition.

2. *The brachiophores and sockets.* All the specimens of *P. bouchardi* studied from numerous localities in the Wenlock Limestone of Wenlock Edge exhibit modifications of the brachiophores and sockets with growth by the addition of secondary shell material.

EXPLANATION OF PLATE 53

Ptychopleurella bouchardi (Davidson). All specimens are from a single bedding plane in the Wenlock Limestone of Coates Quarry, north side of road, 1 mile south-west of Much Wenlock, Shropshire (Grid. Ref. SO/6045.9935). Figs. 8, 9, 10, 11 are ×8; all other figs are ×3.

Fig. 1. NMW.69.96.G1. Interior of brachial valve. Specimen A of text-fig. 2. Note the almost flat notothyrial platform.

Fig. 2. NMW.69.96.G9. Interior of brachial valve. Specimen B of text-fig. 2. Note the low ridge forming the embryonic cardinal process.

Fig. 3. NMW.69.96.G2. Interior of brachial valve. Specimen C of text-fig. 2. Note the slightly lobed cardinal process.

Figs. 4*a–c*. NMW.69.96.G3. Interior, exterior, and lateral views of brachial valve. Specimen D of text-fig. 2. Note the deep sockets, expanded cardinal process, and secondary calcite covering the floor of the valve.

Figs. 5*a*, *b*. NMW.69.96.G4. Interior and exterior of brachial valve. Specimen E of text-fig. 2. Note the bulbous cardinal process, deep sockets, and expanded brachiophores.

Figs. 6*a*, *b*. NMW.69.96.G5. Interior and exterior of brachial valve. Specimen F of text-fig. 2. Note the absence of the cardinal process.

Figs. 7*a*, *b*. NMW.69.96.G6. Interior and exterior of brachial valve. Specimen G of text-fig. 2. Note the absence of the cardinal process.

Fig. 8. Enlargement of the cardinalia of fig. 1.

Fig. 9. Enlargement of the cardinalia of fig. 2. Note the embryonic cardinal process and the fine growth lines across the notothyrial platform.

Fig. 10. Enlargement of the cardinalia of fig. 4*a*. Note the expanded cardinal process and the chevron-shaped growth lines across the notothyrial platform.

Fig. 11. Enlargement of the cardinalia of fig. 7*a*. Note the absence of the cardinal process and the fine growth lines across the notothyrial platform. Compare the growth lines with those in figs. 9 and 10.

Figs. 12*a–c*. NMW.69.96.G7. Interior, exterior, and lateral views of pedicle valve.

Figs. 13*a*, *b*. NMW.69.96.G8. Interior and exterior of pedicle valve.

1

2

3

4a

5a

4b

4c

5b

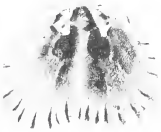

6a

7a

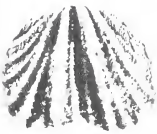

6b

7b

12a

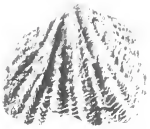

12b

12c

13a

13b

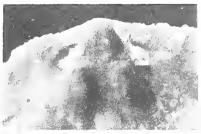

8

9

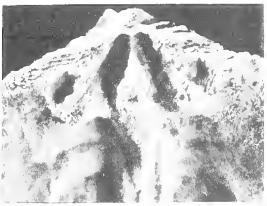

10

11

This results in the building of 'walls' around the rims of the sockets leading to their rounding and apparent deepening, the development of socket pads, and the thickening of the bases of the brachiophores. In the specimens from Coates Quarry, including the aberrant shells F and G, these modifications of the cardinalia by the addition of secondary calcite are generally much more pronounced than in specimens from other localities.

Interpretation

The absence of a cardinal process in two shells, and the extreme modification of the brachiophores and sockets in other specimens from Coates Quarry cannot be regarded solely as a growth feature since these conditions are not seen consistently in shells of comparable size from other localities. Instead it is suggested that the variation observed in these 'abnormal' shells is related partially to the environment in which they lived.

The Wenlock Limestone of Wenlock Edge, and its continuation to Benthall Edge and Lincoln Hill, forms part of a reef complex aligned in a north-east to south-west direction. Scoffin (1965) suggested that a large bioherm which occupies the bulk of the thickness of the Wenlock Limestone around Hilltop (Grid. Ref. SO/5700.9630), about $3\frac{1}{2}$ miles south-west of Much Wenlock, probably acted as a 'barrier' reef. No specimens of *P. bouchardi* have been found by the writer to the south-west of Hilltop in the off-reef area. Coates Quarry lies in the back-reef area about $2\frac{1}{2}$ miles to the north-east of the 'barrier' reef and the specimens described from there were obtained from a thin shale parting on a bedding plane lying immediately adjacent to a large symmetrical bioherm. This and other bioherms in the vicinity probably formed part of an extensive patch reef development in the lee of the 'barrier' reef (Scoffin 1965, p. 190). The bioherms are composed of large colonial corals, stromatoporoids, algae, and crinoids, with interdigitations of skeletal debris and lime mud, while the surrounding bedded sediments consist of biomicrites and biosparites with thin grey shale partings. These deposits together suggest that conditions within and around the bioherms varied from periods of quiet water deposition to periods of moderate agitation, probably by wave action. (The interpretation of the depositional conditions outlined here is based on the classification of Plumley *et al.* 1962; the conditions within the reef area of Wenlock Edge were probably closely analogous with those described by Plumley *et al.* (op. cit., pp. 93–5) in their hypothetical example.) Relatively few other fossils are found immediately adjacent to the bioherms, a factor which supports this interpretation.

Any brachiopods which were to survive the periodical agitation of water in this environment would need relatively thick shells, powerful muscles with large attachment areas, and a strong articulatory mechanism. The specimens of *P. bouchardi* described from Coates Quarry possess all of these features. In some specimens the shell is further thickened by the addition of secondary calcite over the floor of the valve. The large dorsal adductor scars may be clearly seen in the specimens illustrated in text-fig. 2 and Plate 53; it appears that the progressive inflation of the cardinal process in specimens A–E reflects the rapid development of an optimum surface area for the attachment of the diductor bases, while in the aberrant shells F and G the muscle bases covered the whole of the central area of the notothyrial chamber to gain maximum attachment from the earliest growth stage. Thus in 2 specimens a broad, firm attachment area was employed throughout ontogeny as an alternative to the production of a bulbous cardinal process. The deepening of the sockets would produce a strong articulatory

structure while the addition of secondary calcite to the whole of the cardinalia possibly acted as a stabilizer to maintain the shell in its posterior-downward life position. Bowen (1966, p. 1021) suggested a similar function for deposits of secondary calcite in the notothyrial area of specimens of *Atrypa reticularis* (Linnaeus). The few other species of brachiopods associated with *P. bouchardi* in Coates Quarry also exhibit thickening of the shell by the addition of secondary calcite. A few specimens collected by the writer from similar reef-bearing beds along Benthall Edge also possess many of the features described above, including a large cardinal process, but no further specimens have been observed in which the cardinal process is absent.

Lincoln Hill lies some 7 miles to the north-east of the Wenlock Edge 'barrier' reef in the back-reef lagoonal area. Here the abundance of many species of articulated brachiopods and solitary corals in fine biosparite limestones, and the rarity of colonial reef builders, suggests relatively quiet water conditions compared to areas further to the south-west. Under these conditions it appears that the cardinalia of *P. bouchardi* display only the normal features of growth. (Bioherms were probably once present in stratigraphically higher beds at Lincoln Hill, e.g. see Murchison 1839, p. 211, but they have long since been removed by quarrying and there is no evidence that active reef growth took place within the beds exposed today.)

Although the above discussion is based on the study of only a small number of specimens, it nevertheless serves to illustrate that the cardinalia of orthoid brachiopods may vary widely within a single species in different environments. The use of such features as stable characters for purposes of classification should therefore be treated with caution.

Acknowledgements. This work was carried out in the Department of Geology, University College, Swansea, as part of a larger study of British Wenlockian brachiopod faunas. I wish to thank Dr. V. G. Walmsley for his help and guidance, Professor F. H. T. Rhodes for providing research facilities, and Dr. T. P. Scoffin for discussing environmental conditions in the Wenlock Limestone. Financial support from the Sir Richard Stapley Educational Trust and the Natural Environment Research Council is gratefully acknowledged. All the specimens are housed in the Department of Geology, National Museum of Wales, Cardiff.

REFERENCES

BOWEN, Z. P. 1966. Intraspecific variation in the brachial cardinalia of *Atrypa reticularis*. *J. Paleont.* **40**, 1017–22, pl. 118.

DAVIDSON, T. 1847. Observations on some of the Wenlock-limestone Brachiopoda, with descriptions of several new species. *London Geol. Journ.* **1**, 52–65, pl. 12, 13.

MOORE, R. C. 1965 (Ed.). *Treatise on Invertebrate Paleontology, Part H, Brachiopoda.* 2 vols., xxxii + 927 pp., Geol. Soc. Amer. and Univ. Kansas Press.

MURCHISON, R. I. 1839. *The Silurian System, founded on geological researches in the counties of Salop, Hereford, Radnor, Montgomery, Caermarthen, Brecon, Pembroke, Monmouth, Gloucester, Worcester, and Stafford; with descriptions of the coal-fields and overlying formations.* 1–768 (2 vols.), 110 figs; pl. 1–37. London.

PLUMLEY, W. J., RISLEY, G. A., GRAVES, R. W., and KALEY, M. E. 1962. Energy index for limestone interpretation. *In* Classification of Carbonate Rocks. *Mem. Am. Ass. Petrol. Geol.* **1**, 85–107.

SCOFFIN, T. P. 1965. The Sedimentology of the Wenlock Limestone. Unpublished Ph.D. thesis. University of Wales (Swansea).

M. G. BASSETT
Department of Geology
National Museum of Wales
Cardiff, CF1 3NP

Typescript received 3 June 1969

STEREOSCAN OBSERVATIONS ON THE POLLEN GENUS *CLASSOPOLLIS* PFLUG 1953

by Y. REYRE

Abstract. The diagnosis of the pollen formgenus *Classopollis* Pflug 1953 is here emended after both a review of the literature and observation of numerous specimens recovered from Upper Triassic to Middle Cretaceous rocks in the Sahara, Israel, and France. Following a discussion of a proper definition of the species, twelve new species are described. Botanic affinity, taxonomic value, and stratigraphic occurence are also discussed.

Numerous species have been validly assigned to the genus *Classopollis* both before and after the emendation by Pocock and Jansonius (1961). However, among isolated grains of apparently homogeneous assemblages from African or European Mesozoic rocks, it has proved impossible by light microscope to identify these species with certainty. Scanning electron microscope observations indicate four possible reasons: (*a*) the number of potential *Classopollis* species is greater than that of described species, (*b*) inexactness of the majority of specific diagnosis in the description of the exinal structure and sculpture, (c) the hierarchy of characters used to define species is variable depending on the individual author (often it is not indicated), (*d*) it seems that certain species have been defined on the basis of plurispecific assemblages, often unsuspected by the authors themselves. Because of its palaeobotanic and stratigraphic importance, a review of the genus has been undertaken using large assemblages extracted from the following formations: Upper Triassic (above Carnian) in the Tunisian and Algerian Sahara, Infraliassic and Lower Liassic in the Sahara and France (Saintonge, Massif Central), Jurassic and Lower Cretaceous in the Sahara, Israel, and France.

PREVIOUS LITERATURE

The genus *Classopollis* was instituted by Pflug (1953), although some species were previously assigned to other genera. Pocock and Jansonius (1961) presented an extensive review of past works and Boltenhagen (1968) completed this review by a critical survey of the literature.

Couper (1958, pp. 156–7, pl. 28, figs. 2–7) emended the genus *Classopollis* Pflug 1953, considering that Pflug's interpretation was inexact. After observations on pollen of *Pagiophyllum connivens* Kendall, he tried to show that the genus *Classopollis* is a morphographical taxonomic entity including all the species of the type met with in the above-mentioned fossil. Thus he suggested a very wide generic definition in which one must principally note an equatorial endexine thickness and a vague proximal trilete mark; he regarded *P. torosus* Reissinger as the type-species. Klaus (1960, pp. 165–7, pl. 36, figs. 57–60) emended the genus *Corollina* Maljavkina 1949 and included in particular Pflug and Couper's *Classopollis* species. In addition, Klaus suggested his species *Circulina meyeriana* as the type-species of the genus *Circulina* Maljavkina 1949. In his opinion this genus is recognizable by the following characters: a Y-form dehiscence, a distal polar area, a sub-equatorial ring which is not bordered with a thickening,

[Palaeontology, Vol. 13, Part 2, 1970, pp. 303–322, pl. 54–59.]

occasionally parallel folds in the ring zone, and infrastructure without midrib, line, reticulum, or ring (striation ?).

Pocock and Jansonius (1961, pp. 443–4, pl. 1, figs 1–9) emended Pflug's genus, considering the attributions of Couper (1958) and Klaus (1960) as unfounded. They also emended *C. classoides* Pflug which they retained as type-species of the genus, and defined the genus with the following characters: (*a*) distally monoporate, (*b*) exoexine two-layered, (*c*) exoexine absent or much reduced over a circular area surrounding the distal pole and absent or reduced over a triangular area with its centre at the proximal pole, (*d*) intexine frequently bearing a reduced trilete scar, which has no germinal function, (*e*) exine always ornamented by striations, (*f*) the band, usually but not always, marking a zone of exinal thickening. Pettitt and Chaloner (1964) studied by electron microscope pollen grains extracted from a cone of *Cheirolepis muensteri* Schenk. They assigned these grains to the morphographical species *C. torosus* (without naming the author). They established that the exine of *Classopollis* is composite with a lamellate endonexine and a complicated ectonexine within which they distinguished an inner layer (ecn 2), a middle massive layer (ecn 1), and a tegillum. Burger (1966) suggested that the columellars (equivalent to ecn 2 of Pettitt and Chaloner) join in the equatorial belt and are reduced at the rimula. Reyre (1968*d*), using scanning electron microscope observations, established that at least in many cases trilete scars are functional, the outer layer of the exoexine is continuous with an invariable sculpture, the appearance of the grain is explained by variations of the intrastructure (similar to ecn 2 of Pettitt and Chaloner). In different parts of the grain it disappears, resulting in a subequatorial circular furrow, in a distal circular area and also in the proximal triangular area (when that exists); in these places, the outer part of exoexine (tegillum and possibly columellars of Pettitt and Chaloner) collapses and lines the lamellate endonexine which has the shape of a separate internal spheroidal envelope.

DEFINITION OF THE SPECIES

Numerous morphographic species have been described from various stratigraphic periods; they probably corresponded in most cases to different botanical species. However, the assignation of a dispersed *Classopollis* grain to a definite species is always difficult and often impossible.

Table 1 has been assembled from the diagnoses of five authors who have made detailed studies on *Classopollis*. It shows that, strictly, only the two extreme cases of size justify the recognition of two species on this one single character. If, however, one takes into account for each character, only the species in which it is clearly indicated, the number of possibilities for differentiation is one for all the characters except the sculpture where it is four. Table 1 underlines also the concommitant variations which affect the light visible characters. The statistical methods of symbolic dispersion diagrams (Pons 1964) can often record the different types or species an assemblage contains, but do not always permit the assignment of one or a few characters particular to each type.

For example, in the Jurassic and Lower Cretaceous rocks of the Tunisian Sahara, five *Classopollis* groups have been described: L_1, L_2, L_3, *scrabrate-verrucose* group, and *gemmulate* group (Medus and Reyre 1966). However, none can be assigned with any

TABLE 1. Comparative study of published species of the genus *Classopollis*.

Authors	*Species*	*1* *diam.* (μ)	*2* *Rimula*	*3* *trilete mark* (μ)	*4* *pore* (*diam.*) (μ)	*5* *intrastructure*	*6* *exine average*	*7* *thickness equatorial*	*8* *striations*	*9* *band width*	*10* *sculpture*
Couper	*torosus*	24–46	+	+	+	intrapunctate	0·75–1	3	4–7	5–8	scabrate
Pocock and Jansonius	*classoides*	18–24	+	3	12–15	intrapunctate	1–2	?	+	9	?
	belloyensis	30–38	?	?	12	'caniculate'	2	6	8–10	12	?
	minor	21–27	+	5–7	4	'caniculate'	1–3	?	10	6	?
	pflugii	26–33	+	+	?	'caniculate'	1·5	?	7	6	pits
Burger	*torosus*	23–29	+	+	5	intrapunctate	1–2	2·5–3	5–9	7–8	scabrate
	alexi	27–40	+	7–11	9–10	intrapunctate	1·5	1·5–2·5	8–10	10–11	perforate
	multistriatus	24–27	+	?	5	intrapunctate	1	1·5	10–14	8–9	psilate
	echinatus	24–26	+–	?	5	intrapunctate	1·5–2	?	3–5	4	echinate
	hammenii	23–29	–	5	7	intrapunctate	2–2·5	?	3–4	2·5–3	echinate
Groot	*major*	40–50	+–	?	10	?	?	?	+	5·8	granulate
	obidosensis	22–24	?	+	4–8	intrapunctate	?	?	+	4–7	?
Medus and Reyre	L_1	23–32	+	+	4–10	intrapunctate	0·5–1	?	7–11		psilate or scabrate
	L_2	26–39	+	+	4–9	intrapunctate	1–2	?	7–15		psilate
	L_3	18–23	+	+	2–5	massive or intrapunctate	1–2	?	5–11		psilate
	verrucose-scabrate	22–40	+	+	3–10	intrapunctate	1–2	?	7–12		verrucose-scabrate
Number of species recognizable by each single character		0	0	0	0 (1 above 12)	0 1 (massive)	0 1 (0·75)	0 1 (6)	0 1 (11–14)	0 1 (12)	0 4

certainty to definite species, because each has common points with several species depending on the characters under consideration. In addition, except for the gemmulate group, none has a constant individual character which allows a possibility of erecting a new species. L_3 is something like *C. classoides* of Pocock and Jansonius, but the pore diameter is smaller; it also resembles *C. torosus* sensu Burger but it is smaller, psilate, and sometimes massive. In the same way, L_1 resembles *C. multistriatus* Burger, but it is often larger, scabrate, and finer; its pseudopore is larger and the belt can have less striations. Only the *gemmulate* and *scabrate-verrucose* types are theoretically separated on sculpture; the first is easily distinguished but for the second this delicate and variable observation of sculpture cannot be made reliably with a light microscope.

Hierarchical order of use of characters. Two authors have put forward a hierarchical order. Pocock and Jansonius indicate successively the characters (as numbered in Table 1): 6, 2, 7, 8 and 9, 5 or 10 and 1. Their interpretation is not very clear on whether the ornamentation mentioned refers to the sculpture or the intrastructure although it would seem to be the latter because the authors have not mentioned the sculpture of their species. For Burger the order of characters is as follows: 10 and 5 (which can be different on the distal and proximal hemispheres of the grain), 2, 7, 8, and 6. Neither authors have indicated the reasons for their choice. However, the choice of hierarchical order is important, (*a*) to obtain a natural classification of *Classopollis* species (which will be attempted below), and (*b*) because it will be determinative in defining the different species. This fundamental study can only be undertaken on a homogeneous assemblage containing only one species. In fact it is difficult to predict, and experience shows that formations containing only one species are rare. Examples are:

1. Sample from bore-hole Lamarque 1, Aquitaine (Esso France: X = 358, 7; Y = 314, 4), depth 1742 m., Rhetian age (Dupin 1965), contains a *Classopollis* assemblage. Two extreme types are easily distinguishable by light microscope observation of the intrastructure. The first, type A (Pl. 55, figs. 1, 5) is light, almost translucent, with a massive intrastructure. The second, type C (Pl. 54, figs. 9, 11) is darker, with a pseudoreticulate intrastructure which is poorly defined in the area of the equatorial thickening. Between these extreme types, the intrastructure can be finely or poorly pseudoreticulate in the type B (Pl. 54, fig. 10 and Pl. 55, fig. 8).
2. Sample of argillaceous sandstone from bore-hole S_6P_6, Massif Central (B.R.G.M.: X = 566.500; Y = 179.075; Z = 190.90), depth 47·40 m., Hettangian (B.R.G.M. dating), contains a *Classopollis* assemblage of type C only (Pl. 55, figs. 11, 12).

Light microscope observation. Table 2 has been made up by selecting ten grains of each of the three types. It shows for these types whose general appearance and sculpture are perfectly homogeneous, the following points (each character is numbered in Table 2):

1. Size (diameter) is not fixed, but the variation is peculiar to the species $\left(\frac{\text{diameter of the smallest}}{\text{diameter of the largest}} \text{ varies from } \frac{1}{2} \text{ to } \frac{5}{6}\right)$.
2. When there is a circular furrow, it exists in all the grains.
3. Length of laesurae of trilete scar varies as much as 1:4.

TABLE 2. Character variations in the forms A, B, C (see p. 306). Measured characters: 1, size (diameter); 2, circular furrow width; 3, length of laesurae; 4, pseudopore diameter; 6, average exine thickness; 7, equatorial exine thickness; 10, type of stereoscan-visible sculpture.

Forms	1	2	3	4	6	7	10
A	30	1	8	8	—	3	echinulate
	28	—	5	8	—	2·5	micro-echinulate
	30	2·5	2·5	10	1·5	2·5	echinulate
	30	1	3	7·5	—	2·5	,,
	27	1	6	5	2	3	,,
	26	1	7·5	5	—	2·5	,,
	31	2·5	—	10	2	2·5	,,
	27	1	—	8	1·5	2·5	micro-echinulate
	25	1	2·5	4	—	2·5	echinulate
	25	1·5	5	—	1·5	2·5	micro-echinulate
B	27	—	6	7·5	2·5	2·5	grumous-verrucose
	27	1·5	—	6	2·5	1·5	echinulate
	27	1	2·5	—	2·5	—	,,
	25	1	5	7·5	—	2·5	,,
	31	1	6	5	2·5	1·5	,,
	23	1	3	—	2·5	—	,,
	26	1·5	5	—	2	1·5	grumous-verrucose
	23	1·5	5	7·5	2	2·5	echinulate
	30	1·5	8	8	2	2·5	micro-echinulate
	26	1·5	6	6	2	2·5	echinulate
C	24	1	5	6	1·5	—	echinulate
(sample 1)	28	1	—	—	1·5	2·5	,,
	32	1	—	—	1·5	2·5	grumous-verrucose
	34	+	12	10	—	—	,,
	28	+	3	—	1·5	—	echinulate
	28	1	6	5	—	2·5	,,
	26	1	—	8	1·5	2·5	,,
	18	1	4	—	1·5	—	,,
	24	1	—	8	1·5	2·5	grumous-verrucose
	21	1	—	5	—	2·5	echinulate
	28	1	7	—	1·5	—	micro-echinulate
C	30	1	6	5	1·5	2·5	grumous-verrucose
(sample 2)	28	1	—	—	1·5	—	,,
	20	1	—	—	1·5	—	,,
	32	1	8	10	1·5	2·5	,,
	32	1	10	8	1·5	2·5	,,
	28	1	—	—	—	—	,,
	30	1	7	8	1·5	2·5	,,
	24	1	—	—	—	—	,,
	28	1	5	6	1·5	2·5	,,
	26	1	5	6	1·5	2·5	,,

4. Pseudopore diameter varies as much as 2:5.

6, 7. Exinal thickness remains constant at comparable points and especially when there is an equatorial thickening.

Scanning electron microscope observations. Technical conditions for observations of exinal sculpture by the scanning electron microscope has already been set out in detail (Reyre 1968*d*). Results of the observations are as follows:

(*a*) In the case of the sample 2 (optically very homogenous intrastructure) the sculpture of the tegillum is identical in all the grains, grumous-verrucose (Pl. 55, figs. 13, 14).

(*b*) In the sample 1 three types of sculpture are observed. The optical type A can be micro-echinulate (Pl. 55, figs. 3, 7) or echinulate; the optical type B can be micro-echinulate or echinulate (Pl. 55, fig. 10) and rarely verrucose; the optical type C can be rarely micro-echinulate, generally echinulate (Pl. 54, fig. 13) or grumous-verrucose (cf. Pl. 55, fig. 14).

(*c*) Interpretation: the only light microscope visible characters (1–7 in Table 2) cannot establish how many species there are in the sample 1 or how they are distinguishable. Scan observations confirm that there is one species in the sample 2 and establish that there are at least three species in the sample 1. In sample 1 one species is common with the sample 2 (optical type C, grumous-verrucose) and two (optical types A and B, micro-echinulate or echinulate) correspond probably to two closely related botanical species, but one fossil pollen species is made because of the occurrence in the same sample. It thus appears on one hand that light microscope observation alone is generally insufficient to define the ultimate morphographical species, and on the other hand that intrastructure of one species can have a certain variability, generally limited. It also appears that each precise type of sculpture has the properties of one botanical species or a group of closely related species; that suggestion comes from the results established on actual gymnospermous pollen (Reyre 1968*d*) and on higher plants such as the closely related species of the genus *Aristida* L. (Bourreil and Reyre 1968) between which slight variations of outer sculpture can be observed and are peculiar to each species. It comes also from the observation of several homogeneous assemblages of *Classopollis* the sculpture of which is identical for all the grains (as the assemblage C, sample 2).

Inference. In the genus *Classopollis*, the outer sculpture of the grains is at the same time the most consistent and the most distinguishable character of a species; it is the ultimate specific character necessary for diagnosing the species; the consequence is that a diagnosis would not be valid, either from a morphological point of view or from a botanical point of view if it does not show the exine outer sculpture observed by electron microscope.

LIMITS OF THE GENUS

In his generic diagnosis, Couper (1958) extended the genus to all the pollen with an equatorial thickening and a vague trilete scar. The definition of Pocock and Jansonius (1961) was different and narrower, requiring the presence of striations, of a distal pore, and of a proximal triangular area either with or without a trilete aperture. The form-genus *Classopollis* can thus be conventionally limited to the simultaneous presence of the above-mentioned characters. However, this convention could result in a separation of closely related palaeobotanic entities and so we must consider that the absence of each of these characters on one of these pollens excludes it from the genus *Classopollis* when this absence results in either the absence or a notable modification of the other characters.

Striations. Considering the pollen groups A, B, and C, in which no striations are observed on the first two and a vague line arrangement on the third, it can be seen that they all have a pseudopore, a subequatorial circular furrow, an equatorial thickening, and an outer sculpture very similar to that of *Classopollis* with clearly defined and

continuous striations (compare Pl. 55, figs. 8, 10 and Pl. 57, figs. 1, 5). Further, in the succession of types B, A, and C, it is easy to distinguish a progressive passage from a massive intrastructure to pseudostriations. It would be unhelpful to limit the genus *Classopollis* by the actual presence of striations, as Pocock and Jansonius have done.

Equatorial thickening. The pollen shown on Plate 55, figs. 5–7, has no equatorial thickening. It is, however, in all other characters, similar to the grains of the group B, in which it has been included. Pocock and Jansonius (1961), Groot and Groot (1962), and Burger (1965), recorded no equatorial thickening in several of their species with striations.

On account of these two factors I consider that the formgenus *Circulina* (Maljavkina) Klaus 1960 is an exceptional case within the genus *Classopollis*, corresponding to the coincidence of the limiting cases of the two characters, equatorial thickening and ornamentation of the intrastructure.

Trilete scar. Table 2 shows clearly that a homogeneous assemblage can have a variable trilete scar (in particular length of the laesurae). Many assemblages have only a trifid or sinuous fold (Pl. 55, fig. 4) so that it is sometimes impossible, especially with a light microscope, to see a vestigial mark. But all the other characters are similar.

Pseudopore. All *Classopollis* have a more or less distinct pseudopore which is visible in polar view or with a scanning electron microscope. In certain species, however, it is less distinct, especially when the exine is thin. I have so far found only one form with striations but without a pseudopore (Pl. 54, figs. 8, 9) but neither does it have a trilete scar or a circular furrow, and this justifies its inclusion in the genus *Aporina* Naoumova 1937 (in Boltenhagen 1968). The European Jurassic species of the formgenus *Exesipollenites* Balme have a similar pseudopore, but no trilete scar and no circular furrow and they cannot be assigned to the genus *Classopollis*. Also, some species show an outer sculpture similar to that of recent Cupressales (Pl. 59, fig. 5).

THE TYPE SPECIES

I consider the generic name *Classopollis* is valid because the genera *Corollina* Maljavkina 1949 and *Circulina* Maljavkina 1949 were defined too vaguely. Like Pocock and Jansonius (1961) I consider that because of the impossibility of proving the exact similarity of *C. classoides* Pflug with another previously published species, the name of the type-species is *classoides*; but Pflug's diagnosis is inexact.

Of the grains selected for the diagnosis of the *classoides* species, it must be pointed out that the sample studied by Pflug could, in fact, include several species. Thus, even if Pflug's diagnosis is exact, it is impossible to recognize the species he wished to describe since there is no precise indication of the outer sculpture. From comparison of the relevant figures it appears that the species *C. classoides* (Pflug) Pocock and Jansonius 1961 does not correspond to the species represented by Pflug (1953). For reference these authors figure (Pocock and Jansonius 1961, pl. 1) a tetrad (figs. 1, 2) from Pflug's residue but different from the Pflug's *classoides* species by distinctive striations, circular furrow invisible and different intrastructure. They assign to the same species a distinctly intrapunctate grain without distinct striations (fig. 4) and a massive form without

any striations (figs. 6, 7). It seems, therefore, that Pocock and Jansonius have also described a plurispecific assemblage; there is also no precise indication of sculpture. In fact the *Classopollis* type-species has never been fully described. Re-description of the type species *classoides* from Pflug's original residue would be difficult; after chemical or washing operations on this residue in glycerine, how could a grain be chosen? The new species, *C. kieseri* (Pl. 54, figs. 9–14) which resembles Pflug's *classoides* is erected in this paper from new material; but, in practice, for illustrating the genus *Classopollis* it would be preferable to refer to another species showing all the characters proper to this formgenus, striations in particular.

SYSTEMATIC SECTION

Diagnoses and descriptions of the species here described include in the same order all the characters mentioned in Table 1. The high-power Scan micrographs are very important because they show the general disposition of sculptural elements (simple, mixed, double), the similarity or the plurality of shapes and sizes of elements, the shape of these, their length, breadth, and abundance (number of elements on a surface unit). All these characters are mentioned in the same order in the descriptions. The detailed explanation of the method used for describing the exinal sculpture is indicated in a previous paper (Reyre 1968*d*), but see also the text-fig. 2. Light and electron photographs are not always of the same grain; it is difficult to take an immersion photograph of a grain which must be recovered from the liquid before being observed by the scanning electron microscope. However, they always represent grains of the same optical assemblage (which is electronically observed on numerous grains). Holotypes or paratypes of the species here described are preserved at the Geological Laboratory of the National Museum of Natural History, Paris.

Genus APORINA Naumova 1937

Remarks. This genus is separate morphographically, but the corresponding palaeobotanical taxa are closely related to the taxa which produced *Classopolliss* and may be species of the same genus.

Aporina sp.

Plate 54, figs. 1, 2

EXPLANATION OF PLATE 54

Light microscope figures approximately ×1000; Stereoscan figures approximately ×2000 and 10 000.

Figs. 1, 2. *Aporina* sp. 1, L.M. tetrad view showing striations. 2, S.E.M. view on which no pseudopore is observed.

Figs. 3–5. *Classopollis simplex* sp. nov. 3, L.M. holotype, showing massive to micro-alveolate intrastructure. 4, 5, S.E.M., showing the nipples of the outer sculpture.

Figs. 6–8. *Classopollis quezeli* sp. nov. 6, L.M. tetrad holotype, showing striations. 7, 8, S.E.M. holotype showing the outer double sculpture rough with bowls.

Figs. 9–14. *Classopollis kieseri* sp. nov. 11, L.M. paratype, showing pseudovermiculate to pseudoreticulate intrastructure, trilete scar, subequatorial circular furrow, pseudopore and exinal thickness. 9, 10, L.M. paratypes, figures very similar to that of Pflug. 12–14, S.E.M. holotype, showing outer sculpture of exine, hairy with spines; S.E.M. paratype, showing the trilete scar.

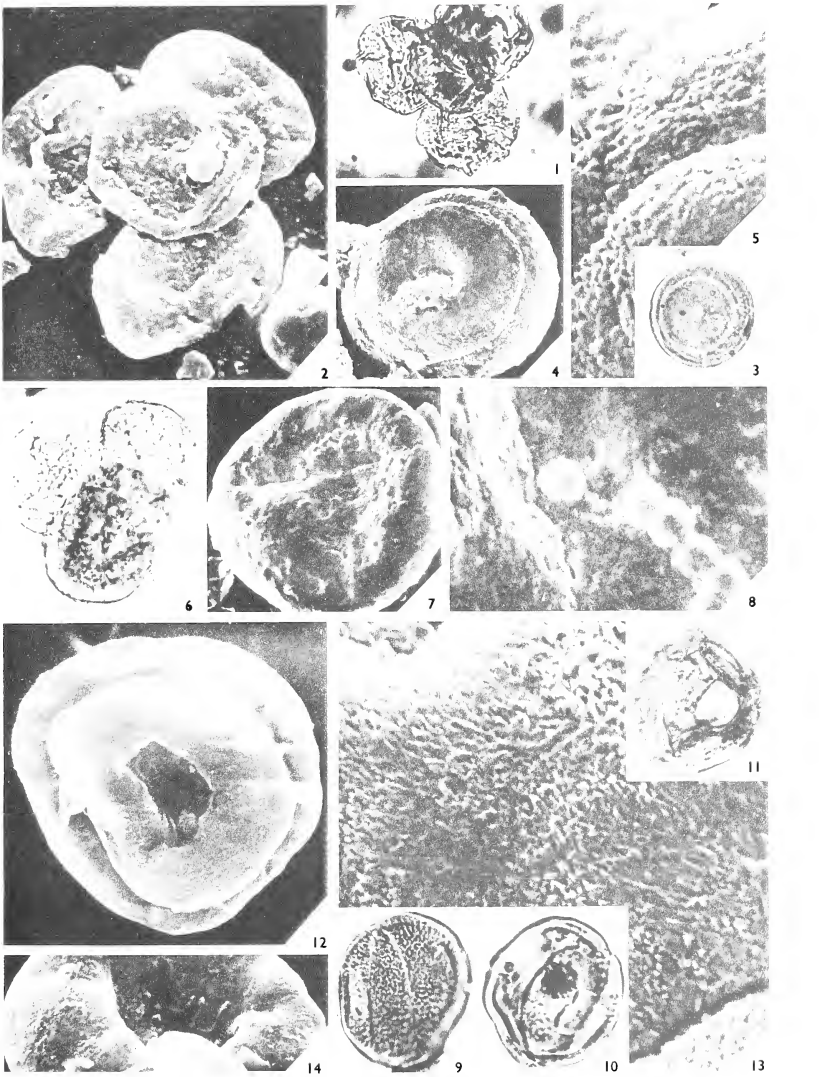

REYRE, Triassic and Jurassic *Classopollis*

Description. No subequatorial furrow; no trilete scar; no pseudopore; intrastructure massive; average exinal thickness 0·5 μ; equatorial thickening 1 μ; 4–6 striations 6 μ; band width 4–5 μ. Sculpture simple, isomorphous, nearly isodiametric, slightly rough and nearly psilate.

Size range. 17–22 μ (28 specimens).

Stratigraphic position. Upper Triassic (post-Carnian) of the Sahara; bore-hole ON_1 (X = 31° 46′ 07″, Y = 6° 25′ 36″, Z = 140 m.), depth 2660 m.

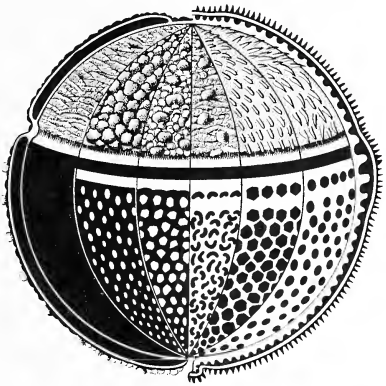

TEXT-FIG. 1. Outer sculpture (designed on the distal hemisphere above); from left to right: rugose, verrucose, mixed, double, echinulate or hairy with sticks, echinulate or hairy with needles or spines. Intrastructure (designed on the proximal hemisphere—below): from left to right: massive, alveolate, reticulate, vermiculate, pseudoreticulate, punctate.

Genus CLASSOPOLLIS Pflug 1953 emend.

Text-fig. 1

Emended diagnosis. More or less spherical prepollens with, both more or less marked, a distal circular pseudopore and a proximal trilete scar; this latter is clearly visible, but sometimes it is vestigial or a sinuous (or trifid) crease takes its place; often it is open and it appears to have had a germinal function (unlike the pseudopore). Exine is two-layered with distinct endoexine and exoexine. Endoexine is shaped into an internal spheroidal separate envelope. Exoexine composition is variable on different parts of the grain; it is composed of an inner complicated layer which constitutes the light microscope visible intrastructure and a tegillum. The tegillum is shaped into a separated outer envelope present all over the grain and covered with an outer sculpture uniformly distributed on the whole surface of the grain. Intrastructure is massive, alveolate, punctate, vermiculate or pseudovermiculate, reticulate or pseudoreticulate but can be absent, reduced, thickened, and differently organized on different parts of the grain;

it is absent or reduced at the distal pole (pseudopore) or only along the circular line surrounding it, absent along a subequatorial line (circular furrow) and sometimes at the proximal pole (triangular area), generally thickened in the equatorial zone of the grain under the circular furrow (equatorial band) where the intrastructure elements are organized into more or less continuous striations.

Remarks. Two reasons justify this emendation: (*a*) in respect of the generic diagnosis of Pocock and Jansonius the present emended diagnosis takes into account the actual knowledge on the structure of *Classopollis* grains; this is important for the understanding of the species and allows recognition and definition of the different species or records by consideration of precise characters. (*b*) the limits of the formgenus *Classopollis* are different from those indicated in the diagnosis of Pocock and Jansonius.

Classopollis simplex sp. nov.

Plate 54, figs. 3–5

Diagnosis. Subequatorial circular furrow present; trilete scar present, length of laesurae 3–6 μ; pseudopore diameter 2–4 μ ; intrastructure massive to micro-alveolate; average exinal thickness 1 μ; no equatorial thickening; no striations. Sculpture simple-mixed, isomorphous, heterodiametric, with nipples; nipple height 0·1–0·2 μ, breadth 0·2–0·3 μ, abundance 12 per μ^2. Many elements overlap a little the bases of the nipples; they are also less rounded nipples, 4 μ high.

Size range. 18–24 μ (40 specimens).

Holotype. Plate 54, figs. 3–5; size 20 μ.

Stratigraphic position. Upper Triassic (post-Carnian) of the Sahara; bore-hole ON_1 (X = 31° 46′ 07″, Y = 6° 25′ 36″, Z = 140 m.), depth 2660 m.

Classopollis quezeli sp. nov.

Plate 54, figs. 12–14

Diagnosis. Subequatorial circular furrow present; trilete scar vestigial; pseudopore diameter 4 μ; intrastructure massive (to micro-alveolate); average exinal thickness less than 1 μ (bowls not included); equatorial thickening 1 μ; 4–5 striations; band width 5 μ. Sculpture double, heteromorphous, heterodiametric, rough with bowls; processes height 0·1–0·2 μ; breadth 0·1–0·2 μ; bowls 0·9–1 μ.

EXPLANATION OF PLATE 55

Light microscope figures approximately ×1000; Stereoscan figures approximately ×2000 and 10 000.

Figs. 1–10. *Classopollis kieseri* sp. nov. 1, L.M. paratype, showing massive intrastructure and equatorial thickening. 2, 3, S.E.M. view of same grain showing small spines of outer sculpture. 4, S.E.M. view of same grain showing outer layer of exoexine lacerated at the proximal pole. 5, L.M. view of a paratype without equatorial thickening. 6, 7, S.E.M. view of same grain, sculpture micro-echinulate. 8, L.M. holotype, showing micropseudoreticulate intrastructure and sinuous circular furrow. 9, 10, S.E.M. holotype, showing sculpture echinulate, hairy with needles.

Figs. 11–14. *Classopollis chateaunovi* sp. nov. 11, L.M. paratype, showing vague pseudostriations. 12, L.M. holotype, showing pseudoreticulate intrastructure and pore. 13, 14, S.E.M. holotype, showing grumous-verrucose sculpture.


4

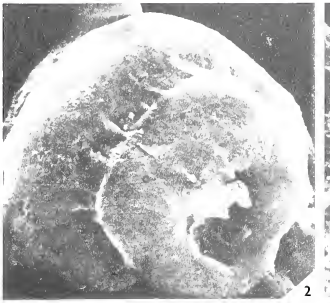
2

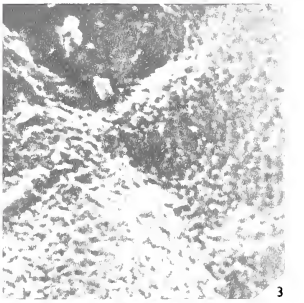
3

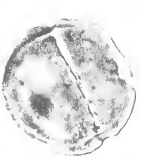
1

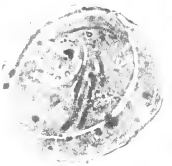
5

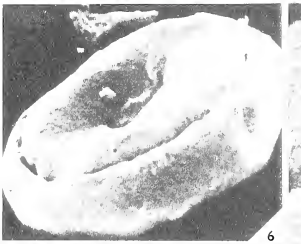
6


7


9

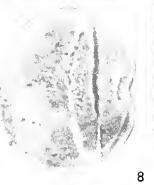
8

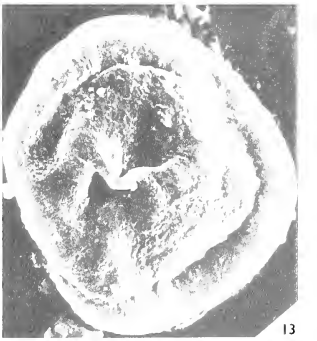
13

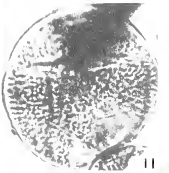
11

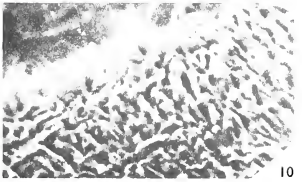
10


12

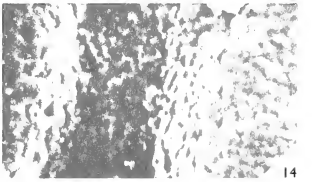
14

REYRE, Jurassic *Classopollis*

Size range. 18–24 μ (36 specimens).

Holotype. Plate 54, figs. 12–14; size 23 μ.

Stratigraphic position. Upper Triassic (post-Carnian) of the Sahara; bore-hole ON_1 (X = 31° 46′ 07″, Y = 6° 25′ 36″, Z = 140 m.), depth 2660 m.

Remarks. Processes are rounded so that the surface seems nearly mammilated.

Classopollis kieseri sp. nov.

Plate 54, figs. 9–13; Plate 55, figs. 1–10

Diagnosis. Subequatorial circular furrow present, narrow (1 μ) or wide (to 3 μ) by distortion and often sinuous; functional trilete scar present, length of laesurae 2·5–10 μ; pseudopore diameter 4–10 μ; intrastructure massive, pseudoreticulate or finely so; average thickness 1·5 μ; equatorial thickening 1·5–2·5 μ; no striations, to vaguely defined pseudostriations; band width 8–10 μ. Sculpture simple, isomorphous, isodiametric, micro-echinulate to echinulate (hairy with little needles); varying from grain to grain, needle height 0·1–0·5 μ, breadth 0·1–0·2 μ, abundance 9 per μ^2 (large needles) to 80 per μ^2 (small needles).

Size range. 21–(28)–34 μ (100 specimens).

Holotype. Plate 55, figs. 8–10; size 31 μ.

Stratigraphic position. Hettangian, bore-hole Lamarque I, Aquitaine, (X = 358, 7; Y = 314, 4), depth 1742 m.

Remarks. By scan observation of the sculpture it seems that there are three closely related species, in which the spines or needles are constant on any one grain but may be very small (micro-echinulate, Pl. 55, fig. 7), medium (Pl. 55, fig. 3) or larger (echinulate, Pl. 55, fig. 10); but these characters do not each correspond to one precise intrastructure type. For this reason and because of their simultaneous occurrence in the same sample one *Classopollis* species is made.

C. kieseri resembles *C. classoides* Pflug 1953 in many characters visible on the illustrations of this species. In Pflug 1953, plate 16, figs. 29, 30 show a pollen finely pseudoreticulate, with a sinuous circular furrow, a pseudopore, a trilete scar not visible but suspected, an exine thickness of 2 μ without striations.

Classopollis chateauneuvi sp. nov.

Plate 55, figs. 11–14

Diagnosis. Subequatorial circular furrow present; trilete scar present, length of laesurae 5–12 μ; pseudopore diameter 5–10 μ; intrastructure pseudoreticulate; average exinal thickness 1·5 μ; equatorial thickening 2·5 μ; only vague pseudostriations; band width 8 μ. Sculpture simple, isomorphous, isodiametric, grumous-verrucose; breadth of grumes 0·2–0·3 μ.

Size range. 20–32 μ (100 specimens).

Holotype. Plate 55, figs. 12–14; size 31 μ.

Stratigraphic position. Hettangian, Massif Central, bore-hole B.R.G.M. S_6P_6 (X = 566.500, Y = 179.075, Z = 190, 91), depth 47·40 m.

Classopollis bussoni sp. nov.

Plate 56, figs, 1–4

Diagnosis. Subequatorial circular furrow present; trilete scar present, length of laesurae 3–10 μ; pseudopore diameter 4–10 μ; intrastructure finely punctate; average exinal thickness 0·5–1 μ; equatorial thickening 1 μ; 7–11 striations; band width 7 μ. Sculpture simple, isomorphous, isodiametric, rugose-verrucose; height of warts 0·2 μ, breadth 0·5–0·8 μ.

Size range. 23–32 μ (100 specimens).

Holotype. Plate 3, figs. 1–3; size 28 μ.

Stratigraphic range. Middle and Late Jurassic and Lower Cretaceous of the Sahara. Holotypes from bore-hole SB 1 (Tunisia, X = 8 g. 21′ 87″ E, Y = 34 g. 91′ 16″ μ, Z = 282 m.), depth 1210 m., Callovian.

Remarks. This species is included in the type L_1 (Medus and Reyre 1966), see Table 1.

Classopollis rarus sp. nov.

Plate 56, figs. 5–7

Diagnosis. Subequatorial circular furrow present, with a prominent swelling; trilete scar vestigial; pseudopore intrastructure reduced at the distal pole, but no well-shaped hollow is observed with electron microscope; intrastructure punctate to pseudoreticulate; average exinal thickness 1 μ; equatorial thickening 2 μ; 7–9 striations; band width 7 μ. Sculpture simple-pargeted, isomorphous, lightly heterodiametric, hairy with short sticks processes with well-rounded tips; height of processes 0·3–1 μ, breadth 0·2–0·5 μ, abundance 15 per μ^2. The pargeted appearance is explained by crowding of processes with the higher projecting above the shorter.

Size range. 23–34 μ (32 specimens).

Holotype. Plate 55, figs. 5–7; size 32 μ.

Stratigraphic position. Lower Portland of Charente, France; bore-hole Vignolles S2 (X = 390.6, Y = 29.3, Z = 15·50 m.), depth 14·80 m.

Classopollis aquitanus sp. nov.

Plate 57, figs. 1–5

Diagnosis. Subequatorial circular furrow present but difficult to distinguish; trilete scar present; pseudopore diameter 5–9 μ; intrastructure clearly reticulate (lumina 1–1·5 μ); average exinal thickness 1 μ; equatorial thickening 1·5–2 μ; 9–10 striations; band width 10 μ. Sculpture simple, isomorphous, heterodiametric, echinulate (hairy with

EXPLANATION OF PLATE 56

Light microscope figures approximately ×1000; Stereoscan figures approximately ×2000 and 10 000.

Figs. 1–4. *Classopollis bussoni* sp. nov. 1, L.M. holotype, view of finely punctate intrastructure and striations. 2, 3, S.E.M. holotype, showing rugose-verrucose outer sculpture with warts. 4, S.E.M. paratype.

Figs. 5–7. *Classopollis rarus* sp. nov. 5, L.M. holotype, showing punctate to pseudoreticulate intrastructure and striations. 6, 7, S.E.M. holotype, showing rounded short sticks of the outer sculpture.

Figs. 8–10. *Classopollis caratinii* sp. nov. 8, L.M. holotype, showing loosely punctate intrastructure, pseudopore, and trilete scar. 9, 10, S.E.M. views showing strongly rough sculpture.

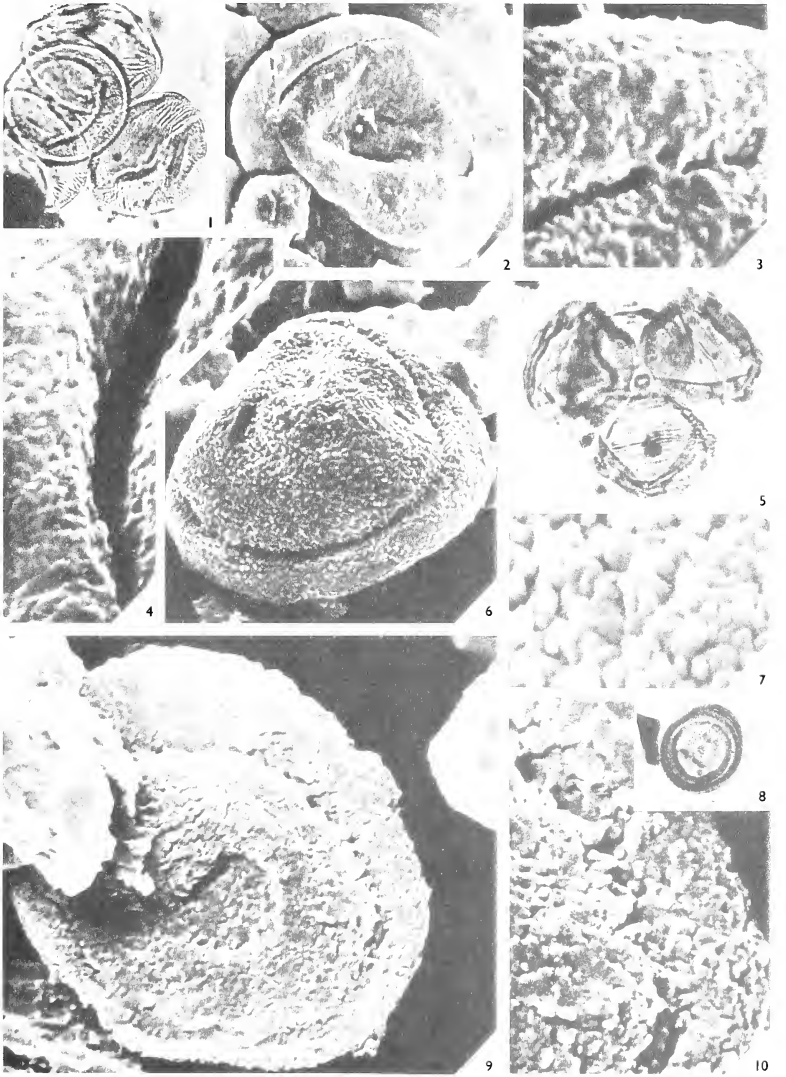
1
2
3
4
5
6
7
8
9
10

spines); height of spines 0·3–0·9 μ, breadth of base 0·1–0·4 μ, abundance 9 per μ^2. Some very short spines among the others.

Size range. 28–36 μ (100 specimens).

Holotype. Plate 57, figs. 1, 4, 5; size 31 μ.

Stratigraphic position. Lower Portland of Charente, France; bore-hole Vignolles S_2 (X = 390.6, Y = 89.3, Z = 15·50 m.), depth 28·80 m.

Classopollis caratinii sp. nov.

Plate 56, figs. 8–10

Diagnosis. Subequatorial circular furrow distinct; trilete scar present, length of laesurae 2·5 μ; pseudopore diameter 4 μ; intrastructure loosely punctate; average exinal thickness 1 μ; equatorial thickening 1·5 μ; 3–4 weak pseudostriations. Sculpture simple, heteromorphous, heterodiametric, strongly rough; height of processes 0·1–0·7 μ, breadth 0·1–1 μ; the shapes of the heteromorphous processes appear to be wrinkles, nipples, warts, blisters, or spines, although no shape is clear.

Size range. 16–20 μ (28 specimens).

Holotype. Plate 57, figs. 8–10; size: 18 μ.

Stratigraphic position. Lower Portland of Charente, France; bore-hole Vignolles S_4 (X = 390.6, Y = 89.3), depth 21·65 m.

Classopollis martinottii sp. nov.

Plate 57, figs. 6–11

Diagnosis. Subequatorial circular furrow present but often difficult to distinguish; trilete scar present, or trace; the outline of the pseudopore is not clearly marked and the intrastructure is only reduced at the distal pole which is often folded in Stereoscan observation; intrastructure finely punctate; average exinal thickness 1 μ; equatorial thickening 1·5 μ; 4–7 striations more or less discontinuous (lining of intra points); band width 5 μ. Sculpture simple, isomorphous, isodiametric echinulate (hairy with spines of which the ends are not sharp but rounded); height of spines 0·4–0·5 μ, breadth of base 0·2–0·3 μ, abundance 14–16 per μ^2.

Size range. 28–33 μ (70 specimens).

Holotypes. Plate 57, figs. 9–11; size 30 μ.

Stratigraphic position. Berriasian-Valanginian of Israel; bore-hole Heletz 2 (E = 115.963, N = 110.807, K.B.+92 m.); depth 1465–71 m.

Remarks. This pollen is not easy to observe optically because of the crowded sculptural elements.

Classopollis pujoli sp. nov.

Plate 58, figs. 1–4

Diagnosis. Subequatorial circular furrow present and large; trilete scar present, or trace; pseudopore diameter 3–4 μ; intrastructure pseudoreticulate; average exinal thickness 1·5 μ; equatorial thickening 2 μ; 5–6 striations; often anastomosing; band

width 6–7 μ. Sculpture simple, isomorphous, isodiametric echinulate (hairy with needles); height of needles 0·6 μ, breadth 0·15 μ, abundance 24 per μ^2.

Size range. 20–6 μ (80 specimens).

Holotype. Plate 58, figs. 1–3; size 22 μ.

Stratigraphic position. Lower Portland of Charente, France; bore-hole Vignolles S_1 (X = 390.6; Y = 89.3); depth 6·80 m.

Remarks. *C. pujoli* differs from *C. hammenii* Burger in the three following characters: circular furrow is more distinct, equatorial thickening more distinct, the tracery of the intrapseudoreticulum is less distinct.

Classopollis mirabilis sp. nov.

Plate 58, figs. 5–11

Diagnosis. Subequatorial circular furrow distinctly present; trilete scar present, or trace; pseudopore diameter 4–12 μ; intrastructure punctate to pseudoreticulate; average exinal thickness 2 μ; equatorial thickening 2·5 μ; 5–6 striations; band width 5–6 μ. Sculpture simple, isomorphous, more or less isodiametric, echinulate (hairy with spines); height of spines 1–1·5 μ, breadth of bases 0·3–0·4 μ, abundance 6 per μ^2.

Size range. 24–36 μ (100 specimens).

Holotype. Plate 58, figs. 8, 10–11; size 35 μ.

Stratigraphic position. Lower Portland of Charente, France; bore-hole Vignolles S_1 (X = 390.6, Y = 89.3); depth 6·80 m.

Remarks. By light microscope observation *C. mirabilis* resembles *C. echinatus* Burger 1966; because of the absence of a clear illustration of the sculpture, it was preferable

---

EXPLANATION OF PLATE 57

Light microscope figures approximately × 1000; Stereoscan figures approximately × 2000 and 10 000.

Figs. 1–5. *Classopollis aquitanus* sp. nov. 1, L.M. holotype, showing reticulate intrastructure, striations, narrow subequatorial circular furrow. 2, S.E.M. tetrad, × 1000. 3, Detail of distal polar area of central grain of tetrad showing vertical appearance of spines. 4, 5, S.E.M. holotype, showing echinulate sculpture, hairy with spines.

Figs. 6–11. *Classopollis martinottii* sp. nov. 6, L.M. paratype, showing finely punctate intrastructure, subequatorial circular furrow, equatorial thickening. 7, 8, S.E.M. views of same tetrad showing end-rounded spines of the echinulate sculpture. 9, L.M. holotype. 10, 11, S.E.M. views of the holotype. (There is a prominent scratch on the negative of fig. 7.)

EXPLANATION OF PLATE 58

Light microscope figures approximately × 1000; Stereoscan figures approximately × 2000 and 10000.

Figs. 1–4. *Classopollis pujoli* sp. nov. 1, L.M. holotype, showing intrastructure, striations, pseudopore, triangular proximal area, and exinal thickness. 2–4, S.E.M. holotype, showing echinulate sculpture, hairy with needles.

Figs. 5–11. *Classopollis mirabilis* sp. nov. 5, L.M. paratype, showing punctate to pseudoreticulate intrastructure. 9, L.M. paratype, showing striations, equatorial thickening, and subequatorial circular furrow, × 2000. 8, L.M. holotype, showing pseudopore. 10, 11, S.E.M. views of same grain showing radially combed strong spines of echinate sculpture.


1


2

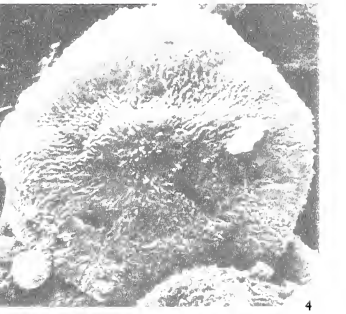
4

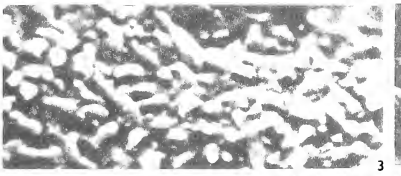
3

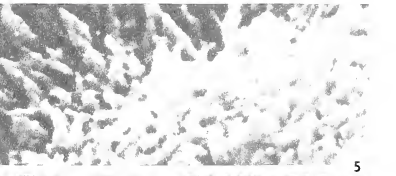
5

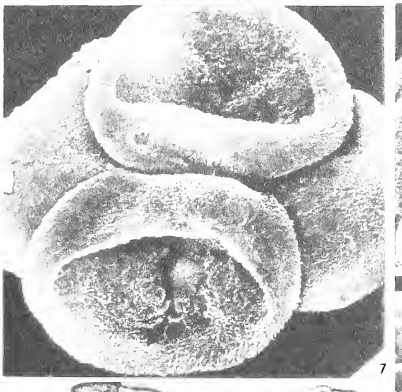
7


10

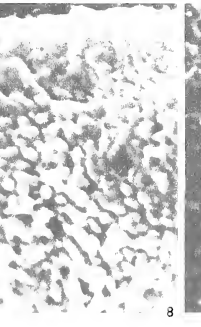
8

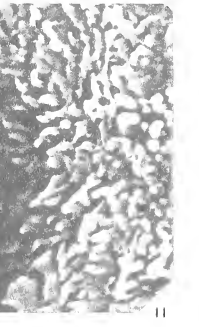
11

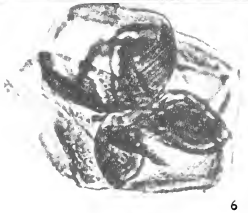
6


9

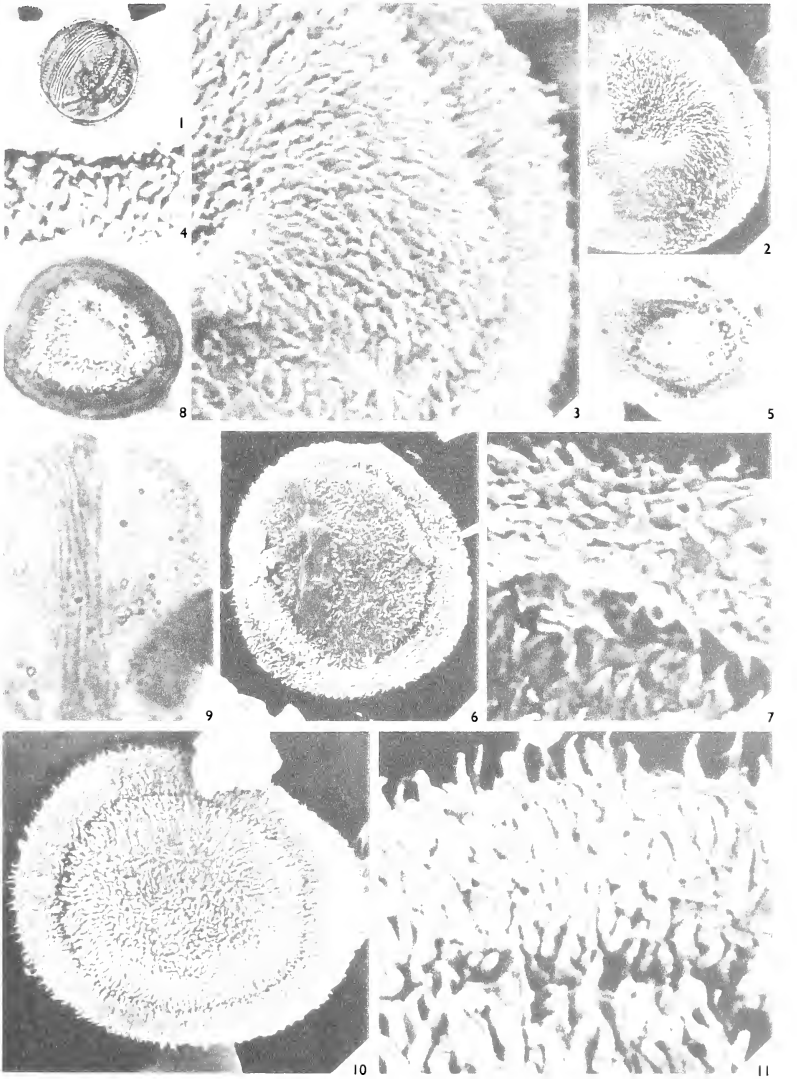

REYRE, Jurassic *Classopollis*

to make a new species. Only scan observation of the *C. echinatus* holotype can indicate whether these species are synonyms or not.

Classopollis noeli sp. nov.

Plate 59, figs. 1–3

Diagnosis. Subequatorial circular furrow present; trilete scar present, length of laesurae 5–12 μ; pseudopore diameter 3–10 μ; intrastructure punctate; average exinal thickness 1 μ; equatorial thickening 2 μ; 7–12 striations, band width 7 μ. Sculpture simple isomorphous, isodiametric, verrucose-pargeted; height of warts 0·2–0·4 μ, abundance 12–15 per μ^2.

Size range. 22–40 μ (100 specimens).

Holotype. Plate 59, figs. 1–3; size 30 μ.

Stratigraphic position. Upper Jurassic to Aptian of the Sahara. Holotype from bore-hole Tamerna 1, Algeria, (X = 4 g. 04′ 03″ E., Y = 37 g. 13′ 72″ N.), depth 1479 m. (Aptian).

Remarks. This species is one of the components of the optical type population 'scabrate-verrucose' (Medus and Reyre 1966).

BOTANICAL AFFINITY AND TAXONOMIC VALUE

Barnard (1968), studying male cones containing *Classopollis*, established that the genus does not belong to the Araucariales; he underlined the similarity between *Cheirolepis muensteri* Schenk cones described by Hörhammer (1933), *Masculostrobus* Seward and those of *Taxus*; however, he put forward no formal conclusion. Perhaps the sculpture of the pollen exine is more significant. Three arrangements of sculptural elements can be recognized: simple (the most common), mixed or double. From observation of the sculpture of Recent gymnosperm pollen (Reyre 1968*d*) it appears that a very important fossil plant taxon is concerned, having at least the rank of an order. Indeed, Cupressales generally have a double sculpture, Taxodiales a mixed sculpture, and Taxales a simple sculpture. Among *Classopollis* simple sculpture is by far the most frequent. However, the elements of the sculpture are, in the main, quite different; the species of recent Taxales show nipples or marked warts, regular and perfectly shaped; on the contrary *Classopollis* show grana, warts, blisters, coarse spines or large distinct needles. In addition, the wide variety of sculpture suggests that there may have been a great number of species; so, if we consider Mesozoic pollen assignable to Taxales for their structural character, we observe a very limited variety of sculpture, as for living Taxales. All these differences seem to show that the plaeobotanical taxon, which produced *Classopollis*, if it had a morphological relationship with *Taxus* (established by observation of the cones), was taxonomically distinct.

In spite of the highly evolved character of the exine, the presence of a proximal trilete scar (sometimes vestigial) is a primitive character. Other Conifers such as Araucariales, Taxodiales, and Taxales no longer show any trace of this ancestral character. Therefore plants which produced *Classopollis* may not be assigned to any Recent order of Coniferales; they corresponded probably to a special and very large fossil taxon having at least the rank of an order. In any case, it is established that *Classopollis* grains were produced by several botanical genera of Coniferales (Barnard 1968).

CLASSIFICATION

Is it possible to establish from pollen a classification likely to indicate the presumed phylums of the palaeobotanical taxon which produced *Classopollis*? Table 3 represents the geographical and stratigraphical distribution of the species described. For each a symbol indicates the nature of the intrastructure, the absence or presence of pseudostriations or distinct continuous striations, the elementary type of sculpture and nature of the elements of this sculpture. If one considers this last character, it can be seen that the rugose-verrucose sculpture (under this name are grouped the psilate, grumous, rugose, and verrucose sculptures) existed in the Sahara from the Late Triassic, and continued to be the most frequent during the Jurassic and Early Cretaceous time. On the contrary, in Aquitaine (France), the echinate sculpture (hairy with points, spines, and needles) is widely represented since the Rhaetian, and undergoes an extreme development during the Early Cretaceous. It should be noted that after the species *C. kieseri* found in Rhaetian and Early Liassic of Aquitaine with echinate sculpture, there follow the Late Jurassic species *C. aquitanus*, *C. pujoli*, *C. mirabilis* which also have an echinate sculpture. In the same way, in the Sahara, the double sculpture of *C. quezeli* of the Late Triassic formations is also to be found in the Early and Middle Jurassic (*gemmulate* type, Medus and Reyre 1966).

In Table 3 the botanical environment indicated results of a personal interpretation of the Stereoscan appearance of pollens (see explanation of Pl. 59). It is remarkable that in the Sahara, where disaccate pollen is almost impossible to find after the Carnian, the succeeding species of *Classopollis* have a rugose-verrucose sculpture, and are principally associated with pollen of Taxales, Araucariales, or Ephedrales. On the other hand, in Aquitaine, numerous echinate species are associated, in the Rhaetian as in the Early Cretaceous times, with pollens that may be compared with that of recent Pinales of Cupressales. It would seem that different groups, linked with different ecological conditions, have each evolved separately.

These different successions of species, during the Mesozoic era, geographically localized with similar sculptures, suggest that sculpture is not an accidental specific character but phyletic.

As for the intrastructure, it may be seen that in each group defined by the sculpture (for example echinate) the massive species are principally founded in the Upper Triassic or the Infraliassic. In the same way the absence of striations or the presence of ill-defined striations (pseudostriations) is the most common at these times, while during the Jurassic and Early Cretaceous one often observes very distinct striations, contrasting with

---

EXPLANATION OF PLATE 59

Light microscope figures approximately $\times 1000$; Stereoscan figures approximately $\times 2000$ and 10 000.

Figs. 1–3. *Classopollis noeli* sp. nov. 1, L.M. holotype, showing punctate intrastructure, striations, and exinal thickness. 2, 3, S.E.M. holotype, showing general shape ($\times 5000$) and verrucose-pargeted sculpture ($\times 12\,500$).

Fig. 4. Mesozoic pollen with a simple sculpture assigned to a fossil species of Taxales (Reyre 1968*d*), $\times 5000$.

Fig. 5. Pollen of a fossil (presumed Cupressales) showing outer sculpture with glomerules (Reyre 1968*d*).

Figs. 6, 7. Pollen assigned to a fossil Mesozoic species of *Araucaria* (Reyre 1968*d*). 6, S.E.M. general shape. 7, S.E.M. view showing sculpture.

1

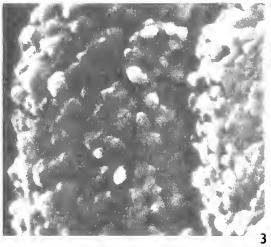

3

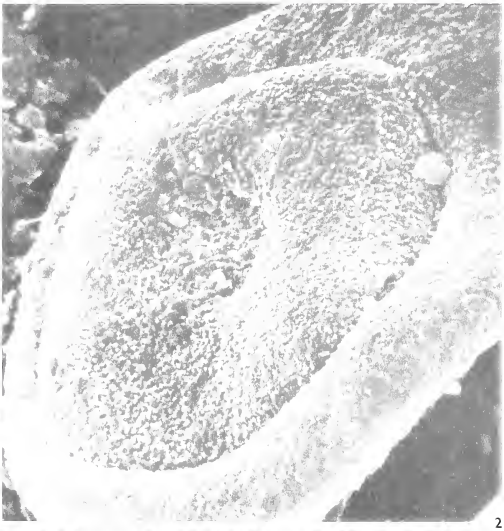

2

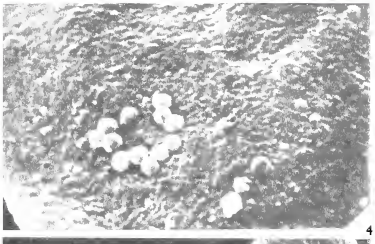

4

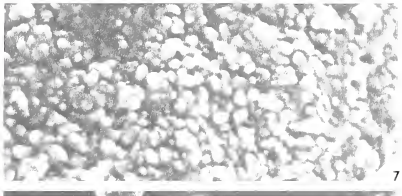

7

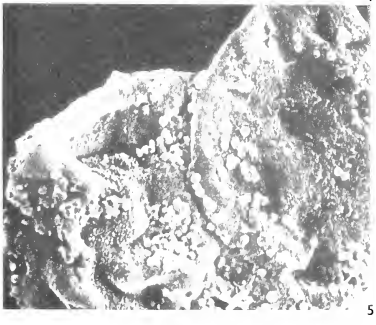

5

6

REYRE, *Classopollis* and other pollen

TABLE 3. Stratigraphic and geographic localization of *Classopollis* species and botanical environment.

	Sahara			Israel			France		
	Species	*Characters*	*Environment*	*Species*	*Characters*	*Environment*	*Species*	*Characters*	*Environment*
Aptian	*noeli*		Gnetales, Ephedrales, Araucariales			Araucariales Taxodiales (Pinales ?) + others			
Barremian	*noeli*	p, s, srv		*martinottii*	mp, Sp, se				
Valanginian	*noeli*	p, s, srv	Araucariales, Bennettittales	*martinottii*	mp, Sp, se				
Berriasian	*bussoni*	p, S, srv							
Lower Portland							*mirabilis*	pr, Sp, se	Pinales, (*Pinus*-, *Abietinae*-, *Tsugae*--*pollenites*) Cupressales
							pujoli	pr, S, se	
							aquitanus	r, S, se	
							caratinii	p, Sp, srv	
							rarus	p(pr), S, se	
Middle to Upper Jurassic	*bussoni*	p, S, srv	Bennettittales Araucariales Taxales (+ others)						
	gemmulate*	p, S, sd							
Upper Liassic	L_3*	mp, S, srv	Araucariales						
Hettangian							*chateaunovi*	pr, Sp, srv	
Upper Triassic (post-Carnian)	*quezeli* *simplex* *Aporina*		no definite				*kieseri*	m (pr), So, se	Pinales
Carnian			Podocarpales						

Explanation. Intrastructure: m, massive; v, vermiculate; mp, micropunctate; p, punctate; pr, pseudoreticulate; r, reticulate. Striations: So, no striations; Sp, pseudostriations; S, striations distinctive. Sculpture: srv, rugose-verrucose; se, echinulate; sm, mixed; sd, double.

TABLE 3. Stratigraphic and geographic localization of *Classopollis* species and botanical environment.

	Sahara			Israel			France		
	Species	*Characters*	*Environment*	*Species*	*Characters*	*Environment*	*Species*	*Characters*	*Environment*
Aptian	*noeli*		Gnetales, Ephedrales, Araucariales			Araucariales Taxodiales (Pinales ?) + others			
Barremian	*naeli*	p, s, srv		*martinottii*	mp, Sp, se				
Valanginian	*noeli*	p, s, srv	Araucariales, Bennettittales	*martinottii*	mp, Sp, se				
Berriasian	*bussani*	p, S, srv							
Lower Portland							*mirabilis*	pr, Sp, se	Pinales, (*Pinus*-, *Abietinae*-, *Tsugae*-*pollenites*) Cupressales
							pujali	pr, S, se	
							aquitanus	r, S, se	
							caratinii	p, Sp, srv	
							rarus	p(pr), S, se	
Middle to Upper Jurassic	*bussoni*	p, S, srv	Bennettittales Araucariales						
	gemmulate*	p, S, sd	Taxales (+ others)						
Upper Liassic	L_3*	mp, S, srv	Araucariales						
Hettangian							*chateauneufi*	pr, Sp, srv	
Upper Triassic (post-Carnian)	*quezeli* *simplex* *Aporina*		no definite				*kieseri*	m (pr), So, se	Pinales
Carnian			Podocarpales						

Explanation. Intrastructure: m, massive; v, vermiculate; mp, micropunctate; p, punctate; pr, pseudoreticulate; r, reticulate. Striations: So, no striations; Sp, pseudostriations; S, striations distinctive. Sculpture: srv, rugose-verrucose; se, echinulate; sm, mixed; sd, double.

the general intrastructure, and without a progressive organization of this intrastructure. It would be necessary to observe all the known *Classopollis* species to affirm the results concerning the distinction of the groups and the internal evolution of them. The remarks above do permit, however, of our advancing the following inferences:

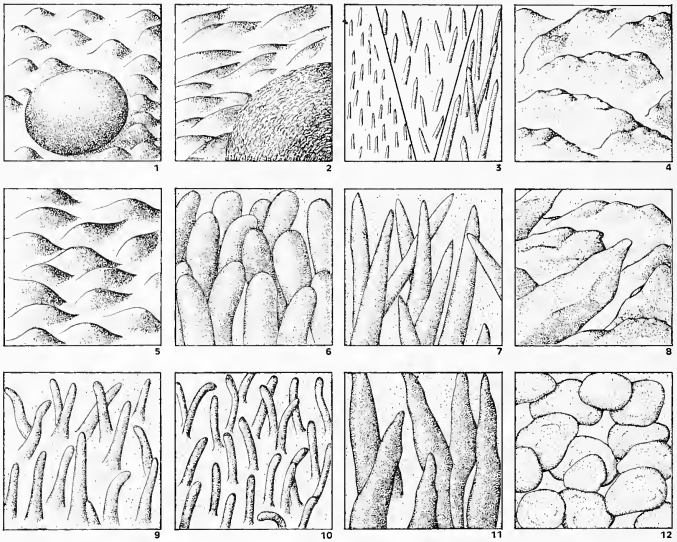

TEXT-FIG. 2. Shape and dimensions of the sculptural elements of the *Classopollis* species described, approximately ×30 000. 1, *simplex*; 2, *quezeli*; 3, *kieseri*; 4, *chateaunovi*; 5, *bussoni*; 6, *rarus*; 7, *aquitanus*; 8, *caratinii*; 9, *martinottii*; 10, *pujoli*; 11, *mirabilis*; 12, *noeli*.

1. *Classopollis* species should be classed according to the exine sculpture. This system seems to be expressive of the botanical entities in the plant group which produced *Classopollis*. From our present knowledge, four groups might be suggested with rugose-verrucose, echinulate, mixed or double structure.

2. The palynological evolution inside each group might be different, but it seems that the massive intrastructure has preceded differentiated intrastructure (alveolate, punctate, reticulate, etc.). This is organized into more and more clear and distinct striations. Thus a species with distinct striations may be considered highly evolved.

Although certain exceptional cases may not confirm this hypothesis, on the whole it seems valid. It explains why species with similar intrastructures can have, in fact, different sculptures; inversely that species with similar sculptures can have dissimilar intrastructures.

Barnard (1968, table 1) described pollen grains assignable to the formgenus *Classopollis* extracted from fossil cones of different palaeobotanical genera; to each genus corresponds a different intrastructure and the scanning observation of these grains should therefore be all the more interesting. But, to discern generic and specific characters, it would be necessary to observe also pollen grains extracted from cones of other species of the same genera.

Conclusion. *Classopollis* grains are the fossilized vestiges of a very important plant group which had, during the Mesozoic, variable radiations and discontinuous evolution according to the geographical province. No species seems to have had a world-wide distribution, but in some countries the abundance and diversity of these pollens in certain periods make them suitable for stratigraphic correlation.

Acknowledgements. I thank Mr. G. Kieser (Compagnie Française des Pétroles), Mr. Chateauneuf (Bureau de Recherches géologiques et minières), Mr. Martinotti ('Lapidoth' Israel Oil Prospectors Corporation), and Mr. Pujol (University of Bordeaux) who have been kind enough to provide me with samples rich in *Classopollis* grains and who have enabled me to mention and describe them. Also I thank Professor R. Laffitte and Miss D. Noël who allowed me to use the electron scanning microscope (Cambridge manufacture, Stereoscan type) at the Geological Laboratory of the National Museum of Natural History of Paris.

REFERENCES

BARNARD, P. D. W. 1968. A new species of *Masculostrobus* Seward producing *Classopollis* from the Jurassic of Iran. *J. Linn. Soc.* (*Bot.*), **61**, 384, 167–76, 1 pl.

BOLTENHAGEN, E. 1968. Revision du genre *Classopollis* Pflug. *Rev. Micropal.* **11**, 29–44, 2 pl.

BOURREIL, P., and REYRE, Y. 1968. Première étude de grains de pollen d'Aristides (Graminées) au microscope électronique à balayage. *C.R. Acad. Sc. Paris*, **267**, 398–401, 2 pl.

BURGER, D. 1965. Some new species of *Classopollis* from the Jurassic of the Netherlands. *Leidse. Geol. Medel.* **33**, 63–9, 3 pl.

—— 1966. Palynology of Uppermost Jurassic and Lowermost Cretaceous strata in the eastern Netherlands. *Leiden*, Groen and Zoon, 276 pp., 39 pl.

COUPER, R. A. 1958. British mesozoic Microspores and Pollen Grains. *Paleontographica*, **103**, B, 75–179, 31 pl.

DUPIN, F. 1965. Contribution à l'étude paléoplanctologique du Jurassique en Aquitaine occidentale. *Act. Soc. Linn. Bordeaux*, **102**, 3B, 1–19.

GROOT, J., and GROOT, CATHERINA. 1962. Plant microfossils from Aptian and Cenomanian deposits of Portugal. *Com. Serv. Geol. Portugal*, **46**, 133–71, 10 pl.

KLAUS, W. 1960. Sporen der karnischen Stufe der ostalpinen Trias. *Jahrb. geol. Bundesanst., Wien*, sond, **5**, 107–83.

MEDUS, J., and REYRE, R. 1966. Contribution à l'étude des grains de pollen appartenant au genre de forme *Classopollis* (Pflug) Pocock et Jansonius. *C.R. Acad. Sci. Paris.* **262**, 2703–6.

PETTITT, J., and CHALONER, W. G. 1964. The ultrastructure of the Mesozoic-Pollen *Classopollis*. *Pollen et Spores*, **6**, 2, 611–20, 1. pl.

PFLUG, H. D. 1953. Zur Entstehung und Entwicklung des angiospermiden Pollens in der Erdgeschichte. *Palaeontographica*, **95B**, 60–171, 10 pl.

POCOCK, S., and JANSONIUS, J. 1961. The pollen genus *Classopollis* Pflug 1953. *Micropaleontology*, **7**, 439–49, 1 pl.

PONS, A. 1964. Contribution palynologique à l'étude de la flore et de la végétation pliocènes de la région rhodanienne. Montpellier, Fac. Sci., 713 p., 3 pl.

REYRE, Y. 1968*a*. Précisions sur la structure et la morphologie des prépollens du genre de forme *Classopollis* (Pflug) Pocock et Jansonius. Conséquences paléobotanique et stratigraphique. *C.R. Sci. Paris*, **266**, 1233–5.

REYRE, Y. 1968*b*. Valeur taxinomique de la sculpture de l'exine des pollens de gymnospermes et de chlamydospermes. *C.R. Sci. Paris*, **267,** 160–1.

—— 1968*c*. Valeur taxinomique de la sculpture de l'exine des pollens fossiles attribués aux gymnospermes ou au chlamydospermes. Ibid., **267,** 488–90.

—— 1968*d*. La sculpture de l'exine des pollens des gymnospermes et des chlamydospermes et son utilisation dans l'identification des pollens fossiles. *Pollen et Spores*, **10,** 197–220, 7 pl.

Y. REYRE
Geological Laboratory
National Museum of Natural History
Paris, France

Typescript received 24 July 1969

PSEUDOCYMOPOLIA, A MESOZOIC TETHYAN ALGA (FAMILY DASYCLADACEAE)

by GRAHAM F. ELLIOTT

ABSTRACT. *Pseudocymopolia* gen. nov. is proposed for certain dasycladaceae ranging from Portlandian to Maestrichtian in age, and from Spain to Borneo geographically. *P. orientalis* sp. nov. is described, and the relationship of the genus to *Cymopolia* discussed.

IN 1959 I described a very distinctive dasyclad alga from the Maestrichtian of Iraqi Kurdistan as *Cymopolia anadyomenea* (Elliott 1959). This alga showed the essential branch-structure seen in *Cymopolia*, but the calcareous segments or units were remarkable externally in swelling periodically into conspicuous annular projections or flanges: at these levels the internal branch-structure was coarser than at the inter-flange levels. These distinctive segments set *C. anadyomenea* apart from all other species of the genus, which ranges from Upper Cretaceous to Recent, but it seemed reasonable to regard the species as an early development before the very conservative morphology of the Tertiary and Recent species was achieved.

During later reporting on the algal microflora of the Bau Limestone of Borneo, random sections of an alga like *C. anadymomenea* were considered to indicate Upper Cretaceous age for the appropriate samples. This was disputed by the field-geologists, for the Bau Limestone is of Upper Jurassic and Lower Cretaceous age, and there was no evidence that the disputed samples were anomalous in position. At this point Praturlon (1964) figured a rare alga from the undoubted Lower Cretaceous of Italy as *C.* aff. *anadyomenea*, and Dr. Radoičić of Belgrade sent me a thin-section of Yugoslav Lower Cretaceous containing fragments of a similar alga. There is a similar record from the Lower Cretaceous of Spain (Champetier, 1967 p. 148). In re-describing *C. anadyomenea* along with other Middle East Dasycladaceae (Elliott 1968), I referred to the Italian Borneo and Yugoslav fossils as examples of 'an apparent homoeomorph' of *C. anadyomenea*.

Recently Dragastan described *Cymopolia jurassica* from the Portlandian of Rumania (Dragastan 1968). This is yet another flanged species, based on good material and carefully distinguished in detail by its author from *C. anadyomenea* Elliott and '*C.* aff. *anadyomenea* Elliott' of Praturlon, the two species available to him in the literature.

It is clear that these flanged forms range from Upper Jurassic to Upper Cretaceous and have a wide Tethyan distribution: Spain, Italy, Yugoslavia, and Rumania in Europe, and Iraq, Afghanistan (Kaever 1965), possibly Tibet (Morellet 1916; Elliott 1968, p. 40), and Borneo in Asia.

A re-examination of the relation of these flanged forms to normal *Cymopolia* spp. is facilitated by the recently described *C. eochoristosporica* (Elliott 1968). This is a key species in dasyclad evolution, for it shows an intermediate stage in the fundamental reproductive evolution of the family. The segments are of normal cymopoliform morphology in proportions and as seen externally, but the internal branches show the

[Palaeontology, Vol. 13, Part 2, 1970, pp. 323–6, pl. 60.]

transition from cladospore to choristospore organization (see Elliott 1968), making it a kind of missing link in algal evolution. This species, from Abu Dhabi in Arabia, is Maestrichtian in age. (It is not the earliest *Cymopolia* known, for the Texan *C. perkinsi* (Johnson 1968), is from the Cenomanian). In Mme Segonzac's recent review of the Pyreneen Thanetian *Cymopolia* spp. (Segonzac 1968), which reached me whilst this was being written, *C. inflataramosa* Segonzac shows a further intermediate stage between *C. eochoristosporica* and *C. elongata* (Defr.) Munier-Chalmas. This detailed study deals fully with the problem of the doubtful morphological validity of *Karreria* Munier-Chalmas, touched on by me in describing the Middle East occurrences of *C. tibetica* Morellet (Elliott 1968), and with the varying inflation of the primary branch in and between different Thanetian and other species.

Since flanged species precede and overlap the primitive true *Cymopolia* spp. in time, it seems doubtful that they are an aberrant early development of *Cymopolia*, as was thought when only the Maestrichtian *C. anadyomenea* was known. They are accordingly referred to *Pseudocymopolia* gen. nov., diagnosed below, and the opportunity is taken to describe the Borneo species, which differs from all the other species, including those not yet fully described.

Pseudocymopolia shows fully developed choristospore organization, at an earlier geological period than the intermediate or developing choristospore structure of the Upper Cretaceous *C. eochoristosporica*. Still earlier, with *Eodasycladus* of the Lias (Cros and Lemoine 1966, 1967), the authors suggest that choristospore organization was apparently achieved by sporangial swelling of one secondary branch in each branch system i.e. a specialized form of cladospory. And Elias (1947) claimed a presumed choristospory in *Permopora* which is Permian in age, though the condition is not apparent from the figures given. Evidently the transition from cladospory to choristospory took place in different genera in different ways at different times geologically.

The relationship of *Pseudocymopolia* to *Cymopolia* is thus not necessarily close, though for taxonomic purposes both genera are placed in the Neomereae Pia 1920 (*Neomeris* appears in the Lower Cretaceous).

Genus *Pseudocymopolia* gen. nov.

Diagnosis. Thick-walled calcified dasyclad units or segments showing prominent external consecutive annular swellings or flanges: numerous crowded verticils of branches which are coarser at flange-levels; each branch showing one short primary giving rise to a globular sporangium and four or more long secondaries. Upper Jurassic to Upper Cretaceous.

Type species. Cymopolia anadyomenea Elliott (Maestrichtian of Iraq).

EXPLANATION OF PLATE 60

Fig. 1. *Pseudocymopolia orientalis* gen. et sp. nov. Longitudinal thin section of slightly distorted segment, ×40. Lower Cretaceous, Bau Limestone; Tebedu Road, Tubiti, Kuching, Sarawak, Borneo. Syntype, reg. no. V.54126.

Fig. 2. *Pseudocymopolia orientalis* gen. et sp. nov. Oblique transverse thin section through terminal thickening of slightly crushed segment, to show branch-structure, ×40. Same locality and horizon. Syntype, reg. no. V.54127.

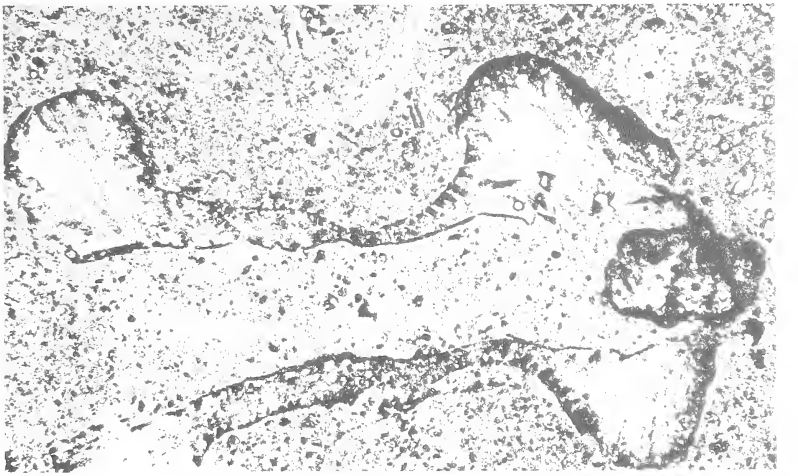

1

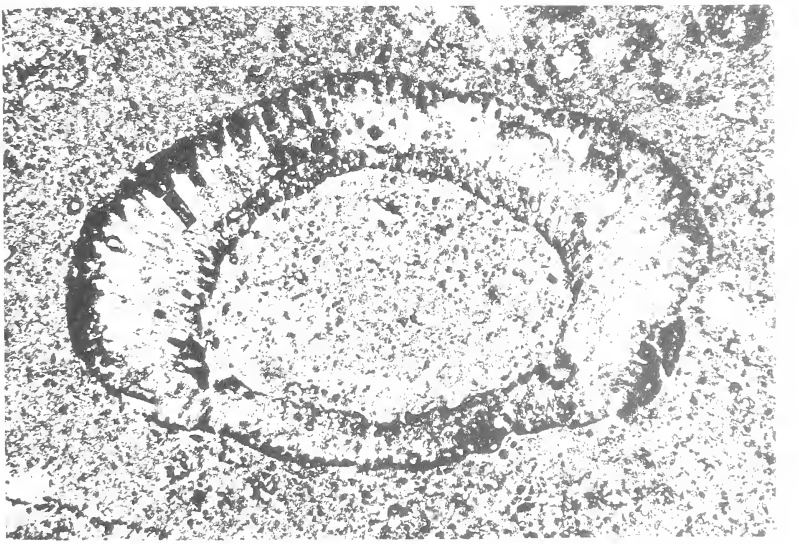

2

ELLIOTT, Mesozoic Dasycladaceae (Algae)

Other species. C. jurassica Dragastan (Upper Jurassic of Rumania), *C.* aff. *anadyomenea* (Praturlon, Lower Cretaceous of Italy), *C.* cf. *anadyomenea* (Radoičić, Lower Cretaceous of Yugoslavia), 'isomorfos de *Cymopolia anadyomenia* Elliott' (Champetier, Lower Cretaceous of Spain), and *P. orientalis* sp. nov. (Lower Cretaceous of Borneo).

Pseudocymopolia orientalis sp. nov.

Plate 60, figs. 1, 2

Description. A *Pseudocymopolia* with dumb-bell-shaped segments showing prominent rounded annular terminal thickenings connected by a much thinner shaft: the diameter of the stem-cell cavity is approximately constant. A small example has a length of 2·86 mm., external diameter at terminal thickening 1·82 mm. (d/D ratio 34%), and external diameter between thickenings 0·78 mm. (d/D ratio 66%). A larger but fragmentary example shows an external diameter across the thickening of 2·76 mm. (estimated length from this 4·33 mm.). In this large fragment the diameter of a primary branch is 0·065 mm., of a secondary branch 0·045 mm., and of a globular sporangium 0·091 mm. The matrix appears to have been stressed and the fossils show slight signs of distortion: some associated organic fragments, presumably more rigid than the alga when buried, show fracturing. The material does not permit a full tabulation of detailed structure dimensions for comparison with *P. anadyomenea* and *P. jurassica*, but the two terminal thickenings only per segment, seems characteristic.

Comparison. P. orientalis differs from *P. anadyomena* in that its thickenings are rounded and not keeled to form a flange. In this it resembles the other Lower Cretaceous and the Jurassic species. The narrow portion of the segment between thickenings is proportionally longer than is normal in other species, and these all differ in showing several thickenings per segment. As with the Italian and Jugoslav Lower Cretaceous species, the Borneo fossil is associated with the problematic non-dasyclad alga *Lithocodium aggregatum* Elliott.

Syntypes. The specimens figured in Plate 60, figs. 1, 2, from the Bau Limestone (Lower Cretaceous) of the Tebedu Road, near Tubiti, 32 miles SSE. of Kuching, Sarawak, Borneo. Brit. Mus. (Nat. Hist.), Dept. Palaeont., reg. nos. V.54126, V.54127.

Other material. Specimens and fragments in thin-sections from the same formation and area.

REFERENCES

CHAMPETIER, Y. 1967. Estudio del Jurásico y del Cretácico de la Sierra de Fontanells (Provincia de Valencia). *Notas Comun. Inst. geol. min. Esp.* **99–100,** 135–76.

CROS, P., and LEMOINE, M. 1966, 1967. Dasycladacées nouvelles ou peu connues du Lias inférieur des Dolomites et de quelques autres régions méditerranéennes. Pt. 1 (1966) *Rev. Micropaléont.* **9,** 156–68, 2 pl.; Pt. 2 (1967) Ibid. **9,** 246–57, 2 pl.

DRAGASTAN, O. 1968. Algues calcaires dans le Jurassique supérieur de Roumanie. *Geol. romana,* **7,** 59–74, 3 pl.

ELIAS, M. 1947. *Permopora keenae*, a new late Permian alga from Texas. *J. Paleont.* **21,** 46–58, pl. 18.

ELLIOTT, G. F. 1959. New calcareous algae from the Cretaceous of Iraq. *Rev. Micropaléont.* **1,** 217–22,

—— 1968. Permian to Palaeocene calcareous algae (Dasycladaceae) of the Middle East. *Bull. Br. Mus. nat. Hist.* (*Geol.*) Suppl. **4,** 111 pp., 24 pl.

JOHNSON, J. H. 1968. Lower Cretaceous algae from Texas. *Prof. Contr. Colo. Sch. Min.* **4,** 71 pp.

KAEVER, M. 1965. Mikropaläontologische Untersuchungen zur Stratigraphie Afghanistans. *Erdöl Kohle Erdgas Petrochem.* **18**, 678–84.

MORELLET, L. 1916. Note sur les algues siphonées verticillées: pp. 47–9 in H. Douvillé, *Le Crétacé et l'Éocène du Tibet central.* Mem. geol. Serv. India Palaeont indica, N.S. **5** (3), 1–52, 16 pl.

PRATURLON, A. 1964. Calcareous algae from Jurassic-Cretaceous limestone of central Apennines (southern Latium–Abruzzi). *Geol. romana*, **2**, 199–206, 1 pl.

—— 1966. Algal assemblages from Lias to Paleocene in Southern Latium–Abruzzi: a review. *Boll. Soc. geol. Ital.* **85**, 167–94.

SEGONZAC, G. 1968. Les *Cymopolia* (Dasycladacées) du Thanétien des Pyrénées. *Bull. Soc. Hist. nat. Toulouse*, **104**, 381–91, pl. 16–18.

G. F. ELLIOTT
Department of Palaeontology
British Museum (Natural History)
London S.W.7

Typescript received 17 July 1969

NEW AND LITTLE-KNOWN PERMIAN AND CRETACEOUS CODIACEAE (CALCAREOUS ALGAE) FROM THE MIDDLE EAST

by GRAHAM F. ELLIOTT

ABSTRACT. Four Codiaceae (calcareous chlorophyte algae) are described from the Middle East. *Anchicodium sindbadi* sp. nov., *Tauridium kurdistanensis* sp. nov., and *Aphroditicodium aurantium* gen. et sp. nov. are from the Permian: *Boueina hochstetteri* Toula (Lower Cretaceous) is a first Middle East record. *Aphroditicodium* is compared with other segmented Codiaceae from Ordovician to Recent, and their characters are tabulated.

AMONGST calcareous green algae the family Codiaceae have shown a much less-detailed and less-varied evolution than the family Dasycladaceae: this arises from the different basic structures peculiar to the two families. In consequence, the Codiaceae, although often abundant, have yielded few fossils of zonal value. Those encountered by me during studies of the calcareous algae of the Middle East have been listed or described (Elliott 1960, 1965); the present note describes four which are new or not previously recorded from the area.

Genus ANCHICODIUM Johnson 1946

Remarks. This Upper Palaeozoic genus was described by Johnson (1946, 1961, 1963). In thin-section it shows the characteristic codiacid pattern of poorly calcified central threads and more heavily calcified marginal radial threads. The macro-structure, however, is unusual in being described as 'a crustose mass from which straight or nearly straight cylindrical stems develop': these stems are unusual in not being segmented so far as is known. In consequence, evaluation of the orientation of random thin sections is often difficult. The Middle East species now described falls in this category, but is clearly an *Anchicodium*.

Anchicodium sindbadi sp. nov.

Plate 61, figs. 3, 4

Description. This species is seen in thin-section as a fragment about 7·5 mm. long and 0·68 mm. wide: it shows one lateral calcified cortical layer only. The fragment is worn and crusted on both sides with obscure organic growths, in part formed by myxophyte algae.

On one side of the fragment the calcite is clear and shows few threads: this is interpreted as part of the pith-like medullary zone of a cylindrical stem, with largely post-mortem calcification. On the other side the calcification, presumed original plant-structure in origin, is crowded with codiacid-like plant threads, parallel to sub-parallel in orientation, and directed more or less at right angles or oblique-transversely to the longitudinal axis of the fragment. The threads are from 0·020 to 0·040 mm. in diameter, the majority typically of 0·026–0·028 mm. diameter, the individual threads varying

[Palaeontology, Vol. 13, Part 2, 1970, pp. 327–333, pl. 61–62.]

somewhat throughout their length. Very few of them show undoubted branching. These features show most clearly in the middle of the fragment: towards the ends the plane of section cuts through the threads transversely, due to the curvature of the piece.

Holotype. The specimen figured in Plate 61, fig. 3, from Permian limestone occurring as derived fragments in the Cretaceous Hawasina Formation (Morton 1959); Jebel Qamar, Peninsular Oman, Arabia. Brit. Mus. (Nat. Hist.), Dept. Palaeont. reg. no. V.54131.

Other material. A second fragment, largely recrystallized, in the same thin section.

Remarks. The Cretaceous Hawasina is full of derived Permian limestone boulders, some of great size, from which a varied Permian microflora and fauna have been obtained. The particular thin-section from which the new *Anchicodium* comes also shows fragments of the dasyclad *Epimastopora*, and pseudopunctate brachiopod debris.

This is the first *Anchicodium* recognized in this area: the record of Elliott (1960) for Iraqi Kurdistan is now found to be a *Tauridium*. The specific name commemorates the legendary Arab traveller, whose voyages from Basra would certainly have touched at this desolate part of Arabia.

Genus *Tauridium* Güvenç 1966

Remarks. This genus, described by Güvenç (1966) from the Permian of Turkey, with type species *T. cuvillieri*, is a typical segmented calcified codiacid. Comminuted debris of what is probably the species described by Güvenç as *T. fragilis* was earlier described by me in error as the 'dasyclad' *Epimastopora minima* (Elliott 1956), from the other side of the Turkish–Iraqi frontier.

Translated diagnosis (free translation from Güvenç). Alga occurring as more or less flattened units, open at their bases. The interiors of these units are uncalcified and hollow (matrix-filled). Only the calcified cortical zone is at present known. This is formed of filaments sometimes oblique, sometimes perpendicular to the outer surface. Regular and constant narrowings and swellings of the filaments give them a characteristic 'moniliform' appearance. The filaments divide dichotomously and their diameters diminish towards the outer surface. Mode of reproduction unknown. Medullary filaments rarely preserved and not well known. (Type species *T. cuvillieri* Güvenç.) Upper Permian: Western Taurus, Turkey.

Tauridium kurdistanensis sp. nov.

Plate 62, figs. 3, 4

1960 *Anchicodium* sp.; Elliott, p. 219.

Description. Rounded-turbinate codiacid segments as seen in thin-section outline and presumed slightly flattened in the three-dimensional segments: length about 2 mm. or

EXPLANATION OF PLATE 61

Figs. 1, 2. *Boneina hochstetteri* Toula. Transverse and longitudinal thin sections of small segments, ×40. Lower Cretaceous, Garagu Formation (Valanginian-Hauterivian); subsurface, Kirkuk no. 116 well, NE. Iraq. Reg. nos. V.54135, V.54136.

Figs. 3, 4. *Anchicodium sindbadi* sp. nov. Permian: from derived fragment in Cretaceous Hawasina Formation; Jebel Qamar, Peninsular Oman, Arabia. Reg. no. V.54131. 3, Longitudinal thin section of holotype, ×15. 4, Portion enlarged, to show thread-detail, ×40.

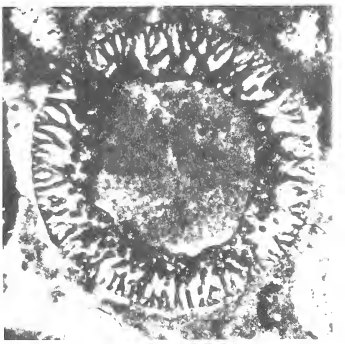

1

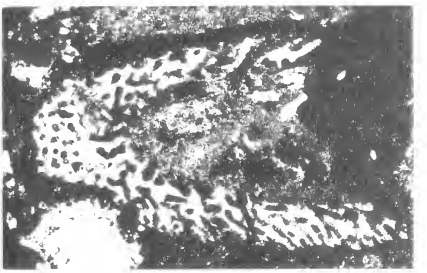

2

3

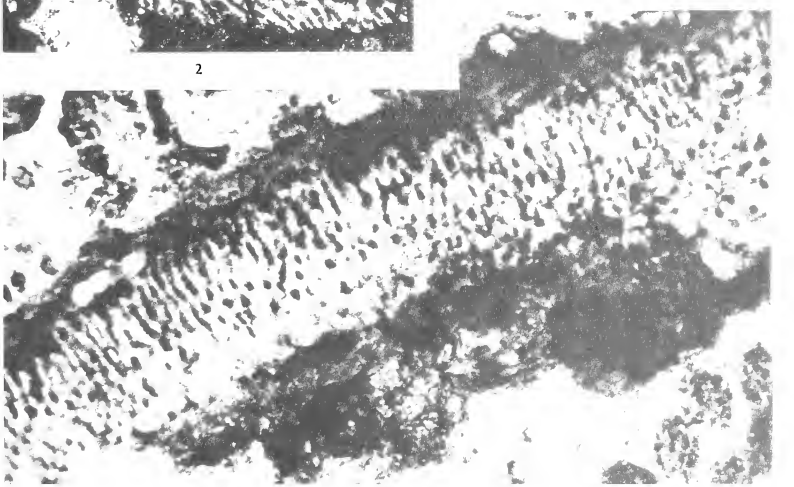

4

ELLIOTT, Permian and Cretaceous Codiaceae (Algae)

more, width about 2 mm. The calcified cortical zone is about 0·6 mm. thick; the interior, now matrix-filled, was filled with largely uncalcified plant matter during life, and by analogy with other species of *Tauridium*, would at best have shown a few weakly calcified medullary threads.

TABLE 1. Dimensions of one swollen and constricted cortical thread throughout its full length. (S = swellings; C = constrictions).

(Inner)	S.	C.	S.	C.	S.	C.	S.	C.	S.	C.	S.	(Outer)
Length	182	26	104	13	104	13	65	39	91	13	52	
Width	78	13-20	52	13	52	20	26	20	26	13	26	microns.

The cortical zone shows very numerous typically codiacid threads showing a repeated 'swollen-and-constricted' pattern throughout their length. They bifurcate repeatedly at angles of from 30° to 60°, the alternating diameters diminishing towards the exterior along all branches. Table 1 gives the dimensions of one thread traced from the interior margin of the cortical zone to the periphery, ignoring all side branches. The threads are crowded, with irregular banded zones of wider spacing due to the concentricity of periodic branching.

Holotype. Specimen shown in Plate 62, fig. 4 from the Zinnar Formation, Permian (? Artinskian); Harur, Mosul Liwa, Northern Iraq. Brit. Mus. (Nat. Hist.), Dept. Palaeont., reg. no. V.54132.

Paratype. Specimen shown in Plate 62, fig. 3 from the Darari Formation, Upper Permian: Ora, Mosul Liwa, Northern Iraq. Brit. Mus. (Nat. Hist.), Dept. Palaeont., reg. no. V.54133.

Other material. Debris has been seen sporadically in other thin-sections from these two formations.

Remarks. *Tauridium kurdistanensis* differs from the type-species in size and shape of segment (*T. cuvillieri* is longer and ellipsoidal), in the much greater thickness of the cortical zone (double or more), and in the more variable and often greater angle of thread-division. From *T. fragilis* Güvenç it is easily distinguishable, this Turkish species being very thin-walled (0·12–0·15 mm.).

The holotype is associated with the coral *Waagenophyllum indicum* (Waagen and Wentzel) var. nov. (Hudson 1958). The paratype is accompanied by the algae *Mizzia velebitana* Schubert, *Gymnocodium bellerophontis* (Rothpl.) Pia, *Permocalculus fragilis* (Pia) Elliott and *P. tenellus* (Pia) Elliott.

Genus APHRODITICODIUM gen. nov.

Diagnosis. Ovoid codiacid segments, probably slightly flattened, showing three distinct zones in section: from within outwards, firstly, a lightly calcified medullary zone of tangled threads more or less longitudinally arranged; secondly, a more heavily calcified cortical zone of irregular branching and obscurely radial threads; thirdly, a very thin, densely calcified subdermal zone showing a single layer of small subdeltoid thread-terminations widening outwards. Type-species *A. aurantium* sp. nov., Permian of Northern Iraq.

Remarks. From the algae of the Permian of Iraqi Kurdistan, a new codiacid is very rare in my experience, but the specimen now described is distinctive.

Aphroditicodium aurantium sp. nov.

Plate 62, figs. 1, 2

1960 *Succodium* sp.; Elliott, p. 219.

Description. Codiacid segment of 2·86 mm. length and 2·21 mm. width, ovoid in near-vertical section with the presumed base incomplete, and interpreted as a terminal segment. It shows clearly marked medullary, cortical, and subdermal zones described below: the measured proportions of these suggest that the section is a near-vertical (slightly oblique) cut of a terminal ovoid segment as stated, and not a more oblique cut of a cylindrical unit. By analogy with similar segmented codiaceae, living and fossil, the segment was likely to be somewhat flattened (thickness less than width). Older (lower) segments from the same plant may well have differed in shape, but have not been seen.

The inner, medullary, zone has a diameter of 0·858 mm. It shows a tangle of indistinct ramifying threads of 0·020–0·026 mm. diameter, more or less longitudinally arranged. This zone was only lightly calcified in life, as in other segmented codiaceae: and is now infilled with secondary calcification.

The cortical zone surrounds the medullary zone except at the base, where the medullary threads united this segment to the preceding one. The cortical zone is from 0·572 to 0·598 mm. thickness, and shows a tangle of more distinct branching and apparently anastomosing threads of similar diameter to the medullary threads (0·020–0·026 mm.). These tangled threads show a very irregular and obscurely radial orientation. The original plant calcification was probably heavier in this zone, thus accounting for the clearer appearance of the threads.

The subdermal layer is very thin, varying from 0·052 to 0·078 mm. in thickness, and shows dense calcification probably of original plant origin. The margin shows a single peripheral layer of fairly close-set thread-terminations, of narrow subdeltoid outline in section and expanding outwards. They have an external diameter of about 0·015 mm., and are seen to taper inwards for about 0·025 mm. They are spaced apart peripherally by about their own diameters. Occasionally, preservation shows their connections with the cortical threads.

Holotype. The specimen figured in Plate 62, figs. 1, 2, from the Zinnar Formation, Permian (? Artinskian–Kungurian); Ora, Mosul Liwa, Northern Iraq. Brit. Mus. (Nat. Hist.), Dept. Palaeont., reg. no. V.54134.

Remarks. Segmented codiaceae are known from the Lower Palaeozoic to the present day. They have in common the tripartite zoning of threads and calcification described above for *Aphroditicodium*, and the classification is largely based on the differences in the characters, at least when dealing with dissociated fossil segments. Table 2 lists the

EXPLANATION OF PLATE 62

Figs. 1, 2. *Aphroditicodium aurantium* gen. et sp. nov. Lr. Permian, Zinnar Formation; Ora, Mosul, N. Iraq. Reg. no. V.54134. 1, Slightly oblique–vertical thin-section of terminal segment (holotype), ×28. 2, Portion of sub-dermal layer enlarged, to show detail, ×84.

Fig. 3. *Tauridium kurdistanensis* sp. nov. Paratype: random thin-section to show thread-detail, ×40. Upper Permian, Darari Formation: Ora, Mosul, N. Iraq. Reg. no. V.54133.

Fig. 4. *Tauridium kurdistanensis* sp. nov. Holotype: oblique–vertical thin-section of segment, ×40. Lower Permian, Zinnar Formation: Harur, Mosul, N. Iraq. Reg. no. V.54132.

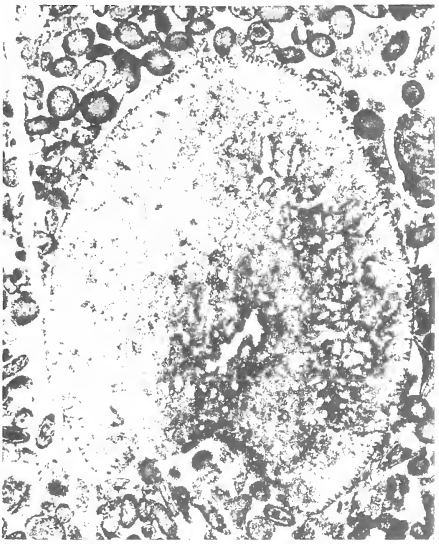

1

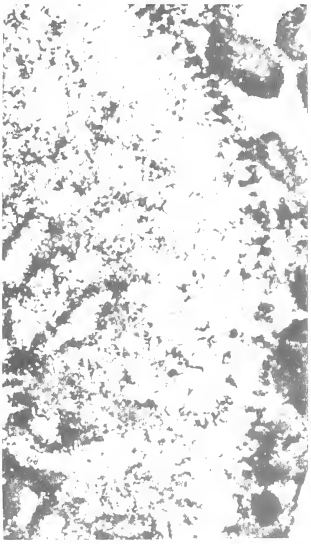

2

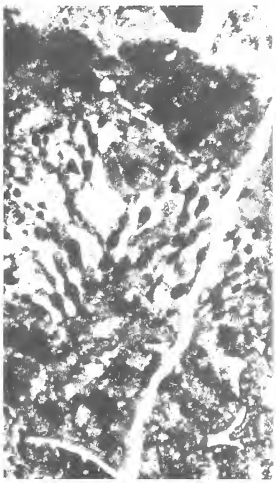

3

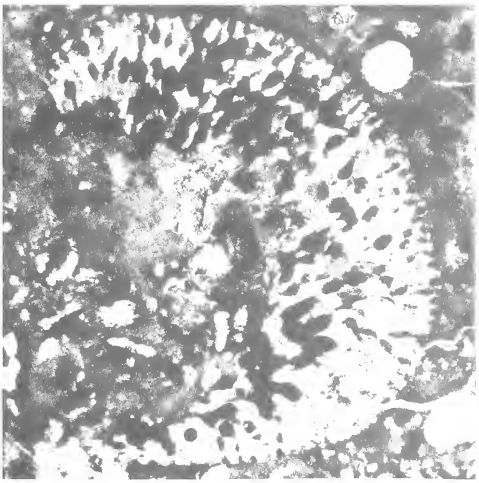

4

differences between the principal genera. These are set out as distinguishable in normal calcified thin-sections. Kozłowski and Kaźmierczak (1968) have recently described *Palaeoporella variabilis* Stolley in detail from acid digests of exceptionally well-preserved material. Detail as normally distinguishable may be seen in Obrhel's comparison of the same species with his new *Maslovina meyenii* (Obrhel 1968). Hurka (1968) who also had access to unusually well-preserved material, decided that *Palaeoporella* is a dasy-

TABLE 2. Key to internal characters of some genera of Codiaceae.

Genus	Author ond Age	Longitudinal Medullary Threads	Rodiol ar Oblique Corticol Threads	Subdermal Zane
Aphroditicodium	Gen. nov. Permian.	Fine, tongled.	Fine, tongled.	Tiny close-set deltoid terminatians.
Arobicodium	Elliott 1957 Jur.-Cret.	Fine, skeinlike.	Fine, branching.	Widening terminotions.
Boueina	Toulo 1884 Jur.-Cret.	Coorse, tangled.	Medium, branching.	Clase-set terminol bronchlets.
Dimorphosiphon	Høeg 1927 Ordovicion.	Coorse, few, straight.	Branching, thinning, radial.	Fine branchlets.
Halimeda	Lomouroux 1812 Cret.-Rec.	Thick, few, close, straight.	Bronching, radial, swallen.	Widening terminotions.
Maslovina	Obrhel 1968 Silurion.	Medium, adjacent.	Medium, bronching, oblique.	Exponded odjocent bronch-terminotions.
Palaeaparella	Stolley 1893 Ord.-Dev.	Fine, stroight.	Branching, thinning, oblique.	Finest bronchlets with terminol widenings.
Succadium	Konishi 1954 Permian.	Fine, skeinlike.	Fine, branching.	Small, flosklike swallen utricles.

cladacean, and not a codiacean, alga. I have not myself had access to material other than in normal calcified limestone preservation: the English Devonian *Palaeoporella* (Elliott 1961) certainly seemed to be a codiacean. A very detailed modern account of *Halimeda* is that of Hillis (1959).

Aphroditicodium is thus seen to be another variant on the basic segmented-codiacid plan. It bears some resemblance to *Succodium*, but the subdermal layer is distinctive. The generic name commemorates Aphrodite, fabled to have risen from the shallow sunlit seas in which living codiaceae thrive; the specific name refers to the segment-shape.

Genus BOUEINA Toula 1884

Remarks. This genus was described from the Lower Cretaceous of Serbia (Toula 1884), and has since been recognized from both Jurassic and Cretaceous in various countries around the Mediterranean and in the Middle East. Although *Boueina hochstetteri* Toula was extremely abundant at the Balkan type locality, and is known also from Italy and France, and the older variety *liasica* occurs as far apart as Algeria and Iraq, this is the first record of the type species in the Middle East.

Boueina hochstetteri Toula 1884

Plate 61, Figs. 1, 2

Description. Represented by clear longitudinal and transverse sections: the central core is missing in both cases. Length of the former is 2·0 mm. incomplete; diameter of the latter 1·2 mm. This is much smaller than the dimensions of the type material, where 2·5–3·5 mm. diameter and up to 10 mm. in length is indicated. The branch-detail of the calcified cortical zone corresponds exactly, however, and the specimens, earlier considered as a new *Arabicodium* sp., are now referred to *B. hochstetteri*. They come from the subsurface Garagu Formation (Lower Cretaceous, Valanginian-Hauterivian) of Kirkuk no. 116 well, north-east Iraq. Associated is debris of the chaetangiacid alga *Permocalculus*, corals and echinoderms.

REFERENCES

ELLIOTT, G. F. 1956. Further records of fossil calcareous algae from the Middle East. *Micropaleontology*, **2**, 327–34, 2 pl.

—— 1957. New calcareous algae from the Arabian Peninsula. Ibid. **3**, 227–330, 1 pl.

—— 1960. Fossil calcareous algal floras of the Middle East with a note on a Cretaceous problematicum *Hensonella cylindrica* gen. et sp. nov. *Q. Jl geol. Soc. Lond.* **115**, 217–32, pl. 8.

—— 1961. A new British Devonian alga, *Palaeoporella lummatonensis*, and the brachiopod evidence of the age of the Lummaton shell-bed. *Proc. Geol. Ass., Lond.* **72**, 251–60, pl. 9, 10.

—— 1965. The interrelationships of some Cretaceous Codiaceae (Calcareous Algae). *Palaeontology*, **8**, 199–203, pl. 23, 24.

GÜVENÇ, T. 1966. Présence d'algues calcaires dans le Permien des Taurus occidentaux (Turquie); description d'un nouveau genre et de quelques espèces. *Rev. Micropaléont.* **9**, 43–49, 2 pl.

HILLIS, L. W. 1959. A revision of the genus *Halimeda* (order Siphonales). *Inst. marine Sci., Univ. Texas*, **6**, 321–403, 12 pl.

HØEG, O. 1927. *Dimorphosiphon rectangulare*: Preliminary note on a new Codiacea from the Ordovician of Norway. *Avh. norske Vidensk Akad*, 1927, no. **4**, 15 pp. 3 pl.

HUDSON, R. G. S. 1958. Permian corals from northern Iraq. *Palaeontology*, **1**, 174–92, pl. 32–5.

HURKA, H. 1968. Über den anatomischen Bau und die systematische Stellung des paläozoischen Algengenus *Palaeoporella* Stolley. *Nova Hedwigia*, **15**, 571–82, pl. 83.

JOHNSON, J. H. 1946. Lime-secreting algae from the Pennsylvanian and Permian of Kansas. *Bull. geol. Soc. Am.* **57**, 1087–1120, 10 pl.

—— 1961. Limestone-building algae and algal limestones. *Publ. Colo. Sch. Min.*, 297 pp. 139 pl.

—— 1963. Pennsylvanian and Permian algae. *Colo. Sch. Min. Quart.* **58**, 211 pp., 81 pl.

KONISHI, K. 1954. *Succodium*, a new Codiacean genus and its algal associates in the late Permian of southern Kyushu, Japan. *J. Fac. Sci., Univ. Tokyo*, (2) **9**, 225–40, 2 pl.

KOZŁOWSKI, R., and KAŹMIERCZAK, J. 1968. On two Ordovician calcareous algae. *Acta palaeont. pol.* **13**, 325–46, 11 pl.

MORTON, D. M. 1959. The geology of Oman. *Proc. 5th Wld Petrol. Congr.* **1**, 277–94.

OBRHEL, J. 1968. *Maslovina meyenii* n.g. et sp. neue Codiacea aus dem Silur Böhmens. *Vest. ústred. Úst. geol.* **43,** 367–70, 2 pl.

STOLLEY, E. 1893. Ueber silurische Siphoneen. *Neues Jb. Miner. Geol. Paläont.* 1893 II, 135–46, pl. 7, 8.

TOULA, F. 1884. Geologische Untersuchungen im westlichen Theile des Balkan und in den angrenzenden Gebieten. X. Von Pirot nach Sofia, auf dem Vitos, über Pernik nach Trn und über Stol nach Pirot. *Sber. Akad. Wiss. Wien,* **88,** (1) 1279–1348, 9 pl.

G. F. ELLIOTT
Department of Palaeontology
British Museum (Natural History
London S.W.7

Typescript received 17 July 1969

THE PALAEONTOLOGICAL ASSOCIATION

PALAEONTOLOGY

The journal *Palaeontology* is devoted to the publication of papers (preferably illustrated) on all aspects of palaeontology and stratigraphical palaeontology. Four parts at least are published each year and are sent free to all members of the Association. Members who join for 1970 will receive Volume 13, parts 1 to 4.

All back numbers are still in print and may be ordered from B. H. Blackwell, Broad Street, Oxford, England, at £3 per part (post free). A complete set, Volumes 1–12, consists of 47 parts and costs £141.

SPECIAL PAPERS IN PALAEONTOLOGY

This is a series of substantial separate works published by the Association. The subscription rate is £6 (U.S. $16.00) for Institute Members and £3 (U.S. $8.00) for Ordinary and Student Members. Subscriptions and orders by members of the Association should be placed through the Membership Treasurer Dr. A. J. Lloyd, Department of Geology, University College, Gower Street, London, W. C. 1, England.

The following *Special Papers* are available. Members may obtain them at reduced rates through the Membership Treasurer. Non-Members may obtain them from B. H. Blackwell, Broad Street, Oxford, England, at the prices indicated.

Special Paper No. 1 (for 1967): Miospores in the Coal Seams of the Carboniferous of Great Britain, by A. H. V. Smith and M. A. Butterworth. 324 pp., 72 text-figs., 27 plates. Price £8 (U.S. $22.00), post free.

Special Paper No. 2 (for 1968): Evolution of the Shell Structure of Articulate Brachiopods, by A. Williams. 55 pp., 27 text-figs., 24 plates. Price £5 (U.S. $13.00).

Special Paper No. 3 (for 1968): Upper Maestrichtian Radiolaria of California, by Helen P. Foreman. 82 pp., 8 plates. Price £3 (U.S. $8.00).

Special Paper No. 4 (for 1969): Lower Turonian Ammonites from Israel, by R. Freund and M. Raab. 83 pp., 15 text-figs., 10 plates. Price £3 (U.S. $8.00).

Special Paper No. 5 (for 1969): Chitinozoa from the Ordovician Viola and Fernvale Limestones of the Arbuckle Mountains, Oklahoma, by W. A. M. Jenkins. 44 pp., 10 text-figs., 9 plates. Price £2 (U.S. $5.00).

Special Paper No. 6 (for 1969): Ammonites from the Mata Series (Santonian–Maestrichtian) of New Zealand, by R. A. Henderson. 82 pp., 13 text-figs., 15 plates. Price £3 (U.S. $8.00).

Special Paper No. 7 (for 1970): Shell Structure of the Craniacea and other Calcareous Inarticulate Brachiopoda, by A. Williams and A. D. Wright. 51 pp., 17 text-figs., 15 plates. Price £1. 10*s*. ($4.00).

SUBMISSION OF PAPERS

Typescripts on all aspects of palaeontology and stratigraphical palaeontology are invited. They should conform in style to those already published in this journal, and should be sent to Mr. N. F. Hughes, Department of Geology, Sedgewick Museum, Downing Street, Cambridge, England, who will supply detailed instructions for authors on request (these are published in *Palaeontology*, **10**, pp. 707–12).

PALAEONTOLOGY

VOLUME 13 • PART 2

CONTENTS

PRINTED IN GREAT BRITAIN AT THE UNIVERSITY PRESS, OXFORD
BY VIVIAN RIDLER, PRINTER TO THE UNIVERSITY

VOLUME 13 · PART 3

Palaeontology

OCTOBER 1970

PUBLISHED BY THE
PALAEONTOLOGICAL ASSOCIATION
LONDON

Price £3

THE PALAEONTOLOGICAL ASSOCIATION

The Association was founded in 1957 to further the study of palaeontology. It holds meetings and demonstrations, and publishes the quarterly journal *Palaeontology* and *Special Papers in Palaeontology*. Membership is open to individuals, institutions, libraries, etc., on payment of the appropriate subscription:

Institute membership	£7·00 (U.S. $20.00)
Ordinary membership	£5·00 (U.S. $13.00)
Student membership	£3·00 (U.S. $8.00)

There is no admission fee. Institute membership is only available by direct application, not through agents. Student members are persons receiving full-time instruction at educational institutions recognized by the Council; on first applying for membership, they should obtain an application form from the Membership Treasurer. All subscriptions are due each January, and should be sent to the Membership Treasurer, Dr. A. J. Lloyd, Department of Geology, University College, Gower Street, London, W.C. 1, England.

COUNCIL 1970–1

President: Dr. W. S. McKerrow, Department of Geology, Oxford

Vice-Presidents: Professor Alwyn Williams, The Queen's University, Belfast
Professor M. R. House, The University, Kingston upon Hull, Yorkshire

Treasurer: Dr. J. M. Hancock, Department of Geology, King's College, London, W.C. 2

Membership Treasurer: Dr. A. J. Lloyd, Department of Geology, University College, Gower Street, London, W.C. 1

Secretary: Dr. W. D. I. Rolfe, Hunterian Museum, The University, Glasgow, W. 2

Editors

Mr. N. F. Hughes, Sedgwick Museum, Cambridge
Dr. Gwyn Thomas, Department of Geology, Imperial College, London, S.W. 7
Dr. Isles Strachan, Department of Geology, The University, Birmingham 15
Dr. R. Goldring, Department of Geology, The University, Reading, Berks.
Dr. J. D. Hudson, Department of Geology, The University, Leicester

Other members of Council

Dr. F. M. Broadhurst, Manchester
Dr. L. R. M. Cocks, London
Dr. R. H. Cummings, Abergele
Dr. D. J. Gobbett, Cambridge
Dr. Julia Hubbard, London
Dr. W. J. Kennedy, Oxford
Dr. J. D. Lawson, Glasgow
Dr. W. H. C. Ramsbottom, Leeds
Dr. P. L. Robinson, London
Dr. E. P. F. Rose, London
Dr. C. T. Scrutton, London
Dr. V. G. Walmsley, Swansea
Dr. A. D. Wright, Belfast

Overseas Representatives

Australia: Professor Dorothy Hill, Department of Geology, University of Queensland, Brisbane

Canada: Dr. D. J. McLaren, Institute of Sedimentary and Petroleum Geology, 3303–33rd Street NW., Calgary, Alberta

India: Professor M. R. Sahni, 98 The Mall, Lucknow (U.P.), India

New Zealand: Dr. C. A. Fleming, New Zealand Geological Survey, P.O. Box 368, Lower Hutt

West Indies and Central America: Mr. John B. Saunders, Geological Laboratory, Texaco Trinidad, Inc., Pointe-à-Pierre, Trinidad, West Indies

Western U.S.A.: Professor J. Wyatt Durham, Department of Paleontology, University of California, Berkeley 4, California

Eastern U.S.A.: Professor J. W. Wells, Department of Geology, Cornell University, Ithaca, New York

The Palaeontological Association, 1970

CONODONTS FROM NEAR THE MIDDLE/UPPER DEVONIAN BOUNDARY IN NORTH CORNWALL

by W. T. KIRCHGASSER

ABSTRACT. Conodonts of the *Polygnathus varcus* (Middle Devonian, Givetian) Zone and the lower (Upper Devonian) and upper part of the Lower *Pol. asymmetricus* Zone (Upper Devonian, Frasnian Iα) are reported from thin turbidite limestones in the upper Trevose Slates, Marble Cliff Beds, and lower Longcarrow Cove Tuffs and Slates, respectively, near Padstow, North Cornwall. The localities include the south side of Trevone Bay and the overturned section along the coast at Marble Cliff. The fauna of the *Schmidtognathus hermanni–Pol. cristatus* Zone, which in Germany marks the Middle/Upper Devonian boundary of the conodont chronology, was not recovered, although some species that enter in that zone (*Pol. cristatus* [?] Hinde, *S. wittekindti* Ziegler and *S. peracutus* (Bryant)) are found in the Marble Cliff Beds, associated with *Palmatolepis transitans* Müller, *Pol. asymmetricus ovalis* Ziegler and Klapper, *Pol. asymmetricus asymmetricus* Bischoff and Ziegler, and abundant *Pol. decorosus* Stauffer *s.l.* The first undoubted Upper Devonian conodonts occur in the Longcarrow Cove Tuffs and Slates near the base of Marble Cliff, where faunas include *Ancyrodella rotundiloba* (Bryant).

REINVESTIGATIONS of ammonoid cephalopods (House 1956, 1961, 1963) from the highly deformed grey slates around Padstow, North Cornwall, have revealed Middle Devonian faunas in rocks long thought to be entirely Upper Devonian in age. Several ammonoid horizons are known in the district and the sequence of faunas enabled House to unravel the stratigraphic succession and establish a correlation with the standard sequence in the Rheinisches Schiefergebirge. Although the broad aspects of the stratigraphy and structure (Gauss 1966, 1967) have been worked out, many parts of the puzzle remain unsolved because of the lack of faunal evidence in critical parts of the succession. This contribution attempts to refine the biostratigraphy of the coastal section near the Middle/Upper Devonian boundary by means of conodonts.

The Middle Devonian Trevose Slates are situated on the southern limb of the St. Minver Synclinorium (House 1961) whose axis lies north of Padstow, within Upper Devonian purple and green slates (upper Frasnian to Fammenian) (text-fig. 1). The grey slates reappearing on the northern limb are overlain by a thick series of pillow lavas (Pentire Point Pillow Lavas) before the entry of purple and green slates. The coastal succession on the southern limb appears to be more complete, and here the Trevose Slates begin in the upper Eifelian (Booby's Bay) and extend into the upper Givetian (Trevone Bay). The fauna of the uppermost Givetian *Maenioceras terebratum* Zone is well represented in the Pentonwarra Point Goniatite Band on the south side of Trevone Bay (House 1963). The fauna of the succeeding lower Frasnian (lowermost Upper Devonian) *Pharciceras lunulicosta* (Iα) Zone has not been found anywhere in the district, but the middle Frasnian *Manticoceras cordatum* (I (β) γ) Zone-fauna is known from several localities, including the dark grey slates at Merope Island (Merope Island Beds), 0·6 miles (1 km.) north of Trevone Bay (House 1961, 1963). Between the Trevose Slates and the Merope Island Beds and situated on the overturned limb of a major recumbent syncline (Gauss 1966) are 220 ft. (67 m.) of alternating limestone and shale exposed at Marble Cliff (Marble Cliff Beds and lower Longcarrow Cove Tuffs and Slates) which are succeeded to the north by grey slates with tuff beds, agglomerate, and minor limestones

[Palaeontology, Vol. 13, Part 3, 1970, pp. 335–54, pl. 63–66.]

(House 1961, House and Selwood 1966). The Marble Cliff succession dips south beneath the dolerite sill that forms the prominent headland north of Trevone Bay.

No ammonoids are known from either the Marble Cliff Beds or Longcarrow Cove Tuffs and Slates, but House (1963) tentatively placed the Middle/Upper Devonian boundary between them, assigning the Marble Cliff Beds to the Givetian largely on the

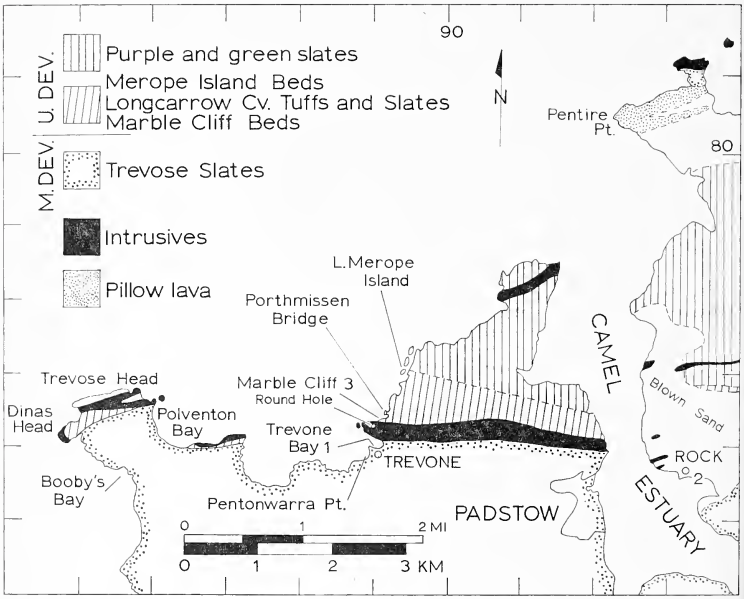

TEXT-FIG. 1. Geological sketch-map of Padstow area showing conodont localities.

evidence of *Wedekindella* (a characteristic Middle Devonian genus) associated with similar limestones to the west at Poventon Bay. House and Selwood (1966, p. 53) recorded an upper Givetian conodont age for the Marble Cliff Beds based on an unpublished preliminary study by F. H. T. Rhodes of a sample collected from loose blocks at the base of the cliff (House 1967, personal communication); this assignment was based on a correlation with the conodont zonation of Bischoff and Ziegler (1957) from the Rheinisches Schiefergebirge. Since the report of Bischoff and Ziegler a more refined conodont zonation has been established within the framework of the standard ammonoid zonation (Ziegler 1958, 1962*a*, 1966*b*). This conodont chronology has proved to be extremely useful for precise inter-continental correlation (see Glenister and Klapper 1966) and it is particularly refined around the Middle/Upper Devonian boundary.

The samples were collected from the coastal sequence around Padstow during the spring tides of October 1967 and January 1968.

CONODONT ZONATION ACROSS THE MIDDLE/UPPER DEVONIAN BOUNDARY

Ziegler (1966*b*), Krebs and Ziegler (1966), Glenister and Klapper (1966), and Orr and Klapper (1968), among others, have thoroughly reviewed the relationship between the conodont zonation and the position of the Middle/Upper Devonian boundary and only a few pertinent details are noted here. In terms of the standard ammonoid zonation in the Rheinisches Schiefergebirge, the top of the Middle Devonian is defined as the top of the *Maenioceras terebratum* Zone and the base of the Upper Devonian as the base of the *Pharciceras lunulicosta* Zone (Iα), with the entry of *Pharciceras*; this boundary has been traditionally equated with the Givetian/Frasnian stage boundary in Belgium, but the correlation has still to be proven. An exact boundary horizon cannot be placed in Germany because there is a gap between the ranges of *Maenioceras* and *Pharciceras*. It is within this critical interval that Ziegler (1966*b*) defined the Middle/Upper Devonian boundary in terms of conodonts.

The *Polygnathus varcus* Zone (*varcus*-Subzone of Bischoff and Ziegler 1957) corresponds to the highest part of the *M. terebratum* Zone and is therefore regarded as uppermost Middle Devonian (Ziegler 1962*b*, p. 16). The *Pol. varcus* Zone begins with the entry of *Pol. varcus* and is characterized by abundant *Pol. varcus* and *Pol. linguiformis* without *Spathognathodus bipennatus*. Wittekindt (1966, pp. 627, 628) subdivided the *Pol. varcus* Zone into a *varcus*-Zone without *Pol. linguiformis transversus* and a succeeding *transversus*-Zone with *Pol. linguiformis transversus*. Because the well-known species *Pol. varcus* and *Pol. linguiformis* dominate the fauna of the *Pol. varcus* Zone as originally defined, and because *Pol. linguiformis transversus* is rare, Krebs and Ziegler (1966, p. 747) preferred an informal subdivision of the *Pol. varcus* Zone into a lower and upper part; this interpretation is followed here.

The *Schmidtognathus hermanni–Polygnathus cristatus* Zone (Ziegler 1966*b*) follows the *Pol. varcus* Zone and comprises the range of *S. hermanni* before the entry of *Pol. asymmetricus* and *Palmatolepis transitans*. The lower boundary of the zone is not precisely defined, as a few early growth stages of *S. hermanni*, as well as forms transitional between *Pol. decorosus s.l.* and *S. hermanni*, occur in horizons that Ziegler regards as still in the *Pol. varcus* Zone (Ziegler (1966*b*, tables 1, 2, p. 659). Above the base of the *S. hermanni–Pol. cristatus* Zone, *S. hermanni* is joined by *Pol. cristatus* and three new species of *Polygnathus* and three of *Schmidtognathus*, but not at a single horizon as implied by Ziegler (1966*b*, text-fig. 2). The details of Ziegler's range-charts show the entry of these species in a staggered sequence, with some of the species (*S. hermanni*, *S. pietzerni*) appearing before *Pol. cristatus*, as in the least condensed Koppen section at Rhenegge near Adorf. Several of these species, in addition to *S. hermanni* and *Pol. varcus*, linger on into the succeeding Lower *Pol. asymmetricus* Zone, whose lower boundary is defined by the entry of *Pol. asymmetricus* and *Pal. transitans*.

The position of the *S. hermanni–Pol. cristatus* Zone relative to the Middle/Upper Devonian boundary is still a problem as the zonal fauna has not been found in rocks bearing ammonoids. In the Rheinisches Schiefergebirge the zone appears to fill the gap

in the ammonoid chronology (Ziegler 1966*b*) and is thus a problematical interval between the Middle and Upper Devonian. It is clear from Ziegler's analysis (pp. 672, 673) that the *S. hermanni–Pol. cristatus* Zone represents an important interval in conodont evolution during which simple ancestral conodonts (*Pol. decorosus s.l.*) gave rise to diverse and morphologically 'advanced' platform conodonts such as *Schmidtognathus* and the *Pol. cristatus* group. *Pol. cristatus* in turn lead to *Pol. asymmetricus*, the stem form of the line leading to *Palmatolepis*, a particularly significant genus in Upper Devonian faunas. Thus in terms of conodont evolution Ziegler (1966*b*, pp. 660, 661) regarded the lower part of the *S. hermanni–Pol. cristatus* Zone (without *Pol. cristatus*) as Middle Devonian and the more diverse upper part as Upper Devonian.

The succeeding Lower *Pol. asymmetricus* Zone is informally subdivided into a lower part and upper part based on the first appearance of *Ancyrodella rotundiloba* (Ziegler 1962*b*, p. 17, 1966*b*, p. 662). Krebs and Ziegler (1966, pp. 748, 749) assembled evidence that proves beyond doubt that the upper part of the Lower *Pol. asymmetricus* Zone (with *A. rotundiloba*) lies within the *Pharciceras lunulicosta* Zone (Iα) and is thus firmly Upper Devonian; this correlation has since been confirmed in Australia (Glenister and Klapper 1966, p. 785) and North America (Orr and Klapper 1968, p. 1069).

Krebs and Ziegler also suggested that the lower part of the Lower *Pol. asymmetricus* Zone probably falls in the *P. lunulicosta* Zone (Iα) but offered no concrete evidence. However, recent ammonoid collections from the classic section at Martenberg near Adorf seem to support this interpretation. In April 1968, Dr. J. Kullmann, in a field party with Professors W. Ziegler, M. R. House, and the author, discovered a new horizon of pharciceratids low down in the Roteisenstein, which narrows the gap in the ammonoid sequence, as typical Middle Devonian ammonoids are found only 0·30 m. below. The new horizon lies within the 1·0 m. interval between Ziegler's (1958) samples 0 (*Pol. varcus* Zone) and 1 (upper part of Lower *Pol. asymmetricus* Zone). It remains to be seen whether the faunas of the lower part of the *Pol. asymmetricus* Zone or the *S. hermanni–Pol. cristatus* Zone can be recovered from the critical interval; Professor Ziegler has made collections and is reviewing the details of the sequence.

The base of the Middle *Pol. asymmetricus* Zone is defined by the first occurrence of *Palmatolepis punctata*, associated with *Pol. asymmetricus*, *A. rotundiloba*, and *A. gigas*, among others; at Martenberg this zone corresponds to the *Pharciceras–Schichten* (Iα) as originally defined by Wedekind (1913). The Middle *Pol. asymmetricus* Zone has been recognized in Australia (Glenister and Klapper 1966, p. 785) and Alberta, Canada (Pollock 1968, p. 442), but its position in other North American sections is difficult to determine because *Palmatolepis punctata* is either not found or is found associated with higher conodont zones equivalent to the *Manticoceras cordatum* (I (β) γ) Zone. Müller and Clark (1967) assigned the Squaw Bay Limestone of Michigan, with *A. rotundiloba* and *Pol. asymmetricus ovalis*, to the Middle *Pol. asymmetricus* Zone but Orr and Klapper (1968, pp. 1068, 1069) disagreed and assigned the Squaw Bay and the supposedly equivalent tongue of the Genundewa Limestone exposed at Eighteenmile Creek, New York, to the upper part of the Lower *Pol. asymmetricus* Zone. In Orr and Klapper's view both horizons have identical faunas, which include *Pol. dengleri* in addition to *A. rotundiloba*. They regard *Pol. dengleri* as the diagnostic species because it has not been reported higher than the upper part of the Lower *Pol. asymmetricus* Zone in the German sequence (Ziegler 1958, tables 2, 10; 1962*b*, p. 17); following this criterion Clark and

Ethington's (1967) fauna from Mary's Mountain, Nevada, should also be reassigned to the upper part of the Lower *Pol. asymmetricus* Zone. Krebs and Ziegler (1966, p. 737) assigned a fauna with *A. rotundiloba* and *A. rugosa* from the Walheim section near Aachen, Germany, to the Middle *Pol. asymmetricus* Zone based on the presence of well-developed pointed anterior lobs in specimens figured as *A. rotundiloba* n. subsp. Krebs and Ziegler (1966). In the present report *A. rotundiloba* n. subsp. is interpreted as an early growth stage variant of *A. rotundiloba* (Bryant) *sensu* Müller and Clark (1967). Krebs and Ziegler's fauna could therefore also correspond to the upper part of the lower *Pol. asymmetricus* Zone, which was the alternative correlation considered by these authors.

CONODONT LOCALITIES

Trevose slates. Thin beds of blue-grey limestone are not uncommon within the grey slates around Padstow, but few horizons can be accurately placed in the generally northward-younging succession. Limestones at several localities, including Trevose Head, Cataclews Point, Padstow, Rock, and further south-east, have long been regarded as equivalent to the well-exposed sequence of closely spaced limestones at Marble Cliff (Reid *et al.* 1910, Dewey 1914). At the type locality, the Marble Cliff Beds are separated from the underlying Trevose Slates by the prominent dolerite sill that extends from Padstow westward to the Trevose Peninsula: on the Trevose Peninsula the Marble Cliff Beds are intruded by the sill. Throughout the area west of the Camel Estuary the critical part of the transition between the Marble Cliff Beds and the Trevose Slates has been obscured by the intrusion, especially where the limestones and shales are adinolized as at Dinas Head and on the peninsula north of Trevone Bay (Fox 1895). The conodont evidence presented here indicates that those limestones lying south of but not directly associated with the sill are older than the Marble Cliff Beds and should be assigned to the Trevose Slates; among these are the limestones around Rock and presumably the limestones with *Agoniatites* and *Wedekindella* from the west and south-west side of Polventon Bay (House and Selwood 1966, p. 53).

Loc. 1. Trevone Bay (SW 890760): Samples 30 and 31. Lower and upper beds of a 2-ft. (0·61 m.) thick series of three limestones alternating with grey slate, dipping south-east in the low cliffs on the south side of the bay. The upper bed (Sample 31) is overlain by 4 ft. (1·22 m.) of slate capped by a prominent 1-foot (0·31 m.) thick bed of brown silty slate. The sequence lies near the top of the Trevose Slates, probably a few feet above the Pentonwarra Point Goniatite Band (Gauss 1968, personal communication).

Loc. 2. Rock (SW 935755): Sample 33. 1-ft. (0·31 m.) thick limestone exposed in the foreshore about 60 yd. (55 m.) east of the sea-wall.

Marble Cliff Beds and Longcarrow Cove Tuffs and Slates. The section at Marble Cliff (Loc. 3: SW 891765) consists of approximately 220 ft. (67 m.) of alternating limestone and shale which are overturned and dip south beneath the dolerite sill (text-fig. 2). There are over 150 individual limestone beds ranging in thickness from less than 1 in. (2·5 cm.) to slightly over 2 ft. (0·61 m.). The thickness of the individual limestones and of the intervening steel-grey shales tends to be constant across the outcrop and the beds are thinner and more widely spaced toward the base of the cliff.

The limestones are light to dark blue-grey bioclastic limestones (packed biomicrite) and are largely composed of fine crinoidal debris. Moulds of *Stylioliua* are common in

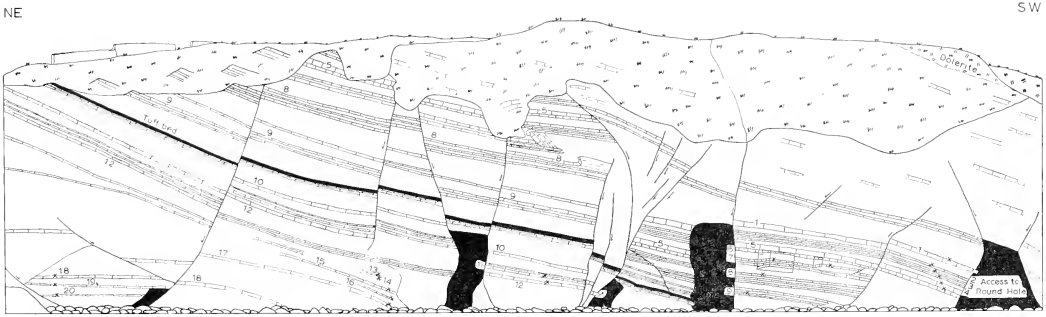

TEXT-FIG. 2. Sketch of Marble Cliff showing sample-horizons and collecting sites (x); the section is not drawn to scale. The outcrop is about 280 yd. (256 m.) long and the cliff is about 150 ft. (46 m.) high.

the residues and at some horizons (notably Sample 17) these are associated with minute pyritic gastropods, bivalves, ostracods, and rare ammonoid fragments. Sole-markings and graded bedding were noted at a few horizons and these features, and the conodont sequence as well, indicate that the succession is overturned. The only distinctive horizon interrupting this monotonous sequence is a light greenish-grey tuff bed in about the middle of the section. Samples 1–14 are from the Marble Cliff Beds and samples 15–20 are from the Longcarrow Cove Tuffs and Slates (text-fig. 3).

Approximately the lower 75 ft. (23 m.) of the Marble Cliff Beds, between Sample 1 and the sill, is inaccessible in the cliff face. Although the lowermost 26 ft. (8 m.) is accessible in the west wall of Round Hole the limestones are too altered to yield significant conodont faunas; only a single fragment was recovered from a sample near the bottom of the Hole, 24 ft. (7·3 m.) above the intrusive contact. Two distinctive groups of limestone, both consisting of three uniformly spaced beds, provide useful reference horizons in the cliff section. The lower set consists of sample-horizons 2, 3, and 4 and the higher set includes sample-horizon 8 at its base. The top of the Marble Cliff Beds is defined as the base of sample-horizon 15, an irregularly bedded 1-ft. (0·31 m.) thick limestone accessible in the north-east part of the outcrop.

The succeeding more argillaceous sequence near the base of the cliff (samples 15–20) is here included in the Longcarrow Cove Tuffs and Slates. This series of thin, widely spaced limestones reappears across a fault in the section at Porthmissen Bridge (opposite Marble Cliff) and continues northward to Longcarrow Cove, where agglomerates and tuffs enter the succession.

The limestones in the Padstow area appear to be turbiditic in origin and may represent bioclastic debris intermittently swept into a deep water pelagic environment (Goldring *et al.* 1968, p. 7), perhaps from centres of reef accumulation in the more tectonically active part of the basin in South Devon. Dineley (1961) proposed this mechanism to explain similar thin-bedded limestones and shales which accumulated in rapidly subsiding troughs immediately surrounding the South Devon reefs. The greater part of these massive reefs or reef-like (Braithwaite 1966) limestones is lower to upper Middle Devonian, although they continue into the lower part of the Upper Devonian (House and Selwood 1966).

ANALYSIS OF THE CONODONT FAUNAS

The Trevose Slate horizons at Trevone Bay (Samples 30, 31) produced a fauna dominated by *Pol. linguiformis* and *Pol. varcus* (text-fig. 4) which is indicative of the uppermost Middle Devonian *Pol. varcus* Zone. A similar fauna recovered from Sample 33 at Rock suggests that the scattered limestones thereabout correlate westward with the Trevose Slates at Trevone Bay rather than with the succession at Marble Cliff. The single specimen of *S. hermanni* from Sample 31 is an early growth stage of an intermediate form between *Pol. decorosus s.l.* and *S. hermanni* and is similar to forms figured by Ziegler (1966*b*) from the uppermost part of the *Pol. varcus* Zone in the Rheinisches Schiefergebirge. The specimens of *Pol. linguiformis* and *Pol. varcus* from the Trevose Slates are remarkably similar to the specimens figured by Rhodes and Dineley (1957) from apparently upper Middle Devonian limestones at Bishopsteignton, South Devon. The remaining less stratigraphically important elements of their fauna are rather different and there

are no other species in common with the Trevose Slate fauna. Matthews (1962) recorded upper Eifelian conodonts from a structurally complicated sequence at Neal Point, Cornwall, on the River Tamar and his report of *Pol. xylus* (= *Pol. varcus*) and *Pol. varcus* suggests that the *Pol. varcus* Zone is also represented.

The fauna of the Marble Cliff Beds (Samples 1–14) corresponds to the lower part of the *Pol. asymmetricus* Zone and thus indicates a probable lower Upper Devonian age for the limestone sequence. Important forms in the diverse but unevenly distributed fauna include *Pol. asymmetricus asymmetricus*, *Pol. asymmetricus ovalis*, *Pol. dengleri*, and *Palmatolepis transitans*. Although the fauna of the *S. hermanni–Pol. cristatus* Zone is not represented there are several holdovers from this and the preceding *Pol. varcus* Zone, including *Pol. varcus*, *Pol. linguiformis*, *Pol. cristatus*, *Pol.* sp. Ziegler (1966*b*, p. 669), *S. wittekindti*, *S. hermanni*?, and *S. peracutus*.

The upper part of the Lower *Pol. asymmetricus* Zone, which corresponds to the lower Upper Devonian *Pharciceras lunulicosta* Zone (Iα), begins at the base of the Longcarrow Cove Tuffs and Slates (Samples 15–20) with the entry of *Ancyrodella rotundiloba*. The fauna is less diverse than that of the Marble Cliff Beds and some stratigraphically important forms which range above the lower part of the Lower *Pol. asymmetricus* Zone were not recovered, such as *Pol. asymmetricus*, *Pol. cristatus*, and *Pal. transitans*. In addition to *A. rotundiloba*, the fauna includes *Icriodus symmetricus*, *Pol. decorosus*, *Pol. foliatus*, *Pol. pennatus*, and *Pol. dengleri*. As noted above, the overlap in the ranges of *A. rotundiloba* and *Pol. dengleri* is diagnostic for the upper part of the Lower *Pol. asymmetricus* Zone.

The conodont sequence at Trevone Bay and Marble Cliff corresponds closely with the sequence in the lower and upper parts of Ziegler's (1966*b*) sections in the Rheinisches Schiefergebirge, especially the Koppen section where the *Pol. varcus* and *S. hermanni–Pol. cristatus* Zones and the entire Lower *Pol. asymmetricus* Zone are represented. *Pol. beckmanni* was not recovered from the Trevose Slates and the Marble Cliff faunas do not include *Pol. caelata*, *Pol. ordinata*, *Spathognathodus sannemanni*, and *Schmidtognathus pietzneri*, among others, but considering the comparative poverty of the Cornish faunas, these absentees do not greatly detract from the overall similarity of fauna and faunal sequence. Because the fauna of the *S. hermanni–Pol. cristatus* Zone was not recovered the Middle/Upper Devonian boundary of the conodont zonation cannot be precisely placed. However, it must roughly correspond to the boundary between the Trevose Slates and the Marble Cliff Beds, that is, within the series of altered rocks associated with the dolerite sill north of Trevone Bay and on the Trevose Peninsula.

Although the bulk of the bioclastic material in the limestones is believed to be turbiditic in origin, there is no evidence to suggest that any elements of the conodont fauna were derived. However, the uneven distribution of species and the preponderance of broken elements would seem to be the result of sorting and current reworking. The few unusually productive horizons (for example Sample 17) are interpreted as lag deposits in which large, robust, or structurally stable elements were relatively concentrated, such as *Icriodus*, *Ancyrodella* and some of the lancet-shaped species of *Polygnathus*. In this respect the fauna of Sample 17 resembles two assemblages Krebs and Ziegler (1966) recovered from detrital reef limestones (lowermost Grenzschiefer) near the Middle/Upper Devonian boundary in the vicinity of Aachen, Germany. Sorting may also account for the absence of the more delicate broad platform elements, such as *Pol. asymmetricus*

and *Palmatolepis*, in samples where they would normally be expected to occur. Thus in cases where the differentiation of adjoining zones or parts of a single zone depends on the ranges of a few diagnostic species that are not closely related and of contrasting morphologies and hydrodynamic property, the precision of correlation of even the furthest offshore facies may be effected by sorting. The collection of large samples from widely spaced points along a horizon will tend to minimize the effect of sorting, but in sections like the Marble Cliff this is not usually possible.

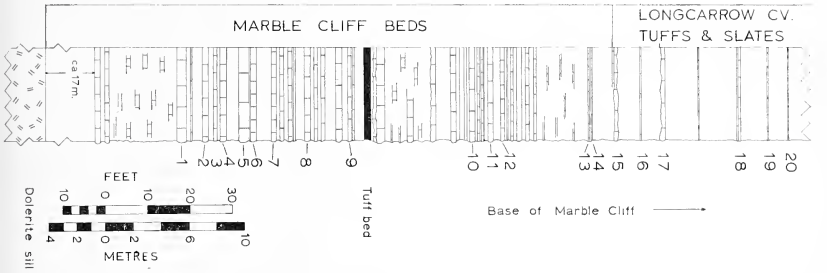

TEXT-FIG. 3. Stratigraphic succession at Marble Cliff showing sample-horizons.

SYSTEMATIC DESCRIPTIONS

The fossils described are deposited in the Sedgwick Museum, Cambridge, where they are numbered SM H9330–H9379. Other material is in the palaeontology collections of the Department of Geology, University of Hull, England.

Ancyrodella rotundiloba (Bryant)

Plate 65, figs. 5, 6, 8, 9

1879 *Polygnathus tuberculatus* Hinde, p. 366, pl. 17, fig. 10 [*non* fig. 9 = lectotype of *Pol. tuberculatus* selected by Bryant (1921, p. 25)].
1921 *Pol. rotundilobus* Bryant, pp. 26, 27, pl. 12, figs. 1–6; text-fig. 7.
1941 *Ancyrodella rotundiloba* (Bryant); Branson and Mehl, p. 202.
1957 *A. rotundiloba* (Bryant); Bischoff and Ziegler, p. 42, pl. 16, figs. 5–12, 14–17.
1958 *A. rotundiloba* (Bryant); Ziegler, pp. 44–5, pl. 11, figs. 11, 12.
1966 *A. rotundiloba rotundiloba* (Bryant); Krebs and Ziegler, pl. 1, figs. 10–13, 15–16.
1966 *A. rotundiloba* (Bryant) n. subsp.; Krebs and Ziegler, pl. 1, figs. 6–9.
1966 *A. rotundiloba rotundiloba* (Bryant); Glenister and Klapper, p. 799, pl. 85, figs. 9–13.
1967 *A. rotundiloba* (Bryant); Müller and Clark, p. 908, pl. 115, fig. 8; pl. 116, figs. 1–5; text-figs. 5, 6.

Material. Eight specimens; SM H9330–H9334.

Remarks. Müller and Clark (1967) have determined the ontogeny and extremes of variation in *A. rotundiloba* from the Squaw Bay Limestone of Michigan. The specimens from the Longcarrow Cove Tuffs and Slates are all relatively early growth stages and compare well with the series c to h (text-fig. 6) in Müller and Clark's ontogenetic scheme.

The Cornish specimens are unusual in having only a few nodes on the upper surface, no secondary keels and an extremely large basal cavity (or pit). In this latter feature, the specimens are perhaps closest to the 'typical' examples of *A. rotundiloba* reported by Krebs and Ziegler (1966) from the Walheim section near Aachen, Germany, particularly the specimen figured by them as Plate 1, figs. 10–11; the two small specimens from the same fauna, figured as *A. rotundiloba* n. subsp. (Pl. 63, figs. 6–7, 8–9), are interpreted as early growth stages of *A. rotundiloba*.

Range. Upper part of the Lower *Pol. asymmetricus* Zone to top of the Middle *Pol. asymmetricus* Zone (Ziegler 1962*b*, pp. 17, 19), corresponding to the Upper Devonian *Pharciceras lunulicosta* Zone (Iα) (Krebs and Ziegler 1966, pp. 748, 749). The entry of *A. rotundiloba* defines the base of the upper part of the Lower *Pol. asymmetricus* Zone. Sample-horizons 15–18, Longcarrow Cove Tuffs and Slates, Marble Cliff.

Palmatolepis transitans Müller

Plate 63, figs. 1, 8

1956 *Palmatolepis* (*Manticolepis*) *transitans* Müller, pp. 18, 19, pl. 1, figs. 1, 2.
1957 *Palmatolepis transitans* Müller; Bischoff and Ziegler, p. 81, pl. 16, figs. 24, 25 [*non* figs. 23, 26, 27 = *Polygnathus asymmetricus asymmetricus* Bischoff and Ziegler].
1958 *Palmatolepis transitans* Müller, Ziegler, p. 66, pl. 1, figs. 9, 11–13; pl. 2, figs. 1–3, 8.

Material. Five specimens; SM H9335, 6.

Remarks. SM H9336 (Pl. 61, fig. 8) differs from typical representatives of *Pal. transitans* in having no clearly differentiated outer lobe and an unusual large flaring basal cavity. This type of basal cavity is also seen in a specimen referred to *Pal. transitans* by Ziegler (1958, p. 2, fig. 2) and is the distinguishing character of *Palmatolepis*? *disparalvea* Orr and Klapper from the *S. hermanni–Pol. cristatus* Zone in Illinois and New York. Ziegler's specimen is from the upper part of the Lower *Pol. asymmetricus* Zone at the Martenberg section, near Adorf, in the Rheinisches Schiefergebirge.

Although the specimen at hand lacks the usually well-defined outer lobe of *Pal. transitans*, it is tentatively assigned to the species because the basal cavity is posterior in

---

EXPLANATION OF PLATE 63

Figs. 1, 8. *Palmatolepis transitans* Müller. 1*a*, *b*, Upper and lower views, SM H9335, Sample 8, Marble Cliff Beds. 8*a*, *b*, Upper and lower views, SM H9336, Sample 8, Marble Cliff Beds.

Fig. 2. *Polygnathus dengleri* Bischoff and Ziegler. *a*, *b*, Upper and lower views, SM H9351, Sample 13, Marble Cliff Beds.

Figs. 3, 7, 10. *Pol. cristatus* (?) Hinde. Specimens are from the Marble Cliff Beds. 3*a*, *b*, Upper and lower views of early growth stage, SM H9339, Sample 8. 7*a*, *b*, Upper and lower views, SM H9340, Sample 1. 10, Upper view, SM H9341, Sample 2.

Fig. 4. *Pol. cf. Pol. rugosus* Huddle. *a*, *b*, Upper and lower views, SM H9365, Sample 17, Longcarrow Cove Tuffs and Slates.

Fig. 5. *Pol. decorosus* Stauffer *s.l.* Lower view of early growth stage with large, flaring basal cavity, illustrating transition to *Schmidtognathus* Ziegler, SM H9342, Sample 8, Marble Cliff Beds.

Fig. 6. *Pol. linguiformis* Hinde. *a*, *b*, Upper and lower views of fragment, SM H9357, Sample 15, Longcarrow Cove Tuffs and Slates.

Fig. 9. *Pol. asymmetricus asymmetricus* Bischoff and Ziegler. *a*, *b*, Upper and lower views, SM H9337, Sample 1, Marble Cliff Beds.

All magnifications × 50.

1a

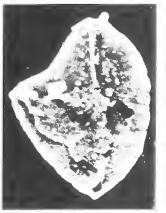

1b

2a

2b

3a

3b

4a

4b

5

6a

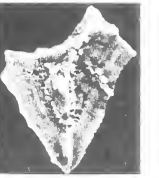

6b

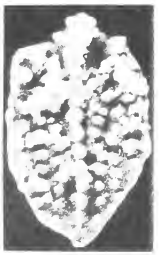

7a

7b

8a

8b

9a

9b

10

KIRCHGASSER, Conodonts from North Cornwall

position, the carina is only slightly curved, and it has an azygous node. It is similar in form to *Pol. asymmetricus asymmetricus* Bischoff and Ziegler, but in that subspecies the basal cavity is anterior (or in some cases central) in position and the azygous node is weakly defined or absent.

The posterior position of the basal cavity in the earliest species of *Palmatolepis* appears to be a more diagnostic character than the degree of development of the outer lobe and asygous node for differentiating the genus from closely related species of *Polygnathus*. In *Pol. asymmetricus* and *Pol. cristatus* the basal cavity is usually anterior or, more rarely, central in position. If one follows Ziegler's (1962*a*, 1966*b*) phylogenetic scheme along the line from variants of *Pol. decorosus* Stauffer *s.l.* to the *Pol. cristatus* group to *Pol. asymmetricus ovalis*, *Pol. asymmetricus asymmetricus*, and finally to *Palmatolepis*, the basal cavity shows a tendency to migrate from an anterior to central position in *Polygnathus* to a posterior position in *Palmatolepis*. There is also a parallel tendency towards a reduction in the size of the basal cavity, so that in possessing the large flaring basal cavity *Palmatolepis*? *disparalvea* and the two specimens discussed above deviate from the main evolutionary line in *Palmatolepis* which leads to *Palmatolepis punctata* Ulrich and Bassler. *Palmatolepis*? *disparalvea* belongs in *Palmatolepis* and is distinguished from *Pal. transitans s.s.* by its strongly differentiated outer lobe and much coarser ornamentation.

Range. Base of Lower *Pol. asymmetricus* Zone to upper part of the *Ancyrognathus triangularis* Zone (Ziegler 1962*b*, pp. 17, 20). Sample-horizons 1–9, Marble Cliff Beds, Marble Cliff.

Polygnathus asymmetricus ovalis Ziegler and Klapper

1957 *Polygnathus dubia dubia* Hinde; Bischoff and Ziegler, p. 88, pl. 16, fig. 19; pl. 21, figs. 1, 2.
1958 *Pol. dubia dubia* Hinde; Ziegler, pp. 57, 58, pl. 1, figs. 1–3, 7.
1964 *Pol. asymmetrica ovalis* Ziegler and Klapper; Ziegler, Klapper, and Lindström, pp. 422, 423.
1966 *Pol. asymmetrica ovalis* Ziegler and Klapper; Ziegler 1966*b*, p. 671, pl. 5, fig. 6.
1966 *Pol. asymmetrica ovalis* Ziegler and Klapper; Glenister and Klapper, p. 828, pl. 87, figs. 8–9.
1967 *Pol. dubius* Hinde; Müller and Clark, p. 916, pl. 115, figs. 5, 6.

Material. Five specimens.

Range. Base of Lower *Pol. asymmetricus* Zone into Upper *Pol. asymmetricus* Zone (Ziegler 1962*b*, table 2). Sample-horizons 1–8, Marble Cliff Beds, Marble Cliff.

Polygnathus asymmetricus asymmetricus Bischoff and Ziegler

Plate 63, fig. 9

1957 *Polygnathus dubia asymmetrica* Bischoff and Ziegler, pp. 88, 89, pl. 16, figs. 18, 20–2; pl. 21, fig. 3.
1958 *Pol. dubia asymmetrica* Bischoff and Ziegler; Ziegler, pp. 57, 58, pl. 1, figs. 4–6, 8, 10.
1964 *Pol. asymmetrica asymmetrica* Bischoff and Ziegler; Ziegler and Klapper in Ziegler, Klapper, and Lindström, p. 423.
1966 *Pol. asymmetrica* Ziegler, 1966*b*, pl. 5, figs. 9, 10.

Material. Eighteen specimens; SM H9337, H9338.

Remarks. According to Ziegler (1962*a*, 1966*b*) *Pol. asymmetricus ovalis* is the stem form of the lineage that gave rise to *Palmatolepis* during the early part of the Late Devonian. The important trends were (1) an increase in platform asymmetry by expansion of the outer side to form a lobe, (2) the development of an azygous node, (3) a reduction in the size of the basal cavity, and (4) migration of the basal cavity to a posterior position on the platform. The last mentioned is here regarded as the most diagnostic feature for differentiating *Palmatolepis* from closely related species of *Polygnathus*. *Pal. transitans* is most closely related to *Pol. asymmetricus asymmetricus*. In *Pol. asymmetricus asymmetricus* the outer side has not developed into a lobe, an azygous node is either missing or weakly developed and the basal cavity is in the centre or anterior part of the platform.

Range. Base to top of *Pol. asymmetricus* Zone (Ziegler 1962*b*, table 2). Sample-horizons 1–8 Marble Cliff Beds, Marble Cliff.

Polygnathus cristatus (?) Hinde

Plate 63, figs. 3, 7, 10

[?] 1879 *Polygnathus cristatus* Hinde, p. 366, pl. 17, fig. 11.
[?] 1921 *Pol. cristatus* Hinde; Bryant, p. 24.
[?] 1933 *Pol. cristata* Hinde; Branson and Mehl 1933*a*, p. 147, pl. 11, fig. 10 [the holotype].
1957 *Pol. cristata* Hinde; Bischoff and Ziegler, pp. 86, 87, pl. 15, figs. 1–7, 10 [*non* figs. 8–9, 11–13, 16 = *Pol. asymmetricus asymmetricus* Bischoff and Ziegler]; pl. 17, figs. 12, 13.
1964 *Pol. cristata* Hinde; Orr, pp. 13, 14, pl. 3, figs. 4–8, 10; text-fig. 4.
1966 *Pol. cristata* Hinde; Ziegler 1966*b*, pp. 670, 671, pl. 4, figs. 17, 18, 19–21 [?], 22, 23; pl. 5, figs. 1, 2, 3–4 [?], 5.
1968 *Pol. cristatus* Hinde; Orr and Klapper, pl. 139, figs. 1–4, 8, 9.

Material. Thirty specimens; SM H9339–H9341.

Diagnosis. The platform is broad and oval-shaped (symmetrical) in outline, with a flattened anterior and pointed posterior margins. The coarse ornamentation on the upper surface is distinctive; rows of discrete rounded nodes are aligned roughly parallel to a gently curved median carina of similar but larger nodes. In late growth stages, the more median rows tend to diverge from the carina near the anterior end, producing furrows on both sides of the carina. The nodes are more irregularly arranged and more closely spaced in late growth stages. The lower surface has a median keel with a well-developed basal cavity located in the anteriormost third of the platform.

Remarks. The name *Pol. cristatus* Hinde rather loosely refers to broad platform conodonts similar to *Pol. asymmetricus ovalis* but which are thicker and more coarsely ornamented. Bischoff and Ziegler (1957) and Ziegler (1966*b*) interpreted *Pol. cristatus* as a highly variable species. They included in the species forms with rather pointed anterior platform margins and more centrally located basal cavities, as well as large forms with relatively small densely packed nodes on the upper surface that are fused into irregular networks or ramifying ridges. These variants were not found in the Marble Cliff Beds. The Marble Cliff specimens are remarkably similar to the specimens figured by Orr (1964) from the *S. hermanni–Pol. cristatus* Zone in the Alto Formation of Southern Illinois.

The assignment of the specimens to *Pol. cristatus* Hinde is questioned because the generally held concept of the species, which focuses on *Pol. cristatus* Hinde *sensu*

Bischoff and Ziegler, is not in accord with Hinde's holotype (British Museum (N.H.) A4319), from the 'Conodont-bed' (= North Evans Limestone) on Eighteenmile Creek, North Evans, New York. In this specimen, which only shows the upper side, the rows of nodes converge posteriorly, and the outermost row parallels the platform margin; also, some of the anterior nodes are clearly fused into ridges. Anteriorly the rows of nodes diverge from the carina to such a degree that the anterior end of the platform appears divided into lobes. These features, which are not seen in the hypotypes or the specimens at hand, are more characteristic of *Ancyrodella* than *Polygnathus*.

Range. *Pol. cristatus* Hinde *sensu* Bischoff and Ziegler ranges from within the *S. hermanni–Pol. cristatus* Zone (Ziegler 1966*b*, p. 675) to the top of the Lower *Pol. asymmetricus* Zone (Bischoff and Ziegler 1957, table 4; Ziegler 1962*b*, p. 19). Sample-horizons 1–8, Marble Cliff Beds, Marble Cliff.

Polygnathus decorosus Stauffer *s.l.*

Plate 63, fig. 5; Plate 64, figs. 1–8

1938 *Polygnathus decorosus* Stauffer, p. 438, pl. 53, figs. 1, 5, 6, 10, 11, 15, 16, 20, 30.
1957 *Pol. foliata* Bryant; Müller and Müller, pp. 1086, 1087, pl. 135, fig. 1.
1957 *Pol. decorosa* Stauffer; Bischoff and Ziegler, p. 87.
1957 *Pol. xyla* Stauffer; Bischoff and Ziegler, p. 101, pl. 5, figs. 11–17.
1964 *Pol. decorosa* Stauffer; Orr, pp. 14, 16, pl. 1, figs. 3, 5, 7; pl. 3, fig. 2.
1966 *Pol. decorosa* Stauffer *s.l.*; Ziegler 1966*b*, pl. 3, figs. 1–4; pl. 4, figs. 1–4; pl. 6, figs. 7–17.
1966 *Pol. xyla* Stauffer; Wittekindt, p. 642, pl. 3, figs. 18, 19.
1966 *Pol. decorosus* Stauffer; Anderson, p. 411, pl. 50, figs. 6–8, 10, 11, 15, 19.
1967 *Pol. foliata* Bryant; Clark and Ethington, p. 61, pl. 7, fig. 7 [*non* pl. 5, fig. 7 = *Pol. foliatus* Bryant].
1967 *Pol. normalis* Miller and Youngquist; Clark and Ethington, p. 63, pl. 4, fig. 3 [*non* pl. 5, fig. 10 = *Pol. foliatus* [?] Bryant].
1967 *Pol. foliatus* Bryant; Müller and Clark, p. 916, pl. 115, fig. 4.

Material. 185 specimens; SM H9342–H9350.

Diagnosis. *Polygnathus decorosus* Stauffer *s.l.* is a morphologically simple polygnathid with a narrow lanceolate platform and relatively long free blade. The unit is moderately to strongly bowed and arched. The ornamentation is weakly developed and consists of nodes or transverse ridges along the platform margins. The free blade is usually uniform in height and carries numerous teeth of nearly equal size and height. In early growth stages (Pl. 64, figs. 1, 2, 7, 8) the platform is symmetrical in outline (the lateral margins are nearly parallel), shorter than the free blade, and the relatively large basal cavity is situated at the point where the free blade joins the platform. In late growth stages (Pl. 64, figs. 3–6) the platform is more asymmetrical, about as long as the free blade, and the basal cavity is less conspicuous and lies posterior of the join between the free blade and the platform.

Remarks. *Pol. decorosus s.l.* is the most common conodont in the faunas from the Marble Cliff. It is an extremely variable species (Ziegler 1966*b*) and many of the Cornish specimens show gradations toward *Pol. foliatus* Bryant and *Pol. pennatus* Hinde and related species. Müller and Müller (1957) regarded *Pol. decorosus* as a synonym of *Pol. foliatus* Bryant. However, in late growth stages of *Pol. foliatus* the platform is broader and distinctly asymmetrical, the ornamentation on the posterior half consists of

numerous small nodes (Bryant 1921, p. 24; Huddle 1934, p. 99), and the teeth on the free blade increase in height anteriorly.

Ziegler (1966*b*) interprets *Pol. decorosus s.l.* as a stem form from which several new species and one genus evolved during late Middle and early Late Devonian time. These forms include: *Pol. varcus* (reduced platform, long free blade), *Pol. foliatus* and *Pol. normalis* Miller and Youngquist (broad, asymmetrical platforms with noded or ribbed ornamentation), *Pol. pennatus* (coarse radially ribbed ornamentation), *Pol. cristatus* group (broad, symmetrical platforms with coarse nodes) and *Schmidtognathus* (large, asymmetrical basal cavity). Compared to *Pol. decorosus s.l.*, these forms also tend to have more highly developed free blades with teeth of varying size and height and well-defined crimps.

Range. Because of the present taxonomic tangle that surrounds *Pol. decorosus* and closely related species (*Pol. foliatus*, *Pol. normalis*, *Pol. pennatus*, among others) and because of their relatively long ranges, these common lanceolate polygnathids have limited biostratigraphic value. *Pol. decorosus s.l.* apparently ranges from the lower Middle Devonian (Wittekindt 1966, table 1) into the upper part of the Upper Devonian (Famennian) (Ziegler 1966*b*, text-fig. 4). Sample-horizons 31, Trevose Slates, Trevone Bay; 33, Trevose Slates, Rock; 1–13, Marble Cliff Beds; and 17, 18, Longcarrow Cove Tuffs and Slates, Marble Cliff.

Polygnathus dengleri Bischoff and Ziegler

Plate 63, fig. 2; Plate 64, fig. 4; Plate 66, fig. 2

1957 *Polygnathus dengleri* Bischoff and Ziegler, pp. 87, 88, pl. 15, figs. 14, 15, 17–24; pl. 16, figs. 1–4.
1966 *Pol. dengleri* Bischoff and Ziegler; Ziegler 1966*b*, pp. 671, 673, pl. 6, figs. 1–6.
1967 *Pol. dengleri* Bischoff and Ziegler; Müller and Clark, p. 916, pl. 115, figs. 3, 7.

Material. Ten specimens; SM H9351–H9353.

Diagnosis. The platform is narrow, oval-shaped, and symmetrical in outline, with a pointed posterior margin. The free blade is short and high. The ornamentation on the flat upper surface consists of weakly developed short transverse ridges along the platform margin; the ridges do not extend into the smooth weakly developed troughs that parallel the median carina.

EXPLANATION OF PLATE 64

Figs. 1–8. *Pol. decorosus* Stauffer *s.l.* 1*a*, *b*, *c*, Upper, lower, and lateral views of early growth stage, SM H9343, Sample 8, Marble Cliff Beds. 2*a*, *b*, *c*, Upper, lower, and lateral views of early growth stage, SM H9344, Sample 8, Marble Cliff Beds. 3, Oblique view of specimen transitional to *Pol. pennatus* Hinde, SM H9345, Sample 8, Marble Cliff Beds. 4, Upper view of late growth stage, SM H9346, Sample 17, Longcarrow Cove Tuffs and Slates. 5*a*, *b*, *c*, Upper, lower, and lateral views of late growth stage, SM H9347, Sample 17, Longcarrow Cove Tuffs and Slates. 6*a*, *b*, *c*, Upper, lower, and lateral view of late growth stage, SM H9348, Sample 17, Longcarrow Cove Tuffs and Slates. 7*a*, *b*, *c*, Upper, lower, and lateral views of early growth stage, SM H9349, Sample 8, Marble Cliff Beds. 8*a*, *b*, *c*, Upper, lower, and lateral views of early growth stage, SM H9350, Sample 8, Marble Cliff Beds.

Fig. 9. *Pol. linguiformis* Hinde. Upper view, SM H9358, Sample 17, Longcarrow Cove Tuffs and Slates.

All magnifications × 50.

1a

1b

1c

2a

2b

2c

3

4

5a

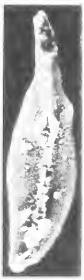

5b

5c

6a

6b

6c

7a

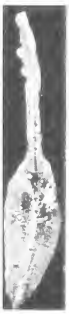

7b

7c

8a

8b

8c

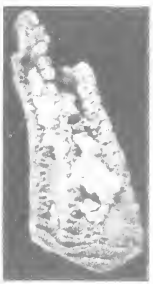

9

KIRCHGASSER, Conodonts from North Cornwall

SERIES	MIDDLE DEVONIAN	UPPER DEVONIAN?																			UPPER DEVONIAN					
STAGE	GIVETIAN																				FRASNIAN					
Ammonoid Zone	*M. terebratum*																				*P. lunulicasta* (Ia)					
Conodont Zone	*Pol. varcus*	Lower *Pol. asymmetricus*																								
		lower part																			upper part					
Conodont species / Sample	TREVOSE SLATES	MARBLE CLIFF BEDS																			LONGCARROW CV TUFFS & SLATES					
	30 31 33	1 2 3 4 5 6 7 8 9 10 11 12 13 14 15 16 17 18 19 20																								
Polygnathus varcus Stauffer	3 17 1						1		1				1													24
Pol. linguiformis Hinde	6 36 8				1				1						1		1									54
Pol. spp.	1 4	17 1 2			1	8	1	11		9	1	12	13	6	1		29	1	3							121
Neoprioneadus alatus (Hinde)	1					1			1			1					1									5
Hindeodella spp.	7 1	1 1				2		3				1			1		2	4								23
Roundya spp.	1					1			1																	3
Schmidtognathus hermanni Ziegler	1									1?																2
Pol. decorosus Stauffer s.l.	3 2	8 2 16		1	34	1	56		8	1	10	14					22	5								185
N. pronus (Huddle)	2	1			3		1								1		1									9
Icriodus symmetricus Branson & Mehl	2																2									4
Ozarkodina spp.	2	2 2			2		1										3	1								13
Bryantodus spp.	1	1			4		2	2			3	1					4									18
Pol. asymmetricus ovalis Ziegler & Klapper		1			1		3																			5
Pol. asymmetricus asymmetricus Bischoff & Ziegler		1	4	3	6	1	3																			18
S. wittekindti Ziegler	3	1			1		1				1															7
Pol. cristatus [?] Hinde	6 1 4	1 3 3 12																								30
Palmatolepis transitans Muller	1 1				2	1																				5
Pal. foliatus Bryant	1	1 3 1 2															7									15
Ligonodina spp.	1 1			1	1										1		4									9
Pal. variabilis Bischoff & Ziegler	1				1																					2
S. peracutus (Bryant)						1																				1
Pol. bryanti Huddle						2																				2
Pol. pennatus Hinde						1		1				1?			1?		4									8
Trichonodella sp.						1																				1
B. grandis Bischoff & Ziegler						1																				1
Spathognathodus brevis Bischoff & Ziegler								1																		1
B. pravus (Bryant)								1																		1
Pol. dengleri Bischoff & Ziegler								5				2			1		2									10
Lanchodina sp.								2																		2
B. bicuminatus Bischoff & Ziegler								1									1									2
Lanchodina discreta Ulrich & Bassler									1																	1
Pol. sp. Ziegler									1					1			1									3
Anguladus sp.									1																	1
Ancyrodella rotundiloba (Bryant)															3		4	1?								8
Pol. subserratus Branson & Mehl																	1									1
Pol. cf. Pol. rugosus Huddle																	2									2
Icriodus spp.																	4									4
O. immersa [?] (Hinde)																	1									1
Indeterminate fragments	6 12	4 1 21 2 25 32 2 13 17 7 4 11 19													2		24 28									
Totals	25 77 15	47 7 53 3 32 106 10 126 23 28 6 40 50 7 12 0 120 40 3 0																								
Sample wt. (kg)	5 5 5	1.0 5 1.0 5 5 1.5 5 1.5 5 1.5 1.5 1.5 1.0 5 1.0 5 1.5 1.0 5 5																								

TEXT-FIG. 4. Distribution of conodonts in samples from Trevone Bay, Rock, and Marble Cliff.

Remarks. The specimens are early growth stages and compare most closely with specimens of *Pol. dengleri* figured by Ziegler (1966*b*).

Range. Pol. dengleri enters somewhat above the base of the Lower *Pol. asymmetricus* Zone (Ziegler 1966*b*, tables) and ranges to the top of the zone (Bischoff and Ziegler 1957, table 4; Ziegler 1958, tables 2, 10; Ziegler 1962*b*, p. 17). Sample-horizons 8–13, Marble Cliff Beds, and 15–17, Longcarrow Cove Tuffs and Slates, Marble Cliff.

Polygnathus foliatus Bryant

Plate 65, figs. 1, 2

1921 *Polygnathus foliatus* Bryant, p. 24, pl. 10, figs. 13–16.
1934 *Pol. foliata* Bryant; Huddle, p. 99, pl. 8, figs. 14–17.

[*non*] 1957 *Pol. foliata* Bryant; Bischoff and Ziegler, p. 90, pl. 4, figs. 1–4 [= *Polygnathus* sp. ?]
[*non*] 1957 *Pol. foliata* Bryant; Müller and Müller, pp. 1086, 1087, pl. 135, fig. 1 [= *Pol. decorosus* Stauffer *s.l.*].
1967 *Pol. foliata* Bryant; Clark and Ethington, p. 61, pl. 5, fig. 7 [*non* pl. 7, fig. 7 = *Pol. decorosus* Stauffer *s.l.*].

Material. Fifteen specimens; SM H9354–H9356.

Remarks. See *Polygnathus decorosus* Stauffer *s.l.*

Range. Sample-horizons 1–8, Marble Cliff Beds, and 17, Longcarrow Cove Tuffs and Slates, Marble Cliff.

Polygnathus linguiformis Hinde

Plate 63, fig. 6; Plate 64, fig. 9; Plate 66, fig. 4

1879 *Polygnathus linguiformis* Hinde, p. 367, pl. 17, fig. 15.
1921 *Pol. linguiformis* Hinde; Bryant, p. 25, pl. 11, figs. 1–9; pl. 14, fig. 2.

EXPLANATION OF PLATE 65

Figs. 1–2. *Polygnathus foliatus* Bryant. 1*a*, *b*, Upper and lower views, SM H9354, Sample 17, Longcarrow Cove Tuffs and Slates. 2*a*, *b*, Upper and lower views, SM H9355, Sample 17, Longcarrow Cove Tuffs and Slates.

Figs. 3, 7. *Schmidtognathus wittekindti* Ziegler. 3*a*, *b*, *c*, Upper, lower, and lateral views of early growth stage, SM H9369, Sample 12, Marble Cliff Beds. 7*a*, *b*, Upper and lower views of late growth stage, SM H9370, Sample 1, Marble Cliff Beds.

Fig. 4. *Pol. dengleri* Bischoff and Ziegler. *a*, *b*, Upper and lower views, SM H9352, Sample 8, Marble Cliff Beds.

Figs. 5, 6, 8, 9. *Ancyrodella rotundiloba* (Bryant). Specimens are from the Longcarrow Cove Tuffs and Slates. 5, Upper view of early growth stage, SM H9330, Sample 17. 6*a*, *b*, Upper and lower views, SM H9331, Sample 15. 8*a*, *b*, Upper and lower views, SM H9332, Sample 15. 9*a*, *b*, Upper and lower views of early growth stage, SM H9334, Sample 17.

All magnifications × 50.

EXPLANATION OF PLATE 66

Fig. 1. *Schmidtognathus hermanni* Ziegler. *a*, *b*, *c*, Upper, lower, and lateral views of early growth stage, SM H9368, Sample 31, Trevose Slates, Trevone Bay.

Fig. 2. *Pol. dengleri* Bischoff and Ziegler. *a*, *b*, Upper and lower views, SM H9353, Sample 8, Marble Cliff Beds.

Fig. 3. *Icriodus symmetricus* Branson and Mehl. Upper view, SM H9374, Sample 31, Trevose States, Trevone Bay.

Fig. 4. *Pol. linguiformis* Hinde. *a*, *b*, Upper and lower views, SM H9359, Sample 31, Trevose Slates, Trevone Bay.

Figs. 5, 8. *Bryantodus biculminatus* Bischoff and Ziegler. 5, Lateral view, SM H9371, Sample 8, Marble Cliff Beds. 8, Lateral view, SM H9372, Sample 17, Longcarrow Cove Tuffs and Slates.

Fig. 6. *Hindeodella* sp. Lateral view, SM H9373, Sample 8, Marble Cliff Beds.

Fig. 7. *Neoprioniodus pronus* (Huddle). Lateral view, SM H9376, Sample 8, Marble Cliff Beds.

Figs. 9–11. *Pol. varcus* Stauffer. Specimens are from the Trevose Slates, Trevone Bay. 9*a*, *b*, Upper and lower views, SM H9362, Sample 31. 10*a*, *b*, *c*, Upper, lower, and lateral views, SM H9363, Sample 30. 11*a*, *b*, Upper and lower views, SM H9364, Sample 31.

Fig. 12. *Ozarkodina immersa* [?] (Hinde). Lateral view, SM H9377, Sample 17, Longcarrow Cove Tuffs and Slates.

Fig. 13. *N. alatus* (Hinde). Lateral view, SM H9375, Sample 12, Marble Cliff Beds.

All magnifications × 50.

1a

1b

2a

2b

3a

3b

3c

4a

4b

5

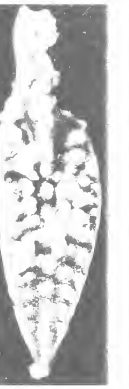

7a

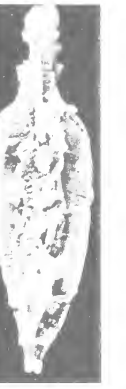

7b

6a

6b

8a

8b

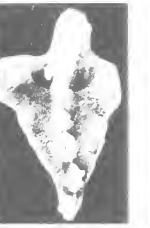

9a

9b


1a


1b


1c


2a


2b


3


4a


4b


5

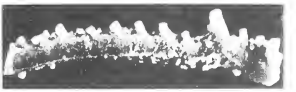
6


7


8


9a


9b

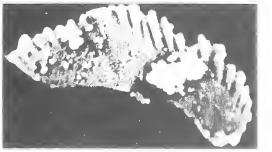
12


10a


10b


10c


11a


11b


13

KIRCHGASSER, Conodonts from North Cornwall

1957 *Pol. linguiformis* Hinde; Rhodes and Dineley, pp. 365, 366, pl. 37, figs. 17–19, 21; pl. 38, fig. 3.
1957 *Pol. linguiformis* Hinde; Bischoff and Ziegler, pp. 92, 93, pl. 1, figs. 1–13; pl. 16, figs. 30–5; pl. 17, figs. 1–8; pl. 19, fig. 18.
1966 *Pol. linguiformis* Hinde; Ziegler 1966*a*, pl. 1, figs. 7–10.
1966 *Pol. linguiformis linguiformis* Hinde; Wittekindt, pp. 635, 636, pl. 2, figs. 10–12.

Material. Fifty-four specimens; SM H9357–H9361.

Remarks. Polygnathus linguiformis Hinde is common and well preserved in the Trevose Slate faunas and comparatively rare in faunas from the Marble Cliff Beds and the Longcarrow Cove Tuffs and Slates. Specimens from the Trevose Slates show extreme ranges in size and in the coarseness of ornamentation. Two of the largest forms (late growth stages) from Sample 31 have two diagonal rows of nodes in the anterior part of the platform, which is a diagnostic feature of *Pol. linguiformis transversus* Wittekindt. However, the two specimens have much more weakly developed ridges than in *Pol. linguiformis transversus* and in all other features they are closest to *Pol. linguiformis* Hinde.

Range. Lower Devonian (Bischoff and Ziegler 1957, p. 93) to top of Upper *Pol. asymmetricus* Zone, (Ziegler 1962*b*, p. 19). Sample-horizons 30, 31, Trevose Slates, Trevone Bay; 33, Trevose Slates, Rock; 3–8, Marble Cliff Beds; and 15–17, Longcarrow Cove Tuffs and Slates, Marble Cliff.

Polygnathus varcus Stauffer

Plate 66, figs. 9–11

1940 *Polygnathus varcus* Stauffer, p. 430, pl. 60, figs. 49, 53, 55.
1940 *Pol. xylus* Stauffer, pp. 430, 431, pl. 60, figs. 42, 50, 54, 65–7, 69, 72–4, 78, 79.
1957 *Pol. varca* Stauffer; Rhodes and Dineley, p. 366, pl. 37, figs. 22, 23; pl. 38, fig. 7.
1957 *Pol. varca* Stauffer; Bischoff and Ziegler, pp. 98, 99, pl. 18, figs. 32–5; pl. 19, figs. 7–9.
[*non*] 1957 *Pol. xyla* Stauffer; Bischoff and Ziegler, p. 101, pl. 5, figs. 11–17 [= *Pol. decorosus* Stauffer *s.l.*].
1966 *Pol. varca* Stauffer; Ziegler 1966*a*, pl. 1, fig. 6.
1966 *Pol. varca* Stauffer; Wittekindt, pp. 639, 640, pl. 3, figs. 5–10.
[*non*] 1966 *Pol. xyla* Stauffer; Wittekindt, p. 642, pl. 3, figs. 18–19 [= *Pol. decorosus* Stauffer *s.l.*].
1966 *Pol. varca* Stauffer; Glenister and Klapper, pp. 830, 831, pl. 95, figs. 12–13 [*non* figs. 14, 15–16 = *Pol. decorosus* Stauffer *s.l.*].

Material. Twenty-four specimens; SM H9362–H9364.

Diagnosis. Pol. varcus has a short, narrow, weakly ornamented platform and an extraordinarily long free blade, up to twice as long as the platform. The ratio of platform length to free blade length appears to remain nearly constant through all growth stages. The sides of the platform are strongly folded upward, forming deep furrows on both sides of the median carina. The free blade is particularly distinctive; it is uniform in height and has a series of 10–20 teeth of variable size and shape but nearly equal height.

Remarks. All of the specimens at hand are intermediate and late growth stages, with markedly asymmetrical platform outlines. Anterior of the platform's midpoint, the margins abruptly constrict, especially on the outer side. The margin on the outer side then flares strongly outward, in a semicircular arc, and joins the free blade at a more anterior position than does the straighter inner margin. The posterior end of the

platform is symmetrical and the margins converge uniformly to a point. In details of platform outline and in development of the free blade, the specimens at hand compare closely with specimens of *Pol. varcus* figured by Rhodes and Dineley (1957) from South Devon and by Bischoff and Ziegler (1957) and Ziegler (1966*a*) from the Rheinisches Schiefergebirge.

Specimens similar to *Pol. varcus* but with longer, more symmetrical and more highly ornamented platforms and shorter free blades with fewer teeth have been interpreted by Bischoff and Ziegler (1957) and Wittekindt (1966) as *Pol. xylus* Stauffer, a species which Glenister and Klapper (1966, p. 831) regard as a synonym of *Pol. varcus*. Forms of this type, for example the specimens figured herein as Plate 64, figs. 2, 7, and specimens of *Pol. varcus* figured by Glenister and Klapper (1966, pl. 95, figs. 14, 15–16) belong in *Pol. decorosus* Stauffer *s.l.* Glenister and Klapper (1966) suggested that in the ontogeny of *Pol. varcus* the length of the platform increases in proportion relative to the free blade and that the ornamentation becomes more highly developed. These changes are not seen in the Cornish specimens, even in the latest growth stages (Pl. 66, fig. 10), and it would seem that their analysis applies more closely to *Pol. decorosus* Stauffer *s.l.* rather than to *Pol. varcus*.

Range. *Pol. varcus* Zone (Bischoff and Ziegler 1957, p. 30) to top of Lower *Pol. asymmetricus* Zone (Ziegler 1962*b*, table 2). Sample-horizons 30–1, Trevose Slates, Trevone Bay; 33, Trevose Slates, Rock; 6–13, Marble Cliff Beds, Marble Cliff.

Schmidtognathus hermanni Ziegler

Plate 66, fig. 1

1966 *Schmidtognathus hermanni* Ziegler 1966*b*, pp. 664, 665, pl. 3, figs. 5–26.

Material. Two specimens; SM H9368.

Remarks. The figured specimen from the Trevose Slates (Sample 31) is an early growth stage and has the enlarged flaring basal cavity and narrow weakly ornamented platform of *Schmidtognathus hermanni*. *S. hermanni* developed from variants of *Pol. decorosus* Stauffer *s.l.* with enlarged basal cavities during the Late Middle Devonian; the link between these species is clearly seen in early growth stages (Ziegler 1966*b*, pl. 3, figs. 1–12).

Range. Base of *S. hermanni–Pol. cristatus* Zone into the lower part of the Lower *Pol. asymmetricus* Zone (Ziegler 1966*b*, p. 657). Ziegler (1966*b*, tables 1, 2, p. 659) also reports *S. hermanni* from the uppermost part of the *Pol. varcus* Zone. Sample horizons 31, Trevose Slates, Trevone Bay and 10, Marble Cliff Beds, Marble Cliff.

Schmidtognathus wittekindti Ziegler

Plate 65, figs. 3, 7

1966 *Schmidtognathus wittekindti* Ziegler 1966*b*, pp. 665, 666, pl. 1, figs. 11–16; pl. 2, figs. 1–10.

Material. Seven specimens; SM H9369–H9370.

Remarks. The specimens at hand are distinguished from a closely related species, *S. peracuta* (Bryant), by their narrower platform and very high free blade with the highest teeth in the middle.

Range. Upper part of the *S. hermanni–Pol. cristatus* Zone into the upper part of the Lower *Pol. asymmetricus* Zone (Ziegler 1966*b*, p. 666, text-fig. 2). Sample-horizons 1–12, Marble Cliff Beds, Marble Cliff.

Acknowledgements. I particularly wish to thank Professor M. R. House for introducing me to the geology of North Cornwall and for his generous assistance through all phases of the investigation. I also thank Dr. G. Gauss for providing unpublished structural data on the area and for his assistance in the field. I gratefully acknowledge the technical assistance of Mr. J. Goldspink and Mr. B. Nettleton and the field assistance of Mr. J. Senior. Dr. R. H. Bate kindly made available the Hinde and Bryant conodont collections at the British Museum (Natural History). The project was undertaken as part of a year of research at University of Hull, supported by a Fulbright–Hays Grant.

REFERENCES

ANDERSON, W. I. 1966. Upper Devonian conodonts and the Devonian-Mississippian boundary of north-central Iowa. *J. Paleont.* **40**, 395–415, pl. 48–52.

BISCHOFF, G. 1956. Oberdevonische Conodonten (to Iδ) aus dem Rheinischen Schiefergebirge. *Notizbl. hess. Landesamt. Bodenforsch.* **84**, 115–37, pl. 8–10.

—— and ZIEGLER, W. 1957. Die Conodontenchronologie des Mitteldevons und des tiefsten Oberdevons. *Abh. hess. Landesamt. Bodenforsch.* **22**, 1–136, pl. 1–21.

BRAITHWAITE, C. J. R. 1966. The petrology of Middle Devonian limestones in South Devon, England. *J. sedim. Petrol.* **36**, 176–92.

BRANSON, E. B. and MEHL, M. G. 1933*a*. A study of Hinde's types of conodonts preserved in the British Museum. *Univ. Mo. Stud.* **8**, 133–56, pl. 11–12.

—— —— 1933*b*. Conodonts from the Grassy Creek Shale of Missouri. Ibid. **8**, 171–259, pl. 13–21.

—— —— 1941. The recognition and interpretation of mixed conodont faunas. *Denison Univ., Bull., J. Sci. Lab.* **25**, 195–209.

BRYANT, W. L. 1921. The Genesee conodonts. *Buffalo Soc. Nat. Sci.* **13**, 1–59, pl. 1–16.

CLARK, D. L. and ETHINGTON, R. L. 1967. Conodonts and zonation of the Upper Devonian in the Great Basin. *Mem. geol. Soc. Am.* **103**, 1–94, pl. 1–9.

DEWEY, H. 1914. The geology of North Cornwall. *Proc. Geol. Ass., Lond.* **35**, 154–79.

DINELEY, D. L. 1961. The Devonian System in South Devonshire. *Fld Stud.* **1**, 121–40.

—— and RHODES, F. H. T. 1956. Conodont horizons in the west and south-west of England. *Geol. Mag.* **93**, 242–8.

ETHINGTON, R. L. 1965. Late Devonian and Early Mississippian conodonts from Arizona and New Mexico. *J. Paleont.* **39**, 566–89, pl. 67–8.

FOX, H. 1895. Notes on the cherts and associated rocks of Roundhole Point (Permizen Point), Cataclews Point, and Dinas Head, west of Padstow. *Trans. R. geol. Soc. Cornwall*, **11**, 687–724.

GAUSS, G. A. 1966. Some aspects of the slaty cleavage in the Padstow area of N. Cornwall. *Proc. Ussher Soc.* **1**, 221–4.

—— 1967. Structural aspects of the Padstow area, North Cornwall. Ibid. **1**, 284–5.

GLENISTER, B. F. and KLAPPER, G. 1966. Upper Devonian conodonts from the Canning Basin, Western Australia. *J. Paleont.* **40**, 777–842, pl. 85–96.

GOLDRING, R. and others. 1968. Devonian of southern Britain. *Int. Symp. Devonian System, Calgary*, **1**, 1–14.

HINDE, G. J. 1879. On conodonts from the Chazy and Cincinnati Group of the Cambro-Silurian, and from the Hamilton and Genesee-Shale divisions of the Devonian, in Canada and the United States. *Q. Jl geol. Soc. Lond.* **35**, 351–69, pl. 15–17.

HOUSE, M. R. 1956. Devonian goniatites from North Cornwall. *Geol. Mag.* **93**, 257–62.

—— 1961. The Devonian succession of the Padstow area, North Cornwall. *Abstr. Proc. Conf. Geol. Geomorph. SW Engld, 1960*, 4–5.

—— 1963. Devonian ammonoid successions and facies in Devon and Cornwall. *Q. Jl geol. Soc. Lond.* **119**, 1–27, pl. 1–4.

—— and SELWOOD, E. B. 1966. Palaeozoic palaeontology in Devon and Cornwall, in *Present views on some aspects of the geology of Cornwall and Devon*. Blackford, Truro, 45–86, pl. 1–4.

HUDDLE, J. W. 1934. Conodonts from the New Albany Shale of Indiana. *Bull. Am. Paleont.* **21,** 1–136, pl. 1–12.

KREBS, W. and ZIEGLER, W. 1966. Über die Mitteldevon/Oberdevon-Grenze in der Riffazies bei Aachen. *Fortschr. Geol. Rheinld Westf.* **9,** 731–54, pl. 1–2.

MATTHEWS, S. C. 1962. A Middle Devonian conodont fauna from the Tamar Valley. *Proc. Ussher Soc.* **1,** 27–8.

MÜLLER, K. J. 1956. Zur Kenntnis der Conodonten-Fauna des europäischen Devons, 1. Die Gattung *Palmatolepis. Abh. senckenb. naturforsch. Ges.* **494,** 1–70, pl. 1–11.

—— and CLARK, D. L. 1967. Early Late Devonian conodonts from the Squaw Bay Limestone in Michigan. *J. Paleont.* **41,** 902–19, pl. 115–18.

—— and MÜLLER, E. M. 1957. Early Upper Devonian (Independence) conodonts from Iowa, part I. Ibid. **31,** 1069–1108, pl. 135–42.

ORR, R. W. 1964. Conodonts from the Devonian Lingle and Alto Formations of southern Illinois. *Circ. Ill. St. geol. Surv.* **361,** 1–28, pl. 1–4.

—— and KLAPPER, G. 1968. Two new conodont species from Middle-Upper Devonian boundary beds of Indiana and New York. *J. Paleont.* **42,** 1066–75, pl. 139–40.

POLLOCK, C. A. 1968. Lower Upper Devonian conodonts from Alberta, Canada. Ibid. **42,** 415–43, pl. 61–4.

REID, C., BARROW, G. and DEWEY, H. 1910. The geology of the country around Padstow and Camelford. *Mem. geol. Surv. U.K.* 1–120.

RHODES, F. H. T. and DINELEY, D. L. 1957. Devonian conodont faunas from southwest England. *J. Paleont.* **31,** 353–69, pl. 37–8.

STAUFFER, C. R. 1938. Conodonts of the Olentangy Shale. Ibid. **12,** 411–43, pl. 48–53.

—— 1940. Conodonts from the Devonian and associated clays of Minnesota. Ibid. **14,** 417–35, pl. 58–60.

ULRICH, E. O. and BASSLER, R. S. 1926. A classification of tooth-like fossils, conodonts, with the descriptions of American Devonian and Mississippian species. *Proc. U.S. natn. Mus.* **68,** 1–63, pl. 1–11.

WEDEKIND, R. 1913. Die Goniatitenkalke des unteren Oberdevon von Martenberg bei Adorf. *Sber. Ges. naturf. Freunde Berl.* **1,** 23–77, pl. 4–7.

WITTEKINDT, H. 1966. Zur Conodontenchronologie des Mitteldevons. *Fortschr. Geol. Rheinld Westf.* **9,** 621–46, pl. 1–3.

ZIEGLER, W. 1958. Conodontenfeinstratigraphische Untersuchungen an der Grenze Mitteldevon/Oberdevon und in der Adorfstufe. *Notizbl. hess. Landesamt. Bodenforsch.* **87,** 7–77, pl. 1–12.

—— 1962*a*. Phylogenetische Entwicklung stratigraphisch wichtiger Conodonten-Gattungen in der *Manticoceras*-Stufe (Oberdevon, Deutschland). *Neues Jb. Geol. Paläont. Abh.* **114,** 142–68.

—— 1962*b*. Taxionomie und Phylogenie Oberdevonischer Conodonten und ihre stratigraphische Bedeutung. *Abh. hess. Landesamt. Bodenforsch.* **38,** 1–166, pl. 1–14.

—— 1966*a*. Zum höchsten Mitteldevon an der Nordflanke des Ebbesattels. *Fortschr. Geol. Rheinld Westf.* **9,** 519–38, pl. 1–2.

—— 1966*b*. Eine Verfeinerung der Conodontengliederung an der Grenze Mittel-/Oberdevon. Ibid. **9,** 647–76, pl. 1–6.

—— KLAPPER, G. and LINDSTRÖM, M. 1964. The validity of the name *Polygnathus* (Conodonta, Devonian and Lower Carboniferous). *J. Paleont.* **38,** 421–3.

W. T. KIRCHGASSER
Department of Geology
State University College
Potsdam, N.Y. 13676
U.S.A.

Final typescript received 11 December 1969

NOTE ADDED IN PROOF

Professor W. Ziegler has informed the writer that he has a paper in press with Dr. J. Kullmann on their restudy of the Martenberg section in which they demonstrate that the boundary between the *M. terebratum* and *P. lunulicosta* zones corresponds to the boundary between the lower and upper parts of the *S. hermanni–Pol. cristatus* Zone. This correlation places the succeeding lower part of the Lower *Pol. asymmetricus* Zone (and the Marble Cliff Beds) firmly in the Upper Devonian.

THE CHELONIAN *RHINOCHELYS* SEELEY FROM THE UPPER CRETACEOUS OF ENGLAND AND FRANCE

by JANICE I. COLLINS

ABSTRACT. The Cretaceous chelonian genus *Rhinochelys* Seeley 1869, which is based on skull material, has been reinvestigated. The foundations for Lydekker's original specific descriptions are shown to be inadequate and new diagnostic features for the genus and species are established. Only three British species are recognized: the type species *R. pulchriceps* (Owen 1851), *R. elegans* Lydekker 1889, and *R. cantabrigiensis* Lydekker 1889. *R. amaberti* Moret 1935 from La Fauge Valley, near Grenoble, France, is compared with the British species. A general description of the skulls and mandibles is given. The taxonomic position of *Rhinochelys* is assessed and the genus is referred to the family Protostegidae, subfamily Chelospharginae. The skulls are compared with those of other Cretaceous turtle genera of the Protostegidae and Cheloniidae and a relationship is suggested. It is suggested that carapace and plastral material originally described as *Chelone* (*Cinochelys*) *benstedi* (Mantell 1841) probably belongs to *Rhinochelys*.

THE chelonian genus *Rhinochelys* was erected by Seeley (1869) for the type skull of *Chelone pulchriceps* Owen 1851, from the Lower Cenomanian Cambridge Greensand. Lydekker (1889) amended the description of the type species and described five new species of *Rhinochelys* (*R. macrorhina*, *R. elegans*, *R. cantabrigiensis*, *R. jessoni*, and *R. brachyrhina*) on skull material from British strata, ranging in age from Albian to Upper Cenomanian. In addition to these properly described and named species, an additional fifteen species were named but not described by Seeley (1869); they are therefore *nomina nuda*, so that the correct taxonomic positions of these specimens is not established. The type material of all these British species is housed in the British Museum (Natural History) and the Sedgwick Museum, University of Cambridge. The only other species known, *R. amaberti*, was described by Moret (1935) from the Vraconien of La Fauge Valley, near Grenoble, France.

The taxonomic position of *Rhinochelys* is at present uncertain. Seeley (1869) thought it showed emydian affinities; Lydekker (1889) considered that it resembled the pleurodires. Williston (1898) thought that it was probably related to his genus *Desmatochelys* and family Desmatochelyidae, from the Cretaceous of Kansas, and Romer (1956) also placed *Rhinochelys* in this family. However, Zangerl and Sloan (1960) suppressed the Desmatochelyidae when they showed, on the evidence of post-cranial material, that *Desmatochelys* has close affinities to the Cheloniidae.

As a result of the availability of new material, it is now possible to provide a more thorough description of *Rhinochelys*. Examination and detailed comparison of the British type specimens and of the other skulls of *Rhinochelys* has also permitted a new assessment of the validities and synonomies of the species and of the taxonomic position of the genus. This in turn has suggested that post-cranial material, known from the same deposits as the skull material, may in fact also belong to the genus *Rhinochelys*, the carapace of which is otherwise unknown.

[Palaeontology, Vol. 13, Part 3, 1970, pp. 355–78, pls. 67–69.]

TAXONOMY OF THE GENUS *RHINOCHELYS*

Generic diagnosis. Skull has slight posterior emargination and no ventral emargination. Squamosal not in contact with parietal; blunt ant-orbital beak; nasal and prefrontal bones distinct; prefrontals excluded from narial margin and from meeting medially; epidermal sulci cross frontal and maxilla. No secondary palate; posterior margin of internal nares formed by maxillae and palatines; vomer divides internal nares as sharp ridge and extends only short way between palatines; palatines meet medially; grinding (triturating) surface of maxillae and premaxillae has broad lingual ridge and deep groove in midline; pterygoids very narrow, emarginate and meet along their length, palatal surface slightly ridged; basisphenoid narrowly triangular and not ridged on palate.

Type species. Chelone pulchriceps Owen 1851, p. 8, pl. vii, figs. 1–3. Lower Cenomanian Cambridge Greensand, Barnwell, near Cambridge.

Holotype. B55775, Sedgwick Museum, Cambridge.

Remarks. As noted, twenty-two species have been ascribed to *Rhinochelys* by Owen, Seeley, Lydekker, and Moret, but only seven have been described. When Lydekker (1889) described his five new species and redescribed *R. pulchriceps* he used the following diagnostic features:

1. Size and shape of the external nares.
2. Size and shape of the nasal.
3. Inclusion of the prefrontal in the narial margin.
4. Depth of the premaxillae.
5. Swelling on the prefrontal.
6. The angle that the premaxillae make with the palate edge in profile.
7. Presence of a hook on the tip of the upper jaw.
8. The ratio of the height to the overall length of the skull.

The size and shape of the nares and nasal bones are variable features and too individual to be of use in distinguishing species.

The inclusion of the prefrontal in the narial margin was considered to be a feature of *R. brachyrhina* and *R. jessoni*. Close examination of the type of *R. brachyrhina* (text-fig. 4) reveals that the specimen is very worn and that the nares are enlarged until most of the nasals have been lost. The suture between the nasal and maxilla practically borders the nares, but it is clear that the prefrontal is definitely excluded from contributing to the narial margin. The suture lines on the very well-preserved type of *R. jessoni* (text-fig. 3) are not very distinct, but it can be seen with a lens that the maxilla and nasal meet and exclude the prefrontal from the narial margin, as in all the other specimens examined.

The depth of the premaxillae was used to distinguish *R. macrorhina* from *R. elegans*. The type of *R. macrorhina* (text-fig. 5*d*) is a poorly preserved snout with an eroded jaw edge. The bone is eroded for about half the depth of the premaxillae, which is evident from the structure of the triturating surface of the palate. The relative depth of the premaxillae is, in any case, subject to individual variation.

A peculiar lateral swelling on the prefrontal was thought to be present in *R. elegans* alone. This area does not, however, appear to be more swollen on this specimen than on any other.

Although the first five characters used by Lydekker are not reliable, the remaining three (i.e. the height/length ratio, the angle that the premaxillae make with the palate edge, and the presence or absence of a hooked tip to the upper jaw), divide the British types into three groups, as can be seen from Table 1. Although these features can therefore be used as specific characters, Lydekker's descriptions are not comprehensive enough for practical purposes. The position becomes clear, however, when these features are defined as follows:

1. The height Y (height measured just anterior to the orbits) relative to the length Z (length between the frontal/parietal suture and the jaw tip).
   Relative height $= (Y/Z) \times 100$.
2. The angle between the anterior surface of the premaxillae and the edge of the palate, as seen in profile. (This is referred to as the premaxillary angle.)
3. The presence or absence of a hooked tip to the upper jaw.

The measurements used are shown in text-figs. 1, 2.

Nevertheless these characters alone are not considered sufficient to assign all the specimens to valid species, and other distinctions were therefore sought. The following features are thought to be sufficiently distinct and constant to be of value:

4. The width X (width just posterior to the orbits) relative to the length Z.
   Relative posterior width $= (X/Z) \times 100$.
5. The angle between the two maxillae. (This is referred to as the 'jaw angle'.)
6. The presence or absence of a ridge over the maxillary sulcus.
7. The convexity or straightness of the premaxillae in profile.

Table 1 shows all these features as they appear on the type species, Lydekker's types, Seeley's named skulls, and on *R. amaberti* taken from Moret's plates and figures (1935, pl. 27, figs. 1–4). (Names in square brackets are the *nomina nuda* of Seeley.)

From Table 1 it can be seen that the British specimens fall into three groups and that none is referable to *R. amaberti*.

In the first group, *R. pulchriceps*, the relative width is over 100 but this is measurable on one specimen only; the relative height (47–51), is the lowest in the groups; the jaw angle is broad (72–80°); the premaxillary angle is acute (70–74°); there is no ridge over the maxillary sulcus; the premaxillae are straight in profile; and there is no hooked tip to the upper jaw.

In the second group, *R. elegans*, [*R. mastocephalus*], [*R. stenicephalus*], *R. brachyrhina*, *R. macrorhina*, the relative width (91–96), is the narrowest in the three groups, as it does not exceed 100; the relative height (51–61) is greater than that of the first group; the jaw angle (50–60°) is narrower than that of the first group; the premaxillary angle (80–90°) is not quite a right-angle; there is no ridge over the maxillary sulcus; the premaxillae are straight in profile; and there is no hook to the tip of the upper jaw. *R. brachyrhina* and *R. macrorhina* are poorly preserved snouts; however, they do not show any features of the other groups, and are therefore doubtfully included here.

In the third group, *R. cantabrigiensis*, *R. jessoni*, [*R. cardiocephalus*], [*R. dayi*], [*R. eurycephalus*], [*R. platyrhinus*], [*R. rheporhinus*], [*R. sphenicephalus*], the relative width is the broadest of the three (87–108); the relative height (59–63) is the greatest of the three; the jaw angle (42–56°) is slightly narrower than that of the second group; the

premaxillary angle equals or exceeds a right angle; it is the only group with a ridge over the maxillary sulcus, a convex profile to the premaxillae, and a hooked tip to the upper jaw.

TABLE 1. Skull measurements of *Rhinochelys* (a—absent, p—present, s—straight, c—curved)

Types	$\frac{X}{Z}\times 100$	$\frac{Y}{Z}\times 100$	*Jaw angle* (in degrees)	*Premaxillary angle* (in degrees)	*Ridge over sulcus*	*Premaxillary profile*	*Hooked tip*
R. pulchriceps	107	51	72	74	a	—	a
R. pulchriceps	—	47	80	70	a	s	a
R. elegans	96	57	57	85	a	s	a
R. elegans	—	56	60	80	a	s	a
[*R. mastocephalus*]	95	61	54	88	a	s	a
[*R. stenicephalus*]	91	55	50	86	a	s	a
R. brachyrhina	—	61	—	—	a	—	—
R. macrorhina	—	51	—	90	a	s	—
R. cantabrigiensis	107	62	50	90	p	c	p
R. jessoni	99	63	55	97	p	c	p
[*R. cardiocephalus*]	87	61	45	94	p	c	p
[*R. dayi*]	93	59	52	98	p	c	p
[*R. eurycephalus*]	105	58	50	101	p	c	p
[*R. platyrhinus*]	108	60	42	92	p	c	p
[*R. rheporhinus*]	—	—	56	95	p	—	—
[*R. sphenicephalus*]	100	60	44	93	p	c	—
R. amaberti	135	65	?105	93	a	s	a

In *R. amaberti* the relative width (135) is very broad; the relative height (65) is greater than that of the British types; the jaw angle is obtuse (?105°) and very much broader than that of the others; the premaxillary angle agrees with the third group but there is no ridge over the maxillary sulcus; the profile of the premaxillae is straight, and there is no hooked tip to the upper jaw.

Thus we have three distinct British species, *R. pulchriceps*, *R. elegans*, and *R. cantabrigiensis*. The names used are the senior taxa in the groups.

Abbreviations. The following abbreviations are used: British Museum (Natural History)—BMNH; Sedgwick Museum, University of Cambridge, SM; Institute of Geological Sciences, GSM. The material used in the charts includes the following specimens in addition to those mentioned:
R. pulchriceps. BMNH 2224, R1806, 2236, R2232: Isolated lower jaws: 46373, R2238, 35184, R35185, 47211, 49920, R793. SM B55771, B55772, B55779, B55811.
R. elegans. BMNH 35193, R2225, 41796, 46371, 46371*a*, 35194, 35197, R27, R2228, R2229, R2230, R2231, R2237, 35195. SM B55773, B55776, B55780, B55784, B55792, B55798, B55800.
R. cantabrigiensis. BMNH R1558, R2227, R2233, R2234, 35196. SM B55774, B55781, B55782, B55783, B55785, B55786, B55787, B55788, B55791, B55793, B55795, B55799, B56572, B56573, B56574, B56576, B56580.

Rhinochelys pulchriceps (Owen 1851)

Plate 67, figs. 1–8; Plate 68, figs. 1–2

1851 *Chelone pulchriceps* Owen, p. 8, pl. 7, figs. 1–3.
1869 *R. pulchriceps* (Owen); Seeley, p. xviii.
1869 *R. dacognathus* Seeley, p. xviii.
1889 *R. pulchriceps* (Owen); Lydekker, p. 230, pl. 8, fig. 1.

Holotype. Skull lacking lower jaw, SM B55775.

Measurements. Holotype, over-all length 58·5 mm., width 40 mm.

Horizon and locality. Lower Cenomanian Cambridge Greensand, Barnwell, near Cambridge.

Diagnosis. Skull shallow, height *Y* less than half length *Z*; jaw angle broadly acute; premaxillary angle acute; profile of premaxillae straight; area over maxillary sulcus smooth; no hooked tip to upper jaw.

Rhinochelys elegans Lydekker 1889

Plate 68, figs. 3–7

1889 *R. elegans* Lydekker, p. 230, pl. 8, fig. 4.
1869 *R. mastocephalus* Seeley, p. xviii.
1869 *R. stenicephalus* Seeley, p. xviii.
1889 *R. brachyrhina* Lydekker, p. 231, pl. 8, figs. 3, 3*a*.
1889 *R. macrorhina* Lydekker, p. 230, pl. 8, fig. 7.

Holotype. Skull lacking lower jaw, BMNH 2226.

Measurements. Holotype, over-all length 64 mm., width 39·8 mm.

Horizon and locality. Lower Cenomanian Cambridge Greensand, near Cambridge.

Diagnosis. Skull high and narrow, height *Y* about three-fifths length *Z*; width *X* less than length *Z*; jaw angle narrow; premaxillary angle just less than right-angle; profile of premaxillae straight; no ridge over maxillary sulcus; no hooked tip to upper jaw.

Rhinochelys cantabrigiensis Lydekker 1889

Plate 68, figs. 8–16

1889 *R. cantabrigiensis* Lydekker, p. 230, pl. 8, figs. 2, 2*a*, 2*b*.
1889 *R. jessoni* Lydekker, p. 231, pl. 8, figs. 6*a*, 6*b*.
1869 *R. cardiocephalus* Seeley, p. xviii.
1869 *R. dayi* Seeley, p. xviii.
1869 *R. eurycephalus* Seeley, p. xviii.
1869 *R. platyrhinus* Seeley, p. xviii.
1869 *R. rheporhinus* Seeley, p. xviii.
1869 *R. sphenicephalus* Seeley, p. xviii.

Holotype. Skull lacking lower jaw, BMNH 43980.

Measurements. Holotype, over-all length 42·5 mm., width 32·5 mm.

Horizon and locality. Lower Cenomanian Cambridge Greensand, near Cambridge.

Diagnosis. Skull high, broad, domed, height *Y* about three-fifths length *Z*; jaw angle narrow; premaxillary angle is right-angle or greater; profile of premaxillae convex; heavy ridge over maxillary sulcus; tip of upper jaw slightly hooked.

It must now be considered whether these diagnoses are supported by any other material.

In the collections examined, there are a further forty skulls which can be assigned to *Rhinochelys*. The specific features of these are carefully tabulated on text-fig. 9.

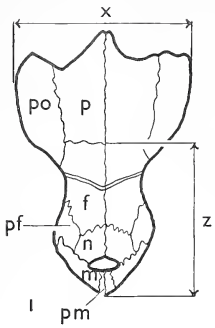

1

3

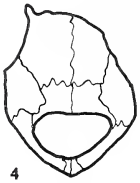

4

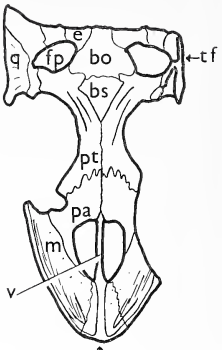

7

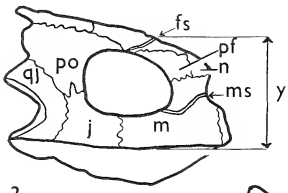

2

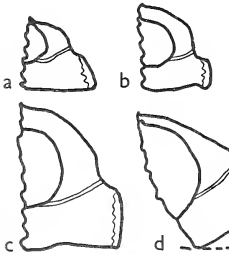

5

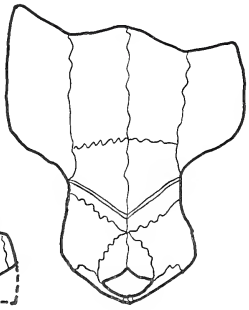

6

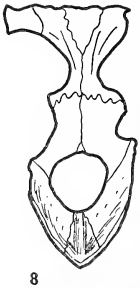

8

Synopsis of text-fig. 9.

Fig. A. The jaw angle is broader in *R. pulchriceps* (66–80°) than in *R. elegans* (49–80°) and *R. cantabrigiensis* (40–63°). The figure for *R. amaberti* may be distorted as the measurement has been taken from a photograph, but the jaw-angle appears to be obtuse and very much broader than the other species at ?105°.

Fig. B. The relative height of *R. pulchriceps* (43–51) is less than that of the other three species, *R. elegans* (51–76), *R. cantabrigiensis* (50–66), and *R. amaberti* (65).

Fig. C. The premaxillary angle in *R. pulchriceps* is acute (63–77°). It is generally just less than a right-angle in *R. elegans* (80–100°), but in *R. cantabrigiensis* (89–105°) and *R. amaberti* (93°) it is slightly obtuse.

Fig. D. Only two specimens of *R. pulchriceps* are sufficiently well preserved to allow the relative width to be used, but these differ widely. The relative width in *R. elegans* (74–97) does not exceed 100; however in *R. cantabrigiensis* this relative width is 87–109, i.e. the width *X* is generally in excess of the length *Z*, although there is a slight overlap. *R. amaberti* at 135 is very much broader.

In the few specimens with concurrent measurements, the other specific features are present and well defined. It is inevitable that there is a degree of variation within a biological group, but the majority in each species can be clearly differentiated using proportional measurements and angles alone. For a list of the other material used see p. 358.

The evidence presented here shows that these skulls can also be placed in three groups which agree with the specific diagnoses, and that all are distinct from *R. amaberti*. Analysis of these specimens also shows additional differences between the palate and mandible of *R. pulchriceps* and those of *R. elegans* and *R. cantabrigiensis*. In the formation of the ridges and grooves there are differences between the palate of the type of *R. pulchriceps* (Pl. 67, fig. 3, text-fig. 7) and those of two other specimens, one referable to *R. elegans* (SM B55792) (text-fig. 8) and the other to *R. cantabrigiensis* (SM B56574).

In *R. pulchriceps* the lingual ridge runs alongside the median groove and appears to join the cutting edge anteriorly. The anterior tip of the premaxillae is notched. The mandibles which fit the broad-angled jaw, and can be referred to *R. pulchriceps*, have a sharp median crest which extends right across the symphysis.

TEXT-FIGS. 1–8.

Figs. 1, 2. *R. elegans* SM B55776. 1, Dorsal view, ×1; 2, Lateral view, ×1. *Z*, length from the frontal-parietal suture to the jaw tip; *X*, width just behind the orbits; *Y*, depth just anterior to the orbits

Fig. 3. Type of *R. jessoni* showing the prefrontals are excluded from meeting medially, ×1.

Fig. 4. Type of *R. brachyrhina* showing the prefrontals are excluded from the narial edge.

Fig. 5. Profile of the beaks. *a*, *R. pulchriceps*; *b*, *R. cantabrigiensis*; *c*, *R. elegans*; *d*, Reconstructed beak of *R. macrorhina*.

Fig. 6. *R. amaberti* (after Moret 1935, pl. xxvii, fig. 1).

Fig. 7. *R. pulchriceps*, palatal view, ×1.

Fig. 8. *R. elegans*, palatal view, ×1.

Explanation of abbreviations: *bo*, basioccipital; *bs*, basisphenoid; *f*, frontal; *fs*, frontal sulcus; *fp*, fenestra postotica; *g*, premaxillary groove; *j*, jugal; *m*, maxilla; *ms*, maxillary sulcus; *n*, nasal; *p*, parietal; *pa*, palatine; *pm*, premaxilla; *po*, postorbital; *pf*, prefrontal; *pt*, pterygoid; *qj*, quadratojugal; *q*, quadrate; *tf*, tympanic fossa; *v*, vomer.

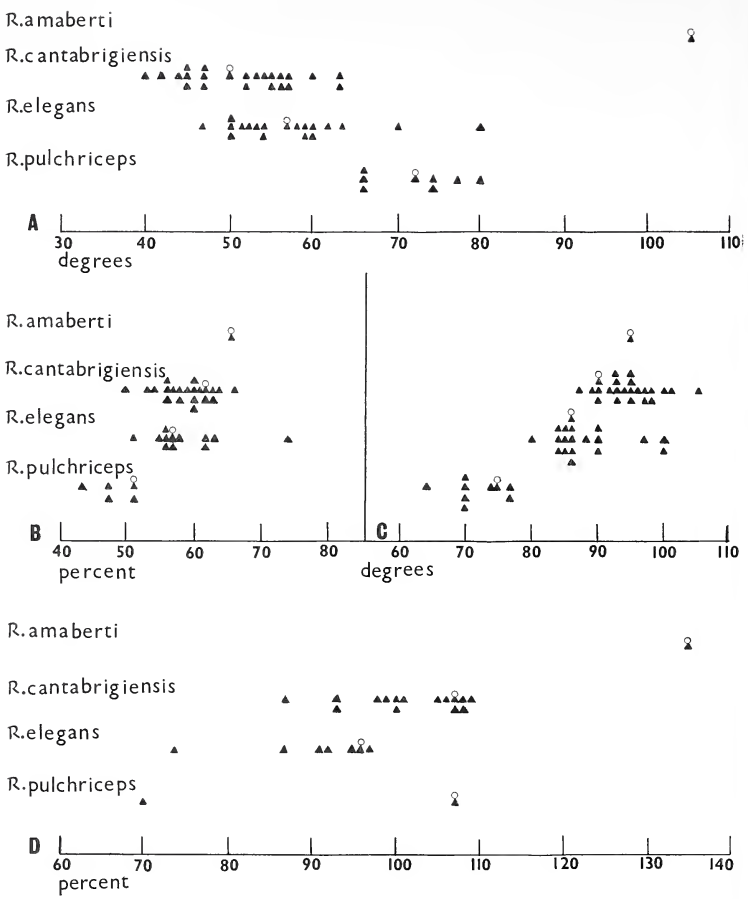

TEXT-FIG. 9. Each triangle represents an individual measurement. All those belonging to the same species are placed along a single horizontal line; where more than one individual has the same measurements, further triangles are added above or below this horizontal line. Measurements derived from the type-specimens of valid species are distinguished by a circle above the triangle.

A, angle between the maxillae: the jaw angle.

B, proportion of height Y to length Z; $(Y/Z) \times 100$.

C, angle between the premaxillae and the palate edge: the premaxillary angle.

D, proportion of width X to length Z: $(X/Z) \times 100$.

On the other two palates, the lingual ridge does not join the cutting edge but is separated by the confluent grooves. The premaxillae are not grooved at the tip. The narrower mandibles, which can be referred to either of these species, have median crests which extend only part of the way across the symphysis, leaving the tip smooth.

One other of Seeley's types, *R. dacognathus* (SM B55809, B55810) can be referred to *Rhinochelys*. The 'type' consists of two mandible tips each with a broad symphysis, smooth ventral surface and a sharp median crest on the grinding surface which extends across the symphysis to the tip. The angle between the rami is broad. These specimens are here referred to *R. pulchriceps*.

R. graptocephalus Seeley is a poorly preserved posterior region of a skull and is indeterminate. The other *nomina nuda*, *R. colognathus*, *R. dinerognathus*, *R. grypus*, *R. leptognathus*, and *R. platycephalus*, are all mandibles of various sorts, but none of these is referable to *Rhinochelys*.

Using the new basis for distinguishing the species, it is evident that *R. anaberti* is a separate species although known by only one specimen. The following features are mentioned by Moret (1935) in his description: the skull is flat on top, not domed, and has a greater relative posterior width than *R. elegans*; the premaxillae form a right-angle with the palate edge and are straight in profile, not convex. To this can be added the following observations taken from his plate (op. cit., pl. 27): the jaw angle is obtuse, about 105°, and there appears to be no ridge over the maxillary sulcus.

CRANIAL MORPHOLOGY OF *RHINOCHELYS*

In the preceeding taxonomic study, the different specimens which in the past have been placed in the genus *Rhinochelys* have been either rejected from, or accepted into, the genus, and the species composition of the genus has been established. It is therefore now possible to use those specimens which belong in the genus to make a detailed study of the cranial morphology of *Rhinochelys*.

Generic description

The skulls are small to medium size (30–60 mm. long) with width about two-thirds of the length. The posterior edge is emarginate to a depth of about a third of the length of the parietal. The temporal fossa is well roofed over by the parietal, postorbital, and squamosal. The squamosal does not meet the parietal. The frontal extends to form part of the rim of the orbit and meets the nasal and prefrontal anteriorly. The prefrontal and nasal are distinct. The prefrontals are moderate in size, do not meet medially and do not form part of the narial margin. The nasal is moderately large; it meets the frontal posteriorly, the prefrontal postero-laterally, the maxilla antero-laterally, and forms the posterior margin of the external nares. The external nares are oval in shape, with the long axis running horizontally. The antorbital beak is blunt and not produced. The premaxillae meet in a sharp angle. The maxilla extends from the nares to meet the jugal in the posterior part of the lower orbital rim to form a jugo-maxillary bar. The jugal forms the postero-ventral and posterior rim of the orbit. It extends dorsally to meet the postorbital and posteriorly to meet the quadratojugal. The quadratojugal bounds the tympanic fossa anteriorly and antero-dorsally. The tympanic fossa is notched postero-ventrally for the passage of the columella from the incisura columella auris.

Palate

The palate is flat and there is no secondary palate. The maxillae and premaxillae form a broad grinding surface which borders the internal nares. This surface is grooved internally from the cutting edge, and passes into a broad ridge on the lingual margin. There is a deep groove at the midline which would oppose the crest on the mandible. The posterior margin of the internal nares is formed by the palatines and maxillae. The vomer divides the internal nares, forming a sharp ridge, and extends only a short way between the palatines. The palatines meet medially and meet the maxillae laterally; there is a dorsal extension which meets the ventral projections of the nasal and prefrontal to form the anterior orbital wall. The orbito-palatal edge of the palatine is deeply notched; this area is not well preserved on any specimen but it does not appear that this notch was surrounded by bone to make a posterior palatine foramen, although the notch would serve the same function (Pl. 67, figs. 3, 8). The pterygoid does not join the maxilla. The two pterygoids meet medially and are narrow, emarginate and slightly ridged. The basisphenoid is exposed as an antero-posteriorly elongate triangle and is flat. The basioccipital is broad anteriorly, narrow posteriorly, and level with the palate.

Epidermal sulci

Two pairs of sulci are evident on all the skulls. One crosses the maxillae from the orbits to the nares, running posteriorly and slightly ventrally. The other crosses the frontal, near to the frontal-nasal suture, as a sinuous curve from the orbits, anteriorly to the midline.

On a small skull of *R. cantabrigiensis* (SM B55791) the dorsal surface is further subdivided into a larger number of scutes by well-marked epidermal sulci. The prefrontal scute is divided into two by a straight sulcus and in addition there are a frontal, parietal, and two postorbital scutes clearly marked (Pl. 68, fig. 16).

Mandible

The mandibles are preserved on two skulls, one referable to *R. elegans* (SM B55776, text-fig. 2) and the other to *R. cantabrigiensis* (SM B55791, Pl. 68, figs. 14, 15). The

EXPLANATION OF PLATE 67

Figs. 1–5. *Rhinochelys pulchriceps*. Skull of type species, SM B55775. Dorsal, palatal, anterior, and lateral views, ×1. Fig. 2 is an enlarged view of the tympanic fossa.
Fig. 6. *R. pulchriceps*. BMNH 2224, lateral view, ×1.
Figs. 7, 8. *R. pulchriceps*. BMNH R1806, dorsal and lateral views, ×2.

EXPLANATION OF PLATE 68

Figs. 1, 2. *R. pulchriceps*. BMNH R1806, lateral and anterior views, ×2.
Fig. 3. Type skull of *R. macrorhina* (*R. elegans*). BMNH 35193, lateral view, ×1.
Fig. 4. Type skull of *R. brachyrhina* (*R. elegans*). BMNH R2225, anterior view, ×1.
Figs. 5–7. *R. elegans*. Holotype skull, BMNH 2226; dorsal, lateral, and anterior views, ×1.
Figs. 8–10. *R. cantabrigiensis*. Holotype skull, BMNH 43980; dorsal, lateral, and anterior views, ×1.
Figs. 11–13. Type skull of *R. jessoni* (*R. cantabrigiensis*). BMNH R2227; dorsal, lateral, and anterior views, ×1.
Figs. 14–16. *R. cantabrigiensis*. SM B55791; lateral, ventral showing the lower jaw, and dorsal views, ×1.

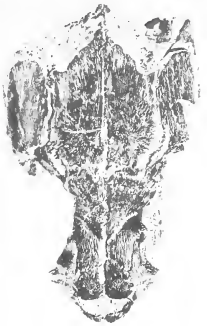

1

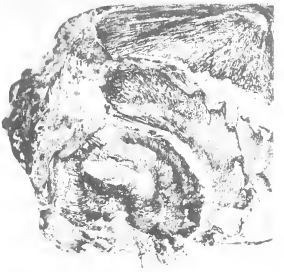

2

3

6

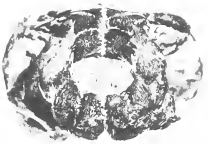

4

5

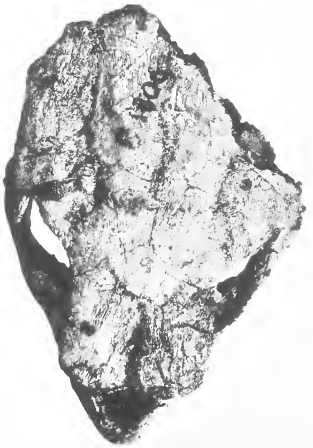

7

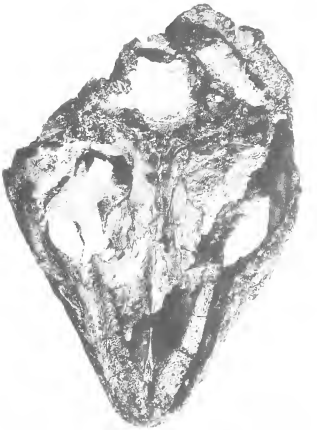

8

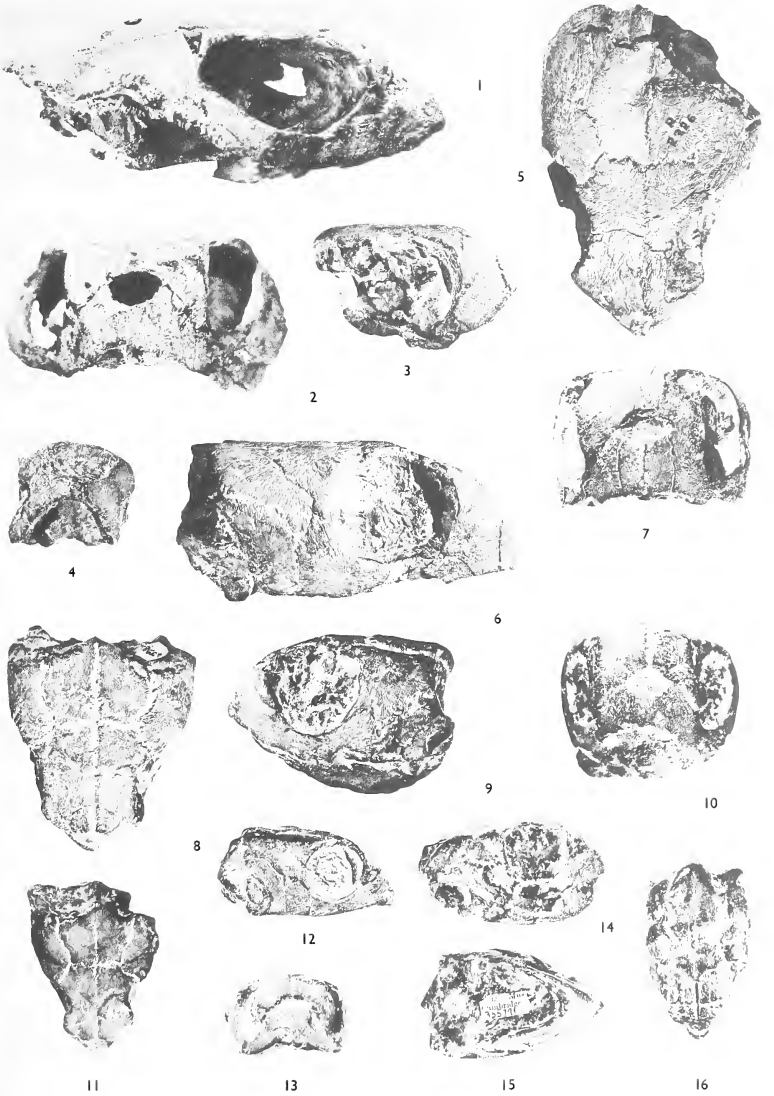

COLLINS, *Rhinochelys*

angle between the mandibular rami is about 5° less than the jaw angle. The symphysis is well fused and long, about a third of the length of the rami. The ventral surface of the symphysis is smooth and tapers in an even curve at an angle of about 40° from the grinding surface. The posterior depth at the symphysis is about half the symphysial length. The lateral medial surfaces of the rami meet ventrally to form a very sharp ridge. The sutures between the bones are indistinct due to poor preservation.

Pieces of mandible, showing the grinding surface at the symphysis but otherwise similar to the articulated mandibles, are fairly commonly recorded. Text-fig. 10 shows a mandible (BMNH R401) from the Chalk of Weymouth, Dorset. The grinding surface is concave with a sharp median crest at the symphysis, and deeply grooved with sharp marginal ridges along the rami.

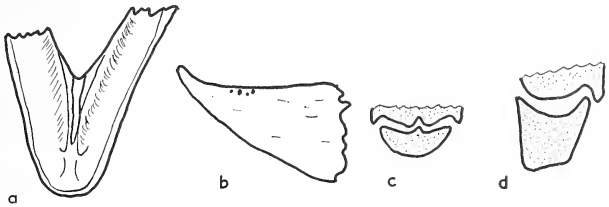

TEXT-FIG. 10. Mandible BMNH R401. *a*, dorsal view of symphysis; *b*, lateral view of anterior part; *c*, transverse section of mandibular symphysis and maxillae; *d*, cross-section of jaw rami and maxilla.

Braincase

The posterior part of a large skull (SM B94606) (text-figs. 11, 12; Pl. 69, figs. 1–4) with part of a maxilla, premaxilla, and vomer of *Rhinochelys* is recorded from the Upper Senonian, Quadrata zone of Shawford, Hampshire (loc. 1086; Brydone 1912, p. 100).

All external features preserved agree with the generic characters of *Rhinochelys* as defined above, but there is not enough evidence to allocate it to a species. Most of the brain cavity and otic capsule are well preserved and show structures which have not as yet been described in *Rhinochelys*. A natural mould in chalk of the upper brain cavity is also preserved (Pl. 69, fig. 4).

Description. A heavy ridge runs across the inner surface of the roofing bones of the temporal fossa, from the anterior part of the brain cavity to the posterior rim of the orbit. The area is thus divided into lachrymal and temporal surfaces. A faint ridge is discernible in the recent *Chelonia*. The ventral extension of the parietal meets the pterygoid ventrally, and the prootic and supraoccipital posteriorly. It forms the anterior side wall of the brain cavity. The suture between the pterygoid and parietal is indistinct and it is uncertain whether an epipterygoid is present or not.

The trigeminal nerve foramen is kidney-shaped and does not extend above the level of the otic capsule. Posteriorly it is bordered by the prootic dorsally and by the quadrate ventrally.

The prootic forms a small part of the wall of the brain case. It projects laterally with a heavy anterior ridge to form the anterior roof of the otic capsule. The stapedial (temporal) canal passes through it near the posterior margin.

The supraoccipital is partially preserved, but the crest is broken. It forms the roof of the posterior part of the brain cavity. The opisthotic is an irregularly shaped bone, extending between the prootic anteriorly, the squamosal laterally, the exoccipital postero-ventrally, and the supraoccipital dorsally. It forms the posterior roof of the otic capsule and part of the dorsal edge of the fenestra postotica.

The exoccipital forms the edge of the foramen magnum medially and of the fenestra postotica laterally. It meets the supraoccipital dorsally, the opisthotic dorso-laterally and the basioccipital ventrally. It does not appear to meet the pterygoid laterally, nor does it extend over the basioccipital to form the posterior floor of the brain cavity.

The quadrate forms the lateral part of the otic capsule. The tympanic fossa is concave with a deep notch and groove, the incisura columella auris, on the posterior margin. Ventrally the bone meets the lateral extension of the pterygoid. The articular condyle is eroded. A fragment of squamosal lies over the quadrate and forms the roof of the stapedial canal.

Brain cavity. The basioccipital forms the floor of the posterior part of the brain cavity. It is concave and broad, with a median anterior ridge which terminates abruptly in a knob, the basi-tuberculi basalis, at the basisphenoid suture. Deep grooves flank this knob, and the area posterior to it is rough. Hypoglossal nerve foramina open into the postero-lateral part of this surface.

The basisphenoid is in two parts and forms the anterior floor of the brain cavity. Posteriorly the bone is broad and concave, the surface is rough with a small median crest which tapers out midway. The clinoid processes are two small peaks on the anterior rim of the main part of the bone and flank the dorsum sellae. The dorsum sellae is vertical and forms a beak which protrudes into the fossa hypophysis. The basisphenoidal rostrum is long, narrow, and grooved; it terminates abruptly in a vertical oval face. It lies over the suture between the pterygoids and is flanked on either side by the sulcus cavernosus. The abducens nerve foramen lies in the dorsum sellae just below the clinoid process.

Otic capsule. The otic capsule is open posteriorly by a wide fenestra postotica, postero-laterally into the tympanic fossa by the incisura columella auris, and anteriorly into the sulcus cavernosus by the carotid canal. The main part of the capsule is divided into three cavities, the cavum labyrinthicum (inner ear cavity) and the medial and lateral parts of the cavum acustico-jugulare (acoustic-jugular cavity).

The inner ear cavity is antero-medial to the other two; it opens into the brain cavity by a large hiatus acusticus, and into the acoustic-jugular cavity by the fenestra ovalis. In the roof lie the three cavities for the semicircular canals: the opisthotic recess posteriorly, the supraoccipital recess medially, and the prootic recess anteriorly. A thin septum of bone separates the inner ear cavity from the medial part of the acoustic-jugular cavity. This septum is pierced by a large oval fenestra perilymphatica.

The medial part of the acoustic-jugular cavity is pear-shaped and lies posterior to the inner ear cavity. It narrows medially and opens into the brain cavity by a small round

anterior jugular foramen and opens into the main part of the acoustic-jugular cavity, laterally, by an oval posterior jugular foramen. This foramen, and the fenestra ovalis beside it, are completely surrounded by bone, and the septum which divides these is fused to the cavity floor. In the Recent cheloniids this bony septum is free of the cavity floor and is completed by cartilage.

The lateral part of the acoustic-jugular cavity is the largest of the three. There is a lateral groove over the floor which passes anteriorly into the carotid canal between the pterygoid, quadrate, and prootic. This canal joins the sulcus cavernosus medial to the trigeminal nerve foramen, and carried the carotid artery and lateral head vein. The stapedial artery passed dorsally from this cavity, through a canal between the prootic and squamosal bones into the temporal fossa.

Brain cast. The chalk formed a natural cast of the upper brain cavity which is partly preserved. The cerebral lobes are faintly discernible and are 11·2 mm. wide, the olfactory lobes lie 12 mm. anteriorly and are 5 mm. wide. The hind region of the brain is flexed ventrally at an angle of 30° from the anterior part.

Measurements. Posterior width 60 mm., height 37 mm.

Discussion

The internal structure of this skull is of chelonioid type and can be compared with skulls of other marine turtle families, the Toxochelyidae, the Cheloniidae, both described from the Cretaceous of North America, and the Recent Dermochelyidae. (The internal cranial morphology of the Protostegidae is not well enough known for comparison to be possible.) There are morphological differences which need emphasizing although the precise significance of these is uncertain.

The passage of the carotid artery and lateral head vein through the acoustic-jugular cavity is essentially simple. In the cheloniids and toxochelyids, the blood vessels are enclosed in the pterygoid and enter the skull close to the occipital condyle. In the Recent cheloniids the basisphenoid, anterior part of the basioccipital, and the pterygoid are thickened, dropping the posterior part of the palate. The ventral surface of the basioccipital, instead of being horizontal as in *Rhinochelys*, is inclined at an angle of 30°. The pterygoid has incorporated the blood vessels within itself and these pass into the sulcus cavernosus much as in that of *Rhinochelys*, but in a toxochelyid skull described by Zangerl (1953*b*, p. 152) the internal carotid passes directly into the basisphenoidal rostrum and does not enter the sulcus cavernosus. The projection of the dorsum sellae into the fossa hypophysis is found also in the Recent *Eretmochelys*, but in other cheloniids and toxochelyids the dorsum sellae is sloped and concave. The basisphenoid and exoccipital are both extended laterally in the cheloniids and the exoccipitals fuse together across the dorsal surface of the basioccipital.

It seems possible that the more complex and sturdier cheloniid skulls could have evolved from a simple condition such as that of *Rhinochelys*. On investigating the skull of a Leathery Turtle, it became clear that this too could have evolved from a skull like *Rhinochelys* but not through the cheloniids or toxochelyids. Apart from specialized features which can only be related to the group, the *Dermochelys* skull is more like the skulls of the Chelonioidea than any other Cryptodire. The basic pattern of the skull is

very similar in the two groups but *Dermochelys* shows a remarkable simplicity and similarity to *Rhinochelys* in the features that have been discussed. The palate is primary and the posterior part is not thickened but is flat. The carotid artery and lateral head vein pass through the acoustic-jugular cavity and are not enclosed in the pterygoid. The

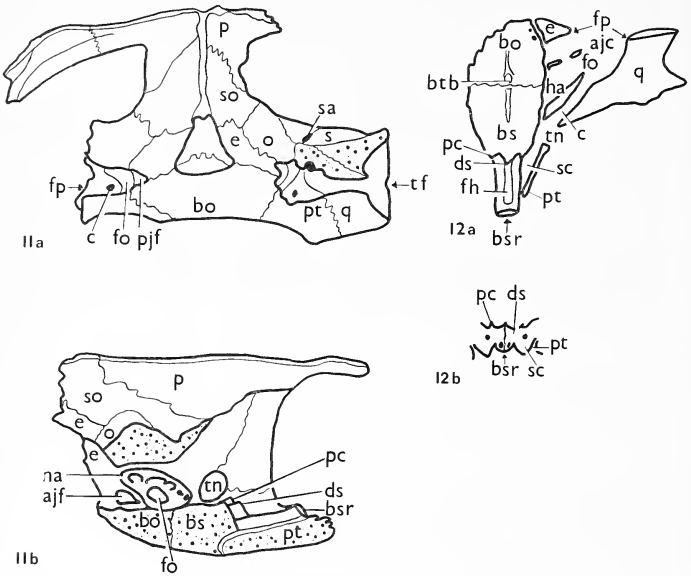

TEXT-FIGS. 11, 12. *Rhinochelys* sp. Upper Chalk skull, SM B94606. 11*a*, posterior view, ×1; 11*b*, lateral view with otic capsule removed, ×1; 12*a*, dorsal view of the floor of the brain cavity and plan of the otic capsule; 12*b*, anterior view of the dorsum sellae looking along the basisphenoidal rostrum. Explanation of abbreviations: *ajc*, acoustic-jugular cavity; *ajf*, anterior jugular foramen; *bsr*, basisphenoidal rostrum; *btb*, basituberculi basalis; *c*, carotid canal; *ds*, dorsum sellae; *fh*, fossa hypophysis; *fo*, fenestra ovalis; *fp*, fenestra postotica; *ha*, hiatus acusticus; *o*, opisthotic; *pc*, clinoid process; *pjf*, posterior jugular foramen; *s*, squamosal; *sa*, stapedial arterial canal; *sc*, sulcus cavernosus; *so*, supra-occipital.

structure of the basioccipital (except in the floor of the brain cavity), pterygoid, and exoccipital are similar to *Rhinochelys*. Zangerl (1953*a*) suggested that the Leathery Turtles could have descended from the Protostegidae; such a relationship might explain this similarity, but it could alternatively be a general, primitive, condition retained by both genera.

So far I have briefly discussed the differences within the superfamily, which are not very extensive. It is far more interesting to demonstrate the developing pattern of

structural changes. The *Rhinochelys* skull, as the first record of the Chelonioidea (Cox *et al.* 1967), is conveniently placed for such a study. Although 'modernized' in type, this skull is uncomplicated by extra bone growth as is seen in the later cheloniids, and is still close enough to the primitive stock to retain a simplicity of structure.

The chelonian skull is specialized in the formation of an acoustic-jugular cavity and a tympanic fossa. All known chelonians possess these features in one form or another, except the primitive Triassic *Proganochelys*.

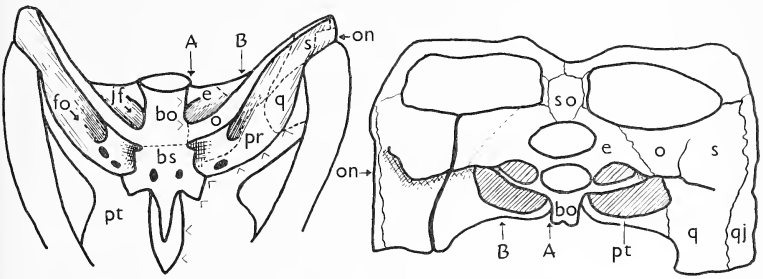

TEXT-FIGS. 13, 14. *Proganochelys quenstedti*. 13, posterior part of the palate. 14, occiput. Reconstructed from Parsons and Williams (1961, pl. 5, 6). Magnification not stated. Explanation of abbreviations: *jf*, jugular foramen; *on*, otic notch; *pr*, prootic.

Photographs of a well-preserved skull of *Proganochelys quenstedti* Baur, housed in the Museum of Natural History at Stuttgart, were published by Parsons and Williams (1961). While a full description of the skull has yet to be published, the photographs are clear and show that the acoustic-jugular cavity is not floored, but is a simple concavity in the back of the skull, very similar to that found in other primitive reptiles. Parsons and Williams (p. 91) briefly discuss this and say:

> a cultriform process is plainly visible between the separated pterygoids. Posteriorly also the situation is primitive; the quadrate ramus of the pterygoid does not send any flange inward to floor the cranio-quadrate passage as on all other known turtles, and the foramina for the *vena capitis lateralis*, the internal carotid, and the stapedial artery, as well as the *fenestra ovalis* are all exposed in ventral view.

In text-figs. 13 and 14 I have interpreted this region of the skull of *Proganochelys*, using the photographs shown in Parsons and Williams (1961, pl. 5, 6) but showing only features which are well defined. The arrows indicate the areas and direction of growth of the bones which would be required to produce the morphology of this region as found in *Rhinochelys*. In *Proganochelys* there are two large fenestrae opening laterally. One, close to the condyle, is the jugular foramen; the other, antero-lateral to this, is the fenestra ovalis. Anteriorly there are two foramina on one side but only one is apparent on the other. One of these is for the stapedial artery and the other possibly for the lateral head vein. The pair of foramina on the basisphenoid could possibly be the internal carotid foramina; however these are placed in a different position from normal. In the

modern chelonians the internal carotid artery enters the basisphenoid through the dorsum sellae; it is possible that the change of position of these foramina is caused by the medial and posterior growth of the pterygoid.

The basisphenoid is slightly proud of the floor of the inner ear cavity as there is a distinct shadow laterally. The basipterygoid processes are sutured anteriorly and laterally to the pterygoids. The pterygoid sends only a thin bar posteriorly and laterally to the quadrate. The articular condyle is level with the occipital condyle.

The otic notch is simply curved and open. It seems to be bordered by the quadratojugal anteriorly and the squamosal dorsally and is lined by the quadrate. The quadrate appears to be in a primitive vertical plane.

The bar of bone which separates the jugular foramen from the fenestra ovalis is probably part of the opisthotic and this bone probably also extends anteriorly to the prootic, flooring the inner ear cavity. These conditions would then be similar to those in *Rhinochelys* where the opisthotic forms the bony septum between the medial acoustic cavity and the inner ear cavity, and floors the latter.

As far as I can see, to reach the condition seen in *Rhinochelys*, the following developments have taken place:

The basioccipital has grown at point *A* laterally to point *B*. It lies ventral to the other bones and has grown alongside the opisthotic bar forming the floor to an extended 'jugular canal' (medial acoustic-jugular cavity), and joins the opisthotic level with the floor of the inner ear cavity, and the pterygoid at point *B*. This 'jugular canal' is completed by the exoccipital which has extended from point *A*, laterally, to form a posterior wall. This canal opens into the brain cavity by the anterior jugular foramen and into the main part of the acoustic-jugular cavity by the posterior jugular foramen.

The pterygoid has grown along its entire posterior margin. It has extended backwards to floor the lateral concavity and so forms the acoustic-jugular cavity. Posteriorly it meets the basioccipital, underlies the floor of the inner ear cavity, completely surrounds the basisphenoid (except posteriorly), and encloses the internal carotid and the lateral head vein between itself, the prootic, and the quadrate. Medially the pterygoids have grown under the basipterygoid processes and the cultriform process, and the internal carotid enters the basisphenoid through the cultriform process, dorsal to the pterygoids.

The quadrate fills the otic notch and forms the tympanic fossa. The articular condyle is pushed anteriorly. In *Rhinochelys*, the original position of the otic notch is suggested by the curved quadratojugal.

TAXONOMIC POSITION OF *RHINOCHELYS*

Having described the cranial morphology of *Rhinochelys*, it is now possible to use this information in attempting to establish to which family the genus belongs. Seeley (1869) said quite simply that the genus had emydian affinities, but gave no reason for this remark. The modern concept of the Testudinidae (Romer 1956, Loveridge and Williams 1957) emphasizes the following features: the presence of a squamosal antrum, the fenestra postotica is almost closed, the pterygoid meets the maxilla, and the nasal bones are absent. Since none of these features is present in *Rhinochelys*, there seems to be no reason for further considering this relationship.

Lydekker (1889) considered that the genus was probably pleurodiran and gave the following reasons: distinct nasals are present only in the Chelydidae, the palatines unite in the midline only in the Pelomedusidae, and there is the same relationship of bones around the internal nares as in *Pelomedusa*. He said also that the narrow palatines and pterygoids and complete roofing of the temporal fossa was more like the Cryptodires than the Pleurodires. However, since Lydekker's time, there has been a major revision of the taxonomy of the Chelonia, and there are diagnostic features of the Pleurodires in the present concept (Romer 1956) which are not present in *Rhinochelys*. These are: the absence of a descending process of the prefrontal, the broad pterygoid with a rolled up lateral expansion, and the meeting between the quadrate and the basisphenoid. On this basis there seems to be little evidence of relationships between *Rhinochelys* and this group of families.

In his description of *Desmatochelys* Williston (1898) compared it with *Rhinochelys* and referred them both to his new family, the Desmatochelyidae. This was followed by Romer (1956). Zangerl and Sloan (1960) suppressed the Desmatochelyidae when they demonstrated the affinities of *Desmatochelys* to the Cheloniidae, on post-cranial material. The relationship between the two genera is discussed below.

Thus *Rhinochelys* has not been satisfactorily assigned to any family, and this will now be considered using modern taxonomy.

Firstly, there can be little doubt that *Rhinochelys* belongs to the superfamily Chelonioidea, which is in the suborder Metachelydia of Zangerl (1969). The characteristics of this superfamily as given by Romer (1956) are as follows: temporal region well roofed; premaxillae unfused; vomer meets premaxilla, separates internal nares and separates the palatines; parietal with descending process; epipterygoid present; pterygoids constricted at mid-length, broadly in contact with one another and separate the basisphenoid from the palatine; pterygoid not in contact with the maxilla. *Rhinochelys* shows all these features except that the vomer does not separate the palatines.

The three families in the Chelonioidea (the Cheloniidae, the Toxochelyidae, and the Protostegidae) are all recorded from the Cretaceous. The position of *Rhinochelys* is shown most clearly by tabulating the condition in respect of a number of cranial features in *Rhinochelys* and in each of these three families. The features of the Toxochelyidae and the Protostegidae are taken from Zangerl (1953 *a*, *b*), and Wieland (1900), and of the Cheloniidae from Loveridge and Williams (1957).

As can be seen from Table 2, *Rhinochelys* has the salient features of the Protostegidae, especially the structure of the mandible and palate, and is best referred to this family. The Protostegidae contains two subfamilies, the Protosteginae (large, highly specialized genera) and the Chelospharginae (two small and primitive genera, *Chelosphargis* and *Calcarichelys*). *Rhinochelys* is obviously neither large nor specialized; in fact it is distinctive in its lack of specialization, which fits in with the subfamily Chelospharginae as diagnosed by Zangerl (1953*a*, p. 128):

> Small blunt straight premaxillary beak. Frontal bones large and with lateral processes towards orbital rims. Prefrontal bones excluded from sagittal contact by nasal bones. Otic and exoccipital area very similar to the condition in cheloniid turtles. Symphysis mandibuli long, with rami fused even in juvenile individuals. Slight, but sharp, sagittal crest on the triturating surface of lower jaw.

The skull of *Calcarichelys* is not known. The skull of *Chelosphargis* has been described by Zangerl (1953*a*, pp. 81–4, figs. 21*a–d*, 22). Comparing this with *Rhinochelys*, the close

relationship between the two genera is unmistakable. The shape of the temporal roofing bones, the ant-orbital beak, the primary palate, the structure of the lower jaw and the epidermal sulci crossing the maxilla and the dorsal bones, are closely comparable in the two genera. Unfortunately the palate and otic region on the specimens of *Chelosphargis* are not preserved in any detail. The occipital region on one specimen, however, is described by Zangerl (op. cit., p. 82), who states that this region resembles *Chelonia* rather than *Dermochelys*, although in his figures 22*a*, *b*, the exoccipital does not appear to contribute to the occipital condyle as it does in *Chelonia*.

TABLE 2. Comparison of cranial features of *Rhinochelys*, Protostegidae, Toxochelyidae and Cheloniidae (a—absent, p—present)

	Rhinochelys	*Protostegidae*		*Toxochelyidae*	*Cheloniidae*
		Chelosphargina	*Protosteginae*		
Postorbital extends back to squamosal tip	a	unknown	a	p	a
Prefrontals meet dorsally	a	a	p	p	p
Vomer separates the palatines	a	unknown	a	p	p
Palatine fenestra	a	unknown	a	p	a
Pterygoids joined to maxillae or jugals	a	unknown	a	maxillae	jugals
Secondary palate	a	a	a	a and p	p
Mandibular symphysis very wide, about one-third length of the rami	p	p	p	a	a
Sharp symphysial ridge	p	p	p	a	a and p

RELATIONSHIP OF *RHINOCHELYS* TO OTHER CRETACEOUS TURTLES

In establishing the family position of *Rhinochelys*, the skull structure of the Recent Cheloniidae is used. All the criteria of this family are based upon the structure of the limbs, girdles, and plastron. The cheloniid method of locomotion apparently underwent little change after its development (Zangerl 1953*b*), but the structure of other parts of the skeleton, including the skull, seems to have been subjected to evolutionary experiment over the long period of time involved. From North America there are two other genera of Cretaceous turtles, *Corsochelys* Zangerl (1960) and *Desmatochelys* Williston (1894), which have been placed in the Cheloniidae on the evidence of the postcranial skeleton. The skulls in these genera show features which are not present in later cheloniids. Table 3 demonstrates the similarities and differences between these two genera, *Rhinochelys*, *Chelosphargis*, and the Recent cheloniids and advanced protostegids.

Corsochelys and *Desmatochelys* closely resemble *Rhinochelys* and *Chelosphargis* but do not display the distinctive protostegid mandible and palate (where preserved), and show cheloniid features. Thus there are four unspecialized genera in the Cretaceous showing distinct features of two families (the Cheloniidae and the Protostegidae) but also possessing many common features which are not shared by the more advanced members of these families. It seems logical to surmise that they have inherited these features from a common ancestry.

TABLE 3. Comparison of cranial features of *Rhinochelys*, *Chelosphargis*, *Desmatochelys*, *Corsochelys*, Recent Cheloniidae and advanced Protostegidae (a—absent, p—present)

	Rhinochelys	*Chelosphargis*	*Desmatochelys*	*Corsochelys*	*Recent Cheloniidae*	*Advanced Protostegidae*
Similarities						
Nasal bones present	p	p	p	p	a	a
Squamosal separated from the parietal	p	—	p	p	a	a
Prefrontals excluded from meeting medially	p	p	p	—	a	a
Primary palate	p	p	p	—	a	p
Vomer does not separate the palatines	p	—	p	—	a	p
Frontal extends to the rim of the orbit	p	p	p	p	a (except in *Chelonia*)	a
Exoccipital does not meet the pterygoid nor extend over the basioccipital	p	—	—	p	a	—
Differences						
Quadratojugal extends to orbital rim	a	—	p	—	a	a
Epidermal sulci	p	p	a	—	a	a
Flat palate	p	—	concave	—	secondary	p
Wide mandibular symphysis	p	p	a	—	a	p

CARAPACE AND PLASTRAL MATERIAL POSSIBLY BELONGING TO *RHINOCHELYS*

A number of remains of carapaces and plastra is known from the Albian to Turonian of south-east England. Unfortunately skull material is not associated with any of these. However, these carapaces and plastra appear (as will be shown) to be of chelospharginid type and, now that *Rhinochelys*, from the same area and deposits, is known to be a chelospharginid, it seems worth investigating the possibility that this material belongs to *Rhinochelys*. The first specimen to be described was a small, probably juvenile, carapace which Mantell (1841) named *Emys benstedi*. Owen (1841) transferred it to the genus *Chelone* and also considered that it was sufficiently distinct to merit subgeneric status, naming it *Cimochelys*. This has been used as a generic name by Zangerl (1960).

Description. The type-specimen of *Emys benstedi* is BMNH 28706. This has been broken and part of the carapace is lost. Other material which appears to be related includes BMNH 39112 (text-fig. 15), R1350, 47210 (text-fig. 16); GSM442; SM B20607.

The type material has unfortunately been partly lost since it was described, and therefore the following description is taken from Owen's figured specimen BMNH 39112 (1851, pp. 7–8, pl. 3) which in all points resembles what remains of the type, the original description, and the figures.

The carapace is heart-shaped with moderate fontanelles and a sharp neural keel which is flattened anteriorly. The sides slope more or less straight from the neurals to the peripherals. The neurals are rectangular, very narrow, long, and of even size, except the eighth, which is triangular and half the length of the seventh. The sutures between the costals and between the neurals correspond, instead of being offset as in the Cheloniidae. The costals are straight, slope at a steep angle and, about halfway along their length, taper into broad striated ribs which continue to taper until they articulate in deep pits in the inner surface of the peripherals. The 2nd peripheral is thin and flat and lies across the front of the carapace. The 3rd is flat anteriorly but broadens posteriorly to become deeply triangular in cross-section; it is crescent-shaped and forms the broad curved angle of the carapace. The 4th–6th peripherals are deeply triangular in cross-section with a convex dorsal and a concave ventral surface. Each peripheral has a deep medial pit in the inner surface for the rib articulation. The 7th–11th peripherals have shallower cross-sections. The medial border of these bones is smooth. The 8th neural, suprapygal, pygal, 11th peripheral, 8th costal and rib, together form a solid bony posterior to the carapace.

Epidermal shield sulci cross the 1st, 3rd, 5th, and 7th costal and neural bones (the 1st neural is not preserved but was presumably the same). These sulci form three small peaks across the neural keel. Each peripheral is notched on the outer margin by a sulcus which gives a serrated appearance to the carapace edge, especially posteriorly.

Plastron. The description of the plastron is taken from the type-specimen. The hyo- and hypoplastra only are preserved and are subrectangular in outline with a moderate

EXPLANATION OF PLATE 69

Figs. 1–4. *Rhinochelys* sp. SM B94606. 1, Occiput, ×1. 2, Lateral view of the brain cavity with the otic capsule removed, ×1. 3, Enlarged view of the hiatus acusticus, inner ear cavity, and the anterior jugular foramen. 4, Dorsal view of a natural cast of the upper brain cavity, ×1.

4

3

2

1

fontanelle in the centre. The hyoplastra are the smaller and meet medially with long digitations, and laterally and posteriorly with short fine digitations. The digitations bordering the fontanelle are fine anteriorly and become larger posteriorly, forming twelve or so large fingers between the hypoplastra. The posterior margin of these plates has two long fingers of bone curving backwards and inwards. In BMNH 47210, from the Gault of Folkestone, Kent (text-fig. 16), the posterior part of the plastron is concave, dipping steeply in from the sides to a depth of 10 mm. Comparison with the Recent turtles suggests that this is probably a male sexual character.

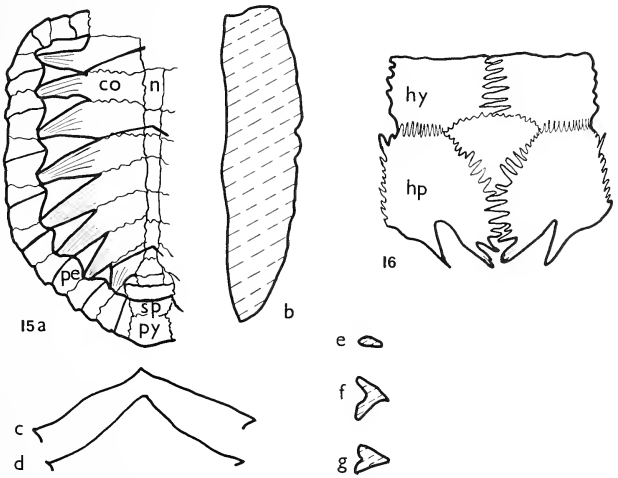

TEXT-FIGS. 15, 16. *Cimochelys benstedi*. 15, BMNH 39112; *a*, reconstructed carapace, ×0·5; *b*, longitudinal section; *c*, anterior transverse section; *d*, posterior transverse section; *e*, cross-section through the second peripheral; *f*, cross-section through the fourth peripheral; *g*, cross-section through the ninth peripheral. 16, Plastron, BMNH 47210, reconstructed ventral view, ×0·5. Explanations of abbreviations: *co*, costal; *n*, neural; *hy* hyoplastron; *hp*, hypoplastron; *pe*, peripheral; *py*, pygal; *sp*, suprapygal.

Discussion. The material was originally described by Mantell (1841) as *Emys benstedi*, although the plastron resembled that of the marine turtles. Mantell considered that the carapace was like that of the juvenile *Emys* because the ribs diminish in width towards the circumference, which might indicate a gradual growth and tendency towards complete infilling of the interspaces. He also pointed out that in marine turtles the broad part of the rib is sharply demarcated from the linear part. However, the carapace in the Testudinidae is usually solid even in juveniles and is very different from *Emys benstedi*. The neurals are hexagonal and generally broader than long; the peripherals are solid and double wedge-shaped with a thin dorsal plate under which lies the tip of the rib;

they are not triangular in cross-section nor open medially. The plastron is not reduced and forms a solid bony plate which is well fused to the carapace.

Owen (1841, 1851) placed the species in *Chelone* on the following points: the carapace is pointed posteriorly with moderate fontanelles, narrow neurals and peripherals which do not join to the plastron; the central fontanelle of the plastron is more like that of the marine turtles than that of *Emys*. He considered, at this time, that most marine turtles belonged to the genus *Chelone*. However, he suggested a subgeneric name, *Cimochelys*, as he believed that these specimens had particularly close affinities to the Emydidae.

Since Owen's time, marine turtles of three families have been described from the Cretaceous: the Protostegidae, Toxochelyidae, and Cheloniidae. The characteristics of *Cimochelys* may therefore now be compared with those of the members of these three families.

At family level, *Cimochelys* has the following features in common with the Protostegidae: narrow, long, rectangular neurals; sharp neural keel; neural and costal sutures coincide; gradual demarcation between the costal plates and the ribs; and subrectangular (rather than saddle-shaped) hyo- and hypoplastra. In none of these features is it like the Toxochelyidae or the Cheloniidae. Next, comparing *Cimochelys* with the two subfamilies in the Protostegidae, it may be noted that it is like the Chelospharginae, and unlike the Protosteginae, in the lack of reduction of its carapace and plastron, and in the absence of digitations along the medial border of the peripherals (Zangerl 1953*a*, p. 128). The differences in the other two genera in the Chelospharginae (*Chelosphargis* and *Calcarchelys*) and *Cimochelys* appear to lie mainly in the degree of formation of the peaks on the neural keel and serrations around the posterior edge of the carapace. In *Calcarichelys* these appear to be accentuated, but *Chelosphargis* is relatively smooth.

Thus the carapace material is characteristic of the Protostegidae, subfamily Chelospharginae, and closely related to *Chelosphargis* and *Calcarichelys*. Since the *Rhinochelys* skulls from similar deposits are also related to these genera, it is suggested that *Cimochelys benstedi* could be the missing post-cranial material of *Rhinochelys*.

Synonomy.

1841 *Emys benstedi* Mantell, pp. 153–8, pl. 11, 12.
1841 *Chelone* (*Cimochelys*) *benstedi* (Mantell); Owen, pp. 176–7.
1851 *Chelone benstedi* (Mantell); Owen, pp. 1–11, pl. 6–8.

SUMMARY

A critical examination of all available British material of the Cretaceous turtle *Rhinochelys* reveals the inadequacy of Lydekker's descriptions and generic diagnosis. Three species only are truly distinguishable; of these, two species (typified by the types of *R. elegans* and *R. cantabrigiensis*) comprise the bulk of the collections, while *R. pulchriceps* is the least common. *R. jessoni* is considered to be a junior synonym of *R. cantabrigiensis*, and *R. macrorhina* and *R. brachyrhina* are considered to be junior synonyms of *R. elegans*. The cranial distinctions between these species are restated and they are compared with the French species *R. amaberti*. Charts of angles taken about the skull and proportional measurements reveal characteristic differences between the three species. These are definable even if superficial features have been eroded. The charts are also of value when handling skulls of different growth stages as there appears to be little

ontogenetic variation. A very finely preserved brain case and otic capsule of *Rhinochelys* is described from the Chalk of Hampshire.

The posterior part of the palate and occiput of a skull of *Proganochelys quenstedti* Baur has been reconstructed from the photographs in Parsons and Williams (1961, pl. 5, 6). The obvious features are discussed and a possible mode of development of the skull into that described in *Rhinochelys* is suggested.

Rhinochelys is referred to the family Protostegidae, subfamily Chelospharginae, mainly on the evidence of the mandible and palate structure. It is compared with the skulls of other Cretaceous turtles and a close relationship in the cranial morphology between the primitive protostegids and the primitive cheloniids is clearly shown.

Since no associated post-cranial material is recorded, all generic and specific descriptions are based on skulls. Carapace and plastral remains have been described from the Upper Cretaceous of south-east England as *Chelone* (*Cimochelys*) *benstedi* (Mantell 1841). These are referable to the same subfamily as *Rhinochelys* and are provisionally referred to the same genus.

The Protostegidae, hitherto restricted to the Late Cretaceous of North America, is extended in range to the Albian–Turonian of Europe.

Acknowledgements. I would like to thank Dr. C. B. Cox (King's College, London) for his patient help with the manuscript; also Dr. A. Charig and Mr. C. Walker (British Museum (Natural History)), Dr. C. Forbes and Mr. A. G. Brighton (Sedgwick Museum, Cambridge), Mr. B. MacWilliams (Norwich Castle Museum, Norwich), and Mr. C. Wood (Institute of Geological Sciences) for access to and loan of specimens; and the Photographic Department, British Museum (Natural History) and Mr. E. Kentish for preparing the photographs.

REFERENCES

BRYDONE, R. M. 1912. *The Stratigraphy of the Chalk of Hants.* London, 116 pp., pl. 1–3.

COX, C. B. *et al.* 1967. Reptilia, *in* HARLAND, W. B. *et al.* (eds.) *The fossil record*, London (Geological Society), 698 pp.

KESTEVEN, H. L. 1910. The anatomy of the head of the green turtle *Chelone midas. J. Proc. R. Soc. N.S.W.* **44,** 368–400, pl. 20–33.

LOVERIDGE, A. and WILLIAMS, E. E. 1957. Revision of the African tortoises and turtles of the suborder Cryptodira. *Bull. Mus. comp. Zool. Harv.* **115,** 163–557, pl. 1–18.

LYDEKKER, R. 1889. On remains of Eocene and Mesozoic Chelonia and a tooth of (?) *Ornithopsis. Q. Jl geol. Soc. Lond.* **45,** 227–46, pl. 8.

MANTELL, G. 1841. On the fossil remains of turtles, discovered in the Chalk Formation of South-East England. *Phil. Trans. R. Soc.* **131,** 153–8, pl. 11, 12.

MORET, L. 1935. *Rhinochelys amaberti*, nouvelle espèce de tortue marine du Vraconien de la Fauge, près du Villard-de-Lans (Isère). *Bull. Soc. géol Fr.* **1,** 605–19, pl. 27, 28.

OWEN, R. 1841. Report on the British Reptiles. *Rep. Br. Ass. Advmt Sci.*, 60–204.

—— 1851. A Monograph on the Fossil Reptilia of the Cretaceous Formations. *Palaeontogr. Soc.* [*Monogr.*] **1,** i–vi, +118, pl. 1–37.

PARSONS, T. S. and WILLIAMS, E. 1961. Two Jurassic turtle skulls: a morphological study. *Bull. Mus. comp. Zool. Harv.* **125,** 43–107, pl. 1–6.

ROMER, A. S. 1956. *Osteology of the Reptiles.* Chicago, xxi+772 pp.

SEELEY, H. G. 1869. *Index to the fossil remains of Aves, Ornithosauria, and Reptilia from the Secondary System of Strata arranged in the Woodwardian Museum of the University of Cambridge.* Cambridge, i–xxiii+143 pp.

WIELAND, G. R. 1900. The skull, pelvis and probable relationships of the huge turtles of the genus *Archelon* from the Fort Pierre Cretaceous of South Dakota. *Am. J. Sci.* **9,** 237–51, pl. 2.

WILLISTON, S. W. 1898. *Desmatochelys lowi. Univ. geol. Surv. Kans.* **4** (1), 353–69, pl. 73–78.

ZANGERL, R. 1953*a*. The vertebrate fauna of the Selma Formation of Alabama. Pt. 3, The turtles of the family Protostegidae. *Fieldiana, Geol. Mem.*, 59–133, pl. 5–8.

—— 1953*b*. The vertebrate fauna of the Selma Formation of Alabama. Pt. 4, The turtles of the family Toxochelyidae. Ibid. 137–277, pl. 9–29.

—— 1960. The vertebrate fauna of the Selma Formation of Alabama. Pt. 5, An advanced cheloniid sea-turtle. Ibid. 281–312, pl. 30–33.

—— 1969. The turtle shell, *in The biology of the Reptilia* (eds. C. GANS, A. D'A. BELLAIRS, and T. PARSONS). London and New York, 311–39.

—— and SLOAN, R. E. 1960. A new specimen of *Desmatochelys lowi* Williston, a primitive cheloniid sea-turtle from the Cretaceous of South Dakota. *Fieldiana, Geol.* **14**, 7–40, pl. 1, 2.

JANICE I. COLLINS
63 Oakhurst Grove
E. Dulwich
London, S.E. 22

Final typescript received 16 September 1969

THE SHELL STRUCTURE, MINERALOGY AND RELATIONSHIPS OF THE CHAMACEA (BIVALVIA)

by W. J. KENNEDY, N. J. MORRIS, *and* J. D. TAYLOR

ABSTRACT. The superfamily Chamacea is a group which has constantly confused systematists concerning its relationship with other bivalves. Various authors have related it to the Cardiacea, Veneracea, Crassatellacea, Lucinacea, and the rudists (Hippuritacea).

Most classifications have placed the Chamacea with the rudists; Newell (1965) placing them into the Hippuritoida, a relationship which Yonge (1967) considers beyond doubt. From a review of hard and soft part anatomy, especially shell-structure, dentition, and mineralogy, it seems likely that the Chamacea arose from a group of byssate *Cardita* in the early or middle Cretaceous. Similarities to the rudists are the result of convergent adaptions to a similar mode of life, and there is no real indication of relationship.

The Chamacea should be removed from the order Hippuritoida and placed in the order Veneroida.

THE Chamidae are the sole bivalve family placed in the Superfamily Chamacea (Newell 1965). They are a small group of cemented or secondarily free bivalves which have attracted the attention of zoologists for many years because of the problem of their origins and systematic position. Despite this attention, the systematics of the Recent species is in a very confused state.

Many authors have inferred that the Chamacea are closely related to the rudists (i.e. Odhner 1919, Yonge 1967) and the most recent review of bivalve classification (Newell 1965) places them in the Order Hippuritoida, together with the Megalodontacea and Hippuritacea. We describe the shell structure and mineralogy of recent and fossil Chamidae below, and discuss the use of these features and the nature of the soft part anatomy to determine the natural relationships to other bivalve superfamilies. We have demonstrated elsewhere (Taylor, Kennedy, and Hall 1969) that shell structure and mineralogy are constant features within bivalve superfamilies, and that they are of value in assessing relationships within the Bivalvia.

The Chamacea are characteristic inhabitants of tropical and sub-tropical seas, although some species, such as *Chama pellucida* Broderip, range into cooler temperate waters along the coast of California (San Francisco), but are also present in warmer waters. One species, *Chama gryphina* Lamarck, is present in the Mediterranean.

Chama usually inhabits rocky shores, and is a typical member of the coral reef community. Individuals usually live cemented on rocky surfaces or upon dead coral. Coral-dwelling *Chama* species are usually found on the underside of coral colonies. Most species inhabit the sublittoral and sublittoral fringe environments, but some are intertidal.

Arcinella arcinella (Linnaeus), a Caribbean species, is usually found free living on a coarse gravel substrate (Nicol 1952) but occasionally cemented adults of this species are found. The loss of cementation in *Arcinella* is secondary, for traces of attachment are always to be seen on the juvenile parts of the shell. Certain fossil species such as

[Palaeontology, Vol. 13, Part 3, 1970, pp. 379–413, pl. 70–77.]

Chama calcarata Deshayes from the Calcaire Grossier of the Paris Basin (Eocene, Lutetian), a shell sand facies, also show this secondary loss of cementation.

THE SHELL

1. *General morphology*. The Chamacea are generally inequivalve, asymmetrical, the free valve being the smaller. The lower valve is usually convex and the upper valve is frequently more or less flattened (Pl. 70, fig. 1). Many early Chamacea are rather less inequivalve than extant forms. The secondarily free genus *Arcinella* (Pl. 70, fig. 2) has returned to a more or less equivalve state. The shell of the Chamacea is thick; the umbones are prosogyrous; attachment can be by either valve.

Shell ornament is variable. Some species bear irregular, concentric lamellae, which may be long and foliaceous (Pl. 70, fig. 4); others are spinose, or have irregular, low squamae. Some species have radial ribs as well as concentric lamellae. Ornament varies considerably with environmental conditions such as site of cementation, exposure to wave action and encrusting biota. *Arcinella* is the only genus which consistently bears long spines. Some specimens of *Chama* show a shallow groove running from the umbo to the posterior ventral margin; this is often marked by a supression of strong sculpture. A well-marked, heart-shaped lunule is present in *Arcinella* (Pl. 70, fig. 2).

The interior margin of the shell is frequently crenulate, while the area between the shell edge and the pallial line may be marked by irregular radial grooves and ridges, which are the impressions of the radial masculature of the mantle (Jaworski 1928).

The pallial attachment area (pallial line) is wide, and the dorsal side is overlapped irregularly by inner shell layer. The adductor muscle pads are massive and translucent; they and the pallial line fluoresce blue under ultra-violet light.

2. *Shell geometry*. Growth in the Chamacea has been considered by Yonge (1967) in terms of radial, transverse, and tangential growth components, as discussed by Owen (1953*a*). As they stand, these terms are purely qualitative and have not been mathematically defined. As such they are of limited use in the discussion of shell form.

Lison (1949) described shell coiling in mathematical terms, and more recently Raup (1966) using the same logarithmic spiral, has provided a more comprehensive scheme for the quantitative description of shell coiling. Thus four basic parameters may be used to define the general form of the coiled shell. These are: the shape of the generating curve (S), the whorl expansion rate (W), the distance of the generating curve from the axis (D),

EXPLANATION OF PLATE 70

Fig. 1*a*. *Chama macerophylla* Gmelin, Recent, West Indies, cemented to a pebble, ×1. 1*b*, as above, view of right valve, ×1.

Fig. 2. *Arcinella arcinella* (Linnaeus), Recent, West Indies, dorsal view showing lunule, cementation site and prodissoconch (arrow), ×1. 2*a*, as above, lateral view of right valve showing spinose ornament on radial ribs, ×1.

Fig. 3. *Chama pellucida* Broderip, Recent, California, view of inner surface of valve, showing outer translucent calcitic prismatic layer, ×1.

Fig. 4. *Chama frondosa* Broderip, Recent, West America, showing extreme development of frondose squamae, ×1.

Fig. 5. *Gyropleura cenomanensis* d'Orbigny, Cenomanian, Le Mans, France, cemented to valve of *Scabrotrigonia*, ×1·25.

1a

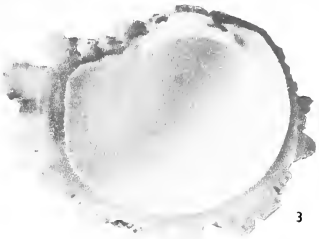

3

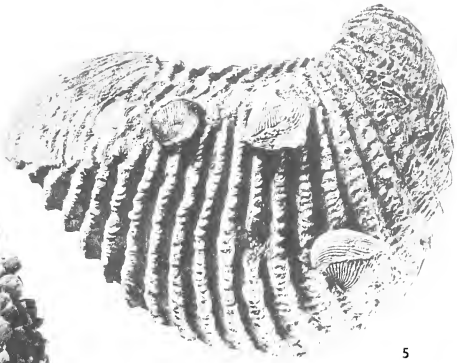

5

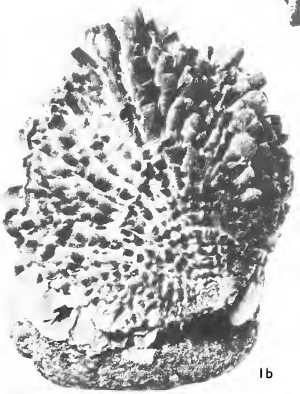

1b

2a

2b

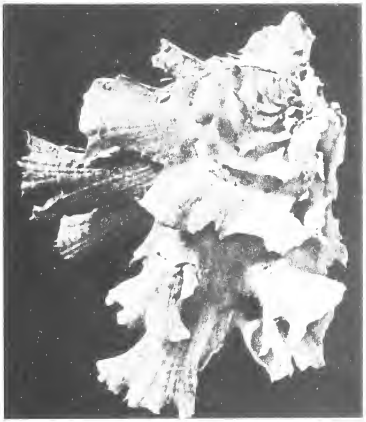

4

KENNEDY, MORRIS and TAYLOR, Chamacea

and the rate of whorl translation parallel to the coiling axis (T) (for full details and derivation see Raup 1966). For most bivalves D is small, and in the Chamacea it is approximately zero. The shape, S, of the generating curve is difficult to define mathematically and is not considered here.

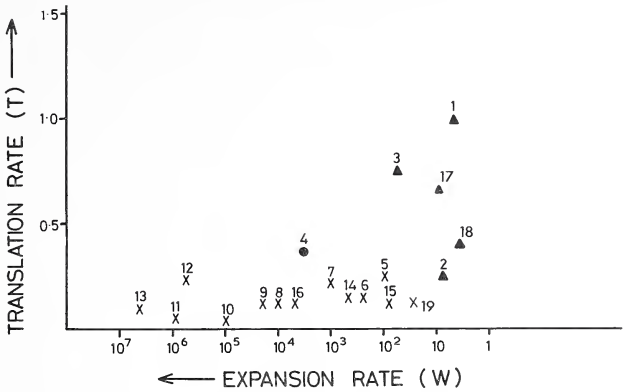

TEXT-FIG. 1. Shell geometry of the Chamacea in relation to other bivalves. Expansion rate (W) plotted against translation rate (T) for a series of uncemented bivalves (x), cemented Chamidae (▲), and the secondarily free *Arcinella arcinella* (●).

Key to numbers:

1, 2. *Chama imbricata* (1 = upper valve, 2 = lower valve).
3. *Chama plicata* Sowerby. Upper valve.
4. *Arcinella arcinella* (Linnaeus). Both valves.
5. *Fragum unedo* (Linnaeus).
6. *Hippopus hippopus* Linnaeus.
7. *Trigonia pectinata* Lamarck.
8. *Codakia tigerina* (Linnaeus).
9. *Mytilus galloprovincialis* Lamarck.
10. *Chlamys varia* Linnaeus.
11. *Gloripecten pallium* (Linnaeus).
12. *Lima squamosa* Lamarck.
13. *Pinctada margaritifera* (Linnaeus).
14. *Crassatella decipiens* Reeve.
15. *Cerastoderma edule* (Linnaeus).
16. *Tellina virgata* (Linnaeus).
17, 18. *Chama gryphina* (Lamarck). (17 = lower valve, 18 = upper valve).
19. *Cardita bicolor* Reeve.

Accurate measurements of W and T are difficult to make in the Chamacea because of the irregular growth form, ornament, and the corroded nature of most shells. Measurements of W and T on *Chama gryphina* Lamarck (text-fig. 1) show that the expansion rate of the lower valve lies between $10^{0.5}$ and $10^{0.9}$, and that of the upper valve is approximately 10. The translation rate of both valves is less than 1. In a specimen of *Chama plicata* Sowerby, where the umbo of the lower valve is strongly enrolled, the translation rate lies between 3·0 and 3·5 whereas that of the upper valve is less than 0·5. Measurements of *Arcinella arcinella* (which has reverted to the uncemented mode of life) show an expansion rate for both valves of approximately $10^{3.5}$. The translation rate is almost zero.

As can be seen from text-fig. 1 the expansion rate of both valves of the cemented Chamacea is low, usually between 10 and 10^2. In 'normal' free-living bivalves such as the Cardiacea and Veneracea, and in *Arcinella*, the expansion rate usually lies between 10^2 and 10^4.

It is clear that the translation rate of any one individual will be variable, according to the substrate upon which original cementation took place. Some repositioning during growth is evident in the attached valve of many individuals, with consequent changes in the translation rate.

3. *The ligament*. The ligament of the Chamacea is opisthodetic, massive, external, but often sunk into a deep groove.

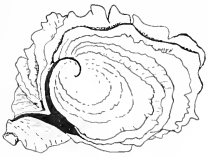

TEXT-FIG. 2. Sketch of *Chama broderipi* Reeve (with strongly enrolled umbos), Recent, Pacific. To show degree of ligament splitting. (Ligament in black.)

The enrolment of the umbonal area causes the ligament to be widely split towards the anterior; each half of the split ligament curls back into the umbones (text-fig. 2).

Three ligament layers are present, an outer thin periostracum, a lamellar layer, and an inner fibrous layer. The outer lamellar layer is thick and wide, and the inner layer is calcified and aragonitic (Pl. 77, fig. 1).

The ligamental splitting is more pronounced than in other bivalves (Stasek 1963 *a*, *b*). Yonge (1967) states that this anterior splitting is due to the rate of growth of the ligament posteriorly exceeding the rate of growth of the valves; this does not seem meaningful as an explanation. The splitting is rather a result of the interumbonal growth produced by the low expansion rate of shell coiling, coupled with a small translation rate. The degree of splitting depends upon the translation rate, which may be rather higher in cemented Chamacea than in the free *Arcinella*. A similar degree of ligamental splitting as is seen in the Chamacea is present in *Glossus* (Owen 1953*b*).

During growth of the shell the ligament elongates in a posteriorward direction. Previously deposited sections of the ligament are overlain by the posteriorward growth of the massive hinge plate.

DEVELOPMENT

The dissoconch stages of Chamacea show a markedly different shell form to that of the adult.

Dissoconchs were examined on very small cemented individuals of *Chama*. Odhner (1919) figured and described some precementation dissoconchs (text-fig. 3, Pl. 71, figs. 1–5). In *Arcinella arcinella* the large dissoconch can frequently be seen preserved at the tips of the umbones on adult shells (Pl. 71, fig. 3).

The first of the shell growth stages is the prodissoconch, formed during the veliger stage. Part of this may be formed by the shell gland rather than the mantle edge. In the Chamacea examined, *Chama pellucida* Broderip, *Chama* sp., and *Arcinella arcinella*, the prodissoconchs (Pl. 71, figs. 1–5) are highly convex, subcircular in outline, translucent, and ornamented only by growth-lines. The form of the prodissoconch indicates a larva either feeding entirely upon the egg yolk during the planktonic stage

(i.e. lecitotrophic), or having direct development and some sort of brood protection (Ockelmann 1962). Yonge (1967) indicates that larval incubation could conceivably occur in *C. pellucida* and *C. exogyra* Conrad.

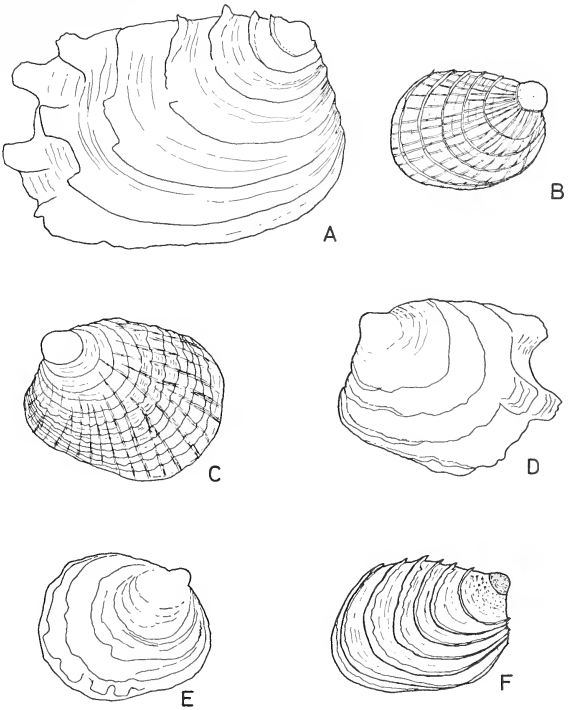

TEXT-FIG. 3. Prodissoconchs and dissoconchs of Recent Chamidae. A. *Arcinella arcinella* (Linnaeus), after Odhner (1919), ×60. B. *Chama pellucida* Broderip, Recent, California, ×60. C. *Chama pusilla* (Odhner), after Odhner (1919), ×40. D, E. *Chama gryphina* Linnaeus, after Odhner (1919), ×60. F. *Chama* sp. East Indies, ×70.

The sharp boundary between prodissoconch and dissoconch (Pl. 71, fig. 2) marks the settlement of the animal on to a substrate. The dissoconch which is secreted by the mantle in the Chamacea is uncemented, equivalve and possesses a sculpture and morphology differing from that of the adult. This stage usually lasts until the young *Chama* is from 0·5 to 1·5 mm. long, but in *Arcinella arcinella* the dissoconch may be prolonged until the individual is 2·5 mm. long. The dissoconch stage is terminated by cementation.

Dissoconch shape is somewhat variable, although a subrectangular or ovate outline is usual (text-fig. 3). Sculpture may consist of thin, widely spaced concentric ribs, as in *Arcinella arcinella* (Pl. 71, fig. 3), in which the outermost parts of the ribs may be projected into small squamae. A similar ornament is seen in *Chama gryphina*.

'*Pseudochama*' *pusilla* Odhner dissoconchs have reticulate ornament (Odhner 1919); *Chama reflexa* Reeve and *C. jukesi* Reeve dissoconchs (Odhner 1919) have radiating ribs. Anthony (1905) figures an unidentified *Chama* dissoconch with fine radiating and concentric ribs. *Chama pellucida* (Pl. 71, fig. 1) has an ornament of fine radiating ribs crossed by about six larger concentric ribs. The early stages of the dissoconch in an unnamed *Chama* show a peculiar pitted ornament (Pl. 71, fig. 5), although the rest of the dissoconch bears concentric ribs only (Pl. 71, fig. 4).

The dentition of the dissoconch is known only from *Arcinella arcinella* (Odhner 1919), *Chama pellucida* (Dall 1903), and an unidentified species (Anthony 1905). In all of these, two cardinals are present in each valve.

An interesting feature of the dissoconch is the subrectangular shape, with a reduced anterior and an elongated posterior portion (text-fig. 3). It is well known that a byssate existence influences the shape of bivalves (Yonge 1962); thus in the Arcacea and some Carditidae a rectangular shape with a long ventral margin is developed. In some *Cardita* species there is a reduction in the anterior part of the animal, which is also seen in the Mytilacea. This purely morphological evidence strongly suggests that the dissoconch stage of some species of *Chama* is byssally attached prior to cementation. The presence of a much larger dissoconch in *Arcinella arcinella* suggests that the byssate existence was prolonged in this species. Unlike most other Chamacea *Arcinella arcinella* inhabits sandy substrates, and the long precementation byssate life may be an insurance against the choice of an unfavourable cementation site.

DENTITION AND INVERSION

Study of the dentition of the Chamacea has given rise to much controversy in the past. The reason for this confusion is that some Chamacea can cement themselves by either the left or the right valve. As a result of attachment by the right valve, the hinge teeth normally present in the left valve appear in the same number and positions in the right valve. As Davis (1935) has pointed out, confusion arises in the interpretation of the teeth of this family by attempting to number teeth in these reversed individuals as though they were in a normal right valve. There are many records of species of *Chama* being attached by either the left valve or the right valve, and even those species which are

EXPLANATION OF PLATE 71

Figs. 1, 2. *Chama pellucida* Broderip, Recent, California. 1, Prodissoconch, dissoconch and early adult shell. Note radial and concentric ornament on dissoconch, very different from the squamaceous ornament of the adult. Scanning electron-micrograph, ×140. 2, Detail of the sharp contact between the larval prodissoconch and the dissoconch. Notice close bunching of growth lines as feeding ceases prior to metamorphosis. Scanning electron-micrograph, ×700.

Fig. 3. Prodissoconch and dissoconch of *Arcinella arcinella* Linnaeus, Recent, West Indies showing concentric ornamentation. Scanning electron-micrograph, ×80.

Figs. 4, 5. Prodissoconch and dissoconch of *Chama* sp. from East Indies. 4, Scanning electron-micrograph, ×80. 5, Detail showing the contact between the prodissoconch and the dissoconch, with peculiar pitted ornamentation of the dissoconch. Scanning electron-micrograph, ×340.

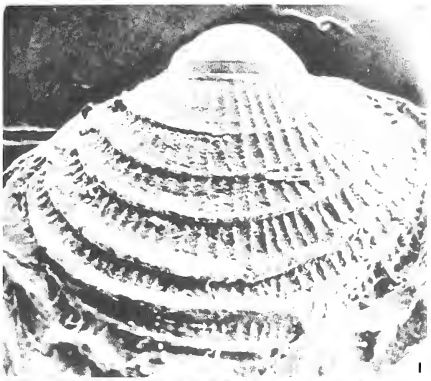

1

2

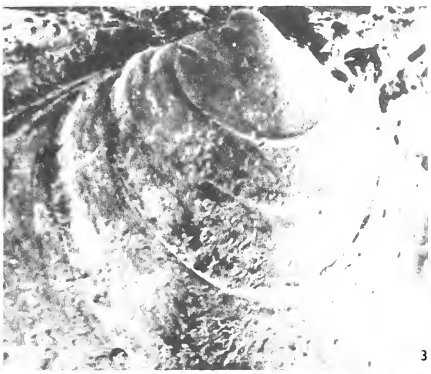

3

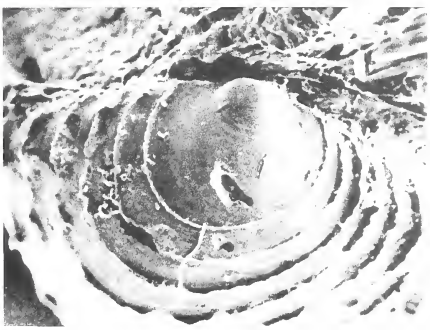

4

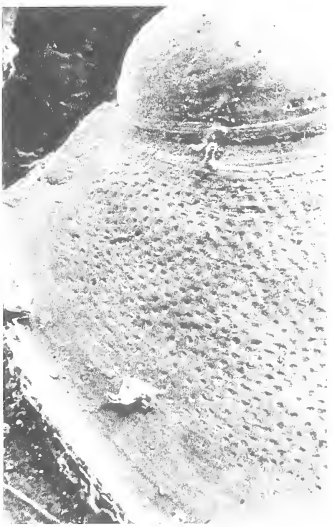

5

KENNEDY, MORRIS and TAYLOR, Chamacea

usually attached by one valve sometimes show attachment by the other (Bayer 1943, Palmer 1928, Yonge 1967). *Chama calcarata* (Eocene, Paris Basin) shows attachment by left and right valves in approximately equal proportions, and this type of variation, plus others noted above, makes the use of the generic name *Pseudochama* Odhner 1919 for those species attached by the right valve of very doubtful validity.

Yonge (1967) stated that it is impossible to homologize the cardinal teeth of the Chamacea with those of other heterodont bivalves because of the great modifications caused by 'tangential growth'. The teeth of many recent species of *Chama* are indeed greatly modified in the adult stage, and it is perhaps easier to study dentition in some of the less modified, fossil forms. The hinge notation used here is that elaborated by Boyd and Newell (1968) from the Steinmann notation, in which every articulating ridge, prominence or depression of the hinge is numbered. This notation system is more objective than that of Bernard (1895) and Munier-Chalmas (1895) which requires knowledge of the ontogenetic development within each family.

The Boyd and Newell system is flexible and is readily convertable to the Bernard system when homologous teeth are recognized. The two valves are illustrated beak to beak with the right valve above the left valve (following Bernard) so that the posterior of the valves lies to the left. The notation is devised to be directly comparable with this. The right valve hinge is expressed by the upper of two lines of symbols and, in both lines, the symbols are arranged from left to right to reflect a traverse along the hinge from the posterior extremity to the anterior extremity. All the structures of the articulating surfaces are indicated. The arabic numeral '1' represents teeth or potentially articular ridges. Inconspicuous or dubious teeth are indicated in brackets. Depressions in the articulating surface which generally function as tooth sockets are indicated as an '0'. Vertical lines, discontinuous in doubtful cases, are used to delimit cardinal from lateral teeth. Various letters such as 'r', 's', 'n', and 'e' are added to represent positions of the resilium, septum, nymph, and elastic ligament, etc.

The basic *Chama* dentition is Bernard's 'lucinoid' type. The hinge notation of *Chama calcarata* (Eocene, Paris Basin) can be expressed as shown below, and in Plate 72, fig. 2:

Right valve	0 1	n (0) (1) 0 1 0 1	
Posterior	———	———	Anterior.
Left valve	1	n (0) (1) 0 1 0 1 0	

n = ligament nymph

In the left valve the anterior cardinal is large and solid, and the posterior cardinal is long and curved. In the upper right valve, the anterior cardinal is small and ill defined, and the posterior cardinal is long and curved. They are separated by a socket for the reception of the large anterior cardinal of the left valve. Extra articulating ridges are developed between the posterior laterals and the nymphs. They are indicated in parentheses.

This species can be compared with the Recent species *Chama macerophylla* shown below and in Plate 72, fig. 1:

Right valve	0 1 n 0 1 0 1	
Posterior	———	Anterior.
Left valve	1 (0) n 1 0 1 0	

In the left valve the massive cardinal tooth is very large and grooved. The sockets for the reception of the cardinals of the right valve have fused to form an arcuate socket isolating the cardinal. In the right valve a comparable fusion of the two cardinals has taken place forming a single arcuate tooth. Loss of laterals has also occurred.

In *Arcinella arcinella* (an inverse form) a similar notation occurs, with the fusion of the cardinals and sockets:

Right valve	n 1	0 1 0	
Posterior			Anterior.
Left valve	n 0	1 0 1	

It will be shown below that the dentition of the early Chamacea shows great resemblances to that of the Carditacea.

ANATOMY

Studies on the anatomy of several species of Chamacea have been made by Anthony (1905), Pelseneer (1911), Grieser (1913), Odhner (1919), and most recently by Yonge (1967) who studied *Chama pellucida* and *C. exogyra*. The general anatomical features of the soft parts are summarized below.

The mantle is similar to that of most bivalves, except that the three marginal folds are rather small. The mantle is fused by the inner fold only, to form posteriorly the inhalent and exhalent siphons, and at the anterior to delimit the more extensive pedal gape. The very short siphons represent extensions of the fused inner mantle fold. Yonge (1967) stated that the mantle dorsal to the pedal gape is fused at the inner fold and the inner part of the middle fold. A laterally compressed flap of mantle projects between the valves in the hinge area, forming the mantle isthmus, the termination of which secretes the ligament. The radial musculature of the mantle, which leaves radial markings on the inner shell surface, has been described by Jaworski (1928).

The mantle is attached to the shell by the broad, entire line of pallial muscles, and the adductor muscles. Other, local, points of attachment on the general outer mantle surface are described below. The adductor muscles are large and subequal. The anterior adductor is usually the larger, and curves ventrally to occupy most of the area immediately within the pedal gape.

The foot is small, compressed, and usually pointed. Yonge (1967) considers that the function of the foot is to assist in the cleansing of the mantle cavity, in particular the

---

EXPLANATION OF PLATE 72

Fig. 1. *Chama macerophylla* Gmelin, Recent, Bermuda. BMNH 1911.12.21.1322.3. *a*, Right valve, hinge teeth, ×2. *b*, left valve, ×2. Abbreviations: C, cardinal teeth; L, lateral teeth; n, ligament nymph; add, adductor muscle scar.

Fig. 2. *Chama calcarata* Deshayes, Eocene, Lutetian, Grignon, France. *a*, Right valve, showing hinge teeth, ×2. *b*, Left valve, ×2.

Fig. 3. *Chama* sp. Maastrichtian, Cotentin, France. Silicone rubber cast, ×2.

Fig. 4. *Chama haneri* Zittel, Cretaceous, Senonian Gosau Beds, Gosau, Austria. ×0·75. *b*, dorsal view.

Figs. 5, 6. *Ciplyella pulchra* (Ravn), Cretaceous, Danian, Faxe, Denmark ×1. 5, internal cast, left valve. BMNH L13601. 6, anterior view, BMNH L25558.

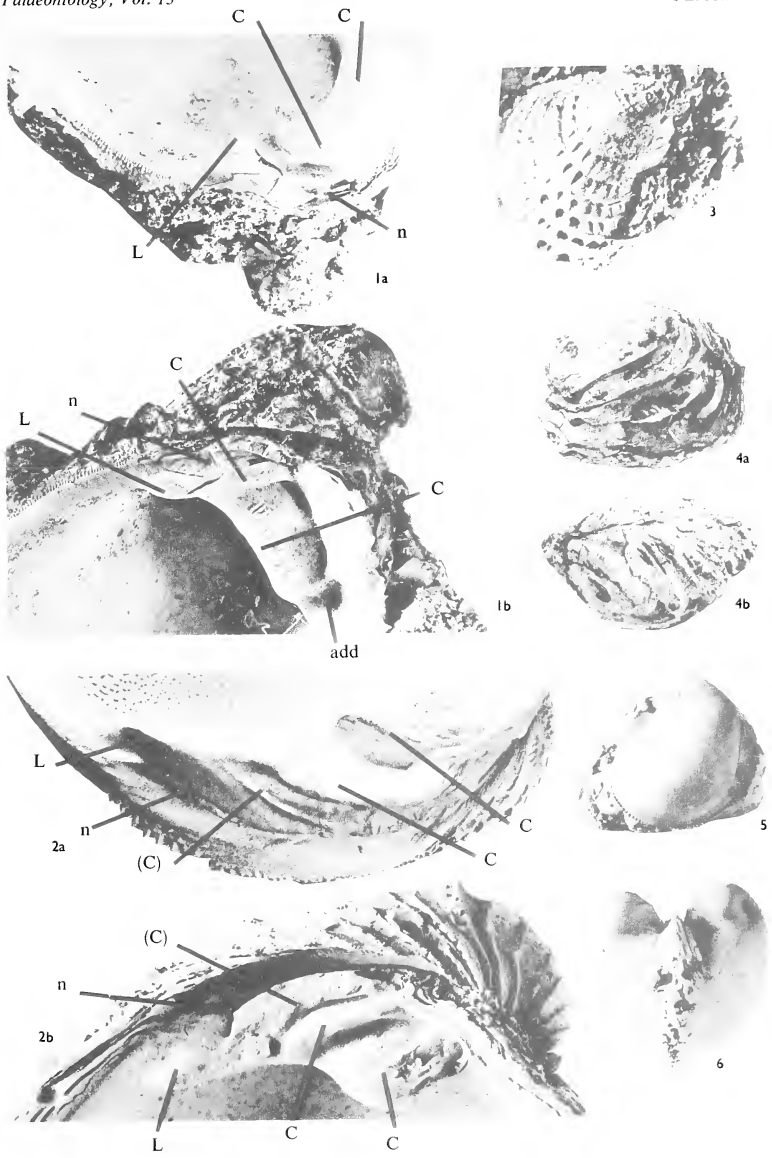

KENNEDY, MORRIS and TAYLOR, Chamacea

area round the anterior adductor muscle. The posterior pedal retractor muscles are attached near the dorsal end of the adductor muscle.

The ctenidia are typically eulamellibranch and have been described in great detail by Odhner (1919). They are highly plicate, and the gill ciliation pattern is type C (1) of Atkins (1937). The labial palps are small, and correspond to type 2 of Stasek (1963*c*), in which the ventral tips of the outermost filaments of the inner demibranches are inserted on to, and fused to, a distal oral groove. The stomach has been discussed by Purchon (1958, 1960) who places the stomach of two species in his types IV and V respectively. A more recent study by Dinamani (1967) places the stomach of *Chama* in his type III*a*.

Other features of the gut, heart, kidneys, nervous and reproductive systems have been described by Grieser (1913) and Odhner (1919).

GEOLOGICAL HISTORY

The generic name *Chama* was used by early workers for many different groups of Cretaceous bivalves, including rudists, *Exogyra*, and other oysters. Pictet and Campiche (1864–7), Stoliczka (1870), and Kutassy (1934) have removed many of these; of the remainder, only five appear to be valid *Chama* species.

Chama coquandi Vidal (1877, 92, pl. 3*a*, fig. 1) is a remarkable Campanian species, in need of reinvestigation. It is inequivalve, but shows no traces of a cementation area, there is no trace of an external ligamental groove or of muscle scars on the internal mould, and the hinge is unknown. The morphology of the valve margin (Vidal 1877, pl. 4, fig. 6) is comparable to that seen in other *Chama* species.

Chama haueri Zittel (1865, 147, pl. 7, figs. 3 *a–c*; see herein Pl. 72, fig. 4) and *C. detrita* Zittel (1865, 147, pl. 7, figs. 4 *a–b*) from the Gosau Beds, Austria, of Senonian age; *C. callosa* Noetling (1902, 50, pl. 12, figs. 9–10) from the Upper Cretaceous of Baluchistan; and *C. toeroeki* Pethö (1906, 269, pl. 19, figs. 15–16) from the Upper Cretaceous of Hungary are all good *Chama* species.

C. haueri is based on material retaining the shell, *C. detrita* on internal moulds. From our knowledge of variation in other species, these are probably synonyms, the trivial name *haueri* taking priority. *C. callosa* may also be a synonym.

All these Cretaceous forms are similar in having an ornament of concentric lamellae (Pl. 72, figs. 3, 4).

Douvillé (1913, 453) also records Chamidae from the Upper Cretaceous of France, but from horizons above that of the Gosau material. We have also seen an undescribed form from the Calcaire à baculites (Maastrichtian) of Cotentin, France (Pl. 72, fig. 3).

Chama angulosa d'Orbigny (1844, 690, pl. 464, figs. 8–9), *Chama gasoli* Vidal (1877, 93, pl. 4, figs. 7 *a–b*), and *C. moritzi* Strombeck (1863, 156) are all species of *Gyropleura*. *C. spondyloides* Bayle (1856, 365, pl. 14, fig. 1) is a monopleurid rudist. *C. triedra* Pictet and Campiche (1867, 5, pl. 140, figs. 4–5) and *C. gracilicornis* Pictet and Campiche (1867, 6, pl. 140, figs. 6–7) are both diceratid rudists. *C. boulei* Basse (1933, 43, pl. 7, fig. 6) is probably a *Spondylus*. *C. deplanata* Stoliczka (1870, 235, pl. 22, fig. 5) is probably a *Plicatula*. *C. bifrons* Griepenkerl (1899, 362, pl. 7, fig. 2), *C. costata* Roemer (1841, 67, pl. 8, fig. 20), *C. multicostata* Wegner (1905, 192, text-fig. 19), and *C. geometrica* Roemer (1840, 35, pl. 18, fig. 39) are all oysters.

Chama cretacea d'Orbigny (1846, 689, pl. 463, figs. 1–2) is generically indeterminate, but does not seem to be a *Chama*. *Chama suborbiculata* d'Orbigny (1822, 100), is not figured. whilst d'Orbigny's description is brief. It may be a *Chama*, but is best regarded as a *nomen dubium* until re-studied.

Little is known of *Chama* in Danian, Montian or Thanetian rocks. *Ciplyella pulchra* (Ravn) (1902, 127, pl. 4, figs. 12–15) from the Danian Koralkalk of Denmark seems to belong to the Monopleuridae (see p. 409). *Chama ciplyensis* Vincent (1928, 104, pl. 5, fig. 17) from the Danian or Montian Poudingue de Ciply of Belgium is little known. The description of its adductor scars suggest that it is a genuine *Chama*. *Chama ancestralis* Cossmann (1908, 44, pl. 1, figs. 38–40) from the Montian Calcaire Grossier of Belgium is known from two specimens only and needs reinvestigation.

In the Eocene *Chama* becomes much more common, being represented by such familiar forms as *Chama squamosa*, *C. lamellosa*, and *C. gigas*.

Arcinella (type species *Chama arcinella* Linnaeus) is a tropical American chamid which appears in the early Miocene of the Florida region. It is thought to be derived from the early to middle Miocene species *Chama draconis* Dall (Nicol 1952).

Most of the fossil occurrences of *Chama* are in association with rich shallow marine faunas of tropical or subtropical aspect.

C. exogyra and *C. pellucida* occur associated with cooler water faunas, as do living members of the same species.

SHELL STRUCTURE AND MINERALOGY

Shells of more than thirty species of recent and fossil Chamidae were examined in connection with this work.

Mineralogical determinations were carried out by means of standard X-ray diffraction techniques. Optical examinations of shell structure were made on shell interiors, fractured sections, acetate peels of polished and etched sections (method in Kummel and Raup 1965), and petrographic thin sections.

Fine structure was studied on surfaces, fractured and polished and etched sections, which were examined with a Cambridge Instrument Company 'Stereoscan' scanning electron microscope.

The shell of most species examined is wholly aragonitic, with a two-layered shell. Exceptions are *Chama pellucida* and *Chama exogyra* which have an additional outer prismatic calcite layer. The significance of this is discussed below.

The results of our observations are summarized in Table 1. It will be seen that we use the terms inner, middle, and outer shell layers. This is an entirely topographic, and thus unambiguous division. We reject Oberling's (1964) use of the terms ectostracum, mesostracum, and endostracum for three-layered shells, mesectostracum and mesendostracum for two-layered shells as this implies homology between layers in different shells. It further suggests that two-layered shells may be derived from three-layered forms.

As well as speaking of shell layers, we have adopted Oberling's (1964) term *myostracum* for the peculiar blocky prismatic aragonite laid down under sites of muscle attachment, i.e. the pallial, pedal, and adductor myostraca.

(*a*) *Structure of the crossed-lamellar layer.* Crossed-lamellar structure forms the outer shell layer of most species (text-fig. 4), but the middle layer of *Chama pellucida* and *C. exogyra* (text-fig. 5).

Conventional microscopy shows the inner surface of the shell layer as a series of elongate, branching, interdigitating lenses. These lenses are arranged with their long axes running concentrically, i.e. essentially parallel to the shell margin over most of the shell.

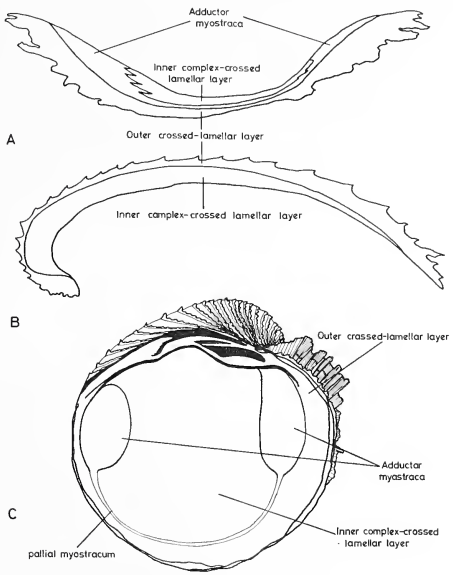

TEXT-FIG. 4. (A) Transverse section, (B) longitudinal section, and (C) interior of *Chama macerophylla* Gmelin to show distribution of shell layers.

More variable orientations are developed on spines, squamae, and in the umbonal region. These lenses correspond to the outcrop of the first order lamels of Bøggild (1930).

In section first-order lamels run normal to the inner surface of the shell layer (Pl. 73, fig. 1). Traced towards the shell exterior they twist and turn however, producing complicated patterns. The first-order lamels branch and interdigitate in sections in much the same way as they do on shell interiors. A strong, interlocking structure is thus produced.

First-order lamels are up to several millimetres long and of the order of 0·5 mm. thick. Sections and peels show a striking colour banding, adjacent lamels being straw-yellow or red-brown in colour.

Within each first-order lamel (text-fig. 6*b*) there are sheet-like second-order lamels (Bøggild 1930). These are in turn built of minute laths, about 1 μ in diameter and some

TABLE 1. Shell structure and mineralogy of recent and fossil Chamacea

Species	*Horizon and locality*	*Mineralogy*	*Outer layer*	*Inner layer*	*Myostraca* *Pallial*	*Adductor*	*Observations*
Chama haueri Zittel	Senonian, Gosau, Austria	Aragonite	Crossed-lamellar	Complex crossed-lamellar with sheets of myostracal-type prisms	Prismatic	Prismatic	
Chama calcarata Lamarck	Lutetian, Chaumont en Vexin, France		Crossed-lamellar	Complex crossed-lamellar with sheets of myostracal-type prisms	Prismatic	Prismatic	
Chama calcarata Lamarck	Lutetian, Mouchy, France		Crossed-lamellar	Complex crossed-lamellar with sheets of myostracal-type prisms	Prismatic	Prismatic	Myostracal sheets in inner layer locally folded (see text)
Chama lamellosa Lamarck	Lutetian, Damercy, France	Aragonite	Crossed-lamellar	Complex crossed-lamellar with sheets of myostracal-type prisms	Prismatic	Prismatic	
Chama gigas Deshayes	Lutetian, Grignon, France		Crossed-lamellar	Complex crossed-lamellar with sheets of myostracal-type prisms	Prismatic	Prismatic	Myostracal sheets in inner layer similar to those in *C. calcarata*
Chama selseiensis S. V. Wood	Lutetian, Brackle-sham, England		Crossed-lamellar	Complex crossed-lamellar with sheets of myostracal-type prisms and myostracal pillars	Prismatic	Prismatic	
Chama turgida Lamarck	Basal Auversian, Chavençon, France		Crossed-lamellar	Complex crossed-lamellar with sheets of myostracal-type prisms and myostracal pillars	Prismatic	Prismatic	Scattered tubules in inner layer
Chama fimbriata Defrance	Auversian, Auvers, France		Crossed-lamellar	Complex crossed-lamellar with sheets of myostracal-type prisms	Prismatic	Prismatic	
Chama papyracea Deshayes	Auversian, Auvers, France		Crossed-lamellar	Complex crossed-lamellar with sheets of myostracal-type prisms	Prismatic	Prismatic	
Chama squamosa Solander	Bartonian, Barton, England		Crossed-lamellar	Complex crossed-lamellar with sheets of myostracal-type prisms	Prismatic	Prismatic	Scattered tubules in inner layer
Chama squamosa Solander	Ludian, Chavanion, France		Crossed-lamellar	Complex crossed-lamellar with sheets of myostracal-type prisms and myostracal pillars	Prismatic	Prismatic	Scattered tubules in inner layer

Chama aquitanica Cossman and Pissarro	Aquitanian, Villandrani, Italy	Crossed-lamellar	Complex crossed-lamellar with sheets of myostracal-type prisms	Prismatic	Prismatic	
Chama sp.	Miocene, San Domingo	Crossed-lamellar	Complex crossed-lamellar with sheets of myostracal-type prisms	Prismatic	Prismatic	
Chama crassa Chenu	Pliocene, Florida	Crossed-lamellar	Complex crossed-lamellar with thin sheets of myostracal-type prisms	Prismatic	Prismatic	Scattered tubules in inner layer
Chama heilprini (Nicol)	Plio-Pleistocene, La Belle, Florida	Crossed-lamellar	Complex crossed-lamellar with sheets of myostracal-type prisms and myostracal pillars	Prismatic	Prismatic	Scattered tubules in inner layer
Chama brocchii Deshayes	Pleistocene, Astigiana, Italy	Crossed-lamellar	Complex crossed-lamellar with sheets of myostracal-type prisms	Prismatic	Prismatic	Scattered tubules in inner layer
Chama gryphina Lamarck	Pleistocene, Piedmont, Italy	Crossed-lamellar	Complex crossed-lamellar with sheets of myostracal-type prisms	Prismatic	Prismatic	
Chama gryphina Lamarck	Pleistocene, Astigiana, Italy	Crossed-lamellar	Complex crossed-lamellar with thin sheets of myostracal-type prisms	Prismatic	Prismatic	
Chama nivalis Reeve	Pleistocene, Berbera, Somalia	Crossed-lamellar with scattered myostracal pillars	Complex crossed-lamellar with sheets of myostracal-type prisms and myostracal pillars	Prismatic	Prismatic	Myostracal pillars in the inner parts of the outer layer; scattered myostracal pillars in inner layer. Tubules in inner layer
Chama pulchella Reeve	Pleistocene, Berbera, Somalia	Crossed-lamellar	Complex crossed-lamellar with sheets of myostracal-type prisms and myostracal pillars	Prismatic	Prismatic	Tubules in inner layer
Arcinella arcinella antiquata (Dall)	Miocene, Colombia	Crossed-lamellar	Complex crossed-lamellar with sheets of myostracal-type prisms	Prismatic	Prismatic	
Arcinella trachyderma (Pilsbry and Johnson)	Miocene, San Domingo	Crossed-lamellar	Complex crossed-lamellar with sheets of myostracal-type prisms	Prismatic	Prismatic	

TABLE 1. Shell structure and mineralogy of recent and fossil Chamacea

Species	*Horizon and locality*	*Mineralogy*	*Outer layer*	*Inner layer*	*Myostraca* *Pallial*	*Adductor*	*Observations*
Chama haueri Zittel	Senonian, Gosau, Austria	Aragonite	Crossed-lamellar	Complex crossed-lamellar with sheets of myostracal-type prisms	Prismatic	Prismatic	
Chama calcarata Lamarck	Lutetian, Chaumont en Vexin, France		Crossed-lamellar	Complex crossed-lamellar with sheets of myostracal-type prisms	Prismatic	Prismatic	
Chama calcarata Lamarck	Lutetian, Mouchy, France		Crossed-lamellar	Complex crossed-lamellar with sheets of myostracal-type prisms	Prismatic	Prismatic	Myostracal sheets in inner layer locally folded (see text)
Chama lamellosa Lamarck	Lutetian, Damercy, France	Aragonite	Crossed-lamellar	Complex crossed-lamellar with sheets of myostracal-type prisms	Prismatic	Prismatic	
Chama gigas Deshayes	Lutetian, Grignon, France		Crossed-lamellar	Complex crossed-lamellar with sheets of myostracal-type prisms	Prismatic	Prismatic	Myostracal sheets in inner layer similar to those in *C. calcarata*
Chama selseiensis S. V. Wood	Lutetian, Brackle-sham, England		Crossed-lamellar	Complex crossed-lamellar with sheets of myostracal-type prisms and myostracal pillars	Prismatic	Prismatic	
Chama turgida Lamarck	Basal Auversian, Chavençon, France		Crossed-lamellar	Complex crossed-lamellar with sheets of myostracal-type prisms and myostracal pillars	Prismatic	Prismatic	Scattered tubules in inner layer
Chama fimbriata Defrance	Auversian, Anvers, France		Crossed-lamellar	Complex crossed-lamellar with sheets of myostracal-type prisms	Prismatic	Prismatic	
Chama papyracea Deshayes	Auversian, Auvers, France		Crossed-lamellar	Complex crossed-lamellar with sheets of myostracal-type prisms	Prismatic	Prismatic	
Chama squamosa Solander	Bartonian, Barton, England		Crossed-lamellar	Complex crossed-lamellar with sheets of myostracal-type prisms	Prismatic	Prismatic	Scattered tubules in inner layer
Chama squamosa Solander	Ludian, Chavanion, France		Crossed-lamellar	Complex crossed-lamellar with sheets of myostracal-type prisms and myostracal pillars	Prismatic	Prismatic	Scattered tubules in inner layer

Chama aquitanica Cossman and Pissarro	Aquitanian, Villandraut, Italy		Crossed-lamellar	Complex crossed-lamellar with sheets of myostracal-type prisms	Prismatic	Prismatic	
Chama sp.	Miocene, San Domingo		Crossed-lamellar	Complex crossed-lamellar with sheets of myostracal-type prisms	Prismatic	Prismatic	
Chama crassa Chenu	Pliocene, Florida		Crossed-lamellar	Complex crossed-lamellar with thin sheets of myostracal-type prisms	Prismatic	Prismatic	Scattered tubules in inner layer
Chama heilprini (Nicol)	Plio-Pleistocene, La Belle, Florida		Crossed-lamellar	Complex crossed-lamellar with sheets of myostracal-type prisms and myostracal pillars	Prismatic	Prismatic	Scattered tubules in inner layer
Chama brocchii Deshayes	Pleistocene, Asti-giana, Italy		Crossed-lamellar	Complex crossed-lamellar with sheets of myostracal-type prisms	Prismatic	Prismatic	Scattered tubules in inner layer
Chama gryphina Lamarck	Pleistocene, Pied-mont, Italy		Crossed-lamellar	Complex crossed-lamellar with sheets of myostracal-type prisms	Prismatic	Prismatic	
Chama gryphina Lamarck	Pleistocene, Asti-giana, Italy		Crossed-lamellar	Complex crossed-lamellar with thin sheets of myostracal-type prisms	Prismatic	Prismatic	
Chama ovalis Reeve	Pleistocene, Berbera, Somalia		Crossed-lamellar with scattered myostracal pillars	Complex crossed-lamellar with sheets of myostracal-type prisms and myostracal pillars	Prismatic	Prismatic	Myostracal pillars in the inner parts of the outer layer; scattered myostracal pillars in inner layer. Tubules in inner layer
Chama pulchella Reeve	Pleistocene, Berbera, Somalia		Crossed-lamellar	Complex crossed-lamellar with sheets of myostracal-type prisms and myostracal pillars	Prismatic	Prismatic	Tubules in inner layer
Arcinella arcinella antiquata (Dall)	Miocene, Colombia		Crossed-lamellar	Complex crossed-lamellar with sheets of myostracal-type prisms	Prismatic	Prismatic	
Arcinella trachyderma (Pilsbry and Johnson)	Miocene, San Domingo		Crossed-lamellar	Complex crossed-lamellar with sheets of myostracal-type prisms	Prismatic	Prismatic	

Specie	*Horizon and locality*	*Mineralogy*	*Outer layer*	*Inner layer*	*Myostraca* *Pallial*	*Adductor*	*Observations*
Arcinella arcinella arcinella (Linnaeus)	Pliocene, Caloosa-hatchee, Florida		Crossed-lamellar	Complex crossed-lamellar with sheets of myostracal-type prisms	Prismatic	Prismatic	
Arcinella arcinella (Linnaeus)	W. Florida	Aragonite	Crossed-lamellar	Complex crossed-lamellar	Thin prismatic	Thick prismatic	Layers of myostracal-type prisms present in inner layer; other specimens have myostracal pillared tubules
Chama aspera Reeve	Indian Ocean	Aragonite	Crossed-lamellar	Complex crossed-lamellar	Thin prismatic	Thick prismatic	Myostracal pillars in inner layer
Chama brassica Reeve	Philippines	Aragonite	Crossed-lamellar	Complex crossed-lamellar	Thin prismatic	Thick prismatic	Thin bands of myostracal-type prisms and tubules in the inner layer
Chama gryphina Lamarck	Mediterranean	Aragonite	Crossed-lamellar	Complex crossed-lamellar	Thin prismatic	Thick prismatic	Myostracal pillars and scattered tubules in inner layer; some specimens have bands of myostracal-type prisms in this layer
Chama iostoma Reeve	Aden	Aragonite	Crossed-lamellar	Complex crossed-lamellar	Thin prismatic	Thick prismatic	Abundant myostracal pillars and scattered pillars in inner layer. Other (? pedal) myostraca in some sections
Chama lazarus Wood	Mombasa, E. Africa	Aragonite	Crossed-lamellar	Complex crossed-lamellar	Thin prismatic	Thick prismatic	Abundant myostracal pillars and scattered tubules in the inner layer. Tubules may be present in the marginal parts of the outer layer. The internal ligament is aragonitic
Chama nubea Reeve	Philippines	Aragonite	Crossed-lamellar	Complex crossed-lamellar	Thin prismatic	Thick prismatic	Abundant radially elongate myostracal pillars and scattered tubules in the inner layer

Chama sarda Reeve	W. Indies	Aragonite	Crossed-lamellar	Complex crossed-lamellar	Thin prismatic	Thick prismatic	Myostracal pillars and scattered tubules in the inner layer
Chama spinosa Broderip	Dunken Island, Cape York, Queensland	Aragonite	Crossed-lamellar	Complex crossed-lamellar	Thin prismatic	Thick prismatic	Tubules present in the inner layer; myostracal pillars occur in some specimens
Chama spondylodes Menke	Queensland	Aragonite	Crossed-lamellar	Complex crossed-lamellar	Thin prismatic	Thick prismatic	Tubules, sheets of myostracal-type prisms and myostracal pillars are present in the inner layer; the latter extend into the outer layer
Chama macerophylla Gmelin	W. Indies	Aragonite	Crossed-lamellar	Complex crossed-lamellar	Thin prismatic	Thick prismatic	Myostracal pillars and abundant tubules in the inner layer
Chama corrugata Broderip	Ecuador	Aragonite	Crossed-lamellar	Complex crossed-lamellar	Thin prismatic	Thick prismatic	The inner layer has a rather coarse fabric, and myostracal pillars in the umbonal area
Chama radians Lamarck	W. Indies	Aragonite	Crossed-lamellar	Complex crossed-lamellar	Thin prismatic	Thick prismatic	Abundant myostracal pillars in the inner layer

				Middle layer	*Inner layer*	*Myostraca*	
						Pallial	*Adductor*
Chama pellucida Broderip	California	Aragonite and Calcite	Granular/prismatic calcite	Crossed-lamellar aragonite	Complex crossed-lamellar aragonite	Thin prismatic aragonite	Thin prismatic aragonite

Specie	*Horizon and locality*	*Mineralogy*	*Outer layer*	*Inner layer*	*Myostraca* *Pallial*	*Adductor*	*Observations*
Arcinella arcinella arcinella (Linnaeus)	Pliocene, Caloosa-hatchee, Florida		Crossed-lamellar	Complex crossed-lamellar with sheets of myostracal-type prisms	Prismatic	Prismatic	
Arcinella arcinella (Linnaeus)	W. Florida	Aragonite	Crossed-lamellar	Complex crossed-lamellar	Thin prismatic	Thick prismatic	Layers of myostracal-type prisms present in inner layer; other specimens have myostracal pillared tubules
Chama aspera Reeve	Indian Ocean	Aragonite	Crossed-lamellar	Complex crossed-lamellar	Thin prismatic	Thick prismatic	Myostracal pillars in inner layer
Chama brassica Reeve	Philippines	Aragonite	Crossed-lamellar	Complex crossed-lamellar	Thin prismatic	Thick prismatic	Thin bands of myostracal-type prisms and tubules in the inner layer
Chama gryphina Lamarck	Mediterranean	Aragonite	Crossed-lamellar	Complex crossed-lamellar	Thin prismatic	Thick prismatic	Myostracal pillars and scattered tubules in inner layer; some specimens have bands of myostracal-type prisms in this layer
Chama iostoma Reeve	Aden	Aragonite	Crossed-lamellar	Complex crossed-lamellar	Thin prismatic	Thick prismatic	Abundant myostracal pillars and scattered pillars in inner layer. Other (? pedal) myostraca in some sections
Chama lazarus Wood	Mombasa, E. Africa	Aragonite	Crossed-lamellar	Complex crossed-lamellar	Thin prismatic	Thick prismatic	Abundant myostracal pillars and scattered tubules in the inner layer. Tubules may be present in the marginal parts of the outer layer. The internal ligament is aragonitic
Chama nubea Reeve	Philippines	Aragonite	Crossed-lamellar	Complex crossed-lamellar	Thin prismatic	Thick prismatic	Abundant radially elongate myostracal pillars and scattered tubules in the inner layer

Chama sarda Reeve	W. Indies	Aragonite	Crossed-lamellar	Complex crossed-lamellar	Thin prismatic	Thick prismatic	Myostracal pillars and scattered tubules in the inner layer
Chama spinosa Broderip	Dunken Island, Cape York, Queens-land	Aragonite	Crossed-lamellar	Complex crossed-lamellar	Thin prismatic	Thick prismatic	Tubules present in the inner layer; myostracal pillars occur in some specimens
Chama spondylodes Menke	Queensland	Aragonite	Crossed-lamellar	Complex crossed-lamellar	Thin prismatic	Thick prismatic	Tubules, sheets of myostracal-type prisms and myostracal pillars are present in the inner layer; the latter extend into the outer layer
Chama macerophylla Gmelin	W. Indies	Aragonite	Crossed-lamellar	Complex crossed-lamellar	Thin prismatic	Thick prismatic	Myostracal pillars and abundant tubules in the inner layer
Chama corrugata Broderip	Ecuador	Aragonite	Crossed-lamellar	Complex crossed-lamellar	Thin prismatic	Thick prismatic	The inner layer has a rather coarse fabric, and myostracal pillars in the umbonal area
Chama radians Lamarck	W. Indies	Aragonite	Crossed-lamellar	Complex crossed-lamellar	Thin prismatic	Thick prismatic	Abundant myostracal pillars in the inner layer

				Middle layer	*Inner layer*	*Myostraca* *Pallial*	*Adductor*
Chama pellucida Broderip	California	Aragonite and Calcite	Granular/prismatic calcite	Crossed-lamellar aragonite	Complex crossed-lamellar aragonite	Thin prismatic aragonite	Thin prismatic aragonite

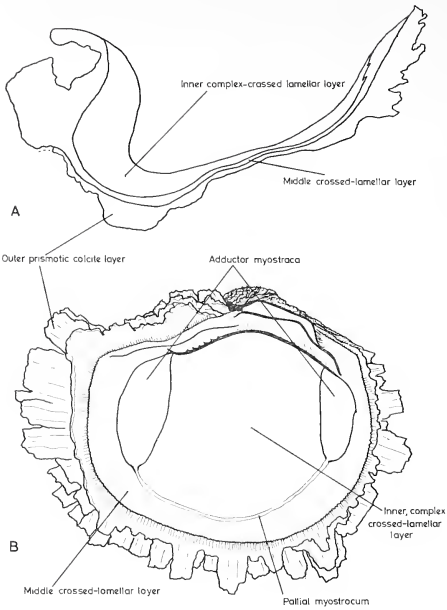

TEXT-FIG. 5. (A) Longitudinal section and (B) interior of *Chama pellucida* Broderip to show the distribution of shell layers.

EXPLANATION OF PLATE 73

All sections are acetate peels.

Fig. 1. Outer crossed-lamellar layer of *Arcinella arcinella* (Linnaeus), showing first-order lamels aligned normal to the shell interior in the inner part of the layer (lower), and the 'bladed' outer part where they are aligned parallel to the shell interior. Radial section, ×32.

Fig. 2. Radial section inner complex crossed-lamellar layer of *Chama calcarata* Deshayes showing cone shaped depressions in myostracal sheets, ×32.

Fig. 3. Planar section through the adductor myostracum of *Chama lazarus* Wood, ×100.

Fig. 4. Contact between the outer crossed-lamellar layer (left) and the adductor myostracum of *Chama radians* Lamarck, radial section, ×80.

Fig. 5. Myostracal pillars in the inner, complex crossed-lamellar layer of *Chama radians* Lamarck. Radial section, ×80.

Fig. 6. Radial section of the inner complex crossed-lamellar layer of *Chama lazarus* Wood, ×20.

Fig. 7. Myostracal sheets in the inner complex crossed-lamellar layer of *Chama lamellosa* Lamarck, ×80.

Fig. 8. Contact between the outer, prismatic, calcitic layer (top) and the middle aragonite crossed-lamellar layer of *Chama pellucida* Broderip, ×80.

Fig. 9. Planar section of the outer prismatic, calcitic layer of *Chama pellucida* Broderip, ×80.

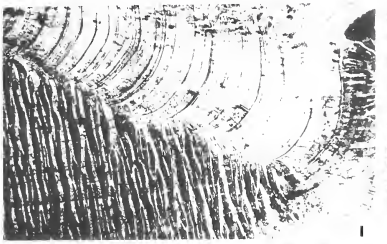
1

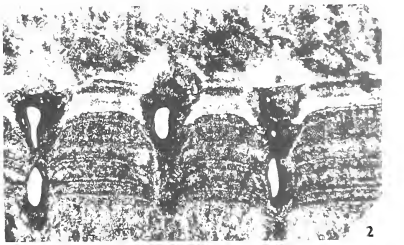
2

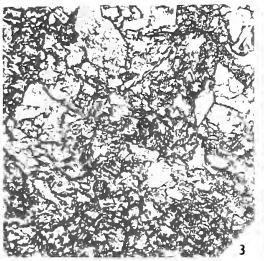
3

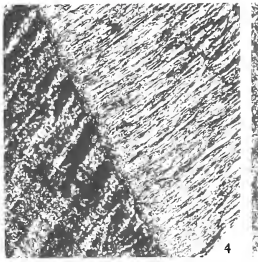
4

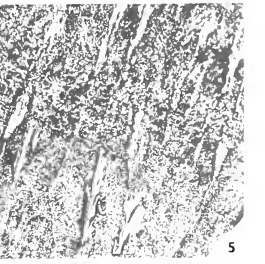
5

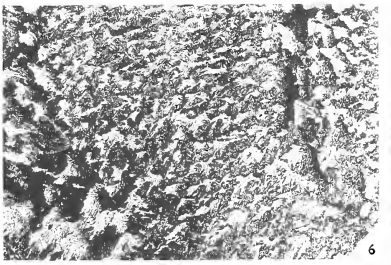
6

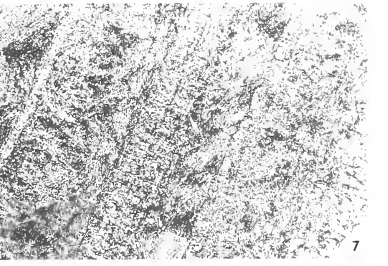
7

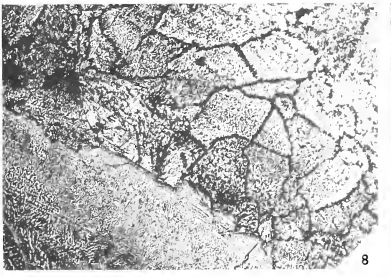
8


9

KENNEDY, MORRIS and TAYLOR, Chamacea

tens of microns long, joined in side-to-side contact. These sheets of laths, i.e. second-order lamels, lie normal to the sides of the first-order lamels, the long axes of the laths being parallel to the plane of the first-order lamels.

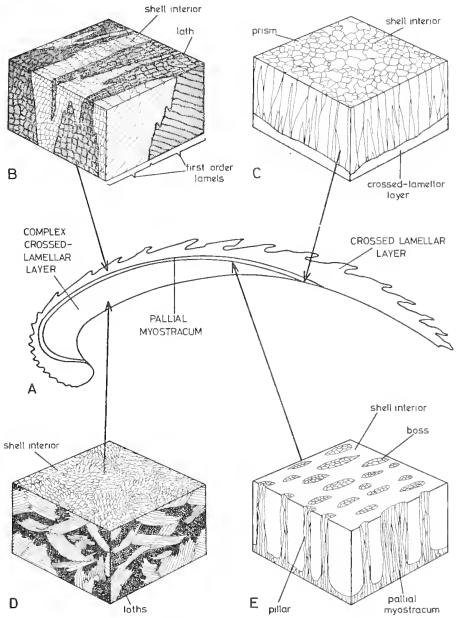

TEXT-FIG. 6. Radial section of a typical *Chama* (A) with block diagrams to show the microstructure of the crossed-lamellar layer (B), pallial myostracum (C), complex crossed-lamellar layer (D), and myostracal pillars (E).

Second-order lamels are inclined to the shell interior, with opposite inclinations of dip in adjacent first-order lamels. Optical work suggests that the whole layer is built of crystallites with only two crystallographic orientations.

These observations are summarized in text-fig. 6*b*. Fine structure is shown in Plate 74, fig. 1.

As well as the carbonate, there is a well-developed proteinaceous organic matrix in the crossed-lamellar layer (Pl. 74, fig. 2). This is intimately associated with the carbonate, surrounding each lath of the crossed-lamellar structure. Unlike the regular, fenestrate sheets of nacre organic matrix (Grégoire 1957, 1959, 1960, 1967), crossed-lamellar matrix has a much more open, irregular structure.

The variation in attitude of first-order lamels seen in sections is a result of their growth normal to the secreting surface, i.e. the marginal parts of the mantle. Where this is variable in form, as in ribs, or in the reflected margin of *Arcinella*, irregularities will develop. Indeed, in *Arcinella*, growth of lamels normal to the surface of the margin produces a structure which superficially resembles the composite prismatic structure developed in the Lucinacea (Pl. 73, fig. 1).

(*b*) *Structure of the complex crossed-lamellar layer*. Complex crossed-lamellar structure forms the inner shell layer of all Chamacea. We use 'complex crossed-lamellar' in the original sense of Bøggild (1930). It is thus equivalent to 'complex' structure of Oberling (1964), which is not to be confused with 'complex' of Bøggild (1930)!

This shell structure type is built of the same basic building blocks as crossed-lamellar structure, i.e. minute laths (Text fig. 6*d*). Instead of building first-order lamels, the laths build much more irregular blocks (Pl. 73, fig. 6; Pl. 74, fig. 3), and many different attitudes and orientations of laths are present within the layer.

In some sections, small irregular patches of radiating laths are recognizable. MacClintock (1967) has described these as sections of spherulitic growth. His patelloid structures are, however, different in detail from structures present in bivalves.

(*c*) *Structure of the prismatic layer*. An outer, calcite prismatic layer is present in two recent species of *Chama*, *C. pellucida*, and *C. exogyra*. The occurrence in *C. pellucida* has been noted by previous workers (Lowenstam 1954 *a*, *b*, 1963, 1964; Kennedy and Taylor 1968), but the present record from *C. exogyra* represents only the second occurrence of calcite in extant bivalves other than the Pteriomorpha.

However, matters are far from simple in respect of these two species.

Examination of the type specimens of *C. exogyra* and *C. pellucida* (in the collections of the British Museum (Natural History)) shows that the specimens appear distinctive. *C. pellucida* is rounded in outline, is 'normal' (i.e. attached by the left valve), and bears striking translucent squamae. *C. exogyra* is irregular, elongate, reversed (i.e. attached by right valve), and lacks conspicuous squamae. Other specimens of *C. exogyra* we have examined show rather more conspicuous ridges, and are 'normal'—attached by the left valve. These normal specimens closely resemble *C. pellucida*, whilst reversed *C. pellucida* closely resembles *C. exogyra*.

These similarities, the identical and highly unusual mineralogy and structure, together with the similar geographical range of the two species (Yonge 1967) plus the problems

---

EXPLANATION OF PLATE 74

All figures are scanning electron-micrographs.

Fig. 1. Polished, etched (HCl) radial section of the middle crossed-lamellar layer of *Chama pellucida*, showing three adjacent first-order lamels, ×700.

Fig. 2. As above, showing contact between the outer prismatic layer (left) and the middle crossed-lamellar layer; notice the lace-like organic matrix network, ×700.

Fig. 3. Fractured section of the inner complex crossed-lamellar layer of *Chama radians*, showing laths joined into second-order lamels having variable orientations, ×240.

Fig. 4. Inner shell surface of *Chama radians*, showing the outcrop of myostracal prisms, ×1,100.

Fig. 5. Polished, etched (HCl) radial section of the outer prismatic layer of *Chama pellucida*, ×700.

Fig. 6. Inner shell surface of *Chama radians* showing the opening of a tubule, ×2,250.

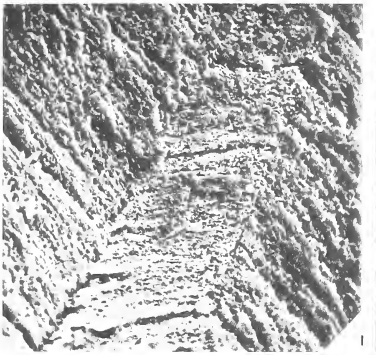
1

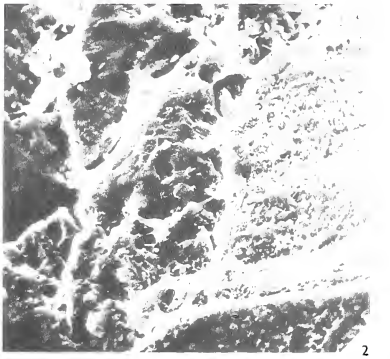
2

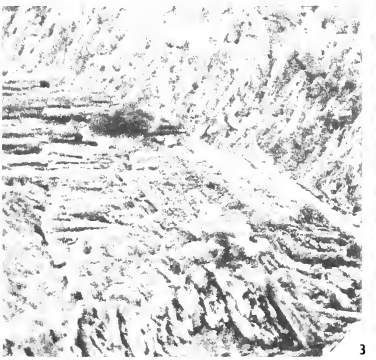
3

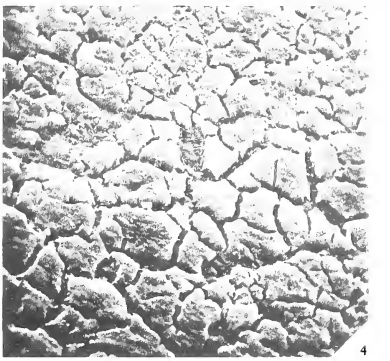
4

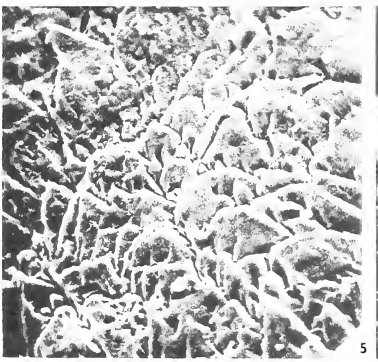
5

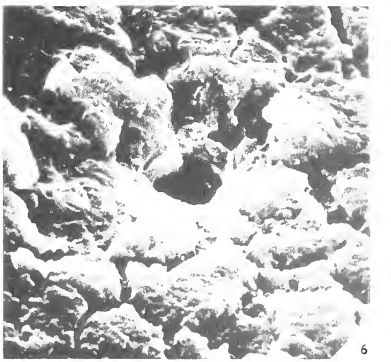
6

of inversion in the Chamacea generally, have led us to suspect that these species may be synonymous. This is, however, a field problem, which we cannot resolve on the basis of material available to us.

In both species the structure of the outer prismatic layer is very similar, and different from that occurring in all other extant bivalves. In hand specimen, the layer has a distinctive, translucent, 'pellucid' appearance (Pl. 70, fig. 3).

In peels and thin sections (Pl. 73, figs. 8 and 9) it appears grey against the browns and yellows of the adjacent crossed-lamellar layer. It is built up of minute, irregular, blade-like prisms, which are orientated more or less normally to the mantle and shell interior at the time of secretion. The prisms are rather variable in their attitude (in part as a result of their being involved in ribs and squamae), and are arranged into blocks with irregular polygonal outlines (Pl. 73, fig. 8). These larger blocks pass into extinction quite irregularly, and there is thus no uniformity of attitude within the blocks.

These observations are confirmed by electron-microscopy. In fractured sections, the large prism blocks show prominent transverse striae, and are clearly built up of smaller units (Pl. 77, fig. 2). Etching brings out these smaller units (Pl. 74, fig. 5), which correspond to the fine prisms seen at optical level. These fine prisms are surrounded by sheaths of organic matrix, but there are no thick conchiolin sheets such as characterize the other prismatic calcite layer of *Pinna*, *Pinctada*, and many other bivalves.

(*d*) *Structure of the myostracal layers.* These layers show similar features in all Chamacea we have examined. At optical level (Pl. 73, figs. 3, 4, 5, 7) myostraca are a characteristic grey colour, contrasting with the adjacent shell layers. The myostraca are built up of prisms, with highly irregular outlines. These prisms are orientated with their long axes normal to the surfaces of the myostracum, with crystallographic axes lying in the same direction (text-fig. 6*c*). There are no well-developed interprismatic protein walls, but thin organic matrix envelopes surround each prism.

The pallial myostracum is a thick sheet, extending into the umbo (text-fig. 6*a*). The adductor myostraca are thick, well-developed pads. In addition to these features, areas of myostracal structure are present in the Chamacea away from well-authenticated areas of muscle attachment. Sheets of myostracal-type prisms are present within the inner shell layer of many species, and represent interruption of deposition of normal shell fabric (Pl. 73, fig. 7). This may be due to periodic attachment of the mantle surface, but there is no direct evidence for this, although structure and fluorescence properties are identical with those of normal myostracum. Pillar-like areas of myostracal structure, called myostracal pillars (Taylor, Kennedy, and Hall 1969) occur in the inner layer of most species of Chamacea and in the crossed-lamellar layer of a few species (Table 1).

These pillars appear in sections as elongate ovoids or strips of myostracal structure, the long axes running normally to the shell interior (Pl. 73, fig. 5). In the inner layer they usually extend upwards from the pallial or adductor myostracum (text-fig. 6*c*).

On shell interiors, myostracal pillars outcrop as minute bosses, usually 0·5–1·0 mm. in diameter, or as elongate ovals, often arranged in lines radiating from the umbo.

Electron-microscopy shows that the surfaces of the bosses consists of a series of irregular prisms, corresponding to those seen at optical level (Pl. 74, fig. 4). The prisms are separated by grooves, of uncertain origin.

Sections of the mantle of *Chama jukesii* reveal the presence of minute papillae all over

the mantle surface, corresponding in size and distribution to the myostracal pillars of the shell. These papillae result from elongation of the normal mantle cells, and we take them to be sites of additional shell and mantle attachment.

A peculiar modification of the sheets of myostracal type prisms present in the inner shell layer is seen in *Chama calcarata* and *Chama gigas*. Here, the inner surface of the inner shell layer is pitted. These pits correspond to depressions in the surfaces of the myostracal sheets (Pl. 73, fig. 1), and presumably reflect another mode of shell/mantle attachment.

(*e*) *Layer contacts*. Crossed-lamellar and complex crossed-lamellar layers are separated by the pallial and adductor myostraca. There is usually a transition zone at the layer/myostracum contact, rich in organic matrix. The organic matrix of the myostracum and the crossed-lamellar or complex crossed-lamellar layers is in structural continuity. There is often a complex interdigitation of adductor myostracum and shell layers (text-fig. 4*a*). This is probably the result of slight shifting of the animal within its shell during growth.

The contact of the crossed-lamellar layer and the outer prismatic layer of *C. pellucida* and *C. exogyra* shows several unusual features (Pl. 73, fig. 8). The surface at contact is minutely corrugated, the corrugations apparently originating at the shell margin, as a reflection of the position of the pallial muscles. They are subsequently buried below the middle layer, filled by a thin zone of fine-grained aragonite, rich in organic matrix (Pl. 74, fig. 2). Elsewhere, this layer is replaced by a complex and irregular junction with minute angular crystals protruding into the crossed-lamellar layer, as though a highly irregular surface was grown over by crossed-lamellar structure. These relationships closely resemble the results of partial recrystallization of aragonite to calcite.

The organic matrix of prismatic and crossed-lamellar layers is in direct structural continuity.

(*f*) *Tubules*. Many species of Chamacea possess the remarkable shell feature which Oberling (1964) described as tubules (Pl. 74, fig. 8).

These are minute cylindrical perforations, only a few microns in diameter, which open at the interior surface of the shell and penetrate the shell layers. Tubules are a primary feature of the shell (Oberling 1964; Taylor, Kennedy, and Hall 1969), and appear as minute hollow cylinders penetrating the finest elements of the shell fabric (Pl. 74, fig. 8). On the shell interior, *Chama* tubules lie in minute pits. The function of tubules is at present unknown.

(*g*) *Ligament*. The ligament of the Chamacea is calcified and aragonitic, as in other bivalves with calcified ligaments (Lowenstam 1964; Taylor, Kennedy, and Hall 1969) (Pl. 77, fig. 1).

(*h*) *Banding*. All shell layers show prominent daily growth bands (Panella and MacClintock 1968).

COMPARISON OF THE CHAMACEA WITH OTHER GROUPS

The systematic position of the Chamacea has always been in doubt. Consideration of their affinities in the past was not helped by the allotment to this superfamily of several other cemented bivalves such as the rudists and the pandoraceans, *Cleidothaerus* and

Myochama. However, as it stands today, the superfamily Chamacea can be considered a homogeneous group.

The Chamacea have been related to the Lucinacea (Douvillé 1912, Nicol 1952), Carditacea (Dall 1903), the Cardiacea (Anthony 1905), Crassatellacea (Boehm 1891), Veneracea (Fischer 1886), and to the Hippuritacea (see references in Odhner 1919, Newell 1965, Yonge 1967). Of all these possibilities that of relationship to the rudists is the most commonly held. Odhner (1919) came to this conclusion after a detailed study of *Chama*, and Cox (1960) in deference to the thoroughness of Odhner's work accepted the conclusion but thought they should constitute a separate superfamily.

The similarities of the Chamacea to the various superfamilies listed above are discussed below. A summary of some of the more easily tabulated characters of possible relatives amongst living bivalve superfamilies is given in Table 2. The affinities with the extinct rudists are more difficult to examine because of the lack of soft parts, but Yonge (1967) has made certain inferences concerning rudist soft parts based on a study of the inner shell morphology.

1. *Comparison with the Carditacea*

Two distinct groups can be recognized within the Carditacea.

(*a*) The *Venericardia* group, which are burrowers with generally rounded shell outlines. The hinge plate is short and high, and the ornamentation usually consists of radial ribs.

(*b*) The *Cardita* group, consisting of byssate forms, ovoid to subrectangular in outline. The hinge plate is usually elongate and the anterior adductor muscle is somewhat reduced. The ornament is usually of radial ribs, but some species can produce squamae. This group contains many tropical species associated with coral reefs and rocky shores.

It is to this second group that the Chamacea may be compared. As can be seen from Table 2 some soft part characters such as the degree of mantle fusion and the gill plication are different, but others, such as labial palps and stomach types, are similar.

The greatest similarity between the Chamacea and the Carditacea is seen in shell characters such as the shell structure, dentition, ornament, and the similarity of the uncemented dissoconch of *Chama* to the adult byssate *Cardita*.

Thus the outer shell layer of the Carditacea consists of crossed-lamellar structure, with rather fine first-order lamels. The inner layer is built up of complex crossed-lamellar structure. Myostracal pillars are present in most species; in some the pillars are confined to the inner layer but in others they occur in both layers. Myostracal-type prisms can also be present, as fine sheets interbanded with complex crossed-lamellar structure in the inner layer. Tubules were present in all the species we have examined.

The dentition of the Carditidae shows striking similarities to that of the Chamacea. Both families have a 'lucinoid' dentition. The notation for *Cardita variegata* Bruguière, Recent, Seychelles is:

Right valve	n 0 1 0 1 0	1
Posterior	———————	Anterior
Left valve	n 0 1 0 1	0 1
	D	d

TABLE 2. Main features of the bivalve superfamilies Chamacea, Carditacea, Lucinacea, Crassatellacea, Cardiacea, and Veneracea

		Shell structure characters								
Superfamily	*Mode of life*	*Outer layer*	*Middle layer*	*Inner layer*	*Myostracal pillars*	*Myostracal sheets*	*Tubules*	*Ligament*	*Hinge teeth*	*Mantle fusion*
CHAMACEA	Cemented	*Crossed-lamellar	—	Complex crossed-lamellar	Present	Present in some	Present	External opisthodetic	Lucinoid	Inner fold
CARDITACEA	Byssate or burrowing	Crossed-lamellar	—	Complex crossed-lamellar	Present in some	Present in some	Present	External opisthodetic	Lucinoid	Inner fold fused between inhalent/exhalent areas
LUCINACEA	Burrowing	Composite prismatic	Crossed lamellar	Complex crossed-lamellar	Rare	Present in some	Rare	Sub-internal	Lucinoid	Inner fold
CRASSATELLACEA	Burrowing	Crossed-lamellar	—	Homogeneous in Crassatellidae, prisms in Astartidae	Absent	Present in Astartidae	Absent	Astartidae: external opisthodetic Crassatellidae: internal resilium	Cyrenoid	Inner fold, fusion at point between exhalent/inhalent areas
CARDIACEA	Burrowing	Crossed-lamellar	—	Complex crossed-lamellar	Absent	Thin sheets in inner layer	Absent	External opisthodetic	Lucinoid	Inner fold and inner surface of middle fold
VENERACEA	Burrowing, rarely byssate	Crossed-lamellar homogeneous	—	Complex crossed-lamellar or homogeneous	Absent	Thin sheets in inner layer of some species	Absent	External opisthodetic	Cyrenoid	Inner fold and inner surface of middle fold

* *C. pellucida* and *C. exogyra* have an outer prismatic calcite layer, middle crossed-lamellar layer and inner complex-crossed lamellar layer.

Superfamily	*Siphons*	*Labial palp Ctenidia Grade (Stasek 1963c)*	*Gill type (Ridewood 1903)*	*Gill cilia (Atkins 1937)*	*Stomach type (Purchon 1958, 1960)*	*Stomach type (Dinamani 1967)*	*External ornament*
CHAMACEA	Short inner fold	Type 2	Plicate	C 1	4 and 5	3*a*	Radial and concentric squamae, or spinose
CARDITACEA	No siphons	Type 2	Non-plicate	Not examined	4	3*a*	Radial ribs, some squamate and reticulate
LUCINACEA	If siphon present then inner fold	Type 3	Non-plicate homorhabdic	G 1	4	Not examined	Concentric, some radial and reticulate
CRASSATELLACEA	No siphons	Type 3 (Crassatellidae) Type 1 (Astartidae)	Non-plicate	C 1	4	Not examined	Concentric, costae and striae
CARDIACEA	Inner and middle fold	Type 2	Plicate heterorhabdic	C 1	5	3	Radical ribs or concentric, some spines
VENERACEA	Inner and middle fold	Types 2 and 3	Plicate heterorhabdic	C 1 and C 2	5	3	Concentric, some radial, reticulate or spinose

TABLE 2. Main features of the bivalve superfamilies Chamacea, Carditacea, Lucinacea, Crassatellacea, Cardiacea, and Veneracea

		Shell structure characters								
Superfamily	*Mode of life*	*Outer layer*	*Middle layer*	*Inner layer*	*Myostracal pillars*	*Myostracal sheets*	*Tubules*	*Ligament*	*Hinge teeth*	*Mantle fusion*
CHAMACEA	Cemented	*Crossed-lamellar	—	Complex crossed-lamellar	Present	Present in some	Present	External opisthodetic	Lucinoid	Inner fold
CARDITACEA	Byssate or burrowing	Crossed-lamellar	—	Complex crossed-lamellar	Present in some	Present in some	Present	External opisthodetic	Lucinoid	Inner fold fused between inhalent/exhalent areas
LUCINACEA	Burrowing	Composite prismatic	Crossed lamellar	Complex crossed-lamellar	Rare	Present in some	Rare	Sub-internal	Lucinoid	Inner fold
CRASSATELLACEA	Burrowing	Crossed-lamellar	—	Homogeneous in Crassatellidae, prisms in Astartidae	Absent	Present in Astartidae	Absent	Astartidae: external opisthodetic Crassatellidae: internal resilium	Cyrenoid	Inner fold, fusion at point between exhalent/inhalent areas
CARDIACEA	Burrowing	Crossed-lamellar	—	Complex crossed-lamellar	Absent	Thin sheets in inner layer	Absent	External opisthodetic	Lucinoid	Inner fold and inner surface of middle fold
VENERACEA	Burrowing, rarely byssate	Crossed-lamellar homogeneous	—	Complex crossed-lamellar or homogeneous	Absent	Thin sheets in inner layer of some species	Absent	External opisthodetic	Cyrenoid	Inner fold and inner surface of middle fold

* *C. pellucida* and *C. exogyra* have an outer prismatic calcite layer, middle crossed-lamellar layer and inner complex-crossed lamellar layer.

Superfamily	*Siphons*	*Labial palp Ctenidia Grade (Stasek 1963c)*	*Gill type (Ridewood 1903)*	*Gill cilia (Atkins 1937)*	*Stomach type (Purchon 1958, 1960)*	*Stomach type (Dinamani 1967)*	*External ornament*
CHAMACEA	Short inner fold	Type 2	Plicate	C 1	4 and 5	*3a*	Radial and concentric squamae, or spinose
CARDITACEA	No siphons	Type 2	Non-plicate	Not examined	4	*3a*	Radial ribs, some squamate and reticulate
LUCINACEA	If siphon present then inner fold	Type 3	Non-plicate homorhabdic	G 1	4	Not examined	Concentric, some radial and reticulate
CRASSATELLACEA	No siphons	Type 3 (Crassatellidae) Type 1 (Astartidae)	Non-plicate	C 1	4	Not examined	Concentric, costae and striae
CARDIACEA	Inner and middle fold	Type 2	Plicate heterorhabdic	C 1	5	3	Radical ribs or concentric, some spines
VENERACEA	Inner and middle fold	Types 2 and 3	Plicate heterorhabdic	C 1 and C 2	5	3	Concentric, some radial, reticulate or spinose

and for *Cardita tenuicosta* Sowerby, Cretaceous (Albian), Gault, Folkestone (Pl. 75, fig. 1)

Right valve	1 0 1 n	0 1 0	
Posterior	———	———	Anterior.
Left valve	0 1 0 n	0 1 0 1	

If these are compared with that of a relatively unmodified *Chama* from the Eocene, striking similarities are seen. The subsequent modification of the teeth in *Chama* has been associated with the cemented habit. Both early *Chama* and recent *Cardita* have one stout anterior cardinal and a long arcuate posterior cardinal.

Radial ribbing is the most frequent ornamentation pattern of Carditidae but some byssate species such as *Cardita crassicostata* Reeve can develop large squamae (Pl. 75, fig. 4). Many Cretaceous species such as *Fenestricardita fenestrata* (Forbes) (Pl. 75, fig. 6) have a reticulate ornament. *Cardita distorta* Reeve, a Red Sea species which lives byssally attached amongst coral, has become inequivalve and very *Chama*-like in appearance (Pl. 75, fig. 5).

The external opisthodetic ligament of the Carditidae is frequently sunk between the dorsal valve margins. A similar condition is seen in several heterodont superfamilies, including the Chamacea.

The dissoconch of the Chamacea shows striking resemblances to the byssate Carditidae (text-fig. 3, Pl. 71, fig. 1) both externally and internally, including the dentition. These similarities could, however, be morphological convergence as the result of the byssate attachment.

Certain adult Cretaceous carditid genera show a remarkable similarity in morphology to the dissoconchs of some Recent *Chama* species. For instance *Fenestricardita fenestrata* (Forbes) (Pl. 75, fig. 6), Aptian, England, while being a typical carditid shell shape has an ornament very similar to that shown on many *Chama* (Pl. 71).

The less-common *Trapezicardita* (Casey 1961, p. 581; Keeping 1883, pl. 6, figs. 5*a* and *b*; Woods 1907, p. 148, pl. 28, figs. 12–15) from the Upper Aptian of England, has the same ornament. More interestingly it has the shell shape of the Recent byssate Carditidae. It is possibly these or similar carditids that are the ancestors of the Chamacea.

2. *Comparisons with the Lucinacea*

Douvillé (1912) proposed that the Chamacea were derived from the Lucinacea during the late Cretaceous. This view was supported by Nicol (1952) on the basis of shell morphology.

EXPLANATION OF PLATE 75

Fig. 1. *Cardita tenuicosta* Sowerby, Cretaceous (Albian), Gault, Folkestone, England. *a*, right valve showing hinge teeth; *b*, left valve. Both ×4.
Abbreviations: C, cardinal teeth; L, lateral teeth.
Fig. 2. *Cardita beaumonti* var. *amelliae* d'Archiac, Upper Cretaceous, Ga'ara, Ruthbah, Iraq. Right valve, BMNH LL22245; ×0·75.
Fig. 3. *Mytilicardia crassicosta* Lamarck, Pleistocene, Limestone creek, Gleneig River, Victoria. BMNH L6570, ×1.
Fig. 4. *Mytilicardia crassicosta* Lamarck, Recent, New Holland. Left valve, ×2.
Fig. 5. *Cardita distorta* Reeve, Recent, Red Sea. *a*, Type, BMNH 1963686/2, ×1·5. *b*, Dorsal view.
Fig. 6. *Fenestricardita fenestrata* (Forbes) Cretaceous, Aptian, Sevenoaks, England. Left valve, BMNH L23280, ×3.

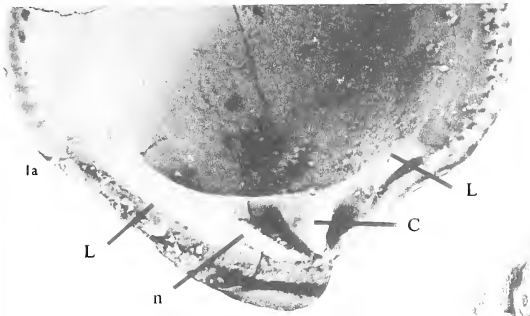

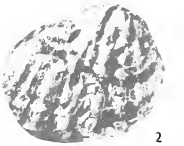

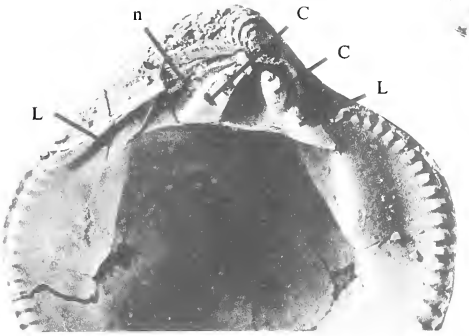

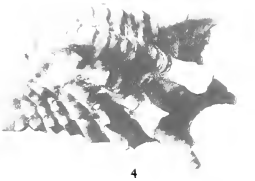

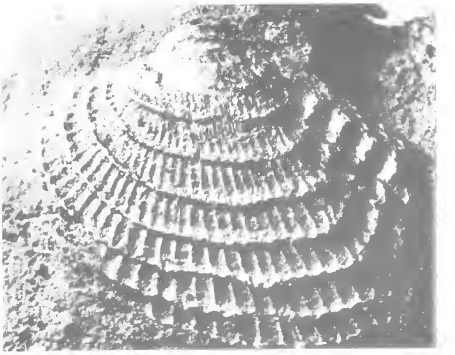

KENNEDY, MORRIS and TAYLOR, Chamacea

This apparent resemblance between the Lucinacea and the Chamacea is well seen only in *Arcinella*. Some Lucinacea have a groove on the posterior part of the exterior of the shell running from the umbo to the postero-ventral margin. This is reflected on the inside of the shell as a low ridge at the anteriorward termination of the posterior adductor muscle scar, and is present at the shell margin as a slight nick. A similar groove on the exterior surface is seen in some Chamacea, although it is often obscured by the irregular surface ornament. The function of this exterior groove and internal ridge is uncertain, but it may be associated with the insertion of the posterior adductor muscle.

In many Lucinacea and a few species of *Chama* the ventral end of the anterior adductor muscle scar is detached from the pallial line (text-fig. 7) and extended in an anterior direction. Allen (1958) has shown that in the Lucinacea the elongate anterior adductor muscle is ciliated, and serves as a preliminary sorting area for food particles brought in by the anterior inhalent current. This anterior inhalent current is peculiar to the Lucinacea. In the Chamacea however, both inhalent and exhalent siphons are situated at the posterior end. Yonge (1967) has described how the foot of *Chama pellucida* protrudes and moves dorsally along the outer surface of the anterior adductor muscle, as in other cemented genera, assisting in the cleansing of the anterior mantle cavity. The elongation in this instance is thus possibly related to the facility of mantle cleansing.

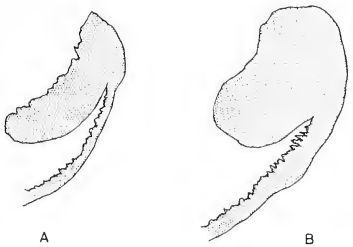

TEXT-FIG. 7. Diagram of the anterior adductor muscle pad and pallial line of (A) *Codakia punctata* Linnaeus and (B) *Chama macerophylla* Gmelin to show the comparable detachment of the ventral end of the muscle pad in the Lucinacea and Chamacea.

As can be seen from Table 2 the labial palps, gill type, and gill cilia of the Lucinacea differ from those of the Chamacea, while they have the anterior inhalent current. Some species have a small posterior exhalent siphon which, although formed by fusion of the inner mantle fold, has a unique inversion retraction mechanism.

The shell of the Lucinacea consists of three layers. There is an outer composite prismatic layer, a middle crossed-lameller layer, and an inner complex crossed-lamellar layer. This arrangement has been present since the Lower Lias (as in *Lucina limbata* Terquem and Piette) at least. Myostracal pillars are not found, although thin sheets of myostracal-type prisms may be present in the inner layer. Tubules are very rare; we have found them only in the genus *Codakia*. Here, tubules, larger and sparser than in other bivalve groups, are found penetrating the inner shell layer only.

The dentition is primitively 'lucinoid' but many Lucinacea have lost teeth, and some are edentulous. The hinge notation for *Lucina pensylvanica* Linnaeus and *Codakia punctata* (Linnaeus) are given below:

Lucina pensylvanica (Linnaeus)

Right valve	0 1 0 1 n	(1) 0 1 (0) (1) 0 1	0 1 0
Posterior			Anterior.
Left valve	1 0 1 n	0 1 0 1 0	1 0 1

Codakia punctata (Linnaeus)

Right valve	(1)	ne nc nc	1 0 1	1 0
Posterior				Anterior
Left valve	(1) (0) (1)	ne nc nc	(1) 0 1 (0)	1 0 1

ne = ridge-bearing elastic ligament.
nc = ridge-bearing calcified ligament.

This pattern shows similarities to the Chamacea but also to the Carditacea.

All living species of Lucinacea are burrowers, and fossil forms seem to have been so since the Ordovician (McAlester 1965). Shell ornament varies from fine concentric growth-lines to radial ribs or a reticulate pattern. The sculpture is always fairly subdued.

3. *Comparisons with the Crassatellacea*

The superfamily Crassatellacea is divided into three families, the Crassatellidae, Astartidae, and Cardiniidae. The first two families are extant but the latter family became extinct during the Jurassic.

The Astartidae and Crassatellidae show rather different characters, and Boyd and Newell (1968) have suggested that the Crassatellacea may have had a diphyletic origin.

Both the Crassatellacea and the Astartacea have a two-layered shell. The outer layer of both consists of crossed lamellar structure. The inner layer of the Crassatellacea is homogeneous, whereas that of the Astartacea is made up of 'myostracal type' prisms with only small traces of complex crossed-lamellar structure. The shell structure characters of the Astartidae have been present since the Lower Jurassic.

The dentition of the Crassatellacea has been related to both the 'lucinoid' and 'cyrenoid' patterns. Boyd and Newell (1968) have recently re-examined the dentition of this superfamily. They find that recent examples of Crassatellidae and Astartidae have rather similar hinges. For the crassatellid *Hybolophus speciosus* (Adams) the notation is:

Right valve	1 0 (1) e r	1 0 1 0 1	1 0 1	
Posterior				Anterior
Left valve	1 0 1	e r	(0) 1 0 1 0	(1) 0 1

e = elastic ligament.
r = resilifer.

For *Astarte castanea* Say:

Right valve	1 0 (1) n	1 0 1 0 (1)	1 0 1	
Posterior				Anterior.
Left valve	1 0 1	n	0 1 0 1 (0)	(1) 0 1

Thus both examples have rather more complex hinge teeth structures than any of the early Chamacea.

The ligament of the Astartidae is external and opisthodetic but in the Crassatellidae there is an internal resilium.

The sculpture of both families is concentric, frequently with raised costae but they are often smooth or concentrically striate. Radial sculpture is never developed.

Members of both the Crassatellidae and Astartidae are shallow burrowers.

4. *Comparison with the Cardiacea*

The Chamacea were considered to have arisen from the Cardiacea by Anthony (1905). His evidence was based primarily upon the ctenidia and the hinge teeth.

It can be seen from Table 2 that although the main shell layers in the Chamacea and Cardiacea are similar, neither tubules nor myostracal pillars are developed in the latter.

Cardiacean dentition is of a 'lucinoid' pattern, but with well-developed laterals as well as the usual cardinals. The development of these widely spaced laterals is a characteristic of the group. The hinge of *Acanthocardia aculeata* (Linnaeus) can be expressed as:

Right valve	1 0 1 (0) n	1 0 (1)	1 0 1
Posterior			Anterior
Left valve	1 0 1 n	0 1 0	1 0

and *Fragum unedo* (Linnaeus)

Right valve	1 0 1 n	0 1 0	1 0 (1)
Posterior			Anterior.
Left valve	1 0 (1) n	1 0 1	1 0 1 0

A hinge which, contrary to the opinion of Anthony (1905), is not like that of *Chama*.

The ctenidia of the Cardiacea, although similar to those of *Chama*, show similarities to several other heterodont groups (Table 2).

All recent species of Cardiacea are shallow burrowers, although the Eocene genus *Lithocardium* which gave rise to the Tridacnacea was in all probability a byssate form.

The first Cardiacea appeared in the Upper Trias and have been distinct since, early members appearing morphologically very like Recent species.

5. *Comparison with the Veneracea*

The Chamacea were related to the Veneracea by Fischer (1887), who considered that the dissoconch stage of *Arcinella* showed similarities of external sculpture to the adult *Venerupis*.

Table 2 shows that many of the anatomical characters of the Veneracea are quite different from those of the Chamacea. The stomachs according to the classification of both Purchon (1958, 1960) and Dinamani (1967) are quite different. Mantle fusion is much more extensive in the Veneracea, fusion being by way of the inner mantle folds and the inner surface of the middle fold. Well-developed siphons are formed from these regions of the mantle.

The dentition of the Veneracea is typically of the 'cyrenoid' pattern, with three cardinals in each valve. This is an altogether more complex dentition than that found in the Chamacea. The notation of *Callistina plana* (Sowerby) from the Albian is:

Right valve	n $\overbrace{0\,1\,0\,1}$ 0 1 0 1	(0) (1) 0 1 0	
Posterior			Anterior
Left valve	n 0 1 0 1 0 1 0	1 0 (1)	

and *Notochione columbiensis* (Sowerby), Recent, Ecuador:

Right valve	(n)	(0) (1) 0 1 0 1 0 1 0	
Posterior			Anterior.
Left valve	n	(1) 0 1 0 1 0	

The Veneracea have an outer crossed-lamellar shell layer and an inner layer usually consisting of homogeneous structure, although in some species it is complex crossed-lamellar. The outer layer shows certain distinctive characters. Because the shell margin is frequently reflected, the first-order lamels of the outer part of the crossed-lamellar layer are arranged radially. They become arranged concentrically when traced inwards, and appear vertical in radial section. Frequently they grade into homogeneous structure at the shell interior. The outer layer thus appears to be built of three distinct shell structures. Both tubules and myostracal pillars are absent.

Most members of the Veneracea are burrowers, and a pallial sinus is developed in many species. However, some species such as *Gafrarium* can under unfavourable conditions, become byssate.

The ornamentation of the shell is mainly concentric, but reticulations, spines and squamae can be developed.

6. *Comparison with the rudists*

It is generally thought that the origin of the rudists lies in the Megalodontacea, a Silurian to Lower Cretaceous group of pachydonts, one of which, *Pachyrisma* (Lower to Upper Jurassic), became cemented, and gave rise to *Diceras* (Oxfordian to Tithonian) and subsequently the rest of the rudists (Cox 1933, Dechaseaux 1952).

Derivation of the Chamacea from the Hippuritacea (Turonian to Maastrichtian) and Radiolitidae (Aptian to Maastrichtian) is unlikely. These forms, with their extensive changes in symmetry, the massive conical lower valves and lid-like upper valves, the porous calcitic shell layers, and the atrophied ligaments, are morphologically too divergent to be considered the ancestors of the Chamacea. Similar arguments can be applied to the Caprinidae (Aptian to Maastrichtian).

Greater resemblance to the Chamacea is shown by the Monopleuridae, Diceratidae, possibly the Requinidae, some Caprotinidae, and the Megalodontacea.

(*a*) *Megalodontacea.* Members of this family were uncemented, and considering the reduction of the anterior part of the shell, were apparently byssally attached.

The shell structure of some well-preserved examples was examined. Examples of *Megalodon pumilis* Benecke and *Pachymegalodon crassus* Böhm from the Lower Lias of Valle del Paradiso, Crezzana, Italy, showed a two-layered aragonitic shell, with an outer homogeneous layer and an inner homogeneous to complex crossed-lamellar layer. The two layers are separated by the prismatic trace of the pallial myostracum. Some thin sheets of myostracal type prisms are present in the inner layer. Specimens of *Durga trigonalis* Böhm, from the Lias near Verona, Italy, are badly recrystallized, but show what was an originally wholly aragonitic shell with two homogeneous layers separated by the trace of the pallial myostracum.

The hinge teeth of Megalodontidae show the pachydont condition, with massive cardinals, the notation for *Eumegalodon cucullatus* (J. Sow.) and *Pachyrisma grande* (Morris and Lycett) is shown below and in Plate 76, fig. 4; Plate 77, fig. 3.

Eumegalodon cucullatus:

Right valve	(1) 0 1 n	0 (1 0 1 0 1 0 1 0 1 0 1) 0	
Posterior	———	———	Anterior.
Left valve	0 1 (0) n	1 (0 1 0 1 0 1 0 1 0 1 0) 1	

The traces of small teeth and sockets (bracketed above) between the two large teeth of the left valve are remnants of an original actinodont condition.

Pachyrisma grande:

Right valve	1 0 n	(0) 1 0 1	(1) 0 1	
Posterior	———	———	———	Anterior.
Left valve	0 1 n	0 1 0	0 1	

In these early derivatives of the actinodonts the ligament and its nymph are basically dorsal to the hinge teeth. Although the dentition appears to be disrupted into cardinals and laterals it is a modified actinodont dentition. The apparent cardinals and laterals are not necessarily homologous with those found in the veneroid type of heterodont dentition.

As is the case with the other rudist families discussed, this is a typical pachydont dentition with a reduced number of large cardinal-like teeth often with their greatest dimension vertical in relation to the plane between the valves.

Both species show a rather more complex notation than that of early Chamacea. Furthermore, the arrangement of the more massive teeth seen in this family is very distinctive.

(*b*) *Diceratidae*. This family can be derived directly from the Megalondontacea; changes in the geometry, dentition, and musculature result from the acquisition of the cemented habit.

The dentition is simplified from the megalodontid pattern of *Pachyrisma*. The smaller anterior teeth are lost. The large tooth in the left valve and the two large teeth in the right valve become larger, longer and twisted. These changes are reflected externally by the exogyriform shape of the shell.

The notation of *Diceras arietum* Lamarck is shown below and in Plate 76, fig. 1.

Right valve	1 0 n	1 0 1	
Posterior	———	———	Anterior.
Left valve	0 1 n	0 1 0	

We have not found any specimens of *Diceras* well enough preserved to determine the original shell structure.

The rudists were cemented by either the right or the left valve and evolved a virtual inversion of dentition in later forms. Some later forms attached by the left valve have a single tooth in that valve and two teeth in the right valve, while forms attached by the right valve have one tooth in the right valve and two in the left valve. It is this point of resemblance with the Chamacea which has most impressed palaeontologists and zoologists. However, early ribbed oysters could be attached by either valve, but later oysters

are attached only by the left valve. It would thus seem that cementation by either valve may be a characteristic of the early history of cementation within a group. Resemblance of *Diceras* to the Chamacea is thus purely coincidental.

(*c*) *Requieniidae*. This family shows certain features (such as the hinge teeth) in common with the Diceratidae, but additional modifications such as siphonal bands and accessory cavities appear.

Moderately unaltered specimens of *Apricardia toucasi* (d'Orbigny) from the Lower Campanian of Var, France, show an outer, calcitic prismatic layer, and middle and inner aragonitic homogeneous layers. Thin prism sheets are seen in the inner layer.

(*d*) *Caprotinidae* (Neocomian–Turonian). Many species in this family are small and exogyriform with an ornament of radial ribs. Together with the Monopleuridae they show the closest morphological resemblance to *Chama* among the rudists.

Material sufficiently unaltered for shell structure studies was not available, but it seems that *Caprotina semistriata* (d'Orbigny) from the Cenomanian of Le Mans had an outer calcitic layer and an inner aragonitic layer or layers.

The pattern of teeth has changed from that of *Diceras* by a foreshortening of the hinge plate, increase in size of the posterior tooth in the left valve, near atrophy of the ligament, and loss of the anterior tooth in the right valve. These changes are associated with the reduction of the free valve to a cap-shaped or opercular form. The notation can be expressed as below:

Right valve (fixed)	$\overset{\frown}{0}10\,1\,0$	
Posterior	———	Anterior.
Left valve (free)	$101\,0\,\underset{\smile}{1}$	

The position of the ligament in *Caprotina* is indicated by an infolding of the shell wall, marked by a shallow groove on the outer surface. The ligament is disposed vertically in relation to the valve commissure, so that the functional distance is therefore very short. It is doubtful whether the ligament in this case was a very effective mechanism for the opening of the valves. No comparable ligamental structure is found in the Chamacea.

EXPLANATION OF PLATE 76

Fig. 1. *Diceras arietum* Lamarck. Jurassic (Oxfordian), Chatel-Censoir, Yonne, France, BMNH L33915, ×1. *a*, right valve, *b*, left valve.

Fig. 2. *Caprotina semistriata* (d'Orbigny). Cretaceous, Cenomanian, Le Mans, France, ×2. *a*, left (free) valve. BMNH L96200. *b*, right (cemeted valve) BMNH L96203.

Fig. 3. *Eumegalodon cucullatus* (J. Sowerby). Devonian, Paffrath, Cologne, Germany. ×2. *a*, right valve; *b*, left valve. Abbreviations: C, cardinal; L, lateral; n, ligament nymph; aa, anterior adductor muscle scar.

EXPLANATION OF PLATE 77

Fig. 1. Fractured section of the inner calcified ligament of *Chama macerophylla* Gmelin. Scanning electron-micrograph, ×1000.

Fig. 2. Fractured section of the prismatic layer of *Chama pellucida* Broderip. Scanning electron-micrograph, ×280.

Fig. 3. *Pachyrisma grande* Morris and Lycett, Jurassic, Great Oolite, Minchinhampton, England. ×0·5. *a*, Left valve showing hinge teeth; *b*, Right valve. Abbreviations: C, cardinals; L, laterals; n, ligament nymph; aa, anterior adductor muscle scar.

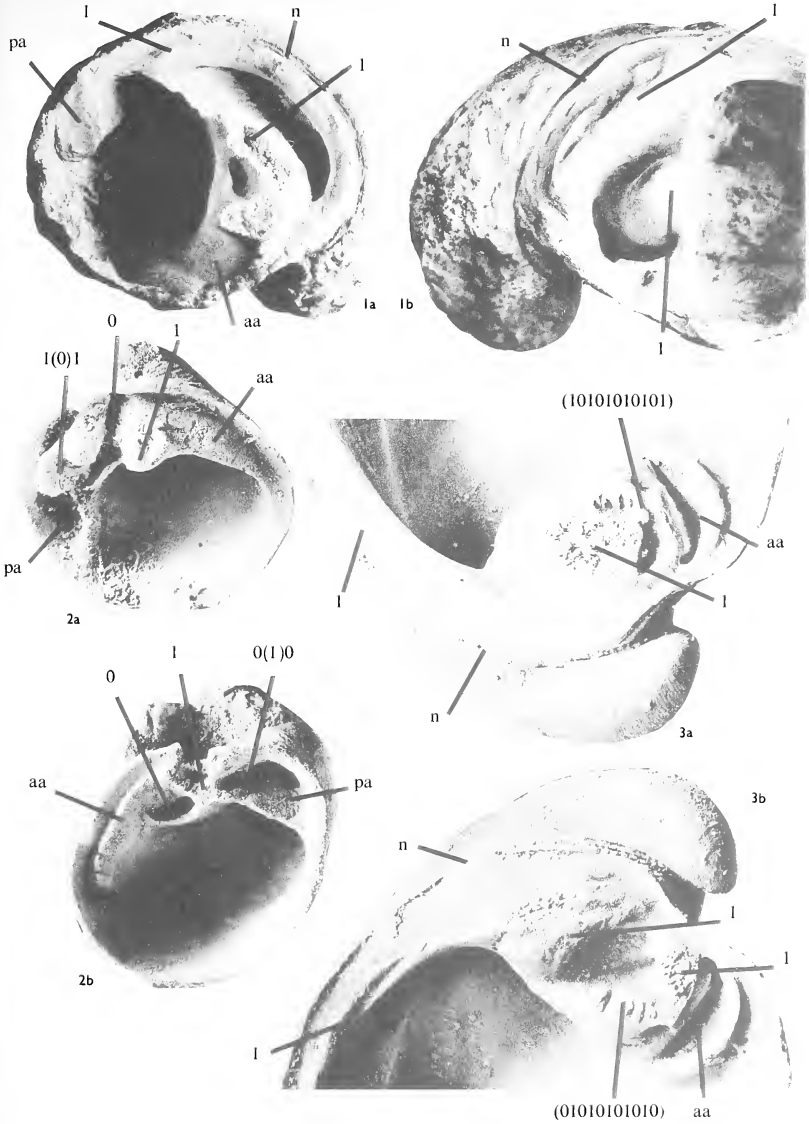

KENNEDY, MORRIS and TAYLOR, Chamacea

1

2

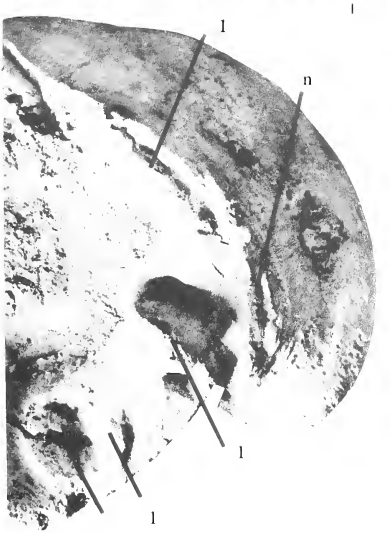

3a

3b

KENNEDY, MORRIS and TAYLOR, Chamacea

(*e*) *Monopleuridae* (Kimmeridgian–Danian). The Monopleuridae can be derived from the Diceratidae through *Valletia*. Certain members of this family, for example *Gyropleura cenomanensis* (d'Orbigny) (Pl. 70, fig. 5) and *Ciplyella pulchra* (Ravn) (Pl. 72, fig. 5), show remarkable similarity in morphology to *Chama*. They are small to medium-sized, strongly exogyriform and radially ribbed. *Ciplyella pulchra* has commonly been considered to be a *Chama*, but the form of the adductor scars and the near atrophy of the ligament show that it is a rudist closely related to *Gyropleura* (N. J. M. and J. D. T., *in. litt.*).

The dentition of the Monopleuridae resembles that of the Caprotinidae, but without the incipient splitting of the posterior tooth in the left valve seen in *Caprotina* (Pl. 76, fig. 2).

The teeth of *Gyropleura* are illustrated in a sketch by Deschaseaux (1952, 335, text-fig. 177). *Gyropleura cornucopiae* (d'Orbigny) from the Middle Cenomanian of north-western Europe, and *G. inequirostrata* (Woodward) from the Campanian and Lower Maastrichtian of the same area, have a similar arrangement. The dentition of *Monopleura* (Deschaseaux 1952, 335, text-fig. 176) is also not significantly different.

The notation of *Gyropleura cornucopiae* (d'Orbigny) is shown below:

Right valve (fixed)	0 1 0	
Posterior	———	Anterior.
Left valve (free)	1 0 1	

As is the case with the other rudist families discussed, this is a typical pachydont dentition with no differentiation into heterodont cardinals and laterals. It contrasts remarkably with the dentition of the earlier Chamacea. The teeth of *Chama calcarata*, for example (Pl. 72, fig. 2), although twisted to lie sub-parallel to the line of the ligament, still diverge slightly below the umbones and in the fixed valve may be matched tooth for tooth with many fossil and recent Carditidae.

No well-preserved material was available for shell structure studies. Specimens of *Gyropleura cenomanensis* from the Cenomanian of Le Mans, France, however, appear to have an aragonitic inner layer or layers and a calcitic outer layer. The preservation of a specimen of *Gyropleura inequirostrata* (Woodward) from the Upper Campanian Chalk of Sidestrand, Norfolk, England, indicates the same arrangement.

Major differences occur in the adductor musculature between the Chamidae and the Monopleuridae together with all other rudists. In the Megalodontacea, the posterior adductor scar is associated with a plate or myophoric septum (Pl. 76, fig. 3) which seems to add strength to the shell in the form of a buttress. The anterior adductor scar is in the form of a shallow, cup-shaped socket (Pl. 76, fig. 3; Pl. 77, fig. 3). In *Diceras*, the animal becomes attached by one valve and presumably takes up a posture reclining on one side. The umbones become widely separate, each valve becoming cornucopia shaped. The adductor musculature attachment has had to compensate in order to remain near normal to the direction of adduction. This compensation took the form of certain modifications of the muscle attachment area. In the Caprotinidae and the Requeniidae, the anterior adductor scar occurs on a raised platform in either valve so that the actual length remains at a minimum. At the same time this muscle became extended parallel to the valve margins. The posterior adductor muscle attachment sank deeper into the space between the myophoric septum and the hinge plate in the Requeniidae. In the

Caprotinidae, the same septum joined with the hinge plate to form a deep accessory cavity to house the posterior adductor muscle. In the Monopleuridae both the posterior and the anterior muscles form elongate scars on raised platforms which tend to form extensions to the hinge plate. They are somewhat less prominent in the fixed valve. The Monopleuridae retain a somewhat reduced posterior myophoric septum.

In marked contrast to these developments in the rudists, the adductor muscle scars of the Chamidae are broadly similar to those of most other heterodont groups, except that the dorsal portion of the anterior adductor scar of both valves impinges somewhat upon the hinge plate.

The resemblance of *Gyropleura* and other Monopleuridae to *Chama* is merely that of convergent adaptions to the same cemented mode of life under similar habitat conditions. Similar exogyriform shapes are found in totally unrelated bivalves, e.g. Ostreacea, Pandoracea, Spondylidae, Unionacea, and the Chamacea.

DISCUSSION

From the comparison of the Chamacea with their possible relatives, it appears to us that amongst these groups only the superfamilies Carditacea and Lucinacea are likely to be closely related.

The rudists, for so long considered closely related to the Chamacea show certain similarities, but these are only the result of convergence because of the cemented habit.

The shell structure characters of the Carditacea match exactly those of the Chamacea (except for the development of calcite in *C. pellucida* and *C. exogyra*), whereas the Lucinacea have an extra outer shell layer. The dentitions of the Chamacea, Lucinacea, and Carditacea are all very similar. Certain shell morphology features such as the shape of the anterior adductor muscle scar, and the groove on the exterior, suggest similarities with the Lucinacea.

The Carditacea, however, contain many species which are byssally attached, and are asymmetrical; some are inequivalve. The Lucinacea are all burrowers. The Lucinacea and the Carditacea have had a distinct history at least as far back as the Ordovician (McAlester 1965).

The weight of evidence suggests to us that the Chamacea were derived from a byssate *Cardita* during the late Cretaceous. *Chama haueri*, the first authenticated *Chama*, is a 'good' *Chama* but rather less inequivalve than many Recent species. Transitional forms (other than the assumption of the byssate habit) between Carditacea and Chamacea are lacking; however, if the *Cardita* origin is not accepted, then possible transitional forms are not found between the Chamacea and any other group. However, possibly byssate *Cardita* are common in the Cretaceous, for example forms from the Upper Cretaceous of Ga'ara, Ruthbah, Iraq (BMNH LL2245–8) labelled *Cardita beaumonti* var. *amelliae* d'Archiac. They are thick-shelled, subrectangular in shape with coarse radial and concentric ornament, on which short spines are developed (Pl. 75, fig. 2). Although perhaps too late in time to be thought of as ancestral to the Chamacea, they show the forms among which the origin of the group should be sought. An alternative would be probably byssate forms such as *Fenestricardita* (Pl. 75, fig. 6).

The superfamily Chamacea should be removed from the Order Hippuritoida and placed in the Veneroida.

Acknowledgements. Our best thanks are to Messrs. R. J. Cleevely and C. P. Nuttall for much useful discussion, and to Mr. A. E. Rixon for considerable assistance in preparing fossil material.

We thank the staff of the British Museum (Natural History) electron microscopy unit, under the direction of Mr. B. Martin, for their assistance, and Dr. A. Hall for help with mineralogical determinations.

REFERENCES

ALLEN, J. A. 1958. On the basic form and adaptations of habitat in the Lucinacea (Eulamellibranchia). *Phil. Trans. R. Soc., Ser. B.* **241,** 421–48.

ANTHONY, R. 1905. Influence de la fixation pleurothétique sur la morphologie des mollusques acéphales dimyaires. *Ann. Sci. nat. (Zool.)* **1,** 165–346.

ATKINS, D. 1937. On the ciliary mechanisms and interrelationships of Lamellibranchs. Part III. Types of Lamellibranch gills and their food currents. *Q. Jl Microsc. Sci.* **79,** 375–421.

BASSE, E. 1933. Faune Malacologique du Cretacé supérieur du sud-ouest de Madagascar. *Annls Paléont.* **21** (3–4), 1–80, pl. 1–9.

BAYER, F. M. 1943. The Florida species of the family Chamidae. *Nautilus*, Philad. **56,** 116–24.

BAYLE, M. E. 1865. Notice sur une nouvelle espèce du genre *Chama. J. Conch., Paris*, (2) **5,** 365–70, pl. 14.

BERNARD, F. 1895. Première note sur le développement et la morphologie de la coquille chez les Lamellibranches. *Bull. Soc. géol. Fr.* (3) **23,** 104–54.

BØGGILD, O. B. 1930. The shell structure of Mollusks. *K. danske Vidensk. Selsk. Skr.* (Afd. 9) **2,** 233–326.

BÖHM, G. 1891. Megalodon, Pachyerisma und Diceras. *Ber. Naturforsch. Gesellsch.* Freiburg. **6,** 33–56.

BOYD, D. W. and NEWELL, N. D. 1968. Hinge grades in the evolution of crassatellacean bivalves as revealed by Permian genera. *Am. Mus. Novit.* **2328,** 52 pp.

CASEY, R. 1961. The stratigraphical palaeontology of the Lower Greensand. *Palaeontology*, **3,** 487–621 pl. 77–84.

COX, L. R. 1933. The Evolutionary History of the Rudists. *Proc. Geol. Ass., Lond.* **44** (4), 379–88.

—— 1960. Thoughts on the Classification of the Bivalvia. *Proc. malac. Soc. Lond.* **34,** 60–88, 2 figs.

DALL, W. H. 1903. Contribution to the Tertiary fauna of Florida. Part IV. *Trans. Wagner free Inst. Sci. Philad.* **3,** 1219–1654.

DAVIS, A. M. 1935. The Composition of Tertiary Faunas. *Tertiary Faunas.* 1. London (Mollusca, pp. 116–356).

DESCHASEAUX, C. 1952. Classe des Lamellibranches. *In* PIVETEAU, J., *Traité de Paléontologie*, 2, 790 pp. Paris.

DINAMANI, P. 1967. Variation in the stomach structure of the Bivalvia. *Malacologia*, **5** (2), 225–68.

D'ORBIGNY, A. 1842. Quelques considérations zoologiques et géologiques sur les Rudistes. *Annls. Sci. nat.* (Ser. 2) **17** (zool.), 173.

—— 1844–7. *Paléontologie Française, Terrain Crétacé 3* (*Lamellibranchia*), 804 pp., 489 pl., Masson, Paris.

—— 1848–51. Ibid. 4 (*Brachiopoda*), 390 pp., pls. 490–599, Bertrand, Paris.

—— 1912. Un essai de classification phyllogénique des Lamellibranches. *C.r. hebd. Séanc. Acad. Sci., Paris*, **154,** 1677–81.

—— 1913. Classification des Lamellibranches. *Bull. Soc. géol. Fr.* (4) **12,** 419–67.

FISCHER, P. H. 1880–7. Manuel de Conchyliologie et de Paléontologie conchyliologique. *Histoire naturelle des Mollusques vivants et fossiles*, 1008 pp. Paris.

GRÉGOIRE, C. 1957. Topography of the organic components in Mother of pearl. *J. biophys. biochem. Cytol.* **3** (5), 797–808.

—— 1959. Conchiolin remnants in mother of pearl from fossil Cephalopoda. *Nature, Lond.* **184,** 1157–8.

—— 1960. Further studies on structure of the organic components in mother-of-pearl, especially in Pelecypods. (Part I) (I). *Bull. Inst. r. Sci. nat. Belg.* **36** (23), 1–22, 5 pls.

—— 1967. Sur la structure des matrices organiques des coquilles de mollusques. *Biol. Rev.* **42,** 653–88.

GRIEPENKERL, O. 1889. Die Versteinerungen der Senonen Kreide von Königslutter im Herzogthum Braunschweig. *Palãont. Abh.* **4,** 305–418, pl. 34–44.

GRIESER, E. 1913. Über die Anatomie von *Chama pellucida* Broderip. *Zool. Jb.* Suppl. bd. **13,** Fauna Chilensis, **4,** 207–80.

JAWORSKI, E. 1928. Untersuchungen über den Abdruck der Mantelmuskulatur bei den Ostreiden und Chamiden und die sog. Cirrhenabdrücke. *Neues Jb. Miner. Geol. Paläont. Beile.* Bd. Abt. **B59,** 327–56, pl. 20–4.

KEEPING, W. 1883. *The Fossils and palaeontological affinities of the Neocomian deposits of Upware and Brickhill,* 164 pp., 8 pls. Cambridge.

KENNEDY, W. J. and TAYLOR, J. D. 1968. Aragonite in rudists. *Proc. geol. Soc. Lond.* **1645,** 325–31.

KUMMEL, B. and RAUP, D. M. 1965. *Handbook of Palaeontological Techniques,* 852 pp. San Francisco and London.

KUTASSY, A. 1934. Pachydonta mesozoica (Rudistis exclusis). *Fossilium Cat.* Pars Animalia, **68,** 202 pp.

LINNAEUS, C. 1758. *Systema Naturae per Regna Tria Naturae.* Sc. Ed. Decima, Holmiae.

LISON, L. 1949. Recherches sur la forme et la mécanique de développément des coquilles des lamellibranches. *Mem. Inst. r. Sci. nat. Belg.* (Ser. 2) **34,** 1–87.

LOWENSTAM, H. A. 1954*a*. Environmental relations of modification compositions of certain carbonate secreting marine invertebrates. *Proc. natn. Acad. Sci. U.S.A.* **40** (1), 39–48, 3 figs.

—— 1954*b*. Factors affecting the aragonite–calcite ratios in carbonate-secreting marine organisms. *J. Geol.* **62,** 284–322, text-figs. 1–15.

—— 1963. Biologic problems relating to the composition and diagensis of sediments. In *The Earth Sciences; Problems and Progress in Current Research,* 138–95, 14 figs. Chicago.

—— 1964. Coexisting calcites and aragonites from skeletal carbonates of marine organisms and their strontium and magnesium contents. In *Recent researches in the fields of hydrosphere, atmosphere and nuclear geochemistry,* 373–405. Tokyo, Maruzen.

MCALESTER, A. L. 1965. Systematics, affinities, and life habits of *Babinka,* a transitional Ordovician lucinoid bivalve. *Palaeontology,* **8** (2), 231–46, pl. 26–8.

MACCLINTOCK, C. 1967. Shell structure of Patelloid and Bellerophontoid gastropods (Mollusca). *Bull. Peabody Mus. nat. Hist.* **22,** 142 pp. 32 pls.

MORRIS, N. J. 1967. Scaphopoda and Bivalvia, chapter 17. In *The Fossil Record. A symposium with documentation.* Geol. Soc. London, 469–77.

MUNIER-CHALMAS, E. C. P. A. 1895. Deuxième note préliminaire sur la charnière des Mollusques acéphales. *C. r. somm. séanc. Soc. géol. Fr.* (3) **23** (for 1895), liii–lvi.

NEWELL, N. D. 1965. Classification of the Bivalvia. *Am. Mus. Novit.* **2206,** 1–25.

NICOL, D. 1952. Revision of the Pelecypod genus *Echinochama. J. Paleont.* **26,** 803–17, pl. 118–19.

NOETLING, E. 1902. Fauna of the Upper Cretaceous (Maestrichtian) beds of the Mari Hills. *Mem. geol. Surv. India, Palaeont. indica,* **1** (3), 1–79, pl. 1–23.

OBERLING, J. J. 1964. Observations on some structural features of the Pelecypod shell. *Mitt. naturf. Ges. Bern.* **NF.20,** 1–63.

OCKELMAN, K. W. 1962. Developmental types in marine bivalves and their distribution along the Atlantic coast of Europe. *Proc. First Europ. Malac. Congr.* 25–35.

ODHNER, N. H. 1919. Studies on the morphology, the taxonomy and the relations of recent Chamidae *K. svenska Vetensk.-Akad. Handl.* **59** (3), 1–102.

OWEN, G. 1953*a*. The shell in the Lamellibranchia. *Q. Jl microsc. Sci.* **94** (1), 57–70, 8 figs.

—— 1953*b*. The biology of *Glossus humanus* (L.) (*Isocardia cor* Lam.). *J. mar. biol. Ass. U.K.* **32,** 85–106.

PALMER, R. H. 1928. The Rudistids of southern Mexico. *Occ. Pap. Calif. Acad. Sci.* **14,** 137 pp.

PANELLA, G. and MACCLINTOCK, C. 1968. Biological and environmental rhythms reflected in Molluscan shell growth. *J. Paleont.* **42** (5), 64–79, pl. 1–9.

—— —— and THOMPSON, M. N. 1968. Paleontological Evidence of Variations in length of Synodic Month since late Cambrian. *Science, N.Y.* **162,** 792–6.

PELSENEER, P. 1911. Les lamellibranches de l'expédition du Siboga. Partie anatomique. *Siboga Exped.* **53a,** 1–126.

PETHÖ, J. 1906. Die Kreide-(Hypersenon-)Fauna des Peterwardeiner (Petervarader) Gebirges (Furska Gora). *Palaeontographica,* **52,** 57–331.

PICTET, E. J. and CAMPICHE, G. 1864–7. Description des Fossiles du Terrain Crétacé des environs de Sainte-Croix. Troisième partie, classe des Mollusques acéphales. *Matér. Paléont. Suisse,* Genève (4) **1,** 1–558, pl. 99–139.

PURCHON, R. D. 1958. The stomach in the Eulamellibranchia; stomach type IV. *Proc. zool. Soc. Lond.* **131**, 487–525.

—— 1960. The stomach in the Eulamellibranchia; stomach types IV and V. Ibid. **135**, 431–89.

RAUP, D. M. 1966. Geometric analysis of shell coiling; General problems. *J. Paleont.* **40** (5), 1178–90.

RAVN, J. P. J. 1902. Molluskerne i Danmarks Kridtaflegringer. 1 Lamellibranchiater. *K. dansk. Vidensk. Selsk. Skr.* (6 Raekke) **9**, 73–138, pl. 1–4.

RIDEWOOD, W. G. 1903. On the structure of the gills of the Lamellibranchiata. *Phil. Trans. R. Soc., Ser. B.* **195**, 147–284.

ROEMER, F. A. 1840. *Die Versteinerungen des Norddeutschen Oolithen-Gebirges. Ein Nachtrag*, 59 pp., 20 pl. Hannover.

—— 1841. *Die Versteinerungen des Norddeutschen Kreidegebirges*, 145 pp., 16 pl. Hannover.

STASEK, C. R. 1963*a*. Orientation and form in the bivalved Mollusca. *J. Morph.* **112**, 195–214.

—— 1963*b*. Geometrical form and gnomonic growth in the bivalved Mollusca. Ibid. **112**, 215–31.

—— 1963*c*. Synopsis and discussion of the association of ctenidia and labial palps in the bivalved mollusca. *Veliger*, **6**, 91–7.

STOLICZKA, F. 1870–1. Cretaceous fauna of southern India. The Pelecypoda, with a review of all known genera of this class, fossil and recent. *Mem. geol. Surv. India Palaeont. indica*, 537 pp., 50 pls.

STROMBECK, A. von, 1863. Ueber die Kreide am Zeltberg bei Lüneberg. *Z. dt. geol. Ges.* **15**, 156.

TAYLOR, J. D., KENNEDY, W. J. and HALL, A. 1969. The shell structure and mineralogy of the Bivalvia: Introduction, Nuculacea—Trigonacea. *Bull. Br. Mus. (nat. Hist.)*, Zoology, Suppl. 3, 125 pp., 25 pls.

VIDAL, L. M. 1877. Nota acerca del sistema cretacés de los Pirineos de Cataluna, Cámidos y Rudistos. *Boln. Comn. Mapa geol. Esp.* **4** (2), 92, pl. 1–7.

WEGNER, T. 1905. Die Granulater Kreide des westlichen Münsterlandes. *Z. dt. geol. Ges.* **57**, 112–232.

WOODS, H. 1904–13. A monograph of the Cretaceans Lamellibranchia of England, vol. 2. *Palaeontogr. Soc.* (Monogr.), p. 148, pl. 28, figs. 12–15.

YONGE, C. M. 1962. On the primitive significance of the byssus in the Bivalvia and its effects in evolution. *J. mar. biol. Ass. U.K.* **42**, 113–25.

—— 1967. Form, habit and evolution in the Chamidae (Bivalvia) with reference to conditions in the Rudists (Hippuritacea). *Phil. Trans. R. Soc. Ser. B.* **252**, 49–105.

ZITTEL, K. A. 1865. Die Bivalven der Gosaugebilde in der Nordöstlichen Alpen. 1. Dimyaria. *Denkschr. Akad. Wiss. Wien* **24**, 105–98.

THE SKULL OF *FABROSAURUS AUSTRALIS*, A TRIASSIC ORNITHISCHIAN DINOSAUR

by RICHARD A. THULBORN

ABSTRACT. The skull of *Fabrosaurus australis* is described in detail. This study is based upon previously undescribed specimens from the late Triassic Red Beds of Lesotho.

The presence of a predentary bone at the mandibular symphysis substantiates Ginsburg's concept (1964) of *Fabrosaurus* as a member of the order Ornithischia—though there is no evidence for any close relationship between *Fabrosaurus* and the Liassic *Scelidosaurus*. Certain cranial features (the toothed premaxilla, the interparietal suture) indicate that *Fabrosaurus* should be referred to the family Hypsilophodontidae of the suborder Ornithopoda. Ornithischian origins and ornithopod phylogeny are re-examined in the light of new evidence from *Fabrosaurus*. *Fabrosaurus* seems to be a fairly direct antecedent of *Hypsilophodon* and appears to fulfil many of the requirements of a genuine 'archetypal' ornithischian.

PRIOR to this decade only a few and fragmentary fossils were available to permit of clarification of early ornithischian history. Faced with this lack of information several investigators tended to simplify the problem by selecting the well-known Wealden ornithopod *Hypsilophodon* as an ornithischian 'archetype' and by attempting to derive the varied ornithischian faunas of the later Mesozoic from similar hypothetical ancestors. This scheme, though useful, is unsatisfactory because of the late stratigraphic occurrence of *Hypsilophodon*—which appears later than stegosaurs and iguanodonts and is roughly contemporary with the earliest ankylosaurs and psittacosaurs. The anomalous situation of *Hypsilophodon* within such a scheme is quite clear—it is geologically younger than (or at least coeval with) those dinosaurs whose ancestry it is supposed to represent. It is in view of this unsatisfactory situation that adequate knowledge of early ornithischians, such as *Fabrosaurus*, becomes of critical importance.

The genus *Fabrosaurus* was established by Ginsburg (1964) on the basis of a tooth-bearing jaw fragment from the late Triassic Red Beds of Lesotho (then Basutoland). Ginsburg concluded, from the appearance of the teeth in the holotype, that *Fabrosaurus* was an ornithischian dinosaur related to the Liassic *Scelidosaurus*. Unfortunately the affinities of *Scelidosaurus* itself are far from clear. This large armoured dinosaur is often quoted as a fore-runner of the stegosaurs (e.g. Romer 1956); recent opinion tends, however, to confirm *Scelidosaurus* as an ankylosaur ancestor (Romer 1968).

The new materials described below considerably amplify knowledge of the *Fabrosaurus* skull and permit reconsideration of this reptile's affinities.

MATERIAL AND METHODS

Two specimens are described. These are listed below with brief notes on their preservation and contents; their original field numbers are given and will be used hereafter for reference.

Specimen B. 17. Three large blocks and numerous small pieces of matrix containing many cranial and post-cranial bones (though few are in natural articulation). At least two individuals are present—the smaller one being more complete.

[Palaeontology, Vol. 13, Part 3, 1970, pp. 414–32.]

Specimen B. 23. A well-preserved and slightly crushed skull (text-fig. 1) with parts of both mandibular rami. The snout is lacking and the teeth are poorly preserved.

These specimens were collected by Dr. K. A. Kermack and Mrs. F. Mussett during the 1963–4 expedition from University College, London, to Basutoland. Both specimens are preserved in the collection of the Zoology Department at University College, London.

Specimen B. 17 was collected from the Red Beds of the Stormberg Series on the northern flank of Likhoele Mountain, near the settlement of Mafeteng in western Lesotho, about 40 miles south-south-west of Maseru, the capital. Skull B. 23 was taken from a hillside exposure, also in the Red Beds, between Fort Hartley and Cutting Camp in south-west Lesotho, some 75 miles south of Maseru. The Red Beds are generally supposed to be of Upper Triassic age.

The bones, preserved in soft, white calcareous material, are enclosed in a tough medium-grained sandstone of bright red colour. The specimens were at first prepared by the use of acetic and formic acids (as described by Kermack 1956). It subsequently became clear that these acids, though effective, have certain disadvantages—they readily attack fossil bone, they have offensive smells and they may (if specimens are not very thoroughly washed after immersion) cause the formation of hard white efflorescences. Thus a saturated solution of sodium citrate in water was employed as an equally effective alternative. Since this solution does not attack bone as readily as formic or acetic acids the specimens were safely immersed in it for periods of up to 24 hours.

DESCRIPTION

General appearance of the skull. Specimen B. 23 is only slightly damaged and adequately demonstrates the general appearance of the *Fabrosaurus* skull (text-fig. 1). This incomplete skull has the following dimensions: maximum length, 94 mm.; maximum width (across frontals), 48 mm.; maximum height (with mandible), 40 mm. Fragments from assemblage B. 17 (text-figs. 2, 3) represent skulls of roughly similar size.

The skull is of typical archosaurian aspect—diapsid, with large circular orbits and extensive antorbital vacuities. The long and tapered snout affords the skull a triangular profile whilst the occipital surface, inclined at about 60° relative to the long skull axis, faces slightly in a dorsal direction. The small and elliptical upper temporal fenestra opens dorsally; the lateral fenestra is larger, faces laterally and is almost crescentic in outline due to the forwards extension of the quadrate.

Skull bones. To facilitate description the skull bones are considered in arbitrary groups (after Romer 1956).

(i) *Tooth-bearing bones.* The tip of the snout, formed by paired *premaxillae* (text-figs. 1, 6, 8), is laterally compressed and has a V-shaped outline in dorsal view. Each premaxilla is extended dorsally into two processes separated by the large and oval external naris. The broad pre-narial process is directed dorsally and slightly to the rear; its contact with the nasal cannot be observed—though it is likely (since the nasals are very extensive) that this process was not very tall. The long and acutely pointed post-narial process extends postero-dorsally at about 50° relative to the tooth row and is tightly sandwiched between the nasal and the maxilla on the side of the snout.

The bar-like dentigerous part of the *maxilla* (text-figs. 1–4 and 8) is about 7 mm. deep (skull B. 23) and has a flat lateral surface. The maxilla extends posteriorly to underlie the anterior ramus of the jugal—the two bones being separated by a long, straight, and oblique suture. A broad and flat process extends postero-dorsally from the front of

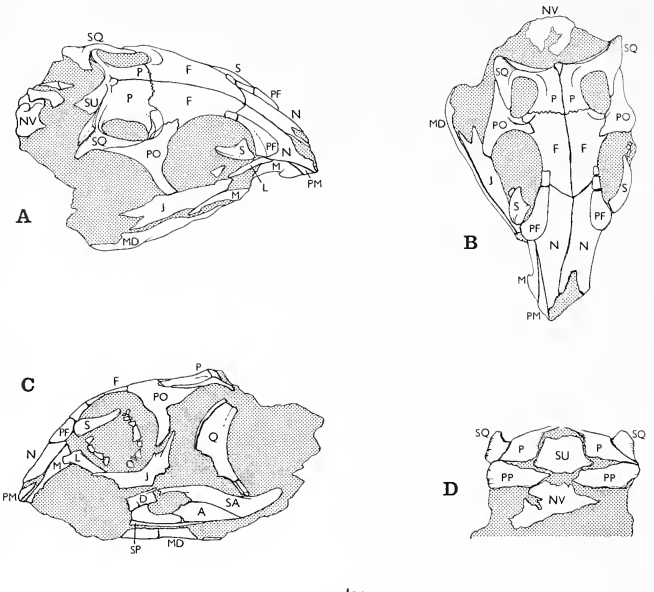

TEXT-FIG. 1. *Fabrosaurus australis*. Skull B. 23 as preserved. ×0·75. Matrix indicated by regular stippling. A, right dorso-lateral view; B, dorsal view; C, left lateral view; D, occipital view.

A, angular; D, dentary; F, frontal; J, jugal; L, lacrimal; M, maxilla; MD, mandible; N, nasal; NV, fragments of cervical vertebrae; P, parietal; PF, prefrontal; PM, premaxilla; PO, postorbital; PP, paroccipital process; Q, quadrate; S, supra-orbital; SA, surangular; SP, splenial; SQ, squamosal; SU, supra-occipital.

the maxilla so as to define the antero-ventral angle of the shallow, triangular antorbital vacuity. The thin bony wall medial to the vacuity is a simple sheet-like extension of the maxilla; this wall is gently convex in a vertical direction and is broken postero-ventrally by a small rounded notch.

(ii) *Skull roofing bones*. Paired *nasal* bones (text-figs. 1, 8) form the roof of the snout and meet in a long and straight median suture. The nasal is at least as long as the frontal and attains its maximum width (12 mm. in skull B. 23) close to the anterior tip of the

adjacent prefrontal. Anterior to the prefrontal the nasal curves down from the nearly flat skull roof to form part of the facial region. Posteriorly the nasal overlaps the frontal —the line of junction running postero-laterally from the mid-line.

Paired *frontal* bones (text-figs. 1, 8) form the skull roof between the orbits. Each frontal is roughly quadrilateral in outline, about 31 mm. long (skull B. 23) and is slightly arched in a longitudinal direction. At its postero-lateral corner the dorsal surface of the

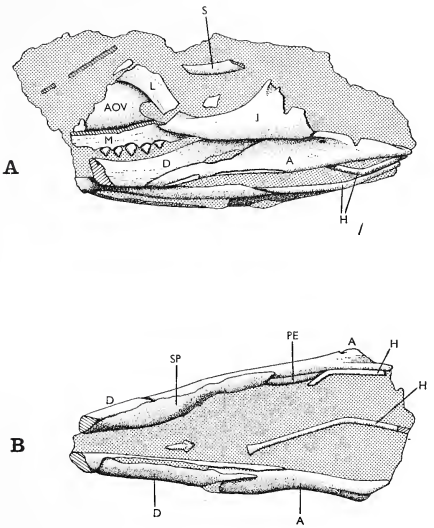

TEXT-FIG. 2. *Fabrosaurus australis*. Partial skull from assemblage B. 17. ×1. Matrix indicated by regular stippling. A, left lateral view; B, ventral view. AOV, antorbital vacuity; H, ossified first ceratobranchials; PE, pre-articular. Other letters as for text-fig. 1.

frontal bears a deeply impressed crescentic pit which defines the anterior limit of the upper temporal opening. Anterior to this pit the dorsal tip of the postorbital is set into a deep V-shaped notch in the lateral edge of the frontal. The posterior tip of the prefrontal occupies a shallow groove in the antero-lateral corner of the frontal. The thin, sharp, and arched lateral edge of the frontal forms the overhanging upper rim of the orbit.

Paired *parietals* (text-figs. 1, 8) form the broadly convex zone of skull roof between the upper temporal openings. Each parietal is firmly joined to the frontal of the same side by a sinuous transverse suture and is extended postero-laterally as a vertical sheet of bone between the occipital surface and the upper temporal opening. The lateral tip

of this expanded portion is applied to the posterior face of the squamosal. The very distinct inter-parietal suture is quite straight and is confluent with that between the frontals.

(iii) *Circumorbital bones.* The *jugal* (text-figs. 1, 2, 8) is gracefully arched to the exterior and has slender processes directed anteriorly, posteriorly, and dorsally. The anterior branch, roughly circular in cross-section, extends to the postero-ventral angle of the antorbital vacuity; its rounded dorsal edge forms the lower rim of the orbit whilst its recessed ventral margin accommodates the postero-dorsal edge of the maxilla. The

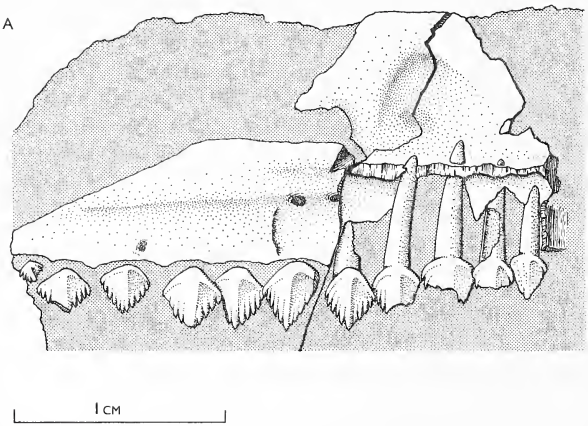

TEXT-FIG. 3. *Fabrosaurus australis.* Isolated right maxilla from assemblage B. 17. ×4. Matrix indicated by regular stippling. Lateral view.

broader posterior jugal ramus is damaged in all examples and its extent cannot be determined The tapered dorsal branch of the jugal is inclined slightly to the rear and is distinctly twisted (the lateral surface being turned to the front).

The tri-radiate *postorbital* (text-figs. 1, 8) curves over from the side of the skull on to its dorsal surface, the dorsal and ventral branches of the bone defining the postero-dorsal corner of the orbit. In this region the rim of the orbit is thickened and bears, on the medial surface, a small cavity. The flat and slender ventral branch of the post-orbital occupies a long and shallow groove on the dorsal ramus of the jugal. The shorter and broader antero-dorsal branch is set into the postero-lateral corner of the frontal above whilst the third, posterior, branch meets an anterior extension of the squamosal to form the stout horizontal bar between superior and lateral temporal openings.

The *lacrimal* (text-figs. 1, 2, 8) is a small bar of bone, some 10 mm. long, which runs anteror-dorsally on the side of the skull from the anterior tip of the jugal. Its antero-ventral edge thus defines the posterior limit of the antorbital vacuity. The lacrimal is

inclined at about 45° relative to the line of the tooth row and is broader in front (6 mm.) than behind (4 mm.).

The *prefrontal* (text-figs. 1, 8) is a long, narrow, flattened, and strap-like bone forming the margin of the skull roof from a point midway over the orbit to the area where lacrimal, nasal, and maxilla all meet above the antorbital vacuity. Left and right prefrontals are completely separated by the frontals and nasals. The narrow posterior tip of the bone is set into a notch in the antero-lateral edge of the frontal whilst the broadly rounded anterior end overlies the nasal. The thin and sharp lateral edge of the prefrontal forms the antero-dorsal rim of the orbit; anteriorly this edge is thickened and planed off to form an attachment surface for the supra-orbital.

(iv) *Bones of the cheek region.* The *squamosal* (text-figs. 1, 8) forms the lateral and posterior margins of the upper temporal opening and is extended postero-laterally to overlap the upper end of the quadrate. A tapered triangular portion runs forwards to meet the posterior ramus of the postorbital—the two bones being separated above the lateral temporal opening by a long, straight, and oblique suture. Posteriorly the squamosal turns sharply in a medial direction to form the postero-lateral corner of the skull roof. This corner is acutely pointed and is ornamented with deeply incised transverse striae. The posterior face of the squamosal is overlain by a plate-like portion of the parietal forming the dorso-lateral part of the occiput. A very slender ventral process from the squamosal is applied to the anterior edge of the quadrate. Though the only example of this process (on the left side of skull B. 23) is damaged it is clear that it extended down the front of the quadrate for at least half the height of this latter.

No *quadrato-jugal* has been recovered. Its probable form is indicated in the skull reconstruction (text-fig. 8).

A single *quadrate* is preserved (text-fig. 1). This example, on the left side of skull B. 23, is damaged antero-ventrally and has suffered slight displacement to the front. The quadrate is a latero-medially compressed plate of bone which is noticeably twisted—the lateral surface being turned to the rear at the ventral end. The thickened and buttress-like posterior margin is arched to the front; at its ventral end this buttress is transversely expanded to form a thick and roller-like condyle lying some 7 or 8 mm. below the level of the maxillary teeth. The sheet-like and slightly concave anterior part of the bone projects into the lateral temporal opening—accounting for the narrow outline of the opening. The dorsal tip of the quadrate fits tightly into a depression in the ventral surface of the squamosal.

(v) *Bones of the palate.* In the incomplete skull from assemblage B. 17 (text-figs. 2, 4) the right half of the palate is exposed in dorsal aspect. The bones displayed (pterygoid, ectopterygoid, palatine, and vomer) appear to have suffered little distortion or displacement. The palate seems to have been quite long, narrow, and moderately vaulted. A narrow inter-pterygoid vacuity is inferred whilst post-palatine fenestrae must (if present at all) have been very small.

The palatal (anterior) ramus of the tri-radiate *pterygoid* is a long, low vertical blade which runs forwards close to the mid-line. This paper-thin and sharp-edged process is 17 mm. long and nearly 3 mm. high. It is separated from the mid-line by the vomer—an arrangement which suggests that left and right palatal rami were not in contact and implies the existence of a narrow inter-pterygoid vacuity. Posteriorly the palatal ramus merges, by means of a sharp flexure, with the medial edge of the widely expanded quadrate

ramus of the pterygoid. This latter ramus, a triangular sheet of bone about a millimetre thick, presumably extended postero-laterally to meet the medial face of the quadrate in normal reptilian fashion. Anteriorly the quadrate ramus is constricted and runs into the third, transverse, ramus from the pterygoid. This transverse ramus is represented in specimen B. 17 only by a fragment of bone overlying the dorsal surface of the palatine. The dorsal surface of this constricted zone between quadrate and transverse rami bears a short and shallow longitudinal groove which doubtless accommodated a posterior extension of the ectopterygoid. The ectopterygoid is represented, in fact, by a small scale-like fragment of bone overlying the anterior end of this groove. An extremely similar arrangement is seen in a variety of reptiles—e.g. phytosaurs (Camp 1930), pelycosaurs (Romer and Price 1940), pseudosuchians (Walker 1961).

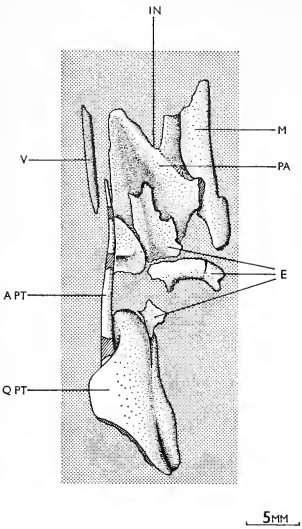

TEXT-FIG. 4. *Fabrosaurus australis*. Right half of palate in partial skull from assemblage B. 17 (see also text-fig. 2). Dorsal view, ×2. Matrix indicated by regular stippling.

APT, anterior (palatal) ramus of pterygoid; E, ectopterygoid (fragments); IN, rear margin of internal naris; M, maxilla; PA, palatine; QPT, quadrate ramus of pterygoid; V, vomer.

The *ectopterygoid* lies anterior to the pterygoid and seems to be considerably smaller than this latter (though its full extent is not clear owing to breakage). Its posterior extension on to the pterygoid is described above. An equally thin anterior extension overlies the middle of the depressed dorsal surface of the palatine. In addition the ectopterygoid is produced laterally as a short (5 mm.), stout, and curved bar which serves to brace the medial surface of the maxilla.

The *palatine* is situated anterior to the pterygoid and antero-medial to the ectopterygoid. There is no trace of any (post-palatine) vacuity between palatine and ectopterygoid. A slender antero-lateral process from the palatine is applied to the medial surface of the maxilla; medial to this the deeply embayed anterior edge of the palatine represents the rear margin of the internal naris. Medial and posterior to the internal naris the palatine forms an extensive sheet of bone, some 9 mm. wide, which is flexed into a deep trough running postero-laterally. The floor of this trough contains the thin anterior part of the ectopterygoid whilst its medial edge meets the tip of the anterior pterygoid ramus.

The *vomer* is represented (specimen B. 17) by a sheet-like fragment of bone, 12 mm. long and 5 mm. high, which lies vertically in the mid-line between the palatines.

(vi) *Bones of the occiput* (text-figs. 1, 8). The account is based upon skull B. 23. In this skull the ventral parts of the occiput are obscured by fragments of cervical vertebrae and cannot (for the present at least) be described. The occipital surface is inclined, at

about 60° relative to the long axis of the skull, so that it faces dorsally as well as posteriorly. It is quite broad (44 mm. across the squamosals) and not exceptionally high (38 mm. including quadrate).

The dorsal part of the occiput is formed, in its central region, by the median *supra-occipital*. This transversely arched bone is of quadrilateral outline, some 15 mm. high, and attains a maximum width (ventrally) of 14 mm. Since its ventral margin is damaged it is difficult to estimate how far this bone contributed to the border of the foramen magnum. The lateral edge of the supra-occipital meets the posterior face of the *parietal* —forming the dorso-lateral part of the occiput. Towards the margin of the occiput the parietal overlaps the posterior face of the *squamosal*—which curves away on to the side of the skull. The intervening suture runs ventro-laterally, roughly parallel with that between supra-occipital and parietal. The ventro-lateral corner of the supra-occipital meets the dorsal edge of the *exoccipital*, which extends laterally away from the foramen magnum as the long (14 mm.) and stout paroccipital process. The expanded lateral tip of this process is doubtless composed of the *opisthotic* bone, though there is no suture serving to separate this from the confluent exoccipital. The paroccipital process is arched very slightly to the anterior; it is directed laterally, and almost imperceptibly in a ventral direction, to terminate in a vertically expanded sheet which is applied to the posterior face of the squamosal.

(vii) *Bones of the mandible* (text-figs. 1, 2, 5, 8). A composite description is derived from all available examples. Each long and slender mandibular ramus is slightly arched to the exterior in its middle and anterior regions. The jaw has a length of about 92 mm. (estimated for skull B. 23) and is latero-medially compressed—so that cross-sections are of elliptical outline. The retroarticular portion is extended as a salient finger-like process whilst the coronoid apophysis is little more than an indistinct rounded eminence on the dorsal surface. A widely open external mandibular fenestra lies at mid-height and just in front of the coronoid process. This opening is of lenticular outline, measuring 8 mm. (maximum length) by 3 mm. (maximum height). A similar, though larger, fenestra in the medial jaw surface is located slightly anterior to the external one.

The jaw rami are joined anteriorly by means of the median *predentary*. This scoop-shaped bone has the outline, in ventral view, of a blunt arrow-head—being composed of a large median portion bearing two smaller lateral processes or 'wings'. The median portion, some 10 mm. long and 4 mm. wide, extends posteriorly between the left and right dentary bones (though it is not clear if these were completely separated).

Behind the predentary the *dentary* bone forms the anterior two-thirds of the lateral jaw surface. This lateral surface is convex in a vertical direction and is confluent ventrally with the broadly rounded inferior margin of the jaw. Posteriorly the dentary ends in a wide V-shaped notch defining the anterior limit of the external mandibular fenestra. Above the fenestra the dentary overlies the surangular; below the opening it overlaps the angular and is drawn out posteriorly as a thin and flattened process applied to the thick ventral margin of the jaw. The dentary also forms the anterior third of the medial jaw surface. This surface is generally similar to the lateral surface just described and shows no indications of any foramina adjacent to the tooth row. Posteriorly this medial dentary surface is overlain by the paper-thin anterior part of the splenial.

The *splenial* forms the ventro-medial surface of the jaw behind the dentary and is extended posteriorly as a thin tongue-like process on the ventral surface of the

retro-articular process. In the middle of the jaw ramus the splenial is widely expanded to form the greater part of the medial surface—except dorsally, where a narrow zone of the underlying dentary is exposed adjacent to the tooth row. This central region of the medial jaw surface is generally flat; posteriorly it is depressed, leading down into the large inner mandibular fenestra.

The *angular* forms the postero-ventral part of the jaw, below the surangular and behind the dentary. The lateral surface of the bone is generally flat, curving round ventrally to merge with the thick inferior margin of the jaw. Angular and surangular are separated

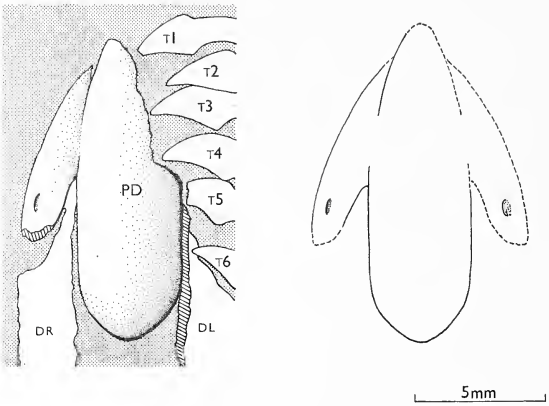

TEXT-FIG. 5. *Fabrosaurus australis*. Mandibular symphysis from assemblage B. 17. Ventral view, ×5. Matrix indicated by regular stippling, broken edges by diagonal shading.

DL, left dentary; DR, right dentary; PD, predentary; T1 to T6, left premaxillary teeth numbered from front.

by a distinct suture from the posterior angle of the external jaw fenestra. This suture runs obliquely in a postero-dorsal direction so that the angular and surangular appear to form roughly equal portions of the lateral jaw surface. Posteriorly this same suture is down-curved—so that a slender process from the angular underlies the retro-articular process (formed predominantly of the surangular).

The *surangular*, overlying the angular, forms the retro-articular process and the postero-dorsal limit of the external jaw fenestra. Since the retro-articular process is deflected medially the lateral surface of the surangular is convex from front to back. This lateral surface is demarcated from the dorsal margin of the retro-articular process by a thick and dorsally arched ridge. The long (10 mm.) and tapered retro-articular process has a bluntly rounded tip and is drawn out medially into a horizontal flange nearly 5 mm. wide. The ventral surface of this flange is gently excavated whilst its most medial tip is extended ventrally as a short and blunt projection.

In front of the retro-articular process, on the dorsal jaw surface, lies the glenoid fossa—a broad and shallow transverse groove. This region of the jaw is doubtless formed by an *articular* element, though the sutures which might define its limits cannot be discerned. Medial to the angular lies the *pre-articular* bone; little may be said of this apart from the fact that it seems to be of rather limited anterior extent.

(viii) *Accessory skull elements.* The partial skull from assemblage B. 17 (text-fig. 2) has a pair of slender rod-like bones preserved between the mandibles. That of the right side lacks only the posterior tip and has a length of 28 mm.; it is marked with fine longitudinal striae and has a diameter of 1·5 mm. Its anterior end is slightly inflated (to a diameter of 2·5 mm.) whilst the bone is sharply flexed in the middle—the ends diverging at about 150°. These curved bony rods are the ossified *first ceratobranchials*—which are, as Romer (1956) points out, the parts of the hyoid complex most frequently encountered in fossil reptiles.

The right orbit of skull B. 23 (text-fig. 1) contains a single undamaged *sclerotic plate.* This is paper-thin, roughly triangular (narrowest anteriorly) and is bent so that its lateral surface is concave from dorsal to ventral edges. It has a length of 4 mm. and a maximum width of 2·5 mm. The left orbit of the same skull contains fourteen similar plates (or parts of plates) which are disposed in overlapping arrangement to form a circle (mean diameter 12 mm.) ventral to the supra-orbital bone.

Each orbit of skull B. 23 also contains a long (20 mm.) and rod-like *supra-orbital* bone which is arched to the exterior. Anteriorly the bone is truncated by a facet for attachment to that part of the orbital rim formed by the thickened lateral edge of the prefrontal. The right supra-orbital has been displaced medially; that within the left orbit shows more clearly the natural relationships of the bone.

Dentition

The teeth are described from specimen B. 17 alone. Skull B. 23 contains teeth which are unmistakably those of *Fabrosaurus*, but these are so poorly preserved that they yield little useful information. In the following descriptions the terms used in dentistry will be employed. The tooth surface facing outwards, towards the lips, is termed *buccal*; the surface directed inwards, towards the tongue, is *lingual.* That surface facing the jaw symphysis is *mesial* whilst the surface facing the jaw articulation is *distal.* The tip of the root is defined as the *apex* of the tooth whilst the other, masticatory, end of the tooth is termed *occlusal.*

Premaxillary teeth (text-figs. 5, 6, 8). The left premaxilla from assemblage B. 17 bears six teeth (text-fig. 6), apparently the full complement. The most posterior tooth in this example displays a long and narrow root of circular cross-section and illustrates the thecodont mode of tooth implantation. Each crown appears in buccal profile as a tall (3·5 mm.) and slightly rounded triangle where the acute occlusal tip is slightly recurved. The last two premaxillary crowns are shorter than those in front and foreshadow the squat triangular crowns in the maxilla. At the alveolar margin the crown is distinctly inflated to the exterior and attains a maximum mesio-distal width of nearly 2 mm. The rest of the transversely convex buccal surface is perfectly smooth (save for an extremely faint vertical ridge near the occlusal end).

The smooth and convex lingual surface is marked, near the distal edge, with a distinct vertical furrow. The distal edge of the crown is considerably thinner and sharper than

the mesial edge. The fifth premaxillary crown (from the front) has its distal edge ornamented with minute denticles; in the last (6th) crown both mesial and distal edges are finely denticulate. These posterior teeth thus form a transition to the obviously denticulate maxillary teeth.

Maxillary teeth (text-figs. 2, 3, 7, 8). The best-preserved example of the maxilla (text-fig. 3) bears eleven teeth—so that their original number might be estimated at thirteen

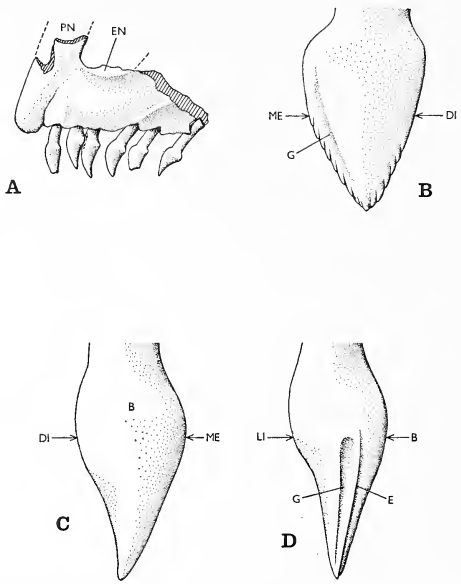

TEXT-FIG. 6. *Fabrosaurus australis*. The premaxilla and its teeth. A, Left premaxilla from assemblage B. 17. Lateral view ×2·5. EN, inflected ventral margin of external naris; PN, pre-narial ramus. B, Last (6th) crown in left premaxilla. Buccal view, ×10. DI, distal edge; G, furrow; ME, mesial edge. C, D, Buccal and distal views of an anterior crown from the right premaxilla. Both ×10. B, buccal surface; E, sharp distal edge; LI, lingual surface. Other letters as above.

or fourteen. In buccal (or lingual) profile each crown has the outline of a low and symmetrical triangle where the occlusal tip is formed by the intersection of slanting mesial and distal edges. The largest crowns, in the middle of the tooth row, are about 3 mm. tall and have similar mesio-distal widths; the smallest crowns, 1–1·5 mm. tall, are situated at the rear of the maxilla and are perfect replicas of the larger ones.

Each crown is compressed in a bucco-lingual direction and has its inclined mesial and distal edges ornamented with very characteristic denticles. These short and blunt denticles are all parallel and none exhibits any curvature or 'hooking' at its tip. The

median denticle is similar to those flanking it and is not appreciably enlarged; there are about seven denticles to each side (mesial and distal) of the median one. The denticles are all of similar size—though locally a very small 'accessory' denticle may be intercalated between two otherwise normal ones.

The smooth and transversely convex buccal crown surface is strongly inflated close to the junction with the root; ill-defined transverse ridges link this swollen area with the most mesial and distal of the marginal denticles. The lingual surface is noticeably flatter than the buccal surface and bears a very faint median ridge. In mesial or distal

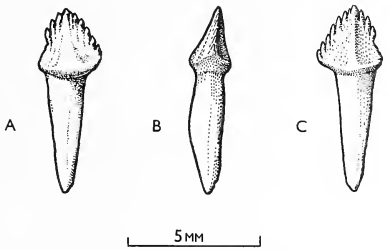

TEXT-FIG. 7. *Fabrosaurus australis*. Cheek tooth from assemblage B. 17. A, buccal view; B, mesial or distal view; C, lingual view. All ×5.

view (text-fig. 7) it may be seen that the whole crown is slightly deflected in a lingual direction and that there is a weak constriction where the crown joins the narrower root.

Dentary teeth. These are identical to the maxillary teeth. They are of equivalent number and exhibit precisely comparable marginal denticles.

Arrangement of the teeth. Premaxillary, maxillary, and dentary teeth all have their crowns completely enamelled and are all disposed in simple marginal rows. Where the dentigerous bones are broken transversely small replacement teeth may be observed close to the lingual sides of the functional teeth.

Teeth extend right to the front of the premaxilla whilst the predentary is toothless. It may also be observed that the teeth in any jaw bone alternate both in size and in situation. The smaller crowns are regularly intercalated between larger ones (which are also located slightly nearer the lateral margin of the jaw).

The *Fabrosaurus* dentition is heterodont—the teeth in the premaxilla differing radically in appearance from the cheek teeth (i.e. those in maxilla and dentary). This change in form between the premaxillary and maxillary teeth is not abrupt but is marked by the appearance, at the rear of the premaxilla, of transitional crowns which are of intermediate shape and bear weakly developed marginal denticles.

DISCUSSION

The systematic position of Fabrosaurus

The materials described above may safely be referred to the genus *Fabrosaurus* since the teeth of this reptile are highly distinctive and are unlikely to be mistaken for those

of coeval ornithischians (or, for that matter, for those of Triassic saurischians). Ginsburg (1964) inferred ornithischian affinities for *Fabrosaurus* on the evidence of the cheek teeth alone. The identification (above) of a diagnostic predentary bone at the mandibular symphysis fully substantiates the concept of *Fabrosaurus* as an ornithischian dinosaur.

The next matter is to assign *Fabrosaurus* to a particular suborder (and, subsequently, to a family) within the Ornithischia. On the basis of dental similarities Ginsburg suggested that *Fabrosaurus* might be allied to the Liassic *Scelidosaurus*. There are, indeed, basic resemblances between the teeth in these two animals; in both cases the completely enamelled crown is compressed in a bucco-lingual direction and possesses an angular and denticulate occlusal margin formed by the intersection of inclined mesial and distal edges. Teeth conforming to this general description are, however, encountered throughout the order Ornithischia and cannot be taken as diagnostic of particular suborders or families. Such teeth are seen, for example, in ornithopods (*Hypsilophodon*), in stegosaurs (*Stegosaurus*), in ceratopsians (*Triceratops*), and in ankylosaurs (*Edmontonia*). These dental characters, though suggestive of ornithischian affinities for *Fabrosaurus*, do not provide sound evidence of any immediate relationship with *Scelidosaurus*. Further, there are numerous minor distinctions between the teeth in these two animals. The blade-like *Scelidosaurus* tooth is much taller than that in *Fabrosaurus* and tends to a distinct asymmetry; the marginal denticles of the *Scelidosaurus* tooth are much more variable in size, are distinctly 'hooked' at their tips, and are arranged in a divergent (rather than parallel) pattern. These differences are, however, of no real use in any attempt to assign the two animals to specific subordinal groups—a direct consequence of the basic conservatism of tooth structure within the Ornithischia.

Amongst ornithischian dinosaurs the skull of *Fabrosaurus* resembles most closely that of the Lower Cretaceous *Hypsilophodon* (as figured by Galton 1967). The pronounced similarities with *Hypsilophodon* indicate that *Fabrosaurus* should be placed alongside this former genus in the family Hypsilophodontidae of the suborder Ornithopoda. *Fabrosaurus* falls naturally into this category (reserved for ornithopods of primitive aspect) when one considers that certain of its cranial features (e.g. the toothed premaxilla, the inter-parietal suture) are decidedly atypical of ornithischian dinosaurs and may best be matched in the thecodont reptiles—putative ancestors of the Ornithischia.

Though the skulls of *Fabrosaurus* and *Hypsilophodon* are essentially similar in construction there are several minor distinctions. The post-narial process of the *Hypsilophodon* premaxilla separates the nasal from the maxilla on the side of the snout; in *Fabrosaurus*, in contrast, the maxilla is in contact with the nasal for a short distance in front of the orbit. Similar contact between maxilla and nasal is seen, incidentally, in thecodonts such as *Euparkeria* and *Sphenosuchus*.

The *Fabrosaurus* maxilla is distinguished from that of *Hypsilophodon* by its shallowness and by its lack of any longitudinal recess above the tooth row. The large and widely open antorbital vacuity is triangular in *Fabrosaurus*, sub-circular in *Hypsilophodon*. The *Fabrosaurus* lacrimal is straighter and is not arched over the antorbital vacuity.

The upper temporal openings of the *Fabrosaurus* skull are separated by a broad and flat zone of skull roof; in *Hypsilophodon*, and in most other ornithopods, there is only a very narrow zone between these skull openings. The *Fabrosaurus* parietals are divided by a distinct median suture. This very unusual feature, which cannot be matched in *Hypsilophodon* (where the parietals are fused in normal ornithischian fashion), is seen

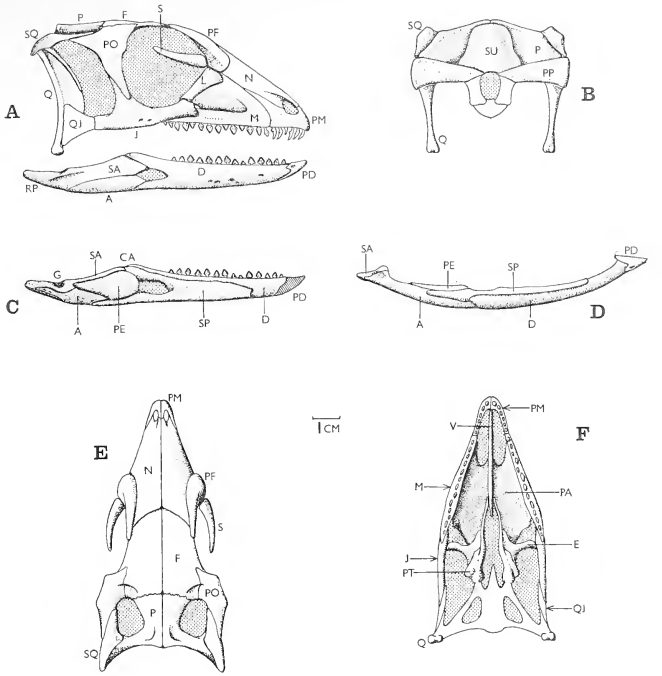

TEXT-FIG. 8. *Fabrosaurus australis*. Reconstruction of skull. All figures ×0·5. A, right lateral view of whole skull. B, occipital view. C, medial view of left mandible. D, ventral view of left mandible. E, dorsal view. F, palatal view.

Lettering as for text-fig. 1, except for: CA, coronoid apophysis; E, ectopterygoid; G, glenoid fossa; PA, palatine; PD, predentary; PE, pre-articular; PT, pterygoid; QJ, quadrato-jugal; RP, retro-articular process; V, vomer.

Following parts are not known and are shown in generalized fashion—quadrato-jugal, bones around foramen magnum, prearticular, ventral surface of brain-case.

also in *Euparkeria* and, more unexpectedly, in *Protoceratops* (Brown and Schlaikjer 1940).

The *Fabrosaurus* mandible is generally similar to that of *Hypsilophodon* though the retro-articular portion is rather more prominent and the coronoid eminence is distinctly less well developed.

The 6 teeth in the *Fabrosaurus* premaxilla extend to the front of the snout; *Hypsilophodon* has 5 premaxillary teeth (Galton 1967) and these are preceded by a wide

edentulous space. The cheek teeth of *Hypsilophodon* (numbering 10 or 11 in maxilla or dentary) are distinguished from those of *Fabrosaurus* (numbering 13 or 14) by their greater height, their prominent surface ridging and the very marked variation in size of their marginal denticles.

Ornithischian origins

The presence of ornithischians in late Triassic sediments certainly suggests that the origins of the group are to be sought at some considerably earlier date. This concept of

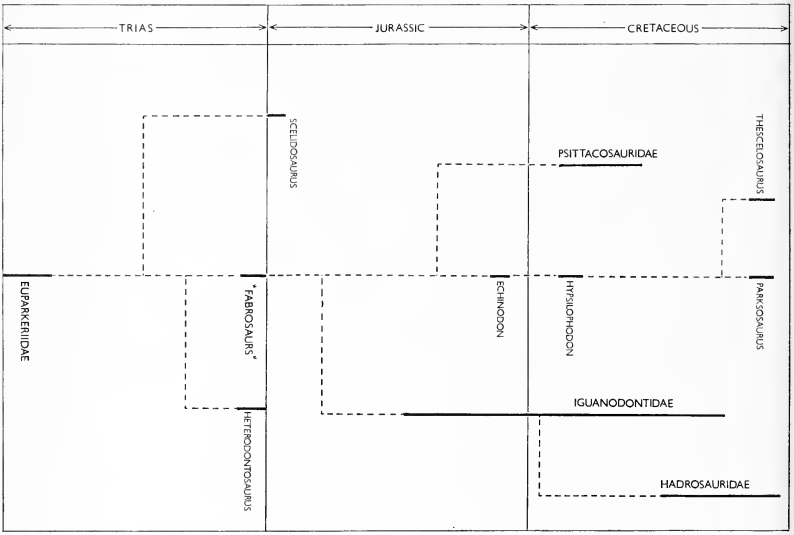

TEXT-FIG. 9. Suggested phylogeny for the Ornithopoda. The 'FABROSAURS' (*Fabrosaurus*, *Tatisaurus*, *Pisanosaurus*) are referred to the family Hypsilophodontidae together with *Heterodontosaurus*, *Echinodon*, *Hypsilophodon*, *Parksosaurus*, and *Thescelosaurus*.

a very early start to ornithischian history, whilst unsupported by fossil evidence, is reinforced simply by the geographic and structural diversity of the known Triassic ornithischians—*Fabrosaurus*, *Geranosaurus* (Broom 1911), and *Heterodontosaurus* (Crompton and Charig 1962) from southern Africa; *Tatisaurus* (Simmons 1965) from China; *Pisanosaurus* (Casamiquela 1967) from South America.

The skulls of *Geranosaurus*, *Pisanosaurus*, and *Tatisaurus* are known only from fragments; the better-known *Heterodontosaurus* skull has a remarkably specialized dentition including 'canine' teeth. Thus it is natural to turn to the relatively well-known and unspecialized *Fabrosaurus* skull in the search for persistent primitive features which

might be indicative of ornithischian ancestry. There are, in fact, only a few characters in *Fabrosaurus* which are noticeably atypical of later ornithischians and which might justifiably be termed primitive. Several cranial features, including the widely open antorbital vacuity, the large external mandibular fenestra and the weakly developed coronoid process, may be closely paralleled in a wide range of thecodont reptiles (e.g. *Ornithosuchus*, *Euparkeria*, *Stagonolepis*). It is immediately evident that such features are of no practical use in any attempt to locate the possible ancestors of the Ornithischia —simply because of their very frequent occurrence in diverse members of the Thecodontia. Similarly the inter-parietal suture of the *Fabrosaurus* skull is matched in numerous thecodonts (*Euparkeria*, *Ornithosuchus*, *Machaeroprosopus*, etc.) and gives no precise clue as to ornithischian origins.

Ewer (1965) supports the general contention advanced by Broom (1913) that the thecodont family Euparkeriidae probably includes the ancestors of all the major lineages of later archosaurs—including the Ornithischia. Whilst saurischian dinosaurs may be derived from hypothetical *Euparkeria*-like ancestors with no very excessive stretching of the imagination it is considerably more difficult to derive ornithischians from the same source—mainly because of irreconcilable differences in ankle and pelvis structure (see Ewer 1965). Whilst it is reasonable to assume that the ancestry of the Ornithischia extends back *ultimately* into the Euparkeriidae this still does not clarify the problem of ornithischian history between Lower and Upper Trias. The members of the Euparkeriidae exhibit no obvious trend towards the ornithischian state of organization whilst the earliest known ornithischians, such as *Fabrosaurus*, present very few primitive characters. Due largely to inadequacies of information concerning Middle Triassic archosaur faunas there is a very considerable hiatus between the Euparkeriidae and the earliest ornithischian dinosaurs. There are, in consequence, no apparent 'intermediates' between the Lower Triassic *Euparkeria* and the Upper Triassic *Fabrosaurus*.

The outlines of ornithopod phylogeny

It is probable that all of the varied ornithischian types of the later Mesozoic have arisen from ancestors which are to be grouped, ultimately at least, within the Hypsilophodontidae. This scheme is quite reasonable since any later ornithischians (most particularly the iguanodonts and the hadrosaurs) may be derived from hypothetical *Hypsilophodon*-like ancestors without any great difficulty. This much, at least, of ornithischian history is fairly clear and has been adequately expressed by earlier authors (e.g. Romer 1945).

Pronounced cranial similarities between *Fabrosaurus* and *Hypsilophodon* have already been noted. *Fabrosaurus*, rather than *Hypsilophodon*, would seem to fulfil the requirements of a genuine ornithischian 'archetype'—simply by virtue of its much earlier stratigraphic location. The basic resemblances between these two dinosaurs also indicate that they are linked in an evolutionary sense—i.e. *Hypsilophodon* appears to be a fairly direct descendant of *Fabrosaurus*. *Echinodon*, a diminutive reptile from the British Purbeck, constitutes a very satisfactory intermediate between *Fabrosaurus* and *Hypsilophodon*, both in relative stratigraphic position and in morphology. *Echinodon* was originally described as a lizard (Owen 1861); it shows, however, thecodont implantation of the teeth (not acrodont or pleurodont as in true lizards), cheek teeth of ornithischian aspect,

and the 'special foramina' described by Edmund (1957) as characteristic of ornithischian dinosaurs. The premaxillary teeth of *Echinodon* point to hypsilophodont affinities.

These three dinosaurs (*Fabrosaurus*, *Echinodon*, *Hypsilophodon*) represent a hypsilophodont lineage persisting from the late Trias to the Lower Cretaceous. *Parksosaurus*, from the North American end-Cretaceous, appears to be the latest known representative of this lineage. These hypsilophodonts retain primitive features (e.g. the premaxillary teeth) which are not encountered in other ornithischians and which demonstrate the need for coherence of these forms in any evolutionary scheme. This same lineage is shown, in consequence, at the core of the 'evolutionary tree' of the ornithopods (text-fig. 9).

Heterodontosaurus, with its peculiarly specialized dentition, represents the earliest evolutionary divergence from the basic hypsilophodont stock. Since both *Fabrosaurus* and *Heterodontosaurus* are referred to the family Hypsilophodontidae it is probable that these two shared a common ancestry at some date earlier in the Trias, implying, in turn, that ornithischian origins were monophyletic. This latter inference is strengthened by the essential homogeneity of structure throughout the Ornithischia.

Tatisaurus and *Pisanosaurus* appear to have unspecialized dentitions and may be regarded as fairly close relatives of *Fabrosaurus*. The great geographic range of this 'fabrosaur' group points to some pre-Upper Triassic episode of migrations and dispersal. Since most known Triassic ornithischians come from southern Africa the centre of this hypsilophodont dispersal might reasonably be expected to occur in this region. This impression of a centre of origin might, however, merely reflect former intensity of interest, and of collecting, in the African Trias. At any rate the 'fabrosaurs' appear to have been much more adaptable and successful than *Heterodontosaurus* and the (perhaps) allied *Geranosaurus*, characteristics that one would naturally anticipate in the 'root-stock' of the ornithischian dinosaurs. *Heterodontosaurus* seems, in contrast, to have been a very specialized and localized (African only) off-shoot of the basic hypsilophodont lineage. Whilst the 'fabrosaurs' successfully faced the environmental changes concomitant with the close of the Triassic period, *Heterodontosaurus* did not, presumably because it was adapted for a very specific mode of life. There are no apparent post-Triassic derivatives of *Heterodontosaurus*.

The first armoured and quadrupedal ornithischians, exemplified by *Scelidosaurus*, appear at the beginning of the Jurassic. The disappearance at the end of the Trias of armoured, quadrupedal, and herbivorous pseudosuchians such as the aetosaurs (Walker 1961) might, in fact, be explained in terms of competition from similarly adapted ornithischians. The derivatives of *Scelidosaurus*, if there be any, cannot be determined at present.

At some date early in the Jurassic the *Fabrosaurus–Hypsilophodon* line of hypsilophodonts gave rise to the larger and more specialized iguanodonts. Known iguanodont remains extend from the Middle Jurassic (*Cryptodraco*) into the late Cretaceous (*Craspedodon*) and it is probable that there are several distinct evolutionary lines within this family itself—though these may not be discussed here. The arrangement shown (text-fig. 9) is in direct contrast to the scheme proposed by Colbert (1951)—where it is suggested that *Hypsilophodon* might have arisen from a 'camptosaurid stem'.

Ostrom (1961) has suggested that the hadrosaurs might have been derived from *Camptosaurus*-like iguanodonts by way of intermediates like the poorly known *Claosaurus*. This scheme is utilized here (see text-fig. 9).

Towards the close of the Jurassic period the basic hypsilophodont stock, exemplified at this point in time by *Echinodon*, gave rise to several small ornithopod types which are of decidedly primitive aspect (e.g. *Laosaurus*, *Nanosaurus*). At roughly the same time a number of diminutive forms (*Psittacosaurus*, *Protiguanodon*) emerged from a (presumably) similar source to become highly suggestive of ceratopsian ancestry.

The basic hypsilophodont stock persisted to the very end of the Cretaceous period with the appearance of *Parksosaurus*. The last divergence from this lineage, just before the extinction of dinosaurs in general at the end-Cretaceous, is represented by *Thescelosaurus*. *Thescelosaurus* possesses a femur which is longer than the tibia (the reverse being true in the otherwise comparable *Parksosaurus*); this feature suggests that *Thescelosaurus* might have filled an ecological niche similar to that previously exploited by the iguanodonts (which had a similar tibio-femoral ratio). If this is so it constitutes evidence that some form of iterative evolution (involving repeated divergences from a main stem towards a single goal) was an operative factor in ornithopod history.

It may be concluded that *Fabrosaurus* and its allies represent the earliest known portion of a hypsilophodont lineage which extended through the greater part of the Mesozoic era and which gave rise, even if indirectly, to well known and very specialized ornithischian groups—iguanodonts, hadrosaurs, ceratopsians, and the like. The 'fabrosaurs' appear, in fact, to fulfil the requirements of genuine ornithischian 'archetypes'. *Heterodontosaurus* seems, in contrast, to represent an early and rather specialized hypsilophodont divergence which failed to survive the close of the Triassic period.

Acknowledgements. My particular thanks go to Dr. K. A. Kermack, of the Department of Zoology, University College London, for allowing me to work upon the unique specimens described above. I am also indebted to Dr. A. J. Charig, of the British Museum, Natural History, for permitting me to examine specimens in his care (*Heterodontosaurus*, *Echinodon*, and *Scelidosaurus*). Miss S. J. Plummer has kindly read and criticized the manuscript. This work was made possible through provision of a research grant from the Natural Environment Research Council.

REFERENCES

BROOM, R. 1911. On the dinosaurs of the Stormberg, South Africa. *Ann. S. Afr. Mus.* **7**, 291–308.

—— 1913. On the South African pseudosuchian *Euparkeria* and allied genera. *Proc. Zool. Soc. Lond.* 1913, 619–33.

BROWN, B. and SCHLAIKJER, E. M. 1940. The structure and relationships of *Protoceratops*. *Ann. N.Y. Acad. Sci.* **40**, 133–266.

CAMP, C. L. 1930. A study of the phytosaurs. *Mem. Univ. Calif.* **10**, 1–161.

CASAMIQUELA, R. M. 1967. Un nuevo dinosaurio ornitisquio triasico (*Pisanosaurus mertii*; Ornithopoda) de la formacion Ischigualasto, Argentina. *Ameghiniana, Rev. Asoc. Pal. Argent.* **4**, 47–64.

COLBERT, E. H. 1951. Environment and adaptations of certain dinosaurs. *Biol. Rev.* **26**, 265–84.

CROMPTON, A. W. and CHARIG, A. J. 1962. A new Ornithischian from the Upper Triassic of South Africa. *Nature, Lond.* **196**, 1074–7.

EDMUND, A. G. 1957. On the special foramina in the jaws of many Ornithischian dinosaurs. *Royal Ontario Mus. Div. Zool. Pal. Contr.* **48**, 1–14.

EWER, R. F. 1965. The anatomy of the Thecodont reptile *Euparkeria capensis* Broom. *Phil. Trans. R. Soc. Lond.*, **B248**, 379–435.

GALTON, P. M. 1967. On the anatomy of the ornithischian dinosaur *Hypsilophodon foxii*. Ph.D. thesis, King's College, University of London.

GINSBURG, L. 1964. Découverte d'un Scélidosaurien (Dinosaure ornithischien) dans le Trias supérieur du Basutoland. *C. r. hebd. Séanc. Acad. Sci., Paris*, **258**, 2366–8.

KERMACK, K. A. 1956. Tooth replacement in mammal-like reptiles of the suborders Gorgonopsia and Therocephalia. *Phil. Trans. R. Soc.* **B240,** 95–133.

OSTROM, J. H. 1961. Cranial morphology of the hadrosaurian dinosaurs of North America. *Bull. Am. Mus. nat. Hist.* **122,** 35–196.

OWEN, R. 1861. On the Reptilia of the Wealden and Purbeck Formations. Part V. *Palaeontogr. Soc.* [Monogr.].

ROMER, A. S. 1945. *Vertebrate paleontology*, 2nd ed. Chicago, 687 pp.

—— 1956. *Osteology of the reptiles.* Chicago, 772 pp.

—— 1968. *Notes and comments on vertebrate paleontology.* Chicago, 304 pp.

—— and PRICE, L. W. 1940. Review of the Pelycosauria. *Spec. Pap. Geol. soc. Amer.* **28.**

SIMMONS, D. J. 1965. The non-Therapsid reptiles of the Lufeng Basin, Yunnan, China. *Fieldiana, Geol.* **15,** 1–93.

WALKER, A. D. 1961. Triassic reptiles from the Elgin area: *Stagonolepis*, *Dasygnathus* and their allies. *Phil. Trans. R. Soc.* **B244,** 103–204.

A RHAETO-LIASSIC FLORA FROM AIREL, NORTHERN FRANCE

by M. MUIR *and* J. H. A. van KONIJNENBURG-van CITTERT

ABSTRACT. An assemblage of fossil plants from the Upper Triassic/Liassic of Airel (Manche), Northern France, is recorded, and two new species, *Hirmerella airelensis* sp. nov. and *Classopollis harrisii* sp. nov., are described and figured. *In situ* and dispersed pollen is compared and a lycopod megaspore and microspore described. The assemblage is compared with others from France and Wales.

THE plant material described in this paper was recovered from some sandy, light-grey clay collected from Airel in the Carentan basin, near Caen, France. Various suggestions have been made about the age of the deposit (Larsonneur 1962, 1963) ranging from Norian to Hettangian. The assemblage is limited, but is generally comparable with the assemblages described by Levet-Carette (1964) and Briche, Danzé-Corsin, and Laveine (1963) from deposits in the neighbourhood of the Boulonnais. Their material came from fissure-fillings in the Carboniferous, while our material appears to be lacustrine, the plants being associated with ostracods and charophytes (Larsonneur 1963).

The macrofossils are in a remarkably good state of preservation; they are almost uncompressed, and the spiral leaf arrangement is evident. Leafy shoots, fragments of leaves, female cone-scales, male cone axes, fragments of microsporophylls, and separate pollen masses were recovered and are here described. Dispersed megaspores, microspores, and pollen from the clay were also examined.

Methods of study. Selected macrofossils were treated by maceration in Schulze's solution followed by dilute ammonia. The male cone fragments were recovered by bulk maceration of the clay, which was disintegrated in water, and then treated with Schulze's solution. Specimens were then mounted in glycerine, and examined and photographed with a Leitz Ortholux microscope. Some of the macrofossil cuticles, pollen masses, and megaspores (both macerated and unmacerated) were mounted on Durofix, coated with gold/palladium and examined on a Cambridge Instrument Company 'Stereoscan' scanning electron microscope.

The microfossils were recovered by a standard method, i.e. disintegration of the clay in H_2O_2, followed by HCl, HF, and HCl treatment. The residue was then macerated in concentrated nitric acid and washed in distilled water. The microspores were then mounted in glycerine jelly and examined and photographed in a Zeiss photomicroscope.

SYSTEMATIC DESCRIPTIONS

Genus HIRMERELLA Hoerhammer emend. Jung

Type species. *H.* (*Cheirolepis*) *muensteri* (Hoerhammer) Jung.

Hirmerella airelensis sp. nov.

Plate 78, figs. 1–5; Plate 79, fig. 2; Plate 80, fig. 1; text-fig. 1A

[Palaeontology, Vol. 13, Part 3, 1970, pp. 433–42, pl. 78–80.]

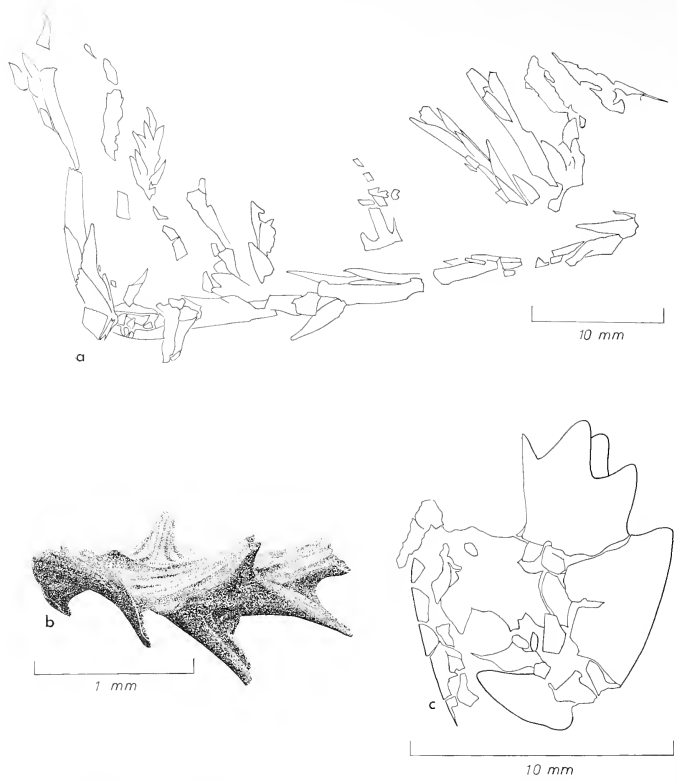

TEXT-FIG. 1. *Hirmerella airelensis* sp. nov. *a*, Holotype; ×2·5. *b*, Isolated male cone axis; ×30. *c*, Partly broken female cone scale, ×5.

Holotype. Specimen 2845: division of Palaeobotany and Pollen-morphology, Museum and Herbarium of the State University of Utrecht.

Diagnosis. Leaves spirally arranged; rather variable; free part 2–5 mm. long, 2–4 mm. wide, leaf-base cushion 2–3 mm. long, 2–4 mm. wide. Cuticle from 1 to 8 μ thick, usually about 4–6 μ; margin scarious, especially near the apex. Upper cuticle: stomata mostly arranged in short longitudinal rows, but some irregularly scattered; rows separated laterally by 3–10 epidermal cells in thin cuticles, 2–6 in thick ones; stomata within rows separated longitudinally by 2–10 epidermal cells in thin cuticles, 1–6 in

thick ones; guard cells sunken, not usually visible; 4–6 subsidiary cells forming a thick, raised ring around the guard cells, often striated and, especially in the thick cuticles, papillate; encircling cells present but not clear; normal epidermal cells in rows, papillate, varying from rectangular with thin walls, to almost square with thick walls; thick walls often pitted. Lower cuticle similar to the upper, but with more stomata, and with few papillae on the epidermal cells.

Description. The material consists of a large number of well-preserved small shoots, usually not more than 2 cm. long. Most of the material is uncompressed and shows the spiral arrangement of the leaves very well.

The leaves vary considerably in size and proportions, from rather long narrow ones, with a large free part, and a rather thin cuticle, to broader ones with a short free part and a rather thick cuticle. All kinds of intermediates between these two extremes have been found. We believe that the long narrow leaves are immature, whilst the broader ones are older, although they may represent sun and shade leaves. It is known that the young and old leaves of recent conifers commonly differ considerably in cuticle thickness and size of the epidermal cells (Napp-Zinn 1966). We very often find *Classopollis harrisii* sp. nov. pollen grains sticking to the thicker cuticles, which reinforces our opinion that they are older leaves.

Discussion and comparison. These shoots can certainly be placed within the genus *Hirmerella*, but they differ in some respects from the type species *Hirmerella muensteri.*

In *H. muensteri*, the cells of the upper cuticle do not have papillae, while in our species, these are prominent. There are more, and longer, rows of stomata, and the stomata are more closely crowded together within rows in *H. muensteri* than *H. airelensis* (Plate 78, fig. 6); the stomata appear to be indistinguishable in the two species.

The presence of male and female cone-scales and of pollen grains which resemble those of *H. nuensteri* confirm the placing of the new species within the genus *Hirmerella.*

This material resembles very closely that described by Lewarne and Pallot (1957) and Harris (1957) from the Rhaeto-Liassic of Cnap Twt, South Wales, although these authors did not mention papillae on the upper cuticle, but thickenings. Re-examination of the material shows the 'central thickenings' to be papillae, and the stomata are rather widely spaced in short rows. Although the Welsh material agrees more in morphology with our species, it was referred to *Cheirolepis* (now *Hirmerella*) *muensteri.* Lemoigne (1967) has described some leafy shoots from Saint Fromond (Manche) in the same region of the Carentan Basin as Airel. Although they were referred to the 'Cupressales', in their over-all morphology and cuticular detail, they appear to be identical with our material. The stomata are very similar, and papillae are present as well. There seems to be no basis for their assignation to the 'Cupressales', and we believe that they should be placed in *Hirmerella airelensis* sp. nov.

Our material is closely comparable with that described by Chaloner (1962) from the Henfield borehole. He found that the isolated leaves are similar in all respects with those from Cnap Twt described by Lewarne and Pallot (1957) and Harris (1957). He mentions the papillae on the epidermal cells, but refers his material to *Cheirolepis muensteri.* We believe that these leaves, although fragmentary could be referred to *Hirmerella airelensis.*

Wood (1961) describes *Cheirolepis muensteri* from Lyme Regis, Dorset, England. While his material is similar to ours, it differs in having very thick cuticles (15–20 μ) and not showing papillae on the walls of the epidermal cells.

Isolated female cone-scales. About ten isolated female cone-scales were found (text-fig. 1c). Among them are a few isolated bract scales which yield good cuticles. The cuticles are like those of *Hirmerella muensteri* as described by Hirmer and Hoerhammer (1934) except that they show papillae on the upper (outer) sides of the cells, which are the same as those occurring on the vegetative shoots.

Some ovuliferous scales were found too, showing a clear five-fold division (see text-fig. 1c). In one case, a six-fold division was observed, the middle appendage being split. No complete seeds were discovered, but one megaspore membrane (7 mm. long) was found in a bulk maceration.

The female cone-scales agree closely with those of *Hirmerella muensteri* except for the papillae on the cuticle of the bract scale, and demonstrate that this new fossil conifer must be placed within the genus *Hirmerella*. Harris (1957) stated that he had found female cone-scales like those of *Hirmerella muensteri*, but he does not give any description or drawing. There are no preparations of female cone-scales in his material kept at

---

EXPLANATION OF PLATE 78

All transmitted light photographs of macerated cuticles.

Figs. 1–5. *Hirmerella airelensis* sp. nov. 1, Upper cuticle, showing papillae in the cells; ×250. 2, Thin lower cuticle, showing stomata; ×250. 3, Stoma, showing striations on the subsidiary cells; ×750. 4, Detail of epidermal cells showing pitting of walls; ×750. 5, Cell outlines and stomatal arrangement at edge of upper and lower cuticle; ×250.

Fig. 6. *Hirmerella muensteri* (Schenk) Jung. Cell outlines and arrangement of stomata, for comparison with fig. 5; note absence of papillae; ×250.

EXPLANATION OF PLATE 79

Figs. 1, 3. Stereoscan photographs of pollen mass of *Classopollis harrisii* sp. nov. 1, General morphology of the whole mass; ×300. 3, Morphology of single grain (centre), with series of pustules on surface representing collapse of outer surface of wall over the coarse bacula; ×1500.

Fig. 2. Stereoscan photograph of edge of cuticle of *Hirmerella airelensis* sp. nov., showing the papillae, and three stomata arranged in a row; ×250.

Fig. 4. Pollen mass of *Classopollis harrisii* sp. nov. showing an immature grain with a thin wall and tetrad mark; ×1000.

Figs. 5–8. *Classopollis harrisii* sp. nov.; ×1000. 5. Very immature grain showing prominent triradiate mark, and weakly developed wall structure. 6, Smooth inner body, isolated by pressing the cover slip. 7, Co-type of dispersed pollen species, showing all general features. 8, Holotype of dispersed pollen species, showing coarse baculae clearly.

EXPLANATION OF PLATE 80

Fig. 1. *Hirmerella airelensis* sp. nov., slightly compressed shoot showing leaf arrangement; Stereoscan photograph, ×25.

Fig. 2–5. *Bacutriletes tylotus* (Harris) Potonié. 2, Stereoscan photograph showing the general morphology and triradiate mark; ×200. 3, Transmitted light photograph of B.M. specimen V 32623 of Lewarne and Pallot, for comparison with fig. 2; ×200. 4, Detail of fig. 2; ×400. 5, Detail of fig. 3; ×400.

Figs. 6, 7. *Heliosporites reissingeri* (Harris) Chaloner 1969. 6, Detail of spine and surface; ×1000. 7, whole grain; ×600.

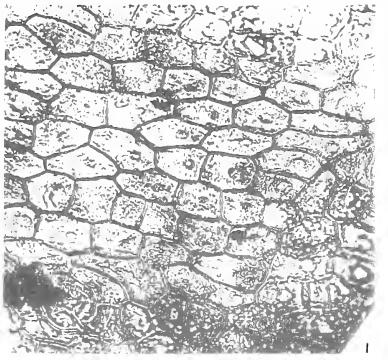
1


2

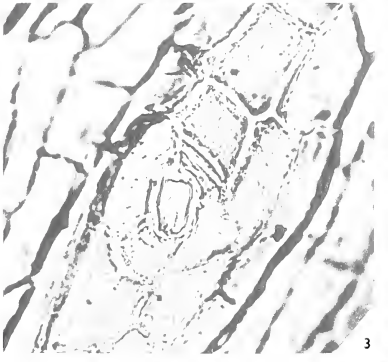
3

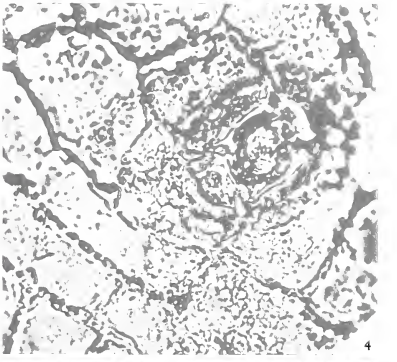
4


5

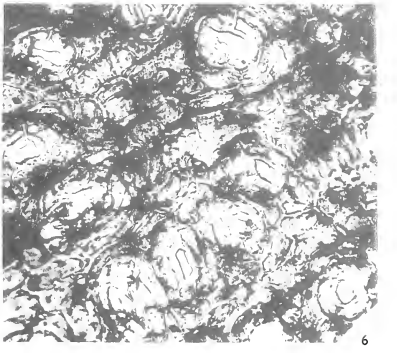
6

MUIR and VAN KONIJNENBURG VAN CITTERT, Mesozoic conifer cuticles

1

2

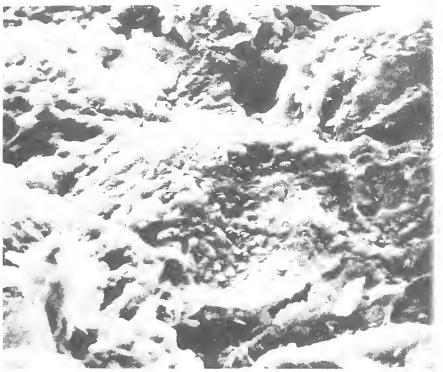

3

4

5

6

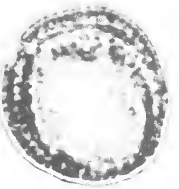

7

8

MUIR and VAN KONIJNENBURG VAN CITTERT, Mesozoic conifer pollen

1

2

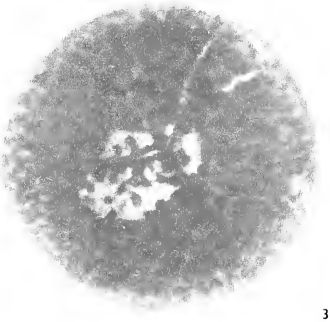

3

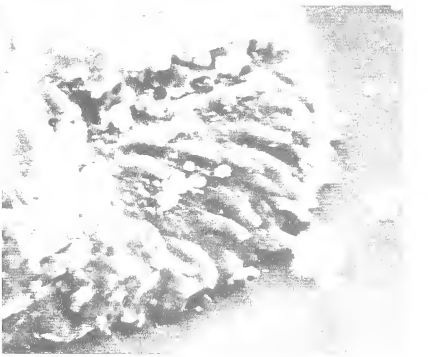

4

5

6

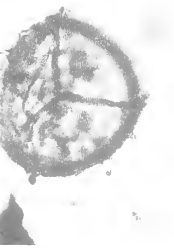

7

MUIR and VAN KONIJNENBURG VAN CITTERT, Mesozoic conifer and spores

the British Museum (Natural History), where all the other Rhaeto-Liassic material is deposited, and so comparison with Harris's material is not possible.

The female cone-scales described by Lemoigne (1967) are papillate, but have eight appendages, and so appear to differ somewhat from the Airel specimens, but the illustrated specimens appear to be broken, and may, in fact, only have five or six appendages.

Isolated male cones. Fragments of male cones are common in the Airel material, but no complete cones have been found, here or elsewhere. There is one isolated male cone axis (3 mm. long), showing the spiral arrangement of the microsporophylls clearly, but there are no microsporophylls adhering (text-fig. 1B). Isolated microsporophylls are common, but none of them has the pollen sacs attached. Microsporophyll heads are almost peltate, the stalk being slightly tilted and attached nearer to the base. They are about 2 mm. long and 2·5 mm. wide. Just below the stalk, there are two regions (one on either side) which are very sunken and polished, indicating the places of attachment of the pollen sacs. The Cnap Twt material of Harris (1957) also had two attachment areas. In *Hirmerella muensteri* (Hoerhammer 1933, Hirmer and Hoerhammer 1934, Jung 1968), however, there are up to twelve pollen sacs on one microsporophyll. Barnard (1968) found a situation similar to this in his material from the Liassic of Iran.

Isolated pollen sacs are also found, usually about 1·5 mm. long, 0·5 mm. wide, and almost circular in section. The wall of the pollen sac is very thin (*c.* 0·5 μ) and composed of rectangular cells. They yield pollen grains in different stages of maturity which are described under *Classopollis harrisii* sp. nov.

These isolated male cone fragments can be assigned with reasonable certainty to *Hirmerella airelensis* sp. nov. since the leaves are the only macrofossils in this material. The evidence of association is thus strong. Harris (1957) also described male cone fragments from Cnap Twt which he attributed to *Cheirolepis muensteri*, by far the most common macrofossil in that assemblage, although he found some dispersed cuticles of other species as well.

We believe that those fragments can be attributed to *Hirmerella airelensis* instead of *H. muensteri* because of their association with the leaves. Both male cone fragments differ from *H. muensteri* in having probably only two pollen sacs in each microsporophyll, while *H. muensteri* has a ring of twelve on each microsporophyll.

Genus CLASSOPOLLIS Pflug 1953

Type species. C. classoides Pflug 1953.

Classopollis harrisii sp. nov.

Plate 79, figs. 1, 3–7

Holotype. Specimen 2845A: division of Palaeobotany and Pollen Morphology, Museum and Herbarium of the State University of Utrecht.

Dimensions. Maximum diameter 37·0 μ; minimum diameter 22·2 μ; average size 25·6 μ. Holotype: maximum diameter 37·0 μ; minimum thickness of wall 1 μ; maximum thickness of wall 6 μ.

Diagnosis. Pollen grains spherical; characterized by an equatorial thickening which is divided off from the distal polar area by a thin ring furrow; no striations visible; no

distal pore seen; proximally triradiate, tetrad mark usually not distinct; exine two-layered; outer layer tegillate; inner layer thin, indistinct. Exine varies in thickness from 1 to 6 μ.

Description. These well-preserved grains can clearly be placed within the genus *Classopollis*, but are distinguished from previously described species by the absence of equatorial striations, and by the apparent absence of a distal pore (Plate 79, figs. 7, 8). The pollen grains have never been observed in tetrads, and this too is a distinctive feature. It can be separated from *Circulina meyeriana* Klaus 1960 by the prominent exine structure in *C. harrisii*.

Discussion. Almost the entire assemblage of dispersed spores from this locality consists of *Classopollis harrisii* sp. nov. (over 99% of the entire assemblage). This is typical of Rhaeto-Liassic assemblages, and less common earlier, suggesting that the assemblage is more likely to be Rhaetian than Norian.

The dispersed pollen grains can be closely compared with most of the pollen *in situ* in the pollen sacs and pollen masses associated with *Hirmerella airelensis* sp. nov., but the *in situ* pollen shows considerable variation. This probably reflects different stages in the development of the pollen grains. None of the pollen found, whether *in situ*, or dispersed, occurs in tetrads. This suggests that the grains went through the stage of tetrad formation before sporopollenin was deposited, and only separated grains are preserved. This would also tend to explain why the tetrad mark is not well developed on many grains.

We have found *in situ* some very small grains (11·1 μ to 18·5 μ maximum diameter) which all possess very thick-walled, smooth inner bodies. The inner bodies are completely spherical and rarely show any sign of either a tetrad mark or distal pore; sometimes, they possess an equatorial thickening which has no internal structure, although it is occasionally delimited by a ring furrow. The wall structure of the outer body is poorly developed, and the wall material is rather thin (Plate 79, fig. 5).

In the same pollen mass are more mature grains which still possess an inner body, but this is rather thin-walled and has no equatorial thickening (Plate 79, fig. 6). The outer layer of the exine has become thicker and its tegillate structure has become much more obvious. The equatorial region of the outer wall is frequently detached from the inner body, and the furrow ring clearly developed. Occasional striated grains are found at this stage of development.

In sporangia with mature grains, the inner body is almost undetachable, either because it is very thin, or because it has become closely attached to the outer layer. No striations are visible, but the ring furrow is very distinct. The dispersed pollen recovered from the clay is exactly like this. Inner bodies are only occasionally visible.

Comparison. These spores agree well with those described by Harris (1957) from the Rhaeto-Liassic of Cnap Twt and Ewenny, South Wales. He described the inner body of the grains and commented that its variability of preservation may be due to preservation of the intine 'partly impregnated with oil'. The electron microscope studies of Pettitt and Chaloner (1964) on *Classopollis* from Cnap Twt, show the presence of an internal layer corresponding to the inner body, as well as the coarse inwardly pointing baculae of the outer wall. These baculae can be seen on the Stereoscan photographs of

pollen in pollen masses (Plate 79, figs. 1, 3) standing up as positive projections with the external layers of the exine collapsed over them. Our pollen grains agree in size with those of Harris, and the only difference appears to be that Harris described thin areas on the inner bodies which he believed to represent the polar regions. However, we believe that our grains are similar to those described by Harris, if not identical; Harris did not name a species.

Classopollis harrisii sp. nov. differs from *C. belloyensis* Pocock and Jansonius 1961 in the lack of separation of the two layers of exine in the mature grains.

Rioult and Levet-Carette (1966) described three species of *Classopollis* under the generic name of *Classopollenites* from Cotentin, and assigned a Lower Lias age to the assemblage. In spite of the near geographical position, none of these species appear to be identical with *C. harrisii*: *Classopollenites tripartitus* is triangular in outline, and is ascribed by Rioult and Levet-Carette to the Pteridosperms, although not with any great certainty.

Classopolleuites (*Classopollis*) *classoides* Pflug is equatorially striated and although the wall structure of *Classopollenites minor* is similar to that of *C. harrisii*, it is described as having a prominent tetrad mark, and distal pore.

Pollen associated with *Brachyphyllum scottii* Kendall 1948 resembles *C. harrisii* sp. nov. closely, being normally non-striate, but has much finer wall structure, and occasionally occurs in tetrads. The *Masculostrobus* pollen described by Barnard (1968) associated with *Brachyphyllun expansum* from Iran differs from ours in the large number of striations on the equatorial thickening.

Genus BACUTRILETES (van der Hammen 1954) Potonié 1956

Type species. B. (*Triletes*) *tylotus* (Harris 1935) Potonié (1956).

Bacutriletes tylotus (Harris 1935) Potonié 1956

Plate 80, figs. 2–5

1935 *Triletes tylotus* Harris, p. 162.
1956 *Bacutriletes tylotus* (Harris) Potonié, p. 35.
1957 *Triletes tylotus* Harris; Lewarne and Pallot, p. 77, fig. 3 A, D.
1962 *Bacutriletes tylotus* (Harris) Potonié; Marcinkiewicz, p. 471.

Dimensions. Maximum diameter 475 μ; minimum diameter 350 μ (10 specimens); height of spines 20–5 μ; width of spines 6–12 μ; spines separated by distances of 5–10 μ.

Description. Our megaspores are very similar to those described by Lewarne and Pallot (1957). The triradiate mark is indistinct, but slightly elevated (illustrated fig. 3A of Lewarne and Pallot, but not described). The spines show a slight characteristic cross striation, also described from the Welsh material.

Discussion and comparison. The only megaspore comparable with this species is *Triletes sparassis* Murray 1939, from which it differs in the size and shape of the ornamentation. *Bacutriletes tylotus* has much more distinct spines.

Genus HELIOSPORITES Schulz 1965

Type species. H. altmarkensis Schulz 1965.

Heliosporites reissingeri (Harris 1957) Chaloner 1969

Plate 80, figs. 6, 7

1950 Cf. *Selaginella kraussiana* Reissinger, p. 104, pl. 12, fig. 28.
1957 *Lycospora reissingeri* Harris, p. 305, fig. 6, A, D.
1969 *Heliosporites reissingeri* (Harris 1957) Chaloner 1969.

Dimensions (10 specimens). Maximum over-all diameter, 49 μ; minimum over-all diameter, 35 μ; average width of cingulum, 10 μ; average length of spines, 10 μ.

Diagnosis. Harris (1957) gave a full diagnosis for this species, but the striations on the contact faces were not seen.

Description. The spores are clearly identical with those described by Harris (1957) as *Lycospora reissingeri.* A new combination of *Heliosporites reissingeri* (Harris 1957) has been proposed by Chaloner (1969).

CONCLUSIONS

The resemblance of this material to that described by Lewarne and Pallot (1957) and Harris (1957) and to the pollen studied by Pettitt and Chaloner (1964) from the fissure depths of Cnap Twt, Glamorgan, is remarkable. The cuticles of our material, with their distinctive stomatal arrangement and papillae are similar to those described from Wales. The male cones and pollen masses are also identical, and although our assemblage is rather restricted, the dispersed spores and pollen are also the same. We believe that the association of organs is so strong that the conclusion that the leafy shoots, female cone-scales, male cone fragments, and dispersed pollen grains come from one and the same plant is inescapable.

Unlike Lemoigne (1967) we do not believe that his (and our) material is Cupressalean. His assignment was based mainly on the wood fragments he found; Mr. van der Burgh studied some of our wood fragments and looked at Lemoigne's illustrations, and he believes that wood of this type may occur not only in the Cupressaceae, but probably also in other fossil conifer families such as the Voltziaceae and Cheirolepidaceae. The wood fragments described by Harris (1957) also look very like Lemoigne's and ours although our material was not fusainised. It does appear, therefore, on the evidence of association, that the wood fragments also belong to the same plant as the leaves, female cone-scales, male cone fragments, and pollen.

Heliosporites reissingeri and *Bacutriletes tylotus* have been found associated both at Airel and Cnap Twt, and this leads us to suggest that they represent the megaspores and microspores of one lycopodiaceous plant.

In our material we have evidence of a large amount of the *Hirmerella* conifer, which must have comprised almost a pure stand, and a lesser amount of the lycopod. The more varied assemblage found by Harris (1957) in the fissure fillings, which are comparable with those of the Boulonnais from which a plant assemblage was described by Briche

et al. (1963) and Levet-Carette (1964), probably includes plant fragments washed in from some distance away, while our material, being lacustrine, is probably more or less local in origin.

Acknowledgements. We are grateful to Mr. Robin Stevenson, Kingston College of Advanced Technology, Great Britain, and the 1966 year of geology students from the University of Utrecht, the Netherlands, for collecting this material for us; also to Mr. Rypkema who made the drawings.

REFERENCES

BARNARD, P. D. W. 1968. A new species of *Masculostrobus* Seward producing *Classopollis* pollen from the Jurassic of Iran. *J. Linn. Soc. Lond.* (*Bot.*) **61**, (384), 167–76.

BOLTENHAGEN, E. 1968. Révision du *Classopollis* Pflug. *Rev. Micropaléont.*, **11**, 29–44.

BRICHE, P., DANZÉ-CORSIN, P. and LAVEINE, J.-P. 1963. Flore infraliassique du Boulonnais (macro- et microflore). *Mém. Soc. géol. Nord*, **13.**

CHALONER, W. G. 1962. Rhaeto-Liassic plants from the Henfield Borehole. *Bull. geol. Surv. G.B.*, **19**, 16–28.

—— 1969. Triassic spores and pollen, TSCHUDY, R. H. and SCOTT, R. A. (eds.) *Aspects of Palynology*. John Wiley, New York.

HARRIS, T. M. 1935. The fossil flora of Scoresby Sound, East Greenland. Part IV. *Medd. Grønland*, **112**, (1). 1–176.

—— 1957. A Rhaeto-Liassic flora in South Wales. *Proc. Roy. Soc. Lond.*, **B147**, 289–308.

HIRMER, M. and HOERHAMMER, L. 1934. Zur weiteren Kenntnis von *Cheirolepis* Schimper und *Hirmeriella* Hoerhammer mit Bemerkungen über deren systematische Stellung. *Palaeontographica*, **B79**, 67–84.

HOERHAMMER, L. 1933. Über die Coniferen-Gattungen *Cheirolepis* Schimper und *Hirmeriella* nov. gen. aus dem Rhaet-Lias von Franken. *Bibl. Bot. Stuttgart*, **107**, 1–34.

JUNG, W. W. 1968. *Hirmerella muensteri* (Schenk) Jung nov. comb., eine bedeutsame Konifere des Mesozoikums. *Palaeontographica*, **B122**, 56–93.

KENDALL, M. W. 1949. On a new conifer from the Scottish Lias. *Ann. Mag. nat. Hist.*, Ser. 12, **2**, 299–307.

KLAUS, W. 1960. Sporen der karnischen Stufe der Ostalpinen Trias. *Jb. Geol. Bundesanst. Wien*, Sonderbd., **5**, 107–84.

LARSONNEUR, C. 1962. Faciès, Faune, et Flore du Keuper supérieur-Rhétien dans la région d'Airel (Manche), Bordure sud du Bassin de Carentan. *Mém. Soc. Sci. Nat. et Math. Cherbourg*, **50**, 72–116.

—— 1963. Contribution à l'étude du Trias supérieur du Bassin de Carentan (Manche). *Bull. Soc. Linn. Normandie*, Sér. 10, **4**, 23–32.

LEMOIGNE, Y. 1967. Paléoflore à Cupressales dans le Trias-Rhétien du Cotentin. *C.R. Acad. Sci. Paris*, Sér. D, **5**, 715–18.

LEVET-CARETTE, J. 1964. Étude de la microflore infraliassique d'un sondage effectué dans le sous-sol de Boulogne-sur-mer (Pas-de-Calais). *Ann. Soc. géol. Nord*, **83**, 101–28.

LEWARNE, G. and PALLOT, J. M. 1957. Mesozoic plants from fissures in the Carboniferous Limestone of South Wales. *Ann. Mag. nat. Hist.*, Ser. 12, **10**, 72–9.

MARCINKIEWICZ, T. 1962. Rhaetian and Lias Megaspores from borehole Mechowo near Kamień Pomorski. *Inst. Geol. Prace*, **30**, 3, 469–94.

MURRAY, N. 1939. The Microflora of the Upper and Lower Estuarine Series of the East Midlands. *Geol. Mag.* **76**, 478–89.

NAPP-ZINN, K. 1966. Anatomie des Blattes, I. Gymnospermen. *Encyclopedia of Plant Anatomy*, **8** (1), 1–369.

PETTITT, J. M. and CHALONER, W. G. 1964. The ultrastructure of the Mesozoic pollen *Classopollis*. *Pollen et Spores*, **4**, 611–20.

POCOCK, S. A. J. and JANSONIUS, J. 1961. The pollen genus *Classopollis* Pflug 1953. *Micropaleontology*, **7**, 439–49.

POTONIÉ, R. 1956. Synopsis der Gattungen der Sporae dispersae. I. Teil, Sporites. *Beih. Geol. Jahrb.* **23**, 1–163.

REISSINGER, A. 1950. Die 'Pollenanalyse' ausgedehnt auf alle Sedimentgesteine der geologischen Vorgangenheit. Zweiter Teil. *Palaeontographica*, **B90**, 99–126.

RIOULT, M. and LEVET-CARETTE, J. 1966. Microflore infraliassique du Cotentin. *Ann. Soc. géol. Nord*, **85**, 283–99.

SCHULZ, E. 1962. Sporenpaläontologische Untersuchungen zur Rhät-Lias-Grenz in Thüringen und der Altmark. *Geologie*, **11**, (3), 308–510.

—— 1967. Sporenpaläontologische Untersuchungen Rhätoliassischer Schichten in Zentralteil des Germanischen Beckens. *Paläont. Abh.*, **B2**, (3), 427–633.

WOOD, C. J. 1961. *Cheirolepis muensteri* from the Lower Lias of Dorset. *Ann. Mag. nat. Hist.*, Ser. 13, **4**, 505–10.

MARJORIE MUIR
Geology Department
Imperial College
Prince Consort Road
London, S.W. 7

JOHANNA H. A. van KONIJNENBURG-van CITTERT
Division of Palaeobotany
Museum and Herbarium
University of Utrecht
Utrecht, The Netherlands

Revised typescript received 20 October 1969

CALCAREOUS ALGAE NEW TO THE BRITISH CARBONIFEROUS

by GRAHAM F. ELLIOTT

ABSTRACT. The first British records of two Lower Carboniferous algal taxa known from the U.S.S.R. and elsewhere are given: *Ungdarella deceanglorum* sp. nov., representing the Ungdarellaceae, an extinct red algal family; and *Exvotarisella maponi* gen. et. sp. nov., representing the tribe Bereselleae of the family Dasycladaceae (green algae). *U. deceanglorum* is from the Visean of Wales, probably lower D_2 Zone: *E. maponi* comes from the D_2 Zone of Northumberland. *Exvotarisella* is considered to be structurally the most advanced genus of the Bereselleae.

DURING an examination of that part of the Garwood collection of fossil algae in the British Museum (Natural History) two interesting occurrences were noted of algae described from Russia and well known from elsewhere, but not until now from Britain. The genera represented are *Ungdarella*, referable to the Rhodophyceae or red algae but not to any living family of this class, and a new genus of the dasycladacean tribe Bereselleae (Chlorophyceae or green algae). Both occur in this country in the Lower Carboniferous, Visean, D_2 Zone, and are now described below.

RHODOPHYCEAE

Family UNGDARELLACEAE Maslov 1956

Genus UNGDARELLA Maslov 1950

Remarks. This genus was described by Maslov (1950) from the Russian Upper Carboniferous and subsequently recognized in Iraq, Turkey, Austria, Spain, the north-west African Sahara, and the U.S.A. with a total range of Lower Carboniferous (Visean) to Upper Permian (Toomey and Johnson 1968). It is a calcified branching twig-like form, compared by Maslov and others in internal structure with two living non-calcified red algae, *Ahnfeldtia* and *Cystoclonium*, though not identical with either nor referable to the families Phylloporaceae and Rhodophyllidaceae to which they belong.

Ungdarella deceanglorum sp. nov.

Plate 81, figs. 1–5

Diagnosis. Small slender species of *Ungdarella*, with almost completely uncalcified medullary zone, and with less conspicuous cortical cell-detail than in other species.

Description. Calcified cylindrical branching thallus, twig-shaped, branches near-circular in cross-section and slightly irregular, length about 3 mm. or more (2·86 mm. seen), diameter often 0·26 mm. (0·14–0·39 mm. seen). Branching at irregular intervals, the angle of divergence ranging from 45 to 110°. Internally the thallus shows a thick calcified cortical zone surrounding an uncalcified central medullary zone: this latter is almost always a third or a little less of the outer diameter. Thus in specimens of the common diameter of

[Palaeontology, Vol. 13, Part 3, 1970, pp. 443–50, pl. 81–83.]

0·26 mm. the medullary zone is 0·078 mm. diameter, surrounded by a cortical zone 0·091 mm. thick. This medullary zone is filled with clear calcite, or with strings and groups of dolomite crystals. In other species of *Ungdarella* this zone is occupied by calcified medullary cells, arranged in single or several axial strings, though not as heavily calcified as the cells of the outer, cortical zone. In two sections only of the British species it was possible from the arrangement of the dolomite crystals, colour of the calcite, etc., to measure single presumed medullary cells: they were 0·045–0·050 mm. long by 0·020 mm. wide, and 0·039 mm. long by 0·026 mm. wide. Both were central in position, and it is uncertain whether the remainder of the uncalcified medullary space was occupied by parallel strings of similar cells, or whether it formed the place of origin of the divergent cortical cells before they became calcified. This uncalcified medullary zone distinguishes *U. deceanglorum* from other species of the genus, whose authors were able to measure and describe medullary cells when sufficient material was available (cf. *U. uralica*, Pl. 83, fig. 6).

The cortical cells are well calcified and form the whole thickness of the outer zone. They show as close-packed parallel single strings or files of cells, inclined at an acute angle of 10–15° to the long axis of the branch, so that they traverse a considerable length before reaching the exterior. A slight irregularity is occasioned by sporadic division, the new cell-strings continuing close-packed with the others. The individual cells are about 0·016 mm. long and 0·013–0·014 mm. wide, squarish in cross-section but in sections taken adjacent to and below the sites of thallus-branching the proportions alter: examples are 0·013 mm. long by 0·020 mm. wide, and 0·010 mm. long by 0·013 mm. wide. The main lateral cell-walls are much more conspicuous than the transverse septa in vertical section. In oblique transverse sections the steep inclination of the cell-strings occasions a curious appearance, one side of the section showing a concentric structure and the other an irregularly radial one.

U. deceanglorum has the characteristic thin-section appearance of other species of the genus: a bleached wood or watered silk effect. The cell-details of *Ungdarella* are not conspicuous as in the Solenoporaceae or Corallinaceae, and in *U. deceanglorum* this negative character is especially marked.

Holotype. The specimen figured in Plate 81, fig. 1 from the Lower Carboniferous, White Limestone Division, probably Lower D_2: Bron-heulog Quarry, Trefor Rocks, 1½ miles east of Llangollen, Denbighshire, Wales. (Wedd 1927, pp. 109, 129, 148.) Brit. Mus. (Nat. Hist.), Department of Palaeontology, reg. no. V55400.

EXPLANATION OF PLATE 81

Figs. 1–5. *Ungdarella deceanglorum* sp. nov. Lower Carboniferous. White Limestone Division, probably lower D_2; Bron-heulog Quarry, Trefor Rocks, Llangollen, Denbighshire, Wales. All from reg. no. V55400. 1, Holotype, longitudinal section showing branching of thallus, fine oblique divergent files of cortical cells, and medullary zone replaced by light transparent calcite or dark dolomite crystals. Other, random cuts in section; ×30. 2, Longitudinal section of another branching specimen; ×30. 3, Longitudinal and transverse sections, the former showing files of cortical cells, and medullary zone replaced by transparent calcite with central string of dolomite crystals suggesting original single string of large medullary cells; ×40. 4, Two transverse sections, slightly oblique; the larger showing clearly the radial appearance of cortical cell-structure on one side of the section and concentric appearance on the other, typical of such sections; ×40. 5, Another longitudinal section showing layered appearance of cortical cells, and medullary zone replaced in different areas by light transparent calcite or areas of dark dolomite crystals; ×40.

1

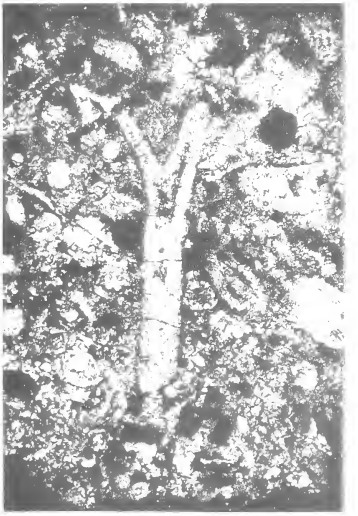

2

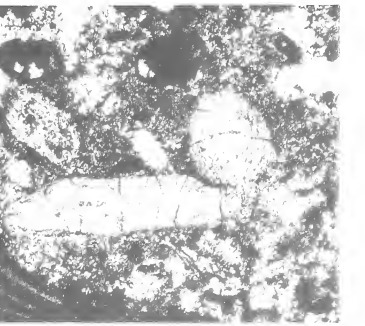

3

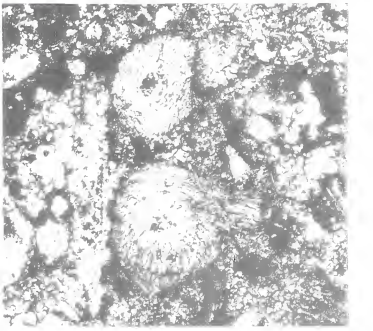

4

5

ELLIOTT, Carboniferous Rhodophyceae (Algae)

Paratypes. The specimens figured in Plate 81, figs. 3, 4; from the same thin-section as the holotype.

Other material. Numerous other random sections.

Remarks. Toomey and Johnson (1968) gave detailed comparison-tables for structures and measurements of all described *Ungdarella* spp. up to date. *U. deceanglorum* is a smaller, more slender species, with smaller cortical cells, than both the type *U. uralica* Maslov, and the other Visean species *U. maslovi* Chanton. The non-calcified medullary zone of the British species is characteristic. The species throws no light on the disputed basal attachment in this genus (Toomey and Johnson 1968, p. 560), and no reproductive structures have been recognized.

Of the two living non-calcified red algae with which *Ungdarella* has been compared, *Ahnfeldtia* shows irregularly concentric rings of secondary thickenings, considered to be in part associated with successive dichotomies (Fritsch 1945, p. 495). In *U. deceanglorum* the apparent concentricity arises from the angle of cut across the normal cortical cells. *Cystoclonium* shows near-vertical medullary cells, but those of the cortex are much more irregular and directed outwards at a much greater angle from the branch-axis than in *U. deceanglorum*. Although these comparisons are valid, and *Ungdarella* probably was a red alga, the relationship is not necessarily close.

Associated in the type thin-section are small foraminifera, brachiopod, and echinoderm debris, and the dasycladacean alga *Koninckopora inflata* (de Kon.) Wood.

The specific name commemorates the old British tribe of Deceangli, whose territory in Roman times lay in what is now Flintshire and part of Denbighshire.

CHLOROPHYCEAE-BERESELLEAE

The Bereselleae are a tribe of tiny dasycladacean algae of Carboniferous age, the genera mostly described from the U.S.S.R., and reviewed by Kulik (1964), and later recognized from rocks of the same age in Turkey and in the north-west African Sahara.

The British examples now recorded were first noted in a Garwood Collection thin-section labelled 'Oxford Limestone, Bean Bed, base D_2; Northumberland'. This is a well-known band at the base of the Lower Carboniferous Middle Limestone Group in the Northumberland Province: the limestone contains small partly pyritic organic nodules with *Girvanella*, first recognized and studied by Garwood. Search in the collection produced a limestone specimen labelled similarly to the thin-section, but further annotated by Garwood. From this it appears that the limestone came from one of two old exposures of the Oxford Limestone at Wisplaw. This locality is four miles north-north-east of Alnwick, Northumberland; the old exposures are mentioned in Carruthers (1930, p. 46). The Oxford from which the limestone takes its name is a tiny locality four miles south of Berwick-on-Tweed. Further thin-sections cut from the limestone were closely similar to the original section, and showed more Bereselleae.

Subsequent discoveries, summarized and discussed in a recent study of the Lower Limestone Group of the Otterburn, North Tyne area of Northumberland by Frost (1969), have shown that the Oxford Limestone does not mark the base of the D_2 Zone, which occurs considerably below this (Frost 1969, pp. 299–301, fig. 6). The Oxford limestone is therefore not basal D_2 as Garwood considered, but well within this zone. The nodules with *Girvanella* are determined by Frost as *Osagia* (Twenhofel 1919), a

form-genus applied to some Palaeozoic nodular associations of small algal filaments and encrusting nubeculariform foraminifera (cf. Johnson 1946, 1947).

CHLOROPHYCEAE

Family DASYCLADACEAE Kützing 1843 orth. mut. Hauck 1884

Tribus BERESELLEAE Maslov and Kulik 1956

Genus EXVOTARISELLA gen. nov.

Diagnosis. Large atypical member of the Bereselleae showing primary, secondary, and tertiary branches as in the subgenus *Trinodella* but with thick primary and secondary branches (unlike *Trinodella* where all branches are uniformly thin), and with tertiary branches much longer than primary and secondary branches (in *Trinodella* the primary branches are longer than the secondary and tertiary branches). Lower Carboniferous, D_2: Northumberland, England. Type-species: *E. maponi* sp. nov.

Exvotarisella maponi sp. nov.

Plate 82, figs. 1–5, Plate 83, figs. 1–5

Description. Calcareous hollow dasyclad cylinder, straight or gently curved, of up to 5 mm. or more length (5·096 mm. seen broken), with diameters of 0·26–0·45 mm. external and 0·104–0·195 mm. internal (d/D 40–47%). Verticils of horizontally directed lateral branch-systems, each estimated to contain 14–20 primary branches. The verticils are set 0·039–0·065 mm. apart along the stem-cell cavity; between them the stem-cell cavity constricts slightly, to give a regular internal annulation. In general the detailed dimensions are more or less proportional to external size, but relatively long, slim specimens occur noticeably. Primary branches of about 0·026 mm. diameter at the stem-cell, extending outwards for 0·026 mm. before bifurcating. Secondary branches diverging at about 45°, with diameter of 0·013 mm. and length of 0·026 mm.; tertiary branchlets about 0·005 or 0·006 mm. diameter, but 0·052–0·078 mm. long. Each primary probably divides into four secondaries, and each secondary probably into four tertiaries: possibly with some variation in this character.

Holotype. The specimen figured in Plate 82, fig. 2; from the Lower Carboniferous, Northumberland Middle Limestone Group, Oxford Limestone, D_2 Zone: Wisplaw, Alnwick, Northumberland. Brit. Mus. (Nat. Hist.), Dept. Palaeont., reg. no. V55393.

EXPLANATION OF PLATE 82

Figs. 1–5. *Exvotarisella maponi* gen. et. sp. nov. Oxford Limestone, Bean Bed; Lower Carboniferous, D_2 Zone. Wisplaw, Alnwick, Northumberland. 1, Longitudinal section of slightly curved and sinuous large example, ordinary preservation, ×30; reg. no. V55398. 2, Holotype, slightly oblique transverse section, pyritic preservation, showing pyrite-filled branch-structure with primary, secondary, and tertiary branching, ×60; V55393. 3, Paratype; oblique-transverse section, pyritic preservation, showing internal annulation and pyrite-filled primary, secondary, and tertiary branches, ×60; V55399. 4, Longitudinal section of slightly sinuous individual, ordinary preservation, ×40; V55391. 5, Slightly oblique transverse section, pyritic preservation, individual with long, slim, atypical branches (cf. *Dvinella* or *Trinodella*), ×60; V55396.

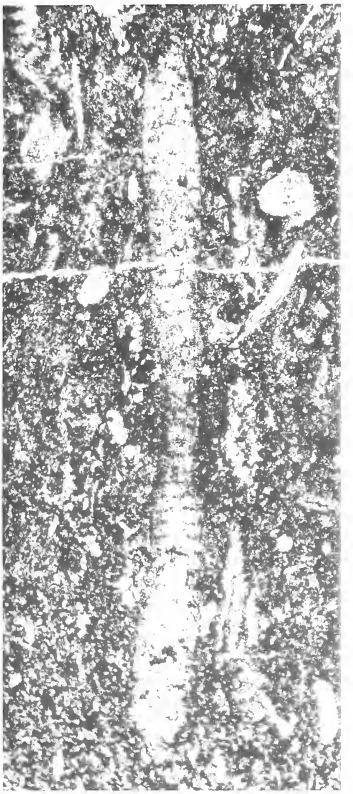

1

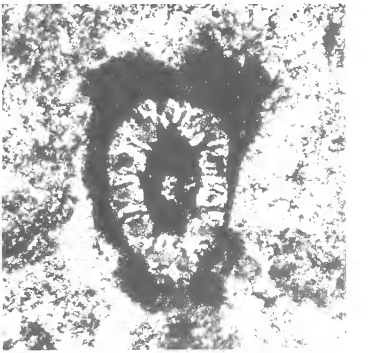

2

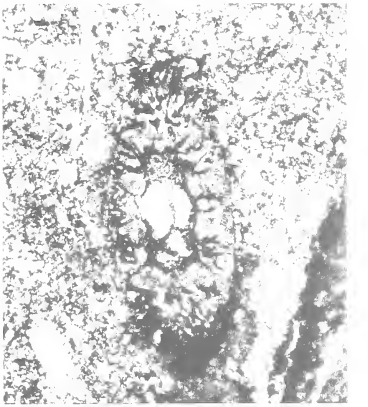

3

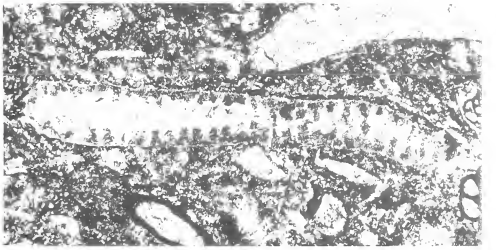

4

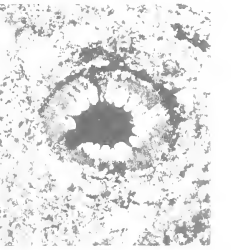

5

ELLIOTT, Carboniferous Chlorophyceae (Algae)

Paratype. The specimen figured in Plate 82, fig. 3; same locality and horizon as holotype. Brit. Mus. (Nat. Hist.) Dept. Palaeont., reg. no. V55399.

Other material. Very numerous sections in seventeen thin-sections prepared from the same sample.

Remarks. Although the general appearance of members of the Bereselleae is characteristic, distinction between the component genera is often difficult. This is due to the extreme fineness and close grouping of the lateral branches, so that the exact nature of the preservation is very important.

Of the five genera or subgenera of the Bereselleae described hitherto, *Beresella*, *Samarella*, and *Goksuella* show various groupings of single lateral branches (primaries): in *Dvinella* these primaries divide once into several secondaries, and in *Trinodella* these

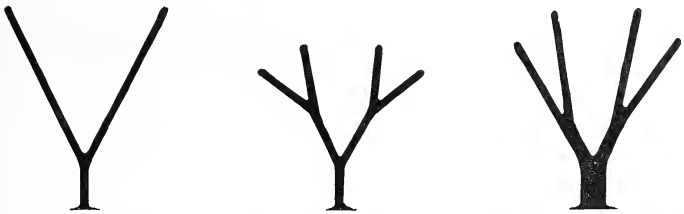

TEXT-FIG. 1. Diagrammatic two-dimensional representation of branching in *Dvinella*, *Trinodella*, and *Exvotarisella* (left to right). There are at least four branches at each point of division in the actual three-dimensional specimens, and the relative branch-lengths vary between different species of *Dvinella* and similarly between species of *Trinodella*.

in turn divide into tertiaries (Maslov and Kulik 1956, Güvenc 1966). *Goksuella* is set apart by a branching thallus; in all the others the thallus is a single, straight or curved, rod-like structure.

In the Northumberland fossils preservation is usually poor for elucidation of detail; in thin-section the areas of branch-structure, representing consecutive verticils, appear as grey truncate cones, amorphous or with the branch-structures indistinct. Calcite crystals may be continuous from the stem-cell filling into the replacement calcite of the walls, so that the boundary is only traceable by a faint colour-change. Some of the branches have the appearance of division, but this could be due to bunched primaries.

There exists a minority of specimens showing partial pyritic preservation, usually found in the vicinity of the organic partly pyritic nodules with *Girvanella* and encrusting organisms. Here again, preservation has been capricious, and in most cases the pyrites fills the stem-cell, or encrusts the outer surface of the tubular dasyclad, but does not penetrate into the branch-systems. It is only with the very small minority of specimens showing pyritic branch-infilling that the diagnostic reference may be made. These show primaries branching into secondaries with great clearness, but care has to be taken to distinguish between true tertiary branching and the regions of apparent overlap between bunched secondaries (cf. *Dvinella*, Khvorova 1949). Thus the tertiary branching characteristic of *Trinodella* and *Exvotarisella* can be definitely seen only on very few specimens, which appear to be favourably orientated sections of those showing secondary branching

as in *Dvinella*. The earlier portions (lower thallus) of individuals of *Trinodella* and *Exvotarisella* may by analogy with other dasyclads be expected to show simpler, *Dvinella* structure only, as mentioned below (p. 449).

The position is, then, that definite Bereselleae are not uncommon in the Oxford Limestone of Wisplaw. The minority of individuals which are preserved to show fine detail are all recognizable as the new genus or may be supposed to be so. None of the others show equal clarity of detail to be definitely referable to other genera. It would seem reasonable, therefore, to suppose that all are referable to the one genus and species, though there are one or two doubtful individuals. The types chosen show fine detail and in this respect are not typical of the majority of the specimens: the branch-dimensions given above under 'Description' are based on the former. It is true that in Saharan Carboniferous rocks examined by me more than one genus of Bereselleae occurs in the same section, but in these Bereselleae are so abundant as to make up an appreciable portion of the rock-volume. In the Northumberland rock they form a minor element only.

Exvotarisella maponi is easily distinguishable from another tiny English Carboniferous dasyclad, *Nanopora anglica* (Wood 1964), which shows simple straight primaries set almost equidistantly, and not bunched.

Exvotarisella differs from the three species of *Trinodella* tabulated by Kulik (1964), by its large size, thickened primary and secondary branches, and in the differing relative proportional lengths of primary, secondary, and tertiary branches and branchlets, though this last character differs between the species of *Trinodella*. The branch-thickening is important: in most Bereselleae the branches are of uniform thickness, usually about 0·002 or 0·005 mm. diameter, whether single, or dividing once as in *Dvinella* or twice as in *Trinodella*. Only in *Dvinella gracilis* Kulik are the secondaries of lesser diameter than the primaries. *Trinodella* is less common than *Dvinella* and is placed by the Russians as a subgenus of the latter. In an interesting correlation between the structure of the Bereselleae and their ecology (based on the nature of the sediments in which the fossils occur) Kulik (1964) supposed that the coarser sediments in which *Dvinella* and *Trinodella* are preserved indicate shallow, disturbed-water environments. In these the tendency to formation of a more massive calcareous dasycladacean envelope with fewer verticils led to a compensatory mechanism for assimilation by division of the lateral branches. From this point of view, their branching is simply a variant of the densely clumped, thin, single branches of the more simple genera, which flourished in deeper quieter waters.

EXPLANATION OF PLATE 83

Figs. 1–5. *Exvotarisella maponi* gen. et. sp. nov.; Oxford Limestone, Bean Bed, Lower Carboniferous, D_2 Zone, Wisplaw, Alnwick, Northumberland. 1, Thin-section of rock showing several examples of *Exvotarisella*, normal preservation, ×30; reg. no. V55395. 2, Transverse section of example showing incomplete pyritic penetration of branch-system, ×60; V55395. 3, Transverse section, slightly distorted individual, with good pyritic penetration of part of the branch-system, ×60; V55396. 4, Longitudinal section, showing pyrite-filled stem-cell with very little pyritic penetration of the branches, ×40; V55394. 5, Longitudinal section, curved individual, normal preservation apart from pyritic filling of part of the stem-cell adjacent to pyritized organic nodule (portion seen top right), ×30; V55397.

Fig. 6. *Ungdarella uralica* Maslov; Longitudinal section of fragment to show coarse cell-structure and well-calcified medullary cells (for comparison with *U. deceanglorum*), ×40; Zinnar Formation, Permian (Artinskian-Kungarian), Ora, Mosul Liwa, northern Iraq.

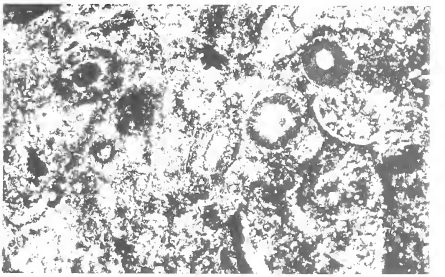

1

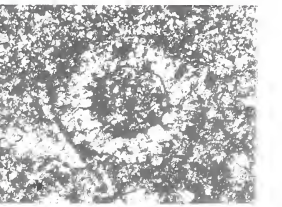

2

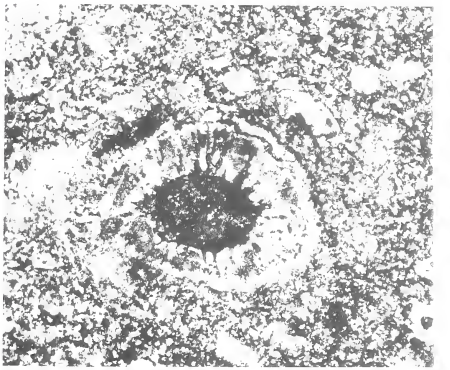

3

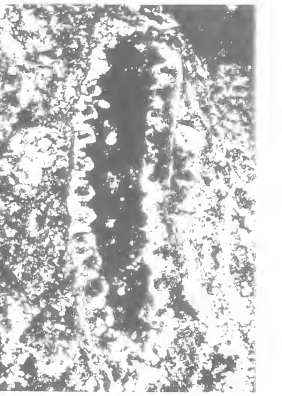

4

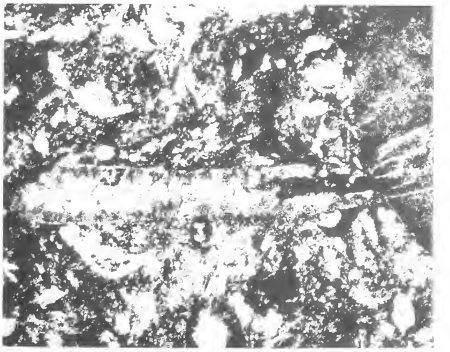

5

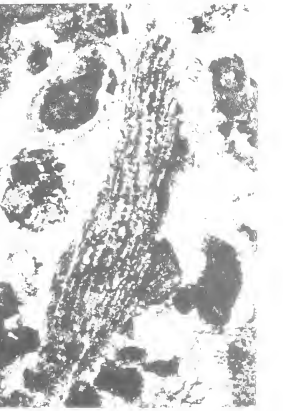

6

ELLIOTT, Carboniferous Chlorophyceae (Algae)

In *Exvotarisella*, however, the thickening of short primaries and secondaries followed by sprays of longer tertiaries, and the larger size of the thallus, shows a trend known in many other genera and part of the main stream of dasyclad evolution, leading to transfer of the sporangial bodies from stem-cell to side-branches (Pia 1920, Rezak 1959, Elliott 1968). From this point of view *Exvotarisella* is the most advanced genus of the Bereselleae, and if it did not share in the general extinction of its tribe, it is the one most likely to have evolved into something else.

Trinocladus of the Cretaceous and Palaeocene (Pia 1936, Elliott 1968) is a genus in which swollen primaries and secondaries are followed by tertiary branchlets. It is known that this full branch-development occurred in the later-formed portions only of the plant, the older earlier portions showing simpler branch-structure only. It seems very likely that this occurred in *Exvotarisella* also.

The English genus and species are dedicated to Mapon, the Celtic Apollo, once worshipped in the region of Hadrian's Wall, Northumberland, and elsewhere.

REFERENCES

CARRUTHERS, R. G. *et al.* 1930. The geology of the Alnwick district. *Mem. Geol. Surv. Engl. Wales*, expl. sheet 6.

CHANTON, N. 1966. Nouvelle contribution à l'étude des algues calcaires du Carbonifère saharien. *Bull. Soc. géol. Fr.* (7) **7,** 402–9, pl. 8.

ELLIOTT, G. F. 1968. Permian to Palaeocene calcareous algae (Dasycladaceae) of the Middle East. *Bull. Br. Mus. nat. Hist.* (*Geol.*), Suppl. **4.**

EMBERGER, J. 1958. Note préliminaire sur les algues du Carbonifère du Sahara occidental. *C.r. somm. Séanc. Soc. géol. Fr.*, 1958, **2,** 16–17.

FRITSCH, F. E. 1945. *The structure and reproduction of the algae*, vol. 2. Cambridge.

FROST, D. V. 1969. The Lower Limestone Group (Viséan) of the Otterburn District, Northumberland. *Proc. Yorks. geol. Soc.* **37** (3), 13, 277–309, pl. 9, 10.

GÜVENÇ, T. 1966. Représentants des Bereselleae (Algues calcaires) dans le Carbonifère de Turquie et description d'un nouveau genre: *Goksuella* n.g. *Bull. Soc. géol. Fr.* (7)7, 843–50, 1 pl.

JOHNSON, J. H. 1946. Lime-secreting algae from the Pennsylvanian and Permian of Kansas. *Bull. geol. Soc. Am.* **57,** 1087–120, 10 pls.

—— 1947. *Nubecularia* from the Pennsylvanian and Permian of Kansas. *J. Paleont.* **21,** 41–5, pl. 17.

KHVOROVA, I. V. 1949. A new genus of Dasycladaceae from the Middle Carboniferous of the Moscow Tectonic Valley. *Dokl. Akad. Nauk SSSR*, **65,** 749–52. (In Russian.)

KULIK, YE. L. 1964. Beresellids from the Carboniferous of the Russian Platform. *Paleont. Zhurn.*, 1964, **2,** 99–114, pl. 8. (In Russian.)

MASLOV, V. P. 1950. La valeur des Algues rouges pour la stratigraphie de l'U.R.S.S. *Dokl. Akad. Nauk SSSR*, **70** (1). (In Russian.)

—— 1956. Nouvelle famille d'Algues rouges fossiles et deux nouveaux genres de Cyanophycées fossiles du Carbonifère. Ibid. **107** (1), 151–4. (In Russian.)

—— and KULIK, YE. L. 1956. Nouvelle tribu d'Algues (Bereselleae) du Carbonifère de l'U.R.S.S. Ibid. **106,** 126–9. (In Russian.)

PIA, J. 1920. Die Siphoneae Verticillatae vom Karbon bis zur Kreide. *Abh. zool. bot. Ges. Wien*, **11** (2), 263 pp., 8 pl.

—— 1936. Calcareous green algae from the Upper Cretaceous of Tripoli (North Africa). *J. Paleont.* **10** (1), 3–13, pl. 1–5.

REZAK, R. 1959. New Silurian Dasycladaceae from the southwestern United States. *Colo. Sch. Min. Quart.* **54** (1), 115–29, pl. 1–4.

TOOMEY, D. F. and JOHNSON, J. H. 1968. *Ungdarella americana*, a new red alga from the Pennsylvanian of southeastern New Mexico. *J. Paleont.* **42,** 556–60, pl. 75, 76.

TWENHOFEL, W. H. 1919. Pre-Cambrian and Carboniferous algal deposits. *Am. J. Sci.* (4), **48**, 339–52.

WEDD, C. B. *et al.* 1927. The geology of the country around Wrexham; Part 1. *Mem. Geol. Surv. Engl. Wales*, expl. sheet 121.

WOOD, A. 1964. A new dasycladacean alga, *Nanopora*, from the Lower Carboniferous of England and Kazakhstan. *Palaeontology*, **7**, 181–5, pl. 31, 32.

GRAHAM F. ELLIOTT
Department of Palaeontology,
British Museum (Natural History)
London S.W. 7

Typescript received 29 October 1969

FERTILE RHYNIOPHYTINA FROM THE LOWER DEVONIAN OF BRITAIN

by DIANNE EDWARDS

ABSTRACT. A new genus *Steganotheca* is erected to include plants from the Downtonian of South Wales with naked dichotomously branching axes and terminal sporangia, which are longer than wide, sharply truncated apically, and with tapering bases. Comparison is made with other members of the Rhyniophytina (Banks 1968). Sterile Silurian axes probably belonging to the same genus are briefly mentioned. The first occurrence of *Cooksonia* in the Lower Old Red Sandstone of Scotland, consisting of naked dichotomously branching axes terminating in oval to circular sporangia, is described from the Cairnconnan Group of the Lower Devonian in Angus; it is placed in a new species.

THE fossils described in the first part of this paper were collected from the Capel Horeb Quarry, Breconshire. Although the majority, including all the fertile ones, were found at the eastern end of the quarry in the lowest of the Long Quarry Beds in the grey Downtonian of the Lower Old Red Sandstone (Potter and Price 1965), some were collected from the older Ludlovian rocks (Lower Whitcliffian). The plants are preserved as heavily carbonized compressions in which little structure can be detected. They were treated in the way described by Edwards (1968), but bulk maceration of the rock was relatively unsuccessful. All the fossils and preparations have been deposited at the National Museum of Wales, Cardiff.

Although *Cooksonia* is commonly found in the Downtonian and Breconian rocks of South Wales and the Welsh Borderland, it has hitherto not been recorded from Scotland. The fertile specimens described in the second part of this paper were all collected at Aberlemno quarry near Turin Hill, Angus. Two of the specimens are in my possession while the third, which is designated the holotype is housed in the Royal Scottish Museum. Also found in this Quarry are *Zosterophyllum myretonianum*, *Prototaxites*, and *Parka*. The plants, associated with occasional fish and eurypterid fragments, are preserved as pinkish-red impressions in a fine-grained, grey sandstone. Very occasionally casts of axes are present or a film of granular carbon covers the specimen. In neither case does structure remain, and the account presented here is merely a description of the fossils immersed in 70% alcohol and examined using a hand lens or binocular microscope. Some of the plants have been developed by removing the covering rock layer with tungsten steel needles.

Most of the rock was collected from the tips on the floor of the quarry, but some fossils were also visible on the quarry face where a hard jointed sandstone is interbedded with the shale and softer fissile sandstone layers in which the plants are found. The rocks form part of the Cairnconnan Group of the Dittonian of the Lower Old Red Sandstone of Angus, probably equivalent to the Gedinnian of Europe (Waterston 1965).

SYSTEMATIC DESCRIPTION

Family RHYNIACEAE Kidston and Lang 1919

Genus STEGANOTHECA gen. nov.

Type species. *Steganotheca striata* sp. nov.

[Palaeontology, Vol. 13, Part 3, 1970, pp. 451–61, pl. 84–87.]

Diagnosis. Naked dichotomously branching axes with erect terminal sporangia. Sporangia longer than wide with tapering bases and truncated apices; apices formed by terminal lens-shaped structure of coaly material; sporangia with almost parallel sides.

Steganotheca striata sp. nov.

Plate 84, figs. 1–6, Plate 85, figs. 1–8

Diagnosis. Axes with at least four dichotomies, 0·4–0·8 mm. wide, with central line. Surface longitudinally striated. Sporangia 1·8–2·7 mm. long and 1·0–1·5 mm. wide; tapering at base; apex truncated; apex formed by terminal lens-shaped structure of coaly material, up to 0·25 mm. thick; surface of sporangium obliquely striated; parallel sides.

Locality. Capel Horeb Quarry, abandoned quarry on the A40 between Trecastle and Llandovery Nat. Grid. Ref. SN 844323.

Horizon. Long Quarry Beds, Grey Downtonian, Lower Old Red Sandstone of South Wales.

Holotype. Specimen 69·64 G32a and counterpart; Department of Geology, National Museum of Wales, Cardiff; Plate 84, figs. 1, 2, 5, 6, Plate 85, fig. 1.

Description of specimens. Most information was obtained from three fertile specimens found in a fine-grained grey sandstone, interbedded with micaceous layers.

(*a*) Specimen 69.64.30a and b (Pl. 84, figs. 3, 4). This fossil consists of a slightly flexuous branching system of over-all length 5·0 cm. The width of the axes remains almost constant through three successive dichotomies ranging between 0·7 mm. at the base and 0·5 mm. distally, where each axis widens into the base of a sporangium. The axis surface is striated, representing perhaps the outlines of epidermal or cortical cells. A faint central line is sometimes seen when the rock is held at a suitable angle to the incident light. The reconstruction given in text-fig. 1 is derived from part and counterpart. The sporangia are cup-shaped, 2·5 mm. high and 1·5 mm. wide on average. The coaly residue in the truncated sporangium apex is much thicker than that in the rest of the sporangium wall, forming a terminal lens-shaped structure (Pl. 85, fig. 4). The coaly residue from the axes, sporangia, and distal thickened region was macerated in Schulze's solution for several days, but no structure was discernible.

(*b*) Specimen 69.64.G31a and b (Pl. 85, figs. 2, 3). This specimen consists of an axis 0·4–0·5 mm. wide and 18 mm. long which dichotomises once. One of the branches ends

---

EXPLANATION OF PLATE 84

Figs. 1–6. *Steganotheca striata* sp. nov. 1, 2, Dichotomously branching fertile axes, 69.64.G32a and b; ×1·2. 3, 4, 69.64.G30a and b; ×1·2. 5, 6, Sporangia from 69.64.G32a; ×7·7.

EXPLANATION OF PLATE 85

Figs. 1–8. *Steganotheca striata* sp. nov. 1, Sporangia from 69.64.G32a; ×7·7. 2, 3, Sporangium and counterpart, 69.64.G31a and b; ×8; note the conspicuous striations in fig. 2 and the thickened apical region in fig. 3. 4, Cup-shaped sporangium with apical thickening, 69.64.G30a; ×8. 5, 6, Sterile Downtonian axes from Capel Horeb, 69.64.G33, ×1·2; 69.64.G34, ×7·5. 7, Cells from Downtonian axis recovered after maceration, 69.64.G35; ×430. 8, Film pull of Downtonian axis showing cell walls, 69.64.G36; ×126.

1

2

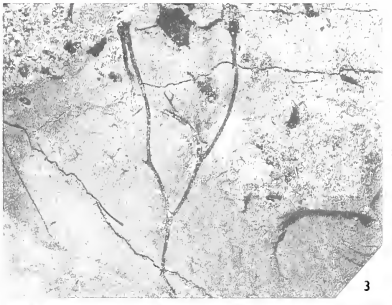

3

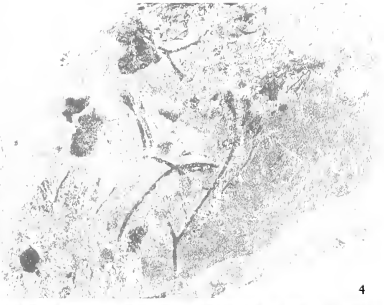

4

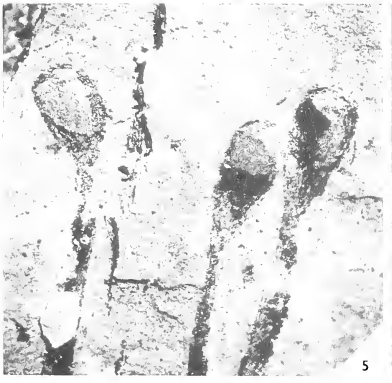

5

6

EDWARDS, Early Devonian Rhyniophytina


1


2

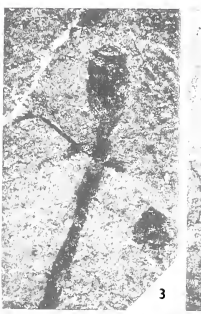
3


4


5


6


7


8

EDWARDS, Early Devonian Rhyniophytina

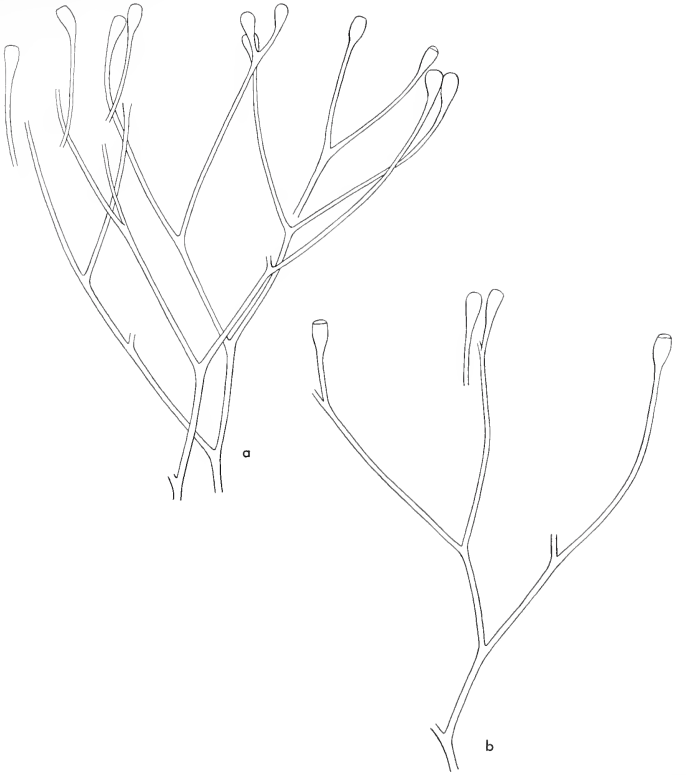

TEXT-FIG. 1. Reconstructions of *Steganotheca striata* sp. nov. *a*, Drawn from 69.64.G32a and b; ×1·8 *b*, Drawn from 69.64.G30a and b; ×1·8.

in a sporangium 1·8 mm. high and 1·0 mm. wide. The axis surface is longitudinally striated. The sporangial features described above are again clearly seen here (Pl. 85, fig. 3). In addition, the sporangium surface is striated, with the lines running diagonally across the sporangium. This is most clearly seen in the counterpart (Pl. 85, fig. 2). The heavily carbonized distal region is not present on the latter.

(*c*) Specimen 69.64.G32a and b (Pl. 84, figs. 1, 2). A reconstruction of the plant is given in text-fig. 1. It consists of a 'bushy' three-dimensional branching system in which at least ten of the axes end in sporangia. Branching is dichotomous with a wide angle

(*c.* 60°) at each branching point. The axes vary between 0·5 and 0·8 mm. in diameter. The sporangia are, on average, 2·4 mm. high (ranging between 2·0 and 2·7 mm.) and 1·2 mm. wide (1·0–1·5 mm.). The majority have truncated tips (Pl. 84, figs. 5, 6) with heavily carbonized areas similar to those already described. A few, however, are rounded at the apices (Pl. 85, fig. 1). These are also unusual in that they terminate very short lengths of axis above the ultimate dichotomy. It is therefore suggested that these oval sporangia are immature ones, though it should be noted that they are no smaller than the others.

Summary of description. Steganotheca striata is a small bushy plant, at least 5·0 cm. high, consisting of naked, dichotomously branching axes with terminal sporangia. Its basal parts are unknown. Branching is strictly dichotomous, with the angle at the branching point ranging between 45° and 75°. The length of axis above a branching point is approximately the same in both arms, and the branches terminating in sporangia are of equal length. The distance between the sporangium and last branching point is usually long compared with the distances between successive dichotomies. The sporangia themselves are almost twice as long as wide. Their apices are truncated and terminate with a heavily carbonized lens-shaped region. The base of each sporangium is not clearly defined. No spores have been isolated and very little is known of the structure of the sporangium wall.

Associated with the fertile specimens are numerous short lengths of axis, the majority being Y-shaped, but some unbranched and some with two successive dichotomies. These axes are approximately the same width as the fertile ones (average 0·55 mm. in the former, 0·6 mm. in the latter) and the angles at branching points are similar. It is therefore probable that these fragments belong to the same genus as the fertile ones (Pl. 85, figs. 5, 6).

Nearly all the axes have faint surface striations which probably represent the outlines of elongate cells of the epidermis or cortex. A thin central strand is seen on some of the sterile axes, but this is more obvious on film pulls of axes, because the coaly residue of the central area forms a continuous band, while that of the remainder of the axis is cracked and often incomplete. Pieces of rock-bearing axes have been macerated and the carbon recovered cleared with Schulze's solution. Fragments of carbon have also been picked off the rock and film pulls and cleared in the same way. No tracheids have been seen. Very occasionally film pulls bear the remains of cell walls, those running parallel to the long axis of the branch being most often preserved. They are 9–20 μ apart, the distance tending to vary proportionally with the width of the axis. Very narrow axes are 10–12 cells wide. Occasionally transverse end walls are seen. These are perpendicular or oblique to the longitudinally running walls (Pl. 85, fig. 8).

Little or no cuticle is recovered on maceration. Some fragments of a 'stringy' nature are sometimes found. These are most probably the longitudinal walls described above. There is no definite cellular structure visible, but occasionally two walls meet suggesting tapering cells (Pl. 85, fig. 7).

Other material. Plant fragments in the Silurian (Ludlovian) part of the quarry are surprisingly abundant. They are found in a very fine-grained, grey sandstone, but unlike the Downtonian plants are not associated with micaceous layers. The remains fall into

three categories: (*a*) Some bedding planes are almost completely covered with small pieces of axis and patches of coaly residue (Pl. 86, fig. 2). (*b*) Slightly longer axes are concentrated sporadically, sometimes in the depressions of ripple marks, and are again associated with patches of coaly residue (Pl. 86, fig. 1). (*c*) Isolated fragments sometimes over 2·0 cm. long with one or two dichotomies are found scattered throughout the deposit (Pl. 86, fig. 3).

These Silurian axes look very similar to the Downtonian ones. They range from 0·7 to 0·1 mm. in width (on average 0·4 mm.). Surface striations and central strands are often seen. Film pulls and maceration products showed similar cellular organization (Pl. 86, figs. 4–7). No tracheids have been found. In the absence of fertile specimens it cannot be determined with certainty that these axes belong to *Steganotheca*.

Discussion. Banks (1968), in his new classification of the psilophytes, divided the group into three subdivisions. The one relevant to this discussion is the Rhyniophytina in which plants with terminal sporangia (*sensu* Kidston and Lang 1917) are placed. Banks has included two families in a single order, the Rhyniales. In the Rhyniaceae, the terminal sporangia are 'usually fusiform and may dehisce longitudinally' (Banks 1968, p. 76) while in the Cooksoniaceae they are globose. Because there is considerable variation in sporangial shape within both the families recognized by Banks, in this paper I prefer to compare all the genera with solitary terminal sporangia included in the Rhyniophytina, with the plants from Capel Horeb.

In the Rhynie Chert flora (Kidston and Lang 1917, 1919), *Rhynia major* and *R. gwynne-vaughanii* both have terminal sporangia which are longer than they are wide on dichotomously branching naked axes. The sporangia of *R. major* are considerably larger than those in *Steganotheca* but those in *R. gwynne-vaughanii* are of comparable size. *Horneophyton lignieri* sporangia are columellate, while the sporangia are branched. Since the Rhynie plants are petrifactions and unknown in the compressed state, comparison is difficult. It seems probable however that, if preserved as compressions, the two *Rhynia* species, at least, would have well-defined sporangia with good distinction between sporangium and axis, and rounded apices.

The genus *Sporogonites* (Halle 1916), although investigated by a number of workers, is still somewhat of an enigma. On present evidence, it is unlikely that it is a vascular plant. The elongate, obovoid sporangia, terminating long, unbranched axes are larger than those in the Welsh plant. The sporangium apex is rounded and the tapering base merges into the thick upper part of the stalk. The sporangium is longitudinally grooved and columellate. It may be difficult to understand why *Sporogonites*, with its clearly defined sporangial characters, should not be eliminated immediately from this discussion. Cookson (1949) pointed out that, in heavily compressed fossils, the columella and ridges are unlikely to be preserved, and concluded that the critical character is whether or not the axis is branched. The Capel Horeb specimens have branched axes and none of the distinctive characters seen in *Sporogonites*.

Hicklingia edwardii (Kidston and Lang 1923) from the Middle Old Red Sandstone of Scotland with its almost spherical sporangia differs from the older plant in sporangial shape and arrangement. In *Taeniocrada decheniana* (Kräusel and Weyland 1930) the terminal sporangia are larger, and borne in clusters on flat ribbon-shaped axes. The dimensions of the Lower Devonian genus *Eogaspesiea* (Daber 1960) are similar to those

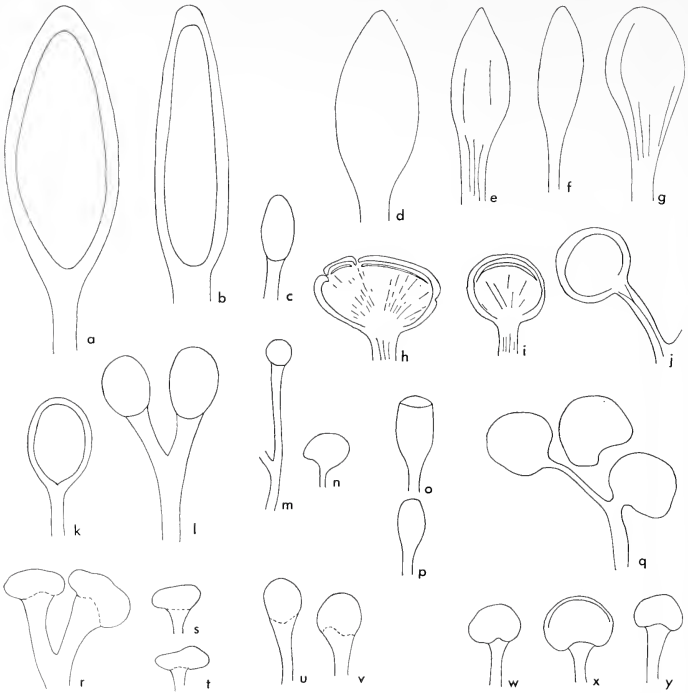

TEXT-FIG. 2. Diagrams to show variation in sporangium shape and size in certain Rhyniophytina; ×4. *a*, *b*, *Rhynia major* (Kidston and Lang 1919); inner line shows extent of spore cavity and is not a thickened border. *c*, *R.gwynne-vaughani* (Kidston and Lang 1917, 1919). *d–g*, *Sporogonites exuberans* (Halle 1916). *h–j*, *Cooksonia crassiparietilis* (Yurina 1964). *k*, *l*, *Cooksonia* sp. (Croft and Lang 1942). *m*, *n*, *Cooksonia* sp. (Obrhel 1962). *o*, *p*, *Steganotheca striata* sp. nov. *q*, *C. rusanovii* (Ananiev 1959, 1960). *r–t*, *C. pertonii* (Lang 1937). *u*, *v*, *C. hemisphaerica* (Lang 1937). *w–y*, *C. caledonica* sp. nov.

in *Steganotheca*, but the sporangia are oval. *Hedeia corymbosa* (Cookson 1935), another Lower Devonian genus, resembles *Steganotheca* because the dichotomously branching axes terminate in elongate sporangia with their tips all at the same level forming a corymb-like arrangement. In *Hedeia*, however, the whole system is compacted to form a definite fructification. In addition, it differs in sporangial shape and size.

When Lang erected the genus *Cooksonia* in 1937, he distinguished it from early genera on the basis of sporangial shape. From his diagnosis, any plant assigned to the genus should have a combination of the following characters: (1) terminal, short, wid

sporangia, (2) dichotomously branched, naked axes, (3) central vascular cylinder composed of annular tracheids. Of these, in my opinion, the most significant and definitive are the short and wide sporangia. There has been a tendency to place any poorly preserved Lower Devonian fossils, where the sporangia are terminal and few anatomical details are known, in the genus *Cooksonia*. The variation in sporangial shape and size is illustrated in text-fig. 2. On the basis of sporangial shape, the Capel Horeb fossils are clearly not assignable to the genus *Cooksonia*. Heard (1939), however, described a single fertile specimen from the Downtonian of the Capel Horeb locality, in which dichotomously branching axes terminated in 'capsule-like' sporangia (5 mm. long by 2 mm. wide). There is little doubt in my mind that this fossil, named *Cooksonia downtonensis* by Heard, should be transferred to the new genus, *Steganotheca*. The lack of distinction between sporangium and stalk might account for the discrepancy in sporangial length. The impression of the plant gained from Heard's illustrations supports my conclusion. In addition, in the line-drawing of the fertile specimen, published by Høeg (1967) at the tip of the left-hand sporangium is a lens-shaped region, limited by a dotted line, which corresponds to the apical feature described above. Heard, however, did not mention this apical feature, nor the oblique striations on the sporangium wall. The morphological nature of this apical thickening is questionable. It is possible that it was similar to the operculum of a bryophyte, but it is unlikely that it could ever be stated with certainty that it was concerned with dehiscence. It is equally possible that the thickness of coaly residue is a preservation feature produced by compression of the flat top of the sporangium. Oxidation of various parts of the sporangia have yielded nothing.

In conclusion the fossils described above present a new combination of characters, not seen in any of the above genera. The new genus *Steganotheca* is therefore erected to include fragments of plants which possess the following characteristics: (*a*) Dichotomously branched, naked axes; (*b*) Erect terminal sporangia, longer than wide with parallel sides, truncated apices and bases tapering into the axes beneath; (*c*) Fine striations running obliquely across the sporangium wall; (*d*) Thick, heavily carbonised, lens-shaped region at sporangium apex.

Heard's specimen has not been made the type of this new taxon, because his material is missing and, secondly, because the new fossils show the distinctive sporangial characters not mentioned in Heard's specific diagnosis.

Genus COOKSONIA Lang 1937

Type species. Cooksonia pertonii.

Original diagnosis. Dichotomously branched, slender, leafless stems with terminal sporangia that are short and wide. Epidermis composed of elongated, thick-walled cells. Central vascular cylinder consisting of annular tracheids.

Cooksonia caledonica sp. nov.

Plate 87, figs. 1–10

Diagnosis. Incomplete plant at least 6·7 cm. high. Naked dichotomously branching axes 0·4–1·8 mm. wide (average 0·65 mm.). Terminal spherical to oval sporangia, some

also reniform. Border (0·1–0·2 mm. wide) sometimes present. Globose sporangia 1·2–2·0 mm. high (average 1·7 mm.) by 1·3–2·2 mm. wide (average 1·8 mm.). Oval ones 1·1–1·8 mm. high (average 1·6 mm.) by 1·8–3·0 mm. wide (average 2·4 mm.). Axis widens slightly below sporangium.

Locality. Aberlemno Quarry, Aberlemno, approximately 1½ miles north-north-west of Turin Hill, Angus; Nat. Grid Ref. 527551.

Horizon. Cairnconnan Group, Dittonian Stage Lower Old Red Sandstone of Scotland.

Holotype. Specimen R.S.M. 1967. 30. 2P and C; Royal Scottish Museum, Edinburgh.

Description of specimens. Very occasionally scattered among the long, relatively unbranched axes of *Zosterophyllum myretonianum* were found narrower dichotomously branching axes, which in the absence of fertile parts, would be assigned to the form genus, *Hostimella*. One piece of rock and its counterpart (R.S.M. 1967.30. 2P and C), found by Dr. C. D. Waterston, was completely covered with these axes lying parallel to each other (Pl. 87, figs. 1, 3). The longest exposed axis was 4·0 cm. long. The slightly flexuous axes branch dichotomously, with an angle of 55–60° at the branching point. Longitudinal striations are sometimes visible on the surfaces of the axes, but what could definitely be called a central strand has not been seen.

A slightly asymmetrical positioning of the branches above a dichotomy indicates a tendency to pseudomonopodial branching, but there is no inequality of axis diameter.

Scattered in the matrix and sometimes attached to short lengths of axis are circular to oval bodies, presumably sporangia (Pl. 87, figs. 5, 6–10). The globose ones measure, on average, 1·8 mm. wide and 1·7 mm. high, while the oval sporangia are 2·4 mm. wide and 1·6 mm. high on average. The height of all the sporangia is slightly less than the width. Occasionally a narrow border less than 0·1 mm. wide extends around the convex margin of the sporangium (Pl. 87, fig. 8). In profile, this is either apparent as a ridge separated from the rest of the sporangium by a sharp depression, or as a groove (Pl. 87, fig. 8). This border could be removed easily.

One specimen (Pl. 87, fig. 10) appears to represent two sporangia almost superimposed, but only one subtending axis is visible. It is possible that this is in fact a dehisced

EXPLANATION OF PLATE 86

Figs. 1–7. Sterile axes from Silurian at Capel Horeb. 69.64.G37; ×2·3. 2, 69.64.G38; ×5. 3, 69.64.G39; ×7·7. 4, Axis recovered on film pull, central strand indicated by arrow; 69.64.G40, ×126. 5, Film pull of axis with longitudinal cell walls and transverse banding (indicated by arrows), the latter are formed because the carbon tears when the film pull is removed and are not tracheidal thickenings; 69.64.G41, ×430. 6, 7, Film pulls from axes showing cell walls, 69.64.G42 and G43; ×126.

EXPLANATION OF PLATE 87

Figs. 1–10. *Cooksonia caledonica* sp. nov. 1, R.S.M. 1967.30.2P before uncovering; ×1·1. 2, Specimen illustrated in fig. 1 showing dichotomously branching axes with terminal sporangia; ×1·1. 3, R.S.M. 1967.30.2C; Sterile axes with isolated sporangia indicated by arrows; ×0·9. 4, Sporangium from specimen DE 33/22; note pad of tissue in base of sporangium; ×7·7. 5, Isolated almost circular sporangium (R.S.M. 1967.2C); ×8. 6, Sporangia as in fig. 2; ×8. 7–10, Isolated sporangia (R.S.M. 1967.30.2P and C); ×8; 7, Oval sporangium with axis entering its base. 8, Oval sporangium with border, here represented by a depression. 9, Globose sporangium. 10, Two superimposed sporangia or single dehisced sporangium.

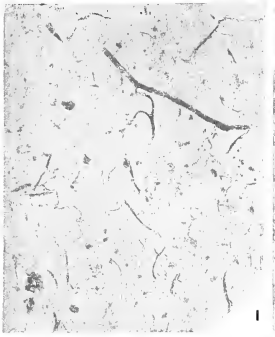

1

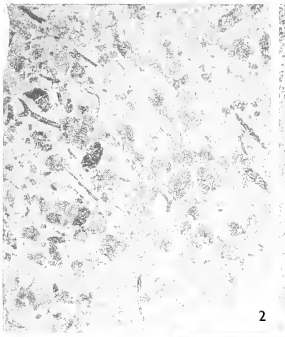

2

3

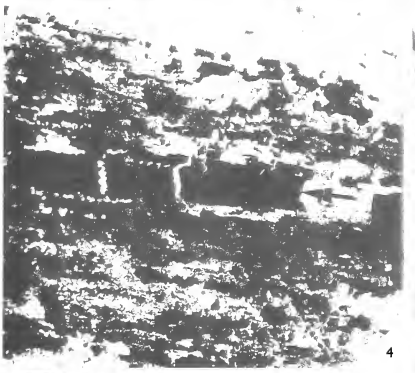

4

5

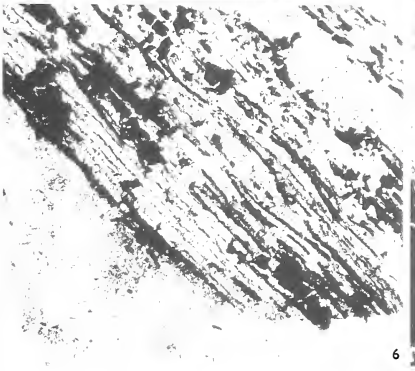

6

7

EDWARDS, Silurian (Ludlovian) plants


1


2


4


5


3

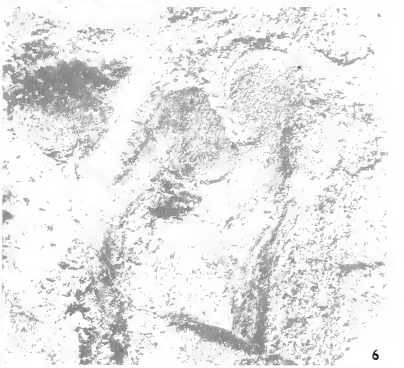
6

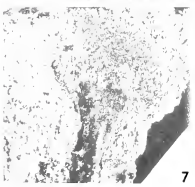
7

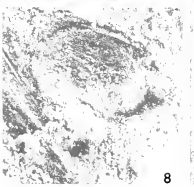
8

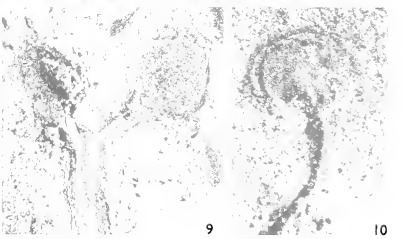
9 10

EDWARDS, Early Devonian Rhyniophytina

sporangium, split into two valves, although the original assumption should not be ignored. The variation in sporangial shape is illustrated in text-fig. 3. In some cases, the tip of the axis extends a short way into the base of the sporangium.

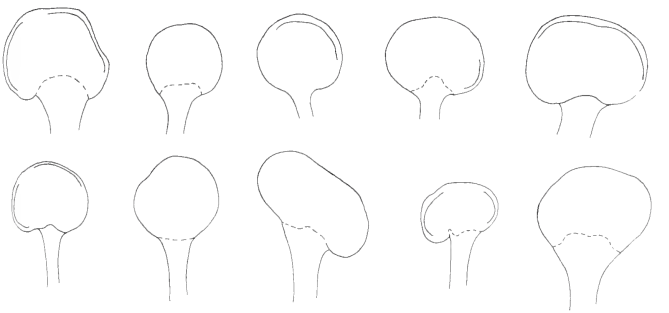

TEXT-FIG. 3. Diagrams showing variation in size and shape of sporangia of *Cooksonia caledonica* sp. nov.; ×9.

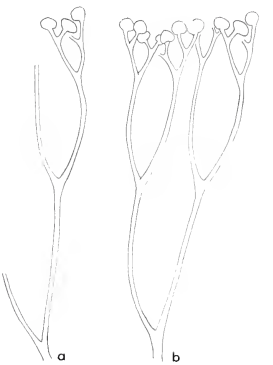

TEXT-FIG. 4. *a*, Drawing of *Cooksonia caledonica* sp. nov. from R.S.M. 1967.30. 2P; ×1. *b*, Reconstruction on the plant; ×1.

One branching system, on uncovering, was found to exhibit four orders of branching with a distinct decrease in axis diameter from base to apex. The most complete part terminated in three relatively large sporangia (Pl. 87, figs. 1, 2, 6). Text-fig. 4*a* shows what has actually been seen, but text-fig. 4*b* is a probable reconstruction of the plant assuming that the branching pattern seen in text-fig. 4*a* is repeated. This assumption is supported

by the fact that a row of sporangia, of which the attached ones form one end, is visible on the specimen.

Specimen DE 33/22 in my own collection is again fertile. Here an axis, 0·6 mm. wide at its base, dichotomises once and one branch terminates in an oval to reniform sporangium 1·7 mm. wide and 1·2 mm. high. The axis increases in width just below the sporangium and forms a pad of tissue (1·0 mm. wide) in its base (Pl. 87, fig. 4). This is particularly noticeable on the counterpart where the sporangium itself is fainter. In another specimen (DE 33/19) a dichotomously branching system bears a single, here almost spherical sporangium, 1·5 mm. high and 1·6 mm. wide. The axis widens into the sporangium base. No border is present.

Discussion. This Scottish plant is clearly a member of the genus *Cooksonia* and comparison with the four species already placed in the genus shows that it differs sufficiently to be a new species (text-fig. 2).

In *C. pertonii* (Lang 1937) the sporangia are more irregularly shaped than in the Scottish plant and a border has not been seen. The latter differs from *C. hemisphaerica* (Lang 1937) and the plants designated *Cooksonia* sp. by Croft and Lang in 1942, both in sporangial shape and size. Not enough is known about Ananiev's *Cooksonia rusanovii* (Ananiev 1959, 1960) described from rather fragmentary remains. Although sporangial shape is similar to that in the new plant, the arrangement of sporangia in the Russian specimens is different and even suggests that the plants belong to another genus.

In sporangial characters the Scottish plant most closely resembles *C. crassiparietilis* described by Yurina (1964) from the Lower Devonian of Karaganda, U.S.S.R. One of her specimens consists of a naked dichotomously branching axis about 2 cm. long, varying in width between 1·5 mm. and 4·0 mm., the latter below a branching point. The terminal sporangia are reniform to circular in shape, and are 3·5–5·67 mm. wide and 2·75–4·50 mm. high. Each sporangium has a thickened border and the surface is ornamented by fine ribs diverging from the point of attachment. The wall itself is three-layered. Spiny spores have been isolated. These sporangia, although much larger, are similar in shape to those in the Scottish plant. An odd feature of the Russian specimens is that more than one, presumably vascular, strand is visible in the axis immediately below a sporangium. There is no indication of this in the Aberlemno specimens.

In conclusion, it is considered that the new Scottish *Cooksonia* differs sufficiently from the existing species to warrant the erection of a new species.

Acknowledgements. I thank Dr. K. R. Sporne for his advice throughout this work and Dr. C. D. Waterston for his generosity in allowing me to work on the Aberlemno flora. Most of this research was carried out during the tenure of an N.E.R.C. fellowship and the Ethel Sargent Research Fellowship at Girton College, Cambridge.

REFERENCES

ANANIEV, A. R. 1959. Die wichtigsten Fundstellen von Devonflora im Ssajan-Altaj Berggebiete. Tomsk. [In Russian; German summary.]

—— 1960. Age of the Izik and Shunet Suites according to the flora on the northern slope of Batenevo Ridge. *Trudy tomsk. gos. Univ.* **146**, 5–28, 4 pls. [In Russian; N.L.L. Translation Service.]

BANKS, H. P. 1968. The early history of land plants. *In* Evolution and environment; a symposium presented on the one hundredth anniversary of the foundation of the Peabody Museum of Natural History at Yale University, DRAKE (ed.). New Haven and London (73–107, figs. 1–9).

COOKSON, I. C. 1935. On plant remains from the Silurian of Victoria, Australia, that extend and connect floras hitherto described. *Phil. Trans. R. Soc. Lond.* **B225,** 127–48, 2 pls.

—— 1949. Yeringian (Lower Devonian) plant remains from Lilydale, Victoria, with notes on a collection from a new locality in the Siluro–Devonian period. *Mem. natn. Mus. Vict.* **16,** 117–31, 3 pls.

CROFT, W. N. and LANG, W. H. 1942. The Lower Devonian flora of the Senni Beds of Monmouthshire and Breconshire. *Phil. Trans. R. Soc. Lond.* **B221,** 131–63, 3 pls.

DABER, R. 1960. *Eogaspesiea gracilis* n.g. n. sp. *Geologie*, **4,** 418–25, 2 pls.

EDWARDS, D. 1968. A new plant from the Lower Old Red Sandstone of South Wales. *Palaeontology*, **11,** 683–90, 3 pls.

HALLE, T. G. 1916. Lower Devonian plants from Röragen in Norway. *K. svenska Vetensk Akad. Handl.* **57,** 1–46, 4 pls.

HEARD, A. 1939. Further notes on Lower Devonian plants from South Wales. *Q. Jl. geol. Soc. Lond.* **95,** 223–9, 2 pl.

HØEG, O. A. 1967. Psilophyta. In *Traité de Paléobotanique*, vol. 2, BOUREAU, E. (ed.). Paris. [In French.]

KIDSTON, R. and LANG, W. H. 1917. On Old Red Sandstone plants showing structure from the Rhynie Chert Bed, Aberdeenshire. Part I. *Rhynia Gwynne-Vaughani*, Kidston and Lang. *Trans. R. Soc. Edinb.* **51,** 761–84, 10 pls.

—— 1919. Part II. Additional notes on *Rhynia Gwynne-Vaughani* Kidston and Lang; with descriptions of *Rhynia major* n. sp. and *Hornea lignieri* n.g., n.sp. Ibid. **52,** 603–27, 10 pls.

—— 1923. Notes on fossil plants from the Old Red Sandstone of Scotland. I. *Hicklingia Edwardi*. Ibid. **53,** 405–7, 1 pl.

KRÄUSEL, R. and WEYLAND, H. 1930. Die Flora des deutschen Unterdevons. *Abh. preuss. geol. Landesanst.* N.F. **131,** 1–92, 14 pls.

LANG, W. H. 1937. On the plant remains from the Downtonian of England and Wales. *Phil. Trans. R. Soc. Lond.* **B227,** 245–91, 7 pls.

OBRHEL, J. 1962. Die Flora der Přídolí-Schichten (Budňany-Stufe) des mittelböhmischen Silurs. *Geologie*, **11,** 83–97, 2 pls.

POTTER, J. F. and PRICE, J. H. 1965. Comparative sections through rocks of Ludlovian–Downtonian age in the Llandovery and Llandeilo districts. *Proc. geol. Ass., Lond.* **76,** 379–402.

WATERSTON, C. D. 1965. Old Red Sandstone. In *The geology of Scotland*, CRAIG, G. (ed.). Edinburgh.

YURINA, A. L. 1964. New Devonian species of the genus *Cooksonia*. *Paleont. Zh.* (Special Reprint No. 1), 107–13, pl. 15. [In Russian.]

DIANNE EDWARDS
Botany Department
University College of South
Wales and Monmouthshire
Cathays Park
Cardiff

Typescript received 16 December 1969

AMMONITES OF THE GENUS *ACANTHOCERAS* FROM THE CENOMANIAN OF ROUEN, FRANCE

by W. J. KENNEDY *and* J. M. HANCOCK

ABSTRACT. Although *Acanthoceras* only forms a minority of the ammonites from the Craie de Rouen, the locality is important as being the type locality of *Acanthoceras rhotomagense*, the type species of the genus and the most oft-quoted species. This study shows that almost all the *Acanthoceras* from Rouen can be regarded as one variable species which can be conveniently divided into five varieties, only one of which, *A. rhotomagense* var. *clavatum*, is new. *A. rhotomagense* is a widespread species and marks an horizon low in the Middle Cenomanian. *Acanthoceras basseae* sp. nov., also from Rouen, is a rarity.

WELL-PRESERVED fossils from the chalk at Rouen were described as early as 1822 by Cuvier and Brongniart. Casual references in the literature and labels in museums show that it has been much collected from ever since, but there are few descriptions of the section. The best is still that of Bucaille in Lennier (1880) quoted by Jukes-Browne and Hill (1903, p. 253), but there are also brief descriptions by Dollfus and Fortin (1911) and Follet (1943). Jefferies (1963, fig. 10) showed the position of the fossil-rich horizon in relation to the Plenus Zone. The section given here (fig. 1) is based on our own field notes.

The Cenomanian Chalk of Normandy contains several glauconitic horizons, well shown in the coast sections at St. Jouin and Cap de La Hève. These glauconitic developments are probably reflections of local differential uplift, on top of which sedimentation was relatively slow. Some of these glauconitic developments are accompanied by phosphatisation. It is one such bed at Côte St. Catherine in Rouen which has yielded the many fossils commonly known as the fauna of the Rouen Chalk; strictly, the Craie de Rouen includes all the chalk at Rouen below that with *Inoceramus labiatus* and Hébert (1884) even included the beds containing '*Ammonites*' *inflatus* and *Turrilites bergeri* that we should now consider Upper Albian.

As far as we know from our own field work, there is only one horizon at Rouen itself which contains well-preserved, light-brown, phosphatic internal moulds. All museum specimens used in this study are in a similar preservation, or have traces of phosphatic test, and we have ignored the few specimens labelled 'Rouen' in other preservations. When we refer to 'the Rouen fauna' we mean that from the fossil-rich bed.

SYSTEMATIC DESCRIPTIONS

Family ACANTHOCERATIDAE Hyatt 1900

Genus ACANTHOCERAS Neumayr 1875

(= *Metacanthoplites* Hyatt 1900)

Type species. Ammonites rhotomagensis Brongniart ex Defrance MS in Cuvier and Brongniart 1822; designated by De Grossouvre 1894.

[Palaeontology, Vol. 13, Part 3, 1970, pp. 462–90, pl. 88–97.]

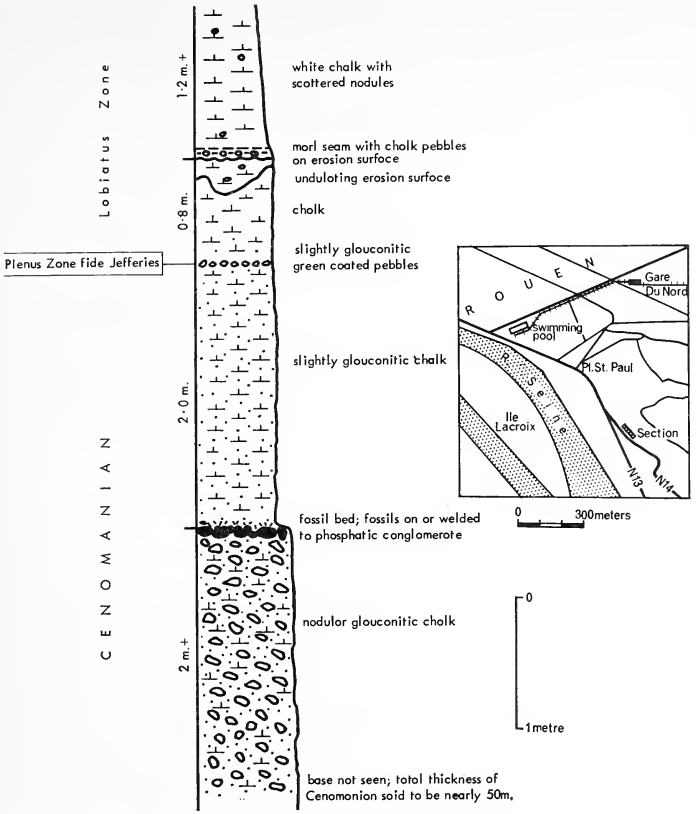

TEXT-FIG. 1. Vertical section showing the stratigraphical position of the fossil-bed of the Craie de Rouen at Côte St. Catherine, Rouen. Sketch-map shows the position of an exposed section.

Generic characters. Decorated ammonites, rather evolute: whorl height normally 6·5–12·5 times as great as the depth of the impressed area, not changing markedly with age but commonly becoming slightly more evolute.

Intercostal whorl section is roughly square sometimes slightly depressed, not changing appreciably during ontogeny. The whorl section through the ribs is markedly angular, commonly on some variant of a square with diagonals cutting the corners; sides may be parallel or diverging slightly towards the umbilicus.

The ribs are strong, generally straight, showing a weak forward projection. Most ribs begin on the umbilical slope, are nearly always strong on the lower part of the sides where they commonly, but by no means invariably, develop a bullate tubercle. Near the top of the side there is a tubercle developed that is the most persistent series in the genus, sometimes developing into great spires; only in one aberrant species, '*A*'. *cornigerum* Crick, are they lost.

Above this upper lateral tubercle is the angular shoulder, on which the ribs show a further forward projection, and nearly terminate at a series of ventro-lateral tubercles, although there is usually a weak connecting rib across the venter between pairs of ventro-lateral tubercles. This connecting rib is sometimes lost in the middle or later stages of ontogeny. The upper lateral and ventro-lateral tubercles may be bullate or clavate or neither. The venter is flat. On the early whorls there is a siphonal tubercle which may persist as strongly as the ventro-lateral tubercles to considerable diameters, but more commonly weakens and disappears before a diameter of 100 mm. is reached.

The above two paragraphs apply to full-length (primary) ribs. In young individuals there are one, or more rarely two, shorter (secondary) ribs intercalated between any two primary ribs. Such ribs begin gently, above the level of the basal lateral tubercles on the primary ribs, and thereafter behave as primary ribs. The persistence of secondary ribs varies greatly from species to species, and in some forms (which might be better classified as *Calycoceras*) lasts throughout the septate stage.

In some species the ribbing weakens slowly during ontogeny, but the very slight amount of change in any features during the ontogeny of the septate portion was even noted by Brongniart (1822).

Acanthoceras is a large genus growing up to a third of a metre or more in diameter. Such large specimens have generally been obtained from the Chalk, and it is not always possible to say from these how much space is occupied by the adult body chamber.

De Grossouvre (1894) in amending and restricting Neumayr's genus, laid stress on the suture line: 'Je réserverai donc le nom générique d'*Acanthoceras* aux formes à lobes et selles large, de forme approximativement rectangulaire, dont le premier lobe latéral présente une fourche terminal nettement accusée, et je prendrai comme type de ce genre *Acanthoceras rhotomagense*.' We would add that the lateral lobe is narrow compared with the first lateral saddle in the middle of which an accessory lobe, nearly half as long as the first lateral lobe, is commonly developed; neither de Grossouvre (1894, fig. 12) nor d'Orbigny (1841, pl. 106, fig. 3) shows this adequately.

All the above description is based on internal moulds, and it should be noted that the shell of *Acanthoceras* is thick (possibly as much as 2 mm. in some large specimens) so that the appearance of an individual with the shell is somewhat different from the mould. On the shell the second-order ribs, for example, begin lower on the sides, and even the first-order ribs are stronger on the umbilical slope than is apparent from the mould. Moreover, the shell possesses decoration not present on the mould: strong striations parallel to the ribbing are common (see Sharpe 1855, pl. 16, fig. 2*a*). In addition there is sometimes a faint longitudinal striation.

Relations with other genera. Even as restricted by De Grossouvre (1894) *Acanthoceras* at first included many forms which are today separated generically. Indeed, every genus in the family, with the exception of *Mammites* Laube and Bruder, 1886, has been erected

since 1894. Happily, only a few of these newer genera are liable to be confused with *Acanthoceras* s.s.

Mantelliceras Hyatt, 1903; type species *Ammonites mantelli* J. Sowerby; Lower Cenomanian. This genus is the ancestor of *Acanthoceras*, but probably by way of *Calycoceras*. Early writers tended to distinguish *Mantelliceras* by the absence of siphonal tubercles, but this distinction can only be used on juveniles. More distinctive of *Mantelliceras* is the persistence of short ribs, the disappearance of lower ventro-lateral tubercles at diameters of 80 mm. or earlier (in rare individuals it may last longer), and the disappearance of all tuberculation on the adult, maturity usually being reached at much smaller sizes than in *Acanthoceras*; moreover, some species of *Mantelliceras*, including the type, possess mid-lateral tubercles.

Calycoceras Hyatt, 1900; type species *Ammonites navicularis* Mantell; Middle to Upper Cenomanian. *Calycoceras* appears to be derived from *Mantelliceras* early in the Middle Cenomanian by the development of a siphonal tubercle, and by increasing the relative strength of the umbilical ribbing or bullae. *Calycoceras* retains the short ribs and ventral ribbing of *Mantelliceras* but develops (in some species) the angular whorl section of *Acanthoceras*, and like *Acanthoceras* often loses the siphonal tubercles long before the ventro-lateral ones. Hence some *Calycoceras* can only be distinguished with certainty from *Mantelliceras* by strong umbilical bullae, e.g. *Calycoceras cottreaui* (Collignon), *C. nitidum* (Crick). However, there are some species of *Mantelliceras* which also have umbilical bullae in the middle stages, e.g. *Mantelliceras lymense* (Spath) (Pervinquière 1907, pl. 16, fig. 16) that Spath (1926) thought was an Upper Cenomanian *Eucalycoceras*. These distinctions still leave forms whose generic attribution is difficult. Thus *Acanthoceras whitei* Matsumoto from southern India, figured by Kossmat (1897, pl. 1, fig. 1), which retains short ribs to a diameter of nearly 100 mm., and whose ribbing does not weaken on the venter, might be better assigned to *Calycoceras*. In *Acanthoceras* gr. *jukes-brownei* (Spath) short ribs are retained to a diameter of more than 300 mm.

Euomphaloceras Spath, 1923; type species *Ammonites euomphalus* Sharpe, 1855; Middle and Upper Cenomanian. *Euomphaloceras* develops from *Acanthoceras* in the Middle Cenomanian by the intercalation of extra ribs or extra tubercles on the venter, e.g. '*Acanthoceras*' *inermis* Pervinquière (= *A. evolutum* Spath). We figure examples of these transitional forms from Rouen (Pl. 92, fig. 4; Pl. 93, fig. 1).

Protacanthoceras Spath, 1923; type species *Ammonites Bunburianus* Sharpe; Middle and Upper Cenomanian. The stratigraphically persistent distinctive feature of this tiny genus, is the triple row of equal-sized clavae, rather closely spaced on the venter. On the adult body chamber of some species these tubercles fuse into smooth chevron-ribs across the venter. The early species (where the genus is diverging from *Acanthoceras*) grade into flat-sided spinose *Acanthoceras*. As has been remarked by Thomel (Porthault *et al.* 1966) *Protacanthoceras* has also been misused for species such as *Eucalycoceras harpax* (Stoliczka) which have strong ribbing on the sides, and grow to a much greater size.

Plesiacanthoceras Haas, 1964 (= *Paracanthoceras* Haas, 1963, non Furon, 1935); type species *Metoicoceras Wyomingensis* Reagan 1924. We agree with Matsumoto and Obata (1966) in regarding this as a synonym of *Acanthoceras*. Haas gave two distinctions: (i) the ventral tubercles 'are, even at an early stage, very inconspicuous and strongly clavate and then assume the aspect of an intermittent keel which soon fades away'. This

could be part of a description of the holotype of *Acanthoceras rhotomagense*. (ii) 'Also the ribs persist into maturity in *A. rhotomagense*, in contrast to the present form.' The abundant European and African material shows that the persistence or disappearance of ribs may be no more than a sub-specific difference. Moreover, in *Acanthoceras wyomingense* (Reagan) itself low, broad ribbing persists at least to a diameter of 220 mm.

Acanthoceras rhotomagense (Brongniart)

The *Acanthoceras rhotomagense* population from Rouen can be divided into 5 morphological varieties as described below. The general features of the population are: *Acanthoceras* with between 15 and 30 ribs per whorl; short ribs are only present in early growth-stages; the siphonal tubercle is lost early in development. Compressed individuals have weak ribs and tubercles, but as the degree of inflation increases, the tuberculation and ribbing become progressively stronger.

Acanthoceras rhotomagense (Brongniart 1822) forma typica

Plate 88, figs. 1–5; Plate 89, fig. 1; text-figs. 2, 6*b*, 7

1822 *Ammonites Rhotomagensis* Brongniart, p. 606, pl. 6, fig. 2.
?1867 *Ammonites Rothomagensis* Lamk; Guéranger pars; pl. 2, figs. 2 and 6 only.
1912 *Acanthoceras rhotomagensis* Defrance in Brongniart; Douvillé, fiche 238.
1956 *Acanthoceras chasca* Benavides-Cáceres, pp. 466–7, pl. 53, figs. 1–4.

Lectotype. Selected by Douvillé (1912); the specimen figured by Brongniart in Cuvier and Brongniart 1822, pl. 6, fig. 2, now in the Sorbonne, Paris.

Diagnosis. Acanthoceras with flat sides, barely depressed to barely compressed whorl sections, and 21–3 ribs per whorl. The short ribs are lost at an early growth-stage (normally by about 40 mm. diameter). There are moderately strong umbilical bullae,

---

EXPLANATION OF PLATE 88

All figures are of natural size. Specimens are coated with ammonium chloride. All ammonites are from the fossil-bed of the Craie de Rouen.

Figs. 1–5. *Acanthoceras rhotomagense* Brongniart. 1*a*, 1*b*, Side and ventral view of R8. 2*a*, 2*b*, Ventral and side view of S14. 3*a*, 3*b*, 3*c*, Ventral, front and side views of a plaster-cast of the lectotype in the Sorbonne; cast kindly provided by Mme É. Basse de Ménorval. 4*a*, 4*b*, Side and front views of a juvenile, A635f. 5, Original figures of the lectotype by Brongniart in Cuvier and Brongniart, 1822, pl. 6, fig. 2.

Figs. 6*a*, *b*. *Acanthoceras rhotomagense* intermediate between var. *subflexuosum* Spath and var. *clavatum* var. nov. Front and side views of S11.

EXPLANATION OF PLATE 89

All figures are of natural size except fig. 3*c*. Specimens are coated with ammonium chloride.

Figs. 1*a–c*. *Acanthoceras rhotomagense* (Brongniart); from quarry on Chard side of boundary fence, ½ mile north of Tytherleigh, near Chardstock, Devon; presumably from the Middle Cenomanian basement bed of the Chalk; ventral, front and side views of C 73088.

Figs. 2*a*, *b*. *Acanthoceras rhotomagense* var. *sussexiense* (Mantell); from fossil-bed of the Craie de Rouen; individual showing change from normal to pathological condition; front and side views of C 74797.

Figs. 3*a–e*. Spinose *Calycoceras* with an *Acanthoceras* nucleus; from fossil-bed of the Craie de Rouen. *a*, *b*, Side and ventral views. *c*, Side view ×2. *d*, *e*, Side and ventral views, all of S9.

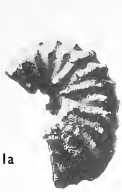
1a


1b


2a

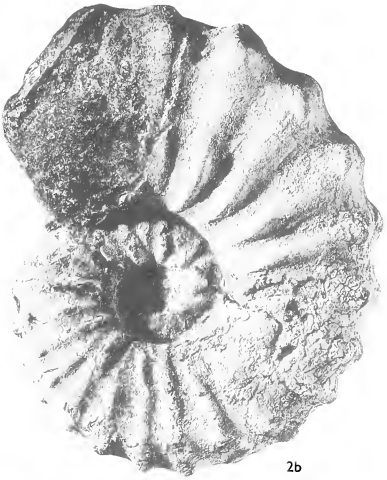
2b


6a


3a


3b


3c


6b


4a


4b

5

KENNEDY and HANCOCK, *Acanthoceras* from Rouen

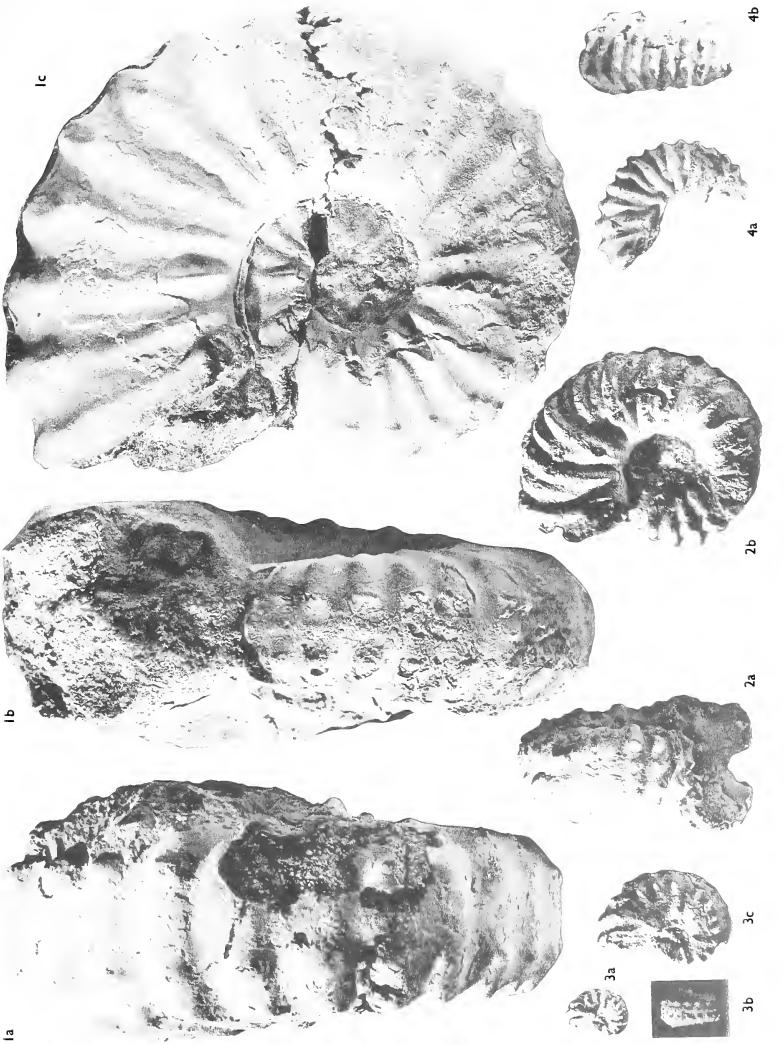

KENNEDY and HANCOCK, *Acanthoceras* from Rouen

round to clavate lower ventro-lateral tubercles, clavate upper ventro-lateral and siphonal tubercles. The siphonal tubercles are lost early in ontogeny.

Description of lectotype. The lectotype is a small, wholly septate, phosphatic internal mould. The umbilicus of one side of the specimen is filled by phosphatised sediment.

The specimen is moderately evolute, about two-fifths of the previous whorl being covered. The whorl section is barely depressed; in intercostal section the sides are flat, the shoulders round, and the venter flat. The costal section is polygonal, approximately a square with the corners truncated, the flat sides slightly convergent; the shoulders are flat and the venter is slightly depressed. The umbilicus is small, quite deep, with a round, undercut wall and a round shoulder.

There are 21–2 ribs at a diameter of 38·5 mm., alternating more or less regularly long and short. Each long rib arises at the umbilical seam, strengthens across the umbilical wall and develops an elongate umbilical bulla on the lowest part of the side. On the sides the ribs are moderately strong, becoming increasingly prominent as the diameter increases. They are straight, and slightly narrower than the interspaces. All bear a well-marked lower ventro-lateral tubercle which is slightly bullate. This is connected by a strong, round, forwardly directed rib to a slightly clavate and stronger upper ventro-lateral tubercle. The ribs are slightly depressed between these two tubercles.

The upper ventro-lateral tubercles are connected across the venter by a broad, low, round rib, lower than the upper ventro-lateral tubercles, and bearing a clavate siphonal tubercle. This siphonal tubercle is weaker than the upper ventro-lateral tubercles even at the earliest stage visible (approx. 15 mm.).

The shorter ribs arise gently some way up the sides and become equal to the long ribs at the shoulder and across the venter. Some are tenuously connected to the umbilical tubercles of the long ribs. The last three ribs are all long.

The suture is simple and of normal *Acanthoceras* type.

Discussion. This form is an intermediate between *A. rhotomagense* var. *subflexuosum* and *A. rhotomagense* var. *sussexiense.* If it had not been the type form of the genus we should not have felt it necessary to give a name to it; its characters are not sufficiently distinctive for it to be easy to assign a specimen to it. It is not even a common form like *A. rhotomagense* var. *sussexiense*: indeed, we have been unable to find anywhere another specimen identical with the lectotype. This is the more disturbing when one recalls that the lectotype is relatively small (less than 40 mm. in diameter) so that the ontogeny may be somewhat different from what we believe. However, we have seen sufficient closely comparable material to be certain that: (i) This is a variety which loses its shorter ribbing at a comparatively early stage: the last three ribs on the type all start at the umbilical edge, but in other specimens short ribs can occur later than this—to diameters of 50–60 mm. (ii) This is not the variety which gives rise to the Mid-Cenomanian *Euomphaloceras*: these all seem to be offshoots of *A. rhotomagense* var. *sussexiense* whatever detailed pattern the extra decoration on the venter takes.

There is an adult specimen in the Rouen museum (uncatalogued but labelled 7 on one side) with a diameter of 375 mm., although the aperture is missing and there is only a quarter whorl of body chamber (which has begun to become more evolute). On the body chamber, which begins at 305 mm., the angular whorl shape seen on phragmocones is maintained; the two ventro-lateral tubercles are joined by a rib of about the same

height, whilst pairs of upper ventro-lateral tubercles are set only 27 mm. apart across the ventral depression. On the septate portion the ventro-lateral tubercles are not clavate, and the umbilical bullae are no more than abrupt terminations of the bottom end of the ribs. The ribbing is directed slightly forward.

We figure an adult specimen from England (WJK 2466) which is very close to *A. rhotomagense* although slightly transitional to *A. rhotomagense* var. *clavatum* in that the ventro-lateral tubercles on the late septate portion are clavate (text-figs. 6*b*, 7). The body chamber occupies two-thirds of the last whorl, and the aperture is simple, with

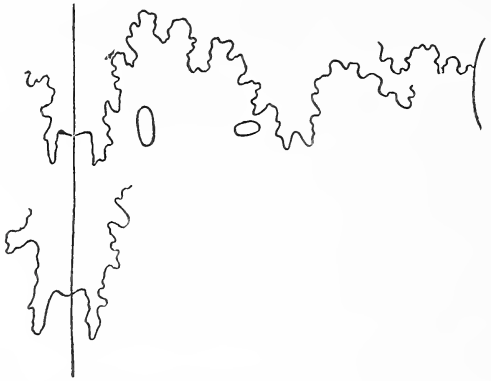

TEXT-FIG. 2. Suture line of the lectotype of *Acanthoceras rhotomagense* (Brongniart). After Douvillé 1912; magnification not stated.

a gently sinuous margin. The tubercles weaken on the body chamber, as strong, sharp ribs develop which pass right across the venter. This body chamber decoration is similar in many species of *Acanthoceras*, making it difficult to identify isolated body chambers.

Both Mantell's and Brongniart's works were published in 1822. We have accepted the general view that Brongniart's *Ammonites rhotomagensis* has priority over Mantell's *Ammonites sussexiensis* (see Sharpe 1853–6, p. 34). This view is not invalidated by the fact that Brongniart had already seen Mantell's plates whilst he was writing his own work; and Mrs. Mantell's execrable figures of this species could never have given Brongniart the idea he was describing a closely allied form.

A. rhotomagense is distinguished from *A. r.* var. *sussexiense* by the more compressed whorl section, weaker umbilical and lower ventro-lateral tubercles, giving an impression of longer ribs; the siphonal tubercle is also lost earlier.

It is distinguished from *A. r.* var. *subflexuosum* by the stronger tuberculation, more widely spaced ribs, and commonly by the narrower, flat venter.

Acanthoceras adkinsi Stephenson (1953, pp. 200–1, pl. 47, figs. 3, 4) is very close to *A. rhotomagense* differing with certainty only in the maintenance of short ribs to a

diameter of at least 74 mm. The slightly greater whorl compression of *A. adkinsi* cannot itself be regarded as even a subspecific difference.

Acanthoceras stephensoni Adkins (1928, p. 246, pl. 31, figs. 1, 2) which Matsumoto and Obata (1966) say 'is closely allied to the broadly ribbed variety of *A. rhotomagense*', is distinguished by flat, unribbed flanks.

Acanthoceras rhotomagense var. *subflexuosum* Spath 1923

Plate 90, figs. 1–4; text-fig. 8

1826 *Ammonites rhotomagensis* Defrance; J. de C. Sowerby v. 6, p. 25, pl. 515, fig. 1.
1867 *Ammonites Rothomagensis* Lamk; Guéranger pars, pl. 2, figs. 1 and 5 only.
1923 *Acanthoceras subflexuosum* sp. nov.; Spath, p. 144.
?1940 *Acanthoceras* cf. *subflexuosum* Spath; Fabre, p. 233.
1951 *Acanthoceras subflexuosum* Spath; Wright and Wright, p. 28.

Holotype. BM 43983a, from the Lower Chalk of Sussex (figured by J. de C. Sowerby 1826, v. 6, pl. 515, upper figure), original designation by Spath 1923, p. 144 n. 3.

Diagnosis. This is a form of *Acanthoceras rhotomagense* with a similar degree of compression to *A. rhotomagense* but with a broader, faintly round, venter. The tuberculation, other than some umbilical bullae, is weaker. The ribbing is slightly denser (typically 25–9 ribs per whorl), and is distinctly, albeit weakly, flexuous.

Description of holotype. The holotype is a small, slightly distorted and abraded, limonite-coated, composite internal mould in grey chalk. Most of the inner whorls and all the ornament of one side have been destroyed. The suture is not visible.

The holotype is moderately evolute, about a quarter of the previous whorl being covered. The whorl section is compressed; in intercostal section the sides are flat and almost parallel, the ventro-lateral shoulders broadly round and the venter flat. The costal section is compressed-polygonal, with the greatest breadth at the umbilical bullae. The umbilicus is small, moderately deep, with a steep umbilical wall and round umbilical shoulder. There are 28 ribs at a diameter of 58 mm., alternating more or less regularly long and short. The long ribs appear to arise at the umbilical seam, strengthen across the umbilical wall, and develop into elongate umbilical bullae just outside the umbilical shoulder. On the sides the ribs are strong, broad, and round, as wide or slightly narrower than the interspaces. The ribs are gently flexed, each passing slightly forwards across the lower part of the sides, and then backwards to a very weak bullate lower ventro-lateral tubercle, then forwards again to a weak clavate upper ventro-lateral tubercle. The venter is rather narrow, with a row of weak clavate siphonal tubercles, connected to the similar upper ventro-lateral tubercles by low, broad, round ribs, separated by narrow interspaces. The shorter intercalated ribs extend across the upper two-thirds of the flank and the venter.

Discussion. This name was introduced by Spath without any description. The holotype is both a juvenile and an extreme variant of this variety, having unusually strong ribs and being unusually compressed, although this latter character may be very slightly exaggerated by crushing.

The ribbing in this variety is weak, but that in *Acanthoceras flexuosum* Crick is even weaker. Moreover, the ribbing on Crick's species has a rather strong forward

TABLE 1. Measurements of *Acanthoceras*: all specimens are from the fossil bed in the Craie de Rouen except the holotype of *A. rhotomagense* var. *subflexuosum*, the lectotypes of *A. r.* var. *sussexiense* and *A. r.* var. *confusum*, the paralectotype of *A. r.* var. *confusum*, C73088, and WJK 2466.

Collection key: S = Sorbonne; A = École des Mines, Paris; C (or number without prefix) = British Museum (Natural History); GSM = Institute of Geological Sciences, London; CC = J. M. Hancock collection; R or WJK = W. J. Kennedy collection.

Measurements of diameter, whorl height, and whorl width have been made between ribs; equivalent measurements across ribs are obviously greater. When ribbing and tubercles are taken into account, whorl sections often appear more compressed than intercostal measurements of whorl height and whorl width would indicate. a. = approximately.

Specimen	*Diameter*	*Whorl height*	*Whorl width*	*Width of umbilicus*	*Number of ribs on last whorl*	*Number of primaries*	*Number of secondaries*
Acanthoceras rhotomagense forma typica							
Holotype (Sorbonne)	37·8	17	19·6	8·3	21	11	10
S13	60·5	27	27·8	16·6	19	13	6
S14	87	37·3	39 a.	15·8	22	15	7
S31	85·5	(34·5)	(37·8)	28	18 a.	14 a.	4 a.
S18	39	17·4	20	11	22	10	12
A636	32	16	18 a.	8·5	23	11 a.	12 a.
A646	74·5	32	33 a.	21	22	18 a.	4 a.
R6		24	26				
Rouen Mus. adult	375 a.	132			23	23	0
C73088	109	42·5		36	25	21	4
Acanthoceras rhotomagense intermediate between var. *clavatum* and *rhotomagense* s.s.							
S24	52·6	20·7	21·8	15·6	21	13	8
S25	85·6	35·9	36·7	25·3	23	17 a.	6 a.
A645	48·0	20·3	21·5	13·8 a.	22–3 a.	11 a.	11 a.
A649	80·0	32·5	35·9	25·5	17	13	4
A659	62·9	25·7	27 a.	19·8	18	14	4
WJK 2466	270	90	95	100	20	20	0
Acanthoceras rhotomagense var. *clavatum*							
Holotype							
A660	90·8	36·7	38·3	27·7	22 a.	17 a.	5 a.
S15		35·2	34·5				
S21	60·8	26·6	23·9	15·9	20–1	9–10 a.	
S22		29·6	29·1	19·2	20 a.		
S23	74·3	29·8	29·6	21·7	20 a.		
Acanthoceras rhotomagense var. *subflexuosum*							
Holotype							
43983a	59·0	26·2	23·0	15·4	28–9	14 a.	14 a.
S3	114·5	45·2	49·5 a.	34·4	27		
S4	107	44·0	48·4	33·4	26	22	4
S10B	14	6·2	7		17–18 a.		
A642	59·4	26·6	28·5	16 a.	29–30	19	10–11
A651	54·7	24·9	26	14·8	27	12–14	13–15
A663	109·6	45·7	46·5	32·9	30	20–2	8–10
C74792	18·4	9·7	9	3·5	19		
Acanthoceras rhotomagense aff. var. *sussexiense-subflexuosum*							
A682	80	32·5	41 a.	23·7	27	17	10

Specimen	*Diameter*	*Whorl height*	*Whorl width*	*Width of umbilicus*	*Number of ribs on last whorl*	*Number of primaries*	*Number of secondaries*
Acanthoceras rhotomagense var. *subflexuosum* transitional to *A. r.* var. *clavatum*							
S11	59·6	25·1	24·3 a.	15·0	24		
Acanthoceras rhotomagense var. *sussexiense*							
Lectotype BM 5691	145	54·7	62	52·2	23–4	23–4	0
C1030	200	74·8	69·5	72	20	20	0
S1	98·7	36·3	47·5	31·2	24 a.		
S10A	26·5	11·2	13·8	7	17 a.		
S20	60·6	26	29·6	18·7	25	15	10
S26	49	20·6	26·5	15·9	19	16	3
S27	97·6	36	49·8		25		
S28	18·8	8·7	10·7	4·6	18	8	10
S29	26·3	10·4	14·3	7·5 a.	18		
S33	45·2	19·1	23·7	12·6	20 a.	11 a.	9 a.
A635	19·6	8·2	10·5	4·8	17	8	9
A654	92	36·3	43½ a.	36	23	22	1
A655	115	45	58	39·5	25	13–15	10–12
R3		18·6	21·8				
R11		42	50				
CC710	47	19	22·8	14·6	19	14	5
CC711		23·6	26·6				
Acanthoceras rhotomagense aff. var. *sussexiense*							
C74799	27	12·7	15	7·7	15	12	3
A644	47	20	23 a.	14·8	15	10 a.	5 a.
A674	36·8	14·9		11·2	16	9	7
Acanthoceras rhotomagense var. *confusum*							
Lectotype Guéranger, pl. 3, fig. 1					20	19 or 20	0 or 1
Paralectotype Guéranger, pl. 2, fig. 4	(70) assuming figures × 1	(26·5)		(23)	20	20?	0?
S8	90·5	34	43·5	26·8	18	14 a.	4 a.
S10D	14·2	5·3	7·9	3·2	15	8	7
S17	36	14·3	20·6	10	18 a.	13 a.	5 a.
A635d	20·3	8	12·8 a.	4·9	17	9 a.	7 a.
A637	28·1	12	16·2	7·6	16	12	4
A647	61·4	24	33½ a.	19·3	18	11	7
A653	124	51·5	68 a.	48	18	18	0
C74791	66	28	30	22	21	15	6
Transitions between *Acanthoceras rhotomagense* var. *clavatum* and *Acanthoceras adkinsi*							
S19	60	28·2	26·6	13·7	25	13	12
A650	54·2	24·3		14·0	29	12	17
CC712	51·4	24·5	22 a.	13 a.	29 a.		
Acanthoceras basseae							
Holotype S5	70·0	24·8	27·5	16·3	21	14–15	6–7
S16		21·5	24·1				
A684	49·4	21·4 a.	23·5 a.	15·3	18 a.		

sweep, and smaller but sharper lower ventro-lateral tubercles (although the sharpness may well be because the shell is preserved). *A. flexuosum* at the least is a closely allied species.

Acanthoceras adkinsi Stephenson (1953, pl. 47, figs. 3, 4) apparently belongs to the *Acanthoceras rhotomagense* group; it differs from *A. rhotomagense* var. *subflexuosum* in having fewer ribs (23 instead of 25–9); BMNH C74794 from Rouen appears to be an intermediate.

Acanthoceras rhotomagense var. *sussexiense* (Mantell 1822)

Plate 89, fig. 2; Plate 91, figs. 1–2; Plate 92, figs. 1–2; text-figs. 3, 4, 5, 6*a*

1822 *Ammonites Sussexiensis* Mantell, pp. 114–15, pl. 20, fig. 2.
1854 *Ammonites Rhotomagensis* Defrance; Sharpe, pp. 33–4, pl. 16, figs. 1*a–c*, 3*a*, *b* (figs. 2*a*, *b* transitional to *A. r. rhotomagense*).

EXPLANATION OF PLATE 90

All figures are of natural size except fig. 3*b*; all specimens are coated with ammonium chloride.

Figs. 1*a–c*. *Acanthoceras rhotomagense* var. *subflexuosum* Spath; from Lower Chalk of Lewes, Sussex. Side, front, and ventral views of the holotype 43983a.

Figs. 2*a*, *b*. *Acanthoceras rhotomagense* aff. var. *subflexuosum* Spath; unusually inflated juvenile from the fossil-bed of the Craie de Rouen. Front and side views of A635e.

Figs. 3*a–c*. *Acanthoceras rhotomagense* var. *subflexuosum* Spath; juvenile from the fossil-bed of the Craie de Rouen. *a*, *c*, Front and side views. *b*, Side view ×2, of S10B.

Figs. 4*a*, *b*. *Acanthoceras rhotomagense* var. *subflexuosum* Spath; from the fossil-bed of the Craie de Rouen. Side and front views of A663.

EXPLANATION OF PLATE 91

All figures are of natural size. Specimens are coated with ammonium chloride.

Figs. 1*a*, *b*. *Acanthoceras rhotomagense* var. *sussexiense* (Mantell); from the Lower Chalk of Hamsey, Sussex. Side and front views of the lectotype, BM 5691.

Figs. 2*a*, *b*. *Acanthoceras rhotomagense* var. *sussexiense* (Mantell); from the fossil-bed of the Craie de Rouen. Side and front views of A635a.

Fig. 3. *Acanthoceras* aff. *rhotomagense* (Brongniart) transitional to a spinose *Calycoceras*; from the fossil-bed of the Craie de Rouen. Side view of S18 (front view in Pl. 97, fig. 3).

EXPLANATION OF PLATE 92

All figures are of natural size. Specimens are coated with ammonium chloride. All from the fossil-bed of the Craie de Rouen.

Figs. 1*a*, *b*. *Acanthoceras rhotomagense* var. *sussexiense* (Mantell); Side and front views of A654; note slight asymmetry in the position of the siphonal tubercle in this individual.

Figs. 2*a*, *b*. *Acanthoceras rhotomagense* var. *sussexiense* (Mantell); Side and front views of a juvenile, S28.

Figs. 3*a*, *b*. *Acanthoceras* aff. *rhotomagense* var. *sussexiense* (Mantell). Ventral and side views of A674; note the narrow venter, relatively compressed whorl, and low rib density.

Figs. 4*a*, *b*, *c*. *Euomphaloceras* sp. close to *Acanthoceras rhotomagense* var. *sussexiense* (Mantell); Front, side, and ventral views of S6; note the rounded whorl-section and the intercalation of extra ventral tubercles.

Figs. 5*a*, *b*. An intermediate between *Calycoceras* and *Acanthoceras*. Side and front views of C74795.

Figs. 6*a*, *b*. *Acanthoceras* aff. *rhotomagense* var. *sussexiense* (Mantell). Side and front views of C74799, paralectotype of *Acanthoceras hippocastanum* (J. de C. Sowerby); note low rib density combined with relatively narrow venter.

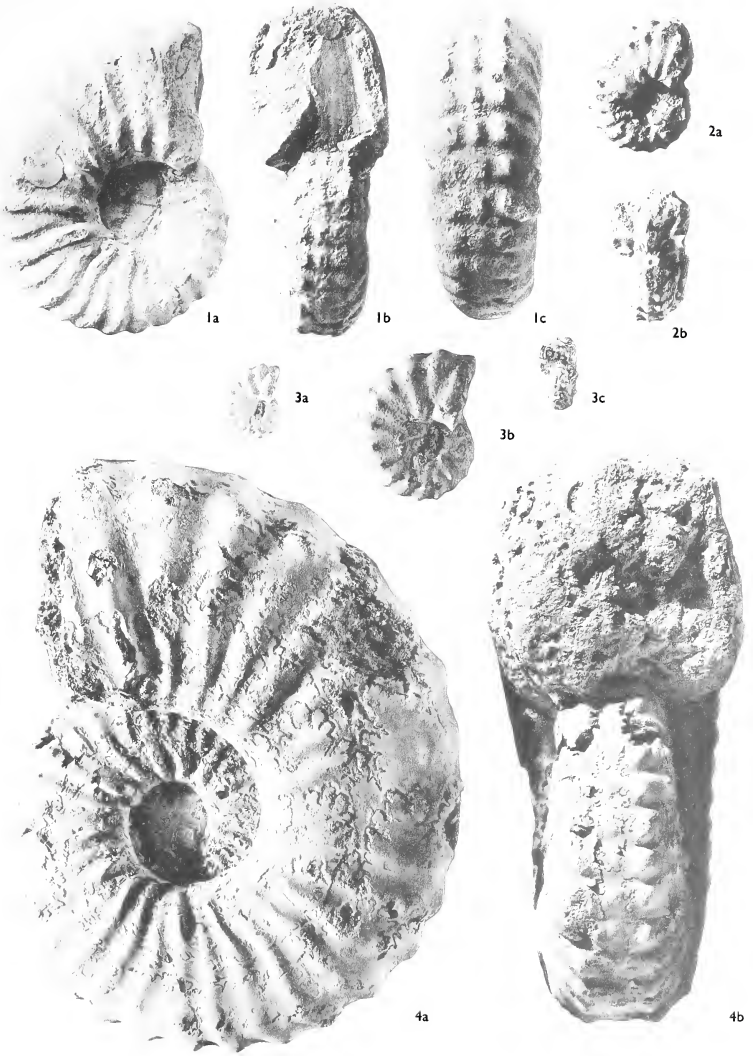

KENNEDY and HANCOCK, *Acanthoceras* from Rouen

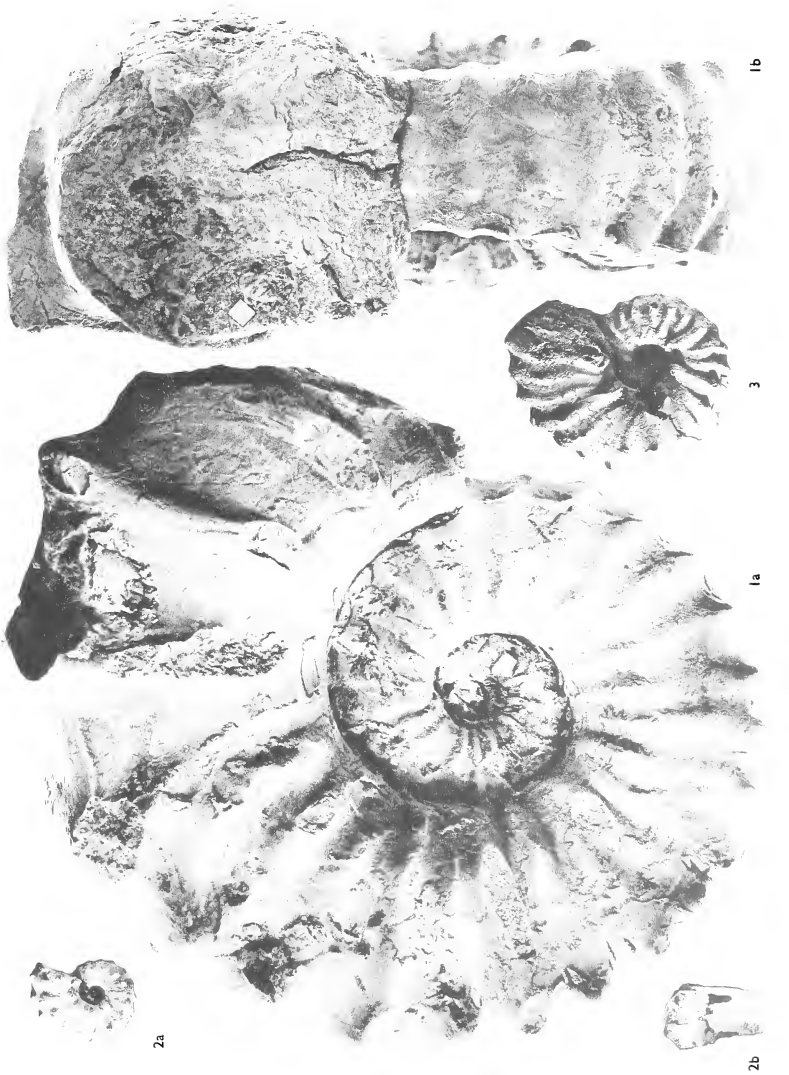

KENNEDY and HANCOCK, *Acanthoceras* from Rouen


1a


2a


2b


1b


3a


4a

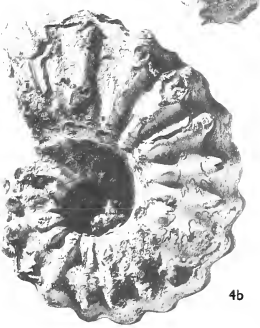
4b


4c


5a


5b


6a


6b


3b

KENNEDY and HANCOCK, *Acanthoceras* from Rouen

non 1854 *Ammonites Sussexiensis* Mantell; Sharpe, p. 34, pl. 15, fig. 1 (= *Enomphaloceras inerme* (Pervinquière)).
1863 *Ammonites rhotomagensis* Brongniart; Pictet pars; pl. 2, figs. 1*a–e* only.
1878 *Acanthoceras rhotomagensis* Brongniart; Bayle, pl. 63, figs. 1–3; ?4–5.
non 1923 *Acanthoceras sussexiense*; Spath, p. 144 n.
1926*a* *Acanthoceras vectense* Spath, p. 82.
1931 *Acanthoceras hippocastanum* Sow; Collignon, pl. 4, fig. 1.
1951 *Acanthoceras vectense* Spath; Wright and Wright, p. 28.
1951 *Acanthoceras sussexiense* (Mantell); Wright and Wright, p. 28.
1963 *Acanthoceras mirialampiense* Wright, p. 606, pl. 84, fig. 3; pl. 85, fig. 1.

Lectotype (here selected). BM 5691 from the Lower Chalk of Hamsey, Sussex, bearing Mantell's original green label, 'xx, 2'. This is possibly the original of Mantell 1822, pl. xx, fig. 2. Two smaller specimens (BM C.73637, 5690) in the Mantell collection labelled *Ammonites sussexiensis* belong elsewhere.

Diagnosis. Form of *Acanthoceras rhotomagense* characterized by a more depressed quadrate whorl section than *A. rhotomagense* itself, with strong, dense, rounded, slightly rursiradiate instead of prorsiradiate ribs, all of which are long in the middle and later growth stages. There are strong umbilical bullae and lower and upper ventro-lateral tubercles, the latter two rows fusing in the adult, and a small siphonal tubercle weakening in the middle and later stages.

Description of lectotype. This is a large, very well-preserved if slightly distorted, composite internal mould in grey chalk, with a rusty limonitic coat. Just under half the later whorl is body chamber, where the specimen develops pathological ribbing.

The coiling is evolute, about a fifth or a sixth of the previous whorl being covered. The whorl section is depressed, with the greatest breadth at the umbilical bullae; rounded quadrangular in intercostal section, with flat sides, broadly round shoulders, and a flat venter; costal section trapezoidal-polygonal. The umbilicus is broad and moderately deep, the umbilical wall round and undercut, and the shoulder round. There are 23 ribs per whorl at 77 mm. diameter, 25 at 134 mm., and 24 at 150 mm. The specimen is pathological beyond 130 mm.

All the visible ribs are long; each arises at the umbilical seam, strengthens across the umbilical wall and develops a strong umbilical bulla just outside the umbilical shoulder. The bulla is developed to a varying degree on different ribs, strengthening with increasing diameter. The ribs also become stronger with increasing diameter; they are more or less straight across the whorl sides, broad and round, equal to or slightly wider than the interspaces, subdued at mid-flank, rectiradiate in the earlier growth stages, rursiradiate in the later stages. Each rib bears a strong, slightly spinose lower ventro-lateral tubercle. From this tubercle the ribs project slightly forwards across the shoulder to a clavate upper ventro-lateral tubercle. Upwards of a diameter of 120–30 mm. the two ventro-lateral tubercles increasingly coalesce. The ribs are broad, round, and continuous across the venter, and up to a diameter of 90 mm. there is a weak clavate siphonal tubercle. At greater diameters this tubercle is lost. There is a weak siphonal depression at diameters of 120 mm. upwards.

The last septum is at a diameter of 120 mm., where there is the median siphonal depression on the ribs and the ventro-lateral tubercles have almost coalesced. The type has been damaged in life at the beginning of the secretion of its final body chamber, and as a result has developed irregular ventral ribbing, an irregularity which becomes more

pronounced on later parts of the body chamber. There are thus only four ribs on the last quarter whorl. These ribs are high, distant, and very much narrower than the interspaces, with a strong umbilical bulla and a lower ventro-lateral tubercle now flat and horn-like. There is an upper ventro-lateral tubercle present on the penultimate rib.

Discussion. The lectotype can be matched with the better-preserved material from Rouen, where it is the commonest form. This material shows that the changes during ontogeny are relatively slight (as is usual in *Acanthoceras*), the strong ornament being present from the earliest stages (see Pl. 92, fig. 2). Thus the siphonal tubercle only weakens very slowly, and during most growth stages is as strong as, or only a little weaker than the upper ventro-lateral tubercles, which are themselves weaker than the lower ventro-lateral tubercles.

There is some degree of variation in the density of the ribbing: 22–6 ribs per whorl. There is considerable variation in the persistence of short-ribbing which disappears within the range 37–60 mm. diameter.

With less inflation (sometimes accompanied by weaker decoration) there are transitions to *A. rhotomagense* (e.g. École des Mines A 658). Transitions to *A. rhotomagense* var. *confusum* are more common: in these there is increasing spinosity, fewer ribs, and sometimes increasing rib strength.

Being common, *A. rhotomagense* var. *sussexiense* has often been figured, usually under other names, particularly *A. rhotomagense* (e.g. Wright (in Arkell *et al.* 1957, L415, fig. 7) has used the figure of Bayle (1878) to illustrate the type species). *A. vectense* Spath (1926*a*) is a synonym: the apparent differences arise from the pathology of the lectotype of *A. r.* var. *sussexiense*; the holotype of *A. vectense* (GSM 7756) shows well the backward sweep of the ribs in the later stages (text-figs. 3, 4).

Those *Acanthoceras* from Rouen which show any development of *Euomphaloceras*-like multituberculation or rib insertions on the venter, are all close to *A. r.* var. *sussexiense* in general style of ornament (Pl. 92, fig. 4; Pl. 93).

Acanthoceras crassiornatum Crick (1907, p. 185) differs in having coarser, more widely spaced ribbing, a more compressed whorl section, and more strongly clavate upper ventro-lateral tubercles.

Acanthoceras robustum Crick (1907, p. 189) has weaker, broader, more widely spaced ribs, with all tubercles, except the siphonal series, weaker.

Acanthoceras quadratum Crick (1907, p. 192, pl. 13, fig. 2) has only 21 ribs at a diameter of 108 mm. compared with 25 in the lectotype of *A. rhotomagense* var. *sussexiense*.

Acanthoceras aff. *rhotomagense* var. *sussexiense* (Mantell)

Plate 92, figs. 3, 6

We have seen a number of specimens which have the decoration of *A. rhotomagense* var. *sussexiense* but which are markedly more compressed. In this respect they are transitions to *Acanthoceras simulans* Spath (Schlüter 1871, pl. 7, fig. 3), although that species has multiple siphonal tuberculation.

Acanthoceras hippocastanum (J. de C. Sowerby) (lectotype, herein designated, is the original specimen figured by Sowerby (1829, pl. 514, fig. 2, GSM 37667)) was based upon

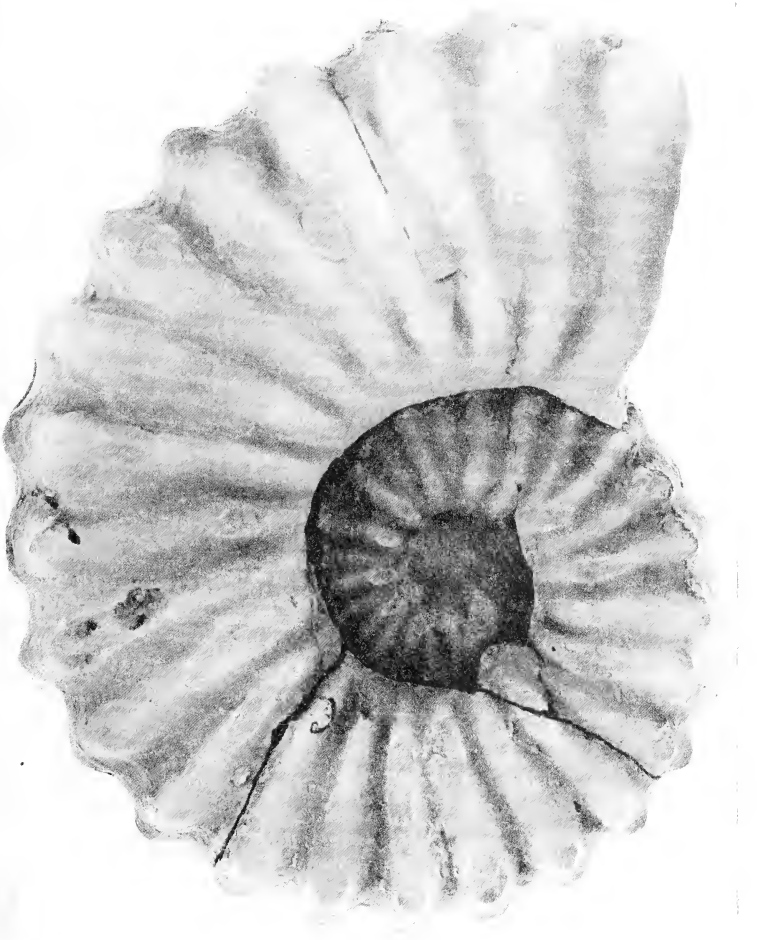

TEXT-FIG. 3. *Acanthoceras rhotomagense* var. *sussexiense* (Mantell). From Bonchurch, near Ventnor, Isle of Wight; horizon unrecorded. Side view of GSM 7756, the holotype of *Acanthoceras vectense* Spath. ×1.

TEXT-FIG. 4. *Acanthoceras rhotomagense* var. ***sussexiense*** (Mantell). Front and ventral view of specimen in fig. 3, the holotype of ***Acanthoceras*** *vectense* Spath. × 1.

TEXT-FIG. 5. *Acanthoceras rhotomagense* var. *sussexiense* (Mantell). From the fossil-bed of the Craie de Rouen. Side view of C1030; ×1.

two specimens; the paralectotype (C74799) figured in Plate 92, fig. 6, is from Rouen, and is better referred to as *A.* aff. *rhotomagense* var. *sussexiense*.

Acanthoceras rhotomagense var. *confusum* (Guéranger 1867)

Plate 94, figs. 1–4; Plate 95, fig. 1

1856 *Ammonites hippocastanum* Sowerby; Sharpe, pp. 37–8, pl. 17, figs. 4*a*, *b*, *c*; figs. 3*a*, *b* represent a form halfway to *A. r. sussexiense*.
1863 *Ammonites rhotomagensis* Brongniart; Pictet pars, pl. 2, figs. 2*a–c* and 3 only.
1867 *Ammonites confusus* Guéranger, pp. 5, 6, pl. 2, fig. 4; pl. 3, fig. 1; pl. 8, fig. 1.
non 1907 *Acanthoceras confusum* Guéranger; Pervinquière, p. 268, pl. 13, figs. 4*a*, *b*.
?1907 *Acanthoceras quadratum* Crick, p. 192; pl. 13, fig. 2.

Lectotype. The lectotype, herein designated, is the specimen figured by Guéranger (1867) in plate 3, fig. 1 and plate 8, fig. 1, from Guéranger's 'Zone à *Perna lanceolata*' in the lower part of the Middle Cenomanian of the Sarthe. We have been unable to find this specimen in the Musée de Tessé at Le Mans, and it is probably lost. Guéranger did not provide a scale for his plates but the magnification of plate 3 is almost certainly in the range 0·3–0·4. The paralectotype specimen figured in plate 2, fig. 4, is also probably lost. We reproduce Guéranger's figures in Plate 94.

Diagnosis and description. This is a form of *Acanthoceras rhotomagense* which is more depressed, and more strongly tuberculate than *A. rhotomagense* var. *sussexiense*, and which has only 19–21 ribs per whorl. The lectotype is an adult with the last 2–3 ribs of the body chamber distinctly approximated and all tuberculation lost.

Discussion. This variety represents a continuation of the trend towards coarser ribbing and stronger ornament seen in *A. rhotomagense* var. *sussexiense*, from which it is distinguished by the fewer (and sometimes heavier) ribs and a general clumsy appearance.

EXPLANATION OF PLATE 93

All figures are of natural size; both specimens are coated with ammonium chloride.

Figs. 1*a*, *b*, 2*a*, *b*. *Euomphaloceras* transitional from *Acanthoceras rhotomagense* var. *sussexiense* (Mantell), showing intercalation of extra ribs on the relatively rounded venter.

Figs. 1*a*, *b*. From the fossil-bed of the Craie de Rouen; front and side views of S2.

Figs. 2*a*, *b*. From Nogent-le-Rotrou (Eure et Loir); horizon unknown but matrix suggests Craie de Théligny (Middle Cenomanian). Ventral and side views of A657; note that the intercalatory ribs on the venter carry tubercles of equal strength to those on the primary ribs.

EXPLANATION OF PLATE 94

All figures except 1 and 2 are of natural size. Specimens except those in figs. 1 and 2 are coated with ammonium chloride.

Figs. 1 and 2. *Acanthoceras rhotomagense* var. *confusum* (Guéranger); from the upper part of the Sands with *Perna lanceolata* (lower part of Middle Cenomanian) in the Sarthe.

Fig. 1. Lectotype; copy of Guéranger 1867, pl. 3; upper figure; reduction unknown.

Fig. 2. Paralectotype; copy of Guéranger 1867, pl. 2, fig. 4; magnification unknown but possibly natural size.

Figs. 3*a–e*. *Acanthoceras rhotomagense* var. *confusum* (Guéranger); from the fossil-bed of the Craie de Rouen. Various views of different growth stages of the same juvenile, S10D.

Figs. 4*a*, *b*. *Acanthoceras rhotomagense* var. *confusum* (Guéranger); from the fossil-bed of the Craie de Rouen. Side and front views of A647.

Figs. 5*a*, *b*. *Acanthoceras* transitional between *rhotomagense* var. *clavatum* var. nov. and *adkinsi* Stephenson; from the fossil-bed of the Craie de Rouen. Side and ventral views of A650.

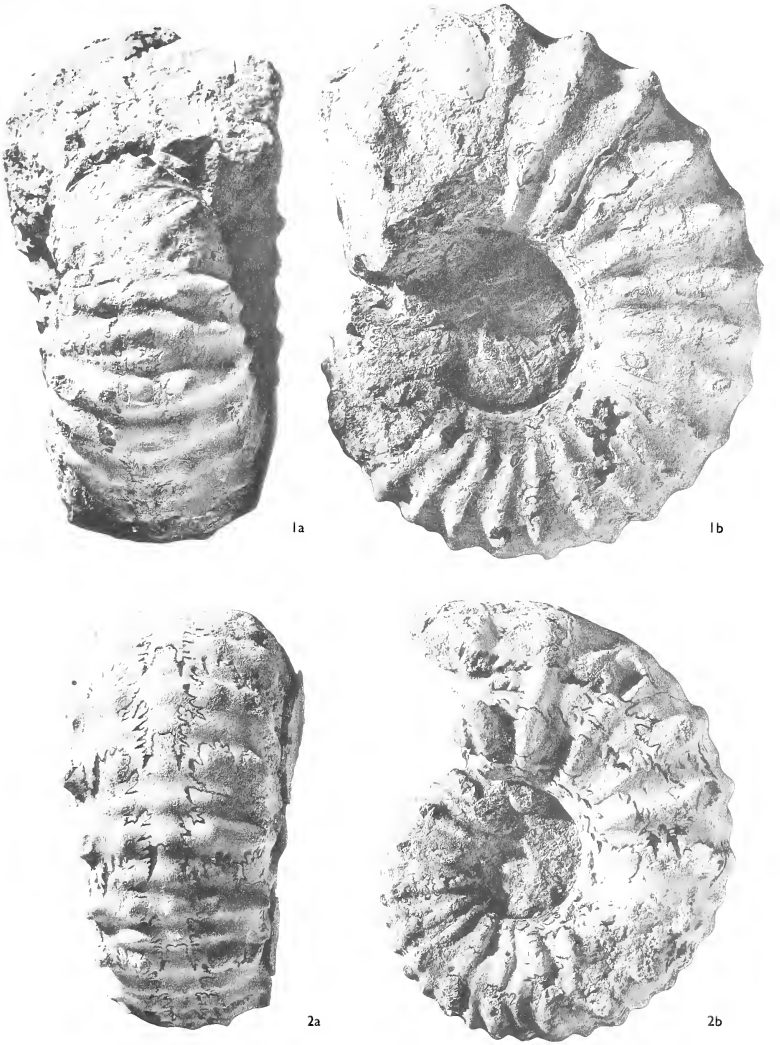

KENNEDY and HANCOCK, *Acanthoceras* from Rouen

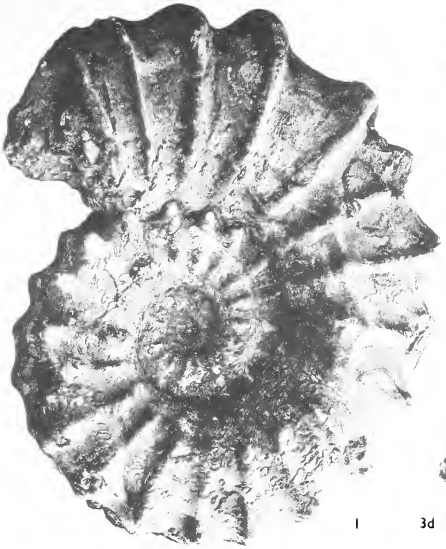

1

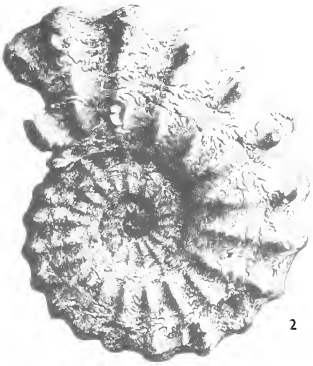

2

3d

3a

3b

3c

3e

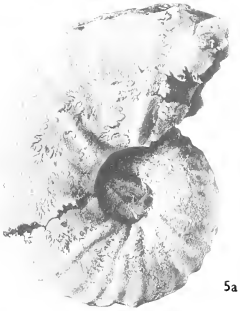

5a

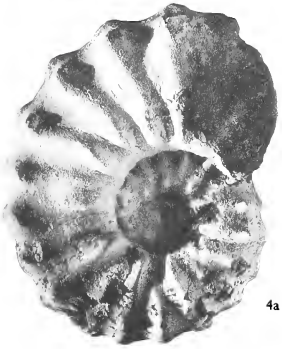

4a

4b

5b

KENNEDY and HANCOCK, *Acanthoceras* from Rouen

There are many transitions between the two varieties. As with most coarsely ornamented ammonites there is much variation in the detail of the decoration.

As can be seen from the synonymy, and from an examination of museum collections, this variety has been frequently mis-identified as *Acanthoceras hippocastanum* (J. Sowerby) which is a much younger species of the Naviculare Zone (Upper Cenomanian). It differs from *A. rhotomagense* var. *confusum* in (i) being adult at small diameters (perhaps one-fifth of the size of an adult *A. r.* var. *confusum*); (ii) being more inflated; (iii) retaining alternately short and long ribs throughout; (iv) retaining strong siphonal tubercles throughout; (v) ribbing between lower and upper ventro-lateral tubercles remaining weak. Of all figures purporting to represent *A. hippocastanum*, only Sowerby's original can in truth be referred to that species.

Acanthoceras jukes-brownei (Spath) and *A. whitei* Matsumoto both differ in retaining alternately short and long ribs throughout the septate portion.

Acanthoceras latum Crick (1907, 195, pl. 12, fig. 2, 2*a*) is a closely allied species with a rapidly expanding whorl section, fewer ribs (about 15 per whorl) which are generally weaker, a much broader venter, and particularly large spinose lower ventro-lateral tubercles. *A. quadratum* Crick has weaker ribbing than the average individual but is probably synonymous.

Acanthoceras confusum tunetana Pervinquière (1907, 268–9, pl. 13, figs. 4*a*, *b*) is a form with few ribs (17 per whorl) and finger-like horns in the position of the lower ventro-lateral tubercles, but no other tubercles: it is best considered as a separate species.

Acanthoceras sherborni Spath (= *Ammonites cenomanensis* Sharpe non d'Archiac) is close to *A. r.* var. *confusum*; the type is lost. The chief differences of *A. sherborni* are: (i) slightly fewer ribs (17 at a diameter of 155 mm.—Sharpe's figure is reduced); (ii) greater compression; (iii) the apparent loss of the lower ventro-lateral tubercle giving rise to squarer shoulders. Some of these features could be exaggerated by the imperfect preservation in the Lower Chalk of Dover.

Acanthoceras rhotomagense var. *clavatum* var. nov.

Plate 96, figs. 2–3; Plate 97, fig. 5

Holotype. A660 in the École des Mines, Paris, from the Craie de Rouen, Ste Catherine, Seine-Maritime, France, here figured as Plate 96, fig. 2.

Diagnosis. A compressed form of *Acanthoceras rhotomagense* with 21–3 weak ribs per whorl which loses umbilical bullae early in ontogeny; has weak, rounded lower ventro-lateral tubercles, and very large, markedly clavate upper ventro-lateral tubercles on each side of a depressed venter.

Description. The holotype is a well-preserved, wholly septate, phosphatic internal mould, retaining traces of phosphatised shell. It is evolute, about two-fifths of the previous whorl being covered. The whorl section is compressed, with the greatest breadth just below mid-flank. The sides are broadly rounded in intercostal section, with a narrow, high, round venter.

There are an estimated 21 ribs on the outer whorl, nearly all of which extend down to the umbilical edge. They are weak close to the umbilical wall, and strengthen across the

sides, so that they reach a maximum development at mid-flank, although there is much variation in the strength of the early formed part of the rib. The ribs are slightly flexuous, and narrower than the interspaces. Each bears a low, round lower ventro-lateral tubercle which weakens with increasing diameter. This tubercle is connected by a low, forwardly directed rib to a very large clavate upper ventro-lateral tubercle, which becomes more pronounced as the diameter increases. These upper ventro-lateral tubercles form closely spaced pairs across the venter, and rise high above the intervening flat siphonal area. There are traces of a weak, spirally elongate, siphonal swelling.

The early whorls are poorly visible but show that variation in rib strength was much more marked up to a diameter of about 35 mm., whilst a distinct siphonal tubercle (as strong as the upper ventro-lateral tubercles) was present.

The suture line is well preserved, and is of normal *Acanthoceras* type (see Pl. 96, fig. 2*a*).

Discussion. The strong upper ventro-lateral clavae, weak ribs, and compressed section are the distinctive features. We have seen two specimens transitional to *A. rhotomagense*. There are also specimens transitional to *A. rhotomagense* var. *subflexuosum* in some of which much of the ribbing is exceptionally weak.

A. rhotomagense var. *clavatum* resembles *A. wintoni* Adkins and the 'plesiotype' of

---

EXPLANATION OF PLATE 95

Both figures are of natural size, and the specimen is coated with ammonium chloride.

Figs. 1*a*, *b*. *Acanthoceras rhotomagense* var. *confusum* (Guéranger); from the fossil-bed of the Craie de Rouen. Front and side views of A653; the last suture is at a diameter of approximately 110 mm.

EXPLANATION OF PLATE 96

All figures are of natural size. Specimens are coated with ammonium chloride. All are from the fossil-bed of the Craie de Rouen.

Figs. 1*a–c*. *Acanthoceras* intermediate between *A. rhotomagense* (Brongniart) and *A. rhotomagense* var. *clavatum* var. nov. Side, ventral and front views of A659.

Figs. 2*a–c*. *Acanthoceras rhotomagense* var. *clavatum* var. nov. Side, ventral and front views of the holotype A660.

Fig. 3. *Acanthoceras rhotomagense* var. *clavatum* var. nov. Side view of a paratype S21.

EXPLANATION OF PLATE 97

All figures are of natural size. All specimens are coated with ammonium chloride except fig. 2*a*. All ammonites are from the fossil-bed of the Craie de Rouen.

Figs. 1*a*, *b*. *Acanthoceras basseae* sp. nov. Side and front views of the holotype S5.

Figs. 2*a–c*. *Acanthoceras* aff. *basseae* sp. nov. Ventral, front and side views of a specimen in the Muséum d'Histoire Naturelle de Rouen. The close spacing of the clavate tubercles on the venter, and the rapid disappearance of these tubercles shown in the ventral view, mean that this ammonite could equally well be referred to *Protacanthoceras*.

Fig. 3. *Acanthoceras* aff. *rhotomagense* (Brongniart) transitional to a spinose *Calycoceras*. Front view of S18 (side view in Pl. 91, fig. 3).

Figs. 4*a*, *b*. *Protacanthoceras* sp. Side and front views of C 74796.

Figs. 5*a*, *b*. *Acanthoceras basseae* sp. nov. Ventral and side views of a paratype A684.

Fig. 6. *Acanthoceras rhotomagense* var. *clavatum* var. nov. Front view of S21 (side view on previous plate).

Figs. 7*a*, *b*. *Protacanthoceras* sp. Side and front views of A52.

Figs. 8*a*, *b*. *Acanthoceras basseae* sp. nov. Ventral and side views of a paratype S16.

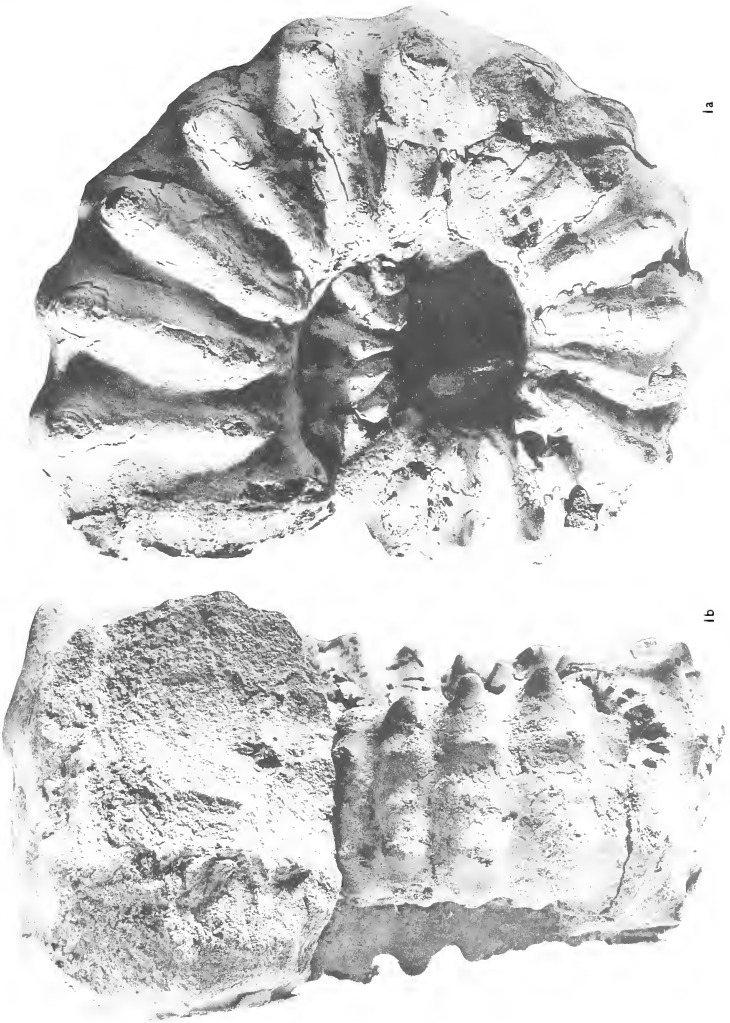

KENNEDY and HANCOCK, *Acanthoceras* from Rouen

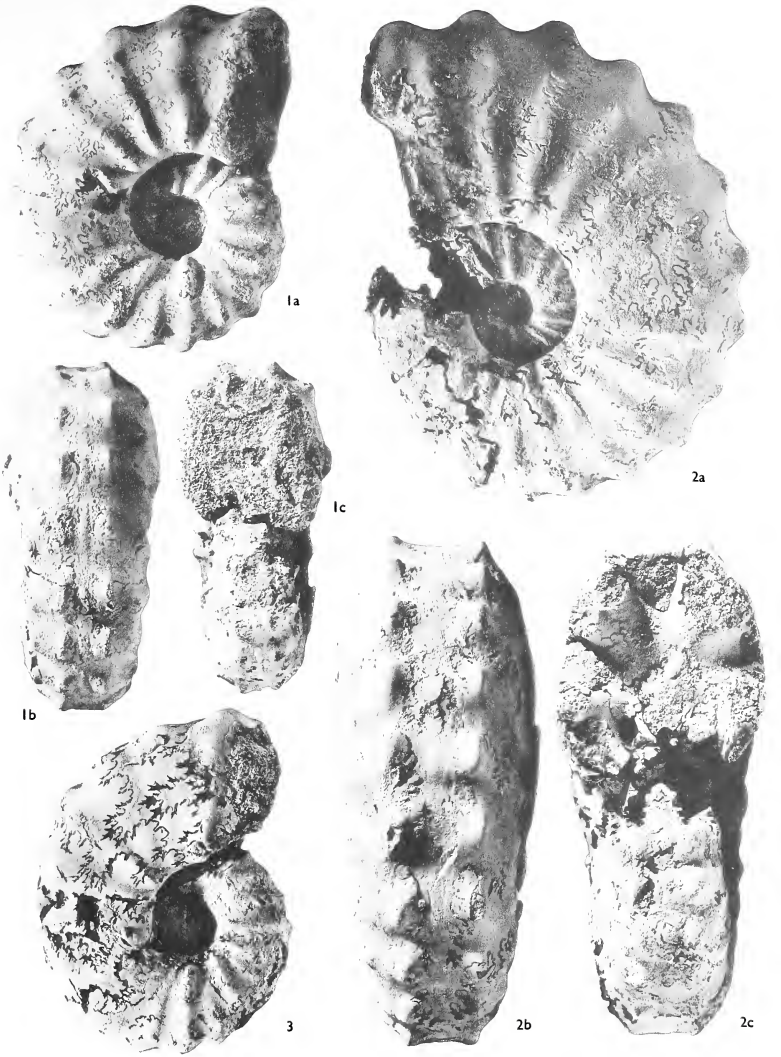

KENNEDY and HANCOCK, *Acanthoceras* from Rouen

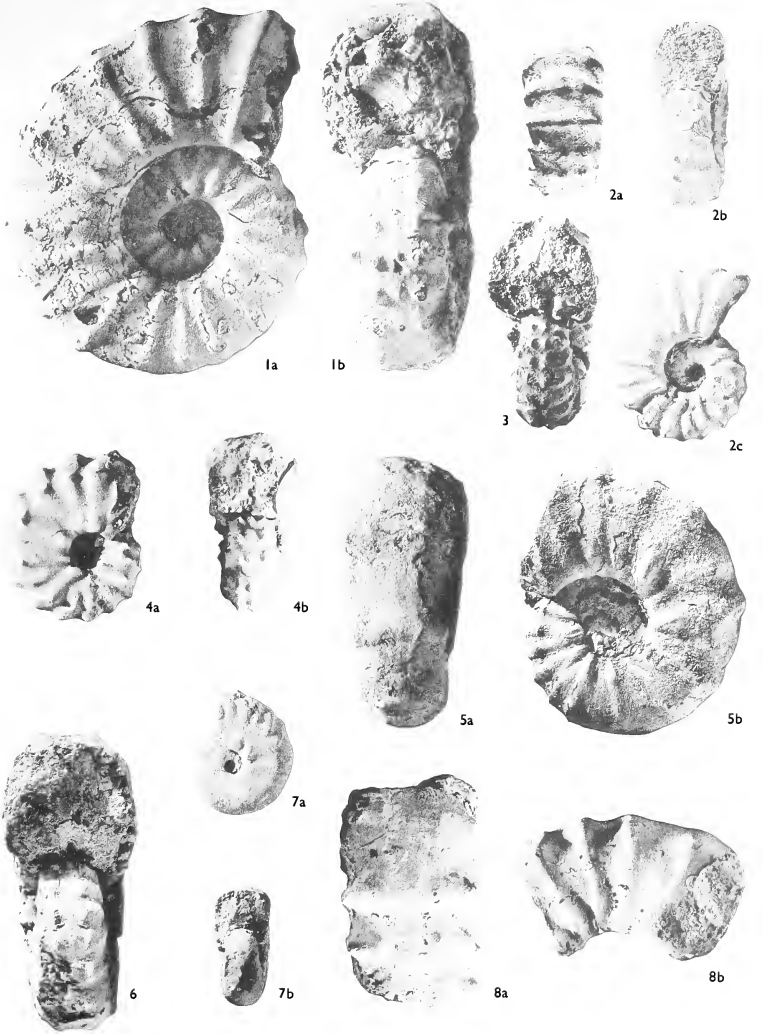

KENNEDY and HANCOCK, *Acanthoceras* from Rouen

Stephenson is even closer (1953, pl. 45, figs. 7, 8; pl. 46, fig. 1). However, in *A. rhotomagense* var. *clavatum* there are more ribs, the siphonal tubercle weakens and disappears much earlier, the ribbing on the venter is weaker (it is also weak in Stephenson's plesiotype), short ribs are absent beyond diameters of 60 mm. (and often do not reach that), and most individuals have flatter sides. *Acanthoceras* very close to *A. wintoni* occur in the Chalk basement bed at Snowdon Hill, Chard, Somerset.

There is an allied form (authors' collections, e.g. cc560) from Snowdon Hill, Chard, in which the lower ventro-lateral tubercles are completely lost, which is homeomorphous with *Mantelliceras couloni* except for the lack of short ribs.

Acanthoceras basseae sp. nov.

Plate 97, figs. 1, 4

Holotype. The unregistered specimen (bearing our label '5') in the collection of the Sorbonne figured as Plate 97, fig. 1, from the Craie de Rouen, Ste Catherine, Seine-Maritime, France.

Diagnosis. Slightly compressed, evolute, square-whorled, slowly expanding *Acanthoceras* with 18–22 ribs per whorl.

Description. The holotype is a well-preserved phosphatic internal mould, the last third of the outer whorl being body chamber. It is evolute, about a sixth of the previous whorl being covered. The whorl section is slightly compressed, with the greatest breadth at the umbilical bullae. The intercostal section is trapezoidal (the sides diverging towards the umbilicus) with rounded corners. The costal section is similar, but the corners of the trapezium are truncated.

There are 21–2 ribs on the outer whorl, most of which extend down to the umbilical seam. They are weak across the umbilical wall; 12–13 develop a pronounced, transversely elongate umbilical bulla of varying strength at or just outside the umbilical shoulder, five lack the bulla, and four arise just below mid-flank. The ribs pass across the sides with gentle flexure, weakening at mid-flank, and connect to a round lower ventro-lateral tubercle which weakens with age. This is connected by a strong rib to a weakly clavate upper ventro-lateral tubercle, which also weakens with age. A very faint low rib extends across the venter, bearing a low clavate siphonal tubercle which again weakens with age.

The early whorls are well exposed, and show strong umbilical bullae on long ribs which alternate with shorter ribs or ribs which extend to the umbilicus as mere striae. Occasional ribs branch in twos from an umbilical bulla.

The suture line is of normal *Acanthoceras* type.

Discussion. There are no transitions from *A. basseae* to any of the forms of *A. rhotomagense* described above, the slowly expanding whorl size giving all specimens a characteristic and immediately recognizable almost serpenticone appearance.

Three other specimens can be accommodated here: an unregistered fragment in the Sorbonne (our number 16); A684 in the École des Mines (Pl. 97, fig. 4), both topotypes; and an English specimen from Eastbourne (ex. J. Parmenter collection no. 7670) from the same horizon as the Rouen fossil bed.

The three complete specimens all have body chambers, whilst the other fragment is small, suggesting that this was a small species.

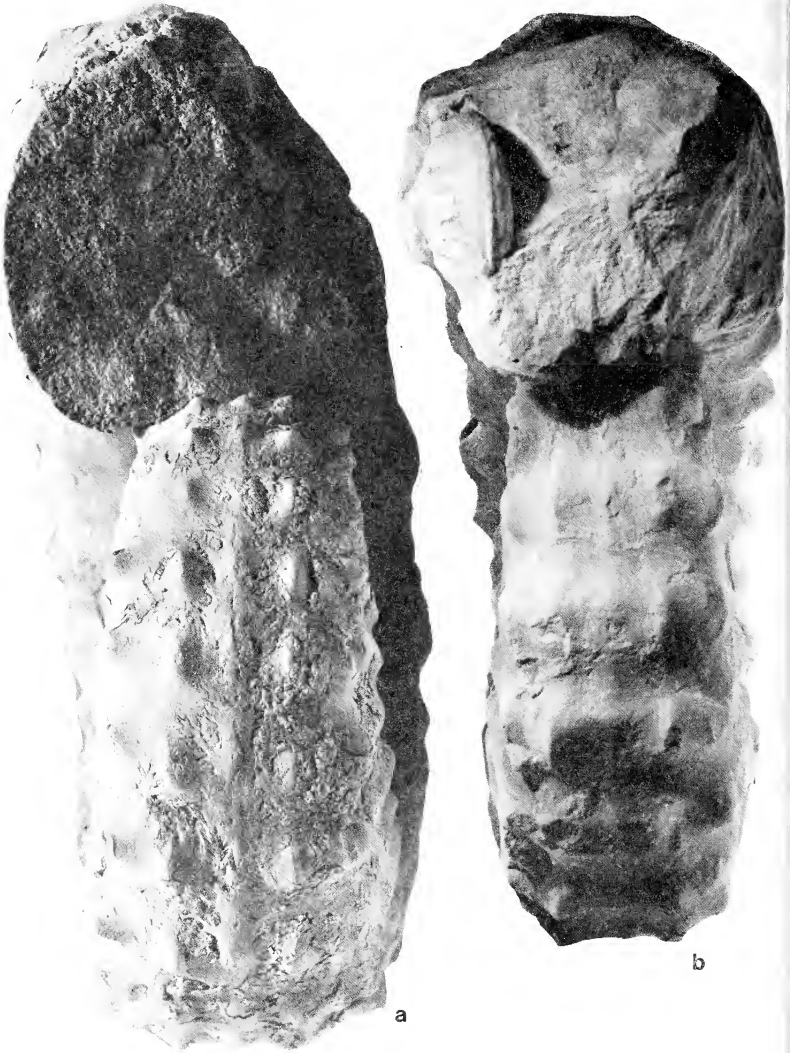

TEXT FIG. 6 (*see opposite*)

TEXT-FIG. 7. Side view of the same ammonite figured in text-fig. 6*b*. ×0·57.

TEXT-FIG. 6. *a*, *Acanthoceras rhotomagense* var. *sussexiense* (Mantell). Front view of specimen in text-fig. 5. *b*, *Acanthoceras rhotomagense* (Brongniart) transitional to *A. r.* var. *clavatum* var. nov. From Band 10 in the Lower Chalk at Folkestone = *Turrilites acutus* assemblage-horizon of the Rhotomagense Zone which is slightly higher than the fossil-bed of the Craie de Rouen. Front view of WJK 2466. ×0·66.

TEXT-FIG. 8. *Acanthoceras rhotomagense* var. *subflexuosum* Spath. From Band 9 of the Lower Chalk at Folkestone, Kent = the *Turrilites costatus* assemblage-horizon of the Rhotomagense Zone. Side view of WJK 5138. ×0·86.

There is also a specimen in the Natural History Museum at Rouen (Pl. 97, fig. 2) which is transitional between this species and *Protacanthoceras* in that it shows an early and very rapid loss of all ventral tuberculation whilst retaining ventral ribbing which is becoming chevron-shaped.

There is some superficial resemblance between *A. basseae* and *A. sherborni* (the type of which, as already noted, is lost). Sharpe's figure shows that the ribbing is more regular in *A. sherborni*, and the species is not adult until a much greater size.

GENERAL COMPOSITION OF THE AMMONITE FAUNA

Out of some 90 ammonites that we ourselves have collected at Rouen or were given as a general collection by Dr. R. P. S. Jefferies, more than two-thirds are *Sciponoceras* gr. *baculoide* (Mantell), *Turrilites costatus* Lamarck and transitions to *T. acutus* Passy, and *Schloenbachia coupei* (Brongniart) and varieties. The following, in order of abundance by genus, comprise less than a third: *Scaphites* (chiefly *S. obliquus* J. Sowerby), *Acanthoceras rhotomagense*, *Calycoceras gentoni* (Brongniart), *Hamites* (*Stomohamites*) *simplex* d'Orbigny, *Anisoceras* sp., *Puzosia* sp., *Austiniceras* sp.

As shown in this paper, museum collections also contain *Acanthoceras* transitional to *Euomphaloceras* and *Protacanthoceras*.

We have seen in the Rouen museum: *Forbesiceras* including *F. largilliertianum* (d'Orbigny), *Acompsoceras*, and several rarities we could not identify at sight (possibly Gaudryceratinae). Follet 1943 (quoted in Sornay (1959)) records a number of other forms of which the following are stratigraphically significant: *Calycoceras naviculare* (Mantell), *Mantelliceras* cf. *tuberculatus* (Mantell), *Hyphoplites falcatus* (Mantell). These may be misidentifications, or are not from the Rouen fossil bed (some museum specimens labelled 'Rouen' are undoubtedly from another bed), or represent *remanié* material such as occurs in other chalk basement beds.

AGE OF THE FAUNA

As early as 1858 Saemann recognized a 'niveau à *Ammonites rotomagensis*' in the middle part of the Cenomanian of Le Mans. This effectively Middle Cenomanian dating of the Rouen fauna is in complete agreement with the list by one of us (Hancock 1959) of the ammonites from the Sables at Grès du Mans à *Scaphites equalis* et *Turrilites costatus*.

Detailed collecting from southern England by one of us (Kennedy 1969) has provided some subdivisions of the Middle Cenomanian. The Rouen fossil bed corresponds to an horizon in the lower part of the Middle Cenomanian characterized by *Acanthoceras rhotomagense*, *Turrilites costatus* common and *T. acutus* uncommon, *Sciponoceras* abundant (and in south-east England abundant *Orbirhynchia* gr. *mantelliana*) called the *T. costatus* faunal horizon (Table 2).

Superposition in the Lower Chalk of south-east England, shows that within a metre above the horizon of the *T. costatus* assemblage occurs a *T. acutus* assemblage which is to be found in a better preservation in the Chalk basement bed at Snowdon Hill, Chard, in Somerset. In this younger fauna *Turrilites acutus* is common and *T. costatus* rare, *Calycoceras* is more common and includes spinose species of the group of *C. newboldi spinosum* (Kossmat), and *Sciponoceras* is normally rare.

It is of interest to compare the *Acanthoceras* of the two faunas. Many of the individuals in the *T. acutus* assemblage cannot at present be distinguished from some forms in the earlier *T. costatus* assemblage, e.g. *A. rhotomagense*, *A. r.* var. *sussexiense* and *A. r.* var. *confusum*, but the assemblage as a whole is different: in particular the *T. acutus* assemblage includes species we have not seen from Rouen, including: *A. flexuosum* Crick, *A. deciduum* Hyatt? (although the type is said to be from Rouen), *A.* aff. *wintoni* Adkins, *A.* aff. *sherborni* Spath.

TABLE 2. Cephalopod zonation of the Cenomanian stage in southern England and northern France. The horizons at which ammonites have been found are limited to those beds in which preservation has occurred; there may be other faunal horizons to be discovered in both the Mantelli and Rhotomagense Zones.

Zone	Faunal Horizons	beds mentioned in paper
Actinocamax plenus	Metaicaceras gaurdani	
	Metaicoceras geslinianum	
Calycaceras naviculare	(clear subdivisians nat yet recagnised in narth-west Europe; far south-east France, see Thamel in Parthault et al 1966)	
Acanthaceras rhatamagense	Acanthaceras jukes-brawnei	
	Turrilites acutus	Chalk basement bed, Snowdon Hill.
	Turrilites costatus	fassil bed, Craie de Rauen. 'Zane à Perna lancealata'.
Mantelliceras mantelli	Mantelliceras dixani	
	Mantelliceras saxbii	
	Hypaturrilites carcitanensis	

The horizon of the Rouen fauna in the Normandy coast sections is still slightly uncertain. Jukes-Browne and Hill (1903, p. 253) equated it with their bed 14 at St. Jouin (= bed 7 of Lennier = Zone à Scaphites of Cayeux 1951 = bed 8 of Rioult 1961). Moreover, M. Cayeux has kindly shown one of us four specimens of *Acanthoceras* from this bed, three of which are forms of *Acanthoceras rhotomagense* and the fourth is *Acanthoceras* transitional to *Protacanthoceras*. But the same bed is said to contain both *Mantelliceras* and *Hyphoplites* of the Lower Cenomanian. We suspect that the Rouen fauna comes from the upper part of this 4-m. bed. The records of Rioult (1961) suggest that the Rouen fauna is also occurring in his bed 10.

In Texas the whole fauna from the Lewesville member of the Tarrant Unit, described by Stephenson (1953), is very close, but is probably slightly younger. This conclusion is

supported by the occurrence of *Turrilites* aff. *acutus* (= *T. dearingi* Stephenson) in the same fauna.

The fauna from the north end of False Bay in Zululand, described by Crick (1907), is slightly enigmatic. Apart from species not known elsewhere, much of the fauna correlates with the *Turrilites acutus* assemblage, but *A. quadratum* Crick is probably synonymous with *A. r. confusum* and *A. latum* Crick is close. It is at least possible that several horizons are represented.

CONCLUSIONS

An examination of *Acanthoceras* populations from the Middle Cenomanian Craie Chloritée of Rouen shows that most individuals belong to a single species, *Acanthoceras rhotomagense*. This species is highly variable: some individuals are compressed, with weak ribs and tubercles, others are inflated, expanding rapidly, and bearing coarse ribs and tubercles. Five names are useful to describe the population, as shown in text-fig. 9.

In accommodating almost the whole range of *Acanthoceras* from Rouen into five varieties, we have been influenced not only by numerous transitional specimens between varieties, but by the existence of individuals which combine characters of apparently disparate varieties. Thus, whilst *A. r.* var. *sussexiense* apparently grades naturally into *A. r.* var. *confusum*, a specimen such as BMNH C74791 combines the general decoration of *A. r.* var. *confusum* with a rib count and a whorl compression of *A. rhotomagense*. Such anomalous forms are sufficiently common to highlight the danger of creating new species of *Acanthoceras* on the basis of single specimens. This variation is comparable to that seen in many Cretaceous ammonites we have examined. Thus there is no doubt that many *Calycoceras*, *Mantelliceras*, and *Schloenbachia* assemblages, at present divided into many 'species', represent but a single population.

It is also clear that *Acanthoceras* populations from successively higher horizons can be recognized elsewhere. Thus the faunas from Snowdon Hill, Chard (Somerset), are from a slightly higher horizon, and show a slightly different population structure. It is possible to collect individual specimens from this locality which fall within the range of the Rouen material, although the populations differ. These sort of observations make detailed synonymies difficult, because individual specimens from unknown horizons elsewhere in the world may hardly bear separation from the forms named here, although the populations whence they are derived may have a structure quite different from the Rouen assemblage. This seems to be one of the greatest difficulties of ammonite systematics. *Acanthoceras* as described by Crick (1907), Stephenson (1953), and Wright (1963) are particularly difficult to place in this respect.

We should regard the following *Acanthoceras* as being of the *rhotomagense* group: *A. adkinsi* Stephenson, *A. bellense* Adkins, *A. crassiornatum* Crick, *A. expansum* Crick, *A. flexuosum* Crick, *A. hazzardi* Stephenson?, *A. laticostatum* Crick, *A. latum* Crick, *A. munitum* Crick, *A. quadratum* Crick, *A. robustum* Crick, *A. sherborni* Spath, *A. stephensoni* Adkins, *A. tapara* Wright, *A. tarrantense* (Adkins), *A. wintoni* Adkins. These are characterized by: (i) early loss of short ribs so that all the ribs are the same length on middle and late growth stages; (ii) loss of the siphonal tubercle during growth; (iii) flat sides. They characterize the early part of the Middle Cenomanian.

This group of ammonites has an almost world-wide distribution in the Middle Cenomanian. It certainly occurs in north-west Europe, South Africa, Madagascar,

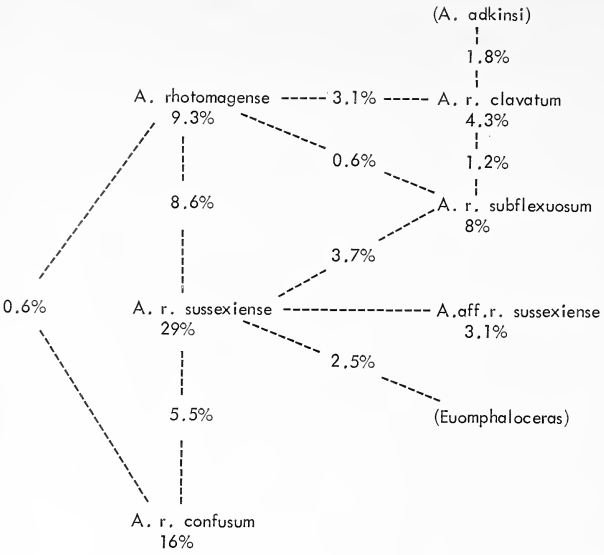

TEXT-FIG. 9. Diagrammatic relation between varieties of *Acanthoceras* found in the Craie de Rouen with percentages of the different forms based on the identification of 162 specimens, mainly in museum collections. Percentages set half-way between two names represent intermediate forms.

Australia, Peru, and Texas. It is apparently absent in the western interior of the United States where its place is possibly occupied by *A. amphibolum* Morrow and its relatives; Matsumoto and Obata (1966) suggest that *A. hazzardi* of Texas is probably conspecific with *A. amphibolum*.

Acanthoceras such as *A. jukes-brownei* and *A. whitei* retain alternately long and short ribs to large diameters, and in our experience characterize the upper part of the Middle Cenomanian.

Acanthoceras hippocastanum is an Upper Cenomanian form as discussed on p. 479.

When *Acanthoceras* from Britain are fully described there seems little doubt that a far more rational taxonomy will prevail, whilst international correlation of the divisions of the Middle Cenomanian will be possible.

Acknowledgements. This work would not have been possible without the help of the staff at the following museums: the Sorbonne, Paris (Dr. M. Beauvais; Mme É. Basse de Ménorval helped us greatly in finding specimens, and had casts of the lectotype of *Acanthoceras rhotomagense* made for us); the

École des Mines, Paris (Mme D. Létia); Muséum d'Histoire Naturelle de Rouen (M. J. Foucher and M. Leclerc); British Museum (Natural History) (Dr. M. K. Howarth and Mr. D. Phillips); the Institute of Geological Sciences (Dr. R. Casey). M. L. Cayeux kindly allowed us to use his private collection.

We are indebted to Mr. C. W. Wright for encouragement, advice, and the use of his outstanding collection of Cretaceous ammonites. We are grateful to Miss H. Cooper for help with the photography.

Dr. Kennedy started his work on the English species whilst in receipt of a studentship from the Natural Environment Research Council.

Abbreviations. See explanation of table 1.

REFERENCES

ADKINS, W. S. 1928. Handbook of Texas Cretaceous fossils. *Univ. Texas Bull.* **2838,** 385 pp., 37 pls.

ARKELL, W. J. *et al.* 1957. Cephalopoda Ammonoidea. *Treatise on invertebrate paleontology*, L4. Kansas.

BAYLE, E. 1878. Fossiles principaux des Terrains. *Explication de la Carte géologique de la France*, **4** (1), 158 pls.

BENAVIDES-CÁCERES, V. E. 1956. Cretaceous system in northern Peru. *Bull. Amer. Mus. nat. Hist.* **108,** 353–494, pl. 31–66.

CAYEUX, L. 1951. L'étage Cénomanien au Cap de la Hève–La Zone à Scaphites. *Bull. Soc. géol. Normandie*, **41,** 5–6.

COLLIGNON, M. 1931. Paléontologie de Madagascar 16 — La faune du Cénomanien à fossiles pyriteux du nord de Madagascar. *Ann. Paléont.* **20,** 43–104, pl. 5–9.

CRICK, G. C. 1907. The Cephalopoda from the deposit at the north end of False Bay, Zululand. *Geol. Surv. Natal and Zululand*, Third Report.

CUVIER, G. and BRONGNIART, A. 1822. Description géologique des couches des environs de Paris . . . In CUVIER, G., *Recherches sur les Ossemens Fossiles*, **2,** 239–648, 18 pls.

DOLLFUS, G. F. and FORTIN, R. 1911. Le Crétacé de la région de Rouen. *Congrès millénaire normand*, 20 pp.

DOUVILLÉ, R. 1912. Ammonites rhotomagensis. *Palaeont. Universalis*, **238.**

FABRE, S. 1940. Le Crétacé supérieur de la Basse-Provence occidentale 1: Cénomanien et Turonien. *Ann. Fac. Sci. Marseille* (2), **14,** 355 pp., 10 pls.

FOLLET, A. 1943. Note paléontologique sur le Cénomanien de la Côte-Sainte-Catherine. *Bull. Soc. Amis Sci. nat. Rouen*, **79,** 42–8.

GROSSOUVRE, A. de. 1894. Recherches sur la Craie Supérieure 2: Les ammonites de la Craie Supérieure. *Mém. Carte géol. dét. Fr.*

GUÉRANGER, E. 1867. *Album paléontologique du département de la Sarthe*, Le Mans, 20 pp., 25 pls.

HAAS, O. 1963. *Paracanthoceras wyomingense* (Reagan) from the Western Interior of the United States and from Alberta (Ammonoidea). *Amer. Mus. Novit.* **2151,** 19 pp.

—— 1964. *Plesiacanthoceras*, new name for *Paracanthoceras* Haas, 1963 *non* Furon, 1935. *J. Paleont.* **38,** 610.

HANCOCK, J. M. 1959. Les ammonites du Cénomanien de la Sarthe. *Comptes Rend. Cong. Soc. Sav.— Dijon 1959 — Colloque sur le Crétacé Supérieur Français*, 249–52.

HÉBERT, E. 1884. *Notions générales de Géologie*, 110 pp., fig. 54. Paris.

HYATT, A. 1900. Cephalopoda. In ZITTEL's *Textbook of Palaeontology* (1st English edition, EASTMAN (ed.)), 502–604.

—— 1903. Pseudoceratites of the Cretaceous. STANTON, T. W. (ed.). *Mon. U.S. geol. Surv.* **44,** 351 pp., 47 pls.

JEFFERIES, R. P. S. 1963. The stratigraphy of the *Actinocamax plenus* Subzone (Turonian) in the Anglo-Paris Basin. *Proc. Geol. Ass., Lond.* **74,** 1–33.

JUKES-BROWNE, A. J. and HILL, W. 1903. The Cretaceous Rocks of Britain **2**: The Lower and Middle Chalk of England. *Mem. geol. Surv. U.K.* 568 pp.

KENNEDY, W. J. 1969. The stratigraphy and correlation of the Lower Chalk of south-east England. *Proc. Geol. Ass., Lond.* **80,** 459–560.

KOSSMAT, F. 1897. Untersuchungen über die Südindische Kreideformation (pt. 2). *Beitr. Paläont. Geol. Öst.-Ung. Or.* **11,** 1–46, pl. 1–8.

LAUBE, C. C. and BRÜDER, G. 1887. Ammoniten der böhmischen Kreide. *Palaeontographica*, **33,** 217–39, pl. 23–29.

LENNIER, G. 1880. Exposition Géologique et Paléontologique du Havre en 1877. *Bull. Soc. géol. Normand.* **6**, 869 pp., 6 pl.

MANTELL, G. 1822. *The fossils of the South Downs.* London.

MATSUMOTO, T. and OBATA, I. 1966. An Acanthoceratid Ammonite from Sakhalin. *Bull. Nation. Sci. Mus., Tokyo*, **9**, 43–52, pl. 1–4.

ORBIGNY, A. D'. 1840–2. *Paléontologie Française.* Terrains Crétacés **1**: Céphalopodes. 662 pp., 148 pls.

PERVINQUIÈRE, L. 1907. Études de Paléontologie Tunisienne **1**: Céphalopodes des terrains Secondaires. *Carte Géologique de la Tunisie.*

PICTET, F.-J. 1863. Mélanges Paléontologiques 1. *Mém. Soc. Phys. Hist. nat. Genève*, **17**, 1–39, 8 pls.

PORTHAULT, B., THOMEL, G., and VILLOUTREYS, O. de. 1966. Étude biostratigraphique du Cénomanien du bassin supérieur de l'Esteron (Alpes-Maritimes). *Bull. Soc. géol. Fr.* (7) **8**, 423–9, pl. 8–11.

RIOULT, M. 1961. Problèmes de géologie Havraise. *Bull. Soc. géol. Normand.* **51**, 1–17.

SAEMANN, L. 1858. Note sur la distribution des Mollusques fossiles dans le terrain crétacé du département de la Sarthe. *Bull. Soc. géol. Fr.* (2) **15**, 500–24.

SCHLÜTER, C. 1871. Cephalopoden der oberen deutschen Kreide (pt. 1). *Palaeontographica*, **21**, 1–24, pl. 1–8.

SHARPE, D. 1853–7. Description of the fossil remains of Mollusca found in the Chalk of England 1: Cephalopoda. *Palaeontogr. Soc.* [*Monogr.*].

SORNAY, J. 1959. Le Cénomanien. In BASSE DE MENORVAL, E. et SORNAY, J., Généralités sur les faunes d'ammonites du Crétacé supérieur Français. *Comptes Rend. Cong. Soc. Sav. — Dijon 1959 — Colloque sur le Crétacé Supérieur Français*, 7–26.

SOWERBY, J. de C. 1823–46. *The Mineral Conchology of Great Britain.* **4** (*pars*)—**7**, pl. 384–648. London.

SPATH, L. F. 1923. On the Ammonite Horizons of the Gault and Contiguous Deposits. *Summ. Progr. geol. Surv. G.B.* **1922**, 139–49.

—— 1926*a*. On New Ammonites from the English Chalk. *Geol. Mag.* **63**, 77–83.

—— 1926*b*. On the Zones of the Cenomanian and the Uppermost Albian. *Proc. Geol. Ass., Lond.* **37**, 420–32.

STEPHENSON, L. W. 1953. Larger Invertebrate Fossils of the Woodbine Formation (Cenomanian) of Texas. *Prof. Pap. U.S. geol. Surv.* **242**, 226 pp., pl. 8–59.

WRIGHT, C. W. 1963. Cretaceous ammonites from Bathurst Island, Northern Australia. *Palaeontology*, **6**, 597–614.

—— and WRIGHT, E. V. 1951. A survey of the fossil Cephalopoda of the Chalk of Great Britain. *Palaeontogr. Soc.* [*Monogr.*].

W. J. KENNEDY
Department of Geology and Mineralogy
Parks Road
Oxford OX1 3PR

J. M. HANCOCK
Department of Geology
King's College
Strand
London W.C. 2

Final typescript received 9 February 1970

ULTRASTRUCTURE OF THE PROTEGULUM OF SOME ACROTRETIDE BRACHIOPODS

by GERTRUDA BIERNAT *and* ALWYN WILLIAMS

ABSTRACT. Electron microscopic studies of the exteriors of a number of acrotretacean genera show that their protegula were ornamented by shallow pits, usually with a coarser set, about 2 μm in diameter, partially or completely segregated from one another by groups of smaller ones about 300 nm across. The pattern is identical with the mould of a bubble raft, and consideration of the structure of the periostracum of living terebratellaceans suggests that the pits ornamenting the acrotretacean protegulum are the moulds of a highly vesicular periostracum up to 3 μm thick with a thin (10 nm) inner sealing membrane. Such a periostracum would have afforded larvae extra buoyancy immediately prior to their settlement on the substrate. The absence of pit ornamentation from the adult shell is believed to indicate the development of an inner sealing membrane which was sufficiently thick to mask the vesicular nature of the adult periostracum. Nothing comparable with this ornamentation is known in other Acrotretida, although the protegulum of *Eoconulus*, which may be an aberrant craniacean, included a mineral mesh of regular, alternating, circular holes about 8 μm in diameter which have been attributed to differential secretion beneath a non-vesicular periostracum comparable with that covering living *Crania*.

THE brachiopod shell usually bears traces of important ontogenetic changes in composition, structure, and secretory rates because resorption by the mantle is restricted to internal surfaces of the valves. In Recent species, the topography of external surfaces reflects growth variation at an ultrastructural level, and although the exteriors of calcareous-shelled fossils are usually masked by adherent micritic calcite of diagenetic origin, those of extinct chitino-phosphatic inarticulate brachiopods can normally be freed of such accretionary deposits by differential etching in acetic acid. The diagenetic processes which allow for this fortunate circumstance are not well understood. Presumably, the chitin and protein of the periostracum and of those layers alternating with apatite within the shell, break down into organic complexes which persist as continuous sheets to preclude any gross recrystallisation of the calcium phosphate, either in continuity with, or independently of, the rock matrix. Consequently even ultramicroscopic details of the topography of the external mineral or organic surfaces of most fossil inarticulates, may, in favourable conditions, be preserved for examination. This fact became evident in a survey of some Acrotretida under the scanning electron microscope. Except for Recent specimens of *Crania* and *Discinisca*, all acrotretide shells examined have been etched out of a variety of sediments; yet many show, to differing degrees of perfection, a previously unsuspected ornamentation of pits on the external surface of the protegulum. As will be shown, the pits may be interpreted as moulds of the undersurface of a distinctive type of periostracum which has its counterpart in living Terebratulida and which may even have contributed to the buoyancy of acrotretide larvae during the planktonic phase of their existence.

In the text, references are made to the protegular structure of a number of undescribed species. Formal systematic accounts of these will be published in due course by G. Biernat, who is currently investigating the Ordovician Inarticulata of Poland.

Materials and methods. The section of the periostracum illustrated in this paper was prepared by fixing a young *Waltonia inconspicua* (Sow.) in 3% gluteraldehyde made up in 3% sodium chloride buffered

[Palaeontology, Vol. 13, Part 3, 1970, pp. 491–502, pl. 98–101.]

to pH 7·2 with phosphate buffer. Material was subsequently decalcified in 5·5% EDTA, washed with sucrose, and treated for 1 hour with 1% osmic acid; all these solutions were buffered to pH 7·2 with phosphate buffer. Following dehydration, the specimen was embedded in Epon-Araldite resin and the sections stained with alcoholic uranyl acetate and aqueous lead citrate. Surfaces of dried periostracum were replicated for the transmission electron microscope by casting them in cellulose acetate strips which, before being dissolved away, were shadowed with gold-palladium at 1 to 1 and coated in carbon. Shell surfaces and sections studied under the 'Stereoscan' scanning electron microscope, were coated with gold-palladium.

THE PROTEGULUM

The protegulum is usually described as the first-formed shell of the brachiopod, secreted simultaneously over the entire surfaces of both mantles in the larval or early post-larval stages of development. The precise sequence of events leading to its appearance, however, is poorly known. Percival (1944, pp. 9–10) reported that, subsequent to the attachment of the larva of *Waltonia inconspicua* (Sow.) and during the last stages of enclosure of the anterior lobe by the reversing mantle, there is 'clear evidence of the formation of a hard shell'. At this stage in development the shell is about 120 μm long and consists of an outer periostracum and an inner layer of calcite crystallites. The protegulum of *Notosaria nigricans* (Sow.) has the same two-layered structure and is also secreted at about the same time after the settling of the larva on the substrate (Percival 1960, p. 448). In contrast, the protegulum of living inarticulates is, as far as is known, secreted before larval attachment. According to Yatsu (1902, p. 31) the mantle lobes of the larva of *Lingula unguis* (Linneus) are differentiated from a rudimentary ring-like flap when the larva is free-swimming. They then secrete a thin chitinous shell in one piece which is folded across the posterior margin to form a pair of semicircular valves about 140 μm in radius. Similarly, the protegulum is known to have been secreted in the youngest free-swimming larva of *Pelagodiscus* or any other discinid yet recovered (Chuang 1968, p. 265) and to have been present in the earliest identifiable individuals of *Crania* and *Discinisca* which were already attached to the substrate (Williams and Rowell *in* Williams *et al.* 1965, p. H50). Despite this difference in the timing of the deposition of the protegulum relative to the free-swimming stage in brachiopod ontogeny, correlation of the skeletal successions shows that the secretory regimes of the outer epithelium of the rudimentary mantle lobes follows the same sequence in widely different species. Studies of newly formed cells at the mantle edge of articulate brachiopods (Williams 1968) as well as unpublished observations of the mantle generative zones in *Lingula* and *Glottidia*, suggest that the first-formed cover of the outer epithelium is likely to have been always a mucopolysaccharide. Such a cover is probably maintained by continuous exudation over the entire surface of the larva until the outer and pedicle epithelia become differentiated and secrete the first persistent layer of the exoskeleton. Over the outer epithelium of the mantle lobes, this layer, the periostracum, is invariably composed of protein and/or chitin. The first-formed periostracum is exuded very rapidly and may immediately become the seeding sheet for deposits of calcite or apatite crystallites. Consequently it is always possible for the outer surface of such a mineral layer to form a mould of the topography of the inner periostracal surface, especially when that surface is only a sealing membrane about 10 nm thick.

The structure of the fossil protegulum is invariably incomplete and its precise boundaries may not be determinable even on the umbones of well-preserved shells. In general,

all external covers of organic origin are lost from the surfaces of fossil shells through the processes of weathering and diagenesis, and only the inner mineral layer remains. Indeed in those specimens where the protegulum was exclusively organic in composition, a mould could be the only surviving trace of the structure and this condition may be characteristic of some of the species discussed below. There is no infallible guide for determining the limits of the protegulum on adult shells. Protegula are known to range from less than 100 to more than 1000 μm in length, and from semi-elliptical to subcircular in outline. The outline is usually accentuated as a distinct step in the general profile of the umbones so that protegula appear to sit on the apices of the valves as extra-skeletal pieces. More importantly, no growth-lines should occur on the surface of a protegulum because it is secreted simultaneously over the entire mantle lobe. This criterion and the expectation that the protegular outline is normally accentuated have been used for the identification of acrotretide protegula.

THE ACROTRETACEAN PROTEGULUM

The fabric of the protegulum of an undescribed species of *Torynelasma* may be taken as typifying that of acrotretacean protegula in general. The ventral protegulum, which is about 100 μm wide (Pl. 98, fig. 1), is not ornamented by raised concentric ridges characteristic of the adult shell, but by a series of shallow circular to elliptical pits (Pl. 98, fig. 2). The pits vary in diameter by more than a factor of ten, although they actually fall into two grades. The coarser pits range from 2 to 4·5 μm in diameter and are separated from one another by ridges, about 350 nm wide, which swell out into flattened areas, up to 4 μm wide, intervening between groups of coarser pits. These flattened areas, as well as some of the ridges, bear the finer grade of pits which are about 350 nm in diameter. All pits are more or less flat-bottomed and about one-tenth as deep as the maximum diameter. The entire fabric of pits and ridges is preserved in apatite crystallites (each about 175 nm in diameter) which are stacked normal to the surface. The junction between the protegulum and later shell is abrupt; within a micron of being fully developed the pits pass into very shallow dimples which in turn give way to the first concentric ridges ornamenting the surface of adult shells (compare Pl. 98, fig. 5). The pits are impressed on the external surface of a mineral layer or lamina, about 2 μm thick, which is underlain by up to six laminae of comparable thickness (Pl. 98, fig. 3). These laminae are composed of apatite crystallites stacked more or less normal to their external and internal surfaces. They are separated from one another by gaps about 170 nm wide which were probably occupied by organic sheets. The entire fabric is reminiscent of laminar deposition in the craniaceans (Williams and Wright, in press), although the mineral constituent is calcium phosphate not calcium carbonate, and the accretion of laminae may involve continuous vertical growth of densely distributed apatite seeds instead of the spiral growth of calcite rhombohedra.

Sampling among other members of the Acrotretacea suggests that the protegular pit pattern of *Torynelasma* is characteristic of the superfamily. Sixteen species belonging to twelve genera, ranging in age from Middle Cambrian to late Ordovician, have provided the information given in Table 1. In addition, the protegular surface of *Ceratreta hebes* Bell from the Upper Cambrian Dry Creek Shale of Montana showed identifiable traces of pits although they were too poorly preserved to be accurately measured or

figured. In all species the protegulum, which varied in maximum diameter from 90 to 135 μm, was ornamented by pits fundamentally the same in structure and arrangement as those of *Torynelasma*. There is a variation in the size and distribution of pits, which may ultimately prove to be of systematic value. Thus the pits ornamenting the surface of the protegula of *Conotreta* (Pl. 99, fig. 1), *Linnarssonella* (Pl. 99, fig. 2), *Myotreta* (Pl. 98, figs. 5, 6), and *Rhysotreta* (Pl. 98, fig. 4) are comparable in size range with those

TABLE 1. The ranges of larger pits (*a*) and the diameter of smaller pits (*b*) forming the ornamentation on the protegula of the listed species. The horizons and locations of the specimens providing these data are given in descriptions of plates except for the unfigured *Scaphelasma septatum* Cooper and *Torynelasma toryniferum* Cooper, both of which were represented by topotypic material from the mid-Ordovician Pratt Ferry Formation, Pratt Ferry, Alabama.

	(*a*) *larger pits* (μm)	(*b*) *smaller pits* (*nm*)
Angulotreta postapicalis Palmer	about 1·5	—
Apsotreta expansa Palmer	1·0–2·3	—
Conotreta depressa Cooper	1·25–2·5	450
Curticia minuta Bell	0·8–3·2	320
Ephippelasma sp.	0·8–1·69	600
Linnarssonella girtyi Walcott	1·9–3·8	—
Myotreta cf. *crassa* Goryansky	2·0–4·6	500
Prototreta sp.	0·96–1·6	320
Rhysotreta corrugata Cooper	1·55–3·1	300
Scaphelasma septatum Cooper	0·9–3·0	300
Scaphelasma sp.	1·1–2·3	700
Spondylotreta concentrica Cooper	0·8–1·7	150
Spondylotreta sp.	0·7–2·0	—
Torynelasma sp.	2·2–4·5	360
Torynelasma toryniferum Cooper	1·2–2·3	380

of *Torynelasma*, whereas the coarser grades found in *Ephippelasma* (Pl. 99, fig. 3), *Prototreta* (Pl. 99, fig. 4), *Scaphelasma* (Pl. 99, fig. 5), and *Spondylotreta* (Pl. 100, fig. 3) are significantly smaller. There are also differences in the frequency distribution of the coarser pits, which are more closely packed together in *Conotreta*, *Myotreta*, and *Prototreta*, so that intervening flattened areas bearing clusters of fine pits, as in *Torynelasma*, are comparatively rare. In *Prototreta*, the fine pits appear to have been obliterated in

EXPLANATION OF PLATE 98

Scanning electron micrographs.

Figs. 1–3. Various aspects of protegulum of pedicle valve of *Torynelasma* sp., Arenig marly limestone, Bartoszyce, Peribaltic Depression, Poland. 1, lateral view of exterior of protegulum (×625). 2, arrangement of pits on exterior of mid-region of protegulum (×5800). 3, laminar layering of mineral parts of protegulum as seen on fracture surface more or less normal to shell with exterior to top of micrograph (×2700).

Fig. 4. Details of pit arrangement in mid-region of exterior of protegulum of topotypic pedicle valve of *Rhysotreta corrugata* Cooper (1956), mid-Ordovician Pratt Ferry Formation, Pratt Ferry, Alabama (×6500).

Figs. 5, 6. Exterior of dorsal protegulum of *Myotreta* cf. *crassa* Goryansky (1969), Arenig marly limestone, Bartoszyce, Peribaltic Depression, Poland. 5, junction between protegulum and adult (bottom left-hand corner) shell (×1300). 6, detail of pits on left lateral part of surface (×2600).

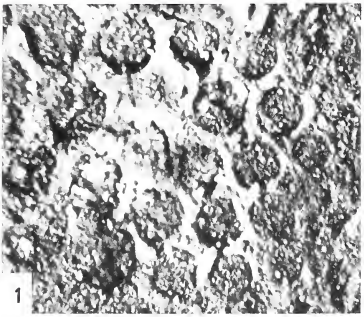
1

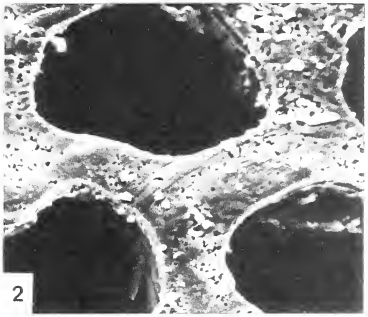
2

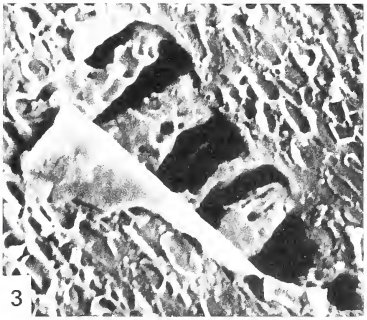
3

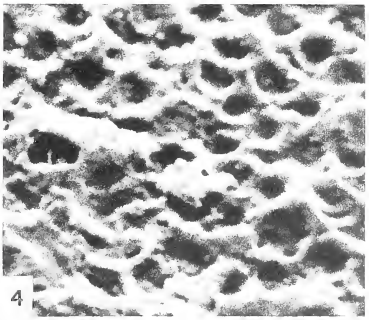
4

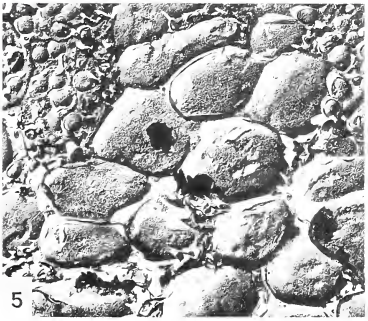
5


6

BIERNAT and WILLIAMS, Ultrastructure of acrotretide protegula

most parts of the protegulum by recrystallization, and the rare occurrence of such pits in other Cambrian stocks has been attributed to diagenesis rather than a natural suppression of their development. There is certainly evidence of a gross recrystallization affecting even the coarser grades of pits in *Linnarssonella* where outlines indicative of hexagonal prisms have been superimposed here and there on a relict pattern of normally distributed subcircular pits.

A profound change in the distribution of pit ornamentation in early *Spondylotreta* seems, also, to be attributable to post-mortem alteration of the shell. In *S. parva* Wright (1963, p. 238) and S. *concentrica* Cooper (Pl. 100, fig. 3) from the Ashgillian and Porterfield limestones of Ireland and Alabama respectively, the pit pattern, although variably preserved in both species, is seen to be normally developed and restricted to the protegulum; but in an undescribed species of *Spondylotreta* from Tremadocian cherts of Poland, pits were found over the entire shell surface. In the specimen examined, the protegulum was ornamented by an array of pits with diameters ranging from 600 nm to 2 μm and a density count of 23 per 100 μm^2 in the mid-region (Pl. 100, fig. 4). Pits of similar size and depth, but with half the frequency distribution of those in the protegulum, also occur in the adult shell where they are limited to those exposed parts of the outer surfaces of overlapping lamellae which must have been covered by periostracum (Pl. 100, fig. 5). Despite this evidence, we believe pits on the adult shell, at least, to be solution features, because the specimens bearing them had been dissolved out of the cherts by hydrofluoric acid, and valves of *Helmersenia* and *Siphonotreta* recovered during the same operation bore similarly distributed pits (Pl. 100, fig. 6). It is still possible that the pits were formerly the sites of surface depressions which originated during shell deposition and were only enlarged during etching. This we believe to be unlikely, and we attribute the denser distribution of pits in the protegulum of the Tremadocian *Spondylotreta* to the existence of a normal array of pits, on which was superimposed a pattern of solution hollows, like those on the adult part of the shell.

No acrothelidid species has been examined but the protegulum of *Curticia*, the monotypic representative of the third acrotretacean family, is known to be pitted in the same way as that of acrotretids (Pl. 100, figs. 1, 2). It would, therefore, be surprising if the protegulum of any acrotretacean proved not to be so ornamented.

INTERPRETATION

In seeking an explanation for these distinctive arrays of pits, attention must be paid to a number of clues like the depth of the pits, their possible relationship to a restored periostracum comparable with those of living brachiopods, and to any similarities between such patterns and naturally occurring structures. In relation to their diameter and the thickness of the shell, the pits are undeniably shallow. In *Myotreta*, *Spondylotreta*, *Rhysotreta*, and *Torynelasma*, the depth of a pit appears not to be more than one-fifth of the diameter, and less than 1 μm absolutely compared with thickness of about 15 μm for the shell underlying the protegulum in adult valves. Hence the pits are not endopunctae in the sense that they were occupied by epithelial extensions persisting throughout life. Nor is it likely that they were exopunctae if the implication is that the pits were temporary sites of caecal extensions of the outer epithelium, possibly acting as food storage centres, which later became sealed off by shell deposition after

withdrawal of the caeca. Terminal branches of mantle papillae penetrating the shell of living Terebratulida and Craniacea correspond to specialized microvilli and vary only narrowly in diameter immediately beneath the periostracum. In fact, the particular pattern of size variation must surely also preclude any possibility that the pits afforded accommodation for patches of specialized epithelium thereby facilitating some function of the mantle, like sensitivity to changes in light or hydrostatic pressures.

In our estimation, the distribution of pits is in itself a key to their origin. The patterns are exactly matched in bubble rafts formed on the surfaces of liquids by groups of relatively large bubbles which are partially or completely separated from one another by clusters of smaller ones. The only difference is that the surface of a raft is compositely convex, whereas that of the protegulum is compositely concave as though it were the mould of a bubble raft. The difference becomes important when one considers the nature of the periostracum that must once have covered the protegular surface. In all brachiopods, the inner sealing membrane of the periostracum acts as the seeding surface of the first apatite or calcite crystallites secreted by the epithelium; and it follows that, if the crystallites form a bubble raft mould, the inner membrane of the periostracum must have been one of the bounding surfaces of such a raft. Further inferences about the periostracum can now be made. Assuming that the vesicles making up the periostracal

EXPLANATION OF PLATE 99

Scanning electron micrographs.

Fig. 1. Details of pit arrangement in mid-region of exterior of protegulum of topotypic pedicle valve of *Conotreta depressa* Cooper (1956), mid-Ordovician Pratt Ferry Formation, Pratt Ferry, Alabama (×3900).

Fig. 2. Recrystallization superimposing a crystal fabric, as in centre of micrograph, on a pit pattern in mid-region of dorsal protegulum of *Linnarssonella girtyi* Walcott (see Bell and Ellinwood (1962)), Upper Cambrian Morgan Creek Member, Blanco Co., Texas (×2600).

Fig. 3. Distribution of pits on exterior of ventral protegulum of *Ephippelasma* sp., Llanvirn shales, Bartoszyce, Peribaltic Depression, Poland (×2600).

Fig. 4. Details of pitted ornamentation in mid-region of ventral protegulum of *Prototreta* sp., Middle Cambrian Meagher Limestone, Horseshoe Hill, Montana (×6250).

Fig. 5. Details of pitted ornamentation in mid-region of dorsal protegulum of *Scaphelasma* sp., Llanvirn marls, Ketrzyn, Peribaltic Depression, Poland (×6000).

Fig. 6. Traces of pitted ornamentation on external surface of damaged protegulum of topotypic pedicle valve of *Apsotreta expansa* Palmer (1954), Upper Cambrian Riley Formation, Llano Co., Texas (×2600).

EXPLANATION OF PLATE 100

Scanning electron micrographs.

Figs. 1, 2. General view and detail of pitted ornamentation on mid-region of exterior of protegulum of topotypic brachial valve of *Curticia minuta* Bell (1941) Upper Cambrian Pilgrim Formation, Little Belt Mountain, Montana (×2500, ×6250 respectively).

Fig. 3. Distribution of pits in mid-region of exterior of protegulum of topotypic pedicle valve of *Spondylotreta concentrica* Cooper (1956), mid-Ordovician Pratt Ferry Formation, Pratt Ferry, Alabama (×6500).

Figs. 4, 5. Exterior of brachial valve of *Spondylotreta* sp., Tremadoc cherts, Wysoczki, Holy Cross Mountains, Poland. 4, distribution of pits in relation to recrystallized fabric in mid-region of protegulum (×6000). 5, presence of pits only on those parts of overlapping lamellae that make up external surface of adult shell (×1700).

Fig. 6. Distribution of external pits near margin of ventral protegulum of *Siphonotreta* cf. *acrotretomorpha* Goryansky (1969), Tremadoc cherts, Wysoczki, Holy Cross Mountains, Poland (×1300).

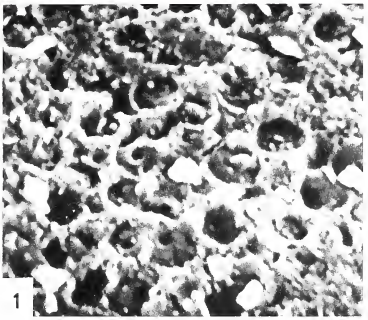
1

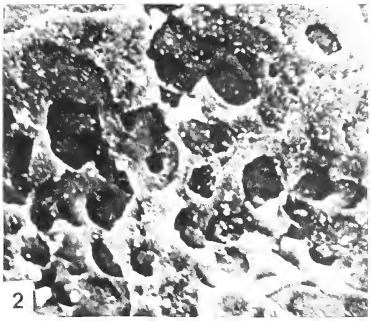
2

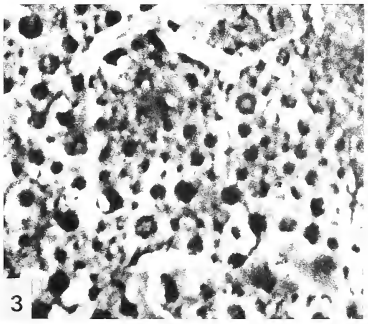
3

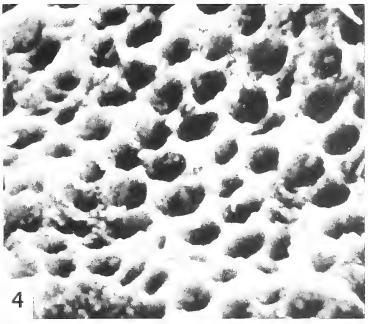
4

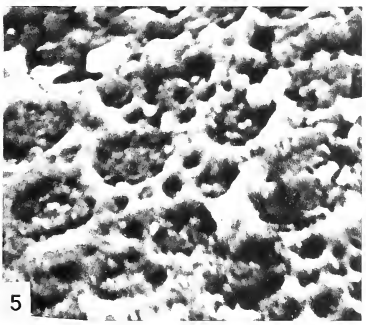
5

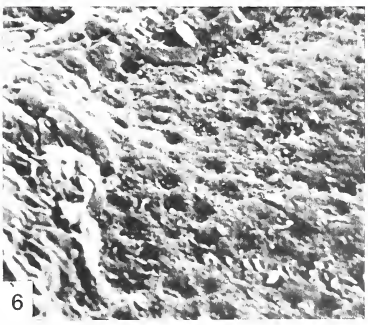
6

BIERNAT and WILLIAMS, Ultrastructure of acrotretide protegula

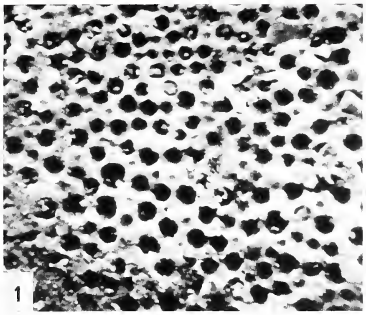
1

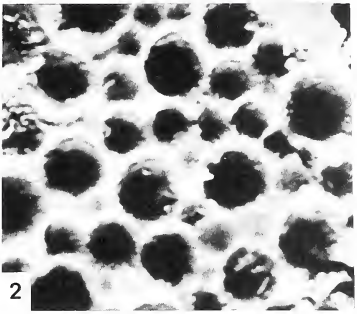
2

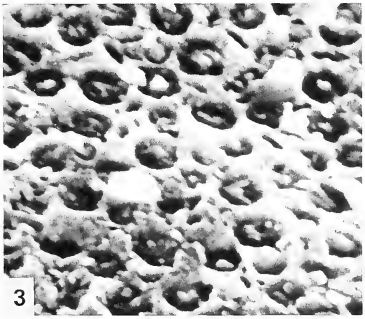
3

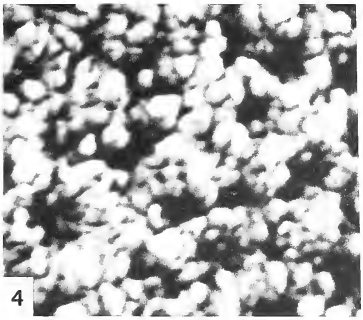
4

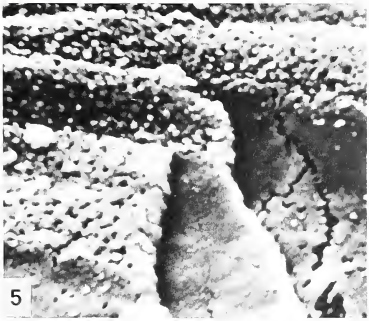
5

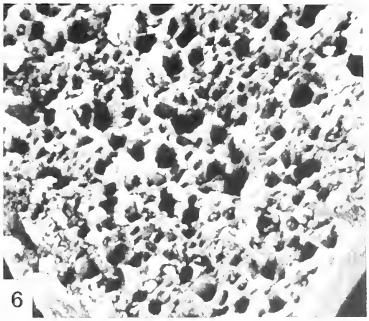
6

BIERNAT and WILLIAMS, Ultrastructure of acrotretide protegula

bubble raft had not been flattened, and that the bounding membranes were not much thicker than 20 nm, the larger vesicles can be estimated to have been up to 5 μm in diameter and would have constituted the thickest part of the periostracum (text-fig. 1).

Information now available about the periostracum of living Terebratulida shows that none of these inferences is unreasonable, although the estimated maximum thickness is greater than any yet known for Recent species. The terebratellacean periostracum

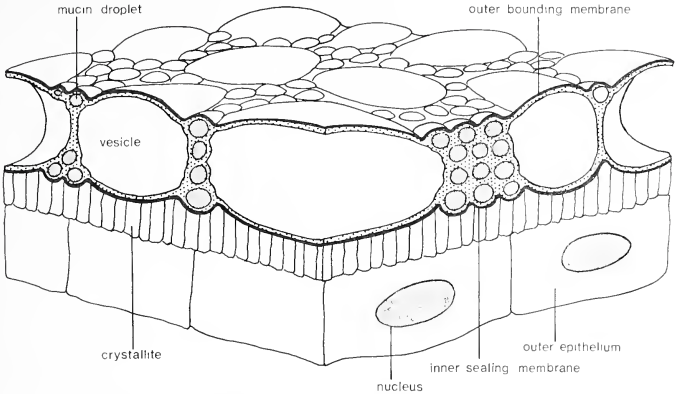

TEXT-FIG. 1. Diagrammatic restoration of the organic parts of the acrotretacean protegulum to show the inferred relationship between the periostracum and the underlying layer of calcium phosphate crystallites.

has already been described (Williams 1968, p. 276) as consisting of an array of level-topped protein rods which arise from a series of labyrinthine protein partitions (Pl. 101, fig. 6). These partitions, which are extensions of the outermost part of a triple unit membrane forming the base of the periostracum, enclose smaller mucin spheroids and larger, more irregularly shaped vesicles. The inclusions are shown in section in Plate 101, fig. 6 and in external surface views of dried periostracum in Plate 101, figs. 4, 5, where they form patterns strikingly like those on the acrotretacean protegulum. Even the dimensions are comparable with those estimated for *Ephippelasma*, *Prototreta*, and *Scaphelasma*, ranging from 240 nm to 2 μm for vesicles and from 200 to 380 nm for mucin inclusions in the periostraca of four living species [*Macandrevia cranium* (Müller), *Magasella sanguinea* (Leach), *Terebratalia transversa* (Sowerby), and *Waltonia inconspicua* (Sowerby)]. Indeed the consistently smaller size of inclusions in the Terebratulida undoubtedly accounts for much of the discrepancy in the thickness of the periostracum, which is not usually greater than about 1·5 μm in the species cited. Moreover the flat-bottomed nature of many of the protegular pits in acrotretaceans suggests that the larger inclusions, at least, were partially collapsed during deposition of the crystallite mould so that thicknesses of about 3 μm may have been more characteristic of the superfamily.

Despite the inferred likeness between the acrotretacean and terebratellacean periostraca, the primary shell of living terebratellaceans does not, as far as is known, bear any superficial ornamentation that faithfully reflects the internal vesicular structure of the covering periostracum (Pl. 101, fig. 3). The reason for this apparent lack of moulding lies in the thickness of the basal layer of adult terebratellacean periostracum, which may be up to 100 nm thick and obviously polymerizes as a fairly rigid, even foundation for the rest of the periostracum. Indeed when the basal layer is less than 40 nm thick it shows signs of being moulded to periostracal inclusions (Pl. 101, fig. 6). Consequently it seems reasonable to conclude that the inner sealing membrane of the periostracum covering the acrotretacean protegulum was probably not much more than about 10 nm thick.

The attribution of topographic differences in the external surfaces of shells to variation in the thickness of the periostracal sealing membrane may explain the absence of pit ornamentation from the surface of adult shells. The periostracum covering the adult shell of acrotretaceans may have been similar in microstructure to that over the protegulum; but exudation of a significantly thicker sealing membrane by the post-larval mantle lobes may have masked the vesicular fabric of the middle periostracal layer, and so precluded the secretion of mineral moulds of such a microstructure.

In summary, then, the periostracum of acrotretaceans is inferred to have consisted mainly of a relatively thick layer (up to 3 μm) crowded with protein-bounded vesicles and mucin droplets such as are found in the periostracum of living Terebratulida (text-fig. 1). No information is available about the outer membrane although it may have been fibrillar like those known in living species. The inner sealing membrane, however, is likely to have been very thin (say 10 nm) in the protegula and relatively thick (up to 100 nm) in the adult shells of all acrotretaceans.

THE PROTEGULA OF OTHER ACROTRETIDA

To date it has been possible to examine only a few genera belonging to the Discinacea and Siphonotretacea, although a recently completed study by Williams and Wright (in press) of the Craniacea affords a comprehensive survey of that group.

The periostracum of living *Crania anomala* (Müller) consists of a mucopolysaccharide layer up to 5·5 μm thick, bounded by an outer membrane bearing fibrillar rods, and a

EXPLANATION OF PLATE 101

Figs. 1–4, scanning electron micrographs. Figs. 5, 6, transmission electron micrographs.

Fig. 1. Regular distribution of pits on mid-region of exterior of protegulum of brachial valve of *Eoconulus* sp., Llanvirn Kundsky member, Abja, W. Estonia (×1400).

Fig. 2. Exterior of pedicle valve showing mineral meshwork in young part of valve of *Dictyonites perforata* Cooper (1956), mid-Ordovician Pratt Ferry Formation, Pratt Ferry, Alabama (×625).

Figs. 3, 4. Exterior of brachial valve of *Waltonia inconspicua* (Sow.), Lyttleton Harbour, New Zealand. 3, torn piece of periostracum turned to one side to show underlying surface of primary shell in young part of valve (×5250). 4, vesicular nature of periostracum affects topography of outer sealing membrane in more mature shell (×12 000).

Fig. 5. Single stage negative replica of periostracum of *Terebratalia transversa* (Sow.), Seattle Harbour, Washington, showing vesicular nature of middle layer (×14 200).

Fig. 6. Section of young periostracum of *Waltonia inconspicua* (Sow.), Lyttleton Harbour, New Zealand, showing moulding of inner sealing membrane (below) to two larger vesicles and a smaller mucin droplet between them (×45 000).

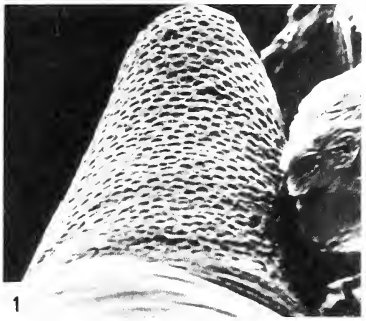
1

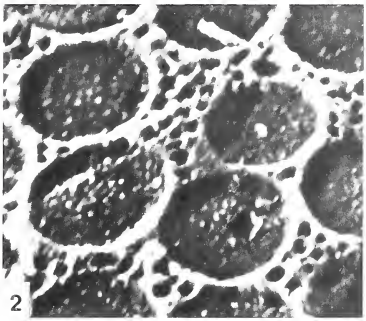
2

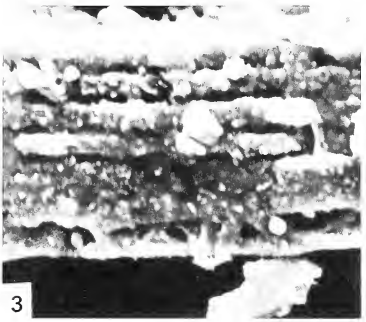
3

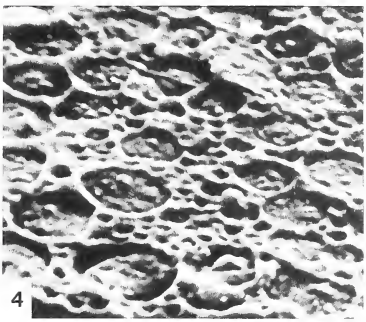
4

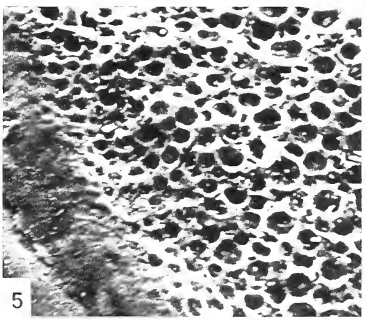
5


6

BIERNAT and WILLIAMS, Ultrastructure of acrotretide protegula

thin inner membrane of protein. The mucopolysaccharide layer is devoid of vesicular structures so that the inner surface is evenly disposed; and it is appropriate that no pit ornamentation is found on any external surface of living *Crania*, nor is it known on any fossil craniacean.

In contrast, the protegulum of *Eoconulus* is ornamented by an array of shallow, flat-bottomed circular pits varying in diameter from 5·5 to 11·5 μm and up to 750 nm deep (Pl. 101, fig. 1). The pattern is different from that characteristic of the Acrotretacea in that, as far as it has been possible to observe, the pits are regularly spaced in alternate rows and segregated from one another by flattened ridges (about 1·3 μm wide) which do not bear traces of finer pits, although the specimen examined was sufficiently well preserved to reveal a fabric of apatite crystallites each about 400 nm across. Among living Terebratulida, no periostracal fabric is known which involves the arrangement of vesicles in regular arrays. On the contrary, the pattern is inconsistent with the processes leading to the exudation of vesicles by outer epithelium. In the circumstances, it seems more reasonable to interpret this pattern as representing a truly differential secretion of calcium phosphate by the epithelium. The function of such a mineral mesh is unknown. Presumably while apatite crystallites were being secreted to form the mineral framework, exudation of periostracum continued in those areas that ultimately appear as pits and formed discrete circular pads internally to the periostracum as shown in text-fig. 2. In all respects except size, the mineral framework of the protegulum of *Eoconulus* is envisaged as having been very like that of the adult shell of *Dictyonites* (Pl. 101, fig. 2). Examination of *D. perforata* Cooper has shown that the protegular surface is not pitted and that the bars forming the open mineral network of the adult shell are similarly free of ornamentation apart from the inevitable interstitial gaps between the apatite crystallites constituting the bars. Even the circular pores defined by the apatite network must also have been occupied by a thickened pad of the inner sealing membrane of the periostracum in the way inferred for the protegulum of *Eoconulus*.

Study of two siphonotretacean stocks suggests that this superfamily may have been characterized by an external ornamentation of pits. Specimens of both genera, however, were dissolved from Tremadocian cherts by hydrofluoric acid and, like those of *Spondylotreta* recovered by the same process, have to be interpreted with caution. Valves of *Siphonotreta* were much better preserved than those of *Helmerseuia* and are figured here (Pl. 100, fig. 6) although a similar pattern of pits also occurs on the exteriors of the latter. As in *Spondylotreta*, the entire surface of the shell of *Siphonotreta*, including the sides of the spines, are ornamented by densely distributed pits ranging in diameter from 1 to 3 μm. There are even indications of clusters of finer pits which are less than 1 μm in diameter. Yet we still think it reasonable to assume that the pits, like those in the adult shell of *Spondylotreta*, are solution phenomena.

The remaining superfamilial group to be considered, the Discinacea, is represented by a number of living species, one of which (*Discinisca strigata* Broderip from Costa Rica) was available for study. Unpublished researches on this species show that the periostracum has a complex lamellar structure on an ultramicroscopic scale, but no vesicles accumulate in this cover and neither the protegulum nor the adult shell has pitted surfaces. Extinct discinaceans examined include *Orbiculoidea nitida* Phillips from the Carboniferous Shales of Capel Rig, Gore, Scotland, and *Schizotreta* sp. from Tremadocian cherts of the Holy Cross Mountains, Poland. In these species too there were

no traces of a microscopic external ornament other than the usual granular appearance of the crystallite fabric, and it seems safe to assume that a pattern of microscopic pits never developed on the discinacean shell.

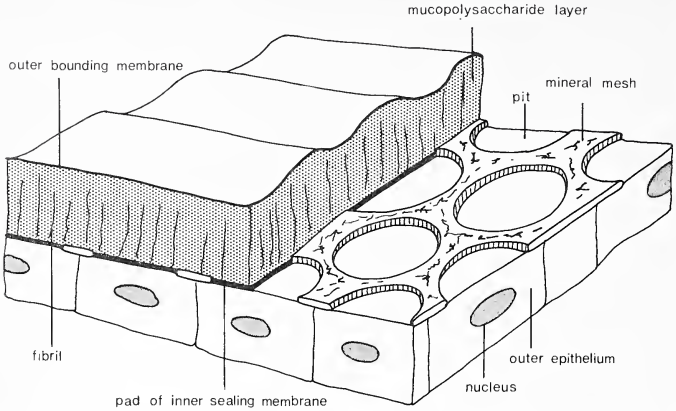

TEXT-FIG. 2. Diagrammatic restoration of the organic parts of the protegulum of *Eoconulus* to show the inferred relationship between the periostracum and the underlying mesh of calcium phosphate crystallites.

CONCLUSIONS

Ignoring the pitted aspect of the entire external shell surface of *Spondylotreta*, *Siphonotreta*, and *Helmersenia*, which was almost certainly effected by hydrofluoric acid, a scrutiny of the exteriors of thirteen acrotretacean genera indicates that their protegula were always ornamented in a distinctive way. The species examined range in age from Middle Cambrian to Upper Ordovician and, since the pattern is best interpreted as the mineral mould of a highly vesicular periostracum with a thin inner sealing membrane, the first-formed shells of all acrotretaceans are assumed to have been so covered. The dense distribution of pits and the size of those moulds presumed to have accommodated the larger subspherical vesicles, suggest that the protegular periostracum was effectively a bubble raft between 1 and 3 μm thick. Such a periostracum could have imparted buoyancy to planktonic larvae during the later stages of their development, thereby promoting the dispersion of the species.

As already mentioned, the absence of pitted ornamentation from the external surface of the adult shell does not necessarily preclude the continued secretion of a vesicular periostracum. Exudation of a thickened inner sealing membrane would not only have masked the bubble raft effect of the middle periostracal layer, but also shown the same transition from one condition to the other through a zone of ill-defined traces of pits as are seen in Plate 98, fig. 5. Such a thickening would have coincided, not so much with

a change from a planktonic to a benthic or epiplanktonic mode of life, as with the first appearance of a pair of circumferential outer mantle lobes contributing cells by a 'conveyor belt system' to the expanding ventral and dorsal mantles. The inferred sequence of secretion of the periostracum along the inner face of the outer mantle lobe has been illustrated in text-fig. 3. Thus, the difference between the surface ornamentation of the protegulum and adult shell in acrotretaceans is envisaged as reflecting a prolongation of one of the phases of a secretory regime, although the sequence of phases remained constant.

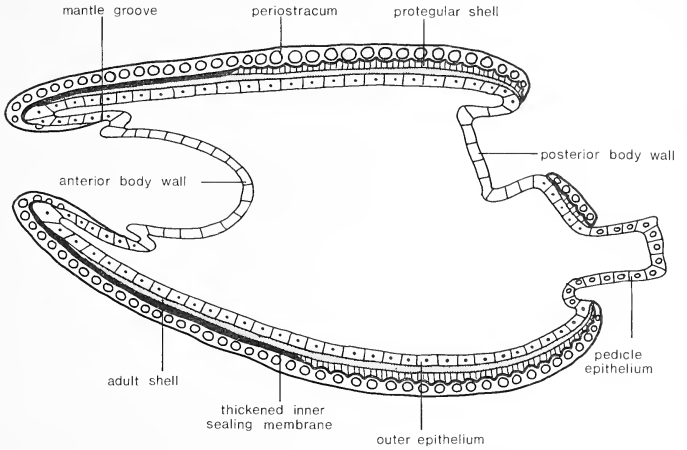

TEXT-FIG. 3. Diagrammatic reconstruction of a very young acrotretacean (lophophore and other organs omitted) to show the inferred relationship between the change in the thickening of the inner sealing membrane of the periostracum and the micro-ornamentation of the mineral shell.

Stratigraphic and morphological evidence favours the acrotretaceans as ancestral to the three other superfamilial groups comprising the Acrotretida (Williams and Rowell *in* Williams *et al.* 1965, p. H172). Ultrastructural comparisons of the shell, however, do not afford any further information on affinity. In respect of the relationship between the thickness of the inner sealing membrane of the periostracum and the topography of the underlying mineral layer, it is noteworthy that the sealing membranes of both *Discinisca* and *Crania* are only about 10 nm thick, but in neither species is the periostracum vesicular, and the underlying mineral shell surface lacks a pitted ornamentation. This condition seems also to have been characteristic of the protegular mineral shell of all extinct discinacean and craniacean species so that it seems reasonable to assume that the protegula of those stocks, too, was covered by a similar periostracum. Yet nothing is known about the derivation of the featureless mid-periostracal layers of *Discinisca* and *Crania* which consist solely of fibrils scattered in a polysaccharide matrix. Judging

from the structure of the periostracum of living articulates (Williams 1968, p. 274), a vesicular periostracum is the more prevalent condition; and, since it seems to have covered the protegula of acrotretaceans, the simple periostracum of the later-appearing discinaceans and craniaceans may represent a paedomorphic substitution in the larval stage of their development. Further study of better-preserved siphonotretaceans will have to be undertaken to determine whether they belonged to the discinacean or acrotretacean stage of development, or whether they were characterized by the neotenous persistence of a larval vesicular periostracum throughout life, so that the entire shell surface was pitted in the manner of the acrotretacean protegulum.

Acknowledgements. We are greatly indebted to Professor W. C. Bell (University of Texas), Dr. Howard Brunton (British Museum (Nat. Hist.)), Dr. G. A. Cooper (U.S. National Museum), and A. J. Rowell (University of Kansas) for promptly responding to urgent requests and sending us vital American and British material for examination, thereby greatly enlarging the scope of this paper. Much of the electron microscopy was carried out on a 'Stereoscan' scanning electron microscope supplied through a N.E.R.C. grant, and to that Research Council we extend our thanks as we do also to Dr. Jean Graham for assistance in the preparation of the text-figures and to Dr. Katharine McClure for cutting the sections of the periostracum of *Waltonia*.

REFERENCES

BELL, W. C. 1941. Cambrian brachiopoda from Montana. *J. Paleont.* **15,** 193–255.

—— and ELLINWOOD, H. L. 1962. Upper Franconian and Lower Trempealeanan Cambrian trilobites and brachiopods, Wilberns Formation, Central Texas. *J. Paleont.* **36,** 385–423.

CHUANG, S. H. 1968. The larvae of a discinid (Inarticulata, Brachiopoda). *Biol. Bull.* **135,** 263–72.

COOPER, G. A. 1956. Chazyan and related brachiopods. *Smithson. Misc. Coll.* **127,** 1–1245.

GORYANSKY, W. U. 1969. *Inarticulate brachiopods from the Cambrian and Ordovician beds of the northwest of the Russian Platform.* 173 pp. NEDRA, Leningrad.

PALMER, A. R. 1954. The faunas of the Riley Formation in Central Texas. *J. Paleont.* **28,** 709–86.

PERCIVAL, E. 1944. A contribution to the life-history of the brachiopod *Terebratella inconspicua* Sowerby. *Trans. R. Soc. N.Z.*, **74,** 1–23.

—— 1960. A contribution to the life-history of the brachiopod *Tegulorhynchia nigricans. Q. J. Microscop. Sci.* **101,** 439–57.

WILLIAMS, A. 1968. A history of skeletal secretion among articulate brachiopods. *Lethaia*, **1,** 268–87.

—— *et al.* 1965. *Treatise on invertebrate paleontology* (ed. MORE, R. C.): *Part H, Brachiopoda.* 927 pp. Lawrence (Univ. of Kansas).

—— and WRIGHT, A. D. 1970. Shell structure of the Craniacea and other calcareous inarticulate brachiopoda. *Spec. Pap. Palaeont. No. 7.*

WRIGHT, A. D. 1963. The fauna of the Portrane Limestone. 1. The inarticulate brachiopods. *Bull. Brit. Mus.* (*Nat. Hist.*) *Geol.* **8,** 221–54.

YATSU, N. 1902. On the development of *Lingula anatina. J. Coll. Sci. Tokyo*, **17,** 1–112.

GERTRUDA BIERNAT
Polska Akademia Nauk
Zaklad Paleozoologii
Warszawa
Al. Zwirki i Wigury 93

ALWYN WILLIAMS
Department of Geology
The Queen's University of Belfast
Belfast BT7 1NN
Northern Ireland

Typescript received 18 November 1969

A NEW TRIONYCHID TURTLE FROM THE BRITISH LOWER EOCENE

by R. T. J. MOODY *and* C. A. WALKER

Abstract. A new trionychid turtle, *Eurycephalochelys fowleri* gen. et sp. nov., is described from a skull found in the Bracklesham Beds (Cuisian, Lower Eocene) of Sussex. Comparisons are made between this first known trionychid skull from the British Eocene, and other fossil and Recent members of the Trionychidae.

In 1966 Mr. R. Fowler discovered the first known skull of a British Eocene trionychid in the Cakeham Beds of the Bracklesham Beds at East Wittering, Sussex.

Shell remains of trionychid turtles in the Lower to Upper Eocene deposits of England are fairly common and have been described as several new species of the genus *Trionyx* Geoffroy 1809. However, only a few indeterminate fragments of skulls have been found. Skull and shell have never been found together, so that the new specimen cannot be related to the previously described fossil forms. For this reason, and because of the considerable differences between this skull and Recent trionychid skulls, we have elected to place it in a new genus.

It may be that future finds of skulls associated with post-cranial material will enable at least some of the species of *Trionyx* based on British Eocene turtle shells to be transferred to the new genus; it may even be that *E. fowleri* will prove to be conspecific with one of those. Similarly it is possible that *Eurycephalochelys* may be congeneric with some genus of Eocene trionychid from elsewhere, known at present only from the remains of its shell.

Suborder CRYPTODIRA

Superfamily TRIONYCHOIDEA Fitzinger 1826

Family TRIONYCHIDAE Bell 1828

The following trionychid characters are seen in the new genus: Temporal region emarginate, with no contact between parietal and squamosal. Premaxillae fused. Postorbital small; naso-palatine foramen large; palatine fenestra present but small. Pterygoids make contact with maxillae and are separated from each other by basisphenoid. Quadrate encloses stapes.

Genus EURYCEPHALOCHELYS gen. nov.

Type species. Eurycephalochelys fowleri gen. et sp. nov.

Diagnosis. Quadrate condyle situated relatively far back, so that it lies well behind stapedial foramen, well behind level of foramen magnum, and more or less at level of back of basioccipital, with occipital condyle projecting only a short distance behind it. Forwardly directed flange of quadrate almost horizontal.

[Palaeontology, Vol. 13, Part 3, 1970, pp. 503–10, pl. 102.]

Internal maxillary foramen in medial wall of vertically rising part of maxilla. Jugal bar originates well below lowest point of orbital margin. Foramen magnum, and brain cavity immediately anterior thereto, wider than high.

Snout region short and broad, with distance from tip of premaxilla to front of orbit much greater than antero-posterior diameter of orbit. Maxilla very deep, depth probably much greater than vertical diameter of orbit. Postorbital bar narrow, slopes backwards and upwards. Area of quadrate exposed on dorsal surface not larger than area of prootic but of approximately equal size. Tympanic cavity shallow. Steep sides of choanal vault rounded.

Eurycephalochelys fowleri sp. nov.

Plate 102, figs. 1–5

Diagnosis. The only species of its genus.

Material. Holotype only, BMNH R8445, an almost complete skull without lower jaw. Cast in the collection of Mr. R. Fowler (Moschatel, Church Road, East Wittering, Sussex).

Occurrence. An oyster bed within the Cakeham Beds, Bracklesham Beds, Cuisian (Lower Eocene); foreshore at East Wittering, Sussex.

Measurements (in millimetres).

Actual length (premaxilla—occipital condyle)	157
Estimated total length, including supra-occipital spine	215
Maximum actual width (quadrate—quadrate)	132
Width across external nares	23
Tip of premaxilla—front of orbit	42
Minimum depth of maxilla beneath orbit	30
Maximum length of orbit	26
Estimated depth of orbit	26
Estimated length of anterior palatine foramen	8
Estimated length of intermaxillary suture	13
Estimated length of choanae	17
Width across choanae	20
Maximum width across maxillae in palatal view	87
Maximum dimension of articulating surface on quadrate	29

Condition of preservation. The specimen is an almost entire skull lacking the lower jaw. It has been slightly crushed dorso-ventrally at the posterior end and the whole bone surface is partially eroded, making sutures difficult to see.

The single, median premaxilla and the maxillae are almost complete. The frontals and prefrontals are lost. Both jugals are damaged; on each side the process reaching up towards the postorbitals is eroded and most of the jugal bar is missing. The parietals are complete posteriorly and laterally. The prootics, opisthotics, and quadrates are present on both sides with little distortion. Only the basal part of the supraoccipital is preserved, the sagittal crest having been lost. The squamosals are lacking but their suture scars on the quadrates are clearly visible. The palate is incomplete but the approximate

---

EXPLANATION OF PLATE 102

Eurycephalochelys fowleri gen. et sp. nov. BMNH R8445. Views of skull; 1, palatal; 2, occipital; 3, dorsal; 4, left lateral; all $\times\frac{1}{2}$. 5, quadrate showing the position of the stapedial foramen, $\times 1$.

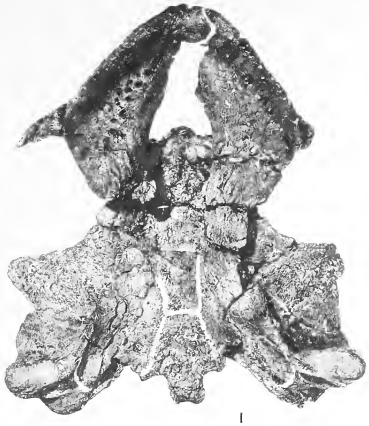

1

4

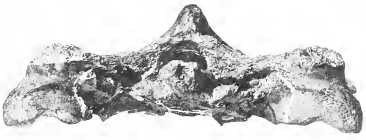

2

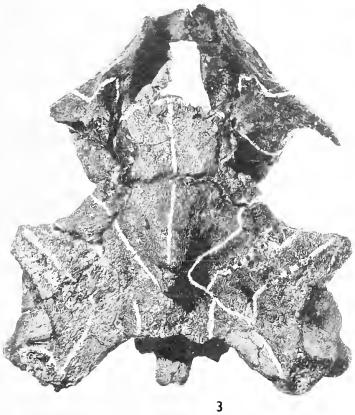

3

5

MOODY and WALKER, Trionychid turtle

margins of the anterior palatine foramen can be seen. The pterygoids are imperfect and only part of the basisphenoid remains. The ventral surfaces of the parietals are badly preserved whilst the articular areas of the quadrates are worn. Erosion of the occipital region has obscured the sutures.

Description. There is a large internal maxillary foramen (text-fig. 1) in the medial wall of the maxilla, bordered dorsally by the maxillary-jugal suture and antero-medially by a ridge which forms the inner edge of the orbital floor. This ridge sweeps upwards anteriorly to form an acute angle with the orbital rim.

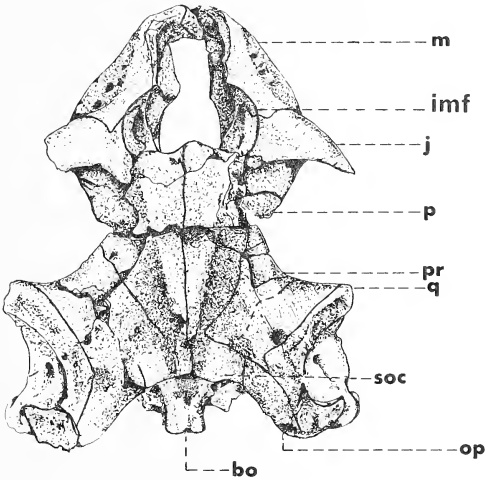

TEXT-FIG. 1. *Eurycephalochelys fowleri* gen. et sp. nov. BMNH R8445. Dorsal view of skull, × ½. *Abbreviations*: *bo*, basioccipital; *bs*, basisphenoid; *imf*, internal maxillary foramen; *j*, jugal; *m*, maxilla; *op*, opisthotic; *p*, parietal; *pm*, premaxilla; *pr*, prootic; *pt*, pterygoid; *q*, quadrate; *soc*, supraoccipital.

A dorsal view of the skull (text-figs. 1, 5A) shows that the lateral surface of the anterior region faces upwards as well as outwards, displaying a series of maxillary foramina a short distance above the cutting edge and running parallel to it. Posteriorly, the lateral surface of the parietal is rounded and slopes gently to the prootic. The area of that part of the quadrate which is normally exposed on the dorsal surface is not larger than the area occupied by the prootic, but is of approximately equal size. There appears to be no sutural contact between the prootic and opisthotic on the dorsal surface of the skull; however, the bone surface in this region is very eroded and the exact location of the sutures must remain in doubt.

A lateral view of the specimen (text-figs. 2, 5B) shows that the facial angle is steep and the flexure of the skull quite pronounced. The distance from the tip of the premaxilla

to the anterior edge of the orbit is greater than the antero-posterior orbital diameter. The maxilla is very deep, its depth probably exceeding the vertical diameter of the orbit. The jugal bar originates well below the lowest point of the orbital margin, being directed outwards and downwards as well as backwards. The postorbital bars, although worn, seem to have been narrow and slope backwards and upwards much as in *Cyclanorbis* Gray 1852.

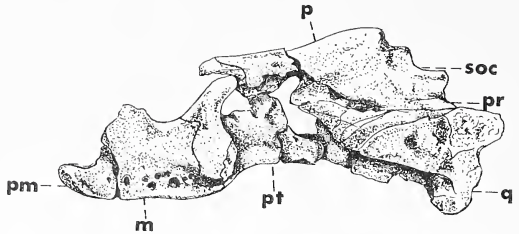

TEXT-FIG. 2. *Eurycephalochelys fowleri* gen. et sp. nov. BMNH R8445. Left lateral view of skull, $\times \frac{1}{2}$. Abbreviations as in text-fig. 1.

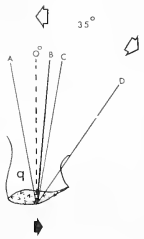

TEXT-FIG. 3. Diagram showing position of stapedial foramen (A–D) in various trionychids relative to quadrate condyle. A, *Chitra*; B, *Trionyx*, *Lissemys*, *Cyclanorbis* and ? *Pelochelys*; C, *Cycloderma*; D, *Eurycephalochelys*.

The most important feature of the skull, shown clearly in this view, is the position of the articular region of the quadrate in relation to the stapedial foramen. The articulation lies well behind and below the stapedial foramen, so that a line connecting the two would form an angle of 35° with the perpendicular (in other trionychids it lies almost immediately beneath it) (text-fig. 3); it lies well behind the level of the foramen magnum (instead of anterior to it); and it lies more or less at the antero-posterior level of the back of the basioccipital, with the occipital condyle projecting only a short distance behind it (instead of at the level of the front of the basioccipital, with the occipital condyle projecting far behind it). The forwardly directed flange of the quadrate, which rises to meet the quadratojugal, is almost horizontal (instead of oblique).

The palate (text-figs. 4, 5c) is the least complete region of the skull. The premaxilla is relatively large ventrally, forming the central portion of the blunt snout. The maxillae are broad with gently sloping surfaces running from the cutting edge to the triturating area, each reaching its maximum width at the level of the jugal bar. Although the vomer and most of the palatines are missing, the approximate form of the central area of the palate can be indicated (text-fig. 5). The intermaxillary suture would have been of

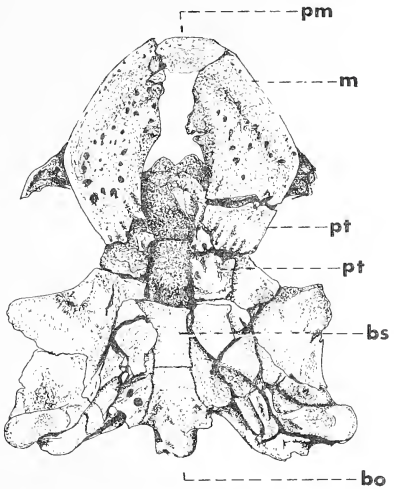

TEXT-FIG. 4. *Eurycephalochelys fowleri* gen. et sp. nov. BMNH R8445. Palatal view of skull, $\times \frac{1}{2}$. Abbreviations as in text-fig. 1.

medium length, but somewhat shorter than the length of the choanae, which are more anterior in position than in *Trionyx*. The lateral slope into the choanal vault is rounded and quite steep. The suture between the basioccipital and the basisphenoid lies anterior to the articular surfaces of the quadrates, whereas in related trionychids it lies as far back as the condyles or even slightly posterior to them.

The occiput cannot be described in great detail because of the damage caused by weathering. There is evidence of an ascending process on the pterygoid running up towards the opisthotic, but it is not possible to say whether those two elements actually met; the prootic fenestra would nevertheless have been at least partly divided. The shape of the foramen magnum and the brain cavity immediately anterior to it is wider than high; other genera of this group show the reverse condition. The only clearly traceable suture in this view is that between the quadrate and the pterygoid, which is normal in position.

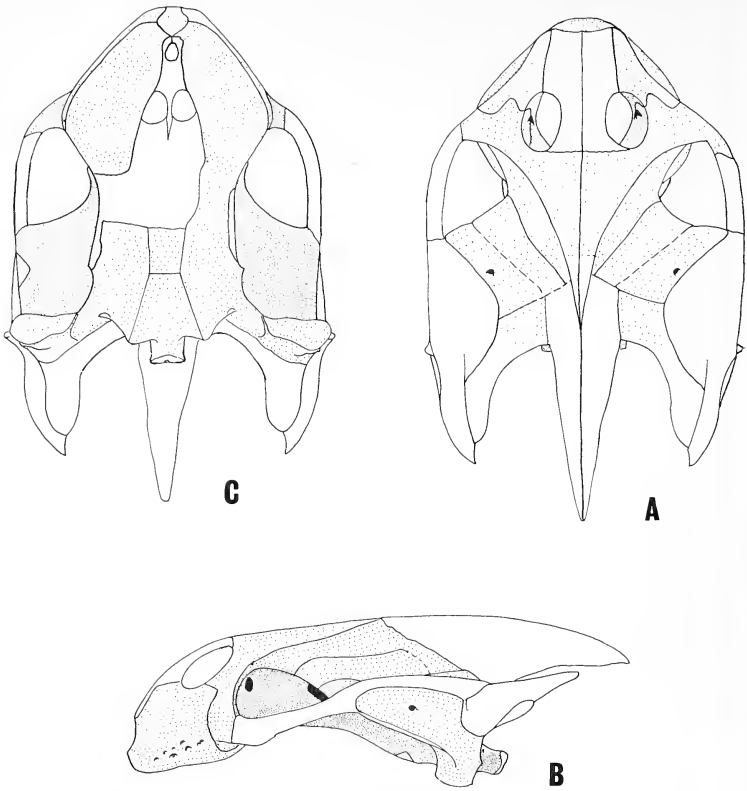

TEXT-FIG. 5. *Eurycephalochelys fowleri* gen. et sp. nov. BMNH R8445. Reconstruction of skull; A, dorsal; B, lateral; C, palatal.

Remarks. The main characters of the genus *Eurycephalochelys* which separate it from other trionychids are listed in the first paragraph of the diagnosis. In some details it resembles *Trionyx*, in others *Cyclanorbis* or *Cycloderma* Peters 1854. The palate is superficially like that of *Trionyx*, but in *Eurycephalochelys* the choanae are further forward, their anterior margins lying far in front of the widest part of the maxilla; indeed, in this feature *Eurycephalochelys* comes midway between *Trionyx* and *Cyclanorbis*. The choanae are longer than the intermaxillary sutures in *Eurycephalochelys*, *Cyclanorbis*, and

Cycloderma, but shorter in *Trionyx*; their form would have been round or oval in *Eurycephalochelys*, elongate in *Cycloderma*. (The form and length of the choanae are based on our reconstruction.)

There was almost certainly a sutural contact between the pterygoid and opisthotic in *Eurycephalochelys*. It may be noted that this contact is also present in *Cycloderma* and *Cyclanorbis* (*Eurycephalochelys* appears to be closer to the latter in its detailed form) but absent in *Trionyx* and *Chitra* Gray 1844. Loveridge and Williams (1954) figured a Recent specimen of *Trionyx triunguis* (Forskål 1775) with such a feature (AMNH 36599).

Only one other species of trionychid has been described from the Bracklesham Beds: *Trionyx bowerbanki* Lydekker 1889. The holotype (BMNH 38960) consists of an imperfect nuchal plate with a form of sculpturing rather different from that typical of *Trionyx*. This species may prove to be conspecific with *E. fowleri* when associated material comes to light.

The only trionychid which is known from the European Eocene and which includes both skull and shell material is a specimen from the Upper Montian of Trieu de Leval (Hainault, Belgium), housed in the Institut Royal des Sciences Naturelles de Belgique (no. 1.720). Dollo (1909) listed this specimen as *T. levalensis*, but he never actually described it and the name must be considered a *nomen nudum*. We have examined the skull fragments and are convinced that it is quite different from the skull described here.

Conclusions. Eurycephalochelys shows similarities to several genera, but the lack of comparative material makes it impossible to relate it to anything else at present.

Acknowledgements. We wish to thank Mr. R. Fowler for making this specimen available for description; Dr. A. J. Charig (British Museum (Natural History)) for criticising the manuscript; Dr. G. E. Quinet (Institut Royal des Sciences Naturelles de Belgique) for the photographs of the Dollo specimen, *Trionyx levalensis*, which we later examined; the American Museum of Natural History for the loan of the type skull of *Trionyx tritor* Hay 1908; and Messrs. T. Parmenter and F. Greenaway for taking the photographs.

Abbreviations. BMNH—British Museum (Natural History); AMNH—American Museum of Natural History.

REFERENCES

BELL, T. 1828. Characters of the Order, Families, and Genera of Testudinata. *Zool. J.* **3**, 513–16.

DOLLO, L. 1909. The fossil vertebrates of Belgium. *Ann. N.Y. Acad. Sci.* **19** (1), 99–119.

FITZINGER, L. J. F. J. de. 1826. *Neue Classification der Reptilien nach ihren natürlichen Verwandtschaften.* Wien.

FORSKÅL, P. 1775. *Descriptiones Animalium.*

GEOFFROY ST.-HILAIRE, E. F. 1809. Sur les tortues molles, nouv., genre sous le nom de *Trionyx* et sur la formation des carapaces. *Ann. Mus. Hist. nat. Paris*, **14**, 1–20, pl. 1–5.

GRAY, J. E. 1844. *Catalogue of the tortoises, crocodiles and amphisbaenians in the collection of the British Museum.* London.

—— 1852. Descriptions of a new genus and some new species of tortoises. *Proc. zool. Soc. Lond.* 133–5.

—— 1873. Notes on mud-tortoises (*Trionyx* Geoffroy) and the skulls of different kinds. Ibid. 38–72.

HAY, O. P. 1908. The fossil turtles of North America. *Publ. Carneg. Inst.* **75**, 529–32, figs. 687–9.

LOVERIDGE, A. and WILLIAMS, E. E. 1957. Revision of the African tortoises and turtles of the Suborder Cryptodira. *Bull. Mus. Comp. zool. Harv.* **115** (6), 164–577, pl. 15–18

LYDEKKER, R. 1889. *Catalogue of the fossil Reptilia and Amphibia in the British Museum* (*Natural History*). London, **3**, 3–23.

OWEN, R. and BELL, T. 1849. Fossil Reptilia of the London Clay and of the Bracklesham and other Tertiary beds. Chelonia. *Palaeontogr. Soc.* [*Monogr.*], 45–61, fig. 19.

PETERS, W. K. H. 1854. Übersicht der auf seiner Reise nach Mossambique beobachteten Schildkröten. *Mber. dt. Akad. Wiss. Berl.* 215–16.

R. T. J. MOODY
Department of Geology and Geography
Kingston Polytechnic
Penrhyn Road
Kingston upon Thames
Surrey

C. A. WALKER
Department of Palaeontology
British Museum (Natural History)
Cromwell Road
London
S.W. 7

Typescript received 7 November 1969

THE PALAEONTOLOGICAL ASSOCIATION

PALAEONTOLOGY

The journal *Palaeontology* is devoted to the publication of papers (preferably illustrated) on all aspects of palaeontology and stratigraphical palaeontology. Four parts at least are published each year and are sent free to all members of the Association. Members who join for 1969 will receive Volume 13, Parts 1 to 4.

All back numbers are still in print and may be ordered from B. H. Blackwell, Broad Street, Oxford, England, at £3 per part (post free). A complete set, Volumes 1–12, consists of 47 parts and costs £141.

SPECIAL PAPERS IN PALAEONTOLOGY

This is a series of substantial separate works published by the Association. The subscription rate is £6 (U.S. $16.00) for Institute Members and £3 (U.S. $8.00) for Ordinary and Student Members. Subscriptions and orders by members of the Association should be placed through the Membership Treasurer, Dr. A. J. Lloyd, Department of Geology, University College, Gower Street, London, W.C. 1, England.

The following *Special Papers* are available. Members may obtain them at reduced rates through the Membership Treasurer. Non-members may obtain them from B. H. Blackwell, Broad Street, Oxford, England, at the prices indicated.

Special Paper No. 1 (for 1967): MIOSPORES IN THE COAL SEAMS OF THE CARBONIFEROUS OF GREAT BRITAIN, by A. H. V. Smith and M. A. Butterworth. 324 pp., 72 text-figs., 27 collotype plates. Price £8 (U.S. $22.00), post free.

Special Paper No. 2 (for 1968): EVOLUTION OF THE SHELL STRUCTURE OF ARTICULATE BRACHIOPODS, by Alwyn Williams. 55 pp., 27 text-figs., 24 collotype, plates. Price £5 (U.S. $13.00).

Special Paper No. 3 (for 1968): UPPER MAESTRICHTIAN RADIOLARIA OF CALIFORNIA, by Helen P. Foreman. 82 pp., 8 collotype plates. Price £3 (U.K. $8.00).

Special Paper No. 4 (for 1969): LOWER TURONIAN AMMONITES FROM ISRAEL, by R. Freund and M. Raab. 83 pp., 15 text-figs., 10 plates. Price £3 (U.K. $8.00).

Special Paper No. 5 (for 1969): CHITINOZOA FROM THE ORDOVICIAN VIOLA AND FERNVALE LIMESTONES OF THE ARBUCKLE MOUNTAINS, OKLAHOMA, by W. A. M. JENKINS. 44 pp., 10 text-figs., 9 plates. Price £2 (U.S. $5.00).

Special Paper No. 6 (for 1969): AMMONOIDEA FROM THE MATA SERIES (SANTONIAN–MAASTRICHTIAN) OF NEW ZEALAND, by R. A. Henderson. 82 pp., 13 text-figs., 15 plates. Price £3 (U.S. $8.00).

Special Paper No. 7 (for 1970): SHELL STRUCTURE OF THE CRANIACEA AND OTHER CALCAREOUS INARTICULATE BRACHIOPODA, by A. WILLIAMS and A. D. WRIGHT. 51 pp., 17 text-figs., 15 plates. Price £1·50 (U.S. $4.00).

SUBMISSION OF PAPERS

Typescripts on all aspects of palaeontology and stratigraphical palaeontology are invited. They should conform in style to those already published in this journal, and should be sent to Mr. N. F. Hughes, Department of Geology, Sedgwick Museum, Downing Street, Cambridge, England, who will supply detailed instructions for authors on request (these are published in *Palaeontology*, **10**, pp. 707–12).

PALAEONTOLOGY

VOLUME 13 • PART 3

CONTENTS

VOLUME 13 · PART 4

Palaeontology

DECEMBER 1970

PUBLISHED BY THE
PALAEONTOLOGICAL ASSOCIATION
LONDON

Price £3 (from 1971, £5)

THE PALAEONTOLOGICAL ASSOCIATION

The Association was founded in 1957 to further the study of palaeontology. It holds meetings and demonstrations, and publishes the quarterly journal *Palaeontology* and *Special Papers in Palaeontology*. Membership is open to individuals, institutions, libraries, etc., on payment of the appropriate annual subscription:

Institute membership . . .	£7. 0*s*. (U.S. $20.00) (from 1971, £10)
Ordinary membership . . .	£5. 0*s*. (U.S. $13.00)
Student membership . . .	£3. 0*s*. (U.S. $8.00)

There is no admission fee. Institute membership is only available by direct application, not through agents. Student members are persons receiving full-time instruction at educational institutions recognized by the Council; on first applying for membership, they should obtain an application form from the Membership Treasurer. All subscriptions are due each January, and should be sent to the Membership Treasurer, Dr. A. J. Lloyd, Department of Geology, University College, Gower Street, London, W.C. 1, England.

COUNCIL 1970–1

President: Dr. W. S. McKerrow, Department of Geology, Oxford

Vice-Presidents: Professor Alwyn Williams, The Queen's University, Belfast
Professor M. R. House, The University, Kingston upon Hull, Yorkshire

Treasurer: Dr. J. M. Hancock, Department of Geology, King's College, London, W.C. 2

Membership Treasurer: Dr. A. J. Lloyd, Department of Geology, University College, Gower Street, London, W.C. 4

Secretary: Dr. W. D. I. Rolfe, Hunterian Museum, The University, Glasgow, W. 2

Editors

Mr. N. F. Hughes, Sedgwick Museum, Cambridge
Dr. Gwyn Thomas, Department of Geology, Imperial College, London, S.W. 7
Dr. Isles Strachan, Department of Geology, The University, Birmingham 15
Dr. R. Goldring, Department of Geology, The University, Reading, Berks.
Dr. J. D. Hudson, Department of Geology, The University, Leicester

Other members of Council

Dr. F. M. Broadhurst, Manchester
Dr. L. R. M. Cocks, London
Dr. R. H. Cummings, Abergele
Dr. D. J. Gobbett, Cambridge
Dr. Julia Hubbard, London
Dr. W. J. Kennedy, Oxford
Dr. J. D. Lawson, Glasgow
Dr. W. H. C. Ramsbottom, Leeds
Dr. P. L. Robinson, London
Dr. E. P. F. Rose, London
Dr. C. T. Scrutton, London
Dr. V. G. Walmsley, Swansea
Dr. A. D. Wright, Belfast

Overseas Representatives

Australia: Professor Dorothy Hill, Department of Geology, University of Queensland, Brisbane

Canada: Dr. D. J. McLaren, Institute of Sedimentary and Petroleum Geology, 3303–33rd Street NW., Calgary, Alberta

India: Professor M. R. Sahni, 98 The Mall, Lucknow (U.P.), India

New Zealand: Dr. C. A. Fleming, New Zealand Geological Survey, P.O. Box 368, Lower Hutt

West Indies and Central America: Mr. John B. Saunders, Geological Laboratory, Texaco Trinidad, Inc., Pointe-à-Pierre, Trinidad, West Indies

Western U.S.A.: Professor J. Wyatt Durham, Department of Paleontology, University of California, Berkeley 4, California

Eastern U.S.A.: Professor J. W. Wells, Department of Geology, Cornell University Ithaca, New York

THE GRAPTOLITE FAUNA OF GRIESTON QUARRY, NEAR INNERLEITHEN, PEEBLESSHIRE

by P. TOGHILL *and* I. STRACHAN

ABSTRACT. The graptolite fauna of the Upper Llandovery beds at Grieston Quarry, Peeblesshire, is described. It includes *Glyptograptus*? *nebula* sp. nov. (the youngest British diplograptid yet found) and *Monograptus drepanoformis* sp. nov. The relationship of the type *Monoclimacis griestoniensis* association to the *griestoniensis* Zone recorded elsewhere is discussed.

GRIESTON QUARRY (NT 3130 3618), 1 mile WSW. of Innerleithen, Peeblesshire, lies in an area of steeply dipping Upper Llandovery greywackes (Gala Group of Lapworth 1870) and has long been known for yielding relatively abundant graptolites indicative of a higher level in the Llandovery than any of the surrounding area. The quarry provided the type specimens of *Monoclimacis* [*Graptolites*] *griestoniensis* (Nicol 1850), and although this species is now an Upper Llandovery zone fossil (Wood 1906), there has been no review of the Grieston Quarry fauna since Nicol's original (1850) account.

Nicol first recorded graptolites from Grieston (1848, p. 204) but gave little information and no specific names. His main account (1850, pp. 53–5) was in fact quite detailed, including joint directions, but it did not include a map and in some cases it is difficult to relate exact horizons in the present quarry with his descriptions. He recorded three graptolite horizons but thought the highest of these might be a repetition due to faulting. The rest of his account consisted of a general discussion of the Silurian rocks of south-east Scotland and the structure of the whole Southern Uplands, ending with notes on the graptolites. His fauna included *Graptolites sedgwickii*, *G. distans*, *G. tenuis*, *G. convolutus*, *G. ludensis*, and the new species *G. griestoniensis*. The last three were described in some detail along with another form from nearby Thornilee Quarry. In conformity with the knowledge of the period, he correlated the Grieston Slates with the Llandeilo flags of Wales.

Lapworth (1870, p. 206) placed the 'Slates of Thornilee and the Grieston' at the top of his Gala Group, and recorded from Grieston Quarry, in addition to Nicol's fauna, *Diplograptus* sp., *Graptolites colonus*, and *Retiolites geinitzianus*. In his later detailed work, 'On Scottish Monograptidae', Lapworth (1876) recorded some of his monograptids from Grieston Quarry, including *Monograptus priodon*, *M. barrandei*, *M. exiguus*, *M. crispus*, and *M. convolutus* var. *proteus*. Remarkably, he did not accept *M. griestouiensis* as a valid species, but considered it (1876, p. 350) to be a peculiar view of *M. hisingeri* (Carruthers) (= *nudus* Lapworth). However, Elles and Wood (1911, pp. 413–14) accepted the species without question, and presumably with Lapworth's approval. Peach and Horne (1899, p. 206) gave few details of the quarry and gave as a fauna: *Monograptus priodon*, *M. convolutus*, *M. vomerinus*, *M. sedgwickii*, and *Retiolites geinitzianus*. Elles and Wood figured specimens of *M. priodon*, *M. acus*, *M. nudus*, *M. griestoniensis*, and *R. geinitzianus* from Grieston.

[Palaeontology, Vol. 13, Part 4, 1970, pp. 511–21, pls. 103–105.]

The fauna described below is based mainly on Nicol's original collection from Grieston Quarry, which he donated to various institutions, together with collections made later by Nicholson, B. M. Wright, and Lapworth, as well as the authors.

LITHOLOGIES AND FAUNA OF GRIESTON QUARRY

The quarry exposes 43 m. (140 ft.) of flaggy greywackes which dip consistently north-west at between 60° and 65°. The detailed succession comprises alternations of greyish-green flaggy shales and fine- to medium-grained greyish-green and bluish-grey greywackes, with occasional nodular horizons. The greywackes, which are normally up to 0·9 m. (3 ft.) thick, but occasionally thicker, contain abundant small-scale sole markings, showing the strata to be the right way up. Some of the finer-grained greywackes, and all of the shales, split into uniform flags or 'slates', and these have been quarried in the past for roofing material.

The quarry is affected by a set of joints striking at 10°, and two joint planes in particular are conspicuous features on the quarry face. Both of these are mineralized and slickensided, and although Nicol thought one at least was a fault, there appears to have been little or no displacement along them. The more easterly of these cuts the lower part of the section and dips E. 10° S. at 80°. The second dips at 37° in the same direction and its face forms the present western limit of the quarry.

Nicol (1850, p. 54) recorded three fossiliferous horizons, two lower beds 3·1 m. (10 ft.) apart, and a third 21–24 m. (70–80 ft.) higher. As a fault intervened (in fact the more easterly of two major joints) he thought the third bed may have been a repetition of the first or second. The lowest bed '. . . a bed of slate . . . lately opened' contained the best-preserved graptolites, but the middle bed contained *Graptolites sedgwickii* in abundance. We have located the majority of Nicol's original collection, which comprises large slabs of bluish-grey greywacke containing well-preserved specimens, and likely to have come from the 'lowest bed of slate' which was being freshly worked at the time.

We have recently found this horizon 3·7 m. (12 ft.) above the base of the section, near the eastern corner of the quarry, and have collected large slabs of greywacke with well-preserved graptolites, and clearly the same material as in Nicol's collection. Another less-fossiliferous horizon occurs only 0·9 m. (3 ft.) above the base of the section, but we have been unable to find any other fossiliferous horizons in situ.

However, there are fragments in the quarry talus of fossiliferous micaceous greywacke, quite unlike the lithology of the main fossil horizon, but which matches closely collections made from Grieston by Nicholson, Wright, and Lapworth, not long after Nicol's original investigations. This lithology has not yet been found *in situ* on the quarry face. It may be from Nicol's middle or highest horizon, but we are referring to all this material as horizon 2, and the horizon of Nicol's original collection as horizon 1.

The fine-grained greywacke slabs of Nicol's collection, and samples collected by us from horizon 1, 3·7 m. (12 ft.) above the base of the section contain the following common species: *Monoclimacis griestoniensis* (Nicol), *Monograptus priodon* (Bronn), and *Monograptus spiralis* (Geinitz) sensu Elles and Wood, together with rarer examples of *M. discus* Törnquist, *Retiolites geinitzianus angustidens* Elles and Wood, *Pseudoplegmatograptus obesus* (Lapworth), and one example of *Diversograptus*? sp.

The micaceous greywackes of horizon 2 yield the following common species: *Monograptus drepanoformis* sp. nov., *M. priodon*, *M. spiralis*, *Pristiograptus nudus* (Lapworth), and *Glyptograptus*? *nebula* sp. nov., together with rarer examples of *Monoclimacis griestoniensis*, *Retiolites geinitzianus angustidens*, and *Pseudoplegmatograptus obesus*.

These two horizons show some notable differences in their fauna. In particular *Monoclimacis griestoniensis* is only common at horizon 1. *Monograptus discus* is restricted to horizon 1, whereas *M. drepanoformis*, *Pristiograptus nudus*, and *Glyptograptus*? *nebula* are common at, but restricted to, horizon 2.

THE AGE OF THE GRIESTON QUARRY BEDS

The fauna listed above represents an horizon in the *griestoniensis* Zone (Upper Llandovery) as defined at Trannon (Wood 1906, pp. 657–60), and as well as the zone species the following are common to both localities: *Pristiograptus nudus*, *Monograptus discus*, *M. spiralis*, and *M. priodon*. It is worth noting that the Trannon area itself has not been reviewed since 1906. The highest fossiliferous band of the *griestoniensis* Zone at Trannon yields *Monoclimacis vomerinus crenulata*, the zone species of the overlying *crenulata* Zone. This species is absent at Grieston, and so is *Monograptus marri*, a species common to all but the highest horizon of the *griestoniensis* Zone at Trannon. It seems likely that the exact horizon of the Grieston Quarry beds may be immediately below the highest fossiliferous beds of the *griestoniensis* Zone at Trannon (Wood 1906, p. 658).

The terms 'Grieston Slates' and 'Grieston Shales' have been applied to the beds of Grieston Quarry, the former term by Nicol (1850) and Lapworth (1870), and the latter by the Geological Survey (Peach and Horne 1899). Both Nicol and Lapworth considered that the term Grieston Slates could be applied to strata outcropping along the strike north-east and south-west of Grieston Quarry. Until a detailed investigation into the whole of the Gala Group is carried out in this area it seems unlikely that any term applied to the beds exposed in the quarry can be safely applied outside its confines. Thus we feel it is best to refer to the beds in the quarry as a horizon within the Gala Group (probably near the top). Lapworth himself expressed some doubt as to whether his divisions within the Gala Group had anything more than local geographical significance (1870, pp. 206–7).

Although the exact relationships of the beds of Grieston Quarry to those of the surrounding area are not yet certain there is no doubt that they contain the youngest (yet proven) graptolite fauna of the area. All the other graptolite localities of the Gala Group to the east and south-east, around Galashiels (Lapworth 1870, pp. 204–9, 279–84; Peach and Horne 1899, pp. 201–6) yield graptolites indicative of the underlying *crispus* and *turriculatus* Zones.

The specimen of *M. vomerinus crenulata* figured by Elles and Wood (1910, pl. 41, fig. 4*d*) from Williamshope, in fact comes from Meigle Quarry, but is a poorly preserved specimen of *M. galaensis* (Lapworth).

Lapworth (1870, p. 280) did not consider that the greywackes to the north of the Grieston slates belonged to the Gala Group as they were not found in the Gala district, and he stated: '. . . the Gala Group may provisionally be considered as terminated by the Thornilee Slates which appear to form the centre of a synclinal'. Thus although he

grouped 'The Slates of Thornilee and the Grieston' together (1870, p. 206) at the top of the Gala Group he must have considered the Thornilee Slates to overlie those of 'the Grieston'.

Between Grieston Quarry and the Ordovician–Silurian boundary 6 miles to the north-west occurs a barren greywacke sequence which presumably must represent the whole of the Llandovery below the *griestoniensis* Zone, so that a major synclinal axis somewhere near to Grieston Quarry seems quite likely, and all the beds north of this axis must young consistently to the south-east.

The whole of this area has a dominant Caledonoid strike (NE.–SW.) and another of the structural problems posed by the area is that at Douglas Burn (Peach and Horne 1899, pp. 141–2), only 6 miles south-west of Grieston Quarry, and on exactly the same strike, occur black graptolitic shales with Ordovician graptolites indicative of the basal Caradoc zone of *Nemagraptus gracilis*. Thus any synclinal axis through Grieston Quarry must rapidly plunge to the north-east.

SYSTEMATIC DESCRIPTIONS

Specimens from various institutions are prefixed as follows: Q, Palaeontology Department, British Museum (Natural History); SM A, Sedgwick Museum, Cambridge; GSM, Geological Survey Museum; GSM Geol. Soc. Coll., Geological Society of London Collection, now in the Geological Survey Museum.

Monoclimacis griestoniensis (Nicol)

Plate 103, figs. 1–5; text-figs. 1*a–h*

1850 *Graptolites griestoniensis* Nicol, p. 63, fig. 2.
1911 *Monograptus griestoniensis* (Nicol); Elles and Wood, pp. 413–14, text-figs. 279*a–f*, pl. 41, figs. 5*a–d*.
1940 *Monoclimacis griestoniensis griestoniensis* (Nicol); Přibyl, p. 10, pl. 3, figs. 1–3.
1945 *Monoclimacis griestoniensis* (Nicol); Waterlot, p. 77, pl. 32, fig. 333.
1952 *Monoclimacis griestoniensis griestoniensis* (Nicol); Münch, pl. 39, figs. 1*a*, *b*.

Lectotype. GSM 11,800 (Pl. 103, fig. 3; text-fig. 1*a*), ?Nicol's type slab, horizon 1, Grieston Quarry, Innerleithen. Figured Elles and Wood 1911, pl. 41, fig. 5*a*.

Discussion of lectotype. It is not clear from Nicol's original two figures whether they are different magnifications of the same specimen, or two different specimens. He may thus have illustrated a holotype or two syntypes, but in any case no specimen in his original collection can be matched exactly with his original figures. Elles and Wood (1911) stated that GSM 11,800 was Nicol's type slab but there seems to be no evidence for this, and in fact Nicol presented his original material, in the form of

---

EXPLANATION OF PLATE 103

Figs. 1–5. *Monoclimacis griestoniensis* (Nicol), horizon 1, Grieston Quarry, Nicol Collection. 1, 2, GSM Geol. Soc. Coll. 6957, ? Nicol's original specimen, figured 1850, p. 63, figs. 2*a*, *b*; 1 ×3; 2, (enlargement of part of same) ×10. 3, Lectotype, GSM 11,800, figured Elles and Wood 1911, pl. 41, fig. 5*a*, ×3. 4, GSM Geol. Soc. Coll. 6957, ×3. 5, SM A21678, figured Elles and Wood 1911, pl. 41, fig. 5*c*, proximal end showing sicula, ×10.

Fig. 6. *Diversograptus*? sp., horizon 1, Grieston Quarry, Nicol Collection, GSM Geol. Soc. Coll. 6957, ×6. Also seen on fig. 4.

Figs. 7, 8. *Pristiograptus nudus* (Lapworth), horizon 2, Grieston Quarry, Wright Collection. 7, Q3078*c*, ×9. 8, Q3081*c*, ×10.

1

2

5

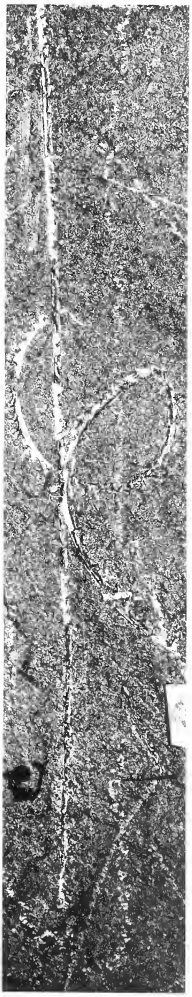

3

4

6

7

8

TOGHILL and STRACHAN, Grieston Quarry

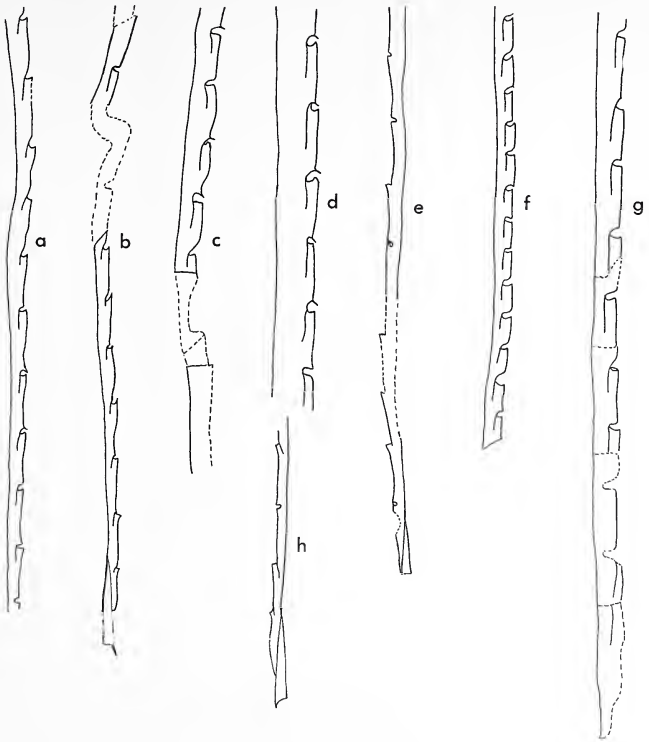

TEXT-FIG. 1. *Monoclimacis griestoniensis* (Nicol), horizon 1, Grieston Quarry, Innerleithen, Peeblesshire. All original Nicol Collection. *f* ×5, remainder ×12. *a*, lectotype GSM 11,800, proximal portion, figured Elles and Wood 1911, pl. 41, fig. 5*a*; *b*, *c*, *d*, SM A21678, figured Elles and Wood 1911, pl. 41, fig. 5*c*; *e*, SM A21681, figured Elles and Wood 1911, p. 413, text-fig. 279*b*; *f*, GSM Geol. Soc. Coll. 6957, possibly Nicol's original specimen (1850, p. 63, fig. 2); *g*, SM A21680, figured Elles and Wood 1911, pl. 41, fig. 5*d*; *h*, SM A21679.

greywacke slabs, to various institutions, including the Geological Society of London. The specimens presented to the latter are now in the Geological Survey Collections, and one of these, GSM Geol. Soc. Coll. 6957, according to their catalogues, contains the type specimen. Indeed one specimen on this slab (Pl. 103, figs. 1, 2; text-fig. 1*f*) compares favourably with Nicol's original drawing, but it is impossible to be certain. In any case Přibyl (1948) selected GSM 11,800, Elles and Wood, 1911, pl. 41, fig. 5*a* as lectotype. This is unfortunate as this specimen is a distal fragment, and better and more complete specimens are available from Nicol's type collection.

Material. Numerous specimens on greywacke slabs from Grieston Quarry (horizon 1) presented by Professor James Nicol to the Geological Society of London, Sedgwick Museum, Geological Survey of Great Britain, and British Museum (Natural History). Rare specimens from horizon 2, Grieston Quarry, B. M. Wright and H. A. Nicholson Collections, British Museum (Natural History).

Diagnosis. Long, slender, straight or slightly arcuate monograptid, up to 0·8 mm. wide, thecae 10–8 in 10 mm. of typical *Monoclimacis* type; proximal thecae showing little curvature and having everted apertures; distal thecae of typical climacograptid shape.

Description. The rhabdosome is long and slender, either straight or showing slight but continuous ventral curvature. The longest fragment is 90 mm. long, but the greatest width is only 0·8 mm. In the most complete specimen (Pl. 103, fig. 5; text-figs. 1*b–d*) the width increases from 0·2 mm. at the first theca to a maximum of 0·7 mm. at th 50, after 75 mm. The sicula is 1·4 mm. long and reaches just past the aperture of the first theca. The thecae number 10–8 in 10 mm., and gradually increase in length from 0·7 to 1·8 mm. after 75 mm. They overlap only $\frac{1}{6}$ at the proximal end but this value increases distally to $\frac{1}{2}$. The proximal thecae are almost straight with only a very slight geniculum, and the apertures are slightly everted. The geniculum becomes distally more pronounced, until the angle between the supra- and infra-genicular walls is 90°, and then the typical *Monoclimacis* appearance is reached. When well preserved the geniculum is produced into a flange which gives the aperture a hooded appearance (text-fig. 1*d*).

Occasionally the rhabdosome is preserved in dorsal or ventral view, and then it has the appearance of a series of vertebrae (Elles and Wood 1911, p. 413, text-fig. 279*f*). This is due to the expansion of the thecae at the aperture, associated with the overlying genicular flange of the next theca.

Remarks. This well-defined species is presumably the ancestor of the main Wenlock vomerinid stock, since it is earlier than *M. crenulata* at Trannon, and other Llandovery forms such as *M. galaensis* can only doubtfully be regarded as monoclimacids (Rickards 1968). This new description agrees with that of Elles and Wood, except that the length of sicula given here, 1·4 mm., is more than twice the 0·6 mm. given by them. One of us (P. T.) has examined specimens of *M. griestoniensis* collected by Wood from Trannon and figured by Elles and Wood (1911, p. 413, figs. *a*, *d–f*). These agree in dimensions with those from Grieston Quarry.

Occurrence and associates. At Grieston Quarry *Monoclimacis griestoniensis* is common on Nicol's original greywacke slabs which presumably come from horizon 1. It is associated commonly with *Monograptus priodon*, *M. spiralis*, and *M. discus*. It only occurs rarely at horizon 2 associated with *Pristiograptus nudus*, *M. drepanoformis* sp. nov. and *Glyptograptus*? *nebula* sp. nov.

EXPLANATION OF PLATE 104

Figs. 1–4. *Monograptus drepanoformis* sp. nov., horizon 2, Grieston Quarry. Fig. 2 Nicholson Collection, remainder Wright Collection. 1, Holotype, Q3072*b*, ×16. 2, Q3089*a*, ×10. 3, Q3073*b*, ×14. 4, Q3081*a*, ×12.

Figs. 5–9. *Monograptus spiralis* (Geinitz) sensu Elles and Wood. Fig. 5, horizon 1; remainder, horizon 2, Grieston Quarry. 5, GSM 11,801, Nicol Collection, ×10. 6, Q3080*a*, ×8, Nicholson Collection. 7, Q3081*b*, ×10, Wright Collection. 8, Q3080*b*, ×8, Nicholson Collection. 9, Q3074*d*, ×6, Wright Collection.

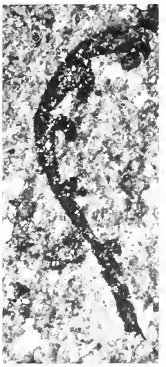

1

2

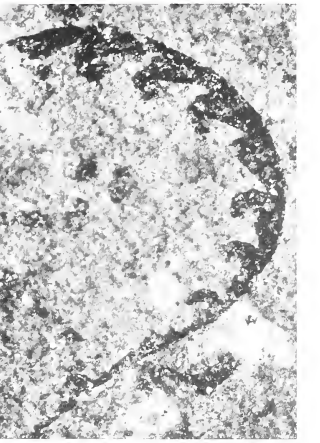

3

4

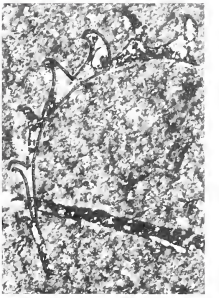

5

6

8

9

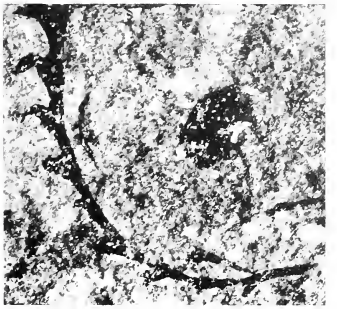

7

TOGHILL and STRACHAN, Grieston Quarry

The type locality is the only well-documented occurrence in Scotland, but the species occurs commonly in the Cross Fell Inlier (Burgess, Rickards, and Strachan 1970). It is common in Wales where it was designated the index fossil for the Upper Llandovery (Tarannon) *griestoniensis* Zone by Wood (1906) in the Trannon area. It has recently been recorded from the Welsh Borderland associated with late Upper Llandovery (Telychian) shelly fossils (Cocks and Rickards 1969). It occurs elsewhere in Europe (Přibyl 1940, Münch 1952); North Africa (Waterlot 1945); and Australia (Thomas and Keble 1933), but has not been recorded from North America.

TEXT-FIG. 2. *Monograptus drepanoformis* sp. nov., horizon 2, Grieston Quarry, Innerleithen, Peeblesshire. All ×7 approx. B. M. Wright Collection except *b*, which is Nicholson Collection. *a*, holotype, Q3072*b*; *b*, Q3089*b*; *c*, Q3081*a*; *d*, Q3073*b*; *e*, Q3079; *f*, Q3081*b*.

Monograptus drepanoformis sp. nov.

Plate 104, figs. 1–4; text-figs. 2*a–f*

Holotype. BMNH Q3072*b* (Pl. 104, fig. 1, text-fig. 2*a*), Grieston Quarry, horizon 2, Innerleithen, Peeblesshire; B. M. Wright Collection.

Material. Numerous specimens from horizon 2, Grieston Quarry.

Derivation of name. Greek, sickle-shaped.

Diagnosis. Short rhabdosome, up to 1 mm. wide, with tight ventral curvature, but slightly recurved dorsally at the proximal end. Thecae with little overlap, 12–10 in 10 mm. with conspicuous open hooks, and a tendency to expand throughout their length giving a triangulate appearance.

Description. The rhabdosome is short, up to 10 mm. and shows conspicuous ventral curvature, although the extreme proximal end is recurved with slight dorsal curvature. The sicula is 1·2 mm. long and reaches as far as the apex of the first thecal hook. The width increases from 0·3 mm. at the widest part of the first theca to a maximum of 0·8–1·0 mm. reached after only 10 thecae. Ten to twelve thecae occur in 10 mm. and these are 1·0 mm. long, including the hooks, and the overlap is always slight. The first two or three thecae have a straight proximal portion which is of constant width passing into a conspicuous open hook at the aperture. The third, or fourth, and later thecae expand throughout their length and thus have a triangulate appearance, but again the apertural region is a conspicuous open hook with the aperture pointing directly backwards.

Remarks. The over-all shape resembles *M. crispus* Lapworth, but the rhabdosome is shorter, and the proximal end not so slender or so recurved. The triangulate distal thecae are similar to *M. flagellaris* Törnquist, but the apertural region is hooked, and not coiled as it is in the latter. Earlier records of *M. crispus* from Grieston Quarry can probably be referred to this new species.

Occurrence and associates. M. drepanoformis occurs commonly at horizon 2 in Grieston Quarry but not on any of Nicol's greywacke slabs from horizon 1. It is associated with *M. priodon*, *M. spiralis*, *Pristiograptus nudus*, and *Glyptograptus*? *nebula* sp. nov.

Monograptus spiralis (Geinitz) sensu Elles and Wood

Plate 104, figs. 5–9; Plate 105, fig. 14

1913 *Monograptus spiralis* (Geinitz); Elles and Wood, pp. 475–6, text-figs. 331*a–c*, pl. 48, figs. 7*a–d*.

Discussion. Elles and Wood (1913) included in *Monograptus spiralis* forms with both regular and irregular curvature, and they remarked on the large size of specimens from the *griestoniensis* Zone. In his review of the genus *Spirograptus*, Přibyl (1944) restricted *Monograptus spiralis* to forms with a very regular spiral curvature, and thus comparable to Geinitz's original figures (1842, pl. 10, figs. 26, 27).

The specimens here referred to *M. spiralis* (Geinitz) sensu Elles and Wood have proximal ends with open spiral curvature (Pl. 104, figs. 5, 7) but distally the curvature can be regular or irregular, and the thecae often appear on the inside of the curved stipe (Pl. 105, fig. 14). Distal fragments (Pl. 104, figs. 8, 9) are often straight, and similar to those figured by Elles and Wood (1913, p. 476, figs. 331*b*, *c*).

Some of these forms are similar in over-all appearance to *Monograptus tullbergi* Bouček, *M. tullbergi spiraloides* (Přibyl) and *M. falx* (Suess), which are recorded from the *griestoniensis* and *crenulata* Zones of Bohemia. However, the proximal end of *M. tullbergi* (Bouček 1931, p. 301, fig. 9*f*) appears to have slender, almost straight thecae, whereas distally the thecae are more hooked than triangulate. The irregularly curved *M. tullbergi spiraloides* appears to have a more robust proximal end (Přibyl 1944, pl. 5, fig. 10) than M. *spiralis* sensu Elles and Wood, as does *M. falx* (Suess) (Přibyl 1944, pl. 5, figs. 1–6).

EXPLANATION OF PLATE 105

Figs. 1–7. *Monograptus priodon* (Bronn). 1 and 2 from horizon 1, remainder from horizon 2, Grieston Quarry. 1, 2, SM A22477, Nicol Collection; 1 ×1; 2, enlargement of part of same, ×8. 3, Q3073*c*, ×9, Wright Collection. 4, Q3083, ×14, Wright Collection. 5, Q3074*e*, ×13, Wright Collection. 6, Q3074*f*, ×13, Wright Collection. 7, Q3077*a*, ×9, Nicholson Collection.

Fig. 8. *Retiolites geinitzianus angustidens* Elles and Wood, horizon 2, Grieston Quarry, Nicholson Collection, Q3089*b*, ×2·5.

Figs. 9–13. *Glyptograptus*? *nebula* sp. nov., horizon 2, Grieston Quarry. 9, 12, Nicholson Collection, remainder Wright Collection. 9, Q3071*a*, ×13. 10, Q3074*b*, ×13. 11, Q3072*a*, ×11. 12, Holotype, Q3071*b*, ×13. 13, Q3075*a*, ×13.

Fig. 14. *Monograptus spiralis* (Geinitz) sensu Elles and Wood, horizon 1, Grieston Quarry, Toghill Collection, Q3111, ×1·5.


1

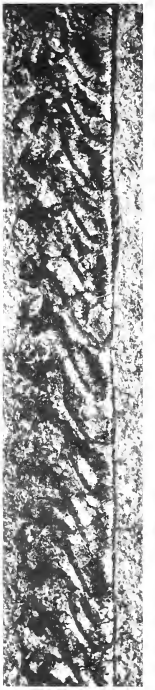
2


3

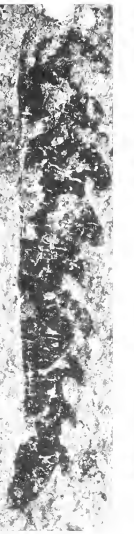
4


5


6


7


9


11


13


8


10


12


14

TOGHILL and STRACHAN, Grieston Quarry

Glyptograptus? *nebula* sp. nov.

Plate 105, figs. 9–13; text-figs. 3*a–l*

1870 *Diplograptus* sp. Lapworth, p. 206.

Holotype. BMNH Q3071*b* (Pl. 105, fig. 12, text-fig. 3*b*), Grieston Quarry, Innerleithen, Peeblesshire, B. M. Wright Collection.

Material. Numerous specimens from horizon 2, Grieston Quarry.

Diagnosis. Short, 'dwarfed' diplograptid with thin 'ghost-like' periderm. Sicula and virgula always conspicuous. Width either uniform at 0·5–0·6 mm. or decreasing somewhat distally. Thecal form often obscure but probably glyptograptid.

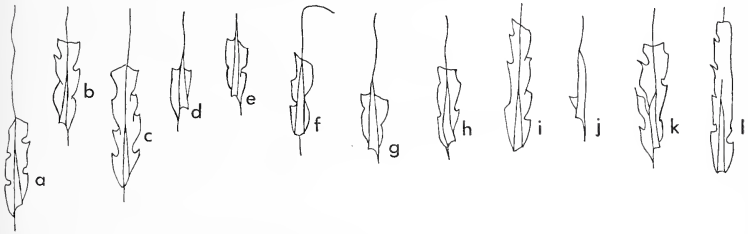

TEXT-FIG. 3. *Glyptograptus*? *nebula* sp. nov., horizon 2, Grieston Quarry, Innerleithen, Peeblesshire. All ×7 approx. *a*, *b*, *i*, H. A. Nicholson Collection, remainder B. M. Wright Collection. *a*, Q3071*a*; *b*, holotype, Q3071*b*; *c*, Q3073*a*; *d*, Q3074*a*; *e*, Q3074*b*; *f*, Q3075*a*; *g*, Q3076*b*; *h*, Q3075*b*; *i*, Q3077; *j*, Q3076*a*; *k*, damaged specimen Q3072*a*; *l*, Q3078*a*.

Description. The rhabdosome is short and narrow, and no specimens longer than 4 mm. have been found. The periderm is very thin so that the sicula and virgula always show through and the latter is always distally prolonged, sometimes to twice the length of the rhabdosome. The sicula is always conspicuous and is relatively long (1·3–1·6 mm.) and robust compared with the whole rhabdosome. It is completely embedded in the rhabdosome and in most cases reaches up to the apertures of the second thecal pair, although the exact position of its apex is sometimes difficult to see.

No more than 5 thecal pairs are ever present, and the width is either uniform at 0·5–0·6 mm. or decreases distally to around 0·4 mm. The thecae themselves are alternate, 0·8 mm. long, and show little overlap. Their shape is rather obscure but appears to vary between a glyptograptid and a climacograptid type, but on the whole are more like the former. The free ventral wall is occasionally produced into a denticle (text-fig. 3*k*).

Remarks. This is the youngest British diplograptid and is presumably the 'small *Diplograptus*' recorded by Lapworth (1870, p. 206) from Grieston Quarry.

Occurrence and associates. This new species is common at horizon 2 in Grieston Quarry, associated with *Pristiograptus nudus*, *Monograptus spiralis*, *M. drepanoformis*, *M. priodon*, and (rarely) *Monoclimacis griestoniensis*. It does not occur on the greywacke slabs

of horizon 1. Wilson (1954, unpublished Ph.D. thesis) recorded a probably identical *Climacograptus* sp. from the *turriculatus* to *griestoniensis* Zones of the Cautley area (NW. Yorkshire).

Notes on some of the remaining fauna

Specimens of *Monograptus priodon* (Bronn) from Grieston Quarry are often well preserved and can be of considerable length. They have been figured by Elles and Wood (1913, pl. 42, figs. 2*a*, *b*), and one specimen figured here (Pl. 105, figs. 1, 2) is that referred to by M'Coy (1851, p. 6) as *Graptolites sedgwickii*. References to *G. sedgwickii* in Nicol's original account can, on a modern basis, be referred to *M. priodon*.

One fragment of *Diversograptus*? has been found on one of Nicol's original slabs (Pl. 103, fig. 6). Although not diversiform this single fragment is similar to branching diversograptids which one of us (P. T.) has collected from the *Cyrtograptus grayi* band of Penwhapple Burn, Girvan.

Acknowledgements. We would like to thank Dr. R. B. Rickards (Sedgwick Museum) and Dr. A. Rushton (Institute of Geological Sciences) for the loan of specimens in their care. We are also grateful to various members of the Ludlow Research Group for advice given on an excursion to Grieston Quarry in September 1969.

REFERENCES

BOUČEK, B. 1931. Preliminary communication on some new species of graptolites from the Silurian of Bohemia. *Vest. st. geol. Ust. csl. Repub.* Prague, **7,** 293–306.

BURGESS, I. C., RICKARDS, R. B. and STRACHAN, I. 1970. The Silurian Strata of the Cross Fell area. *Bull. geol. Surv. Gt. Br.* No. 32, 167–84.

COCKS, L. R. M. and RICKARDS, R. B. 1969. Five boreholes in Shropshire and the relationships of shelly and graptolitic facies in the Lower Silurian. *Q. Jl geol. Soc. Lond.* **124,** 213–38, pl. 9–11.

ELLES, G. L. and WOOD, E. M. R. 1901–18. A monograph of British Graptolites. *Palaeontogr. Soc.* [*Monogr.*].

GEINITZ, H. B. 1842. Über die Graptolithen. *Neues Jb. Miner. Geogn. Geol. Petrefakt*, vol. for 1842, 697–701, pl. 10.

LAPWORTH, C. 1870. On the Lower Silurian Rocks of Galashiels. *Geol. Mag.*, 1 Dec., **7,** 204–9, 279–84.

—— 1876. On Scottish Monograptidae. Ibid. 2 Dec., **3,** 308–21, 350–60, 499–507, 544–52, pl. 10–13, 20.

M'COY, F. 1851. Description of the British Palaeozoic fossils in the Geological Museum of the University of Cambridge. *In* SEDGWICK, A. and M'COY, F. 1851–5. *British Palaeozoic rocks and fossils.* Cambridge, Fasc. **1,** 1–184.

MÜNCH, A. 1952. Die graptolithen aus dem Anstehenden Gotlandium Deutschlands und der Tschechoslowakei. *Geologica, Berl.* **7,** 1–157, pl. 1–62.

NICOL, J. 1848. On the geology of the Silurian rocks in the valley of the Tweed. *Q. Jl geol. Soc. Lond.* **4,** 195–209.

—— 1850. Observations on the Silurian Strata of the south east of Scotland. Ibid. **6,** 53–65.

PEACH, B. N. and HORNE, J. 1899. The Silurian rocks of Britain. **1,** Scotland. *Mem. geol. Surv. U.K.* Glasgow.

PŘIBYL, A. 1940. Revise ceskych graptolitu rodu *Monoclimacis* Frech. *Rozpr. ceske. Akad. Ved. Umeni*, Sect. 2, **50,** No. 23, 1–19, pl. 1–3.

—— 1944. The Middle-European monograptids of the genus *Spirograptus* Gurich. Ibid., Sect. 2, **54,** No. 19, 1–46, pl. 1–11.

—— 1948. *Bibliographic index of Bohemian Silurian graptolites*, Prague.

RICKARDS, R. B. 1968. The thecal structure of *Monoclimacis*? *galaensis. Lethaia*, **1,** 303–9.

THOMAS, D. E. and KEBLE, R. A. 1933. The Ordovician and Silurian Rocks of the Bulla-Sunbury area and discussion of the sequence in the Melbourne area. *Proc. R. Soc. Vict.* **45,** 33–84.

TÖRNQUIST, S. L. 1892. Undersökninger öfver Siljansområdets Graptoliter. II, Monograptidae. *Acta Univ. Lund*, **28,** no. 10, 1–47, pl. 1–3.

WATERLOT, G. 1945. Les graptolites du Maroc. Part 1. *Protectorat de la République Française au Maroc, Service Géologique. Notes et Mémoires*, no. 63, 1–112, pl. 1–50.

WILSON, D. W. R. 1954. The stratigraphy and palaeontology of the Valentian Rocks of Cautley (Yorks W.R.). Unpublished Ph.D. thesis, University of Birmingham.

WOOD, E. M. R. 1906. The Tarannon Series of Tarannon. *Q. Jl geol. Soc. Lond.* **62**, 644–701.

PETER TOGHILL
Department of Palaeontology
British Museum (Natural History)
Cromwell Road
London S.W. 7

ISLES STRACHAN
Department of Geology
University of Birmingham
Edgbaston
Birmingham 15

Revised typescript received 20 February 1970

THE EMUELLIDAE, A NEW FAMILY OF TRILOBITES FROM THE LOWER CAMBRIAN OF SOUTH AUSTRALIA

by K. J. POCOCK

ABSTRACT. Study of the adult morphology and the ontogeny of a new group of trilobites from the Lower Cambrian of South Australia has led to the erection of 2 new genera, *Emuella* and *Balcoracania*, each with 2 species, which are considered to belong to a new family, here named the Emuellidae. The members of this family are characterized by a unique combination of cephalic and thoracic features; the cephalon possesses a complete set of functional sutures of the ptychopariid type, long crescentic eye lobes widely separated from the glabella, and a geniculate posterior border; the thorax is divided into a short prothorax, in which the 6th segment is macropleural and fused to the 5th, and an extremely long opisthothorax containing numerous segments. The family is here included in the suborder Redlichiina.

Study of the ontogeny of two of the species has allowed the cephalic development to be subdivided into stages, which are related, where possible, to meraspid degrees. The fused 5th and 6th segments are released as a unit into the thorax, and the macropleural spine of the 6th has not been observed in the transitory pygidium.

The formation of the opisthothorax results from an abrupt reduction of the space available for the pleurae of segments succeeding the macropleural segment. The macropleural segment serves the role of protection, aids stability, and in the larval stages possibly buoyancy; the fusion of this segment to the preceding assists in control of the former.

The Emuellidae are considered to preserve the structure of possible ancestors of the Olenellina on one hand, and the Redlichiina on the other.

THE trilobites described in this paper were first found by Dr. B. Daily of the Geology Department, University of Adelaide, on the western side of Cape D'Estaing, Kangaroo Island, South Australia (Daily 1956). Subsequently the author discovered a second locality on the eastern side of the Cape (Pocock 1964, p. 459). In 1961, Messrs. Dalgarno and Johnson, of the Geological Survey, South Australian Department of Mines, made a remarkable discovery of a similar trilobite, near Blinman, in the Flinders Ranges, South Australia. Further work by the author has located related trilobites in Kangaroo Island, and extended the known range of occurrence in the Flinders Ranges.

GEOGRAPHIC AND STRATIGRAPHIC DISTRIBUTION

The known occurrences of members of the group are restricted to Lower Cambrian rocks of the Adelaide Geosyncline. They are, however, widely separated geographically, one locality being in the eastern portion of the Flinders Ranges, and the others on the northern coast of Kangaroo Island, *c.* 350 miles away.

The Kangaroo Island localities are at Cape D'Estaing, approximately 12 miles W. of Kingscote (text-fig. 1). The fossiliferous beds occur in sections on either side of the Cape, outcropping on wave-cut platforms and in cliffs behind. On the eastern side, in the Emu Bay section of Pocock (1964), *Balcoracania dailyi* gen. et sp. nov. occurs in a zone, approximately 30 ft. thick, near the top of the White Point Conglomerate, in association with a species of *Estaingia*, *Hyolithes*, and an unidentified brachiopod; *Emuella dalgarnoi* gen. et sp. nov. occurs 250 ft. stratigraphically above, in a 2-ft. thick bed within the

[Palaeontology, Vol. 13, Part 4, 1970, pp. 522–62, pls. 106–110.]

Emu Bay Shale and immediately above beds containing *Estaingia bilobata* Pocock and a species of *Redlichia* (Pocock 1964). On the W. side of the Cape, in a section which can be correlated in part with the Emu Bay section, *Emuella polymera* gen. et sp. nov. occurs in a thin bed near the base of the sequence, and *B. dailyi* occurs in the overlying 60 ft. All the fossiliferous beds at this locality occur in the upper part of the White Point Conglomerate (text-fig. 2).

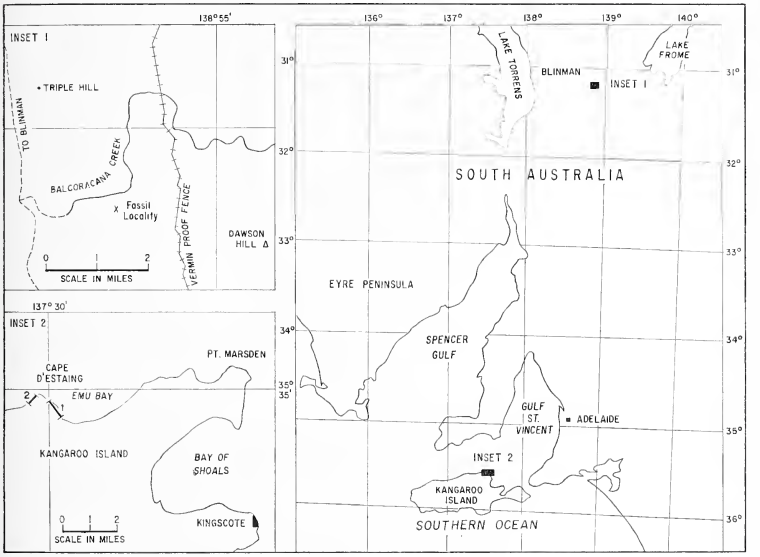

TEXT-FIG. 1. Locality Maps. *Inset* 1, Balcoracana Creek area, Flinders Ranges, South Australia. *Inset* 2, Kangaroo Island, South Australia; 1, Emu Bay section; 2, Cape D'Estaing section.

The Flinders Ranges locality (text-fig. 1) is at Balcoracana Creek, 14 miles ESE. of Blinman. Here *Balcoracania flindersi* gen. et sp. nov. occurs in a 30-ft. thick section of the Billy Creek Formation, approximately 500 ft. above the base.

The White Point Conglomerate and the Emu Bay Shale are considered to be upper Lower Cambrian. The evidence upon which this determination is based was reviewed by Daily (1956) and Pocock (1964).

The Billy Creek Formation is underlain by the Oraparinna Shale of middle Lower Cambrian age (Walter 1967), and overlain by the Wirrealpa Limestone, which Daily (1956) considered lower Middle Cambrian. The Billy Creek Formation at this locality is 3300 ft. thick, and the trilobites occur approximately 2800 ft. below the Wirrealpa Limestone and are thus probably upper Lower Cambrian.

At the present time it is not possible to correlate the Flinders Ranges and Kangaroo Island sections, so the stratigraphic position of *B. flindersi* with respect to the other species is not known.

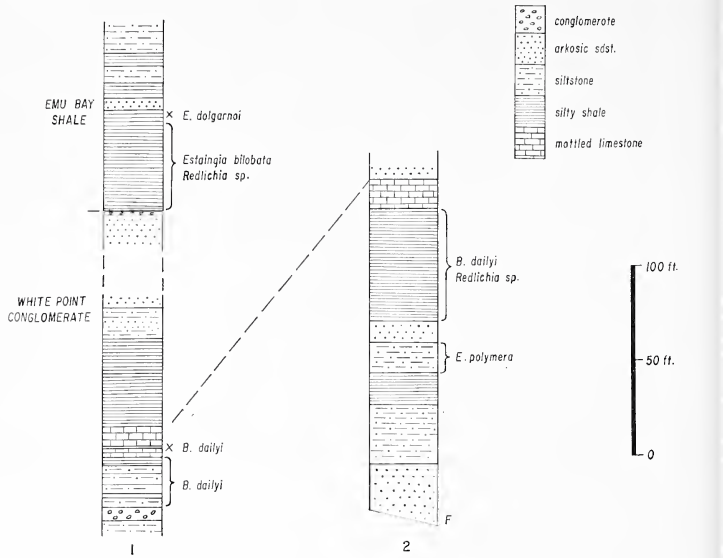

TEXT-FIG. 2. Stratigraphic columns; parts of the stratigraphic successions of Lower Cambrian age of Kangaroo Island, South Australia. 1, Emu Bay section; 2, Cape D'Estaing section.

MODE OF OCCURRENCE

At the Kangaroo Island localities, the trilobites occur on the bedding planes largely as disarticulated moults, interspersed with a few complete individuals. Both larval and adult specimens occur in the collections of *E. polymera* and *B. dailyi*, but only adults of *E. dalgarnoi* have been found. The trilobites occur in fine-grained siltstones or silty shales of slightly varying character.

In the Flinders Ranges, *B. flindersi* occurs in a sequence of greenish-brown tuffaceous shales. Specimens are rare for the greater part of the fossiliferous sequence, and are represented exclusively by moults; however one bed, about 4 in. thick, near the top is richly fossiliferous, one bedding plane being almost covered with complete individuals, both larval and adult. Such an occurrence, in a sequence of sparsely fossiliferous rocks in which only moults are found, combined with the tuffaceous nature of the shale, suggests that the assemblage results from mass mortality, perhaps associated with volcanic activity.

Mass mortality has been invoked many times to explain the nature of some fossil assemblages, and volcanic activity has often been suggested as the cause. Brongersma-Sanders (1957) reviewed this subject, and pointed out the necessity for care in invoking such a phenomenon. In this case, evidence independent of that provided by the presence of tuffaceous material, and the preponderance of complete exoskeletons, is available. The size frequency distribution of the specimens from the bedding plane (text-fig. 3)

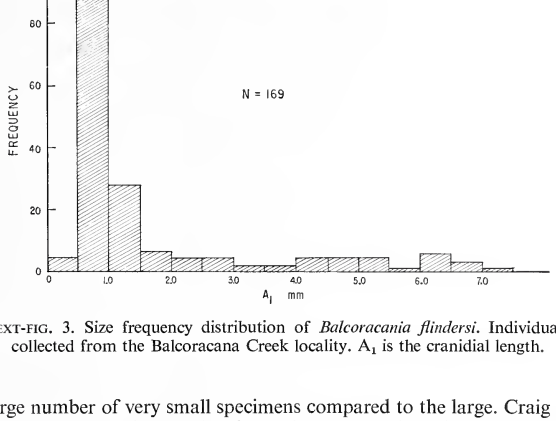

TEXT-FIG. 3. Size frequency distribution of *Balcoracania flindersi*. Individuals collected from the Balcoracana Creek locality. A_1 is the cranidial length.

shows a large number of very small specimens compared to the large. Craig and Oertel (1966) constructed theoretical models for various populations, in terms of size and age frequency distributions, and pointed out that most fossil assemblages differ from theoretical models in the absence of large numbers of young (small) individuals. In addition, mass mortality results in a frozen size frequency distribution of a living population, in which small individuals will be very abundant. The size frequency distribution of *B. flindersi* thus approximates that of a living population in the high proportion of small individuals, and the assemblage probably resulted from mass mortality.

METHODS AND TECHNIQUES

Reconstruction of distorted specimens. Although some degree of distortion and/or flattening is present in all collections, its range is limited and the number of specimens large enough for an accurate reconstruction to be made. Illustrations of reconstructed trilobites, both adult and larval, were made directly from photographs of selected specimens with the aid of a magnifying light table.

Quantitative analysis. A limited statistical analysis of variation has been made using mainly the methods of regression analysis recommended by Shaw (1956). However the parameters for the 'best fit' lines were calculated by the method given by Simpson, Roe, and Lewontin (1960, p. 234).

The measurements on which the analysis is based are given in the Appendix, and the dimensions used are shown in text-fig. 4.

Terminology. The terminology recommended in the *Treatise on invertebrate paleontology*, Part O, *Trilobita* (Harrington *et al.* 1959), is used with some modification, necessitated by the morphology of the trilobites described (text-fig. 4).

The term 'anterior fossulae' has been applied to small depressions in the axial furrows at or near the anterior edges of the glabella (Harrington *et al.* 1959, O120). In the trilobites described below, depressions occur in the axial furrows at their junctions with both the anterior border furrow and the anterior edge of the eye ridge; the term 'anterior furrow fossulae' is applied to the former, and 'eye ridge fossulae' to the latter. In larval forms the informal term 'cheek' is used, owing to the difficulty in distinguishing palpebral and posterior areas in very small specimens; 'cheek furrow' is used to describe

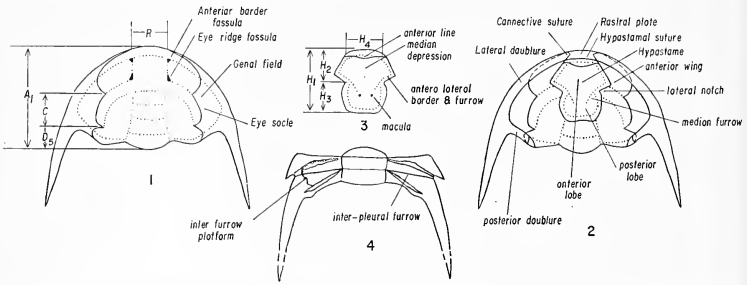

TEXT-FIG. 4. Dimensions measured, terminology, and ventral morphology. 1, Dorsal view of cranidium. 2, Ventral view of cranidium with hypostome in situ. 3, Ventral view of hypostome. 4, Dorsal view of macropleural unit. All diagrams based on specimens of *Balcoracania dailyi*.

a furrow extending onto the cheek from the junction of the axial and glabellar furrows. In the hypostome the terms 'anterior lateral border' and 'border furrow' are applied to the marginal portions between the anterior wing and the lateral notch. The terminology of Shaw and Ormiston (1964) is applied to the librigena. In the thorax, the 6th segment is macropleural and fused to the 5th; the term 'macropleural unit' is applied to this combination and 'interfurrow platform' to the area between the 5th and 6th pleural furrows.

In the systematic description and discussion, all angles are in the horizontal plane, are average values, and are given with reference to the sagittal direction unless otherwise specifically stated.

The widely used terms protaspid, meraspid, and holaspid stages are used. In view of the limited number of protaspides, no division of this stage is applied. Difficulties arise, however, in the application of the meraspid stage. The trilobites described have a short prothorax and an extremely long opisthothorax. Thus in the view of workers who consider the prothorax is homologous to the 'normal' thorax of other trilobites (e.g. Hupé 1953*a*, *c*; Harrington *et al.* 1959), the trilobites described below would have only 5 meraspid degrees, being considered holaspid on the appearance of the 6th (and last) prothoracic segment, with 50 or so articulating opisthothoracic segments still to be released. In addition, at degree 6 the cephalon is still far removed from the adult condition. On the other hand the cephalon does attain the adult condition, except for size, whilst a considerable number of opisthothoracic segments are yet to be released from the transitory pygidium.

The above considerations illustrate that the usual divisions of the stages of larval development are not always easily applicable. If other cases become known in which cranidial development is completed before thoracic development, a formal division of the meraspid period on this basis may become justified. At present, however, in view of the small number of such cases, such a division does not appear justified.

SYSTEMATIC PALAEONTOLOGY

All specimens are deposited in the Palaeontological Collection of the University of Adelaide, South Australia (AUGD, F series).

Suborder REDLICHIINA Harrington 1959 (*in* Harrington *et al.* 1959)
Family EMUELLIDAE fam. nov.

Diagnosis. Small to medium opisthoparian trilobites. Glabella with 3 transglabellar furrows in adult; axial furrows converge from occipital ring to anterior glabellar furrow;

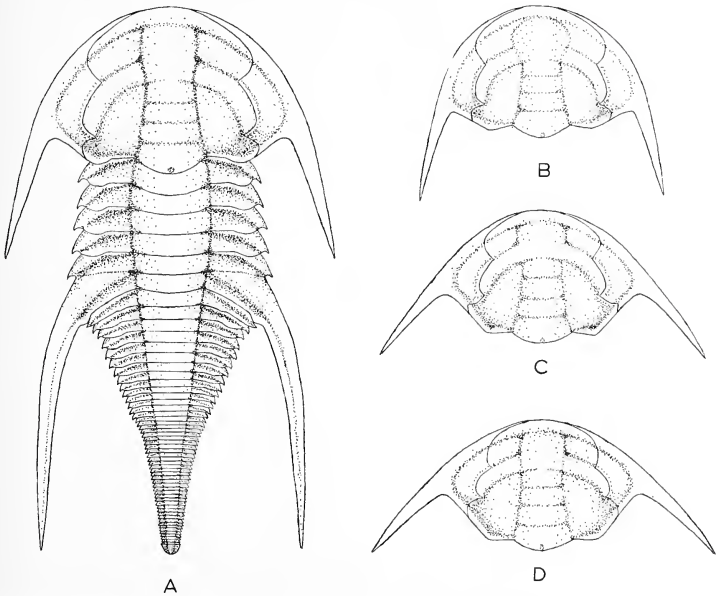

TEXT-FIG. 5. Reconstruction of adult morphology of members of the Emuellidae. A, complete dorsal exoskeleton of *B. dailyi*; B, cranidium of *B. flindersi*; C, cranidium of *E. dalgarnoi*; D, cranidium of *E. polymera*. Magnification × 10.

frontal lobe expanded, rounded laterally; preglabellar field narrow or absent. Eye ridge wide, long, directed slightly postero-laterally, palpebral lobe crescentic. Posterior area with fulcrum. Posterior border with section abaxial to fulcrum directed antero-laterally. Anterior section of facial suture diverges anteriorly to border furrow, curves sharply inwards and crosses anterior border diagonally, before becoming marginal-ventral; connective suture concave abaxially; rostral plate short (tr.), notched laterally; posterior

section of facial suture divergent; hypostomal suture functional. Hypostome with depressed anterior wings; median body with large subtriangular anterior lobe, subdivided anteriorly by median depression; small posterior lobe. Librigena with long genal spine.

Thorax with prothorax of 6 segments, and extremely long opisthothorax of between 42 and 55 segments. Sixth prothoracic segment macropleural and fused to 5th. Macropleural spine long, extends to level of pygidium. Pygidium a minute segmented disc, with border entire.

Discussion. The Emuellidae bear similarities to certain of the Olenellidae and Redlichiidae. The Emuellidae share with the Olenellidae the division of the thorax, and macropleurality; they differ in the number of segments and the fusion of prothoracic segments, and with regard to cephalic features in the possession of a complete set of functional sutures. The cephalic features are similar to those of some of the families of the Redlichiina, but the latter lack the characteristic thorax of the Emuellidae.

Genus EMUELLA gen. nov.

Type species. Emuella polymera sp. nov.

Plates 106, 107; text-fig. 5 C, D.

Derivation of name. From Emu Bay, Kangaroo Island, South Australia.

Diagnosis. Preglabellar field absent. Anterior border furrow shallows abruptly anterior to frontal glabellar lobe. Palpebral lobe relatively short, curved. Posterior border with section abaxial to fulcrum directed antero-laterally at 45° and slightly depressed. Librigena with advanced genal spine. Thorax with axis more than half thoracic width; pleurae very short. Pleural furrow terminates before pleural spine. Thorax with at least 48, and known maximum of 58 segments. Strong closely spaced granules on dorsal surfaces.

Emuella polymera sp. nov.

Plate 106; Plate 107, figs. 1, 2; text-fig. 5D.

Derivation of name. 'Polymera'—for numerous thoracic segments.

Holotype. AUGD F16643 (Pl. 106, fig. 1). It was considered essential that a specimen with an articu-

---

EXPLANATION OF PLATE 106

Figs. 1–7. *Emuella polymera* gen. et sp. nov. White Point Conglomerate, Cape D'Estaing, Kangaroo Island, South Australia. 1, Holotype, F16653, ×10; internal mould of cephalon and thorax; cranidium sagittally compressed, librigenae rotated, macropleural spines incomplete. 2, F16643, ×14; incomplete internal mould of cephalon and thorax; posterior portion of opisthothorax missing. 3, F16645*a*, ×6; incomplete internal mould of cranidium; right posterior area asymmetrically distorted. 4, F16645*b*, ×6; counterpart of fig. 3, showing ornament of cranidium, structure of palpebral lobes. 5, F16648, ×9·5; internal mould of cranidium showing anterior furrow and eye ridge fossulae. 6, F16658, ×20; external mould of hypostome and attached rostral plate; rostral plate incomplete but anterior section of right connective suture can be seen. 7, F16647, ×9; internal mould of librigena showing the long posterior section of the facial suture, the changes in convexity of the genal field, and the widening of the doublure adjacent to the connective suture; the mould of the lateral border is incomplete and collapsed onto that of the doublure.

1

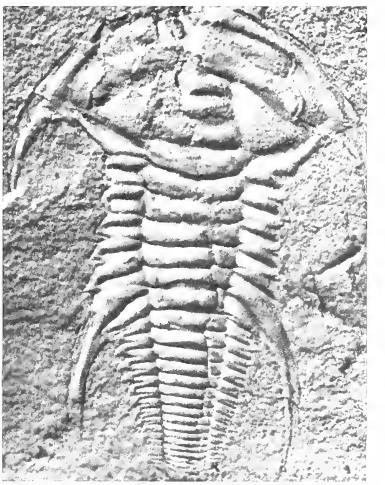

2

3

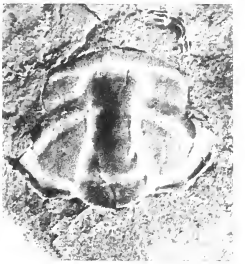

4

7

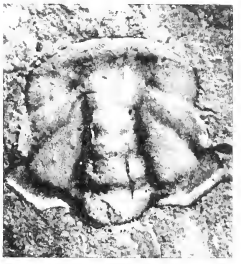

5

6

ated cephalon and thorax be chosen. Although isolated cranidia show some diagnostic features much better, they were not selected for the above reason.

Dimensions of holotype. Length of cranidium 2·8 mm.; palpebral width of cranidium 3·7 mm.; length of prothorax 1·6 mm.; over-all sagittal length of specimen 9·0 mm.

Material. Approximately 50 internal and external moulds, mainly disarticulated.

Occurrence. White Point Conglomerate, upper section of formation; on W. side of Cape D'Estaing, Kangaroo Island, South Australia.

Diagnosis. Axial furrows converge evenly from posterior edge to anterior glabellar furrow; furrows deep, distinct around slightly expanded frontal glabellar lobe. Glabellar furrows shallow, indistinct. Anterior cranidial border furrow almost transverse. Palpebral lobe short, highest at mid point, posterior end opposite middle glabellar furrow or lobe. Posterior border constant width, abaxial section directed antero-laterally at 40°. Posterior border furrow even depth. Anterior section of facial suture diverges anteriorly at 10°. Axial rings of prothorax rise sharply to posterior, with first 4 bearing sagittal, elongate nodes on posterior margin. Thorax with at least 48 segments.

Description. Cephalon subtrapezoidal in outline, gently convex (tr. and sag.). Cranidium gently convex (tr.). Glabella with 3 transglabellar furrows; axial furrows converge evenly from posterior margin to anterior glabellar furrow, diverge and curve around slightly expanded frontal lobe. Preglabellar furrow confluent with anterior border furrow, straight or slightly curved anteriorly. No preglabellar field. Glabella strongly convex (tr.), with slight median ridge extending to anterior glabellar furrow; gently convex (sag.), highest at anterior glabellar lobe, slopes down steeply to anterior border furrow, more gently to posterior. Occipital furrow transverse, or curves slightly to posterior, narrowest and deepest abaxially. Transglabellar furrows shallow and indistinct, posterior and middle furrows almost transverse, anterior furrow curves slightly forwards (Pl. 106, figs. 3, 4). Occipital ring approximately half mid palpebral cranidial width, widest sagitally; posterior edge curves outwards, half sagittal width projecting beyond margins of fixigenae. Length (sag.) of glabellar lobes decreases from posterior to anterior, but frontal lobe longest. Axial furrow slightly to deeply impressed below fixigena from posterior margin to eye ridge, rises and becomes indistinct over eye ridge, deeply impressed from eye ridge to anterior border furrow. Anterior furrow fossulae present at junctions of axial furrows and anterior border furrow (Pl. 106, figs. 3–5). Anterior border medium width, gently convex. Anterior border furrow almost transverse across cranidium (Pl. 106, fig. 3), moderately deep and narrow abaxially, shallows and broadens abruptly, anterior to frontal lobe (Pl. 106, figs. 3–5).

Eye ridge wide, long, gently convex, (tr. and exsag.), directed to posterior at 20° to transverse direction; anteriorly almost grades into gently downsloping frontal area, marked only by indistinct furrow, posteriorly slopes steeply down to distinct furrow continuous with palpebral furrow and aligned abaxially with anterior glabellar furrow (Pl. 106, fig. 4); degree of separation of eye ridge from frontal lobe by axial furrow varies considerably. Palpebral lobe short, less than $\frac{1}{4}$ glabellar length, anterior end opposite anterior glabellar furrow, posterior end opposite middle glabellar lobe (Pl. 106, figs. 3, 4); moderately convex (exsag.), convex upwards with mid point highest; slopes up steeply from palpebral furrow becoming convex (tr.); separated indistinctly from eye ridge by change in convexity (Pl. 106, figs. 4, 5), in some large specimens by indistinct furrow. Palpebral furrow deep, wide, slopes down to posterior. Palpebral area slightly convex (tr.), horizontal to down-sloping posteriorly. Posterior area long (exsag.), almost as wide (tr.) as occipital ring, with distinct fulcrum at opposite posterior end of palpebral furrow. Posterior border narrow, convex, even width; horizontal and transverse from axial furrow to fulcrum; abaxial to fulcrum, slightly downsloping and directed antero-laterally at approximately 40° to postero-lateral corner of cranidium (Pl. 106, figs. 3, 4). Posterior border furrow originates at base of axial furrow, widens abaxially (confluent with posterior end of palpebral furrow); deep adjacent to border, shallows away from it; over-all shape triangular (Pl. 106, figs. 3–5).

Anterior section of facial suture diverges anteriorly at 10°, curves sharply inwards at border furrow, crosses anterior border diagonally to intersect anterior edge opposite junction of axial and border furrows (Pl. 106, figs. 3, 5), then marginal ventral; connective sutures cross doublure, concave abaxially (Pl. 106, fig. 7). Palpebral section of facial suture short, convex abaxially, diverges to posterior at 15°; posterior section relatively long, slightly convex abaxially, diverges to posterior at 50°, and slopes down to cut posterior border opposite posterior glabellar furrow (Pl. 106, figs. 3–5).

Librigena (Pl. 106, fig. 7) with long genal spine. Lateral border moderately convex (tr.), approx. $\frac{1}{3}$ mid-palpebral width of librigena. Lateral border furrow distinct, rises steeply to border and slopes up gently to genal field abaxially; curves sharply inwards near base of genal spine, continuous with posterior border furrow, becomes wider and deeper adaxially. Posterior border narrow, convex, continuous with posterior border of fixigena, slopes down abaxially to join lateral border. Genal field slopes up gradually from border furrows, becomes convex upwards at mid width (tr.), then forms narrow horizontal or slightly depressed surround, below vertically upturned adaxial edge forming eye socle. Genal spine long, advanced (Pl. 106, fig. 2), moderately wide at base, tapers slowly and curves inwards towards posterior; subcentral ridge extends posteriorly.

Cephalic doublure same width as borders. Rostral plate crescentic, length (tr.) equal to maximum width of frontal glabellar lobe, notched abaxially (Pl. 106, fig. 6). Doublure of librigena convex ventrally, widens and flattens immediately posterior to connective suture (Pl. 106, fig. 7); lateral doublure continuous with posterior doublure around base of genal spine. Ventral side of genal spine flat to slightly rounded. Occipital ring with narrow, almost vertical doublure.

Hypostome (Pl. 106, fig. 6; text-fig. 4) with median body subdivided into large subtriangular anterior lobe, and smaller subrectangular posterior lobe. Median body surrounded by furrows and narrow upturned borders; lateral notch towards anterior. Median furrows straight, converge to posterior, not reaching sagittal line. Posterior section of anterior lobe of median body strongly convex (tr.), continuous sagittally with posterior lobe, slopes down anteriorly and divides into 2 down-sloping ridges directed antero-laterally and separated by median concave depression; abaxially ridges slope steeply down to prominent anterior wings. Anterior border slopes up from border furrow, trapezoidal in shape; anterior edge curves slightly forwards along line of hypostomal suture; abaxial section slopes downwards and postero-laterally at 50° to anterior wing. Anterior border furrow slightly convex forwards in central portion, slopes down postero-laterally to anterior wings. Anterior lateral border furrow straight, directed postero-laterally, slopes up from anterior wing to lateral notch; very narrow anterior lateral border. Median furrow originates at posterior end of anterior lateral furrow. Posterior lobe of median body strongly convex (tr.), parallel-sided to slightly tapering posteriorly; postero-lateral corners rounded with prominent bosses; lobe slopes down steeply to lateral border furrows, more gently to posterior border furrow. Lateral border furrow originates abaxial to median furrow, deepens to posterior with fossulae near posterior end; lateral border slopes up steeply from furrow, convex outwards forming shoulder. Posterior border relatively wide (sag.), horizontal (sag. and tr.), posterior lateral corners rounded. Posterior border furrow distinct abaxially, absent sagittally where ridge slopes down from posterior lobe across furrow; small fossulae in furrow abaxial to ridge.

Rostral plate attached along hypostomal suture to median section of anterior border of hypostome; anterior wings free (Pl. 106, fig. 6). Hypostome extends posteriorly to level of posterior glabellar furrow when in situ.

Cranidial ornament of closely spaced granules with pointed tips covers all dorsal surfaces except furrows (Pl. 106, fig. 4). Librigena with long, slightly wrinkled, subparallel terrace lines on posterior and most of lateral doublure; become less regular, and anastomose adjacent to connective suture; pattern of terrace lines on rostral plate unknown. Ventral surface of genal spine with longitudinally

---

EXPLANATION OF PLATE 107

Figs. 1, 2. *Emuella polymera* gen. et sp. nov. White Point Conglomerate, Cape D'Estaing, Kangaroo Island, South Australia. 1, F16649, ×5; internal mould of complete prothorax and incomplete opisthothorax, showing articulating half rings and pleural spines of most segments. 2, F16651, ×8; internal mould of left side of macropleural unit and some opisthothoracic segments, showing long pleural spine and almost completely unmodified posterior pleural band of 5th segment.

Figs. 3–6. *Emuella dalgarnoi* gen. et sp. nov. Emu Bay Shale, Emu Bay, Kangaroo Island, South Australia. 3, F16660, ×4·5; almost complete internal mould; right connective suture visible, imprint of hypostome on frontal glabellar lobe. 4, Holotype, F16659, ×8; almost complete internal mould; cephalon slightly compressed sagittally, right librigena rotated clockwise, posterior segments of opisthothorax tilted to anterior. 5, F16661, ×5·5; external mould of cranidium, showing ornament and muscle scars on occipital and glabellar furrows. 6, F16661, ×18; detail of latex mould of specimen in fig. 5; showing posterior border and border furrow, and sutural ridge.

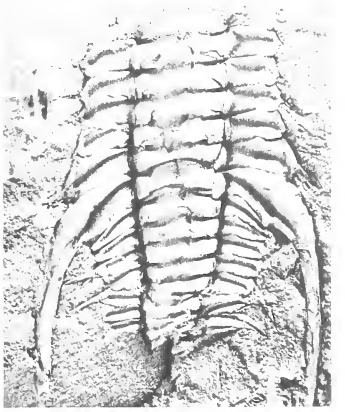

1

2

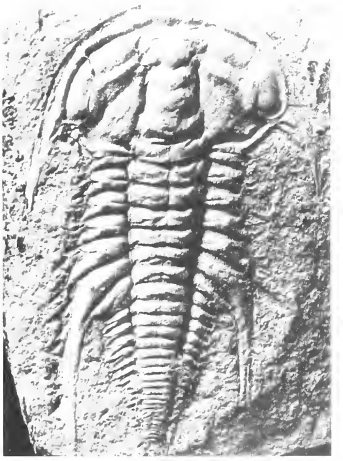

3

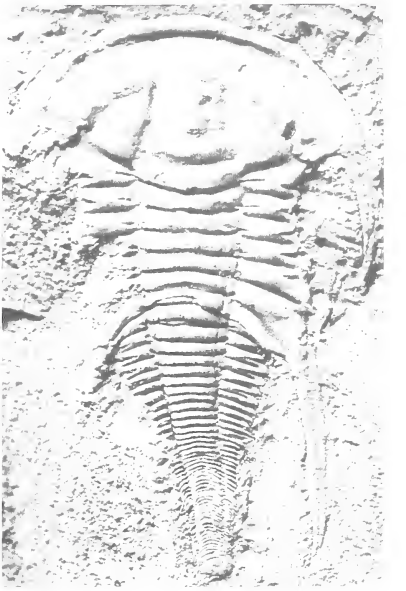

4

5

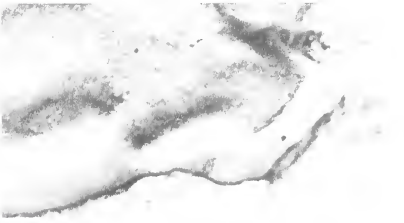

6

elongate granules in subparallel rows. Occipital ring bears sagittal, longitudinally elongate tubercle on posterior margin (Pl. 106, figs. 3, 4).

Thorax (Pl. 106, figs. 1, 2; Pl. 107, figs. 1, 2) with prothorax of 6 segments, with macropleural 6th fused to 5th, and opisthothorax of at least 42 segments (Pl. 106, fig. 1). Axis more than half total thoracic width, almost parallel sided to 4th segment then tapers evenly to posterior; moderately to gently convex (tr.), steep abaxially, rather flat sagittally; axial furrows distinct. Pleurae geniculate, very short (tr.), with pleural spines.

Prothoracic segments 1–4 similar; axial ring narrow (sag.), gently to moderately convex (tr.), rises from transverse furrow to posterior edge, with small sagittal node on posterior edge; transverse furrow with deep apodemal slit abaxially, widens and shallows abaxially (Pl. 107, figs. 1, 2); articulating half ring crescentic, $\frac{3}{4}$ width axial ring (sag.), central portion flat, horizontal, abaxially slopes down to axial furrows (Pl. 107, figs. 1, 2). Pleura strongly geniculate, fulcrum less than half length (tr.) from axial furrow. Pleural furrow shallow, wide adaxially, tapers diagonally across pleura, terminates before pleural spine; slopes up steeply to anterior pleural band, more gently to posterior band. Anterior pleural band widens to fulcrum, abaxially slopes down and out to form facet; extreme antero-lateral corner becomes horizontal (Pl. 107, fig. 2). Posterior pleural band narrow, convex, even width. Anterior and posterior pleural bands abaxially produced into short pleural spine notched at base; spine of 1st segment very short, slightly oblique to posterior situated at mid width (tr.) of pleura (Pl. 107, fig. 1); succeeding segments with spines progressively longer, directed more strongly backwards and situated more posteriorly (Pl. 106, fig. 2; Pl. 107, fig. 1). Pleurae progressively lengthen towards posterior (Pl. 106, fig. 2; Pl. 107, fig. 2). Doublure extends to base of pleural spine.

Macropleural unit consists of 5th and 6th segments, 5th segment similar to preceding segments; axial ring rises steeply to posterior, normal width sagittally; pleura wider, longer than 4th; pleural furrow more oblique, deeper, slopes up almost vertically to anterior, more gently to posterior; anterior pleural band widens more rapidly, facet larger, and fulcrum more strongly developed (Pl. 107, fig. 2); posterior band even width; pleural spine longer than preceding, near posterior edge of pleura (Pl. 107, figs. 1, 2). Line of fusion of pleurae of 5th and 6th sharp, with posterior pleural band of 5th unmodified (Pl. 107, fig. 2) to indistinct (Pl. 106, fig. 1). 6th segment macropleural; axial ring normal, posterior edge almost transverse; transverse furrow deep with strong apodemal slits abaxially, shallows sagittally; apodemal slit extends onto pleural field for short distance (Pl. 107, fig. 1); interpleural furrow extends from slit to base of 5th pleural spine; articulating half ring crescentic, $\frac{3}{8}$ width axial ring; pleural furrow originates adaxial and slightly posterior to extremity of apodemal slit (Pl. 106, fig. 2), widens slightly and deepens to fulcrum, then tapers abruptly and terminates forming notch (Pl. 107, fig. 2); furrow slopes up vertically to anterior, more gently to posterior; ventrally furrow appears as pronounced ridge at angle to apodeme, directed strongly to posterior; anterior pleural band widens rapidly abaxial to fulcrum, slopes down and out, extreme antero-lateral corner forms horizontal flap fused to 5th just adaxial to base of pleural spine (Pl. 107, fig. 1, 2); interfurrow platform asymmetrically convex (exsag.), slopes up gently from 5th pleural furrow, horizontal centrally, then drops almost vertically to 6th pleural furrow; posterior pleural band raised, convex, even width, with distinct notch at base of macropleural spine, just abaxial to fulcrum (Pl. 107, fig. 2); macropleural spine wide, extremely long, tapers gradually and curves inwards to posterior (Pl. 106, fig. 2; Pl. 107, fig. 1), convex to V-shaped anteriorly, flattens to posterior, median ridge extends from posterior edge of interfurrow platform down spine; spine formed by anterior and posterior pleural bands of 6th segment extends to level of pygidium. Doublure of macropleural unit extends from antero-lateral corner of 5th, across base of 5th spine to notch on posterior border of 6th.

Axial ring of 1st opisthothoracic segment similar in size and morphology to normal prothoracic axial ring (Pl. 107, fig. 1); pleura blade shaped, curved to posterior following posterior edge of 6th segment, fulcrum less than $\frac{1}{3}$ length (tr.) from axial furrow; pleural furrow wide, deep, diagonal, tapers to point just abaxial to notch of 6th; furrow slopes up steeply to anterior, moderately steeply to posterior; anterior pleural band overlapped by posterior band of 6th when articulated (Pl. 107, fig. 1) posterior pleural band convex, raised; pleural spine relatively long, advanced slightly to parallel curve of posterior edge of 6th, curves to posterior; formed by anterior and posterior pleural bands. Succeeding segments with pleurae progressively shorter and more transverse (Pl. 106, fig. 2); pleural spines long, directed progressively more to posterior and becoming less advanced; fulcrum migrates adaxially and pleurae become more strongly geniculate to posterior (Pl. 106, fig. 2; Pl. 107, fig. 1). At least 42

segments in opisthothorax; most posterior segments extremely narrow (sag.), lack distinct pleural furrows (Pl. 107, fig. 1). Doublure of pleurae extends to base of pleural spines.

Thoracic ornament of granules similar to those of cephalon, distributed evenly and closely spaced on dorsal surfaces.

Pygidium unknown.

Emuella dalgarnoi sp. nov.

Plate 107, figs. 3–6; text-fig. 5c.

Derivation of name. After Mr. R. C. Dalgarno, joint discoverer of the Flinders Ranges locality.

Holotype. AUGD F16659 (Pl. 107, fig. 4). Specimen shows almost complete thorax and pygidium articulated to a cephalon, which although slightly distorted, displays most of the diagnostic characters.

Dimensions of holotype. Length of cranidium 3·6 mm.; mid-palpebral width of cranidium 4·8 mm.; length (sag.) of prothorax 2·3 mm.; over-all sagittal length 11·3 mm.

Material. Approximately 20 internal and external moulds; 3 almost complete specimens, 1 well-preserved cranidium, remainder very fragmentary.

Occurrence. Upper part of Emu Bay Shale, Emu Bay, Kangaroo Island, South Australia.

Diagnosis. Axial furrows converge strongly from posterior margin to occipital furrow, slightly converging to almost parallel to anterior glabellar furrow, then shallow around moderately expanded frontal glabellar lobe. Transglabellar furrows wide, shallow, distinct. Anterior cranidial border furrow curves to anterior. Palpebral lobe relatively short, posterior end opposite posterior glabellar furrow. Posterior border widens from axial furrow to fulcrum, directed antero-laterally at 45°; low, narrow ridge extends from posterior lateral corner of cranidium along line of posterior section of facial suture. Posterior border furrow with notch abaxial to fulcrum. Anterior section of facial suture diverges anteriorly at 20°. Axial rings of prothorax without nodes. Thorax with 58 segments.

Discussion. E. dalgarnoi is distinguished from *E. polymera* by the possession of a longer palpebral lobe and consequent differences in the posterior section of the facial suture. The structure of the posterior border and border furrow also differs greatly, with *E. dalgarnoi* having a distinct notch at the fulcrum and a low ridge along the line of the posterior section of the facial suture. The anterior section of the facial suture is noticeably more divergent in *E. dalgarnoi* than in *E. polymera*.

Description. Axial furrows converge strongly from posterior margin to occipital furrow, converge slightly (Pl. 107, fig. 4) to almost parallel (Pl. 107, fig. 5) to anterior glabellar furrow, then diverge and curve around moderately expanded frontal glabellar lobe. Frontal glabellar lobe occasionally with slight anterior median depression resulting in bilobed appearance (Pl. 107, fig. 5). Occipital furrow curves slightly to posterior, moderately deep and wide abaxially, narrows and shallows abruptly sagittally; muscle spots at adaxial ends of broad portion of furrow (Pl. 107, fig. 5). Transglabellar furrows similar to occipital, posterior furrow curves slightly to posterior, middle transverse, anterior furrow curves slightly to anterior (Pl. 107, fig. 5). Occipital ring approximately half mid-palpebral cranidial width, constant width, projects very little beyond posterior margin of fixigena. Axial furrow very slightly impressed, deepest at junction with glabellar furrows, anteriorly reaches anterior border furrow, with small anterior furrow fossula at junction (Pl. 107, fig. 5). Anterior border furrow curves to anterior, shallowest opposite frontal glabellar lobe. Eye ridge wide, directed to posterior at 30° to transverse line. Palpebral lobe relatively short, less than $\frac{1}{3}$ glabellar length, anterior end opposite anterior glabellar lobe, posterior end opposite posterior glabellar furrow; slopes up steeply from palpebral furrow, flat on adaxial side, becomes convex dorsally; slightly convex (exsag.) with highest point towards posterior end (Pl. 107, fig. 3, 5); continuous with eye ridge. Palpebral furrow very wide, slopes down to posterior, but with small fossula alongside mid point of ridge. Posterior area relatively long (exsag.), $\frac{2}{3}$ width (tr.) occipital ring, with fulcrum opposite posterior end of palpebral lobe (Pl. 107, figs. 3, 5). Posterior border transverse from axial furrow to fulcrum, widens and rises rapidly, anteriorly drops steeply to border furrow, outer edge concave to posterior (Pl. 107, fig. 6); abaxial to fulcrum, border directed antero-laterally at 45°, width constant; upper surface horizontal, anteriorly drops

vertically to border furrow. Narrow ridge, below level of posterior border, extends from posterior lateral corner, along line of posterior section of facial suture (Pl. 107, figs. 5, 6). Posterior border furrow widens to fulcrum, then with distinct notch (Pl. 107, figs. 5, 6); abaxially slopes down slightly, continuous with furrow running along base of sutural ridge (Pl. 107, fig. 6).

Anterior section of facial suture diverges anteriorly at approximately 20°; rostral plate same width (tr.) as frontal glabellar lobe, notched laterally (Pl. 107, fig. 3). Posterior section of suture relatively long, diverges to posterior at 45°; section from palpebral ridge to posterior border straight, then sharply convex abaxially across border (Pl. 107, figs. 5, 6).

Cranidial ornament of pointed granules; closely spaced on glabellar lobes, borders, eye lobes; sparsely distributed on palpebral area of fixigena, anterior lateral sections of cranidium; absent in all furrows (Pl. 107, figs. 5, 6). Paired muscle spots present on abaxial portions of occipital and glabellar furrows (Pl. 107, figs. 5). Genal field of librigena with scattered granules.

Hypostome unknown.

Thorax with axis approximately half total thoracic width. Maximum number of 52 opisthothoracic segments observed (Pl. 107, fig. 4). Pygidium (Pl. 107, fig. 4) minute furrowed disc, without distinct division into axial and pleural fields; 4 or 5 furrows, transverse sagittally, curving to posterior abaxially; entire lateral and posterior borders.

Genus BALCORACANIA gen. nov.

Type species. Balcoracania dailyi sp. nov.

Plate 109; text-figs. 5A, B

Derivation of name. After Balcoracana Creek, Flinders Ranges, South Australia.

Diagnosis. Preglabellar field narrow, down-sloping, or absent. Palpebral lobe long, crescentic. Posterior border with section abaxial to fulcrum directed antero-laterally at 60°, and strongly depressed. Librigena with genal spine only slightly advanced. Thorax with axis less than half thoracic width. Pleural furrows terminate at base of pleural spines. Thorax with 53–61 segments. Fine closely spaced granules on dorsal surfaces.

Discussion. The cephala of *Balcoracania* differ from those of *Emuella* in having a longer palpebral lobe and consequently shorter posterior section of the facial suture; the abaxial section of the posterior border is much more strongly depressed and not directed forward as strongly. With regard to the thorax, in *Balcoracania* the axis is narrower than in *Emuella*, and the pleural furrows extend to the base of the spines.

Balcoracania dailyi sp. nov.

Plates 108, 109; text-fig. 5A

Derivation of name. After Dr. B. Daily, who first discovered members of this group.

Holotype. AUGD F16663 (Plate 108, fig. 1). Specimen is only one known with the cephalon articulated to a reasonably complete thorax.

Dimensions of holotype. Length of cranidium 4·7 mm.; mid-palpebral width of cranidium 4·4 mm.; length of prothorax 3·4 mm.; over-all sagittal length of specimen 13·4 mm.

Material. Approximately 150 internal and external mounds, mostly isolated cranidia, librigenae, thoracic segments, and several hypostomes.

Occurrence. Upper section of White Point Conglomerate, W. side of Cape D'Estaing, Kangaroo Island, South Australia.

Diagnosis. Axial furrows converge moderately from posterior margin to middle glabellar furrow, almost parallel to anterior glabellar furrow, then curve indistinctly around slightly expanded frontal

glabellar lobe. Preglabellar furrow indistinct, almost transverse; narrow (sag.) downsloping preglabellar field. Prominent anterior border fossulae. Glabellar furrows distinct only laterally.

Description. Cephalon subsemicircular in outline, moderately convex (tr. and sag.). Cranidium moderately convex (tr.). Axial furrows converge moderately from posterior margin to middle glabellar furrow, almost parallel to anterior glabellar furrow, then curve around very slightly expanded frontal glabellar lobe. Glabella strongly convex (tr.), weak median ridge extends from posterior to anterior glabellar furrows; gently convex (sag.), highest at anterior glabellar lobe, slopes down steeply to preglabellar field, more gently to posterior. Occipital furrow deepest abaxially, curves slightly to posterior (Pl. 108, fig. 2). Transglabellar furrows distinct abaxially, but very shallow and indistinct sagittally (Pl. 108, fig. 5); posterior furrow directed slightly to posterior abaxially, transverse sagittally (Pl. 108, fig. 1); middle furrow transverse; anterior furrow directed slightly to anterior abaxially. Occipital ring less than half mid-palpebral, cranidial width, maximum width sagittally, posterior edge convex to posterior; posterior half of ring projects beyond margin of fixigenae (Pl. 108, figs. 2, 3). Frontal glabellar lobe with central portion flat to slightly convex, occasionally with anterior median depression, giving bilobed appearance. Axial furrow slightly impressed below fixigena from posterior margin to eye ridge, rises and becomes indistinct over eye ridge, not impressed on sides of frontal lobe, anteriorly joins anterior border furrow (Pl. 108, figs. 2, 3, 5). Deep anterior furrow fossulae at junction of axial and anterior border furrows (Pl. 108, fig. 5). Preglabellar furrow very indistinct, almost transverse; narrow (sag.) down-sloping preglabellar field (Pl. 108, figs. 2, 5). Anterior border medium width, margin convex to anterior; abaxially convex, raised, but flattens and widens opposite frontal glabellar lobe (Pl. 108, fig. 2). Anterior border furrow moderately deep and narrow abaxially, rises abruptly, broadens and shallows opposite frontal glabellar lobe (Pl. 108, figs. 2, 5).

Eye ridge wide, long, directed to posterior at 25° to transverse line. Palpebral lobe wide (tr.), long, approximately $\frac{3}{4}$ glabellar length, anterior end opposite anterior glabellar lobe, posterior end opposite occipital furrow or posterior half of posterior glabellar lobe; lobe slopes up flatly from palpebral furrow, abaxial edge convex upwards and outwards; rises to posterior with posterior end high above posterior area (Pl. 108, figs. 3, 5); lobe indistinctly separated from eye ridge by change in convexity or occasionally by indistinct longitudinal furrow. Palpebral furrow wide, deepens and slopes down steeply to posterior. Palpebral area slightly inflated, slopes down to posterior border furrow. Posterior area short (exsag.), wider (tr.) than occipital ring, depressed, with fulcrum opposite posterior end of palpebral lobe (Pl. 108, figs. 2, 4); horizontal from axial furrow to fulcrum, slopes down steeply abaxial to fulcrum. Posterior border directed slightly to posterior from axial furrow to fulcrum, antero-laterally at 50–55° abaxial to fulcrum. Posterior border furrow widens abaxially, deep adjacent to border, shallows away from it; almost straight-sided, confluent abaxially with palpebral furrow (Pl. 108, figs. 3, 4).

Anterior section of facial suture diverges anteriorly at 25°, curves sharply inwards at border furrow, crosses anterior border diagonally; from point where facial suture cuts anterior cranidial edge, connective sutures cross doublure, sharply concave abaxially (Pl. 108, fig. 7). Rostral suture marginal ventral. Palpebral section of facial suture convex abaxially, diverges at 15° to posterior. Posterior

---

EXPLANATION OF PLATE 108

Figs. 1–8. *Balcoracania dailyi* gen. et sp. nov. White Point Conglomerate, Cape D'Estaing, Kangaroo Island, South Australia. 1, Holotype, F16663, ×8; external mould of almost complete specimen; macropleural spines incomplete, posterior segments of opisthothorax and pygidium missing. 2, F16665*a*, ×6; internal mould of cranidium showing preglabellar field, fossulae, posterior area; both palpebral lobes incomplete. 3, F16665*b*, ×6; counterpart of specimen in fig. 2; showing palpebral lobes. 4, F16664, ×18; internal mould of portion of cranidium showing posterior area; mould of the abaxial section of posterior border removed to show that of doublure. 5, F16666, ×8; internal mould of cranidium showing anterior border furrow and eye ridge fossulae. 6, F16667, ×9·5; detail of specimen in fig. 8, showing ornament of lateral librigenal doublure. 7, F16669, ×3·5; internal mould of anterior section of librigenal border and doublure, showing the courses of the connective suture and the anterior section of the facial suture, and the ornament. 8, F16667, ×7; internal mould of librigena, with moulds of lateral border and most of posterior border missing, showing lateral and posterior doublures respectively, and convexity of genal field.

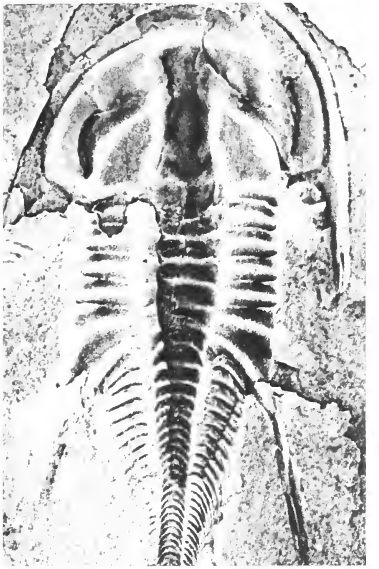

1

2

3

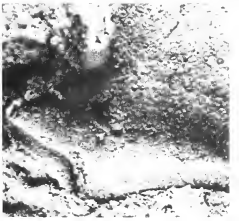

4

5

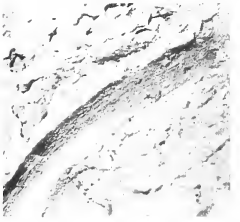

6

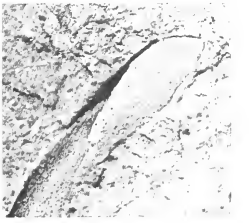

7

8

section relatively short, diverges to posterior at 55°, slopes down stecply to posterior border furrow, then curves sharply inwards across border (Pl. 108, figs. 3, 8). Posterior lateral corner of cranidium opposite occipital furrow (Pl. 108, figs. 2).

Librigena (Pl. 108, figs. 6–8) with long genal spine, slightly advanced. Lateral border furrow curves sharply inwards near base of genal spine, continuous with posterior border furrow; widens, deepens and slopes down adaxially (Pl. 108, fig. 8). Posterior border narrow, convex, high above furrow adaxially, slopes down abaxially to join lateral border. Genal field slopes up gradually and rather flatly from border furrow, sharply upturned at adaxial edge to form eye socle; moderately convex (exsag.), posterior lateral section slopes down steeply (Pl. 108, fig. 8).

Cephalic doublure same width as border anteriorly and laterally; posterior fixigenal doublure tapers rapidly to point just abaxial to fulcrum (Pl. 108, fig. 4). Rostral plate equal in length (tr.) to maximum width of frontal glabellar lobe. Doublure of librigena moderately to strongly convex, widens and flattens adjacent to connective suture (Pl. 108, fig. 6). Lateral and posterior librigenal doublures continuous (Pl. 108, fig. 8). Ventral side of genal spine slightly rounded to flat.

Hypostome (Pl. 109, figs. 4, 5) similar in basic morphology to that of *E. polymera*, but differs or illustrates more clearly the following features: anterior wings very prominent, depressed; wing processes visible in well preserved specimens (Pl. 109, fig. 4); position of wing results in anterior lateral border and furrow being directed postero-laterally (Pl. 109, fig. 5) or transversely (Pl. 109, fig. 4). Anterior border wide, steeply upsloping, crossed by narrow line in some specimens (Pl. 109, fig. 4); line symmetrically concave about sagittal line, abaxially intersects anterior edges at extremities of hypostomal suture. Median furrow with macula at posterior end (Pl. 109, fig. 5). Posterior lobe of median body strongly convex (tr.), parallel sided (Pl. 109, fig. 4) or tapers slightly to posterior; posterior lateral corner rounded, with prominent boss (Pl. 109, fig. 5). Lateral border up-sloping with small shoulder at mid length (Pl. 109, fig. 5); border furrow with very deep fossula below shoulder.

Cranidial ornament of fine granules covering all dorsal surfaces; occipital ring with elongate sagittal node on posterior edge (Pl. 108, fig. 3); terrace lines on extreme outer edges of anterior and lateral borders (Pl. 108, fig. 3). Librigena with fine granules on genal field, adaxial portion of lateral border, and dorsal surface of genal spine (Pl. 108, fig. 7); abaxial portion of lateral border with wrinkled terrace lines, separated by subparallel rows of elongate granules becoming more numerous towards genal spine (Pl. 108, fig. 7); lateral and posterior doublures with long regular terrace lines, become anastomosing adjacent to connective suture (Pl. 108, figs. 6, 8); ventral surface of genal spine with elongate granules in parallel rows. Rostral plate with terrace lines.

Thoracic axis narrow, less than half thoracic width, pleurae correspondingly long (tr.) (Pl. 108, fig. 1). Axial furrows converge slightly from 1st to 6th segment, rapidly converge to about mid length (sag.) opisthothorax, then almost parallel to level of pygidium (Pl. 108, fig. 1). Axial rings of prothoracic segments rise only slightly to posterior, without nodes (Pl. 108, fig. 1). Pleurae of segments 1–4 equal length (tr.). Pleural furrow diagonal, tapers abaxial to fulcrum, terminates at base of pleural spine (Pl. 108, fig. 1). Pleural spine formed by anterior pleural band only. Anterior pleural band slopes down antero-laterally abaxial to fulcrum to form facet; no modification to antero-lateral corner (Pl. 109, figs. 1, 2). Macropleural unit with line of fusion of pleurae generally indistinct, marked by slight furrow to base of 5th pleural spine (Pl. 109, fig. 3) or almost completely effaced (Pl. 109, fig. 1); anterior pleural band of 6th slopes down to join 5th pleural spine without modification (Pl. 109, fig. 1). Thorax with 53 segments.

Pygidium minute, furrowed, borders entire.

Discussion. B. dailyi is easily distinguished from the species of *Emuella* by the possession of a narrow, down-sloping, preglabellar field, and a long palpebral lobe, the structure of which also differs.

Balcoracania flindersi sp. nov.

Plate 109, figs. 7, 8; text-fig. 5B

Derivation of name. From the Flinders Ranges, South Australia.

Holotype. AUGD F16683 (Pl. 109, fig. 7). Specimen with articulated cephalon and thorax.

Dimensions of holotype. Length of cranidium 3·7 mm.; mid-palpebral width of cranidium 4·5 mm.; length of prothorax 2·7 mm.; over-all sagittal length 10·1 mm.

Material. Approximately 280 replaced tests, internal and external moulds; exoskeletons mainly articulated, but some disarticulated elements.

Occurrence. Lower part of the Billy Creek Formation, Balcoracana Creek, Flinders Ranges, South Australia.

Diagnosis. Axial furrows converge evenly from posterior margin to anterior glabellar furrow, then curve out and around markedly expanded frontal glabellar lobe. No preglabellar field or anterior border fossulae. Transglabellar furrows distinct, deep.

Description. Axial furrows converge evenly from posterior margin to anterior glabellar furrow, then curve out and around markedly expanded frontal glabellar lobe. Occipital furrow, transglabellar furrows deep, distinct; posterior furrow convex to posterior, middle transverse, anterior furrow convex to anterior (Pl. 109, figs. 7, 8). Occipital ring less than half mid-palpebral cranidial width. Frontal glabellar lobe markedly expanded, rounded laterally and anteriorly; reaches anterior border furrow; no preglabellar field; anterior border and border furrow unmodified; no anterior furrow fossulae (Pl. 109, figs. 7, 8). Palpebral lobe long (exsag.), wide (tr.), crescentic; anterior and opposite anterior glabellar lobe, posterior and opposite occipital furrow. Palpebral area usually highly inflated, slopes down steeply to posterior.

Thorax (Pl. 109, figs. 6, 8) with long opisthothorax; maximum number of 61 thoracic segments observed.

Discussion. B. flindersi is primarily distinguished from *B. dailyi* by the morphology of the anterior part of the cranidium, by the degree of expansion of the frontal glabellar lobe, absence of preglabellar field, and anterior furrow fossulae. It is clearly distinguished from the species of *Emuella* by the length of the palpebral lobe and the structure of the posterior area of the fixigena, especially the strong depression of the section abaxial to the fulcrum.

A comparison of the morphology of the adults of the four species is presented in Table 1, and of the adult cephala in text-fig. 5.

Intraspecific variation. In all collections some sort of deformation has taken place, and this factor must be considered in an evaluation of the intrinsic variation of the species. The range of morphological variation is approximately the same for the various characters or groups of characters in each of the species. The following groups exhibit a correlated variation:

EXPLANATION OF PLATE 109

Figs. 1–6. *Balcoracania dailyi* gen. et sp. nov. White Point Conglomerate, Cape D'Estaing, Kangaroo Island, South Australia. 1, F16679, ×10; internal mould of left side of macropleural unit and 1st opisthothoracic segment, showing an articulating facet and pleural spine of 5th segment, and extension of apodemal slit onto interfurrow platform along line of fusion of pleurae. 2, F16678, ×9·5; external mould of portion of thorax showing ornament. 3, F16680, ×10; internal mould of left side of macropleural unit; extent of doublure shown by gap surrounding mould from base of 5th spine to notch on posterior border of 6th segment. 4, F16673, ×8; internal mould of hypostome and detached rostral plate; hypostome with maculae and prominent postero-lateral bosses; rostral plate with notched abaxial ends. 5, F16671, ×10; internal mould of hypostome showing anterior line, depressed anterior wings, and deep fossulae in lateral borders. 6, F16676, ×5; portion of external mould of macropleural unit and 1st opisthothoracic segment, showing articulating half rings, prominent junction of apodeme and pleural furrow, and overlap of posterior pleural band of 6th over anterior pleural band of opisthothoracic segment.

Figs. 7, 8. *Balcoracania flindersi* gen. et sp. nov. 7, Holotype, F16683, ×10; internal mould of cephalon and incomplete thorax; cranidium with imprint of hypostome and rostral plate. 8, F16655, ×5; several almost complete specimens on bedding plane.

1

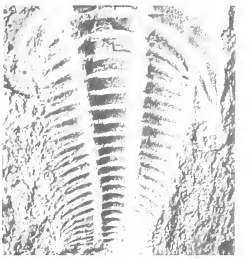

2

3

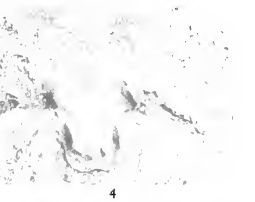

4

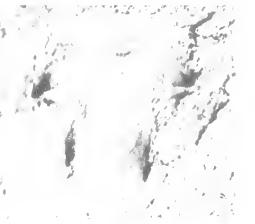

5

6

8

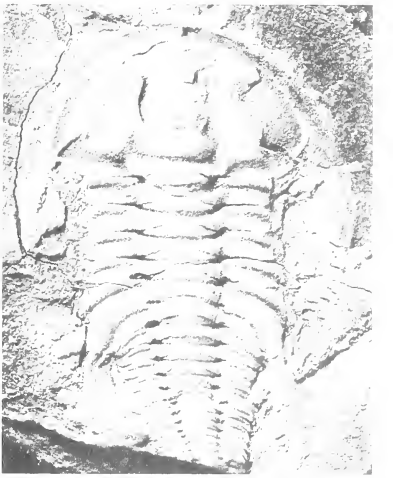

7

POCOCK, Lower Cambrian Emuellidae

(*a*) Convexity of the palpebral area and the degree of impression of the surrounding axial and palpebral furrows: the palpebral area varies from almost flat (tr.) to highly convex; in the former case the furrows are only slightly impressed or are represented merely by a change in slope; in the latter the surrounding furrows are deeply impressed. However it must be remembered that in *B. flindersi* high convexity of the palpebral area appears to represent the norm.

TABLE 1. Comparison of aspects of the morphology of members of the Emuellidea. The limits of variation for these characters are given in the text.

CHARACTER	*EMUELLA POLYMERA*	*EMUELLA DALGARNOI*	*BALCORACANIA DAILYI*	*BALCORACANIA FLINDERSI*
PALPEBRAL LOBE	SHORT, <1/4 GLABELLAR LENGTH; POST END OPPOSITE MIDDLE GLABELLAR LOBE, MIDPOINT HIGHEST	SHORT, > 1/4 AND < 1/3 GLABELLAR LENGTH; POST. END OPPOSITE POST. GLABELLAR FURROW, POST END HIGHEST	LONG, > 1/2 GLABELLAR LENGTH; POST. END OPPOSITE OR JUST ABOVE OCCIPITAL FURROW	DITTO
POSTERIOR AREA (ABAXIAL TO FULCRUM)	SLIGHTLY DEPRESSED	DITTO	STRONGLY DEPRESSED	DITTO
POSTERIOR BORDER (ABAXIAL TO FULCRUM)	ANTERO-LATERALLY AT 40°	ANTERO-LATERALLY AT 45°.	ANTERO – LATERALLY AT 50–55°	DITTO
PREGLABELLAR FIELD	ABSENT	DITTO	NARROW (SAG.), INDISTINCT, DOWNSLOPING	ABSENT
ANT. B FURROW FOSSULAE	PRESENT	DITTO	DITTO	ABSENT
EYE RIDGE FOSSULAE	PRESENT	DITTO	DITTO	ABSENT
ANTERIOR BORDER FURROW	SHALLOWS OPPOSITE FRONTAL GLABELLAR LOBE	DITTO	DITTO	EVEN DEPTH, ABAXIALLY AND SAGITTALLY
TRANSGLABELLAR FURROWS	SHALLOW, INDISTINCT	WIDE, DEEP ABAXIALLY, NARROW, SHALLOW SAGITTALLY	DISTINCT ABAXIALLY, INDISTINCT SAGITTALLY	DEEP, DISTINCT
ANTERIOR SECTION OF FACIAL SUTURE	DIVERGES AT 10°	DIVERGES AT 20°	DIVERGES AT 25°	DITTO
POSTERIOR SECTION OF FACIAL SUTURE	DIVERGES STRONGLY	DIVERGES STRONGLY, WITH LOW SUTURAL RIDGE	DIVERGES MODERATELY	DITTO
WIDTH(TR) OF THORACIC AXIS	>1/2 TOTAL THORACIC WIDTH	APPROX 1/2 TOTAL THORACIC WIDTH	< 1/2 TOTAL THORACIC WIDTH	≤ 1/2 TOTAL THORACIC WIDTH
PLEURAL FURROWS	TERMINATE BEFORE SPINES	DITTO	TERMINATE AT BASE OF SPINES	DITTO
MACROPLEURAL UNIT	ABAXIAL FLAP PRESENT	DITTO	FLAP ABSENT	DITTO
CRANDIAL ORNAMENT	LARGE, POINTED GRANULES, DENSE ON DORSAL SURFACES; OCCIPITAL NODE	DENSE GRANULES ON BORDERS, GLABELLA, AND EYE LOBES WIDELY SPACED ON PALPERAL AREA, ABSENT IN FURROWS, OCCIPITAL NODE	FINE, DENSE GRANULES ON DORSAL SURFACES, OCCIPITAL NODE	DITTO
PROTHORACIC NODES	PRESENT ON SEGMENTS 1 – 4	DITTO	ABSENT	DITTO
NO. THORACIC SEGMENTS	AT LEAST 48	58	53	61

(*b*) Junction of the eye ridge and frontal glabellar lobe: this appears to be the most variable of all characters and the most difficult to distinguish between genuine and spurious variation. The eye ridge may be almost completely separated from the frontal lobe by the axial furrow, or join it without significant interruption; this appears largely independent of the degree of impression of the axial furrow elsewhere. However, the eye ridge is never completely separated from the glabella.

(*c*) Frontal glabellar lobe, preglabellar and anterior border furrow: the outline and convexity of the frontal glabellar lobe varies considerably in *B. dailyi*, and to a lesser extent in the other species. The outline varies from slightly rounded laterally, with an almost straight anterior edge, to almost circular, being correlated respectively to high and low convexity (sag. and tr.). An important variant is a slightly bilobed outline, resulting from a shallow anterior median depression. In all except *B. flindersi*, forms with high convexity of the frontal lobe have the section of the anterior border furrow opposite the lobe raised with respect to its abaxial sections, and thus have more distinct

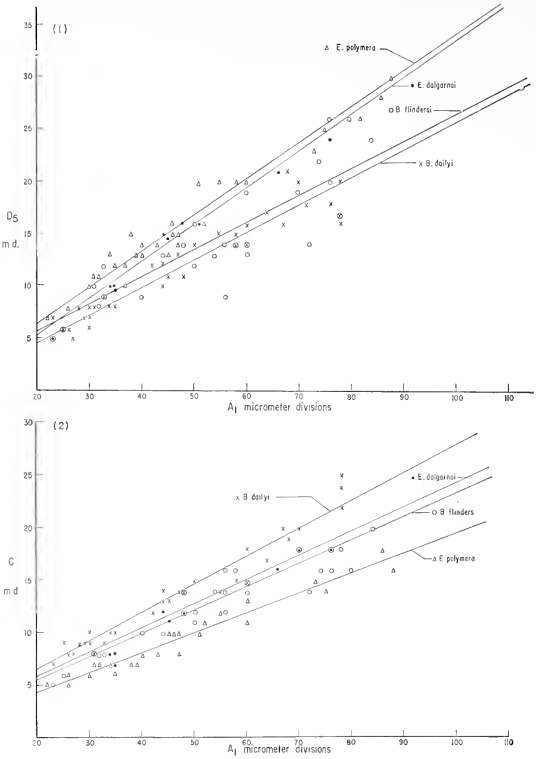

TEXT-FIG. 6. Scatter diagrams and 'best fit' lines for adults of the Emuellidae. A_1, the total cranidial length plotted against (1) D_5, the occipital post-palpebral length; (2) C, the palpebral length. All dimensions given in micrometer divisions where 1·00 mm. = 32 micrometer divisions. The symbol ● denotes specimens of *B. dailyi*, × specimens of *B. flindersi*, ○ specimens of *E. polymera*, and Δ those of *E. dalgarnoi*.

border fossulae than those forms with low convexity. In *B. dailyi* high convexity of the lobe is also associated with a slightly longer (sag.) preglabellar field.

(*d*) The length and level of the palpebral lobe, and morphology of the posterior limb: although the differences in these morphological characteristics form the primary basis for discrimination of the genera and species, each species has a considerable and occasionally overlapping range.

Quantitative analysis. Limited analysis was undertaken, primarily to provide a quantitative description of the species and additionally to supplement the purely qualitative discrimination of the genera and species.

Qualitative work suggests that the length of the palpebral lobe, and in particular the position of its posterior end, are important for the taxonomic discrimination of the genera and species, although a considerable range of intraspecific variation is observed. Accordingly these characters were selected for analysis, the occipital post-palpebral length (D_5) and the palpebral length (C) being plotted against the cranidial length (A_1) and 'best fit' lines fitted (text-fig. 6); the values for the dimensions are given in the Appendix, and the equations of the 'best fit' lines in Table 2.

TABLE 2. The equations of the 'best fit' lines, calculated by the method (Bartlett's method) given by Simpson, Roe, and Lewontin (1960, p. 234). A_1 is the total cranidial length, C is the palpebral length, and D_5 is the occipital post-palpebral length.

	A_1-D_5	A_1-C
E. polymera	$D_5 = -0{\cdot}4+0{\cdot}34A_1$	$C = 0{\cdot}4+0{\cdot}19A_1$
E. dalgarnoi	$D_5 = -1{\cdot}8+0{\cdot}35A_1$	$C = 1{\cdot}3+0{\cdot}23A_1$
B. flindersi	$D_5 = 0{\cdot}3+0{\cdot}26A_1$	$C = 1{\cdot}1+0{\cdot}22A_1$
B. dailyi	$D_5 = -0{\cdot}7+0{\cdot}26A_1$	$C = 0{\cdot}7+0{\cdot}27A_1$

The plot of occipital post-palpebral length against cranidial length indicates that the two genera can be clearly distinguished quantitatively on the basis of the position of the posterior end of the palpebral lobe. However the parameters obtained for *E. dalgarnoi* are somewhat anomalous, in that the gradient of the 'best fit' line is not significantly different from that of *E. polymera*. The small number of specimens in the sample of *E. dalgarnoi* may be a factor affecting the values of the parameters. The plot of palpebral length against cranidial length, however, shows that the two species can be distinguished quantitatively on the basis of their palpebral lengths. The anomalous values for *Balcoracania flindersi* suggest that the anterior end of the palpebral lobe is lower than in the other species, and this can be verified both qualitatively and quantitatively.

ONTOGENY

Larval stages are known for the species *B. flindersi*, *B. dailyi*, and *E. polymera*. *B. flindersi* is represented by over 150 specimens, and the major features of the ontogeny were elucidated by a study of this material; *B. dailyi* is adequately represented by 30 specimens, but only a few specimens of *E. polymera* are known. The order of description of the ontogenies thus differs from that of the adults.

The methods and procedures adopted vary slightly depending upon the size and nature of the sample, but are basically similar to those described below.

All specimens were prepared, measured, photographed, and described individually. A reconstruction of an early meraspid cranidium was made, and compared with a holaspid cranidium on a modified D'Arcy Thomson diagram (text-fig. 7), using the techniques described by Palmer (1957, p. 106). The line of least 'distortion' is the line of bilateral symmetry, and specifically the length of the glabella increases at a rate most nearly equal to that of absolute size. However the length of the glabella is very difficult to measure accurately on extremely small specimens, and the cranidial length (A_1) is used

instead as the standard dimension. The use of this dimension involves some error, as the anterior border appears and develops during ontogeny; however, it is considered that the practical advantage of accurate measurement offsets the theoretical disadvantages. The morphology of each specimen is then tabulated against cranidial length (in ascending order). Examination of the table and the D'Arcy Thompson grid shows that several characters underwent progressive change with increase in cranidial length; of these, three were selected, the anterior border and border furrow, the palpebral lobe,

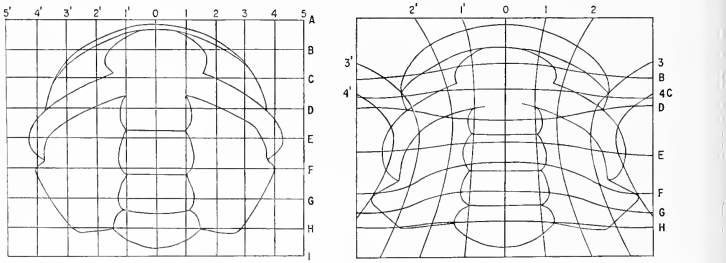

TEXT-FIG. 7. Proportional change in dorsal cephalic features of *B. flindersi* during development. Left, Cranidium of Stage II; Right, Holaspid cranidium.

and the anterior section of the facial suture. On the basis of the changes, subclasses were distinguished for each of the three characters, and the size ranges of each subclass noted. Considerable overlap in the range of the subclasses existed, as the characters change at different rates; however, it was found that the sets of data could be combined to give a number of stages of cranidial development, with an acceptable maximum overlap of the cranidial lengths (Tables 3, 6).

The development of the meraspid thorax is incompletely known, and although related, where possible, to stages of cranidial development, is described separately (Tables 4, 7).

The hypostomes present range in length upwards from 0·50 mm., and it is evident that at least the specimens in the lower part of the range have been separated from larval cranidia. Two problems arise: to match the hypostomes with the equivalent cranidia and thus to stages of cranidial development, and to determine an upper size limit, below which the hypostomes may be considered as 'larval'.

Examination of adult specimens of cephala with hypostomes '*in situ*' or close to that position, shows that the posterior edge of the hypostome reaches approximately the level of the posterior glabellar furrow. The sagittal length of the hypostome is thus slightly less than $\frac{3}{4}$ of the cranidial length (A_1), and accordingly an upper limit for the length of larval hypostomes can be fixed. It is unwise, however, to apply this factor to smaller specimens, as it is well known (Whittington 1957, 1959) that the hypostome is proportionately larger in the larval stages than in the adult in some cases. It is therefore necessary to find some dimension of the hypostome which can justifiably be assumed to bear a constant relationship to some dimension of the cranidium, over the

complete ontogeny. In the adult, the hypostome is attached to the posterior edge of the rostral plate, along the line of the hypostomal suture. Thus the length of the posterior edge of the rostal plate is equal to that of the anterior edge of the hypostome, excluding the anterior wings, which are free (text-fig. 4). As it can be assumed that the functional relationship between the rostral plate and hypostome does not change, the relationship between the two dimensions is fixed throughout ontogeny.

The length of the anterior edge of the rostral plate can be measured directly from the cranidium in most cases, as there is a slight change in curvature at the point where the facial suture intersects the anterior edge of the border, and it is from this point that the connective suture originates. The lengths of the anterior and posterior edges of the rostral plate can be taken as identical, within the limits of mensurational error. The length of the articulating section of the anterior edge of the hypostome (H_4) can be measured directly in most cases.

On the above basis, the hypostomes may be matched with a range of cranidia, and thus to a stage of cranidial development (Tables 5, 8).

The resulting descriptions and tabulations are subjective to some extent, owing to (*a*) the gradational nature of the morphological changes; (*b*) the size overlap between morphological subclasses; (*c*) overlap in size between meraspid degrees; and (*d*) method of allotting hypostomes to cranidial stages. However it is considered that, in general, an accurate representation of the ontogeny results.

Ontogeny of Balcoracania flindersi

(*a*) *Development of the cephalon* (Table 3)

Stage I: Cranidial lengths 0·38–0·49 mm. (includes the protopygidium in this stage): protaspides (text-fig. 8 I). Only 3 specimens were found, smaller than the size range for meraspides of degree 0, and only 1 of these was well enough preserved to verify the presence of the protopygidium. However the position of the specimens prevented adequate photography. The specimen is subelliptical in outline, and almost hemispherical, being slightly flat sagittally. It is divided into a large cephalon (or cranidium) and a narrow (sag.) protopygidium by a transverse line. The axis is narrow, flat to slightly depressed, and is defined for the posterior $\frac{3}{4}$ of its length by distinct parallel furrows, and for the remainder by indistinct furrows diverging at 45°. The axis is divided into 5 rings by indistinct transverse furrows, the most anterior furrow being at the point of divergence of the axial furrows. Cheek furrows are present, but indistinct.

The protopygidium is narrow (sag.), approximately $\frac{1}{4}$ the total length (sag.). The axis tapers posteriorly, but is indistinct.

Stage II: Cranidial lengths 0·50–0·64 mm.; meraspid degrees 0–1 (text-fig. 8 II; Pl. 110, figs. 2–4). Numerous specimens falling within this size range have distinct occipital rings and posterior margins, showing them to be meraspid cranidia. Two specimens with attached transitory pygidia, and 1 meraspid degree 1, are included within this range.

The cranidium is subcircular in outline, sagittally subhorizontal, margins steeply down-sloping. The glabella is moderately convex (tr.), $\frac{1}{3}$ the maximum cranidial width; the glabellar and occipital furrows are all distinct and transverse, with an additional indistinct furrow, aligned with the anterior edge of the eye ridge, partially subdividing the frontal lobe (pre-anterior furrow). The axial furrows are parallel from the posterior margin to the anterior furrow or slightly pinched in at the latter, then diverge at about 45° to the anterior edge. The frontal glabellar lobe is thus expanded to the anterior (although partially subdivided). The eye ridge is distinct, directed slightly to the posterior, and steeply down-sloping abaxially. The palpebral lobe is very short, depressed below the level of the cheek and downsloping abaxially; no distinct palpebral furrow; the posterior end of the lobe is opposite the anterior glabellar lobe or middle glabellar furrow. The cheek has a narrow (exsag.) subhorizontal

portion then slopes steeply downwards abaxially and posteriorly. The cheek furrows are short and parallel the eye ridge (Pl. 110, fig. 2). The posterior border is geniculate, with a short transverse section, and a longer section directed antero-laterally at 25–30°, almost to the base of the palpebral lobe. The anterior sections of the facial sutures converge strongly, intersecting the anterior edge at the same places as the axial furrows, the posterior sections are extremely short and diverge at about 30°.

TABLE 3. Larval development of *B. flindersi* based upon stages of development of the cranidium.

CHARACTER	STAGE I	STAGE II	STAGE III	STAGE IV	STAGE V	STAGE VIa	STAGE VIb	STAGE VIc
FRONTAL GLABELLAR LOBE	SUB – TRIANGULAR	SIDES ROUNDED SLIGHTLY	SIDES ROUNDED	ROUNDED	UNCHANGED	UNCHANGED	UNCHANGED	UNCHANGED
ANTERIOR BORDER	ABSENT	ABSENT	ABSENT OR MINUTE, DOWN – SLOPING STEEPLY	NARROW, DOWNSLOPING	CONVEX ABAXIAL – LY, HORIZONTAL SAGITTALLY	UNCHANGED	UNCHANGED OR NARROW, CONVEX RAISED.	CONVEX, RAISED, NARROW TO MEDIUM
ANTERIOR BORDER FURROW	ABSENT	ABSENT	ABSENT	ABSENT	DISTINCT ONLY ABAXIALLY	UNCHANGED	UNCHANGED, OR EVEN DEPTH	EVEN DEPTH
PALPEBRAL LOBE	INDISTINCT, DEPRESSED	DOWNSLOPING ABAXIALLY, BELOW CHEEK LEVEL; 0·17 GLAB. LENGTH	HORIZONTAL, BELOW CHEEK LEVEL; 0·2 GLABELLAR LENGTH	CONVEX, BELOW CHEEK LEVEL; 0·23 GLABELLAR LENGTH	CONVEX, SLIGHTLY BELOW CHEEK LEVEL 0·27 GLABELLAR LENGTH	CONVEX, SAME LEVEL AS CHEEK; 0·30 GLABEL- LAR LENGTH	UNCHANGED, 0·33 GLABELLAR LENGTH	UNCHANGED
PALPEBRAL FURROW	ABSENT	ABSENT	INDISTINCT	DISTINCT	UNCHANGED	IMPRESSED	UNCHANGED	UNCHANGED
POSTERIOR END OF PALPEBRAL LOBE	OPPOSITE ANT. GLABELLAR FURROW	OPPOSITE ANT LOBE – POST. FURROW	OPPOSITE MIDDLE FURROW – MIDDLE LOBE	OPPOSITE MIDDLE LOBE – POST. FURROW	OPPOSITE POST FURROW	UNCHANGED	OPPOSITE POST. FURROW – POST. LOBE	OPPOSITE POST. LOBE–OCCIPITAL FURROW
POSTERIOR BORDER (ABAXIAL TO FULCRUM)	ABSENT	DIVERGES AT 25 – 30°	DIVERGES AT 30 – 35°	DIVERGES AT 35 – 40°	DIVERGES AT 40 – 45°	UNCHANGED	DIVERGES AT 45–50°	DIVERGES AT 50 – 55°
POSTERIOR BORDER FURROW	ABSENT	INDISTINCT	DISTINCT, STRONGLY GENICULATE	MODERATELY GENICULATE	WEAKLY GENICULATE WIDENS ABAXIALLY	UNCHANGED	STRAIGHT, WIDENS ABAXIALLY	UNCHANGED
GENAL SPINE	—	—	EXTREMELY SMALL	EXTENDS TO LEVEL OF 1 ST. OR 2ND SEGMENT	—	—	—	EXTENDS TO LEVEL OF 5 TH. SEGMENT
ANTERIOR SECTION OF FACIAL SUTURE	?	CONVERGES	CONVERGES	CONVERGES SLIGHTLY	SAGITTAL TO ANTERIOR BORDER FURROW	UNCHANGED OF DIVERGES	DIVERGES SLIGHTLY	DIVERGES MODERATELY
LENGTH OF CRANDIUM (A_1)	0·38 – 0·49mm. (12 – 15·5mic divs.)	0·50 – 0·64mm. (16 – 20·5mic. divs.)	0·65 – 0·79mm (21 – 25·5mic divs.)	0·80 – 0·94mm. (26 – 30·5mic. divs.)	0·95 – 1·24mm. (31 – 39·5mic divs.)	1·25 – 1·36mm. (40 – 43·5mic divs.)	1·37 – 1·49mm (44 – 47·5mic divs.)	1·50 – 3·16mm. (48 – 100 mic divs.)
MERASPID DEGREE	(PROTASPIS)	0 – 1	(1) – 2 – 3	(3) – 4 – 6	7 – 11 – ?	?	?	16? – 18 – 53 – (60)

Stage III: Cranidial lengths 0·65–0·79 mm.; meraspid degrees (1), 2 and 3 (text-fig. 8 III; Pl. 110, figs. 5, 6). The axial furrows are deeply impressed, from the posterior edge to the anterior glabellar furrow, faint over the eye ridges, then indistinct on the sides of the frontal lobe. The frontal lobe is rounded laterally, and either reaches the anterior edge, or an extremely narrow, down-sloping anterior border. In the latter case the border and the lobe are separated by a distinct change in slope. The frontal lobe is subdivided by a pre-anterior furrow. The palpebral lobe is short, subhorizontal (tr. and sag.), depressed below cheek level, and with an indistinct palpebral furrow; the posterior end of the lobe is opposite the middle glabellar furrow or just below it. The cheek furrows parallel the eye ridges. The posterior border is horizontal, and separated from the cheek by a distinct border furrow; the border is again strongly geniculate, with the abaxial section directed antero-laterally at 30–35°. The anterior sections of the facial sutures converge strongly, and the posterior sections are very short and diverge at 45°.

The librigena has a small genal spine, which is directed almost sagittally to level of the occipital furrow.

Stage IV: Cranidial lengths 0·80–0·93 mm.; meraspid degrees (3), 4, 6 (text-fig. 8 IV; Pl. 110, figs. 7–9). Axial furrows converge slightly to anterior glabellar furrow, then curve out and around an expanded frontal lobe which is separated from the anterior edge by a narrow down-sloping anterior border. The palpebral lobe is convex (tr. and exsag.), below the level of the cheek, and separated from it by

a distinct palpebral furrow. The posterior end of the lobe is opposite the middle glabellar lobe or posterior furrow. The cheek is wider and flatter than in previous stages; cheek furrows parallel the eye ridge. The posterior border is convex, geniculate, with the abaxial section directed antero-laterally at 35–40°. The librigenal spine reaches the level of the 1st or 2nd thoracic segment.

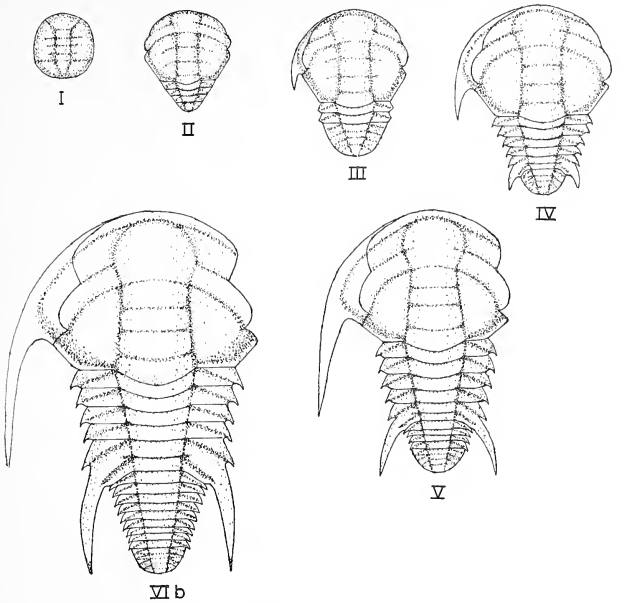

TEXT-FIG. 8. Development of *B. flindersi*. Roman numerals indicate the stage of cranidial development as described in the text. I, protaspis; II, meraspis, degree 0; III, meraspis, degree 2; IV, meraspis degree 6; V, meraspis, degree 10; VI*b*, meraspis, degree 15. Magnification constant at approximately ×50.

Stage V: Cranidial lengths 0·94–1·24 mm.; meraspid degrees 7–11 (text-fig. 8 v; Pl. 110, figs. 10, 11). The frontal glabellar lobe is rounded, and slopes down to a distinct anterior border furrow. The anterior border is convex abaxially, but narrows and flattens opposite the frontal lobe. The axial and palpebral furrows are deeply impressed and the cheek sometimes shows traces of furrows. One exceptionally well-preserved specimen shows the anterior cheek furrow extending from the middle glabellar furrow to the posterior end of the palpebral lobe, and retains traces of the pre-anterior glabellar furrow. The palpebral lobe is convex (tr. and exsag.), slightly below the level of the cheek, and with its posterior end opposite the posterior glabellar furrow or posterior lobe. The posterior border furrow is deep, weakly geniculate, widens abaxially and becomes confluent with the palpebral furrow. The abaxial section of the posterior border is at 40–45°. The anterior section of the facial suture is directed sagittally to the border furrow, then crosses the border diagonally to cut the anterior

edge opposite the sides of the frontal lobe; the posterior sections are short, diverging, and slightly convex abaxially.

The librigena has a distinct lateral and posterior border and furrow. The genal spine extends to the level of the 4th thoracic segment.

Stage VIa: Cranidial lengths 1·25–1·36 mm.; includes at least meraspid degree 12 (Pl. 110, fig. 12). The length of the frontal glabellar lobe is $\frac{1}{3}$ of the total glabellar length. The palpebral lobe is relatively long, on approximately the same level as the cheek, and with its posterior end opposite the posterior glabellar furrow and lobe. The abaxial section of the posterior border is at 40–45°. The anterior section of the facial suture is directed sagittally or diverges slightly to the anterior border furrow.

Stage VIb: Cranidial lengths 1·37–1·50 mm. (text-fig. 8 v*ib*; Pl. 110, fig. 13). The anterior border is unchanged or becomes convex, with the same width abaxially and sagittally. The posterior end of the palpebral lobe is opposite the posterior glabellar furrow or lobe. The abaxial section of the posterior border is at 45–50°. The anterior section of the facial suture diverges slightly to the anterior border furrow.

Stage IVc: Cranidial lengths 1·50–3·16 mm.; includes meraspides of degrees 18–55 (Pl. 116, figs. 14, 15). The cephala of this group have basically attained the holaspid morphology. With increase in size the anterior border continues to widen and the length of the frontal glabellar lobe decreases in proportion to the total glabellar length. The posterior end of the palpebral lobe is opposite the posterior lobe or occipital furrow, the abaxial section of the border is at 50–55°, and the anterior sections of the facial sutures are divergent.

(*b*) *Development of the thorax* (Table 4)

Degree 0 (2 specimens). The transitory pygidium is triangular in shape, with its maximum width (tr.) at the anterior edge which articulates with the posterior edge of the cranidium between the fulcral points. The axial furrows are shallow and taper to a point on the posterior edge. The pleural field slopes down strongly abaxially, and there is a continuous lateral and posterior margin. The axis is subdivided into 3 or 4 rings in one specimen, and 3 in the other; in both specimens the anterior part of the pleural field is indistinctly furrowed.

Degrees 1–4. The prothoracic segments released from the transitory pygidium possess normal axial and articulating half rings, and geniculate pleurae. At degree 1, the pleural furrows are poorly developed

---

EXPLANATION OF PLATE 110

Figs. 1–15. *Balcoracania flindersi* gen. et sp. nov. 1, F16700, ×17; larval hypostome, matched with cranidial, Stage IV. 2, F16687, ×15; cranidium, Stage II, showing cheek furrows. 3, F16688, ×15; meraspis, degree 0, Stage II. 4, F16689, ×15; cranidium, Stage II, showing distinct palpebral lobes. 5, F16690, ×15; cranidium, Stage III, showing distinct cheek furrows. 6, F16691, ×15; meraspis, degree 3, Stage III. 7, F16692, ×15; cranidium, Stage IV, showing narrow down-sloping anterior border. 8, F16693, ×15; crushed and asymmetrically distorted meraspis, degree 6, Stage IV. 9, F16694, ×15; meraspis, degree 6, Stage IV. 10, F16695, ×15; cranidium, stage V, showing distinct cheek furrows. 11, F16696, ×15; incomplete meraspis, degree 11, Stage V. 12, F16697, ×15; cranidium, Stage VI*a*, showing pre-anterior lateral glabellar furrows. 13, F16698, ×15; cranidium, Stage VI *b*. 14, F16699, ×15; meraspis, degree 18, Stage VI*c*; cephalon partly exfoliated, librigenae slightly displaced, portion of opisthothorax and transitory pygidium missing. 15, F16682, ×15; holaspid cranidium, partly exfoliated.

Figs. 16–18. *Emuella polymera* gen. et sp. nov. 16, F16701, ×15; cranidium. 17, F16702, ×15; cranidium showing minute anterior border, anterior position of palpebral lobes. 18, ×3; portion of bedding plane showing F16701–2 in relation to a holaspid cephalon.

Figs. 19–22. *Balcoracania dailyi* gen. et sp. nov. 19, F16703, ×15; cranidium, Stage I. 20, F16704; cranidium, Stage II, showing posterior position of palpebral lobe. 21, F16705, ×15; incomplete cranidium, Stage III, showing distinct development of anterior border and border furrow. 22, F16706, ×15; meraspis, degree 10, Stage IV, showing transitory pygidium with entire margins.


1

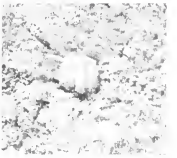
2


3


4

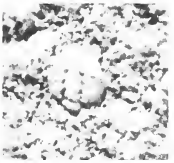
5


6


7


8


9


10


11


12


13


14


15

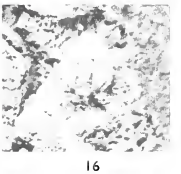
16


17


18


19

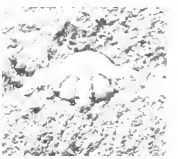
20


21


22

and pleural spines have not been observed; at degrees 2–4, the furrows become more distinct and spines develop. The axial furrows converge evenly to the posterior and are aligned with those of the pygidium; the pleurae are progressively shorter (tr.) to the posterior, and their abaxial ends are aligned with the lateral borders of the pygidium.

The morphology of the transitory pygidium is basically as for degree 0, with very little increase in absolute size. The number of rings on the axis varies from 3 to 4, and the pleural field shows the pleural and interpleural furrows of the two most anterior segments; posteriorly the furrows are indistinct.

TABLE 4. Development of the meraspid thorax and transitory pygidium in *B. flindersi*. A_1, total cranidial length of the articulated cephalon is given in micrometer divisions where 1·00 mm. = 32 divisions.

Meraspid degree	*Cranidial length* (A_1)	*Cephalic stage*	*Segments in transitory pygidium*
0	17	II	3
0	17	II	3–4
1	20	II	4
1	21	III	5
2	23	III	2–3
3	24	III	3–4
3	25	III	2–3
3	26	IV	3
3	26	IV	3
4	26	IV	3
4	27	IV	1
6	28	IV	3
6	29	IV	1–2
6	29	IV	6
6	30	IV	1–2
6	30	IV	4
10	34	V	2
11	38	V	3
18	67	VI*c*	3
18	72	VI*c*	3–4
19	72	VI*c*	3
27	80	VI*c*	3
53	100	VI*c*	3–4

Degree 6 (4 specimens). The prothorax has already attained the characteristic adult morphology; the 5th segment is fused to the macropleural 6th, with the line of fusion visible on the interfurrow platform. The macropleural spine extends to the posterior edge of the transitory pygidium, curving inwards slightly at the posterior end. The axis tapers strongly but evenly to the posterior. The pleurae shorten progressively from the 1st to the 5th segment. The anterior edge of the transitory pygidium articulates with the posterior edge of the 6th between the notches on the posterior border.

Degrees 10–55. The prothorax is as described for degree 6; the opisthothoracic segments are normal. The pleural furrows are generally more distinct towards the anterior, and in the higher degrees do not occur on most of the posterior opisthothoracic segments and the transitory pygidium. The transitory pygidium may have up to 6 distinct axial rings, but generally only the 2 most anterior segments are distinct on the pleural field. The absolute size of the pygidium increases little.

(*c*) *Development of the hypostome* (Table 5)

The hypostome attains the adult morphology when its length (sag.) is approximately 1·45 mm.; from this point onwards the only change is an increase in size. Independent confirmation is given by the fact that the length of the cranidium matched with a hypostome of this size falls within the size range of

Stage VI*c*, the stage in which the cranidium attains the holaspid condition. Changes during ontogeny primarily affect two groups of characters: (*a*) the size and position of the anterior wings; the position is expressed by the ratio of lengths (sag.) from the anterior edge respectively to the level of the anterior wings and to the level of the lateral notch; (*b*) the shape of the posterior lobe of the median body.

The smallest hypostome is matched with cranidia in the upper portion of the size range of Stage III and the lower portion of Stage IV. The posterior lobe of the median body is triangular with the bounding lateral furrows converging to the posterior from the lateral notch. The anterior wings are very small, only slightly depressed, and the ratio of lengths is 1:2, i.e. the wings are towards the anterior end. With increase in size the posterior lobe becomes subrectangular, with a transverse posterior border furrow developing; the anterior wings become more pronounced and depressed, and move progressively to the posterior, the ratio changing to 2:3 (Pl. 110, fig. 1).

TABLE 5. Development of the hypostome in *B. flindersi*. H_1 is the sagittal length of the hypostome, H_4 is the transverse length of the hypostomal suture, R_1 is the transverse length of the rostral suture and A_1 is the total cranidial length; all measurements are expressed in micrometer divisions where 1·00 mm. = 32 divisions. H_4, measured on the hypostome, is approximately equal to R_1, which is measured on the cephalon; thus for any given value of H_4, a range of values for A_1 can be obtained. The hypostome can then be matched to the equivalent stage (or stages).

H_1	H_4 (= R_1)	A_1 *of equivalent cephalon*	*Cephalic stage*
18	15	24–28	III, IV
19	16	28–32	IV, V
26	18	30–34	IV, V
27	18	30–34	IV, V
29	20	34–36	V
32	21	34–38	V
32	22	40–43	VI*a*
35	24	42–43	VI*a*
38	27	45–46	VI*b*
38	28	45–46	VI*b*
42	30	47–57	VI*c*
46	32	55–67	VI*c*

Ontogeny of Balcoracania dailyi

(*a*) *Development of the cephalon* (Table 6; text-fig. 9)

Stage I: Cranidial lengths 0·50–0·70 mm.; all specimens appear to be meraspid cranidia (text-fig. 9 1; Pl. 110, fig. 19).

The cranidium is subcircular in outline with steeply down-sloping margins. The glabella is moderately convex (tr.) and narrow; the glabellar furrows are distinct and transverse. The axial furrows are deep posteriorly, subparallel but pinched in sharply at the anterior glabellar furrow; anteriorly the furrows are faint, diverging around an expanded frontal glabellar lobe. The frontal lobe reaches the anterior edge, and is partially subdivided by short pre-anterior glabellar furrows. The eye ridge is distinct, directly slightly to the posterior, and slopes steeply downwards abaxially. The palpebral lobe is short, depressed below the cheek level, horizontal (sag. and tr.), and is only indistinctly defined by a palpebral furrow; the posterior end of the lobe is opposite the middle glabellar furrow or lobe. The cheek is narrow, steeply down-sloping abaxially and posteriorly, and is subdivided by cheek furrows parallel to the eye ridge. The posterior border is narrow, horizontal or slightly downsloping, and separated from the cheek only by a change in slope. The border is geniculate with short transverse section and a longer section directed antero-laterally at 25–30°. The anterior sections of the facial suture converge strongly to intersect the anterior edge at its junctions with the axial furrows. The posterior sections are extremely short, and curved.

TABLE 6. Larval development of *B. dailyi* based upon stages of development of the cranidium.

CHARACTER	*STAGE I*	*STAGE II*	*STAGE III*	*STAGE IV*	*STAGE V*
FRONTAL GLABELLAR LOBE	SUB-TRIANGULAR	SLIGHTLY ROUNDED ABAXIALLY	ROUNDED ABAXIALLY	UNCHANGED	UNCHANGED
ANTERIOR BORDER	ABSENT	NARROW, DOWNSLOPING STEEPLY	CONVEX ABAXIALLY, HORIZONTAL TO SLIGHTLY DOWNSLOPING SAGITTALLY	BORDER CONVEX, SLIGHTLY RAISED	UNCHANGED
ANTERIOR BORDER FURROW	ABSENT	INDISTINCT OR ABSENT	INDISTINCT SAGITTALLY, DISTINCT ABAXIALLY	DISTINCT, WITH BORDER FURROW FOSSULAE	UNCHANGED
PREGLABELLAR FIELD	ABSENT	ABSENT	ABSENT	MINUTE	NARROW, DOWNSLOPING
PALPEBRAL LOBE	BELOW CHEEK LEVEL, DOWNSLOPING ABAXIALLY, 1/4 GLABELLAR LENGTH	BELOW CHEEK LEVEL, CONVEX (SAG. AND TR.) 1/4 GLABELLAR LENGTH	SAME LEVEL AS CHEEK, CONVEX, BETWEEN >1/4 & <1/3 GLABELLAR LENGTH	ABOVE CHEEK LEVEL, CONVEX, 1/3 GLABELLAR LENGTH	UNCHANGED
PALPEBRAL FURROW	ABSENT TO INDISTINCT	DISTINCT	DISTINCT, IMPRESSED	UNCHANGED	UNCHANGED
POSTERIOR END OF PALPEBRAL LOBE	OPPOSITE MIDDLE GLABELLAR LOBE	OPPOSITE MIDDLE LOBE-POSTERIOR FURROW	OPPOSITE POSTERIOR FURROW	OPPOSITE POSTERIOR FURROW-POSTERIOR LOBE	OPPOSITE POSTERIOR LOBE-OCCIPITAL FURROW
POSTERIOR BORDER (ABAXIAL TO FULCRUM)	DIVERGES AT 30°	DIVERGES AT 35–40°	DIVERGES AT 40–45°	DIVERGES AT APPROX 50°	DIVERGES AT 50–55°
POSTERIOR BORDER FURROW	INDISTINCT	DISTINCT, MODERATELY GENICULATE	WEAKLY GENICULATE	STRAIGHT, WIDENS ABAXIALLY	UNCHANGED
ANTERIOR SECTION OF FACIAL SUTURE	CONVERGES SLIGHTLY	SHORT SECTION DIRECTED SAGITTALLY	DIVERGES SLIGHTLY	DIVERGES MODERATELY	UNCHANGED
GENAL SPINE	–	–	–	MINUTE, EXTENDS TO LEVEL OF POSTERIOR BORDER OF 1ST–2ND SEGMENT	LENGTHENS RAPIDLY TO ATTAIN ADULT CONDITION
LENGTH OF CRANIDIUM (AX)	0·50–0·70mm (16–22·5mic divs)	0·72–0·92mm (23–29·5mic divs)	0·94–1·14mm (30–36·5mic divs)	1·16–1·48mm (37–47·5mic divs)	1·50–2·90mm (48–93mic divs)
MERASPIS DEGREE	–	–	–	6–10	(11)–12–39–(52)

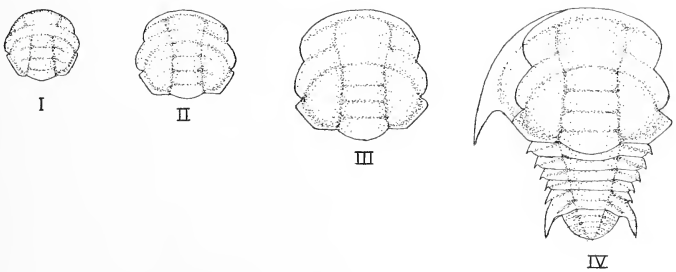

TEXT-FIG. 9. Development of *B. dailyi*. Numerals indicate stages of cranidial development as described in the text. I, II, and III, meraspid cranidia; IV, meraspis, degree 6. Magnification constant at approximately ×50.

Stage II: Cranidial lengths 0·72–0·93 mm. (text-fig. 9 II; Pl. 110, fig. 20). The axial furrows converge evenly from the posterior edge to the anterior glabellar furrow, then diverge around an expanded and rounded frontal glabellar lobe. The frontal lobe is separated from the anterior edge by a narrow downsloping anterior border. The palpebral lobe is convex (tr. and exsag.), below the cheek level, but distinctly defined by a palpebral furrow; the lobe is relatively long (¼ glabellar length) with the posterior edge opposite the posterior glabellar furrow or just anterior to it. The cheek is wider (tr.) than in Stage I, less steeply down-sloping; the cheek furrows are indistinct. The posterior border is narrow, convex, and the border furrow is distinct. The abaxial portion of the border is directed antero-laterally

at 35–40°. The anterior sections of the facial suture are directed sagittally for a short distance before curving inwards; the posterior sections are short, diverging and slightly convex abaxially.

Stage III: Cranidial lengths 0·94–1·14 mm. (text-fig. 9 III; Pl. 110, fig. 21). The frontal glabellar lobe is rounded laterally, and slopes down to an anterior border furrow. The anterior border is narrow, slightly raised and convex abaxially, horizontal to slightly down-sloping opposite the frontal lobe. The anterior border furrow is distinct abaxially, shallow and indistinct opposite the frontal lobe. The palpebral lobe is convex (tr. and exsag.), on the same level as the cheek, and defined by a distinct palpebral furrow; the posterior end is opposite the posterior glabellar furrow. The abaxial section of the posterior border is directed antero-laterally at 40–45°; the posterior border furrow is slightly curved. The anterior sections of the facial suture diverge slightly to the border furrow.

Stage IV: Cranidial lengths 1·16–1·48 mm.; specimens falling within this size range include both cranidia and cephala with attached thoraces and pygidia, of degrees 6–13 (text-fig. 9 IV; Pl. 110, fig. 22).

The frontal glabellar lobe is rounded. The anterior border is narrow and convex, both abaxially and sagittally; the border furrow is deep abaxially, but shallows abruptly opposite the frontal lobe, with small anterior furrow fossulae. A minute, down-sloping preglabellar field is present, but not distinctly separated from the frontal lobe. The palpebral lobe is above the cheek level, about $\frac{1}{3}$ of glabellar length, with its posterior end opposite the posterior glabellar furrow or lobe. The abaxial section of the posterior border is directed antero-laterally at 50°. The posterior border furrow is almost straight, widening abaxially and sloping downwards abaxially. The anterior section of the facial suture diverges at 10° to the border furrow.

The librigena is narrow (tr.) with the genal spine very short, extending through the size range from the level of the posterior border to that of the 1st or 2nd thoracic segment.

TABLE 7. Development of the meraspid thorax and transitory pygidium in *B. dailyi*. A_1, total cranidial length of the articulated cephalon is given in micrometer divisions where 1·00 mm. = 32 divisions.

Meraspid degree	*Cranidial length* (A_1)	*Cephalic stage*	*Segments in transitory pygidium*
6	38	IV	3
6	40	IV	4–5
6	40	IV	4
6	44	IV	3
10	45	IV	4–5
10	48	V	3
12	48	V	5
13	46	V	4–5
13	48	V	5
14	50	V	4–5
17	54	V	3
21	53	V	3–4
22	61	V	9
24	75	V	4–5
28	75	V	7–8
35	115	V	4
39	107	V	6

(*b*) *Development of the thorax* (Table 7)

No meraspis of a degree less than 6 is known from this species. The development from this degree is basically the same as in *B. flindersi*, but a greater variation in the number of segments in the transitory pygidium is observed, both within a degree and between degrees. Three specimens of degree 6 show 3 or 4 axial rings, and 1 or 2 complete sets of pleurae on the pygidium, but another specimen shows 6 distinct, and at least 1 indistinct axial rings, and 3 distinct sets of pleurae; the 2 most anterior segments appear fully formed, but their abaxial ends are continuous with the lateral border of the pygidium.

1 specimen of degree 21 possesses a pygidium with 9 distinct axial rings; the anterior 3 segments are completely formed, and appear to be only semi-ankylosed to each other and the rest of the pygidium. In this specimen the pygidium is 40% longer than in others with a normal complement of segments.

(*c*) *Development of the hypostome* (Table 8)

The changes taking place during the development are similar to those in *B. flindersi*. The smallest hypostome is matched with a cranidium of Stage I, and the smallest with the holaspid morphology with a cranidium larger than those of Stage IV.

TABLE 8. Development of the hypostome in *B. dailyi*. Explanation as for the table 5.

H_1	H_4 (= R_1)	A_1 *of equivalent cephalon*	*Cephalic stage*
20·5	12	19–21	I
22	16	23–25	II
25	18	25–28	II
25	20	28–35	II, III
28	20	28–35	II, III
33	22	35–38	III, IV
39	28	44–47	IV
42	29	48–50	IV
45	29	48–50	IV
53	39	69–	IV

Ontogeny of Emuella polymera (Plate 110, figs. 16–18)

Only 10 specimens of this species are known which are considered larval, and of these, only 2 retain the meraspid thorax. Accordingly the development is not divided into stages, as with the species of *Balcoracania*.

The smallest specimen found had a sagittal length of 0·40 mm., and appears to be a protaspis; however it is badly preserved and details are obscure. At a cranidial length of about 0·67 mm., a narrow down-sloping border appears in front of the frontal glabellar lobe, the palpebral lobe is below cheek level and extends posteriorly to the level of the middle glabellar lobe, and the anterior section of the facial suture has a very short sagittally directed section; one specimen of this size (Pl. 110, fig. 16) shows a pre-anterior glabellar furrow, and cheek furrows. This cranidial size corresponds to meraspid degree 1. At about 0·88 mm., the anterior border has become horizontal abaxially, the palpebral lobe extends to the level of the middle glabellar furrow, and the frontal lobe is outlined by deep axial furrows. A well preserved specimen shows that the cheeks are still furrowed. With further increase in size from 1·00 to 1·40 mm., the anterior border becomes horizontal to slightly convex, the border furrow develops fossulae, the palpebral lobe extends just beyond the middle glabellar furrow, and the anterior sections of the facial suture become slightly divergent. A meraspid degree 7 is included in this range. At approximately 1·7 mm., the cranidium exhibits the holaspid morphology.

No hypostomes which could be considered larval are known.

Discussion

The studies of the ontogenetic development of the three species reinforces the basis of the taxonomic discriminations made on the adult morphology; in particular, the species of *Balcoracania*, which are morphologically very close in the adult, can be clearly discriminated by their ontogenetic development.

The cephala of the three species undergo similar types of changes during their ontogeny, but the individual changes occur at different rates in each species. Thus the cranidia exhibit different combinations of characters at a given age (measured against cranidial length). In addition other features which are characteristic of the adult of the

species appear or are attained at some stage during the ontogeny. In *E. polymera* the characteristic relative length and position of the palpebral lobe is attained at an extremely early stage. In contrast, the preglabellar field which characterizes *B. dailyi* develops rather late compared with other features.

The size at which the cephalon attains the holaspid morphology differs in the genera. In *E. polymera* it is reached at a cranidial length of 1·7 mm., in the species of *Balcoracania* at 1·5 mm.

The development of the thorax is extremely similar in all species. It follows the general pattern outlined by Whittington (1957, 1959), with two important modifications; the release of the macropleural unit, and the change from prothoracic to opisthothoracic segments. With regard to the macropleural unit, it is significant that in *B. flindersi* where numbers are sufficient for all stages of early meraspid development to be represented, no meraspis of degree 5 has been discovered. It is evident that the 5th and 6th segments develop together in the transitory pygidium, and are released into the thorax as a unit. At degree 6, the 6th segment is already macropleural, and the spine reaches the level of the posterior edge of the transitory pygidium. However no trace of the macropleural spine has been found in transitory pygidia of degrees 0–4, indicating that the spine develops very rapidly, ostensibly during the period of the moult at which the macropleural unit is released into the thorax.

After the release of the macropleural unit into the thorax, there occurs a change in the size of the segments released, and the opisthothorax develops.

In all species the length of the transitory pygidium and the number of segments, as indicated by the number of furrows on the axis, vary both within an individual degree and between degrees (Tables 4, 7). Also the length of the cranidium varies considerably for a given degree, and considerable overlap may occur between successive degrees; 3 specimens are known of degree 3 with a range of cranidial lengths which overlaps that for specimens of degrees 4 and 6. It thus appears that segments may be added to the transitory pygidium during individual degrees, implying the occurrence of more than one moult within a degree. In addition, in meraspides of degree 6 or more, specimens occur with considerably more segments in the transitory pygidium than the average. In these cases the most anterior 2 or 3 segments appear to be fully formed, and only semi-ankylosed to the pygidium. It thus seems probable that in the development of the opisthothorax, more than one segment may occasionally be released during some moults.

Comparison of the rates of cephalic and thoracic development raise some points of interest. At degree 6 the cranidium has a length of 0·88 mm. in *B. flindersi*, but 1·25 mm. in *B. dailyi*; the cranidial development is thus further advanced in *B. dailyi* at this stage of thoracic development. In both species, however, the cranidium attains the holaspid condition at a cranidial length of 1·50 mm.; in *B. flindersi* this stage is reached at degree 16, and in *B. dailyi* at degree 13. The larval development of the thorax is thus far from complete and significantly lags behind that of the cranidium.

FUNCTIONAL MORPHOLOGY

The characters of the thorax of the Emuellidae are analysed on a basis of function, both in the adult trilobite and during development, and an attempt is made to seek causes framed in terms of adaptation.

Division of the thorax. The division of the thorax into a prothorax, characterized by a constant number of segments with normal pleurae, and an opisthothorax with a variable number of segments with pleurae clearly reduced in size, was previously only known in the Olenellidae (Hupé 1953*a*, *b*, *c*, 1955; Harrington *et al.* 1959).

In the Olenellidae the number of prothoracic segments varies from 11 in *Neltneria*, to 17 in *Fallotaspis* and *Nevadia*. The number of opisthothoracic segments differs more widely, from 2 to 30, but in general is low.

The division of the thorax has been considered to be a primitive character and to be lost in more advanced trilobites (Hupé 1953*a*, *b*; Harrington *in* Harrington *et al.* 1959). The number of segments in the opisthothorax has also been equated to the degree of 'primitiveness', those with many segments being considered the least evolved. In addition, the prothorax has been considered homologous to the thorax of normal trilobites, because of the fixity of the number of segments, and the opisthothorax as homologous with the pygidium. In most of the Olenellidae in which the prothorax is relatively long and multisegmented, and the opisthothorax short and with only a few segments, the homology may seem justified. However in *Paedeumias robsonensis* (Burling), in which the opisthothorax is as long as the prothorax and contains more than twice the number of segments, it appears difficult to justify its homology with the normal pygidium. It is even more difficult in the case of the Emuellidae where the opisthothorax is twice the length of the prothorax, and has between 48 and 55 segments; in addition the prothorax contains only 6 segments. It is considered that such a homology is inaccurate, or at least misleading.

In attempting to explain the phenomenon on the basis of functional morphology, three questions must be faced; why does the change occur, at what point does it take place, and what causes the eventual termination of segmentation? An attempt is made to answer these questions with reference to the Emuellidae, and to test the validity of the resulting hypothesis by comparison with the Olenellidae.

In the prothorax of the Emuellidae, the posterior edges of the first 4 normal segments are directed transversely, but those of the 6th segment are directed postero-laterally, from the axial furrow to the notch at the base of the macropleural spine. If the 7th segment is to articulate in the normal fashion with the posterior edge of the 6th, its pleurae must necessarily be reduced in length, as the axial ring can only have normal taper. It is considered that in this case, it is the abrupt space reduction, consequent upon the change in direction of the posterior border of the macropleural segment, which initiates the change in the nature of the segments released from the transitory pygidium.

In the adult, the segments of the opisthothorax form a perfectly graded series between the posterior border of the 6th segment and the anterior pygidial border (text-fig. 5A). In the ontogeny of the Emuellidae, meraspid degree 6 shows the transitory pygidium articulating with the posterior border of the 6th, in the same relative position and manner as does the 7th segment in the adult, and displaying a perfect gradation with the prothorax (text-fig. 8). In succeeding meraspid degrees, the absolute size of the transitory pygidium increases only very slightly, whilst that of the 6th segment increases more rapidly, and the opisthothorax remains perfectly graded with respect to both. Thus the release of segments from the transitory pygidium ceases when the ratio of the lengths (tr.) of the posterior border of the 6th and the anterior pygidial border becomes constant. It is notable in this connection that in the ontogeny of the Emuellidae, the

cephalon attains the holaspid condition whilst segments are still being released into the opisthothorax.

In the Olenellidae, only *Neltneria* has the last prothoracic segment macropleural, and it is notable that the number of prothoracic segments is less than in other members of the family. In *Neltneria* the posterior edges of the pleurae of the 11th segment have only very short transversely directed sections before the spine curves to the posterior; thus the space available for pleurae of succeeding segments is reduced. In addition the mechanics of articulation necessitate a progressive inclination of the pleurae to the posterior, with the last opisthothoracic segment having its pleurae wrapped around the sides of the pygidium. In the Olenellinae and *Fallotaspis*, it is the 3rd prothoracic segment which is macropleural. The posterior edge of the macropleural segment is transverse for most of its length, thus it does not cause an abrupt decrease in the space available for succeeding segments. However it does reduce the space, and causes the pleurae of succeeding segments to be progressively inclined to the posterior, and it appears to be this factor which finally causes a change in the nature of the segments released. As this is a more gradual process than in the Emuellidae, a greater number of prothoracic segments are released. In the Olenellidae which possess an opisthothorax, but not macropleural spines, e.g. *Elliptocephala*, *Nevadia*, the segments have pleurae progressively inclined to the posterior, and possessing long pleural spines. In those without division of the thorax, e.g. *Holmia*, the pleurae are again inclined progressively to the posterior, but do not possess long pleural spines; consequently space reduction does not reach a critical point.

It is thus considered that the division of the thorax can be explained as a response to a space reduction, either abrupt or gradual, which necessitates a change in the nature of the segments, in order to maintain the ability to articulate freely. It may be significant however, that the phenomenon has only been observed in Lower Cambrian trilobites. Possibly only primitive trilobites had this ability, or that more advanced ones solved similar problems in a less dramatic fashion.

Macropleurality. This feature occurs in many Cambrian and post-Cambrian families. In the Cambrian it is widespread, with most genera of some families exhibiting this feature; these include the Olenellidae, Neoredlichiidae, Bathynotidae, Paradoxididae, Zancanthoididae, and Dolichometopidae. In post-Cambrian families, such as the Shumardiidae, Asaphidae, Remopleurididae and Cyclopygidae, expression of the feature is usually confined to a single genus.

In the Emuellidae the last segment of the prothorax is macropleural. The spine, which is formed by both anterior and posterior pleural bands, tapers gradually to the posterior, curving inwards slightly, and extending to the level of the posterior edge of the pygidium or just beyond it. The doublure of the segment extends from the base of the pleural spine of the 5th, to which the 6th is fused, to the notch on the posterior border of the 6th. The spine is thus hollow, almost flat on top, slightly V-shaped to rounded below.

In the ontogeny of the Emuellidae, the spine appears abruptly at meraspid degree 6, without having previously appeared in the transitory pygidia of earlier degrees. The general form is the same as in the adult, with the spine extending to the level of the posterior edge of the transitory pygidium. In succeeding degrees, the length of the spine increases to maintain the same relative position.

In view of the high correlation between the lengths of the macropleural spine, and the opisthothorax and pygidium at all ontogenetic stages, it is considered that the spine serves both to stabilize and protect the opisthothorax. In a rest position on the sea floor, the flattish base of the spine would be opposed to the bottom, rather than the delicate pleural spines.

Hupé (1950, 1953*c*) suggested that the macropleural segment is the genital segment containing the gonopores on the basis that as the trilobites themselves are primitive, they are near the original condition where gonads and gonopores are metameric, and would be localized on segments of particularly primitive character. Hupé considered that the macropleural segments are the most primitive because of their narrow axis, and then compared the position of the macropleural segments in trilobites with the position of the gonopore in the Insecta, Myriapoda, Crustacea, and Chelicerata (Hupé 1950, fig. 7*a*), concluding that the opisthogoneate and progoneate tendencies of the 'Atennulata' existed in trilobites in the Lower Cambrian.

There is little evidence that the macropleural segments are the most primitive; in fact in any one trilobite it is the macropleural segment which, by definition, is the most specialized. There is no evidence of a structure on the dorsal surface of the macropleural segment which could be interpreted as a gonopore; thus if the gonopore is located on the ventral side, some modification of the ventral morphology might be expected. However, in the Emuellidae, the doublure of the segment is strictly comparable in structure and position to that of normal prothoracic segments. If it is assumed that the gonopores were carried in the soft ventral integument, there seems to be no reason why the macropleural segment alone should carry them. The suggestion, based on comparison with a hypothetical annelid ancestor, that the gonopores will occur on most, if not all thoracic segments (Raymond 1920, and others), appears the more reasonable.

The contention by Hupé (1953*b*) that macropleural segments in Lower Cambrian trilobites have two preferred positions, one anterior and one posterior, appears to have greater validity. The Olenellidae are characterized by having the 3rd prothoracic segment macropleural, the Emuellidae and *Neltneria* the last. Other related families display a similar division, but at least 2 genera (*Olenelloides* and *Bathyuriscidella*) possess 2 macropleural segments, more or less symmetrically placed in the thorax. The significance of the apparent division is not known.

In all genera whose adults possess macropleural segments, and whose ontogeny is known, the macropleural segment either appears in the transitory pygidium and is released at the appropriate meraspid degree (Olenellidae, *Shumardia*), or develops suddenly at the time of release from the transitory pygidium. In no known case does the macropleural segment develop after release into the thorax. This implies that the segments have some adaptive significance in the larval stages or that sexual maturity is very precocious. Hupé (1953*c*, p. 116), whilst allowing a possible secondary adaptive function connected with pelagic life, considered that the presence of such segments would be almost universal if this were the case; he accordingly considered sexual maturity to be precocious, and that a presumed change from allometric to isometric growth during the early meraspid period marked this change (1953*b*, p. 121). However, this alleged change is based on little data, is unsupported by statistical testing, and in any event is not necessarily indicative of sexual maturity. Therefore it is considered that the first alternative, that of adaptation to a pelagic existence is the more likely possibility.

Indeed Hupé's reasons, i.e. lack of universality, for rejecting this as the primary cause, apply equally well to the interpretation of the macropleural segments as genital.

In *Paradoxides* (Westergard 1936, Whittington 1957, 1959) the 1st and 2nd segments are both strongly macropleural when they first appear, but regress during meraspid development, the 1st more rapidly than the 2nd, so that at degree 15 (Whittington 1957, fig. 5*b*) only the 2nd is macropleural. In the adult, the 2nd segment is only weakly macropleural. The same sort of phenomenon occurs in both the Olenellidae and Redlichiidae, and may be comparable to the regression, during the same period, of the fixigenal and intergenal spines of the Olenellidae and Paradoxididae. Whittington (1957, p. 450) has attributed to the latter a role of support and buoyancy in a supposed pelagic life. It is reasonable to suggest that the macropleural spines had a similar adaptive function. In the Emuellidae it seems probable that the spines also served a protective function, a role which continued into the adult stages. However, the retention of the macropleural spines in adults of most genera raises several problems. The spines may retain a function of stabilization or protection in some cases, but in others they occur in genera belonging to families in which the other members appear well adapted to their habitat and mode of life, e.g. *Octinellus* in the Illaenidae. The question thus arises as to whether the adaptive function is secondary or not. In this context Hupé's suggestion as to the primary function cannot be dismissed.

Raw (1953) suggested that the presence of macropleural spines is related to merocyclism inherited from a polychaete ancestor, occurring most frequently in primitive forms and becoming lost when the segments achieve a graded condition. Macropleurality undoubtedly occurs most commonly amongst Lower Cambrian forms, but even here it is difficult to match macropleurae with cycles of segmentation. Raw (1953, p. 94) cited *Olenelloides armatus* (Peach) as an example where one macropleural segment alternates with two normal segments. This genus is generally regarded as aberrant, but even here it is necessary to consider the cephalic spines as representing macropleurae. Palmer (1957, p. 111) attempted to apply merocyclism to *Olenellus* and *Paedeumias*, but found it necessary to combine it with the hypothesis of secondary segmentation (Størmer 1941) in order to fit merocycles. The presence of contiguous macropleural segments in the larval stages of *Paradoxides* and other genera casts grave doubts on Raw's concept. In post-Cambrian trilobites the sporadic occurrence of macropleural segments in more than one position affords another difficulty; in *Acidaspis*, Hupé (1950) listed seven species with five different positions of the macropleural segment.

Manton's studies on the functional morphology of modern arthropods are interesting in the above context, since she concludes that body form is largely determined by locomotory habits (Manton 1952, 1960, 1964).

Fusion of thoracic segments. The Emuellidae have the 5th and 6th segments of the prothorax fused together. Only one other genus, *Bathynotellus*, shows a similar fusion of segments within the thorax, and in addition one of the segments involved is macropleural. However, it is believed that there is a different functional basis for the fusion in the two cases.

In the Emuellidae the fusion of the otherwise normal 5th segment to the 6th appears to be simply a device to increase the muscular control over the long macropleural spine, and so aid in support and stability. The apodemal slit of the 6th is very strongly de-

veloped, and the fusion of the 5th allows its abaxial extension onto the inter-furrow platform. It also allows the elongated apodemal slit to abut against the adaxial end of the 6th pleural furrow, so that ventrally it forms a large transverse apodeme buttressed by an accessory ridge. On the pleural field, the development of a horizontal flap between the anterior lateral corner of the 6th and the pleural spine of the 5th (*E. polymera*) appears to be a strengthening device.

In *Bathynotellus*, the thorax has 13 segments, but the posterior ones are fused into a unit which has 3 axial rings and a macropleural spine; the pygidium is large, and its articulation with the macropleural unit is similar to that between the macropleural unit and transitory pygidium of meraspid degree 6 of the Emuellidae. In order to understand the situation in *Bathynotellus*, it is necessary to consider the allied genus *Bathynotus*.

Bathynotus has a thorax of 13 segments, with the 11th macropleural, the posterior 2 with considerably reduced pleurae, and a large pygidium. The macropleural spine is directed posteriorly, and in combination with the pygidium reduces the space available for the development of the pleurae of the two segments between them. It has been suggested above that a similar space reduction has resulted in the development of an opisthothorax in the Emuellidae and Oleneliidae. However, the large pygidium in the Bathynotidae suggests that they were more advanced than the other two groups, and had stabilized the number of thoracic segments. The reduced segments thus cannot perhaps be homologized with a true opisthothorax, which is always associated with a small pygidium. It is evident that the problem was solved in a different way, by fusion of the two posterior segments to the macropleural 11th. Thus the 11th, 12th, and 13th segments in *Bathynotus* are homologous with the macropleural unit of *Bathynotellus*.

TAXONOMIC POSITION

The genera *Emuella* and *Balcoracania* possess a unique combination of cephalic and thoracic morphology that sets them apart from other groups of trilobites, and it is proposed that they should be placed in a separate taxon of familial rank, the Emuellidae.

The relation of the Emuellidae to other taxa can only be judged on morphological similarity. Some of the diagnostic characters of the family are found only in Cambrian trilobites, others occur in both Cambrian and post-Cambrian trilobites. However, when assessing the taxonomic position of the family, similarities in Cambrian and particularly Lower Cambrian trilobites are accorded most weight.

The combination of diagnostic characters of cephalon, thorax, and pygidium in the Emuellidae imposes certain conditions on the type of comparison which can validly be made. In particular, it is considered that the presence of a large pygidium largely invalidates comparisons based on the cephalon alone, and this is used as a premise for detailed comparisons of the cephala which follow.

The taxonomic position is assessed with regard both to features of adult morphology, and of ontogenetic development.

Comparisons of adult morphology

(*a*) *Thorax and pygidium.* The division of the thorax is known, apart from the Emuellidae, in some members of the Olenellidae. The occurrence and nature of the division in this family has already been discussed, but in general the genera are usually

characterized by a long prothorax (11–17 segments), and a short opisthothorax, the exception in the latter case being *Paedeumias robsonensis* (Burling), which has at least 29 opisthothoracic segments.

The occurrence of macropleurality has also been discussed. The presence of such segments in genera of so many obviously unrelated families casts grave doubts on the taxonomic value of this character, unless used in association with other thoracic features. In this context, the combination of macropleurality and thoracic division in some members of the Olenellidae is particularly important.

The Bathynotidae also show a combination of thoracic features similar to the Emuellidae, particularly *Bathynotellus*, in which fusion of segments is combined with macropleurality. However, it has been suggested above that the similarities are largely the result of convergence, and additionally the presence of a large pygidium in *Bathynotellus* precludes a close relationship.

(*b*) *Cephalon*. In the cephalon of the Emuellidae, the combination of sutural pattern, structure of the eye lobes, and of the posterior limb, constitute the essential diagnostic features; the glabellar shape is of lesser importance.

The sutural pattern consists of functional rostral, connective, hypostomal, and facial sutures. The cephalon is of the 'ptychopariid' type in the terminology of Rasetti (1952), and is considered to be the primitive type from which all others are secondarily derived (Harrington *in* Harrington *et al.* 1959, pp. 68, 158). Many taxa have members of this type, and those with Cambrian representatives include the Redlichiacea, Ellipsocephalacea, Paradoxididae, and Ptychopariidae.

The eye lobes consist of wide, essentially continuous eye ridges and palpebral lobes, extending in crescents from the frontal glabellar lobe, with the palpebral sections widely separated from the glabella. Genera of many families possess similar eye lobes, with the Cambrian groups Dolerolenidae, Ellipsocephalidae, Protolenidae, Bathynotidae and Ptychopariidae bearing the greatest resemblance.

The geniculate posterior limb of the Emuellidae appears to have no parallel in any other Cambrian family.

The glabella tapers forward to the anterior glabellar furrow, but has a variably expanded frontal glabellar lobe. The ontogeny of the members of the Emuellidae, together with the presence of variants with a bilobed frontal glabellar lobe, suggests that this shape may be due to the persistence of a larval characteristic into the adult. Thus the presence of an expanded frontal lobe in other genera does not necessarily mean a close relationship; conversely a regularly tapering glabella need not indicate a distant relationship.

The over-all morphology of the cephalon is most similar to some members of the Dolerolenidae, Protolenidae, and Ptychopariidae. Of these, the genera *Dolerolenus*, *Bergeroniellus*, and *Estaingia* of the so-called protolenoids, *Protolenus* of the undoubted Protolenidae, and members of the Antagminae, are probably the closest. In addition some of the Olenellidae are discussed, because of special similarities in the thorax to the Emuellidae.

Dolerolenus differs from the Emuellidae in the possession of an evenly tapering glabella, the faintness of the eye ridges, and the length of the posterior limb which is also transversely directed; the genal spine is also much shorter and not advanced.

Bergeroniellus and *Estaingia* resemble the group in the structure and position of the eye lobes, with the subgenera *B.* (*Bergeroniaspis*) and *B.* (*Olekmaspis*) being the closest. The glabella of *Estaingia* approaches the shape of that of *Balcoracania dailyi* in particular. The shape of the glabella of *Bergeroniellus* varies slightly, but is generally slightly tapering to the anterior. Both genera differ from the Emuellidae in the presence of wide preglabellar fields and transverse posterior limbs. *Protolenus* is similar to *Estaingia* except for a narrower preglabellar field and evenly tapering glabella, and so shares most of the above dissimilarities.

Of the Antagminae, *Eoptychoparia*, *Poulsenia*, and *Proliostracus* have a tapering glabella, and eye lobes similar to the Emuellidae. *Poulsenia*, in particular, has only a short preglabellar field, and the frontal lobe bears a similar relationship to the anterior border furrow, as does *B. dailyi*. The anterior sections of the facial sutures cut diagonally across the border, and vary from slightly divergent (*Eoptychoparia*), to rather strongly converging (*Poulsenia*). In all genera the posterior limb is in marked contrast to that of the Emuellidae.

In the Olenellidae the major differences are associated with the sutural pattern, the eye lobes and the posterior border.

(*c*) *Conclusions*. The strong similarities in the thorax of the Olenellidae and the Emuellidae suggest a close relationship, but the indications are that the latter are probably the more primitive group. The structure of the cephalon also suggests that the Olenellidae are the more advanced, as the 'olenellid' sutural pattern is now thought to have been secondarily derived from the 'ptychopariid' type, which is displayed by the Emuellidae (Hupé 1953*a*, Harrington *in* Harrington *et al.* 1959). Together these features suggest that an 'emuellid' stock may have given rise to the olenellid branch. This, however, does not settle the question of their placement within the existing taxonomic framework, for the very presence of the characters which suggest this relationship precludes the placement of the Emuellidae within the suborder Olenellina.

The other groups which show similarities to the Emuellidae belong to suborder Redlichiina (Dolerolenidae, Protolenidae), suborder Bathynotina (Bathynotidae), and suborder Ptychopariina (Antagminae). Of these, the Bathynotidae and the Antagminae exhibit the least similarities to the Emuellidae. Accordingly it is suggested that the family be placed in the suborder Redlichiina.

Within the suborder the position is not clear. The Dolerolenidae and the Protolenidae bear approximately the same degree of over-all similarity to the Emuellidae, but are placed in different superfamilies (Poulsen *in* Harrington *et al.* 1959), the Dolerolenidae in the Redlichiacea, and the Protolenidae in the Ellipsocephalacea. In addition the Dolerolenidae are thought to be transitional between the two superfamilies (Sdzuy 1959), and the protolenoids (*Bergeroniellus*, *Estaingia*) transitional between the Ellipsocephalacea and the Paradoxidacea (Öpik 1961, Pocock 1964).

Comparisons of developmental history

Whittington (1957, p. 462) stated that 'the nature of the developmental history and the morphology of the protaspis . . . offer additional criteria for judging relationships between families and larger groups'. The ontogenies of the Emuellidae are compared with those known from groups which, on the basis of holaspid morphology, appear

to be related: the Olenellidae, Redlichiidae, Dolerolenidae, Protolenidae, and Ptychopariidae.

Protaspides have not yet been recognized in the Olenellidae, but the meraspid development is broadly known from the investigations of Whittington (1957, 1959) and Palmer (1957). The ontogeny of *Redlichia chinensis* (Walcott) has been studied by Kobayashi and Kato (1951); at least one protaspis and several meraspides are described. The ontogeny of the Dolerolenidae is not well known but Kobayashi and Kato (1951, text-fig. 1) illustrated several protaspides of *Dolerolenus*, redrawn from Bornemann (1891). In the Protolenidae, Suvorova (1956) described larval stages of *Lermontovia* and *Bergeroniellus*; all specimens appear to be meraspid cranidia. Protaspides of *Strenuella*, a related protolenid, have been described by Kautsky (1945). Amongst the Ptychopariidae, the ontogeny of *Sao* is well known (Whittington 1957).

A comparison of the ontogenies of the families listed above with those of the Emuellidae, appears to affirm the degree of relationship deduced from the holaspid morphology, but fails to solve the problems which arise. Of the families considered, the protaspides and early meraspides (considered to be of greatest diagnostic value) of the Ptychopariidae are furthest from those of the Emuellidae. The remaining families are all members of the Order Redlichiida, and thus some similarity is to be expected.

In these families there is a similar reduction of the size of the frontal glabellar lobe, but to varying and generally greater degrees than in the Emuellidae, and a similar development of the anterior border and preglabellar field. The presence of a preglabellar field in the meraspides of all groups is not considered a major difference, as in the Emuellidae its initial development can be seen in *B. dailyi*. The most important remaining characters of the protaspides and early meraspides are the cheek furrows, bilobation of the frontal glabellar lobe, and the fixigenal spines. The Emuellidae have distinct cheek furrows, occasional bilobation, but lack fixigenal spines; the Redlichiidae have distinct furrows, definite bilobation, but also appear to ack spines; the Dolerolenidae, although very incompletely known, appear to possess only the cheek furrow; the Olenellidae have furrows and spines, but apparently lack the bilobation; the Protolenidae lack cheek furrows, but are bilobed, and some, but not all, species have fixigenal spines. It is thus apparent that all families bear some relationship to each other, but the degree of relationship is difficult to determine.

It is accordingly considered that the placement of the Emuellidae in the suborder Redlichiina is reasonably based, but its superfamilial position is best left open for the present.

EVOLUTION

Intrafamilial relationships. On the basis of adult morphology, *E. dalgarnoi* is intermediate between *E. polymera* and the species of *Balcoracania*; the morphology of the palpebral lobe, the posterior limb and the facial sutures, all lie between the limits for these structures in the other species. However, with so few species and incomplete stratigraphic information, further speculation is unwise.

Evolutionary position of the Emuellidae. In the possession of a ptychopariid sutural pattern, thick long eye lobes, expanded frontal glabellar lobe, long thorax combining

macropleurality and division, and a diminutive pygidium, the Emuellidae appear to be very primitive, and must be placed near the origin of redlichiid evolution.

It has been suggested that the Olenellina have evolved from a redlichiid-like trilobite with a ptychopariid sutural pattern (Hupé 1953*a*, Harrington *in* Harrington *et al.* 1959). The Emuellidae possess such a cephalon, and combine with it thoracic features which are shared only with some of the Olenellina, i.e. long, multisegmented thorax, division into pro- and opisthothorax, and macropleurality. Although the known members of the Emuellidae occur far too high in the Cambrian to be direct ancestors, they exhibit all the features which might be expected of such an ancestor. Thus, the Olenellina may have evolved from an 'emuellid'-type ancestor by migration and eventual loss of the facial sutures, and by reduction of the opisthothorax. Other members of the Redlichiida may have evolved from a similar ancestral stock by loss of the opisthothorax, retention of the basic sutural pattern, reduction of the frontal glabellar lobe, and development of the preglabellar field. The loss of the opisthothorax is foreshadowed in some of the Olenellina, and the development of the preglabellar field in *B. dailyi*. It is interesting to note that the changes taking place in the early meraspid stages of members of the Redlichiina are strikingly similar to the complete ontogeny of the Emuellidae.

Acknowledgements. I am indebted to Professor M. F. Glaessner (University of Adelaide) for supervising the work and critically reading the manuscript; Professor H. B. Whittington (Sedgwick Museum, Cambridge) and Professor A. R. Palmer (State University of New York, Stonybrook) for advice throughout this study and reading sections of the manuscript; and Dr. M. Wade and Dr. B. McGowran (University of Adelaide) for general discussions of the subject.

Dr. B. Daily (University of Adelaide) kindly lent material from his own collections; and Mr. T. A. Barnes (Director, South Australian Department of Mines) authorized the release to the University of material in his department.

This research work formed part of a thesis submitted for a Ph.D. degree, University of Adelaide. The Department of Geology, University of Malaya, assisted in the preparation of the manuscript.

APPENDIX

Measurements of selected dimensions of adult specimens of the Emuellidae. All measurements are given as micrometer divisions where 1·00 mm. = 12 divisions.

1. *Emuella polymera*

A_1	C	D_5	A_1	C	D_5
16	2	6	45	10	13
22	5	7	46	10	15
26	6	8	46	10	16
26	5	8	47	10	15
30	6	10	47	8	14
31	7	11	51	10	20
32	7	11	52	11	16
34	7	13	55	12	20
35	6	12	58	10	20
37	8	10	60	13	20
37	8	12	60	11	20
38	7	15	73	15	23
39	7	13	75	14	25
40	8	14	82	14	26
40	8	13	86	18	28
43	8	14	88	16	30
43	9	14			

2. *Emuella dalgarnoi*

A_1	C	D_5	A_1	C	D_5
34	8	10	51	13	16
35	7	9	66	16	21
35	8	10	70	18	20
44	12	15	76	18	24
45	11	14	106	22	38
48	12	16			

3. *Balcoracania flindersi*

A_1	C	D_5	A_1	C	D_5
23	5	5	58	16	14
25	6	6	60	14	19
31	8	10	60	15	15
32	8	8	60	14	14
33	8	9	60	14	19
33	8	12	60	14	13
40	10	9	70	18	19
44	10	13	72	14	14
48	12	14	72	20	18
48	14	13	74	16	22
50	11	12	76	18	26
50	12	16	76	16	20
54	14	13	78	18	17
56	16	14	80	16	26
56	14	9	84	20	24
56	12	14			

4. *Balcoracania dailyi*

A_1	C	D_5	A_1	C	D_5
23	7	7	47	14	13
25	9	6	48	14	11
26	8	6	50	15	14
27	8	5	55	14	15
28	9	8	58	15	15
29	9	7	58	15	14
30	10	7	60	15	14
30	9	8	60	18	16
30	10	6	64	17	17
31	8	8	67	20	16
33	9	9	68	19	21
34	10	8	70	20	20
35	10	8	70	20	20
42	12	12	72	20	18
44	13	12	76	20	18
44	14	10	78	24	16
45	13	11	78	22	17
			78	25	20

REFERENCES

BORNEMANN, J. G. 1891. Die Versteinerungen des cambrischen Schichtensystems der Insel Sardinien, Abt. 2. *Nova Acta Acad. Leop. Carol.* **56,** 427–528, pl. 19–28.

BRONGERSMA-SANDERS, M. 1957. Mass mortality in the sea, *in Treatise on marine ecology and paleoecology*, ed. HEDGPETH, J. W., Mem. Geol. Soc. Am. **67**.

CRAIG, G. Y. and OERTEL, G. 1966. Deterministic models of living and fossil populations of animals. *Q. Jl geol. Soc. Lond.* **122,** 315–55.

DAILY, B. 1956. The Cambrian in South Australia; *in* El sistema Cambrico, su palaeogeografi yel problema su base. *20th Int. geol. Congr., Mexico*, **2,** 91–147.

HARRINGTON, H. J. *et al.*, 1959. *In* MOORE, R. C., ed., *Treatise on invertebrate paleontology*, Part O, *Arthropoda 1.* Geol. Soc. Am. and Univ. Kansas Press.

HUPÉ, P. 1950. Á propos des segments macro-pleuraux des trilobites. *Bull. Soc. géol. Fr.*, ser. 5, **20,** 191–3.

—— 1953*a*. Contribution à l'étude du Cambrien inférieur et du Précambrian III de l'Anti-Atlas marocain. *Notes Mém. Serv. géol. Maroc*, **103,** 402 pp., 24 pl.

—— 1953*b*. Classification des trilobites. *Annls Paléont.* (Paris), **39,** 62–168 (1–110).

—— 1953*c*. Classe des Trilobites, *in* PIVETEAU, J., *Traité de Paléontologie*, Masson (Paris), **3,** 44–246.

—— 1955. Classification des trilobites. *Annals Paléont.* (Paris), **39,** 91–325 (111–345).

KAUTSKY, F. 1945. Die Unterkambrische Fauna ven Aistfakk in Lappland. *Geol. För. Stockh. Förh.* **67** (441), 129–211.

KOBAYASHI, T. and KATO, F. 1951. On the ontogeny of *Redlichia chinensis*, with description of *Alutella nakmurai* new gen. and sp. *J. Fac. Sci. Tokyo Univ.*, ser. 2, **9,** 355–493, pl. 1–9.

MANTON, S. A. 1952. The evolution of arthropodan locomotory mechanisms. Part 2, General introduction to the locomotory mechanisms of the arthropods. *J. Linn. Soc.* (*Zool.*), **42,** 93–117.

—— 1960. Concerning head development in arthropods. *Biol. Rev.* **35,** 265–82.

—— 1964. Mandibular mechanisms and the evolution of arthropods. *Phil. Trans. R. Soc.*, ser. B, **247,** 1–183, pl. 1.

ÖPIK, A. A. 1961. The geology and palaeontology of the headwaters of the Burke River, Queensland. *Bull. Bur. Miner. Resour. Geol. Geophys. Aust.* **53**.

PALMER, A. R. 1957. Ontogenetic development of two olenellid trilobites. *J. Paleont.* **31,** 105–28, pl. 19.

POCOCK, K. J. 1964. *Estaingia*, a new trilobite genus from the Lower Cambrian of South Australia. *Palaeontology*, 7, 458–71, pl. 75, 76.

RASETTI, F. 1952. Ventral cephalic sutures in Cambrian trilobites. *Am. J. Sci.* **250,** 865–98.

RAW, F. 1953. The external morphology of trilobites. *J. Paleont.* **27,** 82–129.

RAYMOND, P. E. 1920. The appendages, anatomy and relationships of trilobites. *Mem. Conn. Acad. Arts Sci.* 7, 169 pp.

RŮŽIČKRA, R. 1943. Příspěvek k ontogenii děských Paradoxidu a rodu *Sao*. *Vest. Král. české spol. Nauk, tř. Math.-Přír.* 1–142, pl. 1–5.

SDZUY, K. 1959. Dir unterkambrische Trilobiten-Familie Dolerolenidae. *Senckenberg. leth.* **40,** 389–407.

SHAW, A. B. 1956. Quantitative trilobite studies. I, The statistical description of trilobites. *J. Paleont.* **30,** 1209–24.

—— 1957. Quantitative trilobite studies. II, Measurement of the dorsal shield of non agnostidean trilobites. Ibid. **31,** 193–207.

SHAW, F. C. and ORMISTON, A. 1964. The eye socle of trilobites. Ibid. **38,** 1001–2.

SIMPSON, G. G., ROE, A., and LEWONTIN, R. C. 1960. *Quantitative zoology*. New York.

STØRMER, L. 1941 (1942) Studies in trilobite morphology. II, The larval development, the segmentation and sutures, and their bearing on trilobite classification. *Norsk geol. Tidskr.* **21,** 49–164, 2 pl.

SUVOROVA, N. P. 1956. Cambrian trilobites from the eastern Siberian Platform, Part 1. Protolenidae. *Trudÿ paleont. Inst. Akad. Nauk S.S.S.R*, **63,** 1–158, 12 pl. [in Russian].

WALTER, M. R. 1967. Archaeocyatha and the biostratigraphy of the Lower Cambrian Hawker Group, South Australia. *J. geol. Soc. Aust.* **14,** 139–52, pl. 7, 8.

WESTERGARD, A. H. 1936. *Paradoxides oelandicus* beds of Oland. *Sver. geol. Unders. Afh.*, (6) **394**, 1–66, pl. 1–12.

WHITTINGTON, H. B. 1957. The ontogeny of trilobites. *Biol. Rev.* **32**, 421–69.

—— 1959. *In* MOORE, R. C., ed., *Treatise on invertebrate paleontology*, Part O, *Arthropoda I*. Geol. Soc. Am. and Univ. Kansas Press.

K. J. POCOCK
Department of Geology
University of Malaya
Kuala Lumpur
Malaya

Typescript received 23 January 1970

THE EVOLUTION OF THE HETEROMYARIAN CONDITION IN THE DREISSENACEA (BIVALVIA)

by BRIAN MORTON

ABSTRACT. Inspection of the valves of living members of the Corbiculacea and Dreissenacea and fossil Dreissenacea in the collections of the British Museum (Natural History) has revealed that the evolution of the heteromyarian form in present-day Dreissenacea in all probability arose from an established isomyarian corbiculid stock.

Descriptions of the taxa examined are given, and the stages in the evolution of the Dreissenacea discussed.

Dreissena polymorpha Pallas was first encountered in the River Volga and the Black Sea in 1754 by Pallas, who being struck by the superficial similarity of the animal to members of the Mytilacea named it *Mytilus polymorphus*. In 1835 Van Beneden established that it differed fundamentally from true mytilids and suggested the generic name *Dreissena*. Gray (1840) was responsible for separating *Dreissena* even further from the mytilids by suggesting that it should be placed in a separate superfamily, the Dreissenacea.

Toureng (1894*a*, *b*) showed, on the basis of the structure of the central nervous system and blood vascular system that *Dreissena* was not related to *Mytilus*, whilst Atkins (1937) and Purchon (1960) respectively showed that on the basis of the structure of the ctenidia and stomach the Mytilacea and Dreissenacea are unrelated. Yonge and Campbell (1968) showed that *Dreissena* is very different from the mytilid *Septifer* which has, like *Dreissena*, its anterior adductor muscles inserted on a shell shelf situated near the umbo. It is now generally considered that the similarities which exist between *Dreissena* and the Mytilacea are the result of convergent evolution of the heteromyarian condition in the two groups.

The possession by *Dreissena* of so many anatomical features that are typically 'eulamellibranch' (Morton 1969*a*) suggests that the close relatives of *Dreissena* should not be sought amongst the 'filibranch' bivalve phylogenies but amongst other eulamellibranchs. Taylor *et al.* (1970) have shown that on the basis of the microstructure of the shell, *Dreissena* is most like members of the Corbiculacea. This observation supports the grouping by Newell (1965) of the Dreissenacea with, amongst others, the Corbiculacea in the suborder Articina.

Fossil Dreissenacea in the collections of the British Museum (Natural History) and present day Dreissenacea and Corbiculacea were studied to discover if there is any evidence for the hypothesis of a common ancestry between the isomyarian Corbiculacea and the anisomyarian Dreissenacea. The methods of classification of the Bivalvia (Newell 1965) and of the Dreissenacea adopted by Keen (1969) are used in this paper.

To facilitate discussion of the evolutionary history of the Dreissenacea, short descriptions and simple figures of the left valves of some of the taxa examined follows.

[Palaeontology, Vol. 13, Part 4, 1970, pp. 563–72.]

DESCRIPTION OF SHELLS

Superfamily DREISSENACEA Gray *in* Turton 1840
Family DREISSENIDAE Gray *in* Turton 1840 (ICZN No. 76)

Genus DREISSENA Beneden 1835 (ICZN No. 872)

Subgenus *Dreissena* s.s.
Dreissena (*Dreissena*) *polymorpha* (Pallas)

Text-fig. 1

Material. A large collection of recent specimens from reservoir No. 2, Walthamstow, London.

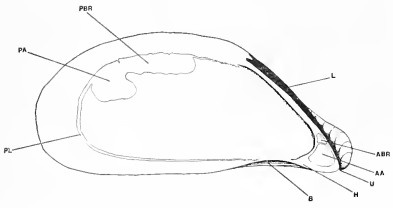

TEXT-FIG. 1. *Dreissena polymorpha*. Interior view of left valve. (For key to lettering see p. 571.)

Description. Shell solid, slightly inequivalve; inequilateral, beaks in anterior half; subtriangular, elongated and swollen; flattened ventrally, with byssal notch anteriorly. Specimens up to 5·0 cm. in length. No internal nacreous layer, ligament internal, extending along dorsal line less than ½ distance of posterior margin. Hinge plate without teeth. Anterior adductor and anterior byssal retractor muscles located on hinge plate, adjoined to each other. Anterior adductor smaller than posterior; pallial line not indented by sinus. Margin smooth; growth rings well defined; colour yellowish or brown, marked with zigzag alternating bands of brown and yellow.

Mode of life. Byssally attached, epifaunal, in shallow fresh and estuarine waters.

Range. Eocene—Recent. Old World.

Subgenus *Dreissenomya* Fuchs 1870
Dreissena (*Dreissenomya*) *aperta* (Deshayes) 1836

Text-fig. 2

Material. One specimen from the Upper Tertiary, Pontian (Bosphorian) of the Stoichitza valley, Cocorova-Mehedintzi, Rumania. BMNH LL 18451.

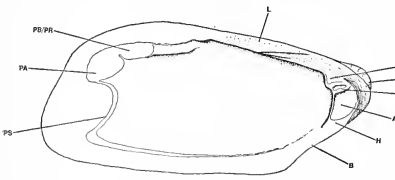

TEXT-FIG. 2. *Dreissena* (*Dreissenomya*) *aperta*. Interior view of left valve. (For key to lettering see p. 571.)

Description. Shell solid, equivalve; inequilateral, beaks in anterior half; tending to be rectangular or broadly oval with posterior margins rounded, enlarged and gaping. Well-defined byssal notch anteriorly; specimen 2·5 cm. in length. No internal nacreous layer to shell. Ligament internal, extending along dorsal line ½ distance of posterior margin. Hinge plate with two rudimentary cardinal teeth. Anterior adductor and anterior byssal and/or anterior pedal retractor muscle scars located on hinge plate on each side of and closely adjoined to cardinal teeth. Anterior and posterior adductor muscle scars of approximately equal size; pallial line with well-defined sinus. Margin smooth.

Inferred mode of life. Bysally attached, infaunal, siphonate, apparently associated with such non-marine forms as *Theodoxus* and the aberrant non-marine Cardiacea. In fresh and estuarine waters.

Range. Miocene–Pliocene. Old World.

Genus CONGERIA Partsch 1885

Congeria subglobosa Partsch

Text-fig. 3

Material. One specimen from the Miocene of Nussdorf, near Vienna. BMNH L22134.

Description. Shell solid, equivalve; inequilateral, beaks in front of mid-line directed forwards; angular, nearly square in outline. Specimen 8·5 cm. long; no internal nacreous layer to shell. Ligament internal, extending along dorsal line almost $\frac{1}{2}$ length of posterior margin. Growth-lines distinct, well-defined byssal notch. Hinge plate with single poorly developed cardinal tooth, covered in life by anterior adductor muscle. Anterior byssal and/or anterior pedal retractor muscle scar also located on hinge plate, posterior to anterior adductor muscle scar. Anterior adductor muscle scar smaller than posterior. Pallial line not indented by sinus. Margin smooth.

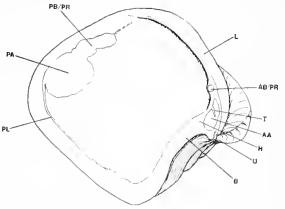

TEXT-FIG. 3. *Congeria subglobosa.* Interior view of left valve. (For key to lettering see p. 571.)

Inferred mode of life. Bysally attached, infaunal, in fresh and estuarine waters.

Range. Oligocene–Pliocene. Old World.

Congeria zsigmondyi Halad

Text-fig. 4

Material. Eleven specimens from the Miocene of Sangenfeld, Temes, Hungary. BMNH L71758–68.

Description. Shell solid, equivalve; inequilateral, beaks in anterior half; angular, rhomboidal in outline. Specimen 2·5 cm. in length; no internal nacreous layer to shell. Ligament internal extending along dorsal line $\frac{1}{2}$ distance of posterior margin. Byssal notch anteriorly. Hinge plate without teeth. Anterior adductor and anterior byssal and/or pedal retractor muscles located on hinge plate, latter posterior to anterior adductor and having its insertion on 'hinge lobe' projecting down from hinge plate. Anterior adductor muscle scar smaller than posterior. Pallial line not indented by sinus. Margin smooth.

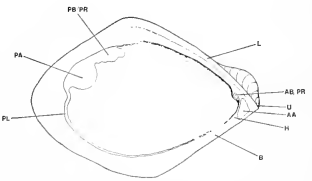

TEXT-FIG. 4. *Congeria zsigmondyi.* Interior view of left valve. (For key to lettering see p. 571.)

Inferred mode of life. Byssally attached, infaunal, in fresh and estuarine waters.

Range. Oligocene–Pliocene. Old World.

Congeria subcarinata botenica Andrusov

Text-fig. 5

Material. A single specimen from the Miocene of the Pricăles valley, Susitza-Mehedintzi, Rumania. BMNH, unregistered.

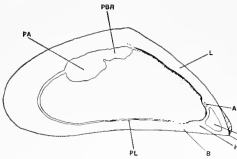

TEXT-FIG. 5. *Congeria subcarinata botenica*. Interior view of left valve. (For key to lettering see p. 571.)

Description. Shell solid, equivalve; inequilateral, beaks in anterior half; approximately triangular in outline, flattened ventrally and with anterior byssal notch. Specimen 5·5 cm. in length. No internal nacreous layer to shell. Ligament internal, extending along dorsal line almost $\frac{1}{2}$ distance of posterior margin. Hinge plate without teeth. Anterior adductor and anterior byssal and/or pedal retractor muscles located on hinge plate, latter posterior to anterior adductor. Anterior adductor muscle scar smaller than posterior. Pallial line not indented by sinus. Margin smooth.

Inferred mode of life. Byssally attached, epifaunal, in fresh and estuarine waters.

Range. Oligocene–Pliocene. Old World.

Congeria triangularis Partsch

Text-fig. 6

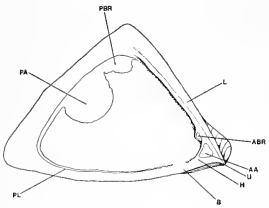

TEXT-FIG. 6. *Congeria triangularis*. Interior view of left valve. (For key to lettering see p. 571.)

Material. Four specimens from the Miocene, Pontian of Radmanest, Krasso, Hungary. BMNH L71686–9.

Description. Shell solid, equivalve; inequilateral, beaks in anterior half; sharply triangular in outline, flattened ventrally and with anterior byssal notch. Specimen 4·0 cm. in length. No internal nacreous layer to shell. Ligament internal, extending along dorsal line almost $\frac{1}{2}$ distance of posterior margin. Hinge plate without teeth. Anterior adductor and anterior byssal and/or pedal retractor muscles located on hinge plate, latter posterior to anterior adductor and having its insertion on 'hinge lobe' projecting down from hinge plate. Anterior adductor muscle scar much smaller than posterior. Pallial line not indented by sinus. Growth-lines distinct. Margin smooth.

Inferred mode of life. Byssally attached, epifaunal, in fresh and estuarine waters.

Range. Oligocene–Pliocene. Old World.

Genus MYTILOPSIS Conrad 1858

Mytilopsis sallei (Recluz)

Text-fig. 7

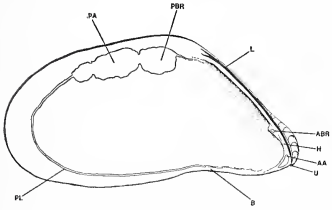

TEXT-FIG. 7. *Mytilopsis sallei*. Interior view of left valve. (For key to lettering see p. 571.)

Material. A large collection of recent specimens from Visakhapatnam harbour, India, where they seem to have recently been introduced from Central America.

Description. Shell brittle, equivalve; inequilateral, beaks in anterior half; subtriangular, elongated, not swollen; slightly flattened ventrally, convex dorsally. Well defined byssal notch anteriorly. Specimen 1·4 cm. in length. No internal nacreous layer to shell. Ligament internal, extending along dorsal line less than $\frac{1}{2}$ distance of posterior margin. Hinge plate without teeth. Anterior adductor and anterior byssal retractor muscles inserted on hinge plate, latter posterior to anterior adductor and having its insertion

on 'hinge lobe' projecting down from hinge plate. Anterior adductor muscle scar smaller than posterior. Pallial line not indented by sinus. Margin smooth.

Mode of life. Byssally attached, epifaunal, in shallow estuarine and sea waters.

Range. Upper Oligocene–Recent. Central America and India.

Other species in the genus *Mytilopsis* include:

Mytilopsis leucophaeta Conrad	Eastern North America.
Mytilopsis cochleata Kickx	Northern Europe.
Mytilopsis africanus Beneden	West Africa.

All the above mentioned species bear a very close resemblance to *M. sallei* and for this reason are not described or illustrated.

DISCUSSION

One of the most characteristic features of the shell of *Dreissena* (text-fig. 1) is the possession of a shell shelf upon which is inserted the anterior adductor muscle and the anterior byssal retractor muscle. Amongst other bivalves the same type of structure occurs in the Mytilid genus *Septifer*, although in this genus only the anterior adductor muscle has its insertion upon the shelf (Yonge and Campbell 1968). It has been suggested by Yonge and Campbell (1968) that the possession of this structure in these two stocks is the result of convergent evolution by adaptation to similar modes of life. It would seem that the forward extension of the umbones and the extremes of ventral (morphologically anterior) flattening in these two species has necessitated the evolutionary development of an anchorage, other than the valve itself, for the anterior adductor muscles. Yonge and Campbell pointed out that the possession of this shelf in these two genera not only permits the retention of the anterior adductors but enhances their function. They also suggested that the formation of the shell shelf in these two genera was achieved by a pushing forward of the mantle tissues in the region just within the area of insertion of the anterior adductors. This process (although perhaps only occurring in isolated instances in the Mytilacea, e.g. *Septifer*) is a feature of all fossil and living Dreissenacea. It is suggested that the shell shelf in the Dreissenacea has a deep evolutionary significance and is homologous to the hinge plate of other bivalves.

Taylor *et al.* (1970) showed that the detailed structure of the shell of *Dreissena polymorpha* most closely resembles that of certain corbiculids. Inspection of fossil Dreissenacea similarly suggests the possibility of a common ancestry for these two groups of bivalves.

Each valve of *Corbicula* possesses two adductor muscle scars of approximately equal size and two smaller pedal retractors. The shell is equilateral, with a small internal ligament, and three cardinal teeth lying on the hinge plate immediately below the umbo (text-fig. 8A). In another corbiculid, *Villorita cyprinoides*, the first signs of anterior flattening are seen, accompanied by extension of the ligament and posterior region of the shell. This has resulted in this species in the reduction of the anterior portion of the hinge plate and the movement of the anterior adductor and pedal retractor muscles towards the umbo. The extension of the dorsal (posterior) region of the shell has resulted in the greater development of the posterior adductor and pedal muscles, relative to the anterior muscles (text-fig. 8B).

Yonge (1962) showed that bivalves in many phylogenies have retained into adult life an essentially larval characteristic, the byssus, and that the neotenous retention of

this structure has, in many cases, influenced the form of the shell. The effect of the retention of the byssus in forms essentially similar to present-day *Villorita* would have been to produce forms in which the processes of ventral flattening were extreme, necessitating not only a change in mode of life but also of function of some organ systems. The fossil record shows some Driessenacea in which these changes can be observed; and although these forms have become extinct, it is suggested that they may represent stages through which the ancestors of present-day Dreissenacea passed.

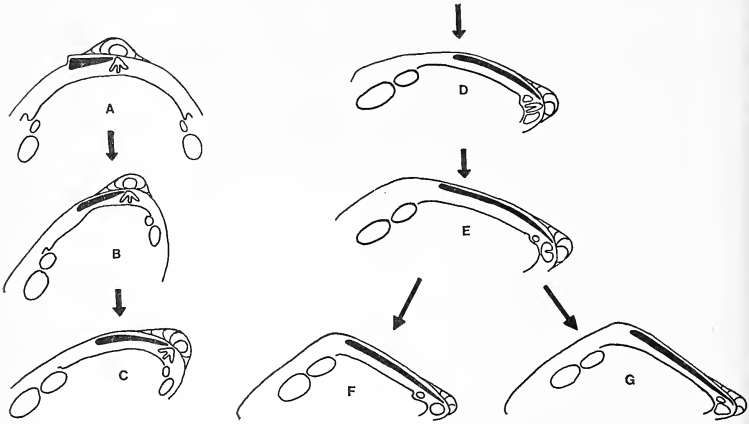

TEXT-FIG. 8. Diagram showing the possible course of evolution of the heteromyarian form in the Dreissenacea, from an isomyarian ancestor. A, *Corbicula*; B, *Villorita*; C, Hypothetical; D, *Dreissenomya*; E, *Congeria zsigmondyi*; F *Mytilopsis*; G, *Dreissena polymorpha*.

Dreissenomya aperta (text-figs. 2, 8D) possesses a rectangular-shaped shell, in which the anterior (ventral) margin has only a small degree of flattening, whereas the posterior (dorsal) margin is extended, with elongation of the ligament and enlargement of the posterior adductor and posterior byssal and/or pedal retractor muscles. In addition there is a well-defined pallial sinus, indicating that the animal had long siphons, and was therefore adapted to an infaunal mode of life. Anteriorly the presence of a byssal notch shows that the animal was attached to the substratum. The coexistence of a pallial sinus and byssal notch can perhaps be explained by the animal living attached to a solid substratum, but either partly or wholly buried by a surface covering of mud or silt. Yonge and Campbell (1968) noted that *Dreissena polymorpha*, although attached to stones by its byssus, is frequently found covered in mud and silt, alive and well. Situated on the hinge plate of *Dreissenomya* are the scars of the anterior muscular system, the anterior adductor muscle lying over and below (anterior to) the most anterior of the two cardinal teeth. Above (posterior to) the cardinal teeth is the muscle

scar that represents the site of insertion of the anterior byssal and/or pedal retractor muscles.

The neotenous retention of the byssus in the ancestors of the Dreissenacea and the Corbiculacea must also have had an accompanying effect upon the relative importance of the pedal retractor muscles. Whereas in the burrowing Corbiculacea pedal retractors were necessary for the movements of the foot associated with burrowing, in the essentially epifaunal Dreissenacea their importance is diminished as the foot has ceased to be an organ of locomotion [except for the first year of life (Morton 1969*c*)] and is now merely used as a tool for the planting of byssal threads. In order for the byssus to fulfil its function as an anchor to the animal, enlargement of the byssal retractor muscles has occurred. It seems possible that the retention of the byssus in the ancestors of the Dreissenacea also resulted in a change in importance of different areas of mesoderm, so that the emphasis was displaced from development of pedal retractors to development of byssal retractors. Yonge (1962) showed that a small byssal gland is present in certain members of the Sphaeriacea. Assuming that this gland possesses at least a presumptive muscle mesoderm, then it is no big step to accept the view that the retention of the byssus caused preferential development of byssal muscles instead of pedal muscles in the ancestors of the Dreissenacea.

Congeria subglobosa shows another facet of the development of the heteromyarian form in the Dreissenacea. The shell is almost square in outline, and extremely solid. It seems unlikely that this bivalve could lead an epifaunal mode of life, since, although possessing a byssus, movement of water would put a great strain upon the byssal apparatus. The animal was probably attached to stones, but was covered by mud or silt. The anterior adductor muscle scar (text-fig. 3) surrounds a vestigial cardinal tooth, whilst the muscle scar of the anterior byssal and/or pedal retractor muscle is situated slightly further posteriorly than in *Dreissenomya*. Ventral flattening of an animal similar to *C. subglobosa* would result in the hypothetical creation of a form very similar to the living Dreissenacea. Perhaps representing a stage in the development of this form is *C. zsigmondyi*, in which the ventral margin of the shell is very much flatter (text-fig. 4), although the animal was in all probability a burrower. The anterior adductor muscle scar occupies the now familiar position underneath the umbo, whilst the anterior byssal and/or pedal retractor muscle scar is situated on a 'hinge lobe' projecting down from the hinge plate. Apart from the lack of ventral flattening this animal is very similar to *Mytilopsis* (text-fig. 7). Ventral flattening has been accomplished in *Congeria triangularis* (text-fig. 6) resulting in a form very similar to *Mytilopsis*.

Congeria subcarinata botenica (text-fig. 5), however, although flattened ventrally, is slightly different from *C. zsigmondyi* and *C. triangularis* in that the muscle scar of the anterior byssal retractor is not situated on a 'hinge lobe' but on the hinge plate itself near the anterior adductor muscle scar, a situation very similar to that in *Dreissena polymorpha* (text-fig. 1). It would seem that in the Dreissenacea, the positioning of the insertion of the anterior byssal retractor muscle has proceeded in two separate ways. Text-fig. 8 indicates a possible way in which the heteromyarian form could have evolved in the Dreissenacea. From a corbiculid type, e.g. *Corbicula* (text-fig. 8A), the elongation of the posterior border of the shell (caused not by the retention of the byssus, but probably so as to give greater efficiency in feeding whilst burrowing) has resulted in a form characterized by *Villorita* (text-fig. 8B) in which the evolutionary modification

of the anterior adductor muscular system has begun. This condition is extended in a hypothetical stage (text-fig. 8C) in which the progressive elongation of the posterior border of the shell and reduction in the anterior border has brought the anterior muscles on to the hinge plate and nearer the umbo. The effect of the neotenous retention of the byssus upon such an animal would have enhanced the evolutionary changes already started in the Corbiculacea, and perhaps produce a whole range of animals all basically pre-adapted to the future development of an epifaunal mode of life. Most became extinct, and only a few species have survived to the present day.

Dreissenomya (text-fig. 8D) and *Congeria zsigmondyi* (text-fig 8E) are extinct forms that show the way in which the heteromyarian condition could have evolved in the Dreissenacea. The insertion of the anterior byssal retractor on the hinge plate itself in such fossils as *C. subglobosa* and *C. subcarinata botenica* and present-day *Dreissena polymorpha* (text-fig. 8G) probably marks an evolutionary divergence from such forms as *C. zsigmondyi*, *C. triangularis* and present-day species of *Mytilopsis* (text-fig. 8F), in which the insertion of this muscle has progressed even further posteriorly along the hinge plate, with the formation of a 'hinge lobe' specially for its insertion. This adaption undoubtedly improves the efficiency of action of the byssal retractor. It is significant in separating *Dreissena* from *Mytilopsis*.

The evolution of the heteromyarian condition in the Dreissenacea is presumed to have taken place under conditions that differed from those in which *Dreissena* now lives. Yonge and Campbell (1968) suggested that it probably occurred in the intertidal or shallow sublittoral regions in the sea and that subsequently acquired powers of osmoregulation allowed the animals to migrate up rivers into fresh waters. Morton (1969*a*) supported this view. It is envisaged that the marine ancestor of both the Corbiculacea and the Dreissenacea underwent adaptive radiation, producing a wide range of forms capable of surviving in a variety of habitats. The ancestors of the present day Veneracea and Glossacea remained in the sea, while the ancestors of the Corbiculacea and Dreissenacea invaded estuaries, and there underwent further radiation. During their period in the sea the ancestors of the Corbiculacea and Dreissenacea left some forms on the sea-shore, e.g. *Mytilopsis*, and in estuaries, e.g. *Dreissena* (Morton 1969*b*), *Corbicula japonica* (Fuji 1957), and *Villorita cyprinoides* (Dinamani 1957). *Dreissena* has, in some localities, also invaded fresh waters, where it is ideally adapted to the exploitation of rocky surfaces. *D. polymorpha* is probably as cosmopolitan in the fresh waters of the Old World as *Mytilus* is in the seas. The fossil infaunal Dreissenacea probably represent distant relatives of *Dreissena* and *Mytilopsis* which reflect the evolutionary trend in these two forms. The evolution of the Corbiculacea and Dreissenacea in many ways parallels the evolution within the Unionacea, both groups having given rise to burrowing forms, e.g. *Sphaerium* and *Anodonta*, and epifaunal forms, e.g. *Dreissena* and *Etheria*.

The heteromyarian condition in present day Dreissenacea is a direct consequence of the evolutionary trend described which, it is suggested, proceeded from an established eulamellibranch stock. Available evidence suggests that the ancestors of the modern corbiculids gave rise to forms which ultimately produced the species of *Mytilopsis*, and *Dreissena polymorpha*. The neotenous retention in these genera of primitive characters, e.g. the byssus and a free swimming veliger larva, has made them extremely successful in the exploitation of rocky surfaces of fresh and estuarine waters. The evolution of the

heteromyarian form in the Dreissenacea mirrors in many ways the evolution of the same form in the filibranch Mytilacea.

Summary. It is considered that the evolution of the heteromyarian form in the Dreissenacea, culminating in the evolution of such recent forms as *Dreissena polymorpha* and species of *Mytilopsis* has taken place comparatively recently and from established eulamellibranch stock.

The neotenous retention of the byssus in forms ancestral to the modern Corbiculacea has contributed the greatest influence to this process. The effect of this process upon the ancestral isomyarian parent stock has been:

1. The extension of the posterior border of the shell, and ligament.
2. Reduction of the anterior (ventral) border.
3. Passage of the anterior adductor muscle and anterior byssal and/or pedal retractor muscles on to the hinge plate, with a corresponding reduction in the development of the cardinal teeth.
4. The relatively greater development of the posterior adductor and posterior byssal and/or pedal retractor muscles.
5. An increase in importance of the byssal retractors compared with the pedal retractors.

Stages in this evolutionary transition from an isomyarian to a heteromyarian form can be seen in fossil Dreissenacea.

Acknowledgements. I am indebted to Drs. J. D. Taylor and N. J. Morris (British Museum (Natural History)), for advice in the preparation of this paper; Professor R. Turner (Harvard University) for supplying specimens of *Mytilopsis*, and Professor R. D. Purchon (Chelsea College of Science and Technology) for discussion on the evolution of the Dreissenacea. The work was supported by a research studentship at the Chelsea College of Science and Technology.

Key to lettering

AA	Anterior adductor muscle scar
AB/PR	Anterior byssal and/or pedal retractor muscle scar
ABR	Anterior byssal retractor muscle scar
B	Byssal notch
H	Hinge plate
L	Ligament
PA	Posterior adductor muscle scar
PB/PR	Posterior byssal and/or pedal retractor muscle scar
PBR	Posterior byssal retractor muscle scar
PL	Pallial line
PS	Pallial sinus
T	Cardinal tooth
U	Umbo

REFERENCES

ATKINS, D. 1937. On the ciliary mechanisms and interrelationships of Lamellibranchs. Part III: Types of lamellibranch gill and their food currents. *Q. Jl microsc. Sci.* **79**, 375–421.

DINAMANI, P. 1957. On the stomach and associated structures in the backwater clam, *Villorita cyprinoides* (Gray) var. *cochinensis* (Hanley). *Bull. cent. Res. Inst. Univ. Kerala*, **5**, 123–48.

FUJI, A. 1957. Growth and breeding season of the brackish-water bivalve, *Corbicula japonica*, in Zyusan-Gata Inlet. *Bull. Fac. Fish., Hokkaido Univ.* **8**, 178–84.

GRAY, J. E. 1840. *In* TURTON, W. *Manual of land and freshwater shells of the British islands*, 2nd ed., 277.

KEEN, M. 1969. *In* MOORE, R. C., ed., *Treatise on invertebrate paleontology*, Part. N, *Bivalvia*. Geol. Soc. Am. and Univ. Kansas Press.

MORTON, B. S. 1969*a*. Studies on the biology of *Dreissena polymorpha* Pall. 1, General anatomy and morphology. *Proc. malac. Soc. Lond.* **38**, 301–21.

—— 1969*b*. Ibid. 3, Population dynamics. Ibid. **38**, 471–82.

—— 1969*c*. Ibid. 4, Habits, habitats, distribution and control. *Water Treatment and Examination*, **18**, 233–40.

NEWELL, N. D. 1965. Classification of the Bivalvia. *Am. Mus. Novit.* No. 2206, 1–25.

PURCHON, R. D. 1960. The stomach in the Eulamellibranchia; stomach types IV and V. *Proc. zool. Soc. Lond.* **135**, 431–89.

TAYLOR, J. D., KENNEDY, W. J. and HALL, A. 1970. The shell structure and mineralogy of the Bivalvia. Part 2, Chamacea–Poromyacea, Conclusions. *Bull. Brit. Mus.* (*Nat. Hist.*). *Zool.* (in press).

TOURENG, M. 1894*a*. Sur le système nerveux du *Dreissensia polymorpha*. *C. r. hebd. Séanc., Acad. Sci., Paris*. **118**, 544.

—— 1894*b*. Sur l'appareil circulatoire du *Dreissensia polymorpha*. Ibid. **118**, 929–30.

YONGE, C. M. 1962. On the primitive significance of the byssus in the Bivalvia and its effects in evolution. *J. mar. biol. Ass. U.K.* **42**, 113–25.

—— and CAMPBELL, J. I. 1968. On the heteromyarian condition in the Bivalvia with special reference to *Dreissena polymorpha* and certain Mytilacea. *Trans. R. Soc. Edinb.* **68**, 21–43.

BRIAN MORTON
Department of Zoology
The University
Hong Kong

Revised typescript received 14 April 1970

A NEW TRINUCLEID TRILOBITE FROM THE UPPER ORDOVICIAN OF NEW SOUTH WALES

by K. S. W. CAMPBELL *and* GWENDA J. DURHAM

ABSTRACT. The new genus and species of trinucleid trilobite *Parkesolithus gradyi* described herein is the first member of the family to be described from Australia though there have been occasional records of occurrences. It is found in Upper Ordovician siltstones near Parkes, New South Wales.

IN 1967 Dr. A. E. Grady discovered numerous specimens of a trinucleid trilobite in poorly outcropping black siltstones on the property of Mr. S. K. Mill, 'New Durran', approximately 15 miles W. of Parkes, New South Wales (grid reference 598899 Forbes 1:250 000 Topographical Sheet). Parkes is situated approximately 170 miles WNW. of Sydney. Ordovician rocks have been suspected to occur in the area for more than half a century (Andrews 1910). Recently an extensive Late Ordovician fauna of brachiopods, trilobites, ostracods, and conodonts has been discovered in the vicinity of the trilobite locality (Packham 1967). These have been recovered from an unnamed limestone that lies an unknown distance stratigraphically below the trinucleid-bearing siltstone. Packham has suggested that the limestone fauna is of late Wilderness age in terms of the American sequence, or Gisbornian in terms of the Australian graptolite sequence.

Associated with the trinucleids are a few poorly preserved brachiopods and numerous specimens of the graptolites *Orthograptus truncatus socialis* (Lapworth), *O. truncatus intermedius* Elles and Wood and *Climacograptus* cf. *scharenbergi* Lapworth. These indicate an Eastonian (Caradocian) age which is consistent with Packham's determination of the age of the under-lying limestone.

No trinucleids have been described previously from Australia. There are, however, various records of the group, for example 'a cryptolithid close to *Eirelithus*' from probable Middle Ordovician siltstones in Tasmania (Banks 1962), 'fragmentary trinucleids' in the limestone mentioned above from Parkes (Packham 1967), and *Trinucleus* from the Upper Ordovician Cliefden Caves Limestone and Malongulli Formation of central New South Wales (Packham *et al.* 1969, pp. 80–1).

The text-figure and the plate are the work of Mrs. J. A. Davis and Mr. L. Seeuwen respectively.

SYSTEMATIC DESCRIPTION

Family TRINUCLEIDAE Hawle and Corda 1847
Subfamily CRYPTOLITHINAE Angelin 1854
Genus PARKESOLITHUS gen. nov.

Type species. Parkesolithus gradyi sp. nov. from an unnamed formation in the Upper Ordovician, west of Parkes, N.S.W.

Diagnosis. Cephalon similar in shape to that of *Cryptolithus*; small eye tubercles present just medial to the highest point of the cheek and opposite the anterior edge of furrow 2p;

[Palaeontology, Vol. 13, Part 4, 1970, pp. 573–80, pl. 111.]

glabella with furrow 1p formed of a double pit, and 2p and 3p almost imperceptible externally but forming distinct, strongly arcuate muscle areas internally; occipital ring sharply crested but not produced into a spine; glabella and cheeks unornamented; upper lamella with pit rows E_1, E_2, I_1, and I_4 (and usually I_2) continuous around the entire structure, and I_3 present laterally; regularity of pit rows lost on postero-lateral parts of fringe; a strong continuous list present between E_1 and E_2; lower lamella with very weak girder. Thorax with 6 segments. Pygidium subtriangular in outline; 8+ weak axial rings; 7+ pleural ribs weak but distinct; posterior border prominent and steep.

Remarks. We accept the subfamilial divisions of the Trinucleidae proposed by Whittington (1941) with the addition of the Hangchungolithinae of Lu. The shape of the glabella, the deep but small glabellar furrows 1p that are in close juxtaposition to the occipital furrow, the very weak furrows 2p, the virtual absence of the furrows 3p, the flat to gently concave dorsal fringe, and the absence of radial sulci on the fringe, all indicate that *Parkesolithus* is more closely related to the Cryptolithinae than any of the other subfamilies. Eye tubercles are not normal in members of this subfamily as it is at present constituted (Whittington *in* Moore 1959). We are not inclined to place much weight on this feature, however, since eye tubercles do occur in such genera as *Eirelithus* Lamont.

If, as most workers believe, the number of E rows of pits on the fringe is of fundamental taxonomic importance, *Parkesolithus* is closely related to *Broeggerolithus* Bancroft. However, there are considerable differences. The preglabellar fringe of *Broeggerolithus* has E_{1-2} and I_{1-2} complete; I_3 is introduced laterally and usually forms the innermost row, though I_4 is occasionally present inside it. In *Parkesolithus*, on the other hand, E_{1-2}, I_{1-2}, and I_4 are continuous in front of the glabella and I_3 is introduced between I_2 and I_4 antero-laterally (see discussion under the specific description for the identification of I_{3-4}). The two genera also differ in the following: the pronounced list between E_1 and E_2 on the upper lamella of *Parkesolithus* does not occur in *Broeggerolithus*; 2 p in *Parkesolithus* is deeper than in *Broeggerolithus*; the girder is much stronger in *Broeggerolithus*; the postero-lateral margin of the cephalon is turned back to form a large triangular genal angle in *Parkesolithus*, but is almost transverse in *Broeggerolithus*; the genal spines are directed obliquely outwards in *Broeggerolithus* but almost directly backwards in *Parkesolithus*. In our opinion these differences outweigh the similarity of the two E rows.

In the shape of the cephalon, glabella, genal spines, glabellar furrows, muscle scars, and pygidium *Parkesolithus* is closely comparable to *Cryptolithus*, but there are many differences in the fringe and girder structure. Typical species of *Cryptolithus* have a single E row, fewer complete I rows, new I rows introduced against the cheek rather than between existing rows, and a pronounced girder on the lower lamella. There are, however, species doubtfully assigned to *Cryptolithus* that have some features in common with *Parkesolithus*, the best known being *C.? bedinanensis* Dean (1967) from the Caradocian Bedinan Formation of Turkey. On the upper lamella of the fringe this species has a distinct list inside the outermost row of pits, and many specimens have four continuous rows of pits in front of glabella whereas most species of *Cryptolithus s.s.* have three. *Parkesolithus* has five. Furthermore, the insertion of new rows takes place antero-laterally between existing rows rather than against the cheek (Dean, pl. 4, figs.

4, 5, 6, 8). However, examination of the material convinces us that Dean was correct in interpreting the position of the girder as inside the outermost row of pits as is normal for *Cryptolithus*. His plate 3, fig. 7 tends to emphasize unduly the pseudogirders inside the girder proper. We are not inclined, therefore, to place *C.? bedinanensis* in *Parkesolithus* despite the above-mentioned similarities.

Parkesolithus gradyi sp. nov.

Plate III, figs. 1–15

Material. Holotype 21293; paratypes 21288–9, 21295a–b, 21301, 21304, 21306, 21308–10, 21315a–b, 21318a–b, 21321a–b, 21327a–c, 21328, 21331–4, 21337a–b. Geology Department, Australian National University Collection.

Description

Cephalon. Outline semicircular, approximately twice as wide as long (sag.); no accurate estimate of height available because of distortion; lateral margins at genal angle parallel and extend into genal spines which are faintly convex outwards and extend almost straight backwards; genal spines posterior to fringe approximately equal to median length of cephalon, unornamented and almost square in cross-section with a faint furrow along the ventral surface and an even fainter one along the dorsal surface; precise termination of spine not observed but spine tapers very gradually over its anterior three quarters and then more rapidly.

Ratio of length to width of glabella is approximately 3:2 (variation cannot be determined owing to crushing); outline expands slightly to 1p and then more rapidly, giving a mildly pyriform outline; greatest width and height located about two-thirds of the length of the glabella from the occipital furrow; anterior margin gently rounded and only slightly deflecting the continuous rows of pits on the fringe.

Occipital ring narrow and convex in posterior profile, sharply crested on the posterior half in sagittal profile; no occipital spine; axial furrow broad and shallow, deepening laterally into small occipital pits which are located inside the axial furrow; occiput considerably lower than the anterior portion of the glabella and about one-tenth of the length of the glabella. Glabellar furrow 1p of two pits lying in the same shallow depression on the lateral slope of the glabella; the more posterior pit moderately deep and circular medially but with a shallow antero-lateral extension, and situated immediately in front of the tiny occipital pit; the more anterior one is two or three times larger, shallower and oval in outline with the long axis directed antero-medially well up on the flanks of the glabella, the deeper posterior portion almost in contact with the posterior depression. 2p situated on the lateral slope of the glabella directly anterior to the oval depression of 1p, scarcely visible externally, but internally forming a shallow horseshoe-shaped ridge open posteriorly, the posterior extremities being slightly more prominent than the remainder. 3p a very faint comma-shaped depression on the slope of the glabella slightly more than midway along its length, the deeper part of the depression being higher on the slope of the glabella and the long axis pointing medially. All three pairs of depressions lie inside the axial furrow.

Axial furrows parallel, broad, shallow, and straight except for a slight curvature at the widest point of the glabella; anterior pits small and separated from the fringe by a low ridge. No ornament on the glabella and no median tubercle.

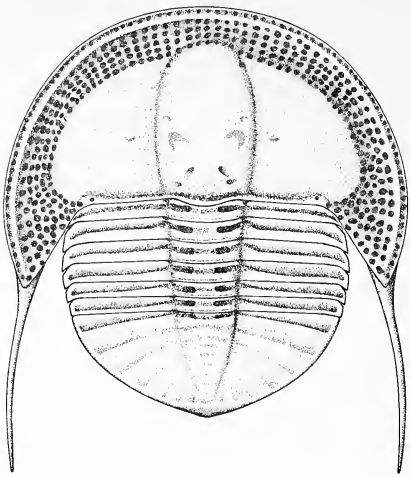

TEXT-FIG. 1. Reconstruction of *Parkesolithus gradyi* gen. et sp. nov.

Cheeks slightly convex with the highest point near the postero-lateral corner; cheeks distinctly lower than the glabella and slope away gently medially to the axial furrow and more steeply to the fringe; posterior border furrow moderately deep; a shallow extension of the posterior border furrow present a short distance along the posterior border beyond the fulcrum; most specimens with a tiny pit (separate from the fringe pits but probably one of them) in the triangular space between the posterior border, the posterior border furrow and the inner edge of the fringe (see Pl. 111, figs. 14–15).

EXPLANATION OF PLATE 111

Parkesolithus gradyi gen. et sp. nov.

Fig. 1. Latex cast of the first two thoracic segments; ×2; 21304 ANU.
Fig. 2. Latex cast of ventral surface showing the pleural tips and the broken apodemes; ×1·4; 21318a ANU.
Figs. 3 and 4. Latex cast of ventral surface showing complete apodemes; ×2 and ×4; 21301 ANU.
Fig. 5. Latex cast of dorsal surface; ×2; 21308 ANU.
Fig. 6. Latex cast of exterior of pygidium; ×3·5; 21332 ANU.
Figs. 7 and 8. Latex casts of dorsal surfaces of two cephala; 7 is a juvenile holaspid; ×5 and ×1·4; 21310 and 21334 ANU.
Fig. 9. Latex cast of dorsal surface cephalon; ×2; 21327a ANU.
Fig. 10. Mould of internal surface of thorax, pygidium and lower lamella; ×1·5; 21315a ANU.
Fig. 11. Latex cast of dorsal surface of thorax and pygidium, and ventral surface of lower lamella; ×1·5; 21315b ANU.
Fig. 12. Latex cast of dorsal surface of pygidium; ×1·9; 21289b ANU.
Fig. 13. Latex cast of ventral surface of cephalon showing lower lamella; ×1·6; 21309 ANU.
Figs. 14 and 15. Internal moulds of two cephala; ×1·5, ×2; 21295a and 21293 ANU.


1


3

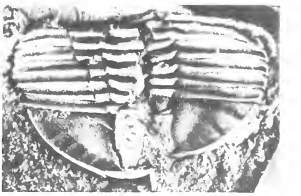
5


2


4


6


7

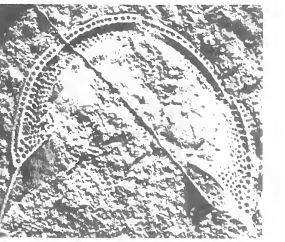
8

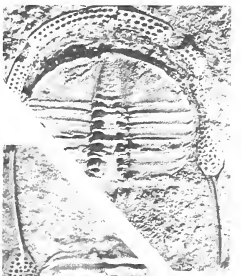
10

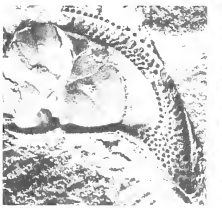
9

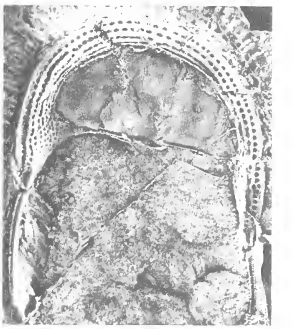
13


12

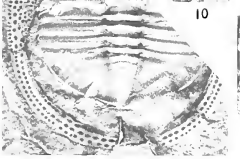
11

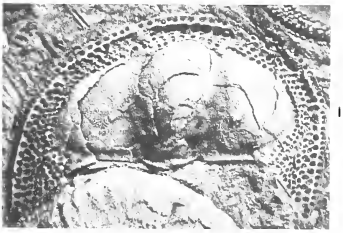
14

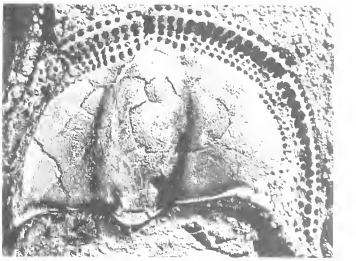
15

CAMPBELL and DURHAM, *Parkesolithus gradyi* gen. et sp. nov.

Pair of small circular eye tubercles opposite the anterior edge of furrow 2p, on the inner slope of the cheeks *c.* one-quarter of the distance from the axial furrow to the fringe; no ornamentation on cheeks but extremely faint eye ridges extend from the eye tubercles anteromedially to the axial furrow opposite the 3p muscle scar on some specimens.

Posterior border short, highest along the sharp posterior edge and sloping gently forwards into the symmetrical posterior border furrow; border longer (exsag.) behind the first few pits on the fringe and then gradually fades away laterally; posterior border of fringe almost straight and inclined at an angle of 45° to posterior border of cheeks; articulatory furrow along posterior border very shallow, if present at all. Doublure on the occipital ring very short and with a slightly thickened edge.

Upper lamella of fringe. Anteriorly and antero-laterally fringe slopes gently down for half its width then turns up slightly, resulting in a gently concave fringe with the inner and outer margins being on the same level. Laterally and postero-laterally fringe less concave, especially its inner part which actually becomes convex and very steep near the posterior border, and is on a much higher level than the still slightly concave outer part; a prominent concentric ridge developed inside E_1 around the entire circumference except in the most posterior part of the genal angle where it fades out abruptly; fringe narrowest in front of the glabella; on all specimens E_1, E_2, I_1, and I_4 complete in front of glabella; on most specimens I_2 also complete; I_3 never complete and most anterior pits of this row inserted near the line of the axial furrow, i.e. about R_{4-7}; I_4 bent distinctly forwards in front of the glabella on all specimens, but I_2 only slightly distorted if at all. Anteriorly and antero-laterally pits radially arranged; three or four innermost rows usually arranged radially as far back as a line joining the eyes; in this region radial arrangement of pits sometimes gives a false impression of weak sulci; anterior radial rows straight, antero-lateral ones slightly arcuate. Laterally and postero-laterally, pits mostly irregularly arranged with many additional ones inserted. Normally ten pits present along the posterior border of the fringe. All pits approximately the same size but outermost row and innermost row smaller on some specimens.

Pit count (half-fringe)

Row	*No. of pits*	*Mean*	*No. of specimens*
E_2 (outermost row)	38–44	42	9
E_1 (first row inside ridge)	30–6	32	7
I_1—I_2	30–6	31	7

Other rows too irregular to count.

Lower lamella of fringe. Girder at very weak angulation, only slightly stronger than the weak pseudogirders on either side; girder continued down along genal spine as the inner ventral carina on some specimens (Pl. 111, fig. 13) but not on others (Pl. 111, fig. 11); outer ventral carina of the spine is a continuation of the outer fringe margin; no sign of any prominent ridge or furrow between E_1 and E_2 corresponding to the ridge on the upper lamella.

Thorax. Six segments in the thorax; axis tapers slightly towards the pygidium; axial furrow shallow, deeper at the back than the front of each segment giving a regular

notched appearance; axial ring short (sag. and exsag.), axially one-third of the total length of the segment; ring rises steeply from the articulating furrow to a crest, immediately behind which is a shallow furrow that extends the full width of the ring.

Deep transverse slit-like apodemal pits set well in from the axial furrow with a slight depression on their outer and a much deeper one on their inner margin; apodemes set about mid-length on the segment; articulating furrow symmetrical with a uniform slope anterior and posterior and a well-rounded base; articulating half-ring on all segments short, on the anterior segment its anterior margin being almost transverse but on subsequent segments gently convex forwards; articulatory processes relatively short.

Pleurae of third and fourth segments *c.* 1·75 times as wide as the axis; anterior and posterior pairs slightly shorter than the middle pair; anterior pleurae shorter so as to fit against the posterior border of the cheeks and fringe of the cephalon. Anterior edges of the first pleural segment on opposite sides of fulcrum set at an angle of 45°; posterior edge also bends slightly posteriorly at fulcrum; pleural tip moderately sharp. On more posterior segments angulation of pleural tip progressively less pronounced; last segment with a blunt almost square pleural tip, a virtually straight posterior edge and an anterior edge with only a slight angulation close to the pleural tip. Fulcrum moves progressively outwards on more posterior segments and on the last one is almost at the extremity; pleural furrow on anterior segment of uniform length (exsag.) throughout, deepest at the axial furrow, shallowing laterally and then deepening again towards the pleural tip; furrow transverse between the axial furrow and the fulcrum, then curving posteriorly to terminate almost on the posterior edge of the pleural tip; furrows progressively broader and shallower on more posterior segments (and have progressively more rounded lateral terminations) until on the last segment the furrow occupies most of the segment surface. Posterior band on anterior segment lanceolate and flat-topped; on second segment of uniform length (exsag.) and sharp crested; on third segment unusually high and sharp crested and diminishing in size distally to fulcrum; and on segments four, five, and six, triangular in outline, rounded on top, and progressively shorter (exsag.).

Tips of pleurae downturned to form an almost vertical lateral doublure; no inflected ventral doublure present. Apodemes on all segments strong; all transverse and with a distinct swelling and ventral projection at their median end; some also with a much smaller lateral swelling.

Pygidium. Two to three times as wide as long depending on size (the larger are relatively wider) with subtriangular axis extending to the posterior margin; eight definite rings visible on the dorsal surface, and possibly one or two more on exceptionally well-preserved specimens, the more posterior ones being very faint; rings deflected forwards medially, the amount of deflection decreasing posteriorly; anterior ring furrows deepest laterally but longest sagittally, the most anterior one almost bisecting the anterior ring; on more posterior segments ring furrows visible only on the medial part of the axis; articulating half ring short but with a pronounced arcuate anterior outline. Axial furrow broad, shallow, and only slightly deepened opposite the ends of the more anterior ring furrows.

Anterior margin of the pleural regions of the pygidium straight and sharp; inner half of pleural region smooth and gently concave except on the most anterior segment where it is almost flat; outer half gently concave and rising to a sharp ridge on the posterior

border; outside this ridge doublure widest and gently convex on either side of the axis, but more steeply sloping and progressively narrower postero-laterally and laterally, becoming vertical at the anterior end of the pygidium; line of border ridge arcuate but actual posterior margin of pygidium sub-triangular; axis meets border ridge posteriorly producing a gently rounded crest on the ridge; very fine terrace lines on the posterior doublure fading medially behind the axis.

Seven 'pleural ribs' readily distinguished; ribs clearly marked only in the outer half of the pleural field, straight to slightly curved in outline and symmetrically sloping front and back; ribs meet border ridge at their distal extremities but do not interrupt crest of ridge; extremely delicate interpleural furrows occasionally seen and cut obliquely across these 'pleural ribs' which are thus seen to be composed of the posterior band of a given segment adaxially and the anterior band of the next succeeding segment distally (see text-fig. 1).

Pair of deep apodemal pits in the first ring furrow set well in from the axial furrow; on each side of second ring furrow a pair of ovate, subequal, slightly raised muscle scars reach two-thirds of the distance to the median line from the axial furrow; on subsequent ring furrows outer scar of pair tends to maintain its size whereas the inner one gradually diminishes, but on most posterior furrows outer scar also diminishes rapidly; paired arrangement probably maintained right to posterior extremity; eleven pairs of scars (in addition to the apodemes) present on largest and most complete specimen.

Remarks. The material is all crushed to some extent so that it is difficult to determine the exact proportions of the various structures, or in many specimens such details as the pit arrangement on parts of the fringe. With regard to the latter character, however, enough specimens are known for us to be confident of the interpretation given above. We may have been unconventional in the way that we have interpreted the interruption of I_3 and the continuity of I_4 in front of the glabella. Some authors may prefer to interpret I_3 as continuous and I_4 as interrupted. In our opinion this would be unjustified since it is possible to consider the I_4 pits as forming a continuous, but gently flexed row in front of the glabella in all specimens, whereas continuity cannot be considered for I_3 without an angular change in direction of the row. But even more important is the fact that on some specimens, particularly 21321a–b, the pits of the I_3 row diminish in size towards the line of the axial furrow and the row wedges out between I_2 and I_4, the pits of which retain their normal size. It is also worth noting that on one specimen, 21328C, I_2 fails immediately in front of the glabella, but on nine others it appears to be complete.

The girder is variably developed but is always weak and virtually indistinguishable from the ridges on either side. It has been recognized by its continuity with the carina on the venter of the genal spine and/or by the slight change in slope of the lamella on its inner side. In most specimens there is no doubt about its recognition. Take, for example, the specimen figured on Plate 111, fig. 11. The carina on the genal spine does not continue strongly into any one of the ridges, though it could continue into the outermost ridge only by a distinct flexure. On the other hand, on the antero-lateral and anterior parts of the specimen the second ridge in from the margin marks a change in slope of the inner and outer parts of the lamella. The normal situation is

shown on Pl. 111, fig. 13. In our opinion it is not possible to interpret any ridge other than the one inside the second row of pits as the girder on any of our specimens.

The radial arrangement of the pits which occurs on the anterior and antero-lateral parts of the fringe often does not extend across the E_1–E_2 ridge to row E_2, and on several specimens the pits of this latter row are definitely offset. The regularity of all rows tends to break down postero-laterally. Sometimes it is not possible to recognise even E_1, and occasionally there is an odd pit on the ridge between E_1 and E_2.

There may possibly be some doubt about our interpretation of the glabellar furrows and muscle scars. We have chosen to use the terminology 1p to 3p for these structures despite the fact that the anterior ones can scarcely be described as furrows. The occipital apodeme is very small and shallow and could easily be overlooked. The double structure in front of it that we have labelled 1p, is clearly the homologue of 1p together with the posterior muscle scar of Whittington's (1968) interpretation of *Cryptolithus*. Since in all other trinucleids on which the glabellar furrows are clearly defined they are three in number, and since the two pits in question lie more or less in the one depression, it seems unlikely that they represent separate glabellar furrows.

Finally, we have chosen to refer to the downturned edge of the pygidium and the corresponding parts of the pleural tips as the doublure rather than the border as is the usual practice. These parts carry terrace lines as is normal on the doublure; there is no completely inflected exoskeleton such as might be expected if the parts in question are really the border; and the sharp crest around the extremities of the pygidium corresponds with the border of other trilobites. It seems clear to us therefore that the doublure has been modified in shape to serve some special function in the trinucleoids.

REFERENCES

ANDREWS, E. C. 1910. The Forbes–Parkes Goldfield. *Mineral Resour. N.S.W.* **13**, 1–109.

BANKS, M. R. 1962. Ordovician System, *in* SPRY, A. H. and BANKS, M. R., eds., Geology of Tasmania. *J. geol. Soc. Aust.* **9**, 147–76.

DEAN, W. T. 1967. The correlation and trilobite fauna of the Bedinan Formation (Ordovician) in south-eastern Turkey. *Bull. Br. Mus. nat. Hist. Geol.* **15**, (2), 83–123, pl. 1–10.

PACKHAM, G. H. 1967. The occurrence of shelly Ordovician strata near Forbes, New South Wales. *Aust. J. Sci.* **30** (3), 106–7.

—— *et al.* 1969. *In* PACKHAM, G. H., ed., The geology of New South Wales. *J. geol. Soc. Aust.* **16**, 1–654.

WHITTINGTON, H. B. 1941. The Trinucleidae—with special reference to North American genera and species. *J. Paleont.* **15**, 21–41, pl. 5–6.

—— 1959. *In* MOORE, R. C., ed., *Treatise on invertebrate paleontology*, Part O, *Arthropoda I.* Geol. Soc. Am. and Univ. Kansas Press.

—— 1968. *Cryptolithus* (Trilobita): specific characters and occurrence in Ordovician of eastern North America. *J. Paleont.* **42**, 702–14, pl. 87–9.

K. S. W. CAMPBELL
GWENDA J. DURHAM
Geology Department
Australian National University
Canberra, A.C.T.
Australia

Typescript received 29 December 1969

ZOARIAL MICROSTRUCTURES OF TWO PERMIAN SPECIES OF THE BRYOZOAN GENUS *STENOPORA*

by JOHN ARMSTRONG

ABSTRACT. The zooecial walls of *Stenopora ovata* Lonsdale and *S. crinita* Lonsdale consist of laminae which are built of variably shaped and variably disposed tabular units. It is suggested that the acanthopores of *S. crinita* and *S. ovata* are rods of calcite that together with the surrounding wall laminae were deposited by the stenoporid zooids. The mechanisms of growth of the laminae and their components are discussed.

TRADITIONALLY the laminae that comprise the skeletons of members of the bryozoan orders Cyclostomata, Trepostomata, Cryptostomata, and Cystoporata (i.e. Boardman's and Cheetham's (1969) tubular Bryozoa) have been interpreted as growth surfaces. Laminae were believed to have been added to the skeleton one layer at a time with the depositing epithelium paralleling the laminae. However, Boardman and Cheetham (1969) have now recognized exceptions to this growth model in Pliocene to Recent heteroporid Cyclostomata. Whereas the wall laminae of many tubular Bryozoa are convex distally (e.g. *Stenopora* herein), the laminae making up the walls of these heteroporid skeletons, together with the appearances of the skeletal components on zooecial surfaces, suggest that calcium carbonate was added simultaneously to the exposed edges of numerous laminae. Such laminae enlarge in an edgewise direction and are oblique to growth surfaces. For zoaria having distally convex wall laminae, Boardman and Towe (1966) had suggested that the laminae were in fact deposited layer by layer, each layer being essentially completed before the succeeding one was initiated. In this scheme, the depositing epithelium parallels the laminae that it is secreting. Nevertheless, as a result of their findings from Recent heteroporid specimens, Boardman and Cheetham (1969) speculated that 'quite possibly many Bryozoa having laminae that closely parallel depositing epidermis will prove to have shingled and edgewise crystal development'.

Results presented herein were obtained from a study of two species of the trepostomatous genus *Stenopora* in which the wall laminae are convex distally. The work was undertaken to detail the characteristics of laminar parts of the skeletons of these species and to determine the nature of acanthopores which occur in the zooecial walls. One specimen (F15872) of *Stenopora ovata* Lonsdale and one specimen (F60038) of *Stenopora crinita* Lonsdale were used; both specimens now being retained in the type collections of the Department of Geology, University of Queensland. The illustrations in Plates 112 and 113 are optical photomicrographs of thin sections and the photographs in Plates 114 to 117 are electron-micrographs of polished sections (Pl. 114–16) and broken skeletal surfaces (Pl. 117). The polished sections were cut perpendicular to (transverse section) and parallel to (vertical section) the direction of growth of the zooecia. The surfaces of the sections were polished with a sequence of abrasives finishing with a 1-μm. diamond abrasive. Before replication, the surfaces of the sections were etched for a few seconds with a mixture of 1% nitric acid in ethyl alcohol. The normal two-stage carbon replicating technique was employed; the intermediate medium being nitrocellulose. The broken surfaces used were obtained by splitting the zooecial walls and directly replicating, without any polishing or etching, the fractured surface. Shadowing of the replicas at angles of approximately 30° was with 1 to 1 mixtures of gold and palladium.

[Palaeontology, Vol. 13, Part 4, 1970, pp. 581–7, pls. 112–117.]

ZOARIAL STRUCTURE

The zoaria of *Stenopora ovata* and *S. crinita* consist of zooecial tubes separated by laminar walls containing acanthopores.

The zoarium of the studied specimen of *Stenopora crinita* is massively branching with a broad immature zone surrounded by a mature zone about one half as wide. The branches are up to 8 cm. in diameter. Zooecial tubes are polygonal and their walls are usually thin (Pl. 113, fig. 7). No diaphragms are present in any of the zooecia and annular thickenings of the walls occur only in the mature zone where they are small and widely separated. Acanthopores are present only at wall junctions.

The zoarium of the studied specimen of *Stenopora ovata* is encrusting a brachiopod shell and is about 1 cm. thick. Zooecial tubes are polygonal to smoothly rounded and lack diaphragms. Annular thickenings of the walls are well developed throughout the zoarium (Pl. 113, figs. 3, 4). Acanthopores are present only at wall junctions (Pl. 112, figs. 1–3).

LAMINAR MICROSTRUCTURE

The zooarial walls of *Stenopora* are composed of laminae of the order of 1–5 μm. thick (Pl. 115, fig. 6; Pl. 117, figs. 1–4). In vertical sections perpendicular to the walls the laminae are convex distally (Pl. 113, figs. 3, 4, 6; Pl. 114, fig. 2; Pl. 115 figs. 1, 2: Pl. 116, figs. 1–3). Laminae successively overlie each other both in the walls and annular thickenings and they terminate at the surfaces of the walls (Pl. 113, figs. 3, 4, 6; Pl. 114, figs. 1, 2; Pl. 115, fig. 2). In transverse section the laminae are also arched and they are convex away from the closest inter-zooecial angle (Pl. 114, fig. 1; Pl. 115, fig. 3). Because the laminae are convex distally, transverse sections of the zooecia often show the walls with apparently non-laminated central regions bordered on each side by a zone having an obvious laminar structure (Pl. 114, fig. 1). This apparent layering of the wall is simply the result of sectioning a series of parallel sharply convex laminae. Towards the surfaces of the walls the laminae are perpendicular to transverse sections, whereas medially the tangential relationship between the wall laminae and the section yields the massive appearance of this part of the wall. Adjacent to acanthopores the laminae are deflected distally (Pl. 113, figs. 1, 2, 5) and they comprise a series of 'cone-in-cone' structures. Transverse sections usually reveal the laminae concentrically arranged around acanthopores (Pl. 112, figs. 1, 2; Pl. 114, fig. 5; Pl. 115, figs. 4, 5) although in the walls of the specimen of *Stenopora crinita* this concentric arrangement is not developed except

EXPLANATION OF PLATE 112

Figs. 1–3. *Stenopora ovata* Lonsdale. F15872, transverse sections of the zoarium illustrating zooecia and acanthopores. 1, ×60. 2, ×250. 3, ×25.

EXPLANATION OF PLATE 113

Figs. 1–5. *Stenopora ovata* Lonsdale. F15872. 1, vertical section parallel to wall illustrating an acanthopore and the adjacent inclined wall laminae, ×95. 2, enlargement approximately by 3 of part of the acanthopore in fig. 1. 3, 4, moniliform appearance of zooecial walls in vertical section, both ×85. 5, vertical section parallel to wall illustrating acanthopores and wall laminae, ×60.

Figs. 6 and 7. *Stenopora crinita* Lonsdale. F60038. 6, vertical section of thickened portion of a zooecial wall illustrating disposition of the wall laminae, ×60. 7, transverse section of zoarium illustrating the thin walled polygonal zooecia with inorganic lining, ×20.

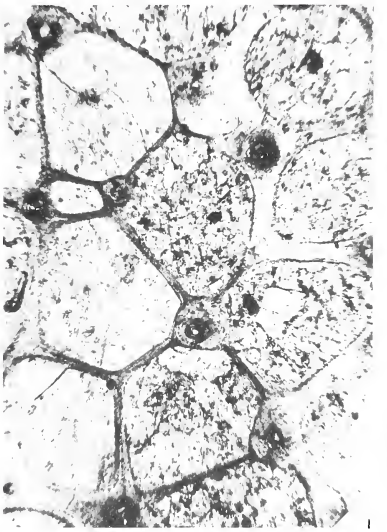

1

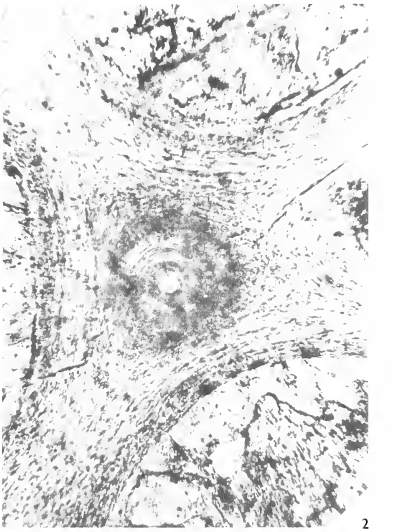

2

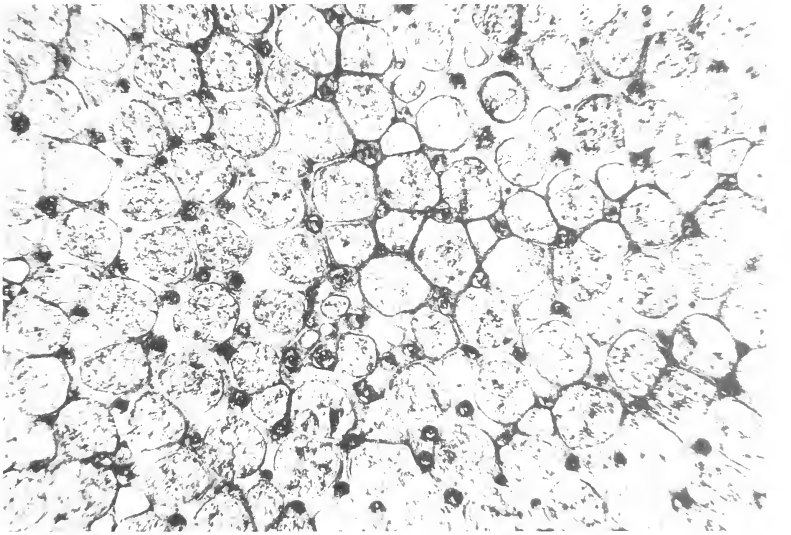

3

ARMSTRONG, Bryozoan microstructure

1

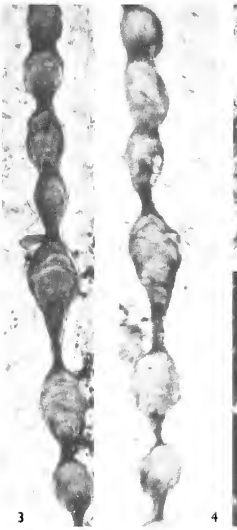

3 4

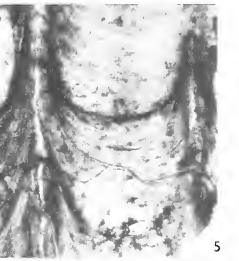

5

6

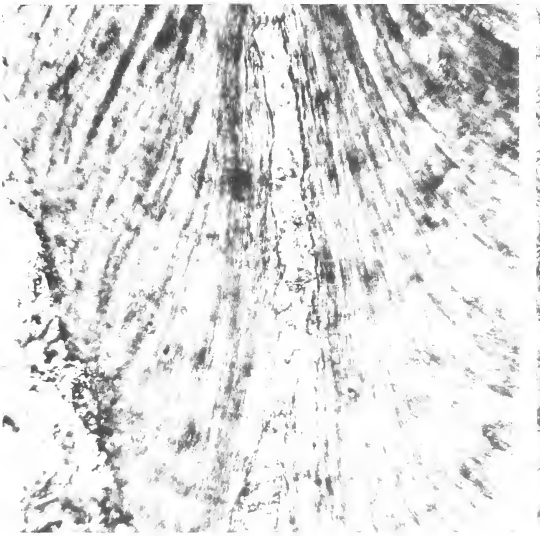

2

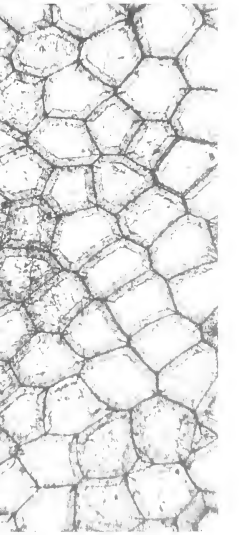

7

ARMSTRONG, Bryozoan microstructure

in thicker parts of the walls (Pl. 114, figs. 3–5). Growth-lines and annular thickenings in the walls of the zooecia of *Stenopora ovata* and *S. crinita* are concave distally reaching their most distal points at the inter-zooecial wall junctions (Pl. 113, fig. 5).

Longitudinal sections of the walls immediately distal to the annular thickenings of *Stenopora crinita* show the wall with a massive central portion that is surrounded by one or more laminae, the number of laminae increasing distally (Pl. 116, figs. 1–3). This massive material was present above all of the examined annular thickenings of *S. crinita* and although its origin is conjectural, the consistent appearance of the material seems to suggest that it was a primary deposit laid down by the stenoporid zooids. Similar massively granular regions occur above some of the annular thickenings of *Stenopora ovata* (Pl. 115, figs. 1, 2). Above other annular thickenings of *S. ovata* there appear to be superimposed laminae like those in normal parts of the walls.

The components making up the laminae of *Stenopora crinita* were observed in replicas of broken surfaces of the walls. The laminae are built of tabular units which are two to five times wider than they are thick, and twice to many times longer than they are wide (Pl. 117, figs. 1–4). Boundaries between the tabular units of a lamina are marked by grooves in the surface of the lamina. The laminae consist of both irregularly and regularly shaped units. Surfaces of the laminae sometimes bear ridges, and these seem to be associated only with the more regular laminar units (Pl. 17, figs. 1, 2). The surfaces of the regular units are also often marked with fine chevron-shaped ridges and grooves (Pl. 117, figs. 1, 2). Armstrong (1969) described a somewhat similar situation in the shells of the strophomenid brachiopods *Streptorhynchus pelicanensis* and *Terrakea solida*. The shells of these species consist of thin sheets, each of which is composed of tabular blade-like units. The blades of a particular sheet are parallel to each other, but almost invariably they are not parallel either to the blades in contiguous sheets above and below or to the blades in adjacent coplanar sheets. Surfaces of the sheets are covered with crossing sets of parallel ridges and grooves (Armstrong 1969, pl. 57, fig. 3; pl. 58, figs. 1, 2), the grooves representing the boundaries between the blades of that sheet and the ridges being the parts of that sheet which have infilled the inter-blade grooves in the base of the sheet above.

ACANTHOPORES

Commonly occurring in the skeletons of bryozoans are structures referred to as acanthopores. Bassler (1953) defined an acanthopore as a 'cylindrical tube adjoining zooecial walls and parallel to them in growth; formed of cone in cone layers with narrow central tubule which may be crossed with minute diaphragms; position often marked superficially by projecting spines', and he stated that they 'undoubtedly represent zooids with some definite function' (Bassler 1953, p. G 91). Previously, in discussing the morphology of trepostomatous zoaria, Cumings and Galloway (1915) had referred to acanthopores as 'hollow thick walled tubules'. They speculated that the small spines formed by the projection of acanthopores beyond the surface of the zoarium had a protective function (Cumings and Galloway 1915, pl. 15, figs. 51, 52). Subsequent to Bassler (1953) many references to, and definitions of, acanthopores have implied their tubiform nature Boardman 1960, pp. 28, 29; Ross 1961, pp. 21, 32, text-fig. 7; Ross 1966, p. 112; Boardman and Utgaard 1966, p. 1087; Cuffey 1967, p. 53). Recently, however, Tavener-Smith (1969) has suggested that acanthopores in the

trepostomatous *Leioclema asperum* are solid rods of calcite and that they did not house accessory zooids. Tavener-Smith implies that the calcite of the acanthopores of this species is of zooidal rather than inorganic origin.

The structures termed acanthopores in the studied specimens of *Stenopora* are so identified because they consist of apparently 'tubular' structures running parallel to the zooecia in the walls (Pl. 112, figs. 1–3; Pl. 113, figs. 1, 2). The wall laminae dip away from the acanthopores in a proximal direction (Pl. 113, figs. 1, 2, 5). In the studied specimen of *S. ovata* the acanthopores vary from 10 to 60 μm. in diameter with 90% of them being between 10 and 40 μm. and 70% having a diameter between 15 and 25 μm. Boundaries between the acanthopores and the surrounding wall laminae are abrupt and well defined (Pl. 113, fig. 2; Pl. 114, figs. 3–5; Pls. 115, figs. 4, 5). Longitudinal sections of acanthopores show the rods of calcite to be continuous and to lack indications of growth surfaces (Pl. 114, fig. 6). Laminae do not seem to be continuous into acanthopores. In longitudinal sections adjacent to acanthopores (Pl. 114, fig. 2) there is a zone in which the boundaries between the laminae are widely spaced. In these areas, the laminae, being tangential to the adjacent acanthopore, are almost parallel to the section and consequently they simulate an elongate massive structure that is occasionally crossed by growth lines. Tavener-Smith's (1969) figure 6 is similar to Plate 114, fig. 2 herein and may also have been adjacent to rather than in an acanthopore. All acanthopores in the studied specimens of *Stenopora ovata* and *S. crinita* consist of an apparently homogeneous calcite rod and none are occupied by the sedimentary and carbonate mineral infillings that occur in the zooecia of these specimens. Carbonate minerals in the zooecia of the studied specimens of *Stenopora ovata* and *S. crinita* include calcite, ferroan calcite, and ferroan dolomite, whereas the zooecial walls and acanthopores consist only of calcite. These facts suggest that the calcite of the acanthopores has not been secondarily introduced and there seems little doubt that the acanthopores of *Stenopora ovata* and *S. crinita*, like those of *Leioclema asperum* described by Tavener-Smith (1969) were never minute tubes. Indeed, the nature of the acanthopores in *Stenopora ovata* and *S. crinita* can only be reconciled with the viewpoint that the calcite of both the acanthopores and the wall laminae was deposited by the stenoporid zooids. Conceivably, as Tavener-Smith (1969) suggested, many of the 'calcite filled tubules' constituting the acanthopores of other bryozoans might also be of zooidal rather than inorganic origin.

The rods of calcite and the laminae of the zooecial walls probably owe their different

EXPLANATION OF PLATE 114

Figs. 1–6. *Stenopora crinita* Lonsdale. F60038. 1, transverse section of wall. Closest wall junction was in direction of lower right corner of figure, ×500. 2, vertical section of wall adjacent to an acanthopore, ×750. 3, 4, 5, wall junctions containing acanthopores, all ×250. 6, vertical section of zooecial wall illustrating an acanthopore. Massive calcite in left part of wall is the acanthopore, ×750.

EXPLANATION OF PLATE 115

Figs. 1–6. *Stenopora ovata* Lonsdale. F15872. 1, 2, vertical sections of the distal portions of annular thickenings, ×1000 and ×500 respectively. 3, transverse section of wall close to its junction with other walls; this junction is located in direction of base of figure, ×250. 4, 5, transverse sections of wall junctions with acanthopores, ×350 and ×250 respectively. 6, laminae that make up walls of zooecia, ×3000.

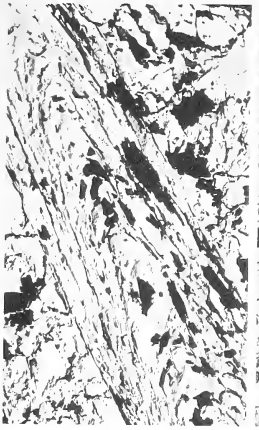

1

2

3

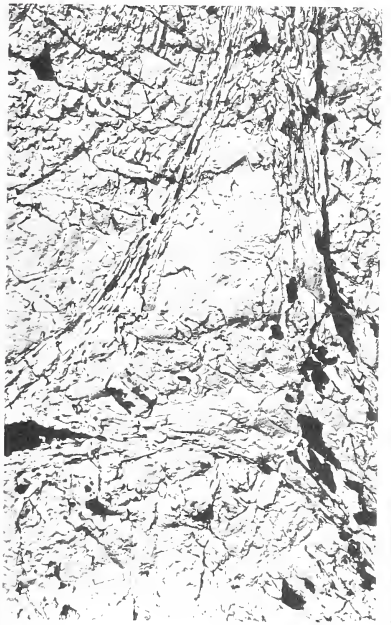

4

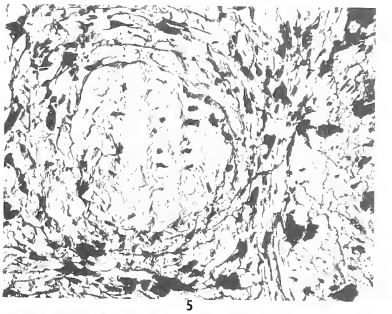

5

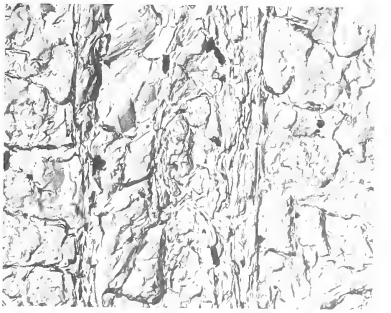

6

ARMSTRONG, Bryozoan microstructure

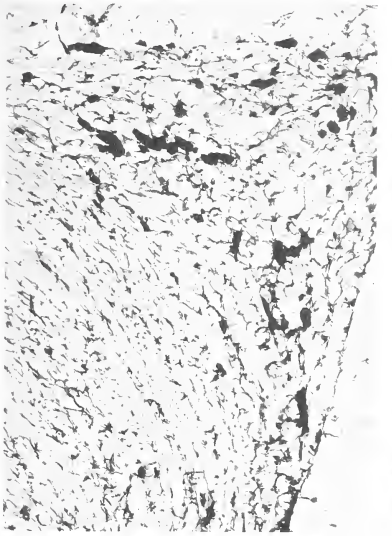

1

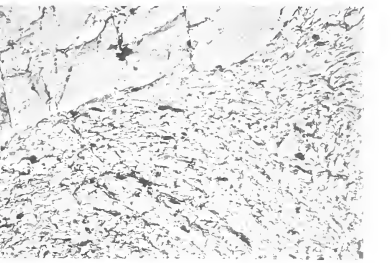

2

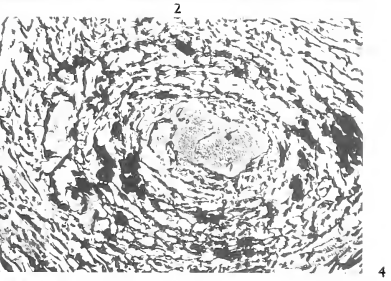

4

3

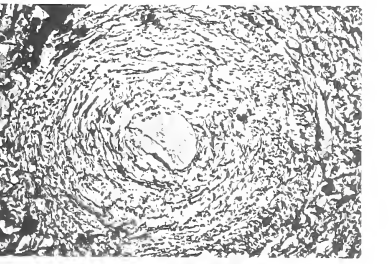

5

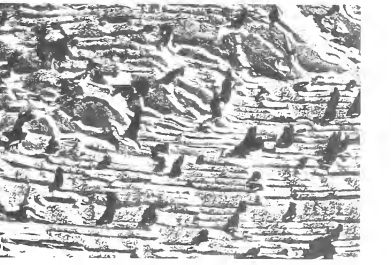

6

ARMSTRONG, Bryozoan microstructure

natures to the different biological conditions attendant to their deposition. Doubtless, considerations about the mode of formation of acanthopores cannot be divorced from speculations about their function. Both Bassler (1953) and Cuffey (1967) support the view that acanthopores, as tubes, must have housed specialized zooids. The fact that the acanthopores of *Stenopora ovata* and *S. crinita* consist of rods of calcite does not necessarily rule out this possibility, for such 'heterozooids' could conceivably have produced a continuous deposit of calcite. However in view of the size of the acanthopores of the studied specimens of *Stenopora* (they are between 10 and 60 μm. in diameter) there would seem little likelihood that these acanthopores could have housed discrete individuals. The calcite of these acanthopores is probably the secretory product of areas of specialized zooidal epithelium.

In this context it is interesting to note the amazing similarity between the acanthopores of *Stenopora* and the taleolae of the pseudopunctae that occur in many brachiopod shells.

Pseudopunctae consist of rods of calcite (taleolae) inclined obliquely forwards into the shell. Around them the sheets of the shell are deflected towards the interior of the shell to form cone-in-cone-like structures. Transverse sections of pseudopunctae show the taleolae concentrically surrounded by the deflected sheets of the shell. Taleolae were enlarged by the addition of calcite to their exposed ends on the internal surface of the shell. The textural similarity between the calcite of taleolae and the calcite forming the areas of attachment of the adductor and diductor muscles in brachiopod shells lead to suggestions that taleolae were the loci of attachment of small tendons or tonofibrils (Williams 1953, 1956, 1968; Williams and Rowell 1965; Armstrong, in press).

In the studied specimens of *Stenopora* the acanthopores are unique because of the probable manner of their deposition. Whereas the wall laminae are thought to have been deposited both successively and by edgewise growth (see later), it seems that calcium carbonate could have been continuously added to the distally exposed ends of acanthopores throughout the life of a stenoporid colony. In view of the similarity between acanthopores and taleolae, and considering the suggested function of taleolae, the possibility that epithelial differences account for the distinctive aspects of acanthopores and laminae, together with the inference that the deposition of the calcium carbonate of acanthopores once initiated could have continued on uninterrupted, enable speculation that acanthopores may have served some attachment type of function. Tavener-Smith (1969) has discussed the relationships inferred to have existed between the zooarium and the epithelial tissues of the trepostomatous *Leioclema asperum*. Loci of attachment for the frontal epithelium (see Tavener-Smith 1969, fig. 1) of stenoporid soft parts would probably have been most conveniently located along the distal edges of the walls. Acanthopores could have served such an attachment purpose in addition to having the protective function envisaged by Cumings and Galloway (1915), Tavener-Smith (1969) and other authors.

GROWTH

Boardman and Cheetham (1969, text-fig. 2) have discussed three possible modes by which the wall laminae of the tubular bryozoa may be deposited. They suggest that wall laminae which are convex proximally are deposited in edgewise directions with calcium carbonate being added simultaneously to the distal edges of numerous laminae. Evidence for this growth mechanism is obtained from recent heteroporid specimens.

Carbon replicas taken from the surfaces of the zooecial walls of these specimens show the edges of numerous laminae to which calcium carbonate seems to be being added (Boardman and Cheetham 1969, pl. 28, figs. 2, 3). The resulting laminae are obliquely inclined to the depositing epithelium. After studying a recent species of the Cyclostomata with distally convex wall laminae Boardman and Towe (1966) suggested that from one to a few laminae were concurrently being added to the wall surface by the development and coalescence of seeds of calcite on the surface of an earlier formed lamina. The laminae produced are parallel to the depositing epidermis and are coincident with growth-lines. Boardman and Cheetham (1969) speculated that such a growth mechanism is also suggested by the appearance of the surfaces of the laminae on the walls of *Denispora corrugata* (Boardman and Cheetham 1969, pl. 28, fig. 1). In this illustration small crystals seem to have formed on the surface of an already existing lamina. The components of this lamina are visible and they are irregularly shaped and of variable size (Boardman and Cheetham 1969, pl. 28, fig. 1). The third possible mode of laminar growth is depicted in Boardman's and Cheetham's (1969) text-fig. 2c. Boardman and Cheetham speculate that the laminae in some tubular bryozoa with distally convex wall laminae may also have been enlarged in an edgewise direction. In this scheme the wall laminae begin axially and aborally, and extend distally by edgewise growth.

The walls and acanthopores of *Stenopora* were presumably deposited by epithelial cells comprising tissue referred to by Tavener-Smith (1969, fig. 1) as inner epithelium. Although *Stenopora* lacks diaphragms, the relationship which existed between its soft parts and its skeleton was probably similar to that depicted by Tavener-Smith for *Leioclema asperum*. Irregular laminar units like those in parts of Plate 117, fig. 3 are similar to the irregular units making up the lamina in Boardman's and Cheetham's (1969) plate 28, fig. 1, and those authors consider that the lamina in the latter figure was formed by the coalescence of numerous small crystals established on the preceeding lamina. Conceivably the parts of the laminae of *Stenopora crinita* with irregularly shaped components were deposited in this manner. However, the more regularly shaped units like those which possess the chevron markings (Pl. 117, figs. 1, 2) strongly resemble the units making up the edgewise growing laminae in Boardman's and Cheetham's plate 28, figs. 2, 3. The occurrence of ridges on the surfaces of the laminae consisting of these more regular units in *Stenopora crinita* may be significant. Possibly because of the concurrent growth of several laminae, the calcium carbonate being added to a particular lamina was able to infill the inter-component grooves in the base of the next overlying laminae. Growth of one lamina at a time, where each lamina was essentially completed before the first crystals of the succeeding lamina were established, would not have permitted this to occur. Thus the available evidence seems to suggest that the walls of *Stenopora crinita* grew both by the successive addition of some laminae

EXPLANATION OF PLATE 116

Figs. 1–3. *Stenopora crinita* Lonsdale. F60038, vertical sections of the distal portions of annular thickenings of the walls. ×250, ×250, and ×500 respectively.

EXPLANATION OF PLATE 117

Figs. 1–4. *Stenopora crinita* Lonsdale. F60038. Views of the surfaces of several of the laminae that make up the walls of the zooecia. Note the ridges and the chevron-shaped markings in figs. 1 and 2 (see p. 583), figs. 1–3, ×500. fig. 4, ×1500.

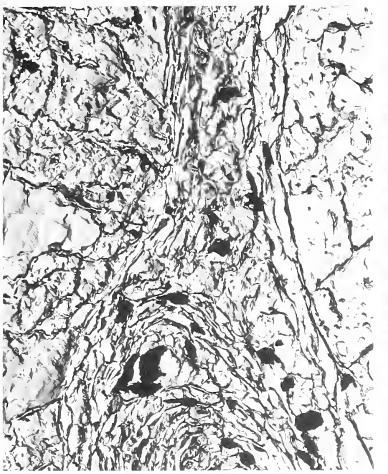

1

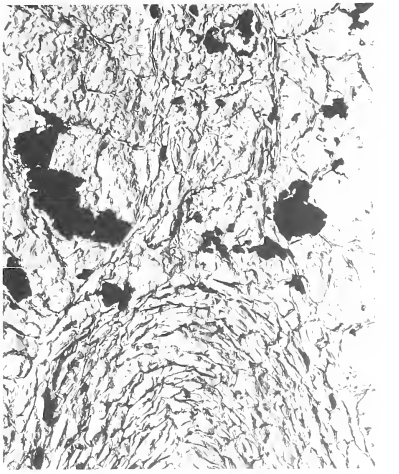

2

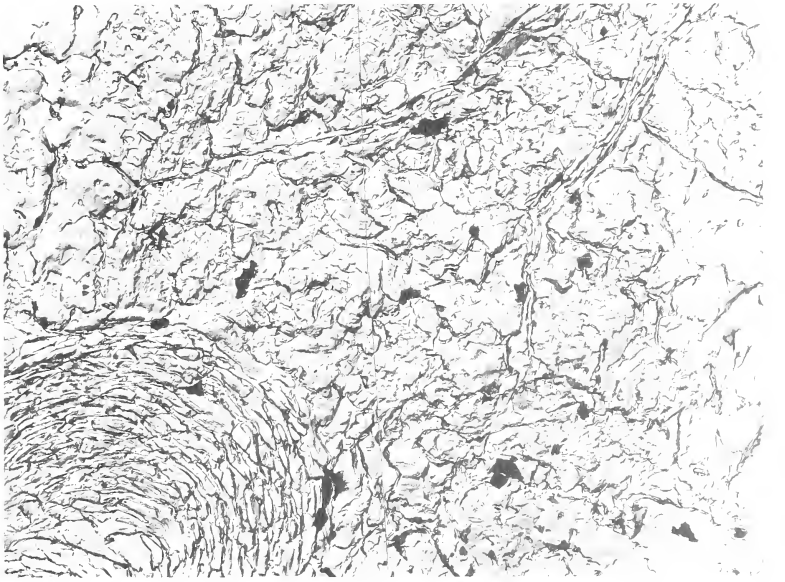

3

ARMSTRONG, Bryozoan microstructure

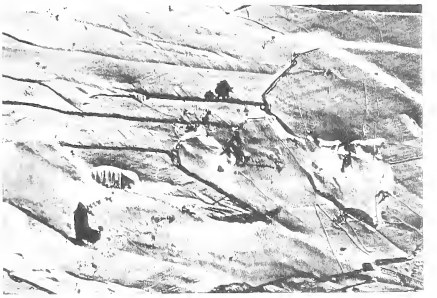

1

2

3

4

ARMSTRONG, Bryozoan microstructure

and by the edgewise enlargement of other laminae. It is unknown, however, whether the different growth mechanisms envisaged for the laminae of *Stenopora crinita* were restricted to different parts of the walls, and it is difficult to develop a model with both types of growth occurring in the same skeleton.

Considerably more work will be required before the growth of stenoporid skeletons is completely understood, and undoubtedly, much data about the distribution and directions of growth of the edgewise and successively growing laminae in the zooecia will be obtained when growing surfaces of zooecial walls are able to be studied.

Acknowledgements. I am grateful to Professor Dorothy Hill, F.R.S. and Dr. J. S. Jell, Department of Geology, University of Queensland, and Dr. R. Wass, Department of Geology, University of Sydney, for reading the manuscript and offering several helpful suggestions. Mr. Bob Grimmer of the Electron Microscope Unit at the University of Queensland carried out all of the preparative work.

REFERENCES

ARMSTRONG, J. 1969. The crossed-bladed fabrics of the shells of *Terrakea solida* (Etheridge and Dun) and *Streptorhynchus pelicanensis* Fletcher. *Palaeontology*, **12**, 310–20.

—— in press. Microstructure of the shell of the brachiopod, *Wyndhamia clarkei*.

BASSLER, R. S. 1953. Bryozoa. *In* MOORE, R. C., ed., *Treatise on invertebrate paleontology*, Part G. Geol. Soc. Am. and Univ. Kansas Press. 253 pp.

BOARDMAN, R. S. 1960. Trepostomatous Bryozoa of the Hamilton Group of New York State. *Prof. Pap. U.S. geol. Surv.* **340**, 87 pp.

—— and CHEETHAM, A. H. 1969. Skeletal growth, intracolony variation, and evolution in Bryozoa: A review. *J. Paleont.* **43**, 205–33.

—— and TOWE, K. M. 1966. Crystal growth and lamellar development in some recent cyclostome Bryozoa. *Spec. Pap. geol. Soc. Am.* **101**, p. 20.

—— and UTGAARD, J. 1966. A revision of the Ordovician bryozoan genera *Monticulipora*, *Peronopora*, *Heterotrypa*, and *Dekayia*. *J. Paleont.* **40**, 1082–1108.

CUFFEY, R. J. 1967. Bryozoan *Tabulipora carbonaria* in Wreford megacyclothem (Lower Permian) of Kansas. *Paleont. Contr. Univ. Kans.* **43**, Bryozoa, Article 1, 96 pp.

CUMINGS, E. R. and GALLOWAY, J. J. 1915. Studies of the morphology and histology of the Trepostomata or monticuliporoids. *Bull. geol. Soc. Am.* **26**, 349–74.

ROSS, J. P. 1961. Ordovician, Silurian, and Devonian Bryozoa of Australia. *Bull. Bur. Min. Resour. Aust.* **50**, 172 pp.

—— 1966. The fauna of the Portrane Limestone, IV: Polyzoa. *Bull. Br. Mus. nat. Hist.* Geol. **12**, 109–35.

TAVENER-SMITH, R. 1969. Wall structure and acanthopores in the bryozoan *Leioclema asperum*. *Lethaia*, **2**, 89–97.

WILLIAMS, A. 1953. North American and European stropheodontids: their morphology and systematics. *Mem. geol. Soc. Am.* **56**, 67 pp.

—— 1956. The calcareous shell of the Brachiopoda and its importance to their classification. *Biol. Rev.* **31**, 243–87.

—— 1968. Evolution of the shell structure of articulate brachiopods. *Spec. Pap. Palaeont.*, No. 2, 55 pp.

—— and ROWELL, A. J. 1965. Brachiopod anatomy. *In* MOORE, R. C., ed., *Treatise on invertebrate paleontology*, Part H, *Brachiopoda*. Geol. Soc. Am. and Univ. Kansas Press, pp. 6–155.

J. ARMSTRONG
Union Oil Dev. Corp.
P.O. Box H 68
Australia Square
Sydney
N.S.W. 2000

Typescript received 29 January 1970

VARIATION OF BIVARIATE CHARACTERS FROM THE STANDPOINT OF ALLOMETRY

by ITARU HAYAMI *and* AKIHIKO MATSUKUMA

ABSTRACT. In fossil biometry simple ratios between two linear measurements have been frequently applied as a third variable for representation of the variation of a bivariate character. Theoretically, however, it is obvious that its frequency distribution is sometimes strongly influenced by the heterogeneity of sample, especially the age distribution of a fossil population, and is apt to be artificially skewed and platykurtic. In order to analyse the real state of frequency distribution of bivariate characters and to apply further advanced statistical techniques for taxonomic identification and discrimination, it may be necessary to use some other index which is little, or preferably not at all influenced by growth. In this respect the diagonal distance from each point to the reduced major axis on a double logarithmic scatter diagram may be a more desirable index, if a single power function represents the relative growth of the organism. The advantage of this method is also recognized empirically by a comparative study on an actual fossil sample of *Glycymeris rotunda* from the Pliocene of central Japan. Some comments are given as to the definition of isometry and allometry.

MODERN palaeontology focuses on the population rather than the individual. A biometrical study of individual variation seems to be important, primarily because it may offer fundamental and objective information for the consideration of classification and evolution. There are various kinds of individual variation which are controlled by different factors. As classified by Mayr, Linsley, and Usinger (1953) and again by Mayr (1969), some are genetic and the others are non-genetic. Here we intend to discuss mainly non-sex-associated continuous variation and methods for the representation of bivariate characters in a population. It is no doubt important to consider from a biological viewpoint whether the variation is genetic or non-genetic. Unfortunately, however, the distinction is usually not easy in fossils. We presume that such bivariate characters as are discussed here might be controlled both by genes and environments.

Various kinds of characters may be used for the representation of continuous variation. In neontology individual variation can be well recognized on the basis of a univariate character, if the population proves to be composed of individuals of almost the same age. This method is logically appropriate and certainly applicable also in palaeontology, if the character does not change as the organism grows. For instance, the number of simple radial ribs of bivalves can be regarded as a good character. Such characters are, however, usually restricted to count, whereas linear measurements themselves are hardly applicable as the growth-invariant index.

Many previous authors have shown histograms of bivariate characters in order to express the individual variation, taking the simple ratio between pairs of linear measurements as the index. Ratios are, in fact, often more useful than linear measurements in taxonomy. It is, however, obvious that this conventional method bears some theoretical difficulties, because such a ratio may change to some extent through the growth of organism. In this respect the dynamic concept of relative growth should be introduced in the study of individual variation. We have been devoting ourselves to seek good indices for the representation of bivariate characters from the standpoint of allometry.

[Palaeontology, Vol. 13, Part 4, 1970, pp. 588–605.]

As such indices may deserve general application in palaeontology, we intend to discuss the problem in some detail and to evaluate them on the basis of some actual data.

PROBLEMS

When one intends to discuss the continuous variation of a sample and to apply any advanced statistical techniques for the estimation of the nature of a population, it may be necessary as an initial condition to recognize or presume normal frequency distribution of characters. Therefore, one should select the most adequate and meaningful index for each character especially carefully and strictly in order to represent the variation with the combination of two variables.

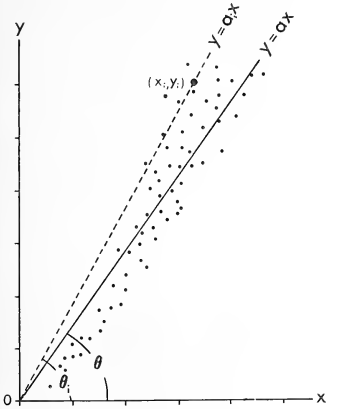

TEXT-FIG. 1. Hypothetical scatter diagram showing the concept of isometric variation, where the simple ratio y/x is applied as an index. $a_i - a$ or $\tan\theta_i - \tan\theta$ means the deviation for an arbitrary individual.

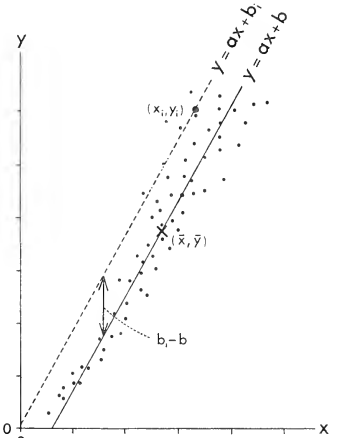

TEXT-FIG. 2. Hypothetical scatter diagram showing the concept of 'initial index variation'. The line $y = ax+b$ is the reduced major axis for a sample. $b_i - b$ means the deviation for an arbitrary individual.

The ratio between two linear measurements, which is the simplest index, has been used frequently in fossil biometry. Many authors distinguished one species from another on the basis of the difference of mean simple ratios. Some biometricians applied Student's t-test for the discrimination of populations. In this case, as shown in text-fig. 1, the relation of a linear equation:

$$y = a_i x \tag{1}$$

is presumed for the growth of each individual. If the average value of a_i is defined as a, the growth of a typical individual is represented by the following equation:

$$y = ax \tag{2}$$

In this case $a_i - a$ or $\tan\theta_i - \tan\theta$ is regarded as the deviation of bivariate character from the mean. We may provisionally call this expression *isometric variation*.

Some authors (e.g. Omori and Utashiro 1954) suggested another statistical method to show the variation of a sample, where the following linear equation was regressed by means of the least-squares criterion from all the given individuals:

$$y = ax + b. \tag{3}$$

They presumed that the slope a is nearly constant in one species and that the initial index (y-intercept) b is a variable mainly related to the intraspecific or geographic variation. In that method, although the presumption of the constancy of a is quite dubious, the growth of each individual would be expressed by the following formula:

$$y = ax + b_i \tag{4}$$

where b_i or $b_i - b$ is regarded as the index for the variation (text-fig. 2).

Such an estimation of variation on the basis of either the slope or the initial index of a linear equation is, however, generally inadequate, because the relative growth of an organism is not necessarily linear. The simple ratio between two linear measurements is actually variable as the organism grows. The histograms of isometric variation would be apt to be flat-topped (platykurtic) and skewed in comparison with the ideal normal distribution, if the sample were composed of individuals of different ages (text-fig. 3).

There are several methods for obtaining a regressed line of best-fit. As discussed by Teissier (1948), Kermack and Haldane (1950), Imbrie (1956), Miller and Kahn (1962), and others, the method of reduced major axis seems to be more reasonable and advantageous in biometrical studies than the conventional regression analysis y on x or x on y. In a statistical study of Cenozoic *Argopecten*, Waller (1969) found empirically that the reduced major axis fits a greater variety of point distributions than Bartlett's line.

The slope of the reduced major axis is given as:

$$a = \frac{s_y}{s_x} = \sqrt{\left(\frac{\Sigma y^2 - \bar{y}\Sigma y}{\Sigma x^2 - \bar{x}\Sigma x}\right)} \tag{5}$$

where s_x and s_y are the standard deviations of x and y respectively. If the two variables of the equation (3) are substituted by the mean values of x and y, the initial index of this axis is readily determined. Incidentally, the slopes of ordinary regressed lines of y on x and x on y are given by $r.s_y/s_x$ and $s_y/r.s_x$ respectively, where r is the correlation coefficient between two variables. Because r is positive and smaller than 1, the gradient of the reduced major axis is equal to the geometric mean of the slopes of two ordinary regressed lines. Therefore, the reduced major axis is also intuitively more reasonable than ordinary regressed lines, if the two variables are equal in dimensions.

The initial index of the linear equation, however, may be biologically meaningless, even if it is obtained by the method of reduced major axis. Moreover, it is a great difficulty for the methods of 'initial index variation' that the state of the frequency distribution is strongly influenced by the heterogeneity of the sample, especially by the age distribution within a population. This may be a serious objection in comparing fossil populations, because the age distribution must be controlled not only by the biological condition but also by sorting in the process of sedimentation.

On the other hand, it is much more reasonable to consider that a pair of variables,

which are closely related to growth, increase approximately in accordance with a non-linear function. This relation has long been called allometry (or heterogony) (Huxley 1932, Huxley and Teissier 1936, Gould 1966). In this respect isometry is better

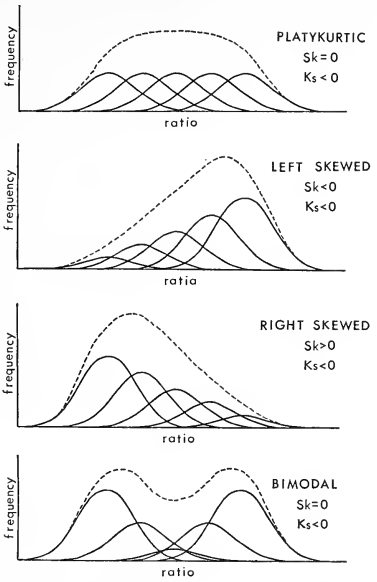

TEXT-FIG. 3. Hypothetical frequency distributions of heterogeneous samples, showing artificially platykurtic, skewed and bimodal tendencies.

regarded as a special case of allometry. Since the pioneer work of Nomura (1926), a power equation:

$$y = \beta x^{\alpha} \tag{6}$$

has been generally applied in the study of allometry, where the exponent α is called the specific growth ratio (or relative growth coefficient) and β the initial growth index. The adequacy of this function has been recognized empirically in many organisms.

As pointed out by some authors (e.g. Shimizu 1959, Röhrs 1961, Gould 1966), the method of study of ontogenetic allometry may be classified broadly into two categories: one is the direct examination of individual relative growth, and the other is the estimation of average relative growth deduced from many individuals of various growth stages. The former is no doubt more advantageous than the latter in many respects (Gould 1966, Obata 1967), but cannot be pursued in the study of fossils, unless the

morphology of every growth stage is preserved in an individual. Furthermore, we must treat the sample representing a population instead of the individual in a quantitative study of variation. In other words we should focus on the population allometry, paying attention also to the individual growth.

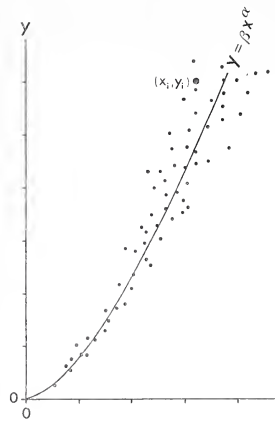

TEXT-FIG. 4. Hypothetical scatter diagram showing the concept of allometric variation of a bivariate character. The power function $y = \beta x^{\alpha}$ represents the average allometry for a sample.

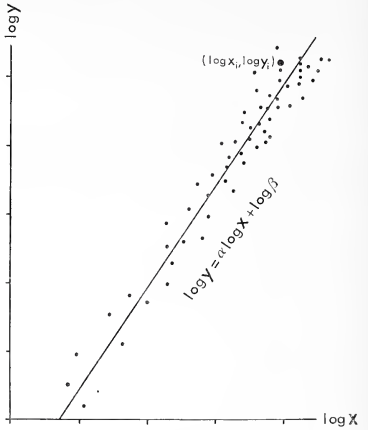

TEXT-FIG. 5. Data of text-fig. 4 plotted as $\log x$ $\log y$ on a double logarithmic paper ($X = \log x$, $Y = \log y$).

The allometric equation (6) is just equivalent to the following linear equation:

$$\log y = \alpha \log x + \log \beta. \tag{7}$$

The equation of average ontogenetic allometry for a sample can be obtained by the regression of $\log y$ on $\log x$ (or vice versa) or more desirably by the method of reduced major axis with transformation of the original linear measurements into logarithms. Imbrie (1956) showed empirically that better results would be obtained by the method of reduced major axis and by the transformation of original bivariate data into logarithms. As exemplified in text-figs. 4 and 5, it is reasonable to consider that the deviation for each individual is well represented by some standardized distance from the line of average allometry (= reduced major axis). Although there are several different methods to measure the deviation, we like to discuss the frequency distribution of the distance collectively in terms of *allometric variation*.

REPRESENTATION OF ALLOMETRIC VARIATION

In order to recognize allometric growth it is convenient to plot the original bivariate data on a double logarithmic paper (see text-fig. 5). If a linear relation was expected

between log x and log y in the scatter diagram by intuition or high value of correlation coefficient, a power equation for the average ontogenetic allometry could be justified.

Sometimes, however, the average relative growth of an organism might better be regarded as a more complicated function. Some authors have expressed such a relation by the composition of connected lines of different slopes, where 'di or poly-phasic allometry' might be suggested. In such a case the sample may better be split, though artificially, into several classes of different ontogenetic stages in accordance with the expected 'critical point(s)', before the equation of average ontogenetic allometry is determined. Simpson, Roe, and Lewontin (1960, p. 413) and many others introduced such a procedure. In the study of average allometry, however, this state may hardly be discriminated from the gradual change of specific growth ratio. Therefore, precise examination on the individual relative growth may be also necessary for the recognition of 'poly-phasic allometry'. This problem was discussed on a theoretical and biological basis by Gould (1966). He is of the opinion that the so-called 'poly-phasic allometry' and 'critical point(s)' are usually nothing but pure artifacts of an improper procedure [personal communication from Dr. S. J. Gould (17 September 1969)].

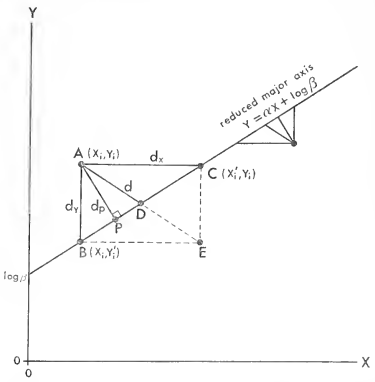

TEXT-FIG. 6. Various distances from the reduced major axis. A (X_i, Y_i) are the coordinates for an arbitrary individual. d_Y (= AB): Y-distance; d_X (= $\overline{AC}$): X-distance; d (= $\overline{AD}$): diagonal distance; d_P (= $\overline{AP}$): perpendicular distance.

Many authors have assumed that α is constant in one population or even in one species and that β is related principally to the individual or geographic variation. Actually, however, the value of α must vary to some extent among individuals of the same population. This is, in fact, a very troublesome problem, because the variability of α could not be clarified without a detailed analysis of individual growth. Therefore, it is not quite adequate to discuss the variation by means of the initial growth indices for individuals on the assumption of strictly parallel lines to the line of average allometry.

More adequate and easily measurable index is the actual distance from each point to the line of average allometry (the reduced major axis) on a double logarithmic scatter diagram (text-fig. 6). At least five kinds of measurements are available for the distance, namely, Y-distance, X-distance, diagonal distance, perpendicular distance, and triangle-root distance. They can be computed in the following manner:

1. Y-distance (d_Y). The distance measured parallel to the Y-axis. If log y and log x are substituted by Y and X respectively, the equation of average allometry (7) is transformed into the following simple formula:

$$Y = \alpha X + \log \beta. \tag{8}$$

When the coordinates for the point B are designated as (X_i, Y'_i), the Y-distance for an arbitrary individual is obviously given as:

$$d_Y = Y_i - Y'_i = Y_i - \alpha X_i - \log \beta. \tag{9}$$

This index was applied already by Richards and Kavanaugh (1945) and quoted by Simpson, Roe, and Lewontin (1960) in relation to the analysis of 'di-phasic' allometry.

2. X-distance (d_X), the distance measured parallel to the X-axis. If the coordinates for the point C are defined as (X'_i, Y_i), the X-distance is represented as:

$$d_X = X'_i - X_i = \frac{Y_i - \log \beta}{\alpha} - X_i. \tag{10}$$

3. Diagonal distance (d). Imbrie (1956) suggested that one of the most reasonable indices for the deviation is the diagonal distance ($\overline{AD}$) from each point to the line of average allometry which is determined by the method of reduced major axis. This index could be calculated in the following manner:

$$\overline{AD} = \tfrac{1}{2}\overline{AE} = \frac{\sqrt{\{(\overline{AB})^2 + (\overline{AC})^2\}}}{2}.$$

Therefore,

$$d = \frac{\sqrt{(d_Y^2 + d_X^2)}}{2} = \frac{(Y_i - \alpha X_i - \log \beta)\sqrt{(\alpha^2 + 1)}}{2\alpha}. \tag{11}$$

4. Perpendicular distance (d_P). This is of course the shortest distance ($\overline{AP}$), which is measured perpendicularly from each point to the line of average allometry. It is actually similar to the deviation in the method of 'major axis', where the line of best-fit is obtained by minimizing the sum of the squares of the perpendicular distance. Kermack and Haldane (1950) and Imbrie (1956) pointed out its inappropriateness for the determination of the line of average allometry, because its slope may change with the unit of measurement. In discussing the deviation from the already determined line of average allometry, however, this distance seems to be one of the meaningful indices. Because ΔPBA is a similar figure to ΔABC (see text-fig. 6), the value of perpendicular distance can be determined in the following manner:

$$\frac{\overline{AP}}{\overline{AB}} = \frac{\overline{AC}}{\overline{BC}}, \qquad \overline{AP} = \frac{\overline{AB}.\overline{AC}}{\overline{BC}} = \frac{\overline{AB}.\overline{AC}}{\sqrt{\{(\overline{AB})^2 + (\overline{AC})^2\}}}.$$

Therefore,

$$d_P = \frac{d_Y . d_X}{\sqrt{(d_Y^2 + d_X^2)}} = \frac{Y_i - \alpha X_i - \log \beta}{\sqrt{(\alpha^2 + 1)}}. \tag{12}$$

5. Triangle-root distance (d_R). A reduced major axis is obtained by minimizing the sum of the areas of triangles ΔABC. Therefore, the square root of the area of each triangle may be also a useful index for the deviation, although it can be hardly measured directly on a scatter diagram

$$d_R = \sqrt{\left(\frac{\overline{AB}.\overline{AC}}{2}\right)} = \sqrt{\left(\frac{d_Y . d_X}{2}\right)} = \frac{Y_i - \alpha X_i - \log \beta}{\sqrt{(2\alpha)}}. \tag{13}$$

The actual values of these distances are always positive for the points above the line of average allometry and always negative for those below the line. This may be a convenient nature for further statistical treatment.

As readily recognized from the formulae (9)–(13), the values of these distances are completely proportional to one another.

$$d_Y : d_X : d : d_P : d_R = 1 : \frac{1}{\alpha} : \frac{\sqrt{(\alpha^2+1)}}{2\alpha} : \frac{1}{\sqrt{(\alpha^2+1)}} : \frac{1}{\sqrt{(2\alpha)}}. \tag{14}$$

Therefore, the following relation is also recognized as to the absolute values of distances for an arbitrary individual:

$$|d| \geqslant |d_R| \geqslant |d_P|. \tag{15}$$

The value of sample standard deviation also depends upon the above proportional expression (14). Consequently one would obtain essentially the same pattern of frequency distribution, whatever distances might be applied as the index. Every distance may be applicable for the representation of variation, but, we think, the diagonal distance is the best, when the two variables are the same in dimensions. However, provided that one variable is dependent on the other (whorl height of coiling shell versus volution number for example), it may be desirable to apply the Y-distance from the ordinary regressed line (Y on X).

Generally speaking, the degree of variability should be expressed on the basis of the value of sample standard deviation (s) in comparison with the sample mean (M), as Pearson's coefficient of variation (V) is defined as:

$$V = \frac{100s}{M}. \tag{16}$$

In discussing the variability of the distance from the reduced major axis, Teissier (1948) gave the following expression for the variance of diagonal distance, using the vector sum of d_Y and d_X:

$$s_d^2 = \tfrac{1}{2}\{(1-r)(s_X^2+s_Y^2)\} \tag{17}$$

where s_X and s_Y are the sample standard deviations of X and Y, and r is the the correlation coefficient between the two variables. As discussed by Imbrie (1956), the value of the variability of d should be represented by the value of s_d in comparison with the joint mean of $\bar{X}$ and $\bar{Y}$.

$$V_d = \frac{100s_d}{\sqrt{(\bar{X}^2+\bar{Y}^2)}} = 100\sqrt{\left\{\frac{(1-r)(s_X^2+s_Y^2)}{2(\bar{X}^2+\bar{Y}^2)}\right\}}. \tag{18}$$

(Imbrie (1956) actually gave the coefficient of variability for twice the diagonal distance of the present usage.) In applying this parameter to this coefficient we could discuss the variability of a bivariate character. It is generally supposed that the variability of diagonal distance is smaller than that of the simple ratio, if the relative growth of an organism is better represented by a power function than a linear equation.

AN EMPIRICAL EVALUATION OF ALLOMETRIC VARIATION ON THE BASIS OF ACTUAL DATA

As discussed above, it is theoretically certain that the variation of distance from the line of average allometry (reduced major axis in double logarithmic field) is a more desirable representation for a bivariate character than that of a simple ratio. We might be able to recognize the advantage of the former method also empirically, if these two methods were applied independently to the same sample. In the present article we intend to take a fossil sample of *Glycymeris* (Bivalvia) as an illustrative example.

The following is the basic information about the sample here analysed.

Specific name. *Glycymeris rotunda* (Dunker).

Locality. Loc. 4, Ugari, Fukuroi City, Shizuoka Prefecture, central Japan (collected by A. Matsukuma). This is probably the same as Loc. 525 described by Makiyama (1941).

Horizon. Hosoya tuffaceous siltstone member of the Kakegawa group.

Age. Kechienjian stage (Pliocene).

Statistical sample. Only right valves were used. The sample is composed of 203 individuals which were collected randomly from a fossil bed. They consist of individuals of quite various size, although smaller ones are relatively abundant (see text-fig. 8).

For the sake of convenience the following characterization is applied for the linear measurements and related auxiliary variables (see also text-fig. 7).

x: The length of the dental plate measured from the umbo to the posterior extremity.
y: The length of the dental plate measured from the umbo to the anterior extremity.
z: The simple ratio between the two linear measurements (y/x).
X: The common logarithms of x [$X = \log x$].
Y: The common logarithms of y [$Y = \log y$].

The values of x and y were measured strictly along the direction parallel to the basal line of ligament area. The mensuration was carried out by means of a specially designed comparator which was recently introduced by Shuto (1969, p. 49).

1. *Analysis of isometric variation*

From the bivariate data of the 203 individuals the following fundamental values were calculated in relation to the isometric variation:

$$\bar{z} = \frac{1}{203}\sum \frac{y_i}{x_i} = 1{\cdot}16651,$$

$$s_z = \sqrt{\left\{\frac{\Sigma(z_i - \bar{z})^2}{202}\right\}} = 0{\cdot}11788,$$

$$V_z = \frac{100 s_z}{\bar{z}} = 10{\cdot}105.$$

As shown in text-fig. 9 and also in Table 1, the null hypothesis for goodness-of-fit of the actual data to a normal distribution is accepted.

Kurtosis is the property of being more pointed or flatter than a normal curve. As noted by Simpson, Roe, and Lewontin (1960, pp. 146–7), the best measure of kurtosis (Ks) is given as follows:

$$Ks = \frac{\Sigma(x_i - \bar{x})^4}{N s^4} - 3, \tag{19}$$

where N is the number of individuals and s the sample standard deviation. In this case we obtained the following value as the kurtosis coefficient for the distribution of z:

$$Ks = \frac{\Sigma(z_i - \bar{z})^4}{203 s_Z^4} - 3 = -0{\cdot}5257.$$

Because the value is negative, the distribution is flatter than the normal curve and may be said to be platykurtic. We presume that this tendency is partly due to the gradual

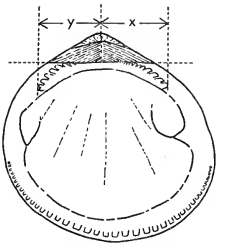

TEXT-FIG. 7. Linear measurements (in millimetres) adopted in the present study. *x*: The length of dental plate from the umbo to the posterior extremity; *y*: The length of dental plate umbo to the anterior extremity.

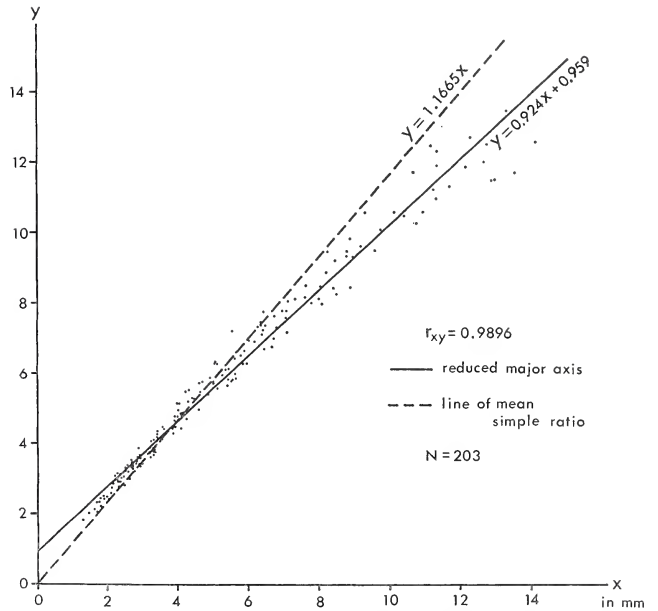

TEXT-FIG. 8. Scatter diagram for a sample of *Glycymeris rotunda* (Dunker) from a fossil bed of the Kakegawa group at Loc. 4, Ugari, Fukuroi City, Shizuoka Pref., Japan. The reduced major axis does not fit to the original bivariate data especially in small individuals.

change of z through the growth of each individual. In fact, the average value of z is much larger in smaller individuals than in larger ones.

Skewness is a parameter showing the property of asymmetric frequency distribution. It is commonly given as:

$$Sk = \frac{\Sigma(x_i - \bar{x})^3}{Ns^3}. \tag{20}$$

TABLE 1

Calculation of χ^2 for goodness-of-fit of the observations of z to a normal distribution

Simple ratio (y/x)		Normal probability	Observed frequency (O_i)	Expected frequency (E_i)	$\frac{(O_i-E_i)^2}{E_i}$
$\bar{z}-3s_z \sim \bar{z}-2s_z$	(0·8128∼0·9307)	0·0215	5	4·36	0·0939
$\bar{z}-2s_z \sim \bar{z}-s_z$	(0·9307∼1·0486)	0·1359	32	27·59	0·7049
$z-s_z \sim \bar{z}$	(1·0486∼1·1665)	0·3413	64	69·28	0·4024
$\bar{z} \sim \bar{z}+s_z$	(1·1665∼1·2844)	0·3413	71	69·28	0·0427
$\bar{z}+s_z \sim \bar{z}+2s_z$	(1·2844∼1·4023)	0·1359	30	27·59	0·2105
$\bar{z}+2s_z \sim \bar{z}+3s_z$	(1·4023∼1·5202)	0·0215	1	4·36	2·5894
Total		0·9974	203	202·46	4·0438

$$\chi^2 = \sum \frac{(O_i-E_i)^2}{E_i} = 4{\cdot}04 \quad \text{[with 3 degrees of freedom].}$$

$\chi^2_{0\cdot05(\nu=3)} = 7{\cdot}81.$

$0{\cdot}25 < P < 0{\cdot}30.$

For reference: If the data of z are regrouped to interval $0{\cdot}5s_z$, the result of χ^2 test is as follows:

$\chi^2 = 11{\cdot}95$ [with 7 degrees of freedom]

$\chi^2_{0\cdot05(\nu=7)} = 14{\cdot}07.$

$0{\cdot}10 < P < 0{\cdot}15.$

This coefficient is positive in a right-skewed distribution and negative in a left-skewed distribution. In the present sample the following value was obtained for the skewness of the distribution of z.

$$Sk = \frac{\Sigma(z_i-\bar{z})^3}{203s_Z^3} = -0{\cdot}2250.$$

The left-skewed distribution is possibly related to the sample heterogeneity especially the relative abundance of small individuals.

Incidentally, we obtained the following values as to the correlation coefficient between the two linear measurements and the reduced major axis.

$r_{xy} = 0{\cdot}9896$ [0·9862—0·9921 for the 95 per cent confidence interval],

$y = 0{\cdot}924x + 0{\cdot}959.$

2. *Analysis of allometric variation*

The reduced major axis (best-fitted line of average allometry) for the present sample was determined in the following manner:

$$\bar{X} = 0{\cdot}64791, \qquad \bar{Y} = 0{\cdot}71253,$$

$$s_X = 0{\cdot}25213, \qquad s_Y = 0{\cdot}21411.$$

The following value was obtained for the correlation coefficient between X and Y:

$$r_{XY} = 0{\cdot}9948 \text{ [0·9931—0·9961 for the 95\% confidence interval]}.$$

Therefore, the correlation between the two variables is very significant. The slope of reduced major axis is given by the formula (5),

$$\alpha = \frac{s_Y}{s_X} = \frac{0{\cdot}21411}{0{\cdot}25213} = 0{\cdot}84920.$$

From the formula (8), $\log \beta = Y - \alpha X$.

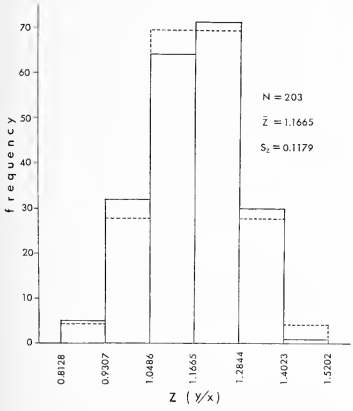

TEXT-FIG. 9 Frequency distribution of z (= y/x). The broken lines show the expected values in theoretical normal distribution.

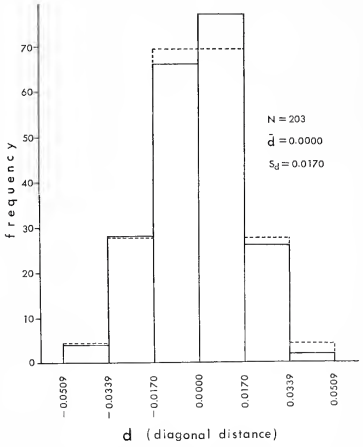

TEXT-FIG. 10. Frequency distribution of d (diagonal distance from the reduced major axis). The broken lines show the expected values in theoretical normal distribution.

By the substitution of $\bar{X}$ and $\bar{Y}$,

$$\log \beta = 0{\cdot}71253 - 0{\cdot}84920 \times 0{\cdot}64791 = 0{\cdot}16232.$$

Therefore, the reduced major axis for the present sample is represented by the following equation:

$$Y = 0{\cdot}84920X + 0{\cdot}16232 \quad \text{or} \quad y = 1{\cdot}4532x^{0{\cdot}84920}.$$

The standard error of the slope (α) is given as:

$$\sigma_\alpha = \alpha \sqrt{\left(\frac{1-r^2}{N}\right)} = 0{\cdot}84920 \times \sqrt{\left(\frac{1-0{\cdot}9948^2}{203}\right)} = 0{\cdot}00608.$$

Consequently, the interval of α with 95% confidence is:

$$\alpha \pm 1{\cdot}96\sigma_\alpha = 0{\cdot}84920 \pm 0{\cdot}01192.$$

Therefore, the relative growth is certainly allometric. The diagonal distance (d), which

is measured from each point to this reduced major axis in a double logarithmic field, is given as:

$$d = \frac{(Y_i - \alpha X_i - \log \beta)\sqrt{(\alpha^2+1)}}{2\alpha} = 0{\cdot}77245(Y_i - 0{\cdot}84920X_i - 0{\cdot}16232).$$

The computation of d for 203 individuals results in:

$$\bar{d} = 0{\cdot}00002 \quad \text{[negligible]}$$

$$s_d = 0{\cdot}01697.$$

TABLE 2

Calculation of χ^2 for goodness-of-fit of the observations of d to a normal distribution

Diagonal distance (d)		Normal probability	Observed frequency (O_i)	Expected frequency (E_i)	$\frac{(O_i-E_i)^2}{E_i}$
$\bar{d}-3s_d \sim \bar{d}-2s_d$	$(-0{\cdot}0509 \sim -0{\cdot}0339)$	0·0215	4	4·36	0·0297
$\bar{d}-2s_d \sim \bar{d}-s_d$	$(-0{\cdot}0339 \sim -0{\cdot}0170)$	0·1359	28	27·59	0·0061
$\bar{d}-s_d \sim \bar{d}$	$(-0{\cdot}0170 \sim 0)$	0·3413	66	69·28	0·1553
$\bar{d} \sim \bar{d}+s_d$	$(0 \sim 0{\cdot}0170)$	0·3413	77	69·28	0·8603
$\bar{d}+s_d \sim \bar{d}+2s_d$	$(0{\cdot}0170 \sim 0{\cdot}0339)$	0·1359	26	27·59	0·0916
$\bar{d}+2s_d \sim \bar{d}+3s_d$	$(0{\cdot}0339 \sim 0{\cdot}0509)$	0·0215	2	4·36	1·2774
Total		0·9974	203	202·46	2·4204

$$\chi^2 = \sum \frac{(O_i-E_i)^2}{E_i} = 2{\cdot}42 \quad \text{[with 3 degrees of freedom].}$$

$\chi^2_{0{\cdot}05(\nu=3)} = 7{\cdot}81.$

$0{\cdot}40 < P < 0{\cdot}50.$

For reference: If the data of d are regrouped to interval $0{\cdot}5s_d$, the result of χ^2 tests is as follows:

$\chi^2 = 10{\cdot}00$ [with 7 degrees of freedom].

$\chi^2_{0{\cdot}05(\nu=7)} = 14{\cdot}07.$

$0{\cdot}15 < P < 0{\cdot}20.$

If the formula (18) were applied for the estimation of variability, the coefficient of variation might be shown:

$$V_d = \frac{100s_d}{\sqrt{(\bar{X}^2+\bar{Y}^2)}} = \frac{1{\cdot}697}{\sqrt{(0{\cdot}6479^2+0{\cdot}7125^2)}} = 1{\cdot}762.$$

As shown in text-fig. 10 and also Table 2, the frequency distribution of d is also regarded as normal. The distribution seems to be also platykurtic in view of the negative value of kurtosis coefficient:

$$Ks = \frac{\Sigma(d_i-\bar{d})^4}{203s_d^4} - 3 = -0{\cdot}3570.$$

The skewness for the distribution of d is given as:

$$Sk = \frac{\Sigma(d_i-\bar{d})^3}{203s_d^3} = -0{\cdot}0292.$$

It means a slightly left-skewed distribution.

3. *Comparisons and discussions*

Now, we intend to compare the result obtained by the method of diagonal distance with that by the method of simple ratio. The obtained value of sample correlation coefficient between X and Y is significantly higher than that between x and y. We presume that the appropriateness of the index for a bivariate character is indicated to a certain extent by the smallness of the coefficient of variation. Although direct comparison may not be meaningful, the value of V_d is obviously much smaller than V_z.

The result of χ^2 test for the frequency distribution of d supports the null hypothesis of a normal distribution. The value of χ^2 (with the same degrees of freedom) is more or less smaller and the probability for a normal distribution higher than those for the distribution of z (Tables 1 and 2). In this respect the pattern of histogram of d is more safely assumed to fit a theoretical normal curve than is that of z.

As to the coefficients of kurtosis and skewness, a similar assumption is possible. The values of *Ks* and *Sk* indicate that the frequency distribution of d is less platykurtic and less left-skewed than that of z.

As indicated in text-fig. 8, neither the isometric line, $y = 1{\cdot}16651x$, nor the reduced major axis, $y = 0{\cdot}924x + 0{\cdot}959$, fits the original bivariate data. On the other hand, as shown in text-fig. 11, the reduced major axis in double logarithmic field seems to represent well the relative growth of this sample. Therefore, so far as the present sample is concerned, monophasic allometry is well recognized. Judging from the comparative data aforementioned, it is concluded empirically that the diagonal distance from the reduced major axis is a more desirable index for the expression of a bivariate character than is the simple ratio between two variables.

STATISTICAL DEFINITION OF 'ISOMETRY' AND 'ALLOMETRY'

In order to identify or to discriminate samples purely statistically, Imbrie (1956) and Miller and Kahn (1962) introduced a method of significance test for the difference of two reduced major axes. It is, in fact, a very useful method, if the relative growth of each sample shows monophasic allometry.

The standard errors of the slopes or reduced major axes are given as:

$$\sigma_{\alpha_1} = \alpha_1 \sqrt{\left(\frac{1-r_1^2}{N_1}\right)} \tag{21}$$

$$\sigma_{\alpha_2} = \alpha_2 \sqrt{\left(\frac{1-r_2^2}{N_2}\right)} \tag{22}$$

where α_1 and α_2 are the slopes of two reduced major axes, r_1 and r_2 are the correlation coefficients between two variables and N_1 and N_2 are the numbers of individuals in respective samples. Provided that the numbers of individuals are not too small, one can recognize by means of the following value whether the difference of slopes is significant or not

$$Z = \frac{\alpha_1 - \alpha_2}{\sqrt{(\sigma_{\alpha_1}^2 + \sigma_{\alpha_2}^2)}}. \tag{23}$$

If $|Z| < 1{\cdot}96$, the difference of slopes is not significant with 95% confidence, and if $|Z| > 1{\cdot}96$, the two samples can be discriminated by the difference of specific growth ratio.

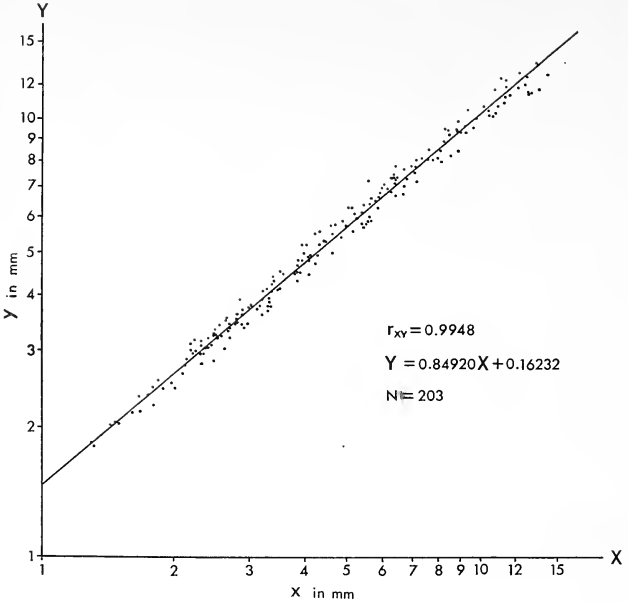

TEXT-FIG. 11. Double logarithmic scatter diagram for a sample of *Glycymeris rotunda* (Dunker) [the same sample as shown in text-fig. 8.] Because the reduced major axis fit well to the data, the relative growth can be regarded as monophasic.

Applying the method of this significance test, we can define statistically the terms of 'isometry' and 'allometry'. In the case of ideal isometry, though such a state is actually non-existent, the slope is, of course, strictly equal to 1 without error. Consequently, if the value of Z is calculated by the following equation:

$$Z = \frac{\alpha - 1}{\sigma_\alpha} = \frac{\alpha - 1}{\alpha\sqrt{\{(1-r^2)/N\}}} \tag{24}$$

one can judge with 95% confidence whether the relative growth is isometric or allometric, as follows:

if $-1{\cdot}96 < Z < 1{\cdot}96$, the null hypothesis for 'isometry' would be accepted,

if $Z < -1{\cdot}96$, negative allometry would be suggested, and

if $Z > 1{\cdot}96$, positive allometry would be suggested.

Because the simple ratio between two variables is an index on the assumption of isometry, the allometric variation is certainly a more reasonable representation than the

isometric one, if the null hypothesis were rejected by the above-mentioned significance test.

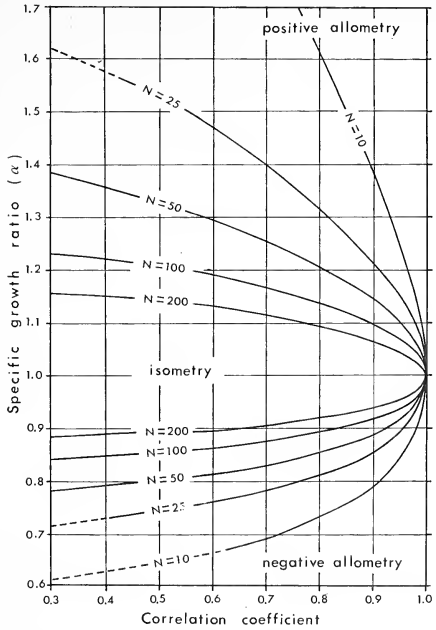

TEXT-FIG. 12. Statistical discrimination of 'isometry' and 'allometry'. *N*: number of individuals. Confidence 95%.

CONCLUDING REMARKS

It would be logically inadequate to discuss the variation of a bivariate character without considering the relative growth of the organism, if the sample is composed of individuals of various growth stages. If the simple ratio between two linear measurements were used as the index, we might have much trouble in analysing the real state of variation, especially in applying advanced statistical techniques for the recognition of a normal distribution of character and random sampling as well as taxonomic identification or discrimination. As pointed out by Simpson, Roe, and Lewontin (1960), a platykurtic and skewed distribution may be due to the heterogeneity of sample. In the analysis of bivariate characters it is necessary to apply an index which is less influenced by the age distribution.

On the other hand, if the organism proved to grow approximately in accordance with a simple power function, the individual variation within a sample could be analysed more reasonably by means of the distance from each point to the line of average allometry on a double logarithmic scatter diagram. Although at least five kinds of distance (d_Y, d_X, d, d_P, and d_R in this paper) are available for the index, this representation may be collectively called allometric variation. It is believed that this representation is more advantageous than the conventional method of simple ratio in the following respects:

1. The coefficient of variation may be reasonably small in comparison with that of simple ratio.
2. The standard deviation, skewness, and kurtosis as well as the shape of the histogram may be scarcely, if not at all influenced by the age distribution in a population and other sample heterogeneity.
3. Normal frequency distribution of bivariate characters would be recognized more reasonably on a firm basis.
4. The tendency for artificially skewed and platykurtic distribution could be avoided.
5. A comparison between different samples could be well based on the significance test for the difference of slopes and positions of reduced major axes. This procedure was fully explained by Imbrie (1956, pp. 235–8). The contingency of age distribution in samples might be negligible also in this case.
6. As pointed out by Gould (1966), the study of average allometry may not be an adequate approach to individual ontogeny, when strong natural selection takes place. The present analysis of allometric variation, however, is considered to be sometimes informative also for the consideration of the influence of natural selection and environmental factors.

The advantage of this method is also recognized empirically by a comparative study in which a sample of fossil *Glycymeris* from the Pliocene of Japan is treated as an illustrative example.

As noted by Kotaka (1953), the method of rejection ellipse may be a useful method for taxonomic identification and discrimination of fossil populations. In discussing the relation of characters on the basis of simple ratios, however, this approach may bear some difficulty, unless the ontogenetic transformation and the age distribution of samples are sufficiently considered.

On the contrary it may be an objection that the present method is somewhat time-consuming to justify its general application. More complicated techniques would be required in the organisms showing 'polyphasic' allometry. The recent rapid development of computers, however, would make the application easy, and, we believe, biometricians should not mind taking this trouble.

Acknowledgements. We express our sincere thanks to Dr. Stephen Jay Gould of Harvard University and Dr. Norman D. Newell of the American Museum of Natural History for their invaluable suggestion about the method of the reduced major axis and for their kind supervision of the manuscript. Acknowledgements are also due to Professor Tatsuro Matsumoto, Professor Ryuzo Toriyama, Dr. Tsugio Shuto, Mr. George Kato, and Mr. Tomowo Ozawa of the Department of Geology, Kyushu University; Professor Akio Kudo, Miss Kami Honda, and Mr. Kiyoshi Kawazu of the Department of Mathematics of the same university; and Dr. Ikuwo Obata of the National Science Museum (Tokyo) for their kind assistance and fruitful discussions.

REFERENCES

GOULD, S. J. 1966. Allometry and size in ontogeny and phylogeny. *Biol. Rev.* **41**, 587–640.

HUXLEY, J. S. 1932. *Problems of relative growth.* 276 pp. London.

—— and TEISSIER, G. 1936. Terminology of relative growth. *Nature*, **137**, 780–1.

IMBRIE, J. 1956. Biometrical methods in the study of invertebrate fossils. *Bull. Am. Mus. Nat. Hist.* **108**, 215–52.

KERMACK, K. A. and HALDANE, J. B. S. 1950. Organic correlation and allometry. *Biometrika*, **37**, 30–41.

KOTAKA, T. 1953. Variation of Japanese *Anadara granosa*. *Trans. Proc. Pal. Soc. Japan* [N.S.], **10**, 31–6.

MAKIYAMA, J. 1941. The Kechienjian fauna series no. 1: Evolution of gastropod genus *Siphonalia* etc. *Mem. Fac. Sci., Kyoto Imp. Univ.* [B], **16**, 75–93.

MAYR, E. 1969. *Principles of systematic zoology*. 428 pp. New York.

—— LINSLEY, E. G., and USINGER, R. L. 1953. *Methods and principles of systematic zoology*. 336 pp. New York.

MILLER, R. L. and KAHN, J. S. 1962. *Statistical analysis in the geological sciences*. 483 pp. New York.

NOMURA, E. 1926. An application of $a = kb^n$ in expressing the growth relation in the freshwater bivalve *Sphaerium lieterodon* Pils. *Sci. Rep. Tohoku Imp. Univ.* [4], **2**, 57–62.

OBATA, I. 1967. Notes on relative growth in palaeontology. *Fossils* (14), 20–39 [in Japanese].

OMORI, M. and UTASHIRO, T. 1954. Some problems on the variation of *Pecten albicans*. *Seibutsu-kagaku*, special volume (for evolution), 16–22 [in Japanese].

RICHARDS, O. W. and KAVANAUGH, A. J. 1945. The analysis of growing form. pp. 180–230. In *Essays on growth and form*, LE GROS CLARK, W. E. and MEDAWAR, P. B., eds., Oxford.

RÖHRS, M. 1961. Allometrieforschung und biologische Formanalyse. *Zeit. Morph. Anthrop.* **51**, 289–321.

SHIMIZU, S. 1959. *Relative growth*. 287 pp. Tokyo [in Japanese].

SHUTO, T. 1969. Neogene gastropods from Panay Island, the Philippines. *Mem. Fac. Sci., Kyushu Univ.* [D], **19**, (1), 1–250, pl. 1–24.

SIMPSON, G. G., ROE, A., and LEWONTIN, R. C. 1960. *Quantitative zoology*, revised ed. 440 pp. New York.

TEISSIER, G. 1948. La relation d'allométrie: sa signification statistique et biologique. *Biometrics*, **4**, 14–48.

WALLER, T. R. 1969. The evolution of the *Argopecten gibbus* stock (Mollusca: Bivalvia), with emphasis on the Tertiary and Quaternary species of eastern North America. *Paleont. Soc. Mem.* **2**, [*J. Paleont.*, **43**, Suppl. to No. 5], 1–125, pl. 1–8.

ITARU HAYAMI
AKIHIKO MATSUKUMA
Department of Geology
Faculty of Science
Kyushu University
Fukuoka 812, Japan

Typescript received 12 February 1970

THE MORPHOLOGY AND MICROSTRUCTURE OF *ZELLANIA DAVIDSONI* MOORE (BRACHIOPODA), FROM THE MIDDLE JURASSIC OF ENGLAND

by P. G. BAKER

ABSTRACT. Investigation of Oolite Marl samples from the mid Cotswolds has yielded occasional minute brachiopods which are undoubtedly specimens of the little-known species *Zellania davidsoni* Moore 1855. The material studied has enabled determination of the correct orientation, growth, development, and microstructure of the shell and provides the first record of the internal morphology of the pedicle valve. Adolescent and adult shells may be recognized, which enables the mode of development of certain internal structures to be determined. Sectioned material shows that the shell of *Z. davidsoni* is differentiated into primary and secondary layers of a type which, although unusual, may be reconciled with the shell of primitive terebratulides. Although *Z. davidsoni* occurs together with thecidellinids the form of the shell is thought to be indicative of a sheltered environment. Microstructural features exhibited by shells support the view that *Zellania* is of terebratellacean affinity. The paper records the probable location of Moore's type specimens, missing since before 1927.

Zellania is a rare, little-known micromorphic brachiopod genus of uncertain affinities, which occurs in the Jurassic of England. Material of the species *Z. davidsoni* (Moore 1855) has been obtained during a study of the brachiopod fauna of the Oolite Marl (Upper Aalenian, *murchisonae* zone) of the Cotswolds, South England.

Information on *Z. davidsoni* is singularly lacking. The account in the *Treatise on Brachiopoda* has perpetuated a misinterpretation of the type material by Moore in his original description.

Of the specimens of *Z. davidsoni* figured in the *Treatise* (fig. 741, 1*a–c*, H857) and presumably, in the absence of the types, taken from Moore (1855), 1*a* is in fact a pedicle valve and 1*b* figures the exterior of a brachial valve.

The type specimens of *Z. davidsoni* were found to be missing from the Moore collection, held in Bath City Reference Library, when it was catalogued by Dr. Wallis in 1927. The only zellanid material in the collection was a tube containing three specimens identified as types of *Zellania oolitica* Moore, ref. no. M3036. Study of these specimens reveals that they bear little resemblance to any of the published figures (Moore 1860, Davidson 1874) of *Z. oolitica* but are certainly specimens of *Z. davidsoni* bearing a very close resemblance to Moore's figured types. The author is of the opinion therefore, that it is the type material of *Z. oolitica* which is missing and inadvertently represented by the specimens of *Z. davidsoni* (M3036) which should be reinstated as the types of *Z. davidsoni*.

The rarity of *Z. davidsoni* in the Oolite Marl is indicated by the fact that the collection of specimens over a period of more than four years has yielded only two complete pedicle valves, four complete brachial valves and twenty-eight complete specimens, together with numerous brachial and a few pedicle valve fragments. It is possible that the rarity of the species may be, in part, an artefact of the fragility of the shell. The rarity of the pedicle valve is undoubtedly due to its form and lack of the strengthening effect

[Palaeontology, Vol. 13, Part 4, 1970, pp. 606–18, pls. 118–120.]

of structures such as the ridge and septum which occur in the brachial valve. The weakness of the pedicle valve may be gauged by the fact that it is often crushed into the brachial valve during compaction of the sediment. The observations contained in this paper are therefore based on a very small collection. However, the uniformity of character exhibited by the material studied indicates that the observations are nevertheless valid.

Acknowledgements. The author is indebted to Dr. J. D. Hudson, Department of Geology, the University of Leicester, for supervision of the preparation of this paper. Thanks are due to Mr. G. McTurk for preparing the stereoscan negatives and to Mr. P. Pagan, City of Bath Reference Library for access to zellanid material from the Moore collection. I wish to thank Professor P. C. Sylvester-Bradley for use of the research facilities of the Department of Geology, the University of Leicester.

Registration of material. The material figured in this paper, together with original and duplicate peels is to be housed in the museum collection of the Department of Geology, the University of Leicester, under the catalogue numbers quoted.

PREPARATION OF MATERIAL

The material studied was obtained during the collection of thecidellinids from the Oolite Marl. A detailed account of the preparation of Oolite Marl residues and the investigation techniques employed, is given in Baker (1969) with minor amendments in Baker (1970).

Early attempts to section *Z. davidsoni* by the methods employed for *M. granulosa* were unsuccessful because peculiarities of the microstructure of the shell allowed blocks of shell to be lifted away during the production of cellulose acetate peels. This, combined with the relatively very thin zellanid shell and poorly consolidated matrix led to rapid disaggregation of the shell layers. Vacuum embedding was tried with considerable success but some difficulty with peel bubbling was still encountered owing to the porous matrix. This can be eliminated by running hot paraffin wax on to the specimen prior to each successive stage of sectioning. The wax soaks into the matrix and solidifies. The wax overlying the shell material is, of course, removed as the block is ground preparatory to re-etching but sufficient wax remains in the matrix to act as an effective sealant.

MORPHOLOGY

Information concerning the morphology of *Zellania davidsoni* is limited. The accounts in Moore (1855) and in the *Treatise on Brachiopoda* (1965) concern only the brachial valve and need some amplification. Detailed examination of the internal ridges (Moore 1855) (inner ridges, Treatise) of the brachial valve in serial transverse section (Pl. 120, fig. 7) shows that they are structurally ridges (by definition, Williams 1965 H152), though appearing more in the manner of outwardly inclined flanges (Pl. 118, fig. 7; text-figs. 1B, 2K–P). They occupy a position similar to that of the sub-peripheral rim of thecidellinids (Baker 1969) but arise in a different manner (Baker 1970) and apparently performed a function similar to the lophophore platform of the plectambonitacean *Leptellina*. There is no evidence that the structure seen in the brachial valve of *Z. davidsoni* is any way related to the lophophore platform of *Leptellina*. It is by definition not a flange. It performed a function different from that of the thecidellinid

sub-peripheral rim. In order to avoid confusion therefore, it is proposed to refer to the structure as a *sub-marginal ridge*.

Figures of the interior of the brachial valve in Moore, C. (1855) and Elliott (in Moore, R. C. 1965) indicate a depression at the end of the median septum (clearly visible in specimen M3036). Studies show that the septum is a hollow structure for much of its length (Pl. 119, figs. 1–3, text-figs. 1B, 2P–R) and that the floor of the cavity is endopunctate in the normal manner (Pl. 119, fig. 1). It is proposed to refer to this cavity as an *intra-septal cavity*. Counterparts of the sub-marginal ridge and median septum are found in the pedicle valve and it is proposed to term them *lateral ancillary ridges* and *ancillary septum* respectively.

Growth and external morphology. Z. davidsoni (Pl. 118, figs. 1–4) is a very small form. The growth is mixoperipheral, leading to a strophic condition, with a rectimarginate commissure. The width : length ratio of the shell is in the order of 1·2 : 1 and specimens rarely exceed 1·3 mm. in length. Specimens in which the protegulum (Pl. 118, fig. 4) and growth-lines are visible, show that the width:length ratio does not change appreciably throughout the life of the animal. Small forms, here correlated with adolescents (Pl. 118, fig. 6), are almost biconvex. During growth the pedicle valve retains its convexity but the brachial valve shows a declining vertical growth component (Rudwick 1959) so that adults have a characteristic plano-convex lateral profile (Pl. 118, fig. 2). The adult shell outline is typically shield-shaped (Pl. 118, fig. 1) but subject to some variation, adolescents particularly having a more rounded outline (Pl. 118, fig. 5). The interareas are anacline and relatively well developed, the dorsal interarea being only slightly smaller than that of the pedicle valve. The pedicle opening (Pl. 118, fig. 4), as stated in the *Treatise on Brachiopoda*, is amphithyridid and it is relatively very large. Stereoscan photomicrographs reveal that the feeble striate ornamentation of shells is in fact a series of radially arranged fissures (Pl. 119, figs. 7, 8) penetrating the primary shell but not extending down into the secondary shell layer. At ×250 magnification incipient striae are found to be present on smooth shells also.

Z. davidsoni is unusual in that the umbo of the brachial valve projects posteriorly to a greater degree than the umbo of the pedicle valve and gives the appearance of being

EXPLANATION OF PLATE 118

Stereoscan photomicrographs of *Zellania davidsoni* Moore, from the Oolite Marl, Westington Hill Quarry near Chipping Campden. All specimens coated with evaporated aluminium before photography.

Figs. 1–4. Brachial, lateral, anterior and posterior views of an adult specimen (37530), showing the shield-shaped outline, fig. 1; the posterior extension of the brachial umbo and plano-convex lateral profile, fig. 2 (tilt angle 88°); the rectimarginate commissure, fig. 3; the interareas, protegula and large amphithyridid pedicle opening, fig. 4. ×60.

Fig. 5. Pedicle view of an adolescent shell (37531) showing the rounded profile. Shell surface coated with crystallites. ×66.

Fig. 6. Near lateral view of an adolescent shell (37532) showing the relatively more biconvex lateral profile. ×60.

Fig. 7. Interior view of an adult brachial valve (37533) showing the cardinal process, sockets, and the sub-marginal ridge and hollow median septum with denticulate anteriors. ×55.

Fig. 8. Interior view of an adolescent brachial valve (37534) showing the short sub-marginal ridge and short median septum with no intra-septal cavity. ×60.

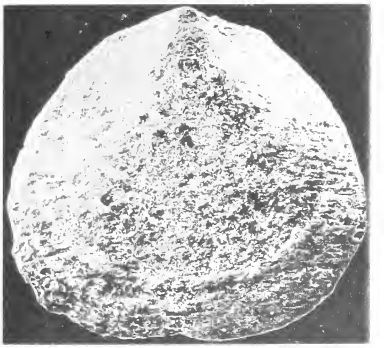

1

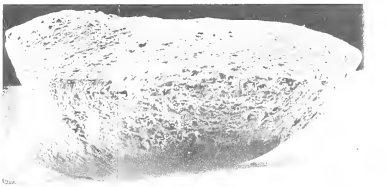

2

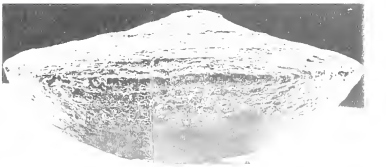

3

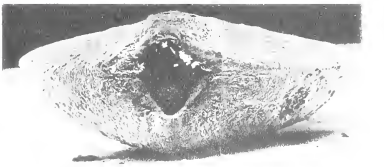

4

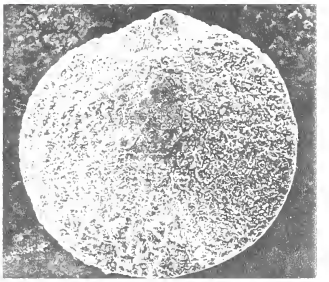

5

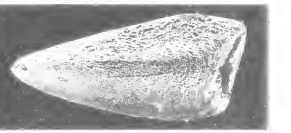

6

7

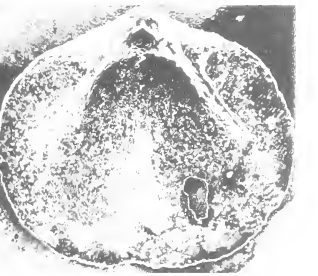

8

BAKER, *Zellania davidsoni*

a pedicle valve, probably accounting for the error in the *Treatise* (Elliott, in Moore 1965, H857). The significance of this arrangement in terms of life-attitude will be discussed later.

Interior. Brachial valve. The adult brachial valve (Pl. 118, fig. 7) is regularly endopunctate, with a large notothyrium. Its internal morphology is dominated by the sub-marginal ridge and a hollow median septum. These structures were present in the valves of all sizes studied, although degree of development was found to vary. In smaller specimens the ridge terminates in the lateral zones of the shell. The cardinal process is very small and transversely concave in a manner similar to that of thecidellinids (Baker 1969, text-fig. 2B) but not contributing to the formation of socket ridges (Pl. 119, fig. 1; text-fig. 2A–D). The muscle pattern is not known but two depressions at the base of the cardinal process may represent diductor muscle scars. The socket ridges are very prominent (Pl. 119, fig. 2) and in fact bound the notothyrium, the outer socket ridge being represented by the edge of the dorsal interarea. In none of the stereoscanned material has the granulation described by Moore (1855) been seen. Certain shells however, show the development of crystallites on the internal surface and it is possible that it is to these that Moore was referring. If, in fact, the specimens M3036 are the types of *Z. davidsoni* this speculation becomes virtual certainty. The interior of the brachial valve represented has this crystallite covered surface and has been coated with glue, obviously for the purpose of repairing the damaged median septum. The optical effect of the glue-coated crystallites is to produce an apparently granular interior. The presence of this septum is important as Davidson 1874, p. 113, states that in *Z. oolitica* there is no indication of the presence of a septum in either valve.

Interior. Pedicle valve. The pedicle valve (Pl. 119, figs. 4, 5) is concave, endopunctate, with a large open delthyrium bounded by what may presumably be regarded as tooth ridges although the teeth themselves are very weakly developed. They appear as two posteriorly arching flaps, almost indistinguishable from the secondary shell material of the ventral interarea and invariably broken in separated valves. The apex of the delthyrium is occupied by a concave plate, lying between the tooth ridges on the floor of the valve in the position of a pedicle collar. Serial sections show the development of a small ridge, the lateral ancillary ridge (text-fig. 2I–N) also sub-marginal in position and situated in the postero-lateral and lateral zones of the shell (Pl. 119, fig. 6). The orientation of these ridges is such that they abut against the edge of the sub-marginal ridge when the valves are closed. There are no visible muscle scars but transverse sections of shells show a callus on the floor of the valve which may have been the site of muscle scars. From the anterior of this thickened region, a thin blade-like septum extends almost to the anterior of the valve (text-fig. 1D) and is almost in contact with the median septum when the valves are closed.

Development of structures. On the basis of faunal analyses conducted for other studies, *Z. davidsoni* may be regarded as comprising approximately 0·04% of the brachiopod fauna of the Oolite Marl in Westington Hill Quarry (Baker 1969); and even if the number of specimens is drastically reduced by fragmentation it is indeed a rare species. Any attempt at detailed ontogenetic studies would therefore be fruitless. Owing to the delicate nature of the shell, valves are usually fragmented but sufficient material has

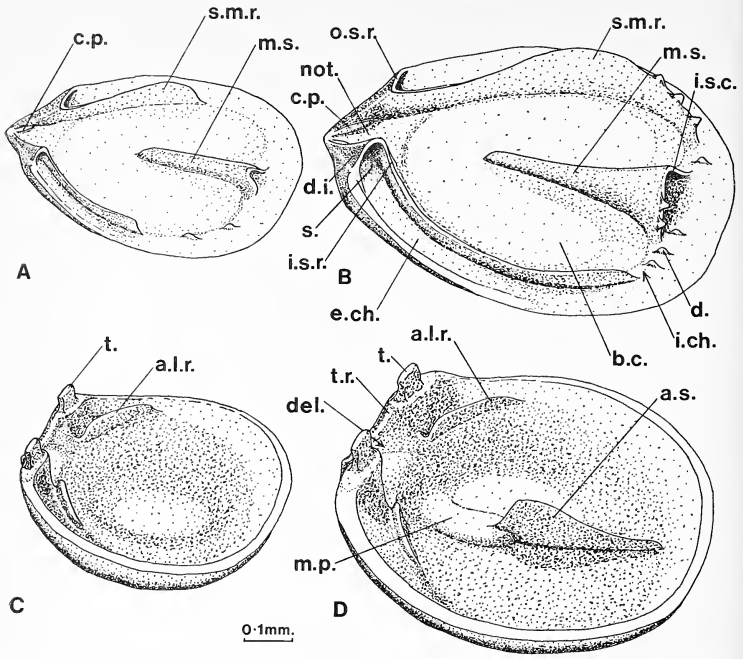

TEXT-FIG. 1. Three-quarter profile reconstructions from photomicrographs and serial sections to illustrate the internal morphology of the determinable growth stages of *Z. davidsoni*. A, B adolescent and adult brachial valves. C, D adolescent and adult pedicle valves. a.l.r. ancillary lateral ridge, a.s. ancillary septum, b.c. brachial cavity, c.p. cardinal process, d. denticle, del. delthyrium, d.i. dorsal interarea, e.ch. exhalent channel, i.ch. inhalent channel, i.s.c. intra-septal cavity, i.s.r. inner socket ridge, m.p. muscle platform, m.s. median septum, not. notothyrium, o.s.r. outer socket ridge, s. socket, s.m.r. sub-marginal ridge, t. tooth, t.r. tooth ridge.

been recovered to enable determination of the mode of development of various structures and the recognition of certain growth stages (text-fig. 1A–D).

It is possible to distinguish specimens which, by their invariably smaller size, although morphologically similar to the larger shells, may be regarded as adolescent forms. The largest shells do not exceed a length of 1·4 mm. and the argument that they represent adults is essentially that outlined in earlier studies (Baker 1969). The primitive aspect of the cardinalia and the small size, together with the form of the pedicle opening and probable form of the lophophore, suggests that, like the thecidellinids, *Zellania* is the product of neotenous modification.

Development of the sub-marginal ridge and median septum. Existing accounts state that the inner ridges (sub-marginal ridge) are reflexed anteriorly into a posteriorly directed septum. In fact, adolescent brachial valves show that the sub-marginal ridge and median septum arise separately (Pl. 118, fig. 8), and are extended anteriorly as growth proceeds.

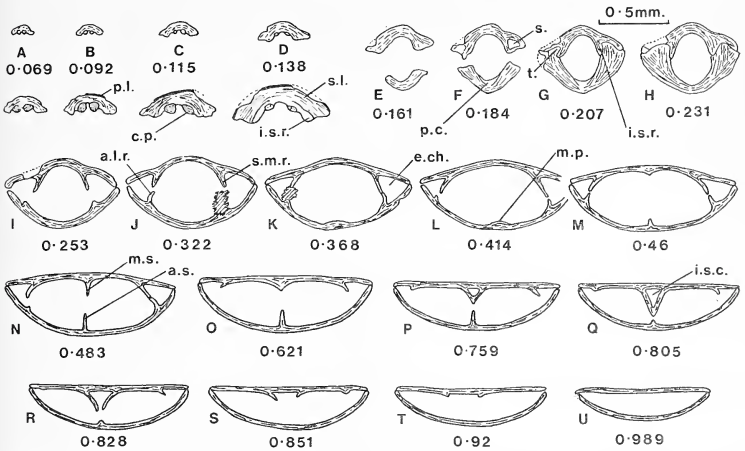

TEXT-FIG. 2. Drawings prepared from microprojected cellulose acetate peels of serial transverse sections through *Z. davidsoni* showing the morphological features in section. Number indicates distance o section in mm. from the brachial umbo. A–D reproduced at ×2 scale to show microstructure. Apparently thick pedicle valve, F–H due to obliquity of valve posteriorly relative to the plane of section (see Westbroek 1969). Recrystallization shaded. a.l.r. ancillary lateral ridge, a.s. ancillary septum, c.p. cardinal process, e.ch. exhalent channel, i.s.c. intra-septal cavity, i.s.r. inner socket ridge, m.p. muscle platform, m.s. median septum, p.c. pedicle collar, p.l. primary layer, s. dental socket, s.l. secondary layer, s.m.r. sub-marginal ridge, t. tooth.

At this adolescent stage of development the sub-marginal ridge extends little more than half the length of the valve and the median septum is a low structure, extending from near the anterior margin, posteriorly, about half-way to the cardinal process. It is only hollow at the extreme anterior end.

In adult brachial valves the sub-marginal ridge extends almost to the anterior margin and may extend in the direction of the median septum as a row of denticles (Pl. 118, fig. 7). The posterior termination of the median septum however, maintains a constant position relative to the socket ridges and cardinal process (Pl. 118, figs. 7, 8). Increase in the size of the structure must therefore, be achieved by addition of material at the anterior end and, as the walls diverge, so the intra-septal cavity increases in size.

Serial sections (Pl. 120, fig. 7; text-fig. 2K–P) show that the ridge, on the evidence of the orientation of fibres, develops from the floor of the valve. Therefore, both the ridge and median septum, in terebratuloid terms, represent ascending elements, a point of

significance in consideration of affinities. The ridge increases in size by the simple incrementa, addition of secondary material. Exactly how this occurs is not clear, but the development of denticles may be an initial feature of the anterior extension of the sub-marginal ridge and also the median septum (Pl. 119, fig. 3). Posteriorly the sub-marginal ridge forms the inner socket ridges, and the dental sockets are obviously much deepened as the ridge develops.

The sub-marginal ridge is not vertical but directed outwards (Pl. 119, fig. 2; text-fig. 2 K–P). As material is added at the summit therefore, the size of the brachial cavities must be increased. A similar trend is exhibited by the median septum. As it increases in height, the walls become more divergent (Pl. 119, figs. 1–3; text-figs. 1B, 2P–R) so that the intra-septal cavity increases in size. The result of this development pattern is the development of a border morphologically similar to that of certain thecidellinids (Baker 1969) but differing structurally and with no migration as encountered in the sub-peripheral rim of *Moorellina granulosa* (Moore) (Baker 1970).

Development of the pedicle valve. The two complete pedicle valves discovered, judging from their small size, apparently belonged to adolescent individuals. The teeth are missing but the only discernable difference between these and the valves of serially sectioned larger forms appears to be a relative decrease in the prominence of the lateral ancillary ridges as the sub-marginal ridge of the brachial valve becomes more well developed. The development of the callus on the valve floor and the development of the thin ancillary septum are apparently late ontogenetic features as they are not seen in adolescent valves of the size studied.

MICROSTRUCTURE

The material studied shows that in *Z. davidsoni* the endopunctate shell, although very thin, was clearly differentiated into primary and secondary layers (Pl. 119, fig. 8; Pl. 120,

EXPLANATION OF PLATE 119

Stereoscan photomicrographs of specimens of *Zellania davidsoni* Moore. Material of all figures coated with evaporated aluminium before photography.

Fig. 1. Interior view of a brachial valve fragment (37535) showing the endopunctation and cardinal process. The left dental socket is damaged and the hollow anterior region of the median septum has been broken away to reveal the endopunctate floor of the intra-septal cavity. ×60.

Fig. 2. Profile view of specimen (37535) to show the relative prominence of the inner socket ridges bounding the notothyrium, the inclined sub-marginal ridge, left, and the divergent anterior of the median septum. Angle of tilt 70°. ×65.

Fig. 3. Enlarged view of specimen (37533) to show detail of the denticulate anterior of the hollow median septum and sub-marginal ridge. ×110.

Fig. 4. Interior view of an adolescent pedicle valve (37536). Detail obscured by a heavy coating of crystallites but the left lateral ancillary ridge is just visible, upper left. Teeth missing. ×58.

Fig. 5. Posterior view of specimen (37536) showing the delthyrium bounded by tooth ridges. Angle of tilt 57°. ×70.

Fig. 6. Profile view of the interior of a fragment of an adolescent pedicle valve (37537) showing the lateral ancillary ridge, centre-left. Angle of tilt 70°. ×150.

Fig. 7. Enlarged portion of the exterior of the brachial valve of specimen (37538) showing the radial fissuring of the primary shell layer. ×400.

Fig. 8. Stereoscan photomicrograph of a cellulose acetate peel of a transverse section through the shell of specimen (37543) showing the fissures in the prismatic primary layer, upper, and the fibrous secondary layer. Section location: Pedicle valve, right antero-lateral sector. ×1080.

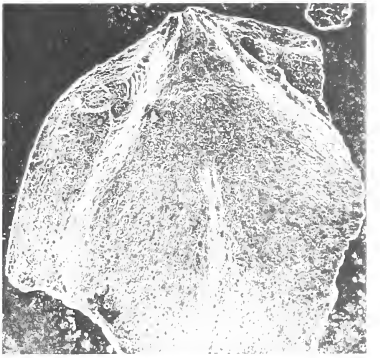

1

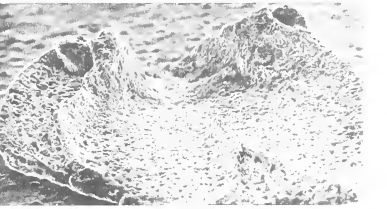

2

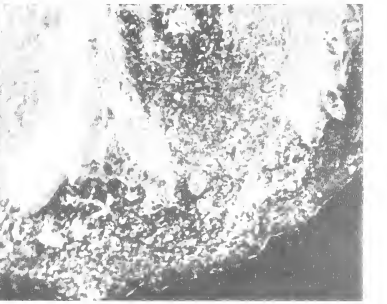

3

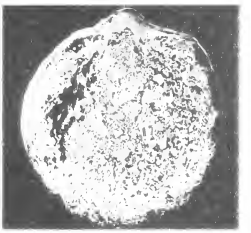

4

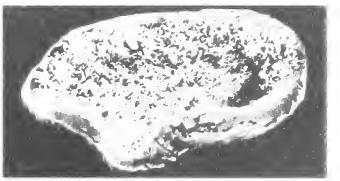

5

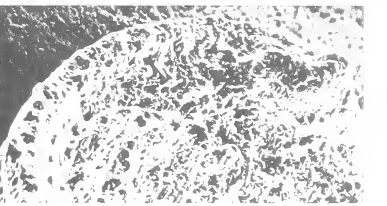

6

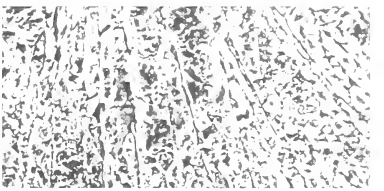

7

8

BAKER, *Zellania davidsoni*

fig. 2). Although the punctae deflect the secondary fibres in a normal (Williams 1968*a*) terebratulide manner (Pl. 120, figs. 5, 6), the microstructure of the layers themselves differs from the normal terebratulide pattern.

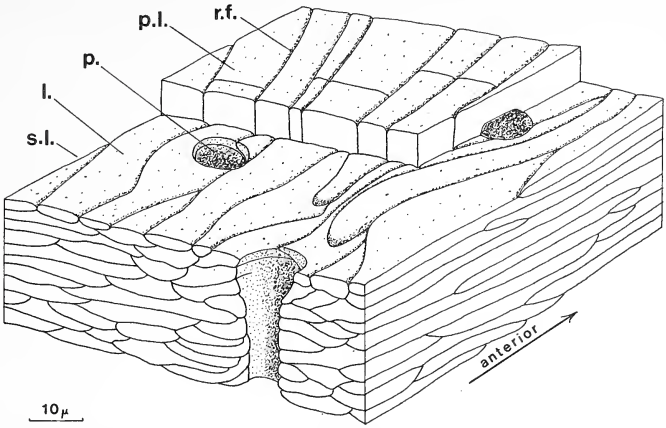

TEXT-FIG. 3. Block reconstruction of the shell of *Z. davidsoni* from photomicrographs of cellulose acetate peels, to show the form of the primary layer and the orientation and variability of the fibres of the secondary layer. l. lamina, p. puncta, p.l. primary layer, r.f. radial fissure, s.l. secondary layer.

Primary layer. The zellaniid primary layer is thin and apparently of an unusual type. Reference has already been made to the radially arranged fissures in the primary shell (Pl. 119, figs. 7, 8; Pl. 120, fig. 1). In transverse sections (Pl. 119, fig. 8) the shell material is seen to be of crystalline type and without the normal pitted appearance described by Williams (1968*a*). The persistence of the radial arrangement of the fissures and their failure to penetrate the secondary layer must indicate a more than coincidental relationship with the primary shell material. The radial pattern is relieved at intervals by cross-joints so that the primary layer in effect, consists of a series of sub-rectangular blocks of prismatic calcite (text-fig. 3). The primary layer is usually poorly preserved because the physical characteristics described contribute to its easy removal mechanically, as evidenced by the difficulties encountered during the preparation of cellulose acetate peels.

Secondary layer. Stereoscan photomicrographs of etched secondary shell surfaces and investigation by horizontal, transverse, and longitudinal serial sections, shows that the secondary shell mosaic also is of rather unusual type. Even the most careful orientation of sectioned material has failed to produce anything approaching a typical (Williams 1968*a*) terebratulide or spiriferide transverse mosaic except at the base of the teeth

(horizontal sections). Horizontal (Pl. 120, fig. 4) and transverse (Pl. 120, fig. 5) sections show that the secondary shell material appears typically as a series of sheets or very broad (20–30 μm. wide) laminae which are, in longitudinal section, disposed with normal (Williams 1956, 1966, 1968*a*) secondary orientation relative to the primary layer (Pl. 120, fig. 8). Horizontal sections show that the orientation of laminae changes rapidly, so that, in places, a zigzag rather than a spiral arc (Williams 1968*a*) secondary growth mosaic is produced.

General observations. At present the origin and purpose of the radial fissuring is unknown, but it may represent the diagenetic expression of some peculiarity in the mode of deposition of the primary shell material. The uncertainty of whether the fissures are of primary or diagenetic origin is obviously a point of considerable importance because, if primary, the features indicate in *Zellania* the existence of a new type of primary shell material. Owing to the rarity of material resolution of the problem will be difficult. A certain amount of indirect evidence is available: (*a*) shells coated with crystallites, and in which some recrystallization has obviously occurred, show obliteration of the fissuring effect, (*b*) the fissures are most clearly seen in the best-preserved material, (*c*) they are a pronounced feature of all horizontal sections through the primary layer and (*d*) it is difficult to envisage a diagenetic process which would, universally, affect the primary layer to such an extent, with no apparent effect on the secondary layer. Williams (1968*b*) suggests that the finely crystalline covering of *Billingsella* represents the recrystallized primary layer. Similar recrystallization may have occurred in *Zellania*, but it is odd that the line of demarcation between recrystallized and unaltered material should be so

EXPLANATION OF PLATE 120

Stereoscan photomicrographs of *Zellania davidsoni* Moore. Material of all figures coated with evaporated aluminium before photography and all, with the exception of fig. 3, taken from cellulose acetate peels.

Fig. 1. Horizontal section through the primary shell layer of specimen (37540) showing the radially arranged fissures and block-like nature of the primary shell. Section location: Brachial valve, anterior sector. ×1200.

Fig. 2. Horizontal section through the shell of specimen (37541) showing the primary/secondary layer junction, broken line. Shell partially recrystallized. Section location: Brachial valve, left antero-lateral sector. ×1200.

Fig. 3. External surface of specimen (37542) from which the primary layer has been removed, showing detail of the fibre mosaic at the external surface of the secondary shell layer. Normal proximal, centre right, and laminar distal, centre, regions of fibres are visible. Figure location: Brachial valve, left antero-lateral sector. ×900.

Fig. 4. Oblique section through the secondary shell layer showing endopunctae and the secondary fibres arranged as overlapping laminae. Section location. Brachial valve, right lateral sector. Section orientation: Parallel with the plane of the commissure. ×550.

Fig. 5–7. Transverse sections through specimen (37543).

Fig. 5 shows the primary layer, upper and the fibres of the secondary layer deflected by punctae. Section location: Brachial valve, right antero-lateral sector. ×540.

Fig. 6. Enlarged section to show detail of an endopuncta and deflected secondary fibres. Section location as Fig. 5. ×2000.

Fig. 7. Transverse section through the sub-marginal ridge showing the orientation of the secondary fibres. Section location. Brachial valve, right lateral sector. ×400.

Fig. 8. Longitudinal section through specimen (37544) showing the orientation of the secondary fibres relative to the primary shell layer, lower. Section location: Pedicle valve, 0·086 mm. to the left of the mid-line. ×1000.

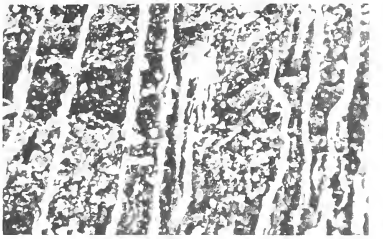

1

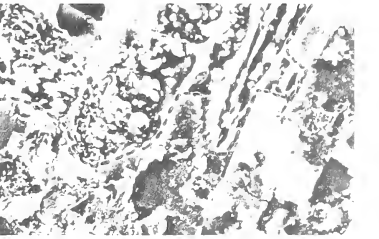

2

3

4

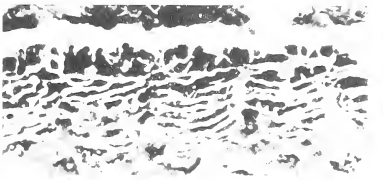

5

6

7

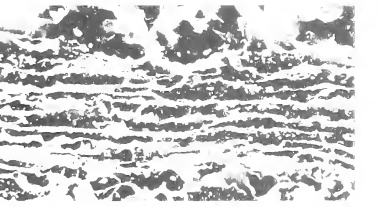

8

BAKER, *Zellania davidsoni*

abrupt, and also that the structure is present in all sections involving primary shell. Williams (1968*a*, p. 31) states that the primary layer of all specimens of *Spiriferina walcotti* (Sow.) examined is recrystallized but that the secondary shell is normally well preserved. He notes a strong lineation in the primary layer (Williams 1968*a*, pl. 11, fig. 5) normal to the shell surface and is of the opinion that this lineation may represent an original fabric. The evidence available, therefore, indicates that the microstructure of the zellanid primary layer is of secretory rather than diagenetic origin. Some transverse sections of secondary shell (Pl. 120, fig. 6) are very similar to the recrystallized secondary mosaic of *Nisusia fergusensis* (Williams 1968*b*, p. 487). However, if recrystallization in *Zellania* extended below the primary layer, so that some of the secondary fibres have been recrystallized whilst retaining their morphological characteristics, the observed features of the primary layer may also be regarded as original.

The zellaniid laminae are curiously like the flared fibres of *Moorellina granulosa* (Moore) described in Baker (1970, p. 84). In *M. granulosa*, only the distal ends of the fibres are affected but in *Z. davidsoni* this expansion has a tachygenetic expression and affects all but the extreme proximal end of the fibre. The unmodified proximal ends of some secondary fibres (Pl. 120, fig. 3) are similar to the secondary fibres (Williams 1968*a*, pl. 7, fig. 4) of *Terebratulina caput-serpentis* (Linné). However, the microstructure of the shell as a whole most closely resembles that of the stringocephalacean *Mutationella podolica* (Siemiradzki), illustrated in Williams (1968*a*, pl. 11, figs. 1–3).

PALAEOECOLOGY

Z. davidsoni occurs together with thecidellinids and other, larger, brachiopods; the probable environment of the thecidellinids is discussed in Baker (1969). It may be argued that *Zellania*, by association, occupied the same environment. The close morphological similarity between certain internal characters of *Zellania* and thecidellinids has been noted, but it has been clearly shown that the structures arise in different ways and probably performed different functions. Morphological similarity produced by convergent evolution is to be expected if the animals did occupy a similar environment. However, there are certain features of the organization of *Z. davidsoni* which render the above argument hazardous.

Analysis of the microstructure of the thecidellinid *Moorellina granulosa* in functional terms (Baker 1970) reveals the development of a reinforced shell which is entirely in agreement with the turbulent environment suggested by Ager, Baker, and Nekvasilová (in Baker 1969). The pedicle opening of *Z. davidsoni* is disproportionately large relative to the size of the animal. *Moorellina* is a cemented form and it is possible that *Zellania* required a large pedicle for anchorage. However, the shells of the two genera are in direct contrast. In *M. granulosa* the shell is thick and reinforced. In *Z. davidsoni* the shell is thin and very brittle; so brittle in fact that shells are often crushed by a degree of compaction of sediment which does not deform *Moorellina* at all. Such a shell could not survive in anything other than a sheltered environment. Dr. J. D. Hudson (personal communication) has suggested that *Zellania* may have occupied a sheltered microenvironment, e.g. protected cavities under large shells (*Ostrea*, etc.). This would afford protection whilst the animal was alive but when the pedicle decayed the shell would be liberated into the turbulent general environment. The cardinal process and teeth of

M. granulosa are strongly developed. The cardinal process of *Zellania* is small and the teeth are very fragile so that unless transportation of the shell occurred before the musculature of the animal decayed, the valves would almost certainly become disarticulated. It seems likely that the musculature would decay before the pedicle, thus allowing separation of the valves. Of the material collected however, complete specimens are the most common although the broken teeth of the pedicle valves and perforations in some brachial valves (Pl. 118, figs. 7, 8) do indicate a degree of abrasion consistent with some transportation.

There exists therefore, the apparent anomaly of a strong pedicle and a weak shell. Analysis of the shell characters of *Z. davidsoni* in environmental terms is indicative of a sublittoral mud-grade environment (Ager 1965) into which the thecidellinids, the organodetrital remains and the peri-reefal brachiopods (Baker 1969) were drifted. It is possible to reconcile a large (rather than strong) pedicle with this view, as it would afford anchorage in a soft substratum, although the anatomy of the pedicle itself is unlikely ever to be described.

The association of micromorphic brachiopods with shell debris is noted by Swedmark (1967) who records the occurrence of *Gwynia capsula* (Jeffreys) in a sub-tidal mineral sand containing a high proportion of fine broken shell. In this environment the animal apparently seeks the shelter of serpulid tube fragments.

Circumstantial evidence is provided by speculation concerning the life-attitude and the functional significance of the internal structures of *Zellania*. Analysis of the growth habit of *M. granulosa* indicates a growth pattern designed to lift the brachial apparatus away from the attachment surface (Baker 1970). This growth habit requires that the brachial valve be uppermost in position. The posteriorly projecting brachial umbo of *Z. davidsoni* may indicate similar orientation. The convex pedicle valve, possibly partially buried in the sediment, would enable the dorsally oriented, relatively plate-like brachial valve to be lifted clear of the sub-stratum (text-fig. 4A). This hypothesis is supported by a consideration of the functional significance of the sub-marginal ridge and ancillary structures. From a consideration of the thecidellinid brachial apparatus it is probable that the inner surface of the sub-marginal ridge and the sides of the median septum (text-figs. 4B, C) supported a simple schizolophe (Rudwick 1968). Study of brachiopod feeding mechanisms (Rudwick 1965, H206) indicates that in schizolophous forms the valves gape fairly widely and the filaments form a bell-like inhalent chamber. If *Zellania* occupied a mud-grade environment it is possible that under certain conditions, e.g. high turbidity, the valves did not gape as widely as normal. The denticulate anterior of the brachial valve (text-fig. 1B) may, therefore, represent the point of entry of the inhalent current when the valves were almost closed (text-figs. 4A, C). In this case it is thought that the exhalent apertures were situated postero-laterally in the zones occupied by the lateral ancillary ridges. The current flow would now be influenced by the degree of gape of the valves, as the exhalent apertures would be closed as the sub-marginal ridge and lateral ancillary ridges came together (text-fig. 4A). The virtual compartmentation of the shell (text-fig. 2) must have some significance and may be an expression of the lack of turbulence in the water, thus assisting in the separation of the inhalent and exhalent currents produced by the filaments of the lophophore.

These arguments, of course, apply equally well to occupation of a sheltered microenvironment but it is considered that the sum of the morphological and microstructural features of *Z. davidsoni* favours the postulated mud-grade environment.

AFFINITIES

The close morphological similarity between the internal characters of *Zellania* and thecidellinids has been noted, but it has been clearly shown that the structures arise in different ways, and therefore contradict Moore's (1855) view that thecideaceans and *Zellania* are related. In the *Treatise*, *Zellania* is tentatively linked with the terebratellaceans. The material studied shows all degrees of preservation but there is little doubt that the secondary mosaic is of modified terebratulide or spiriferide type. The similarity

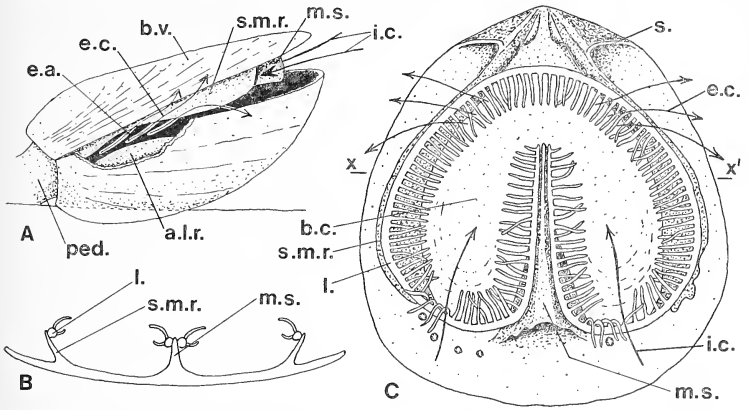

TEXT-FIG. 4. A. Diagrammatic reconstruction of the possible life-attitude of *Z. davidsoni* with the valves gaping slightly. A small portion of the pedicle valve is omitted to show the postulated exhalent aperture. B. Transverse section through X–X', fig. C. to show the postulated position of the schizolophe relative to the sub-marginal ridge and median septum. C. Diagrammatic representation of the interior of a brachial valve of *Z. davidsoni* showing the probable form and position of the lophophore and inhalent and exhalent apertures. a.l.r. ancillary lateral ridge, b.c. brachial cavity, b.v. brachial valve, e.a. exhalent aperture, e.c. exhalent current, i.c. inhalent current, l. lophophore, m.s. median septum, ped. pedicle, s. socket, s.m.r. sub-marginal ridge.

between some secondary fibres of *Z. davidsoni* and secondary fibres of *Terebratulina caput-serpentis* (Linné), and the similarity between the primary shell of *Zellania* and *Spiriferina walcotti* (Sow.), has been noted. The sub-marginal ridge is very like the loop of stringocephalids such as *Rensselandia johanni* (Hall) in a sessile position. However, the shell microstructure of *Z. davidsoni* appears to most closely resemble that of the Lower Devonian stringocephalacean *Mutationella podolica* (Siemiradzki). Studies strongly indicate that the secondary shell mosaics of even distantly related brachipods may show a similar initial development pattern, although subsequently diverging. The evidence presented in the present paper, although not solving the problem of immediate affinity, indicates that the microstructure of *Zellania* may partially recapitulate the phylogeny of the genus. It is generally accepted that recapitulation in organisms can occur, although

its value as an evolutionary criterion is open to criticism. If it is possible for the secretory regime of the secondary fibres to recapitulate phylogeny, accompanied by tachygenesis, the process may be arrested and the evidence thus preserved in neotenous forms such as *Zellania*. The dorsal cardinalia are of billingsellacean type, i.e. primitive, and work in progress, on very young terebratulides, shows that the initial development of the cardinal process of *Moorellina*, *Zellania*, and terebratulides follows the same pattern and supports the hypothesis of recapitulation.

Stehli (in Moore 1965, H739) derives both the Terebratulidina and Terebratellidina from mutationellin ancestors. The shell of *Zellania* shows mutationellin affinities. Owing to the enormous time-gap it would be ambitious to suggest that *Zellania* is descended from a stringocephalacean ancestor. However, consideration of features such as the recapitulatory nature of secondary fibre secretion, the development of the submarginal ridge from ascending elements and the typical endopunctation certainly suggest that *Z. davidsoni* may be closely related to terebratellacean stock.

REFERENCES

AGER, D. V. 1965. The adaptation of Mesozoic brachiopods to different environments. *Palaeogeography, Palaeoclimatol, Palaeoecol*, **1**, 143–72.

BAKER, P. G. 1969. The ontogeny of the thecideacean brachiopod *Moorellina granulosa* (Moore) from the Middle Jurassic of England. *Palaeontology*, **12**, 388–99.

—— 1970. The growth and shell microstructure of the thecideacean brachiopod *Moorellina granulosa* (Moore) from the Middle Jurassic of England. Ibid., **13**, 76–99.

DAVIDSON, T. 1874. Supplement to the British Jurassic and Triassic Brachiopoda, 4, 113, Suppl. Pl. 11. *Palaeont. Soc.* (*Monogr.*), *London*.

ELLIOTT, G. F. 1965. *Zellania*. *In* MOORE, R. C., ed., *Treatise on invertebrate paleontology*, Part H, *Brachiopoda*, H857. Geol. Soc. Am. and Univ. Kansas Press.

MOORE, C. 1855. On new Brachiopoda from the Inferior Oolite of Dundry. *Proc. Somerset Arch. Nat. Hist. Soc.* **5** (for 1854), 107–28, pl. 1.

RUDWICK, M. J. S. 1959. The growth and form of brachiopod shells. *Geol. Mag.* **96**, 1–24.

—— 1965. Ecology and Palaeocology. In MOORE, R. C. ed., *Treatise on invertebrate paleontology*, Part H, *Brachiopoda*, H199–213. Geol. Soc. Am. and Univ. Kansas Press.

—— 1968. The feeding mechanisms and affinities of the Triassic brachiopods *Thecospira* Zugmayer and *Bactrynium* Emmrich. *Palaeontology*, **11**, 329–60.

STEHLI, F. G. 1965. Palaeozoic Terebratulida. In MOORE, R. C., ed., *Treatise on invertebrate paleontology*, Part H, *Brachiopoda*, H730–40. Geol. Soc. Am and Univ. Kansas Press.

SWEDMARK, B. 1967. *Gwynia capsula* (Jeffreys) an articulate brachiopod with brood protection. *Nature*, 213, 1151–52.

WESTBROEK, P. 1969. The interpretation of growth and form in serial sections through brachiopods, exemplified by the trigonorhynchiid septalium. *Palaeontology*, **12**, 321–32.

WILLIAMS, A. 1956. The calcareous shell of the Brachiopoda and its importance to their classification. *Biol. Rev.* **31**, 243–87.

—— 1966. Growth and structure of the shell of living articulate brachiopods. *Nature*, *Lond.* **211**, 1146–8.

—— 1968*a*. Evolution of the shell structure of articulate brachiopods. *Spec. Pap. Palaeont.* **2**, 55 pp.

—— 1968*b*. Shell-structure of the billingsellacean brachiopods. *Palaeontology*, **11**, 486–90.

—— *et al.*, 1965. Glossary of morphological terms. *In* MOORE, R. C., ed., *Treatise on invertebrate paleontology*, Part H, *Brachiopoda*, H139–55. Geol. Soc. Am. and Univ. Kansas Press.

P. G. BAKER
Department of Biological Sciences
Derby and District College of Technology
Kedleston Road
Derby, DE3 1GB

Typescript received 6 February 1970

TEREDINID (BIVALVIA) PALLETS FROM THE PALAEOCENE OF NORTH AMERICA

by ALAN M. CVANCARA

ABSTRACT. Well-preserved teredinid pallets from the Cannonball Formation (Danian) of North America are the oldest known for that continent and constitute the second occurrence for the Palaeocene. The Cannonball pallets establish the existence of the extant genus, *Nototeredo*, in the earliest Palaeocene. All Cannonball teredinids are included within *N. globosa* (Meek and Hayden).

FOSSIL teredinid bivalve mollusks are represented usually by globular shells or calcareous tubes lining borings in wood. Unfortunately these structures are of very little taxonomic use (Turner 1966, pp. 61, 64–5). The pallets, hard structures at the base of the siphons for closing the tube, are used primarily for generic and specific determination. Because fossil pallets are discovered rarely, the purpose of this paper is to describe and illustrate well-preserved specimens from the Cannonball Formation (Palaeocene) of central North America (North Dakota).

The Cannonball pallets are the oldest known in North America; elsewhere only in Iraq have they been taken from rocks as old as the Palaeocene (Elliott 1963). Turner (1966, p. 14–17) has reviewed the fossil record of the Teredinidae and noted the relatively few occurrences of pallets from the Tertiary.

The Cannonball Formation is a clastic sequence, of up to 1300 m. (Fox and Olsson 1969, p. 1397) of largely poorly consolidated, light greyish-green sandstone and medium to very dark grey mudstone. I have synthesized the detailed stratigraphy elsewhere (Cvancara 1965). Recently, the age of the Cannonball, based on planktonic foraminiferids, has been assigned as earliest Palaeocene or early Danian (Fox and Olsson 1969, p. 1400). Macrofossils of the Cannonball consist mostly of gastropod and bivalve mollusks, (Stanton 1920, Cvancara 1966), with few crustaceans (Holland and Cvancara 1958) and small coelenterates (Vaughan 1920). Vertebrate fossils, with the exception of shark teeth, are generally rare.

The specimens figured in this paper are deposited at the University of Michigan Museum of Paleontology (UMMP).

SYSTEMATIC DESCRIPTION

Class BIVALVIA Linnaeus 1758
Family TEREDINIDAE Rafinesque 1815
Genus NOTOTEREDO Bartsch 1923

Type species. Teredo edax Hedley 1895.

Diagnosis. Pallets oval to broadly oval, with short stalk. Blade thin, outer face convex, inner face concave. Blade segmented, with segments closely packed and appearing arranged concentrically near tip, where small depression may be present. Shells like

[Palaeontology, Vol. 13, Part 4, 1970, pp. 619–22, pl. 121.

those of *Teredo*, *Lyrodus*, and *Bankia*. Tubes concamerate at posterior end. (After Turner 1966, p. 78; only those characters apparent in fossil species are included.)

Nototeredo globosa (Meek and Hayden) 1858

(for synonymy see Cvancara 1966, p. 350)

Diagnosis. Pallets (Pl. 121, figs. 4, 6–9, 11, 13) elongate, flattened-spoonlike. Stalk hollow, exposed part very short, only about $\frac{1}{6}$ of total length of pallet. On inner face of blade, stalk evidenced as only low, rounded ridge, almost imperceptible on distal half of blade.

Hypotypes. UMMP 47370 and 57578–86.

Material. See Cvancara (1966, p. 357) for all material; twenty-two, mostly incomplete, pallets are included.

Remarks. Teredinids in the Cannonball Formation are evidenced largely by shells (Pl. 121, figs. 1–3, 5, and 10) and tubes, which may be concamerate (Pl. 121, fig. 12). The tubes line borings which occur in well-preserved petrified wood or in very fine-grained sandstone and sandy claystone in which little, if any, of the wood structure remains.

Thin-sections were cut of teredinid-bored wood from six Cannonball localities (including localities 1 and 4, listed below under *Occurrence*). All wood specimens from the six localities were from the lower middle or lower part of the formation. Because of preservation inadequate for details essential for accurate identification, the taxonomy of the bored wood is uncertain. However, both 'hardwoods' and softwoods' are represented, and five species are apparently demonstrated from the six localities. Either *Sequoia* or *Metasequoia* is possibly present, and perhaps *Magnolia*, taken at localities 1 and 4.

Pallets were found at two localities, associated with the *Magnolia*? wood at locality 4 and with unidentified wood at locality 2. At both localities they have been noted in direct association with shells (Pl. 121, figs. 11 and 13, and Cvancara 1966, pl. 9, fig. 28). Pallets were found usually attached to the sides of tubes and they, with the shells, were encrusted uncommonly with calcite (Pl. 121, fig. 11).

EXPLANATION OF PLATE 121

Nototeredo globosa (Meek and Hayden). Cannonball Formation, Palaeocene. All figures are ×4 unless otherwise indicated.

Figs. 1–3. Right exterior, posterior and dorsal views of conjoined valves. Hypotype. UMMP 47370; locality 1.

Figs. 4, 7. Outer and inner faces of two different pallets. Hypotypes, UMMP 57578 and UMMP 57581, respectively; locality 2.

Fig. 5. Interior of left valve. Hypotype, UMMP 57579; locality 2.

Figs. 6, 9. Oblique and proximal views of two pallets in tube. Hypotype, UMMP 57580; locality 2.

Fig. 8. Outer face of pallet attached to tube. Hypotype, UMMP 57582; locality 2.

Fig. 10. Exterior of right valve in tube. Hypotype, UMMP 57583; locality 1.

Fig. 11. Two valves and two pallets, all calcite-encrusted, attached to tube. Hypotype, UMMP 57584; locality 4; ×2.

Fig. 12. Concamerate tubes, that on extreme left with a calcite-encrusted valve. Hypotype, UMMP 57585; locality 3; ×2.

Fig. 13. Tubes with shell and pallets; one tube (left) has conjoined valves and a single pallet and another (right) contains two pallets. Hypotype, UMMP 57586; locality 2.


1


2


3


4


5


6


7


8


9


10

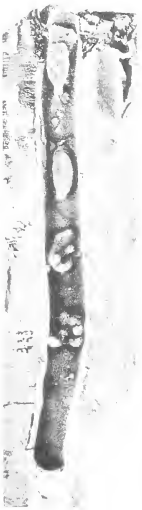
11

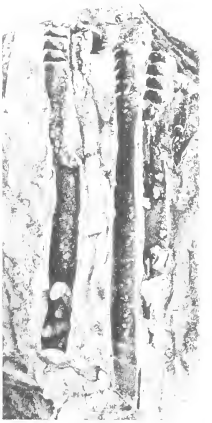
12


13

CVANCARA, Paleocene *Nototeredo*

I have placed all Cannonball teredinid material within *Nototeredo globosa* (Meek and Hayden) although pallets, for assignment to *Nototeredo*, have been taken only at two localities. The specific name '*globosa*' was based originally upon tubes and shells, but it is retained because it was the first name applied to teredinid specimens now known to occur in the Cannonball Formation. I have chosen to assume that all Cannonball teredinid shells, tubes, and pallets were secreted by the same species unless further pallet finds should indicate otherwise.

Occurrence. Pallets have been collected from the middle and lower middle parts of the Cannonball Formation, whereas other teredinid specimens have been taken essentially throughout the unit. Although I have noted teredinid material from 28 Cannonball localities, the specimens illustrated here are from the following four localities:

1. South-facing hillside, NW¼ sec. 26, T. 139 N., R. 81 W., north-west edge of Mandan Foundry, off north end of 12th Avenue Northeast, Mandan, Morton County, North Dakota; University of Michigan accession, 1961/Tpa-23. Lower part of Cannonball Formation.
2. South-facing (left) cutbank of Heart River, SE¼ sec. 10, T. 138 N., R. 83 W., about 7·4 air km. west-south-west of Mandan, Morton County, North Dakota; University of Michigan accession 1962/Tpa-10. Middle part of Cannonball Formation.
3. South-facing, upper part of Mitchell Butte, SW¼ sec. 7, T. 134 N., R. 83 W., about 2 air km. east-south-east of Flasher, Morton County, North Dakota; University of Michigan accession, 1961/Tpa-10. Lower middle part of Cannonball Formation.
4. West-facing (right) cutbank of Heart River, near centre of sec. 21, T. 136 N., R. 86 W., about 6·5 air km. south of Almont, Grant County, North Dakota; University of Michigan accession, 1962/Tpa-28. Lower middle part of Cannonball Formation.

SIGNIFICANCE OF CANNONBALL PALLETS

As noted in the introduction, the Cannonball pallets are the oldest known in North America and the second occurrence recorded from the Palaeocene. Those reported from the Palaeocene of Iraq (Elliott 1963) were described from thin-sections of petrified wood; the Cannonball specimens have been taken from empty tubes and can be studied directly.

The Cannonball specimens also establish the existence of the genus *Nototeredo* at least as early as earliest Palaeocene. This genus is presently world-wide and occurs in fully marine, tropical to cold temperate seas. The Cannonball species is closest to the living *N. norvagica* Spengler which probably occurs largely along the Atlantic European Coast and in the Mediterranean (Turner 1966, pp. 16, 78, and 258).

Acknowledgements. I wish to thank Dr. R. D. Turner, Harvard College, for aid in the generic assignment of the Cannonball teredinids. Dr. C. A. Arnold, University of Michigan, identified the teredinid-bored wood. Dr. F. D. Holland, Jr., University of North Dakota, critically reviewed the manuscript.

REFERENCES

CVANCARA, A. M. 1965. Bivalves and biostratigraphy of the Cannonball Formation (Paleocene) in North Dakota. Unpubl. Ph.D. Dissertation, Univ. Michigan, Ann Arbor, 470 pp., 10 pl.

—— 1966. Revision of the fauna of the Cannonball Formation (Paleocene) of North and South Dakota. Part 1. Bivalvia. *Contr. Univ. Mich. Mus. Paleont.* **20**, 277–374, pl. 1–9.

ELLIOTT, G. F. 1963. A Paleocene teredinid (Mollusca) from Iraq. *Palaeontology*, **6**, 315–17, pl. 51–2.

FOX, S. K., JR. and OLSSON, R. K. 1969. Danian planktonic Foraminifera from the Cannonball Formation in North Dakota. *J. Paleont.* **43**, 1397–1404, pl. 168–9.

HOLLAND, F. D., JR., and CVANCARA, A. M. 1958. Crabs from the Cannonball formation (Paleocene) of North Dakota. *J. Paleont.* **32,** 495–505, pl. 74.

STANTON, T. W. 1920. The fauna of the Cannonball marine member of the Lance formation. *Prof. pap. U.S. geol. Surv.* 128–A, 1–60, pl. 1–9.

TURNER, R. D. 1966. *A survey and illustrated catalogue of the Teredinidae (Mollusca: Bivalvia).* Cambridge, Mass. 265 pp.

VAUGHAN, T. W. 1920. Corals from the Cannonball marine member of the Lance formation. *Prof. pap. U.S. geol. Surv.* 128–A, 61–6, pl. 10.

ALAN M. CVANCARA
Department of Geology
University of North Dakota
Grand Forks
North Dakota 58201
U.S.A.

Typescript received 7 February 1970

THE DENTITION AND MUSCULATURE OF SOME MIDDLE ORDOVICIAN (LLANDEILO) BIVALVES FROM FINISTÈRE, FRANCE

by MARGARET A. BRADSHAW

ABSTRACT. The dentition and musculature of palaeotaxodontid and palaeoheterodontid bivalves from the Middle Ordovician of Finistère is described. These characters suggest that a number of species currently grouped in the genus *Ctenodonta* show closer affinity to *Cardiolaria*, *Praeleda*, and *Tancrediopsis*. The two species of *Praeleda* examined are considered to have had a reversed (nuculoid) orientation. The palaeoheterodontids *Redonia deshayesi* and *Actinodonta naranjoana* exhibit reduction of hinge teeth during ontogeny, due to fusion and resorption. An early Palaeozoic bivalve phylogeny is suggested, based on the development of the dentition within this fauna.

THE Middle Ordovician bivalves of the Crozon Peninsula (Finistère) have been referred to in many publications. Earlier work was summarized by Kerforne (1901), who attributed the forms present to species described from beds of similar age in Portugal and Spain (Ribeiro, Sharpe, and Jones 1853, de Verneuil and Barrande 1855). Subsequent work has been summarized and expanded by Babin (1966) in a major work on the Palaeozoic Mollusca of Brittany.

The present work is more detailed and restricted to bivalves. Particular attention has been given to the dentition and its development during ontogeny, and to accessory muscle scar patterns.

This study is based on material from coastal sections near La Mort Anglaise (831487 and 838495) and south-east of Crozon (912441). These grid references refer to square UU of the U.T.M. international grid. The most perfectly preserved bivalves are found as disarticulated valves in numerous thin fossil bands in shales, and are present as internal and external moulds. Isolated steinkerns sometimes occur outside these fossil bands. The most prolific beds were found in the Schistes de Morgat (Llandeilo). A more detailed description of the nature of these fossil bands and their constituents can be found in Bishop, Bradshaw, Renouf, and Taylor (1969).

The bivalves frequently show tectonic distortion, and identification on general shape alone is therefore unsound. The dentition, combined with the positioning of the accessory muscle scars, was found to be more reliable.

The Llandeilian bivalves of the Crozon Peninsula were listed by Babin (1966) as: Order Palaeotaxodonta: *Ctenodonta bussacensis* (Sharpe) 1853, *Ctenodonta ciae* (Sharpe) 1853, *Ctenodonta costae* (Sharpe) 1853, *Ctenodonta ribeiroi* (Sharpe) 1853, *Ctenodonta britannica* Babin 1966, *Palaeoneilo hopensacki* (de Verneuil and Barrande) 1855, *Palaeoneilo beirensis* (Sharpe) 1853, *Palaeoneilo ctenodontoides* Babin 1966; Order Pantodontida: *Actinodonta naranjoana* (de Verneuil and Barrande) 1855, *Redonia deshayesi* Rouault 1851, emend. Gouzien 1934.

The placing of many of the palaeotaxodontids in the genus *Ctenodonta* is not supported by a comparison with the type species, *Ctenodonta nasuta* (Hall). The

[Palaeontology, Vol. 13 Part 4, 1970, pp. 623–45.]

palaeotaxodontids of the Crozon Peninsula exhibit several small, but significant, differences amongst themselves, and a revised list of the more abundant palaeotaxodontids is suggested:

Sub-class PALAEOTAXODONTA
Order NUCULOIDA

Cardiolaria beirensis (Sharpe) 1853.
Tancrediopsis ezquerrae (Sharpe) 1853.
Praeleda ciae (Sharpe) 1853.
Praeleda costae (Sharpe) 1853.

Each genus of the fauna is reviewed separately in the following pages. As *Ctenodonta ribeiroi* and *Ctenodonta britannica* are inadequately represented in the material collected, they are not discussed. The description of each species refers to the actual shell, but the accompanying figures are of internal moulds, as the dentition in many cases was too delicate to withstand the making of latex casts.

In all accompanying illustrations the muscle scars are indicated as follows: Anterior adductor muscle—AA; Posterior adductor muscle—PA; accessory muscles—a. Other symbols used are explained in the figure captions. With incomplete specimens the suggested outline has been dotted in.

All figured specimens have been deposited in the museum of the Department of Geology, University of Canterbury, New Zealand.

Orientation. The orientation of the palaeotaxodontids was deduced from the nature of the teeth along the hinge line and the positions of the accessory muscle scars. Two orientations are present, a normal orientation as shown by *Cardiolaria beirensis* and *Tancrediopsis ezquerrae*, and a reversed (nuculoid) orientation shown by *Praeleda costae* and *Praeleda ciae*. A fuller explanation is given at the beginning of the section on the reversed forms.

PALAEOTAXODONTIDS OF NORMAL ORIENTATION

Cardiolaria beirensis (Sharpe) 1853

Text-figs. 1–4

1853 *Nucula beirensis* Sharpe, p. 150, pl. 9, figs. 11–12.
1853 *Nucula bussacensis* Sharpe, p. 151, pl. 9, figs. 13–14.
1855 *Nucula hopensacki* de Verneuil and Barrande, p. 989, pl. 28, fig. 8.
1876 *Ctenodonta beirensis* de Tromelin and Lebesconte, p. 654.
1876 *Ctenodonta bussacensis* de Tromelin and Lebesconte, p. 683.
1886 *Ctenodonta beirensis* Barrois, p. 680.
1886 *Ctenodonta bussacensis* Barrois, p. 685.
1901 *Ctenodonta beirensis* Kerforne, p. 194.
1901 *Ctenodonta bussacensis* Kerforne, p. 195.
1901 *Ctenodonta hopensacki* Kerforne, p. 196.
1912 *Palaeoneilo hopensacki* Douville, p. 439, fig. 6.
1934 *Ctenodonta bussacensis* Gouzien, p. 179.
1966 *Ctenodonta bussacensis* Babin, p. 45, text-figs. 5 and 6; pl. 1, figs. 4 and 5.
1966 *Palaeoneilo hopensacki* Babin, p. 73, text-figs. 23 and 24; pl. 11, figs. 10 and 11.
1966 *Palaeoneilo beirensis* Babin, p. 74, text-figs. 25; pl. 11, fig. 9.

The general morphology and dentition of *Cardiolaria beirensis* is clearly illustrated in text-figs. 1–4. The most significant point concerning the dentition is the marked

difference in adult forms between the anterior and posterior series of teeth. The anterior teeth are few (4–6 in adult), massive, and vary amongst themselves in shape, size and position. The posterior teeth are more numerous (15–20 in adult), uniform in size and placement, and usually chevron in shape. In the adult the posterior series of teeth tends to override the anterior, and there is resorption in this region. The dentition undergoes appreciable change during ontogeny. Recrystallization has destroyed the dentition of individuals smaller than 5 mm. in length and 3·5 mm. in height, but at this size the two series of teeth are almost indistinguishable, appearing continuous (text-fig. 1). With increase in size the two series of teeth become more distinct and discontinuous (text-fig. 2). With further growth the overriding of the first anterior tooth by the proximal end of the posterior series becomes emphasized, and the two series become separated by a narrow flat region (text-figs. 3 and 4).

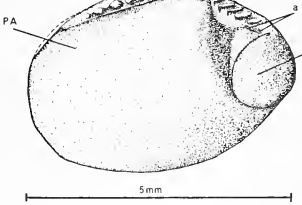

TEXT-FIG. 1. *Cardiolaria beirensis*. Internal mould of a juvenile right valve showing simple, continuous dentition. Pointed umbo missing. The unequally impressed musculature and the strong anterior myophoric plate are already distinct at this stage. Note the general similarity of tooth shape and size. The anterior teeth appear slightly thicker and more oblique to the dental plate. Specimen B. 10. Llandeilo. G.R. 838495.

Fusion of anterior teeth in the left valve accompanies the growing discordance between the two series of teeth. In medium-sized individuals (approx. 1·3 cm. length, 1 cm. width) a bifid tooth opening ventrally is situated in the left valve. Certain specimens indicate that this bifid tooth is composed of a chevron tooth fused to a smaller, ridge-like tooth that lies ventral and posterior to it (illustrated by the opposite valve in text-fig. 3). In the right valve a corresponding spike-like tooth lies between two normally developed teeth, close to the ventral margin of the dental plate. In only one medium-sized valve has a bifid tooth been seen in the right valve. This specimen (text-fig. 2) was obtained from beds older than the bulk of the material studied. A larger valve of identical shape from the same horizon shows no trace of the bifid tooth.

In the largest forms available (text-fig. 4) the bifid tooth is retained, and the flat region between the two series of teeth appears prominent. This featureless area is interesting as *Cardiolaria* is the only palaeotaxodontid member of the Crozon Peninsula bivalve fauna to exhibit a well-marked area where resorption of teeth occurs. Bernard (1896) records the progressive resorption of teeth adjacent to the internal ligament of Tertiary and modern nuculids. The featureless area of *Cardiolaria beirensis* does not resemble the clearly defined resilifer of modern palaeotaxodontids, but it may indicate a very early stage in the migration of the external ligament onto the hinge plate.

The adductor muscle scars of *Cardiolaria beirensis* are rounded and equal in size, although the anterior scar is much more deeply impressed. The posterior pedal accessory muscle scar is too feeble to be visible, but those to the anterior, adjacent to the adductor scar, are very prominent. These accessory scars lie in the thickness of the myophoric plate where it abuts the hinge plate (text-figs. 1, 2). Most specimens appear to possess only one anterior pedal accessory muscle scar, but very well-preserved specimens

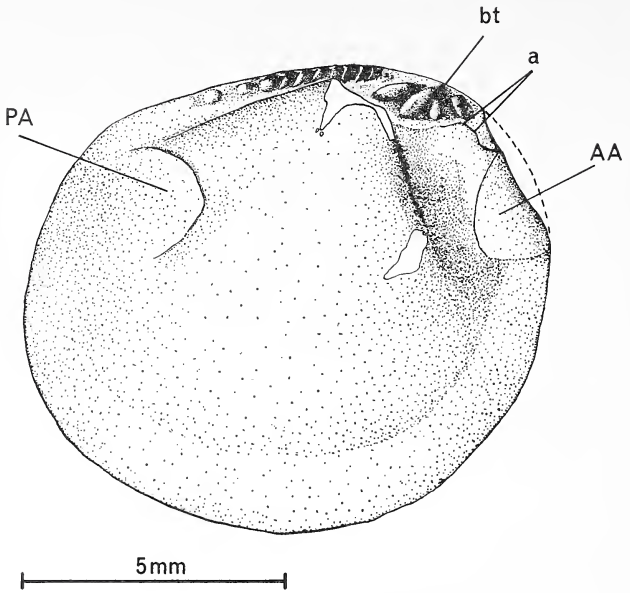

TEXT-FIG. 2. *Cardiolaria beirensis*. Young adult. Internal mould of right valve, umbonal region missing, showing the developing differences between the anterior and posterior series of teeth. The extreme posterior teeth are obscured. The mould of a bifid anterior tooth (bt—appearing as socket) and the position the two anterior pedal muscle scars are indicated. Specimen K.3. Llanvirn. G.R. 803469.

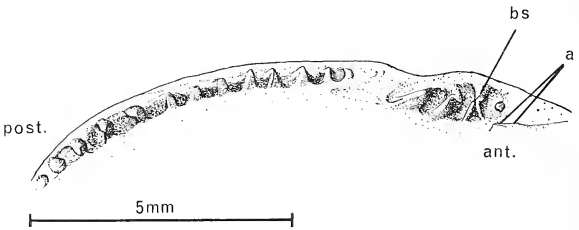

TEXT-FIG. 3. *Cardiolaria beirensis*. Internal mould of right valve (hinge only) showing anterior and posterior teeth and the area of resorption between them. The mould of an anterior bifid socket is indicated (bs). Specimen B.4. Llandeilo. G.R. 838495.

indicate it to be composed to two juxtaposed elliptical scars lying with their common long axes sub-parallel to the anterior part of the hinge plate. In these specimens a smaller scar is also present between the juxtaposed scars and the anterio-dorsal edge of the anterior adductor muscle scar. The close grouping of these scars is further indication of the normal orientation of *Cardiolaria*. The two elongate, juxtaposed scars

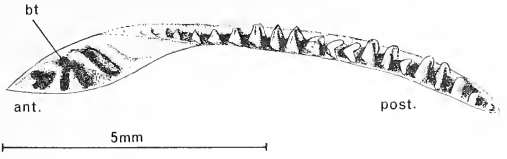

TEXT-FIG. 4. *Cardiolaria beirensis*. Internal mould of the hinge region only of a large left valve, showing the hinge plate clearly composed of two distinct dental sections. The few anterior teeth are massive, and the mould of a bifid tooth (bt) is indicated. The regular posterior teeth are numerous and vary from an asymmetrical chevron shape with a longer ventral limb, to ridge-like below the umbo. Both series of teeth show resorption where the posterior series overrides the anterior series. Specimen A.8. Llandeilo. G.R. 831487.

resemble the anterior protractor and retractor found in *Acila divaricata* figured by Driscoll (1964, fig. 3). The accompanying smaller scar in *Cardiolaria*, which is slightly ventral to these scars, is probably the smaller anterior protractor also visible in *Acila divaricata*.

Discussion. *Cardiolaria beirensis* is here interpreted as including *Ctenodonta beirensis*, *C. bussacensis*, and *C. hopensacki* of previous authors. Originally the three species were based on differences in general shape, but these characters alone have proved of little value in distorted faunas.

Babin (1966) has attempted to distinguish the species on the nature of the sub-umbonal teeth together with detailed variation in shape. However, he admits that without the sub-umbonal teeth the forms are difficult to distinguish in distorted faunas. Since the character of these teeth is related to stages in ontogeny, the maintenance of separate species can no longer be supported. Babin divides the three species into two genera, *Ctenodonta* and *Palaeoneilo*, which he places in two separate subfamilies, Ctenodontinae and Palaeoneilinae. He considers the former to be characterized by continuous teeth below the umbo and the latter by two series discontinuously arranged below the umbo.

However, McAlester (1968) describes the lectotype of *Palaeoneilo*, *Palaeoneilo constricta* (Conrad), as having 'fine taxodont dentition' a characteristic that is borne out by his illustrations (pl. 15, especially fig. 15). The teeth are continuous along the hinge, and the illustrated specimens appear in no way similar to *Ctenodonta hopensacki* or *C. beirensis*. Furthermore, the range of *Palaeoneilo* is generally accepted as being Devonian–Triassic.

The specific name *beirensis* is retained on the grounds of priority (Sharpe 1853, p. 150),

but the species possesses no characters attributable to the type species of *Ctenodonta*, *Ctenodonta nasuta* (Hall). It does, however, show striking resemblances to the type species of *Cardiolaria* (*Cardiolaria barrandei*) figured by McAlester (1968, pl. 10), having the same distinct anterior myophoric plate and the two unequal series of teeth. For this reason *Ctenodonta beirensis* is here transferred to the genus *Cardiolaria*.

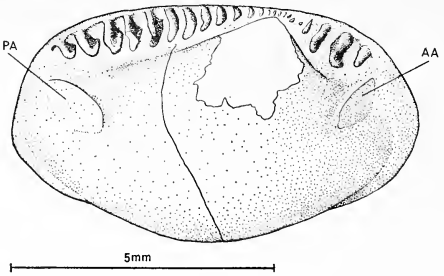

TEXT-FIG. 5. *Tancrediopsis ezquerrae*. Internal mould of a right valve, tilted to show the dental plate. The chevron-shaped posterior teeth decrease steadily in size towards the umbo below which they are ridge-like and low. The series is straight except just anterior of the umbo. The anterior teeth are fewer in number and show abrupt decrease in size at both ends of the series. The highest posterior tooth is equal in size to the highest anterior tooth. The junction of the two series is visible anterior of the umbo. Specimen A.12. Llandeilo. G.R. 831487.

Tancrediopsis ezquerrae (Sharpe) 1853

Text-figs. 5, 6

1853 *Nucula ezquerrae* Sharpe, p. 149; pl. 9, fig. 7.
1876 *Ctenodonta ezquerrae* de Tromelin and Lebesconte, p. 624.
1886 *Ctenodonta ezquerrae* Barrois, p. 680.
1901 *Ctenodonta ezquerrae* Kerforne, p. 196.
1966 *Ctenodonta costae* Babin, p. 52, text-figs. 13, 14, 15; pl. 1, figs. 6 and 7.

Unlike the other palaeotaxodontids of the fauna which possess teeth of different size and shape on each side of the umbo, the dentition of *Tancrediopsis ezquerrae* is very uniform in shape and size. The teeth are arranged in two series with more teeth present in the posterior series (text-fig. 5). The arrangement of the teeth on the two parts of the dental plate is closer to that in *Cardiolaria* than in *Praeleda*. The dentition appears continuous along the hinge plate but well-preserved specimens with the sub-umbonal region unobscured show that the two series are slightly offset (text-fig. 5). There is no indication of resorption in this region.

Young specimens of *Tancrediopsis ezquerrae* possess teeth that are pustule-like in shape rather than chevron. With increase in size of the individual the chevron shape develops with the formation of a strong groove down the side of the tooth facing away from the umbo.

The sub-equal adductor muscle scars are situated at the distal ends of the hinge plate beyond the last teeth. A distinct pedal accessory muscle scar is present close to each adductor muscle scar (text-fig. 6). In both cases the accessory scar lies adjacent to the edge of the hinge plate, and the posterior pedal scar is more obviously dorsal to its related adductor muscle scar than is the anterior pedal scar.

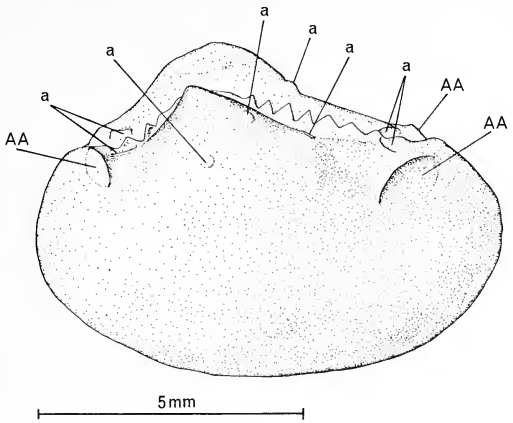

TEXT-FIG. 6. *Tancrediopsis ezquerrae*. Left side view of articulated internal moulds showing the characteristic oval shaped adductor muscle scars whose long axes converge ventrally, and the positions of the accessory muscle scars. Specimen 0·5. Llandeilo. G.R. 806468.

In addition three umbonal scars have been consistently observed. Two of these lie along the dorsal side of the umbonal cavity close to the hinge plate (text-fig. 6). The position of these scars is interesting as McAlester (1963) mentions faint impressions just below the posterior hinge plate in *Tancrediopsis contracta* which he suggests may represent pedal or visceral muscle scars. A further umbonal muscle scar lies ventrally placed in the umbonal cavity and is level with the adductor muscle scars.

Discussion. The general morphology of *Ctenodonta ezquerrae* of previous authors has little in common with the type species *Ctenodonta nasuta*, and it would seem more desirable to place the species in another genus.

McAlester (1963, p. 4) writes: 'The name *Tancrediopsis* will, however, probably prove useful in the future as a generic sub-division of the heterogeneous assemblage of Ordovician forms now included in "*Ctenodonta*".' It is suggested that *Ctenodonta ezquerrae* has closer affinities with *Tancrediopsis* than any other genus described to date.

The oval, dorsally impressed adductor muscle scars of *Ctenodonta ezquerrae* are very similar to those preserved in the type species *Tancrediopsis contracta* (Salter) which

have long axes also converging ventrally. The strongly inflated valves, the regular but faint growth-lines, and the strong chevron teeth almost continuous along the hinge, are additional similarities. As in *Tancrediopsis contracta*, two distinct pedal muscle scars are present in *Ctenodonta ezquerrae* adjacent to the umbonal edge of the adductor muscle scars.

Although *Ctenodonta ezquerrae* does not possess the almost equilateral valves of the type species of *Tancrediopsis*, nor the two sub-equal series of teeth, the author feels that it has closer affinities to *Tancrediopsis* than to any other described genus of palaeotaxodontid, and transfers it accordingly.

PALAEOTAXODONTIDS OF REVERSE ORIENTATION

Orientation. A general discussion on the problem of palaeotaxodontid orientation would be inappropriate in a paper of this type. A separate contribution is in preparation.

However, with regard to the forms described here, the dentitions of *Praeleda* and *Cardiolaria* indicate that their orientations are opposite. In *Cardiolaria* the larger chevron teeth are always found along the shorter side of the valve on a plate whose inner edge is straight or arched dorsally (text-fig. 4). *Praeleda* is the reverse. The largest teeth are found on the longer side of the valve, but still on a plate whose inner edge is arched ventrally. The lower ridge-like teeth are present on a narrower plate, arched dorsally (text-fig. 7). It has been shown above that *Cardiolaria* has a normal orientation as indicated by the grouping of certain accessory muscle scars.

Where the shape of the teeth can be established in detail, the relative movement of the two valves can be determined and the position of the external ligament and regions of maximum opening inferred (the latter probably determined by the retraction of a large foot as in modern *Nucula*). The inferred positions in *Praeleda* and *Cardiolaria* are opposite.

Consequently, in the descriptions of *Praeleda*, the shorter end will be referred to as posterior, and the extended end as anterior.

Despite tectonic distortion, *Praeleda costae* and *Praeleda ciae* can be readily distinguished from each other by the shape and disposition of the teeth and the relative positions of the accessory muscle scars.

Praeleda costae (Sharpe) 1853

Text-figs. 7–10

1853 *Nucula costae* Sharpe, p. 149, pl. 9, fig. 4.
1855 *Nucula costae* de Verneuil and Barrande, p. 989.
1876 *Ctenodonta costae*? de Tromelin and Lebesconte, p. 641.
1886 *Ctenodonta costae* Barrois, p. 680.
1891 *Ctenodonta costae* Barrois, p. 189, pl. 1, fig. 6.
1901 *Ctenodonta costae* Kerforne, p. 196.
1934 *Ctenodonta costae* Gouzien, p. 179.
1966 *Palaeoneilo ctenodontoides* Babin, p. 76, text-figs. 26–8; pl. 1, figs. 9–10; pl. 11, figs. 6, 12, 13.

In *Praeleda costae* (text-fig. 7) the two series of teeth are arranged at an angle to each other on the hinge plate, the junction lying just anterior to the umbo. Seventeen to

twenty-two teeth are usually present along the adult hinge, either divided equally between the two series or with more in the posterior series. Those in the anterior series are large and prominent, possessing an inconsistent chevron shape. The most anterior teeth commonly show the more usual curved chevron form with angles directed towards the umbo, but in many specimens the teeth closer to the umbo show a reversal of this shape with angles directed away from the umbo. The posterior teeth are low and ridge-like,

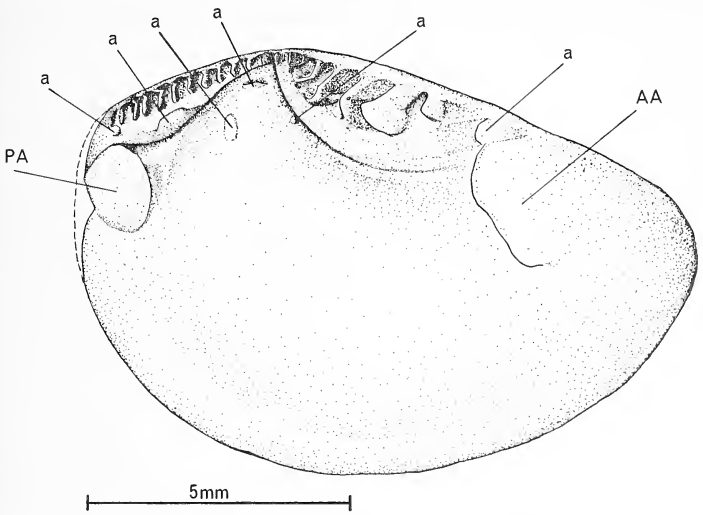

TEXT-FIG. 7. *Praeleda costae*. Internal mould of right valve, anterior to right, showing muscle scars and the two different types of teeth on each side of the umbo. Specimen 0·1. Llandeilo. G.R. 806468.

frequently curved with the concave side towards the umbo. In some cases the teeth appear to have a grossly asymmetrical form with the ventral limb developed at the expense of the dorsal limb. Where this form is visible the angle of the chevron is directed towards the umbo.

In juvenile forms of *Praeleda costae* (text-fig. 8) the adductor muscle scars are rounded and equal, but in the adult (text-fig. 7) the anterior adductor scar is larger and oval in shape with its long axis roughly parallel with the anterio-dorsal margin of the shell. In addition five pedal accessory muscle scars are usually visible. Three of these are umbonal in situation commonly arranged in the form of a triangle with its apex ventral and the base slanting downwards anteriorly. The scar closest to the umbo is frequently the strongest. A pedal accessory scar is present at the distal end of the anterior hinge plate, adjacent and dorsal to the anterior adductor muscle scar. Another prominent

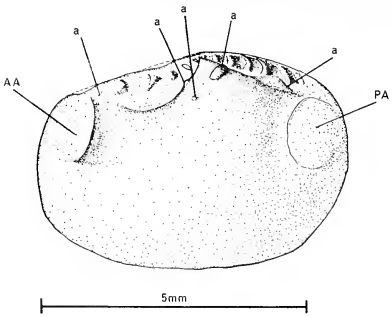

TEXT-FIG. 8. *Praeleda costae*. Internal mould of small left valve, anterior to left, showing early dentition and muscle scars. Specimen F.30. Llandeilo. G.R. 912441.

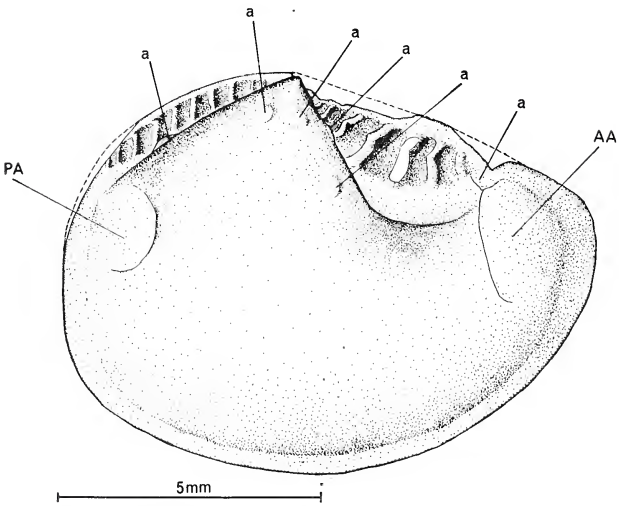

TEXT-FIG. 9. *Praeleda costae*. Internal mould of distorted right valve, anterior to right. Note accessory muscle scars. Specimen C.1.b. Llandeilo. G.R. 912441.

accessory scar lies half-way along, and ventral to, the posterior part of the hinge plate. This scar is quite isolated from the posterior adductor scar, and its position is characteristic of the species.

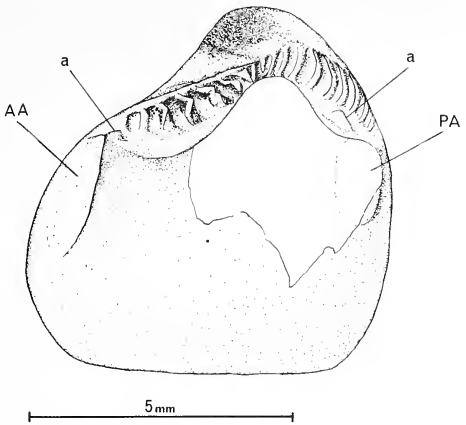

TEXT-FIG. 10. *Praeleda costae*. Internal mould of a distorted left valve, anterior to left, showing a more concordant junction between the two series of teeth than is usual for this species. Part of the external mould of a pronounced lunule is also visible. Specimen F.31.b. Llandeilo. G.R. 912441.

Praeleda ciae (Sharpe) 1853

Text-figs. 11, 12

1853 *Nucula ciae* Sharpe, p. 149, pl. 9, fig. 5.
1876 *Ctenodonta ciae* de Tromelin and Lebesconte, p. 641.
1886 *Redonia ciae* Barrois, p. 659.
1901 *Ctenodonta ciae* Kerforne, p. 195.
1923 *Ctenodonta ciae* Kerforne, p. 180.
1966 *Ctenodonta ciae* Babin, p. 49, text-figs. 10–12; pl. 1, fig. 9.

The teeth of *Praeleda ciae* are fewer than in *Praeleda costae*, and are arranged without disruption along the hinge plate (text-fig. 11). Approximately 16 teeth are present in the adult, either divided equally between the two series or with slightly more in the anterior series. The teeth of the anterior series have a clear, regular chevron form, curved in profile with angles directed towards the umbo. They merge steadily into the small ridge-like sub-umbonal teeth, which in turn pass posteriorly into the low, ridge-like posterior teeth.

In the adult the adductor muscle scars are unequal, the anterior scar being larger and oval in shape with its long axis roughly parallel with the anterio-dorsal margin of

the shell. Five pedal accessory muscle scars are generally visible. Two of these are found dorsal and adjacent to both adductor muscle scars. A further three scars are present in the umbonal region, usually situated in a straight line slanting downwards towards the anterior. The lowest scar is frequently the strongest.

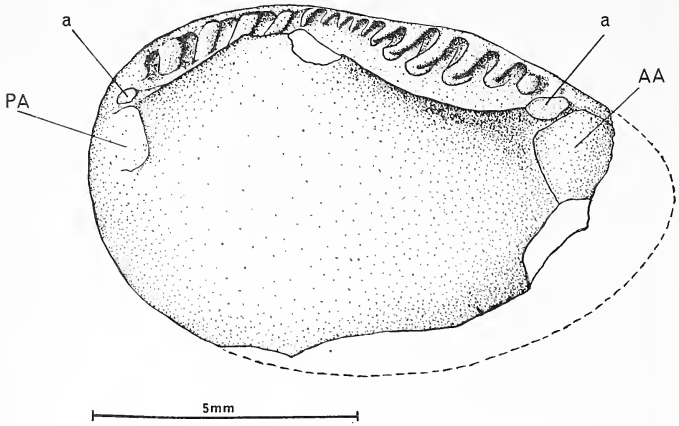

TEXT-FIG. 11. *Praeleda ciae*. Internal mould of right valve, anterior to right and tip of umbo missing. The anterior teeth are prominent and curved, the posterior teeth lower and ridge-like. The two series are continuous below the umbo where the teeth are low and ridge-like. Specimen B.19. Llandeilo. G.R. 838495.

Comparisons. Praeleda costae is particularly interesting as it is the more variable of the two species and sometimes exhibits a dental plate similar to that of *Praeleda ciae*, e.g. text-fig. 10. The two patterns of dentition are fundamentally similar, and only seem different because of variations in the relative growth-rates of the two portions of the hinge plate, which have a direct bearing on their angular relationship.

The pattern of accessory muscle scars in the two species is basically similar, but their different development in each has allowed them to be used for specific definition. An internal mould of average preservation will only show the strongest of the accessory scar impressions, and a distinctive pattern is obvious in each species. But certain well-preserved specimens of each species show numerous accessory scars in a basically similar pattern. The right valve of *Praeleda costae*, in text-fig. 9, shows the usual triangular arrangement of umbonal accessory scars. However, there is an additional scar in the middle of the base line so that this line resembles the usual pattern of umbonal scars found in *Praeleda ciae*. In text-fig. 7, a right valve of *Praeleda costae*, an additional small accessory scar is visible dorsal to the posterior adductor scar and closely adjacent to the distal posterior teeth. This appears to be the pedal scar commonly preserved in *Praeleda ciae* next to the posterior adductor scar. In text-fig. 12, a right valve of *Praeleda ciae*,

a prominent umbonal accessory scar is present half-way along the umbonal cavity and adjacent to the posterior hinge plate. It is suggested that this scar is comparable to the posterior accessory scar found in *Praeleda costae* close to the posterior teeth and half-way along the series.

Discussion. Ctenodonta ciae, *C. costae*, and *C. ezquerrae* were all recorded from the Llandeilian of the Crozon Peninsula by Kerforne (1901). However, Babin (1966)

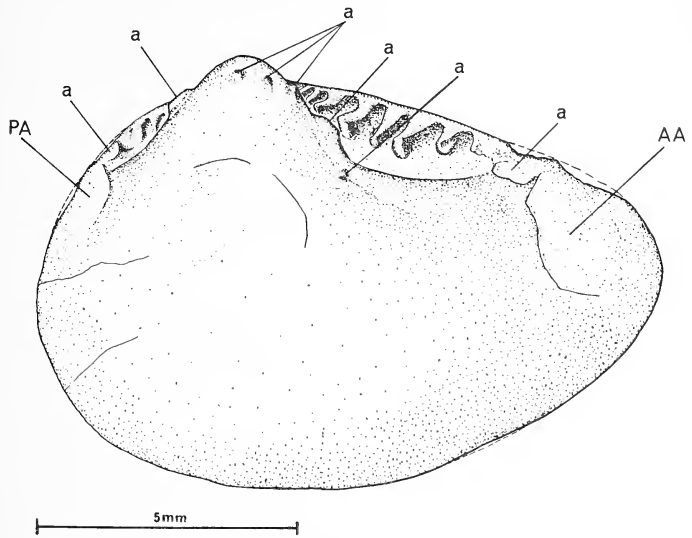

TEXT-FIG. 12. *Praeleda ciae*. Internal mould of right valve, anterior to right. The specimen is slightly crushed, but otherwise well preserved, showing numerous umbonal accessory muscle scars. The curved anterior teeth are also distinct. Specimen C.6. Llandeilo. G.R. 912441.

regarded *Ctenodonta ezquerrae* as a synonym of *Ctenodonta costae* in his sub-family Ctenodontinae. At the same time he erected a new species *Palaeoneilo ctenodontoides* in his second sub-family the Palaeoneilinae.

Babin's figures of *Ctenodonta costae* are in no way similar to photographs of the holotype from Bussaco housed in the British Museum on which the Crozon identification were based. On the contrary, his figures closely resemble photographs of the holotype of the distinctive *Ctenodonta ezquerrae*. In addition, his figures of the newly erected species *Palaeoneilo ctenodontoides* are identical to the holotype of *Ctenondonta costae*, and for these reasons it would appear that the species *Palaeoneilo ctenodontoides* Babin is invalid.

In common with the other palaeotaxodontids of the Crozon Peninsula fauna, *Ctenodonta ciae* and *Ctenodonta costae* show little similarity to the type species *Ctenodonta nasuta*, and would be best included in another genus.

The two forms show closest resemblances to *Praeleda* Pfab in general shape, dentition and accessory muscle scars. The type species *Praeleda compar* (Barrande) figured by McAlester (1968, pl. 7) appears very similar to *Ctenodonta ciae*. The dentition is in two series, and although more teeth are present to the posterior, the larger teeth are found to the anterior. A distinct pedal accessory scar is visible dorsal to the anterior adducted muscle scar, and in Paratype B (pl. 7, figs. 7 and 9) three umbonal accessory scars are also visible in a line slanting towards the anterior. The three umbonal scars are also obvious in an illustration by Pfab (1934, pl. III, fig. 2).

McAlester (1969) has listed *Praeleda* as a synonym of *Deceptrix*, but there are reasons for retaining this genus. *Praeleda compar*, *P. costae*, and *P. ciae* seem to form a group of species more closely related to each other than they are to *Deceptrix*. There is also similarity between *Praeleda* and the contemporaneous genus *Praenucula*. Whereas *Deceptrix* shows a sub-circular, equilateral form, all three species of *Praeleda*, and *Praenucula*, exhibit an anteriorly elongate shape. Although the inflation of the umbo varies within *Praeleda costae*, *P. ciae*, the anteriorly elongate shape is constant. Variation in the dentition is more common. Although the dentition of some individuals of *Praeleda* (e.g. *Praeleda costae*, text-fig. 7) is remarkably similar to *Deceptrix*, others are quite different and approach *Praenucula*. It is highly likely that these two Ordovician genera were ancestral to later Palaeozoic forms such as *Deceptrix*, and the anteriorly elongate bivalves with an internal ligament such as *Nuculanella*.

PALAEOHETERODONTIDS

Actinodonta naranjoana (de Verneuil and Barrande) 1855

Text-figs. 13–15

1855 *Arca naranjoana* de Verneuil and Barrande, p. 989, pl. 26, fig. 12.
1901 *Arca*? *naranjoana* Kerforne, p. 194.
1901 *Dolabra lusitanica* Kerforne, p. 194.
1923 *Arca*? *naranjoana* Kerforne, p. 180.
1966 *Actinodonta naranjoana* Babin, p. 233, text-fig. 60; pl. x, figs. 5, 7, 11.

Five to seven teeth are generally present in each valve of *Actinodonta naranjoana*. These vary in both length and orientation but give a crude impression of radiating ventrally from below the umbo, the shortest teeth being in the centre of the series (text-fig. 15). It seems unwise to use the terms 'cardinal' and 'lateral', to describe the teeth, as these have associations with the true heterodonts, and in the strictest sense imply that the lateral teeth extend posteriorly or anteriorly beyond the external ligament. This does not appear to be the case in *Actinodonta naranjoana*. Furthermore, lateral and cardinal teeth are regarded as being distinctly separate from each other, usually having different orientations. The author considers it undesirable to number these teeth in any way until the affinities of *Actinodonta* are better known.

The posterior teeth are elongate, extending from the umbo to the posterior adductor scar. They are for the most part parallel with the dorsal margin, and are crenulated

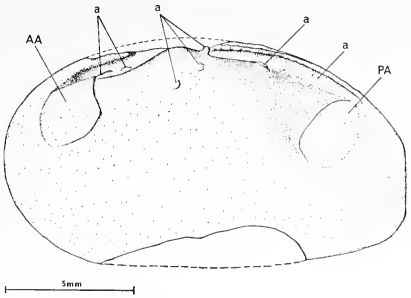

TEXT-FIG. 13. *Actinodonta naranjoana*. Internal mould of well-preserved left valve, hinge incomplete, showing general morphology and pattern of adductor and accessory muscle scars. Specimen C. 14. Llandeilo. G.R. 912441.

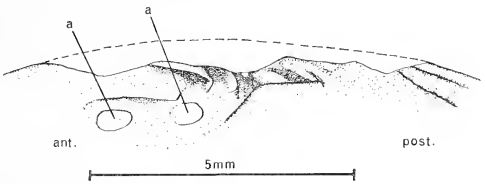

TEXT-FIG. 14. *Actinodonta naranjoana*. Internal mould of sub-umbonal and anterior hinge regions of left valve showing dentition. Part of the proximal end of the elongate socket is visible to the right. Each of the four anterior sockets (appearing as teeth) have different forms owing to varying stages in the bending of a simple ridge. Just posterior of the umbo tip are two distinct sockets that become fused in other forms. Two anterior accessory muscle scars (anterior retractor and protractor) are clearly visible anterior to the umbo. Specimen C.24. Llandeilo G.R. 912441.

along the anterior two-thirds of their length. Two such elongate teeth are present in the left valve and one in the right valve.

The most anterior tooth on the hinge is strong, and parallel with the dorsal margin. The following two or three teeth towards the umbo show a gradual change in orientation to one almost at right-angles to the dorsal margin (text-figs. 14, 15). The pattern of these teeth suggest a vague similarity to the lateral and cardinal teeth of the true heterodonts, although the analogy is incomplete. The short perpendicular teeth of *Actinodonta* are formed from the flexed tip of a longer plate that is almost parallel to the dorsal margin (see particularly text-fig. 14). There would thus appear to be 2 or 3 anterior cardinals and one anterior lateral in *Actinodonta*. However, it should be remembered that all these teeth of different orientation have in fact formed from different dental lamellae.

In the right valve of *Actinodonta*, in addition to the teeth described above, there is a short tooth below the umbo parallel to the proximal end of the long posterior tooth. This tooth provides evidence for fusion along the dental plate. In some forms two such teeth are visible below the umbo (text-fig. 14). However, in others these appear to have become reduced to a single tooth of two distinct fused components (text-fig. 15). In other forms only a single smooth-tipped tooth is visible. In a single specimen fusion has also been observed among the anterior teeth of the right valve. The ventral tips of two adjacent teeth have become fused to form a chevron-shaped tooth opening dorsally, the reverse of a similar process observed in *Cardiolaria*.

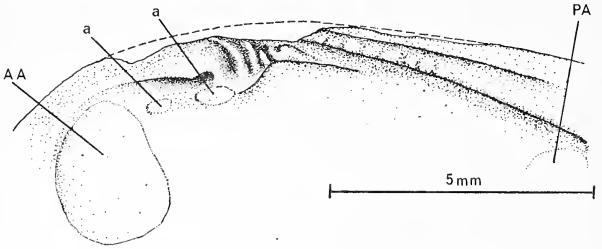

TEXT-FIG. 15. *Actinodonta naranjoana*. Internal mould of the hinge region of a left valve showing a dental plate possibly further developed than that shown in fig. 14. The anterior sockets (appearing as teeth) have become differentiated into three that are almost at right-angles to the dorsal margin, and one that is parallel to it. Between these and the long posterior socket is a single socket that clearly shows two fused sections. The anterior adductor and anterior accessory muscle scars are distinct. Specimen C.14.b. Llandeilo. G.R. 912441.

The pattern of muscle scars commonly visible in *Actinodonta naranjoana* is shown in text-fig. 13. The two closely positioned anterior accessory pedal scars visible in text-figs. 13, 14, and 15, are strongly reminiscent of the two juxtaposed anterior pedal scars present in both *Cardiolaria beirensis* and *Redonia deshayesi*. The umbonal accessory scars of *Actinodonta naranjoana* show a similarity in pattern to those observed in *Tancrediopsis ezquerrae* (text-fig. 6), and to some extent, those found in *Redonia deshayesi* (text-fig. 20).

Redonia deshayesi Rouault 1851, emend. Gouzien 1934

Text-figs. 16–21

1851 *Redonia deshayesi* Rouault, p. 364, figs. 1, 2.
1851 *Redonia duvaliana* Rouault, p. 365, fig. 1, 2.
1853 *Redonia deshayesiana* Sharpe, pl. 9, fig. 1.
1853 *Redonia duvaliana* Sharpe, pl. 9, fig. 2.
1955 *Redonia deshayesiana* de Verneuil and Barrande, pl. 16, fig. 10.
1855 *Redonia duvaliana* de Verneuil and Barrande, pl. 16, fig. 11.
1876 *Redonia deshayesiana* de Tromelin and Lebesconte, p. 641.
1876 *Redonia duvaliana* de Tromelin and Lebesconte, p. 641.

1901 *Redonia deshayesiana* Kerforne, p. 198.
1901 *Redonia duvaliana* Kerforne, p. 198.
1934 *Redonia deshayesi* Gouzien, p. 179.
1934 *Redonia duvali* Gouzien, p. 180.
1966 *Redonia deshayesi* Babin, p. 246, text-fig. 67; pl. x, figs. 13–16.

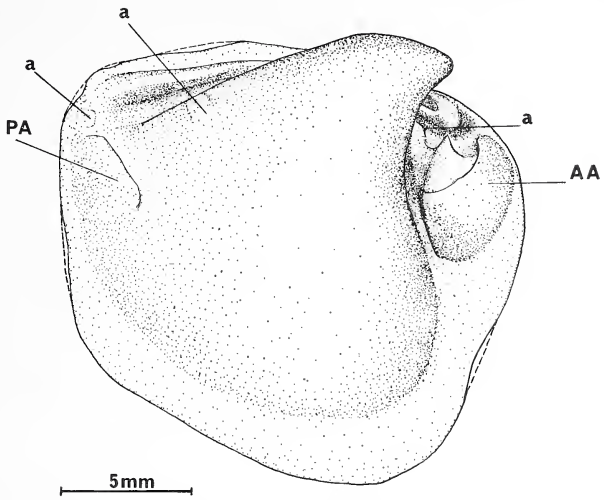

TEXT-FIG. 16. *Redonia deshayesi*. Internal mould of distorted adult right valve, showing the inequilaterally placed prosogyral umbo, and the strong anterior myophoric plate. The pallial line is simple and the anterior musculature more deeply impressed than the posterior. The mould of a chevron socket is visible anterior to the umbo, and a long socket posterior to it. Specimen A.4. Llandeilo. G.R. 831487.

The general morphology of *Redonia deshayesi* is shown in text-figs. 16–21. Previous descriptions of this genus have contained little detail on the nature and development of the dental plate.

Two teeth and two sockets are present in each valve of *Redonia deshayesi*, and all show a similar oblique orientation to the dental plate. In the left valve of an adult *Redonia deshayesi* (text-fig. 17) a strong asymmetrical chevron tooth is present below the umbo. Posterior to this and following the same oblique orientation is an elongate tooth persisting as far back as the posterior adductor muscle scar. The two limbs of the chevron tooth form an acute angle opening posteriorly, and the tooth is highest at its angulation. The dorsal limb of the chevron is extremely short, and the bulk of the tooth is formed by the longer ventral limb which lies nearly parallel to that part of the hinge immediately below the umbo.

In the right valve of an adult *Redonia deshayesi* (text-fig. 16) a strong, short, ridge-like tooth exists below the umbo posterior to a deep, chevron-shaped socket. The second tooth of this valve is situated close to the posterior adductor muscle scar, and though elongate, is shorter than the posterior tooth of the left valve. The posterior teeth of both valves terminate dorsally against what is considered to be the site of an external, opisthodetic ligament.

Whereas members of Palaeotaxodonta show an increase in the number of teeth with age, *Redonia* indicates reduction of teeth during ontogeny.

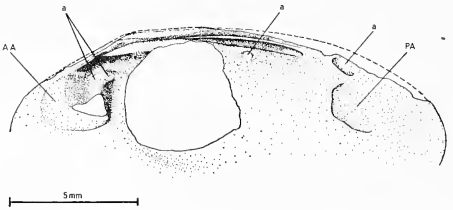

TEXT-FIG. 17. *Redonia deshayesi*. Internal mould of adult left valve showing dentition, and adductor and accessory muscle scars. Umbonal region missing. Specimen B.17. Llandeilo. G.R. 838495.

As mentioned previously, recrystallization has obliterated the detail from hinges of very young individuals. In forms approx. 5·5 mm. in length, 4 mm. in height (text-figs. 18, 19) an extra pustule-like tooth is present in each valve anterior to the teeth retained in the adult. At this size the adult teeth are already elongate, though the chevron tooth of the left valve appears only as a ridge with a very small dorsal limb curving round the anterior tip of the adjacent socket.

Fusion between the chevron tooth and the anterior pustule-like tooth occurs during growth of the individual. The angle of the chevron moves anteriorly as a result of this fusion and appears constricted before the process is completed (text-fig. 21). In consequence the anterior pustule-like tooth of each valve becomes obliterated, and in the adult left valve all evidence of fusion has disappeared.

Partial fusion between the posterior teeth is also obvious in *Redonia deshayesi*, similar to that already observed in *Actinodonta naranjoana*. This can be best seen by studying the internal moulds of sockets. In text-fig. 17 the moulds of two sockets (appearing as teeth) are visible, the most posterior socket mould appearing to overlap and touch that to the anterior. In text-fig. 20 the most anterior long socket mould (mould of pit-like socket also present) appears slightly bifid, and a distinct ridge extends along its dorsal flank posteriorly to merge into the second socket mould. Thus, fusion between the tips of two oblique posterior teeth appears to have taken place in the right adult valve of *Redonia* and is most obvious in younger individuals.

The musculature of *Redonia* is clearly visible in text-figs. 16–21. Two anterior pedal accessory muscle scars are visible adjacent to the adductor scar where the myophoric plate abuts the hinge plate, but these frequently have the appearance of a single narrow

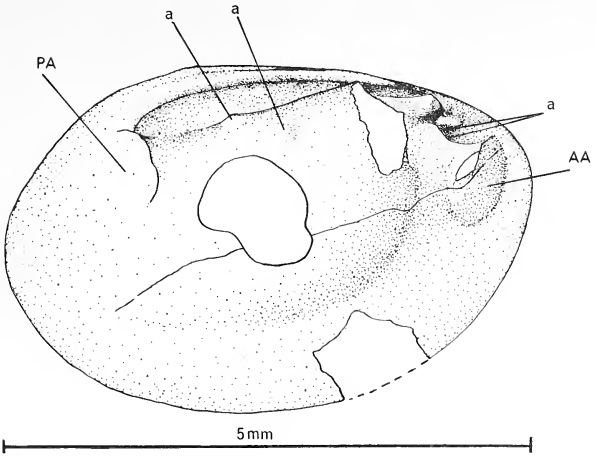

TEXT-FIG. 18. *Redonia deshayesi.* Internal mould of young right valve showing an extra socket (appearing as a tooth) to the anterior. Umbo of specimen missing. Specimen F.23.a. Llandeilo. G.R. 912441.

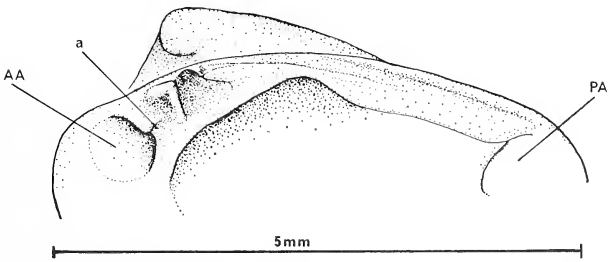

TEXT-FIG. 19. *Redonia deshayesi.* Artificial cast of specimen F.23.a shown in fig. 15. Note the strong myophoric plate and the impressed anterior adductor muscle scar with adjacent accessory scars. The distinct chevron-shaped tooth to the anterior is not present in the adult. Llandeilo. G.R. 912441.

scar with its long axis oblique to, and converging anteriorly on, the hinge plate (text-fig. 17). Well-preserved specimens of *Redonia* show these scars to be slightly oval and juxtaposed, showing a strong resemblance to those in *Cardiolaria beirensis.* A comparison with *Acila divaricata* figured by Driscoll (1964, fig. 3) would suggest that one of these scars is an anterior protractor muscle scar, and the other the anterior retractor muscle

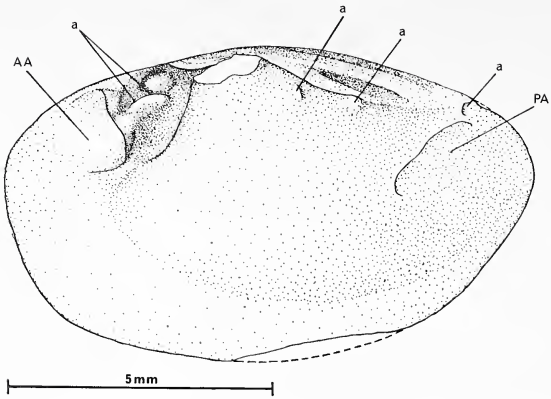

TEXT-FIG. 20. *Redonia deshayesi.* Internal mould of young left valve showing additional socket (appearing as a pustule-like tooth) to the anterior. Adductor and accessory muscle scars are clearly visible. Specimen J.5. Llandeilo. G.R. 912441.

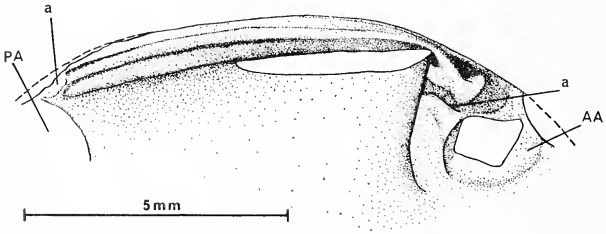

TEXT-FIG. 21. *Redonia deshayesi.* Internal mould of right valve showing form of dentition following the fusion of anterior teeth in the left valve with the mould of the chevron socket appearing constricted. Specimen F.18. Llandeilo. G.R. 912441.

scar. The smaller anterior protractor scar visible in *Cardiolaria beirensis* has not been observed in *Redonia deshayesi.* In addition, a posterior pedal accessory scar is often visible adjacent to the dorsal edge of the posterior adductor muscle scar (text-figs. 16, 17, 20). Two further accessory scars have been observed in the umbonal region (text-figs. 16, 18, 20), resembling those visible in *Actinodonta naranjoana* (text-fig. 13). It is highly likely that *Redonia* developed from a form with a dental plate similar to that of *Actinodonta.* The fusion of teeth in both forms follows a similar pattern but has been more extreme in *Redonia.*

DISCUSSION OF THE EVOLUTIONARY RELATIONSHIPS OF THE CROZON PENINSULA BIVALVE FAUNA

From the variety shown by Ordovician bivalves it seems likely that at least two, and perhaps three, ancestral stocks, with basically different dental patterns, had evolved from the early Mollusca during the Cambrian.

Following Vogel (1962) and Babin (1966) it is suggested that one ancestral stock was almost equilateral, with a dental plate bearing a simple ridge on each side of the umbo parallel to the dorsal margins. Forms such as *Lamellodonta* (Cambrian) and *Babinka* (Ordovician) probably developed from this stock. The origins of *Lyrodesma* may also lie here.

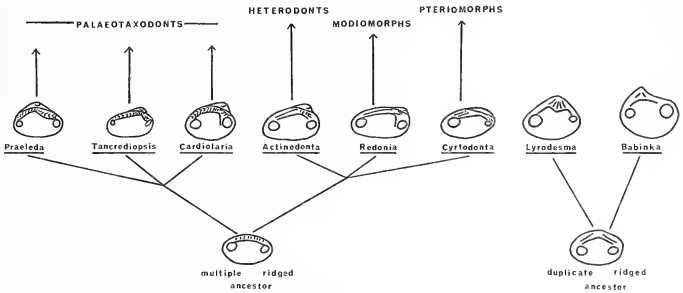

TEXT-FIG. 22. The Crozon Peninsula bivalves in a suggested Lower Palaeozoic phylogeny.

The second ancestral stock may have had a multiple-ridged dental plate, each ridge either perpendicular to the dorsal margin or slightly oblique to it (text-fig. 22). It may have shown some resemblance to juvenile forms of *Cardiolaria beirensis* (text-fig. 1).

The developing dentition of the Crozon Peninsula bivalves indicate two main lines of development from such a multiple-ridged ancestral stock (text-fig. 22). One trend is marked by a simple increment in teeth as the animal grows, the other by a tendency towards reduction in teeth by fusion and resorption. The diverse forms seen in the Ordovician fauna represent cladogenesis within these two lines. At its simplest these two lines can be viewed in terms of Douvillé's 'active' and 'burrowing' branches of bivalve evolution.

Active forms would tend to develop chevron teeth from the primitive dentition to counter the stresses produced by foraging. The most active types probably used a large foot for ploughing through sediment and labial proboscides for food collection, in a manner similar to modern *Nucula*. The primitive opisthodetic ligament and the need for a large anterior opening during retraction of the foot would encourage the development of a differentiated dental plate with larger anterior teeth as seen in *Praeleda*. The anterior part of the shell would tend to become enlarged to provide protection and accommodation. Later Palaeozoic bivalves with a reversed orientation and an internal ligament probably developed from these forms.

Another branch of this line, represented by *Cardiolaria*, may have evolved towards a secondary burrowing condition. The inherited 'active' type of dentition would become modified. With a change in the direction of growth within the valve and less frequent protrusion and retraction of the foot, there would be no tendency to increase the number of large anterior teeth. The myophoric plate and deeply impressed anterior musculature of *Cardiolaria* probably reflect its mode of life. Since the adductor muscles are used to close the shell, the anterior adductor, strengthened by the adjacent plate, suggests a more violent and sudden action by this muscle than its posterior counterpart. If *Cardiolaria* still possessed the anterior inhalent current associated with certain palaeotaxodontids, the action would produce an abrupt cleansing current out of the posterior region of the shell.

Tancrediopsis may represent a third branch, distinct from *Praeleda* and *Cardiolaria*. *Tancrediopsis* has a dentition similar to that of later siphonate nuculanids, and may have been a burrowing bivalve.

The second major line, in which tooth resorption and fusion takes place, appears to be represented by burrowing forms (text-fig. 22). The dentition of *Actinodonta* in particular suggests modification of the ancestral dental plate by elongation of its posterior components and flexing of some anterior teeth. When clear (text-figs. 14, 15), the curved anterior teeth have one long and one short limb. It is not difficult to envisage that resorption at the junction of the two limbs, to leave them isolate, would result in a dentition associated with the heterodontids.

Actinodonta and *Redonia* appear to be closely related, the latter showing a greater reduction of teeth. In addition, the general morphology of *Redonia* closely resembles that of *Cardiolaria*, particularly in the possession of a deeply impressed anterior musculature and an anterior myophoric plate. They could be regarded as homeomorphs. *Actinodonta* shows some parallels with *Tancrediopsis* in its musculature, and it is possible that both forms had posterior inhalant currents.

The cyrtodontids are generally accepted as being closely related to the later pteriomorph bivalves. From the trends reviewed in the Crozon Peninsula fauna it seems likely that they evolved during the Cambrian from the hypothetical multiple-ridged ancestor, in a slightly different direction from *Actinodonta* and *Redonia*, rather than from the duplicate ridged form.

Acknowledgements. The author gratefully acknowledges the help of the British Museum of Natural History for supplying photographs of type material. Acknowledgement is also due to Dr. R. Carter for his helpful and critical reading of the manuscript, and to Mr. D. Jones for the preparation of photographs from the original figures. The author would like to thank Professor M. Gage for the use of facilities in the Department of Geology, University of Canterbury. The author is also grateful to Dr. J. D. Bradshaw for initiating interest in the Ordovician bivalves, and for his helpful and tolerant criticism of the manuscript and many useful discussions.

REFERENCES

BABIN, C. 1966. *Mollusques Bivalves et Céphalopodes du Paléozoique Armoricain*, 472 pp. Brest.

BARROIS, C. 1886. Compte rendu de la réunion extraordinaire de la Societé dans le Finistère. *Bull. Soc. géol. Fr.* 3E, **14**, 652–78.

—— 1886. Constitution de la rade de Brest. Ibid., **14**, 678–707.

—— 1891. Mémoire sur la faune du Grès Armoricain. *Ann. Soc. géol. Nord.* **19**, 134–237.

BERNARD, F. 1896. Deuxième note sur le developpment et la morphologie de la coquille chez les lamellibranches. (Taxodontes). *Bull. Soc. géol. Fr.* 3E, **24,** 54–82.

BISHOP, A. C., BRADSHAW, J. D., RENOUF, J. T., and TAYLOR, R. T. 1969. The stratigraphy and structure of part of Western Finistère. *Q. Jl geol. Soc. Lond.* **124,** 309–48.

COX, L. R. 1960. Thoughts on the classification of the Bivalvia. *Proc. malac. Soc. London,* **34,** 60–88.

DOUVILLÉ, H. 1912. Classification des Lamellibranches. *C.R. Somm. Soc. géol. Fr.* 4E, **12,** 7.

DRISCOLL, E. G. 1964. Accessory muscle scars, an aid to protobranch orientation. *J. Paleont.* **38,** 61–6.

GOUZIEN, V. 1934. Contribution à l'étude géologique de la presqu'ile de Crozon suivant la voie ferrée de Telgruc à Camaret. *Bull. Soc. géol. Minér. Bret.* (1930), 176–91.

KERFORNE, F. 1901. *Étude de la region silurique occidentale de la Presqu'ile de Crozon.* Thèse Fac. Sci. Paris. Imp. Simon, Rennes, 234 pp.

—— 1923. Étude stratigraphique de la vallée de l'Ille entre Saint-Médard. *Bull. Soc. géol. Minér. Bret.* **41,** 78–194.

MCALESTER, A. L. 1963. Revision of the type species of the Ordovician nuculoid pelecypod genus *Tancrediopsis. Postilla,* Yale Peabody Mus. **74,** 1–19.

—— 1964. Preliminary suggestions for a classification of nuculoid bivalves. *J. Paleont.* **38,** 397–400.

—— 1968. Type species of paleozoic nuculoid bivalve genera. *Mem. geol. Soc. Amer.* **105.** 143 pp.

—— 1969. In MOORE, R. C., ed., *Treatise on invertebrate paleontology,* Part N, *Mollusca* 6, *Bivalvia,* **1** and **2** 951 pp. Geol. Soc. Am. and Univ. Kansas Press.

NEWELL, N. D. 1965. Classification of the Bivalvia. *Am. Mus. Novit.* 2206, 25 pp.

PFAB, L. 1934. Revision der Taxodonta des bohmischen silurs. *Palaeontographica,* A. **80,** 195–253.

RIBEIRO, C., SHARPE, D., and JONES, T. R. 1853. On the Carboniferous and Silurian formations in the neighbourhood of Bussaco, Portugal. *Q. Jl geol. Soc. Lond.* **9,** 135–61.

ROUAULT, M. 1850–51. Mémoires sur le terrain paléozoique des environs de Rennes. *Bull. Soc. géol. Fr.,* 2E, **8,** 358–99.

DE TROMELIN, G. and LEBESCONTE, P. 1876. Essai d'un catalogue raisonné des fossiles siluriens des departments de Maine-et-Loire, de la Loire-Inférieure et du Morbihan avec observations sur les terrains paléozoiques de l'Ouest. *Congrès. Ass. Fr. Av. Sci., Nantes* (1875), 601–61.

—— 1876. Presentation de fossiles paléozoiques du department d'Ille-et-Vilaine et note additionelle sur la faune silurienne de l'Ouest de la France. Ibid. 683–7.

DE VERNEUIL and BARRANDE C. 1855. Descriptions des fossiles trouves dans les terrains silurien et devonien d'Almaden, d'une partie de la Sierra Morena et des Montagnes de Toledo. *Bull. Soc. géol. Fr.* 2E, **12,** 182–203.

VOGEL, K. 1962. Muscheln mit Schlosszahnen aus dem spanischen Kambrium und ihre Bedeutung für die Evolution de Lamellibranchiaten. *Abhandl. Math. Nat. Kl. Acad. Wiss. und Lit. Mainz,* 192–244.

MARGARET A. BRADSHAW
c/o Department of Geology
University of Canterbury
Christchurch
New Zealand

Final typescript received 1 April 1970

DINOPHYTON, A PROBLEMATICAL NEW PLANT GENUS FROM THE UPPER TRIASSIC OF THE SOUTH-WESTERN UNITED STATES

by SIDNEY R. ASH

ABSTRACT. *Dinophyton* gen. nov. is based on ultimate and penultimate shoots bearing spirally arranged, outward directed, linear leaves and on some associated, bilaterally symmetrical organs superficially resembling pinwheels. The pinwheels have four arms and bear an empty cup-like structure at the centre. Cuticles of the pinwheels are very similar to those of the shoots and it is concluded that the two organs belonged to the same plant. The function of the pinwheel is uncertain; it may have been seedbearing or possibly had a role in vegetative propagation. *Dinophyton* does not resemble any known plant when all of its characters are considered and for this reason is tentatively assigned to the gymnosperms. The type species, *D. spinosus* sp. nov., has been collected from ten localities in rocks of Late Triassic age in Texas, New Mexico, and Arizona.

TWO of the more common plant fossils found in the Upper Triassic Chinle Formation and Dockum Group of the south-western United States are described in this report. One resembles the shoot of a modern conifer with medium-sized needle-leaves (see text-fig. 2A). The other looks superficially like a pinwheel with four arms or a leaf whorl of *Annularia* (see Pl. 124, figs. 1–6). Close examination shows, however, that the structure is bilaterally, not radially, symmetrical and actually more closely resembles an upside-down Latin cross (see text-fig. 2B). Cuticular study demonstrates that the two fossils probably are parts of the same plant, although the function of the bilaterally symmetrical structure is questionable. Possibly it bore an ovule but since that can not be proven at this time the structure will be referred to as a pinwheel. Neither the shoot nor the pinwheel can be identified with any known plant, fossil or living, so they are both referred to *Dinophyton spinosus* gen. et sp nov.

Although the early Mesozoic gymnosperms of the world are poorly known it is apparent that a number of unusual forms developed during this important time in plant history. Their classification and relationships are uncertain and it is difficult to assign many of them to presently recognized groups. *Dinophyton* is assigned tentatively to the gymnosperms because further classification of the fossil would be premature and must await the results of future research.

Cuticles used in this study were prepared by the standard maceration technique as follows: Compressions and coaly material were placed in concentrated nitric acid and potassium chlorate for a few hours. Then the cuticles were washed with water and cleared with dilute ammonia. Any rock material that still adhered to them after maceration was removed by placing the specimens in concentrated hydrofluoric acid for a day or so. Several of the fairly complete fossils were embedded in plastic but the majority of the material was mounted unstained in glycerine jelly. All slides and specimens have been deposited in the U.S. National Museum (USNM), Washington, D.C.

Previous investigations. Plant fossils of Late Triassic age have been known from the south-western United States for many years. They occur mainly in the Chinle Formation

[Palaeontology, Vol. 13, Part 4, 1970, pp. 646–63, pls. 122–124.]

in New Mexico and Arizona although a few have been collected from a generally equivalent unit, the Dockum Group in west Texas. A number of palaeobotanists have worked on this flora but over-all progress has been slow and erratic and it is apparent that there is still much to learn about these plants.

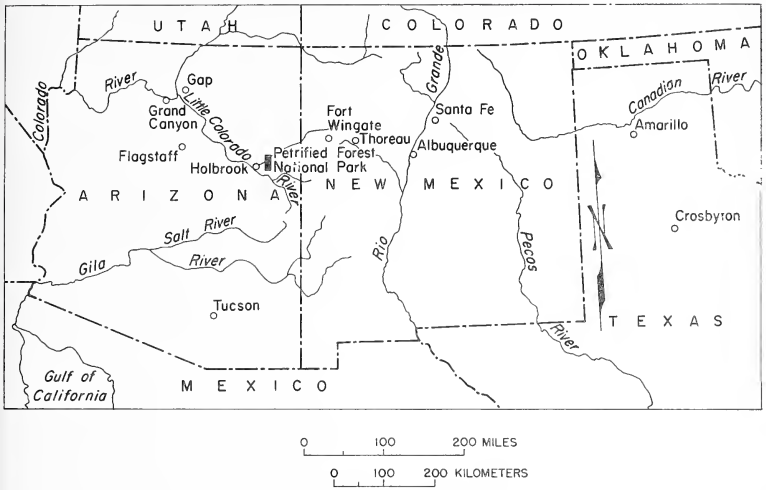

TEXT-FIG. 1. Index map of the south-western United States.

The principal report on the Triassic plants of the Southwest was published by Daugherty (1941). A detailed review of the flora and a history of its investigation were published recently (Ash 1970*a*, *b*, *c*). These reports show that the Chinle Formation contains 51 well-characterized species. The Dockum contains 6 species, 5 of which also are known from the Chinle Formation. Only two species in the Chinle and Dockum floras occur in any other formation and it appears that the floras in the Chinle and Dockum are more closely related to each other than to any other flora.

LOCALITIES

Specimens of the shoot of *D. spinosus* and the pinwheel have been collected from ten different localities in the Upper Triassic rocks of west-central Texas, west-central New Mexico, and east-central and north-central Arizona (text-fig. 1). The distance between the easternmost locality (in Texas) and the westernmost (in north-central Arizona) is about 700 miles. In Texas the fossils occur in the Dockum Group; in New Mexico and Arizona they occur in the Chinle Formation. Both units are considered more or less equivalent (Reeside *et al.* 1957, p. 1464) and a chart showing the currently

accepted nomenclature and correlation of the subdivisions of the two units is given in Table 1. The approximate stratigraphic level of the ten localities mentioned in this report are also indicated on the correlation chart.

Texas. The remains of both the shoot of *D. spinosus* and the pinwheel have been collected from a locality in west-central Texas about 15 miles south-east of Crosbyton in the drainage of Home Creek. They occur in a discontinuous bed of brownish mudstone in the lower part of the Tecovas Formation of the Dockum Group and about 20 ft. above the Permian rocks in that area. Hand specimens of the mudstone frequently show poorly preserved plant remains including fragments of the new species, the bennettite *Otozamites powelli* and some small, round unidentified seeds. Bulk maceration of the mudstone, however, yields many fragments of the distinctive cuticle of *D. spinosus*. Most of the fragments are large enough to show that both the shoot and the pinwheel are present at the locality. Scale leaves of several unidentified conifers and the cuticles of a number of large and unknown leaves were also noted in the bulk macerations from the locality.

New Mexico. All of the localities in New Mexico which have yielded specimens of *D. spinosus* are in the west-central part of the state and in the Monitor Butte Member of the Chinle Formation. A few well-preserved examples of the shoot and the pinwheel have been collected from a locality approximately 4 miles south-west of Thoreau in sec. 13, T. 13 N., R. 14 W. They occur in a bed of soft, greenish, sandy mudstone in the lower part of the Monitor Butte Member and are associated with several other plant fossils including a fern resembling *Cladophlebis reticulata*, *Otozamites powelli*, and some unidentified leaves and seeds.

Many shoots and pinwheels have been collected from four localities about 1 mile south of the Fort Wingate Trading Post. Two are in beds of soft greenish mudstone and sandstone in the lower part of the Monitor Butte Member where it is exposed in road cuts along the highway from Fort Wingate to McGaffey. They have been assigned USGS fossil plant locality numbers 10058 and 10059 and part of the flora they contain has been described recently (Ash 1967, 1970*a*). It includes the ferns *Todites fragilis Cynepteris lasiophora*, *Phlebopteris smithii*, *Wingatea plumosa*, *Clathropteris walkeri*, and *Cladophlebis daughertyi*, the bennettite *O. powelli* and several unidentified leaves, seeds, and fragmentary cones. Two localities in the upper part of the Member have also yielded specimens of *D. spinosus*. One is in a bed of grey mudstone exposed in the badlands a few thousand feet east of the Fort Wingate–McGaffey highway and the two localities mentioned above. It is referred to as USGS fossil plant locality 10061 and a portion of the flora it contains has also been described (Ash 1967, 1968, 1970*a*). That flora includes *T. fragilis*, *C. lasiophora*, *C. daughertyi*, *O. powelli*, *Williamsonia nizhonia*, and a number of unidentified leaves, seeds, and cone scales. Also the wings of an unidentified insect, apparently related to the modern locusts, has been reported from the same locality (Breed 1970).

One of the most productive localities for *Dinophyton* in the Fort Wingate area is on the dissected plateau between the Fort Wingate–McGaffey highway and the badlands containing the previously mentioned locality (no. 10061). The new locality is about 150 ft. west of that locality and is assigned USGS fossil plant locality number 10088. Here the fossils occur in a bed of dark brown shale which is about 5 ft. thick. These rocks are very fossiliferous and the remains of five new conifers, and several unidentified

TABLE 1. Correlation chart of the Upper Triassic rocks in the southwestern United States. The asterisks (*) mark the approximate stratigraphic position of fossil plant localities containing *Dinophyton*. Chart adapted from Reeside and others (1957, pl. 1).

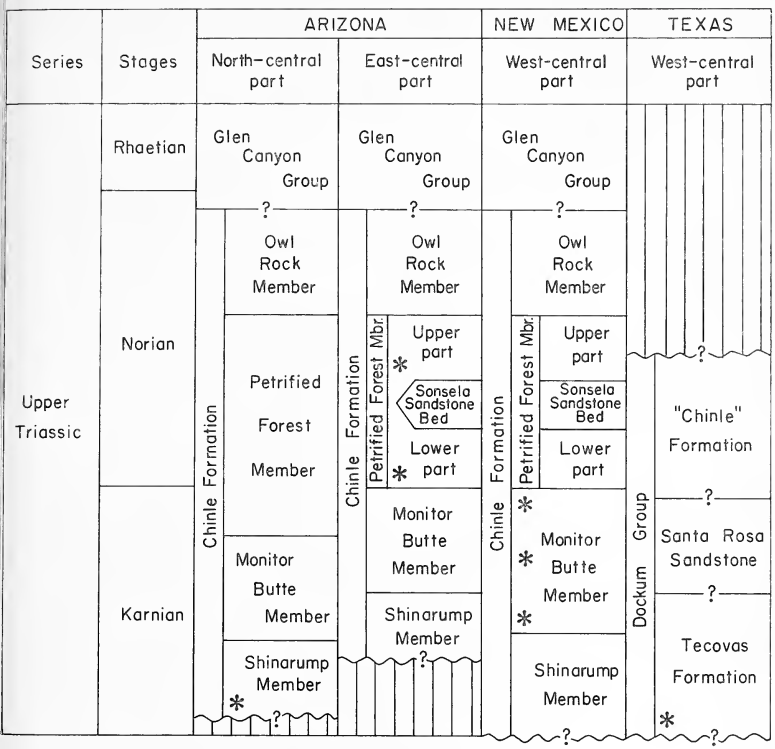

leaves have been collected from them. Other fossils which have been observed there include phytosaur teeth, coprolites of several sizes, and the remains of the branchiopod *Cyzicus* (*Estheria*) sp. The unit is of limited lateral extent and is exposed at only a few other places on the plateau. It is generally a foot or less in thickness at these localities and contains few plant fossils although abundant coprolites and the shells of *Cyzicus* are usually present.

Arizona. At least two of the several fossil leaf localities in Petrified Forest National Park in east-central Arizona contain the remains of *D. spinosus*. One of them is in a thin

layer of paper coal in the lower part of the Petrified Forest Member of the Chinle about 150 ft. below the Sonsela Sandstone Bed and about 20 ft. above the Newspaper Rock Sandstone of Stagner (1941). The locality is in the badlands south of the principal road through the Park in the NE $\frac{1}{4}$, sec. 22, T. 18 N., R. 24 E. (USGS fossil plant locality 10090). Specimens of the pinwheel are particularly abundant at this locality whereas the shoot is uncommon. Remains of many unidentified leaves including those of several conifers are also present in the paper coal. The second locality is in a bed of coaly material and associated sediments in the upper part of the Petrified Forest Member of the Chinle about 90 ft. above the Sonsela Sandstone Bed. It is in a small hill approximately $\frac{1}{2}$ mile west of the principal road through the Park in the NE$\frac{1}{4}$, sec. 29, T. 17 N., R. 24 E. (USGS fossil plant locality number 10089). The coaly material contains abundant plant fossils but most are unidentified. One of the conifers in the flora, however, was recently described as *Pagiophyllum simpsonii* (Ash 1970*d*).

Two localities in the Shinarump Member of the Chinle Formation about 10 miles south-west of the Gap Trading Post at the abandoned A and B uranium mine in north-central Arizona contain large quanities of the foliage of *D. spinosus* but only a relatively few examples of the pinwheel. Several specimens of the penultimate shoots with attached ultimate shoots were collected at both localities but most of the material consists of fragments of just the ultimate shoots. The only other fossils noted at the localities are the shoots of an unidentified scale-leaf conifer and the leaf of *Otozamites powelli*. At these localities fossils are represented typically by limonite encrusted impressions in hard black shale or coarse-grained, tan sandstone. Cuticles are not preserved and identification is based only on the gross morphology of the fossils.

SYSTEMATIC DESCRIPTIONS

Genus DINOPHYTON gen. nov.

Type species. Dinophyton spinosus sp. nov.

Diagnosis. Shoots with many spirally arranged, spreading, needle-like, persistent foliage leaves and a few small leaves. Foliage leaves linear, round in section, containing two parallel veins, apices obtuse to more or less acuminate, base broad, petiole absent. Small leaves clasping, less than 2 mm. long, apices acuminate, attached by entire base. Narrow stumps attached to stem of certain ultimate shoots among typical adult leaves. Possible ultimate female reproductive organ consisting of a pinwheel or cross-shaped structure composed of four appendages and containing a cup which may have held an

---

EXPLANATION OF PLATE 122

Figs. 1–10. *Dinophyton spinosus* gen. et sp. nov. 1, Apical region of penultimate shoot with portions of five ultimate shoots, USNM 43671, ×1. 2–7, Fragments of ultimate shoots. 2, USNM 43672, ×1. 3, USNM 43673, ×1. 4, USNM 43674, ×1. 5, USNM 43675, ×1. 6, USNM 43676, ×1. 7, USNM 43677, ×2. 8–10, Fragmentary penultimate shoots with one or more attached ultimate shoots. 8, USNM 43678, ×1. 9, USNM 43679, ×2. 10, USNM 43680, ×2. Variation in lengths of leaves is from about 1 cm. in figs. 3 and 5 to about 2 cm. in fig. 2. Specimen in fig. 5 is from USGS fossil plant locality 10060; others from USGS fossil plant locality 10061, and all from Monitor Butte Member, Chinle Formation, Fort Wingate area, New Mexico.

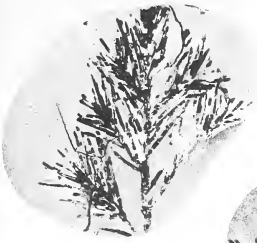

1

2

3

5

4

6

7

8

9

10

ASH, Problematic Triassic plant

ovule. Stomata occurring on both sides of leaf and pinwheel, mostly monocyclic, stomatal pit rectangular, longitudinally orientated. No other parts of the plant are known.

Derivation of name. The name is derived from *diné* which means 'The People' in the language of the Navajo Indians who have inhabited north-western New Mexico and adjacent areas for several hundred years. *Diné* is what the Navajo call themselves.

Dinophyton spinosus sp. nov.

Plates 122–124; text-figs. 2–6

1967 Gymnospermous shoots, Ash, pp. 128–30, fig. 3.
1970*b* Foliage of undescribed conifer, Ash, p. 37, fig. 2f.

Holotype. USNM 43639. Paratypes: USNM 43637, 43638, 43649.

Distribution. The shoot of *D. spinosus* and the pinwheel occur in the Tecovas Member of the Dockum Group near Crosbyton, Texas; in the Monitor Butte Member of the Chinle Formation near Thoreau and Fort Wingate, New Mexico; in the Petrified Forest Member of the Chinle in Petrified Forest National Park, Arizona; and in the Shinarump Member of the Chinle Formation near Gap, Arizona.

Diagnosis. Axis of penultimate shoots 1–2 mm. wide, straight, bearing leaves similar to foliage leaves of ultimate shoots. Ultimate shoots arising alternately at intervals of 15–20 mm. and at an angle of about 35–45° from penultimate shoots, axis about 0·8 mm. wide, bearing many spirally arranged (phyllotaxis probably 2/5), closely set, spreading, outward directed, long, linear foliage leaves and a few, rather small, clasping leaves. Foliage leaves (text-fig. 3) arising from an inconspicuous oval, decurrent leaf cushion about the same width or slightly smaller than leaf, cushion gradually merging with stem. Free part of leaf straight, round in section, projecting at an angle of about 30–50° to stem, about 10–25 mm. long, about 0·35–0·75 mm. broad, sides parallel except in vicinity of base and apex, occasionally narrowing slightly near base to meet leaf cushion, in upper part narrowing abruptly to an obtuse to more or less accuminate apex. Leaf typically containing two veins about 70–90 μm. wide, arising dichotomously from one vein in base of leaf, unbranched, generally parallel except in leaf base where they diverge and in apical region where they unite, resulting vein appears to continue to within a very short distance of apex. Small leaves inconspicuous, concealed by adult leaves, rare, occurring at base of some adult leaves, usually one to three leaves present at one position, small leaves elongate, obtusely pointed, clasping, size ranges from 170–340 μm. wide near base, 500–1700 μm. in length. Narrow stumps about 300 μm. wide, 3–3·5 mm. long arising from stem at several places between foliage leaves on certain shoots.

Cuticle of leaf (text-fig. 4) tough, about 5 μm. thick; cuticle of stem slightly thinner and more delicate, rib-like projections or flanges of cuticle at position of anticlinal walls of epidermal cells, flanges about 3 μm. high. Stomata present on leaf and on stem in approximately equal numbers (about 100 per mm.^{2}), rather widely spaced in poorly defined rows a single stoma wide on leaf and stem. Stomatal rows not sunken, typically separated by 2–5 rows of ordinary epidermal cells, individual stomata in rows separated by 2–6 ordinary epidermal cells. Stomata mostly monocyclic with 2–4 lateral and two terminal subsidiary cells, rarely amphicyclic, subsidiary cells having thickened inner walls, otherwise unmodified except by position, rarely shared, stomatal pit rectangular,

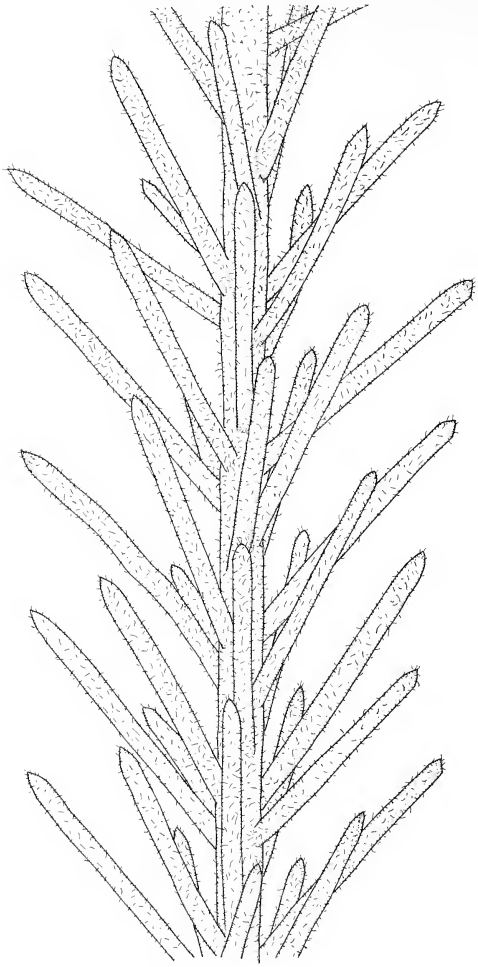

TEXT-FIG. 2A. Reconstruction of part of an ultimate shoot of *Dinophyton*, approximately × 5. The position, size, and number of trichomes is generalized.

about 10–14 μm. $\times$ 3–6 μm., longitudinally orientated, shallow, guard cells slightly sunken, thinly cutinized. Ordinary epidermal cells similar on leaf and stem, longitudinally oriented, polygonal (range noted 7–21 μm. wide, 24–56 μm. long) in and adjacent to margins. Anticlinal cell walls strongly marked, about 1–2 μm. thick, straight to curving with only slight irregularities. Outer periclinal cell walls containing small irregularly distributed pits (usually less than 0·5 μm. in diameter) and often bearing a single, cutinized, simple, usually unicellular hair or low papillae about 7–24 μm. wide at base,

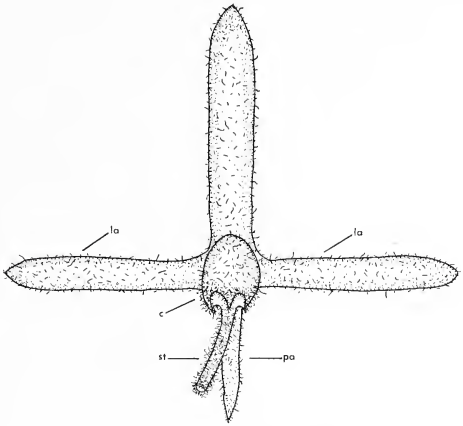

TEXT-FIG. 2B. Reconstruction of the adaxial side of the pinwheel of *Dinophyton* showing the nomenclature used for the several parts of the organ, approximately $\times$ 5. The position, size and number of trichomes is generalized. c, cup; st, stalk; la, lateral appendage; da, distal appendage; pa, proximal appendage.

14–450 μm. long, sides of hair taper gradually from base to acutely pointed apex, base of hair a simple ring on an ordinary epidermal cell. Hypodermal cells having straight to curving walls about 0·5 μm. thick, cells generally rectangular along margins, often about 15 μm. $\times$ 45 μm., elsewhere polygonal, isodiametric to elongate, usual size about 22 μm. $\times$ 30 μm.

Pinwheel organ (?ovuliferous) dorsiventrally flattened, bilaterally symmetrical, consisting of four appendages forming a structure shaped like a pinwheel (text-fig. 5) or more accurately a Latin cross, a small hollow, elipsoidal structure or cup (which might have contained an ovule) positioned at intersection of appendages and a narrow stalk attached to and near proximal end of cup. Cup 2–3 mm. wide, 3–5 mm. tall, long axis orientated along long axis of cross, proximal end open, free part of wall (?integument) divided into three evenly spaced lobes and an elongated stalk-like structure. Lobes acutely pointed, 1·5–2·0 mm. wide and tall, stalk narrows slightly then drawn out into

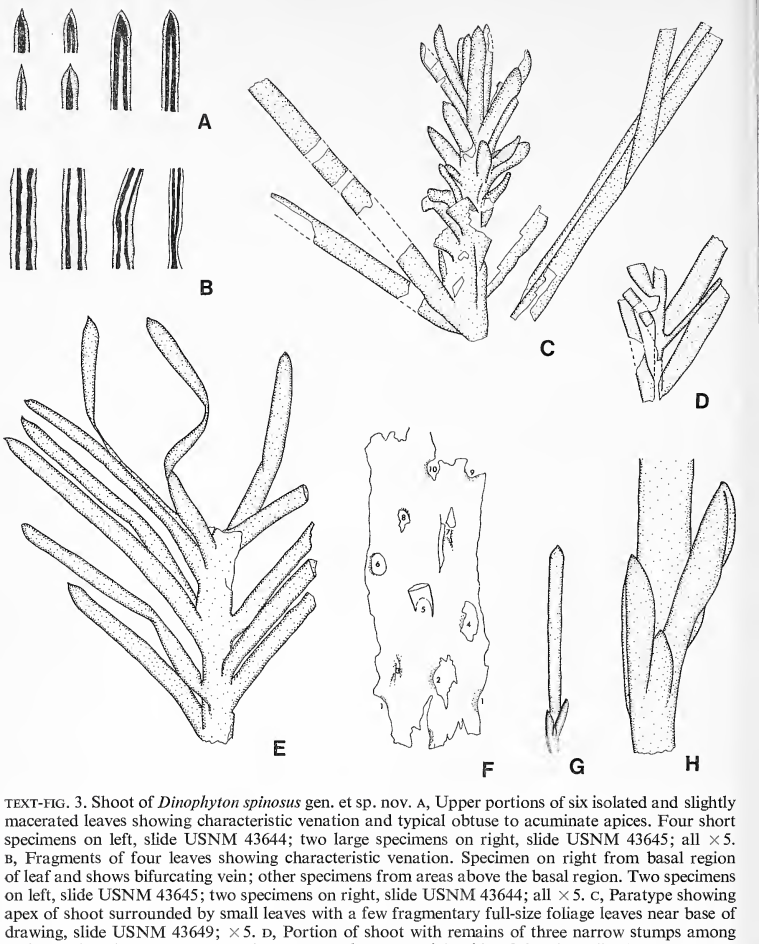

TEXT-FIG. 3. Shoot of *Dinophyton spinosus* gen. et sp. nov. A, Upper portions of six isolated and slightly macerated leaves showing characteristic venation and typical obtuse to acuminate apices. Four short specimens on left, slide USNM 43644; two large specimens on right, slide USNM 43645; all ×5. B, Fragments of four leaves showing characteristic venation. Specimen on right from basal region of leaf and shows bifurcating vein; other specimens from areas above the basal region. Two specimens on left, slide USNM 43645; two specimens on right, slide USNM 43644; all ×5. C, Paratype showing apex of shoot surrounded by small leaves with a few fragmentary full-size foliage leaves near base of drawing, slide USNM 43649; ×5. D, Portion of shoot with remains of three narrow stumps among typical foliage leaves; one stump between two leaves on right side of drawing, slide USNM 43647; ×5. E, Holotype, slide USNM 43639; ×5. F, Exterior of shoot cuticle from which all but the base of one leaf has been naturally broken off. Irregular holes indicate position of leaves and darkly stippled areas are folds in cuticle; numbers indicate leaf sequence; slide USNM 43648, ×10, G, H, Typical foliage leaf with three small leaves at base; slide USNM 43646. G, ×5. H, ×25. Specimens in A–E, G, H from Monitor Butte Member of Chinle Formation, Fort Wingate area, New Mexico. Four short specimens in A, and two specimens on right in B from USGS fossil plant locality 10088; two long specimens in A, two specimens on left in B and specimens in C–E, G, H from USGS fossil plant locality 10061. Specimen in F from USGS fossil plant locality 10089, lower part of Petrified Forest Member, Chinle Formation, Petrified Forest National Park, Arizona. For simplification trichomes are not shown in these drawings.

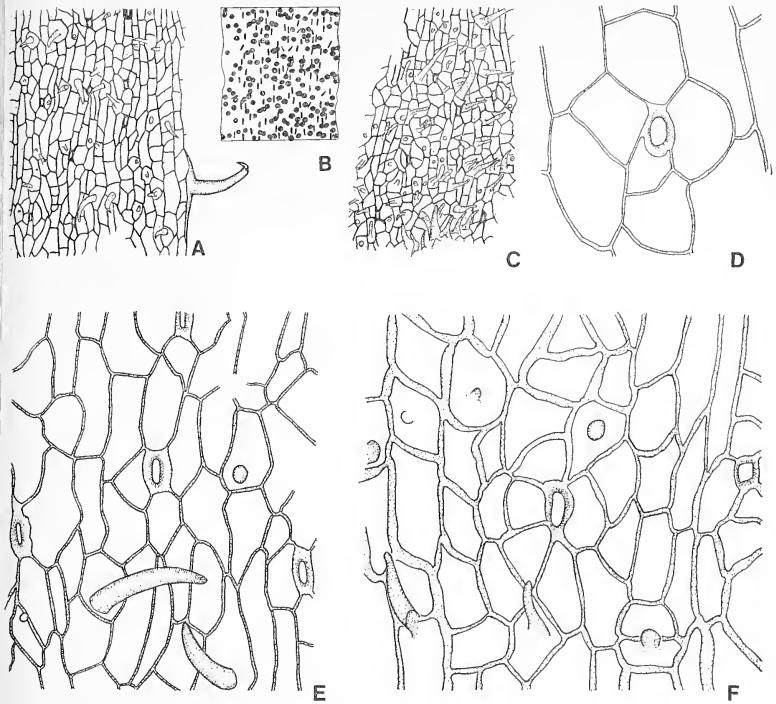

TEXT-FIG. 4. Cuticles of shoot and pinwheel structure of *Dinophyton spinosus* gen. et sp. nov. A, Cuticle of leaf, margin to right; compare with cuticle of pinwheel (text-fig. 6E), epidermal cells generally smaller; slide USNM 43657, ×100. B, Cuticle from typical leaf showing distribution and orientation of stomatal apertures (short lines) and trichomes (large dots); slide USNM 43658, ×25. C, Cuticle from axis of shoot showing stomata and trichomes; cells smaller than on leaf; slide USNM 43655, ×100. D, Stoma on cuticle of pinwheel appendage; slide USNM 43651, ×400. E, Stomata and trichomes on leaf cuticle; slide USNM 43658, ×400. F, Stomata and trichomes on cuticle of pinwheel appendage; slide USNM 43656, ×400. Specimen in A from USGS fossil plant locality 10088, Monitor Butte Member, Chinle Formation, Fort Wingate area, New Mexico. Specimens in B and E from lower part of Tecovas Member, Dockum Group, near Crosbyton, Texas. Specimens in C, D, and F from USGS fossil plant locality 10089, lower part of Petrified Forest Member, Chinle Formation, Petrified Forest National Park, Arizona.

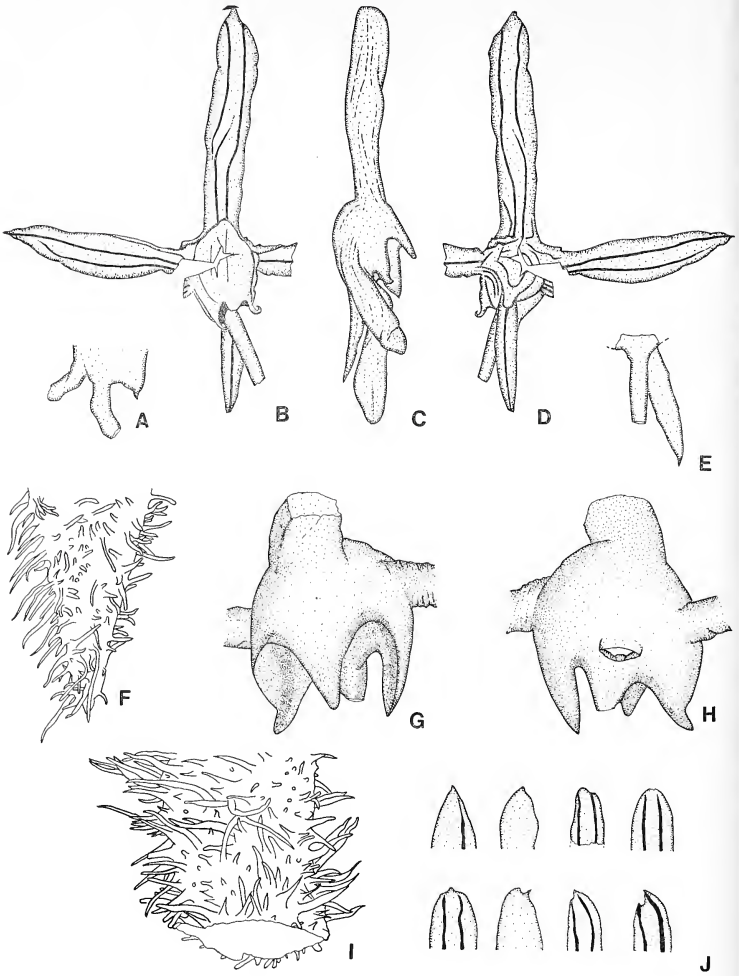

TEXT-FIG. 5.

a long, narrow, linear structure about 0·5–0·7 mm. wide, 2–3 mm. long, broken end not eroded. Appendages linear to oblanceolate, sides generally parallel to subparallel, round in section, apexes usually acute, appendages sometimes slight constricted in basal regions, margins usually entire, occasionally showing low teeth. Lateral appendages of same size (range noted about 1–2 mm. wide, 5–12 mm. long), attached to side of cup, containing two parallel veins. Distal appendage typically slightly longer than lateral appendages (range noted 1–2·5 mm. wide, 9–15 mm. long), attached to distal end of cup, containing two parallel veins about 120 μm. wide; apex sometimes bifurcate for a short distance. Proximal appendage usually shorter and narrower than other appendages, about 1 mm. wide and 4–8 mm. long, attached to back of cup between centre and stalk, containing one vein.

Cuticle of pinwheel (text-fig. 6), except for that lining cup, generally similar to cuticle of leaf. Stomata present on appendages, stalk and exterior of cup in approximate equal numbers (about 50 per mm.^{2}), typically longitudinally orientated, but larger proportion obliquely orientated than on shoot, otherwise identical. Ordinary epidermal cells somewhat larger and more irregular than cells on leaves and stems, epidermal hairs more abundant, especially on cup and stalk, than on shoot. Hypodermal cells present, similar to those on shoot. Upper part of cup and lower part of lobes lined with cuticle, lining extending at least 350 μm. below base of lobes and to within about 100 μm. of the apex of the lobes where it joins typical external cuticle. Internal cuticle delicate, thin, 1 μm. or less in thickness, composed entirely of ordinary epidermal cells, cells mostly polygonal, equidimensional to distinctly elongated, of various sizes, largest noted 30×75 μm. often smaller, elongated cells usually arranged longitudinally in rows, near margins 2–3 rows of rectangular cells (range noted, 7–20 μm. wide, 15–70 μm. long) typically present, anticlinal cell walls about 2–3 μm. thick, straight to curving, smooth, few irregularities, periclinal cell walls smooth, flat. Hypodermal cells present, similar to those on foliage. Female cone as a whole, ovule, male cone, and pollen unknown.

Attribution. Although the shoot of *Dinophyton* and the pinwheel have not been found connected the two structures are attributed to the same plant because of the evidence

---

TEXT-FIG. 5. Pinwheel organ of *Dinophyton spinosus* gen. et sp. nov. A, Obliquely flattened fragment of side and back of a cup showing from left to right, the proximal appendage (slightly distorted), the stalk, and a lateral lobe; slide USNM 43640, ×10. B, D, paratype. B, Adaxial side of pinwheel. D, Abaxial side; specimen unmacerated and broad lines in appendages probably represent veins; slide USNM 43637, ×5. C, Paratype specimen compressed laterally, with front of cup to right, showing both lateral lobes and front lobe of cup; left lateral appendage bent downward nearly completely hiding the stalk; slide USNM 43638, ×5. E, Fragment of back of cup showing stalk at front and proximal appendage behind it; slide USNM 43641, ×10. F, Apex of one lateral lobe of a cup showing typical distribution of trichomes; slide USNM 43642, ×25. G, H, Cup viewed from adaxial and abaxial sides; only bases of four appendages and stalk shown; slide USNM 43643, ×10. I, Broken end of stalk showing typical distribution of trichomes; slide USNM 43654, ×25. J, Upper portions of eight isolated, slightly macerated distal appendages showing apical variation and veins; upper left specimen slide USNM 43659, next to right slide USNM 43661, remainder slide USNM 43660, all ×5. Specimens in A, C, G–I, and second specimen from left in top row of J from USGS fossil plant locality 10089, lower part of Petrified Forest Member, Chinle Formation, Petrified Forest National Park, Arizona. Specimens in B, D–F, and all other specimens in J from USGS fossil plant locality 10088, Monitor Butte Member, Chinle Formation, Fort Wingate area, New Mexico. For simplification trichomes not shown in A–E, G, H, J.

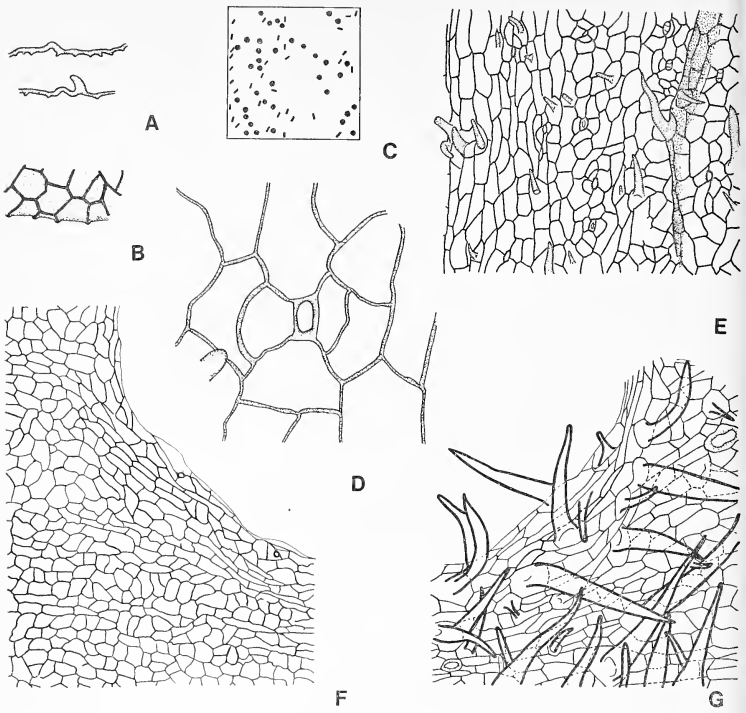

TEXT-FIG. 6. Cuticle of pinwheel of *Dinophyton spinosus* gen. et sp. nov. A, Cross-section of cuticle of distal appendage showing cutinized anticlinal flanges; slide USNM 43650, ×200. B, Fold in lower cuticle of appendage viewed from below showing outlines of polygonal epidermal cells with cutinized anticlinal flanges; slide USNM 43651, ×200. C, One square mm of cuticle of distal appendage showing distribution and orientation of stomatal apertures (short lines) and trichomes (large dots); slide USNM 43651, ×25. D, Stoma, slide USNM 43651, ×400. E, Cuticle from proximal appendage; heavily stippled area near right side represents a fold (cf. leaf cuticle in text-fig. 4); slide USNM 43651, ×100. F, Interior cuticle from a cup lobe; margin marked by narrow elongated cells; note total absence of stomata and trichomes; slide USNM 43652, ×100. G, Exterior cuticle from a cup lobe, margin marked by narrow elongated cells; note stomata and abundant trichomes; slide USNM 43653, ×100. Specimens in A–E from USGS fossil plant locality 10090, lower part of Petrified Forest Member, Chinle Formation, Petrified Forest National Park, Arizona. Those in F and G from USGS fossil plant locality 10088 Monitor Butte Member, Chinle Formation, Fort Wingate area, New Mexico.

of association and the evidence of similar cuticle. Careful collecting has shown that when the remains of one structure are found at a locality examples of the other are always present also. Both the shoot and the pinwheel are now known to occur together in rocks of Late Triassic age at ten localities extending from west-central Texas to north-central Arizona, a distance of about 700 miles. No locality is known where only one of the structures occurs.

The distinctive cuticle of the leaf of *Dinophyton* is easily distinguished from all other Chinle cuticles, the stomata and the papillae being highly characteristic. On the other hand, the resemblance between the cuticles of the shoot of *Dinophyton* and the pinwheel is very close as they agree in: (1) the form and size of stomata; (2) the form and size of the papillae and hairs on the ordinary epidermal cells; (3) the general shape and arrangement of the epidermal cells; (4) the form of the anticlinal walls of the epidermal cells; and (5) the form and size of the tiny pits on the outer periclinal walls of the epidermal cells. Accordingly it is concluded that both the shoots and 'pinwheels' described in this report are parts of the same plant.

Some slight differences have been noted in the cuticles but they are considered unimportant. For example, the epidermal cells are somewhat smaller on the shoot than on the lateral appendages of the pinwheel and the anticlinal walls of the epidermal cells are somewhat thinner on the shoot (about 1–2 μm.) than on the lateral appendages of the pinwheel (about 2–3 μm.). In addition the stomata and papillae are about twice as abundant per square millimetre on the shoot as on the lateral appendages of the pinwheel, but papillae are just as abundant on the stalk of the pinwheel as on the leaf of *Dinophyton*. None of these differences are thought to be significant. Thomas (1925, p. 338), in his study of the Caytoniales, showed that the epidermal cells on the petiole of *Sagenopteris phillipsi* were larger than the epidermal cells on the stalk of the fruit *Caytonia nathorsti*. Nevertheless, he attributed them to the same plant because of several similarities. Harris (1964, pp. 12–13, 23) confirmed Thomas's observations and also attributed the two forms to the same plant. Their findings are just the reverse of mine on *Dinophyton* but it suggests the cell size is not of great importance when there are a great number of similarities as in the present situation. As noted elsewhere in this paper the number of stomata on the two organs may be only an indication of the primary role each played in the life of the plant and are not of importance when attribution is concerned.

Discussion. The function of the stumps (text-fig. 3D) on the ultimate shoot axes of some specimens is uncertain. Possibly they are the bases of the pinwheels but there is no definite information to support this except that the stump and the stalk of the pinwheel are about the same diameter. The ends of the stumps and the stalks are not eroded or worn, suggesting that abscission has taken place. The small leaves at the bases of some of the adult leaves are also of uncertain function. They do not appear to have originated with the stumps, as in the best example of a stump there is no evidence of such leaves. Small leaves are present at the bases of some adult leaves on the same specimen and there is no indication that they surround a stump or any other organ. At present, no special function is attributed to these leaves; perhaps they were merely diminutive leaves; in this connection the shoot apex shown in text-fig. 3C is surrounded by many of the same sort of small leaves.

Isolated but complete leaves of *Dinophyton* are rarely found at any locality. They are uncommon even in the dark, highly fossiliferous shale at locality 10088 and in the coaly material at localities 10089 and 10090. Usually the isolated leaves which are found at these localities are fragmentary, consisting of only the apex and the upper portion of the lamina. A number of short lengths of the ultimate shoot have also been isolated from bulk macerations of material from the same localities. In most of these specimens the leaves were still attached to the axis of the shoots even though they had undergone a certain amount of rough treatment during both deposition and more recently in the laboratory when they were recovered from the rock and macerated. Examinations of these specimens shows that the leaves are still fairly firmly attached to the axis. Actually the upper portions of the leaves are usually missing suggesting that the leaves have more of a tendency to break apart at some point above their base rather than to separate from the axis at the base. A few shoot axes which do not bear leaves were found only in bulk macerations from locality 10090; they are exceptional occurrences. The leaves in these cases typically have not separated cleanly from the axes as irregular holes in the cuticles show where the leaves were attached (text-fig. 3F).

At practically all localities the foliage of *Dinophyton* is represented only by fragments of the ultimate shoot about 5–10 cm. long, rarely longer. A few penultimate shoots with attached ultimate shoots have been found in New Mexico at locality 10061 (see Pl. 123, figs. 8–10) and at the two localities near Gap, Arizona. Most of the foliage referable to *Dinophyton* at these localities, however, consists of short lengths of the ultimate shoots. The comparative rarity of complete, isolated leaves and the common occurrence of specimens of the ultimate shoots with attached leaves suggests that the leaves were normally retained and that the ultimate shoots themselves were deciduous as in some modern members of the Taxaceae, Podocarpaceae, Araucariaceae, and Taxodiaceae.

It is possible that the strands in the leaves of *Dinophyton* which are thought to be veins are actually resin ducts such as occur in the leaves of the modern *Abies lasiocarpa*. Resin ducts in modern conifers, however, usually do not rejoin as the strands do in the leaves of *Dinophyton*. A careful but unsuccessful search was made for evidence of vascular elements in the strands. High magnification showed that they consist mainly of dark, generally structureless material and occasional discontinuous lines which could be anticlinal walls of cells. Usually the strands were visible only in leaves which had been either treated with a commercial bleaching solution for a few hours or had been macerated for about half an hour or less. Continued bleaching or maceration caused them to disappear entirely. In a number of leaves only a single wide strand is present; this could be due to two strands drifting together prior to fossilization giving the appearance of a single strand.

Several lines of evidence seem to indicate that the leaves of *Dinophyton* were round

---

EXPLANATION OF PLATE 123

Figs. 1–9. *Dinophyton spinosus* gen. et sp. nov.; macerated compressions of pinwheel, all ×5. 1, USNM 43670. 2, USNM 43662. 3, USNM 43663. 4, USNM 43664. 5, USNM 43665. 6, USNM 43666. 7, USNM 43667. 8, USNM 43668. 9, USNM 43669. All specimens collected from USGS fossil plant locality 10090 in bed of paper coal, lower part of Petrified Forest Member, Chinle Formation, Teepee Buttes area, Petrified Forest National Park, Arizona.


1


2


3


4


5


6

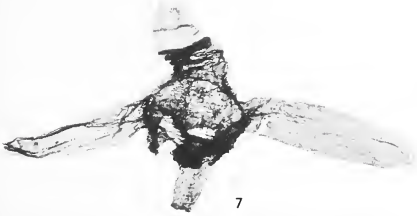
7


8


9

ASH, Problematic Triassic plant

in cross-section and were not flattened appreciably, if at all, during life. The leaf cushion is round to oval on the few shoot axes known that have lost their leaves and also on the many leafy shoots which have been macerated. Apices of the leaves often do not appear to be compressed and look very much like tips of cones. During maceration the leaves swell and become round as if returning to their original shape. Swelling also occurs sometimes when the fossil is embedded in plastic. The leaves do not have specialized margins which typically are found on the edges of most flattened conifer leaves. Finally, the frequency of stomata on the leaves seems to be about the same on all parts of the leaf. The difference in frequency of stomata on the foliage (about 100 per mm.^{2}) and the pinwheel (about 50 per mm.^{2}) is puzzling.

Comparisons. The leaves of *Dinophyton* can be easily distinguished in shape and size from the leaves of all plants in the Chinle Formation (Ash 1970*b*). Only one conifer, *Pagiophyllum* sp. D, could conceivably be confused with *Dinophyton* as they both have leaves of about the same size, but the leaves are distinctly falcate and not linear as in *Dinophyton*. The two species can easily be differentiated on the microscopic level even if only a small fragment of cuticle is available. In *Dinophyton* the stomata are mainly monocyclic and possess small (10–14×3–6 μm.) rectangular stomatal pits, in contrast to the *Pagiophyllum* stomata which are amphicyclic and have comparatively large (20–5×12–15 μm.) oval stomatal pits. In the *Pagiophyllum* the anticlinal walls of the epidermal cells are thicker and more irregular than comparable cell walls on the leaves of *Dinophyton*. Also the outer periclinal walls of the epidermal cells on the leaves contain large angular pits whereas in *Dinophyton* they contain tiny round pits and often bear single, simple papillae. The stomatal pits are overhung by cuticle projections from the subsidiary cells whereas in *Dinophyton* the subsidiary cells do not have any such projections or papillae.

Of plant fossils known to me, *Dinophyton* compares most closely with *Rissika media* Townrow 1967, from the Middle Triassic rocks of South Africa. The gross morphology of the foliage of the two species is remarkably similar (Townrow 1967, pl. 1, fig. E, and Pl. 123, figs. 2–7 of this paper). Both species have leaves of about the same size and with approximately the same proportions. The leaf attachment (spiral with decurrent bases) and the leaf apex (obtuse with an acuminate tip) are very close in certain specimens of the two species. In addition on the microscopic level the anticlinal cell walls of both species are straight and narrow and the cells are usually rectangular to polygonal in shape. In both species the stomata are usually monocyclic with two–four lateral and two terminal subsidiary cells, and the stomatal pits are rectangular.

The two species have dissimilarities which are probably more significant and include round, closely set leaves (1 mm. or less apart) which are not modified by twisting into two lateral rows in *Dinophyton* as against the flat, remotely-set leaves (2–5 mm. apart) which are modified by twisting into two lateral rows in *R. media*. The ultimate shoots of the present species do not seem to bear any small leaves at their base as do the foliar spurs of *R. media*. *Dinophyton* does have small leaves at the base of some adult leaves but they are not present in *R. media*. In *R. media* the stomatal pits are overhung by two to four projections of cutin which extend from the subsidiary cells and walls of the ordinary epidermal cells are smooth; in *Dinophyton* the outer periclinal walls of the ordinary epidermal cells often bear a single, simple cutinized papillae. The apical seed

cones and the three-lobed ultimate seed-bearing structures of *R. media* cannot be matched in *Dinophyton* and it is concluded that the two fossils are not very closely related.

Pinus monophylla is the only conifer I know with leaves which are round in section. The way they are borne on the stem, however, is fundamentally that of the other species of *Pinus* and different from *Dinophyton* where they arise directly on the stem. Apart from having stomata with rectangular pits on all surfaces the cuticle of *P. monophylla* is unlike that of *Dinophyton*.

The shoots of the new species resemble those of many other fossil and Recent conifers and taxads but in no case in all characters. Many genera have narrow leaves but most are dorsiventrally flattened and the leaves, though arranged spirally, curve basally to bring them into the horizontal plane. The narrow leaves contain one vein in contrast to the leaves of *Dinophyton* which apparently have two veins. Two separate veins would be unusual in a conifer leaf less than 1 mm. in width but the 'veins' of *Dinophyton* may be merely two woody strands of a single 'mid vein' as it is ordinarily called in a living conifer.

It is the microscopic features which are so anomalous. In conifers with dorsiventrally flattened needle leaves the stomata are limited to a band on each side of the mid-rib and confined to the lower side; occasionally they are on both sides but the upper commonly has fewer. In only *P. monophylla* are there stomata on all sides of the leaf in about equal numbers. The equal frequency of stomata on the leaves and stem is anomalous as conifer stems bearing needles have but few stomata on the stem, for the leaves are the specialized photosynthetic organs. The form of the stoma (in a pit surrounded by 4–6 unspecialized subsidiary cells) and their arrangement in short longitudinal files is easy to match in living and fossil conifers of various families but is not exclusive to conifers. It is for example seen in *Czekanowskia* (?Ginkgoales) and in *Stenopteris* (?Pteridosperms.) In many genera (Taxaceae, *Sciadopitys*, etc.) strong outgrowths occur on the subsidiary cells which might almost be called 'trichomes' but are not so named. In some conifers and taxads small outgrowths from the marginal cells of the leaf are frequent, and they form microscopic teeth; but in none does one see flat subsidiary cells and strong, hollow, conical outgrowths on the ordinary epidermal cells (properly called trichomes). This feature is foreign to conifer and taxad families and gives the cuticle a strange aspect. Very similar trichomes are seen in certain *Stenopteris* species and in a good many Ginkgoales but there, if trichomes occur, the subsidiary cells are usually more or less papillate.

The strange little pinwheel structure is perhaps very incompletely known; I have assumed that it originally bore an ovule, but another possibility is that it is a vegetative reproductive unit, a kind of bulbil (cf. *Lycopodium selago*) in which case it is perhaps of

EXPLANATION OF PLATE 124

Figs. 1–10. *Dinophyton spinosus* gen. et sp. nov. 1–6, Compressions of pinwheel. 1, USNM 43681, ×1. 2, USNM 43682, ×1. 3, USNM 43683, ×2. 4, USNM 43684, ×2. 5, USNM 43681, ×2. 6, USNM 43685, ×2. 7–10, Cuticle of distal appendage of pinwheel, slide USNM 43686, ×250. Specimens in figs. 1–6 from Monitor Butte Member, Chinle Formation, Fort Wingate area, New Mexico; figures 1, 2, 4, 5 from USGS fossil plant locality 10061, 3 from USGS fossil plant locality. 10060, 6 from USGS fossil plant locality 10058. Cuticle in figs. 7–10 from USGS fossil plant locality 10090 in bed of paper coal, lower part of Petrified Forest Member, Chinle Formation, Teepee Buttes area of Petrified Forest National Park, Arizona.

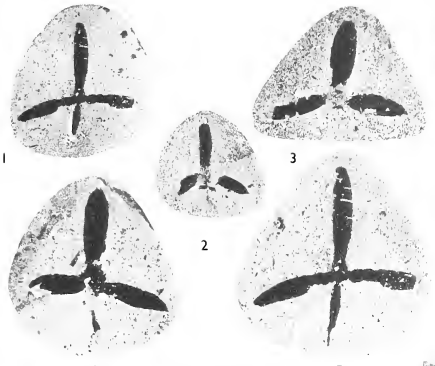

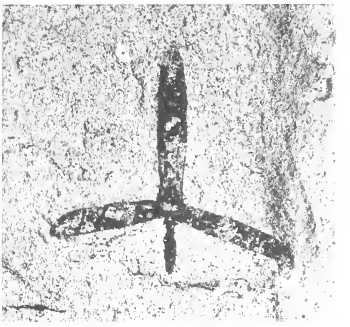

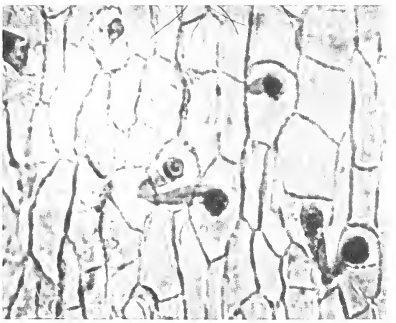

ASH, Problematic Triassic plant

less taxonomic significance. No bulbil occurs in the conifers or taxads, but *Dinophyton* has not yet been proved to be either. It is reasonable to regard the four little outgrowths or appendages as small leaves and these could well have surrounded an ovule. One possibility is that the structures were attached singly on ordinary vegetative shoots but it is only suggested by a few examples of outgrowths or stumps which might be pedicels. Certainly if these organs bore a median ovule it is unlike the ovuliferous part of any known conifer or taxad.

Summary. *Dinophyton* has more features in common with the conifers and taxads than with any other group, but in detail the shoots are distinct by having: (1) a cuticle uniform over the whole surface of the leaves and stem; (2) many trichomes all over the leaf and the stem; and (3) stomata all over the leaf and the stem. The curiously shaped detached organs here called 'pinwheels' do not at present help at all in placing *Dinophyton*, but it seems reasonable to regard *Dinophyton* as a gymnosperm of unknown affinities.

Acknowledgements. The advice of Professor T. M. Harris and Dr. P. D. W. Barnard, the University of Reading, and Dr. H. N. Andrews, the University of Connecticut is acknowledged with thanks. I am grateful to Mr. Charles Bonner, Hays, Kansas for helping with the preparation of the reconstruction of an ultimate shoot of the fossil in text-fig. 2A and to Dr. Donald Becker, Fremont, Nebraska who prepared the thin sections used in text-fig. 6A. The assistance given me by the Museum of Northern Arizona, Flagstaff in the collecting of material for this report is appreciated.

REFERENCES

ASH, S. R. 1967. The Chinle (Upper Triassic) megaflora, Zuni Mountains, New Mexico. *New Mexico Geol. Soc. 18th Ann. Field Conf. Guidebook*, 125–31.

—— 1968. A new species of *Williamsonia* from the Upper Triassic Chinle Formation of New Mexico. *J. Linn. Soc. Lond.* (Bot.), **61**, 113–20, pl. 1.

—— 1970*a*. Ferns from the Chinle Formation (Upper Triassic) in the Fort Wingate area. New Mexico. *U.S. Geol. Survey Prof. Paper* **613-D**, 1–52, 5 pl.

—— 1970*b*. Review of the plant megafossils. In *Symposium on the Chinle Formation*. Mus. N. Arizona.

—— 1970*c*. History of paleobotanical investigations. Ibid.

—— 1970*d*. *Pagiophyllum simpsonii*, a new conifer from the Chinle Formation (Upper Triassic) of Arizona. *J. Paleont.* **44**.

BREED, WILLIAM. 1970. The Invertebrates. In *Symposium on the Chinle Formation*. Mus. N. Arizona.

DAUGHERTY, L. H. 1941. The Upper Triassic flora of Arizona. *Carnegie Inst. Wash. Publ.* **526**, 1–108, pl. 1–34.

GREEN, F. E. 1954. *The Triassic deposits of northwestern Texas.* Ph.D. Dissertation, Texas Tech. College, Lubbock, pp. 1–196, pl. 1–15.

HARRIS, T. M. 1964. *The Yorkshire Jurassic flora, II, Caytoniales, Cycadales and Pteridosperms.* Brit. Mus. (Nat. Hist.), 212 pp., 7 pl.

REESIDE, J. B. *et al.* 1957. Correlation of the Triassic formations of North America, exclusive of Canada. *Geol. Soc. Am. Bull.* **68**, 1451–1513.

STAGNER, H. R. 1941. Geology of the fossil leaf beds of the Petrified Forest National Monument. In DAUGHERTY, L. H. 1941. *Carnegie Inst. Wash. Publ.* **526**, 9–17.

THOMAS, H. H. 1925. The Caytoniales, a new group of angiospermous plants from the Jurassic rocks of Yorkshire. *Phil. Trans. R. Soc.* **213 B**, 299–363, pl. 11–15.

TOWNROW, J. A. 1967. On *Rissikia* and *Mataia*, podocarpaceous conifers from the lower Mesozoic of southern lands. *Pap. Proc. R. Soc. Tasm.* **101**, 103–36, pl. 1–2.

SIDNEY R. ASH
Weber State College
Ogden, Utah, U.S.A.

Typescript received 20 January 1970

ON THE ORIGIN OF THE CLYMENID AMMONOIDS

by M. R. HOUSE

ABSTRACT. The stratigraphical and morphological evidence relating to the abrupt appearance of the endosiphonate clymenids in the early Famennian (Upper Devonian) is reviewed. An origin from goniatites of the *Tornoceras* stock is suggested. A series of morphologically intermediate forms is described from the earliest Upper Famennian of the Holy Cross Mountains of southern Poland. This series leads to *Tornia*, a new genus here described, which is homoeomorphic with *Platyclymenia* but with a ventral siphuncle. Attention is drawn to the fact that some clymenids show a ventral siphuncle in their early ontogeny.

THE origin of the Upper Devonian endosiphonate clymenids, or Clymeniina, has been the subject of considerable past speculation. There have been some, even recently, who would derive the group direct from the Nautiloidea. But these have usually avoided the implications of their enthusiasm. The traditional view, essentially since Branco's classic ontogenetic work of 1890, has been to consider them as derived from the goniatites, but some have preferred a monophyletic, others a polyphyletic origin. The purpose of this paper is to review the stratigraphical and morphological evidence bearing on the subject and to describe, from the earliest Upper Famennian of southern Poland, certain goniatites which seem to be transitional between the Tornoceratidae and the earliest clymenids. These may provide a solution to the problem.

From their sudden first appearance in the early Upper Famennian the clymenids diversified rapidly as is indicated by an accompanying diagram (text-fig. 1) based mainly on the work of Wedekind and Schindewolf. Evolutionary diversification is both in shell form and suture pattern. Extremes in shell form are reached by the bizarre triangular *Soliclymenia* and trilobed *Wocklumeria*. Sutural variation grades from the utter simplicity of *Platyclymenia* to the multilobed *Sphenoclymenia*, superficially homoeomorphic with *Beloceras* but of distinct ontogeny, and *Wocklumeria* and *Epiwocklumeria* with ventral sutures closely homoeomorphic with *Imitoceras*. Their diversity was short lived. The close of the Famennian saw the extinction of the group. Clymenid evolution and sutural derivation has been described at length by Schindewolf in a series of papers: he favours a monophyletic origin of the group and has produced substantial evidence to support this (Schindewolf 1937, 1949*a*, *b*, 1955).

Münster (1831, p. 182) was the first to recognize the endosiphonate clymenids which he described under the name *Planulites* (*non* Parkinson 1822), a name later corrected to *Clymenia* (Münster *in* Goldfuss 1832, p. 489). It is unfortunate that the apt name *Endosiphonites* (Ansted 1838, p. 416) proposed as an alternative during the description of Cornish material is invalid. The complex nomenclatorial history of *Clymenia* and its relatives has been reviewed by Schindewolf (1949, p. 63; 1955, p. 418 et seq.) and Turner (1962).

OPINIONS ON CLYMENID AFFINITY

Following von Buch's use of siphuncle position to separate nautiloids from the ammonoids, Münster placed *Planulites* and *Clymenia* with the former. This view was

[Palaeontology, Vol. 13, Part 4, 1970, pp. 664–76, pls. 125–126.

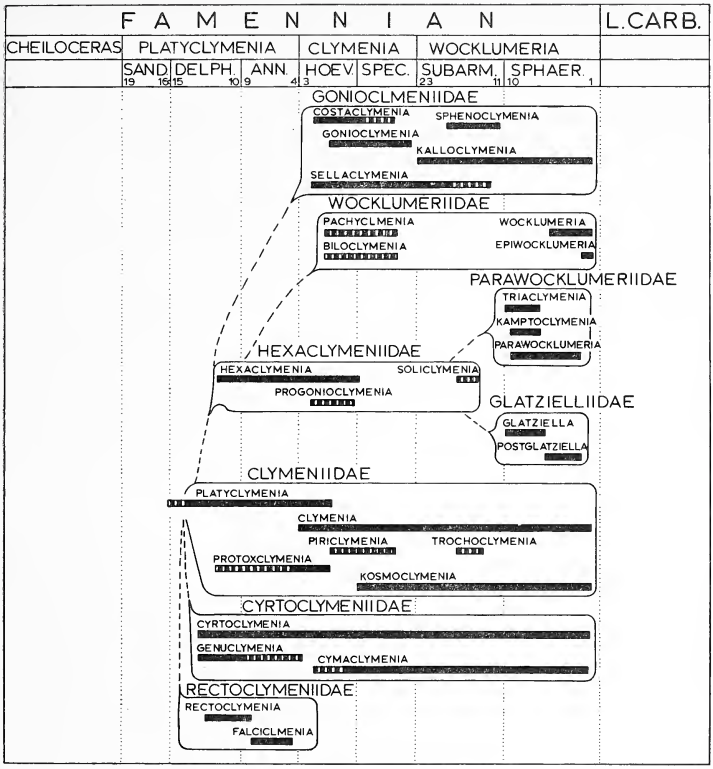

TEXT-FIG. 1. Diagram showing the ranges of genera and families of the Clymeniina. The family groupings are those of Schindewolf (*in* Moore 1957). Pecked lines indicate ranges which are uncertain. The numbers for the Delphinus to Hoevelensis Zones correspond to bed numbers of Wedekind (1908) at Enkeberg: those for the Subamata to Sphaeroides Zones are those of Schindewolf (1937) at the Hönnetal railway cutting.

curiously strengthened when Edwards (1849, p. 50) erected the Family Clymenidae with *Clymenia* and the Tertiary *Aturia* only, being misled by the sutural similarities of the latter with the *Kosmoclymenia* group. Although the relations with *Aturia* were soon disentangled, clymenid affinities were usually given in early textbooks, following Münster, as with the Nautiloidea, for example by Roemer (in Bronn 1859–6, p. 495),

Sedgwick and McCoy (1851–5, p. 312, 401), Woodward (1851–6, p. 87), Blake (1882, p. 36) and others. But a current of disagreement was growing, led by Quenstedt (1849, p. 68) and followed by Hyatt (1883–4), Nicholson and Lydekker (1889, p. 853), Hoernes (1886, p. 400) who gave clear placing of the group with the Ammonoidea even before Branco (1890, p. 34) published his work on the early stages of ammonoids which finally convinced other workers on cephalopods. From 1890 almost all writers have accepted the ammonoid relation as being the most probable. The list includes Foord and Crick (1897), Frech (1890, 1897–1902), Wedekind (1908), Schindewolf (1922, 1955), Miller (1938), Petter (1960), and Bogoslovski (in Ruzhencev, ed., 1962), that is all the most significant contributors on the Devonian Ammonoidea. Recent exceptions are Flower (1961, p. 574) and Donovan (1964, p. 271).

Of those who favoured an origin of the clymenids from typical ammonoids opinion has differed as to their precise source. Frech (1890, p. 399) derived them both (from *Anarcestes* and *Agoniatites*, presumably a generalization, and Schindewolf (1949, p. 206) favouring the anarcestid descent, derived them from *Archoceras* or a related form (1955, p. 422). These views typify the monophyletic standpoint.

Polyphyletic origin of the clymenids found Sobolew (1914*a*, *b*) as its chief exponent. Sobolew sought to derive all the diverse-sutured clymenids from their Devonian goniatite homoeomorphs. The dorsal migration of the siphuncle was held to take place along over ten unrelated lines of descent (see also Schindewolf [1949] since Sobolew's major work is very rare in western libraries: I am indebted to Professor Makowski for a copy). No stratigraphic evidence has been found to support most of these links, and Schindewolf, in several papers, has as a result of ontogenetic work and careful collecting produced a picture of an evolutionary radiation of clymenids from a simple sutured stock of *Hexaclymenia* type. Sobolew's suggestions therefore raise more problems than they solve.

STRATIGRAPHICAL EVIDENCE

Until recently it was supposed that clymenids were represented in the middle Frasnian by the anomalous *Acanthoclymenia* (Frech 1897, p. 177k; Schindewolf 1955), but it has since been demonstrated that *Acanthoclymenia* is a manticoceratid and quite unrelated to the clymenids (House 1961). The elimination of the anomalous Frasnian records clarifies the picture and it is now clear that clymenids enter the stratigraphical record a little above the base of the Upper Famennian and above the *Cheiloceras* Stufe of the German terminology. This has now been demonstrated in unambiguous sections in North Africa (Petter 1960), Spain (Kullmann 1960, 1963), England (House 1963), and Australia (Jenkins 1968), but especially in Germany (Wedekind 1908, Schindewolf 1922, Lange 1929). Similar relations hold in the U.S.A. (House 1962), Canada (House and Pedder 1963) and China (Chang 1958) although in these latter areas less detailed faunal successions have been described.

A brief review will now be given of the main German sequences which have been described showing the entry of the clymenids. This is intended as a nomenclatorial revision and the taxonomic assignments have been corrected as far as possible. The available type material has been re-examined but for Wedekind's material the bed numbers are rarely recorded with the specimens (most labels having been burnt) and

the determinations are based also on his figures and descriptions. Since Wedekind's photographic illustrations are hardly ever given their correct size, and ventral views rarely given, some new illustrations of primary types are given here (Pl. 126).

The first detailed succession described was that on the western part of Enkeberg given by Wedekind (1908, pp. 569–71). The ammonoid sequence is as follows: youngest beds above, oldest below:

Bed 10 (9 cm.): *Platyclymenia* (*Platyclymenia*) *sandbergeri* (Wedekind) (not listed from this bed on p. 621 or on the table), *Rectoclymenia roemeri* (Wedekind), *Cyrtoclymenia involuta* (Wedekind), *P.* (*Pleuroclymenia*) *cycloptera* (Wedekind), *Genuclymenia* (?) *dunkeri* (Münster), *Prolobites delphinus* (G. and F. Sandberger), *Sporadoceras angustisellatum* Wedekind, *S. munsteri* (von Buch), *S. inflexum* Wedekind, *S. discoidale* Wedekind, *Praeglyphioceras pseudosphaericum* Frech, and *Pseudoclymenia planidorsata* (Münster).

Bed 11 (10 cm.): *P.* (*Pl.*) *brevicosta* (Münster), *P.* (*P.*) *steinmanni* (Wedekind), *Cyrtoclymenia angustiseptata* (Münster), *P.* (*P.*) *enkebergensis* (Wedekind), *R. subflexuosa* (Münster), *S. discoidale* Wedekind, *S. münsteri* (von Buch), *S. inflexum* Wedekind, *S. biferum* (Phillips), *Prolobites delphinus* (G. and F. Sandberger), and *Ps. planidorsata* (Münster).

Bed 12 (9 cm.): *P.* (?*P.*) *pompecki* (Wedekind), *C. involuta* (Wedekind), *C. lotzi* (Wedekind), *P.* (*Pl.*) *cycloptera* (Wedekind) (figured here Pl. 126, figs. 8, 9; this specimen may have come from Bed 10, the precise source is not indicated), *G. frechi* (Wedekind), *G. gumbeli* (Wedekind), *G. angelina* (Wedekind) (not recorded from this bed on p. 618), *R. roemeri* (Wedekind), *G. angustiseptata* (Münster), *R. subflexuosa* (Münster), *S. angustisellatum* Wedekind, *S. munsteri pseudosphaericum* Frech, and *Prol. delphinus* (G. and F. Sandberger). *Hexaclymenia hexagona* (Wedekind) (figured here in Pl. 126, figs. 18, 19) was recorded on p. 619 as coming from this bed but was not listed on p. 570.

Bed 13 (11 cm.): *C. lotzi* (Wedekind), *G. phillipsi* (Wedekind) (figured here Pl. 126, figs. 10, 11), *G. frechi* (Wedekind), *S. angustisellatum* Wedekind, *S. munsteri* (von Buch), and *Prol. delphinus* (G. and F. Sandberger).

Bed 14 (12 cm.): *P.* (*P.*) *steinmanni* (Wedekind) (figured here Pl. 126, figs. 6, 7; also recorded from Bed 14 on p. 570 which could have been the source of the figured specimen), *C. involuta* (Wedekind) (recorded from this bed on p. 570 but not on p. 610), and *S. biferum* (Phillips). *G. angelina* (Wedekind) (refigured here on Pl. 126, figs. 14, 15) is recorded from this bed on p. 618 and on the table but not on p. 570. *P.* (*P.*) *sandbergeri* (Wedekind) (figured here Pl. 126, figs. 12, 13) is also recorded from this bed on p. 621 and on the table, but not on p. 570.

Bed 15 (9 cm.) and Bed 16 (15 cm.): no ammonoids recorded.

Bed 17 (9 cm.): *Pseudoclymenia sandbergeri* (Gümbel), *Ps. sandbergeri dillensis* Drevermann, *Ps. dorsatum* (Wedekind), *Dimeroceras padbergensis* Wedekind.

In this succession *Platyclymenia s.s.* and *Cyrtoclymenia* are the first clymenids to appear above beds with abundant *Pseudoclymenia*, *Dimeroceras*, and *Sporadoceras* (Beds 22–17) with *Cheiloceras* abundant lower still (Beds 25–31). Although not relevant to the present discussion the discrepancies in Wedekind's various records and the textual inconsistencies should be noted. Also the magnifications which he gives for his

illustrations are mostly incorrect. The large number of species he erected is also suspicious, and doubtless most of these will be redundant when a modern statistical analysis of the fauna is undertaken.

When the Enkeberg section was revised by Lange (1929) the collecting was not done with the same scrupulous attention to the detailed succession that characterized Wedekind's work, and the stratigraphic revision was at the crude level of zones (as on text-fig. 1) only. One cannot therefore feel other than cautious in accepting some of the changed ranges which he recognized. Thus Lange (1929, p. 16, 97) records *Platyclymenia* (*Varioclymenia*) *kayseri* as common in Zone IIIα, the Sandbergeri Zone, from Wedekind's Beds 19–16, and the entry of other clymenids above in Beds 15–10 is not recorded in detail, and in failing to do so Lange leaves himself open to the suggestion that he did not correctly interpret Wedekind's bed numbers. This matter, however, is a trivial one which will only be resolved by the next reviser of the Enkeberg section. In recording clymenids in Zone IIIα he was following Schindewolf as will be seen below.

Another detailed succession showing the entry of clymenids is the sequence at Hof described by Schindewolf (1922, p. 256; Wurm 1961, p. 118). Here the entry of clymenids is recorded as follows (again taxonomic revisions have been made).

Bed 11 (0·25 m.): *S. discoidale* Wedekind, *S. munsteri* (von Buch), *R. subflexuosa* (Münster), *C. involuta* (Wedekind), *C. wedekindi* Schindewolf, *P.* (*P.*) *sandbergeri* (Wedekind), *P.* (*P.*) *prorsostriata* Schindewolf, *P.* (*Trigonoclymenia*) *crassicosta* (Wedekind), and others.

Bed 10 (1·8 m.): *S. munsteri* (von Buch), *S. discoidale* (Wedekind), *R. rotunda* Schindewolf, *C. sulcata* Schindewolf, *Genu. frechi* (Wedekind), *Genu. borni* Schindewolf.

Bed 9 (*c.* 1·2 m.): *R. sandbergeri* (Gümbel), *Ps. sandbergeri dillensis* (Drevermann), *S. munsteri* (von Buch), *S. contiguum* (Münster), *Praeg. pseudosphaericum* Frech *R.* (?) *kayseri* Drevermann, *C. pulcherrima* (Wedekind), *Genu. frechi* (Wedekind).

Bed 8 (2·5 m.): *Ps. planidorsata* (Münster), *Cheiloceras* sp., *S. biferum* (Phillips).

Schindewolf referred Bed 8 to IIβ, the upper part of the Cheiloceras Stufe (Pompeckji Zone), Bed 9 to IIIα (Sandbergeri Zone), and Beds 10 and 11, and the overlying Bed 12 to IIIβ. Since *Prolobites delphinus* was not recorded it is to be inferred only that the latter group represent the Delphinus Zone.

This review serves to emphasize that the stratigraphical evidence shows that the earliest known clymenids all have sutures showing a lateral lobe and dorsal lobe only (*Platyclymenia s.s. Rectoclymenia, Cyrtoclymenia*) with some (*Genuclymenia*) with a slightly more complex pattern. Later follow the other subgenera of *Platyclymenia* and later still, in the Clymenia Stufe, *Kosmoclymenia* and *Cymaclymenia*. *C. ornata*, an early form of the latter, is illustrated here (Pl. 126, figs. 16, 17): the figured specimen is Münster's, Schindewolf recorded this species in the lower part of Zone Vβ.

ORIGIN FROM THE TORNOCERATIDAE

It is the purpose here to suggest that a group of derivatives of the common Devonian *Tornoceras* stock which occur in the early Upper Famennian are morphologically transitional between typical tornoceratids and the earliest clymenids. The critical fauna

is from the Lower Famennian of Kielce in the Holy Cross Mountains. Some of this is illustrated here (Pl. 125, 126).

The Kielce Tornoceratids

In 1913 Dybczyński published a brief account of a prolific locality for pyritized goniatites in the Holy Cross Mountains on the outskirts of the town of Kielce, from which he had collected over 5000 specimens. Sobolew (1913, 1914*a*, *b*) gave a lengthy account of this fauna with many illustrations, but described them using a complex generic nomenclature based on a root with morphologically descriptive prefixes and suffixes. Sobolew's genera, but not his species, have been declared invalid by Opinion 132 of the ICZN (Schindewolf and others 1936). The pyritic fauna is of great diversity and is almost wholly of early Famennian age. The evidence for this will briefly be discussed.

The main source of the material described by Sobolew was from shales overlying the Frasnian and perhaps earliest Famennian limestones at the Kiedelna quarry. Housing developments have now covered most of the site, but in 1962 the author was able to collect from weathered shales (but not in place) a poor fauna including *Raymondiceras* and *Sporadoceras* (with spiral ornament) confirming that a position succeeding the Cheiloceras Stufe recorded in the quarry below is proven. Fortunately Dr. H. Makowski has kindly made available a collection from Kielce thought to come wholly from the shales overlying the quarry and the Sieklucki's Brickpit there, and which forms the remnants of a pre-war collection of the Geology Department of the University of Warsaw.

Interest here centres on the remarkable suite of tornoceratids and their precise age. Rare early clymenids occur in the fauna and some were figured by Sobolew. The most readily determined tornoceratids are those similar in shell and suture form to *T. crebriseptum* from the Three Forks Shale of Montana (House 1965, p. 115). The Montana fauna contains *Platyclymenia*, *Raymondiceras*, and *Rectoclymenia* and has been referred to the Delphinus Zone. The main source at Kielce would appear to be earlier than this. (The Delphinus Zone is where the clymenids first appear, text-fig. 1). Sobolew's fauna included *Sporadoceras* and *Imitoceras*, both of which, in Germany, enter in the upper half of the Cheiloceras Stufe (Pempeckji Zone). Although there is no reason to suppose that the Kielce pyritic fauna is from a single horizon, the evidence suggests that the fauna studied here covers the range of the Pompeckji and Sandbergeri Zones. That is, the bulk of the fauna correlates with horizons immediately preceding the known entry point of the clymenids. Higher horizons, with clymenids are also known and were mentioned by Sobolew.

SYSTEMATIC PALAEONTOLOGY

The whole of the Kielce material is in need of description but the material at present available is so meagre in comparison with that formerly known and destroyed during the Second World War, that this would be unwarranted at present. Dybczyński (1913) described a number of species and the specific names given by Sobolew are still valid despite the ruling of the ICZN on his genera. The Kielce tornoceratids which are the concern here comprise some belonging to the *Tornoceras crebriseptum* Raymond group,

which perhaps, should be recognized as a new subgenus. Others of the transitional series fall in *Protornoceras* and the end point in which the lateral lobe has ceased to exist except as a vestigal remnant comprise a small group for which the new generic name *Tornia* is here proposed.

Suborder GONIATITINA Hyatt 1884
Superfamily CHEILOCERATACEAE Frech 1897
Family TORNOCERATIDAE Athaber 1911
Genus TORNOCERAS Hyatt 1884

Type species. By original designation *Goniatites uniangulare* Conrad.

Tornoceras (*T.*) *crebriseptum* Raymond Group

Discussion. The tornoceratids which form the starting point of the morphological series leading to *Tornia* belong to a group represented by forms referable to *T.* (*T.*) *crebriseptum* (for a description of the type material see House 1965). The Montana type material already shows evidence, in the internal mould, that the umbilicus is open, although testate specimens may not have been. Were the latter point settled in the affirmative then they should be referred to *Protornoceras* or a new genus group. The suture, with its subdued form and flat ventro-lateral saddle is also distinctive (Pl. 125, fig. 1). Quite closely similar types occur in the Kielce fauna but these differ in showing small constrictions over the venter (Pl. 125, figs. 2–5) which, suturally are even closer to the Montana material. In view of the priority of Raymond's work over that of Dybczyński and Sobolew these may be referred to as *T.* (*T.*) aff. *crebriseptum* pending revision of the whole fauna.

Genus PROTORNOCERAS Dybczyński 1913

Type species. By original designation *Tornoceras* (*Protornoceras*) *polonicum* Dybczyński, 1913, p. 512.

Discussion. The current use applies this generic name to all open umbilicate tornoceratids without the ventro-lateral grooves and other characters which distinguish *Aulatornoceras*. Middle Devonian examples, such as *P. foxi* House (1963 p. 19, pl. 2*a*, *d–g*, text-fig. 8*a–g*) seem clearly to be unrelated directly to those of the Lower Famennian and should, at some stage, receive another generic name. The Polish material forms the type for the genus and some representatives are figured here (Pl. 125, figs. 6–22). Many specific names belong here which we owe to Dybczyński, Sobolew, and Wedekind. The group is a variable one and many of these names will be lost in synonomy when they come to be revised.

The importance in the present context is that as well as showing a progressive opening of the umbilicus the group also shows sutural characters linking it with the crebriseptum

EXPLANATION OF PLATE 125

Figs. 1–5. *Tornoceras* (*Tornoceras*) spp. 1, *T.* (T.) *crebriseptum* Raymond, holotype from the Three Forks Shale of Montana in the Carnegie Museum, Pittsburgh No. 464; ×2. 2–5, *T.* (*T.*) aff. *crebriseptum* (Raymond) from Kielce; 2, ×2·5; 3–5, ×2.

Figs. 6–22. *Protornoceras* spp. 6–8, *P.* cf. *planidorsatum* (Wedekind) from Kielce; ×2. 9–19, *P. simplificatum* (Sobolew) from Kielce; 9, 10, ×2·5, 11–13, ×2, 14–19, ×3. 20–22, *P.* cf. *zuberi* Dybczyński from Kielce; ×2·5.

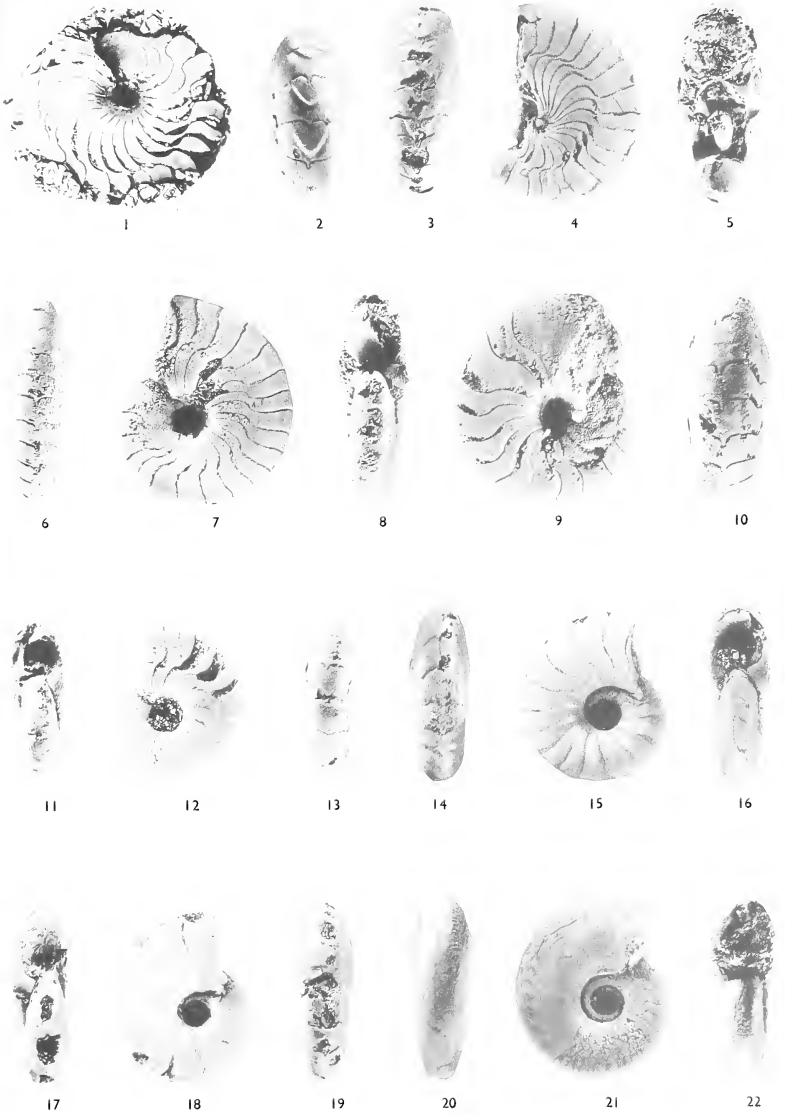

HOUSE, Origin of Devonian clymenid ammonoids

group of *Tornoceras s.s.* Further, in the Polish material all morphological gradations can be seen from sutures typical of *Tornoceras s.s.* to those in which the elements become progressively subdued (text-figs. 2B, C; Pl. 125, figs. 6–20; Pl. 126, figs. 1, 2).

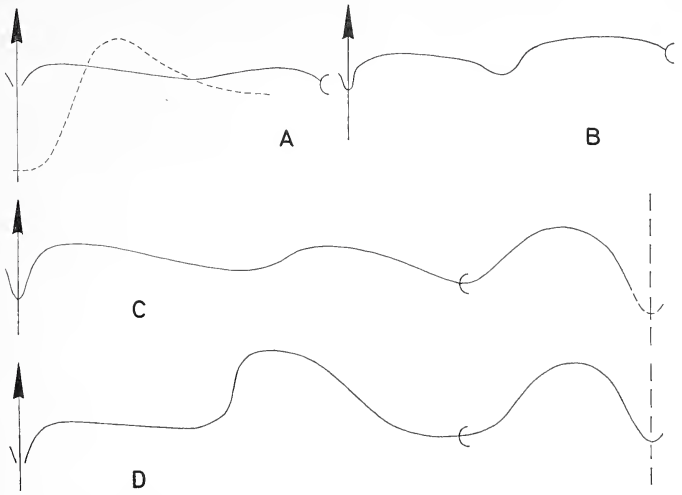

TEXT-FIG. 2. Early Famennian tornoceratids from the Sieklucki Brickpit Kielce, Poland; all ×20. A, *Tornia mirabile* (Dybczyński), suture at 13 mm. diameter. B, *Protornoceras* cf. *zuberi* Dybczyński, suture at 11·9 mm. diameter (also figured on Pl. 125, figs. 21, 22). C, *Protornoceras simplificatum* (Sobolew), suture at 15 mm. diameter (also figured on Pl. 125, figs. 17–18). D, *Tornoceras* (*T.*) aff. *crebriseptum* Raymond, suture at 11·8 mm. diameter (also figured on Pl. 125, fig. 2).

Genus TORNIA gen. nov.

Type species. Here designated *Tornia mirabile* Dybczyński 1913, p. 514, pl. 1, fig. 4, pl. 2, fig. 4.

Diagnosis. Open umbilicate tornoceratids with ventral siphuncle, biconvex growth-lines and mature suture forming a broad shallow lateral lobe, a narrow ventral lobe and a deep linguiform dorsal lobe.

Remarks. Morphologically this form is identical with some platyclymenids apart from the ventral position of the siphuncle. Relic traces of the typical tornoceratid adventitious lobe can be seen in the broad lateral lobe, but this cannot be crossed by a radial line drawn from the umbilicus and in this respect differs from the presumed *Protornoceras* antecedents (e.g. Pl. 125, figs. 21, 22 Pl. 126, figs. 1, 2;), and there is no arched latero-umbilical saddle as is also characteristic of tornoceratids. The genus closely approaches homoeomorphy with the Middle Devonian genus *Agoniatites*.

Tornia mirabile (Dybczyński)

Plate 126, figs. 3–5, text-fig. 2A

Neotype. The holotype having been lost one specimen belonging here will be described and is designated the neotype: this is an internal haematite mould showing some 90° of body chamber. A tendency to orad sutural approximation and evidence of shell thickenings in the body chamber suggest maturity. This specimen is in Professor H. Makowski's collection at the Polski Akademia Nauk, Warsaw.

The shell form (see Pl. 126, figs. 4, 5) is open umbilcate but the earliest whorls are not seen. Experience with this preservation having shown that the inner whorls are rarely shown by sectioning, this has not been risked on the neotype, but moderately evolute early whorls are indicated. The whorl form shows a well-rounded venter, somewhat flat sides and a steep and rounded umbilical shoulder.

Dimensions (in mm.)

	D	WW	WH	UW
Holotype (data from Dybczyński)	17	6	*c.* 8	4
Specimen from Sieclucki's brickpit	16·7 (max.)	—	—	—
(Neotype)	14·4	4·1	5·9	4·3

Growth-lines, as discernible on an internal mould are biconvex, forming a slight salient on the umbilical shoulder, a broad slightly prorsiradiate sinus on the flanks and a short, stubby ventro-lateral salient or short lappet passing to a U-shaped ventral sinus. On the body chamber diffuse shell thickenings appear to have followed the same course.

The sutures vary a little among themselves. A small V-shaped ventral lobe passes to a very broad and weak lateral saddle of slightly varying very shallow depth. Traces of the position of the lateral lobe of the supposed ancestral *Protornoceras* can be discerned as a very slight ventral facing slope on the lower flanks. The dorsal suture has not been seen, but in the nearest *Protornoceras* in which a clear lateral lobe can be seen (Pl. 126, fig. 2), it shows that a typical *tornoceratid* deep lobe was present.

Remarks. This sole neotype specimen from the Sieklucki Brickpit is the end member of the sequence described under *Protornoceras*. The suture is homoeomorphic in its elements

EXPLANATION OF PLATE 126

Figs. 1, 2. *Protornoceras* aff. *zuberi* Dybczyński from Kielce; ×3.

Figs. 3–5. *Tornia mirabile* (Dybczyński) from Kielce; ×2.

Figs. 6–9. *Platyclymenia* (*P.*) Spp. 6, 7, *P.* (*P.*) *steinmanni* (Wedekind), holotype (figured Wedekind 1908, pl. 43, figs. 12, 12a) from Bed 14 at Enkeberg. ×1. Univ. Göttingen Coll. 8, 9, *P.* (?*P.*) *cycloptera* (Wedekind), holotype (figured Wedekind 1908, pl. 43, fig. 11) from Bed 11 or 12 at Enkeberg; ×2, Univ. Göttingen Coll.

Figs. 10, 11. *Genuclymenia phillipsi* (Wedekind), holotype (figured Wedekind 1908, pl. 39, fig. 26, pl. 43, fig. 6) from Bed 13 at Enkeberg; ×2, Univ. Göttingen Coll.

Figs. 12, 13. *Platyclymenia* (*P.*) *sandbergeri* (Wedekind), lectotype here designated (figured Wedekind 1908, pl. 44, figs. 9, 9a; 1914, pl. 2, fig. 7 as *P. wysogorskii* Frech) from Beds 14 to 12 at Enkeberg; ×2, Univ. Göttingen Coll.

Figs. 14, 15. *Genuclymenia angelina* (Wedekind), holotype (figured Wedekind 1908, pl. 44, fig. 6) from either Bed 13 or 14 at Enkeberg; ×1, Univ. Göttingen Coll.

Figs. 16, 17. *Cymaclymenia*(?) *ornata* (Münster); Münster's holotype in the Bayerische Staatssammlung für Paläeontologie und Historische Geologie, Munich; ×2.

Figs. 18, 19. *Hexaclymenia hexagona* (Wedekind), holotype (figured Wedekind 1908, pl. 43, figs. 7, 7a) from Bed 12 at Enkeberg; ×1·78, Univ. Göttingen Coll.

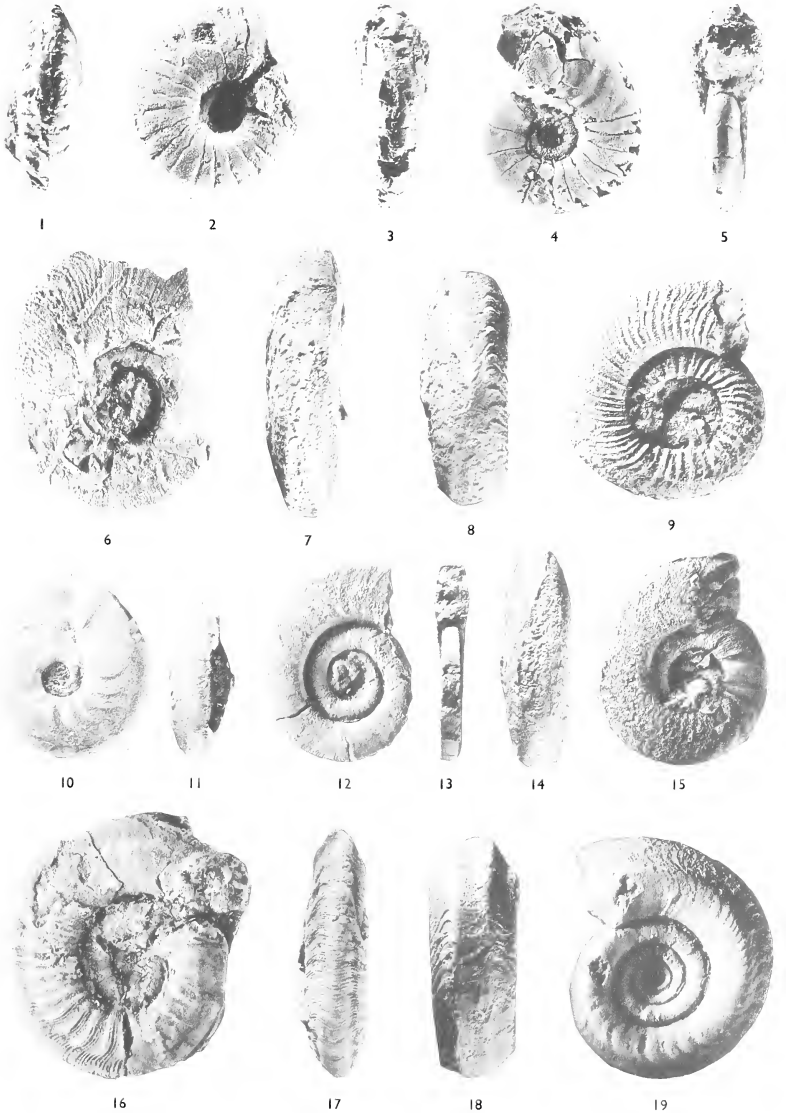

HOUSE, Origin of Devonian clymenid ammonoids

with *Agoniatites*, but the lateral lobe is much shallower. No Frasnian agoniatitids being known, and the *Protornoceras* link being demonstrable, a phylogenetic derivation from *Agoniatites* is not possible. Only the specimen figured by Sobolew as *Gomi-reprotomeroceras* (*Tornoceras*) *alobatum* Sobolew (1913, pl. 9, figs. 5, 6, ?non text-fig. 105) seems also to belong in *Tornia*; but this form is significantly more evolute than the holotype and substantially more so than the neotype specimen here described. However, the involvement of new species within Sobolew's generic formulae is so complex a matter that it is unfortunate that they were not also invalidated by the ICZN. The destruction of his collection in the Second World War renders the use of his names even more difficult and those of Dybczyński are preferred in this case although his collection is also untraced.

The comparison with the varied early clymenids (Pl. 126, figs. 6–19) in shell form and in the course of the growth-lines, and where present, ribbing is sufficiently close to raise no great problems in their derivation from *Tornia*. No other Devonian goniatite shows so close a sutural resemblance to these early clymenids as does *Tornia*. A ventral suture has been demonstrated in the early stages of some clymenids (see references given later) and this suggests that the permanent adoption of the endosiphonate condition falls wholly within the Clymeniina.

SUMMARY AND CONCLUSIONS

The demonstration that the Frasnian *Acanthoclymenia* is not a clymenid concentrates attention on the Lower Famennian sequences where clymenids appear. The Polish fauna of *Protornoceras* and *Tornia* at this level gives a morphological series leading to the earliest known clymenid genera. The reasons for favouring an origin of the clymenids from goniatites rather than nautiloids is summarized below:

1. *The form of the protoconch.* As Branco (1890, p. 35, pl. 7, figs. a–e), Schindewolf (1923, p. 24 et seq.) and others have observed the egg-shaped, often laterally elongate protoconch of the clymenids finds its closest analogy with those of the goniatites. What early stages of Devonian nautiloids homoeomorphic with coiled ammonoids are known, for example centroceratids (Flower 1952), are different. Similarly the form of the prosuture (Branco 1880, pl. 8, fig. 1*b*; Schindewolf 1923, text-fig. 2) is very similar to that of goniatites particularly the *Tornoceras* group (see House 1965).

2. *The lack of an umbilical perforation.* This is the rule in the clymenids and of the goniatites from which it is here argued they are derived. It does not appear to be a character of the groups of nautiloids from which Donovan (1964, p. 271) would derive the clymenids. There is no doubt, however, that information on the early stages of some relevant Devonian nautiloid genera is lacking.

3. *Transitional position of the siphuncle.* As Branco (1880, pl. VII, fig. 3*b*) and Schindewolf (1955, p. 420) have described, some early clymenids show a ventral siphuncle in the early stages. Later the siphuncle migrates to a dorsal position. Sandberger (1853, pl. 6, fig. 1) has illustrated sagittal sections of *Clymenia compressa* showing that in early whorls, but not the earliest, the siphuncle is often well away from the dorsum.

To these factors the present paper adds a description of forms which show evidence of:

4. *Transitional shell form.* The sequence of tornoceratids described here from the

Lower Famennian of Southern Poland shows a progressive opening of the umbilicus and lateral forward projection of the adult aperture which approaches that of the earliest known clymenids.

5. *Transitional Suture Forms.* The same sequence shows a simplification of the *Tornoceras* suture to one showing a deep dorsal lobe, and a shallow lateral lobe: both features of the earliest known clymenid genera. The trend culminates in the new genus, *Tornia*.

6. *Stratigraphic intermediates.* The horizon of the new intermediate forms appears to lie just below the level at which clymenids appear.

It seems to the author that it is the summation of this evidence which makes an origin of the clymenids from goniatites, and a specific origin from the *Tornoceras* stock, probable.

Some comments may be made on another contendor as ancestor, *Archoceras* (Schindewolf 1955) which is a late Frasnian and earliest Famennian genus. For several reasons it does not seem very suitable. There is a clear gap in the record of *Archoceras* before the appearance of clymenids. The sutural pattern of the genus, although simple (House 1962, p. 367, text-fig. 7), is not such as to enable ready derivation of the clymenid suture. The large lateral saddle is directly the reverse of the shallow lateral lobe of the earliest clymenids. Also the deep ventral lobe, combined with a deep dorsal lobe, makes the septum highly arched orad, and hence any migration of the siphuncle across this is difficult to envisage. The suitability of *Tornia* and its relatives is particularly shown here since the septal mid-line actually slopes dorsad along the line of the siphuncle migration. When *Acanthoclymenia* was thought to be a Frasnian clymenid, *Archoceras* did seem to offer attractions, but these have now been lost.

What the functional advantages of a dorsal siphuncle were it is difficult to assess, but the rapid evolution after the inception of the character suggests that the survival value was considerable. The wholesale extinction of the clymenids at the close of the Devonian need not be related to any change in this factor necessarily since goniatite groups are also affected by the extinctions. But during the late Famennian the diversification of the clymenids seems matched by an over-all decline of goniatite stocks. Migration of the siphuncle occurs in other ammonoid groups also (*contra* Donovan 1964, p. 271), for example in the Permian *Pseudoholorites* and *Neoaganides* (Miller and Furnish 1957, p. 1044), but at no other time in ammonoid history does the fully dorsal siphuncle position appear to have been adopted again.

Acknowledgements. Thanks are due especially to Professor H. Makowski for allowing me to study collections in Warsaw and to loan and figure material from his personal collection at the Polski Akad. Nauk: to Dr. G. Biernat and Dr. H. Osmolska for their kindness in guiding me in the Kielce area and the Holy Cross Mountains generally. Also to Professor H. Schmidt and Professor O. H. Walliser for allowing me to photograph Wedekind's type collection at Göttingen and Marburg respectively.

REFERENCES

ANSTED, D. T. 1838. On a new genus of fossil multilocular shells found in the slate rocks of Cornwall. *Trans. Camb. phil. Soc.* **6**, 415–22.

BLAKE, J. F. 1882. *A monograph of British fossil Cephalopoda. Part 1, Introduction and Silurian species.* 248 pp., 31 pl. London.

BRANCO, W. 1880. Beiträge zur Entwicklungsgeschichte der fossilen Cephalopoden. II. Die Goniatiten, Clymenien, Nautiliden, Belemnitiden und Spiruliden, nebst Nachtrag zu Teil I. *Palaeontographica*, **27**, 12–81, pl. 4–11.

BRONN, H. G. 1835–7. *Lethaea geognostica oder Abbildungen und Beschreibungen der für die Gebirgsformationen bezeichnensten Versteinerungen, I.* vi+544 pp., 47 pl. Stuttgart.

CHANG, A. C. 1958. Stratigraphy palaeontology and palaeogeography of the ammonite fauna of the Clymeneenkalk from the Great Khingan. *Acta Palaeont. sin.* **6**, 71–89. (In Chinese with an English summary, pp. 83–9.)

DONOVAN, D. T. 1964. Cephalopod phylogeny and classification. *Biol. Rev.* **39**, 259–87.

DYBCZYŃSKI, T. 1913. Ammonity górnego Dewonu Kielc Wiadmość tymczasowa. *Kosmos, Warsz.* **38**, 510–25.

FLOWER, R. H. 1952. The ontogeny of *Centroceras* with remarks on the phylogeny of the Centroceratidae. *J. Paleont.* **26**, 519–28.

—— 1961. Major divisions of the Cephalopoda. Ibid. **35**, 569–74.

—— 1964. Nautiloid shell morphology. *Mem. Inst. Min. Technol. New. Mex.* **13**, 1–79, pl. 1–6.

FOORD, A. H. and CRICK, G. C. 1897. *Catalogue of the fossil Cephalopoda in the British Museum (Natural History), Part 3.* xxxiii+303 pp. London.

FRECH, F. 1890. *Elemente der Paläontologie.* 848 pp. Leipzig.

—— 1897–1902. *Lethaea geognostica: Theil 1, Lethaea palaeozoica, 2.* xxxiv+788 pp. Stuttgart.

GOLDFUSS, A. G. 1824–43. *Naturhistorischer Atlas.* 512 pp., 452 pl. Dusseldorf.

HOERNES, R. 1886. *Manuel de paléontologie.* 741 pp. Paris.

HOUSE, M. R. 1961. *Acanthoclymenia*, the supposed earliest Devonian clymenid is a *Manticoceras. Palaeontology*, **3**, 472–6, pl. 75.

—— 1962. Observations on the ammonoid succession of the North American Devonian. *J. Paleont.* **36**, 247–84, pl. 43–8.

—— 1963. Devonian ammonoid successions and facies in Devon and Cornwall. *Q. Jl geol. Soc. Lond.* **119**, 1–27, pl. 1–4.

—— 1965. A study in the Tornoceratidae: the succession of *Tornoceras* and related genera in the North American Devonian. *Phil. Trans. R. Soc.* **250B**, 79–130, pl. 5–11.

—— and PEDDER, A. E. H. 1963. Devonian goniatites and stratigraphical correlations in Western Canada. *Palaeontology*, **6**, 491–539, pl. 70–7.

HYATT, A. 1883, 4. Genera of fossil Cephalopoda. *Proc. Boston Soc. nat. Hist.* **22**, 253–338.

JENKINS, T. B. H. 1968. Famennian ammonoids from New South Wales, *Palaeontology*, **11**, 535–48, pl. 104, 105.

KULLMAN, J. 1960. Die Ammonoidea des Devon im Kantabrischen Gebrige (Nordspanien). *Akad. Wiss. Lit. Mainz* (1960), 455–559, pl. 1–9.

—— 1963. Las series devónicas y del Carbonifero inferior con ammonoideos de la Cordillera Cantábrica. *Estudios geol. Inst. Invest. geol. Lucas Mallada*, **19**, 161–91.

LANGE, W. 1929. Zur Kenntnis des Oberdevons am Enkeberg und bei Balve (Sauerland). *Abh. preuss. geol. Landesanst.*, N.F. **119**, 1–132, pl. 1–3.

MILLER, A. K. 1938. Devonian ammonoids of America. *Spec. Paper geol. Soc. Am.*, **14**, vii+262, pl. 39.

—— and FURNISH, W. M. 1957. Permian ammonoids from southern Arabia. *J. Paleont.* **31**, 1043–51, pl. 131, 2.

MOORE, R. C. (ed.) 1957. *Treatise on invertebrate paleontology*, Part L, *Mollusca 4, Cephalopoda Ammonoidea*. Geol. Soc. Am. and Univ. Kansas Press, 490 pp.

MÜNSTER, G. 1831. Le gisement des Nautilacée en Allemagne. *Bull. soc. geol. France*, **1**, 178–183.

NICHOLSON, H. A. and LYDEKKER, R. 1889. *A manual of palaeontology for the use of students*, 3rd ed. Edinburgh and London.

PETTER, G. 1960. Clymenes du Sarah. *Mém. Carte géol. Algér. Paléont.* **6**, 1–58, pl. 1–8.

QUENSTEDT, F. A. 1849. *Die cephalopoden.* Tübingen, 580 pp.

RUZHENCEV, V. E. (ed.) 1962. *Fundamentals of palaeontology*, **5**, 438 pp., 32 pl. Moscow (in Russian).

SANDBERGER, G. 1853. Einige Beobachtungen über Clymenien; mit besonderen Rücksicht auf die westfälischen Arten. *Vereins d. Rhein.* **10**, 1–46, pl. 6–8.

SCHINDEWOLF, O. H. 1922. Beiträge zur Kenntnis des Paläozoicums in Oberfranken, Osthüringen und dem Sächsischen Vogtlande. 1. Stratigraphie und Ammoneen fauna des Oberdevons von Hof a. S. *Neues Jb. Miner. Geol. Paläont.* **49,** 250–357, 393–509, pl. 14–18.

—— 1923. Entwurf einer natürlichen Systematik der Clymenoidea. *Centralbl. Min., Geol. Paläont.* (1923), 23–30, 59–64.

—— *et al.* 1936. Status of the 'Gattungsbezeichnungen' of Sobolew 1914. *Smithson, misc. Collns.* **73** (8), 39, 40.

—— 1937. Zur Stratigraphie und Paläeontologie der Wocklumer Schichten (Oberdevon). *Abh. preuss. geol. Landesanst.*, N.F. **178,** 1–132, pl. 1–4.

—— 1949*a*. Zur Nomenklatur der Clymenien (Cephalop., Ammon.). *Neues Jb. Miner. Geol. Paläont.* Mh. **7,** 64–76.

—— 1949*b*. Zur Phylogenie der Clymenien (Cephalop., Ammon.). Ibid. **7,** 197–209.

—— 1955. Zur Taxionomie und Nomenklatur der Clymenien. Ein Epilog. Ibid. **10,** 417–29.

SEDGWICK, A. and MCCOY, F. 1851–5. *A synopsis of the classification of the British Palaeozoic rocks with a systematic description of the British Palaeozoic fossils in the Geological Museum of the University of Cambridge*. xcviii+iv+viii+661 pp., 25 pl.

SOBOLEW, D. 1914*a*. Skizzen zur Phylogenie der Goniatiten. *Izv. varshav. politekh. Inst.* 192 pp., pl. 1–9 (a Russian translation is dated 1913).

—— 1914*b*. Über Clymenien und Goniatiten. *Paläont. Zeit.* **2,** 1, 248–378, pl. 8–9.

TURNER, J. S. 1962. The type species of *Aganides*, *Clymenia* and *Cyrthoceratites*. *Geol. Mag.* **99,** 183, 4.

WEDEKIND, R. 1908. Die Cephalopoden fauna des höheren Oberdevon am Enkeberge. *Neues Jb. Miner. Geol. Paläont.* **26,** 565–634, pl. 39–45.

—— 1914. Monographie der Clymenien des Rheinischen Schiefergebirges. *Abh. K. Ges. Wiss. Göttingen*, N.F. **10,** 1–73, pl. 1–7.

WOODWARD, S. P. 1851–56. *A manual of the Mollusca; or a rudimentary treatise of recent and fossil shells*. xvi+486 pp., 24 pl. London.

WURM, A. 1961. *Geologie von Bayern*. 556 pp. Berlin.

M. R. HOUSE
Department of Geology
The University
Kingston upon Hull
Yorkshire

Typescript received 15 April 1970

THE TRILOBITES *INCAIA* WHITTARD 1955 AND *ANEBOLITHUS* GEN. NOV.

by C. P. HUGHES *and* A. J. WRIGHT

ABSTRACT. The restudy of British and Peruvian type material together with new material from New Zealand has led to the revision of *Incaia* and to the belief that it represents a distinct trinucleid stock, known at present only from Peru and New Zealand, for which the subfamily Incaiinae is erected. The British species '*Incaia*' *simplicior* Whittard is excluded from the genus and is proposed as the type of *Anebolithus* gen. nov.

As part of a more general study of the Trinucleidae at present being undertaken by Hughes, the Peruvian type material of *Incaia* and British material previously attributed to the genus have been re-examined. Study of a new species of *Incaia* from New Zealand recently recognized by Wright yields data needed to characterize the genus more fully. Whittard (1966, pp. 273–4, text-fig. 9) believed that British material from the Shelve region was congeneric with *Incaia nordenskioeldi* (Bulman 1931) but the present study shows this not to be so. '*Incaia*' *simplicior* Whittard from the Arenig (*Didymograptus hirundo* Zone) of the Shelve Inlier in the Welsh Borderland is proposed as the type species of *Anebolithus* gen. nov.

Incaia is no longer thought to be closely allied to the Trinucleinae and it is believed that it represents a distinct, possibly primitive, trinucleid stock known at present only from South America and New Zealand.

SYSTEMATIC DESCRIPTIONS

Terminology. The terminology applied throughout is essentially that proposed in the *Treatise*, Part O (Harrington, Moore, and Stubblefield 1959). However, the term 'arc' (referring to the pits on the trinucleid fringe, e.g. E_1 arc) is here preferred to Bancroft's (1929) term 'concentric row' (see also Hughes 1970).

Family TRINUCLEIDAE Hawle and Corda 1847
Subfamily INCAIINAE subfam. nov.

Remarks. The small number of arcs, with pits arranged in radial sulci, combined with the development of large lateral eye tubercles, characterize this monotypic subfamily.

Genus INCAIA Whittard 1955

Diagnosis. Incaiinae with semicircular cephalon; simple, narrow fringe with no pits external to the girder; pits of internal series consist of two or three arcs with pits sunk in radial sulci. Glabella typically trinucleid, pyriform and with three pairs of lateral glabellar furrows; no median node. Genal regions with prominent eye tubercles situated close to axial furrows and approximately opposite mid-point of glabella. Genal spines relatively short extending posteriorly a distance equal to the cephalic length. Thorax typically trinucleid. Pygidium relatively long, being only about two and a quarter times as wide as long; pleural fields faintly furrowed; axis well segmented.

[Palaeontology, Vol. 13, Part 4, 1970, pp. 677–90, pls. 127–128.]

Type species. Trinucleus nordenskioeldi Bulman, 1931.

Distribution. The type species is from the Upper Llanvirn of SE. Peru. The only other known occurrence of the genus is from the Caradoc (*Nemagraptus gracilis* Zone) of New Zealand.

Discussion. In 1955 Whittard, working only from Bulman's figures, believed that '*T.*' *nordenskioeldi* was unique in that it possessed a glabella probably without lateral furrows, large eye-tubercles close to the axial furrows and a simple fringe consisting essentially of only two arcs which Whittard interpreted as 'presumably representing E_1 and I_1'. Following the discovery of trinucleids in Shropshire possessing very simple fringes with the girder external to all the pits, Whittard examined the type specimens of *Incaia nordenskioeldi.* He then modified his earlier views regarding the position of the girder, stating (1966, p. 273) that 'there is no indication of a girder separating external from internal series of pits, although the preservation is such that if a girder existed it should be observable; furthermore, in all cases, I_{1-2} occur in close association in sulci, and it would be unreasonable to separate them into E_1 and I_1; finally, surrounding the fringe there is a peripheral tumid border or rolled margin which clearly resembles the peripheral girder of *Myttonia.*' Whittard thus clearly believed that in *I. nordenskioeldi* the girder was external to all the pits.

The present study has reaffirmed Bulman's statement (1931, p. 86) that all the material of *I. nordenskioeldi* consists of internal and external moulds of cranidia with upper lamella, and that no specimens are known with the lower lamella preserved. It is thus a little difficult to understand Whittard's categorical remarks concerning the existence and position of the girder. He apparently believed that the absence of any structure between the two arcs on the upper lamella which might correspond to a girder on the lower lamella, indicated that there was no such girder. Whilst arcuate structures are commonly developed on the upper lamella between the various arcs, these need not correspond to the position of the girder on the lower lamella in any way [for example in *Cryptolithus* (see Whittington 1968, pl. 89, figs. 1, 2)]. Furthermore, the absence of any such arcuate structures on the upper lamella need not mean that a girder is absent (for example in *Trinucleus* and *Stapeleyella*). The other evidence cited by Whittard as supporting his claim of a peripheral girder is also inconclusive. Although the pits of the two main arcs are fairly close together there is ample space for a girder to be developed between them. The so-called 'tumid border or rolled margin' referred to by Whittard is simply a slightly convex marginal rim (Pl. 127, fig. 7). Although not unlike that developed in *Myttonia*, this rim is of little significance as similar rims are present in many trinucleids [for example *Cryptolithus* and *Salterolithus* (see Whittard 1958, pl. 10, fig. 1, pl. 12, fig. 3)]. Thus it is believed neither position nor existence of the girder is determinable from the type material. In the New Zealand species described below the lower lamella is known and the girder is, in fact, positioned external to both the arcs of pits. Since the cephalon of this new species is so similar to that of *I. nordenskioeldi* it is here considered that they are congeneric, and that the girder in *I. nordenskioeldi* is probably peripheral.

The affinities of *Incaia* are rather uncertain. Whittard, who did not attach any great importance to the presence of lateral eye tubercles, believed *Incaia* to be intermediate between *Myttonia* and *Lordshillia*, possessing the peripheral girder of *Myttonia* and the ordered radial arrangement of the fringe pits of *Lordshillia.* The present authors, however, believe the development of lateral eye tubercles (a feature absent in the

majority of trinucleids), together with the fringe characteristics, is of considerable generic importance, and it is held that *Incaia* is in no way closely related to the early Ordovician trinucleids of the Welsh Borderland. Of trinucleids known from other parts of South America and Australasia, none shows any apparent close affinity to *Incaia*. Of these forms, however, the majority are very different from those known from the rest of the world, e.g. *Famatinolithus*, *Guandacolithus* (Harrington and Leanza 1957), '*Cryptolithus*' *empozadensis* (Rusconi 1953), '*Onnia*' *verrucosa* (Rusconi 1956). From Australia the only form known in any detail is a new species (Moors MS. 1966)[1] from New South Wales. This species, while exhibiting some similarities in fringe characteristics to *Lloydolithus* and *Protolloydolithus*, possesses lateral eye tubercles similar to those of *Incaia*.

Thus although our present knowledge is rather scant, it seems possible that many trinucleids from the present southern hemisphere with lateral eye tubercles may have evolved in isolation. This would necessitate an isolated stock of trinucleids within the 'southern province' of Whittington (1966). Some support for such a concept is given by some other trilobite groups, notably the thysanopygid asaphids of South America which also appear to have evolved in isolation. The probable occurrence in the New Zealand Tremadocian of *Pseudohysterolenus* (Wright 1968), otherwise known only from Argentina (Harrington and Leanza 1957), further suggests an early Palaeozoic 'austral' faunal province.

The significance of the lateral eye tubercles with reference to the evolution and origin of the trinucleids is at present uncertain. *Orometopus*, which has eye tubercles, has often been quoted as a probable trinucleid ancestor, but this is by no means established.

Incaia nordenskioeldi (Bulman)

Plate 127, figs. 3, 9, Plate 128, figs. 1, 2

1931 *Trinucleus nordenskiöldi* Bulman, p. 85, pl. 11, figs. 2, 3.
1955 *Incaia nordenskiöldi* (Bulman); Whittard, pp. 31–2.
1966 *Incaia nordenskiöldi* (Bulman); Whittard, pp. 273–4, text-fig. 9.

Diagnosis. *Incaia* having I_{1-2} fully developed with about 16 pits in each arc (half-fringe); occasional pits of I_3 developed, especially posterolaterally; only two or three sulci present between the mid-line and the axial furrow. Eye tubercles slightly posterior of glabellar mid-length. Thorax and pygidium unknown.

Type locality and horizon. Upper Llanvirn between Limpucuni and Itchubamba, SE. Peru (see text-fig. 1).

Bulman (1931, pp. 8–10) discussed the probable location of these two places and concluded that Limpucuni probably lay to the west of San Juan del Oro and that Itchubamba was between Limpucuni and Quiaca. Efforts by the present authors have also failed to discover the exact position of these places. Map B drawn from information supplied by the Royal Geographical Society shows a somewhat different relative positioning of some of the places in the area, but it should be noted that the accuracy of mapping in this area is only to within about 20 minutes both of longitude and latitude. Maps published at about the time of the Nordenskioeld expedition show one track leading northwards from Sandia through Ichubamba (note spelling) and another from Quiaca to San Juan del Oro. This latter one passes through Huich*ull*uni which may be near Limpucuni (Bulman stated 1931, p. 10, 'Huich*iy*uni is said to be near Limpucuni'). It is uncertain whether Ichubamba is equivalent to Itchubamba, but in any case it seems unlikely that the expedition passed through Ichubamba. It is quite

[1] A further new trinucleid is now known from New South Wales (see Campbell and Durham, this issue, pp. 573–80.

feasible however that they may have made a detour off to the west of the Quiaca–San Juan del Oro track and made collections on the ridge that runs up between the two tracks mentioned above. Such collections could then quite well be labelled as 'between Limpucuni and I(t)chubamba.' The exact locality for the type material of *I. nordenskioeldi* must thus remain uncertain.

Material. Ar. 42445a/b (419, 420); Ar. 42446 (418); Ar. 42447 (366); Ar. 42448 (367). Specimens Ar. 42447 and Ar. 42448 are part and counterpart. Numbers given in brackets are original numbers cited by Bulman (1931, p. 86).

Dimensions	A	I	K
Ar. 42445 (419)	4·8	*c.* 11·0	2·3
Ar. 42446 (418)	4·2	*c.* 10·3	2·7
Ar. 42447 (366)	5·5	10·6	3·2

All measurements in millimetres. A—maximum sagittal cephalic length; I—maximum transverse cephalic width; and K—maximum transverse glabellar width.

Discussion. A full redescription is not deemed necessary until new material becomes available, but the following points are of note in addition to the comments already made in the discussion of the genus concerning the position of the girder. All the known specimens are deformed to some extent and are preserved in a rather soft pinkish-brown shale. It is thought that this rather indifferent mode of preservation accounts for the doubtful occurrence of lateral glabellar furrows and it is probable that three pairs of shallow, typically trinucleid lateral glabellar furrows were developed as are known in *I. bishopi* (see below). The rather large, so-called eye tubercles close to the axial furrows however are consistently developed and it is believed that they represent some form of lateral eye (Pl. 128, fig. 2). This is also supported by the New Zealand material. As pit counts can be made with any certainty on only three specimens, the figure of 'about 16 pits' in each arc (half-fringe) given in the diagnosis should not be taken as a truly diagnostic figure. Further specimens almost certainly would indicate some range in the number of pits developed. Bulman (1931) compared *I. nordenskioeldi* with *Trinucleus coscinorrhinus*; differences noted by Bulman between the species would now seem to be of generic or even higher significance.

Incaia bishopi sp. nov.

Plate 127, figs. 1, 2, 4–6, 8; Plate 128, figs. 3, 4, 6–14; text-fig. 3

Diagnosis. Incaia with I_{1-2} fully developed in radial sulci with approximately 23 pits (half-fringe); about 8 sulci between axial furrows; I_3 pits not known with certainty, no

EXPLANATION OF PLATE 127

Figs. 1, 2, 4–6, 8. *Incaia bishopi* sp. nov. All specimens from scree material, Paturau River, New Zealand, locality S3/526, grid ref. 907010 1, Internal mould, VA5a ×3. 2, Dorsal surface of cranidium showing caecae, latex cast, DC350b ×3. 4, Dorsal surface of fringe, latex cast of holotype, VA6b ×5. 5, Internal mould, VA4a ×3. 6, Ventral surface of fringe, latex cast of holotype, VA6a ×4. 8, Internal mould showing three lateral glabellar furrows, VA7 ×4.

Figs. 3, 9. *Incaia nordenskioeldi* (Bulman). All specimens from Upper Llanvirn between Limpucuni and Itchubamba, SE. Peru. 3, Internal mould, Ar. 42446 ×6. 9, Internal mould of holotype, Ar. 42445a ×6.

Figs. 7, 10. *Anebolithus simplicior* (Whittard). Specimen from Mytton Flags, (Arenig), small quarry 160 yd. N. 35° E. of Snailbeach Reservoir, Shropshire, England. grid ref. SJ 377023. 7, Lateral view, 10, Dorsal view of internal mould, holotype GSM102178 ×6.

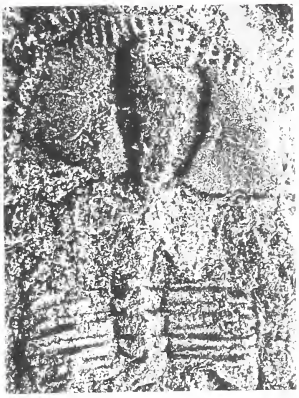

1

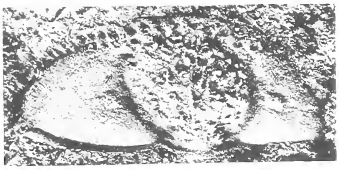

2

3

4

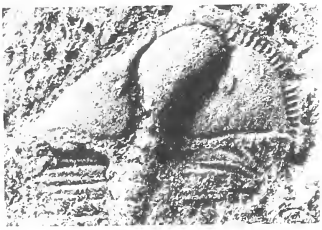

5

6

7

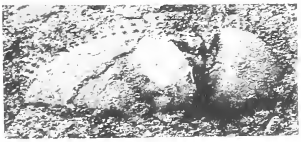

8

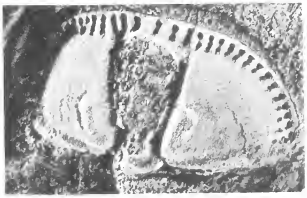

9

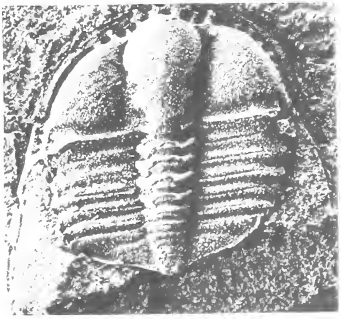

10

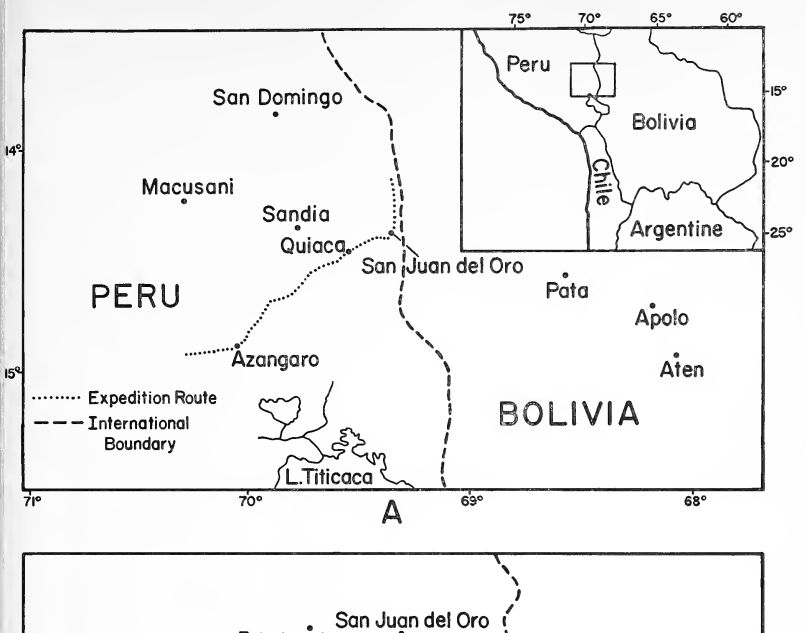

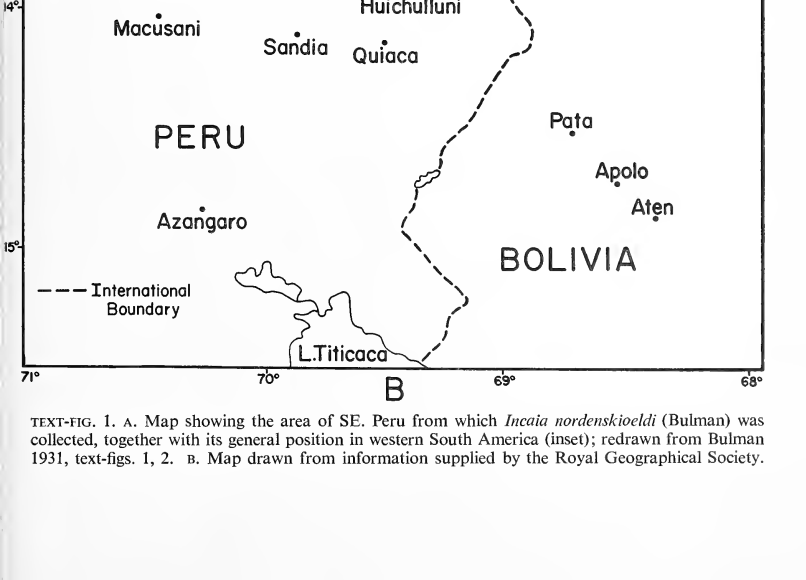

TEXT-FIG. 1. A. Map showing the area of SE. Peru from which *Incaia nordenskioeldi* (Bulman) was collected, together with its general position in western South America (inset); redrawn from Bulman 1931, text-figs. 1, 2. B. Map drawn from information supplied by the Royal Geographical Society.

E arcs developed; 3 pairs of lateral glabellar furrows; median node absent; lateral eye tubercles located at mid-length of cephalon, close to axial furrows; genal caecae sometimes developed. Pygidium with up to 5 weakly developed pleural ribs; up to 16 axial rings.

Localities and material.

S3/526 (Collections GS9504, V1593) Type locality. Scree material, Paturau River. Grid ref. 907010 (909012). Specimens VA4–18, 20–4, 26–72, 74–7, 84, 88–115, 118–20, DC350–2, 354–7.

S3/527 (Coll. GS10209) River boulder, Paturau River, Grid ref. 912024 (912024) (Not 899025 as Cooper [1968, p. 79] stated) Spec. DC358.

S3/552 (Coll. V2710) Scree material, Higgins Branch (tributary of Paturau River). Grid ref. 907971 (909969). Specs. VA78–80, 87.

S3/553 (Coll. V2715) River boulder, Paturau River. Grid ref. 908012 (910015) Specs. VA19, 81–3, 85–6, 121.

S3/554 (Coll. V2716) Scree material, Paturau River. Grid ref. 905006 (907008). Spec. VA73.

All *I. bishopi* material is deformed tectonically, and fine morphological features (such as posterior pygidial axial rings and lateral glabellar furrows) are often obliterated. S3 is the Collingwood sheet of the N.Z. 1:63360 map series. Grid references are taken from the second edition (1967); grid references in brackets are taken from the 1945 edition. Numbers 526, etc., refer to collection or locality numbers on that sheet.

Horizon. Bishop (1965) described the type locality (S3/526) where *Nemagraptus gracilis* is now known to occur (R. A. Cooper pers. comm.), indicating an early Caradoc age. Bishop (1969) proposed the name Golden Bay Group for strata in which all *Incaia bishopi* localities occur (see also Bishop, in press).

Type material. Specimen VA6 (counterparts a and b) is here selected as holotype. Paratypes which are not topotypes are: VA19, VA73, VA78–83, VA85–7, VA121, DC358.

Description. Cephalon semicircular, tending to be relatively wider and more rectangular in smaller specimens (VA65) (see text-fig. 4 and Table 1). Glabella typically trinucleid, being pyriform with hemispherical pseudofrontal lobe, maximum width varying from about one-quarter the cephalic width in small specimens to about one-third in larger individuals (see text-fig. 5). Three pairs of lateral glabellar furrows are developed; posterior pair (VA4, 5, 23, 24) transverse, shallow, constricting the glabella just anterior of the broad, shallow occipital furrow to form a prominent occiput; median

EXPLANATION OF PLATE 128

Figs. 1, 2. *Incaia nordenskioeldi* (Bulman). Both specimens from Upper Llanvirn between Limpucuni and Itchubamba, SE. Peru. 1, Internal mould, Ar. 42447 ×6. 2, Latex cast of holotype, Ar. 42445b ×6.

Fig. 5 ?*Incaia bishopi* sp. nov. From scree material, Paturau River, New Zealand, locality S3/526 grid. ref. 907010. Fringe fragment, VA25×8. Orientation uncertain.

Figs. 3, 4, 6–14. *Incaia bishopi* sp. nov. All from scree material, Paturau River, New Zealand, locality S3/526 grid. ref. 907010 with the exceptions of VA19 and VA121 (figs. 4, 8) which are from a river boulder, Paturau River, New Zealand, locality S3/553 grid. ref. 908012. 3, Ventral surface of fringe fragment showing genal spine, latex cast VA14a ×4. 4, Dorsal surfaces of two pygidia, upper specimen VA19b, lower VA121, latex cast, ×4. 6, Internal mould of pygidium, VA8a ×3. 7, Internal mould of pygidium, VA21a ×4. 8, Internal mould of pygidium, VA19a ×4. 9, Internal mould of glabella showing reticulate ornamentation, VA81 ×5. 10, Internal mould of pygidium, VA9a ×3. 11, Dorsal surface of pygidium, latex cast. DC351b ×3. 12, Internal mould of pygidium, VA10 ×4. 13, Internal mould of pygidium, VA11 ×3. 14, Internal mould of pygidium, VA20a ×4.

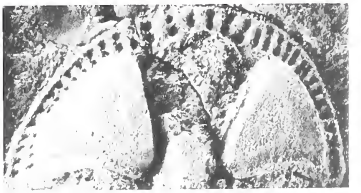

1

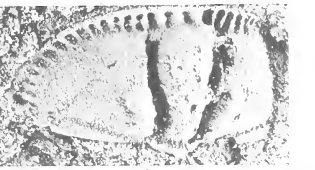

2

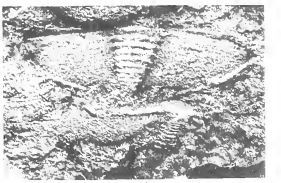

4

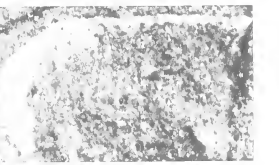

5

3

6

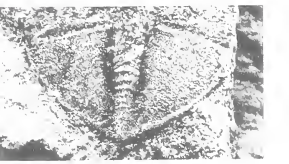

7

8

9

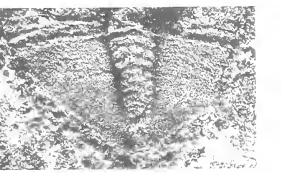

10

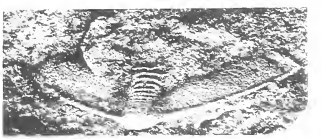

11

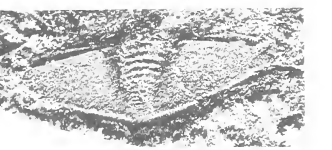

12

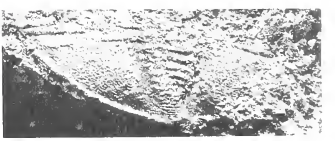

13

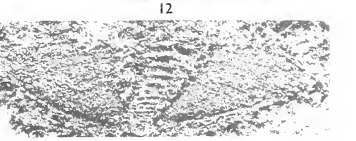

14

HUGHES and WRIGHT, *Incaia* from Peru and New Zealand

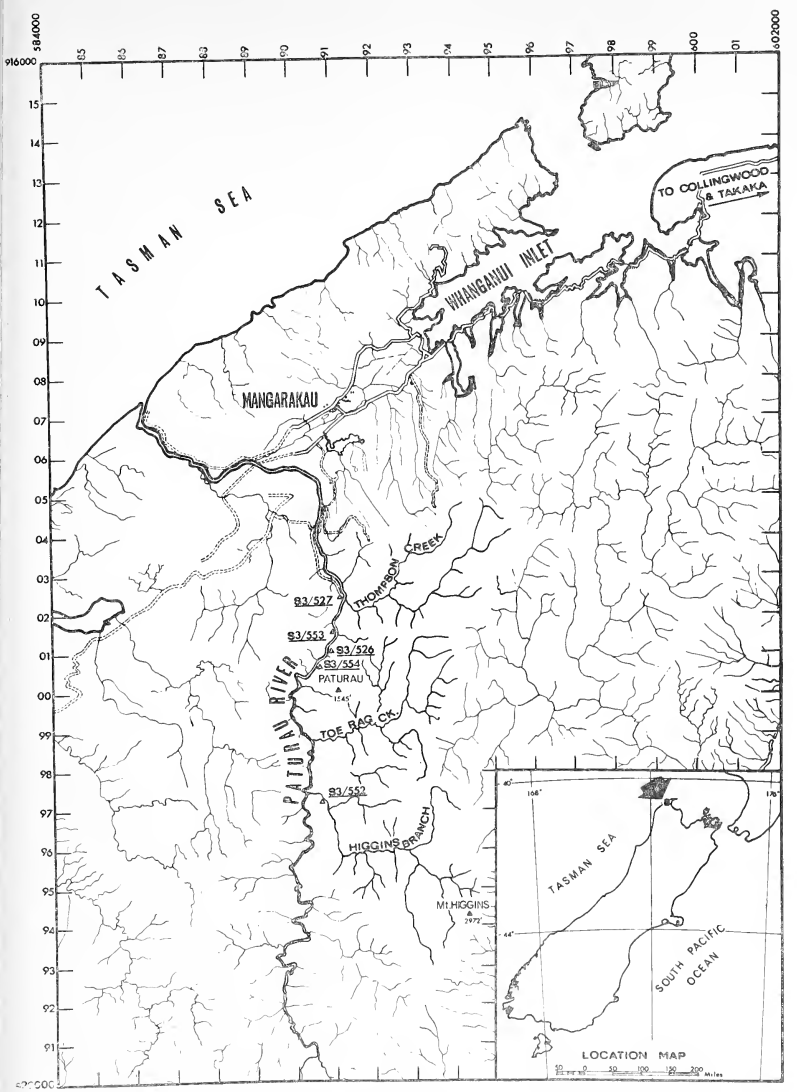

TEXT-FIG. 2. Map showing *Incaia bishopi* localities. Detailed map and 1000-yd. grid are from N.Z.G.S. S3 (Collingwood), 2nd edition.

glabellar furrows just posterior to mid-length of glabella, developed as small shallow rounded depressions; anterior furrows (VA7, Pl. 127, fig. 8) simply small rounded pits. Axial furrows deep anteriorly, with well-developed apodemal pits, shallowing and widening posteriorly. Genal regions moderately convex with simple curving caecae preserved on some specimens (e.g. DC350, Pl. 127, fig. 2; VA26). Eye tubercles prominent in all specimens as slightly elongated (*exsag.*) (VA4, Pl. 127, fig. 5; VA22) ridges located immediately outside the axial furrows at about mid-length of the cephalon.

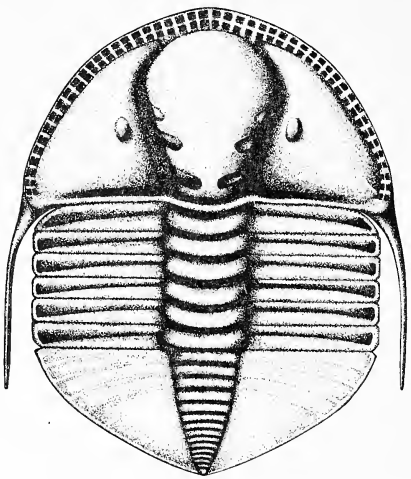

TEXT-FIG. 3. Reconstruction of *Incaia bishopi* sp. nov. in dorsal view; surface ornamentation omitted. Magnification *c.* ×2·5.

Posterior margin straight, border furrow broad and very shallow laterally, merging axially with axial furrows. No occipital spine present.

Fringe slightly convex, with a smooth, weakly concave rim. Width up to 2 mm. (*exsag.*) anteriorly being at a maximum in front of apodemal pits; laterally fringe becomes more steeply declined and narrower. Pits confined to radial sulci which are about as wide and rounded as the intervening ridges. Sulci radially arranged except medially where they are locally divergent (VA5, Pl. 127, fig. 1; VA65). Approximately 23 pits of arcs I_{1-2} are developed on each half-fringe, the two arcs being separated in sulci of the upper lamella by a low rounded ridge which is only very weakly manifested on the intervening ridges and becomes weaker laterally. One poorly preserved specimen (VA65) anteriorly exhibits what may be I_3 pits, but relatively well-preserved specimens (e.g. VA5, 8, 64, DC350) clearly lack such pits. Minor irregularities (perhaps due to tectonic deformation) are present in some specimens (VA30, 73) in the development of

short sulci with only one pit, or a twin pit, developed. Ventral side of lower lamella with angular girder inclined at about 15° to the horizontal (VA6, 15), possessing sparse terrace-lines. Girder continued along the genal spines as an angular ventral edge. Dorsal edge of genal spines, which extend posteriorly for a distance approximately equal to the length of the remainder of the cephalon, is also angular, giving an approximately rhomboidal cross-section. Ventral edge of lower lamella does not lie in a plane;

TABLE 1. Table of the width–length ratios for three cephala and two pygidia of *Incaia bishopi* sp. nov., both before and after correction by the use of Wellman's method (Wellman 1962). All measurements in millimetres.

Specimen No.	Original (deformed) Dimension (mm.)		Uncorrected W:L	Corrected W:L
VA 5 (cephalon)	19·0	11·0	1·73 : 1	2·13 : 1
DC 350 (cephalon)	25·0	10·5	2·38 : 1	1·34 : 1
DC 352 (cephalon)	6·8	4·0	1·70 : 1	2·95 : 1
VA 112 (pygidium)	10·1	5·2	1·94 : 1	2·42 : 1
DC 351 (pygidium)	20·4	6·3	3·24 : 1	1·77 : 1

preglabellar edge and genal flange are relatively dorsally elevated but posterior portion of genal spine approximately coplanar with the rest of the girder (VA6) (see Størmer 1930, p. 106). Suture line apparently intra-marginal except postero-laterally where it becomes dorsal (VA6, 29, 30) cutting across the genal spine without isolating any pits.

External surface of glabella ornamented with a fine reticulate pattern of delicate ridges (VA63; VA81, Pl. 128, fig. 9). Pleural lobes of some pygidia bear fine, close-set pits (see Pl. 128).

Hypostoma unknown.

Thorax typically trinucleid with six segments (VA4, Pl. 127, fig. 5; VA5, Pl. 127, fig. 1; VA16). Axis about one-quarter of total width. Anterior half-ring elevated; axial furrows deep. Pleurae flat, deflected ventrally and posteriorly distally. Pleural furrow expanded laterally, commences near the antero-median angle of pleurae.

Pygidium varies in shape from obtusely sub-triangular (e.g. VA8, Pl. 128, fig. 6) to semi-elliptical (e.g. VA9, Pl. 128, fig. 10). Much of this shape variation however is thought to be due to deformation, and it seems likely that undeformed pygidia were generally slightly more than twice as long as wide, with the smaller individuals being relatively slightly longer (see text-fig. 6). The two pygidia to which Wellman's ingenious method (Wellman 1962) was applied, however, appear to indicate an opposite trend (see Table 1) (see also discussion of biometric data, p. 686). Anterior margin not quite

straight, each side being slightly deflected posteriorly. An elongate triangular anterior border is delimited on each pleural lobe by an angular furrow extending from in front of the anterior axial ring and becoming deeper laterally (VA9, Pl. 128, fig. 10; VA19, Pl. 128, fig. 4). Curvature of postero-lateral margins varies with outline, having a more curved margin in sub-triangular specimens. Axis slightly more convex (*tr.*) than the moderately convex pleural lobes which bear a fine reticulate ornament. Axis varies from one-quarter to one-fifth of width of pygidium, tapers posteriorly to merge into the deflected margin as a broad low swelling. Twelve or thirteen axial rings generally

TABLE 2. Bivariate statistics for the type sample of *Incaia bishopi* sp. nov. A—maximum sagittal cephalic length; B—maximum sagittal glabellar length; I—maximum transverse cephalic width; W—maximum transverse pygidial width; Z—maximum sagittal pygidial length. Measurements are in millimetres.

x:y	x	var. x	y	var. y	r	r_e	α	var. α	a	var. a	n
I:B	16·17	22·966	4·67	2·966	0·93	0·93	1·23	0·0490	0·36	0·0044	6
I:A	15·37	19·697	8·19	7·496	0·91	0·91	1·15	0·0361	0·62	0·0109	8
W:Z	12·12	21·768	5·40	3·554	0·78	0·79	0·91	0·0526	0·40	0·0108	8

present, up to a maximum of sixteen (VA8, Pl. 128, fig. 6; VA11, Pl. 128, fig. 13); inter-ring apodemal pits developed between anterior eight rings. Axial furrows prominent anteriorly, becoming broader, shallower, and more rounded posteriorly. Pleural lobes have up to three to five weakly developed, flat-topped ribs convexly curved anteriorly. Declined border is deepest medially, becoming steeper and lower antero-laterally, terrace-lines present.

Biometrical data. Sufficient data are available for some selected bivariate analyses to be made. Text-figs. 4–6 give plots of the selected parameters, the various bivariate statistics being given in Table 2.

The use of standard bivariate techniques on such distorted material is justifiable provided there was no (primary) current or other orientation of the fossils. However, with tectonically distorted fossils it is impossible to be certain that the (undistorted) material had a random two-dimensional distribution. Therefore this must be assumed. The validity of the statistical approach depends partly on this assumption; it is further assumed that the attitude of the regression line is not affected by the deformation. The small number of specimens may contribute to an erroneous result in the statistical technique (Table 2) as well as the graphic technique (Table 1). Only two bedding surfaces were suitable for study by Wellman's (1962) method in bearing more than one specimen. The lack of agreement between results from the two methods does not indicate where errors occur.

Discussion. This species is of interest as it provides confirmation of the presence of the lateral eye tubercle in *Incaia* and the position of the girder, as well as showing details of the glabella, thorax and pygidium. *I. bishopi* differs from *I. nordenskioeldi* in that it has considerably more sulci medially in front of the glabella (i.e. between the extensions of the axial furrows). Furthermore in *I. nordenskioeldi* the lateral eye tubercle appears to be slightly more posteriorly placed.

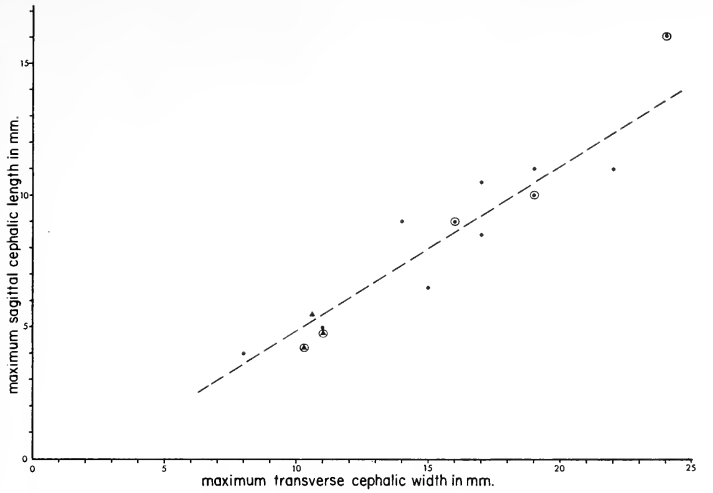

TEXT-FIG. 4. Plot of maximum transverse cephalic width against maximum sagittal cephalic length. ●—*I. bishopi* sp. nov.; ▲—*I. nordenskioeldi* (Bulman). Encircled points indicate that at least one of the measurements is approximate. All data for *I. bishopi* is from topotypic material (S3/526, see p. 682).

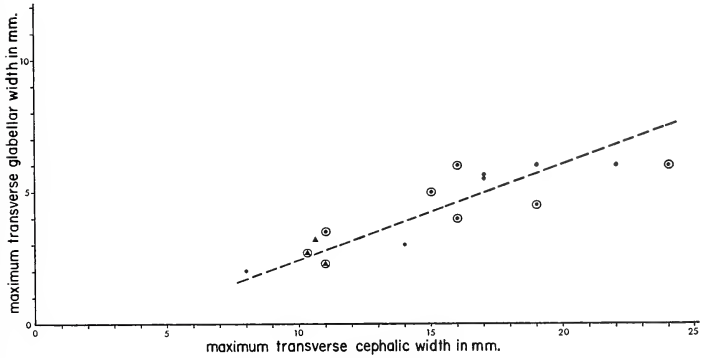

TEXT-FIG. 5. Plot of maximum transverse cephalic width against maximum transverse glabellar width. ●—*I. bishopi* sp. nov.; ▲—*I. nordenskioeldi* (Bulman). Encircled points indicate that at least one of the measurements is approximate. All data for *I. bishopi* is from topotypic material (S3/526, see p. 682).

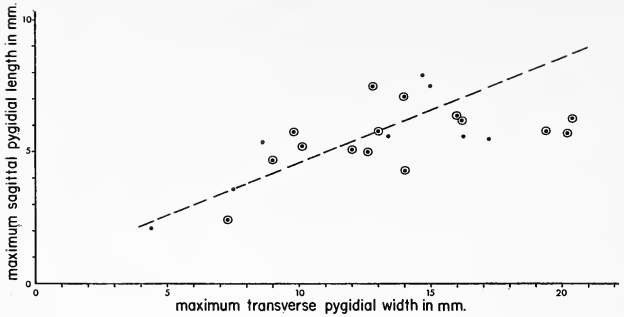

TEXT-FIG. 6. Plot of maximum transverse pygidial width against maximum sagittal pygidial length for *I. bishopi* sp. nov.; all data from topotypic material (S3/526, see p. 682). Encircled points indicate that at least one of the measurements is approximate.

?*Incaia bishopi* sp. nov.

Pl. 128, fig. 5

Locality and material. Specimens VA25, 116, 117 and DC353 from locality S3/526 (see p. 682).

Horizon. As for *I. bishopi* (see p. 682).

Discussion. These four specimens, all fragmental fringe casts, differ from *I. bishopi* in having at least three arcs of pits developed. The best of these specimens (VA25, Pl. 128, fig. 5) is of the same order of size as a cephalon of *I. bishopi* such as VA17 or 65 which almost certainly possess only 2 arcs. However it is known that trinucleid species may exhibit variations in the fringe which may or may not be linked to different growth stages. Thus these specimens of isolated casts of fringe fragments cannot conclusively be said to belong to or differ from *I. bishopi*. No girder is discernable on any of these specimens.

Subfamily TRINUCLEINAE Hawle and Corda 1847
Genus ANEBOLITHUS gen. nov.

Pl. 127, figs. 7, 10

Diagnosis. Cephalon semicircular with simple, narrow fringe with no pits external to the girder; pits of internal series consist of three arcs with pits sunk in radial sulci. Glabella typically trinucleid, pyriform with three pairs of lateral glabellar furrows; median node present. No eye tubercles developed on genal regions. Thorax typically trinucleid. Pygidium about four and a half times as wide as long, pleural fields faintly furrowed anteriorly, axis segmented.

Type species. Incaia simplicior Whittard 1966.

Type locality and horizon. Small path-side quarry in northerly trending valley 160 yd. N. 35° E. of the north-eastern corner of Snailbeach Reservoir, Shropshire, England (grid ref. SJ 377023); Mytton Flags, Arenig (*Didymograptus extensus* Zone) about 2000 ft. above Stiperstones Quartzite.

Distribution. The genus at present is restricted to the type species. However, a further occurrence of the genus is shortly to be described from the lower Llanvirn of the Builth–Llandrindod Inlier (Hughes 1971).

Discussion. Although the details of the fringe are similar to *Incaia*, the lack of large lateral eye tubercles and the presence of a median glabellar node together with other minor morphological features (for full description of morphology see Whittard 1966, pp. 274–6) suggest that *Anebolithus* is closely related to the other Trinucleinae of the Welsh Borderland, e.g. *Bergamia*, *Stapeleyella*, and not to *Incaia*. The combination of peripheral girder and radially disposed pits warrants the erection of *Anebolithus*, which appears to be in an evolutionary series between *Myttonia*, with marginal girder but irregular pits, and *Lordshillia* with radially arranged pits but with one arc external to the girder.

Acknowledgements and abbreviations. One of us (C. P. H.) is grateful to Dr. V. Jaanusson of the Swedish State Natural History Museum, Stockholm for kindly loaning the type specimens of *Incaia*. His thanks are also due to Professor H. B. Whittington and Dr. A. W. A. Rushton for much helpful discussion, and to the Institute of Geological Sciences, London for the loan of Whittard's original material.

Sincere thanks are extended by Wright to the following: D. G. Bishop of the New Zealand Geological Survey who discovered the initial *I. bishopi* locality (S3/526), encouraged work on the fauna and guided Wright to the locality; Dr. R. A. Cooper, N.Z.G.S., who assisted with collecting, provided the determination of *Nemagraptus gracilis* from locality S3/526 and, with W. M. Briggs, Jr., assisted with photographic equipment; Dr. C. A. Fleming who made the N.Z.G.S. collections available for study; Victoria University students who assisted in collecting; E. F. Hardy who drafted text-fig. 2. Field work by Wright was supported by grants, from Victoria University of Wellington and the New Zealand Universities Grants Committee, which are gratefully acknowledged.

Both authors would like to extend their thanks to Mr. John Lewis for his skill in preparing the text-figures other than text-fig. 2.

All relevant specimens are referred to by individual numbers; suffixes a or b indicate counterparts; prefixes denote collection in institutions where material is housed, as follows:

Ar.—Swedish State Natural History Museum, Stockholm.
DC—New Zealand Geological Survey, Lower Hutt.
VA—Geology Department, Victoria University of Wellington, Wellington.
GSM—Institute of Geological Sciences, London.

A copy of all the original measurements made on specimens is lodged with each of the first three of the above institutions together with a further copy in the Geological Society, London.

REFERENCES

BANCROFT, B. B. 1929. Some new species of *Cryptolithus*, (s.l.), from the Upper Ordovician. *Mem. Proc. Manchr. lit. phil. Soc.* **73**, 67–96.

BISHOP, D. G. 1965. Two new Palaeozoic fossil localities in northwest Nelson. *N.Z. Jl Geol. Geophys.* **8**, 1232–3.

—— 1969. S2 Kahurangi (1st edition) 'Geological map of New Zealand' 1:63360. Department of Scientific and Industrial Research, Wellington, New Zealand.

—— (in press) S3 Collingwood (1st edition), ibid.

BULMAN, O. M. B. 1931. South American graptolites with special reference to the Nordenskiöld collection. *Ark. Zool.* **22A** (3) 1–111.

COOPER, R. A. 1968. Lower and Middle Paleozoic fossil localities of north-west Nelson. *Trans. R. Soc. N.Z. Geol.* **6**, 75–89.

HARRINGTON, H. J. and LEANZA, A. F. 1957. *Ordovician trilobites of Argentina*. Dept. Geol. Univ. Kansas, Spec. Pub. 1. 276 pp. 140 figs.

HARRINGTON, H. J., MOORE, R. C. and STUBBLEFIELD, C. J. 1959. Morphological terms applied to Trilobita. In MOORE, R. C. (ed.), *Treatise of invertebrate paleontology*, Part O. Geol. Soc. Am. and Univ. Kansas Press. pp. 117–26.

HAWLE, I. and CORDA, A. J. C. 1847. *Prodrom einer Monographie der böhmischen Trilobiten*. 176 pp., 7 pl. Prague.

HUGHES, C. P. 1970. Statistical analysis and presentation of trinucleid (Trilobita) fringe data. *Palaeontology*, **13**, 1–9.

—— 1971. The Ordovician trilobite faunas of the Builth–Llandrinod Inlier, Central Wales, Part II. *Bull. Br. Mus. nat. Hist.* (Geol.) (in press).

MOORS, H. T. 1966. Some of the stratigraphy and palaeontology of the Cliefden Caves District, near Mandurama. Unpublished M.Sc. thesis, Department of Geology and Geophysics, University of Sydney, Australia.

RUSCONI, C. 1953. Trilobitas ordovicicos y cambricos de Mendoza. *Bol paleont. B. Aires.* (**25**), 1–8, figs. 1–10.

—— 1956. Fosiles ordovicicos de la quebrada de los Bueyes, (Mendoza). *Revta Mus. Hist. nat. Mendoza*, **9**, (1, 2), 2–15, pl. 1.

STØRMER, L. 1930. Scandinavian Trinucleidae, with special reference to Norwegian species and varieties. *Skr. norske Vidensk-Akad.* Mat.-naturv. Kl. 1930, **4**, 1–111, pl. 1–14, figs. 1–47.

WELLMAN, H. W. 1962. A graphical method for analysing fossil distortion caused by tectonic deformation. *Geol. Mag.* **99**, 348–52, pl. 16.

WHITTARD, W. F. 1955. The Ordovician trilobites of the Shelve Inlier, West Shropshire, Part I. *Palaeontogr. Soc.* (*Monogr.*) 1–40, pl. 1–4.

—— 1958. The Ordovician trilobites of the Shelve Inlier, West Shropshire, Part III. Ibid. 71–116, pl. 10–15.

—— 1966. The Ordovician trilobites of the Shelve Inlier, Shropshire, Part VIII. Ibid. 265–306, pl. 46–59.

WHITTINGTON, H. B. 1966. Phylogeny and distribution of Ordovician trilobites. *J. Paleont.* **40**, 696–737.

—— 1968. *Cryptolithus* (Trilobita): Specific characters and occurrence in Ordovician of eastern North America. *J. Paleont.* **43**, 702–14.

WRIGHT, A. J. 1968. Ordovician conodonts from New Zealand. *Nature*, **218**, 1232–6.

C. P. HUGHES
Department of Geology
Sedgwick Museum
Cambridge, CB2 3EQ

A. J. WRIGHT
Geology Department
Victoria University of Wellington
P. O. Box 196
Wellington, New Zealand
Present address:
Department of Geology
Oregon State University
Corvallis, Oregon 97331
U.S.A.

Typescript received 26 February 1970

THE PALAEONTOLOGICAL ASSOCIATION

Annual Report of the Council for 1969–70

MEMBERSHIP. On 31 December 1969 there were 1257 members (717 Ordinary, 111 Student, and 429 Institutional). The net decrease of 73 members since last year is largely explained by the transfer of Institutional Members to Blackwell's agency, resulting in greater financial benefit to the Association. The number of subscriptions through the agency was 282, a net increase of 24 on last year's figure.

FINANCE. During 1969 the Association published *Palaeontology* in four parts at a cost of £9286. Volume 2 has been reprinted at a cost of about £1200, of which £449 has been paid. *Special Papers* 4 and 5 have been published and *Special Paper* 6 is in the press; the total cost of these will be about £2400 of which £1235 has been paid. Administration costs have been slightly higher than usual, but relative to costs of printing have remained small. Good sales of *Special Paper* 2 enabled the Association to repay £552 of the £1000 loan from the Royal Society.

Although the Association only published four parts of *Palaeontology* in 1969 against five parts in 1968, total expenditure rose to £11740, slightly higher than even last year's record level. Each part of *Palaeontology* is costing about £300 more than it was two years ago. Income from subscriptions has fallen slightly, and subscriptions in 1969 only covered 70% of the cost of publishing *Palaeontology*. However, regular sales plus subscriptions paid in arrear covered the other 30%.

Total income in the year was higher than ever because of good sales of *Palaeontology* and *Special Papers*, and exceeded expenditure by £2127. This has been added to the Publications Reserve which stands at £11650. This would be sufficient to publish one volume of *Palaeontology* even after provision has been made for the payment of *Special Papers* in the press. The maturity of £200 5% Defence Bonds and the increased Publications Reserve have enabled the Association to increase and diversify their investments.

Sales of *Special Papers* have been encouraging. There are now 154 regular subscribers, and the earlier numbers have continued to sell well. However, we are still dependent on donations in order to cover the initial costs of printing *Special Papers* and the Association is indebted to: the Shell Oil Co. for a fourth grant of £250 for *Special Papers*; the Hebrew University of Jerusalem for a donation of £540 towards the cost of No. 4; the Esso Oil Co. for a donation of £328 towards the cost of No. 5; and the Victoria University of Wellington, New Zealand for a donation of £100 towards the cost of No. 6.

PUBLICATIONS. The four parts of Volume 12 of *Palaeontology* were published during 1969; they contained 41 papers and consisted of 718 pages and 130 plates. *Special Papers in Palaeontology* 4, 5, and 6 (for 1969) were published; they contain a total of 209 pages and 34 plates.

MEETINGS. Five meetings took place during 1969–70. The Association is grateful to the Council of The Geological Society of London, the Director of the British Museum (Natural History), Professor D. T. Donovan (University College, London), and Professor F. W. Shotton (University of Birmingham) for generously granting facilities for meetings, to Dr. L. R. M. Cocks for leading the field meeting, and to the local secretaries for their efficient services.

a. The *Twelfth Annual General Meeting* was held in the rooms of the Geological Society of London, Burlington House, London W. 1, on Wednesday, 5 March 1969, at 5.00 p.m. The Annual Report of the Council for 1968–9 was adopted and a ballot was held for the election of the Council for 1969–70. Dr. Pamela L. Robinson of University College, London, delivered the *Twelfth Annual Address* on 'Problems in the study of Triassic vertebrates'.

b. A *Field Demonstration Meeting* was held on 'Some Llandovery brachiopod localities in Shropshire', on 3 May 1969; the meeting was organized by Dr. L. R. M. Cocks.

c. A *Demonstration Meeting* on 'Micropalaeontology' was held in conjunction with the 11th European Micropalaeontological Colloquium at the British Museum (Natural History) on Saturday, 20 September 1969 at 2.00 p.m. Dr. C. G. Adams was local secretary.

d. A *Special Discussion Meeting* on a 'Proposal for an archive of palaeontological data' was held at University College, London, on Wednesday 5 November 1969 at 2.00 p.m. The local secretary was Professor D. T. Donovan.

e. A *Symposium* on 'The occurrence and preservation of fossils' was held in the Geology Department, University of Birmingham, from Tuesday to Thursday, 16–18 December 1969. About 85 persons attended to hear fourteen papers and to see fourteen demonstrations. Dr. I. Strachan was local secretary.

Council. The following were elected members of Council of the Association for 1968–9 at the Annual General Meeting on 5 March 1969: *President*: Professor Alwyn Williams, F.R.S.; *Vice-Presidents*: Dr. W. S. McKerrow, Dr. C. Downie; *Treasurer*: Dr. J. M. Hancock; *Membership Treasurer*: Dr. A. J. Lloyd; *Secretary*: Dr. W. D. I. Rolfe; *Editors*: Mr. N. F. Hughes, Dr. Gwyn Thomas, Dr. I. Strachan, Professor M. R. House, Dr. R. Goldring; *Other members*: Dr. F. M. Broadhurst, Dr. L. R. M. Cocks, Dr. C. B. Cox, Mr. D. Curry, Dr. A. Hallam, Dr. Julia A. E. B. Hubbard, Dr. J. D. Hudson, Dr. W. J. Kennedy, Dr. J. D. Lawson, Dr. E. P. F. Rose, Dr. C. T. Scrutton, Dr. V. G. Walmsley, Professor H. B. Whittington.

Circulars. Four Circulars (Nos. 57–60), containing full details of the affairs of the Association, were distributed to Ordinary and Student Members during the year, and to Institutional Members on request.

BALANCE SHEET AND ACCOUNTS FOR THE YEAR ENDING 31 DECEMBER 1969

Liabilities	£	*s.*	*d.*	£	*s.*	*d*
Publications Reserve Account:						
Balance as per annexed account				12 420	17	8
Royal Society Loan				448	0	0
Amounts received in advance						
Subscriptions for 1969				213	19	0
Provision for cost of publication of Palaeontology, Vol. 12, as per Income and Expenditure Account	9286	4	5			
Less Expenditure incurred to 31 December 1969	5764	4	5			
				3522	0	0
Sundry creditors				19	19	0
				£16 624	15	8

Assets	£	*s.*	*d.*	£	*s.*	*d.*
Office Equipment at cost	41	18	2			
Less depreciation to date	25	18	2			
				16	0	0
Investments at cost						
Equities Investment Fund for Charities—1403 units	1798	2	8			
Kirkby Urban District Council	1500	0	0			
Wagon Finance Corporation Limited	3000	0	0			
5½% National Development Bonds	2000	0	0			
Foreign and Colonial Investment Trust Co. Limited 750 5*s.*—Ordinary shares	1073	18	6			
8% City of Chester Loan	1000	0	0			
£500 9% Treasury Stock 1994	482	10	0			
£860 6¾% London County Stock 1974	751	9	4			
Grattan Warehouses Limited 200 5*s.* Ordinary shares	465	15	9			
Westland Aircraft Limited 500 5*s.* Ordinary shares	361	12	9			
Industrial and Commercial Finance Corporation Limited						
£500 'A' Loan Stock	487	10	0			
£200 'B' Loan Stock	120	0	0			
				13 040	19	0
Sundry Debtors and Payments in Advance						
Authors for offprints	370	19	6			
Advance payments for *Palaeontology*, Vol. 13	136	17	9			
For *Palaeontology* offprints	109	3	4			
Income Tax refund—1969 Investment Income	202	12	8			
				819	13	3
Cash at Bank						
Deposit Account	119	10	3			
Current Account—Sheffield	2628	13	2			
„ „ London	–	–	–			
				2748	3	5
				£16 624	15	8

Report of the Auditors to the Members of The Palaeontological Association. We have examined the above Balance Sheet and annexed Income and Expenditure Account which in our opinion give respectively a true and fair view of the state of the Association's affairs as at 31 December 1969 and of its income and expenditure for the year ended on that date.

THORTON BAKER & CO.
Chartered Accountants, Auditors

Income and Expenditure Account
for the year ended 31 December 1969

	£	s.	d.	£	s.	d.
Expenditure						
To Provision for the cost of publication of *Palaeontology*, Vol. 12						
Part 1	2299	13	1			
Part 2	2386	11	4			
Part 3	2300	0	0			
Part 4	2300	0	0			
	9286	4	5			
Add Extra costs						
Vol. 11, Part 5	293	13	0			
	9579	17	5			
Less Overprovision—Volume 11, part 4	29	10	0			
				9 550	7	5
Reprinting back issues				1 463	0	8
Administrative expenses						
Postage and stationery	270	5	5			
Audit Fee	19	19	0			
Duplicating and dispatch of circulars	259	11	6			
Meeting expenses	26	1	0			
Sundries	77	2	6			
Membership Treasurer—Honorarium	52	10	0			
				705	9	5
Depreciation of equipment				6	0	0
Excess of Income over Expenditure for the year, transferred to Publications Reserve Account				2897	16	0
				£14 622	13	6

To Balance as per Balance Sheet				12 420	17	8
				£12 420	17	8

	£	s.	d.	£	s.	s.
Income						
By Subscriptions for 1969	6467	9	7			
Subscriptions for 1968	373	10	9			
				6841	0	4
Sales of Publications						
Gross Income	4218	10	5			
Offprints Profit	431	2	4			
				4649	12	9
Premium on Redemption of 5% Defence Bonds				60	0	0
Investment Income (gross)						
5% Defence Bonds	50	0	0			
Bank Deposit Account	6	13	9			
Equities Investment Fund for Charities	111	18	5			
Wagon Finance Corporation Ltd.	236	4	1			
5½% National Development Bonds	110	0	0			
7·3/8% Kirkby U.D.C.	110	12	6			
Foreign and Colonial Investment Trust Ltd.	8	8	8			
8% City of Chester Loan	15	6	10			
9% Treasury Stock 1994	14	8	9			
Grattan Warehouses Ltd.	6	5	0			
				669	18	0
Special Donations				46	2	10
General Donations						
British Petroleum Co. Ltd.	250	0	0			
Texaco	175	0	0			
Burmah Oil Co. Ltd.	100	0	0			
				525	0	0
Special Papers						
Sales	2147	7	0			
Donations	667	13	5			
Offprints	165	14	5			
	2980	14	10			
Less Cost of Printing	1235	2	0			
				1745	12	10
Miscellaneous Receipts				85	6	9
				£14 622	13	6
By Balance at 31 December 1968				9523	1	8
Add Excess of Income over Expenditure	2897	16	0			
Reprinting Fund written back	–	–	–			
				2897	16	0
				£12 420	17	8

INDEX

Pages 1–173 are contained in Part 1; pages 175–333 in Part 2; pages 335–510 in Part 3; pages 511–691 in Part 4
Figures in **Bold Type** indicate plate numbers.

THE PALAEONTOLOGICAL ASSOCIATION

PALAEONTOLOGY

The journal *Palaeontology* is devoted to the publication of papers (preferably illustrated) on all aspects of palaeontology and stratigraphical palaeontology. Four parts at least are published each year and are sent free to all members of the Association. Members who join for 1970 will receive Volume 13, parts 1 to 4.

All back numbers are still in print and may be ordered from B. H. Blackwell, Broad Street, Oxford, England, at £3 per part (post free). A complete set, Volumes 1–12, consists of 47 parts and costs £141.

SPECIAL PAPERS IN PALAEONTOLOGY

This is a series of substantial separate works published by the Association. The subscription rate is £6 (U.S. $16.00) for Institute Members and £3 (U.S. $8.00) for Ordinary and Student Members. Subscriptions and orders by members of the Association should be placed through the Membership Treasurer Dr. A. J. Lloyd, Department of Geology, University College, Gower Street, London, W. C. 1, England.

The following *Special Papers* are available. Members may obtain them at reduced rates through the Membership Treasurer. Non-Members may obtain them from B. H. Blackwell, Broad Street, Oxford, England, at the prices indicated.

Special Paper No. 1 (for 1967): MIOSPORES IN THE COAL SEAMS OF THE CARBONIFEROUS OF GREAT BRITAIN, by A. H. V. Smith and M. A. Butterworth. 324 pp., 72 text-figs., 27 plates. Price £8 (U.S. $22.00), post free.

Special Paper No. 2 (for 1968): EVOLUTION OF THE SHELL STRUCTURE OF ARTICULATE BRACHIOPODS, by A. Williams. 55 pp., 27 text-figs., 24 plates. Price £5 (U.S. $13.00).

Special Paper No. 3 (for 1968): UPPER MAASTRICHTIAN RADIOLARIA OF CALIFORNIA, by Helen P. Foreman. 82 pp., 8 plates. Price £3 (U.S. $8.00).

Special Paper No. 4 (for 1969): LOWER TURONIAN AMMONITES FROM ISRAEL, by R. Freund and M. Raab. 83 pp., 15 text-figs., 10 plates. Price £3 (U.S. $8.00).

Special Paper No. 5 (for 1969): CHITINOZOA FROM THE ORDOVICIAN VIOLA AND FERNVALE LIMESTONES OF THE ARBUCKLE MOUNTAINS, OKLAHOMA, by W. A. M. Jenkins. 44 pp., 10 text-figs., 9 plates. Price £2 (U.S. $5.00).

Special Paper No. 6 (for 1969): AMMONOIDEA FROM THE MATA SERIES (SANTONIAN–MAASTRICHTIAN) OF NEW ZEALAND, by R. A. Henderson. 82 pp., 13 text-figs., 15 plates. Price £3 (U.S. $8.00).

Special Paper No. 7 (for 1970): SHELL STRUCTURE OF THE CRANIACEA AND OTHER CALCAREOUS INARTICULATE BRACHIOPODA, by A. Williams and A. D. Wright. 51 pp., 17 text-figs., 15 plates. Price £1. 10*s*. ($4.00).

SUBMISSION OF PAPERS

Typescripts on all aspects of palaeontology and stratigraphical palaeontology are invited. They should conform in style to those already published in this journal, and should be sent to Mr. N. F. Hughes, Department of Geology, Sedgwick Museum, Downing Street, Cambridge, England, who will supply detailed instructions for authors on request (these are published in *Palaeontology*, **10**, pp. 707–12).

PALAEONTOLOGY

VOLUME 13 · PART 4

CONTENTS

PRINTED IN GREAT BRITAIN AT THE UNIVERSITY PRESS, OXFORD
BY VIVIAN RIDLER, PRINTER TO THE UNIVERSITY

SMITHSONIAN INSTITUTION LIBRARIES